DEFENSE DOCUMENTATION CENTER

FOR

SCIENTIFIC AND TECHNICAL INFORMATION

CAMERON STATION, ALEXANDRIA, VIRGINIA

DISCLAIMER NOTICE

THIS DOCUMENT IS BEST QUALITY AVAILABLE. THE COPY FURNISHED TO DTIC CONTAINED A SIGNIFICANT NUMBER OF PAGES WHICH DO NOT REPRODUCE LEGIBLY.

This Document Contains
Missing Page/s That Are
Unavailable In The
Original Document

Best
Available
Copy

STRUCTURAL METHODS IN THE THEORY OF CONTROL

AND ELECTRIC AUTOMATION

by A. S. Shatalov

- USSR -

F O R E W O R D
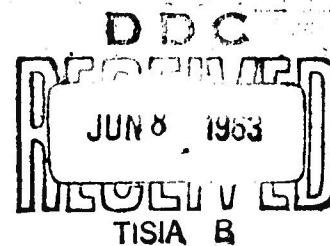
This publication was prepared under contract for the
Joint Publications Research Service as a translation
or foreign-language research service to the various
federal government departments.

The contents of this material in no way represent the
policies, views or attitudes of the U. S. Government
or of the parties to any distribution arrangement.

PROCUREMENT OF JPRS REPORTS

All JPRS reports may be ordered from the Office of Technical
Services. Reports published prior to 1 February 1963 can be provided,
for the most part, only in photocopy (xerox). Those published after
1 February 1963 will be provided in printed form.

Details on special subscription arrangements for JPRS social
science reports will be provided upon request.

No cumulative subject index or catalog of all JPRS reports
has been compiled.

All JPRS reports are listed in the Monthly Catalog of U. S.
Government Publications, available on subscription at $4.50 per year
($6.00 foreign), including an annual index, from the Superintendent
of Documents, U. S. Government Printing Office, Washington 25, D. C.

All JPRS scientific and technical reports are cataloged and
subject-indexed in Technical Translations, published semimonthly by
the Office of Technical Services, and also available on subscription
($12.00 per year domestic, $16.00 foreign) from the Superintendent
of Documents. Semiannual indexes to Technical Translations are
available at additional cost.

STRUCTURAL METHODS IN THE THEORY OF CONTROL

AND ELECTRIC AUTOMATION

- USSR -

[Following is a translation of a Russian-language book by A. S. Shatalov entitled Strukturnyye Metody v Teorii Upravleniya i Elektroavtomatike, Moscow, 1962, pp 1 - 405.]

PART I

The General Theory of Linear Transformations in Continuous Control Systems with Variable and Constant Parameters and Its Application to Elementary Components

PART II

Characteristics of Typical Elements Used in the Automatic Regulation of Power Equipment and in Automatic Control Systems

PART III

Analysis and Synthesis of Linear Continuous
Control Systems

Chapter 10. Precision of Forced Motion

PART IV

Nonlinear and Special Automatic Control Systems

FOREWORD

This book elucidates the problems, essential in practice, of the theory of automatic control and electric automation from the aspect of structural investigation methods. Analyzed is the effect of inner components which characterize the structure of elements and the complex control systems, as well as additional connections employed to obtain stability, precision, and other indices of system.

A mathematical device is described needed in the use of structural methods, based on the Laplace and Fourier conversions, and designed for use in control systems with alternating as well as constant parameters. The majority of these problems are oriented toward solutions by modulation methods.

The complex dynamic processes in electric furnaces, electric machines, electric automatic parts, and synthetized complex control systems are described in a manner understandable to engineers.

The book contains a number of nomograms and calculation tables which facilitate the solution of the problems of analysis and synthesis, mainly on the basis of frequency methods.

The book is intended for engineers and students of higher technical educational institutions, who are specializing in the field of automatic control systems, and may prove useful to designers of electrical machines and parts of electric automatic apparatus, intended for use in automatic control systems.

INTRODUCTION

The higher the level of development of each concrete science, the more clearly the principles of materialistic dialectics that are its nucleus are manifested. Sciences adjoining the theory and technique of automatic control show us, in a number of other sciences, the fruitfulness of application of the principles of materialistic dialectics at the stage of cognition of phenomena -- analysis -- and at the stage of purposefully directed attention to the course of the phenomena -- synthesis.

Of these principles, we will dwell on the principle of examination of phenomena in their interrelation and interconditioning that in application to technique determines the program of investigation drawn up for clarification of all the relations that can be taken into account in control systems, and on a detailed analysis of the elements on which these relations are superimposed.

The simpler the characteristics of the elements, the greater the weight the relation between the elements obtains in a description of the properties of the control system. Only on the basis of analysis of the relations set by the programs, algorithms, etc., does one succeed, in the area of cybernetics, in approaching an understanding of extremely complex phenomena, including some functions of the human brain.

In the problems of the theory of control and electric automation examined in this book, the methods of cognition of the relations within the elements and between the elements of a control system have acquired the name "structural methods."

Their exposition has also determined the main direction of this book.

The approach on the basis of structural methods has proved to be most general in the study of such varied control systems as: linear systems of continuous control with variable parameters; pulse control systems; systems with modulation of the control signal and nonlinear systems under certain particular conditions.

The general mathematical apparatus for the investigation of the

indicated systems is the theory of linear systems with variable parameters. ... In order to explain most clearly the influence of the relations and conditions of the accumulation of the transfer properties of the elements studied when they are combined into circuits it is necessary to apply those mathematical methods which transfer the problem from the area of classical analysis of differential equations, visible with difficulty at the high order peculiar to control systems, especially in the presence of specific elements with variable parameters, with a pulse regime, with modulation and nonlinearities, into a region of algebraic relations where the relations become completely 'transparent.' This is provided: by extension of the method of algebraization of differential equations to the case of systems with variable parameters, by the application of Laplace and Fourier transforms along the argument -- time for systems of linears with constant parameters, along the argument -- displacement for systems of linears with variable parameters, by the application of the same transforms with temporary shift of the argument into a complex plane for systems with modulation, and by the application of a discrete Laplace transform for pulse systems and of a Fourier transform with a functionally varying amplitude of the first harmonics for certain special problems in nonlinear systems. The aggregate of these transforms are generalized in the method of ... transforms developed in this book.

The complexity and variety of the apparatus of mathematical ... used in the theory of control, corresponding to the character of the problems being solved, naturally requires every sort of attraction of mathematical machines to the analysis of the regimes of complex automatic elements and control systems, and the more widely the methods of machine mathematics are introduced, the less becomes the need for explanation of analytical methods. This circumstance is ... into consideration in this book, where many problems ... selected toward their solution on by electronic continuous ... or ... (discrete) differential analyzers. It is here that the ... orientation of the book has proved especially fruitful, ... representations with clearly ... technical and mathematical relations developed ... into the adjustment circuit ... mathematical computer.

... considerable attention has been given to the ... methods of calculation and transformation of the parameters of ... elements and systems, and, on the basis of a number of ... programs ... giving relatively rapid ... of control systems:

b. ... the number of required calculations to ... programs;

... these as additions to the needed area of investigation ... calculations in all boundary conditions.

Since we have paid tribute in this book, in its limited volume, to the principal structural direction, naturally it was necessary at least to clarify and exclude a number of other interesting questions. But this gap is readily filled in, thanks to the presence of splendid books on the theory of control and electric automation by Russian and foreign authors, for example those mentioned in the bibliography. Books of recent years which basically embrace the whole complex of questions of control theory have been put in a separate list accompanying this introduction. Books which develop special directions have been referred to the lists of the literature by chapters.

In the final processing of the manuscript the author had the help of the criticism of Professor Nikolay Il'ich Andreyev, Doctor of Technical Sciences, and the careful editing done by Yevgeniy Borisovich Pasternak, to whom the author expresses his sincere appreciation.

Before the publication of this book the author found it possible to acquaint with its main ideas only a limited circle of engineers who have been interested in the journal articles and textbook of the author, issued in a departmental edition, and also to those who have attended the lecture courses of the author, given in the last ten to fifteen years to student and aspirant groups. Therefore the author sincerely requests all readers to express their opinions about this book, directing them to the address of the publishing house.

Bibliography

1. Solodovnikov, V V (Editor and author of the principal sections), Osnovy avtomaticheskogo regulirovaniya (Principles of Automatic Control), Vol 1, 1954; Vol 2, Parts I and II, 1959, Mashgiz.

2. Popov, Ye P, Dinamika sistem avtomaticheskogo regulirovaniya (Dynamics of Automatic Control Systems), GITTL, 1954.

3. Fel'dbaum, A A, Elektricheskiye sistemy avtomaticheskogo regulirovaniya (Electric Automatic Control Systems), Oborongiz, 1954.

4. Pugachev, V S, Teoriya sluchaynykh funktsiy i yeye primeneniye k zadacham avtomaticheskogo upravleniya (The Theory of Random Functions and Its Application to Problems of Automatic Control), GITTL, 1957.

5. James, H, Phillips, R and Nichols, N, Teoriya sledyashchikh sistem (The Theory of Follow-Up Systems), Foreign Literature Press, 1947.

6. Ch'ien Hsüeh-Sen, Tekhnicheskaya kibernitika (Technical Cybernetics), Foreign Literature Press, 1956.

7. Laning, J Kh and Bettin, R G, Sluchaynyye protsessy v zadachakh avtomaticheskogo upravleniya (Random processes in problems of Automatic Control), Foreign Literature Press, 1958.

8. Traxsell, Dzh, Sintez sistem avtomaticheskogo regulirovaniya (The Synthesis of Automatic Control Systems), Mashgiz, 1959.

9. *Trudy 2-go vsesoyuznogo soveshchaniya po teorii avtomaticheskogo regulirovaniya* (Proceedings of the Second All-Union Conference on the Theory of Automatic Control), Vol 3. Bibliography for the period 1941-1953.

PART I

THE GENERAL THEORY OF LINEAR TRANSFORMATIONS

IN CONTINUOUS CONTROL SYSTEMS

WITH VARIABLE AND CONSTANT PARAMETERS

AND ITS APPLICATION TO ELEMENTARY COMPONENTS

Chapter 1

METHODS OF COMPOSING AND TRANSFORMING LINEAR

DIFFERENTIAL EQUATIONS OF COMPONENTS OF CONTROL SYSTEMS

pp. 3-57

1.1. Forms of Notation of Differential Equations of Connection with Variable and Constant Coefficients

Automatic control systems consist of elements which react with one another by means of relations of different form. Through the elements of the control system and along the lines of communication pass control signals and disturbing effects which bring about changes in the controlled values.

Analysis of the conditions of passage of the signals through the elements of the control system is one of the fundamental questions of the theory of automatic control. We will start the examination of this question from the notation of the mathematical dependences which establish the laws of change of the input and output values in elements of an automatic control system. We will designate:

x_{in} is the control (input) signal;

x_{out} is the output (controlled) value for the investigated ...; we will call the equation connecting the laws of change of the input and output values the equation of connection.

In the majority of cases the equation of connection is a differential equation relative to an unknown x_{in} and a given x_{out} functions of an independent variable, the time t. A large circle of problems in the theory of automatic control is solved by means of a description of the elements of a system by linear differential equations. In this case the properties of the concrete element determine the order of the differential equation and its coefficients, in the general case the variables or in a particular case the constants, corresponding to the character of the physical parameters of the investigated element.

In writing linear differential equations of connection a definite relation can be seen which it is worthwhile explaining at the very beginning.

The classical form of notation

General case:

$$a_n(t)x_{in}^{(n)}(t) + \ldots + a_1(t)x_{in}'(t) + a_0(t)x_{in}(t) =$$
$$= b_m(t)x_{out}^{(m)}(t) + \ldots + b_0(t)x_{out}(t). \quad (1\text{-}1a)$$

The particular case of constancy of the parameters of the element and corresponding coefficients (a_i, b_i) is the equation:

$$a_n x_{in}^{(n)}(t) + \ldots + a_0 x_{in}(t) =$$
$$= b_m x_{out}^{(m)}(t) + \ldots + b_0 x_{out}(t). \quad (1\text{-}1b)$$

The abbreviated form of notation

The operation of single differentiation with respect to time is correspondingly denoted by the symbol D, and the multiple differentiation corresponding by a power of the symbol D, that is

$$\frac{d}{dt} = D, \quad \frac{d^n}{dt^n} = D^n. \quad (1\text{-}2)$$

The symbol of differentiation at the stage of writing and transforming the differential equation of connection is considered as an ordinary multiplier and can be separated from the differentiated

— 6 —

value, thanks to which new forms of notation of the equation of connection are obtained.

In the general case:

$$[a_n(t) D^n + \ldots + a_1(t) D + a_0(t)] x_{in}(t) =$$
$$= [b_m(t) L^m + \ldots + b_0(t)] x_{in}(t); \qquad (1\text{-}3a)$$

and in the case of constancy of the coefficients

$$(a_n D^n + \ldots + a_0) x_{out}(t) =$$
$$= (b_m D^n + \ldots + b_0) x_{in}(t). \qquad (1\text{-}3b)$$

Contracted algebraized form of notation:

General case:

$$\left[\sum_{i=0}^{n} a_i(t) D^i \right] x_{out}(t) = \left[\sum_{j=0}^{m} b_j(t) D^j \right] x_{in}(t). \quad (1\text{-}4a)$$

Particular case:

$$\left(\sum_{i=0}^{n} a_i D^i \right) x_{out}(t) = \left(\sum_{j=0}^{m} b_j D^j \right) x_{in}(t). \quad (1\text{-}4b)$$

Form of notation with use of designations of the algebraized differential polynomials (ADP) (linear operators)

The sums obtained in expressions (1-4) can be written more compactly:

$$a(t, D) = \sum_{i=0}^{n} a_i(t) D^i ; \qquad (1\text{-}5a)$$

$$b(t, D) = \sum_{j=0}^{m} b_j(t) D^j , \qquad (1\text{-}5b)$$

Where the functions on the left sides of (1-5) we will call the el-... differential polynomials (ADP). If we use the designations for the ADP with constant and variable coefficients, we get new forms of notation of the equations of connection:

In the general case:

$$a(t,D)x_{out}(t) = b(t,D)x_{in}(t) \qquad (1\text{-}6a)$$

and in the case of constancy of the coefficients

$$a(D)x_{out}(t) = b(D)x_{in}(t), \qquad (1\text{-}6b)$$

Operator form of notation:

While all the preceding expressions established the connection between the input and output values in the domain of time, the operator form establishes the connection between their Laplace transforms in the region of the complex argument p.

In the general case the equation of connection, converted into a Laplace transform, has the form:

$$\sum_{k=0}^{n} A_{ki}[p^k X_{out}(p)] = \sum_{j=0}^{m} A_{ij}[p^j X_{in}(p)]. \qquad (1\text{-}7a)$$

Here the Laplace-transforms in the region of the argument p, to which the transformations of the input and output values are subject, are distinguished by the symbols A_{ki} and A_{ij}. These transformations depend on the law of change of the variable coefficients, and there-fore the transformations are different in the general case for each coefficient a_i, b_j, and this is additionally noted by the subscripts j and i. The properties of A-transforms for typical laws of change are present in chapter 2.

In the particular case of constancy of the coefficients we have:

$$\sum_{k=0}^{n} a_k p^k X_{out}(p) = \sum_{j=0}^{m} b_j p^j X_{in}(p), \qquad (1\text{-}7b)$$

... the A-transform are reduced to a multiplication of the ... of the controlled value by the operator polynom with the powers p^k and p^j and coefficients a_k and b_j. If we designate the operator polynomials by functions analogous to the ADP in equation (1-6), we get the operator equation in the contracted form:

$$a(p) X_{out}(p) = b(p) X_{in}(p) \qquad (1\text{-}7c)$$

The operator form of notation not only permits designating the differential relationships between the input and output values, but also permits using the most economical form of solution of the given equations. However, at the stage of composing and transforming the equations of connection, other forms of notation often permit obtaining more general and clearer results, and therefore they also will be used in these cases.

We will now dwell on the question of the physical dimensions of the terms of the equations of connection.

Since the differential equation of connection reflects a definite physical process, the controlled values of x_{in} and x_{out} that enter it have a corresponding physical dimension. Agreement of the dimensions of all the terms of the equation is provided by the coefficients of the left side a_i ($i = 0, 1, 2, \ldots, n$) and of the right side b_j ($j = 0, 1, 2, \ldots, m$). At given dimensions of the input (x_{in}) and output (x_{out}) values the dimensions of the lowest coefficients (a_0) and (b_0) are connected by the relationship

$$\left[\frac{a_0}{b_0}\right] = \left[\frac{x_{in}}{x_{out}}\right]. \qquad (1\text{-}8)$$

The dimension of the coefficients in the presence of the derivatives is determined the fact that a single differentiation with respect to time d/dt changes the dimensions of the variable by sec^{-1}, and therefore

$$\left[\frac{a_i}{a_0}\right] = sec^i; \quad \left[\frac{b_j}{b_0}\right] = sec^j.$$

Consequently the subscripts of the coefficients of the differential equation of connection (1-1), equal to the order of the derivative in the presence of which that coefficient is found, show the time dimension of the relationship of that coefficient to the lowest coefficient of the left a_0 or right b_0 side of the equation respectively.

Above were explained only the mathematical dependences which permit describing the course of the processes of change of the controlled values in time, but when there is a passage of the control action through the elements of the system both the physical nature of the control action and its power can also be changed.

If we connect the source of the control action with the executive organ by intermediate elements and provide the necessary amplification of power as a function of the operating conditions of concrete systems and the primary sources of energy, often it is necessary to use intermediate values that are different in their physical nature, for example: electric voltage, hydraulic pressure, the expenditure of air in pneumatic systems, the angle of rotation, linear displacement, etc.

The proper selection of the physical nature of the control action for different sections of a system during necessary amplification of the power is a sufficiently complex task. Its solution requires a qualified engineering approach to the selection of the typical intermediate elements and the design of new elements specifically for certain systems. But even a system made from elements that are of high quality and have the necessary power amplification can prove inoperative if the course of the processes of control in time have not been carefully analyzed.

1.2. Structural Representations and Mathematical Models
Corresponding to the Equations of Connection

In Equations (1-5), (1-6) or (1-8a) we will leave on the left side only the higher derivative of the controlled value, transferring all the other terms to the right side and dividing them by the coefficient $a_n(t)$; then we obtain a form conditionally solvable with respect to the higher derivative:

$$D^i x_{out} = \frac{1}{a_n(t)} \left[\sum_{j=0}^{m} b_j(t) D^j x_{in} - \sum_{i=0}^{n-1} a_i(t) D^i x_{out} \right]. \qquad (1-9)$$

We will introduce a designation of the symbol of integration, the reciprocal of that adopted earlier (1-2) for the differentiation:

$$\frac{1}{D} = \int_0^t \ldots dt, \quad \frac{1}{D^i} = \int_0^t \ldots \int_0^t \ldots (dt)^i, \quad (1-10)$$

then we can obtain from (1-9) a form conditionally solvable with respect to the output value:

$$x_{out} = \frac{1}{D^n a_n(t)} \left[\sum_{j=0}^{m} b_j(t) D^j x_{in} - \right.$$

$$\left. - \sum_{i=0}^{n-1} a_i(t) \frac{1}{D^{i-i}} (D^n x_{out}) \right], \qquad (1\text{-}11a)$$

or

$$x_{out} = \frac{1}{D^n a_n(t)} \{ b(t,D) x_{in} - a^*(t,D) x_{out} \}. \qquad (1\text{-}11b)$$

In Equation (1-11a) several formal complications were intentionally developed which do not change the result but permit more clearly tracing the transformation of the values under investigation. A corresponding graphic representation is given in Figure 1-1.
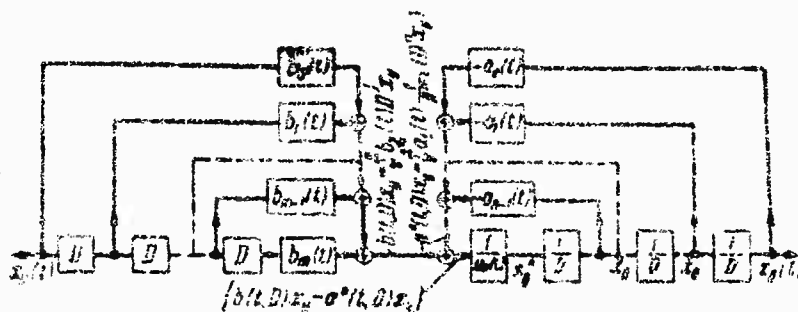
Fig 1-1. Structural representation of a differential equation of connection with variable parameters.

key: $x_y = x_{in}$; $x_B = x_{out}$

In fact, let us consider separately the obtaining of the difference standing in brackets in formula (1-11a) and the process of determining the desired value.

To obtain the expression in brackets, in the figure a row of summators is shown in the center; let the required sum be formed on the output of the last (right) summator; then according to the right end of the figure it is multiplied by the coefficient $1 / a_n(t)$ and passed through n integrators, as shown by the arrows, giving the controlled value x_{out} on the output.

On the left side of the figure is shown the obtaining of the

elementary terms generated by the input action x_{in}; the control signal is differentiated, and then is multiplied by the corresponding variable coefficients, forming the sum $b(t, D)x_{in}$.

On the right side of the figure, thanks to the introduced chain of integrators, all the derivatives of the output value are formed on the lines between the, and are multiplied by the corresponding variable coefficients $a_i(t)$ and arrive at the summators, forming the second sum — $a^*(t, D)z_{out}$. Thus all the connecting lines in the figure are closed, creating jointly with the variable co-factors, the differentiators, integrators, angles (branch points) and summators a structural representation of a system with variable parameters.

We will call the structural representation a graphic analog of an algebraised equation with variable parameters, explaining on the basis of the introduced structural designations the interconnection and interdependence between the individual terms of the equation in the domain of time.

Structural circuit

For an equation with constant coefficients in the structural representation in Figure 1-1 the variable co-factors are replaced by constant coefficients in accordance with equations (1-3b) and (1-4b), and the remaining transformations in the domain of time, peculiar to a structural representation, are preserved without change. If the operator form of notation is taken as a basis (1-7b), the connection between the terms of the equation will now be explained graphically by the structural circuit shown in Figure 1-2. The analogy between formulas (1-3b) and (1-7b) brings about an analogy also between the structures of Figures 1-1 and 1-2, but in the latter the operations of differentiation and integration are replaced by multiplication of the transforms of the signals by p or $1/p$.
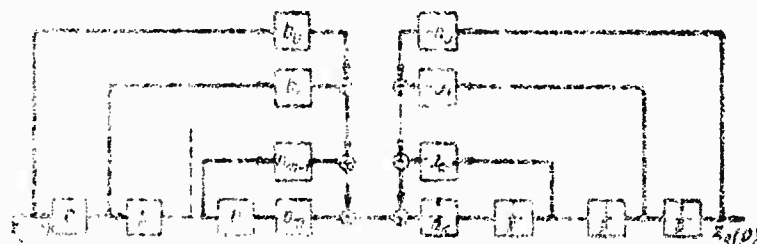
Fig. 1-2. Structural circuit corresponding to an equation of connection with constant parameters.
Key: $z_y = z_{in}$; $z_r = z_{out}$.

The same structural circuit is given to the graphic analog of an operator equation with constant coefficients, explaining the interconnection and interdependence between the transforms of the values

Adjustment Circuit of an electronic model

It is easy to proceed from the structural representation, which excludes all the operations on the controlled and input values in the domain of time, to the adjustment circuit of an electronic model for solution of the equation of connection by modern methods of machine mathematics. In doing so, the real apparatus of the model is introduced instead of the symbols of the structural representation: integrating amplifiers, summing amplifiers, scaled and inverting amplifiers and blocks of variable and constant coefficients. The connecting lines are made in the form of conducting lines along the circuits of parallel summation of voltages. The controlled values are reproduced in the form of voltages in scales coordinated during summation. If we have given the model the starting values or introduced the law of the equation also in the form of the voltage $U_{in} = m_{in} X_{in}$, where m_{in} is the electric scale V/physical dimensions of X, we got on the output of the model the result of solution of the equation of connection, which can be examined on the tube of an oscilloscope or recorded on the tape of an oscillograph.

It is natural that in constructing the adjustment circuit of the model, in addition to the logic of the structural representation it is necessary also to take into consideration the possibilities of the apparatus and the characteristics of the model. Thus, for example, in constructing the structural representation it is possible to make up several variants of circuits, depending on the derivative with respect to which the conditionally solved form of notation of the given initial equations is obtained. The variants will differ in the number of differentiators and integrators and the conditions of superposition of the connections, but mathematically they will remain equivalent. Differentiators are generally not used in explicit form in the circuit of the electronic model, and not every structural representation can be directly replaced by a model without preliminary transformations. We will examine questions of the apparatus and of the transformations of the structural representations later.

And so a mathematical formula -- a differential equation of connection -- can be graphically expressed by a structural representation valuable at the stage of cognition of the character and logic of the connections between the terms of the equation, convenient at the stage of transformations of the equation, replaceable by clear structural transformations, and creating the basis for solution of the equation by modern methods of machine mathematics.

1-3. Composition of a Differential Equation of Connection of
a Component with Constant Parameters According to
the Desired Character of the Process

Let a control system element which participates in the transmission of a control signal, or a measuring element of a control system be examined. During the transmission of a constant control signal x_{in}, on the output of the element, let us assume, it also is required that the constant value x_0, proportional to the control signal be obtained:

$$X_0 = k_{in}^{out} x_{in}. \qquad (1\text{-}12)$$

The proportionality factor k_{in}^{out} can be the amplification factor or the scale coefficient for agreement not only of the values but also of the dimensions of the input and output, which is also marked by its double indexation: the lower index is the input value and the upper is the output value.

A constant deviation on the output, caused by the control signal, we will call the forced motion. In the example under consideration it is defined by a very simple equation (1-12), but in the general case it can also be very complex, according to the demands presented to the system element.

The requirements for forced motion explain only one side of the desired process. In fact, if real physical elements are used the transition to a new, even a constant level of the output value is usually accompanied by transitional processes. The pointer of the measuring instrument, of a galvanometer for example, primarily gives an angular reading proportional to the current (k_{in}^{out} rad/a) and completes several oscillations around its position. The elastic elements of inertial pickups and elements similar to them likewise, as a rule, have an oscillational transitional process. Elimination of the oscillating component often is incompatible with the physical nature of the pickup or other control system element or leads to considerable deterioration of its properties: loss of sensitivity and reduction of its speed of operation. Therefore in the examination of element of such a kind it is necessary to tolerate the oscillational component if it has a damping character, that is, if it disappears in the course of time according to the law

$$x(t) = A e^{-\frac{t}{T}} \sin(\Omega t + \varphi). \qquad (1\text{-}13)$$

giving the constant of the time of damping of the amplitude T sec and the angular frequency Ω sec^{-1} values allowable according to the conditions of functioning of the element in the control system.

The transitional component of the process, accompanying the establishment of the forced component on the output of the unit, we will call the characteristic motion of the unit.

The total change in the output value is equal to the sum of the components of the forced and characteristic motion

$$x_{out}(t) = x_0 + x(t). \qquad (1\text{-}14)$$

Since the requirements for the forced and characteristic motions have been formulated, we will proceed now to composition of the differential equation of connection, in which at first we will compose a homogeneous equation and then a complete one.

The homogeneous differential equation of connection can be obtained by excluding the two arbitrary constants A and φ in the equation of characteristic motion, which is achieved by double differentiation of the equation of free motion (1-13) and corresponding substitutions.

The first differentiation is:

$$\dot{x} = A\left[-\frac{1}{T}e^{-\frac{t}{T}}\sin(\Omega t + \varphi) + \right.$$
$$\left. + \Omega e^{-\frac{t}{T}}\cos(\Omega t + \varphi) \right].$$

Substitution of the value of x from equation (1-13) gives:

$$\dot{x} = -\frac{1}{T}x + A\Omega e^{-\frac{t}{T}}\cos(\Omega t + \varphi).$$

The second differentiation is:

$$\ddot{x} = -\frac{1}{T}\dot{x} + A\Omega\left[-\frac{1}{T}e^{-\frac{t}{T}}\cos(\Omega t + \right.$$
$$\left. + \varphi) - \Omega e^{-\frac{t}{T}}\sin(\Omega t + \varphi) \right],$$

the substitutions

$$A\Omega e^{-\frac{t}{T}}\cos(\Omega t + \varphi) = \dot{x} + \frac{1}{T}x$$

and

$$Ae^{-\frac{t}{T}}\sin(\Omega t + \varphi) = x$$

give:

$$\ddot{x} + \frac{2}{T}\dot{x} + \left(\Omega^2 + \frac{1}{T^2}\right)x = 0,$$

or

$$T^2\ddot{x} + 2T\dot{x} + (1 + \Omega^2 T^2)x = 0. \qquad (1\text{-}15)$$

The dimensions of the coefficients in the presence of the derivatives is clearly evident in the obtained form:

$$[1] = [\Omega^2 T^2] = 0; \quad [2T] = sec; \quad [T^2] = sec^2.$$

In order to proceed from the homogeneous equation to the differential equation of connection with the amplification factor of the unit k_{in}^{out} taken into consideration for the regime that is being established, we eliminate the coefficient at the zero derivative in the left side of homogeneous equation (1-15) and add the equation obtained with equation (1-12), and obtain the complete equation of connection:

$$\frac{T^2}{1 + \Omega^2 T^2}\ddot{x}_{out} + \frac{2T}{1 + \Omega^2 T^2}\dot{x}_{out} + x_{out} = k_{in}^{out} x_{in}. \qquad (1\text{-}16)$$

Let us note once more that the proportionality between the input and output values (1-12) is provided only at the most simple input law $x_{in} = $ constant and only in the regime being established (at $t \rightarrow \infty$) when $\dot{x}_{out} = 0$ and $\ddot{x}_{out} = 0$. In the presence of a more complex input process, it is necessary to solve equation (1-16) anew according to the rules for determination of the forced component.

1-4. Composition of the Differential Equation of Connection According to Given Constant Physical Parameters of the Unit. Linearization.

Let us consider the design of a mobile system of an angular voltage regulator, represented schematically in Figure 1-3. In the voltage stabilization system the regulator is inserted between the output buses of the generator and the circuit of the excitation coil. Its purpose is to transform the voltage oscillations on the buses into reversed-

sign changes in conductivity of the excitation circuit in order to compensate for deviations of voltage on the buses from the rated. In the element under consideration, only part of the path of transmission of the control signal from the current of the electromagnet I (input) to the angle of rotation Θ of the movable lever (output), varying on account of the variable adjustment of the conductivity of the angular columns inserted in the excitation circuit, is analyzed.
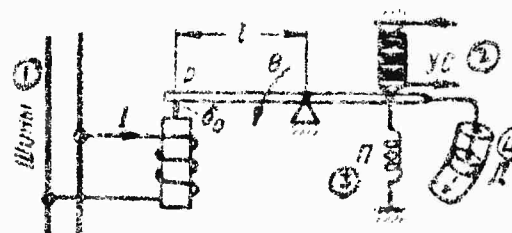
Fig 1-3. Mobile system of an angular voltage regulator. 1- Buses; 2 - Amplifier; 3 - Spring. 4-Damper

In the given case the differential equation of connection is the equation of the dynamic equilibrium of the mobile system (equation of moments) which has the form:

$$ J\ddot{\Theta} + M_2(\dot{\Theta}) + M_1(\Theta) = M(I, \Theta). \qquad (1\text{-}17) $$

Let us examine the values which enter this equation and the conditions of their assignment.

The controlling moment created by the electromagnet is $M(I, \Theta)$.

The moment depends on the current (direct square dependence) and on the tolerance δ (an inverse dependence of a complex character). Since the value of the tolerance is connected with the angle of rotation of the level by the relationship $\delta_0 - \delta = 1 \tan(\Theta - \Theta_0)$, where 1 is the arm of the lever, the moment of the electromagnet can be written directly as a function of the current I and the angle of rotation Θ:

$$ M_{in} = M(I, \Theta). \qquad (1\text{-}18a) $$

Representation of this function is possible in the form of a set of experimentally taken graphs shown in Figure 1-4.

The moment of counteraction of the spring is proportional to the rigidity of the spring and its tension. If the additional elastic moment from the angular columns is taken into consideration, the de-
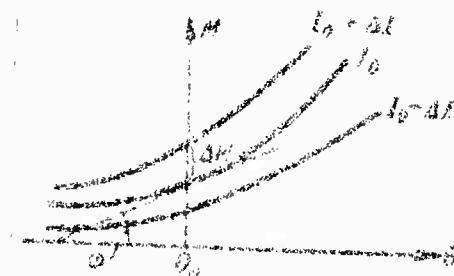
Fig 1-4. (Linearization of the traction)
characteristic of the electromagnet.

pendence of the total moment on the angle of rotation will be non-
linear, which can be written analytically in the form of the function

$$M_1 = F(\theta). \qquad (1\text{-}18b)$$

given, as a rule, also in the form of an experimental graph.

The moment of the viscous friction is determined by the speed of
movement of the damper and its design, and is expressed by the formula

$$M_2(\dot{\theta}) = S_1\dot{\theta} + S_2(\dot{\theta})^2 + \dots, \qquad (1\text{-}18c)$$

which takes into consideration the linear, square and more complex
dependence between the speed and moment.

The dynamic component of the moment $J\ddot{\theta}$ is equal to the product
of the angular acceleration times the moment of inertia of the mobile
part J ($\Gamma \cdot$ cm $\cdot$ sec^2)

$$M_3(\ddot{\theta}) = J\ddot{\theta}. \qquad (1\text{-}18d)$$

[Organization of Equation (1-17)]

In composing equation (1-17) for a real element it was necessary
to take in consideration considerably more complex relationships between
the physical values than is so given by the linear scheme in the
linear part of equations (1-1) or (1-16).

Various forms of these relationships have been given by formulas

(1-18b) and (1-18c), and of a more complex one by (1-18a).

The introduction into the equation of connection of the functional dependence on the controlled value (but not on time) makes the equation nonlinear, and evaluation of the operation of a system with such elements in a broad range of changes in values requires the application of special methods explained in Chapter 13.

However, a nonlinear equation can be reduced to linear notation if the dependences entering it are coarsened in a suitable manner and if the region of change of the controlled values is limited to a narrow zone.

Thus, for dependence (1-18c) it is simple enough to discard the quadratic term, limiting ourselves to the linear component:

$$M_2(\dot{\theta}) = S_a^M \dot{\theta},$$

which gives excellent approximation at small rates of motion.

The damping component S_a^M that enters the linear dependence is equal to the specific moment of viscous friction of the damper per unit of velocity. For its experimental determination it is sufficient, if we apply to the lever of design already encountered the known moment M_{meas} and to note the time t of rotation of the lever at the given angle Θ_{meas}. Then the mean rate of motion of the lever at the measured part is determined by the formula

$$\Omega_{av} = \frac{\theta_{meas}}{t},$$

according to the formula the damping coefficient is

$$S_a^M = -\frac{M_{meas}}{\Omega_{av}} = -\frac{M_{meas}}{\theta_{meas}} \left[\Gamma \cdot c.u \cdot sec \right].$$

For linearization of dependence (1-18b) it is necessary to take into consideration the characteristics of the operation of the voltage regulator, consisting of the fact that it is previously adjusted to the average value of the tolerance or corresponding angle Θ. This value of the angle Θ is a working point relative to which in the future the lever is rotated only at a small angle of deflection $\Delta\Theta$. For small deflections the increment of the moment can be described by the first term of a Taylor series:

$$\Delta M_1 = \left(\frac{df}{d\theta}\right)_{\theta=\theta_0} \Delta\theta. \qquad (1-19)$$

The derivative of the function F, which has the sense the steepness in increase of the moment upon the angle of rotation, we will call at the working point the linearized coefficient of moment of the spring and will designate

$$k_J = \left(\frac{dF}{d\theta}\right)_{\theta=\theta_0}. \qquad (1\text{-}20)$$

If we examine the right side of equation (1-17), we should also take into consideration that during static adjustment of the regulator not only the angle of rotation θ_0 is established, but also the rated voltage on the buses and the current corresponding to it on the coil of the electromagnet I_0. Around this working point in the future the current will obtain only small deviations ΔI. For small deviations the increment in the moment of the electromagnet can be described by two linear terms of the expansion of the function of two arguments $M(I, \Theta)$ in the Taylor series:

$$\Delta M(I, \theta) = \left(\frac{\partial M}{\partial I}\right)_{\substack{I=I_0 \\ \theta=\theta_0}} \Delta I + \left(\frac{\partial M}{\partial \theta}\right)_{\substack{I=I_0 \\ \theta=\theta_0}} \Delta\theta. \quad (1\text{-}21)$$

The partial derivatives at the given working point $\Theta = \Theta_0$ and $I = I_0$ can be provided by the symbols of the steepness S of increase in the moment with respect to the angle and with respect to the current:

$$S_\theta^M = \left(\frac{\partial M}{\partial \theta}\right)_{\substack{I=I_0 \\ \theta=\theta_0}} ; \quad S_I^M = \left(\frac{\partial M}{\partial I}\right)_{\substack{I=I_0 \\ \theta=\theta_0}}. \qquad (1\text{-}22)$$

It is evident from Figure 1-4 that the steepness S_θ^M is equal to the tangent of the angle φ of inclination tangential at the working point $\theta = \theta_0$ to that curve of the set for which $I = I_0$. In Figure 1-4 as the positive direction of reading Θ is assumed the direction opposite the time arrow; in that case the positive increase in Θ corresponds to a decrease in the tolerance. A second steepness S_I^M can be obtained from the same graph if in it, besides the curve corresponding to $I = I_0$ we examine the curve $I = I_0 + \Delta I$ and divide the increment of the function measured on the graph by the increment of the argument: $S_I^M = \Delta M / \Delta I$. If it is desired also to measure this steepness by the inclination of the tangents, the graph in Figure 1-4 must be redrawn on the coordinates I and M at the parameter Θ.

The values of the controlled values at the working points, set during the adjustment of the regulator, naturally satisfy the transformed equation (1-17):

$$\mathcal{J}\ddot{\theta}_c + S_{\theta}^{M}\dot{\theta}_0 + F(\theta_n) = M(I_n, \theta_0), \quad (1\text{-}23)$$

but it would be possible not to write the first two terms on the left side, since the derivatives from the constant value θ_0 equal zero. If now in transformed equation (1-17) the current values of the variables are replaced by the sum of their nominals and increments:

$$\left.\begin{array}{l} I = I_0 + \Delta I; \\ \theta = \theta_0 + \Delta\theta; \\ \dot{\theta} = \Delta\dot{\theta}; \\ \ddot{\theta} = \Delta\ddot{\theta}, \end{array}\right\} \qquad (1\text{-}24)$$

the zero and terms in the right and left sides, which are equal to one another according to (1-21) are contrasted, and relationships ... (1-22) are taken into consideration, we get the linearized equation for the load on at the lever of the regulator in the increments:

$$J\Delta\ddot{\theta} + S_{\dot{\theta}}^{M}\Delta\dot{\theta} + n_{\beta}\Delta\theta = S_{I}^{M}\Delta I + S_{\theta}^{M}\Delta\theta.$$

... after the reduction of similar terms we arrive at the differential equation:

$$J\Delta\ddot{\theta} + S_{\dot{\theta}}^{M}\Delta\dot{\theta} + (b_{\beta} - S_{\theta}^{M})\Delta\theta = S_{I}^{M}\Delta I. \quad (1\text{-}25)$$

Linearization is a powerful means of analysis of complex real dynamic systems, and is always used where the initial values of the variables they represent ... variable in time according to a known program, can be determined in advance by an adjacent or preliminary calculations, and for functions the linear terms of expansion into a Taylor series describe with adequate precision the main parts of the process, which is essential for study of a control system ...

Control Roles and Structural ... of the Rules of Linearization

Since linearization is ... cases it unavoidable in computing equations of components with their physical ..., we will ... remarks and explanations supplementing what has been previously considered.

... ... nd ... separation into linear and nonlinear parts. Let
... ... their steady state signal actual value y. Their assigned values,
which ... the control process name i.e. course, will be designated
... x₀, y₀; deviations from the assigned values are Δx and Δy; then
the complete values of the controlled values are

$$x = x_0 + \Delta x \quad y = y_0 + \Delta y.$$

... the system of differential equations which interconnects the
quantities in a nonlinear system, the total value of y and even its
steady component y₀ can be determined with respect to the assigned
... only by nonlinear methods, but for small increments, the
... which represents the main task in the analysis of stabiliza-
tion ... linear properties and structure corresponding to them
... ... set.

... principle of separation of the controlled values into assigned
... and their increments is illustrated in Figure 1-3. In the upper
... of the figure a nonlinear state is the formation of the input non-
... ... the output constant y₀ ... it is shown below, by sub-
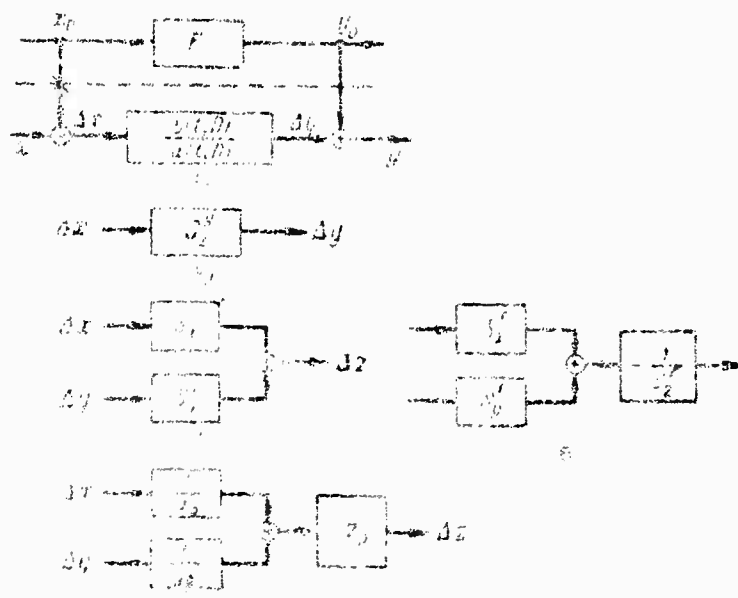
... separate the operating function of increments.

traction from the total value of the input its constant (assigned) part the increment in the input value Δx was obtained; the increment passes through the linearized system and is transformed into the increment of the output value Δy. In order to obtain the total value of the output, it is sufficient to add its increment to the constant part y_0, and this is also indicated in the right side of Figure 1-5a).

The procedure of the transformation of the increments depends on the character of the differential equation of correction for the increments. In the general case it is revealed according to Figure 1-1. In the scheme under consideration, in 1-5a, the linear structure for brevity's sake is conditionally written in the form of a fraction, the numerator and denominator of which are the algebraized differential polynomials of the right and left sides respectively of the equation of correction. In the beginning, as in the preceding examples, we will study only the linear part of the transformations and above all will examine simple questions of the transition to the increments for functional dependences of a static type in accordance with scheme b and the subsequent schemes of Figure 1-5.

The increment of the function of a single argument. The increment of the function $y = F(x)$ consists of:

$$\Delta y = \frac{dF}{dx} \Delta x = S_x^y \cdot \Delta x. \qquad (1\text{-}26)$$

Replacement of the designation of the derivative by that of the steepness $dy/dx = S_x^y$, besides being a more compact form of notation, also has the purpose of emphasizing the constancy of the coefficient S_x^y for a given small zone of change Δx.

This result was already obtained earlier (1-19); it is illustrated in Figure 1-a and does not require further explanations. Somewhat more complex is the case of assignment of an analogous dependence, but in an unclear form $F(x,y) = 0$.

In this case the transition to the increments gives the dependence:

$$\frac{\partial F}{\partial x} \Delta x + \frac{\partial F}{\partial y} \Delta y = 0 \quad \text{or} \quad S_x^F \Delta x + S_y^F \Delta y = 0,$$

whence

$$\Delta y = - \frac{S_x^F}{S_y^F} \Delta x = S_x^y \Delta x. \qquad (1\text{-}27)$$

Increment of the function of two arguments. For a functional dependence of the type

$$z = \varphi(x, y) \qquad (1\text{-}28)$$

transition to the increments gives the formula

$$\Delta z = \frac{\partial \varphi}{\partial x}\,\Delta x + \frac{\partial \varphi}{\partial u}\,\Delta y$$

or

$$\Delta z = S_x^z\,\Delta x + S_y^z\,\Delta y. \qquad (1\text{-}29)$$

The structural scheme of 1-5c corresponds to this formula. Upon the implicit assignment of the same function in the form $F(x, y, z)$ the transition to the increments gives:

$$\frac{\partial F}{\partial x}\,\Delta x + \frac{\partial F}{\partial y}\,\Delta y + \frac{\partial F}{\partial z}\,\Delta z = 0,$$

whence

$$\Delta z = -\frac{1}{S_z^F}(S_x^F\,\Delta x + S_y^F\,\Delta y). \qquad (1\text{-}30)$$

Scheme 1-5d corresponds to the latter formula. This scheme is reduced to scheme 1-5c if it is kept in mind that

$$-\frac{S_x^F}{S_z^F} = S_x^z\;;\quad -\frac{S_y^F}{S_z^F} = S_y^z\,.$$

A quite expanded partial form of the function of the two arguments (1-29) is the product

$$z = xy. \qquad (1\text{-}31)$$

For example, a structural diagram of an electric motor is examined in Chapter 6; in it the magnetic flux is related to the controlled values and the moment proportional to their product is investigated. Analogously the e.m.f. of a generator is proportional to the product of the rate and the magnetic flux.

The formula for linearization of the product (1-31) is very simple:

$$\Delta z = x_0\,\Delta y + y_0\,\Delta x.$$

It is convenient to rewrite this formula for relative increments, dividing both parts of it by $z_0 = x_0 y_0$:

$$\frac{\Delta z}{z_0} = \frac{\Delta x}{x_0} + \frac{\Delta y}{y_0}, \qquad (1\text{-}32)$$

A structural diagram corresponding to formula (1-32) has been constructed in Figure 1-5e.

Thus the linear part of the relative increment of the product is equal to the sum of the relative increments of the factors. This rule is valid for any number of factors.

1-5. Typical Linear Components of Continuous Control Systems with Constant Parameters

1. Classification

Practice has shown that equations of connection of elements of control systems, independently of their design and likewise of the physical nature of the controlling action, in many cases prove to be of the same type. This confirms the validity of the profound thought of V I Lenin: "The unity of nature is discovered in the striking analogousness of differential equations relating to different regions of phenomena" (V I Lenin, Materializm i empiriokrititsizm (Materialism and Empiriocriticism), Gospolitizdat, 4th Edition, Vol 14, Chapter V, Section 5, p 276) in the region of the theory and technique of automatic control.

In the apparatus of the structural analysis of the present-day theory of automatic control, wide use is made of the single-typicity of differential equations of connection for elements that differ in their design and principle of action. The foundations for the development of this apparatus were laid by the Soviet scholar A V Mikhaylov /1/, who suggested classifying all possible elements of automatic control systems according to types of equations of connection and designated a series of typical equations, relating them to typical elementary components.

In order for an element of a control system to be called an elementary component it must possess two properties: first, its differential equation of connection must not be above the second order; secondly, it must possess the property of single-directedness, that is, it must pass the controlling action only in one direction, from the input to the output, and not change its transmission properties when succeeding components are connected into its output, which usually is done when there is an adequate power amplification factor.

In connection with limitation of the order of equations of connection, the number of types of components obtained is relatively small. From these typical components it proves possible to create a structural diagram of any control system, as it is possible to put together a building from typical blocks.

Static components. Components are called static if in them, at
a constant input signal, a constant output value also is established
in the course of time. A necessary condition for obtaining such a
particular solution is the presence of lower terms in the equations
of connection, that is, the condition

$$a_0 \neq 0, \quad \text{and} \quad b_0 \neq 0.$$

Then if, at $t \to \infty$, $x^{(i)} \to 0$ $(i = 1, 2, \ldots, n)$, then

$$a_0 x_0 = b_0 x_{in}.$$

If we change the order of the higher terms of the left and right
sides of equation (1-1) within the limits $0 \leqslant m \leqslant 2$ or $0 \leqslant n \leqslant 2$,
we obtain equations of the zero, first and second orders. The number
of elementary components is exhausted by these combinations, with some
additional limitations.

A classification by order of the equation of connection is given
in Table 1-1.

Table 1-1   Typical Static Components

Порядок уравнения (1)	Форма уравнения (2)	Наименование звена (3)	
0	$a_0 x_b(t) = b_0 x_y(t)$	④	Усилительное
	$a_0 x_b(t) = b_0 x_y(t - \tau)$	⑤	Запаздывающее
1	$a_1 \dot{x}_b + a_0 x_b = b_0 x_y$	⑥	Апериодическое
	$a_0 x_b = b_1 \dot{x}_y + b_0 x_y$	⑦	Формирующее первого порядка
2	$a_2 \ddot{x}_b + a_1 \dot{x}_b + a_0 x_b = b_0 x_y$	⑧	Колебательное
	$a_2 \ddot{x}_b + a_0 x_b = b_0 x_y$	⑨	Резонансное
	$a_0 x_b = b_2 \ddot{x}_y + b_1 \dot{x}_y + b_0 x_y$	⑩	Формирующее второго порядка

1 - Order of equation of connection; 2 - Form of equation; 3 - Desig-
nation of component; 4 - Amplifying; 5 - Delaying; 6 - Aperiodic; 7 -
Boosting of first order; 8 - Oscillating; 9 - Resonant; 10 - Boosting
of second order.

$$x_b = x_{out}; \quad x_y = x_{in}.$$

The group of static components, as is evident from Table 1-1, is extensive. Besides the division into sections with different orders of equations, within each section there are several components with different designations. The designation of the components given in the table is determined by the fundamental character of the characteristic motion of the component.

Astatic components. Components are called astatic if in them a constant input signal determines the rate of increase of the output signal and, consequently, at an unchanged (but not null) input the output value is continuously changing. Such a dependence corresponds to integration of the input value, which is accomplished when there is equality with zero of a lower coefficient in the left side of the equation, that is, at $a_0 = 0$, but $b_0 \neq 0$.

The simplest equation of an astatic component has the form:

$$a_1 \dot{x}_{out} = b_0 \dot{x}_{in}. \qquad (1\text{-}34)$$

Such a component is called an ideal integrating or simply integrating component. If higher derivatives are added on the left side, analogously to the static components presented in Table 1-1, the astatic properties are preserved only within the limit ($t \rightarrow 0$), and the component will not perform an ideal operation of integration and will belong to the category of real integrating components.

Differentiating components. Components are called differentiating in which the output value is determined by the rate of change of the input value. For this to happen in an equation of connection there must be no lower coefficient on the right side, that is, $b_0 = 0$, $a_0 \neq 0$. In contrast with the preceding components, the differentiating component does not pass on a constant signal and usually is used in the ideal form only in auxiliary circuits, and is used in the main control circuit only when connected up in parallel with other components.

The equation of an ideal differentiating component is

$$a_0 x_{out} = b_1 \dot{x}_{in} \qquad (1\text{-}35)$$

Complication of the left side of (1-35) according to Table 1-1 leads to real differentiating components.

2. The Structure of Typical Components

In Figure 1-6 are variants of the structures of typical components, compiled according to their equations of connection, which we will give below in technical form.

The equation of connection of an amplifying component has the
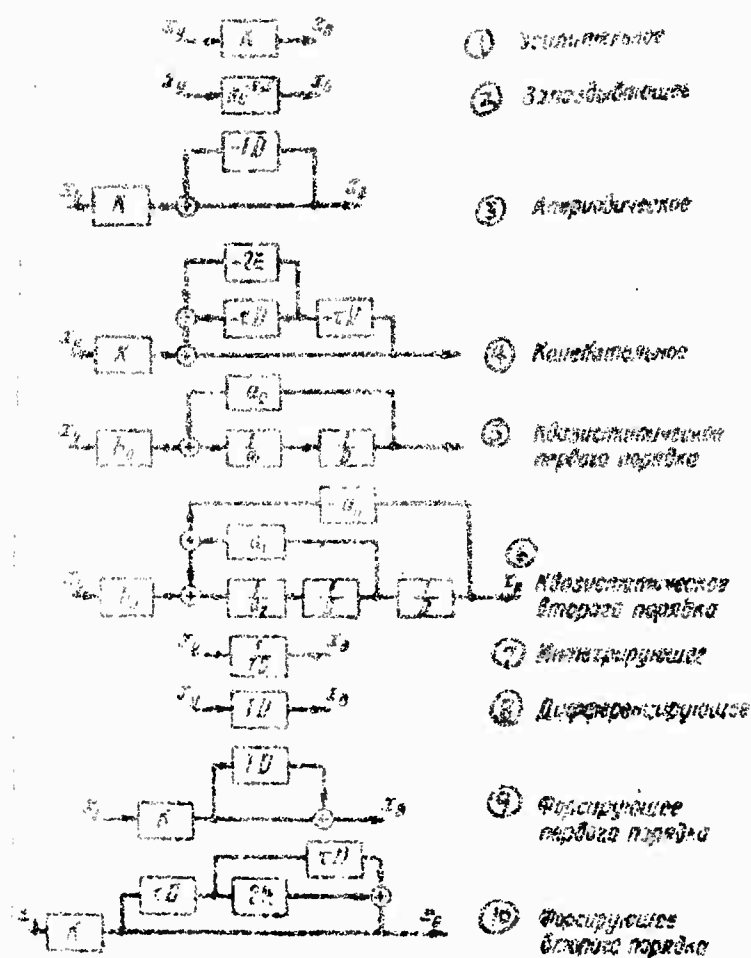
Fig 1-6. The structure of typical components. 1 - Amplifying; 2 - Delaying; 3 - Aperiodic; 4 - Oscillating; 5 - Quasi-static of first order; 6 - Quasi-static of second order; 7 - Integrating; 8 - Differentiating; 9 - Boosting of first order; 10 - Boosting of second order.

$x_1 = x_{out}$; $x_2 = x_{in}$

form:
$$x_{out} = kx_{in} \qquad (1\text{-}36)$$

The equation of connection for the delaying component has the form:
$$x_{out}(t) = kx_{in}(t - c_3) \qquad (1\text{-}37)$$

The process on the output of the delaying component is a repetition of the input process, but with a delay in time by the value τ_3 and a simultaneous change in the scale of the process (amplification) by k times. Thus the delaying component is characterized by two parameters: the time of delay τ_3 and the amplification factor k.

The delaying component amounts to a long line or a circuit replacing it which creates a temporary delay in the transmission of electrical signals; the delaying component is also a hydraulic line, where the transmission of excitations along a column of liquid occurs with a definite speed. Temporary delaying is also observed in the transmission of sound oscillations from beyond the finite speed of sound.

Great delay can be obtained when the signal is recorded and removed on a moving magnetic tape.

A circuit with a large number of aperiodic components also amounts to a delaying component.

The interval of time from 0 to τ_3 after the feeding of the input action is the time of the transitional process. However, this process runs its course within the delaying component: there are no changes in x_{out} observed in that period, and the connection between the input and output is reduced to a temporary displacement and amplification which enter equation (1-37).

Since in equation (1-37) there are no symbols of differentiation, in classificational Table 1-1 the delaying component was put in the category of components of null order. However, the operation of displacement (1-37) can represent an expansion into a Taylor series with respect to the derivative $x_{in}(t)$:

$$kx_{in}(t - \tau_3) = k\left[1 - \tau_3 D + \frac{(\tau_3 D)^2}{2!} - \frac{(\tau_3 D)^3}{3!} \cdots\right] x_{in}(t).$$

(This expansion cannot serve as the basis for the construction of a model of the component, and is used only for explanation of the correspondence between the forms of notation of (1-37) and (1-38).)

If we contract the series, we obtain the compact formula:

$$x_{out}(t) = ke^{-\tau_3 D} x_{in}(t). \tag{1-38}$$

For the aperiodic component the technical form of the equation of connection has the form:

$$T\dot{x}_{out} + x_{out} = kx_{in} \tag{1-39a}$$

where T is the time constant; k is the amplification factor.

If we reduce equation (1-39a) to the form conventionally solved with respect to the output value:

$$x_{out} = kx_{in} - TDx_{out} \qquad (1\text{-}39b)$$

we construct on this a structure with a negative inverse connection corresponding to the second term of the right side of the formula, damping the increase in the output value and proportional to the rate of its change.

In the regime that is established at $x_{out\ est}$ = constant and $\dot{x}_{out}$ = 0 there remains only one term on the $x_{out\ est}$ left side of equation (1-39a): $x_{out\ est} = kx_{in\ 0}$, which characterizes the static amplifying properties of the component.

The presence of the characteristic motion, which prevents instantaneous change of the output value, is caused by the existence of inhibiting factors in the real component. These factors in components that are different in their physical nature appear in the form of moments, forces, voltages, etc., and if the inhibiting action is proportional to the rate of change of the output value, the component becomes aperiodic.

Thus, for example, during the movement of a body in a viscous medium there arise hindering forces of viscous friction proportional to the rate of displacement. If as the output value the study is not of displacement but of the rate of displacement or of rotation, then forces of inertia proportional to the rate of change of the output value will prevent change of the output value. By analogy with mechanical motion the course of the transitional process in aperiodic components of any physical nature also is explained by their inertia and the component itself often is called inertial.

For the oscillating component the differential equation of connection in the technical form has the form:

$$\tau^2 \ddot{x}_{out} + 2\xi\tau\dot{x}_{out} + x_{out} = kx_{in} \qquad (1\text{-}40)$$

where τ is called the conditional time constant and ξ is the relative damping coefficient.

These new parameters can be compared with the coefficients of the equation of the component displaced in Table 1-1, and also with the coefficients of formula (1-16) on the basis of the relationships given in Table 1-2.

If the relative damping coefficient tends toward zero, equation

Table 1-2 Parameters of the Oscillating Component

Соотношения между параметрами ①	Условия существования затухающих колебаний ②
$\tau = \sqrt{\dfrac{a_3}{a_1}} = \dfrac{T}{\sqrt{1+\Omega^2 T^2}} = \xi T$	$4a_0 a_1 > a_1^2$
$\xi = \dfrac{a_1}{2\sqrt{a_2 a_0}} = \dfrac{1}{\sqrt{1+\Omega^2 T^2}} = \dfrac{\tau}{T}$	$\Omega_0 > \dfrac{1}{T}$
$\Omega_0 = \sqrt{\dfrac{a_2}{a_1}} = \sqrt{\dfrac{1}{T^2}+\Omega^2} = \dfrac{1}{\tau}$	$T > \tau$
$T = 2\dfrac{a_3}{a_1} = \dfrac{\tau}{\xi}$	$\xi < 1$
$\Omega T = \dfrac{1}{\xi}\sqrt{1-\xi^2}$	
$\Omega = \sqrt{\dfrac{a_0}{a_2}-\dfrac{a_1^2}{4a_2^2}} = \dfrac{1}{\tau}\sqrt{1-\xi^2} =$	
$= \sqrt{\Omega_0^2 - \dfrac{1}{T^2}}$	

1 – Relations between parameters; 2 – Conditional existence of damping oscillations.

(1-40) will assume the form.

$$\tau^2 \ddot{x}_{out} + x_{out} = k x_{in} \qquad (1-41)$$

From Table 1-2 we have:

$$\Omega_0 = \dfrac{1}{\tau}, \qquad (1-42)$$

where $\Omega_0 = \lim_{\xi \to 0} \Omega$ is the frequency of the nondamping oscillations or the resonant frequency. From formula (1-41), with (1-42) taken into consideration, we get:

$$\dfrac{1}{\Omega_0^2} \ddot{x}_{out} + x_{out} = k x_{in}. \qquad (1-43)$$

The component described by equations (1-41) and (1-43) we will call the resonance component. Its properties correspond to degenerate properties of the oscillating component during tending of the damping toward zero

$$\left(\xi = 0; \quad \frac{1}{T} = 0; \quad a_1 = 0\right).$$

To obtain one of the variants of structure of the oscillating component we reduce equation (1-40) to the form conventionally solved with respect to the output value:

$$x_{out} = kx_{in} - (2\xi\tau D + \tau^2 D^2) x_{out} \qquad (1-44)$$

and construct its structure.

It is obvious that in the regime that is being set up the component transmits a constant input signal with amplification k times, but the establishment of this value is hindered by terms proportional to the rate and acceleration of the output value.

Quasi-static components. We will begin our consideration of the components of this type with a concrete example, continuing the analysis of the voltage regulator considered in 1-4.

In the design of the regulator represented in Figure 1-3, let the increase in the force of attraction of the electromagnet during decrease in the air tolerance be greater than the simultaneous increment of the restorative force of the spring. For convenience in analysis it is worthwhile writing the equation of the moments (1-25) with clearly expressed signs of the coefficients:

$$I\Delta\ddot{\theta} + S_2^M \Delta\dot{\theta} - (S_6^M - k_p)\Delta\theta = S_I^M \Delta I \qquad (1-45)$$

or in the general form:

$$a_2 \ddot{x}_{out} + a_1 \dot{x}_{out} - a_0 x_{out} = b_0 x_{in}$$

We will begin the analysis of this equation with the simplest case, where in a given design of the regulator the moment of the inertial forces is inconsiderable in comparison with other components of the equation of moments and its value can be disregarded.

In that case the equation of connection is simplified:

$$a_1 \dot{x}_{out} - a_0 x_{out} = b_0 x_{in} \qquad (1-46)$$

The formally obtained equation converges with equation (1-39a)

— 32 —

and the coefficients $a_0 \neq 0$ and $b_0 \neq 0$ on the left and right sides of the equation can suggest a real static amplification factor $k = -b_0/a_0$ and the fact that the motion on the output is directed to the side opposite the input action (minus sign).

But such a conclusion would be false: the presence of the coefficients a_0 and b_0 not equal to zero, it is true, makes the equation of connection similar to the equation of the static component, but this is a simulated statism and components of this type are called quasi-static. In fact, if the equation is reduced to the conventionally solved form relative to x_{out}

$$Dx_{out} = \frac{1}{a_1}(b_0 x_{in} + a_0 x_{out}) \qquad (1\text{-}47)$$

then assuming $x_{out} = 0$ at $t = 0$, we find for the initial rate the concrete and positive value:

$$x'_{out}(0) = -\frac{b_0}{a_1} x_{in}(0).$$

Further motion will run its course at an ever-increasing rate.

This concept is clearly illustrated by the structural component constructed according to equation (1-47), from which it is evident that the sum formed on the summator, proportional to the velocity, continuously increases on account of the positive constituent of the output value.

In a real regulator with such parameters the lever quickly arrives at rest upon any small controlling action.

A quasi-static component of the second order has the differential equation of connection

$$a_2 \ddot{x}_{out} - a_1 \dot{x}_{out} + a_0 x_{out} = b_0 x_{in} \qquad (1\text{-}48a)$$

and a structure corresponding to the conventionally solved form

$$D^2 x_{out} = \frac{1}{a_2}\{b_0 x_{in} + [a_1 D - a_0] x_{out}\}. \qquad (1\text{-}48b)$$

The negative sign of the coefficient a_1 in (1-48a) is expressed in the structure of the component by feed of positive values of the rate of the output value on the input of the first integrator, which creates a continuous increase in the amplitude of oscillations on the output of the component. An established solution of the type of (1-??) likewise does not exist in this component.

The appearance in an equation of the second order of other negative coefficients (a_0 or a_2), as follows from the structure, likewise leads to the rise of divergent processes, but these new equations are split into two equations with real coefficients and correspond to a combination of two elementary components.

For the integrating component the equation of connection reflects on the output the proportionality of the rate of the process to the input value:

$$T\dot{x}_{out} = x_{in} \qquad (1\text{-}49)$$

If we transpose the coefficient T to the right side, we get the standard form of the differential equation of connection:

$$\dot{x}_{out} = \frac{1}{T} x_{in} = k_{-1} x_{in} \qquad (1\text{-}50)$$

where the designation of the amplification factor of the component is renamed with respect to the rate k_{-1} sec^{-1}.

For a component of the given type an equation of the integral connection, obtained from the preceding, appears more natural:

$$x_{out} = k_{-1} \int_0^t x_{in} dt = \frac{k_{-1} x_{in}}{D} = \frac{1}{TD} x_{in} \qquad (1\text{-}51)$$

The integrating component at constancy of the input value creates on the output a continuous increase in the output value. This property is not a shortcoming in closed automatic control systems, but on the contrary leads to the attainment of a very high indicator of accuracy.

The equation of connection for the differentiating component has the form:

$$x_{out} = T\dot{x}_{in} = TDx_{in} \qquad (1\text{-}52)$$

and determines its structure.

The coefficient T on the right side of the equation of connection is the amplification factor of the differentiating component. When the physical nature of the input and output values is identical, the amplification factor has the dimension of time, that is, seconds.

At different dimensions of the input and output values the dimensions of the amplification factor are correspondingly complicated. Such a component is used in control systems in auxiliary circuits, and in computers serves for the performance of a mathematical opera-

tion, differentiation.

For the roading component of the first order in the equation of connection

$$x_{out} = k(x_{in} + T\dot{x}_{in}) = k(1 + TD)x_{in} \qquad (1\text{-}53)$$

and the conditions of transmission of the derivative from the input value are reflected in the structure along with the input action.

For the roading component of the second order the right side of the differential equation of connection is supplemented by one more term, proportional to the second derivative from the input value, and the equation assumes the form:

$$x_{out} = k(x_{in} + 2\tau\dot{x}_{in} + \tau^2\ddot{x}_{in}). \qquad (1\text{-}54)$$

The algebraic form of the equation

$$x_{out} = k(1 + 2\tau D + \tau^2 D^2)x_{in} \qquad (1\text{-}55)$$

is used for construction of the structure.

1-5. Circuit Elements of Control Systems and Linear Electronic Models

The components presented in the preceding paragraphs had a relatively simple internal structure. They were constructed according to algebraic equations and reflected elements of the equations and the connections between them.

Integrators, differentiators, and variable and constant coefficients were used as elements of the structures; such structures in the future will be called detailed structures.

The connections between the elements were accomplished by branches from lines -- angles, and at the expense of adjuncts to lines -- summators. All these structural elements and connections, as a rule, do not figure directly in the form of the design elements of a component, and are manifested only in its mathematical description, but the action of these connections, as is evident from the preceding examples, has the same result as the action of real connections if they were realized in the form of separate design elements.

In a single circuit of a control system the connections between the real components will be not only mathematical, but also physical: in the form of cylinders or levers for mechanical controlled values, wires for electrical currents, hydraulic or pneumatic conduits, etc. The selection of these values for lines branching off from the main

path in the general case requires the establishment on the main line
of a   node   which sometimes degenerates into a very simple circuit
combination, for example for the circuit of electrical voltage. The
summation of the real values requires a circuit element -- a summator.

Thus in the complex structure of a control system it is necessary
to expect a mapping of the real constructive connections between the
elements and, when there is a detailing of the structures of the ele-
ments, a mapping of the internal mathematical connections in the ele-
ments themselves. These mathematical and constructive connections,
which are heterogeneous in their physical nature, are reflected iden-
tically in the structure, but this does not cause any misunderstand-
ings in the mathematical and structural analysis.

In modeling also all the connections are materialized identical-
ly into electrical connections between the elements of the model.

We will proceed to a consideration of real circuit elements that
are applied in typical control systems.

1. Nodal Elements

In figure 1-7 is a branching node, or simply a node. If there
is a signal x on some segment of the structural circuit a, all the
rays branching from that section will transmit the same signal x.
Elements of a structural circuit possess the property of unidirectiv-
ity, and therefore the switching in of any number of rays does not
change the value of the signal. But only one line can arrive at the
node.

Typical nodes of real control systems are presented in diagrams
1-7b, c and d.

In the mechanical diagram b the node is realized in the form of
a geared drive with a transmission number equal to 1.

The node for the branching of electrical voltage along circuit
c is realized by a simple tap from the buses of conductors that are
under that voltage. The node during utilization of current as a
controlling value is realized by switching in, in sequence, into a
break of the circuit of the nodal elements, for example, of two mag-
netic amplifier with a single amplification factor. Since one and
the same current x passes through all the amplifiers, there will be
one and the same controlling value in the branches in correspondence
with the structural circuit a. Nodal elements of another physical
nature can be constructed analogously under the condition that they
satisfy the structural diagram a.

2. Summators
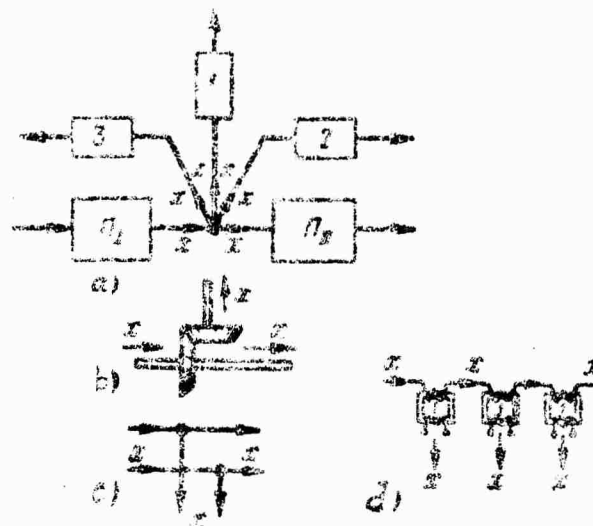
Fig 1-7. Structural representation of some types of nodes.

Summators are shown in Figure 1-8. The signal on the output of a summator is equal to the sum of the input signals. In diagrams a and b are structural representations of summators; in diagrams c, d, e, f, g and h are examples of real elements used in practice as summators.

The angles of rotation (diagram c) are summarized on a mechanical differential. Linear displacements are summarized on a linear lever-type summarizing mechanism (diagram d).

Electrical voltages can be summarized according to the sequential diagram e and according to the parallel diagram f. In the latter case the scale of the sum of $n + 1$ terms is equal, at

$$r_0 = r_1 = \ldots r_n = r$$

to

$$\frac{1}{n + r/r_{n+1} + 1},$$

a scaling amplifier can be used to increase it.

The multigrid tube (diagram g) changes the current under the influence of the total action of the voltages on the grids.

The summation can also be accomplished by means of a magnetic system in accordance with diagram h. The total magnetic flux formed by the currents of the separate windings is used in a magnetic or
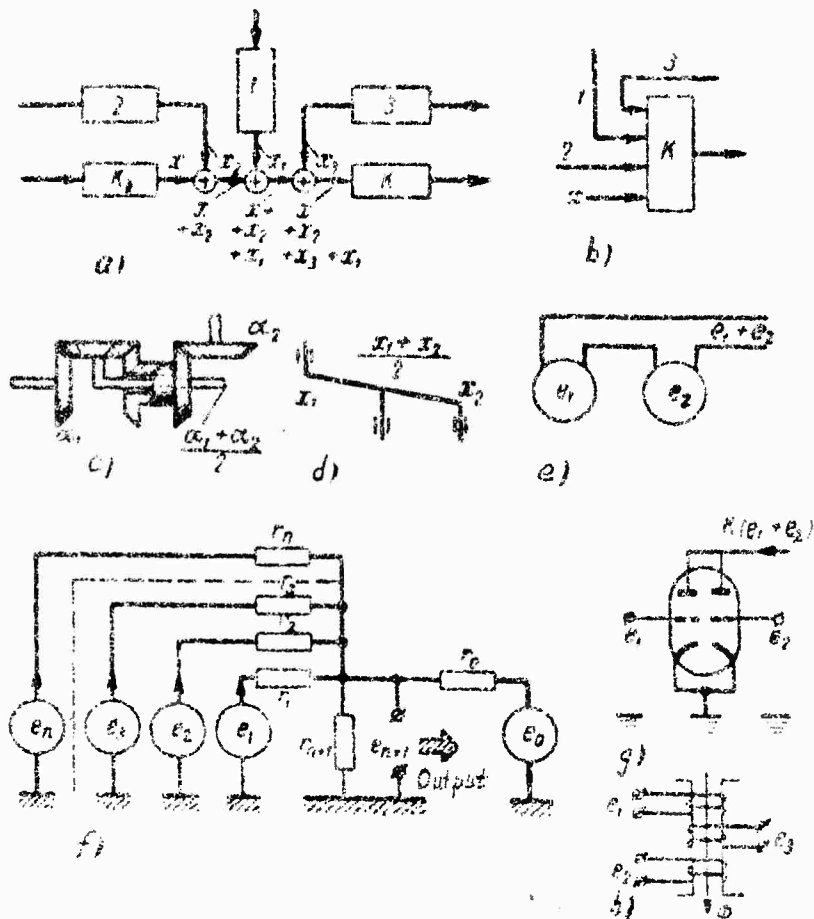
Fig 1-8. Summators. a and b - structure; c and d - conic and lever differentials; e and f - series and parallel diagrams; g - summarizing tube; h - summation of magnetic fluxes.

dynamoelectric amplifier for the creation of the output value (voltage, current) used for further control.

Many more examples of summarizing designs can be presented from various branches of technology; their correspondence to structure a or h is determined by the properties of linearity and undirectivity.

Let us examine in more detail the parallel summation of voltages of the passive design f for input resistances that differ in value. Let $n + 1$ controlled values be summarized, given in the form of the voltages e_k ($k = 0, 1, 2, \ldots, n$). The voltages are fed through the input resistances r_k to the total resistance r_{n+1}, through which

the summary current I_{n+1} will pass under the influence of the enumerated voltages.

Let us determine the components of the current I_k (k = 0, 1, 2, ..., n). Each of them will be determined by the single-type formula

$$I_k = \frac{1}{r_k}(e_k - I_{n+1} r_{n+1})$$

The summary current is

$$I_{n+1} = \sum_{k=0}^{n} I_k = \sum_{k=0}^{n} \frac{1}{r_k} e_k - I_{n+1} r_{n+1} \sum_{k=0}^{n} \frac{1}{r_k}.$$

We will solve this equation with respect to the drop in voltage on the resistance r_{n+1}:

$$I_{n+1} r_{n+1} = \frac{1}{n+1} \sum_{k=0}^{n} \frac{1}{r_k} e_k. \qquad (1\text{-}56)$$
$$\sum_{k=0}^{n} \frac{1}{r_k}$$

Thus it is evident that on the total resistance the voltages of the parallel circuit actually are summarized

$$e_{n+1} = I_{n+1} r_{n+1} = \sum_{k=0}^{n} m_k e_k \qquad (1\text{-}57)$$

with scales determinable by the formula

$$m_i = \frac{\dfrac{1}{r_i}}{\displaystyle\sum_{k=0}^{n} \frac{1}{r_k}} \qquad (1\text{-}58)$$

If all $n + 2$ resistances of the circuit equal one another and $r_k = r = $ constant, then the scale is equal to

$$m_i = \frac{1}{n+2}.$$

The drop in the scale of the circuit with increase in the number of terms is its shortcoming, but it is convenient for the summation of voltages that are formed on the elements with general feed.

2. Summarizing Amplifier

It is possible to preserve the merits of the examined circuit and eliminate the dependence of the scale on the number of terms if we introduce into the circuit an active element -- an amplifier with a large amplification factor.

The transformed circuit is shown in Figure 1-9a. The amplifier has a large amplification factor K and simultaneously changes sign, which is characteristic for amplifiers with an odd number of cascades, considered further in Chapter 5; in this the voltage e_0, which was independent in diagram 1-8c, becomes the output voltage of the amplifier, equal to

$$e_0 = -K e_{n+1} \qquad (1\text{-}59)$$

If we replace in the sum of the voltages (1-56) the term with the zero subscript e_0 by the new value (1-59) and if we group it with the terms on the left side, we get the output voltage of the amplifier:

$$e_{n+1} = \frac{+\sum_{k=1}^{n} \frac{1}{r_k} e_k + \frac{r_0}{K} \sum_{k=1}^{n} \frac{1}{r_k} e_k}{\sum_{k=1}^{n+1} \frac{1}{r_k} + \frac{K}{r_0} \qquad 1 + \frac{1}{K} \sum_{k=0}^{n+1} \frac{r_0}{r_k}} , \quad (1\text{-}60)$$

If the amplification factor now tends toward infinity, the input voltage of the amplifier, in accordance with the preceding formula, tends toward zero, but the output voltage (1-59) is determined according to the rules for finding the limit:

$$e_0 = \lim_{K \to \infty} \frac{-\sum_{k=1}^{n} \frac{r_0}{r_k} e_k}{1 + \frac{1}{K} \sum_{k=0}^{n+1} \frac{r_0}{r_k}} = -r_0 \sum_{k=1}^{n} \frac{1}{r_k} e_k . \quad (1\text{-}61)$$

Consequently, at a large enough amplification factor K, e_0 ceases in fact to depend on the fluctuations of the value of that factor on
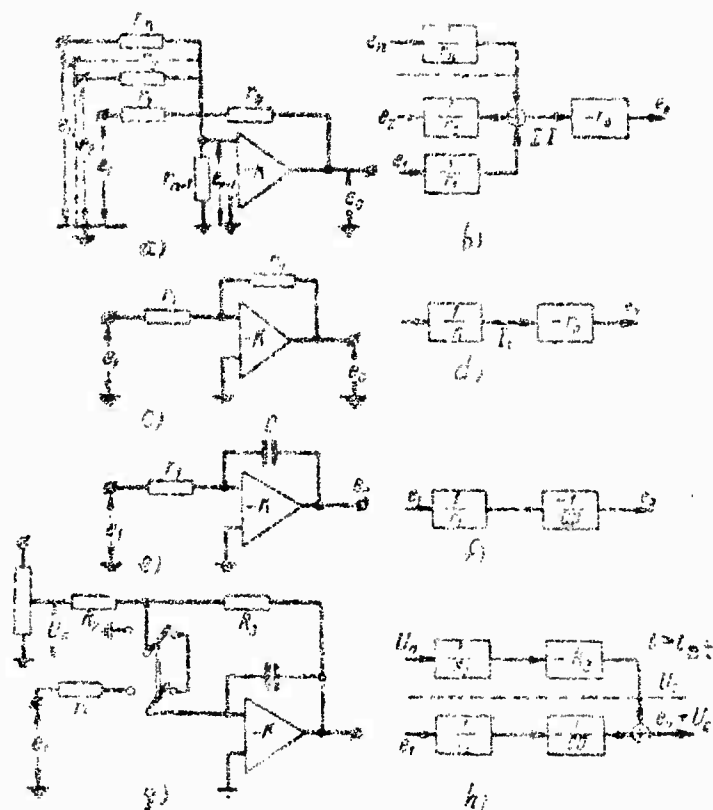
Fig 1-... Electrical and structural diagrams of computing blocks of
a model: a, c, e and g - summating, scaling, integrating, with null
and non-null initial conditions of the amplifier: b, d, f and h -
their structures.

the side of further increase

If we rewrite the obtained formuls in the form:

$$\sum_{k=0}^{n} \frac{z_k}{r_k} = 0 \qquad (1\text{-}62)$$

or

$$c_0 = \sum_{k=1}^{n} \frac{1}{r_k} e_k \cdot (-r_0), \qquad (1\text{-}63)$$

We compared the circuit to structural diagram b of Figure 1-9. It explains the intersecting operating conditions of a circuit with an active element in the regime of a current generator. The essence of this regime is that the voltages that are summed generate currents proportional to the local conductivities ($1/r_i$); they are summed and, having passed through the resistance r_0, which has no effect on the value of the summed current, create in it a voltage drop equal to the output voltage with negative sign.

The summating amplifier of the electronic model operates according to the examined diagram.

a. Scaling Amplifier

At only one input voltage according to Figure 1-9c the amplifier varies its scale and sign proportionally to the input conductivity and the resistance of the feedbock r_0, connecting the output with the input:

$$e_0 = -\frac{r_0}{r_1} e_1 = \frac{1}{r_1} \cdot (-r_0) e_1. \qquad (1\text{-}64)$$

The latter form of notation is used for the construction of structural diagram d of the same figure.

b. Inverting Amplifier

The equality of the resistances $r_1 = r_0$ in the preceding structure make the scale of the amplifier irrelevant, and it is used simply for changing the sign of any of the voltages in the circuit of the model. With respect to the ground stage it is necessary according to the conditions of the algebraic summation on the conditions of closing the circuit.

c. Input of coefficients

Inputs of constant coefficients are usually formed in a model in the form of a one-cascade voltage dividers with a fixed installation, and certain known scale, which is compensated for by inserting a scaling amplifier.

Blocks of coefficients variable in time have controllable computation and a mobile system which switches in the potential axis of the voltage divisor to the output of the block according to the law of a change of the variable coefficient. Their arrangement is described in more detail in the specialized literature, for example [2] and [3].

3. Integrating Amplifier

In diagram e of Figure 1-9 the regime of the current generator conditions a task proportional to the input voltage e_1 of the current across the capacitor, which in this case operates as an integrator, having provided at zero initial charge the transformation of the input voltage according to the dependence:

$$e_0 = \frac{1}{C}\int_0^t I_3\,dt = -\frac{1}{r_1 C}\int_0^t e_1\,dt = -\frac{1}{r_1 CD}\,e_1 , \quad (1\text{-}65)$$

which corresponds to the structure of Figure 1-9f.

Before the start of operation this voltage on the capacitor is equal in modulus to the voltage on the output of the amplifier. This voltage can be led in to the amplifier from an outside source with control by a voltmeter and used in the scale of the model as the initial value of the controlled value required at start-up, formed on the output of the given amplifier and necessary at the start-up of the circuit.

The introduction of the initial conditions into an integrating amplifier is shown in the diagram of 1-9g. When the switch is in the position to the right the capacitor does not participate in the regime that is being established and in it the voltage

$$-U_C = -U_n \frac{R_2}{R_2}$$

is established.

When the switch is in the position to the left the block operates according to diagram e, having developed an increment of voltage (1-65) from the initial level U_C according to the formula

$$e_0 = -\left[U_C + \frac{1}{r_1 CD}\,e_1 \right] \qquad (1\text{-}66)$$

and structural diagram h.

The elements examined are sufficient for a statement of the conditions of modeling of very simple problems. Additional elements will be required further on to the extent of increase in their complexity.

1-7. Equations, Structure and Model of a Component
        with Variable Parameters

Composition of the Equation according to the Desired Character
                    of the Process

    We will set the booster motion of the component analogously to
(1-12) but require that the characteristic motion be subject to the
following dependence:

$$x = A \frac{e^{-\sigma t}}{\Omega t} \sin(\Omega t + \varphi). \qquad (1\text{-}67a)$$

    If we differentiate the transformed equation of the character-
istic motion (1-67a) twice and perform substitutions analogous to
those made in 1-3, we arrive at the result:

$$\frac{d}{dt}(tx) = t\dot{x} + x = Ae^{-\sigma t}\cos(\Omega t + \varphi) - \sigma t x$$

and

$$t\ddot{x} + 2\dot{x} = -\sigma(t\dot{x} + x + \sigma t x) - \Omega^2 t x.$$

    Finally, after transformations, with the character of the boosted
motion (1-12) taken into consideration, we get:

$$t\ddot{x}_{out} + 2(1 + \sigma t)\dot{x}_{out} + [2\sigma + (\Omega^2 + \sigma^2)t]x_{out} =$$
$$= [2\sigma + (\Omega^2 + \sigma^2)t]x_{in}. \qquad (1\text{-}67b)$$

Composition of the Equation of Connection according to the Assigned
                    Physical Parameters

    Let us examine, for an example of oscillation, an airplane in
the vertical plane with respect to the center of mass, occupying in
space the position indicated in figure 1-10. We will designate that:
Θ is the angle constituting the vector of velocity with the horizon;
α is the angle of attack, or the angle constituted by the axis of
the airplane (in relative motion) and the direction of the air
stream oriented along the vector of velocity; ϑ is the pitch angle,
or angle between the axis of the airplane in absolute motion and the

—— 14 ——

Fig 1-10. Angles character-
izing the motion of an
airplane
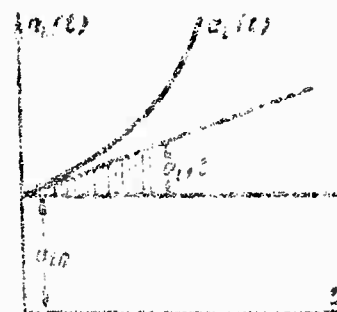
Fig 1-11. Graph of a
variable coefficient.

horizon, and will proceed to the composition of the equation of the
moments. We will write it in the following form:

$$J\ddot{\theta} + S_2^{M}\dot{\alpha} + F(\alpha) = M_{axc} . \qquad (1\text{-}68a)$$

In comparison with equation (1-17), where the concepts of the
absolute and relative angular displacements coincided, in (1-68) they
are different: the inertial moment $J\ddot{\theta}$ is always given in absolute
motion, and the damping S_2^{M} and the stabilizing $F(\alpha)$ moments are
given in functions of turn relative to the stream of air. We will
replace the angle of attack according to the figure by the differ-
ence:

$$\alpha = \vartheta - \theta,$$

and then we get

$$J\ddot{\theta} + S_2^{M}\dot{\theta} + F(\vartheta - \theta) = M_{axc} + S_2^{M}\dot{\theta}. \quad (1\text{-}68b)$$

At a given rectilinear course of the airplane $\Theta = \Theta_0$ and, in
order to be kept in a rectilinear trajectory the airplane must have
a constant angle of attack α_0, providing the vertical component of
the lifting force which, together with the lifting force of the rud-
der, balances the weight of the airplane.

If we linearize the equation of the moments with respect to the
values of ϑ_0 and α_0, we bring it to the form:

$$J\Delta\ddot{\theta} + S_2^{M}\Delta\dot{\theta} + \frac{\partial F}{\partial\alpha}\Delta\vartheta - \frac{\partial F}{\partial\alpha}\Delta\theta = \Delta M_{axc} - S_2^{M}\Delta\dot{\theta}.$$

$$J\Delta\ddot{\vartheta} + S_{g}^{M}\Delta\dot{\vartheta} + S_{n}^{M}\Delta\vartheta = M(t). \qquad (1\text{-}68c)$$

In the latter notation the right side of the equation has been replaced by the reduced disturbing moment, which we will consider the assigned input value.

If the speed of the airplane changes in time, the coefficients S_{g}^{M} and S_{n}^{M}, connected with the aerodynamics of the airplane, likewise will be variable in time; the moment of inertia J can vary in time as a result of decrease in the weight of the airplane in the combustion of fuel. Let one of the variable coefficients vary according to the graph in Figure 1-11; on the graph we can separate the constant component $\alpha_{l,c}$, the part $\alpha_{c,1}t^2$ varying linearly, the part $\alpha_{c,2}t^2$ varying quadratically, etc., that is, we can analytically express the graph by the polynomial of the argument t.

In (1-67c) the variable coefficients were formed by polynomials of the first power, that is, were changed linearly; in the example with the airplane the laws of change of the coefficients can be more complex, for example:

$$S_{a}^{V}(t) = a_{0}(t) = a_{00} + a_{01}t + a_{02}t^2 + \ldots;$$

$$S_{2}^{V}(t) = a_{1}(t) = a_{10} + a_{11}t + a_{12}t^2 + \ldots;$$

$$J(t) = a_{2}(t) = a_{20} + a_{21}t + a_{22}t^2 + \ldots$$

The general notation of the polynomial coefficients of such a type has the form

$$a_{j}(t) = a_{j0} + a_{j1}t + a_{j2}t^2 + \ldots = \sum_{k=0}^{l} a_{jk}t^k \ldots,$$

and the general notation of the differential equation of connection with polynomial coefficients is:

$$\left(\sum_{j=0}^{n} \sum_{k=0}^{l} a_{jk}t^k D^j \right) x_{out} = \left(\sum_{j=0}^{m} \sum_{k=0}^{h} b_{jk}t^k D^j \right) x_{in} \qquad (1\text{-}69)$$
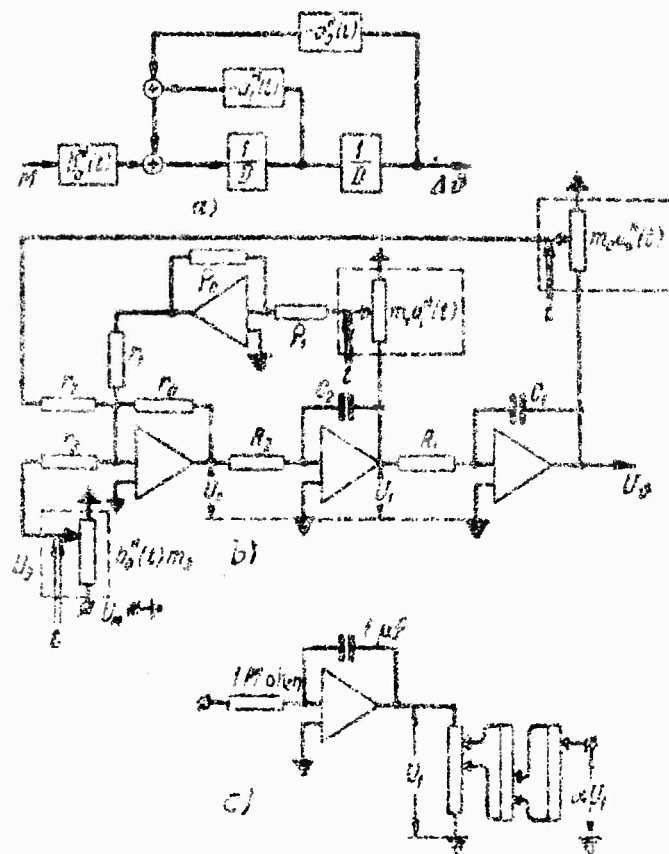
Fig. 1-12. Structural representation and scheme for tuning a model of a component of the 2nd order with variable parameters.

The structure of a component of the second order with variable parameters is also made up according to the principles of Figure 1-1 and is given in Figure 1-12a, where all the coefficients of equation (1-69) $a_1(t)$ and b_0 are normalized by division by the higher coefficient $a_2(t)$ and are designated:

$$b_0^n(t) = \frac{1}{a_2(t)} ; \quad a_0^n(t) = \frac{a_k(t)}{a_2(t)} ;$$

$$a_1^n(t) = \frac{a_1(t)}{a_2(t)} ,$$

after which equation (1-69b) is transformed to the form:

$$\Delta\theta + a_1^n(t)\,\Delta\dot{\theta} + a_0^n(t)\,\Delta\theta = b_0^n(t)\,M(t). \quad (1\text{-}70)$$

Adjustment Circuit of an Electronic Model

The preliminary circuit of the model is obtained directly from the structural representation, all the elements of which, including the summators, are replaced by the computing blocks of the model, given in Figure 1-9, and blocks of variable coefficients. Inverting amplifiers are introduced into the model, supplementing the structural representation. It is evident from Figure 1-12b that in the problem being solved -- the modeling of the equation of the moments -- change of sign was required only in the feedback circuit with the variable coefficient $a_1^n(t)$.

The equation of the model in voltages can be written as the equation of the summing amplifier, for which the sum of the voltages applied on it with its own scales (1-62), including $e_0 = U_0$, is practically equal to zero:

$$\frac{1}{r_0}U_0 - \frac{m_1 a_1^n(t)}{r_1}\,\frac{\rho_0}{\rho_1}\,U_1 + \frac{m_0 a_0^n(t)}{r_2}\,U_0 = \frac{m_3 b_0^n(t)}{r_3}\,U_m.$$

In the coefficients of the equation that has been given participate the scales of the blocks of the variable coefficients m_0, m_1, and m_2 with the dimensions $1/[a_0^n]$, $1/[a_1^n]$ and $1/[b_0^n]$, the conductivity of the input circuits of the summing amplifier $1/r_k$ and the ratio of the resistances ρ_0/ρ_1 of the scaling amplifier, which at $\rho_0 = \rho_1$ becomes simply an inverting amplifier.

The equation of the model, reduced to the output voltage, is ob-

tained from the preceding equation by the substitution:

$$U_9 = - R_1 C_1 \dot{U}_6 = - T_1 \dot{U}_6; \quad U_9 = - R_2 C_2 \dot{U}_5 = = T_1 T_2 \ddot{U}_6;$$

which gives:

$$\frac{T_1 T_2 \ddot{U}_6}{r_0} + \frac{m_1 a_0^n(t) \rho_0 T_1}{r_1 \rho_1} \dot{U}_9 + \frac{m_0 a_0^n(t)}{r_1} U_9 = = \frac{m_3 b_0^n(t)}{r_3} U_M. \qquad (*)$$

The electrical scale of the input disturbance m_M is set, according to the concepts of full utilization of the resources of the model $|U_M|_{max} = 100$ V at the maximal value of disturbance

$$m_M = \frac{100}{M_{max}} \left[\frac{v}{\kappa \Gamma \cdot M} \right].$$

The value inverse to the scale, or the value of a volt of input voltage in units of measurement of disturbance, will be designated

$$k_M = \frac{1}{m_M} = \frac{M_{max}}{100} \frac{\kappa \Gamma \cdot M}{v}.$$

The electrical scale of the solution is set, according to concepts of the greatest possible utilization of the output voltage of the model, at $U_{\vartheta max} = 100$ V.

Since the solution is not previously known, its boosted part can be roughly estimated by the value of the ratio of the lower terms of equation (1-70):

$$\vartheta_0 = \frac{b_0^n(t) M(t)}{a_0^{\Gamma}(t)} = \frac{b_0(t) M(t)}{a_0(t)}. \qquad (**)$$

If we take into consideration the approximateness of the estimate, and also the existence of characteristic motion superimposed on the boosted, in the selection of the electrical scale at the maximum (**) we will divert half of the assumed output voltage of the model, that is, 50 V:

$$m_\vartheta = \frac{50}{|\vartheta_0|_{max}} \frac{v}{rad}.$$

Hence the value of a volt of the output voltage or the coefficient of similarity is

$$k_\delta = \frac{1}{m_\delta} \frac{|\Delta\delta|_{max}}{50} \frac{rad}{V}.$$

The ratio between the parameters of the circuit and the scales of the model. If we perform in the equation of voltages of the model (*) substitution of the variables

$$U_\delta = \frac{\Delta\delta}{k_\delta}; \quad U_i = \frac{\Delta i}{k_i},$$

we get:

$$\frac{T_1 T_2}{r_\delta k_\delta}\Delta\delta + \frac{m_1 \rho_* l_1}{r_{i} \rho_i k_\delta} a_1^r(t)\Delta\delta + \frac{m_0}{r_2 k_i} a_0^k(t)\Delta i =$$

$$= \frac{m_3 b_0^k(t)}{r_i k_M} M$$

For the task of modelling to be solved correctly, the coefficients of the given equation -- the balance of the currents of the model -- must be proportional to the coefficients of the initial equation of the model (1-62b) or the normalized equation (1-70), from which

$$\frac{T_1 T_2}{r_\delta k_\delta} = \frac{m_1 T_1 \rho_*}{r_i \rho_i k_i} = \frac{m_0}{r_2 k_i} = \frac{m_3}{r_i k}.$$

The ratios obtained are basic in the adjustment of the model. They permit varying the parameters of the circuit by reducing some at the expense of others while retaining the derived ratios.

The time constants of the integrating amplifiers T_1 and T_2 can also be estimated from the conditions of complete utilization of the measures of the model with respect to the voltage in the intermediate circuits $|U_1|_{max} = 100$ V and $|U_2|_{max} = 100$ V, if any preliminary estimates at all are available about the characteristic action of the dynamical system being investigated. Thus, for example, it is possible to start from a frequency estimate of the characteristic motion. Let the frequency of the dominant harmonic of the characteristic motion equal Ω. For the amplitude of the characteristic motion on the output of the model, 80 V are reserved. On the input of the integrators of the model are fed the derivatives of the output voltage, which having some change of the forced solution will in practice be close to the derived dominant harmonic of the characteristic motion.

$$U_1 \approx \frac{d}{dt}(T_1 50 \sin \Omega t) = 50 \Omega T_1 \cos \Omega t;$$

$$U_{max} = 50 \Omega T_1;$$

$$U_0 = \frac{d}{dt}(T_2 U_1) = -T_1 T_2 \Omega^2 \sin \Omega t;$$

$$U_{0\ max} = 50 \Omega^2 T_1 T_2.$$

If we completely fill the resources of the model $|U_1{}_{max}| = 100$ V and $|U_0{}_{max}| = 100$ V with these components, we obtain the values of the time constants of the integrating amplifiers:

$$T_1 = \frac{2}{\Omega};$$

$$T_2 = \frac{2}{\Omega^2 T_1} = \frac{1}{\Omega}.$$

The distribution of the amplification factors of integrators between the integrating amplifiers and supplementary blocks. If, as a result of the approximate calculation, the time constants obtained were larger than 1 second, then in a number of types of models it is worthwhile establishing on the integrating amplifier the largest time constant, for example $T = 1$ sec ($R = 1$ Mohm, $C = 1$ μf), and merge the excess of the amplification factor with the voltage divider in the block of the constant coefficient according to diagram 1-12c. The total amplification factor of the two blocks indicated in the figure is equal to $(1/\text{sec})$ a. = α sec^{-1}; if we equate it to the coefficient $-(1/?$? α required by the calculation, we determine the setting of the scale of the block of constant coefficients. Thanks to the use of a three-decade voltage divider in the block, α is established from ? to 1 with precision to the third place.

If the calculated time constants differ from 1 sec, it is necessary to put the nearest large time number from the assortment available in the model and to merge the excess amplification again with the divider or, when there is insufficient amplification to introduce after the integrating amplifier a supplementary scaling amplifier. Let us note that, from the point of view of reducing the instrumental error of the apparatus of the model, it is disadvantageous to use in the circuit adjustments of the integrator with small time constants or scaling amplifiers with large amplification factors, and from these considerations in a number of cases it is necessary to abstain from

complete utilization of the resources of all the intermediate ampli-
fiers.

An Electromechanical Model of an Airplane
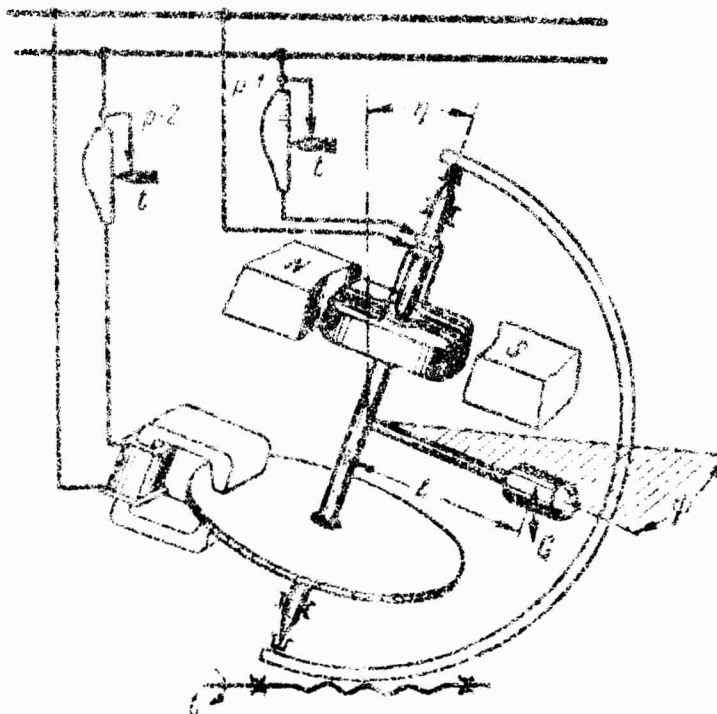
Fig 1-15. An electromechanical model of an airplane.

After the transition to normalized coefficients, equation (1-70)
became to a great extent analogous to the equation of the mobile sys-
tem of the electromagnet (1-17), which provides the possibility of
creating, on the basis of the principles of similarity, a physical
model of the oscillations of an airplane in the form of the oscilla-
tions of a similar electromechanical system.

In the electromechanical model, shown schematically in Figure
1-15:

1) The normalized disturbing moment is set by a magnetoelectri-
cal system in which the loop passed by the assigned current interacts
with constant magnets;

2) the normalized regenerative moment is set by the pendulum, and during inclination of its axis to the vertical at the angle η composed.

$$M = (GL \sin \eta)\sin \psi \approx (GL \sin \eta)\psi; \quad = N$$

3) the normalized damping moment arises in the electromagnetic damper at the expense of eddy currents.

The change in time of the normalized disturbing moment is accomplished by the rheostat R-1.

Change of the normalized damping coefficient is achieved by rheostat R-2.

Change of the normalized coefficient of the regenerative moment is effected by inclination of the axis of oscillation of the pendulum. Displacement of the brushes of rheostats R-1 and R-2 and change of the angle of inclination η in time is effected by the programming mechanism.

The moment of inertia of the mobile part of the system, $L^2(3/g)$ + ... is unchanged and enters into the calculation of all the normalized coefficients.

1-3. Transformation of the Algebraic Equations of the Components with Constant Parameters when they are conclosed in Elementary Circuits

a. Cascade Design

Two components with input values x_1 and x_2 and corresponding output values y_1 and y_2 are called combinations in a cascade design if the output of one (the first, let us say) component is fed to the input of the second component.

We will write the equations of a cascade circuit and the equations of the components according to the designations in Figure 1-14a.

The equation of the circuit is:

$$y_1 = x_2. \qquad (1\text{-}71a)$$

The equation of connection of component No 1 is:

$$a_1(D) y_1 = b_1(D) x. \qquad (1\text{-}71b)$$
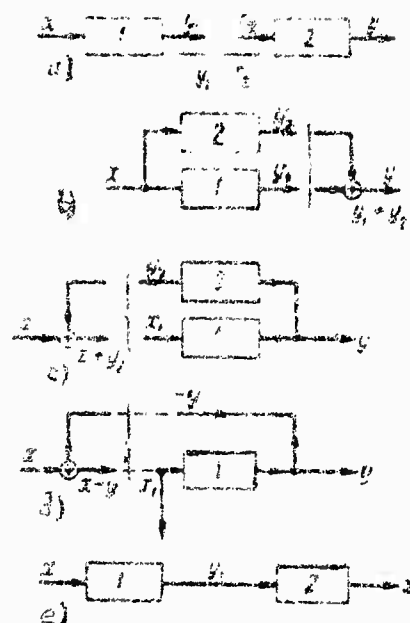
Fig 1-14. Typical forms of connections between components.
a - cascade; b - matching-parallel; c - antiparallel; d -
with single feedback; e - neutral.

The equation of connection of component No 2 is:

$$a_2(D) y = b_2(D) x_2. \qquad (1-71c)$$

If we multiply both parts of equation (1-71b) by $b_2(D)$ and both
parts of equation (1-71c) by $a_1(D)$, add the results and reduce the
total terms according to (1-71a), we get the equation of connection
for the input and output values not only of the individual components
but of the entire circuit:

$$a_1(D) a_2(D) y = b_1(D) b_2(D) x. \qquad (1-72)$$

The order of the equation obtained, on its left and right sides,
is equal to the sum of the orders of the equations of connections of
the components.

B. Matching-parallel Circuit

Two components are called switched in a matching-parallel circuit if they have a common input and their output values are summed, forming an output value for the entire circuit as shown in Figure 1-14b.

We will write, in the designations of circuit b, the equation for the circuit connection and the equation of the components in a form convenient for making up the determinant:

The circuit connection is:

$$y_1 + y_2 - y = 0. \qquad (1\text{-}73a)$$

Component No 1 is:

$$a_1(D)\,y_1 + 0 + 0 = b_1(D)\,x. \qquad (1\text{-}73b)$$

Component No 2 is:

$$0 + a_2(D)\,y_2 + 0 = b_2(D)\,x. \qquad (1\text{-}73c)$$

From which we write at once the equation of connection for the input and output values of the entire circuit:

$$\begin{vmatrix} 1 & 1 & -1 \\ a_1(D) & 0 & 0 \\ 0 & a_2(D) & 0 \end{vmatrix} y =$$

$$= \begin{vmatrix} 1 & 1 & 0 \\ a_1(D) & 0 & b_1(D) \\ 0 & a_2(D) & b_2(D) \end{vmatrix} x,$$

or after transformations:

$$a_1(D)\,a_2(D)\,y = [a_1(D)\,b_2(D) + a_2(D)\,b_1(D)]\,x. \qquad (1\text{-}74)$$

2. Antiparallel Circuit

If the output of one component serves as the input of a second component, and the input of the first component is formed as the sum

* Also called counter-parallel circuit

of the controlling action and the output reaction of the second component, as shown in Figure 1-14c, such a method of inserting the components is called an antiparallel circuit or a feedback circuit. We will make up a system of equations for this circuit.

The circuit connection is:

$$x_1 - y_2 + 0 = x. \qquad (1\text{-}75a)$$

Component No 1 is:

$$b_1(D) x_1 + 0 - a_1(D) y = 0. \qquad (1\text{-}75b)$$

Component No 2 is:

$$0 + a_2(D) y_2 - b_2(D) y = 0. \qquad (1\text{-}75c)$$

We obtain the general equation of connection of the circuit in the form:

$$\begin{vmatrix} 1 & -1 & 0 \\ b_1(D) & 0 & -a_1(D) \\ 0 & a_2(D) & -b_2(D) \end{vmatrix} y =$$

$$= \begin{vmatrix} 1 & -1 & 1 \\ b_1(D) & 0 & 0 \\ 0 & a_2(D) & 0 \end{vmatrix} x_1$$

or after transformation:

$$[a_1(D) a_2(D) - b_1(D) b_2(D)] y = a_2(D) b_1(D) x. \qquad (1\text{-}76)$$

B. Circuit with a single Negative Feedback

A particular case of an antiparallel circuit is that given in Figure 1-14d with algebraized differential polynomials of a feedback circuit equal to -1.

If we substitute $a_2(D) = 1$ and $b_2(D) = -1$ in equation (1-76), we

$$[a_1(D) + b_1(D)]\, y = b_1(D)\, x. \qquad (1\text{-}77)$$

For the same circuit the equation of connection with respect to the difference signal x_1, if we have recomposed the determinant of the right side, we get in the form:

$$\begin{vmatrix} 1 & -1 & 0 \\ b_1(D) & 0 & -a_1(D) \\ 0 & 1 & 1 \end{vmatrix} x_1 =$$

$$= \begin{vmatrix} 1 & -1 & 0 \\ 0 & 0 & -a_1(D) \\ 0 & 1 & 1 \end{vmatrix} x.$$

Expansion of the determinant gives:

$$[a_1(D) + b_1(D)]\, x_1 = a_1(D)\, x. \qquad (1\text{-}78)$$

2. Neutral Cascade Circuit

The cascade circuit given in Figure 1-4a is called neutral if the circuit properties of the first component are neutralized by the second component and the total transmission coefficient of the circuit is equal to 1.

Assuming $y = x$ in equation (1-72), we get adequate conditions of neutralization:

$$\left. \begin{array}{l} a_2(D) = b_1(D); \\ b_2(D) = a_1(D). \end{array} \right\} \qquad (1\text{-}79a)$$

that is, the first and the neutralizing components have identical algebraical differential polynomials in different sides of the equations of connection, for example:

Component No 1 $\qquad a_1(D)\, y_1 = b_1(D)\, x.$

Component No 2 $\qquad b_1(D)\, y = a_1(D)\, x_2.$ $\qquad (1\text{-}79b)$

1-9. The Method of Noncommutative Determinants and Its Application for the Convolution of Circuits Containing Components with Variable Parameters

1. Transformations of variable algebraized differential polynomials

The methods of the preceding section can be applied also to the case of components with variable parameters combined in circuits according to Figure 1-14. The transformations of the algebraized differential polynomials which arise in this case will contain new characteristics in connection with the need to differentiate during the transformations not only controllable values but also variable coefficients. We will examine preliminarily some rules of such transformations which rest on classical methods [4], but with a supplementary development of the symbolics.

4. The Effect of the Symbol of Differentiation on the Product of Two Controllable Values

The product is a particular case of a function of two variables, and therefore differentiation with respect to time can have as an intermediate stage the obtaining of the partial derivatives of that function:

$$D(xy) = \left[\frac{\partial}{\partial x}(xy)\right]\dot{x} + \left[\frac{\partial}{\partial y}(xy)\right]\dot{y}.$$

If we recompose the factors and symbolically take out the differentiated product beyond the brackets, we get

$$D(xy) = \left[\dot{x}\frac{\partial}{\partial x} + \dot{y}\frac{\partial}{\partial x}\right]xy =$$

$$= \left[\frac{d_x}{dt} + \frac{d_y}{dt}\right]xy = [D_x + D_y]xy. \qquad (1\text{-}80)$$

where

$$D_x = \dot{x}\frac{\partial}{\partial x} = \frac{d_x}{dt}$$

and

$$D_y = \dot{y}\frac{\partial}{\partial y} = \frac{d_y}{dt}. \qquad (1\text{-}81)$$

The symbols of differentiation with respect to time D_x and D_y are each addressed to only one of the factors x or y. The second

factor is not subjected to changes from the action of the symbol not addressed to it.

Thus, for example, in (1-80) we put x or y in the brackets; then we have:

$$D[xy] = [\dot{x} + xD_y] y = [yD_x + \dot{y}] x = x\dot{y} + y\dot{x}.$$

E. The Effect of the Symbol of Differentiation on the Product of the Controllable Value and the Variable Coefficient

By analogy with the preceding

$$D[a(t) x(t)] = [D_a + D_x] ax, \qquad (1\text{-}82)$$

where $D_a = \dot{a}\dfrac{\partial}{\partial a} = \dfrac{d_a}{dt}$ is the symbol of differentiation with respect to time, addressed only to the coefficient a(t).

If we insert a in the brackets, we get:

$$D[a(t) x] = [\dot{a} + aD] x. \qquad (1\text{-}83)$$

Here on the right side the symbol of differentiation, addressed to a single variable, is again replaced by the symbol of complete differentiation, since only one controllable value x is located after it.

We will write the formula for multiple differentiation:

$$D^i[a(t; x] = (D_a + D_x)^i ax =$$
$$= \left[D_a^i + iD_a^{i-1}D_x + \frac{i(i-1)}{1\cdot 2} D_a^{i-2}D_x^2 + \ldots + D_x^i \right] ax$$

where

$$D_a^i = \frac{d_a^i}{dt^i}.$$

We will insert a in the brackets

$$D^i[ax] =$$
$$= \left[a^{(i)} + ia^{(i-1)}D + \frac{i(i-1)}{1\cdot 2} a^{(i-2)}D^2 + \ldots + D^i \right] x.$$
$$(1\text{-}84)$$

7. Multiplication of the Algebraized Differential Polynomials

If the controllable value x enters the equation in the form of the sum of derivatives multiplied by variable coefficients

$$b(t, D)x = \sum_{j=0}^{m} b_j(t) D^j x,$$

and then on that side of the equation is assumed to produce supplementary operations of differentiation, multiplication by new variable coefficients and summation

$$a(t, D) b(t, D) x,$$

then in the algebraized form of notation we arrive at a multiple application of formulas of division "D" with supplementary multiplication by the variable coefficients $a_i(t)$. The symbols of differentiation $(1-34)$ with respect to time, addressed to only one of the variables, permit using in this case the formula for multiplication of algebraized differential polynomials; if we separate them from the controllable value and replace D in the initial algebraized differential polynomials by D_x and D in the supplementary ADP by $D_B + D_x$, we get:

$$a(t, D) b(t, D) = a(t, D_B + D_x) b(t, D_x). \qquad (1\text{-}35)$$

We will use the derived rules for algebraized differential polynomials of the second order. Let

$$\left.\begin{aligned}
a(t, D_B + D_x) &= a_2(t)(D_B + D_x)^2 + \\
&\quad + a_1(t)(D_B + D_x) + a_0(t), \\
b(t, D_x) &= b_2(t) D_x^2 + b_1(t) D_x + b_0(t),
\end{aligned}\right\} \qquad (1\text{-}36a)$$

If we perform the multiplication according to $(1-35)$, we get:

$$a(t, D) b(t, D) = a_2(t) b_2(t) D^4 +$$
$$+ (a_2(t) b_1(t) + 2 a_2(t) \dot{b}_2(t) + a_1(t) b_2(t)) D^3 +$$
$$+ (a_2 b_0 + 2 a_2 \dot{b}_1 + a_2 \ddot{b}_0 + a_1 \dot{b}_2 + a_1 b_1 + a_0 b_2) D^2 +$$
$$+ (2 a_2 \dot{b}_0 + a_2 \ddot{b}_1 + a_1 \dot{b}_1 + a_1 b_0 + a_0 b_1) D +$$
$$+ a_2 \ddot{b}_0 + a_1 \dot{b}_0 + a_0 b_0 =$$
$$= (\Sigma_4) D^4 + (\Sigma_3) D^3 + (\Sigma_2) D^2 + (\Sigma_1) D + (\Sigma_0) \quad (1\text{-}36b)$$

Table 1-3. Intermediate Data for the Organization of Calculations in Multiplication of the ADP's $a(t, D)$ and $b(t, D)$.

$a_j \big\backslash D_X^j$		D_X^1	D_X^2	D_X^3	D_X^4	D_X^5	D_X^6	D_X^7	D_X^8	D_X^9	D_X^{10}
a_0	1										
a_1	D_B	1									
a_2	D_B^2	$2D_B$	1								
a_3	D_B^3	$3D_B^2$	$3D_B$	1							
a_4	D_B^4	$4D_B^3$	$6D_B^2$	$4D_B$	1						
a_5	D_B^5	$5D_B^4$	$10D_B^3$	$10D_B^2$	$5D_B$	1					
a_6	D_B^6	$6D_B^5$	$15D_B^4$	$20D_B^3$	$15D_B^2$	$6D_B$	1				
a_7	D_B^7	$7D_B^6$	$21D_B^5$	$35D_B^4$	$35D_B^3$	$21D_B^2$	$7D_B$	1			
a_8	D_B^8	$8D_B^7$	$28D_B^6$	$56D_B^5$	$70D_B^4$	$56D_B^3$	$28D_B^2$	$8D_B$	1		
a_9	D_B^9	$9D_B^8$	$36D_B^7$	$84D_B^6$	$126D_B^5$	$126D_B^4$	$84D_B^3$	$36D_B^2$	$9D_B$	1	
a_{10}	D_B^{10}	$10D_B^9$	$45D_B^8$	$120D_B^7$	$210D_B^6$	$252D_B^5$	$210D_B^4$	$120D_B^3$	$45D_B^2$	$10D_B$	1

1 - Coefficient at D_x^2; 2 - Key

Table 1-3 has been compiled for the more complex factors; from it it is possible to obtain the sums of the coefficients (Σ_i) at the desired powers of D^i in the product of the ADP. For this purpose, in the lower half of the table it is necessary to select the line with the assigned power i, for each element of that line multiply all the elements of the column of the upper half of the table located above the given coefficient, increased by a_k times in the limits $a_0 - a_k \neq 0$, and add the results.

These operations are explained by the key, presented in an open space in the table; for the line D_7^Σ, for example, it is easy to obtain from the table the sum (Σ_2), which takes part in formula (1-86b).

The separation of the desired coefficient can also be done on the basis of a Taylor expansion.

In fact, if we designate the product of the two ADP by a single function:

$$F(t, D) = a(t, D_H + D)b(t, D).$$

If we expand it into a series with respect to the powers $D = D_X$:

$$F(t, D) = F(t, 0) +$$

$$+ \left[\frac{\partial}{\partial D} F(t, 0) \right] D + \ldots + \frac{1}{n!} \left[\frac{\partial^n}{\partial D^n} F(t, 0) \right] D^n,$$

we obtain an expression for the coefficient at D^i in the form

$$(\Sigma_i) = \frac{1}{i!} \cdot \frac{\partial}{\partial D^i} F(t, 0) =$$

$$= \frac{1}{i!} \cdot \frac{\partial^i}{\partial D^i} \{a(t, D_s) b(t, 0)\}. \qquad (1\text{-}87)$$

The substitution of $D = D_{out}$ in $a(t, D)$ and $D = 0$ in $b(t, D)$ naturally is done after the i-th differentiation with respect to D. Thus, for example, for the ADP of (1-86a) at $i = 1$ we have

$$(\Sigma_1) = \frac{\partial}{\partial D} \{(a_2 D^2 + a_1 D + a_0) \cdot (b_2 D^2 + b_1 D + b_0)_{D=0}\}_{D=D_s} =$$

$$= (2a_2 D_a + a_1) b_a + (a_2 D_a^2 + a_1 D_a + a_0) b_1 =$$
$$= 2ab_a + a_1 b_0 + a_2 \dot{b}_1 + a_1 \dot{b}_1 + a_0 b_1.$$

which coincides with the coefficient at D in (1-86b).

It is evident from the examples that have been examined that in the multiplication of the ADP the coefficients of the second factor are differentiated, and the coefficients of the first factor are not subjected to that operation, that is, the product of the variables of the ADP do not possess the property of commutativity:

$$a(t, \ D_a + D_x) b(t, \ D_x) \neq b(t, \ D_a + D_x) a(t, \ D_x). \quad (1-88)$$

D. Coordinating ADP's (CADP)

The inequality (1-88) can be transformed into an equality of the type:

$$a(t, \ D_a + D_x) b(t, \ D_x) = \beta(t, \ D_a + D_x) a(t, \ D_x), \quad (1-89a)$$

or

$$\begin{vmatrix} a(t, \ D_a + D_x) & a(t, \ D_x) \\ \beta(t, \ D_a + D_x) & b(t, \ D_x) \end{vmatrix} = 0, \quad (1-89b)$$

if supplementary algebraic differential polynomials $\alpha(t, \ D)$ and $\beta(t, \ D)$ are selected in a corresponding manner at assigned $a(t, \ D)$ and $b(t, \ D)$. Since the supplementary ADP's equate or coordinate both sides of formula (1-89a), we will call them coordinating ADP's, or CADP's for short, and to designate them in the future we will use the Greek letters.

The conditions of coordination are reduced to a set of time functions for the description of the variable coefficients $\alpha_i(t)$ and $\beta_i(t)$ which satisfy the conditions of (1-89). If we now consider the first factor in this formula as a CADP with the unknown coefficients $\alpha_0(t)$, $\alpha_1(t)$ and $\alpha_2(t)$, it is easy to note that all these coefficients enter the sum $(\sum_i)_\alpha$ linearly at powers of D. In exactly the same way the unknown coefficients $\beta_0(t)$, $\beta_1(t)$ and $\beta_2(t)$ will enter the sum $(\sum_i)_\beta$ during multiplication of the CADP $\beta(t, \ D)$ and the APD $a(t, \ D)$ on the right side of (1-89a). The balance of the coefficients, when there are identical powers of D_x on the left and right sides of (1-89a)

$$(\sum_i)_\alpha = (\sum_i)_\beta \qquad (1-89c)$$
$$i = 0, \ 1, \ 2 \ldots$$

provides the conditions for coordination of both sides of formula (1-89a) and permits determining the unknown functions $\alpha_i(t)$ and $\beta_i(t)$.

In calculating Table 1-4 are expressions for $(\Sigma_i)_\alpha$ borrowed from example (1-85c). Analogous sums for $(\Sigma_i)_\beta$ (the right side of the table were calculated with use of Table 1-3, in which the input coefficients α are replaced by the β coefficients, and the b differential coefficients by the a coefficients.

Thus in calculating table 1-4 five equations were formed, containing six unknowns: α_i, β_i (i = 0, 1, 2).

Since the number of equations per unit is less than the number of unknowns, the solution can be obtained in the form of an expression of all the coefficients through one expressed earlier. If the coefficient $\beta_2(t)$ is given, it can be left in the right side of all the equations of the balances, located in Table 1-4, and columns $\beta_0(t)$ and $\beta_1(t)$ can be carried to the left sides of the equations of balances, the signs of the elements having been changed. Then the determinant of the system of the fifth order is formed from the coefficients of the first five columns (with change of the signs in the last two columns taken into consideration).

$$
\Delta(t) = \begin{vmatrix}
b_0 & \dot{b}_0 & \ddot{b}_0 & -a_0 & -\dot{a}_0 \\
b_1 & b_0 + \dot{b}_1 & 2\dot{b}_0 + \ddot{b}_1 & -a_1 & -a_0 - \dot{a}_1 \\
b_2 & b_1 + \dot{b}_2 & b_0 + 2\dot{b}_1 + \ddot{b}_2 & -a_2 & -a_1 - \dot{a}_2 \\
0 & b_2 & b_1 + 2\dot{b}_2 & 0 & -a_2 \\
0 & 0 & b_2 & 0 & 0
\end{vmatrix}
$$

(1-90a)

Further, by a standard method, the solution is found for all the unknown coefficients, expressed by the coefficient $_2(t)$.

As an example, we will determine the coefficient α_0:

$$
\sigma_0(t) = \begin{vmatrix}
\ddot{a}_0 & b_0 & \ddot{b}_0 & -a_0 & -\dot{a}_0 \\
2\dot{a}_0 + \ddot{a}_1 & b_0 + \dot{b}_1 & 2\dot{b}_0 + \ddot{b}_1 & -a_1 & -a_0 - \dot{a}_1 \\
a_0 + 2\dot{a}_1 + \ddot{a}_2 & b_1 + \dot{b}_2 & b_0 + 2\dot{b}_1 + \ddot{b}_2 & -a_2 & -a_1 - \dot{a}_2 \\
a_1 + 2a_2 & b_2 & b_1 + 2\dot{b}_2 & 0 & -a_2 \\
a_2 & 0 & b_2 & 0 & 0
\end{vmatrix} \frac{\beta_2(t)}{\Delta(t)}
$$

(1-90b)

Table 1.4. Expanded Expressions for Formula (1-39) at $n = m = 2$

$$\sum_{i=0}^{2} a_i(t,D)(C_i + D_i) + \sum_{j=0}^{2} b_j(t,D)C_j = \sum_{k=0}^{2} \beta_k(t,D)C_k + \sum_{k=0}^{4} \alpha_k(t,D)D_k$$

			$a(t,D)\cdot b(t,D)$		Позиция умножения AND Q		$\beta(t,D)\cdot a(t,D)$		
a			a_2	a_1	a_0		β_2	β_1	β_0
a_2^0	D_{2}	1							
a_1	D_1	$2C_0$							
a_0		1	a_2	b_0a_2	b_0a_1	$= a_0b_0$	$a_0\beta_2$		$a_3\beta_2$
D_2^2	a_2	b_0	$b_2^2a_2$	$(b_0+b_2)a_2 +$	b_0a_2	$= a_0\beta_2 +$	$(a_0+a_2)\beta_2 +$	$(a_1+2a_0)\beta_2$	
D_1	b_1	$b_2a_2 +$	$(b_1+b_2)a_2 +$	$(b_0+2b_0)a_2$	$= a_2\beta_2 +$	$(a_0+a_2)\beta_0 +$	$(a_0+2a_1+a_2)\beta_0$		
D_2^2	b_2	0	b_2a_2	$(b_1+2b_2)a_2 +$	$(b_0+2b_1+b_2)a_2$	$= a_2\beta_2$	$(a_1+2a_2)\beta_0$		
D_1^2		0	0	b_2a_2	$(b_1+2b_2)a_2$	$= 0$	$a_2\beta_0$		
A_2^0	b_2	0	0	0	b_2a_2	$= 0$	0		$a_2\beta_2$

1 - Results of multiplication of the AND's

In finding the other coefficients in the determinant of the system the following column is shifted over.

As was mentioned above, the form of the function $\beta_2(t)$ can be set in advance. In the majority of cases it is convenient to assume:

$$\beta_2(t) = 1 \quad \text{See} \ \boxed{3}$$

but obviously in some problems one can assume another substitution -- in the form of a function which, during multiplication of the ADP's, compensates for a more complex dependence contained in the coefficients $\kappa_1(t)$.

The composition of the equations of balances of the coefficients (1-89a) for simple examples can transferred over without Table 1-4 by formulas of the order of (1-87). In all cases the order of the coordinating polynomials must be selected by attaining minimal and equal orders of both parts of equation (1-89a).

Let: the ADP order $a(t, D)$ equal n;
    the ADP order $b(t, D)$ equal m;
    the ADP order $\alpha(t, D)$ be designated by ν;
    the ADP order $\beta(t, D)$ be designated by μ; $\qquad$ (1-91a)

Then, if we assume

$$\begin{aligned} \nu &= n \\ \mu &= m \end{aligned} \quad \qquad (1\text{-}91b)$$

and if we are given one of the functions, for example $\beta_2(t) = 1$, we get an equality of the orders of both sides of (1-89a) and the correspondence of the number of equations with the number of unknowns. If we replace μ and ν from comparison with (1-91b) with one and the same whole number ξ, then since the equality of the orders is not disturbed but the number of equations remains the same

$$m + n + \xi + 1,$$

and the number of unknown functions likewise at $\beta_2(t) = 1$ is

$$m + n + 2\xi + 1,$$

it is evident from this that only the condition $\xi = 0$ is acceptable, since the positive values of ξ create an insufficiency of equations and the negative values of ξ create an excess of the number of equations over the number of unknowns, which makes the equations inconsistent.

2. Construction of the Algebraized System of Equations by
   the Method of Noncommutative Determinants

Let us consider a sufficiently general system of differential
algebraized equations.

$$a_{11}(t, D) y_1 + a_{12}(t, D) y_2 + a_{13}(t, D) y_3 =$$
$$= b_1(t, D) x_1;$$
$$a_{21}(t, D) y_1 + a_{22}(t, D) y_2 + a_{23}(t, D) y_3 =$$
$$= b_2(t, D) x_2; \qquad (1\text{-}92a)$$
$$a_{31}(t, D) y_1 + a_{32}(t, D) y_2 + a_{33}(t, D) y_3 =$$
$$= b_3(t, D) x_3;$$

Here the ADP $a_{ik}(t, D)$ are numbered by columns and rows. We will ex-
clude from the first and second equations the variable value y_1. To
do this we will multiply the first row by CADP $a_{21}(t, D)$ and the second
row by CADP $a_{11}(t, D)$, which we will determine from the solution of the
condition of coordination, analogous to (1-89b), and calculate the
first row from the second. Then we will eliminate from the first and
third equations the same value y_1 by multiplying the first row by CADP
$a_{31}(t, D)$ and the third row by CADP $a_{11}(t, D)$ and calculating the
first row from the third.

We will write the result in the following form:

$$\begin{vmatrix} a_{11}(t, D) & a_{12}(t, D) \\ a_{21}(t, D) & a_{22}(t, D) \end{vmatrix} y_2 + \begin{vmatrix} a_{11} & a_{13} \\ a_{21} & a_{23} \end{vmatrix} y_3 = \begin{vmatrix} a_{11} & b_1 \\ a_{21} & b_2 \end{vmatrix} x_1$$

$$\begin{vmatrix} a_{11}(t, D) & a_{12}(t, D) \\ a_{31}(t, D) & a_{32}(t, D) \end{vmatrix} y_2 + \begin{vmatrix} a_{11} & a_{13} \\ a_{31} & a_{33} \end{vmatrix} y_3 = \begin{vmatrix} a_{11} & b_1 \\ a_{31} & b_3 \end{vmatrix} x_1$$

$$(1\text{-}92b)$$

In developing the determinants of the second order it is necessary
to recall that the CADP's designated by the Greek letters always retain
the first factors in the paired products. After development of the
determinants, new ADP's of a higher order will be obtained, which we
will designate $a_{ir}^0(t, D)$, where the subscript r corresponds to the
number of the excludable value, and the subscript i to the number
of the row (equation) in system (1-92b), transformed after the intro-
duction of these designations into the form

$$a_{12}^0(t, D) y_2 + a_{13}^0(t, D) y_3 = b_{11}^0(t, D) x_1;$$
$$a_{12}^0(t, D) y_2 + a_{13}^0(t, D) y_3 = b_{11}^0(t, D) x_1; \qquad (1\text{-}92c)$$

If we now select the coordinating factors in the form of the CADP $\alpha^*_{12}(t, D)$ and $\alpha^*_{21}(t, D)$ for the two lines of the system (1-89c) and subtract the first from the second row, we will eliminate the controllable value y_2:

$$\begin{vmatrix} a^*_{12}(t, D) & a^*_{13}(t, D) \\ a^*_{21}(t, D) & a^*_{23}(t, D) \end{vmatrix} y_3 = \begin{vmatrix} a^0_{12}(t, D) & b^*_{11}(t, D) \\ a^0_{21}(t, D) & b^*_{21}(t, D) \end{vmatrix} x_1$$

(1-91d)

The answer can be written more compactly

$$a_{11}(t, D) y_3 = b_{11}(t, D) x_1 \qquad (1\text{-}92\text{a})$$

It can readily be noted that transformations (1-92b-e) on the ADP can be performed in isolation from the controllable values and generalized for any number of excludable controllable values. Thus, for the system of equations (1-92a) the result of (1-92e) can be written formally in the following manner:

$$\left| \left| \begin{vmatrix} a_{11}(t, D) & a_{12}(t, D) & a_{13}(t, D) \\ a_{21}(t, D) & a_{22}(t, D) & a_{23}(t, D) \\ a_{31}(t, D) & a_{32}(t, D) & a_{33}(t, D) \end{vmatrix} \right| \right| y_3 =$$

$$= \left| \left| \begin{vmatrix} \ldots & b_{11}(t, D) \\ \ldots & b_{21}(t, D) \\ \ldots & b_{31}(t, D) \end{vmatrix} \right| \right| x_1 \qquad (1\text{-}93)$$

The three vertical lines in the determinants mark those special features which these determinants have which contain terms which are not subject to the principle of commutativity (1-86) during multiplication. The special features are that such determinants, called noncommutative $/9/$ by us, are developed by the method of successive reduction of the order to unity by deleting the first row and the first column and replacement of the remaining a_{ij} elements by second-order determinants of the form

$$\begin{vmatrix} a_{ij} & a_{ik} \\ a_{lj} & a_{lk} \end{vmatrix}$$

as proceeds from the transformations (1-92 and the conditions of solution of the equations of coordination, 1-89).

The number of vertical lines in the designation at unity of the noncommutative determinant is greater than the number of steps of development of the noncommutative determinant until it is converted into an ordinary second-order determinant (1-92b).

Let us consider the example of development of a third-order noncom-

— 68 —

First Step:

a) Solution of the coordination equations:

$$\begin{vmatrix} a_{11}(t,\,D) & a_{11}(t,\,D) \\ x_{21}(t,\,D) & a_{21}(t,\,D) \end{vmatrix} = 0; \qquad \begin{vmatrix} a_{13}(t,\,D) & a_{11}(t,\,D) \\ x_{31}(t,\,D) & a_{31}(t,\,D) \end{vmatrix} = 0.$$

$$(1\text{-}94a)$$

b) Reduction of the order of the determinant to unity:

$$\begin{vmatrix} x_{12} & a_{12} & x_{12} & a_{13} \\ x_{21} & a_{22} & x_{21} & a_{23} \\ a_{13} & a_{12} & x_{13} & a_{13} \\ a_{31} & a_{32} & a_{41} & a_{33} \end{vmatrix} y_3 - \begin{vmatrix} & & \begin{vmatrix} x_{12} & b_{11} \\ x_{21} & b_{21} \end{vmatrix} \\ \cdots & & \begin{vmatrix} a_{13} & b_{11} \\ a_{31} & b_{31} \end{vmatrix} \end{vmatrix} x_1. \quad (1\text{-}94\,b)$$

c) Replacement of elements of the determinants of (1-94b) by new ADF's:

$$a^{\bullet}_{k} = \begin{vmatrix} a_{1,\,i+1} & a_{1,\,k} \\ a_{i+1,\,1} & a_{i+1,\,k} \end{vmatrix}$$

$$\begin{vmatrix} a^{\bullet}_{12}(t,\,D) & a^{\bullet}_{13}(t,\,D) \\ a^{\bullet}_{21}(t,\,D) & a^{\bullet}_{23}(t,\,D) \end{vmatrix} y_3 - 1 \begin{vmatrix} \cdots & b^{\bullet}_{11}(t,\,D) \\ \cdots & b^{\bullet}_{21}(t,\,D) \end{vmatrix} x_1.$$

$$(1\text{-}94\,c)$$

Second Step:

The second step of the development of the determinant of (1-93) is the first step for the noncommutative determinant (1-94c) and contains the same stages "a" - "c":

$$\begin{vmatrix} a^{\bullet}_{12} & a^{\bullet}_{12} \\ a^{\bullet}_{21} & a^{\bullet}_{22} \end{vmatrix} = 0, \qquad\qquad (1\text{-}95a)$$

$$\begin{vmatrix} x^{\bullet}_{12} & a^{\bullet}_{13} \\ x^{\bullet}_{21} & a^{\bullet}_{23} \end{vmatrix} y_3 = \begin{vmatrix} a^{\bullet}_{12} & b^{\bullet}_{11} \\ a^{\bullet}_{21} & b^{\bullet}_{21} \end{vmatrix} x_1; \qquad (1\text{-}95b)$$

$$a_{13}(t,\,D)\,y_3 = b_{13}(t,\,D)\,x_1. \qquad (1\text{-}95c)$$

For a determinant of a higher order the following steps in the reduction of the order are performed analogously to the preceding steps. In the determinant on the right side all the columns coincide with the column of the determinant on the left side except the last; there is no need to calculate them, and it is necessary only to fix the last column, which differs from the determinant of the left side; this also was done in equations (1-94) and (1-95).

Several general algebraic rules are retained for concommutative determinants:

a constant coefficient that is common for a column can be removed according to the sign of the determinant;

a constant coefficient that is common for a row can be removed according to the sign of the determinant;

equal coefficients in the left and right parts of the row can be mutually cancelled, etc.

3. Elementary Transformations of Structural Representations

A. Contraction of a Cascade Circuit

We will consider the parameters of the components in the circuits in Figure 1-14 variable. This is reflected only in the form of notation of the ADF, and for the cascade circuit a that is under consideration. Instead of equations (1-71), we will have:

The circuit connection:

$$x_1 \quad - \quad y_1 \quad + \quad 0 = 0, \tag{1-96a}$$

Component No 1:

$$0 \quad - a_1(t, D) y_1 + \quad 0 \quad = b_1(t, D) c. \tag{1-96b}$$

Component No 2:

$$b_2(t, D) x_2 + \quad 0 \quad - a_2(t, D) y = 0. \tag{1-96c}$$

The number of equations can be shortened at once by elementary substitution (1-96a), but for clarification of the features of the general method we will retain the system of equations with three unknown values: x_2, y_1, and y.

We will write the solution of this system in the form of the non-commutative determinants:

$$\left\| \begin{vmatrix} 1 & -1 & 0 \\ 0 & a_1(t,\,D) & 0 \\ b_2(t,\,D) & 0 & -a_2(t,\,D) \end{vmatrix} \right\| y =$$

$$= \left\| \begin{vmatrix} \cdots & 0 \\ \cdots & b_1(t,\,D) \\ & 0 \end{vmatrix} \right\| x.$$

The first step in the expansion of the non-commutative determinant gives:

$$\left\| \begin{vmatrix} 1 & -1 \\ 0 & a_1(t,\,D) \end{vmatrix} \begin{vmatrix} 1 & 0 \\ 0 & 0 \end{vmatrix} \right\| y =$$
$$\left\| \begin{vmatrix} 1 & -1 \\ b_2(t,\,D) & 0 \end{vmatrix} \begin{vmatrix} 1 & 0 \\ b_2(t,\,D) & -a_2(t,\,D) \end{vmatrix} \right\|$$

$$= \left\| \begin{vmatrix} \cdots & \begin{matrix} 1 & 0 \\ 0 & b_1(t,\,D) \end{matrix} \\ \cdots & \begin{matrix} 1 & 0 \\ b_2(t,\,D) & 0 \end{matrix} \end{vmatrix} \right\| x.$$

Since a part of the elements of the determinant is constant and equal to zero, the coordinating ADP's prove to be equal to the principal ADP's and the formulas are simplified:

$$\left\| \begin{vmatrix} a_1(t,\,D) & 0 \\ b_2(t,\,D) & -a_2(t,\,D) \end{vmatrix} \right\| y = \left\| \begin{vmatrix} \cdots & b_1(t,\,D) \\ \cdots & 0 \end{vmatrix} \right\| x.$$

The second step in the expansion of the non-commutative determinant in the given example is the following:

$$\begin{vmatrix} a_1(t,\,D) & 0 \\ b_2(t,\,D) & -a_2(t,\,D) \end{vmatrix} y =$$
$$= \begin{vmatrix} a_1(t,\,D) & b_1(t,\,D) \\ b_2(t,\,D) & 0 \end{vmatrix} x, \qquad (1\text{-}97a)$$

or

$$\alpha_1(t,\ D)_a + D_y)\,a_2(t,\ D_d)\,y =$$
$$= \beta_2(t,\ D_z + D_x)\,b_1(t,\ D_y)\,x, \qquad (1\text{-}97b)$$

where

$\alpha_1(t,\ D)$ and $\beta_2(t,\ D)$ are the coordinating ADP's; their designation with Greek letters was explained above.

The conditions of coordination are the following:

$$\begin{vmatrix} \alpha_1(t,\ D) & a_1(t,\ D) \\ \beta_2(t,\ D) & b_2(t,\ D) \end{vmatrix} = 0. \qquad (1\text{-}97c)$$

If we find the value of the ADP's which enter equations (1-96b) and (1-96c):

$$a_1(t,\ D) = a_0(t) + a_1(t)\,D + a_2(t)\,D^2;$$
$$b_1(t,\ D) = b_0(t) + b_1(t)\,D + b_2(t)\,D^3,$$

and also if we are given the form of the coordinating ADP's:

$$\alpha_1(t,\ D) = \alpha_0(t) + \alpha_1(t)\,D + \alpha_2(t)\,D^2;$$
$$\beta_2(t,\ D) = \beta_0(t) + \beta_1(t)\,D + \beta_2(t)\,D^2,$$

we find, by using Table 1-5 or -- within limits of the second order -- calculating Table 1-4, by formulas analogous to (1-90b), the variable coefficients in the coordinating ADP's, after which they are determined and by the same token the final equations (1-97a) and (1-97b) are determined, which select the contracted circuit of cascade connection of two components.

Components with derivatives on the right side of equation (1-96b) or (1-96c) sometimes are conveniently presented in the form of a cascade circuit, consisting of two components, by introducing the intermediate value y_0:

$$a(t,\ D)\,y = y_0 = b(t,\ D)\,x\} \equiv$$
$$\equiv \begin{cases} y_0 = b(t,\ D)\,x \\ a(t,\ D)\,y = y_0. \end{cases} \qquad (1\text{-}97d)$$

5. Contraction of a Matching-Parallel Circuit

Matching-parallel circuit b in Figure 1-14, for components with

variable parameters, is written with the following system of equations:

The circuit connection:

$$y_1 \quad + \quad y_2 \quad - y = 0. \tag{1-98a}$$

Component No 1:

$$a_1(t, D)\, y_1 + \quad 0 \quad + 0 = b_1(t, D)\, x. \tag{1-98b}$$

Component No 2:

$$0 \quad + a_2(t, D)\, y_2 + 0 = b_2(t, D)\, x. \tag{1-98c}$$

The solution with respect to y is:

$$\begin{Vmatrix} 1 & - & 1 & - 1 \\ a_1(t, D) & & 0 & 0 \\ 0 & a_2(t, D) & & 0 \end{Vmatrix} y =$$

$$= \begin{Vmatrix} \cdots & 0 \\ \cdots & b_1(t, D) \\ \cdots & b_2(t, D) \end{Vmatrix} x.$$

The first step of expansion of the determinant is:

$$\begin{Vmatrix} \begin{vmatrix} 1 & 1 \\ a_1(t, D) & 0 \\ 1 & 1 \\ 0 & a_2(t, D) \end{vmatrix} & \begin{vmatrix} 1 & -1 \\ a_1(t, D) & 0 \\ 1 & -1 \\ 0 & 0 \end{vmatrix} \end{Vmatrix} y =$$

$$= \begin{Vmatrix} \cdots & \begin{vmatrix} 1 & 0 \\ a_1(t, D) & b_1(t, D) \\ 1 & 0 \\ 0 & b_2(t, D) \end{vmatrix} \end{Vmatrix} x.$$

$$\begin{vmatrix} -a_1(t, D) & a_1(t, D) \\ a_2(t, D) & 0 \end{vmatrix} y = \begin{vmatrix} \cdots & b_1(t, D) \\ \cdots & b_2(t, D) \end{vmatrix} x.$$

The second (last) step is:

$$\left|\begin{array}{cc} -a_1(t,\ D) & a_1(t,\ D) \\ a_2(t,\ D) & 0 \end{array}\right| y =$$

$$= \left|\begin{array}{cc} -a_1(t,\ D) & b_1(t,\ D) \\ a_2(t,\ D) & b_2(t,\ D) \end{array}\right| x, \qquad (1\text{-}99a)$$

or

$$a_2(t,\ D_\beta + D_y)\, a_1(t,\ D_y)\, y =$$

$$= [a_1(t,\ D_\beta + D_x)\, b_2(t,\ D_x) +$$

$$+ a_2(t,\ D_\beta + D_y)\, b_1(t,\ D_y)]\, x. \qquad (1\text{-}99b)$$

Under conditions of coordination

$$\left|\begin{array}{cc} a_1(t,\ D) & a_1(t,\ D) \\ a_2(t,\ D) & a_2(t,\ D) \end{array}\right| = 0. \qquad (1\text{-}99c)$$

C. Contraction of an Antiparallel Circuit

The system of equations in the designations indicated in circuit c of Figure 1-14 is:

The circuit connection:

$$x_1 \qquad - \qquad y_2 \qquad + \quad 0 \qquad = x. \qquad (1\text{-}100a)$$

Component No 1:

$$b_1(t,\ D)\, x_1 \quad + \qquad 0 \qquad - a_1(t,\ D)\, y = 0. \qquad (1\text{-}100b)$$

Component No 2:

$$0 \qquad + a_2(t,\ D)\, y_2 - b_2(t,\ D)\, y = 0. \qquad (1\text{-}100c)$$

The solution with respect to y is:

$$\left|\begin{array}{ccc} 1 & -1 & 0 \\ b_1(t,\ D) & 0 & -a_1(t,\ D) \\ 0 & a_2(t,\ D) & -b_2(t,\ D) \end{array}\right| y =$$

$$= \begin{Vmatrix} \cdot & \cdot & \cdot & 1 \\ \cdot & \cdot & \cdot & 0 \\ \cdot & \cdot & \cdot & 0 \end{Vmatrix} x.$$

The first step in the expansion of the determinant is:

$$\begin{Vmatrix} 1 & -1 \\ b_1(t, D) & 0 \\ 1 & -1 \\ 0 & a_2(t, D) \end{Vmatrix} \begin{Vmatrix} 1 & 0 \\ b_1(t, D) & -a_1(t, D) \\ 1 & 0 \\ 0 & -b_2(t, D) \end{Vmatrix} y =$$

$$= \begin{Vmatrix} \cdots \\ \cdots \end{Vmatrix} \begin{Vmatrix} 1 & 1 \\ b_1(t, D) & 0 \\ 1 & 1 \\ 0 & 0 \end{Vmatrix} x.$$

Here, as previously, repeating elements of the determinant of the system are omitted in the replaced determinant. If we transform the determinant, we get

$$\begin{vmatrix} b_1(t, D) & -a_1(t, D) \\ a_2(t, D) & -b_2(t, D) \end{vmatrix} y =$$

$$= \begin{vmatrix} \cdots & -b_1(t, D) \\ \cdots & 0 \end{vmatrix} x.$$

The final contracted equation of the circuit has the form:

$$\begin{vmatrix} \beta_1(t, D) & -a_1(t, D) \\ a_2(t, D) & -b_2(t, D) \end{vmatrix} y =$$

$$= \begin{vmatrix} \beta_1(t, D) & -b_1(t, D) \\ a_2(t, D) & 0 \end{vmatrix} x, \quad (1\text{-}101a)$$

or

$$[a_2(t, D_u + D_y) a_1(t, D_y) -$$
$$- \beta_1(t, D_u + D_y) b_2(t, D_y)] y =$$
$$= a_2(t, D_u + D_x) b_1(t, D) x \quad (1\text{-}101b)$$

$$\begin{vmatrix} \tilde{\beta}_2(t, D) & b_1(t, D) \\ a_2(t, D) & a_1(t, D) \end{vmatrix} = 0. \qquad (1\text{-}101c)$$

D. Contraction of a Circuit with a Single Negative Feedback

For circuit d of Figure 1-14, $a_2(t, D) = 1$; $b_2(t, D) = -1$ and formulas (1-101a) and (1-101b) are transformed to the form:

$$\begin{vmatrix} b_1(t, D) & -a_1(t, D) \\ 1 & 1 \end{vmatrix} y =$$

$$= \begin{vmatrix} b_1(t, D) & -b_1(t, D) \\ 1 & 0 \end{vmatrix} x, \qquad (1\text{-}102a)$$

$$[a_1(t, D) + b_1(t, D)] y = b_1(t, D) x. (1\text{-}102b)$$

Solving the equation of coordination (1-101c) is not required here, as the ADP's coincide with the CADP's.

For the same circuit the solution of the system of equations (1-100) with respect to the controlling signal x_1 has the form:

$$\begin{vmatrix} 1 & 1 \\ a(t, D) & -b(t, D) \end{vmatrix} x = \begin{vmatrix} 1 & 1 \\ a(t, D) & 0 \end{vmatrix} x,$$

$$(1\text{-}103a)$$

or

$$[a(t, D) + b(t, D)] x_1 = a(t, D) x. (1\text{-}103b)$$

E. Neutralization of a Cascade Circuit

The problem of neutralization is solved for variable ADP's analogously to (1-75), that is, for circuit e in figure 1-14 we have:

Component No 1
$$a_1(t, D) y_1 = b_1(t, D) x.$$

Component No 2
$$b_1(t, D) y = a_1(t, D) x_2.$$

$$(1\text{-}104)$$

All the examples that have been worked out for variable ADP's
are also valid for constant ADP's. This is readily verified by com-
paring the formulas of the present and previous sections and having
in mind that the concept of ADP and CADP coincides for constant coef-
ficients, that is, $a(D) = \alpha(D)$ and $b(D) = \beta(D)$. Where the step of
solution of the coordination equations is absent, the forms of trans-
formations of the coefficients also coincide. Thus formulas (1-102b)
and (1-103b) are valid both for constant and for variable coefficients.

Bibliography

1. Mikhaylov, A V, Method of harmonic analysis in the theory of con-
   trol, Avtomatika i telemekhanika (Automation and Telemechanics),
   1938, No 3.
2. Korn, G A and Korn T M, Elektronnyye modeliruyushchiye ustroystva
   (Electronic Modeling Devices), Foreign Literature Press, 1955.
3. Kogan, B Ya. Elektronnyye modeliruyushchiye ustroystva i ikh
   primeneniye dlya issledovaniya sistem avtomaticheskogo reguliro-
   vaniya (Electronic Modeling Devices and their Use for Investigat-
   ion of Automatic Control Systems), GIFML, 1959.
4. Smirnov, V I. Kurs vysshey matematiki (Course of Higher Mathema-
   tics), GITTL, 1952.
5. SHATALOV, A S, Structural methods of investigation of linear sys-
   tems with variable parameters, Sbornik "Avtomaticheskoye upravle-
   niye i vychislitel'naya tekhnika" (Collection "Automatic control
   and Computer Technique"), No 4, Mashgiz, 1961.
6. Solodov, A V, Structural transformations of linear systems with
   variable parameters, Avtomatika i telemekhanika, No 5, 1961.

Chapter 2

THE PROPERTIES OF THE PROCESSES

IN LINEAR CONTROL SYSTEMS

§2.1. Initial and Displaced Functions

A. Initial Functions

In physical systems, reactions of the system to the input action cannot exist before the moment of application of the action. Therefore in the analysis of the course of a process that has been excited at the output of a system it is natural to adopt the moment of application of the input action as the start of the time reference.

We will designate: ϑ is the moment of application of the input action;

τ is the time from the moment ϑ and admissible as an argument in constructing the output process.

The initial function in the region of the argument τ we will designate $x(\tau)$; it is not equal to zero only in the region of positive values of the argument τ, that is

$$x(\tau) = 0 \quad at \quad \tau < 0;$$

$$x(\tau) = x(\tau) \quad at \quad \tau > 0.$$

The designation in the form of a single bracket at the argument τ distinguishes a special class of right-hand (unilateral functions) in contrast with bilateral functions $x(\tau)$ existing both at $\tau > 0$ and at $\tau < 0$; it marks the moment of origination of a function which must have at that moment a steep front (a jump) along the coordinate or derivative at the moment of equality of the argument to zero.

Initial functions, which describe the output processes of physi

cal systems, at $\tau > 0$ can be continuous functions which have continuous derivatives, for example:

$$x[\tau] = [1 - e^{-\sigma\tau}].$$

A single initial function is called the limit of an initial function (*) at infinite increase of the coefficient σ:

$$1[\tau] = \lim_{\sigma \to \infty} [1 - e^{-\sigma\tau}]. \qquad (2\cdot1)$$

The tendency toward the limit when the values of σ are doubled is shown in Figure 2-1a.

It is evident that $1[\tau] = 1$ at $\tau > 0$ and $1[\tau] = 0$ at $\tau < 0$.

The symbol of the single initial function permits establishing the correspondence between the bilateral function and its right branch:

$$x[\tau] = x(\tau)\, 1[\tau].$$

B. Displaced Functions

If a system is subjected to disturbances, the action of which is begun at different moments of time, than in the study of the joint process excited by these disturbances, from the particular intervals of time τ in each process it is necessary to proceed to a single time t, counted from the characteristic moment of insertion for the physical system, the moment of starting, the moment of transition to the working regime, etc. Consequently, the particular intervals in the preceding formulas must be replaced:

$$\tau = t - \theta. \qquad (2\cdot2)$$

This replacement gives the basis for consideration of a new class of displaced functions.

A function set equal to zero only in the region of values of time greater than θ is called a displaced function $x(t - \theta)$, that is

$$x[t - \theta] = 0 \quad at \quad t < \theta,$$
$$x[t - \theta] = x(t - \theta) \quad at \quad t > \theta.$$

The role of the bracket here is the same as in initial functions: a jump of the function or of its derivatives is observed at the moment of equality of the argument to zero: $t - \theta = 0$ or $t = \theta$.

The exponent (*) can serve as an example of a displaced function.

$$x(t-\vartheta)=1-e^{-\alpha(t-\vartheta)}.$$

A set of graphs of the function (**) for various values of $\mathscr{S}_1$ is shown in Figure 2-1b.

A single displaced function, by analogy with formula (2-1), we will call the limit

$$1(t-\vartheta)=\lim_{\sigma\to\infty}[1-e^{-\alpha(t-\vartheta)}]. \qquad (2\text{-}3)$$

In that case

$$1(t-\vartheta)=0 \quad at \quad t<\vartheta;$$
$$1(t-\vartheta)=1 \quad at \quad t>\vartheta.$$

Multiplication of the two-sided function from the argument $t-\mathscr{S}$ by the single displaced function isolates the right half-branch of the function

$$x(t-\vartheta)=x(t-\vartheta)\;1](t-\vartheta). \qquad (2\text{-}4)$$

C. Contour of a Displaced Function

A geometric displaced function can be represented in the form of a contour, shown for the function (**) in Figure 2-1c. The contour includes all the possible values of the displaced functions at differ-ent values of $\mathscr{S}_1$, replacing graph b. To obtain a displaced function at a given displacement of $\mathscr{S}$ it is sufficient to bring the section of the contour through the plane $\mathscr{S}_1$; then by virtue of the properties of the bisectrix $\tau=0$ the starting point of the graph will be displaced from the start of the time reference $t=0$ by exactly the value of $\mathscr{S}_1$.

To obtain the ordinates of all the displaced functions at one and the same moment of time t, it is sufficient to bring the section of the same contour through the plane t_1. The new argument $\mathscr{S}$, character-izing the displacement of each of the functions, is for this case read along the $\mathscr{S}$-axis, as shown in Figure 2-1c at the bottom. We will in-troduce one more argument: Θ, read in the same plane from point t_1 towards the argument $\mathscr{S}$, so that

$$\theta=t_1-\vartheta. \qquad (2\text{-}5)$$

By virtue of the properties of the cylindrical surface it is easy
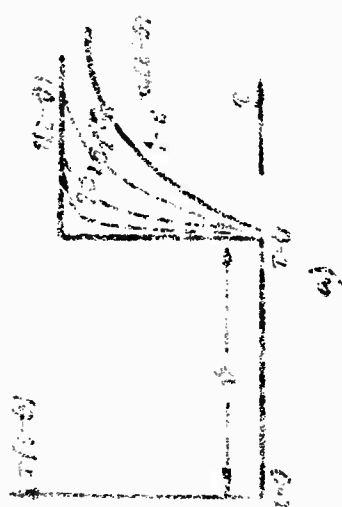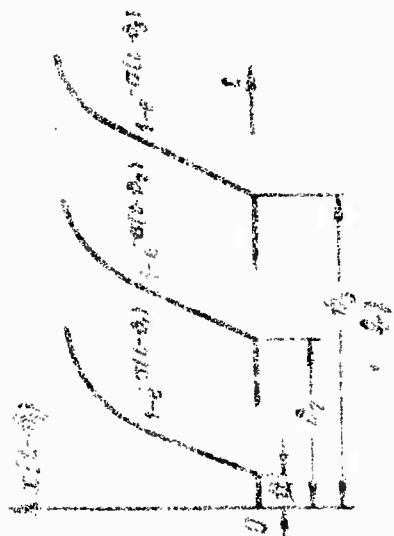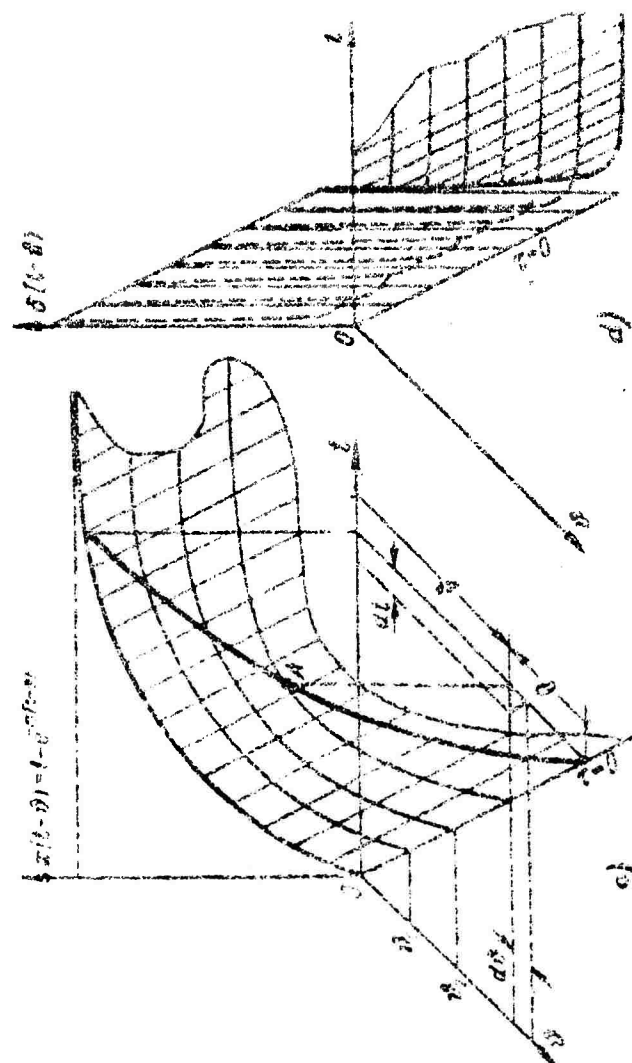
Fig 2-1. Graphs of displaced functions. a - limiting transition to a single displaced function; b - set of graphs for different displacements; c - contour of a displaced function; d - contour of a derivative of a displaced function.

to note that the sections of the contour of the displaced functions
by the planes $\vartheta = 0$ and $t = t_1$ have an identical form, that is, at the
interval $0 - t_1$ the functions

$$x(t) = x(\vartheta), \qquad (2-6)$$

coincide.

The geometric interpretation of the displaced funtion makes it
possible to show a number of its important properties clearly later on.

2-2. Differentiation and Integration of Displaced Functions

A. Equivalent Differentiation

If there is a displacement from the arbitrary point A on the sur-
vace of the contour by $d\vartheta$ and $-d\vartheta$ in the corresponding directions,
then, as shown in Figure 2-1c, the ends of the elementary vectors fall
on one and the same line τ, which creates an identical increase in the
function $x(t - \vartheta) = x(\tau)$ in comparison with its value at point A. Con-
sequently, differentiation of the displaced function with respect to
time can be replaced by equivalent differentiation with respect to the
displacement with change of the sign of the result obtained:

$$\frac{d}{dt} x(t - \vartheta) = - \frac{d}{d\vartheta} x(t - \vartheta); \qquad (2-7a)$$

$$\frac{d^i}{dt^i} x(t - \vartheta) = (-1)^i \frac{d^i}{d\vartheta^i} x(t - \vartheta). \qquad (2-7b)$$

And so, from the equivalence of the sections of the cylindrical
contour of the displaced function there flows an equivalence with ac-
curacy of the sign of the operations of differentiation with repect to
time and with respect to displacement.

The difference between the sections is established only for the
limits of the working regions.

The derivatives of the displaced function are likewise geometri-
cally formed by the contour. For example, for the function (**) we
have:

$$\frac{d}{dt} \left[1 - e^{-a(t-\vartheta)} \right] = a e^{-a(t-\vartheta)}.$$

The contour of the derivative of such a function is shown in Figure 2-1d.

B. Impulses

A real single displaced impulse is called a process of type (***) at an adequately rapid damping ($\sigma \gg 1$):

$$\delta[t - \vartheta] = \sigma e^{-\sigma(t-\vartheta)} \ \sec^{-1}. \qquad (2\text{-}8a)$$

It is designated in the same way as all displaced functions and has a limited argument only on the left (bracket). It is called single because the area of the process M_0 is equal to unity:

$$M_0 = \int_\vartheta^\infty \sigma e^{-\sigma(t-\vartheta)} \, dt =$$

$$= \sigma \int_\vartheta^\infty e^{-\sigma(t-\vartheta)} \, dt = 1.$$

An ideal single displaced impulse (the term "ideal" will be omitted from now on) is the name given the limit of a function (2-8a) at an infinite increase in σ:

$$\delta[t - \vartheta] = \lim_{\sigma \to \infty} \sigma e^{-\sigma(t-\vartheta)} = \frac{\partial}{\partial t} 1[t - \vartheta] \ \sec^{-1}$$

$$(2\text{-}8b)$$

either ± the derivative of the single displaced function with respect to one of the arguments. Since the above-calculated area of the real impulse did not depend on σ, it remains equal to 1 and upon transition to the limit $\sigma = \infty$. In designating the impulse two brackets were used which limit the interval of change of the argument on the left and on the right from the point $t = \vartheta$. However, as before, the impulse remains a right-side process which represents the conditional working zone from ϑ to $\vartheta+$ or from $\vartheta+$ to $\vartheta++$, etc., in which it is convenient in the future to mark by the quantity of plus signs the mutual disposition of the impulse processes existing at the point ϑ.

A single (undisplaced) impulse is designated by

$$\delta[t] = \lim_{\sigma \to \infty} (\sigma e^{-\sigma t}) = \frac{d}{dt} 1[t] \ \sec^{-1}, \quad (2\text{-}8c)$$

or for the argument τ by:

$$\delta[\tau] = \lim_{\sigma \to \infty}[\sigma e^{-\sigma\tau}) = \frac{d}{d\tau} 1[\tau] \, sec^{-1}. \quad (2\text{-}8d)$$

For convenience in comparison with other impulses it is given in Figure 2-2a in the zone $(0++)$ to $(0+++)$.
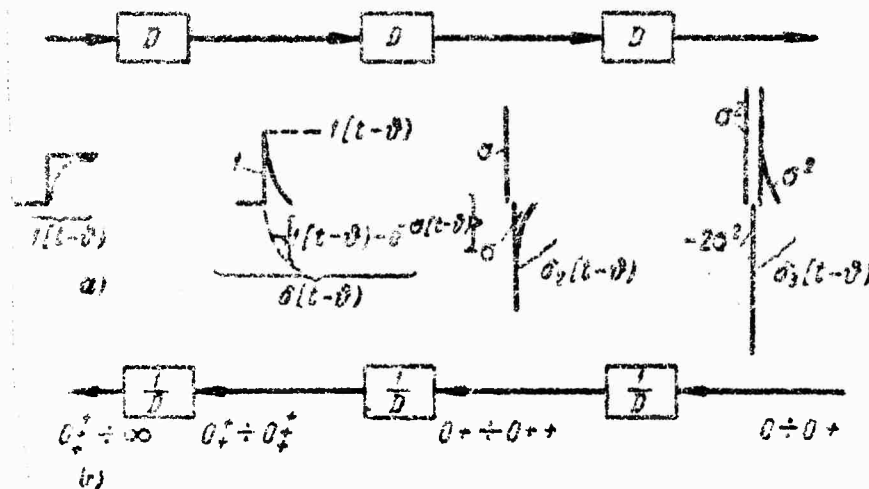
Fig 2-2. Differentiation and Integration of Impulses.

A single displaced impulse of the second order is obtained in the differentiation of an impulse of the second order or double differentiation of a single displaced function, as shown in Figure 2-2a in the zone $(0+)$ to $(0++)$, with conditional anticipation with respect to the first zone.

In order to use the theorems derived above in the differentiation of a real impulse (2-8a), it is convenient to present it in the form of a difference in a graduated displaced function reproducing the front of the impulse, and of an exponential function reflecting its continuous right side·

$$\delta[t - \vartheta) = \sigma \{ 1[t - \vartheta) -$$
$$- [1[t - \vartheta) - e^{-\sigma(t-\vartheta)}]\}.$$

Then according to (2-8a) and (2-8b) the differentiation gives a

85

real impulse of the second order:

$$\delta_2[t - \theta] = \frac{\partial}{\partial t}\delta[t - \theta] =$$

$$= \sigma\left\{\delta[t - \theta] - \sigma e^{-\sigma(t-\theta)}\right\} \; sec^{-2}.$$

A system was obtained with two first-order impulses of different signs, having a total area of zero ($+\sigma - \sigma = 0$), but since the "center of gravity" of the second impulse is displaced relative to the first impulse, the moment of the area M_1, determinable by the formula:

$$M_1 = \int_0^\infty (t - \theta)\,\sigma^2 e^{-\sigma(t-\theta)}dt = 1.$$

is not equal to zero.

The value of the moment does not depend on σ and does not vary during transition to the limit $\sigma \to \infty$. And so, for second-order impulses we have the formulas:

$$\delta_2[t - \theta] = \frac{\partial}{\partial t}\delta[t - \theta] = \frac{\partial^2}{\partial t^2}1[t - \theta] \; sec^{-2};$$

$$(2-8e)$$

$$\delta_2[t] = \frac{\partial}{\partial t}\delta[t] = \frac{\partial^2}{\partial t^2}1[t] \; sec^{-2}. \qquad (2-8f)$$

A third-order impulse can also be replaced by a system of impulses of different signs. Again at the start we get a real third-order impulse, and if we differentiate (2-8a) twice it gives the figure of the process $\delta_3[t - \theta] \; sec^{-3}$, displaced in the zone (0 to 0+), and indicated in Figure 2-2, where the areas of the component impulses are marked. In that case the area M_0 and the moment of first order of the area of impulses M_1 are equal to zero, but the moment of the second order, determinable by the formula

$$M_2 = \int_0^\infty (t - \theta)^2 \sigma^3 e^{-\sigma(t-\theta)}dt = 1.$$

is not equal to zero.

The differentiation examined above does not vary the coefficients when there are impulses which remain equal in size to unity, and so the impulses obtained as a result of further differentiation of a single displaced function are also called single displaced impulses of the corresponding order.

Equivalent Differentiation of Impulses

For a single displaced function and for displaced impulses the differentiation with respect to time can be replaced by equivalent differentiation with respect to the displacement:

$$\delta_1[t - \theta] = \dot{\delta}[t - \theta] = -\frac{\partial}{\partial \theta} 1[t - \theta]; \quad (2\text{-}9a)$$

$$\delta_2[t - \theta] = \ddot{\delta}[t - \theta] = -\frac{\partial}{\partial \theta} \dot{\delta}[t - \theta]; \quad (2\text{-}9b)$$

$$\cdots \qquad \cdots$$

$$\delta_{k+1}[t - \theta] = \delta^{(k)}[t - \theta] =$$

$$= (-1)^k \frac{\partial^k}{\partial \theta^k} \delta[t - \theta] \qquad (2\text{-}9c)$$

C. The Differentiating Properties of Impulses

If an impulse of any order is multiplied by a continuous function

$$\delta^{(k)}[t - \theta] \, x(t),$$

then, since the first co-factor is not equal to zero only at the point $t = \theta$, the product will be equal to zero at all points except $t = \theta$, that is, will also have an impulse character.

For a co-factor in the form of a first-order impulse the product is simply obtained:

$$\delta[t - \theta] \, x(t) = x(\theta) \delta[t - \theta]; \qquad (2\text{-}10a)$$

it corresponds to an impulse with an area equal to the value of the continuous function at the moment of application of the impulse.

For second-order impulses the mechanism of multiplication is more complex in connection with the specifics of the graph of the process $\delta_2(t - \theta)$, shown in Figure 2-2. It is most convenient to obtain the desired product by differentiating the result of (2-10a) with respect to the argument θ and replacing the left side on the basis of the formula of equivalent differentiation (2-9b);

$$\delta_2[t-\theta]\,x(t) = -\frac{\partial}{\partial t}\{\delta[t-\theta]\,x(t)\} = $$

$$= -\frac{\partial}{\partial \theta}\{x(\theta)\,\delta[t-\theta]\}. \qquad (2\text{-}10b)$$

For a co-factor in the form of an impulse of the $(k+1)$-th order, analogous differentiation of the product (2-10a) with an equivalent transition (2-9c) gives:

$$\delta_{\varkappa+1}[t-\theta]\,x(t) = (-1)^{\varkappa}\frac{\partial^{\varkappa}}{\partial \theta^{\varkappa}}\{x(\theta)\,\delta[t-\theta]\}.$$

$$(2\text{-}10c)$$

We will expand the right side of (2-10b) according to the rules for differentiation of a product and proceed from the derivative of the impulse with respect to θ, the physical sense of which can be clarified on the contour of Figure 2-1d, to the derivative with respect to t on the basis of (2-9):

$$\delta_2[t-\theta]\,x(t) = x(\theta)\,\dot{\delta}[t-\theta] - $$

$$- x(\theta)\,\delta[t-\theta].$$

The general formula (2-10c) also is analogously expanded, in which in Chapter 1 it was convenient to introduce designations of derivatives addressed to only one of the co-factors

$$D_x^{\varphi} = \frac{\partial_x}{\partial \theta}, \quad D_{\theta}^{\varphi} = \frac{\partial_{\theta}}{\partial \theta}:$$

$$\delta_{\varkappa+1}[t-\theta]\,x(t) = $$

$$= (-D_x^{\varphi} - D_{\theta}^{\varsigma})^{\varkappa}\,x(\theta)\,\delta[t-\theta].$$

In order not to disregard the change of sign in the transition to the derivatives of the impulse with respect to time (2-9c), it is possible in the general formula (**) to proceed to differentiation with respect to time, having re-established the designation

$$D = \frac{\partial}{\partial t} = -D_{\theta}^{\varphi}:$$

then we obtain:

$$\delta_{\varkappa+1}[t-\theta]\,x(t) = (D - D_x^{\varphi})^{\varkappa}\,x(\theta)\,\delta[t-\theta].$$

$$(2\text{-}10d)$$

In application to a third-order impulse this formula gives the following result:

$$\delta_3 [t - \theta] x(t) = (D - D_r^r)^3 x(\theta) \delta[t - \theta] =$$

$$= (D^3 - 2DD_r^2 + D_r^{r2}) x(\theta) \delta[t - \theta] =$$

$$= x(\theta) \overset{..}{\delta}[t - \theta] - 2\dot{x}(\theta) \delta[t - \theta] +$$

$$+ \ddot{x}(\theta) \delta[t - \theta].$$

Thus impulses of high orders, multiplied by a continuous function, generate a series of impulses of lower orders with moments proportional to the derivatives of the continuous function at the point of application of the impulse. These differentiating properties of impulses can be explained by using the representation of the processes in Figure 2-2, where the displaced co-factors reveal the difference in the displaced values of the function entering the derivatives.

Ordinary Formulas of Differentiation

The derivatives of the displaced impulse and the derivatives make it possible to show clearly the conditions (2-3) of differentiation of functions with the initial front. Let the displaced function be given in the form of the derivative

$$x(t) 1[t - \theta] = x(\theta + \tau) 1[\tau] = x_r[t], \quad (2\text{-}11)$$

where the right side is given an abbreviated designation of the displaced function with an indication of the location of the front r added to the subscript.

If we differentiate the left side of (2-11), we get

$$\frac{d}{dt} \{x(t) 1[t - \theta]\} = \dot{x}(t) 1[t - \theta] +$$

$$+ x(\theta) \delta[t - \theta] \qquad (2\text{-}12a)$$

The first term on the right side coincides with the usual representation of the derivative of a bilateral function, if at such only the usual bilateral front is used; the second term indicates the possibility of formation of an impulse during differentiation of the displaced function if $x(\theta) \neq 0$. The conditions of formation of the second term are explained by formula (2-10a).

We shall continue to differentiate expression (2-12a), but with

consider the first term as the product of the functions, and the second as a function with a constant coefficient:

$$\frac{\partial^2}{\partial t^2}\{x(t)\,1[t-\theta]\} = \ddot{x}(t)\,1[t-\theta] +$$

$$+\,\dot{x}(\theta)\,\delta[t-\theta] + x(\theta)\,\dot{\delta}[t-\theta]. \quad (2\text{-}12\text{b})$$

Repeated differentiation permits obtaining the general formula

$$\frac{\partial^i}{\partial t^i}\{x(t)\,1[t-\theta]\} = x^{(i)}(t)\,1[t-\theta] +$$

$$+\sum_{j=0}^{i-1} x^{(j)}(\theta)\,\delta_{i-j}[t-\theta]. \quad (2\text{-}12\text{c})$$

For a displaced function in the form of (2-4) we obtain the analogous expression:

$$\frac{\partial^i}{\partial t^i}\{x(t-\theta)\,1[t-\theta]\} = x^{(i)}(t-\theta)\,1[t-\theta] +$$

$$+\sum_{j=0}^{i-1} x^{(j)}(0)\,\delta_{i-j}[t-\theta]. \quad (2\text{-}12\text{d})$$

valid also at $\theta = 0$ is:

$$\frac{\partial^i}{\partial t^i}\{x(t)\,1[t]\} = x^{(i)}(t)\,1[t] +$$

$$+\sum_{j=0}^{i-1} x^{(j)}(0)\,\delta_{i-j}[t]. \quad (2\text{-}12\text{e})$$

B. Equivalent Integration of Displaced Functions

If we consider in Figure 2-1c the sections of the contour cut by

the planes $x = 0$, and $t = 0$, it is easy to establish an equality of the areas in these sections, and consequently an equality of the integrals of the form:

$$\int_{0}^{t_1} x(t-\theta)\,dt = -\int_{t_1}^{0} x(t-\theta)\,d\theta. \qquad (2\text{-}13)$$

In application to impulses the limits of integration can be expanded if the designations of functions limited on both sides are used (two brackets). The operation of integration gives a lowering of the order of the impulse at each integration, which makes it possible to write the following formulas of the equivalent integration:

$$\int_{0}^{\infty} \delta(t-\theta)\,dt = -\int_{\infty}^{0} \delta(t-\theta)\,d\theta = 1(t-\theta);$$
$$(2\text{-}14a)$$

$$\int_{0}^{\infty} \delta(t-\theta)\,dt = -\int_{\infty}^{0} \delta(t-\theta)\,d\theta = \delta(t-\theta);$$
$$(2\text{-}14b)$$

$$\cdot \ \cdot \ \cdot \ \cdot \ \cdot \ \cdot \ \cdot \ \cdot \ \cdot \ \cdot \ \cdot \ \cdot \ \cdot \ \cdot \ \cdot \ \cdot \ \cdot \ \cdot$$

$$\int_{0}^{\infty} \delta_{k+1}(t-\theta)\,dt = -\int_{\infty}^{0} \delta_{k+1}(t-\theta)\,d\theta =$$
$$= \delta_{k}(t-\theta). \qquad (2\text{-}14c)$$

In Figure 2-2 the conditions of transformation a third-order impulse in integration performed three times are shown in the form of a chain of the integrators b. These transformation repeat in reverse sequence the conditions of differentiation of a single displaced function by a chain of differentiators. In the same figure, for the case $x = 0$, the intervals are shown at which the impulse functions are conveniently considered to be given. After each integration and reduction of the order of the impulse the interval is conventionally shifted to the right.

2-3. Transient and Weight Functions of First and Zero Order Components

A. A First Order Component with Linearly Varied Parameters

Let us consider the relatively simple particular form of an equation of connection with variable parameters

$$t\dot{x}_{out} + (1 + st)\, x_{out} = x_{in}$$

Here the coefficients on the left side are variable, and on the right side the coefficient is constant and equal to unity:

$$a_1(t) = t; \quad a_0(t) = 1 + st; \quad b_0 = 1.$$

The transient function of a component or linear system is the name given a reaction of a previously not excited component or linear system on a single function. The transient function is designated $h = x_{out}$ at $x_{in} = 1(t - \vartheta)$, which is explained by Figure 2-3a.

The equation of connection composed for the transient function will have the following form in the particular example under consideration:

$$t\dot{h} + (1 + st)\, h = 1(t - \vartheta). \qquad (2\text{-}15a)$$

For the solution it is convenient to proceed from an absolute reading of the time to the interval τ by substitution of $t = \vartheta + \tau$; $dt = d\tau$:

$$(\vartheta + \tau)\dot{h} + [1 + s(\vartheta + \tau)]\, h = 1(\tau). \qquad (2\text{-}15b)$$

and then bring the equation to the normalized form by dividing all its terms by the coefficient at the higher (first) derivative:

$$\dot{h} + \left(\frac{1}{\vartheta + \tau} + s\right) h = \frac{1(\tau)}{\vartheta + \tau}. \qquad (2\text{-}15c)$$

The general solution of the first-order equation of the form

$$\dot{x} + a_0^{*}(t)\, x = n(t) \qquad (2\text{-}16a)$$

is known in the form

$$x = e^{-\int a(t)\,dt} \left[\int n(t)\, e^{\int a(t)\,dt}\, dt + C \right]. \qquad (2\text{-}16b)$$

The determination of the transient function from (2-15a) requires some preparation of the intermediate data:

$$\int a(\tau)\,d\tau = \int \left(\frac{1}{\vartheta + \tau} + \sigma\right) d\tau = \ln(\vartheta + \tau) + \sigma\tau;$$

$$e^{\int a(\tau)d\tau} = (\vartheta + \tau)\,e^{\sigma\tau};$$

$$e^{-\int a(\tau)d\tau} = \frac{1}{\vartheta + \tau}\,e^{-\sigma\tau};$$

$$\int h(\tau)\,e^{\int a(\tau)d\tau}\,d\tau = \int \frac{1}{\vartheta + \tau}\,(\vartheta + \tau)\,e^{\sigma\tau}\,dt = \frac{e^{\sigma\tau}}{\sigma}.$$

Then, if we use formula (2-16b), we get:

$$h(\tau,\ \vartheta) = \frac{e^{-\sigma\tau}}{\vartheta + \tau}\left[\frac{e^{\sigma\tau}}{\sigma} + C\right], \qquad (2\text{-}17a)$$

where it can readily be seen from the character of the right side that the transient function depends on two arguments, and this is also noted on the left side.

To discover the arbitrary constant C it is necessary to find the initial values of the transient function at t = 0+.

From the conditions

$$h(0+,\ \vartheta) = \frac{1}{\vartheta} \quad \text{and} \quad h(0+,\ \vartheta) = 0$$

we find

$$C = -\frac{1}{\sigma}$$

and we make the solution of (2-17a) more precise:

$$h(\tau,\ \vartheta) = \frac{1 - e^{-\sigma\tau}}{\sigma(\vartheta + \tau)}. \qquad (2\text{-}17b)$$

If we now proceed to the argument t, we get:

$$h_\tau(t,\ \vartheta) = h(t - \vartheta,\vartheta) = \frac{1 - e^{-\sigma(t-\vartheta)}}{\sigma t}. \qquad (2\text{-}17c)$$
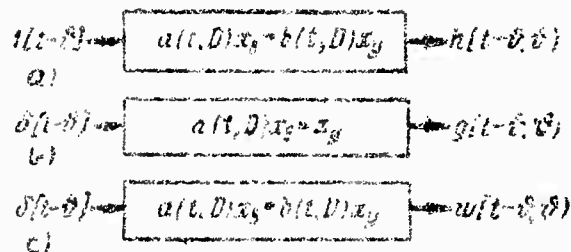
Fig 2-3. Conditions of excitation of transient and weight functions in a linear system.

$$x_B = x_{out} \; ; \; x_y = x_{in}$$

If the solution (2-17c) is obtained for various displacements, it is possible to construct the contour of the transient function on the same coordinates as contour c in Figure 2-1, but it will not be a cylindrical surface, since arguments t and ϑ enter function (2-17c) unequivalently.

The equation of connection composed for the weight function has the following form in the example under consideration:

$$t\dot{g} + (1 + \sigma t)\, g = \delta[t - \vartheta] \qquad (2\text{-}18a)$$

or

$$(\vartheta + \tau)\dot{g} + [1 + \sigma(\vartheta + \tau)]\,g = \delta[\tau]; \qquad (2\text{-}18b)$$

$$\dot{g} + \left(\frac{1}{\vartheta + \tau} + \sigma \right) g = \frac{\delta[\tau]}{\vartheta}. \qquad (2\text{-}18c)$$

Formula (2-10a) is taken into consideration in the normalization of the right side in (2-18c).

The determination of the weight function from the differential equation is done by the general formula (2-16c), in which

$$n(\tau) = \frac{\delta[\tau]}{\vartheta}; \quad \int n(\tau)\, e^{\int a(t)dt}\, dt = 1;$$

the remaining intermediate data can be used from calculation of the transient function, which permits obtaining the solution

$$g[\tau, \vartheta] = \frac{e^{-\sigma t}}{\vartheta + \tau}(1 + C). \qquad (2\text{-}19a)$$

For calculation of the arbitrary constant we will consider the

processes at zero. In the interval 0 to 0+ we have contracted equation (2-18a):

$$\dot{g}[\tau, \vartheta] = \frac{1}{\theta} \delta[\tau],$$

that is, the derivative of the weight function determined at zero. The transition from the derivative to the function itself at the end of the interval is connected with the integration and gives:

$$g[0+, \vartheta] = \frac{1}{\theta}.$$

If we return to (2-19a), we find the arbitrary constant:

$$\frac{1}{\theta} = \frac{1 + C}{\theta}; \quad C = 0,$$

which proves to be equal to zero, and the solution is reduced to the form:

$$g[t, \vartheta] = \frac{e^{-\sigma\tau}}{\theta + x}, \qquad (2\text{-}19b)$$

or after substitution of the argument:

$$g_\tau[t, \vartheta] = g[t - \vartheta, \vartheta] = \frac{1}{t} e^{-\sigma(t-\vartheta)}. \quad (2\text{-}19c)$$

Determination of the Weight Function According to a
   Known Transient Function

The equation for the transient function

$$\ldots a_1(t)\, \dot{h} + a_0(t)\, h = b_0(t)\, 1[t - \vartheta] + \ldots$$

we will differentiate with respect to the displacement $\mathcal{G}$:

$$\ldots a_1(t) \frac{\partial}{\partial \vartheta}[h] + a_0(t) \frac{\partial}{\partial \vartheta}[h] =$$
$$= -b_0(t)\, \delta[t - \vartheta] - \ldots$$

We will carry the minus sign over into the left side and change the sequence of the differentiation:

$$\ldots a_1(t)\frac{\partial}{\partial t}\left[-\frac{\partial h}{\partial \theta}\right]+a_0(t)\left[-\frac{\partial h}{\partial \theta}\right]=$$

$$= b_0(t)\,\delta[t-\theta]+\ldots \qquad (2\text{-}20a)$$

It is evident from the general determination so the weight function and the partial example (2-18a) that the equation obtained is the equation for the weight function, which can be determined from it in the form:

$$w_\tau[t,\theta]=-\frac{\partial}{\partial \theta}h_\tau[t,\theta]. \qquad (2\text{-}20b)$$

It is obvious that, independently of the order of the right and left sides of the differential equation of the component-system connection, the weight function always is equal to the derivative of the transient function with respect to displacement with change of sign.

B. Transient Functions of Typical Components with Constant Coefficients

1. Aperiodic Component

We obtain the transient function of an aperiodic component by solving its differential equation of connection (1-39a) at $x_{in}=1/t)$, that is

$$T\dot{h}+h=k\,1(t). \qquad (2\text{-}21a)$$

After transition to the normalized form:

$$\dot{h}+\frac{1}{T}h=\frac{k}{T}\,1(t) \qquad (2\text{-}21b)$$

the general form of solution of this equation is readily established by formula (2-16b):

$$h=e^{-\frac{t}{T}}\left[ke^{\frac{t}{T}}+c\right].$$

It follows from equation (2-21b) that motion at the output starts with a limited jump of the first derivative:

$$\dot{h}(0+)=\frac{k}{T}. \qquad (2\text{-}21c)$$

Hence $h/(0+) = 0 = k + C$, or $C = -k$.

If the initial velocity (2-21b) had been preserved during the entire course of the process, such a process would be expressed by the equation:

$$x_{int}(t) = k \frac{t}{T}$$

and have a rectilinear graph (Figure 2-4). But the actual process, as follows from the general equation, has an aperiodic character with a changing (decreasing) rate

$$h(t) = k\left(1 - e^{-\frac{t}{T}}\right). \qquad (2\cdot21d)$$

In the same Figure 2-4 has been constructed an exponent tangential to the inclined straight line x_{int} at the start of the coordinates and asymptotically approaching the horizontal straight line $h = k$. The degree of approximation of the process to the asymptote (to the ratio being established for $t = T$, $2T$, $3T$, $4.6T$) is estimated in percentages of k at the following values respectively: 36, 8, 13.5, 5 and 1% respectively.
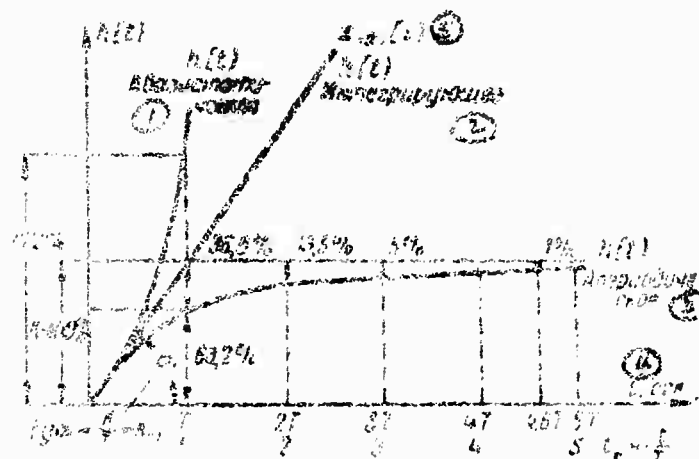
Figure 2-4. Transient functions of first-order components.
1 - Quasi-static; 2 - Integrating; 3 - Aperiodic; 4 - t, sec.;
5 - $x_{int}(t)$.

Thus the form of the transient function in an aperiodic component is wholly determined by the time constant of the component. The time

of transition to the state being established is equal, with an accuracy of ± to 1%, to 3T or 4.6T respectively.

The time constant can be determined from the graph of the transient process by several methods:

On the basis of measurement of the ordinates -- as the time of attainment by the output value of 63.2% of the value being established;

From formula (2.21c) -- as $T = \dfrac{k}{h(\infty)}$ or indirectly by the cotangent of the angle of inclination tangential to the graph at the start of the coordinates $T = k \cot \alpha$; in the given case the tangent is the straight line $x_{init}(t)$;

By starting from the preceding determination -- as the segment between the points of intersection of the asymtote with the tangent and continuation of the ordinate at the point of tangency; the validity of this rule, which is most clear for tangency at the point $t = 0$, is just as readily verified for any point of tangency;

by starting from the time of damping of the entire process to 5 or 1%

$$T = \frac{t_{5\%}}{3} = \frac{t_{1\%}}{4.6} .$$

It also is possible to construct the transient function of an aperiodic component in the relative time t_* measurable in fractions of the base T:

$$t_* = \frac{t}{T} . \qquad (2.22a)$$

In Figure 2-w, on the time scale, a second scale, of the relative time t_* has been presented; in this system of reading, the equation of the transient function of an aperiodic component assumes the form:

$$h(t_*) = k(1 - e^{-t_*}) . \qquad (2.22b)$$

4. A First-Order Quasi-Static Component

We will consider the differential equation

$$Th + h = k1(t) . \qquad (2.23a)$$

as the starting equation for determination of the transient function of a first-order quasi-static component.

For best comparison with the preceding conclusions the coefficients of equation (1-46) have been transformed, so that the notation of 2-23a) and (2-23a) may coincide.

The general solution of the equation according to (2-16b) is:

$$h(t) = e^{\frac{t}{T}}\left[-ke^{-\frac{t}{T}} + C\right). \qquad (2-23b)$$

If we analyze the initial conditions, we arrive at the conclusion of equality to zero of the initial value of the coordinate, $h(0+) = 0$, and of the finiteness of the jump of the first derivative. Thanks to the equality of the coefficients in the equations of both components, the value of the initial derivative $h(0+)$ for the quasi-static component is determined again by formula (2-21b), derived for the aperiodic component. Therefore the inclined straight line $x_{init}(t)$ will serve as the tangent also for the graph of the transient function of a quasi-static component.

If we use in the general solution (2-23b) the condition $h(0+) = +0$, from which it proceeds that $C = k$, we get the equation for the transient function of a first-order quasi-static component:

$$h(t) = k\left(e^{\frac{t}{T}} - 1\right). \qquad (2-23c)$$

A curve (the upper curve) has been constructed in Figure 2-4 according to this equation. For the time values T, 2T and 3T the ordinates of the transient function are 1.72, 6.39 and 20.09 of k respectively.

4. An Integrating Component

If we have assumed in the equations of the aperiodic or quasi-static component a coefficient at the output value equal to zero, $a_0 = +0$, we arrive at the differential equation of the integrating type:

$$T\dot{h} = k \, 1(t). \qquad (2-24a)$$

Its solution is:

$$h(t) = \frac{k}{T} t = \kappa \, t. \qquad (2-24b)$$

The amplification factor of the integrating component was selected in such a way, ($\kappa = k/T$), that the initial values of the deriva-

tives of the integrating component and of the preceding components coincide. Thanks to this the graph of the transient function of the integrating component coincides with the common initial tangent of the two preceding graphs.

The coincidence of the initial segments of the transient functions for all the components which have first-order differential equations of connection is not an accident and is explained by the presence of the integrating component, included by feedbacks in the internal structure of the static and quasi-static components, shown in Figure 1-6 and in Chapter 5.

4. Amplifying and Delaying Components

From formulas (1-36) and (1-37), in accordance with the determination, we obtain the transient functions of the amplifying

$$h(t) = k_y 1(t) \qquad (2\text{-}25)$$

and the delaying

$$h_{10}(t) = k_3 1(t - \tau_3) \qquad (2\text{-}26)$$

components.

Graphs of the transient functions obtained are presented in Figure 2-5.
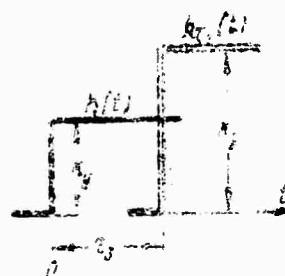
Figure 2-5. Transient functions of the amplifying and delaying components.

5. Weight Functions of Typical Components with Constant Coefficients

a. Aperiodic, Quasi-static and Integrating Components

Having solved the normalized equation

$$\dot{w} + a_0^n w = \frac{k}{T} \delta[t]$$

for the cases

$$a_0^n = \frac{1}{T}, \quad a_0^n = -\frac{1}{T} \text{ and } a_0^n = 0,$$

according to formula (2-16b) we obtain the weight functions of the aperiodic

$$w[t] = \frac{k}{T} e^{-\frac{t}{T}}, \qquad (2\text{-}27)$$

the quasi-static

$$w[t] = \frac{k}{T} e^{\frac{t}{T}} \qquad (2\text{-}28)$$

and the integrating

$$w[t] = \frac{k}{T} 1[t] = k_{-1} 1[t] \qquad (2\text{-}29)$$

components.

The same results can be obtained with respect to known transient functions of the same components by using formula 2-20b). Since the contours of the reactions of components with constant parameters have the form of cylindrical surfaces (depend only on the difference of the arguments t $-\vartheta$), then on the basis of the rules of equivalent differentiation instead of (2-20b) it is possible to obtain a simplified connection between the weight and transient functions:

$$w[t] = \frac{d}{dt} h[t]. \qquad (2\text{-}30)$$

And so, for components with constant parameters, the weight function is equal to the derivative of the transient function according to the argument t or ϑ, which makes no difference by virtue of the independence of the form of the solution on ϑ. Graphs of the weight functions of the components examined are given in Figure 2-6.

2. Amplifying and Delaying Components

Formally the weight function of the amplifying component equals:

$$w[t] = k_y \delta[t]. \qquad (2\text{-}31a)$$

that is, the impulse on the input generates the impulse on the output.

But in real components such a sharp change in the output value always manifests a time constant that has not been taken into consideration. If we designate it $T = 1/\alpha$, assume a single amplification factor $k = 1$ and take into consideration for generality the possible displacement of the impulse, we obtain from (2-27) the weight function in the form:

$$w(t-\theta) = \alpha e^{-T(t-\theta)} = \delta(t-\theta). \quad (2\text{-}31b)$$

This weight function has the contour shown in Figure 2-6d.

From the weight function of a single amplifying component (of a real impulse), by introducing the amplification factor k and directing the time constant toward zero ($T \to \infty$), it is possible to proceed to the weight function of an inertialess amplifier (2-31a).
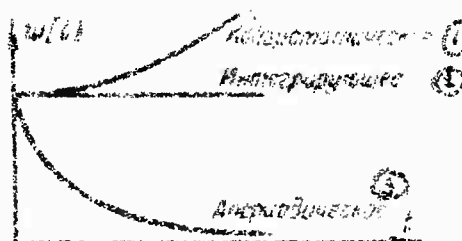
Fig 2-6. Weight functions of a first-order component.
1 - Quasi-static; 2 - Integrating; 3 - Aperiodic.

For the delaying component the weight function has the form of a displaced impulse:

$$w_n(t) = k_2 \delta(t - \tau_2). \quad (2\text{-}32)$$

Graphs of displaced impulses have been considered early in Figure 2-2.

B. Experimental Determination of Transient and Weight Functions

In taking down a transient function on the input of component being tested, constant action of the level x_0 are assigned (which in the general case does not equal 1), sufficiently small in value that the component does not go beyond the limits of the linear characteristics, but substantially exceeds the level of interferences in the input and output devices. The input reaction of the component x_n assumed in this is used to obtain the transient function on the basis of the pro-

$$h = \frac{x_h}{W_0}. \qquad (2\text{-}33)$$

In taking down the weight function, instead of an ideal single impulse on the input of the component, an impulse of area x_0 and duration Δt is assigned. The reduction of the reaction of the component x_w to a single area in order to obtain the weight function is done by proportional recalculation:

$$\omega = \frac{x_w}{W_0}. \qquad (2\text{-}34)$$

The finality of the time interval Δt introduces error into the form of the output process. Thus, for example, for an aperiodic component at $\Delta t = 0.05T$ the ideal weight functions differs from the experimental (2-34) by 2%. At small values of Δt the further course of process (2-34) depends only on the area of the impulse. Thus, for the input actions presented in Figure 2-7 the reaction of the system can be identical (for $t > \Delta t$) if the areas of the impulses are identical and the interval Δt is relatively small.

The experiment can be conducted on an electronic model. In that case the step is given in the form of the input voltage (cf, for example, Figure 1-9), and the impulse -- in the form of equivalent initial conditions on the output integrators of the straight path of the model.
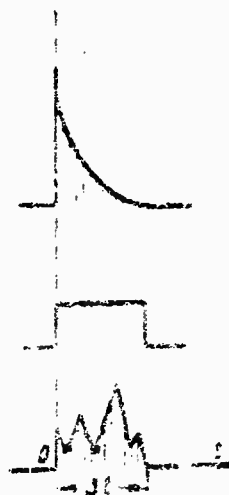
Fig 2-7. Short-period input signals. Identical in regime of consequence.

We have examined the analytical expressions for transient and weight functions of the components, differential equations of which are not above the first order on the left side. It is not economical to solve more complex equations by the classical methods, and for them use will be made of operational methods. In the presence of complication of the right side of the differential equation of connection the classical methods retain their effectiveness, and therefore we will consider further the corresponding additional types of components.

2-4. Transient and Weight Functions of Differentiating and Boosting Components

Having substituted in the equations of the components (1-52), (1-53) and (1-54) the input action in the form of a single function and a single impulse, we obtain expressions for the output reactions of these components.

The differentiating component. The transient function is:

$$h[t] = T\delta[t]; \qquad (2\text{-}35a)$$

the weight function is

$$w[t] = T\delta_1[t]. \qquad (2\text{-}35b)$$

The first-order boosting component is:

$$h[t] = k\{1[t] + T\delta[t]\}; \qquad (2\text{-}36a)$$

$$w[t] = k\{\delta[t] + T\delta_1[t]\}. \qquad (2\text{-}36b)$$

The second-order boosting component is:

$$h[t] = k\{1[t] + 2\tau\delta[t] + \tau^2\delta_2[t]\}; \qquad (2\text{-}37a)$$

$$w[t] = k\{\delta[t] + 2\tau\delta_1[t] + \tau^2\delta_1[t]\}. \qquad (2\text{-}37b)$$

The real differentiating component. We will examine the equation of balance of voltages in the circuit of Figure 2-8, $U_0 + (R_1 + R_2)I = 0$. If we differentiate and proceed in both terms of the left side to the current $I = C\dot{U}_c$, and then to the voltage drop on the output resistance $U_1 = IR_1$, it is possible to obtain the equation of connection of the component:

$$T\dot{U}_1 + U_1 = k\dot{U}, \qquad (2\text{-}38a)$$

where

$$T = (R_1 + R_2)C; \quad k = CR_1 \text{ sec}.$$

The current in the circuit or the output voltage prove in fact
to be proportional to the derivative of the input voltage and the com-
ponent is classed as differentiating, but pure differentiation is at-
tained only at R = 0, which is never attainable in the real circuit,
where the circuit resistance R and the resistance of the conductors are
inescapably present, and therefore the component is called a real
differentiating one.

The transient function of a real differentiating component is the
solution of the equation:

$$Th + h = k\delta[t].\qquad (2\text{-}38b)$$

We will solve at first the contracted equation for the working
zone at zero 0 to 0+:

$$Th = k\delta[t]; \quad h = \frac{k}{T}\delta[t].$$

After integration we find the value of the current h at the end
of the zone:

$$h[0+] = \frac{k}{T},$$

which also will be the initial value for the transient function of the
component damping with respect to the exponent

$$h[t] = \left[\frac{k}{T} e^{-\frac{t}{T}}\right].\qquad (2\text{-}38c)$$

The same solution can be obtained by other methods, by dividing
the real component into two typical ones.

In Figure 2-56 is a possible structure of a real component, ac-
cording to which the input signal proceeds at first through the dif-
ferentiating component with amplification k, as a result of which the
first part of equation (2-38b) is formed

$$n[t] = k\delta[t]; \qquad (*)$$

and the process $n[t]$ acts on the aperiodic component with a single
amplification factor and time constant T according to the formula

$$Th + h = n[t]. \qquad (**)$$

In the figure are shown an intermediate signal at the graduated
input, which according to (*) has the impulse character $k\delta[t]$, and

the reaction of the component (**) on the impulse that can be developed in formula (2-38c).

In circuit c of the same figure the components (*) and (**) are represented, which do not have an effect on the properties of the linear circuit. Then after the first component the process has the form of the exponent $1 - e^{-\frac{t}{T}}$, and after differentiation of it with amplification k the transient function of circuit (2-38c) is again obtained.

The examples examined show that the impulses can manifest themselves not only as a result of actual operation of components (2-35) to (2-37), but likewise are sometimes introduced artificial for convenience in calculations (Figure 2-8b). In that case the impulse has ideal properties: infinite height, zero duration and at the same time is not cut off by real limitations existing in the circuit, since in fact it does not originate in the circuit (Figure 2-8c). The introduction of ideal impulses often leads to simplification of the calculations.

The weight function of the real differentiating component is obtained in solution of the equation

$$T\dot{\omega} + \omega = k\delta_2[t]. \qquad (2\text{-}39a)$$

For the first zone in zero from 0 to 0+, from the contracted equation $T\dot{\omega} = k\delta_2[t]$ we get, after integration,

$$\omega'_+[t] = \frac{k}{T}\delta[t]. \qquad (*)$$

In the second zone 0+ to 0++ the solution will be determined already by the internal properties of the component, that is, by a homogeneous equation, obtainable from (2-39a), of the form:

$$T\dot{\omega}_+[t] + \omega_+[t] = 0, \qquad (2\text{-}39b)$$

since the information about the input action is already exhausted.

Here, as in (*), the additional plus signs in brackets mark the shift of the front of the corresponding initial functions in zero. We will substitute (*) in (2-39b)

$$T\dot{\omega}_+[t] + \frac{k}{T}\delta[t] = 0$$

and integrate within the limits of its zone

$$w[0++] = -\frac{k}{T^2}.$$

The results serves as the initial value for the right branch of the weight function, with the character of a diminishing exponent

$$w[t] = -\frac{k}{T^2} e^{-\frac{t}{T}}. \qquad (**)$$

The complete weight function is obtained by summing (*) and (**):

$$w[t] = \frac{k}{T}\left\{\delta[t] - \frac{1}{T} e^{-\frac{t}{T}}\right\}. \qquad (2\text{-}39c)$$

The solution is readily verified by differentiation of the transient function (2-38c) according to rule (2-12a).

2-5. The Principal Properties of Impulse and Weight Functions

4. The Filtering Properties of Impulses

We will integrate both sides of equation (2-10a) within semi-infinite limits:

$$\int_0^\infty \delta[t - \vartheta] x(t)\,dt = x(\vartheta). \qquad (2\text{-}40a)$$

If we differentiate both sides of the obtained equation with respect to ϑ, introducing this operation in the left side under the sign of the integral, where it can be related only to the impulse, and increasing its order with the change in sign, we get:

for a single differentiation

$$-\int_0^\infty \delta_2[t - \vartheta] x(t)\,dt = \dot{x}(\vartheta). \qquad (2\text{-}40b)$$

for multiple differentiation

$$(-1)^k \int_0^\infty \delta_{k+1}[t - \vartheta] x(t)\,dt = x^k(\vartheta). \qquad (2\text{-}40c)$$

Formulas (2-40 a-c) show that by multiplying by the displaced

first-order impulse and subsequent integration it is possible to filter (separate) a single value of the function for the moment of application of the impulse, and by multiplication by a displaced impulse of the $(k + 1)$-th order in the presence of analogous integration the value is filtered off at the point of application of the impulse of the k-th derivative of the function.

Formulas (2-40 a-c) can serve as the basis for explanation of the term "impulse": a first-order impulse is any short-term process that filters the coordinate of the function, and an impulse of the $(k + 1)$th order is any short-term process that filters the k-th derivative function according to the filtration principles (2-40 a-c).

For example, the filtration of an exponentially diminishing function gives

$$\int_{0}^{\infty} e^{-\gamma t} \delta[t - \theta] \, dt = e^{-\gamma \theta}. \qquad (2\text{-}41)$$

5. Superposition of Reduced Weight Functions

If a component has a single ADP on the right side

$$a(t, D) x_{out} = 1 \cdot x_0$$

then its reaction to the impulse input is called a reduced weight function $\sigma_z(t, \theta)$, obtained from the equation

$$a(t, D) \sigma_z(t, \theta) = \delta(t - \theta). \qquad (2\text{-}42a)$$

If a component has a complex ADP on the right side

$$a(t, D) x_{out} = b(t, D) x_0 \qquad (2\text{-}42b)$$

(see figure 2-10), then in the presence of impulse controlling action all the right side is complicated:

$$a_+(t, \theta) = b(t, D) \delta(t - \theta), \qquad (2\text{-}42c)$$

and the reaction of the component is call a complete weight function $\sigma_z^p(t, \theta)$, obtainable from the equation

$$a(t, D) \sigma_z(t, \theta) = a_+(t, \theta). \qquad (2\text{-}42d)$$

If we substitute the ADP $b(t, D)$ in the form of the sum (2-50)

instead of (2-42c), we get

$$n_z(t, \theta) = \sum_{j=0}^{m} b_j(t)\delta^{(j)}(t - \theta) =$$

$$= \sum_{j=0}^{m} (-1)^j \frac{\partial^j}{\partial \theta^j} \{b_j(\theta)\delta(t - \theta)\}. \qquad (*)$$

According to (2-42a) the action $b(\mathcal{G})\delta(t - \mathcal{G})$ forms a reduced weight function with the scale $b(\mathcal{G})$, and consequently the action

$$\frac{\partial}{\partial \theta} \{b_j(\theta)\delta(t - \theta)\}$$

will bring about the reaction

$$\frac{\partial}{\partial \theta} \{b_j(\theta)g_z(t, \theta)\}.$$

The superposition (*) of the partial reactions gives the complete weight function

$$w_z(t, \theta) = \sum_{j=0}^{m} (-1)^j \frac{\partial^j}{\partial \theta^j} \{b_j(\theta)g_z(t, \theta)\}. \qquad (2-43a)$$

This equality can also be written in an abbreviated form:

$$w_z(t, \theta) = \sum_{j=0}^{m} \{(-D_\theta^z - D_z^y)^j \{b_j(\theta)g_z(t, \theta)\}\}. \qquad (2-43b)$$

where

$$D_\theta^z = \frac{\partial_z}{\partial \theta} ; \quad D_z^y = \frac{\partial_k}{\partial \theta}$$

are the symbols of differentiation with respect to displacement, addressed each one to one of the co-factors.

2-6. The Theorem on the Limit of Superposition of Impulses

We will examine an aperiodic component with the weight function $w(t)$ in the form of the real impulse

$$\delta(t - \theta) = \omega e^{-j(t-\theta)}, \qquad (*)$$

we will lead to the input of the component the given action $x(t)_z$.
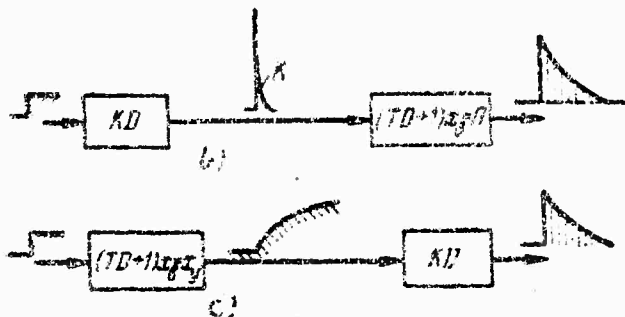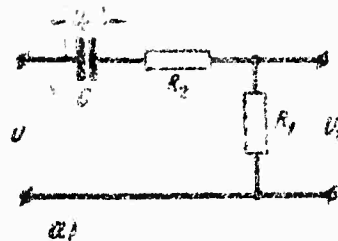
$x_B = x_{out}$; $x_y = x_{in}$

Fig 2-8. Diagram and structure of a real differentiating component.
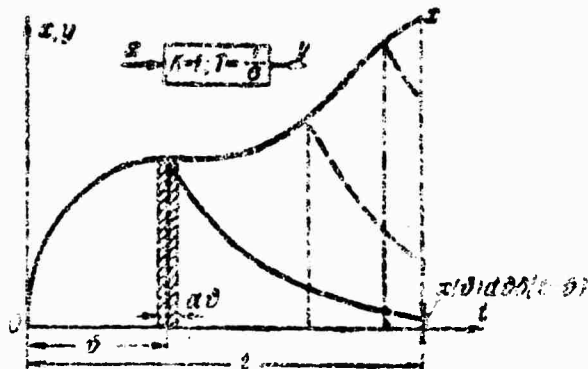
Fig 2-9. The process as a superposition of real impulses.

Knowing the reaction of the component to the impulse t, we can obtain the reaction of the same component to any short-term action. Thus, for example, as is shown in Figure 2-9, an infinitely narrow band with the area $x \cdot x \cdot d \vartheta$ is to be isolated in the given process, the consequence of the term will be determined by its weight function to the scale $x \cdot \vartheta \cdot d \vartheta$. At the moment of time t the reaction of the component of the weight band reaches the value

$$dy = \delta(t - \vartheta) x(\vartheta) d\vartheta$$

-- 110 --

In the figure the elementary reaction (infinitely small in value) is conventionally shown in the scale $\sigma d \vartheta = 1$.

The complete reaction of the component to the complex process $x(t)$ is obtained as superposition of the reactions on the elementary bands:

$$y(t) = \int_0^\infty \delta(t - \vartheta) x(\vartheta) d\vartheta. \qquad (**)$$

We will now direct σ toward infinity. The the aperiodic component becomes an inertialess component (2-31a), but with a single amplification factor. The output of such a component coincides with the input process, and formula (**) assumes the form:

$$x(t) = \int_0^\infty \delta(t - \vartheta) x(\vartheta) d\vartheta. \qquad (2\text{-}44)$$

This formula permits considering the value of the input process at each point $x(t)$ as the limit of superposition of the real impulses $\delta(t - \vartheta)$, conditioned by all the preceding points of the process from $\vartheta = 0$ to $\vartheta = t (0 < t < \infty)$.

Displaced process. In the displaced process $x(t - \vartheta_1)$ at a concrete time segment ϑ_1 the value of the separate points of the process can be determined as before: $x(\vartheta)$, but the orientation of the impulses along the time axis is changed $\delta(t - \vartheta - \vartheta_1)$ and formula (2-44) assumes the form:

$$x_1(t) = \int_0^\infty \delta(t - \vartheta - \vartheta_1) x(\vartheta) d\vartheta. \qquad (2\text{-}45)$$

2-7. The Equation of the Integral Connection. Convolution of the Function.

A. General Case of an Equation with Variable Parameters

The elementary impulse action

$$dx_\eta = \delta(t - \vartheta) x_\eta(\vartheta) d\vartheta, \qquad (*)$$

having excited a component with the weight function

$$\omega(t, \vartheta) = \omega_\eta(t, \vartheta). \qquad (**)$$

brings about an elementary reaction at the moment of time t,

$$d x_{out}(t_1) = w_\tau(t_1, \theta)\, x_{in}(\theta)\, d\theta \qquad (^{***})$$

If now any given input process $x_{in}(t)$ is assumed as a superposition (2-44) of impulses (*), the complete reaction on the output is readily determined as an analogous superposition of elementary reactions $(^{***})$:

$$x_{out}(t_1) = \int_0^\infty w_\tau(t_1, \theta)\, x_{in}(\theta)\, d\theta =$$

$$= \int_0^{t_1} w_\tau(t_1, \theta)\, x_{in}(\theta)\, d\theta. \qquad (2\text{-}46)$$

One of the forms of connection of the output with the input has been obtained on the basis of an integral transformation, and is called the equation of the integral connection. The limits of integration with respect to the argument θ are determined by the working zone 0 to t_1; they are duplicated by the conventional designation of the displaced function. The calculation according to the equation of the integral connection is made for fixed moments of time t_1, t_2... At given analytically simple functions the integrals (2-46) are reduced to tabular; in the presence of complex functions or when any one of them is given by a graph, numerical integration is applied.

If we turn to a geometric representation of the weight function, it is easy to note that in the integral equation of connection the section of the contour used is not along the argument t at θ = constant, but the section perpendicular to it along the argument θ at t_1 = constant. In Figure 2-1c these two mutually perpendicular sections were shown for a cylindrical contour; now for a weight function with variable parameters the contour will not be cylindrical, but the conditions of obtaining the section indicated in Figure 2-10 along the displacement and the conditions of reading the arguments remain the same.

It is possible to express the graph in Figure 2-10 both as a function of the displacement θ and as a function of the argument Θ, which we will call reverse-displacement, since it varies inversely with θ:

$$w_*(t_1, \theta) = w_\tau(t, \theta)\Big|_{\substack{t=t_1 \\ \theta=t_1-\theta}} = w_*(t_1, t_1 - \theta), \qquad (2\text{-}47)$$

where the asterisk subscript designates a new form of notation of the weight function with the variable second argument Θ.

The transition to the new argument, reverse-displacement, can be
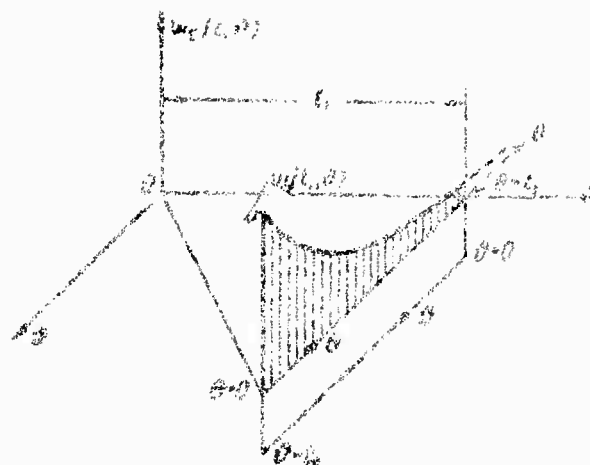
Fig. 2-10. Variation of weight function at fixed time t_1.

... based on the example of the weight function (2-10)

$$w_3(t_1, \theta) = \frac{e^{-2(t_1-\theta)}}{2} \qquad = \left(\frac{1}{2} - e^{-2\theta}\right)$$

If we replace in (2-40) the weight function by the new expression $w_3(t_1, \theta)$, introduce the reverse-displacement argument in the remaining computation

$$x_{in}(\theta) = x_1(t_1 - \theta), \quad d\theta = -d\theta$$

and take into consideration that minus sign of the rearrangement of the ... in integration with respect to θ, we obtain new forms of the ... internal computation:

$$g_o(t_1) = \int_0^{t_1} w_3(t_1, \theta)\, x_{in}(t_1 - \theta)\, d\theta \qquad (2\text{-}48a)$$

$$g_o(t_1) = \int_0^{t_1} w_3(t_1, t_1 - \theta)\, x_{in}(\theta)\, d\theta \qquad (2\text{-}48b)$$

In Figure 2-11a are shown the conditions of the integration ac-
cording to the formula (2-48a), where the disposition of the Ot axis
for the graph x_{in} and $O\Theta$ for the graph w correspond to Figure 2-10,
but the graphs themselves have been expanded onto the common plane
to $\mathcal{Y}$. It can readily be noted that when there is multiplication of
the input functions $w_e(t_1, \Theta)$ and $x_{in}(t_1 - \Theta)$ on the integral (2-48a)
the arguments are calculated from the opposite sides of the interval
0 to t_1, and therefore such equations are called a convolution of the
functions x_{in} and w .

The accumulation of the integral of the convolution is illustrated
by the graph of the function

$$F(\theta) = w_e[(t_1, \theta) x_{in}[(t_1 - \theta),$$

each point of which is obtained in the multiplication of values of the
weight function and input signal that are equidistant from the ends of
the interval 0 to t_1, and its area in the same interval gives the value
of the output process at the point t_1.

We will now consider the case of the representation of a displaced
input process $x_{in}(t - \mathcal{Y})$, the graph of which is shown in Figure 2-11b.
At the same section of the weight function $w_e(t_1, \Theta)$ the accumulation
of the integral of the convolution will occur only within the limits
$0 - \Theta_{in}$, where the upper limit of the integral is connected with the
moment of representation of the input signal by the condition

$$t_{in} = t_1 - \theta_{in}.$$

Since the designation Θ was found to be used for the limit of
integration, we will designate the current value of the reverse-dis-
placement argument along the section of the weight function by the
symbol ξ . Then according to the conditions of convolution the argu-
ment of the input action becomes equal to $\Theta_{in} - \xi$ instead of $t_1 - \Theta$
and instead of (2-48a) we get

$$x_{in}(t_1, \theta_{in}) = \int^{t_{in}} w_e[(t_1, \xi) x_{in}(\theta_{in} - \xi)d\xi. \quad (2-48c)$$

But result written as the function of the two arguments t_1 and Θ_{in}
in difference with the parameter and limit of integration is inter-
preted, first of all, as a description of the accumulation of a certain
mathematical function $x_{in}(t_1, \Theta)$ along the argument Θ at a fixed t_1,
and accordingly, as real values of the output process in the system, ob-
tained at one and the same moment of time t_1 during the action on
the system of single-type processes $x_{in}(t - \mathcal{Y}_{in})$ with different dis-
placements of $\mathcal{Y}_{in}$, that is,
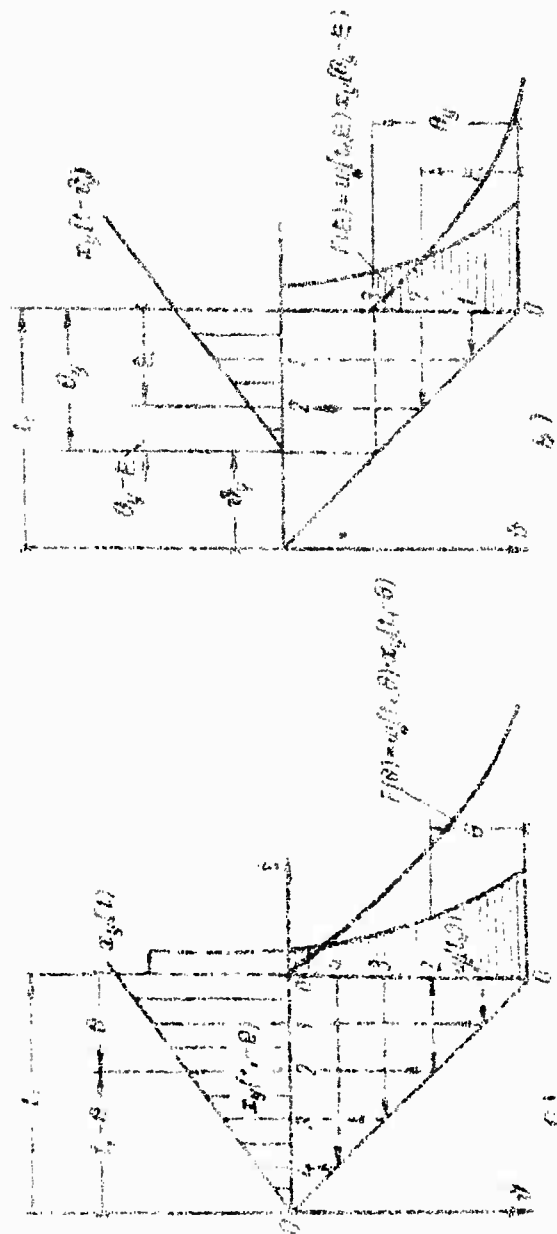
Fig 2.11. Calculation of the output process at the single point t_1 according to the equation of the integral connection by the method of numerical integration.

Key: $X_y = X_{зд}$

$$x_{si}(t_i, \theta_{in}) = x_{si}(t_i, \theta_{ij})\big|_{\theta_{ij}=\cdots=\theta_{in}} =$$

$$= x_{si}(t_i, (t_i - \theta_{in})). \qquad (2\text{-}48\text{d})$$

If the input action is given in the form of a single displaced function

$$x_{ps}(t - \theta_{in}) = 1(t - \theta_{in}),$$

then, if we introduce it into equation (2-48c) in the form of $1(\theta_{in} - \xi)$, we get

$$h(t, \theta_{in}) = \int_0^{\theta_{in}} w(t, \xi) 1(\theta_{in} - \xi) d\xi,$$

or

$$h(t, \theta) = \int^{t-\theta} w_s(t, \xi) d\xi. \qquad (2\text{-}48\text{e})$$

Thus, it is possible to obtain from (2-48c) the transient function (2-48e):

$$\int_0^{t-\theta} \frac{1}{\sigma} e^{-\sigma t} d(\theta) = \frac{1}{\sigma} e^{-\sigma t}\int_{t-\theta} = \frac{1 - e^{-\sigma(t-\theta)}}{\sigma}.$$

B. The Case of an Equation with Constant Parameters

For constant parameters the contour of the weight function is cylindrical. The section along the displacement coincides with the section along time, it does not depend on the second argument and it is obtained from the weight function of a component with the changed argument $t = \theta$ in the interval $0 - \infty$ in the working section $0 - t$:

$$w(\theta) = w(t)\big|_{t=\theta}.$$

In this connection the equation of the integral connection acquires the form:

$$x_{si}(t) = \int_0^t w(\theta) x(t - \theta) d\theta =$$

$$= \int_0^t w(t - \theta)\, x(\theta)\, d\theta. \qquad (2\text{-}49a)$$

For a single undisplaced input we have

$$h(t) = \int_0^t w(\theta)\, 1(t - \theta)\, d\theta = \int_0^t w(\theta)\, d\theta. \quad (2\text{-}49b)$$

Example. Data: a weight function of an aperiodic component

$$w(t) = \frac{1}{T}\, e^{-\frac{t}{T}}$$

and an input process $x_{in} = vt$ (winding with a constant rate). It is required to determine the output process $x_{out}(t)$.

We will ass for the solution formula (2-49a), in which we substitute:

$$w(\theta) = \frac{1}{T}\, e^{-\frac{\theta}{T}};$$

$$x_{in}(t - \theta) = v(t - \theta);$$

then

$$x_{out}(t) = \frac{v}{T}\int_0^t (t - \theta)\, e^{-\frac{\theta}{T}}\, d\theta.$$

In connection with the character of the integrand the output value can be presented in the form of two terms:

$$x_{out} = (x_1 + x_2)\frac{v}{T},$$

where

$$x_1 = \int_0^t te^{-\frac{\theta}{T}}\, d\theta; \quad x_2 = -\int_0^t \theta e^{-\frac{\theta}{T}}\, d\theta.$$

Since in the first integral the integration is made with respect to θ, the value of t can be taken out at the sign of the integral:

$$x_1 = t\int_0^t e^{-\frac{\theta}{T}}\, d\theta = Tt\left(1 - e^{-\frac{t}{T}}\right).$$

The second integral is taken in parts:

$$x_1 = T \int_0^t \hat{v}_0 d\left(e^{-\frac{\vartheta}{T}}\right) = Tv_0 e^{-\frac{t}{T}} - T^2\left(1 - e^{-\frac{t}{T}}\right).$$

And so,

$$x_{\text{out}}(t) = v\left[t - T\left(1 - e^{-\frac{t}{T}}\right)\right] = x_{in} - \epsilon,$$

where

$$\epsilon = vT\left(1 - e^{-\frac{t}{T}}\right),$$

which is illustrated by Figure 2.12.
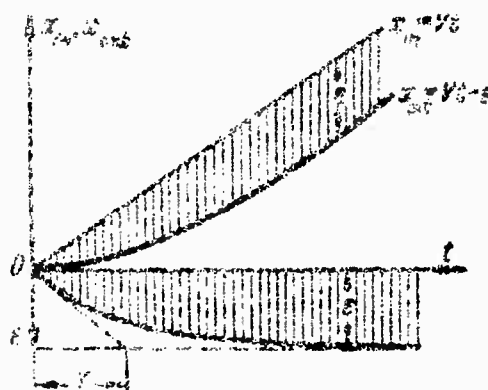
Figure 2.12. Advance of a linearly varying signal through an aperiodic component.

C. Additional Explanations of the Properties of Weight Functions

Terminology. Above, in Section 2-3, weight functions were considered as a special form of reaction of a component to an input impulse and in this connection could be called impulse transient functions. In equations of integral connection these functions already take part in the determination of the reaction of a component to any input signal.

Since in the process of summation (integration) the weight function emerges as a coefficient in each term (impulse), such summation

is called summation with a determined weight for each term (let us

recall that $\sum_{i=1}^{n} \frac{1}{n} x_i$ is called the mean value of x, and the sum

$\sum_{i=1}^{n} \omega_i x_i$ the weighted-mean value of x, if $\sum_{i}^{n} (\omega_i = 1)$.   In ac-

cordance with the role of the function in the equation of the integral
connection it also is called the weight function.

Connection with the Duamel integral. The equation of the inte-
gral connection is a corollary of the Duamel integral, but in its ap-
plication usually in the manuals (e. g., [1] and [2]) under the inte-
gral only the continuous part of the weight functions are introduced,
and the integral from impulse constituents in zero is considered se-
parately in the form of additional terms which reflect the actual in-
itial values of the integral. These conditions are taken into consid-
eration automatically in the complete notation of the weight function.

For example, as the weight function of a real differentiating com-
ponent (k-vha) we determine its transient function

$$ h(t) = \int_0^t \omega(\theta)\, d\theta = \frac{k}{T} \int_0^t \left\{ \delta(\theta) - \frac{1}{T} e^{-\frac{\theta}{T}} \right\} d\theta = $$

$$ = \frac{k}{T}\left(1 + e^{-\frac{\theta}{T}} \Big|_0^t \right) = \frac{k}{T} e^{-\frac{t}{T}}, $$

which agrees with (4-28c).

By the absence of impulse constituents under the integral or at
all limits of these conditions the notations of the equation of the integral
connection and of the Duamel integral coincide.

Parametric weight functions. Weight functions of components with
variable parameters depend on two arguments, the first of which can be
linked with the start of change of the coefficients t or the interval of
time from the moment of application of the impulse τ, and the second,
the displacement ϑ or reverse-displacement Θ. One of the arguments
is fixed and serves as a parameter, and the second remains constant
and with it is accomplished the operation of differentiation or inte-
gration (convolution). The necessary combinations of arguments are
used in different problems, and since in this the weight functions de-

termine one and the same contour w or g, the disposition of the various arguments in them is different, which is marked by the additional indication. In precisely the same way, different designations have been used for the symbol of differentiation with respect to the first and second arguments. A summary of the designations used above, and also to be used in the future, is given in Table 2-1.

2-5. Composition of the Conjugate Differential Equation of Connection

A. Use of Solutions of the Direct Equation of Connection

Questions of the composition of differential equations in the region of time have been considered in Chapter 1. The structural representations obtained according to the differential equations of connection were used for the composition of adjustment circuits of models which solved equations of any complexity, and only very simple equations, for example those given in Section 2-3, are solved analytically. In the latter case the solution of a direct equation containing the arguments t and ϑ can be used to obtain the equation of a section of the contour of a weight function with the plane t, ϑ constant, which enters into the composition of the main body of the equation of integral connection.

To obtain this section of the weight function, a series of direct solutions could also be used for the various moments of application of the input impulses $\delta[t - \vartheta_1]$, $\delta[t - \vartheta_2]$ and $\delta[t - \vartheta_n]$, if a single point $t = t_1$ is selected from each solution (Figure 2-13a). Then in that selection the unchanged parameter will be t_1 and the variable parameter turns out to be ϑ, that is, the points of support of the desired section are determined at the desired values of the argument ϑ or another, Θ, connected with it by the relationship $\Theta = t_1 - \vartheta$.

Graph 2-13b is constructed on the basis of these points of support. If the model is used for the solution, n cut-ins of the model are required at the moments $\tau_0 = \vartheta_1$, $t_0 = \vartheta_2$, $t_0 = \vartheta_n$ with a stop of it each time at the moment $t = t_1$.

B. The Reduced Reversely-Conjugate Equation

To obtain a graph of the desired section of the weight function without recalculation or by a single cut-in of the model, it is necessary to have an equation of connection composed for the new argument, most conveniently of all for the argument Θ of reverse-displacement. In connection with the reversing of the argument, in the future such an equation will be briefly designated the RC equation. The general theory of conjugate equations has been developed in the mathematical literature, for example [3]; its applications have been explained in [4] and [5].
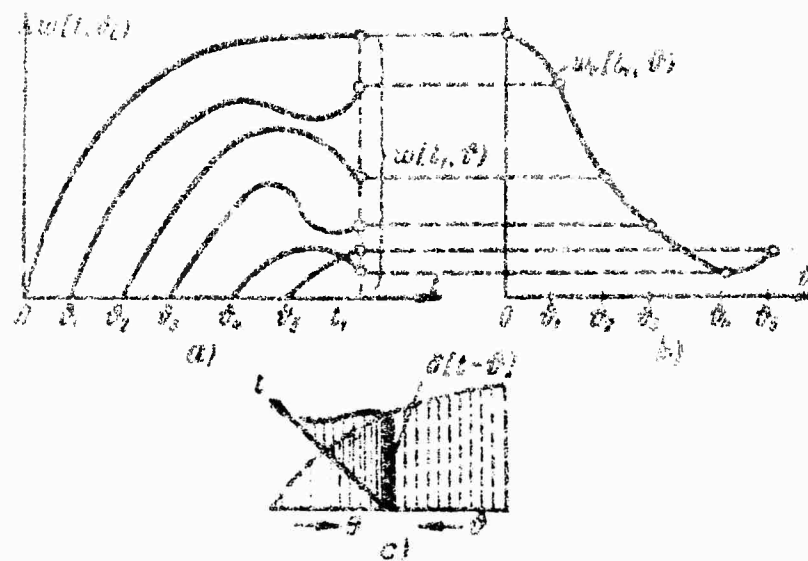
Fig. 2-13.   Illustration of solution of direct and
conjugate equations.

a-Family of curves for direct solutions. b. Selection
of reference points according to argument ϑ .
c-Pulse response common to arguments t and ϑ .

We will show that if the direct equation of the component (system) is reduced to a single ADP on the right side

$$\sum_{i=0}^{n} a_i(t) D^i x_n(t) = x_n(t), \qquad (2\text{-}50a)$$

the RC equations corresponding to it, determining the weight function, has the form:

$$\sum_{i=0}^{n} D^i[a_i(t - \theta) g_i(t, \theta)] = \delta[\theta], \qquad (2\text{-}50b)$$

or in the more compact form of notation:

$$a(D^i, t - \theta) g_i(t, \theta) = \delta[\theta], \qquad (2\text{-}50c)$$

where

$$D^i = \frac{\partial}{\partial \theta}.$$

The transition from the equation of section of the weight function with respect to the argument t to the equation of section with respect to the argument Θ or $\mathcal{Y}$ is explained much more simply if the common point of these two sections, shown in Figure 2-3c, is given in the form of the impulse

$$y[t] = \delta[t - \theta] \qquad (*)$$

and (*) is considered a "process" equally relating both to the section with respect to t and to the section with respect to $\mathcal{Y}$.

If we substitute (*) in (2-50a), we get the input process $x(\xi)$, exciting the impulse on the output:

$$x[t] = \sum_{i=0}^{n} a_i(t) \delta^{(i)}[t - \theta]. \qquad (**)$$

But the input (**) and output (*) processes must satisfy the equation of the integral connection. Here it is convenient to use it in the form of description (2-48b), having replaced, to assure correctness of the following substitutions, the variable of the integration by the arbitrary argument ξ, which does not have an effect on the value of the determined integral and gives as a result:

$$y[t] = \int_0^t g_i(t, t - \xi) x(\xi) d\xi. \qquad (***)$$

We will substitute expression (**) for the input process with the substituted argument, that is,

$$x[\xi] = \sum_{i=0}^{n} a_i(\xi)\delta^{(i)}[\xi - \theta],$$

in formula (***); then with (*) taken into account we get:

$$\delta[t - \theta] = \sum_{i=0}^{n} \int_0^t g_i(t, t - \xi) a_i(\xi) \delta^{(i)}[\xi - \theta] d\xi,$$

On the basis of the filtering properties of the impulse (2-90b), multiplied by the function $\{g_i(t, t - \xi) \cdot a_i(\xi)\} = F(\xi)$, we have:

$$\delta[t - \theta] = \sum_{i=0}^{n} (-1)^i \frac{\partial^i}{\partial\theta^i}\{g_i(t, t - \theta) a_i(\theta)\}.$$

If we substitute $t - \theta = \Theta$, then $a_i(\theta) = a(t - \Theta)$, and finally

$$-\frac{\partial}{\partial\theta} = \frac{\partial}{\partial\Theta} = D^*,$$

we get the RD equation (2-50b) for the section of the weight function along the argument Θ or the more convenient form for calculations:

$$\sum_{i=0}^{n} (D_G^* + D_z^*)^i a_i(t - \theta) g_i(t, \theta) = \delta[\theta]. \quad (2-50b)$$

C. The Total RD Equation and the Structural Representation Corresponding to It

If the direct equation of a component (system) is given in general form (1-4b) then for it the connection between the reduced and total weight functions is given by equation (2-49a).

The RD transformation of the total equation leads to the following system of equations:

$$\sum_{i=0}^{n} D^i\{a_i(t - \theta) g_i(t, \theta)\} = \delta[\theta]; \quad (2-51a)$$

$$w[t, \theta] = \sum_{j=0}^{n} D^{j}\{b_j(t-\theta) g_i[t, \theta]\}. \quad (2\text{-}51b)$$

Equation (2-51a) repeats (2-50b), and equation (2-51b) is obtained from (2-43a) in transition to the argument θ.

In the contracted algebraized form these same equations will assume the form:

$$a(D^*, t-\theta) g_i[t, \theta] = \delta[\theta]; \quad (2\text{-}51c)$$

$$w_i[t, \theta] = b(D^*, t-\theta) g_i[t, \theta]. \quad (2\text{-}51d)$$

It is readily noted that in the conjugate systems, both in the notation of a and b in the form of the sums and in the notation of a and b in the form of the convoluted ADP's, the sequence of the operations is changed in comparison with the direct systems, that is: in the RC systems at the beginning the multiplication is done with the variable coefficients, and then the differentiation of the products according to the argument θ; in addition, in the coefficients the argument is reversed, since after the substitution of $\mathscr{S} = t - \theta$ the decrease in the common argument $\mathscr{S}$, which enters into the coefficients, corresponds to the increment θ.

The structural representation of the RC system is constructed according to equations (2-51 c and b). For this, we find from equation (c) the conventional solution with respect to the higher derivative of the two co-factors:

$$D^{*n}\{a_n(t-\theta) g_i[t, \theta]\} =$$

$$= \delta[\theta] - \sum_{j=0}^{n-1} D^{*j}\{a_j(t-\theta) g_i[t, \theta]\},$$

and then, integrating n times all the terms on the right side, we find the conventional solution with respect to the reduced weight function:

$$g_i[t, \theta] = \frac{1}{a_n(t-\theta)} \left\{ \frac{1}{D^{*n}} \delta[\theta] - \right.$$

$$-\sum_{i=0}^{n-1} \frac{1}{D^{n-i}} \left| a_i(t-\theta) \, g_i(t,\theta) \right| \right\}. \qquad (2\text{-}52)$$

The right side of the structural representation in Figure 2-14a was constructed according to the obtained formula. The left side of the structural representation is constructed directly according to formula (2-51b), that is, the reduced weight function obtained is multiplied by the variable coefficients, and then the products are differentiated the necessary number of times.

If we compare Figure 2-14a with Figure 1-2, we can formulate the simple rule established in [4] for obtaining the RC structural representation according to the direct structure of the system. For this, the following are necessary in the detailed direct system: interchanging the places of the input and output; changing into the reverse direction the signals in all the lines of the direct path and supplementary connections; replacing the summators with nodes and the nodes with summators; considering the argument in the solution, giving the disturbance to the new input in the form of an impulse along the argument θ, and beginning to change the variable coefficients from their values at the moment t_1, that is, $a_i(t_1)$, on the side of decrease of the common argument $t_1 - \theta$ with increase of θ.

Adjustment of the circuit of the electronic model is done according to the structural representation of Figure 2-14. Before start-up of the model all the blocks of variable coefficients are established according to their values at that moment of time for which the section of contour of the weight function along the argument θ is sought, and further the direction of rotation of the blocks is reversed into the side of decrease in the arguments. The conditions of adjustment of the blocks of variable coefficients are shown in diagram 2-14b.

The solution on the output of the model is taken oscillographically in the form of the graph $w_x(t,\theta)$. The machine time plays the role of a variable argument which depicts the argument θ on a 1:1 scale.

Upon starting of the model, the input impulse, as in the model of the direct system, examined in Chapter 1, is replaced by a single initial condition on the output of the first integrator from the right. Supplementary transformations of the structural form to eliminate the differentiating blocks which are unsuitable for modeling are discussed in Chapter 5.

Fig 2-14. Structural representation of a RC system and the rule of reverse of the argument of the block of variable coefficients in the circuit of the model of the RC system.

2-9. Aftereffect in Linear Systems at Input Excitations Limited in Time

1. Reaction at the Interval of Action of the Input Process

If the input process (excitation) is a limited interval of time T, as shown in Figure 2-15, then by virtue of the limited working zone of the change of the argument from the left and from the right

$$x_{in}[t]_T = 0 \quad \text{at} \quad 0 < t < T \qquad (*)$$

the input function $x_{in}[t]_T$ has fronts on the left $t = 0$ and on the right $t = T$, which is marked by the two brackets in the designation of this function.

The reaction at the interval of action of excitation $x_{in}[t]_T$ is determined according to the general equations of the integral connection (2-49c) for variables and (2-49a) for constant parameters:

$$x_{out}[t] = \int_0^t w_v[t, \ t - \theta) \, x[\theta]_T \, d\theta; \qquad (2\text{-}53a)$$

$$x_{out}[t] = \int_0^t w[t - \theta) \, x[\theta]_T \, d\theta. \qquad (2\text{-}53b)$$

Here, since $\alpha \leqslant 1$, the limitation of $x(\theta)$ on the right does not manifest itself and happen.

b. The equation of Integral Connection for the regime
of the Aftereffect

If we extend formulas (2-53) for the region $t > 1$, we get:

$$y(t) = \int_0^T w_0(t, t-\theta) x(\theta) d\theta; \qquad (2\text{-}54a)$$

$$y(t) = \int_0^T w(t-\theta) x(\theta) d\theta. \qquad (2\text{-}54b)$$

The integration is done independently of the value of within the limits $0 - 1$, and therefore the limits of the graph $x(\theta)$ cannot be fixed in formulas (2-54).

It is evident from picture 2-13 that during the calculation of the values of $x(t_1, y(t_1))$, etc., according to the plan examined previously in figure 2-12, graph $x(\theta)$ will be accurately drawn and will permit operations for any sought value of t, and the graph of the weight function in this interval will be given by the constants in the range of weight, embodied in form of sections from $w(t, t-T)$ to $w(t, t)$.

If the weight function $w(t-\theta)$ is expanded in the series

$$w(t-\theta) = w(t) - \dot{w}(t)\theta + \ddot{w}(t)\frac{\theta^2}{2!} + \ldots,$$

then the integral can be transformed:

$$y(t) = w(t)\int_0^T x(\theta) d\theta - \dot{w}(t)\int_0^T \theta x(\theta) d\theta +$$

$$+ \frac{\ddot{w}(t)}{2!}\int_0^T \theta^2 x(\theta) d\theta - \ldots \qquad (2\text{-}55a)$$

To estimate the integrals entering the formula we have to, given w, independently estimate the sum of the area
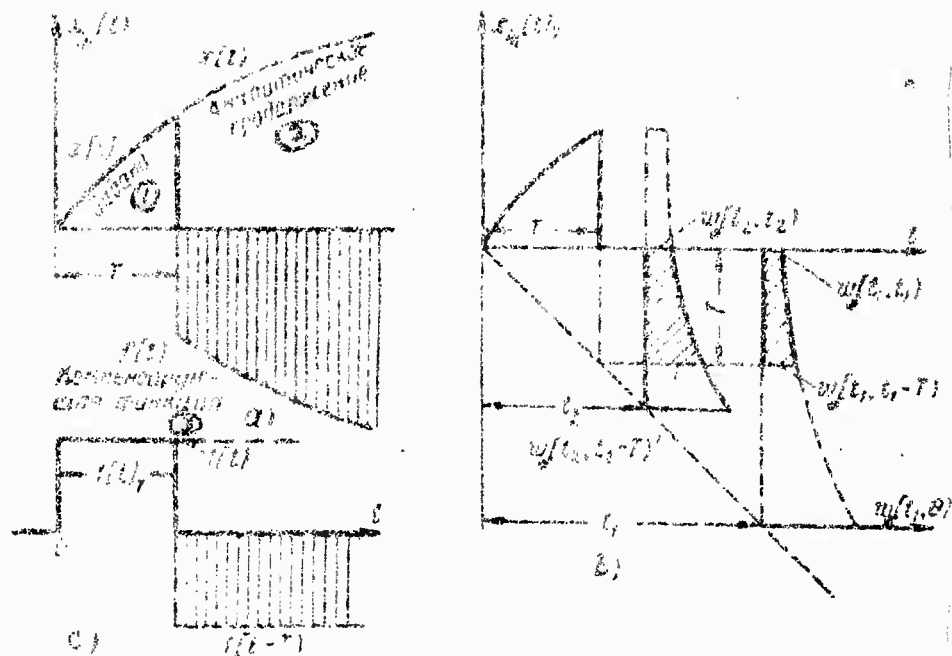
Fig. 8-15. Input process, given for a limited interval.
a — general form; b — for calculation of the output reaction;
c — graduated form; 1 — Given; 2 — Analytical continuation;
3 — Compensating function.

$$M_0^T = \int_0^T x[\theta]\, d\theta = x_0^{cp}\, T;$$

$$M_1^T = \int_0^T \theta\, x[\theta]\, d\theta = \frac{x_1^{cp} T^2}{2!} \dots ; \qquad (^*)$$

$$M_i^T = \int_0^T \theta^i x[\theta]\, d\theta = \frac{x_i^{cp} T^{i+1}}{(i+1)!}$$

$$x_{\text{sr}}(t) = M_0^T \, x(t) - M_1^T \, x'(t) + \frac{M_2^T \, x''(t)}{2!} + \dots \quad (2\text{-}55b)$$

For small intervals T of the action of excitation the following approximation of the formula of the aftereffect is valid

$$x_{\text{sr}}(t) = M_0^T \, x(t), \quad (2\text{-}55c)$$

that is, the reaction to the short impulse approaches the reaction of an ideal impulse of the same area M_0^T. The error of the approximated formula always can be estimated from the discarded terms of expression (2-55b).

Formulas (2-55a) to (2-55c) can also be used for system with variable parameters during expansion of the weight function which enters formula (2-55a) into a series according to the second argument.

C. Method of Expansion of a Limited Input Action into the Sum of Functions Unlimited in Time

The region of the aftereffect can always be considered as the result of superposition of two unlimited and displaced in time actions

$$x(t) \quad \text{and} \quad f(t - T) = f(t).$$

The function $f(T)$ is so selected that at $t > T$ the sum of $x(t)$ and $f(t - T)$ will be identically equal to zero.

$$x(t) + f(t - T) = 0, \quad (*)$$

and this is called a compensating function.

We will present the expression for the compensating function in the form of a series

$$f(t) = -\sum_{i=0}^{n} \frac{x^{(i)}(T) \, t^i}{i!}, \quad (2\text{-}56)$$

to the two input functions $x(t)$ and $f(T)$ correspond the two reactions y_x and y_f, which are determinable by the equations of the integral correction, and their superposition gives the overall output process

$$y = y_x + y_f$$

— 124 —

both in the case $T = T$, where only the first term participates, and in the case of the aftereffect. For the most simple short-term action,

$$x(t) = 1(t) - 1(t - T) = 1(t),$$

shown in the graph of Figure 2-4bc and satisfying condition (*), the process of the output of the system is determined that:

$$y(t) = h(t, 0) - h(t - T, T).$$

If we proceed for the period of the aftereffect to a new reading of the time, we get:

$$y_n(t) = h(t + T, 0) - h(t, T).$$

5. Differential Equation for the Region of Aftereffect

In the majority of cases, in calculation, the aftereffects are abstracted from the conditions of the representation and type of the input action in the previous history, by examining the characteristic motion of the system of equations at the arbitrary values of the output coordinates and its n-1 derivatives at the moment of the time for $t = 0$ for $x(t) = T$, $y^{(i)}(0) = y_0^{(i)}$, $i = 0, 1, 2, \dots, (n - 1)$,

and the equation of connection of type (2-1) becomes homogeneous:

$$\sum_{i=0}^{n} a_i(t) y^{(i)}(t) = 0 \qquad (2-57a)$$

In solving of this equation this solution is understood, that is, the initial motion of the system in the aftereffect without any input action in the period $t \le 0$, as shown in Figure 2-4cd by the solid curve.

With the initial at $y^{(i)}(t)$ are values of the aftereffect the initial state of physical origin.

By the these derivatives at $t \le 0$ at t in equation (2-57a)

$$y_n(T + y_n^{(i)}(0) + \dots = y_n^{(i)}(T - t) \qquad (2-57b)$$

the initial value of the reaction to such process in the region of physical motion for Figure 2-4cd, we determine $t = 0$.
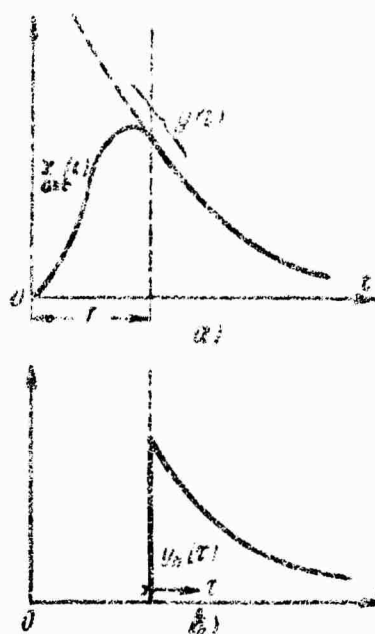
Fig 2-16. Reaction at the interval of action of $x_{out}(t)$, aftereffect $y_f(t)$ and the two-sided analytically continued process $y(t)$.

For the higher derivatives at $n - m \leqslant k \leqslant n - 1$

$$y_n^{(k)}(0+) = x_{out}^{(k)}(T-) - y_f^{(k)}(0), \quad (2\text{-}57c)$$

that is, of the derivatives of the end section of the regime of action, it is necessary to subtract the initial derivatives of the reaction from the compensating function. Information on n initial conditions is sufficient to solve equation (2-57a) on the electronic model.

E. Equivalent Impulse Action for the Formation of the Regime of the Aftereffect as an Initial Process

We will aim at composing, according to equation (2-57a) an equation for the initial functions which gives a solution that coincides with the right half-branch ($t > T$) of the solution of (2-57a). For this, we will form for the output value a dependence analogous to (2-12c), having assumed $\mathscr{S} = T$ and having solved (2-12c) with respect to the derivative of the two-sided function

$$y^{(i)}(t) = y_n^{(i)}(t - T) - \sum_{j=0}^{i-1} y^{(j)}(T) \delta_{i-j}(t - T) \quad (2\text{-}58)$$

we will eliminate the terms obtained in expression (2-58) and transfer the known terms to the right side:

$$\sum_{i=0}^{n} a_i(t) q_{ij}^{(i)}(t-T) = \sum_{i=0}^{n} a_i(t) \sum_{j=0}^{n-1} g^{(j)}(T) \delta_{i-j}(t-T).$$

We will proceed to the algebraized form of notation, transforming the right side according to Formula (2-49):

$$a(t, D) g_1(t-T) =$$

$$= \sum_{i=0}^{n} \sum_{j=0}^{n-1} g^{(j)}(T)(D-D_0^x)^{i-j-1} a_i(T) \delta(t-T).$$

$$(2-59)$$

where $D = \dfrac{d}{dt}$ is the symbol of differentiation with respect to time;

$D_0^x = \dfrac{d}{dx}$ is the symbol of differentiation with respect to the displacement $\left(\dfrac{d}{dx} = \right)$, addressed only to the variable coefficients $a_i(T)$.

Then, the right side of (2-59) is conveniently subdivided into terms, the order of the impulses entering it, by which the exponents at the binomials in powers of D, when ordered:

$$a(t, D) g_0(t-T) = A_0(T) \delta(t-T) +$$

$$+ A_1(T) \delta(t-T) + \ldots + A_n(T) \delta^{n-1}(t-T).$$

$$(2-60a)$$

$$A_0(T) = \sum_{j=0}^{n-1} g^{(j)}(T) \sum_{i=1}^{n} (-D_0^x)^{i-j-1} a_i(T) \Bigg|$$

$$A_1(T) = \sum_{j=0}^{n-1} g^{(j)}(T) \sum_{i=1}^{n} (i-j-1) \times$$

$$\times (-D_0^x)^{i-j-2} a_i(T). \Bigg|$$

$$\ldots \ldots \ldots \ldots \ldots \ldots \Bigg| \quad (2-60b)$$

$$A_{n-1}(T) = \sum_{j=0}^{n-1} y^{(j)}(T) \sum_{i=1}^{n} \times$$

$$\times \frac{(i-j-1)(i-j-2)\ldots(i-j-n+1)}{(n-1)!} \times$$

$$\times (-D_j^\tau)^{i-j-n} a_i(T).$$

We will explain the rules for obtaining the sums entering into (2-60h) on the example of a component of the second order (n = 2).

In Figure 2-17a are illustrated the conditions for obtaining the double sum which forms the coefficients A_0 and A_1.

In this case there are two groups of terms with respect to the order j: for j = 0 and for j = 1.

Summation with respect to the index i gives in each group the same two terms each, but from them only those are considered for which $i - j - 1 \geq 0$, which gives:

$$A_0(T) = y(T)[a_1(T) - \dot{a}_2(T)] + \dot{y}(T) a_2(T).$$

For $A_1(T)$, analogously, only that term for which $i - j - 2 \geq 0$, that is, $i = 2$, $j = 0$, $i - j - 2 = 0$, is considered:

$$A_1(T) = y(T) a_2(T).$$

Finally we have:

$$a(t, D) y_n[t - T] = \{y(T)[a_1(T) - \dot{a}_2(T)] +$$

$$+ \dot{y}(T) a_2(T)\} \delta[t - T] + y(T) a_2(T) \delta_1(t - T).$$

For the case of the constant coefficients in formula (2-60a) it is necessary to discard all the derivatives of the coefficients $a^{(i)}(T)$ and proceed to the argument τ:

$$a(D) y_n[\tau] = \sum_{i=1}^{n} \sum_{j=0}^{n-1} y^{(j)}(T) a_i \delta_{i-j}[\tau] =$$

$$= \delta[\tau]\sum_{j=0}^{n-1} y^{(j)}(T)a_{j+1} + \delta[\tau]\sum_{j=1}^{n-2} y^{(j)}(T)a_{j+2} + \ldots +$$
$$+ \delta^{(n-1)}[\tau]y(T)a_n. \qquad (2\text{-}60\text{c})$$

For a second order component with constant coefficients the equation of aftereffect assumes the form:

$$(a_2 D^2 + a_1 D + a_0)y_n[\tau] =$$
$$= [y(T)a_1 + \dot{y}(T)a_2 + y(T)a_2 D]\delta[\tau]. \qquad (*)$$

If a component in which residues of the regime of aftereffect have not yet been eliminated receives at the moment of time $t + T$ a new prolonged excitation, the regimes of action and aftereffect are superimposed and the general equation of connection assumes the form.

$$a(t, D)y = b(t, D)x + A(T, D)\delta[\tau]. \qquad (2\text{-}61\text{a})$$

where

$$A(T, D) = A_0(T) + A_1(T)D + A_2(T)D^2 + \ldots \qquad (2\text{-}61\text{b})$$

in accordance with formulas (2-60b) for variable coefficients and with the right side of formula (2-60c) for constant coefficients.

In Figure 2-47b a structural explanation is given of the case of complex action upon the component; for this we separate equation (2-61) into two equations:

$$b(t, D)x[t] + A(T, D)\delta[\tau] = \Pi[t]; \qquad (2\text{-}62\text{a})$$
$$a(t, D)y[t] = \Pi[t]. \qquad (2\text{-}62\text{b})$$

The actions $x[t]$ and $\delta[\tau]$ are subject to the operations described symbolically in the form of the variable and constant ADP's according to (2-62a), and equation (2-62b) is solved afterwards in the presence of a complex right side.
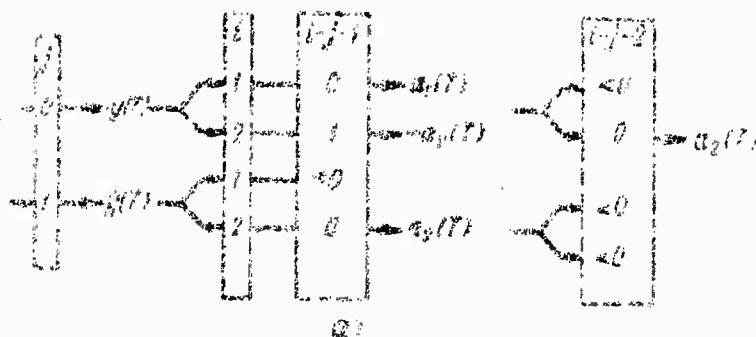
Fig 2-17. For calculation of the regime of aftereffect.
a - rule of calculation of the coefficients of the ADF
A(T, D); b - superposition of the regimes of action and
countereffect.

2. The Regime of Aftereffect as a Linear Form of the Reduced
Weight Function of a Component

We will start from the equation of the regime of aftereffect of
the type,

$$a(t, D)g(t) = A(T, D)\tilde{a}(t) \qquad (2\text{-}63a)$$

and an unknown reduced weight function of the component in the case
of variable coefficients $g_i(t, T)$ and in the case of constant coeffi-
cients $g_i(T)$. Then the solution of (2-63a) relative to y can be
written for the variable coefficients as

$$y(t, T) = \sum_{j=0}^{n-1} A_j(T)(-1)^j \frac{d^j}{dT^j} g_i(t, T) \qquad (2\text{-}63b)$$

and for the constant coefficients as

$$\eta[\tau] = \sum_{j=0}^{n-1} A_j(T) g^{(j)}[\tau]. \qquad (2\text{-}68c)$$

.. Explanation of the Term "Equation of Connection"

All the equations examined above have connected the input act-
ions with the reaction to a given action. Since the reaction to a
given action cannot arise before the application of the action, then
automatically all the conditions in a solution before the supplying
of the action (zero to the left $0-$) are zero conditions. After
the supplying of the action (zero to the right $0+$) the initial val-
ues in the reaction always are not zero values (with respect to the
coordinate or its derivative), but they already enter the solution.
For a delaying component these same considerations relate to the
point $\tau_{delay}+$ and $\tau_{delay}-$. The initial conditions of the regime

of aftereffect $(0-)$ are considered not the "equation of connection
but the equation of aftereffect (2-59), but it also is convenient in
a number of cases to substitute the equivalent equation of connec-
tion (2-68a), which establishes the connection of the reaction $y[\tau]$
with the action $\delta[\tau]$ anew at zero $(0-)$ initial conditions.

2-10. The Composition of a Linear Differential Equation for
the Quadratic Evaluation of the Process

In a number of problems a study is made, not of the process
itself, but of its quadratic evaluation. Thus, for example, if in
a component with an output process in the form of a value of cur-
rent it is necessary to study the power dispersed for heating, the
quadratic evaluation of the process gives the value of the dispersed
power arriving per ohm of resistance. Quadratic evaluations of out-
put processes, which characterize the error of a component or system
(see Figure 2-12), usually more fully take into consideration the
weight of the error or its influence on the efficiency of the control
motion.

We will examine two methods of obtaining a quadratic evaluation:

On the basis of a circuit with a nonlinear element, and

On the basis of creating a linear equation of a special form.

A diagram with a nonlinear element is given in Figure 2-18a for
the case of quadratic evaluation of the solution of equation (2-16a)
upon insertion on the right side of a normalized variable coefficient

$$x[\tau] - a_0^k(s + b)x[\tau] = b_0^k(t + b)x_y[\tau] \qquad (2\text{-}64a)$$

and a given input action in the form of a single displaced impulse $x_{in} = \delta[\tau']$.
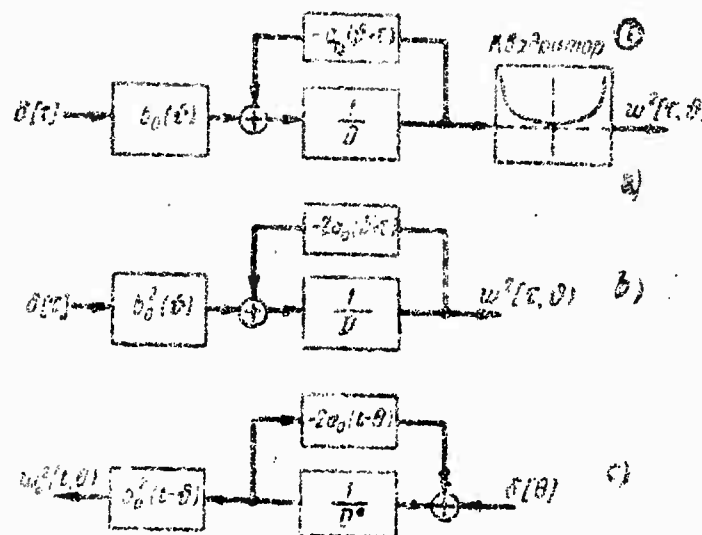
Fig 2-18. Structural forms for obtaining a quadratic evaluation of the weight function of a first-order component with variable parameters. a - diagram with a nonlinear element; b - direct linear diagram; c - linear RC diagram. 1 - Quadrator.

For such a right side the connection between the reduced and complete weight functions is very simple:

$$w[\tau, \vartheta] = b_0^q(\vartheta) g[\tau, \vartheta]. \qquad (2\text{-}64 b)$$

The left side of Figure 2-18a was constructed according to the principles of structural representation, and a supplementary element was inserted in the right side -- a quadrator, the static characteristic of which, shown in the figure within the element, provides the raising of the weight function obtained for the output circuit to the square.

To construct the circuit without a nonlinear element it is ne-

cessary to compose a linear differential equation with respect to the new function — the quadratic evaluation $x^2(\tau)$. We will prepare some correlation from (2-65a) and divide this formula for the derivative of the quadratic evaluation:

$$x[\tau] = x(t) 1[\tau], \qquad (2\text{-}65a)$$

$$\dot{x}[\tau] = \dot{x}(\tau) 1[\tau] + x(0)\delta[\tau]; \qquad (2\text{-}65b)$$

$$x(\tau)\dot{x}[\tau] = x(\tau)\dot{x}(\tau) 1[\tau] + x^2(0)\delta[\tau]; \qquad (2\text{-}65c)$$

$$Dx^2[\tau] = [x^2[\tau]] = 2x(\tau)\dot{x}(\tau) 1(\tau) + x^2(0)\delta[\tau]. \qquad (2\text{-}65d)$$

If we substitute formulas (2-65a) and (2-65d) we will ascertain:

$$[x^2[\tau]] = 2x[\tau]\dot{x}[\tau] - x^2(0)\delta[\tau]. \qquad (2\text{-}65e)$$

Thus, for the initial function the derivative of the quadratic evaluation contains not only the doubled product of the function and its derivative (which more exhaustively characterizes the derivative of the square of a two-sided function), but also the initial impulse with the area $-x^2(0)$ with the negative sign.

We will replace in the obtained formula the first derivative of the output value by its value from formula (2-64a):

$$\dot{x}[\tau] + b_0^2(\tau + \theta)x_0[\tau] - a_0^2(\tau + \theta)x[\tau]. \qquad (2\text{-}66a)$$

then we will arrive at the relationship

$$[x^2[\tau]] + 2a_0^2(\tau + \theta)[x^2[\tau]] =$$

$$= 2b_0^2(\tau + \theta)x_0[\tau]x[\tau] - x^2(0)\delta[\tau]. \qquad (2\text{-}66b)$$

Furthermore, we will proceed from the obtained general formula to the partial case where the component is excited by an impulse and the quadratic evaluation is done for the weight function of the component $w^2[\tau, \theta]$, that is

$$[w^2[\tau, \theta]] + 2a_0^2(\tau + \theta)[w^2[\tau, \theta]] =$$

$$= [2b_0^2(\theta)w[0, \theta] - w^2(0, \theta)]\delta[\tau]. \qquad (2\text{-}67a)$$

or, according to (2-64b)

$$[\omega^3[\tau, \theta)] + 2\alpha_3^8(\tau + \theta)[\omega^2[\tau, \theta)] =$$

$$= \delta_s^2(\theta) g[0, \theta)[2 - g[0, \theta)]\delta[\tau]. \quad (2\text{-}67b)$$

If we also take into consideration that $g(0, \theta) = 1$ in the solution (2-64a), we finally arrive at the linear differential equation with respect to the quadratic evaluation of the weight function:

$$[\omega^3[\tau, \theta)] + 2\alpha_3^8(\tau + \theta)[\omega^2[\tau, \theta)] =$$

$$= \delta_s^2(\theta)\delta[\tau]. \quad (2\text{-}67c)$$

A structural representation has been constructed in Figure 2-19b on the basis of this equation. It can serve as the basis for the adjustment circuit of an electronic model which will contain only linear elements, but will give a solution analogous to Figure 2-19b with a nonlinear element in the presence of pulse input action. It is possible to convince oneself of this also by comparing the analytical solution of equation (2-67c) with the square of the analytical solution of equation (2-64a). For the first-order equation both solutions are obtained rather simply according to formula (2-65b); for equations of higher orders the analytical transformations are more complicated and will be considered in succeeding chapters with further developed mathematical apparatus drawn in.

In conclusion we will formulate for the quadratic evaluation of the weight function the PE equation:

$$\begin{rcases} D^2 g_s^2(\tau, \theta) + 2\alpha_3^8(\tau - \theta) g_s^2(\tau, \theta) = \delta(\theta), \\ \omega_s^2(\tau, \theta) = \delta_s^2(\tau - \theta) g_s(\tau, \theta). \end{rcases} \quad (2\text{-}68)$$

This corresponds to the structural representation in Figure 2-19c. The solution of the PE equation gives a quadratic evaluation of the section of the weight function along the argument θ, that is, the value of the squares of the reaction of the component at the moment of time τ to impulses given in any of the moments of time from θ_{13} to θ_{1n}, at direct substitution of $\theta = \tau - \theta_{1n}$.

Bibliography

1. Krug, K.A. Perekhodnyye protsessy v elektricheskikh tsepyakh
    (Transient Processes in Electrical Circuits), Gosenergoisdat, 1940.
2. Lur'ye, A.I. Operatsionnoye ischisleniye i yego prilozheniye k
    zadacham mekhaniki (Operational Calculus and Its Application to
    Problems of Mechanics), Gostekhizdat, 1950.
3. Stepanov, V.V. Kurs differentsial'nykh uravneniy (Course in Dif-
    ferential Equations), GITTL, 1950.
4. Lanning, J Kh and Bettin, R G, The Use of Analog Computers for
    Statistical Analysis of Systems Variable in Time, Trans. IRE on
    Circuit Theory, March, 1955; issued in translation, Ref. 7 of the
    Introduction; also in: Project Cyclone. Symposium II on Simulation
    and Computing Techniques, Reeves Instrument Corp., N.Y., May 1952.
5. Solodov, A V, Statistical investigation of nonstationary processes
    in linear systems with variable parameters, Avtomatika i telemekha-
    nika (Automation and Telemechanics), 1958, No 4.

Chapter 3

OPERATOR METHODS OF ANALYSIS

OF PROCESSES IN CONTROL SYSTEMS

WITH VARIABLE AND CONSTANT PARAMETERS

pp. 157-187

3.1. Laplace Transform for Processes Displaced and
Compressed in Time

A. The Mathematical L-Component

In the examination of elementary components it was made clear
that the calculation of the process at the output of a component is
readily feasible only in the presence of very simple input laws, and
in the presence of complication of those laws, and especially when a
group of components is joined into a single system, the solution of
differential equations by classical methods becomes extremely tedious.

The question of the simplification of the method of solution of
differential equations by the introduction of symbolic designations
characteristic of operational calculus was first raised by the Russian
scholar M. Ye. Vashchenko-Zakharchenko. In a monograph published by him
at Kiev in 1862, entitled "Symbolic calculus and its application to the
integration of linear differential equations" the basic problems of
modern operational calculus were raised and solved.

In order to obtain a clearer idea of the place of the apparatus
of operational calculus in the theory of control, and of its useful
role in calculations, we will use an algebraic analogy.

Let, for example, the formula $\beta = \alpha^n$ be used for the calculation
of a sought number β according to a given number α. If the exponent
n is zero or is a fractional number, the calculations according to

accomplished, as a rule, by the following processes:

1) Conversion from the value of the output quantities (representation) in α;

2) Transformation of the logarithm (representation) in accordance with the given formula. In the given case — multiplication of the logarithm by the exponent, which gives the logarithm of the output number — the answer is $\log \beta = n \log \alpha$;

3) Conversion from the logarithm of the output number to the original — the number itself (potentiation) $\beta = \log^{-1}\{n \log \alpha\} = \alpha^n$.

All the operations enumerated are illustrated in Figure 5-12.

The apparatus of operational calculus plays the same useful role as the apparatus of taking the logarithm, in permitting transfer from the input process $x_{in}(t)$, which is a certain given function of time from the beginning of the transformation, and then transformation of that representation in accordance with the transfer properties of the component or combination of components that make up the control system, in order to obtain the representation of the output process and, finally, returning again to the original, that is, to the actual output process in the function of time $x_{out}(t)$. The sequence of the operations in this case is illustrated by Figure 5-12. The symbols and $^{-1}$ designate the direct and reverse transformations which transfer the process from the region of the originals (function of time) into the region of the representations and the reverse.

The majority of cases that arise in the theory of automatic control are adequately well solved using the use of Laplace transitions X and their reverse, determinable by the formulas of direct (5-1a) or reverse (5-1b) transformations:

$$X(p) = \int_0^\infty e^{-pt} x(t) dt, \qquad (5\text{-}1a)$$

$$x(t) = \frac{1}{2\pi i} \int_{\sigma-i\infty}^{\sigma+i\infty} e^{pt} X(p) dp \qquad (5\text{-}1b)$$

In both formulas p is the complex number:

$$p = s + j\omega, \qquad (5\text{-}1c)$$

of which a substantial part is positive and provides convergence of the integrand (5-1a):

In that case, as it is not difficult to see, after completion of the operation of integration (3-1a) the variable t disappears and the result will depend only on p, which gives one the right to call the function X(p) a representation of the function x(t). For the original and for the representation of one and the same function we will use identical alphabetical designations, but for the time processes we will use small letters and for the representations capital letters.

The coincidence of the designations must not be considered erroneously as coincidence of the character of the functions describing the original and the representation. The only thing common to these functions is that they reflect one and the same process. This connection is designated

$$X(p) = L\{x(t)\}; \quad x(t) = L^{-1}\{X(p)\} \quad (3\text{-}2a)$$

or

$$X(p) \doteq x(t); \quad x(t) \doteq X(p). \quad (3\text{-}2b)$$

In all the formulas of the relation between the original and the representation, the arrow is directed toward the original.

Since the transition from the original to the representation is connected with operations of integration (3-1a), the series of functions which in the region of time have discontinuities become continuous functions in the region of the argument p.

We will consider, for example, the representation of the impulse $\delta(t - \vartheta)$. If we apply to the impulse transformation (3-1a) and note that the filtering properties of the impulse (2-41) are completely applicable to the function e^{-pt}, we get at once the relation (3-3a) for $\vartheta > 0$ and (3-3b) for $\vartheta = 0$.

$$\delta(t - \vartheta) \doteq e^{-p\vartheta}, \quad (3\text{-}3a)$$

$$\delta(t) \doteq 1. \quad (3\text{-}3b)$$

Suppression of discontinuities of the functions is a great merit of the operator method for the transformation of functions. A still greater merit is simplification of the mathematical operations on the functions, which will be examined in the following section.

It is convenient to consider a direct Laplace transformation as a result of the passage of the process (signal) through the L-component (Figure 3-1b). The reaction of that component to the single displaced impulse is known (3-3a), and since any process on the basis of

formula (2-44) is assumed to be a superposition of displaced impulses with the scales $x(\vartheta)d\vartheta$, it is easy to write the reaction also on the input process $x(t)$:

$$L\{x(t)\} = \int_0^\infty e^{-p\vartheta} x(\vartheta)\, d\vartheta. \qquad (3\text{-}3c)$$

In the obtained formula the superposition (2-44) is repeated for representations of the impulse on the basis of the linearity of the Laplace transform.

Formula (3-3c) does not give a new result in comparison with the basic formula of direct transformation (3-1a), since the determined integral does not depend on the variable integration, but permits understanding the representation of the process as a superposition of the representations of the displaced impulses $e^{-p\vartheta}$ and describes the basic properties of the mathematical L-component in the region of the argument p. In the region of the argument ϑ, on the basis of formula (3-3c), the role of the L-component is reduced to obtaining the signal, a weighted-mean for semi-infinite limits, with the weight function $e^{-p\vartheta}$.
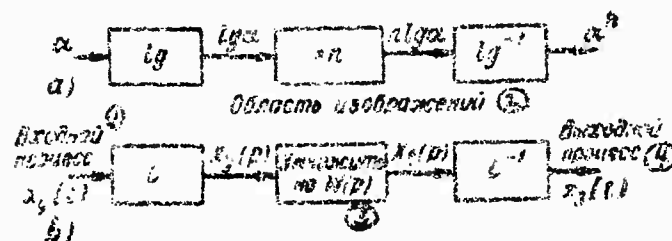
Fig 3-1. Explanation of the principle of transition to representations. 1 - Input process; 2 - Region of representations; 3 - Multiply by W(p); 4 - Output process.

$$x_1 = x_{out}; \quad x_4 = x_{in}$$

2. Properties of Representations of Displaced Functions

The representation of a displaced impulse (3-3d) actually is a function of two arguments:

$$A(p, \vartheta) = e^{-p\vartheta}, \qquad (3\text{-}3d)$$

one of which can be fixed and serve as a parameter. In precisely the same way the representation of any displaced function $x(t - \vartheta_1)$ (example of a displaced function can be seen in Figure 2-1b) will depend on two arguments: $A(p, \vartheta_1)$.

If the representation of the initial function $X(p)$ is known, it is not difficult to obtain the representation of the displaced function $X(x, \vartheta_1)$ on the basis of formula (3-3c), which, with (3-3a) taken into consideration, we write as:

$$X(p) = \int_0^\infty \Delta(p, \vartheta) \, x(\vartheta) \, d\vartheta. \qquad (3\text{-}4a)$$

In accordance with Fig 3-2a it may be considered that the scales of the impulses entering (3-4a) are determined according to an undisplaced function, and the moments of application of the impulses are additionally displaced by the interval ϑ_1, which changes the form of the representation of the impulse:

$$\Delta(p, \vartheta + \vartheta_1) = e^{-p(\vartheta + \vartheta_1)} = e^{-p\vartheta} e^{-p\vartheta_1} \qquad (3\text{-}4b)$$

and leads to the appearance in formula (3-4a) of the co-factor $e^{-p\vartheta_1}$, which is taken out beyond the sign of the integral.

As a result

$$X(p, \vartheta_1) = \Delta(p, \vartheta_1) \, X(p) = e^{-p\vartheta_1} X(p). \qquad (3\text{-}4c)$$

Thus the representation of the displaced process equals the product of the representations of the same initial process and the frontal impulse or representation of the initial process multiplied by $e^{-p\vartheta_1}$.

The initial functions are a special case of displaced functions at zero displacement $\vartheta = 0$. The designation

$$L\{x(t)\} = X(p, 0) = X(p) \qquad (3\text{-}4d)$$

permits having general rules for displaced and initial functions.

4. The Representation of Functions Compressed in Time

Let the representation of the initial function $x(t)$, $L\{x(t)\} = X(p)$ be known. It can readily be noted that the function $x(nt)$ has the same figures of the process but proceeds n times faster. If we turn to Figure 3-2b, we see that the scales of the impulses entering formula (3-4a) can be determined according to the principal function and not the one compressed in time, but the disposition of the impulses will be determined by the new displacement ϑ/n and their area
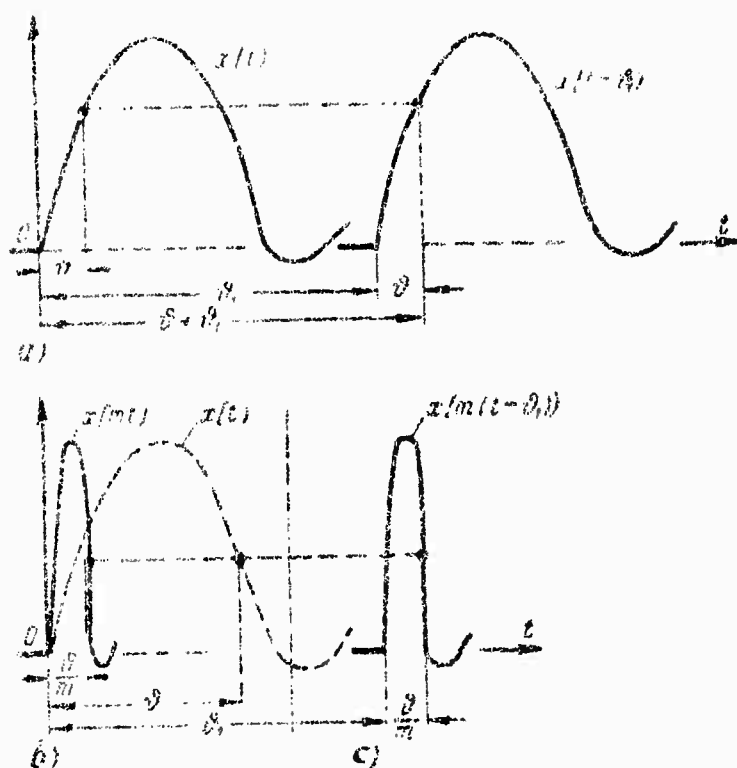
Fig. ... signals of ... slowed and compressed in time

... by ... times, which is reflected in the representa-
... in the following manner:

$$\Delta_n(p, \vartheta) = \frac{1}{m} e^{-\frac{p}{m}\vartheta} = \frac{1}{m}\Delta\left(\frac{p}{m}, \vartheta\right), \quad (3\text{-}5a)$$

... the representation of the impulse to the right
... we note that as a result of integration the
... and will depend on the argument
... of the argument ...

$$L\{x(mt)\} = \frac{1}{m} X\left(\frac{p}{m}\right). \quad (3\text{-}5b)$$

Thus, when the process is compressed in time by m times, its
... and the argument of representation p are reduced by m
times.

— 162 —

If the representation of the displaced process $x_m(t - \mathcal{S})$ is examined, the representation can be found by the formula

$$L\{x[m(t - \vartheta_j)]\} = \frac{1}{m} e^{-p\vartheta} X\left(\frac{p}{m}\right).$$

The deformation of the impulses in this case is illustrated in Figure 4-10.

3-7. The Representation of the Integro-Differential Operations

A. Differentiation

To obtain the representation of the displaced function we will use formula (3-1a), which also leads to a result analogous to (3-4c):

$$e^{-p\vartheta} X(p) = L\{x[t - \vartheta)]\} = $$
$$= \int_0^\infty e^{-pt} x(t - \vartheta)\, dt. \qquad (3\text{-}6)$$

We will differentiate the left and right sides of the obtained formula with respect to ϑ, inserting the operation of differentiation under the sign of the integral:

$$-pe^{-p\vartheta} X(p) = \int_0^\infty e^{-pt} \left\{\frac{\partial}{\partial \vartheta} x(t - \vartheta)\right\} dt. \qquad (?)$$

In addition, on the basis of the formula of equivalent differentiation (2-15) we will proceed to the derivative in time and then we note that on the right side of (4) is written the representation of the derivative of the displaced function which, consequently, constitutes:

$$L\{\dot{x}(t - \vartheta)\} = pX(p, \vartheta). \qquad (3\text{-}7a)$$

If we perform multiple differentiation of (3-6a) with respect to ϑ and use the formula of equivalent differentiation (3-7a), we arrive by an analogous path at the representation of the higher derivatives of the displaced function:

$$L\{x^{(l)}(t - \vartheta)\} = p^l X(p, \vartheta). \qquad (3\text{-}7b)$$

— 165 —

These same formulas are valid also for the initial functions.

$$\dot{x}(t) \div p X(p); \tag{3.8a}$$

$$x^{(k)}(t) \div p^k X(p). \tag{3.8b}$$

In application to the impulses the relations obtained give the following dependences which supplement (3.8a) and (3.8b):

$$\delta_1(t - \theta) \div p e^{-p\theta}; \tag{3.9a}$$

$$\delta_{k+1}(t - \theta) \div p^k e^{-p\theta}; \tag{3.9b}$$

$$\delta_1(t) \div p; \tag{3.9c}$$

$$\delta_{k+1}(t) \div p^k. \tag{3.9d}$$

Thus the operation of differentiation in time requires multiplication of the representation by p, which is illustrated by figure 3.4, a and b.
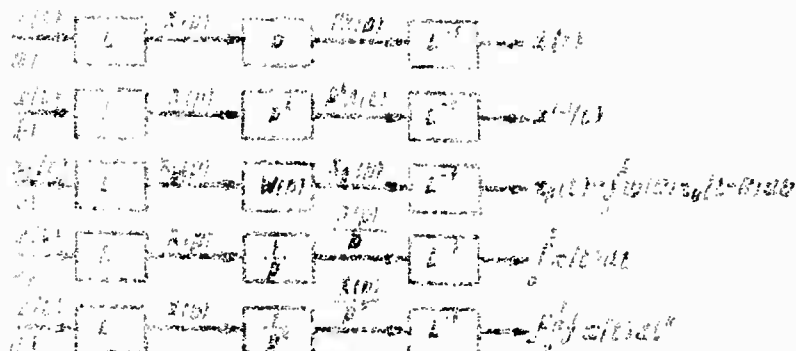
Fig. 3.4. Representation of integro-differential operations.
$x_0 = x_{out}(t); \quad y = \bar{p} > 1.$

C. Convolution

Let the solution of the equation of the integral equation for a component with constant parameters (2.49a) involve all the points of the output process from $t = 0$ to $t = \infty$, for which we will assume the limits of integration to be semi-infinite.

$$X_{out}(t) = \int_0^\infty w(\theta)\, x_{in}(t - \theta)\, d\theta. \qquad (*)$$

In that case, for each concrete point of the process, the integration with respect to the argument θ proceeds as before within the limits $0 - t$, conditioned by the width of the working zone of the displaced function $x_{in}(t - \theta)$.

We will perform a direct Laplace transform (3-1a) on both sides of the equation. Since in $(*)$ the integration is done with respect to θ, and in (3-1a) with respect to t, the operation of direct transformation can be introduced under the sign of the integral $(*)$, which gives:

$$X_{out}(p) = \int_0^\infty w(\theta)\, L\{x_{in}(t - \theta)\}\, d\theta =$$

$$= \int_0^\infty w(\theta)\, e^{-p\theta}\, X_{in}(p)\, d\theta = X_{in}(p) \int_0^\infty w(\theta) \times$$

$$\times e^{-p\theta}\, d\theta = X_{in}(p)\, W(p);$$

finally we have:

$$X_{out}(p) = W(p)\, X_{in}(p), \qquad (3\text{-}10a)$$

where

$$W(p) = L\{w(t)\}. \qquad (3\text{-}10b)$$

The representation of the weight function of the component (3-10b) is called the operator function of transfer (OFT) of the component. On the basis of the elementary transformation (3-10a):

$$W(p) = \frac{X_{out}(p)}{X_{in}(p)} \qquad (3\text{-}10c)$$

it is evident that the OFT is equal to the ratio of the representations of the output and input signals. The conditions of transformation of the representations of the signals by the component are illustrated by Figure 3-14.

If we integrate the left and right sides of formula (3-6) with respect to displacement in the limits from $\vartheta = 0$ to $\vartheta = \infty$, we get:

$$\frac{1}{c} X(p) = \int_0^\infty e^{-pt} \left\{ \int_0^\infty x(t - \vartheta)\, d\vartheta \right\} dt.$$

Now in the left side we have the representation of the integral written in braces on the right side, which, with the limitations of the zone of change of the displacement $\vartheta \leq t$, can be replaced by the single (3-11a) and multiple (3-11b) integrations, which are equivalent for the operations:

$$\int_0^t x(t)\, dt \longleftrightarrow \frac{X(p)}{p}; \qquad (3\text{-}11a)$$

$$\int_0^t \langle \ldots k_{\text{sum}} \ldots \rangle \int_0^t x(t)\, dt^k \longleftrightarrow \frac{X(p)}{p^k}. \qquad (3\text{-}11b)$$

If in accordance with these formulas, illustrated by figures ..., a and b, we take the representation of the images ..., as a basis, then, by multiplying it by $1/p$, we will obtain in the region of the originals, in sequence: a step, linear, quadratic and higher integral functions of t, which gives a new series of relations:

$$1(t) \longleftrightarrow \frac{1}{p}; \qquad (3\text{-}12a)$$

$$(t) \longleftrightarrow \frac{1}{p^2}; \qquad (3\text{-}12b)$$

$$\frac{1}{k}(t^k) \longleftrightarrow \frac{1}{p^{k+1}}; \qquad (3\text{-}12c)$$

$$1(t - \vartheta) \longleftrightarrow \frac{1}{p} e^{-p\vartheta}; \qquad (3\text{-}12d)$$

$$(t - \vartheta) \longleftrightarrow \frac{1}{p^2} e^{-p\vartheta}; \qquad (3\text{-}12e)$$

$$\frac{1}{k}(t - \vartheta)^k \longleftrightarrow \frac{1}{p^{k+1}} e^{-p\vartheta}. \qquad (3\text{-}12f)$$

4. The Equation of Connection

For equations of connection of the type of (1-7b) a description of the input and output processes by the initial and displaced functions is characteristic, since the reaction of the component is studied at a given concrete excitation without taking account of its previous history. In that case, by making Laplace transformations of both sides of equation (1-7b), it is sufficient by virtue of (3-7b) to simply make the substitution

$$D^i = p^i, \qquad (3\text{-}13a)$$

which leads to the operator equation of connection of the type of (1-7b) or (1-7c).

On the basis of these equations the OFT is readily determined according to (3-10c)

$$W(p) = \frac{b(p)}{a(p)} = \frac{\sum\limits_{i=0}^{m} b_i p^i}{\sum\limits_{i=0}^{n} a_i p^i}. \qquad (3\text{-}13\,b)$$

And so the OFT is equal to the ratio of the operator polynomials of the right and left sides of the equation of connection. According to formula (3-13b) the OFT is usually determined more simply than on the basis of use of the direct transformation directly to the weight function (3-10b). The OFT's of typical components are given in Table 3-1.

5. The Equation of Aftereffect

The substitution of (3-13a) in the equation of the aftereffect (2-61) is not admissible, since the continuous (two-sided) functions are differentiated according to formula (2-58); we will present this formula for the case $l = 0$.

$$z_{out}^{(l)}(t) = z_{out}^{-l}(t) - \sum\limits_{j=0}^{l-1} z_{out}^{(j)}(0)\,\delta_{l-j}(t) \qquad (3\text{-}13a)$$

If we proceed to the representations, we can use the substitution

of (3-13a) for the first term of the right side, and substitute according to (3-92) the impulses entering the sum; as a result we obtain the general formula:

$$\dot{x}_{out}^{(i)}(0) \longrightarrow p^i X_{out}(p) - \sum_{j=1}^{i-1} \dot{x}_{out}^{(j)}(0) \, p^{i-j-1} \quad (3\text{-}14b)$$

and the partial correspondences:

$$\dot{x}_{out}(0) \longrightarrow p X_{out}(p) - x_{out}(0); \qquad (3\text{-}14c)$$

$$\ddot{x}_{out}(t) \longrightarrow p^2 X_{out}(p) - x_{out}(0) \, p - \dot{x}_{out}(0). \qquad (3\text{-}14d)$$

If we make a Laplace transformation of the equation of aftereffect (2-57a), on the basis of expressions (3-14) we get:

$$a(p) \, X_{out}(p) = \sum_{i=0}^{n} a_i p^i X_{out}(p) = \sum_{i=0}^{n} \sum_{j=0}^{m} a_i x_{out}^{(j)}(0-) \, p^{i-j-1}.$$

$$(3\text{-}15)$$

This result might have been obtained directly from equation (2-60a), if we subjected it to direct L-transformation. For a second-order equation the preceding formula is simplified:

$$(a_2 p^2 + a_1 p + a_0) \, X_{out}(p) = a_1 x_{out}(0) + a_2 \dot{x}_{out}(0) + a_2 x_{out}(0) p. (^*)$$

C. Structural Circuits of Components Excited by the Input Signal and the Initial Conditions

The placing of a regime of action on a regime of aftereffect, allowable according to the principle of superposition, was illustrated by the general formulas (2-61 a and b). In operator form, for components with constant parameters, the general equation assumes the form:

$$a(p) \, X_{out}(p) = b(p) \, X_{in}(p) +$$

$$+ \sum_{i=1}^{n} \sum_{j=0}^{n} a_i x_{out}^{(j)}(0-) \, p^{i-j-1}, \qquad (3\text{-}16a)$$

where $i - j - 1 \geq 0$.

The structural circuit for this complex case of excitation of the component can be constructed in the form of Figure 3-4a, if the superposition of the reaction on the output of each action is performed:

$$X_{out}(p) = X_{out\ in}(p) + X_{aftereffect}(p)$$

[illegible] form of figure [illegible] 4, as the superposition of the action on [illegible] of [illegible] formulate the general [illegible]
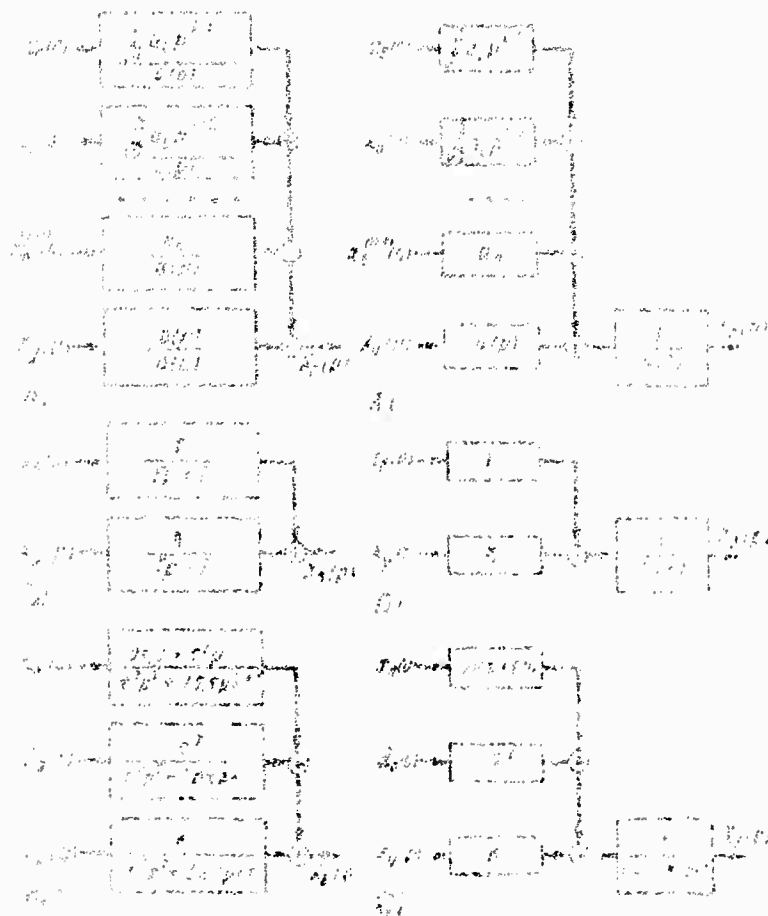
$$X(p) = X_1(p) + x_1(0)\sum_{i=1}^{n} a_i p^{i-1} +$$

$$+ x_2(0)\sum_{i=2}^{n} a_i p^{i-2} + \dots + x_1^{(n-1)}(0)\, a_n.$$

a)
b)
c)

Fig. [illegible] Structural diagrams of components excited by the control signal and initial conditions: a – constant term; b – aperiodic component; c – oscillating component.

[illegible]

Table 2-1   Transfer Functions of Transfer of Typical Components

Название звена	№	Дифференциальное уравнение звена	Переходная характеристика $h(t)$	Передаточная функция $W(p)$
Усилительное	6	$x_0 = k_1 x_1$	$k_1 \cdot 1(t)$	k_1
Запаздывающее	7	$x_0(t) = k_2 x_1(t - \tau)$	$k_2 \cdot 1(t - \tau)$	$k_2 e^{-\tau p}$
Апериодическое	8	$T\dot{x}_0 + x_0 = k_3 x_1$	$\dfrac{k_3}{T} e^{-\frac{t}{T}}$	$\dfrac{k_3}{Tp+1}$
Реальное дифференцирующее	9	$T\dot{x}_0 + x_0 = k_4 \dot{x}_1$	$\dfrac{k_4}{T} e^{-\frac{t}{T}}$	$\dfrac{k_4}{Tp+1}$
Интегрирующее	10	$\dot{x}_0 = k_{-1} x_1$	$k_{-1} \cdot 1(t)$	$\dfrac{k_{-1}}{p}$
Дифференцирующее	11	$x_0 = T\dot{x}_1$	$T\delta(t)$	Tp
Реальное дифференцирующее	12	$T_c \dot{x}_0 + x_0 = T_{\text{д}} \dot{x}_1$	$\dfrac{T_{\text{д}}}{T_c} \delta(t) - \dfrac{T_{\text{д}}}{T_c} e^{-\frac{t}{T_c}}$	$\dfrac{T_{\text{д}} p}{T_c p + 1}$
Форсирующее	13	$x_0 = k_b(x_1 + T\dot{x}_1)$	$k_b[1(t) + T\delta(t)]$	$k_b(1 + Tp)$

Таблица 3.1 (продолжение)

Реальное дифференцирующее звено первого порядка	(15) $T_0 \dot{x}_в + x_в = k_0(\dot{x}_y + T_{д1}\dot{x}_y)$	$k_0\left[\dfrac{T_{д1}}{T_0}\delta(t) + \dfrac{T_0 - T_{д1}}{T_0^2}e^{-\frac{t}{T_0}}\right]$	$\dfrac{k_0(1 + T_{д1}p)}{T_0 p + 1}$
Колебательное (апериодическое) звено $0 < \xi < 1$	(16) $\tau^2\ddot{x}_в + 2\xi\tau\dot{x}_в + x_в = k x_y$	$\dfrac{k}{\tau\sqrt{1-\xi^2}}e^{-\frac{\xi}{\tau}t}\sin\dfrac{t}{\tau}\sqrt{1-\xi^2}$	$\dfrac{k}{\tau^2 p^2 + 2\xi\tau p + 1}$
Неустойчивое колебательное звено $0 < \xi < 1$, $a_3 < 0$	(16') $\tau^2\ddot{x}_в - 2\xi\tau\dot{x}_в + x_в = k x_y$	$\dfrac{k}{\tau\sqrt{1-\xi^2}}e^{\frac{\xi}{\tau}t}\sin\dfrac{t}{\tau}\sqrt{1-\xi^2}$	$\dfrac{k}{\tau^2 p^2 - 2\xi\tau p + 1}$
Резонансное звено	(17) $\ddot{x}_в + \Omega^2 x_в = k_0 x_y$	$\dfrac{k_0}{\Omega}\sin\Omega t$	$\dfrac{k_0}{p^2 + \Omega^2}$
Форсирующее звено второго порядка	(18) $x_в = k_0(x_y + 2\xi\tau\dot{x}_y + \tau^2\ddot{x}_y)$	$k_0[\delta(t) + 2\xi\tau\dot{\delta}(t) + \tau^2\ddot{\delta}(t)]$	$k_0(1 + 2\xi\tau p + \tau^2 p^2)$
Реальное форсирующее звено второго порядка	(19) $T_1 T_2 \ddot{x}_в + (T_1 + T_2)\dot{x}_в + x_в = k_0(x_y + 2\xi\tau\dot{x}_y + \tau^2\ddot{x}_y)$	$k_0\left[\dfrac{\tau^2}{T_1 T_2}\delta(t) + \left(1 - \dfrac{2\xi\tau}{T_1} + \dfrac{\tau^2}{T_1^2}\right)\dfrac{e^{-\frac{t}{T_1}}}{T_1 - T_2} - \left(1 - \dfrac{2\xi\tau}{T_2} + \dfrac{\tau^2}{T_2^2}\right) \times \right.$ $\left. \times \dfrac{e^{-\frac{t}{T_2}}}{T_1 - T_2}\right]$	$\dfrac{k_0(1 + 2\xi\tau p + \tau^2 p^2)}{(T_1 p + 1)(T_2 p + 1)}$

Table 3.1 Operator Designations

1 - Order of differential equation of component; 2 - Name; 3 - Differential equation of connection; 4 - Weight function w(t); 5 - Operator function of transfer; 6 - Amplifying; 7 - Delaying; 8 - Aperiodic; 9 - Quasi-static, first order; 10 - Integrating; 11 - Differentiating; 12 - Real differentiating; 13 - Boosting, 1st order; 14 - Real boosting, 1st order; 15 - Oscillating static; 16 - Oscillating quasi-static; 17 - Resonance; 18 - Boosting, second order; 19 - Real boosting, second order; 20 - Real integrating; 21 - Two differentiating; 22 - Two integrating; 23 - Two aperiodic; 24 - Aperiodic and quasi-static, first order; 25 - Two quasi-static, first order; 26 - Two aperiodic with short $\xi = 1$ bands.

Subscript o= out, subscript y = in

We will compose, for the sake of example, operator equations during complex action for the aperiodic component:

$$(Tp + 1)X_{out}(p) = kX_{in}(p) + T x_{out}(0-) \qquad (3.16\text{b})$$

and for the oscillating component:

$$(t^2 p^2 + 2\xi t p + 1)X_{out}(p) = kX_{in}(p) +$$
$$+ (2\xi t + t^2 p) x_{out}(0-) + t^2 x'_{out}(0-). \qquad (3.16c)$$

These correspond to structural diagrams b and b', c and c' presented in the same figure.

As is evident from the formulas and structural diagrams, the conditions of the aftereffect are all the more complicated, the higher the order of the left side of the equation of the component, that is, the greater is its memory relative to the initial derivative. The component with zero order of the left side with similar memory does not exist and there is no regime of aftereffect for them.

Components with a developed right side have a regime of aftereffect that coincides with the regime of aftereffect of a component with an analogous left side and a single ADF of the right side at identical initial conditions with respect to all derivatives taken into consideration by the equation.

3.4.   Representation of the Product of Two Functions; Lambda-Transformation

In linear problems are considered the products of given functions at two input actions, the products of the controllable (sought) values for a single function or for impulse functions and the products of given variable coefficients for controllable (sought) values and their

derivatives. The latter is the most complex and general problem, and therefore we will begin by considering it.

In the general form of notation of the differential equation of connection (1-1) the variable parameters are given in the form of arbitrary functions of time. Furthermore, we will use representations of the variable parameters the limited class of functions $a(t)$, which we will write in the first column of Table 3-2. The most complex coefficients can be obtained in the form of linear combinations of the tabulated functions.

No limitations are set for the second co-factor in the form of initial functions, under the condition that it has the representation $X(p)$.

First of all we will determine the representation of the product of the function $a(t)$ for a displaced impulse:

$$L\left\{a\left(t\right)\delta\left[t-\theta\right]\right\} = L\left\{a\left(\theta\right)\delta\left[t-\theta\right]\right\} \cdot a\left(\theta\right)e^{-p\theta}. \tag{3-17}$$

As is evident from the formula, the area of impulse $a(\theta)$ determines the scale of its representation.

Representations (3-17), for the examined functions of $a(t)$, are given in the second column of Table 3-2.

Now we will establish what linear transformation in the region of argument p must be undergone by the representation of impulse $\Delta(p, \theta)$ in order that the co-factor $a(\theta)$ be formed. We will designate the sought transformation by Λ and call it the lambda-transformation; then after the determination we have:

$$\Lambda\left\{\Delta(p, \theta)\right\} = L\left\{a\left(t\right)\delta\left[t-\theta\right]\right\}. \tag{3-18a}$$

The lambda-transformations are shown in the determined form in the third column of the same table and are reduced to a displacement of the argument p, separation of a substantial part of the representation in an imaginary or complex displacement, separation of the coefficient at an imaginary part of the displaced function, differentiation or integration of the representation within special limits and to combinations of those operations.

Thus, for example, to obtain the product $\sin \Omega t \cdot e^{-p\tau}$ according to the table it is necessary to make the following transformations:

$a(t)$	$L\{a(t)\delta(t-b)\}$	$\lambda\{\Delta(p,b)\}$
$e^{-\sigma t}$	$e^{-(p+\sigma)b}$	$\Delta(p+\sigma,b)$
$\sin\Omega t$	$\sin\Omega b\,e^{-pb}$	$-\mathrm{Im}\,\Delta(p+j\Omega,b)$
$\cos\Omega t$	$\cos\Omega b\,e^{-pb}$	$\mathrm{Re}\,\Delta(p+j\Omega,b)$
$\sin(\Omega t+\varphi)$	$\sin(\Omega b+\varphi)e^{-pb}$	$\sin\varphi\,\mathrm{Re}\,\Delta(p+j\Omega,b)-$ $-\cos\varphi\,\mathrm{Im}\,\Delta(p+j\Omega,b)$
$e^{-\sigma t}\sin(\Omega t+\varphi)$	$\sin(\Omega b+\varphi)e^{-(p+\sigma)b}$	$\sin\varphi\,\mathrm{Re}\,\Delta(p+\sigma+j\Omega,b)-$ $-\cos\varphi\,\mathrm{Im}\,\Delta(p+\sigma+j\Omega,b)$
t^m	$b^m e^{-pb}$	$(-1)^m\dfrac{d^m}{dp^m}\Delta(p,b)$
$t^m e^{-\sigma t}$	$b^m e^{-(p+\sigma)b}$	$(-1)^m\dfrac{d^m}{dp^m}\Delta(p+\sigma,b)$
$t^m e^{-\sigma t}\sin(\Omega t+\varphi)$	$b^m e^{-(p+\sigma)b}\times$ $\times\sin(\Omega b+\varphi)$	$(-1)^m\dfrac{d^m}{dp^m}\{\sin\varphi\,\mathrm{Re}\,\Delta(p+\sigma+j\Omega)-$ $-\cos\varphi\,\mathrm{Im}\,\Delta(p+\sigma+j\Omega)\}$
$\dfrac{1}{t^m}$	$\dfrac{1}{b^m}e^{-pb}$	$(-1)^m\displaystyle\int_{p}^{\infty}\underset{m}{(\cdots)}\int\Delta(p,b)\,dp^m$
$\dfrac{e^{-\sigma t}\sin\Omega t}{t}$	$\dfrac{e^{-\sigma b}}{b}e^{-pb}$	$\displaystyle\int_{p}^{\infty}\mathrm{Im}\,\Delta(p+\sigma+j\Omega,b)\,dp$
$\dfrac{1}{a+t}$	$\dfrac{1}{a+b}e^{-pb}$	$e^{ap}\displaystyle\int_{p}^{\infty}e^{-ap}\Delta(p,b)\,dp$

$\mathcal{L}\{x(t)\} = L\{x(t)a(t)\}$	$L\{e^{-t}x(t)\}$
$X(p + s)$	$\dfrac{1}{p + s}$
$-\operatorname{Im} X(p + j\Omega)$	$\dfrac{\Omega}{p^2 + \Omega^2}$
$\operatorname{Re} X(p + j\Omega)$	$\dfrac{p}{p^2 + \Omega^2}$
$\sin\varphi\,\operatorname{Re} X(p + j\Omega) - \cos\varphi\,\operatorname{Im} X(p + j\Omega)$	$\dfrac{\Omega\cos\varphi + p\sin\varphi}{p^2 + \Omega^2}$
$\sin\varphi\,\operatorname{Re} X(p + s + j\Omega) - \cos\varphi\,\operatorname{Im} X(p + s + j\Omega)$	$\dfrac{\Omega\cos\varphi + (p + s)\sin\varphi}{(p + s)^2 + \Omega^2}$
$(-1)^m \dfrac{d^m}{dp^m} X(p)$	$\dfrac{m!}{p^{m+1}}$
$(-1)^m \dfrac{d^m}{dp^m} X(p + s)$	$\dfrac{m!}{(p + s)^{m+1}}$
$(-1)^m \dfrac{d^m}{dp^m}\{\sin\varphi\,\operatorname{Re} X(p + s + j\Omega) - \cos\varphi\,\operatorname{Im} X(p + s + j\Omega)\}$	$(-1)^m \dfrac{d^m}{dp^m}\dfrac{(p + s)\sin\varphi + \Omega\cos\varphi}{(p + s)^2 + \Omega^2}$
$(-1)^m \int \cdots \int X(p)\,dp^m$	
$\int \operatorname{Im} X(p + s + j\Omega)\,dp$	$\operatorname{arctg}\dfrac{\Omega}{p + s}$
$\int e^{-sp} X(p)\,dp$	

$$-\ln \Delta (p + j\Omega, \vartheta) = -\ln e^{-(p+j\Omega)\vartheta} =$$

$$= -\ln \{e^{-p\vartheta} (\cos \Omega\vartheta - j\sin \Omega\vartheta)\} = \sin \Omega\vartheta\, e^{-p\vartheta}.$$

Now, if we replace the product with the superposition (2-44),

$$a(t)\, x(t) = \int_0^\infty \delta(t - \vartheta)\, a(t)\, x(\vartheta)\, d\vartheta,$$

we can introduce the Laplace transform under the sign of the integral, since the variable integration does not depend on a parameter of the transform:

$$L\{a(t)\, x(t)\} = \int_0^\infty L\{\delta(t - \vartheta)\, a(t)\}\, x(\vartheta)\, d\vartheta.$$

But it was shown above that the representation of the product of an impulse on a continuous function can be replaced by a lambda-transformation of the representation only of the impulse; consequently

$$L\{a(t)\, x(t)\} = \int_0^\infty \lambda\{\Delta(p, \vartheta)\}\, x(\vartheta)\, d\vartheta =$$

$$= \lambda\left\{\int_0^\infty \Delta(p, \vartheta)\, x(\vartheta)\, d\vartheta\right\}.$$

On the right side of the formula the lambda-transformation as a linear operation in the region of the argument p was carried beyond the sign of the integral, which in accordance with (3-4a) gives:

$$L\{a(t)\, x(t)\} = \lambda\{X(p)\}. \qquad (3\text{-}18b)$$

And so, if the Laplace transform of the arbitrary function $X(p)$ is known, then to obtain the representation of the product of the same function for the variable coefficient $a(t)$ it is necessary to carry out a linear lambda-transformation on the representation $X(p)$. The lambda-transformations for the tabulated coefficients are given in the fourth column.

If $x(t) = 1(t)$ is assumed, that is, $X(p) = 1/p$, then the fourth column of the table can be used simply to obtain the representations of the initial functions located in the first column. For example,

$$\{\cos \Omega t\} \to R\frac{1}{p+j\Omega} = \frac{p}{p^2 + \Omega^2}$$

$$\left[\frac{e^{-\sigma t}\sin\Omega t}{t}\right) \to - \int\limits_{p}^{\infty}\mathrm{Im}\,\frac{dp}{p+\sigma+j\Omega} =$$

$$= \int\limits_{p}^{\infty}\frac{\Omega dp}{(p+\sigma)^2+\Omega^2} = \mathrm{arc\,tg}\left(\frac{\Omega}{p+\sigma}\right).$$

Representations for functions of the form $a(t)\,1(t)$ are in the fifth column.

In Figure 3-5 are the initial harmonic non-damping functions which have a different phase shift, which leads to change in the initial conditions from the right of $x(0+)$, and their representations, taken from the table, are given. For the last column of the table the representation was obtained in [5].

In concluding this section we present an example of application of the lambda-transformation to the product of a displaced impulse of the $(k + 1)$th order for a continuous function [coefficient $a(t)$], which near the point ϑ always can be expanded into a Taylor series:

$$a(t)\,\delta^k[t-\vartheta] = \left[a(\vartheta)+\dot{a}(\vartheta)(t-\vartheta)+\right.$$
$$\left.+\frac{\ddot{a}(\vartheta)(t-\vartheta)^2}{2!}+\dots\right]\delta^k[t-\vartheta].$$

We will make a Laplace transform of the product under consideration

$$\mathcal{L}\{a(t)\,\delta^k[t-\vartheta]\} = \lambda\{p^k\} = \left[a(\vartheta)\,p^k - \right.$$
$$\left.- \dot{a}(\vartheta)\,kp^{k-1} + \frac{\ddot{a}(\vartheta)\,k(k-1)}{2!}\,p^{k-2} + \dots\right]e^{-p\vartheta}.$$

$$(3\text{-}18c)$$

or in a form coordinated with (2-10d):

$$\lambda\{p^k\} = e^{-p\vartheta}\,(p-D^7)^k\,a(\vartheta) \to a(t)\,\delta^{(k)}[t-\vartheta].$$

$$(3\text{-}18d)$$

The operator analysis of transonic flow with variable parameters

If we make a Laplace transform of the equation of ... it is necessary for the representation of each derivative in the Laplace ... together with ... of the equation be substituted ... in accordance with the form of representation of each variable coefficient of that derivative. The general form of the transformed equation (3.xx) has already been given in Chapter 1, Table ... only finds the value or more forms of transformation.

Let us consider in detail the representation or approximation of the coefficients in the form of the power polynomials:

$$a_i(t) = \sum a_{ij} t^j = \sum_{k=0} \frac{a^{(k)}(0) t^k}{k!} \qquad (3.19a)$$

Here the coefficients with the ... indication a_{ij} is the power of the derivative, the exponent of t are the relevant numbers:

$$\frac{a_i^{(k)}(0)}{k!}$$

... in a large interval the coefficients are described with an accuracy adequate for practice by a cubic polynomial:

$$a_i(t) = a_0 + a_1 t + a_2 t^2 + a_3 t^3 =$$

$$= a_i(0) + a_i'(0) t + \frac{a_i''(0)}{2!} t^2 + \frac{a_i'''(0)}{3!} t^3 \qquad (3.19b)$$

Each of the terms entering for one ... upon multiplication by the corresponding derivative, transformed as ..., transforms this representation in accordance with Table ... to a sum of the type:

$$A(p) X(p) = \sum_{k=0} A_k(p) X(p) =$$

$$= \sum (-1)^k a_{k} \frac{d^k}{dp^k} X(p).$$

$$L\left\{a_i(t)\,x^{(i)}(t)\right\} =$$

$$= \sum_{k=0}^{l}(-1)^k\,a_{ik}\,\frac{\partial^k}{\partial p^k}\,p^i X(p). \qquad (3\text{-}19\varepsilon)$$

If formula (3-19c) has been prepared, it is now possible to make a Laplace transform of the entire equation (1-4):

$$\sum_{i=0}^{n}\sum_{k=0}^{l}(-1)^k\,a_{ik}\,\frac{\partial^k}{\partial p^k}\,p^i X_{out}(p) =$$

$$= \sum_{j=0}^{m}\sum_{x=0}^{r}(-1)^x\,b_{jx}\,\frac{\partial^x}{\partial p^x}\,p^j X_{in}(p). \qquad (3\text{-}20)$$

As a result a differential equation is obtained in the region of the representation, the order of which does not depend on the order of the differential equation in the region of time (1-4), and is determined only by the higher degree of the polynomials of t, which represent variable coefficients.

Thus, for example, for an equation of the second order ($n = 2$, $m = 0$), with only the rate of change of the coefficients $l = 1$ taken into account, we have the initial equation:

$$[a_2(0) + \dot a_2(0)\,t]\,\ddot x_{out} + [a_1(0) + \dot a_1(0)\,t]\,\dot x_{out} +$$

$$+ [a_0(0) + \dot a_0(0)\,t]\,x_{out} = n(t) \qquad (3\text{-}21a)$$

and its transformation

$$[a_2(0)\,p^2 + a_1(0)\,p + a_0(0)]\,X_{out}(p) -$$

$$- \frac{\partial}{\partial p}\{[\dot a_2(0)\,p^2 + \dot a_1(0)\,p +$$

$$+ \dot a_0(0)]\,X_{out}(p)\} = \Pi(p). \qquad (3\text{-}21b)$$

which is reduced to an equation of the second order in the region p.

If the coefficients are varied according to more complex laws, it is possible to arrive at a first-order equation in the region p only on the basis of rough approximation. For this purpose we assume

$$\frac{d^k}{dp^k} X(p) = 0 \text{ when } k \geq 2. \qquad (3\text{-}22a)$$

Then for a typical component of equation (3-20) differentiation with respect to p gives:

$$\frac{d}{dp}[p^i X(p)] = i p^{i-1} X(p) + p^i X'(p). \qquad (3\text{-}22b)$$

Further, with limitation (3-22a) taken into consideration

$$\frac{d^2}{dp^2}[p^i X(p)] = i[(i-1) p^{i-2} X(p) + \\ + 2 p^{i-1} X'(p)]; \qquad (3\text{-}22c)$$

$$\frac{d^k}{dp^k}[p^i X(p)] = i(i-1)\ldots(i-k+2) \times \\ \times [(i-k+1) p^{i-k} X(p) + k p^{i-k+1} X'(p)]. \qquad (3\text{-}22d)$$

If we assemble the elements of (3-22d), we get instead of (3-20) a general operator equation of first approximation

$$V(p) X'_{out}(p) + U(p) X_{in}(p) = \Pi(p), \qquad (3\text{-}23a)$$

where

$$U(p) = \sum_{i=0}^{n} \sum_{k=0}^{i} (-1)^k a_{ik} i \times \\ \times (i-1)\ldots(i-k+2) k p^{i-k+1} \qquad (3\text{-}23b)$$

and

$$V(p) = \sum_{i=1}^{n} \sum_{k=1}^{i} (-1)^k a_{ik} i \times \\ \times (i-1)\ldots(i-k+1) p^{i-k}. \qquad (3\text{-}23c)$$

— 165 —

Formally according to (3-23a) it is possible to obtain the representation of the process in brackets:

$$x_{3R}(p) = e^{-\int \frac{U(p)}{V(p)}dp}\left[\int \frac{\Pi(p)}{V(p)}e^{\int \frac{U(p)}{V(p)}dp}dp + C\right].$$

$$(3-24)$$

But this solution is rather difficult to use, and therefore we will consider more obvious methods.

3-6. The Method of Balance of Partial Representations for Solution of Operator Equations

A. Calculating Table for the Coefficients and the Solution in the Form of Polynomials

In an n-th order equation of the type of (3-20), let the right side of the equation contain an impulse of the $(\nu + 1)$th order, higher than the order of equation, n:

$$x_{9R} = \delta^{\nu+1}[t], \quad \nu \geq n;\qquad (3-25a)$$

then in the solution a series of impulses must be expected:

$$x_{5R} = M_{\nu-n}\delta^{(\nu-n)}[t] + M_{\nu-n-1}\delta^{(\nu-n-1)}[t] + \dots$$
$$\dots + M_0\delta[t].\qquad (3-25b)$$

For a second-order equation, for example, of the type of (3-21a), at an input impulse of the fourth order $\nu = 3$, the impulse part of the solution is:

$$x_{5R} = M_1\dot{\delta}[t] + M_0\delta[t].\qquad (*)$$

With the completion of the action of the input impulse the system undoubtedly will perform the transient process $x_{3R}(t)$. If we expand this still unknown process into a Maclaurin series, we obtain the power series:

$$x_{3R} = x_{3R}(0)1[t] + \dot{x}_{3R}(0)[t] +$$

$$+ \frac{\ddot{x}_{3R}(0)[t]^2}{2!} + \dots\qquad (3-25c)$$

in which the initial derivatives of the process are unknown as before.

The complete reaction of the system, with the impulse (3-25b) and prolonged (3-25a) components taken into consideration, is written in the general form:

$$x_w(t) = \sum_{i=0}^{\mu} M_i \delta^i(t) + \sum_{\kappa=0}^{\infty} \frac{x_w^{(\kappa)}(0) t^\kappa}{\kappa!} \quad (3\text{-}25\,d)$$

and for the particular case $\mu = 2$, $\nu = 3$:

$$x_w(t) = M_1 \dot{\delta}(t) + M_0 \delta(t) + \sum_{\kappa=0}^{\infty} \frac{x_w^{(\kappa)}(0) t^\kappa}{\kappa!} \quad (**)$$

We will proceed to make a Laplace transformation in the last two equations:

$$X_w(p) = \sum_{i=1}^{\mu} M_i p^i + \sum_{\kappa=0}^{\infty} \frac{x_w^{(\kappa)}(0)}{p^{\kappa+1}} \quad (3\text{-}26)$$

$$X_w(p) = M_1 p + M_0 + \frac{x_w(0)}{p} + \frac{x_w(0)}{p^2} + \\ + \frac{x_w(0)}{p^3} + \dots \quad (***)$$

and substitute the proposed solution for the special case (***) in equation (3-25b). The result, in view of its unwieldiness, we will consider limited — by lines for the identical coefficients a_{jk} and by columns for the identical degrees p:

$$a_{00} \left[M_1 p + M_0 + \frac{x_w(0)}{p} + \frac{x_w(0)}{p^2} \dots \right];$$

$$+ a_{01} \left[-M_1 + 0 + \frac{x_w(0)}{p^2} \dots \right];$$

$$+ a_{10} \left[M_1 p^2 + M_1 p + x_w(0) + \frac{x_w(0)}{p} + \\ + \frac{x_w(0)}{p^2} \dots \right];$$

$$+ a_{21}\left[-2M_1 p - M_0 + 0 + \frac{\dot{x}_1(0)}{p^2} + \dots\right];$$

$$+ a_{20}\left[M_1 p^3 + M_0 p^2 + x_{out}(0) p + \dot{x}_{out}(0) + \frac{\ddot{x}_{out}(0)}{p} + \right.$$

$$\left. + \frac{\dddot{x}_{out}(0)}{p^2} + \dots\right];$$

$$+ a_{21}\left[-3M_1 p^2 - 2M_0 p - x_{out}(0) + 0 + \right.$$

$$\left. + \frac{\ddot{x}_{out}(0)}{p^2} + \dots\right] = p^3.$$

The identical equality of the left and right sides is assured only when there is coincidence of the coefficients at identical powers p in both sides. We will call the operation of equating the coefficients the balance of the partial representations. The balances begin with the highest power p and are used to determine the sought M_0 and $x_{out}^{(\cdot)}(0)$ entering the proposed solution (***).

The balance for p^3 is: $a_{20}M_1 = 1; \qquad M_1 = \frac{1}{a_{20}}.$

The balance for p^2 is:

$$(a_{10} - 3a_{21})M_1 + a_{20}M_0 = 0. \qquad M_0 = \frac{3a_{21} - a_{10}}{a_{20}}.$$

The balance for p^1 is:

$$(a_{00} - 2a_{11})M_1 + (a_{10} - 2a_{21})M_0 + a_{20}x_{out}(0) = 0;$$

— 184 —

$$\chi_s(0) = \frac{1}{a_{31}^2} \{(2a_{11} + a_{50})a_{60} + (2a_{21} - $$

$$ - a_{10})(5a_{51} - a_{50})\}.$$

The balance for p^0 is:

$$ - a_{11}\,\mathcal{U}_1 + (a_{60} - a_{51})\,\mathcal{K}_0 + (a_{10} - a_{50})\,\chi_s(0) + $$

$$ + a_{10}\,\chi_{s1}(0) = 0.$$

If we continue to solve the balances for negative powers p, we find the desired number of components of series (**), the beginning of which has the form:

$$\chi_s(t) = \frac{1}{a_{50}}\,\delta(t) + \frac{3a_{51}}{a_{51}^2}\,\frac{a_{50}}{a}\,\delta(t) + $$

$$ + \chi_s(0)\,1(t) + \chi_{s1}(0)\,1(t) + \dots$$

It is easily noted that for different forms of equations only the coefficients a_{ij} vary, and their coefficient which enter the equation remain unchanged.

In order to simplify the organization of the calculations Table .. has been compiled, in which the rough coefficients of the equation (**) are given, and also the coefficients obtained as a result of multiplication of series (***) by p^i in accordance with the order of the equation ($i = 1, \dots, 6$) and as a result of differentiation with respect to t in accordance with the power of the argument that approximates the coefficients. A non-complicated order of argument ($k = 0, 1, 2, 3$) is assumed.

If we designate the functions located in the blocks of the table as F_{ij}, where the coordinates of the block are indicated in the index (i is the number of the derivative at which the coefficient stands; j is the exponent in the expansion of the coefficient); Z is the exponent of p; and on the right side the B_k coefficients at the power p^k, we obtain the balance of the partial representations in the form:

$$\sum_{i=0}^{n}\sum_{j=0}^{6} F_{ij}a_{ij} = B_k \qquad (3.2)$$

This served as the basis for the naming of the method adopted by us [1].

It is necessary to start the solution of the equations of balances from the column containing the highest of the possible $(3-25b)$ moments M_ν for the case $\nu \geq n$. If the order of the impulse in the right side is less than the order of the equation or equal to it $(\nu < n)$, the general solution $(3-25d)$ is begun with the $(n - \nu - 1)$th derivative:

$$x_c(t) = \sum_{\varkappa = n - \nu - 1}^{\infty} \frac{x_{out}^{(\varkappa)}(0)}{\varkappa!} (t)^{\varkappa}, \qquad (3\text{-}28a)$$

If the input action is gradual, the solution will contain a still smaller number of lower terms of the series:

$$h(t) = \sum_{\varkappa = n}^{\infty} \frac{x_{out}^{(\varkappa)}(0)}{\varkappa!} (t)^{\varkappa}, \qquad (3\text{-}28b)$$

In that case the solution of the equations of balances is begun at the column containing the lowest initial derivative, the order of which constitutes $\varkappa = n$.

Increase of the order $M_{c\ max}$ or lowering of the order $x_{out}^{(\varkappa\ min)}(t)$ in the proposed solution does not lead to errors, since the verifying balances according to the table columns for high powers p automatically manifest zero and non-zero coefficients.

9. Example of Solution in the Form of a Convergent Series

Let a second-order equations of connection with linearly varying coefficients of the form:

$$\ddot{\psi}(t) + 2[1 + \sigma t]\dot{\psi}(t) +$$
$$+ [2\tau + (\Omega^2 + \sigma^2) t] \psi(t) =$$
$$= [2\tau + (\Omega^2 + \sigma^2) t] x(t).$$

be given for a linear system.

It is required to find the reaction of the system to a displaced impulse, that is, its weight function. First of all we will determine the function for the right side:

$$n(t) = [2\tau + (\Omega^2 + \sigma^2) t] \delta(t - \theta) =$$
$$= [2\tau + (\Omega^2 + \sigma^2) \theta] \delta(t - \theta).$$

It is reproduced by a displaced impulse of a determined area.

As was noted in Section 1-1, it is convenient to assume as the start of the time reading the moment of application of the input action $\tau = 0$. After change of the argument the given equation is transformed:

$$(\theta + \tau)\ddot{y}(\tau) + 2[1 + \sigma(\theta + \tau)]\dot{y}(\tau) +$$

$$+ [2\sigma + (\Omega^2 + \sigma^2)(\theta + \tau)]y(\tau) =$$

$$= [2\sigma + (\Omega^2 + \sigma^2)\theta]\delta(\tau).$$

For the solution we will compile a calculating table analogous to Table 3-2 but with a reduced number of columns in accordance with the type of equations being solved (Table 3-4). In addition, it is convenient to change the places of the columns and rows and to introduce an additional row a_i for notation of the actual values of the coefficients of the equation. The values from the corresponding column of Table 3-4 are put in the window, multiplied by the coefficients of the equation. This permits obtaining by rows ready balances of the partial representations upon writing in the first column not only the lower y but also the coefficient θ corresponding to it. The solution of the balances is written in the last column of Table 3-4 for the first three lines in expanded form and from then on in the form of the sum of the numbers Σz_i in five columns, excluding columns $i = 1$, $k = 0$.

Assuming in the obtained initial values of the derivatives, on the basis of Maclaurin series, we write the solution in the form of a power series:

$$y(\tau, \theta) = \left(\frac{2\sigma}{\theta} + \Omega^2 + \sigma^2\right)\left[\tau - 2\left(\frac{1}{\theta} + \sigma\right)\frac{\tau^2}{2!} + \right.$$

$$+ 6\left(\frac{2}{\theta} + \frac{1}{\theta^2} + \frac{\sigma^2}{2} - \frac{\Omega^2}{6}\right)\frac{\tau^3}{3!} +$$

$$\left. + y^{(IV)}(0)\frac{\tau^4}{4!} + \ldots\right]$$

This series can be condensed:

$$y(\tau, \theta) = \frac{2\sigma + (\Omega^2 + \sigma^2)\theta}{\Omega(\theta + \tau)} e^{-\sigma\tau}\sin\Omega\tau. \qquad (*)$$

Table 3.3 Values of the Functions F_{ik} et Coefficients z_{ik}

Entering the Equation of Balance of Partial Representations (3-27)

i	k	F^6	F^5	F^4	F^3	F^2	F^3	F	
0	0					M_3	M_2	M_1	M_3
	1							$-2M_2$	$-M_1$
	2								$2M_2$
	3								
1	0			M_3		M_2	M_3	M_3	$x(0)$
	1						$-3M_2$	$-2M_3$	$-M_6$
	2							$6M_2$	$2M_1$
	3								$-6M_2$
2	0			M_3	M_1		M_6	$x(0)$	$x(0)$
	1				$-M_2$		$-3M_2$	$-2M_2$	$-x(0)$
	2						$12M_2$	$6M_1$	$2M_2$
	3							$-24M_2$	$-6M_1$

3	0	M_0			M_2	M_1	M_0	$x(0)$	$x(0)$	$x(0)$
	1				$-5M_3$		$-3M_3$	$-2x(0)$	$-x(0)$
	2				$20M_2$		$12M_2$	$6x_2$	$2x(0)$
	3						$-30M_2$	$-24M_3$	$-6M_3$
4	0	M_3		M_2	$x(0)$	M_0	$x(0)$	$x(0)$	$x(0)$
	1			$-6M_2$	$-4M_0$	$-5M_1$	$-3x(0)$	$-5x(0)$	$-x(0)$
	2				$20M_1$	$30M_0$	$12M_0$	$6x(0)$	$2x(0)$
	3				$-120M_0$		$-30M_0$	$-24M_0$	$-x(0)$
5	0	M_0	M_7	M_5	$x(0)$	$x(0)$	$x(0)$	$x(0)$	$x^{(IV)}(0)$
	1		$-8M_1$	$-6M_3$	$-4x(0)$	$-5M_0$	$-3x(0)$	$-2x(0)$	$-5x(0)$
	2			$42M_2$	$20M_0$	$30M_1$	$12x(0)$	$6x(0)$	$2x(0)$
	3			$-120M_2$	$-120M_1$	$-210M_2$	$-30M_0$	$-24x(0)$	$-5x(0)$
6	0	M_7	M_7	M_4	$x(0)$	$x(0)$	$x(0)$	$x^{(IV)}(0)$	$x^{(IV)}(0)$
	1		$-8M$	$-6M_3$	$-4x(0)$	$-5x(0)$	$-3x(0)$	$-2x(0)$	$-x^{(IV)}(0)$
	2		$54M_2$	$42M_3$	$20x(0)$	$30x(0)$	$12x(0)$	$6x(0)$	$2x(0)$
	3			$-135M_3$	$-210M_2$	$-210M_2$	$-30x(0)$	$-24x(0)$	$-6x(0)$

[Right side of table continues on page 175]

Table 3-4   Solution by the Method of Balance of Partial
Representations of Equations

$$(\vartheta + \tau)\ddot{y} + 2[1 + \sigma(\vartheta + \tau)]\dot{y} + [2\sigma + (\Omega^2 + \sigma^2)(\vartheta + \tau)]y = [2\sigma + (\Omega^2 + \sigma^2)\vartheta]\delta[\tau]$$

$H(p)$ \ a_{ik}	$i = 0$	
	$k = 0$	$k = 1$
	$2\sigma + (\Omega^2 + \sigma^2)\vartheta$	$\Omega^2 + \sigma^2$
$[2\sigma + (\Omega^2 + \sigma^2)\vartheta]p^0$	—	—
$0 \cdot p^{-1}$	—	—
$0 \cdot p^{-2}$	$[2\sigma + (\Omega^2 + \sigma^2)\vartheta]\dot{y}$	—
$0 \cdot p^{-3}$	$[2\sigma + (\Omega^2 + \sigma^2)\vartheta]\ddot{y}(0)$	$2(\Omega^2 + \sigma^2)\dot{y}(0)$
$0 \cdot p^{-4}$	$[2\sigma + (\Omega^2 + \sigma^2)\vartheta]\dddot{y}(0)$	$3(\Omega^2 + \sigma^2)\ddot{y}(0)$
$0 \cdot p^{-5}$	$[2\sigma + (\Omega^2 + \sigma^2)\vartheta]y^{(IV)}(0)$	$4(\Omega^2 + \sigma^2)\dddot{y}(0)$

$i=1$		$i=2$		$y^i(0)$
$k=0$	$k=1$	$k=0$	$k=1$	
$2(1-s\theta)$	$2s$	θ	1	
—	—	$\theta \dot{y}(0)$	—	$\dot{y}(0) = \dfrac{2a}{\theta} + \Omega^2 + s^2$
$2(1-s\theta)\dot{y}(0)$	—	$\theta \ddot{y}(0)$	—	$\ddot{y}(0) = -2\left(\dfrac{1}{\theta} + s\right)\dot{y}(0)$
$2(1+s\theta)\ddot{y}(0)$	$2s\dot{y}(0)$	$\theta \dddot{y}(0)$	$\ddot{y}(0)$	$\dddot{y}(0) = 6\left(\dfrac{s}{\theta} + \dfrac{1}{\theta^2} + \dfrac{s^2}{3} - \dfrac{\Omega^2}{3}\right)\dot{y}(0)$
$2(1+s\theta)\dddot{y}(0)$	$4s\ddot{y}(0)$	$\theta y^{(IV)}(0)$	$3\dddot{y}(0)$	$y^{(IV)}(0) = -\dfrac{1}{\theta}\sum_{i=1}^{3} I_{i}$
$2(1+s\theta)y^{(IV)}(0)$	$6s\dddot{y}(0)$	$\theta y^{(V)}(0)$	$3 y^{(IV)}(0)$	$y^{(V)}(0) = -\dfrac{1}{\theta}\sum_{i=1}^{3} I_{i}$
$2(1+s\theta)y^{(V)}(0)$	$8s y^{(IV)}(0)$	$\theta y^{(VI)}(0)$	$4 y^{(V)}(0)$	$y^{(VI)}(0) = -\dfrac{1}{\theta}\sum_{i=1}^{3} I_{i}$

Now we will turn to the basic time reference:

$$y(t - \vartheta, \vartheta) = \omega_2(t, \vartheta) =$$

$$= \frac{2\eta \pm (\Omega^2 + \sigma^2)\,\vartheta}{\Omega_1}\, e^{-\sigma\,(t-\vartheta)} \sin \Omega\,(t - \vartheta). \qquad (**)$$

The given equation did not have derivatives on the right side. If additional terms appear, containing derivatives, it is possible to proceed on the basis of formula (2-43), as we have the solution of the simple equation.

If we know the weight function (**), we can find the reaction (2-43) for any input process. But if the representation of the input process is reduced to a series according to the powers p, the solution can be carried out at once by the method of balance of the partial representations for the complete output process.

Let us dwell briefly on the accuracy of the method of balance of the representations.

1. At a precise analytical assignment of the coefficients in the form of polynomials and in the presence of the possibility of contracting the series which represents the solution, as was obtained in the example given above, there are no errors in principle.

2. If the series is not contracted and it is necessary to use a limited number of terms of the series, the discarded terms give the error. A converging sign-variable series has an error which is less than the first discarded term. If the convergence is attained only in a very small time interval, then actually only the initial part of the process is determined.

3. If the variable coefficients were set not by polynomials, but by experimental graphs or other functions, their approximation by polynomials always will be approximate, with an error that increases in proportion to the interval of approximation at the given power of the polynomial.

4. The possibilities of analytical solution must not be over-estimated. Complex problems with variable parameters are more rapidly solved on electronic models. In that case, Table 3-3 facilitates a rapid discarding of the initial section of the process, and in the presence of impulse actions permits rapidly calculating the equivalent initial conditions that may be introduced into the model.

3. The Determination of Impulse Actions Equivalent to the Assigned Initial Conditions

A similar problem was solved in chapter 2 for equations given in the general form (2-60), and in the same place for a particular example — a second-order component. We will solve the same example by the operational method by means of Table 3-3. Thus the solution of a homogeneous equation

Table 3.5 Calculating Table for the solution of equation
(3-32) in the form of a Series

$f(t)$	$a_i = -1$ $i=0$	$a_i = -2$ $i=1$	$a_i = t$ $i=2$	Преднее уравнений 6-ниже изображения $\bigodot$
$h(t)$	$h(0)$			
$t, p - 1$		$t^2 h'(0)$	$t^2 h'(0)$	$g(0) = \dfrac{k}{\tau}$
$0, p - 2$		$t^2 h''(0)$	$t^2 h''(0)$	$g'(0) = \dfrac{2k}{\tau}$
$6, p - 3$	$h(0)$	$t^2 h^{(IV)}(0)$	$t^2 h^{(IV)}(0)$	$h^{(IV)}(0) = \dfrac{(4k^2 - 1)k}{\tau^4}$
$0, p - 4$	$\bar{h}(0)$	$t^2 h^{(IV)}(0)$	$t^2 h^{(IV)}(0)$	$h^{(V)}(0) = \dfrac{8k(k^2 - 1)k}{\tau^4}$

1. Solution of equations of balance of representations

$$a_2(t)\ddot{x}(t) + a_1(t)\dot{x}(t) + a_0(t)x(t) = 0 \qquad (3\text{-}29)$$

is examined at given initial conditions $x(0)$, $\dot{x}(0)$.

We will translate equation (3-29) into the equation for the initial functions:

$$a_2(t)\ddot{x}(t) + a_1(t)\dot{x}(t) + a_0(t)x(t) =$$
$$= B_0\delta(t) + B_1\dot{\delta}(t), \qquad (3\text{-}30)$$

in which $x(0+)$ and $\dot{x}(0+)$ are unknown and it is required to determine the moments of the impulses in the equivalent input action: B_0 and B_1.

From the conditions of balance according to column p^1 of Table 3-1, in which we use only the rows $k = 0, 1, 2$, we have:

$$a_2(0)\dot{x}(0+) = B_1. \qquad (3\text{-}31a)$$

From the conditions of balance according to column p^0 we get:

$$[a_1(0) - \dot{a}_2(0)]x(0+) + a_2(0)\dot{x}(0+) = B_0. \qquad (3\text{-}31b)$$

The result coincides with the solution of this example in Section 2-9b. The balances according to the remaining columns p^k ($k < 0$) of Table 3-1 give solutions for the subsequent initial derivatives which permit obtaining the process of the aftereffect in the form of a series.

B. Obtaining the Solution in the Form of a Series for a Component with Constant Parameters

In this case in Table 3-1 only the rows $k = 0$ are used. We will calculate for the sake of example the transient function of an oscillatory component according to the equation

$$\ddot{h} + 2\xi\dot{h} + h = \xi 1(t). \qquad (3\text{-}32a)$$

Let us prepare the calculating table.

If we use the data of the last column of the table, we get the transient function in the form of a series:

$$h(t) = k\left\{\frac{1}{2!}\left[\frac{t}{\tau}\right]^3 - \frac{2\xi}{3!}\left[\frac{t}{\tau}\right]^2 + \right.$$

$$+ \frac{(4\xi^2-1)}{4!}\left[\frac{t}{\tau}\right]^4 - \frac{8\xi(\xi^2-1)}{5!}\times$$

$$\left. \times \left[\frac{t}{\tau}\right]^5 + \dots \right\}, \qquad (3\text{-}32\mathbf{b})$$

which can be contracted into a single function (3-43b).

The method of determination of initial sections of processes in systems with variable and constant coefficients permits making the calculation of the entire process by sections [4].

3-7. The Forced Motion of Components with Constant Parameters

A. Separation of the Output Reaction of a Component into Forced and Proper Motion

Let a control process, the representation of which is

$$W(p) = \frac{b(p)}{a(p)},$$

be supplied on the input of a component which has the DFT

$$X_{*}(p) = \frac{\beta(p)}{\alpha(p)}.$$

Then on the output we have:

$$X_{*}(p) = \frac{\beta(p)\,b(p)}{\alpha(p)\,a(p)}.$$

The fraction obtained can be decomposed into the sum of simple fractions if the root-poles z_i of the common denominator $a(z_i)\alpha(z_i) = 0$ are known. But for subsequent derivations it is possible to preserve the individual expressions for the denominator of the representation of the input process and the denominator of the transfer function, and therefore the fraction is divided in all into two terms:

$$X_{out}(p) = \frac{U_x(p)}{\alpha(p)} + \frac{U_{y}(p)}{a(p)} \qquad (3\text{-}33a)$$

with the denominators and representations respectively of the input signal and the DFT of the component. Such a separation is usually successfully made only by grouping the determined very simple fractions in advance.

This separation of the representations corresponds to a separa-

tion of the time process into two parts.

The first part of the process, the representation of which contains only poles of representation of the input process, we will call the forced motion:

$$X_{forc}(p) = \frac{U_x(p)}{a(p)} + x_{forc}(t) \qquad (3-33b)$$

The second part of the process, which has a transfer function in the region of representation of the pole, we will call the proper motion:

$$X_{proper}(p) = \frac{U_{x}(p)}{a(p)} + x_{proper}(t) \qquad (3-33c)$$

Only the forced motion will be examined in this section.

B.   The Case of Elementary Actions Without Short Poles

1.   Exponentially Damping Control Action:

The representation of the input action

$$X_N(p) = \frac{1}{p - \gamma_i} \qquad (3-34a)$$

has a single root of the denominator — the pole $a_i = \gamma_i$. If it is equal to the negative real number $\gamma_i = -\sigma$, then representation (3-34a) corresponds to an exponentially damping process:

$$x_{iN}(t) = e^{-\sigma t}.$$

The representation of the output reaction will be written in full form and in a form separated into components (3-35a):

$$X_{out}(p) = \frac{W(p)}{p - \gamma_i} = \frac{B}{p - \gamma_i} + X_{proper}(p) \qquad (*)$$

The case of non-coincidence of the pole of the input action with no single pole of the OTF of the component is examined; then, if we are rid of the denominator in (*), we arrive at the formula

$$W(p) = B + (p - \gamma_i) X_{proper}(p), \qquad (*)$$

in which for determination of the scale of the forced reaction B it is sufficient to assume $p = \gamma_i$, which gives: $B = W(\gamma_i)$.

— 132 —

Consequently,

$$X_{forc}(p) = \frac{W(\eta)}{p - \eta} = W(\eta) X_{in}(p). \qquad (3\text{-}34b)$$

Thus the forced reaction coincides in form with the input action (3-34a) independently of the OPT of the component, which during the substitution of $p = \eta$ determines only the scale of the forced reaction. The calculations that have been given are illustrated in Figure 3-6a.
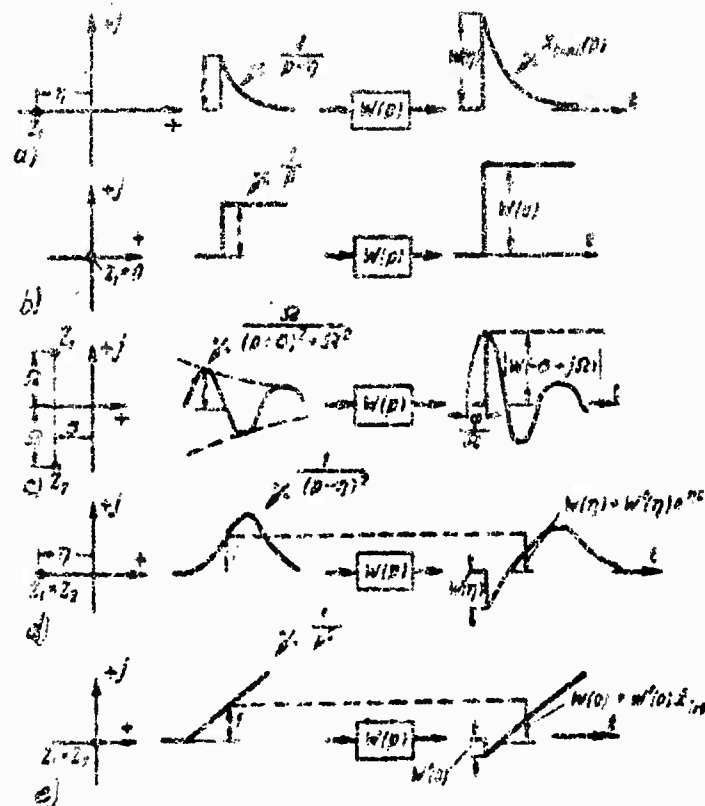
Fig 3-6. Disposition of the poles of the elementary control processes and forced reaction of an arbitrary component.

2. Stepwise Action

For the single input action

$$X_{in}(p) = \frac{1}{p} \doteq 1(t) \qquad (3\text{-}35a)$$

the pole is a zero one, $z_1 = 0$, which permits, from formula (3-34b), obtaining the corollary

$$H_{forc}(p) = \frac{W(0)}{p} \doteq W(0)\,1(t). \qquad (3\text{-}35b)$$

Thus the forced component of the transient function repeats the input step on a scale $W(0)$ for all types of components which do not have zero poles of the OPT (Figure 3-6b).

3. Harmonic Damping Action

The representation of the initial damping sine

$$X_{in}(p) = \frac{\Omega}{(p+\sigma)^2 + \Omega^2} \qquad (3\text{-}36a)$$

(see Table 3-1) has two poles: $z_1 = -\sigma + j\Omega$ and $z_2 = -\sigma - j\Omega$ and can be expanded into the sum of two simple fractions:

$$X_{in}(p) = \frac{1}{2j}\left(\frac{1}{p+\sigma-j\Omega} - \frac{1}{p+\sigma+j\Omega} \right).$$

By virtue of (3-34b) the output reaction will be composed of two complex representations

$$X_{forc}(p) = \frac{1}{2j}\left[\frac{W(-\sigma+j\Omega)}{p+\sigma-j\Omega} - \frac{W(-\sigma-j\Omega)}{p+\sigma+j\Omega} \right], \quad (3\text{-}36b)$$

that is, the complex input processes bring about analogous reactions, in form, with the scale

$$W(-\sigma+j\Omega) \quad \text{or} \quad W(-\sigma-j\Omega).$$

If the real and imaginary parts are separated in the scale coefficients:

$$W(-\sigma+j\Omega) = \operatorname{Re} W(-\sigma+j\Omega) + j\operatorname{Im} W(-\sigma+j\Omega);$$
$$W(-\sigma-j\Omega) = \operatorname{Re} W(-\sigma+j\Omega) - j\operatorname{Im} W(-\sigma+j\Omega),$$

then after transformation the representation of the forced reaction is written in the real form

$$X_{forc}(p) = \frac{\Omega \operatorname{Re} W(-s+j\Omega) + (p+c)\operatorname{Im} W(-s+j\Omega)}{(p+s)^2 + \Omega^2}$$

$$(3\text{-}36c)$$

If the complex representations are also drawn in for the conclusion, there are always two of them, conjugates (3-36b) with mutually suppressing imaginary components.

If we introduce the designations of the module and phase:

$$|W(-s+j\Omega)| = \sqrt{\operatorname{Re}^2 W(-s+j\Omega) + \operatorname{Im}^2 W(-s+j\Omega)},$$

$$\operatorname{tg}\varphi = \frac{\operatorname{Im} W(-s+j\Omega)}{\operatorname{Re} W(-s+j\Omega)},$$

we get the real process:

$$x_{forc}(t) =$$

$$= |W(-s+j\Omega)|\, e^{-st} \sin\left[\Omega t + \operatorname{arctg}\frac{\operatorname{Im} W(-s+j\Omega)}{\operatorname{Re} W(-s+j\Omega)}\right].$$

$$(3\text{-}37)$$

The form of the forced summary reaction is shown in Figure 3-6c. Upon substitution of $\sigma = 0$ the forced reaction on non-damping harmonic action is readily obtained from it, and this will be examined in detail in the following chapter.

C. The Case of Elementary Actions with Short Poles

4. Short Real Poles

The representation of the form

$$X_{in}(p) = \frac{1}{(p-r_1)^m}$$

$$(3\text{-}38a)$$

has identical poles $z_{1 \ldots m} = r_1$ of the m-th shortness and according to Table 3-1 described at $r_1 = -\sigma$ the process

$$X_{in}(t) = \frac{t^{m-1}}{(m-1)!}\, e^{-\sigma t},$$

shown in Figure 3-6 d for $m = 2$.

The complete output reaction, by virtue of the rules of expansion into elementary fractions, must contain both the highest power of $p - r_1$ in the denominator, as well as all the lower:

$$X_{\text{set}}(p) = \frac{W(p)}{(p-\eta)^m} = \frac{B_m}{(p-\eta)^m} + \frac{B_{m-1}}{(p-\eta)^{m-1}} + \cdots$$

$$\cdots + \frac{B_1}{p-\eta} + X_{\text{proper}}(p). \qquad (*)$$

According to the determination, m terms of the expansion relate to the forced reaction, and the last term to proper motion. It is supposed that the poles of the input action do not coincide with a single pole of the OFT of the component.

We will rid ourselves in (*) of the highest power of the denominator:

$$W(p) = B_m + (p-\eta)B_{m-1} + \cdots$$

$$\cdots + (p-\eta)^{m-1}B_1 + (p-\eta)^m X_{\text{proper}}(p).$$

If we differentiate i times ($i = 0, 1, \ldots, m-1$) both sides of the obtained equality with respect to p and make the substitution of $p = \eta$, we find all the scales of the partial representations:

$$B_m = W(\eta);$$

$$B_{m-1} = W'(\eta);$$

$$B_{m-2} = \frac{1}{2!}W''(\eta);$$

$$\cdot \ \cdot \ \cdot \ \cdot \ \cdot \ \cdot \ \cdot \ \cdot$$

$$B_1 = \frac{W^{(m-1)}(\eta)}{(m-1)!}.$$

The general representation of the forced reaction is:

$$X_{\text{forc}}(p) = \frac{W(\eta)}{(p-\eta)^m} + \frac{W'(\eta)}{(p-\eta)^{m-1}} +$$

$$+ \frac{W''(\eta)}{2!(p-\eta)^{m-2}} + \cdots + \frac{W^{(m-1)}(\eta)}{(m-1)!(p-\eta)}. \qquad (3.38\,b)$$

Let us take out of the brackets the representation of the input action (3-38a):

$$X_{\text{forc}}(p) = \left[W(\eta) + W'(\eta)(p - \eta) + \right.$$

$$+ \frac{W''(\eta)}{2!}(p - \eta)^2 + \ldots + \frac{W^{m-1}(\eta)}{(m-1)!}(p - \eta)^{m-1} \left. \right] \times$$

$$\times \frac{1}{(p - \eta)^m}; \qquad (3\text{-}38c)$$

after which it is easy to write the forced reaction in the region time-original:

$$x_{\text{forc}}(t) = e^{\eta t} \left[W(\eta) + W'(\eta)D + \frac{W''(\eta)}{2!}D^2 + \ldots \right.$$

$$\ldots + \frac{W^{m-1}(\eta)}{(m-1)!}D^{m-1} \left. \right] \frac{t^{m-1}}{(m-1)!}. \qquad (3\text{-}38d)$$

In Figure 3-6d, for $m = 2$, is shown the sum of the two components of the forced reaction and is noted the value of the ordinates at the moment of time t_1, for which $x_{in}(t_1) = 1$.

5. Short Zero Poles

The representation of the form

$$X_{in}(p) = \frac{1}{p^m} \qquad (3\text{-}39a)$$

has m zero short poles: $z_{1,2\ldots m} = 0$ and corresponds to the stepwise function of time (Figure 3-6a, $m = 2$):

$$\frac{t^{m-1}}{(m-1)!} = x_{in}(t)$$

If we reason analogously to point 4 and assume $\eta = 0$, we arrive at the formulas for the forced reaction in the region of the representations:

— 197 —

$$x_{\text{Forc}}(t) = \left[W'(0) + W'(0)\, p + \frac{W''(0)}{2!}\, p^2 + \cdots \right.$$

$$\left. \cdots + \frac{W^{(m-1)}(0)}{(m-1)!}\, p^{m-1} \right] X_{in}(p) \qquad (3.39b)$$

and in the region of the originals:

$$x_{\text{Forc}}(t) = W'(0)\, x_{in}(t) + W'(0)\, \dot{x}_{in}(t) +$$

$$+ \frac{W''(0)}{2!}\, \ddot{x}_{in}(t) + \cdots + \frac{W^{(m-1)}(0)}{(m-1)!}\, x_{in}^{(m-1)}(t) \qquad (3.39c)$$

The forced reaction copies the input process with a scale $W(0)$, adding to it components proportional to the rate and the highest derivatives with scales and signs determinable by $W^{(r)}(0)/r!$ — in Figure 3-6e, $W'(0) < 0$.

E. Complex Summary Action

6. The Sum of Elementary Input Actions

On the basis of the principle of superposition in linear systems the sum of the reactions corresponds to the sum of the actions. At any number of elementary input actions their representations can be grouped in a single sum for all the non-short, including the zero and complex, poles, and the actions can be written separately for each new short pole:

$$X_{in}(p) = \sum_{j=0}^{s} \frac{A_j}{p - z_j} + \frac{A_1}{(p - z_1)^2} + \frac{A_2}{(p - z_2)^3} + \cdots$$

$$(3.40a)$$

We will designate the representations of the original correspon-ding to these:

$$x_{in}(t) = \sum_{j=0}^{s} x_j(t) + x_1(t) + x_2(t) + \cdots \qquad (3.40b)$$

Then the representation of the forced reaction is

$$X_{\text{для}}(p) = \sum_{j=0}^{k} W(z_j) X_j(p) + \sum_{j=0}^{k-1} \frac{W^{(j)}(z_j)(p - z_j)^j}{j!} X_j(p) +$$

$$+ \sum_{s=0}^{l-1} \frac{W^{(s)}(z_s)(p - z_s)^s}{s!} X_s(p) + \dots \qquad (3.40с)$$

The original of the forced reaction is reduced to the form

$$x_{\text{для}}(t) = \sum_{j=0}^{N} W(z_j) x_j(t) + \sum_{j=0}^{k-1} \frac{W^{(j)}(z_j)(D - z_j)^j}{j!} x_j(t) +$$

$$+ \sum_{s=0}^{l-1} \frac{W^{(s)}(z_s)(D - z_s)^s}{s!} x_s(t) \qquad (3.40d)$$

Thus for any component the forced reaction is formed of elementary input processes and their derivatives, summated with scales determinable by substitution in the transfer of the component or, in the derivatives with respect to p at the differential of the component, of the numeric representations of the input actions instead of the argument p.

4. The Proper Reaction of Components with Constant Parameters

1. The reaction of a Complex Signal through Elementary Components

1. The aperiodic Component

If a signal $x_V(t)$ excites in a component with the transfer function

$$W(p) = \frac{1}{Tp + 1} \qquad (3.41a)$$

the reaction

$$x_{cs}(p) = \frac{k X_V(p)}{Tp + 1} = \frac{Ch}{Tp + 1} + X_{\text{для}}(p) \qquad (*)$$

which is separable into the proper and forced components.

The proper component copies the weight function of an aperiodic

on the scale c, which is readily found by multiplying (?) by $Tp + 1$:

$$k\,X_{in}(p) = (k + (Tp + 1)\,X_{prep}(p)$$

and substituting $p = -(1/T)$:

$$c = X\left(-\frac{1}{T}\right).$$

From this we get the representation of the proper motion:

$$X_{proper}(p) = X_{s}\left(-\frac{1}{T}\right)\frac{k}{Tp+1} = X_{in}\left(-\frac{1}{T}\right)W(p)$$

(3.41b)

and the original:

$$x_{proper}(t) = X_{in}\left(-\frac{1}{T}\right)\frac{k}{T}e^{-\frac{t}{T}} = X_{in}\left(-\frac{1}{T}\right)\omega(t)$$

(3.41a)

In the presence of any form of the input process it excites the proper motion only in the form of the weight function with the scale c_p equal to the representation of the input action during replacement of p by the pole of the transfer function.

The Oscillating component

For the transfer function of an oscillating component

$$\frac{k}{\tau^2 p^2 + 2\xi\tau p + 1}$$

we find two poles:

$$z_1 = \frac{-\xi + j\sqrt{1-\xi^2}}{\tau},$$

$$z_2 = \frac{-\xi - j\sqrt{1-\xi^2}}{\tau}$$

and expand it into two complex CFF's of the first order

$$\frac{k}{\tau^2 p^2 + 2\xi\tau p + 1} = \frac{k}{\tau^2}\cdot\frac{1}{\ldots} \times$$

- 196 -

$$\times \frac{1}{2j} \left(\frac{1}{p + \frac{\xi - j\sqrt{1 - \xi^2}}{\tau}} - \frac{1}{p + \frac{\xi + j\sqrt{1 - \xi^2}}{\tau}} \right).$$

$$(3\text{-}42a)$$

In these CFI's, in accordance with the case in point 1 of this section, two components of the proper motion are excited:

$$X_{\text{proper}}(p) = \frac{k}{2j\tau\sqrt{1 - \xi^2}} \left[\frac{X_{\text{in}}\left(\frac{-\xi + j\sqrt{1 - \xi^2}}{\tau} \right)}{p + \frac{\xi - j\sqrt{1 - \xi^2}}{\tau}} - \frac{X_{\text{in}}\left(\frac{-\xi - j\sqrt{1 - \xi^2}}{\tau} \right)}{p + \frac{\xi + j\sqrt{1 - \xi^2}}{\tau}} \right]. \qquad (*)$$

If we expand the representation of the input process with displaced argument to the real and imaginary constituents:

$$X\left(\frac{-\xi + j\sqrt{1 - \xi^2}}{\tau} \right) = \operatorname{Re} X_{\text{in}}\left(\frac{-\xi + j\sqrt{1 - \xi^2}}{\tau} \right) + $$

$$+ j \operatorname{Im} X_{\text{in}}\left(\frac{-\xi + j\sqrt{1 - \xi^2}}{\tau} \right),$$

$$X\left(\frac{-\xi - j\sqrt{1 - \xi^2}}{\tau} \right) = \operatorname{Re} X_{\text{in}}\left(\frac{-\xi + j\sqrt{1 - \xi^2}}{\tau} \right) - $$

$$- j \operatorname{Im} X_{\text{in}}\left(\frac{-\xi + j\sqrt{1 - \xi^2}}{\tau} \right),$$

It is possible to reduce the representation of the proper motion (*) to the real form:

$$X_{proper.}(p) = \frac{k}{\tau\sqrt{1-\xi^2}} \times$$

$$\times \frac{\frac{\sqrt{1-\xi^2}}{\tau} \operatorname{Re} X_{in}\left(\frac{-\xi + j\sqrt{1-\xi^2}}{\tau}\right) +}{\left(p + \frac{\xi}{\tau}\right)^2 +}$$

$$\frac{+ \left(p + \frac{\xi}{\tau}\right)\operatorname{Im} X_{in}\left(\frac{-\xi + j\sqrt{1-\xi^2}}{\tau}\right)}{+ \left(\frac{\sqrt{1-\xi^2}}{\tau}\right)^2}$$

by designating

$$\operatorname{tg}\varphi = \frac{\operatorname{Im} X_{in}\left(\frac{-\xi + j\sqrt{1-\xi^2}}{\tau}\right)}{\operatorname{Re} X_{in}\left(\frac{-\xi + j\sqrt{1-\xi^2}}{\tau}\right)},$$

we find, finally, the representation of the proper motion

$$X_{proper}(p) = \frac{k}{\tau\sqrt{1-\xi^2}} X_{in}\left(\frac{-\xi + j\sqrt{1-\xi^2}}{\tau}\right) \times$$

$$\times \frac{\frac{\sqrt{1-\xi^2}}{\tau}\cos\varphi + \left(p + \frac{\xi}{\tau}\right)\sin\varphi}{\left(p + \frac{\xi}{\tau}\right)^2 + \left(\frac{\sqrt{1-\xi^2}}{\tau}\right)^2} \qquad (3\text{-}42\,b)$$

and the original corresponding to it

$$X_{proper}(t) = \frac{k}{\tau\sqrt{1-\xi^2}} X_{in}\left(\frac{-\xi + j\sqrt{1-\xi^2}}{\tau}\right) \times$$

$$\times e^{-\frac{\xi t}{\tau}}\sin\left[\frac{t}{\tau}\sqrt{1-\xi^2} + \operatorname{arctg}\frac{\operatorname{Im} X}{\operatorname{Re} X}\right]. \qquad (3\text{-}42\,c)$$

$$X_{proper}(p) = \frac{k}{\tau \sqrt{1-\xi^2}} \times$$

$$\times \frac{\dfrac{\sqrt{1-\xi^2}}{\tau} \operatorname{Re} X_{in}\left(\dfrac{-\xi + j\sqrt{1-\xi^2}}{\tau}\right) +}{\left(p + \dfrac{\xi}{\tau}\right)^2 +}$$

$$\frac{+\left(p + \dfrac{\xi}{\tau}\right) \operatorname{Im} X_{in}\left(\dfrac{-\xi + j\sqrt{1-\xi^2}}{\tau}\right)}{+\left(\dfrac{\sqrt{1-\xi^2}}{\tau}\right)^2}$$

by designating

$$\operatorname{tg} \varphi = \frac{\operatorname{Im} X_{in}\left(\dfrac{-\xi + j\sqrt{1-\xi^2}}{\tau}\right)}{\operatorname{Re} X_{in}\left(\dfrac{-\xi + j\sqrt{1-\xi^2}}{\tau}\right)},$$

we find, finally, the representation of the proper motion

$$X_{proper}(p) = \frac{k}{\tau\sqrt{1-\xi^2}} X_{in}\left(\frac{-\xi + j\sqrt{1-\xi^2}}{\tau}\right) \times$$

$$\times \frac{\dfrac{\sqrt{1-\xi^2}}{\tau}\cos\varphi + \left(p + \dfrac{\xi}{\tau}\right)\sin\varphi}{\left(p + \dfrac{\xi}{\tau}\right)^2 + \left(\dfrac{\sqrt{1-\xi^2}}{\tau}\right)^2} \qquad (3.42 b)$$

and the original corresponding to it

$$X_{proper}(t) = \frac{k}{\tau\sqrt{1-\xi^2}} X_{in}\left(\frac{-\xi + j\sqrt{1-\xi^2}}{\tau}\right) \times$$

$$\times e^{-\frac{\xi t}{\tau}} \sin\left[\frac{t}{\tau}\sqrt{1-\xi^2} + \operatorname{arctg}\frac{\operatorname{Im} X}{\operatorname{Re} X}\right]. \quad (3.42 c)$$

$$\times \frac{1}{2j} \left(\frac{1}{p + \dfrac{\xi - j\sqrt{1-\xi^2}}{\tau}} - \frac{1}{p + \dfrac{\xi + j\sqrt{1-\xi^2}}{\tau}} \right).$$

$$(3\text{-}42a)$$

In these CFT's, in accordance with the case in point 1 of this section, two components of the proper motion are excited:

$$X_{proper}(p) = \frac{k}{2j\tau\sqrt{1-\xi^2}} \left[\frac{X_{in}\left(\dfrac{-\xi + j\sqrt{1-\xi^2}}{\tau} \right)}{p + \dfrac{\xi - j\sqrt{1-\xi^2}}{\tau}} \right.$$

$$\left. - \frac{X_{in}\left(\dfrac{-\xi - j\sqrt{1-\xi^2}}{\tau} \right)}{p + \dfrac{\xi + j\sqrt{1-\xi^2}}{\tau}} \right] \qquad (*)$$

If we expand the representation of the input process with displaced argument to the real and imaginary constituents:

$$X\left(\frac{-\xi + j\sqrt{1-\xi^2}}{\tau} \right) = \mathrm{Re}\, X_{in}\left(\frac{-\xi + j\sqrt{1-\xi^2}}{\tau} \right) +$$

$$+ j\,\mathrm{Im}\, X_{in}\left(\frac{-\xi + j\sqrt{1-\xi^2}}{\tau} \right),$$

$$X\left(\frac{-\xi - j\sqrt{1-\xi^2}}{\tau} \right) = \mathrm{Re}\, X_{in}\left(\frac{-\xi + j\sqrt{1-\xi^2}}{\tau} \right) -$$

$$- j\,\mathrm{Im}\, X_{in}\left(\frac{-\xi + j\sqrt{1-\xi^2}}{\tau} \right),$$

It is possible to reduce the representation of the proper motion (*) to the real form:

The general formula for the proper action of the oscillating component, expressed by its weight function, shows that the character of the input process determines only the scale

$$\left| X_{in}\left(\frac{-1 + j\sqrt{1-\beta^2}}{2} \right) \right|$$

and phase shift φ of the weight function of the component.

Example 1. Calculation of the weight function of an oscillating component.

$$X_{in}(p) = 1; \quad |X_1| = 1 = \operatorname{Re} X_{in};$$
$$\operatorname{Im} X_{in} = 0; \quad \varphi = 0.$$

According to formula (3-42c) we have:

$$w(t) = \frac{k}{2\sqrt{1-\beta^2}} e^{\frac{-t}{2}} \sin \frac{t}{2}\sqrt{1-\beta^2}, \qquad (3-43a)$$

which coincides with the data of Table 3-1.

Example 2. Calculation of the transient function of an oscillating component.

This is a complex example of the rules laid forth in Sections 3-3 and 3-4. For the proper constituent we prepare the values entering formula (3-42b):

$$X_{in}(p) = \frac{1}{p}; \quad X_{in}\left(\frac{-1 + j\sqrt{1-\beta^2}}{2} \right) =$$

$$= \frac{2}{-1 + j\sqrt{1-\beta^2}};$$

$$|X_{in}| = x_0 = X_0 = \frac{2}{\sqrt{1-\beta^2}}; \quad \operatorname{Re} X_{in} = -2;$$

$$\varphi = \operatorname{arctg} \frac{-\sqrt{1-\beta^2}}{-1} = \pi + \operatorname{arctg} \frac{\sqrt{1-\beta^2}}{-1}$$

$$= \pi + \operatorname{arccos} \beta.$$

If we introduce them into the formula, we get

$$x_2(t) = -\frac{k}{\sqrt{1-\xi^2}} e^{-\frac{t}{\tau}} \sin\left(\frac{t}{\tau}\sqrt{1-\xi^2} + \arccos\xi\right).$$

For the forced constituent we use formula (3-35b):

$$W(0) = k; \quad h_{force}(t) = k \, 1(t).$$

If we sum the proper and forced constituents, we find the transition function of the oscillating component:

$$h(t) = k\left[1 - \frac{e^{-\frac{\xi t}{\tau}}}{\sqrt{1-\xi^2}} \sin\left(\frac{t}{\tau}\sqrt{1-\xi^2} + \arccos\xi\right)\right]. \tag{3-42 b}$$

3. A Second-Order Component

If $\xi > 1$, the poles of the second order transfer function, written in the parameters τ and ξ, equal:

$$z_1 = \frac{-\xi + \sqrt{\xi^2 - 1}}{\tau};$$

$$z_2 = \frac{-\xi - \sqrt{\xi^2 - 1}}{\tau}.$$

The transfer function in this case breaks down into the difference of the two real transfer functions of the first order:

$$\frac{k}{\tau^2 p^2 + 2\xi\tau p + 1} = \frac{k}{2\tau\sqrt{\xi^2-1}} \times$$

$$\times \left(\frac{1}{p + \frac{\xi - \sqrt{\xi^2-1}}{\tau}} - \frac{1}{p + \frac{\xi + \sqrt{\xi^2-1}}{\tau}}\right), \tag{3-44}$$

as shown in Figure 3-7a. This is an aperiodic component with a transfer function described with separated poles:
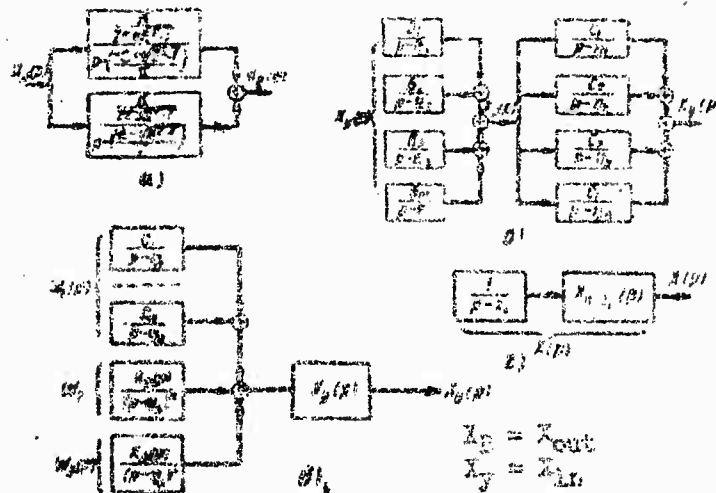
Fig 3-7. Examples of the expansion of the process and OPT's into elementary constituents in the calculation of the forced and proper motion.

$$z_1 = -\frac{1}{T_1}; \quad z_2 = -\frac{1}{T_2}. \qquad (3\text{-}45a)$$

The proper motion of the aperiodic components is obtained analogously by formulas (3-41) in new designations (3-44):

$$X_{1,2}(p) = \frac{k}{2\tau\sqrt{\xi^2-1}} \times$$

$$\times \left[\frac{X_{in}\left(\frac{-\xi+\sqrt{\xi^2-1}}{\tau}\right)}{p+\frac{\xi-\sqrt{\xi^2-1}}{\tau}} - \frac{X_{in}\left(\frac{-\xi-\sqrt{\xi^2-1}}{\tau}\right)}{p+\frac{\xi+\sqrt{\xi^2-1}}{\tau}} \right]; \qquad (3\text{-}45b)$$

$$x_{proper}(t) = x_1(t) + x_2(t) =$$

$$= \frac{k}{2\tau\sqrt{\xi^2-1}} \left[X_{in}\left(\frac{-\xi+\sqrt{\xi^2-1}}{\tau}\right) e^{-\frac{t}{\tau}(\xi-\sqrt{\xi^2-1})} - \right.$$

$$\left. - X_{in}\left(\frac{-\xi-\sqrt{\xi^2-1}}{\tau}\right) e^{-\frac{t}{\tau}(\xi+\sqrt{\xi^2-1})} \right]. \qquad (3\text{-}46)$$

B. The Passage of a Signal Through a Complex Component

4. A Component of the n-th Order

In the proper motion the form of the process determines each pole of the transfer function, and the input signal only conditions the scales of the partial processes associated with each pole of the TFT.

Actually, if a complex TFT is successfully presented in the form of the sum of the TFT's of very simple components, as shown in Figure 3-7c on the right:

$$W(p) = \sum_{i=1}^{n} \frac{C_i}{p - \eta_i}, \qquad (3\text{-}47a)$$

then the proper motion by virtue of (3-45) and the principle of superposition is determined in the form of the sum with the same number of elements:

$$X_c(p) = \sum_{i=1}^{n} \frac{C_i X_{iN}(\eta_i)}{p - \tau_i}, \qquad (3\text{-}47b)$$

$$x_c(t) = \sum_{i=1}^{n} C_i X_{iN}(\eta_i) e^{\eta_i t}. \qquad (3\text{-}47c)$$

For oscillating components and second-order components the partial processes enter the sum (3-47) in the form of (3-42) and (3-46). If there are partial components with short poles in the composition of the TFT, it is expedient to use the conclusions of the preceding section, to present the representation of the input signal in scheme be in the form of the forming block of the input action $X_{iN}(p)$ excited by the impulse $\delta(t) \leftrightarrow 1$. Then if we rearrange the blocks in places, which is allowable in a cascade circuit with constant parameters, we arrive at Figure 3-7c. Now it is not difficult to obtain the constituent of the output reaction of the circuit according to the rules of Section 3-7.

If we consider an TFT analogous in structure to representation (3-40a):

$$W(p) = W_1(p) + W_2(p) + W_3(p) =$$

$$\sum_{j=0}^{N} \frac{C_j}{p - \tau_j} + \frac{K_2(p)}{(p - \tau_n)^k} + \frac{K_3(p)}{(p - q_n)^l}, \quad (3\text{-}47\text{d})$$

then the sought representation of the proper motion will also be analogous to (3-40a):

$$X_{proper}(p) = \sum_{j=0}^{N} X_3(\tau_j) W_{1j}(p) +$$

$$+ \sum_{j=0}^{k-1} \frac{X_{in}^{(j)}(q_n)(p - \tau_n)^j}{i!} W_2(p) +$$

$$+ \sum_{i=0}^{l-1} \frac{X_{in}^{(3)}(q_n)(p - \tau_n)^i}{i!} W_3(p). \quad (3\text{-}47\text{e})$$

Thus in the comparable formulas $X_{in}(p)$ is replaced by $W(p)$, and the reverse.

When there is coincidence of the poles of the input process and of the transfer function of a component, their separation into the poles of the process and component according to to scheme b is not eliminable at the stage of calculation of the process; but this case is examined later in Section 3-10.

3-9. The Initial Section and Neutral Constituent of the Output Process

A. The Limiting Theorems for Components with Constant Parameters

1. Impulses at zero (0 to 0+)

The representation of the output process is given in the form of the fraction:

$$X_{out}(p) = \frac{\beta_\mu p^\mu + \dots + \beta_1 p + \beta_0}{\tau_n p^n + \dots + \tau_1 p + \tau_0}. \quad (3\text{-}48\text{a})$$

If $\mu \geq n$, then in this representation the impulse constituents are included. They are separated by simple division to the formation

of a remainder

$$b_n p^n + b_{n-1} p^{n-1} + \ldots + b_1 p + b_0 \quad \Big| \quad \frac{x_n p^n + x_{n-1} p^{n-1} + \ldots + x_0}{M_{\mu-n} p^{\mu-n} + M_{\mu-n-1} p^{\mu-n-1} + \ldots + M_0}$$

$$\left(b_{n-1} - b_{n-1} \frac{x_n}{x_n} \right) p^{n-1} + \ldots$$

. . . .
. . . .

The remainder is

$$b_{n-1} p^{n-1} + \ldots + b_1 p + b_0$$

The moments of the two highest impulses are:

$$M_{\mu-n} = \frac{b_n}{x_n} ; \qquad (3\text{-}48b)$$

$$M_{\mu-n-1} = \frac{b_{n-1}}{x_n} - \frac{b_n}{x_n^2} x_{n-1} . \qquad (3\text{-}48c)$$

2. Initial Section of a Transient Process

After separation in (3-48a) of the entire part, the remainder term

$$X(p) = \frac{b_m p^m + \ldots + b_1 p + b_0}{a_n p^n + \ldots + a_1 p + a_0} \qquad (3\text{-}49)$$

already contains no impulses, since $m < n$, and therefore in the expansion of the process into series (3-26) we consider only the second sum of the right side:

$$Y(p) = \frac{x(0)}{p} + \frac{\dot{x}(0)}{p^2} + \frac{\ddot{x}(0)}{p^3} + \ldots \qquad (3\text{-}50a)$$

To separate the initial value of the process, it is sufficient to multiply the series (3-50a) by p and then direct p toward infinity, which eliminates all elements of the series other than that sought:

$$x(0) = \lim_{p \to \infty} p X(p). \qquad (3\text{-}50b)$$

It is natural that representation (3-49) will figure in the cal-

oulations, although the properties of series (3-50a) were used in the derivation.

In order to separate the initial value of the first derivative it is necessary not only to multiply series (3-50) by p^2 and proceed to the limit, but likewise to subtract in advance the non-merging first term of the series:

$$\dot{x}(0) = \lim_{p \to \infty} [p^2 X(p) - px(0)]. \quad (3\text{-}50c)$$

Upon further multiplication by the elevating power p the number of lower terms which must be excluded before transition to the limit continuously rises:

$$\ddot{x}(0) = \lim_{p \to \infty} [p^3 X(p) - p^2 x(0) - p\dot{x}(0)]; \quad (3\text{-}50d)$$

$$x^{(k)}(0) = \lim_{p \to \infty} [p^{k+1} X(p) - p^k x(0) -$$

$$- p^{k-1} \dot{x}(0) - \ldots - px^{(k-1)}(0)]. \quad (3\text{-}50e)$$

If this method is compared with the "tabular method" that duplicates it, it must be noted that in calculation by Table 3-3 on the basis of the balance of the numerator and denominator (3-48a), considering the numerator the right side and the denominator the left side of the operator equation of connection, we obtain at once both the impulse constituents of the process and its continuous part, whereupon the number of elements in the calculating formulas always does not exceed the order of the equation.

3. The Neutral (Polynomial) Constituent of the Transition Process

The higher the order of the denominator of representation (3-49) the more complex the process, but for linear systems with constant parameters it always will consist of groups of exponentially damping, exponentially divergent and neutral (not containing exponential co-factors) functions (marked A, B, and C, respectively, in the following):

$$x(t) = \underbrace{\Sigma f_k e^{-\gamma_k t}}_{A} + \underbrace{\Sigma f_i e^{+\gamma_i t}}_{B} +$$

$$+ \underbrace{\Sigma f_k + \sum_{i=0} \frac{x_k^{(i)}(0)}{i!} (t)^i}_{C}. \quad (3\text{-}51a)$$

In the group of neutral processes can be found the harmonic constituents and partial processes describable by the power polynomial of t. It turns out that the latter group of processes

$$X_H(t) = \sum_{l=0} \frac{x_H^{(l)}(0)}{l!} [t]^l; \qquad (3\text{-}51b)$$

$$X_H(p) = \sum_{r=0} \frac{x_H^{(l)}(0)}{p^{l+1}} \qquad (3\text{-}51c)$$

can be found according to the general representation of the process (3-49) on the basis of a simple limiting transition.

Actually, if we proceed from the original (3-51a) to the representation, we separate part of representation (3-51c) that has been studied in detail, having gathered together all the remaining terms:

$$X_c(p) = \frac{x_H^{(v)}(0)}{p^{v+1}} + \frac{x^{(v-1)}(0)}{p^v} + \ldots +$$

$$+ \frac{x_H(0)}{p} + X_{raw}(p). \qquad (3\text{-}51c)$$

If we multiply both parts of the latter equation by p^k ($k = v+1, v, v-1, \ldots$) and proceed to the limit $p \to 0$, we get the special formulas:

$$x_H^{(v)}(0) = \lim_{p \to 0} p^{v+1} X_H(p); \qquad (3\text{-}52a)$$

$$x_H^{(v-1)}(0) = \lim_{p \to 0} \left[p^v X_H(p) - \frac{x^{(v)}(0)}{p} \right] \qquad (3\text{-}52c)$$

and the general formula

$$x_H^{(k)}(0) = \lim_{p \to 0} \left[p^{k+1} X_c(p) \right.$$

$$\left. - \frac{x_H^{(v)}(0)}{p^{v-k}} - \ldots - \frac{x^{(k+1)}(0)}{p} \right]. \qquad (3\text{-}52c)$$

In these domains the neutral part of the process is reconstructed in the form of the polynomial of the $(\gamma-1)$th power (3-51b).

The neutral constituent of this type is preserved in the complete process in the interval from $t = 0$ to $t = \infty$. Close to $t = 0$ it is included in the complete process reconstructed according to formulas (3-43), and its separate calculation presents no interest, but at $t \to \infty$, if all the real parts of the poles of the representation $X_{neu}(n)$ entering expression (3-51a) are negative, the neutral part with increase in t all the more exactly coincides with the complete process and the solution obtained with formula (3-51b) has practical value.

Since the neutral process is given by a polynomial of γth power, the highest of the determinable derivatives is constant, that is, $x_n^{(\gamma)}(0) = x_n^{(\gamma)}(\infty)$, and upon approach of the neutral part to the complete process it is possible to obtain the special formula

$$\lim_{t \to \infty} x^{(i)}(t) = \lim_{p \to 0} p^{i+1} X(p). \qquad (3-53)$$

In the presence of positive real parts of the poles $X_{neu}(p)$ the neutral part does not approach the complete process and its calculation presents no interest.

For stable control systems with constant coefficients the zero poles in the representation of the output process are dependent upon the input action. The expansion of the representation of the output process in poles of the input action gives a group of partial representations of the forced reaction.

Thus the method of limiting transition duplicates the method of finding of the forced reaction for disturbance with zero short poles (3-36).

If we require in (3-36) one representation of the process by the product of the transfer function and the representation of the disturbance (3-39a), we get:

$$x_q^{(-1)}(0) = \lim_{p \to \infty} W(p) = W(0); \qquad (3-54a)$$

$$x_q^{(-2)}(0) = \lim_{p \to \infty} \frac{W(p) - x_q^{(-1)}(0)}{p}; \qquad (3-54b)$$

$$x_q^{(i)}(0) =$$

$$-\lim_{p \to 0}\left| \frac{W(p) - x_W^{(m-1)}(0) - px^{(m-2)}(0) - \ldots - p^{m-x-2}x_W^{(x+1)}(0)}{p^{m-x-1}} \right|.$$

$$(3-54c)$$

Comparison of formulas (3-54) and (3-39) becomes clearer if the OPT is expanded into the series

$$W(p) = W(0) + W'(0)\,p + \frac{W''(0)\,p^2}{2!} + \ldots,$$

$$(3-55)$$

and then the coefficients of the series are determined by the formulas of the limiting transition:

$$W(0) = W(p)\big|_{p=0};\qquad (3-56a)$$

$$W'(0) = \left[\frac{W(p) - W(0)}{p} \right]_{p=0};\qquad (3-56b)$$

$$W''(0) = 2!\left[\frac{W(p) - W(0) - pW'(0)}{p^2} \right]_{p=0};\ (3-56c)$$

$$W^{(x)}(0) = x!\,\times$$

$$\times\left[\frac{W(p) - W(0) - pW'(0) - \ldots - \frac{p^{x-1}}{(x-1)!}W^{(x-1)}(0)}{p^x} \right].$$

$$(3-57)$$

Instead of calculation of the OPT derivatives in the form of complex fractions in (3-49) it sometimes is more convenient to apply the formulas of limiting transition (3-56) and (3-57), where instead of differentiation of the numerator and denominator of the fraction it is necessary only to calculate and reduce by p the lower terms of the numerator and denominator.

A. Initial Section of the Process

For systems with variable parameters it likewise is possible to use formulas (3-X), but with additional transformations. We will separate for this in (3-40) all the terms with constant coefficients (k = 0), will contract in these separate terms the series (3-2x) in the region of the representations in a single function of $X_{out}(p)$ -- the representation of the input process -- and will equate all of the right side:

$$
(a_{00} + a_{10}p + \ldots + a_{n0}p^n)\, X_{out}(p) +
$$

$$
+ \sum_{i=0}^{n} \sum_{k=1}^{l} (-1)^k a_{ik} \frac{\partial^k}{\partial p^k} \times
$$

$$
\times \left\{ p^i \sum_{x=0}^{\infty} x^{(x)}(0)\, p^{-i-x} \right\} = \Pi(p).
$$

We will solve the obtaining equation relative to $X_{out}(p)$:

$$
X_{out}(p) = \frac{\Pi(p) - \sum_{i=0}^{n} \sum_{k=1}^{l} (-1)^k a_{ik} \frac{\partial^k}{\partial p^k}\left\{ p^i \sum_{x=0}^{\infty} x^{(x)}(0)\, p^{-i-x} \right\}}{a_{n0}p^n + a_{n-1,0}p^{n-1} + \ldots + a_{10}p + a_{00}} \qquad (3\text{-}58)
$$

For formula (3-58) it is possible to apply the obtaining transformation (3-X) for determination of the initial derivatives of the output process, in spite of the fact that the sought derivatives are also in the right side:

$$
x^{(x)}(0) = \lim_{p \to \infty} \left\{ \frac{p^{n+1}}{a_n p^n + \ldots + a_{00}} \left[\Pi(p) - \right. \right.
$$

$$
\left. \left. - \sum_{i=0}^{n} \sum_{k=1}^{l} (-1)^k a_{ik} \frac{\partial^k}{\partial p^k}\, p^i \sum_{x=0}^{\infty} x^{(x)}(0)\, p^{-i-x} \right] \right\}.
$$

$$
(3\text{-}59)
$$

In fact, the terms on the right side that contain derivatives higher than the n-th, vanish upon transition to the limit and the following highest derivative, similarly to the solution of the equations of balances, is determined according to the preceding lower derivatives.

These same results are obtained during use of Table 3-3, where the organization of the calculation according to the method of balances is obtained more orderly.

5. The Final Section of the Process

If the variable coefficients have the finite limits

$$\lim_{t \to \infty} a_i(t) = a_i = \text{const}_i, \qquad (3\text{-}60)$$

then with rise in time the equation approaches the equation with constant coefficients a_i, the analysis of which has been stated above.

If the physical coefficients are given for a given interval, then asymptotic solutions outside that interval have no practical value. The methods of determining the process at a concrete point at the end of the interval, and also the case of periodic coefficients, will be examined later.

3-10   Inverse Laplace Transform on the Basis of the Theorem of Expansion

The basic engineering method of Laplace transformation of the representation of the function into the original -- the time function -- is the tabular method. The corresponding representations have already been obtained in the preceding sections for a portion of the functions (see Table 3-1). But for the general expression of representation of the process

$$X(p) = \frac{\beta(p)}{\alpha(p)} =$$

$$= \frac{\beta_m p^m + \ldots + \beta_1 p + \beta_0}{a_n p^n + \ldots + a_1 p + a_0}, \qquad (3\text{-}61)$$

where $\beta(p)$ is the designation of the polynomial of the numerator;
$\alpha(p)$ is the designation of the polynomial of the denominator,
at a high order of the polynomials the table of correspondences "representation-original" would be too unwieldy and inconvenient for use, since a new time function corresponds to each new combination of the coefficients α_i and β_j which change the roots of the denominator.

But if the representation $X(p)$ is successfully presented in the form of the sum of the most simple typical representations

$$X(p) = \sum_{i=1}^{n} X_i(p), \qquad (3\text{-}62)$$

the compilation of the tables for the typical terms is facilitated.

Further, if we have obtained for each partial representation the corresponding partial time function

$$X_i(p) \longrightarrow x_i(t),$$

the summary time process can, on the basis of linearity of the Laplace transform, be presented as the sum of these partial processes:

$$x(t) = \sum_{i=1}^{n} x_i(t). \qquad (3\text{-}63)$$

The operation of expansion of the complex fraction into the terms must begin with the representation of the denominator by the product of the co-factors.

$$a(p) = a_0(p - z_1)(p - z_2)\ldots(p - z_n). \qquad (3\text{-}64)$$

The transition from expression $a(p)$ in the form of the polynomial to the expression in the form of the product requires preliminary determination of the roots of the denominator from the equation $a(p) = 0$. An equation of the n-th power in the general case has n complex roots which are determined, for example, by the method given in [2] or [3, Introduction].

The character of the process depends essentially on the shortness of the roots and on the sign and value of the components of the complex root, and therefore in Table 3-6 are given all the possible varieties of the roots of the denominator of the representation.

We will consider the expansion for nonmultiple real roots. The representation that has the form of a complex fraction, the denominator of which is presented in the form of the product of the co-factors (3-64), can be represented as the sum of the partial fractions:

$$X(p) = \frac{\eta(p)}{\zeta'(p)} = \frac{\beta_m p^m + \ldots + \beta_1 p + \beta_0}{a_n(p-z_1)(p-z_2)\ldots(p-z_n)} =$$

$$= \frac{k_1}{p-z_1} + \frac{k_2}{p-z_2} + \ldots + \frac{k_n}{p-z_n}. \quad (3\text{-}65)$$

Table 3-6   Types of Poles of the Representations of the Processes

Разделение корней ①		
по признаку кратности ②	по наличию вещественной и мнимой составляющих ③	
Некратные Кратные	$\sigma \neq 0$ $\omega = 0$ Вещественные корни ⑥	
4. 5	$\sigma = 0$ $\omega = 0$ Нулевые, корни ⑦	
	$\sigma \neq 0$ $\omega \neq 0$ Комплексные корни ⑧	
	$\sigma = 0$ $\omega \neq 0$ Мнимые корни ⑨	

1 - Separation of the roots; 2 - According to the indication of short-
ness; 3 - According to the presence of real and imaginary components;
4 - Nonmultiple; 5 - Multiple; 6 - Real roots; 7 - Zero roots;
8 - Complex roots; 9 - Imaginary roots.

For the determination of all the coefficients of the expansion of
k_i a single-type method is used which we will illustrate on the example
of k_1.

For this purpose we will multiply all the terms of equation (3-65)
by the denominator of the first partial fraction:

$$\frac{\beta_m p^m + \ldots + \beta_0}{a_n(p-z_2)\ldots(p-z_n)} =$$

$$= k_1 + (p-z_1)\sum_{i=2}^{n}\frac{k_i}{p-z_i}.$$

We will now assume that $p = z_1$; then on the right side of the ob-
tained equality all the terms except k_1 are cancelled, and on the left
side there will be a certain finite expression

$$k_1 = \frac{\beta_m z_1^m + \ldots + \beta_0}{z_1(z_1 - z_2)\ldots(z_1 - z_n)}, \qquad (*)$$

Analogous results can be obtained also for the remaining coefficients of the expansion, whereupon they are usually written in one of the forms given below.

The first form of notation of the coefficient of the expansion is the generalization (*) with preservation of the operation of contraction of the denominator and numerator by $p - z_i$ and subsequent substitution of $p = z_i$

$$k_i = \frac{\beta(p)(p - z_i)}{\alpha(p)}\Big|_{p=z_i} = \frac{\beta(z_i)}{\alpha_{n-z_i}(z_i)} = X_{n-z_i}(z_i), \tag{3-66}$$

where the denominator with the contracted binomial $p - z_i$ is designated $\alpha_{n-z_i}(p)$, and the entire contracted representation $X_{n-z_i}(p)$.

The second form of notation of the coefficient of the expansion is: if it is attempted to substitute $p = z_i$ in (3-66) before the contraction, then we get an indeterminability of the type $0/0$.

If we expand it according to l'Hospital's rule, we get:

$$k_i = \lim_{p \to z_i} \frac{\beta(p) - (p - z_i)\beta'(p)}{\alpha'(p)} = \frac{\beta(z_i)}{\alpha'(z_i)}. \tag{3-67}$$

In the use of this formula it is necessary at first to perform differentiation of $\alpha(p)$ with respect to p and then to substitute $p = z_i$.

Each partial representation corresponds to the exponential time function:

$$\frac{k_i}{p - z_i} = \frac{\beta(z_i)}{\alpha'(z_i)(p - z_i)} \to \frac{\beta(z_i)}{\alpha'(z_i)} e^{z_i t}. \tag{3-68}$$

For the case of a single zero root, which is a particular example of the preceding case, formulas (3-66) and (3-67) are applicable upon substitution of $z_i = 0$.

$$k_1 = \frac{\beta(p)p}{\alpha(p)}\Big|_{p=0} = \frac{\beta(0)}{\alpha'(0)}; \tag{3-69a}$$

$$\frac{k_2}{p} + \frac{\ddot{z}(0)}{\alpha'(0)}\,1(t). \qquad (3\text{-}69b)$$

2. Analogy with the Method of Calculation of Forced Motion

The separation from the general representation of a single co-factor $1/p - z_i$ and the remainder $X_{n-z_i}(p)$ can be illustrated by Figure 3-7 d. Then further transformation according to the calculation of the coefficient of the expansion k_i is done as if the partial process $1/p - z_i$ were the input disturbance for the component with the CFT $X_{n-z_i}(p)$. Therefore, if we assume

$$\left.\begin{array}{l} B_i = k_i; \\ W(p) = X_{n-z_i}(p), \end{array}\right\} \qquad (3\text{-}70)$$

all the formulas of Section 3-7 can be used for calculation of the coefficients of the expansion in the general process.

In addition, the general process can be understood as the sum of the forced reaction of the imaginary components which have the CFT $X_{n-z_i}(p)$ with the co-factors $p - z$ excluded in the denominator, on actions of the type $1/p - z_i$.

3. Aperiodic Resonance

If the input action $1/p - k$ has the pole ξ, which coincides with the pole of the CFT of the component $\beta - \eta$, the representation of the output process leads to the form:

$$\frac{W(p)}{p - \eta} = X_w(p) = \frac{\beta(p)}{(p - \eta)^2 \, x_{n-2}(p)} = \frac{X_{n-1}(p)}{(p - \eta)^2}. \qquad (3\text{-}71)$$

It is impossible here to separate the disturbance from the CFT during the transformations, since then the special properties of the multi pole are disturbed, and it is necessary to separate the entire co-factor $1/(p - \eta)^2$ by separating the remainder of the general representation

$$X_{n-2}(p) = X_w(p)(p - \eta)^2 = W(p)(p - \eta). \qquad (3\text{-}72)$$

Later the problem of determining the coefficients k_i in the terms of the expansion

$$X_\eta(p) = \frac{k_0}{(p-\eta)^2} + \frac{k_1}{p-\eta}$$

is solved according to formulas (3-38) and gives:

$$X_\eta(p) = \frac{X_{n-2}(\eta)}{(p-\eta)^3} +$$

$$+ \frac{X'_{n-2}(\eta)}{p-\eta} + X_{n-2}(\eta) e^{\eta t} t + X'_{n-2}(\eta) e^{\eta t}. \quad (3\text{-}73a)$$

If $\eta = -\sigma$, then

$$x_\eta(t) = X_{n-2}(-\sigma) e^{-\sigma t} t + X'_{n-2}(-\sigma) e^{-\sigma t}. \quad (3\text{-}73b)$$

There are two co-factors in the first term on the right side: the diminishing $e^{-\sigma t}$ and the increasing t. In the regime that is established the product tends to zero, but in the initial section of the process a time splash is observed, in spite of the damping character of the action $e^{-\sigma t}$.

This event, caused by the coincidence of the poles of the input action and the OPF of the component, we will call the aperiodic resonance.

At $\sigma = 0$ the input single function $1/p$, jointly with the integrating argument $1/p$ in the OPT gives the partial output process:

$$x_\eta(t) = X_{n-2}(0)[t] + X'_{n-2}(0) \, 1[t]. \quad (3\text{-}73c)$$

b. Natural Resonance

If the process $1/p^2 + \Omega^2$ acts on a component containing in the OPT the co-factor $1/p^2 + \Omega^2$, the representation of the output process is reduced to the form:

$$X_\omega(p) = \frac{S(p)}{(p^2 + \Omega^2)^2 x_{n-1}(p)}.$$

The contracted representation can be written in the form:

$$X_{n-4}(p) = X_{30}(p)(p^2 + \Omega^2)^2 = -\frac{f(\Omega)}{c_{n-4}(p)} = K(p).$$

The partial representation corresponding to the multiple roots $z_{1,2} = +j\Omega$ and $z_{3,4} = -j\Omega$ we will seek in the form:

$$X_{1+4}(p) =$$

$$= \frac{k_1}{(p-j\Omega)^2} + \frac{k_2}{p-j\Omega} + \frac{k_3}{(p+j\Omega)^2} + \frac{k_4}{p+j\Omega}.$$

For the first two multiple roots, their contracted representation is introduced

$$X_{n-1,2}(p) = \frac{K(p)}{(p+j\Omega)^2}$$

and the coefficients of the expansion are found from the relations

$$k_1 = X_{n-1,2}(j\Omega) = -\frac{K(j\Omega)}{4\Omega^2};$$

$$k_2 = X'_{n-1,2}(j\Omega) = -\frac{K'(j\Omega)}{4\Omega^2} - j\frac{K(j\Omega)}{4\Omega^3}.$$

For the third and fourth multiple roots it is necessary to introduce the new contracted representation

$$X_{n-3,4}(p) = \frac{K(p)}{(p-j\Omega)^2}$$

and the coefficients of the expansion must be obtained by an analogous method:

$$k_3 = X_{n-3,4}(-j\Omega) = -\frac{K(-j\Omega)}{4\Omega^2};$$

$$k_4 = X'_{n-3,4}(-j\Omega) = -\frac{K'(-j\Omega)}{4\Omega^2} - j\frac{K(-j\Omega)}{4\Omega^3}.$$

We will proceed now from the representation x_1 to $x(p)$ with the obtained coefficients $k_1, \ldots, k_4$ to the original:

$$x_{i+1}(t) = \frac{1}{4j\pi} \left\{ \left[-K(j\Omega)i - K'(j\Omega) - \right. \right.$$

$$\left. - j\frac{K(j\Omega)}{\Omega} \right] e^{j\Omega t} + \left[-K(-j\Omega)i - K'(-j\Omega) + \right.$$

$$\left. \left. + j\frac{K(-j\Omega)}{\Omega} \right] e^{-j\Omega t} \right\}.$$

We will expand the exponential functions into the harmonic components according to Euler's formula, and likewise consider that the real parts of the functions $K(j\Omega)$, $K(-j\Omega)$ and correspondingly of the functions $K'(j\Omega)$, $K'(-j\Omega)$ are equal, and the imaginary parts are equal in value but opposite in sign. Then after transformations we get:

$$x_{i+1}(t) = \frac{1}{2\Omega^2} \left\{ \left[\operatorname{Im} K(j\Omega) \sin\Omega t - \right. \right.$$

$$- \operatorname{Re} K(j\Omega) \cos\Omega t \right] t + \left[\operatorname{Im} K'(j\Omega) + \frac{1}{\Omega} \times \right.$$

$$\times \operatorname{Re} K(j\Omega) \right] \sin\Omega t + \left[-\operatorname{Re} K'(j\Omega) + \right.$$

$$\left. \left. + \frac{1}{\Omega} \operatorname{Im} K(j\Omega) \right] \cos\Omega t \right\}. \qquad (3\text{-}74a)$$

The sine and cosine components can be transformed to a single harmonic function shifted in phase:

$$x_{i+1}(t) = \frac{K(j\Omega)}{2\Omega^2} \cdot t \sin\left[\Omega t - \operatorname{arctg}\frac{\operatorname{Re} K(j\Omega)}{\operatorname{Im} K(j\Omega)} \right] +$$

$$+ \frac{1}{2\Omega^2} \left| \operatorname{Im} K'(j\Omega) + \frac{1}{\Omega} \operatorname{Re} K(j\Omega) \right| +$$

$$+ j \left[-\operatorname{Re} K'(j\Omega) + \frac{1}{\Omega} \operatorname{Im} K(j\Omega) \right] \right| \times$$

$$\times \sin\left[\Omega t + \operatorname{arctg}\frac{-\operatorname{Re} K'(j\Omega) + \frac{1}{\Omega}\operatorname{Im} K(j\Omega)}{\operatorname{Im} K'(j\Omega) - \frac{1}{\Omega}\operatorname{Re} K(j\Omega)} \right].$$

$$(3\text{-}74b)$$

Example. Let us examine the passage of the sinusoidal oscilla-
tions $a \sin(\Omega t - \varphi)$ through a resonance component with the trans-
fer function $W(p) = 1/p^2 + \Omega^2$ during coincidence of the frequencies
of the forced and proper oscillations.

The representation of the output process in the given case has
the form:

$$X_o(p) = \frac{a(\Omega \cos \varphi + p \sin \varphi)}{(p^2 + \Omega^2)^2}.$$

Present are the short imaginary roots of the denominator: $z_{1,2} = +$
$j\Omega$; $z_{3,4} = -j\Omega$.

The contracted representation of the examined output process is
$K(p) = a(\Omega \cos \varphi + p \sin \varphi)$. After substitution of $p = j\Omega$ we have
the complex number $K(j\Omega) = a\Omega(\cos \varphi + j \sin \varphi)$, of which the real
and imaginary parts are $\mathrm{Re}\, K(j\Omega) = a\Omega \cos \varphi$; $\mathrm{Im}\, K(j\Omega) = a\Omega \sin \varphi$.

The derivative from the contracted representation equals $K'(p) =$
$= a \sin \varphi$; substitution of $p = j\Omega$, $K'(j\Omega) = a \sin \varphi$ gives:

$$\mathrm{Re}\, k'(j\Omega) = a \sin \varphi; \quad \mathrm{Im}\, k'(j\Omega) = 0.$$

If we substitute the obtained amounts of the real and imaginary
values in the basic formula (3-74b):

$$x(t) = \frac{at}{2\Omega} \cos(\Omega t + \varphi) + \frac{a \cos \varphi}{2\Omega^2} \sin \Omega t.$$

The first (secular) term of this expression tends to infinity,
which corresponds to the case of resonance. The rate of increase in
amplitude of the output oscillations proves to be proportional to the
amplitude of the input oscillations divided by the doubled frequency.

In the case of complex poles of second-order shortness the inves-
tigated roots of the denominator of the representation can be expressed
in the form:

$$z_{1,2} = -s + j\Omega;$$
$$z_{3,4} = -s - j\Omega.$$

In comparison with the case of purely imaginary roots, in com-
plex roots in the representation the argument p obtains a displace-

ment, that is, varies by the value $p - \sigma$. Consequently the new time process will differ from the original process (3-74a) and (3-74b) by the additional co-factor $e^{-\sigma t}$. In addition, naturally, the values of the function $K'(p)$ and $K(p)$ must be calculated for the new argument $-\sigma + j\Omega$. With the observations made taken into consideration we proceed from the relations (3-74a) and (3-74b) to relations with the displaced argument $p + \sigma$ for the case of short complex roots

$$
x_{1+1}(t) = \frac{|K'(-\sigma + j\Omega)|}{2\Omega^2} t e^{-\sigma t} \sin\left[\Omega t - \right.
$$

$$
- \operatorname{arctg} \frac{\operatorname{Re} K'(-\sigma + j\Omega)}{\operatorname{Im} K'(-\sigma + j\Omega)}\right] + \frac{1}{2\Omega^3}\left\{\left[\operatorname{Im} K'(-\sigma + j\Omega) + \right.\right.
$$

$$
+ \frac{1}{\Omega}\operatorname{Re} K(-\sigma + j\Omega)\right] + j\left[-\operatorname{Re} K'(-\sigma + j\Omega) + \right.
$$

$$
+ \frac{1}{\Omega}\operatorname{Im} K(-\sigma + j\Omega)\right]\right\} e^{-\sigma t} \sin\left[\Omega t + \right.
$$

$$
+ \operatorname{arctg} \frac{-\operatorname{Re} K'(-\sigma + j\Omega) + \frac{1}{\Omega}\operatorname{Im} K(-\sigma + j\Omega)}{\operatorname{Im} K'(-\sigma + j\Omega) + \frac{1}{\Omega}\operatorname{Re} K(-\sigma + j\Omega)}\right].
$$

$$
(3\text{-}74c)
$$

4. Application of the Abbreviated Tables for a Reverse Laplace Transform.

It follows from the method of expansion that the character of the functions $x(t)$ elements which reflect the partial components of the solution is determined by the denominator of the representation of the spectrum. However, the different character of the numerator has an influence on the value of each component, too the initial conditions is essentially determined.

The simplest character of the representation is unity.

$$
X(p) = \frac{1}{p^l \prod_{j=1}^{m}(p + c_j) \prod_{k=1}^{n}[(p + \varepsilon_k)^2 + \Omega_k^2]},
$$

and the numerator in the general case can contain zero, real and

complex roots.

If we take into consideration the relatively rare case of multiplicity of the complex and imaginary roots above two, a comparatively short table of the relations can be compiled for the different combinations of parameters of the reduced denominator. For this, in order not to complicate the table with different forms of the numerator of the representation, we will use an expansion of the representation according to its terms.

Let the representation have a complex numerator and tabulated denominator:

$$X(p) = \frac{b_m p^m + \ldots + b_1 p + b_0}{a(p)}.$$

We will perform the division term by term:

$$X(p) = p^m \frac{b_m}{a(p)} + \ldots + p \frac{b_1}{a(p)} + \frac{b_0}{a(p)}. \quad (3\text{-}75a)$$

According to the table of correspondences for the representation with a unit numerator we find the initial original:

$$X_1(p) = \frac{1}{a(p)} \dashrightarrow x_1(t).$$

With the help of the original $x_1(t)$ it is possible to form the summary process, if in accordance with formula (3-75a) differentiate it from 1 to m times, multiply each result by the coefficient c, and summarize the results:

$$x(t) = b_0 x_1(t) + b_1 \dot{x}_1(t) + \ldots + b_m x_1^{(m)}(t). \quad (3\text{-}75b)$$

Although the initial functions are differentiated, until m is less than the order of the denominator n the initial impulses are absent. They appear at $m \geq n$.

As an example we will determine the weight function of a real boosting component of the second order, the representation of which has been given in Table 3-1 in the form:

$$X(p) = \frac{1 + 2\xi\tau p + \tau^2 p^2}{(T_1 p + 1)(T_2 p + 1)}$$

(here $b_0 = a_0 = 1$ is assumed and division is not carried out preliminarily.)

We will use the representation with a single numerator, given in the same table for the case of two aperiodic components:

$$X_1(p) = \frac{1}{(T_1 p + 1)(T_2 p + 1)} \div \frac{e^{-\frac{t}{T_1}} - e^{-\frac{t}{T_2}}}{T_1 - T_2}.$$

If we proceed on the basis of (3-75b) to the actual numerator of the examined example, we get the original:

$$x[t] = \frac{e^{-\frac{t}{T_1}} - e^{-\frac{t}{T_2}}}{T_1 - T_2}$$

$$-\frac{2\xi\tau}{T_1 - T_2}\left(\frac{1}{T_1} e^{-\frac{t}{T_1}} - \frac{1}{T_2} e^{-\frac{t}{T_2}}\right) +$$

$$+\frac{\tau^2}{T_1 - T_2}\left(\frac{1}{T_1^2} e^{-\frac{t}{T_1}} - \frac{1}{T_2^2} e^{-\frac{t}{T_2}}\right) + \frac{\tau^2}{T_1 T_2}\hat{\gamma}[t].$$

After regrouping the terms we get the weight function presented in table 3-1.

The last two columns of Table 3-1 give practically all the correspondences encountered between the original and representation for formations of not greater than the second order. For the determination of the originals of representations with a denominator that has an order $n = 3$ and $n = 4$ in the presence of a unit numerator, Table 3-7 is presented below. In it are the most frequently encountered combinations of real and complex roots within the limits of the indicated order of the denominator.

In the presence of zero and imaginary roots of the representation, the original can be found in the same table by assuming $a = 0$ or $b = 0$.

The correspondences given in Tables 3-1 and 3-7 are sufficient for solution of the majority of problems that are prevalent in practice. In the examination of representations of a higher order it is necessary to use general methods, mainly the method of separation from the complete representation of its abbreviated parts and the finding of each partial process individually. A large number of new correspondences can be found by the method of lambda-transformations, by developing the elements from Table 3-2. The most complete tables in the reference literature are given in [2].

3.11. The Parametric Representation of Processes in Systems with Variable Coefficients

A. The Representation of a Section of a Weight Function Along the Argument t

The weight function of a component with variable parameters depends on two arguments: t and ϑ, which are represented by a contour, an example of which is Figure 2-16. If one of the arguments is considered a fixed parameter, it is possible to transform the section of the weight function along the second argument by a Laplace transform and obtain a parametric representation of the weight function.

For a reduced and complete weight function the representations along the arguments τ and t are designated:

$$G(p, \vartheta) \leftrightarrow g[\tau, \vartheta]; \tag{3-76a}$$
$$W(p, \vartheta) \leftrightarrow w[\tau, \vartheta];$$

$$e^{-p\vartheta} G(p, \vartheta) \leftrightarrow g[t - \vartheta, \vartheta]; \tag{3-76b}$$
$$e^{-p\vartheta} W(p, \vartheta) \leftrightarrow w[t - \vartheta, \vartheta].$$

Let the reduced weight function be determined by the differential equation

$$\sum_{i=0}^{n} a_i(t) g^i[t - \vartheta, \vartheta] = \delta[t - \vartheta]. \tag{3-77a}$$

We will transform the equation, having left on the left side the derivatives only of constant components of the coefficients $a_i(\vartheta)$, and a group of terms containing the variable part of the coefficients $a_i(t) - a_i(\vartheta)$ we will transfer to the right side of the equation:

$$\sum_{i=0}^{n} a_i(\vartheta) g^{i}[t - \vartheta, \vartheta] = \delta[t - \vartheta] - $$

$$- \sum_{i=0}^{n} [a_i(t) - a_i(\vartheta)] g^{i}[t - \vartheta, \vartheta].$$

We will carry out the substitution of the argument $\tau = t - \vartheta$, $\partial/\partial\tau = \partial/\partial t$:

$$\sum_{i=0}^{n} a_i(\vartheta)\, z^{(i)}(\tau,\vartheta) = -\delta[\tau] -$$

$$-\sum_{i=0}^{n} [a_i(\tau+\vartheta) - a_i(\vartheta)]\, z^{(i)}(\tau,\vartheta)$$

and write a Laplace transform along the variable τ :

$$\sum_{i=0}^{n} a_i(\vartheta)\, p^i G(p,\vartheta) =$$

$$= 1 - L\left\{\sum_{i=0}^{n} [a_i(\tau+\vartheta) - a_i(\vartheta)]\, z^{(i)}(\tau,\vartheta)\right\}.$$

$$(3.77b)$$

Although the weight function enters both sides of the obtained equation, as was showed [7], the representation of the weight function can be obtained in the form of the series

$$G(p,\vartheta) = G_1(p,\vartheta) + G_2(p,\vartheta) + \ldots + G_n(p,\vartheta).$$

$$(3.77c)$$

The first approximation $G(p,\vartheta) \approx G_1(p,\vartheta)$ is found as the solution of equation (3.77b) with a simplified right side in the form of the impulse

$$G_1(p,\vartheta) = \frac{1}{\displaystyle\sum_{i=0}^{n} a_i(\vartheta)\, p^i}, \qquad (3.77d)$$

that is, on the basis of an equation with fixed (frozen) coefficients.

The second approximation $G(p,\vartheta) \approx G_1(p,\vartheta) + G_2(p,\vartheta)$ is found as a result of solution of equation (3.77b), on the right side of which the impulse is included, since the solution for it was already found in (3.77d), and instead of the unknown representation $G(p,\vartheta)$ the first approximation $G_1(p,\vartheta)$ was introduced:

$$\sum_{i=0}^{n} a_i(\vartheta)\, p^i G_2(p,\vartheta) = - \sum_{i=0}^{n} A_i \{p^i G_1(p,\vartheta)\}, \quad (3.77e)$$

The form of the lambda-transformation is determined according to relation (3.) and depends on the functional expression of increment of

239

the coefficients. If we use basically the representation of the in-
crement in the form of the series

$$\Delta_\tau a_i(\theta) = \dot{a}_i(\theta)\,\tau + \ddot{a}_i(\theta)\,\frac{\tau^2}{2!} + \dddot{a}_i(\theta)\,\frac{\tau^3}{3!} + \ldots$$

instead of formula (3-78a) we get:

$$\sum_{i=0}^{n} a_i(\theta)\,p^i G_2(p,\theta) = \sum_{i=0}^{n} \dot{a}_i(\theta)\,\frac{\partial}{\partial p}\,[p^i G_1(p,\theta)] -$$

$$- \frac{1}{2!}\sum_{i=0}^{n} \ddot{a}_i(\theta)\,\frac{\partial^2}{\partial p^2}[p^i G_1(p,\theta)] + \ldots$$

From which, with (3-77c) taken into consideration we have

$$G_2(p,\theta) = G_1(p,\theta)\left\{\sum_{i=0}^{n} \dot{a}_i(\theta)\,\frac{\partial}{\partial p}\,[p^i G_1(p,\theta)] -\right.$$

$$\left. - \frac{1}{2!}\sum_{i=0}^{n} \ddot{a}_i(\theta)\,\frac{\partial^2}{\partial p^2}[p^i G_1(p,\theta)] + \ldots\right\}. \quad (3\text{-}78b)$$

The third approximation $G(p,\theta) = G_1(p,\theta) + G_2(p,\theta) + G_3(p,\theta)$
contains an additional term which is determined by a formula analogous
to (3-78b), that is,

$$G_3(p,\theta) = G_1(p,\theta)\sum_{i=0}^{n}\left\{\dot{a}_i(\theta)\,\frac{\partial}{\partial p}\,[p^i G_2(p,\theta)] -\right.$$

$$\left. - \frac{1}{2!}\ddot{a}_i(\theta)\,\frac{\partial^2}{\partial p^2}[p^i G_2(p,\theta)] + \ldots\right\}. \quad (3\text{-}78c)$$

The additional term in the n-th approximation likewise is deter-
mined according to the additional term in the n-1th approximation:

$$G_n(p,\theta) = G_1(p,\theta)\sum_{i=0}^{n}\left\{\left[\dot{a}_i(\theta)\,\frac{\partial}{\partial p} -\right.\right.$$

$$\left.\left. - \frac{1}{2!}\dot{a}_i(\theta)\,\frac{\partial^2}{\partial p^2} + \ldots\right]p^i G_{n-1}(p,\theta)\right\}. \quad (3\text{-}78d)$$

Example. We will consider equation (4-18a) with the argument τ:

$$t\ddot{g} + (1 + \sigma t)g = \delta(t - \theta)$$

The transformed equation with the argument τ is:

$$(\theta + \tau)\dot{g} + [1 + \sigma(\tau + \theta)]g = \delta(\tau)$$

The operator equation of the type of (4-77b) is:

$$(\theta p + 1 + \sigma\theta)G(p,\theta) = 1 - L\{\tau\ddot{g} + \sigma\tau g\}.$$

The first approximation is:

$$G_1(p,\theta) = \frac{1}{\theta(p + \sigma) + 1};$$

$$g_1(\tau,\theta) = \frac{1}{\theta}e^{-\sigma\tau}e^{-\frac{\tau}{\theta}}.$$

The second approximation is:

$$G_2(p,\theta) = G_1(p,\theta)\frac{\partial}{\partial p}\left\{-\frac{p+\sigma}{\theta(p+\sigma)+1}\right\} =$$

$$= \frac{1}{[\theta(p+\sigma)+1]^3};$$

$$g_2(\tau,\theta) = \frac{\tau^2}{\theta^3}e^{-\sigma\tau}e^{-\frac{\tau}{\theta}}.$$

The third approximation. We use (4-77b) for the solution; in this case the coefficients remain the same as for the second approximation, but it is necessary to recalculate the derivatives with respect to p, since they are taken from the representation of the second approximation:

$$\frac{\partial}{\partial p}G_2(p,\theta)(p+\sigma) = \frac{\partial}{\partial p}\cdot\frac{p+\sigma}{[\theta(p+\sigma)+1]^3} =$$

$$= \frac{1 - 2\theta(p+\sigma)}{[\theta(p+\sigma)+1]^4}$$

To substitute these expressions in (5-70b) we obtain:

$$G_2(p, 0) = \frac{1 - 2p(p + a)}{[p(p + a) + 1]^2} \qquad (*)$$

In the transition from the representation to the original we use the rule of expansion according to the terms of the numerator (see the preceding section), namely, we find the original for the representation with the unit numerator

$$\frac{1}{\left(p + a + \frac{1}{6}\right)^5} \div \frac{z^4}{4!} e^{-\left(a + \frac{1}{6}\right)z}.$$

We will determine the representation of the derivative

$$\frac{p}{\left(p + a + \frac{1}{6}\right)^5} \div \left[\frac{z^3}{3!} - \frac{\left(a + \frac{1}{6}\right)z^4}{4!}\right] e^{-az} e^{-\frac{z}{6}},$$

and we obtain the complete original with consideration of the coefficients existing in the starting formula (*)

$$g_2(z, 0) = \frac{1}{6}\left[\left(\frac{3}{6} - \frac{z^3}{4!} - \frac{2z^4}{5!}\right)\right] e^{-az} e^{-\frac{z}{6}}. \qquad (**)$$

If we sum up the obtained functions, we form new terms of the solution in the form of a series:

$$g(z, 0) = e^{-az} e^{-\frac{z}{6}}\left[\frac{1}{6} + \frac{z^3}{2!6^3} - \frac{1}{6} \frac{2z^3}{3!} + \cdots\right]$$

It can be shown that the obtained series is the product of the expansion of the two functions:

$$e^{+\frac{z}{6}} = 1 + \frac{z}{6} + \frac{z^2}{2!6^2} + \frac{z^3}{3!6^3} + \frac{z^4}{4!6^4}$$

$$\frac{1}{1 + 6^{-2}} = \frac{1}{6} - \frac{z}{6^2} + \frac{z^2}{6^3} - \frac{z^3}{6^4} + \frac{z^4}{6^5}$$

Consequently, the solution is reduced to the form:

$$g[\tau, \vartheta] = \frac{e^{-\sigma\tau}}{\tau + \vartheta}, \qquad (3\text{-}79a)$$

or

$$g[t - \vartheta, \vartheta] = \frac{e^{-\sigma(t - \vartheta)}}{t}, \qquad (3\text{-}79b)$$

which coincides with the solution obtained according to (2-19c).

The expansion of the representation of the weight function into a series according to derivatives is especially convenient during slow change of the coefficients. In that case the first approximation (3-77d) at values of the coefficients fixed (frozen) at the point $\mathscr{S}$ is already rather close to the complete solution, and the succeeding steps rapidly converge.

Parametric Representation of the Complete Weight Function

The connection (2-43a) between the reduced and complete weight functions is also preserved for their representations:

$$e^{-p\vartheta} W(p, \vartheta) = \sum_{j=0}^{m} (-1)^j \frac{\partial^j}{\partial \vartheta^j} \{b_j(\vartheta) e^{-p\vartheta} G(p, \vartheta)\}. \tag{3-80a}$$

If we take into consideration the properties of the derivative of the exponential function

$$\frac{\partial}{\partial \vartheta^j} e^{-p\vartheta} = (-p)^j e^{-p\vartheta}. \tag{3-80b}$$

Formula (3-80a) can be transformed:

$$W(p, \vartheta) = \sum_{j=0}^{m} (p - D^{\nabla})^j \{b_j(\vartheta) G(p, \vartheta)\} =$$

$$= \sum_{j=0}^{m} (p - D_{out}^{\nabla} - D_G^{\nabla})^j \{b_j(\vartheta) G(p, \vartheta)\}. \tag{3-80c}$$

B. Representation of the section of the Weight Function Along the Argument Θ

The use of the argument Θ of reverse displacement permits analyzing the desired section of the weight function as an initial function extended to $\Theta = \infty$, although its working limits are defined by the interval 0 to t.

We will introduce for the new argument Θ in the original the correspondingly new argument s in a Laplace transform:

$$W(t, s) = \int_0^{\infty} e^{-s\theta} w(t, \theta) \, d\theta; \qquad (3\text{-}81a)$$

then the parametric representation of the weight functions along the argument Θ is determined from the correspondences

$$g(t, \theta) \doteq G(t, s); \qquad (3\text{-}81b)$$

$$w(t, \theta) \doteq W(t, s), \qquad (3\text{-}81c)$$

where the fixed value t is the parameter.

The calculation of the parametric representation along the argument Θ can be done by the same method of successive approximations (3-??) and (3-78) as the calculation of the parametric representation along the argument t, only instead of the starting differential equation of connection it is necessary to use the RC equation (2-50b and c or 2-51a and b).

Since the method of approximations itself has been stated above in Part I, we will proceed directly to the solution of an example, in the capacity of which we will examine equation (2-18a).

We rewrite this equation in the RC form (2-50c):

$$\frac{\partial}{\partial \theta}[(t - \theta) g(t, \theta)] +$$

$$+ [1 + s(t - \theta)] g(t, \theta) = \delta(\theta) \qquad (3\text{-}82a)$$

and leave on the left side only the constant (independent of Θ) components of the coefficients:

$$t g'(t, \theta) + st g(t, \theta) = \delta(\theta) +$$

$$+ \theta \{ g'(t, \theta) + s g(t, \theta) \}. \qquad (*)$$

Later we seek the solution by the method of successive approximations.

The first approximation is:

$$G_1(t, s) = \frac{1}{T(s + \sigma)}.$$

For succeeding approximations we prepare a representation of the functions found on the right side, with the exception of the impulse δ/Θ:

$$L\{\theta[g'_{s1}(t, \theta) + \sigma g_1(t, \theta)]\} =$$
$$= -\frac{\partial}{\partial s}\{sG_1(t, s) + \sigma G_1(t, s)\}.$$

The additional term of the second approximation is:

$$\frac{G_2(t, s)}{G_1(t, s)} = -\frac{\partial}{\partial s}\left\{\frac{s}{T(s + \sigma)} + \frac{\sigma}{T(s + \sigma)}\right\} =$$
$$= -\frac{\partial}{\partial s}\frac{1}{T} = 0.$$

The additional term of the second approximation proved to equal zero, which guarantees the equality to zero also of the remaining additional terms; therefore the first approximation gives the best possible value of the sought representation:

$$G(t, s) = \frac{1}{T(s + \sigma)}. \qquad (3\text{-}82\,b)$$

If we proceed to the original, we find the process along the argument Θ:

$$g_s(t, \theta) = L^{-1}\{G(t, s)\} = \frac{1}{T}e^{-\sigma\theta}. \qquad (3\text{-}82\,c)$$

In very complex cases, for transition from the representation $G(t, s)$ to the section of the weight function $g(t, \Theta)$ it is necessary to calculate the poles of the representation $s = \sigma_i$, to apply the theorem of expansion and other rules of transformation stated in the preceding sections, and to use the tables of correspondences 3-1 and 3-7, assuming in so doing that $s = p$ and t is a fixed number.

The obtained section of the weight function, first of all, serves as the nucleus in the equation of convolution, and secondly, reflects the state of the real system at the moment of time t, excited by a single displaced impulse applied at the moment of time ϑ, that is,

given for each ϑ the reaction $g_x(t, \vartheta)$ at one point:

$$q = t - \vartheta, \qquad (*)$$

determinable by substitution of this value of the argument in the solution along Θ:

$$g_x(t, \vartheta) = g_x(t, \vartheta)\big|_{t=\vartheta=q} = g_x(t, t - \vartheta). \qquad (3\text{-}82d)$$

In particular, for $\vartheta = 0$ the value of the undisplaced weight function is given only at the point $\Theta = t$, that is,

$$g_x(t, 0) = g_x(t, t) \qquad (3\text{-}82e)$$

etc.

For solution of (3-72a) the substitution of (*) gives:

$$k_T(t, \vartheta) = \frac{e^{-\alpha(t-\vartheta)}}{t} \qquad (3\text{-}82f)$$

or in the case of the undisplaced impulse

$$g_x(t, 0) = \frac{e^{-\alpha t}}{t} \qquad (3\text{-}82g)$$

(see Table 2-1).

The Dynamic Function of Transfer (DFT)

Just as for a system with constant parameters the concept of the DFT was presented through the equation of convolution on the basis of the weight function presented in Section 2-24, analogously for a system with variable parameters the concept of the DFT is directly linked with the equation of convolution (3-44a) and the input process displaced by the value ϑ, from the beginning of change of the variable coefficients of the system.

If this equation is extended to the entire working region of the possible displacements $t > \vartheta$, $\vartheta < t$ or $0 \leqslant \Theta \leqslant t$ and analytically to ϑ which is extended to infinity, then, in order to include all the partial cases in this region the upper limit of integration in (2-44a) must likewise be made infinite:

$$x_{out}(t, \vartheta) = \int_0^\infty x_{in}(t, \vartheta) x_{in}(\vartheta - t) dt. \qquad (*)$$

This substitution does not distort the result, since the actual

244

Integration with respect to ξ is done in the limits of the working zone $0 - \Theta$, determinable by the properties of the displaced function $x_{in}/\Theta - \xi$, which enters the main copy of the integral.

Now we will make a Laplace transform of both parts of (*) along the argument Θ. The left side, in accordance with (3-81a) will be represented as a function of the argument s and the parameter t:

$$X_{out}(t, s) \doteq x_{out}(t, \Theta). \qquad (**)$$

On the right side the operation of transformation is introduced under the sign of the integral and is addressed only to one function, $x_{in}(\Theta - \xi)$, which is a function of Θ:

$$\int_0^\infty w_{in}(t, \xi) L\{x_{in}(\theta - \xi)\}\,d\xi =$$

$$= \int_0^\infty w_{in}(t, \xi) e^{-s\xi} X_{in}(s)\,d\xi. \qquad (***)$$

Here

$$X_{in}(s) \doteq x_{in}(\theta)\,1(\theta) \qquad (3-83a)$$

is the representation of the undisplaced input process, since the fact of displacement is taken into consideration by the separate co-factor $e^{-s\xi}$. The same representation can be otherwise written:

$$X_{in}(s) = X_{in}(\mu)_{\mu=s} = L\{x(\tau)\}_{\mu=s}. \qquad (3-83b)$$

On the basis of the designations (3-81a) and (3-83a) from (**) and (***) we get:

$$X_{out}(t, s) = W(t, s) X_{in}(s). \qquad (3-83c)$$

The inverse Laplace transform

$$L^{-1}\{X_{out}(t, s)\} = x_{out}(t, \theta) \qquad (3-83d)$$

gives the output reaction of the system at the identical point t for the single-type actions $x_{in}(\tau)$ with different displacements:

$$\theta_{in} = t - \theta. \qquad (3-83e)$$

particular of such the general solution (3-53x):

$$x_{out}(t, \theta)_{in; t-\theta_0} = x_{out}(t, t-\theta_0) = x_{out}(t, \theta_0).$$

For example, at the instantaneous input action $(\theta_{in} = 0)$ we have:

$$x_{out}(t) = x_{out}(t, \theta)_{\theta=t} = x_{out}(t, t). \qquad (3\text{-}83h)$$

Thus for systems with variable parameters the role of the PCFT is analogous to the role of the CFT in systems with constant parameters, that is to, it permits obtaining, by the representation of the input process the representation of the output reaction of the system at a fixed moment of time t as a function of a continuously changing displacement of the input process, which we will call the parametric representation of the output process, by analogy with the parametric weight function (see Table 3-1). The principle of obtaining it is explained by the general structural figure shown in Figure 3-8a. Below on Figure 3-8 is shown the passage of the signal the passage of the linearly increasing signal $G_{in}(s) = 1/s^2$ through a variable component with a PCFT determined by equation (3-82b).

For the case illustrated in Figure 3-8b, the parametric representation of the output process is

$$G_0(t, s) = \frac{1}{T(s+a)} \cdot \frac{1}{s^2} = W'(t, s) X_{in}(s). \qquad (*)$$

From it passing to the partial representations according to the rule formula 3-45 we get:

$$X_{out}(t, s) = \frac{W(t, 0)}{s} + \frac{W'(t, 0)}{s^2} + \frac{X_b(-a)}{T(s+a)}$$

$$= \frac{1}{Ts^2} - \frac{1}{s} + \frac{1}{(s)(s+a)}$$

a)

b)

Figure 3-8. Transfer properties of a component with variable parameters: a) general representation; b) partial example.

It is not difficult to proceed from this to the original:

$$L^{-1}\{X_{\omega\varepsilon}(t,s)\} = \frac{1}{\alpha t}\left[\dot{q} - \frac{1}{q} + \frac{1}{q}e^{-qt}\right], \qquad (^{**})$$

If a controlling signal of the same form has displacement, that is, the coefficients of the equation of connection of the component start to vary before the delivery of the input action, then at a time of displacement ϑ_0 the solution of $(^{**})$ will contain a single point of displaced output reaction at $\Theta = t - \vartheta_0$:

$$x_\varepsilon(t,\vartheta_0) = \frac{1}{q} - \frac{\vartheta_0}{\alpha t} - \frac{1 - e^{-q(t-\vartheta_0)}}{q^2 t}, \qquad (^{***})$$

or for an undisplaced input process at $\mathcal{S} = 0$

$$x_\omega(t) = \frac{1}{q} - \frac{1 - e^{-qt}}{q^2 t}, \qquad (^{****})$$

Since both solutions are successfully obtained in latter form, the fixed points t and ϑ_0 naturally can assume any numerical values, which usually is not achieved in solutions in numbers.

Thus the parametric representations of processes possess the properties of ordinary representation when there is fulfilment of the rules of agreement of the solutions according to the arguments Θ and t at the determined points.

Consequently the rules of limiting transition given in Section 3-2 are also applicable to parametric representations.

The Initial Section of a Parametric Output Process

By analogy with (3-80) it is possible to determine the initial derivatives with respect to argument Θ in the original, corresponding to the representation of the parametric output process:

$$\frac{d^k}{d\Theta^k}x_\varepsilon(t,\Theta)_{\Theta=0} = D^k x_\varepsilon(t,0) =$$

$$= \lim_{s\to\infty}[s^{k+1}X(t,s) - s^k x(t,0) - \dots - $$

$$- s x^{(k-1)}(t,0)] \qquad (3\text{-}84a)$$

and to reconstruct the solution in the form of the series

$$x_a(t_1, \theta) = x_a(t_1, 0) + x'_a(t_1, 0)(\theta) +$$

$$+ x''_a(t_1, 0)\frac{(\theta)^2}{2!} + \ldots \qquad (3\text{-}84b)$$

If we now assume $\theta = t_1 - \mathcal{A}_{in}$, we can obtain for a fixed moment of time t the output reaction from the input action, set close to the investigated moment of time $t_1 - \mathcal{A}_{in} = \tau \to 0$, in the form of the series

$$x(t_1, \theta) = x_a(t_1, 0) + x'_a(t_1, 0)\tau +$$

$$+ x''_a(t_1, 0)\frac{\tau^2}{2!} + \ldots$$

with a relatively small number of terms if τ is small enough.

The Neutral Component of a Parametric Output Process

If there are zero poles of $\gamma + 1$-th shortness in the parametric representation of the output process, then in the original there is a neutral component determinable by a polynomial of the γ-th power:

$$x_{aH}(t_1, \theta) = x_{aH}(t_1, 0) +$$

$$+ x'_{aH}(t_1, 0)(\theta) + \ldots + \frac{x_{aH}^{(\gamma)}(t_1, 0)(\theta)^{\gamma}}{\gamma!}; \qquad (3\text{-}84c)$$

the initial derivatives with respect to the argument θ, used in this polynomial, are determined by analogy with formula (3-82c):

$$x_{aH}^{(s)}(t_1, 0) = \lim_{s \to 0}\left[s^{s+1} X(t, s) - \right.$$

$$\left. \frac{x_{aH}^{(0)}(0)}{s^{s+1}} - \ldots - \frac{x_{aH}^{(s+1)}(0)}{s} \right]. \qquad (3\text{-}84d)$$

When the remaining components of the original are damped with rise in θ, (3-84c) approaches the complete solution, and according to it at large enough values of θ after substitution of $\theta = t_1 - \mathcal{A}_{in}$ it is possible to obtain the output reaction at the fixed point t_1 from the input displaced process of the assigned, much earlier studied

$$\text{where } \vartheta_{1n} \ll t_1;$$

$$x_{un}(t, \theta) = x_{un}(t_1, 0) + x'_{un}(t_1, 0)(t_1 - \vartheta_{1n}) + \ldots$$

$$\ldots + \frac{x^{(v)}_{un}(t_1, 0)(t_1 - \vartheta_{1n})^v}{v!}. \qquad (3.84c)$$

The Forced Neutral Component

If the short zero poles have been determined by the input action, the neutral component (3-84c) coincides with the forced reaction of the component (3-79c) and can be written in the form:

$$x_{nfor}(t_1, \theta) = W(t_1, 0) x_{un}(\theta) +$$

$$+ W'(t_1, 0) \dot{x}_{un}(\theta) + \frac{W''(t_1, 0)}{2!} \ddot{x}_{un}(\theta) + \ldots$$

$$(3-85a)$$

The substitution of $\theta = t_1 - \vartheta_{1n}$ gives the forced reaction at the point t of a process displaced by the value ϑ_{1n}.

In the presence of an undisplaced action $\vartheta_{1n} = 0$ the substitution also has a partial character $\theta = t_1$, which leads to the formula:

$$x_{for}(t_1) = W(t_1, 0) x_{un}(t_1) + W'(t_1, 0) \dot{x}_{un}(t_1) +$$

$$+ \frac{W''(t_1, 0)}{2!} \ddot{x}_{un}(t_1) + \ldots \qquad (3-85b)$$

Here again, as in formulas (3-84), only the point t_1, on which the right side $x(t_1)$, was selected, relates to the undisturbed reaction.

In conclusion we will write the expression for the connection between the RMT of the component with a single AIT on the right side and the MT of a component with a developed right side:

$$W(t_1, s) = \sum_{j=0}^{m} \sum_{k=0}^{l} s^j b_{jk} (-1)^k \frac{\partial^k}{\partial s^k} G(t_1, s). \qquad (3-86)$$

This formula follows directly from its input transition to representation along the argument θ and expansion of the coefficients into the series:

$$b_j(t_1 - \theta) = b^*_{j0} + b^*_{j1}\theta + b^*_{j2}\theta^2 + \ldots$$

D. Obtaining the POFT from the Basic Differential
   Equation of Connection

In Figure 3-9 the section of the weight function at t = constant
is presented once more. If ϑ, reverse-displacement, which is lack-
ing in the basic equation of connection, is not introduced into the
consideration of the argument, it is possible to make a Laplace trans-
formation of the function w along the argument $-\vartheta$ (minus ϑ); then
we get the POFT (3-81c), displaced forward with respect to the init-
ial graph w_N by $+t$, which is represented by the additional co-factor
e^{+st}.

$$e^{+st} W(t, s) = \int_{-\vartheta=-t}^{\infty} w_\vartheta [t, \vartheta] e^{-s(-\vartheta)} d(-\vartheta).$$

The transformation includes the dotted part of graph w, which
is an analytical extension of the function into the non-working
region.

By changing the sign we get:

$$e^{st} W(t, s) = \int_{-\infty}^{t} w_\vartheta [t, \vartheta] e^{s\vartheta} d\vartheta. \qquad (3\text{-}87)$$
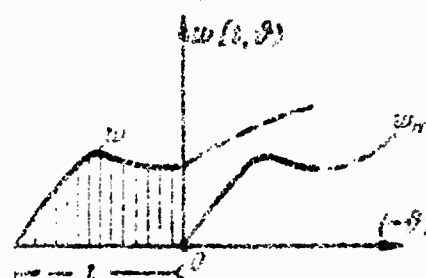
Fig 3-9. Determination of the POFT.

The conditions of integration do not agree with the classical
description of a Laplace transform (3-1), and therefore we will call
this operator an L-transform, noting its peculiarity by the addition-
al subscript ϑ and designating

$$L_\vartheta \{ w_\vartheta [t, \vartheta] \} = \int_{-\infty}^{t} w_\vartheta [t, \vartheta] e^{s\vartheta} d\vartheta \qquad (3\text{-}88)$$

Then the preceding formula is written as:

$$L_\varphi\{w_\varphi(t, \theta)\} = e^{st} W(t, s). \qquad (3\text{-}89)$$

We will take here the complete differential equation of connection, describing its reaction to the impulse:

$$\sum_{i=0}^{n} a_i(t) w^{(i)}(t, \theta) = \sum_{j=0}^{m} b_j(t) \delta^{(j)}(t-\theta)$$

and apply the L_φ-transform to all of its terms (3-88):

$$\sum_{i=0}^{n} a_i(t) D^i\{W(t, s) e^{st}\} = \sum_{j=0}^{m} b_j(t) s^j e^{st}.$$

On the left side the L_φ-transformation according to the second argument was introduced under the sign of differentiation for the first argument, which gave the result (3-89), and on the right side theorem (2-40c) for the filtering properties of the impulse was applied.

If we take into consideration the properties of the derivative of the exponential function (3-80b), we simplify the preceding notation.

$$\sum_{i=0}^{n} a_i(t)(s + D)^i W(t, s) = \sum_{j=0}^{m} b_j(t) s^j. \qquad (3\text{-}90)$$

The obtained differential equation in the region of representations during slow change of the coefficients can be solved by the scheme that follows, by determining the terms of the series

$$W(t, s) = W_1(t, s) + W_2(t, s) + \cdots \qquad (3\text{-}91)$$

by successive approximations.

For the first approximation in (3-90), all the derivatives ($D = 0$) are eliminated, which gives:

$$W_1(t, s) = \frac{\sum_{j=0}^{m} b_j(t) s^j}{\sum_{i=0}^{n} a_i(t) s^i} = \frac{b(t, s)}{a(t, s)}. \qquad (3\text{-}92a)$$

For the second approximation the terms discarded above are transferred to the right side of equation (3-90), where the derivatives are taken from the first approximation that has been found. On the left side, as an unknown, remains the second approximation $W_2(t, s)$, that is,

$$W_2(t, s) = \frac{-1}{a(t, s)} \left\{ [a_1(t) + 2a_2(t)s + \ldots \right.$$

$$+ n s^{(n-1)} a_n(t)] W_1'(t, s) + [a_2(t) + 3a_3(t) s + \ldots$$

$$\ldots + \frac{n(n-1)}{2!} s^{n-2} a_n(t)] W_1''(t, s) + \ldots + a_n(t) W_1^n(t, s),$$

$$(3\text{-}92b)$$

or contracted in the form of the ADP

$$W_2(t, s) = \frac{-1}{a(t, s)} A(t, s + D) W_1(t, s). \qquad (3\text{-}92c)$$

If we develop the latter formula, we obtain for the k-th approximation:

$$W_k(t, s) = \frac{-1}{a(t, s)} A(t, s + D) W_{k-1}(t, s) \qquad (3\text{-}92d)$$

3-12. Calculation of the Process at a Given Point

The use of the precise formula (2-4a), which reflects the filtering properties of the impulse, is difficult for the representations, since for the exclusion of part of the processes prior to a given moment of time there is no suitable equivalent in the region of the representations. (There is no need to confuse the operation of cutting off part of the process with the operation of displacement of the entire process, which has a simple equivalent in the region of the representations.) Therefore we will give an account of the method of approximate filtration of A A Krasovskiy [?].

Let a filtering function be given of the type of:

$$f(t) = e^{-\sigma t}\, t^n, \qquad (3\text{-}93a)$$

characterized by the area

$$M_0 = \int_0^\infty e^{-\sigma t}\, t^n\, dt = \frac{n!}{c^{n+1}}, \qquad (3\text{-}93b)$$

by the moment of the area

$$M_1 = \int_0^\infty e^{-\sigma t}\, t^{n+1}\, dt = \frac{(n+1)!}{\sigma^{n+2}} \qquad (3\text{-}93c)$$

and by the disposition of the center of gravity of the graph of the process

$$x_u = \frac{M_1}{M_0} = \frac{n+1}{\sigma}. \qquad (3\text{-}93d)$$

If we multiply function (3-93a) by the investigated process, integrate the product in semi-infinite limits and divide the integral by the area of the function

$$\frac{\sigma^{n+1}}{n!} \int_0^\infty x(t)\, e^{-\sigma t}\, t^n\, dt \approx x\left(\frac{n+1}{\sigma}\right), \qquad (3\text{-}94a)$$

we get a certain number which indicates how many times the area of the function increased after its multiplication by the desired process. In the case of an ideal impulse this number would be equal to the value of the ordinate of the process at the point of application of the impulse. For the examined function with a sloping maximum we relate this average ordinate to the moment of time corresponding to the center of gravity of the graph of the function: then we obtain the right side of formula (3-94a).

The value of this formula is that all the operations in the region of time have known equivalents in the region of the representations. We will examine these operations.

1. Multiplication by the function $e^{-\sigma t} t^n$ has the equivalent — displacement of the argument p by the value σ and n-times differentiation of the displaced representation with respect to p with change of the sign in accordance with Table 3-2.

2. Integration with a moving upper limit t has the equivalent of multiplication of the representation by $1/p$.

3. Direction of the active limit toward infinity ($t \to \infty$) has the equivalent — multiplication of the representation by p with subsequent limiting transition $p \to 0$ (see (3-53)) at $v = 1$ and in the absence of exponentially divergent components in the process).

All these rules, with consideration of the mutual cancellation of the co-factor $1/p$ and p in parts 2 and 3, lead to the formula

$$x\left(\frac{n+1}{\theta}\right) \approx (-1)^n \frac{\theta^{n+1}}{n!} \frac{d^n}{dp^n} X(p+c)\Big|_{p=0},$$

or

$$x\left(\frac{n+1}{\theta}\right) \approx (-1)^n \frac{\theta^{n+1}}{n!} \frac{d^n}{d c^n} X(c). \quad (3\text{-}94b)$$

If we vary the parameters of our filtering function θ and n, we can obtain new points of the process according to its representation at the moments $n+1/\theta$ etc.

The accuracy of the calculations for the special example have been estimated by G S Pospelov [3] and is about 10% in the case of the exponential desired process.

3-13. Analysis of the Quality of the Process in an Oscillating Component

On the example of an oscillating component, to which control systems periodically important but simple in mathematical description are referred in some cases, or to which the equations of more complex automatic control systems are reduced by a series of permissible simplifications, we conduct an examination of some qualitative evaluations of the processes proceeding in them.

Qualitative evaluations naturally are applied to an independent object or to a completely closed system; in that case they can be linked directly with the various requirements of practice. If a separate component in a complex automatic control system is to be analyzed, the processes in it can be evaluated, not directly, but from the point of view of their effect on the general processes in the automatic control system. These evaluations are more conveniently made, not according to the processes, but according to the different characteristics of the components.

Operator methods are used to a great degree for evaluations of the quality of processes. We will consider only one typical form of

process -- the transient function of a component.

We will consider the component to be assigned the DFT shown in Table 5-1. The equation of the transient function (3-43b) has already been determined.

We will examine the initial section of the transient function.

According to (3-50) we have:

$$h(0) = W(\infty) = \lim_{p \to \infty} \frac{k}{\tau^2 p^2 + 2\xi\tau p + 1} = 0;$$

$$\dot{h}(0) = \lim_{p \to \infty} p W(p) = 0;$$

$$\ddot{h}(0) = \lim_{p \to \infty} \frac{p^2 k}{\tau^2 p^2 + 2\xi\tau p + 1} = \frac{k}{\tau^2};$$

$$\dddot{h}(0) = \lim_{p \to \infty} \left[\frac{p^3 k}{\tau^2 p^2 + 2\xi\tau p + 1} - \frac{pk}{\tau^2} \right] = -\frac{2\xi k}{\tau^3}.$$

The higher initial derivatives were determined in Table 3-5, and according to them a series (3-32b) of representations of the process has been compiled. Figure 3-10 illustrates the approximation of the sum of series (3-32b) with rise in the number of considered terms to the real process for the partial value $\xi = 0.5$. According to the data of Table 3-5 it is possible to evaluate the quality of the initial section of the transient function, by comparing the values of the derivatives with the permissible values.

An established section of the transient function was determined by formula (3-50):

$$h(\infty) = W(0) = k.$$

A complete graph of the transient function, constructed according to (3-43b), is given in Figure 3-11. The initial zone of the function in Figure 3-11 was constructed on the parabola

$$h_{init}(t) = \frac{k\left(\frac{t}{\tau}\right)^2}{2}.$$
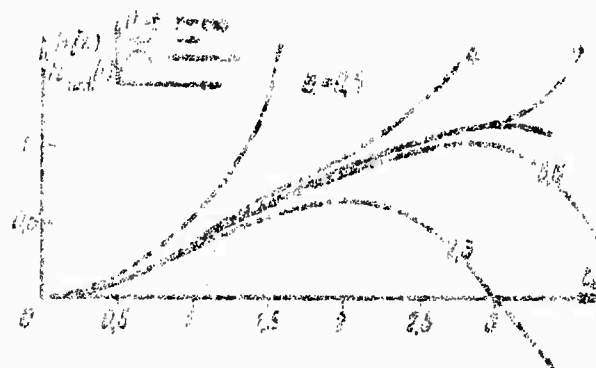
Fig 3-10. Formation of the initial section of a transient function of an oscillating component according to a power polynomial with a limited number of terms.
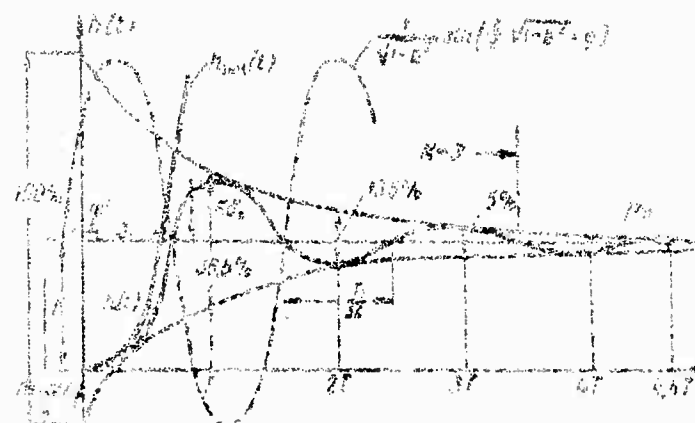
Fig 3-11. A transient function and its components for an oscillating component.

The graph of the process adjoins the parabola in the initial section and then deviates from it and in an oscillating manner approaches the horizontal asymptote $y = k$.

In order that the phase shift $\phi = \arccos \xi$ may be seen clearly, the harmonic component without damping is shown by the dotted line

$$ y = \frac{1}{\sqrt{1-\xi^2}} \sin\left(\frac{t}{T}\sqrt{1-\xi^2} + \varphi\right). $$

If the complete transient function is given experimentally in the form of an oscillogram, it is possible by its graph to determine all the parameters of the oscillating component.

The amplification factor k is determined on the scale of the graph as the distance from the time axis to the asymptote of the damping process.

The proper angular frequency of oscillations Ω is proportional to the frequency f cps, directly calculable by the graph

$$\Omega = 2\pi f,$$

The period of oscillations $1/f = 2\pi/\Omega$ is measured as double the distance between the two adjacent points of intersection of the graph with the asymptote.

The time constant T can be measured by the enveloping amplitude as the distance between any two adjacent points corresponding to the opening of the "damping eddy", equal to 100, 36.8, 13.5 and 5% of the initial opening:

$$\frac{2\xi}{\sqrt{1-\xi^2}} = 2k\cos\varphi.$$

If the time t_s is measured to 5% of the damping, then

$$T = \frac{\tau}{\xi} = \frac{t_s}{3}.$$

The relative coefficient of damping ξ is determined by the phase shift φ of the harmonic component according to the formula

$$\xi = \cos\varphi = \cos(\pi - \Delta_1\Omega).$$

Where Δ_1 is the interval of time from zero to the first intersection of the asymptote.

If the phase shift is not clearly expressed on the graph (oscillogram), ξ can be determined by the ratio of two adjacent amplitudes of the oscillation component. If close to the start the graph of the amplitude has the value

$$A_1 = ke^{-\frac{t_1}{\tau}},$$

the following amplitude is observed through the half-period

$$\frac{\alpha\tau}{\sqrt{1-\beta^2}} = \frac{\pi}{\Omega},$$

and A_2 equals

$$A_2 = A_1 e^{-\frac{\beta}{\tau}\cdot\frac{\pi}{\sqrt{1-\beta^2}}}.$$

It will determine the logarithm of the ratio of the adjacent amplitudes:

$$\ln\frac{A_1}{A_2} = \frac{\pi\beta}{\sqrt{1-\beta^2}}.$$

If we transform, we find:

$$\beta = \frac{1}{\sqrt{1+\left(\dfrac{\pi}{\ln A_1/A_2}\right)^2}}$$

for large dampings $(A_1/A_2) \gg 1$ and

$$\beta = 1 - \frac{1}{2}\left(\frac{\pi}{\ln A_1/A_2}\right)^2,$$

for small dampings $(A_1/A_2) \approx 1$ and

$$\beta = \frac{\ln\dfrac{A_1}{A_2}}{\pi}.$$

The number of waves N from the time of amplitude A_1 calculated from the graph of the graph to the time t, amp $= A_1$ to $t = h$:

$$N = \frac{t \Omega \alpha \tau_p}{\pi \Omega} - 1.$$

$$N \approx Th\Omega - 1 = \beta\sqrt{\frac{1}{\beta} - 1}.$$

if

$$\beta < \frac{1}{\sqrt{\pi}}.$$

Consideration of A as determines a motive direction of the reading amplitude of the system with respect to the ratio of the maximum amount of the initial energy amount that we have gets stored to the value that is under evaluation.

$$\beta = \frac{B_{max}}{B} + h. \tag{3.87}$$

The overcorrection is analytically connected with other parameters of the oscillating component by means of more complex calculations.

In the first place, it is necessary to determine the position of the maximum of the transient function, by equating to zero its first derivative or the weight function (3-43a):

$$\frac{k}{\tau \sqrt{1-\xi^2}} e^{\frac{-\xi t}{\tau}} \sin \frac{t_M}{\tau} \sqrt{1-\xi^2} = 0.$$

Consequently

$$\frac{t_M}{\tau} \sqrt{1-\xi^2} = n\pi.$$

For the first maximum n = 1 and

$$\frac{t_{M1}}{\tau} \sqrt{1-\xi^2} = \pi,$$

or

$$\frac{t_{M1}}{\tau} = \frac{\pi}{\sqrt{1-\xi^2}}. \tag{3-96}$$

In the second place, the value of the maximum is determined by (3-43b)

$$h_M = k \left(1 + e^{-\frac{\xi\pi}{\sqrt{1-\xi^2}}} \right).$$

And, finally, according to (3-95) the relative overcorrection is determined

$$\delta_M = e^{-\frac{\pi\xi}{\sqrt{1-\xi^2}}}. \tag{3-97}$$

The values of the relative overcorrection were calculated according to (3-97) and the graph $\delta_M = f(\xi)$ was contructed in Figure 3-12 for determination of the relative overcorrection by the value of ξ.

We will present one more form of notation of the equation of the transient function of the oscillating component, by introducing in it the relative time, equal to $t_* = t/\tau$, and also by assuming k = 1; then we get:

$$h(t_*) = 1 - \frac{1}{\sqrt{1-\xi^2}} e^{-\xi t_*} \sin (t_* \sqrt{1-\xi^2} + \text{arc} \cos \xi). \tag{3-98}$$
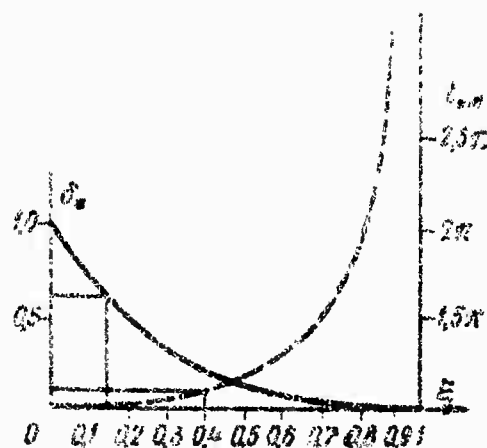
Fig 3-12. Excess value of the first maximum of the transient function of an oscillating component (overcorrection) and time of attainment of the maximum.

The principal convenience of this form of notation is that it is possible on a relative time scale to construct all the possible transient functions as a function of only a single parameter ξ .

The position of the maximum of the characteristic on the relative time scale also depends only on ξ . The values of t_{max} calculated by (3-96) were used for the construction of the dotted line graph in Figure 3-13.

The conditional time constant $\mathcal{T}$ can be determined from (3-96) and the graph

$$\tau = \frac{t_M}{t_{M_0}} = \frac{t_M}{\pi} \sin \varphi$$

or from the other relations given in Table 1-2.

3-14. The Representation of the Quadratic Evaluation of the Process

Let the process $x(t)$ have a representation of the form

$$X(p) = \frac{b''_m p^m + \ldots + b''_1 p + b''_0}{p^n + \ldots + a''_1 p + a''_0} . \quad (3\text{-}99a)$$

We will determine the connection between the representation of the process and the representation of its quadratic evaluation:

$$L\{x^a(t)\} = \Lambda_\Lambda\{X(p)\}. \qquad (3.99b)$$

For this purpose we will compose a linear differential equation, the solution of which for the input impulse is the process being studied

$$(D^n + \ldots + a_1^{\prime\prime} D + a_0^{\prime\prime}) x(t) = b_0^{\prime\prime} \delta(t) +$$
$$+ b_1^{\prime\prime} \delta(t) + \ldots + b_m^{\prime\prime} \delta^{(m)}(t). \qquad (3.99c)$$

For a first-order equation the transition to the equation for the quadratic evaluation was considered in Section 2-10; elevation of the order of the equation in (3.99b) requires the most general approach to the solution of the problem in comparison with formulas (2-64) – (2-67) in the same procedure.

We will consider the conditions of elevation of the order (differentiation) of the derivatives of the initial function $x^{(i)}(t)$ and $x^{(j)}(t)$:

$$x^{(i+1)}(t) = x^{(i+1)}(t) \, 1(t) + x^{(i)}(0) \delta(t);$$
$$x^{(j+1)}(t) = x^{(j+1)}(t) \, 1(t) + x^{(j)}(0) \delta(t)$$

and conditional multiplications of the derivatives of a different order:

$$x^{(i+1)}(t) \, x^{(j)}(t) = x^{(i+1)}(t) \, x^{(j)}(t) \, 1(t) +$$
$$+ x^{(i)}(0) \, x^{(j)}(0) \delta(t); \qquad (*)$$
$$x^{(i)}(t) \, x^{(j+1)}(t) = x^{(i)}(t) \, x^{(j+1)}(t) \, 1(t) +$$
$$+ x^{(i)}(0) \, x^{(j)}(0) \delta(t). \qquad (**)$$

If we now consider the conditions of the differentiation of the product

$$D[x^{(i)}(t) \, x^{(j)}(t)] = [x^{(i+1)}(t) \, x^{(j)}(t) +$$
$$+ x^{(i)}(t) \, x^{(j+1)}(t)] \, 1(t) + x^{(i)}(0) \, x^{(j)}(0) \delta(t)$$

as a single initial function, we note that if the derivative is developed by the formula of Leibniz in the designations of the initial

functions (*) and (**), then it is necessary to exclude the unnecessary impulse:

$$D\left[x^{(i)}(t)\, x^{(j)}(t)\right] = x^{(i+1)}(t)\, x^{(j)}(t) +$$
$$+ x^{(i)}(t)\, x^{(j+1)}(t) - x^{(i)}(0)\, x^{(j)}(0)\, \delta(t).$$
(3-100a)

During coincidence of the orders of the factors $i = j$ we get a partial form of the general dependence:

$$D\left[x^{(i)2}(t)\right] = 2x^{(i)}(t)\, x^{(i+1)}(t) - x^{(i)2}(0)\, \delta(t).$$
(3-100b)

The initial values of the derivatives which form the coefficient before the impulse are determined according to the representation of the process (3-99a) on the basis of the formulas of the limiting transition.

We will examine at first the representation of the process with a unit numerator, that is, in formula (3-99a) we assume $b_0^* = 1$, $a_i^* = 0$ ($i = 1, 2,\ldots n$).

Then

$$x^{(n-1)}(0) = 1; \quad x^{(k)}(0) = 0 \quad \text{at} \quad k < n - 1.$$
(3-100c)

It can readily be noted that in equations (3-100) homogeneous unknowns enter the left and right sides in the form of multiplicable derivatives of different orders. We will introduce a numeration of the different variants of conjugate products; in that case at the beginning we will fix the order of the second factor j, and will vary the order of the first factor from $i = 0$ to $i = j$. Then, if we designate the first combination

$$y_1 = x(t)\, x(t) = x^2(t). \qquad (3\text{-}101a)$$

then for the k-th combination

$$y_k = x^{(i)}(t)\, x^{(j)}(t) \qquad (3\text{-}101b)$$

we will have:

$$k = \frac{1}{2} j(1 + j) + 1 + i. \qquad (3\text{-}101c)$$

Actually, the number of combinations exhausted by the value of the second index, equal to $j + 1$, is determined by a formula of arith-

setic progression, the first term of which, that is, the number of combination for i at $j = 0$ at the order of the second factor equal to $j - 1$, is j and the number of terms of the progression, that is, the number of variants with respect to the index j is j. The sum of the terms of the indicated arithmetic progression also exactly makes up the first term in the right side of formula (3-101c). Moreover, to that sum is added the incomplete number of combinations $i - 1$ for the index i, corresponding to the place of the variant with respect to it in the latter fixed value of the order of the second derivative j.

If we differentiate (3-101b), we note in accordance with formula (3-101a) that in the first term of formula (3-100a) the number of combinations is increased by unity, and in the second term, by $j + 1$, which in the designations of (3-101b) permits writing the result of the differentiation in this manner:

$$\dot{y}_s = y_{s+1} + y_{s+1+j} - x^{(i)}(0) x^{(j)}(0) \delta(t). \qquad (3\text{-}102a)$$

If we add to the numbers i and j the maximal values of $n - 1$, we get at $i \&\ j$ the total number of equations:

$$N = R_{max} = \frac{1}{2}(n-1)n + n = \frac{n(n+1)}{2}. \qquad (3\text{-}102b)$$

Among this group, $n(n-1)/2$ equations with (3-100a) taken into consideration will have the form

$$\left. \begin{array}{l} \text{At } i < j \; \dot{y}_s = y_{s+1} + y_{s+1+j}; \\ \text{At } i = j \; \dot{y}_s = 2y_{s+1+j}; \\ k = 1, 2 \dots \tfrac{1}{2}n(n-1). \end{array} \right\} \qquad (3\text{-}103a)$$

In the succeeding $n - 1$ equations, where

$$j = n - 1, \; k = \frac{1}{2}n(n-1) + i + 1;$$

$$i = 0, 1 \dots n - 2.$$

arising in the form of the factor, the highest derivative is replaced by the value from (3-99c)

$$x^{(n)}(t) = \delta(t) - a_0^n x(t) - a_1^n x(t) - \dots$$
$$- a_{n-1}^n x^{(n-1)}(t)$$

and with (3-103a) taken into consideration the equations assume the form:

$$\dot{y}_k = -y_{k+1} - x^{(i)}(t)[a_0^{ii} x(t) + a_1^{ii} \dot{x}(t) + \ldots + $$
$$+ a_{n-1}^{ii} x^{(n-1)}(t)]. \qquad (3\text{-}103b)$$

In this case the substitution of (3-101b) and (3-101c) for the extreme values of k gives:

At $i = 2$:

$$\dot{y}_{\frac{1}{2} n(n-1)+1} = -y_{\frac{1}{2} n(n-1)+2} - a_0^{ii} y_1 - $$
$$- a_1^{ii} y_2 - a_2^{ii} y_3 - a_3^{ii} y_4 - \ldots - $$
$$- a_n^{ii} y_{\frac{1}{2} n(n-1)+1}; \qquad (3\text{-}103c)$$

At $i = n - 1$:

$$\dot{y}_{N-1} = -y_N - a_0^{ii} y_{\frac{1}{2} n(n-1)} - $$
$$- a_1^{ii} y_{\frac{1}{2} n(n-1)+1} - \ldots - a_{n-1}^{ii} y_{N-1}. \qquad (3\text{-}103d)$$

Finally, for the N-th equation we get:

$$\dot{y}_N = 2 x^{(n-1)}(t) [\delta(t) - a_0^{ii} x(t) - \ldots - $$
$$- a_{n-1}^{ii} x^{(n-1)}(t)] - [x^{n-1}(0)]^2 \delta(t),$$

or in the designations of (3-101c):

$$\dot{y}_N = \delta(t) - 2 [a_0^{ii} y_{N-n+1} + $$
$$+ a_1^{ii} y_{N-n+2} + \ldots + a_{n-1}^{ii} y_N]. \qquad (3\text{-}103e)$$

The preceding system of equations (3.103) a, b, c, d and e, ... is .... and can be correlated into a single equation or from it a solution with respect to the quadratic evaluation y_2 can be obtained directly in operator form.

We will present as an example the determination of the quadratic evaluation for a process that has $n = 2$, $m = 0$ and $b_0^m = 1$ in formula (3.90a).

In this case the total number of equations (3.102a) is

$$N_2 = \frac{2 \cdot 3}{2} = 3.$$

The equation of the process is:

$$\ddot{x}(t) + a_1^u \dot{x}(t) + a_0^u x(t) = \delta(t).$$

The initial values of this process are the following:

$$\dot{x}(0) = 1; \quad x(0) = 0.$$

As a result of this the first equation of type (3.100b) does not have a singular component:

$$\dot{y}_1(t) = [x^2(t)]' = 2x(t)\dot{x}(t) = 2y_3(t). \qquad (3.104a)$$

The second equation of type (3.100a) likewise does not contain ...., but requires replacement of the highest derivative by .... of the equation of the process:

$$\ddot{x}(t) = \delta(t) - a_1^u \dot{x}(t) - a_0^u x(t).$$

After which it assumes the form:

$$\dot{y}_2(t) = x^2(t) - a_1^u x^2(t) - a_0^u x(t)\dot{x}(t) =$$

$$= y_1 - a_0^u y_1 - a_1^u y_2 \qquad (3.104b)$$

The third equation of type (3.100c) requires into introduction of the highest are replacement of the highest derivative.

$$\dot{y}_3(t) = [x^2(t)]' = 2x(t)[\delta(t) - a_1^u \dot{x}(t) -$$

$$- a_0^u x(t)] - x^2(0)\delta(t) = \delta(t) -$$

$$- 2a_1^u y_3 - 2a_0^u y_2. \qquad (3.104c)$$

We shall proceed from the processes $y_i(t)$ to their Laplace transforms $Y_i(p)$ by carrying over all the variables into the left sides of the equations:

$$p Y_1(p) - 2 Y_2(p) = 0;$$

$$a_1^2 Y_1(p) + (p + a_1^2) Y_2(p) - Y_3(p) = 0; \quad (3\text{-}104d)$$

$$2a_1^2 Y_2(p) + (p + 2a_1^2) Y_3(p) = 1.$$

The solution of this system with respect to $Y_1(p)$ will be written in the form of the determinant:

$$Y_1(p) = \frac{\Delta_{31}(p)}{\Delta(p)}, \qquad (3\text{-}104e)$$

where $\Delta(p)$ is the main determinant of the system
$\Delta_{31}(p)$ is the cofactor for the coefficient of the third row of the first column, equal to unity.

We will expand these determinants:

$$\Delta(p) = \begin{vmatrix} p & -2 & 0 \\ a_1^2 & p + a_1^2 & -1 \\ 0 & 2a_1^2 & p + 2a_1^2 \end{vmatrix} = p(p + a_1^2)p \times$$

$$\times (p + 2a_1^2) + 2a_1^2 + 2a_1^2(p + 2a_1^2) - \\ - (p + a_1^2)(p^2 + 2a_1^2 p + 4a_1^2),$$

$$\Delta_{31}(p) = \begin{vmatrix} -2 & 0 \\ p + a_1^2 & -1 \end{vmatrix} = 2.$$

and shall write the expanded expression for the reprsdistribution of the quantity in question:

$$Y_1(p) = \frac{2}{(p + a_1^2)(p^2 + 2a_1^2 p + 4a_1^2)}$$

and according to table 3-2 find the original at $4a_1^2 > a_1^2$

$$x^2(t) = \frac{2e^{-a_1 t}}{4a_0 - a_1^2}(1 + \cos t\sqrt{4a_0 - a_1^2}) =$$

$$= \frac{4e^{-a_1 t}}{4a_0 - a_1^2} \sin^2 \frac{t}{2}\sqrt{4a_0 - a_1^2}.$$

The solution is readily compared with (3-93a) if it is assumed that:

$$k = \frac{1}{a_0^{II}}; \quad \tau = \frac{1}{\sqrt{a_0^{II}}}; \quad \xi = \frac{a_1^{II}}{2\sqrt{a_0^{II}}}.$$

The value of the solution obtained in operator for for the quadratic evaluation naturally rises with increase in the order of the equation described by the process, and is especially manifested in seeking the limiting values of the quadratic evaluation, which in the operator form are limitingly simple.

If the process is given by an expression with a complicated numerator:

$$X(p) = \frac{b_1^{II} p + b_0^{II}}{p^2 + a_1^{II} p + a_0^{II}},$$

then the equation of the process acquires the form:

$$\ddot{x}(t) + a_1^{II} \dot{x}(t) + a_0^{II} x(t) = b_1^{II} \dot{\delta}(t) + b_0^{II} \delta(t)$$

with the initial values:

$$x(0) = b_1^{II}; \quad \dot{x}(0) = b_0^{II} - b_1^{II} a_1^{II};$$

$$\ddot{x}(0) = a_1^{II}(a_1^{II} b_1^{II} - b_0^{II}) - a_0^{II} b_1^{II}.$$

In this case, in making up the first equation, besides the terms contained in (3-104a) it is necessary to take into consideration the impulse component:

$$\dot{y}_1(t) = 2y_2(t) - x^2(0)\delta(t) =$$
$$= 2y_2(t) - b_1^2 \delta(t). \qquad (3-105a)$$

In setting up the second equation we introduce impulses on the

right side of (3-105b) in the first place, on the basis of (3-100a), and secondly, on the basis of replacement of the highest derivative from one equation of the process:

$$\dot{y}_2(t) = y_3(t) - a_0^{\shortparallel} y_1(t) - a_1^{\shortparallel} y_2(t) + x(t) \left[b_1^{\shortparallel} \dot{\delta}(t) + b_0^{\shortparallel} \delta(t) \right] - x(0)\dot{x}(0)\delta(t).$$

All this gives:

$$\dot{y}_2(t) = y_3(t) - a_0^{\shortparallel} y_1(t) - a_1^{\shortparallel} y_2(t) +$$
$$+ x(0) b_1^{\shortparallel} \dot{\delta}(t) - \{\dot{x}(0)[b_1^{\shortparallel} + x(0)] -$$
$$- x(0) b_0^{\shortparallel} \} \delta(t),$$

or with the actual initial values taken into consideration:

$$\dot{y}_2(t) = y_3 - a_0^{\shortparallel} y_1 - a_1^{\shortparallel} y_2 + b_1^2 \dot{\delta}(t) -$$
$$- b_1 (b_0 - 2a_1 b_1) \delta(t). \qquad (3\text{-}105b)$$

For the third equation we will take (3-100c) as a basis, but will form here the impulse components analogously to the second equation:

$$\dot{y}_3(t) = -2a_0^{\shortparallel} y_2 - 2a_1^{\shortparallel} y_3 + \dot{x}(t) \{ b_1^{\shortparallel} \dot{\delta}(t) +$$
$$+ b_0^{\shortparallel} \delta(t) \} - \dot{x}^2(0) \delta(t) = -2 (a_0^{\shortparallel} y_2 +$$
$$+ a_1^{\shortparallel} y_3 + \dot{x}(0) b_1^{\shortparallel} \dot{\delta}(t) - \{ b_1^{\shortparallel} \ddot{x}(0) +$$
$$+ \dot{x}(0) [\dot{x}(0) - b_0^{\shortparallel}] \} \delta(t).$$

After the transition to the actual initial values, we get:

$$\dot{y}_3(t) = -2 (a_0^{\shortparallel} y_2 + a_1^{\shortparallel} y_3) + (b_0^{\shortparallel} - b_1^{\shortparallel} a_1^{\shortparallel}) \dot{\delta}(t) -$$
$$- [2a_1^{\shortparallel} b_1^{\shortparallel} (a_1^{\shortparallel} b_1^{\shortparallel} - b_0^{\shortparallel}) - a_0^{\shortparallel} b_1^2] \delta(t). \quad (3\text{-}105c)$$

The replacement of the processes by their representations gives a system of operator equations in which the left sides coincide with the left sides of relations (3-105a), and the right sides are multiplied. As a result of this the main determinant of the system will

factor for the elements of the first column do not change, but formula (3-105a) obtains the development:

$$Y_1(p) = \frac{1}{\Delta(p)} \left\{ -b_1^{"} \Delta_{11}(p) + [b_1^2 p - \right.$$

$$- b_1(b_0 - 2a_1 b)] \Delta_{21}(p) + \{(b_0^{"} - b_1^{"} a_1^{"}) p - $$

$$\left. - b_1^{"}[2a_1^{"}(a_1^{"} b_1^{"} - b_0^{"}) - a_0^{"} b_1^{"}]\} \Delta_{31}(p). \right. \quad (3-105d)$$

where

$$\Delta_{31}(p) = 2(p + 2a_1^{"});$$

$$\Delta_{11}(p) = (p + a_1^{"})(p + 2a_1^{"}) + 2a_0^{"}.$$

Review of the formulas for the second-order equations (3-104) and (3-105) permits establishing the character of the Δ_Δ-transformation which must be carried out on the representation of the process given in the form of (3-99a) for the transition to the representation of its quadratic evaluation (3-99b):

$$L\{x^2(t)\} = Y_1(p) = \Lambda_\Delta\{X(p)\} = $$

$$= \Lambda_\Delta \left\{ \frac{b_m^{"} p^m + \ldots + b_1^{"} p + b_0^{"}}{p^n + \ldots + a_1^{"} p + a_0^{"}} \right\} = $$

$$= \frac{1}{\Delta(p)} \sum_{i=1}^{n} B_i(p) \Delta_{i1}(p). \quad (3-106)$$

Here $\Delta(p)$ is the main determinant of the system of equations for the quadratic evaluation, composed according to the general procedure indicated by formulas (3-102) and (3-103); $\Delta_{i1}(p)$ is its cofactor for elements of the first column; $B_i(p)$ are the displaced elements of the first column, in which, besides the operator terms, the initial values of the process enter, determined above for a second-order process (3-105a) and calculable in the general case for any process with the attraction of Table 3-3.

Energetic Evaluation of the Process

If we assume, as was noted at the beginning of this section, the square of the process $x^2(t)$ to be an evaluation of its capacity,

It is possible to make an estimate of the energy consumed in the entire process by the formula

$$I_2 = \int_0^\infty x^2(t)\,dt = \int_0^\infty y_1(t)\,dt. \qquad (3\text{-}107a)$$

If we use the rule of limiting transition (3-99) at $\gamma = 0$, the problem of determining the integral (3-107a) in the presence of tendency of the upper limit of the integration toward infinity ($t \to \infty$) can be solved in the region of the representations:

$$I_2 = \lim_{p \to 0} Y_1(p) = Y_1(0) =$$

$$= \lim_{p \to 0} \Delta \left\{ \frac{b_n'' p^n + \ldots + b_0''}{p^n + \ldots + a_1'' p + a_0''} \right\} =$$

$$= \frac{1}{\Delta(0)} \sum_{i=1}^{l} B_i(0)\,\Delta_{1i}(0). \qquad (3\text{-}107b)$$

For damping processes the energetic estimate is expressed by a finite positive number. Thus, for example, in the case of a second-order process, examined above, we get:

$$I_2 = \lim_{p \to 0} \Delta_2 \left\{ \frac{1}{p^2 + a_1'' p + a_0''} \right\} :$$

$$I_2 = \frac{\Delta_{21}(0)}{\Delta(0)} = \frac{\begin{vmatrix} -2 & 0 \\ a_1'' & -1 \end{vmatrix}}{\begin{vmatrix} 0 & -2 & 0 \\ a_0'' & a_1'' & -1 \\ 0 & 2a_0'' & 2a_1'' \end{vmatrix}} = \frac{1}{2a_0'' a_1''}. \qquad (3\text{-}107c)$$

For non-damping processes there is no finite estimate I_2.

The attraction for analysis of the quadratic evaluations of linear methods has permitted examining them in the first part of this book.

Bibliography

1. Sech 3, Rukovodstvo k prakticheskomu primeneniyu preobrazovaniya

Laplasa (Manual for the Practical Application of Laplace Trans-
forms), Fizmatgiz, 1960.

2. Ditkin V A and Kuznetsov P I, Spravochnik po operatsionnomu
   ischisleniyu (Handbook of Operational Calculus), Gostekhizdat,
   1950.

3. Bashkirov D A, Grafoanaliticheskiy metod analiza perekhodnykh
   protsessov v sistemakh avtomaticheskogo regulirovaniya (Graphic-
   Analytic Method of Analysis of Transient Processes in Automatic
   Control Systems), 1950.

4. Shatalov A S, Engineering method of the linear theory of control
   systems with variable parameters, Avtomaticheskoye upravleniye i
   vychislitel'naya tekhnika (Automatic Control and Computer Tech-
   nology), 1959, No 3.

5. Litovchenko Ts G, Analtyical solutions of linear equations des-
   cribing dynamic systems with variable parameters of a single
   class, Avtomatika i telemekhanika (Automation and Telemechanics),
   1961, No 4.

6. Zade L A, Determination of an impulse transient function in vari-
   able systems, J. Appl. Phys., 21, July 1950.

7. Krasovskiy A A and Pospelov G S, Some methods of calculation of
   approximate time characteristics of linear automatic control
   systems, Avtomatika i telemekhanika, 1953, No 6.

8. Pospelov G S, Osnovy avtomatiki (Principles of Automation), 1954.

Chapter 4

FREQUENCY ANALYSIS

pp. 107-150

4-1. Forms of Frequency Characteristics and Their
Analytical Calculation

A. Terminology

The frequency characteristic of a component is an analog of its transfer function for the particular case of a forced regime in the presence of harmonic input action. As was shown in the preceding chapter, in the output reaction of a linear system there always is a constituent the representation of which contains the poles of the input action, that is, a so-called forced constituent. Consequently, for a harmonic action the forced reaction will also be harmonic.

The conditions of excitation of the forced reaction on harmonic control action in a linear component are shown in Figure 4-1. Let us recall that besides this reaction the output process can contain all the partial constituents of the proper motion of the component: the damping, increasing and neutral, determinable by the character of the poles of the transfer function of the component itself.

If all the partial constituents of the proper motion have a damping character, then for a certain interval of time in the regime being established on the output of the component there remains only the forced harmonic constituent. Thus the lower graph in Figure 4-1 forms without any limitations a single forced partial constituent of the output process, or the complete output reaction but with the following limitations: the component has damping proper motion, and the time of observation is greater than the time of damping of the proper motion.

Special frequency characteristics are introduced for evaluation of the transfer properties of the component.

The amplitude-frequency characteristic (AFC) of the component or automatic control system is the name given to the analytically or graphically given function of the frequency $A(\omega)$, which equals the ratio of the amplitude of the forced harmonic oscillations that have been established on the output of the system $A_{out}(\omega)$ to the amplitude of the input oscillations $A_{in}(\omega)$:

$$A(\omega) = \frac{A_{out}(\omega)}{A_{in}(\omega)}. \qquad (4-1)$$

If the input oscillations have a single amplitude, then $A(\omega) = A_{out}(\omega)$ and the amplitude-frequency characteristic is nothing but the dependence of the amplitude of the output oscillations on the frequency. The frequency, as a rule, is expressed in control theory in radians per second, more rarely in cycles per second (periods per second).

It is also convenient to consider the amplitude-frequency characteristic as the amplification factor of the amplitude of oscillations or amplification in modulus in the regime of the harmonic oscillations.
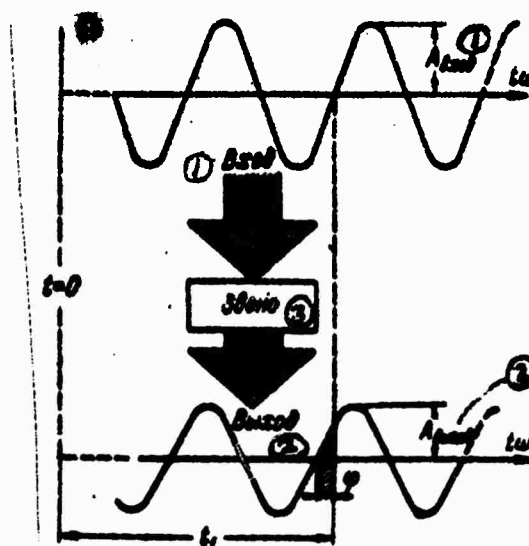
Fig 4-1. Linear component with constant parameters under conditions of harmonic action. 1 - Input; 2 - Output; 3 - Component.

The phase-frequency characteristic (PFC) is the difference between the phases of the output $\varphi_{out}(\omega)$ and input $\varphi_{in}(\omega)$ harmonic

oscillations that have been established:

$$\psi(\omega) = \varphi_{out}(\omega) - \varphi_{in}(\omega). \qquad (4\text{-}2)$$

For illustration of the phase shift, markings have been made on Figures 4-1 on the input and output at the identical moment of time t_1. In the input oscillations the marking fell on the start of the wave, and in the output oscillations at the moment t_1 there already is observed, not a zero, but a certain positive value of the output.

In Figure 4-1 the shift between the input and output oscillations is measured by the interval of time $+\Delta t$. For transition from the time shift to the phase, the known relation

$$\varphi = \frac{2\pi\Delta t}{T} = \omega\Delta t.$$

is used.

The amplitude-phase characteristic. The change in the amplitude and change in the phase of the output oscillations in correspondence with AFC $A(\omega)$ and the PFC $\varphi(\omega)$ can be given in the form of the general complex function:

$$W(j\omega) = A(\omega)\,e^{j\varphi(\omega)}, \qquad (4\text{-}3)$$

representing for the given frequency a vector on a complex plane, the modulus of which corresponds to the amplitude characteristic and the argument of which corresponds to the phase characteristic of the system.

The geometric place of the ends of the vector $A(\omega)^{ej\varphi(\omega)}$, or its hodograph, is a graphic representation of the amplitude-phase characteristic. One of the possible forms of this hodograph is shown in Figure 4-2.

Instead of the term "amplitude-phase characteristic", the term "complex amplification factor" is often used.

Real and imaginary frequency characteristics. The complex amplification factor $A(\omega)e^{j\varphi(\omega)}$, like every complex number, can be expanded into a real and an imaginary constituent:

$$A(\omega)\,e^{j\varphi(\omega)} = P(\omega) + jQ(\omega),$$

which are called the real

$$P(\omega) = A(\omega)\cos\varphi(\omega) \qquad (4.4)$$

and the real

$$Q(\omega) = A(\omega)\sin\varphi(\omega) \qquad (4.5)$$

frequency characteristics respectively.
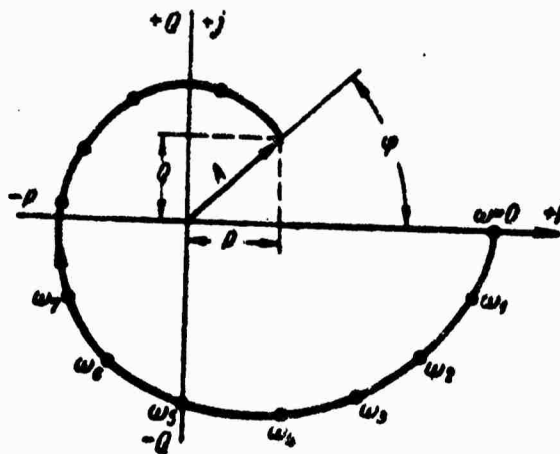
Fig 4-2. Amplitude-phase frequency characteristic --
hodograph of the vector $W(j\omega)$.

The modulus of the complex amplification factor equals the geometric sum of the real and imaginary constituents:

$$A(\omega) = \sqrt{P^2(\omega) + Q^2(\omega)}. \qquad (4.6)$$

B. Calculation of the Frequency Characteristics
    by the OFT of the Component

Let the OPT of a component be given in the form:

$$W(p) = \frac{\sum_{j=0}^{m} b_j p^j}{\sum_{i=0}^{n} a_i p^i}. \qquad (*)$$

Then to obtain the frequency characteristics it is sufficient to turn to the general formula (3-37d), having assumed in it that $\sigma = 0$. This replacement, and likewise the entire conclusion given in Section 3-7, permit giving strict analytical expressions for determination of the various types of frequency characteristics.

The amplitude-phase characteristic, or complex amplification factor, equals the transfer function of the system upon substitution of $p = j\omega$:

$$W(p)_{p=j\omega} = W(j\omega) = A(\omega) e^{j\varphi(\omega)}.$$

The amplitude-frequency characteristic -- the modulus of the complex amplification factor -- can be expressed in the form of the root of the product of the conjugate functions:

$$A(\omega) = |W(j\omega)| = \sqrt{W(j\omega) W(-j\omega)}. \qquad (4-8)$$

The real and imaginary frequency characteristics are the corresponding parts of the complex amplification factor

$$P(\omega) = \operatorname{Re} W(j\omega); \quad Q(\omega) = \operatorname{Im} W(j\omega). \qquad (4-9)$$

The phase-frequency characteristic is a phase of the complex amplification factor

$$\operatorname{tg} \varphi(\omega) = \frac{\operatorname{Im} W(j\omega)}{\operatorname{Re} W(j\omega)}. \qquad (4-10)$$

In using formula (4-10) it is necessary to take strictly into consideration the signs of the numerator and denominator, since according to them is determined the quadrant in which the unknown angle is located. In Figure 4-2, on the axis of the coordinates, the directions are marked for the positive and negative signs of the real and imaginary constituents of the complex amplification factor. Since the general form of the transfer function was determined above in the form

of the ratio of the polynomials from p, the frequency characteristics can also be expressed by the coefficients of the same polynomials.

In the first place, the substitution of $j\omega$ instead of p gives the expanded expression for the amplitude-phase characteristic:

$$W(j\omega) = \frac{b_m (j\omega)^m + \ldots + b_1 j\omega + b_0}{a_n (j\omega)^n + \ldots + a_1 j\omega + a_0}. \qquad (4\text{-}11)$$

In addition, if we have joined in the numerator and denominator the real and imaginary terms, we have

$$W'(j\omega) = \frac{P_{num} + jQ_{num}}{P_{den} + jQ_{den}}, \qquad (4\text{-}12)$$

where

$$P_{num} = b_0 - b_2\omega^2 + b_4\omega^4 - \ldots; \quad Q_{num} = b_1\omega - b_3\omega^3 + b_5\omega^5 - \ldots;$$

$$P_{den} = a_0 - a_2\omega^2 + a_4\omega^4 - \ldots; \quad Q_{den} = a_1\omega - a_3\omega^3 + a_5\omega^5 - \ldots$$

In the second place, multiplication of the denominator of the obtained fraction by the conjugate complex number $P_{denom} - jQ_{denom}$ gives the possibility of separating the real and imaginary frequency characteristics

$$W(j\omega) = \operatorname{Re} W + j \operatorname{Im} W,$$

each of which can be expressed in the following manner:

$$\operatorname{Re} W = \frac{P_n P_3 + Q_n Q_{den}}{P_3^2 + Q_{den}^2} = P(\omega); \qquad (4\text{-}13a)$$

$$\operatorname{Im} W = \frac{Q_n P_3 - P_n Q_{den}}{P_3^2 + Q_{den}^2} = Q(\omega). \qquad (4\text{-}13b)$$

In the third place, expanded expressions for the amplitude-frequency characteristic can be obtained from the preceding formulas:

$$A(\omega) = \sqrt{P^2 + Q^2} = \sqrt{\frac{P_{num}^2 + Q_{num}^2}{P_3^2 + Q_{den}^2}} \qquad (4\text{-}14)$$

D. Regimes of Harmonic Oscillations in Automatic Control Technique

Automatic control systems and their components can in a number of cases be in regimes of harmonic oscillations.

Firstly, the regime of harmonic oscillations can be the basic operating regime of the control system, for example the regime of operation of the gear of a stabilizing platform on the deck of a ship in a period of rolling. In that case the automatic control system -- the stabilization gear of the platform -- must compensate as accurately as possible (must exhaust) for these oscillations.

Secondly, the harmonic oscillations often penetrate the main and auxiliary channels of the control system in the form of a noise signal and are superposed on the relatively smooth, regularly varying working signal. In that case the automatic control system will obviously be all the better the less the harmonic noises are asserted on the output value.

Thirdly, the harmonic oscillations can not only be introduced from without but also can arise within the system itself as a result of complex internal and external connections, mainly feedbacks. In that case, for such a system inclined toward the oscillations, its components are presented the problem of modifying in a corresponding manner the amplitude and phase of those oscillations for their complete liquidation.

Fourthly, the regime of harmonic oscillations can serve as a checking regime which can be given to a system being tested in an adequately simple way and by means of which it is possible to show a number of important properties of any complex automatic control system.

Fifthly, investigation of the regimes of harmonic oscillations of a system at all frequencies, mainly analytical, provides an exhaustive representation of all the dynamic properties of a linear system on the basis of use of a Fourier transformation, to a great extent analogous in its possibilities to the Laplace transform examined in Chapter 3.

From all that has been said it follows that knowledge of the transfer properties of an automatic control system, and above all of its components in a regime of forced harmonic oscillations is very important and necessary.

4-2. Experimental Methods of Taking Down the Frequency Characteristics

A. Harmonic Oscillation Pickups

Various designs of harmonic oscillations pickups, also called sine pickups, are used for experimental investigation of automatic control systems or their components.

Two types of sine mechanical pickups are shown in Figure 4-3. Type a is the ordinary eccentric with constant eccentricity that can be joined to a spring piston pressed against it. The eccentric is brought into rotation from the gear with the controllable rate Ω. The rotation of the eccentric at the given rate Ω is transformed into back-and-forth motion of the piston. The piston rod completes the harmonic oscillation with the frequency ω. The linear oscillations of the rod can be supplied directly to the input of the mechanical elements of the automatic control system; for example, the rod is connected to the piston of an automatic control system, etc. However, in case of need the linear mechanical displacement can be transformed into electric voltage by means of connection of the rot with the brush of a linear potentiometer, as shown in the upper part of diagram a. In that case the voltage between the brush and the midpoint of the potentiometer will also vary sinusoidally and can be supplied to the input of the electric elements of the automatic control system.

The sine pickup (Figure 4-3b) differs from plan a by a device for the creation of a variable eccentrici y by means of a screw pair which provides displacement of the cam connected with the piston along the diameter of the disc. The starting scale of the oscillations, suitable from the point of view of connection of the pickup to the input elements of the automatic control system being investigated, is subjected to change of eccentricity and consequently of amplitude of the harmonic oscillations. Additional features of design b are bilateral connection of the cam to the piston, eliminating the need for spring compression, and a rack and pinion gear in the upper part of the rod, which transforms its linear oscillations into harmonic rotary oscillations of the pickup D.

Two types of electric sine pickups are shown in Figure 4-4. In both pickups the sine dependence of the voltage of the pickup on time is obtained at a uniform rotation of the drive roller.

The pickup of type a creates harmonic oscillations of direct current voltage, more precisely, oscillations of infralow frequency from fractions of a cycle per second to tens of cycles per second. It is made in the form of two plate potentiometers with two end brushes. The brushes complete a uniform rotary motion at a given rate, but the voltage taken from the brushes is varied sinusoidally, since it is proportional not to the angle of the rotation but to its sine (Figure 4-4a).

The pickup of type b assures the creation of modulated harmonic oscillations which are necessary in tests of an automatic control sys-
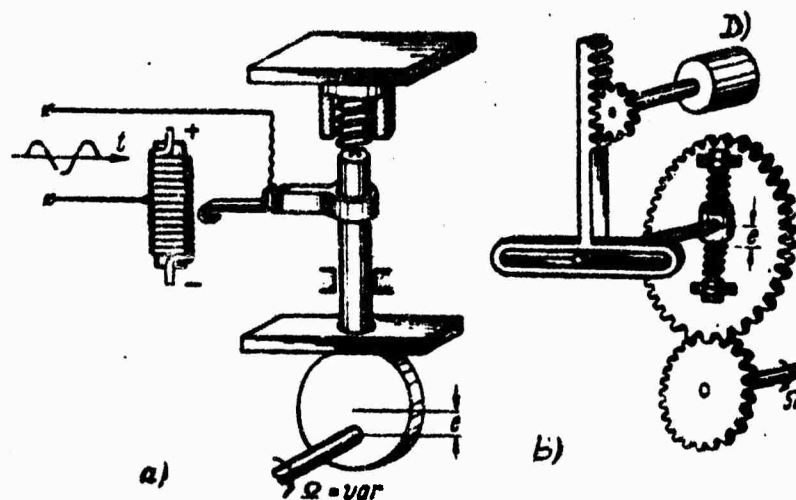
Fig 4-3. Sine mechanisms with electric signal pickups.
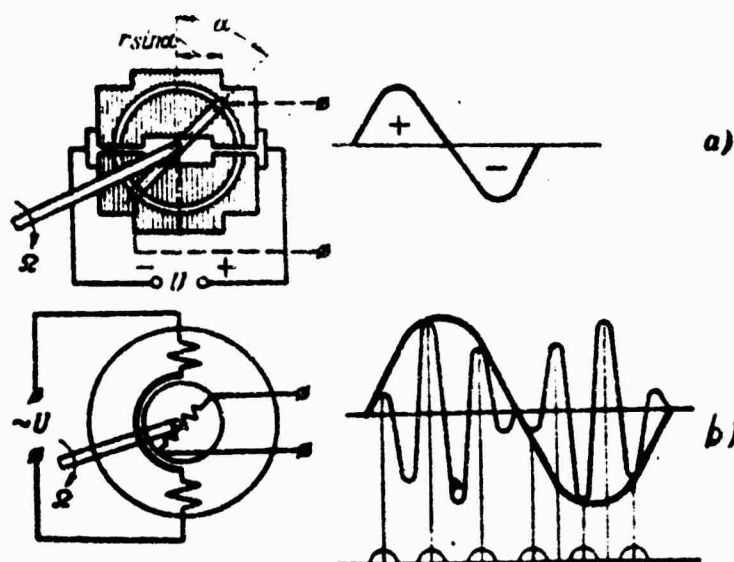
Fig 4-4. Electromechanical sine pickups.

tem with input elements of alternating current. The pickup is a
rotating transformer, the primary winding of which is fed from a
50 - 500 c p s network, and the secondary winding of which is com-
bined with the input of the automatic control system being tested.
The secondary e m f of the transformer has a frequency equal to that
of the network, called the carrier frequency. The amplitude of the
secondary e m f varies proportionally to the sine of the angle of
rotation of the rotor at the beginning of reading of the angle from
the position at which the windings of the stator and rotor are mutu-
ally perpendicular. In addition, during the transition of the ampli-
tude of the emf through zero, the phase of the carrier frequency
varies each time by 180°. When there is uniform rotation of the
rotor the envelope of the secondary emf varies with a frequency of
modulation equal to the frequency of rotation of the rotor, as shown
on the right in diagram b. The carrier frequency in the given case
is only a "filling" graph of the frequency; the automatic control
system being tested will react to the oscillations with a frequency
of modulation shown on the graph in the form of the envelope of the
sinusoid, whereupon the sign of each half-wave of the envelope is
connected with the phase of the filling frequency. On the graph, from
below, the apexes of the positive half-waves of the frequency of the
network are shown for control of the phase of the enveloping frequency.
The coincidence of the phase of this voltage with the phase of the
filling frequency corresponds to the positive half-wave of the enve-
lope, and a difference of 180°, to the negative half-wave.

A sine induction pickup also can be used for automatic control
systems operating on direct current, if its output voltage passes
through a demodulator. In exactly the same way a potentiometric pick-
up, when fed alternating current, can be used as a pickup of an am-
plitude-modulated signal.

Besides the above-considered pickups of harmonic oscillations
with a mechanical drive, electric and electronic generators which are
in a regime of stable oscillations are also used.

B. Diagram of Cut-In of a Registering Arrangement for
   Taking Down Frequency Characteristics by a Direct Method

The frequency characteristics of a component manifest themselves
most simply during the simultaneous registration of input and output
oscillations for each frequency on any type of registering instrument.
If the real region of the infralow frequency oscillations of the com-
ponent being investigated is taken into consideration, it proves pos-
sible for their registration in each separate case to use either mech-
anical recording or electrical recorder or oscillograph; the latter
permit considerable expansion of the region of the frequencies being
registered.

In Figure 4-5a is presented one of the simplest diagrams of a
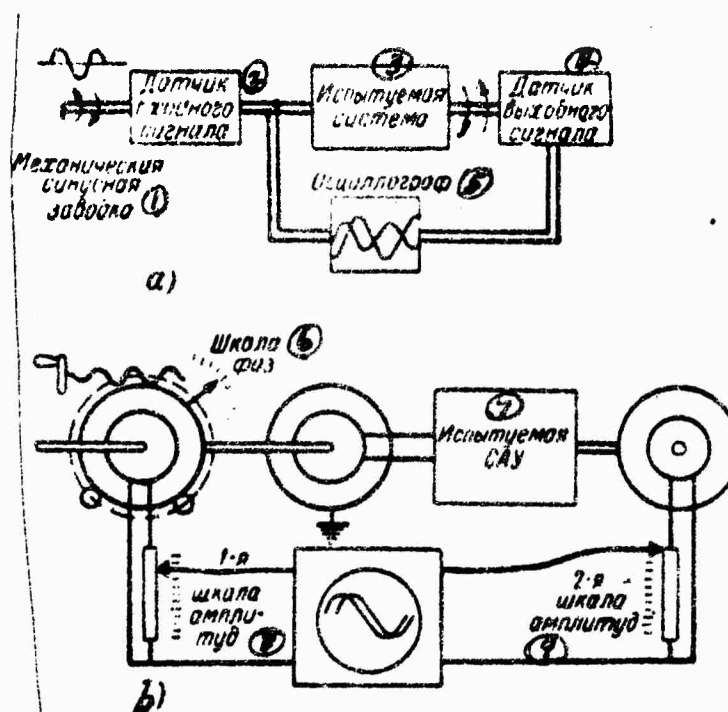
Fig 4-5. Direct and compensated methods of taking off frequency characteristics. 1 - Mechanical sine winding; 2 - Input signal pickup; 3 - System being tested; 4 - Output signal pickup; 5 - Oscillograph; 6 - Scale of phases; 7 - System being tested; 8 - Scale of amplitudes; 9 - Second scale of amplitudes.

similar type with utilization of an electric registering instrument, for example, an oscillograph. The system being tested has an electrical input and mechanical output, for example, and electric motor, controllable by an amplifier. An electrical pickup of harmonic oscillations is connected up with the input of the system. The input oscillations not only enter the system, but at the same time are fed to one loop of the oscillograph. Since the system depicted in the figure has a mechanical output, for registration of the output oscillations it is necessary to transfrom them into electrical voltage. This transformation is readily accomplished, for example, by a potentiometric linear pickup.

The joint registration of the input and output oscillations at previously set scales and agreed starts of reading of the processes permits later on readily determining the phase and amplitude-frequency characteristics. These characteristics can be taken off with a scanning of a loop oscillograph or from the screen of a two-gun

cathode oscilloscope. The recording is made most exactly on tape. The main inconvenience in this is the need to have separate sections of the oscillogram, in some cases rather extended, in order that the oscillations may successfully assume the character being established for each frequency, that is, actually for each point of the frequency characteristic.

Along with the two-gun cathode oscillograph it is possible to use a cathode oscillograph with an electronic commutator for simultaneous obtaining on the screen of the input and output oscillations. The screen of the oscillograph is calibrated in advance for the reading of amplitude and phase, by providing it with a constant or pickup scale network.

C. Diagram of Arrangement for Taking the Frequency Characteristics By a Compensated Method

The principle of the compensated method of measurement will be examined on the example of the circuit depicted in Figure 4-5b.

Let a sine transformer be used as the elements of the loop, for example, one of those shown in Figure 4-4. In that case, to obtain the input electric signal in the form of harmonic oscillations of various frequencies it is sufficient to communicate to the input cylinder a rotary motion with a different speed.

Two pickups of the input harmonic signal (Figure 4-5b, left) enter the composition of the circuit under consideration.

The pickup connected directly with the system investigated has a fixed stator-frame and gives the system a signal constant in amplitude and phase.

The pickup connected with the cathode oscillograph has a rotary body, thanks to which the voltage taken from it can be shifted artificially in phase during rotation of the body, for example, from a worm gear. The amplitude of this signal can be decreased by the voltage divider.

If the automatic control system being tested has a mechanical output in the form of a roller, a linear pickup is connected with it which controls the second beam of the cathode oscillograph.

Work with this circuit, in taking the frequency characteristics, amounts to the following operations:

Establishment of the desired rate of rotation of the pickups, equal to the angular frequency of the input signal (sec^{-1});

Control of the phase by rotation of the body of the pickup until it coincides with the zero points of the input and output sinusoids on the screen of the oscillograph;

Control of the amplitude by the input potentiometer at A $<$ 1 and output potentiometer at A $>$ 1 until the apexes of the half-waves of the input and output sinusoids are equated;

Recording the readings according to the scales of phase and amplitude for the given frequency.

Since the reading is done according to mechanical scales, its accuracy is much higher than in the case of the direct method of measurement, all the more so that the mechanical scales can be provided with so-called verniers or devices for rough and precise reading of the type of vernier. Even in this case, however, accuracy of the order of 1% is attainable with difficulty, since a cathode oscillograph itself has limited accuracy as an indicator of comparison and, moreover, the output oscillations, besides the basic frequency, can contain the highest harmonics, which makes comparison of the output and input oscillations difficult. For practical purposes the accuracy mentioned is completely adequate.

If desired, the oscillograph in that circuit can be replaced by two indicating instruments -- zero wattmeters, if the pickup with the rotating body is provided with two mutually perpendicular networks or windings.

The first zero wattmeter in this case is connected to a single pair of networks or to a single winding of the pickup of input oscillations and to the pickup of output oscillations. The mean deviation of the pointer of the zero wattmeter will be proportional to the cosine of the difference of the phases of the input and output oscillations; by rotation of the body of the pickup it is possible to displace it to zero at a difference in phases equal to 90°. The second zero wattmeter is connected up with the difference in voltages formed on the second coil of the pickup with the rotating body and on the output pickup. This difference, since the compared voltages are in phase, is reduced to zero by displacement of the networks of the potentiometers (see Chapter 14).

The reading of phase and amplitude after adjustment of both zero wattmeters to zero is done by the mechanical scales, just as in the circuit with the oscillograph.

The realization of the indicated circuit on zero-wattmeters, model IK-42, has shown satisfactory results at elevated frequencies. At frequencies below 5 c p s the second harmonic is inadequately smoothed out by the mobile system of the wattmeter and the readings

267

of zero become difficult.

D. Infralow Frequency Registering Apparatus

It is inconvenient to record frequencies measured in cycles per second or fractions of cycles per second on a loop oscillograph or to examine them on a cathode oscillograph due to the necessity of very slow time scanning. This compels the use of special infralow frequency apparatus -- a phasometer and peak voltmeter.

A phasometer, of type NF-1 for example, is based on the principle of measurement of the interval of time between the moments of passage of the input and output sinusoid through zero. The time interval in turn is estimated by a digital computer, which registers the number of waves of oscillations of a stable frequency of 100 cps in the measured interval of time.

The amplitude is measured, for example, by a peak voltmeter of type DVP-1. In the English electronic instrument -- the "Solartron" process analyzer, the real and imaginary characteristics are measured separately by peak voltmeters.

E. Indirect Methods of Determining the Phase-Frequency Characteristic

In the simplest cases the amplitude-frequency characteristic can be taken by means of a single indicating instrument; for taking the phase characteristic a more complex apparatus usually is required. If it is desirable to avoid this, the method of taking two amplitude-frequency characteristics of the given and of an additional system is used.

Usually elementary complements are used; the most extensive of them are given in Figure 4-6.

In diagram a, firstly, the amplitude of the output oscillations 2 is taken, which upon comparison with the input oscillations 1 gives the basic characteristic, and, secondly, the amplitude of the sum of the input and output oscillations 3 is taken. Since the total amplitude 3 depends not only on the constituent amplitudes 1 and 2, but also on the phase shift between them, it is easy to make the latter manifest by measurements of amplitudes 2 and 3. The analytical calculations and nomograms for the calculation are given in Figure 4-6.

F. Taking the Real and Imaginary Frequency Characteristics
    of a Component by Means of Elements of an Electronic Model
    by an Active Method

The essence of the active method [1] is that the component being tested itself participates in the generation of oscillations of a
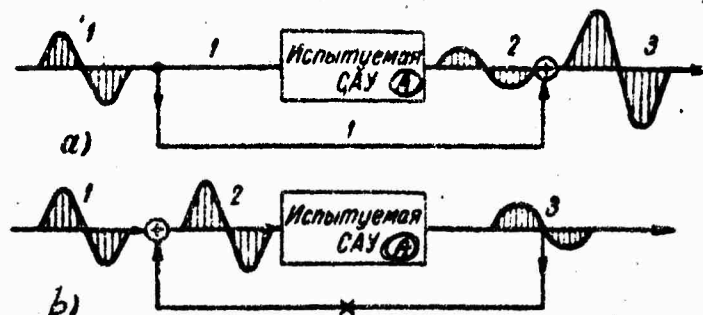
Fig 4-6. Diagrams for experimental determination of two amplitude-frequency characteristics with subsequent calculation of the phase-frequency characteristic by a nomogram. A - Automatic control system being tested.

closed system, by forcing them to dampen or diverge. The behavior of the circuit in a stable state with established oscillations permits determining the unknown frequency characteristics of the component point by point.

Regimes of damping, divergent and stable oscillations are attained in a second-order component in the structural circuit of which (Figure 1-16) the damping coefficient a_1 is assumed to be negative, positive or equal to zero respectively. For the latter case the structural circuit becomes very simple; it is given in Figure 4-7a,b in the form of contours containing the components K, $1/T_1 p$ and $1/T_2 p$.

The general function of transfer of the open contour is:

$$\frac{K}{T_1 T_2 p^2},$$

and the operator equation of connection has the form:

$$a(p) X_{out}(p) = b(p) X_{in}(p)$$

or

$$T_1 T_2 p^2 X_{out}(p) = K X_{in}(p)$$

Upon closing of the contour the left side of the new operator equation, in accordance with equation (1-77), is:

$$M(p) = a(p) + b(p) = T_1 T_2 p^2 + K.$$
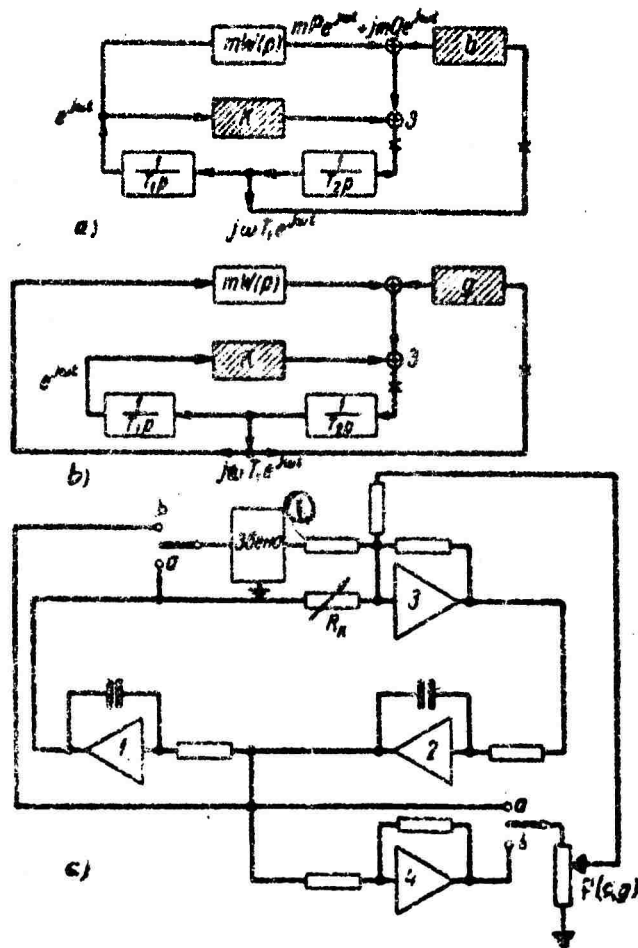
Fig. 4-7. Structural circuit and adjustment circuit of an experimental arrangement for taking the frequency characteristics by an active method.

Key: 1) component

The equation $N(z) = 0$ permits determining the poles of the OFT of the closed system: $z_{1,2} = \pm j\omega$ and expressing the frequency of its damping oscillations through the general amplification factor of the open contour $K/T_1 T_2$:

$$\omega = \sqrt{\frac{K}{T_1 T_2}}. \qquad (4\text{-}18)$$

The system under consideration was realized on elements of an electronic model shown in Figure 4-7c (amplifiers 1, 2 and 3).

By changing the resistances of the circuit it is possible to generate oscillations of a different frequency necessary for taking the frequency characteristics of the tested component point by point.

It is assumed that the tested component has an input and output in the form of an electric voltage, or the study is made, not of the component itself, but of its electronic model. Connecting up the component to circuit c requires a relatively small number of additional elements: two circuits with resistances on the summing amplifier, an inverting amplifier 4, a compensating potentiometer P and two switches, the locations of which, a and b, are in agreement with the configuration of the structural diagrams a and b of the same figure. Therefore we will consider the operation of the circuit of the model c by means of the structural circuits a and b.

1. The taking of the imaginary frequency characteristic of the component $Q(\omega)$. Let the closed contour of the model be constructed at the frequency ω. Then on the input of the integrating component $1/T_1 p$ oscillations are shifted by $+ 90°$ in phase and increased in amplitude by ωT_1 times relative to the output. In symbolic form the oscillations on the input are written by us as $j\omega T_1 A e^{j\omega t}$, and on the output as $A e^{j\omega t}$. After the tested component, connected into the circuit with the scale coefficient m, the harmonic oscillations will have sine and cosine constituents which we also will write in symbolic form:

$$mAe^{j\omega t} W(j\omega) = mAP(\omega) e^{j\omega t} + jmAQ(\omega) e^{j\omega t}.$$

The compensating cosinusoidal signal $jb\omega AT_1 e^{j\omega t}$ is supplied on the input of the summing amplifier 3 from the potentiometer P or in the structural circuit a by the controlled component c. The experimenter, observing the amplitude of the oscillations, selects a value of the compensating voltage at which the process is stable, that is, at which there is no damping or increase in amplitude. This indication is very sensitive, since with the course of time the divergence or damping becomes very noticeably apparent.

After attainment of stability of the oscillations on the basis of the equality

$$j\omega b A T_1 e^{j\omega t} = j m A Q(\omega) e^{j\omega t}$$

the point of the imaginary characteristic is found

$$Q(\omega) = \frac{b T_1 \omega}{m}. \qquad (4\text{-}19a)$$

The uncompensated sine constituent of the output oscillations of the investigated component is summed with the sine constituent that has passed through the amplifying element K, and the total amplification factor becomes equal to

$$[k + m P(\omega)]\frac{1}{T_1 T_2}.$$

Hence the frequency of the oscillations of the closed system departs somewhat from the value of (4-18):

$$\omega' = \sqrt{\frac{k + m P(\omega')}{T_1 T_2}}. \qquad (4\text{-}19b)$$

The difference between the frequencies ω and ω' can be made so conveniently small on account of lowering of the scale m and increase by the same token of the active role of the tested component in the generation of oscillations.

2. Taking the real frequency characteristic of the component $P(\omega)$. In the structure b, which corresponds to the position b of the switches of circuit c, two cosine harmonics from the component and the potentiometer are compensated:

$$j\omega T_1 g A e^{j\omega t} = j\omega T_1 m P(\omega) A e^{j\omega t}.$$

After stabilization of the oscillations this equality is used for determination of the point of the real characteristic

$$P(\omega) = g/m. \qquad (4\text{-}20a)$$

The branch parallel to the components $k/T_1 p$ with respect to the uncompensated sine constituent of the tested component increases the total amplification factor of the open contour to the value

271

$$\left[\frac{k}{T_1} + mQ\left(\omega''\right)\omega''\right]\frac{1}{T_k},$$

which changes the frequency:

$$\left|\omega'' = \sqrt{\frac{|k + mT_1\omega''Q\left(\omega''\right)}{T_1T_k}}.$$

Again the difference between (4-20b) and (4-18) is small at small m. This permits calibrating the model in advance by frequency, taking the scale with the resistance R_k at the selected time constants of the integrating amplifiers T_1 and T_2, and by the values of the characteristics b and g, taking the second scale with the potentiometer P. For agreement of the scales of the potentiometer at different positions of the switch, the amplifier 4 is used not only as inverting but also as scalar.

4-3. General Properties of the Hodographs on a Complex Plane

A. Direct and Inverse Frequency Characteristic

The rule of inversion. The inverse amplitude-phase characteristic is the name given to the characteristic inverse to the basic amplitude-phase characteristic:

$$W_{inv}\left(j\omega\right) = \frac{1}{W\left(j\omega\right)}. \qquad (4\text{-}21$$

On the basis of the general properties of complex numbers it is easy to conclude that the modulus of the inverse characteristic is equal to the inverse value of the modulus of the basic characteristic

$$A_{in}\left(\omega\right) = \frac{1}{A\left(\omega\right)}. \qquad (4\text{-}22)$$

and the phase of the inverse characteristic is equal in value to the phase of the basic characteristic and the reverse of it in sign:

$$\varphi_{in}\left(\omega\right) = -\varphi\left(\omega\right). \qquad (4\text{-}23)$$

The boosting and aperiodic first-order components. A first-order boosting component has the amplitude-phase characteristic obtainable by substitution of $p = j\omega$ from the OFT given in Table 3-1:

$$W\left(j\omega\right) = k\left(1 + j\omega T\right) \qquad (4\text{-}24a)$$

The polygraph of the amplitude-phase characteristic has been plotted on Figure 4-8 (F-1) and contains the constant real constituent

$$P = k \qquad (4\text{-}24b)$$

and the imaginary constituent, linearly varying with rise in the frequency

$$Q(\omega) = kT\omega. \qquad (4\text{-}24c)$$

It is not difficult also to obtain the two remaining characteristics:

АЧХ $\qquad A(\omega) = k\sqrt{1 + \omega^2 T^2}; \qquad (4\text{-}24d)$

ФЧХ $\qquad \varphi(\omega) = \operatorname{arctg} \omega T. \qquad (4\text{-}24e)$

(АЧХ = amplitude-frequency characteristic)
(ФЧХ = phase-frequency characteristic)

The aperiodic component has the following amplitude-phase characteristic, determinable from the transfer function from Table 3-1:

$$W(j\omega) = \frac{k}{1 + j\omega T}. \qquad (4\text{-}25a)$$

From that we get:

AFC $\qquad A(\omega) = \frac{k}{\sqrt{1 + \omega^2 T^2}}; \qquad (4\text{-}25b)$

PFC $\qquad \varphi(\omega) = -\operatorname{arctg} \omega T; \qquad (4\text{-}25c)$

the real frequency characteristic

$$P(\omega) = \frac{k}{1 + \omega^2 T^2}; \qquad (4\text{-}25d)$$

and the imaginary frequency characteristic

$$Q(\omega) = -\frac{kT\omega}{1 + \omega^2 T^2}. \qquad (4\text{-}25e)$$

In constructing hodograph A (Figure 4-8) of the amplitude-phase characteristic of the aperiodic component it was convenient to form it as the inverse characteristic of the boosting component by superimposing the phase in reverse direction and by taking the reverse values of the modulus. The geometric place of the points of the inverse char-
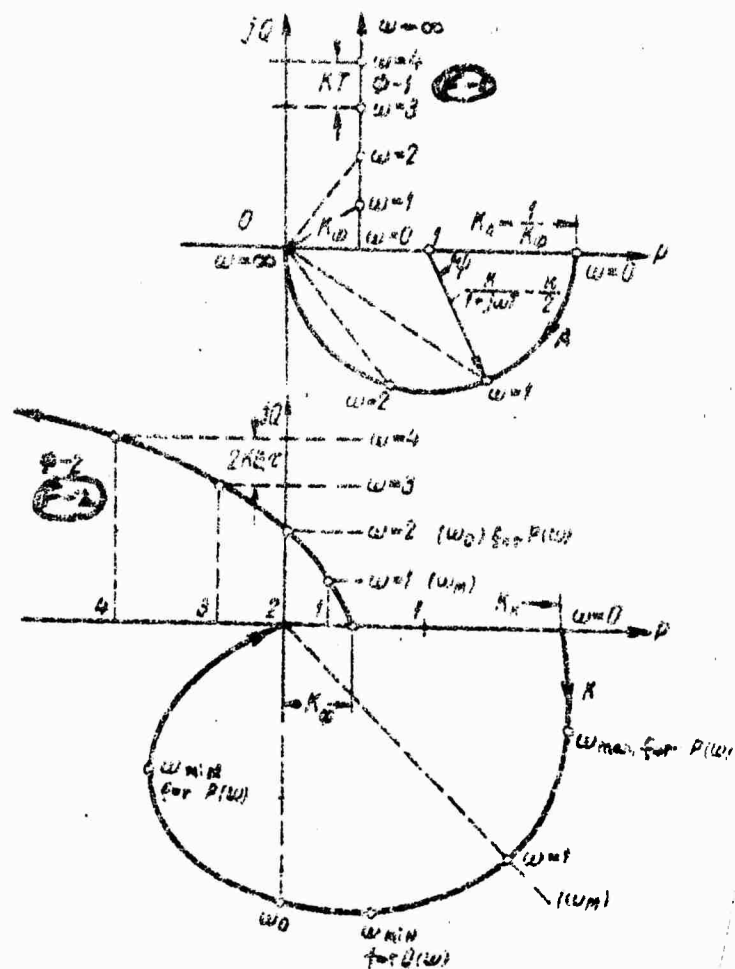
Fig 4-4. Direct and inverse amplitude-phase characteristics of components. F-1: First-order boosting; A: Aperiodic; F-2: Second-order boosting; K - Oscillating.

acteristic is the semi-circle with the radius k/2, located in the fourth quadrant and tangent to the imaginary axis at the start of the coordinates. Actually, if we subtract from the complex transfer function the vector of the center of the circle k/2, as shown in diagram 1, we get:

$$\frac{k}{1+j\omega T} - \frac{k}{2} = \frac{k}{2} \cdot \frac{1-j\omega T}{1+j\omega T}.$$

The modulus of the obtained difference vector is constant and equal to the radius

$$\left| \frac{k}{2} \cdot \frac{1-j\omega T}{1+j\omega T} \right| = \frac{k}{2}.$$

Consequently the hodograph of the vector is a circle with its center on the real axis at the point $k/2$. The angle of rotation of the radius of the vector of this circle is

$$\psi = -2 \text{ arctg } \omega T.$$

Second order boosting and oscillating components. A second-order boosting component, in accordance with Table 3-1, has the amplitude-phase characteristic

$$W(j\omega) = k_\phi (1 - \tau^2\omega^2 + j2\xi\tau\omega). \qquad (4.26a)$$

Its hodograph is the graph F-2, constructed in Figure 4-8 by points. For this purpose the segment k_ϕ was laid out on the positive real semi-axis from the start of the coordinates, and from its end, on the left, a quadratic scale was constructed on which the value of the real constituent $k(1 - \omega^2\tau^2)$ was determined for each frequency. For the construction of the imaginary constituents of the amplitude-phase characteristic, a regular scale of frequencies on the scale $2k\xi\tau$ was plotted on the positive imaginary semi-axis. By summing the real and imaginary constituents geometrically, we get the hodograph of the amplitude-phase characteristic, disposed in the upper semi-circle.

The amplitude-phase characteristic of the boosting component is

$$A(\omega) = k_\phi \sqrt{(1 - \omega^2\tau^2)^2 + 4\xi^2\tau^2\omega^2}. \qquad (4.26b)$$

The amplitude has a minimum at the frequency $\omega_r = \frac{1}{\tau}\sqrt{1 - 2\xi^2}$; the hodograph at this point is closest to the start of the coordinates.

The phase-frequency characteristic is

$$\varphi(\omega) = \text{arctg } \frac{2\xi\tau\omega}{1 - \omega^2\tau^2}. \qquad (4.26c)$$

The real frequency characteristic

$$P(\omega) = k(1 - \omega^2\tau^2) \qquad (4.26d)$$

passes through zero at the frequency $\omega_0 = 1/\tau$. At the same frequency the phase is:

$$\varphi(\omega_0) = \frac{\pi}{2}$$

The imaginary frequency characteristic

$$Q(\omega) = 2\xi\tau\omega \qquad (4\text{-}26e)$$

is a linearly increasing function of the frequency.

The oscillating component. In accordance with Table 3-1 we have the amplitude-phase characteristic

$$W(j\omega) = \frac{k}{1 - \omega^2\tau^2 + j2\xi\tau\omega}. \qquad (4\text{-}27a)$$

For the values of the coefficients

$$\tau_\phi = \tau_\kappa; \ \xi_\phi = \xi_\kappa; \ k_\phi = \frac{1}{R_\kappa}$$

the amplitude-phase characteristic of the oscillating component can be constructed by inversion of the amplitude-phase characteristic of the second-order boosting component. According to the rules of inversion the characteristic is disposed in quadrant symmetric to the quadrants of the amplitude-phase characteristic of the boosting component relative to the real axis, that is, in the lower semi-circle. Its modulus is determined by the inverse value of the amplitude-phase characteristic of the boosting component. At zero frequency the points of both the characteristics lie on the real positive semi-axis, and at $\omega \to \infty$ the amplitude-phase characteristic of the oscillating component arrives at the start of the coordinates. The intersection of the imaginary axis of the two amplitude-phase characteristics occurs at the frequency $\omega_0 = 1/\tau$, which is the frequency of the undamped oscillations.

The amplitude-frequency characteristic is determined by the formula:

$$A(\omega) = \frac{k}{\sqrt{(1 - \tau^2\omega^2)^2 + 4\xi^2\tau^2\omega^2}}. \qquad (4\text{-}27b)$$

At the same frequency, where the correspondences of the characteristic of the boosting component had a minimum, that is, at

$$\omega_M = \frac{1}{\tau}\sqrt{1 - 2\xi^2},$$

the amplitude-frequency characteristic of the oscillating component has the maximum:

$$A_{max}(\omega) = \frac{k}{2\xi\sqrt{1-\xi^2}}$$

and its holograph is farthest removed from the start of the coordinates.

The phase-frequency characteristic has the expression

$$\varphi(\omega) = -\arctan\frac{2\xi\tau\omega}{1-\omega^2\tau^2} \qquad (4\text{-}27c)$$

and is distinguished from the phase-frequency characteristic of the coasting component only by the sign.

The real frequency characteristic

$$P(\omega) = \frac{k(1-\omega^2\tau^2)}{(1-\omega^2\tau^2)^2 + 4\xi^2\tau^2\omega^2} \qquad (4\text{-}27d)$$

passes through zero at the frequency $\omega = 1/\tau$, equal to the proper undamped frequency of oscillations of the component, has a maximum $P_{max} = \dots \xi\sqrt{\dots - \xi}$ at the frequency $\omega_{\dots} = \frac{1}{\tau}\sqrt{\dots - \dots\xi}$ and a minimum $P_{min} = -1/\xi\sqrt{\dots - \xi}$ at the frequency $\omega_{\dots} = \frac{1}{\tau}\sqrt{\dots - \dots\xi}$, and upon further increase of the frequency tends to zero.

The imaginary frequency characteristic

$$Q(\omega) = \frac{-2\xi\tau\omega}{(1-\omega^2\tau^2)^2 + 4\xi^2\tau\omega^2} \qquad (4\text{-}27e)$$

begins and ends with zero values, and at the frequency

$$\omega_{min} = \frac{1}{\tau}\sqrt{\frac{1-2\xi^2 - 2\sqrt{1 - \xi^2 \dots \xi^2}}{\dots}}$$

has a minimum.

The Asymptotic Properties of the Frequency Characteristics

The high-frequency segment of the amplitude-phase characteristic, $\omega \to \infty$, for the reasons described in \dots the highest terms in the numerator and denominator obtain a \dots value and the formula acquires the form:

$$\lim_{\omega \to \infty} W(j\omega) = \lim_{\omega \to \infty} \frac{b_m(j\omega)^m}{a_n(j\omega)^n} = \lim_{\omega \to \infty} \frac{b_m}{a_n}(j\omega)^{m-n}. \qquad (4\text{-}28)$$

Hence the limiting value of the amplitude-frequency character-
istic is

$$A(\infty) = \left| \frac{b_m}{a_n} \right| \lim_{\omega \to \infty} \omega^{m-n}, \qquad (4\text{-}28b)$$

and, depending on the orders of the numerator and denominator, the
amplitude-frequency characteristic can tend to a finite apex, includ-
ing a zero one, or increase in modulus to infinity.

The limiting value of the phase, from the same formula, is

$$\varphi(\infty) = \frac{\pi}{2}(m - n) \left(\text{sign } \frac{b_m}{a_n} \right). \qquad (4\text{-}28c)$$

Thus it is easy to determine the quadrant in which the amplitude-
phase characteristic ends. The fact that the final phase can only be
a multiple of $\pm \pi/2$ is evidence that the amplitude-phase character-
istic must be tangent to one of the axes of the coordinates, if it ends
at the beginning of the coordinates, or must be parallel to one of the
axes if it ends in infinity.

If $m < n$, then $A(\infty) = 0$ and $\varphi(\infty) = -\frac{\pi}{2}(n - m)$, that is, the
amplitude-phase characteristic is tangent to one of the axes of the
coordinates at the start of the coordinates.

If $m = n$, the amplitude-phase characteristic ends at a final seg-
ment of the real axis, since its modulus equals $A(\infty) = |b_m/a_n|$, and
the phase is equal to zero.

If $m > n$, the amplitude-frequency characteristic increases infin-
itely in modulus, and its infinite branch is oriented on one of the
semi-axes corresponding to the value of the phase $\frac{\pi}{2}(m - n)$ (sign
b_m/a_n).

We will apply formula 4-29b) to the hodographs in Figure 4-8.

Components F-1 and F-2 are:

$$A_1(\infty) = \frac{kT}{1} \lim_{\omega \to \infty} \omega^{1-3} = \infty.$$

$$A_2(\infty) = \frac{k\tau^2}{1} \lim_{\omega \to \infty} \omega^{2-0} = \infty.$$

Components A and K are:

$$A_A(\infty) = \frac{k}{T} \lim_{\omega \to \infty} \omega^{0-1} = 0;$$

$$A_K (\infty) = \frac{k}{\tau^2} \lim_{\omega \to \infty} \omega^{0-2} = 0.$$

We will check formula (4-28c) on these same hodographs:

$$\varphi_1 (\infty) = \frac{\pi}{2} (1 - 0) = \frac{\pi}{2} ;$$

$$\varphi_2 (\infty) = \frac{\pi}{2} (2 - 0) = \pi;$$

$$\varphi_A (\infty) = \frac{\pi}{2} (0 - 1) = -\frac{\pi}{2} ;$$

$$\varphi_K (\infty) = \frac{\pi}{2} (0 - 2) = -\pi.$$

The initial segment of the amplitude-phase characteristic, $\omega \to 0$. In the region of low frequencies in (4-11) the lowest terms of the numerator and denominator obtain a determining value. In this, although in the general form of notation of (4-11) the lowest terms are a_0 and b_0, depending on the number of zero roots of the numerator and denominator, part of the lowest coefficients can prove to be equal to zero and the initial value of the amplitude-phase characteristic assumes the form:

$$W(j0) = \lim_{\omega \to 0} \frac{b_\mu (j\omega)^\mu}{a_\nu (j\omega)^\nu} = \frac{b_\mu}{a_\nu} \lim_{\omega \to 0} (j\omega)^{\mu - \nu}. \qquad (4\text{-}29a)$$

Hence

$$A(0) = \left| \frac{b_\mu}{a_\nu} \right| \lim_{\omega \to 0} \omega^{\mu - \nu} \qquad (4\text{-}29b)$$

and

$$\varphi(0) = \frac{\pi}{2} (\mu - \nu) \left(sign \; \frac{b_\mu}{a_\nu} \right). \qquad (4\text{-}29c)$$

The behavior of the amplitude-phase characteristic on the initial section is investigated analogously to the analysis of the final section that has been considered. Some variants of the disposition of the initial section of the amplitude-phase characteristic, depending on the number of zero roots of the numerator and denominator (in the limits $\mu - \nu \le 4$), determinable by the indexes of the lowest coefficients of the polynomials of the numerator and denominator, are given in Figure 4-9. On the hodograph the arrows are always directed toward the side of increase in frequency, so that the initial section being investigated is located at the start (feathering) of the arrows.

All the evaluations obtained related to the boundary sections of
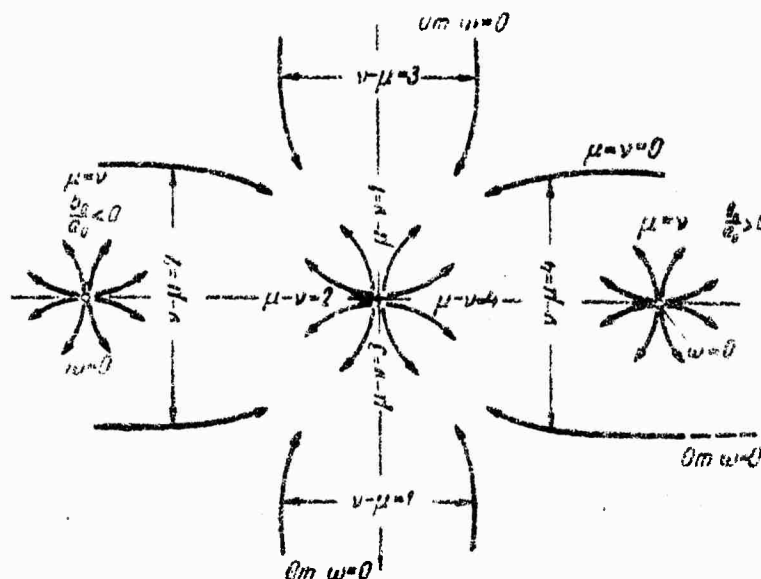
Fig 4-9. Initial sections of the amplitude-phase character-
istic ($\omega \to 0$).

the amplitude-phase characteristic. In order to connect the beginning
and end, it is necessary to construct the entire characteristic by
points by calculation or on the basis of experiment. However, to ob-
tain a general representation of the course of the characteristic,
namely from the angle of rotation of the complex amplification factor,
the hodograph of which is the amplitude-phase characteristic, know-
ledge of the number of roots, different in character, of the numerator
and denominator proves to be sufficient. We will proceed to an exam-
ination of this question.

C. The Angle of Rotation of the Vector of the
   Amplitude-Phase Characteristic

If we know the directions of the initial and final sections of
the amplitude-phase characteristic, we can establish a general express-
ion for the angle of rotation of the amplitude-phase characteristic
during change of the frequency from zero to infinity:

$$\Delta \varphi = \varphi(\infty) - \varphi(0) \pm 2k\pi, \qquad (4\text{-}30)$$

where $k = 0, 1, 2\ldots$

However it does not appear possible in practice to use this expression also for a general estimate of the angle of rotation of the amplitude-phase characteristic until the sign and value of the last term of the formula are determined.

For solution of the question of the total angle of rotation of the amplitude-phase characteristic it is necessary to proceed by another method, by investigating the rotation of the vectors making up the total vector of the amplitude-phase characteristic. For this purpose, using the designation λ_j for zero and z_i for the poles of the transfer function, we write the expression for the amplitude-phase characteristic in a new form:

$$W(j\omega) = \frac{b(j\omega)}{a(j\omega)} = \frac{b_m(j\omega - \lambda_1)\ldots(j\omega - \lambda_m)}{a_n(j\omega - z_1)\ldots(j\omega - z_m)}. \quad (4\text{-}31)$$

Each of the factors of the right side of the type

$$j\omega - \lambda_j \qquad \text{and} \qquad \frac{1}{j\omega - z_i}$$

is an elementary complex vector, the direction of which varies with change in the frequency. It turns out that the character of this change essentially depends on the disposition of the zeros and poles relative to the imaginary axis. We will investigate in detail all the possible variants of disposition of the roots and their influence on the rotation of the elementary vectors.

In the general case the roots of the numerator and denominator are complex numbers which (more precisely, their points forming a complex plane) can be in the left semi-circle, on the imaginary axis and in the right semi-circle.

We will designate the number of roots in the left semi-circle by l, on the imaginary axis by i and in the right semi-circle by r. To distinguish the roots of the numerator and denominator we will give them the subscripts n and d respectively. We will put the obtained system of designations, and also the designations applied above, in Table 4-1.

In Figure 4-10 are shown the rules for counting the angles of rotation of the constituent vectors $(j\omega - \lambda_k)$ for the various kinds of roots.

The total angle of rotation of the vector $W(j\omega)$ is:

$$\Delta\varphi = \frac{\pi}{2}(l_n - l_d - r_n + r_d). \quad (4\text{-}32)$$
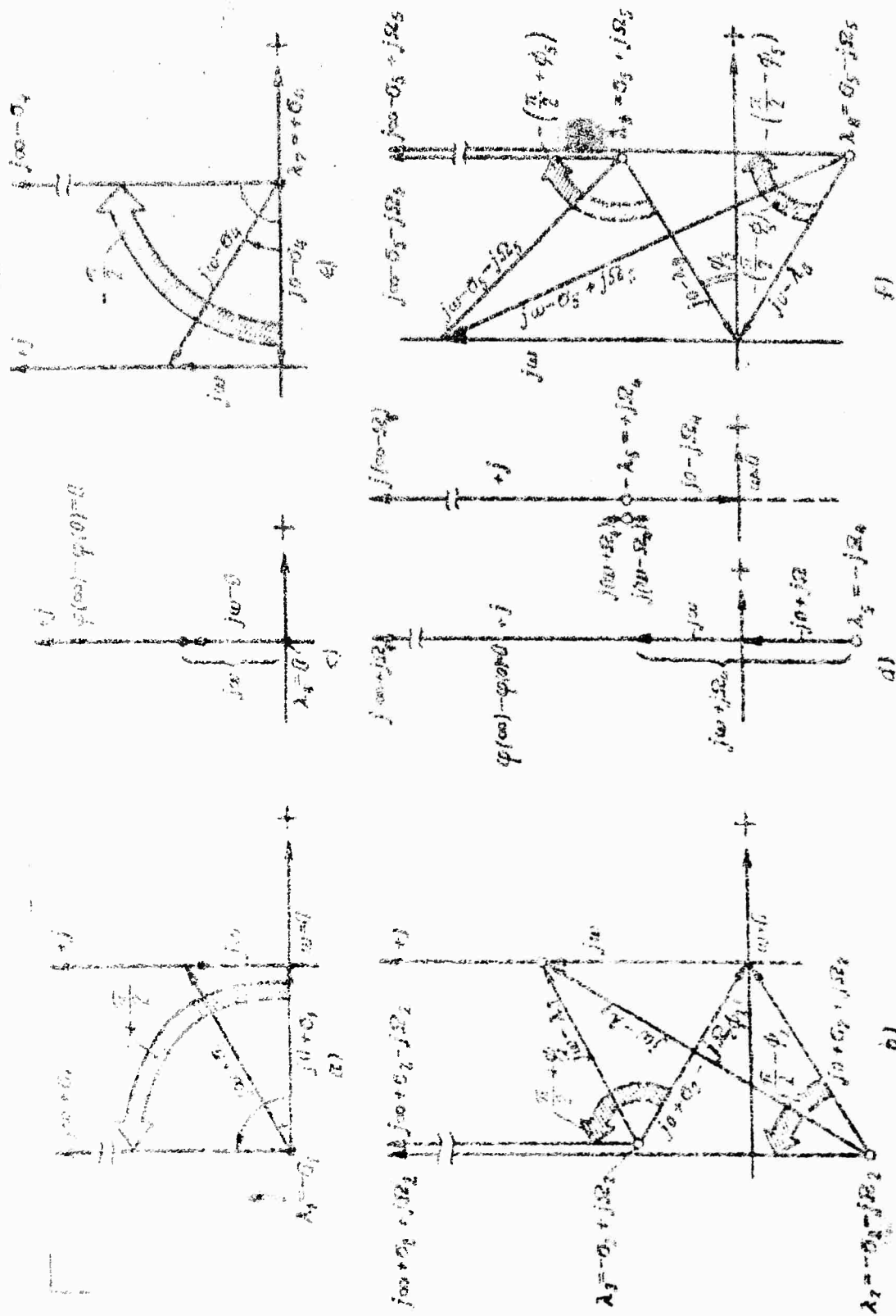
Fig. 4-10. Rotation of elementary vectors $(0 \leq \omega \leq \infty)$

Table 4-1   The Number and Character of Roots of Transfer Functions

Number of Roots	Numerator (zeros)	Denominator (poles)
In the left semi-circle	l_n	l_d
On the imaginary axis Total	i_n	i_d
Zeros	μ	γ
In the right semi-circle	r_n	r_d
Total number	m	n

The zeros and poles lying on the imaginary axis are excluded from consideration in the calculation of the total angle of rotation. The zero roots of the numerator and denominator change the phase of all vectors of the amplitude-phase characteristic at the constant angle $\frac{\pi}{2}$ ($\mu - \gamma$) and deform in modulus the boundary sections of the amplitude-phase characteristic (Figure 4-11); the purely imaginary zeros bring about passage of the amplitude-phase characteristic through the start of the coordinates at the frequency $\omega = \Omega$; the purely imaginary poles cause a break in the amplitude-phase characteristic at the same frequency. In calculating the total angle of rotation of the characteristic passed through the start of the coordinates, it is necessary to calculate separately the angle of rotation of the section of the characteristic from $\omega = 0$ to Ω - and add it to the angle of rotation of the characteristic from Ω + to ∞. In calculation of the angle of rotation of an amplitude-phase characteristic with a break it is necessary in precisely the same way to add separately the angles of torsion of one branch of the characteristic from $\omega = 0$ to the break point and of a second branch from the break point to ∞.

Fig 4-11.   The amplitude-phase characteristic of systems with neutral zeros and poles of a transfer function.
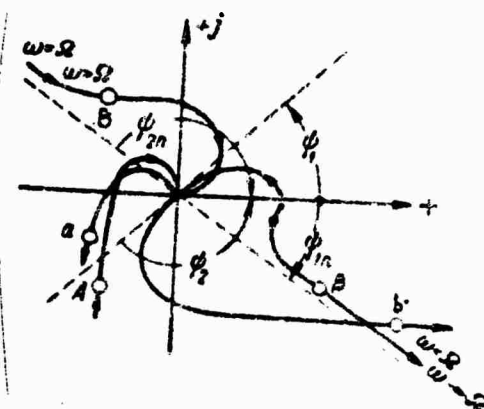
C. The Influence of Small Changes in the Parameters of
Components on the Disposition of the Hodograph on
a Complex Plane

Let η be a constructive parameter of a component which determines the analytical representation of the amplitude-phase characteristic:

$$W(j\omega, \eta) = P(\omega, \eta) + jQ(\omega, \eta) \qquad (4\text{-}33a$$

and the disposition of its hodograph on a complex plane (Figure 4-12).

We will take on the hodograph in the first quadrant the arbitrary point A, corresponding to the frequency ω_1, and determine the tangent of the angle α of inclination tangential to the hodograph at that point:

$$\operatorname{tg} a_1 = \frac{dQ}{dP} = \frac{\dfrac{\partial Q(\omega_1, \eta)}{\partial \omega}}{\dfrac{\partial P(\omega_1, \eta)}{\partial \omega}} . \qquad (*)$$

If the parameter η now obtains the small increment $\Delta\eta$, all the points of the hodograph are displaced. For point A the direction of the displacement is determined by the angle β, the tangent of which equals:

$$\operatorname{tg} \beta_1 = \frac{\dfrac{\partial Q(\omega_1, \eta)}{\partial \eta}}{\dfrac{\partial P(\omega_1, \eta)}{\partial \eta}} . \qquad (**)$$

If we compare formulas (*) and (**) it is easy to establish the side of the old hodograph $W(j\omega, \eta)$ on which the new hodograph $W(j\omega, \eta + \Delta\eta)$ is disposed. For determinability of the formulation we will watch the right side of the hodograph in the direction of increase in frequency. Then the condition of transition of the new hodograph into the hatched region close to the point A is written in the form:

$$\operatorname{tg} a > \operatorname{tg} \beta,$$

which is equivalent to the condition of positiveness of the following determinant:

[see next page]

$$\begin{vmatrix} \dfrac{\partial P(\omega_1, \eta)}{\partial \eta} & \dfrac{\partial P(\omega_1, \eta)}{\partial \omega} \\[3mm] \dfrac{\partial Q(\omega_1, \eta)}{\partial \eta} & \dfrac{\partial Q(\omega_1, \eta)}{\partial \omega} \end{vmatrix} > 0. \qquad (4\text{-}33b)$$

This rule permits the sets of homogeneous hodographs with variable parameters to be oriented in arrangement.
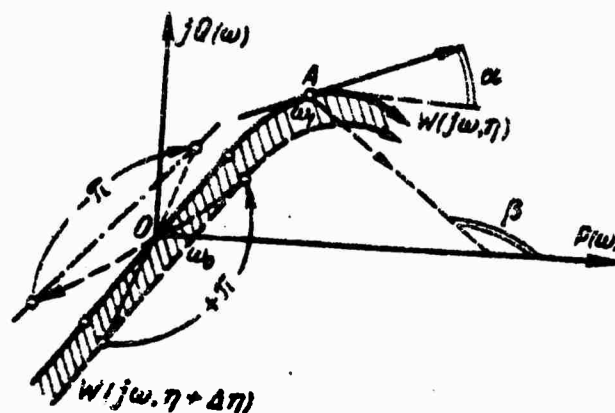
Fig 4-12.   The effect of small changes of the parameter η on the arrangement of the hodograph.

If the hodograph being investigated at a certain frequency passes through the start of the coordinates, there is fulfilment of the condition

$$W(j\omega_0, \eta) = 0$$

or

$$P(\omega_0, \eta) = 0; \quad Q(\omega_0, \eta) = 0. \qquad (***)$$

In that case, small changes in the parameter change the arrangement of the hodograph relative to the start of the coordinates and, if in accordance with the rule given in Section C the transition of the hodograph through the start of the coordinates did not cause increase in the angle of rotation, the passage of the hodograph close to the

start of the coordinates increases the total angle of rotation by + when the start of the coordinates falls in the unhatched zone and reduces the angle of torsion by π when the start of the coordinates falls in the hatched zone.

This is accompanied at the same time by transition of the two neutral roots of the numerator of the OFT into the left or correspondingly the right semi-circle. These regularities can be observed in testing the system according to the method illustrated in Figure 4-7. During the construction of the circuit at an exact value of the parameter $b(g)$, non-damping oscillations are observed in it which correspond to the two neutral poles of the OFT or two neutral zeros of the inverse amplitude-phase characteristic.

Very small changes in the value of the parameter $b(g)$ cause oscillations in the circuit damping or increasing in accordance with the transition of the zeros of the inverse amplitude-phase characteristic of the entire system into the right or left half-plane.

The determinant of (4-33b) is called the Jacobian of the system of equations (***). The transition of the neutral zeros of the OFT into the left half-plane corresponds to the positive Jacobian, and their transition into the right half-plane, to the negative Jacobian at the point ω_0, η. These rules, which were derived for the first quadrant (Figure 4-12), are valid for any hodographs in all quandrants.

4-4. The Frequency Characteristics of Typical Components

On the basis of the general properties of the frequency characteristics the characteristics of typical components were calculated and presented in Table 4-2. A graphic representation of the frequency characteristics of the components is given in Figures 4-13 - 4-16.

Figure 4-13 contains the frequency characteristics of the amplifying and delay components. For the amplifying component the amplitude-phase characteristic degenerates into a single point on the complex plane, lying on the real positive semi-axis at a distance from the start of the coordinates equal to the amplification factor; the phase and imaginary frequency characteristics are identically equal to zero, and the amplitude-frequency characteristic coincides with the real, and they both have the form of horizontal straight lines. For the delay component the amplitude-phase characteristic has the form of a circle, the amplitude-frequency is horizontal, the phase-frequency increases linearly to $\varphi(\infty) = -\alpha$ and the real and imaginary frequency characteristics vary harmoniously with the period

$$\Delta\omega = \frac{2\pi}{\tau_s}.$$
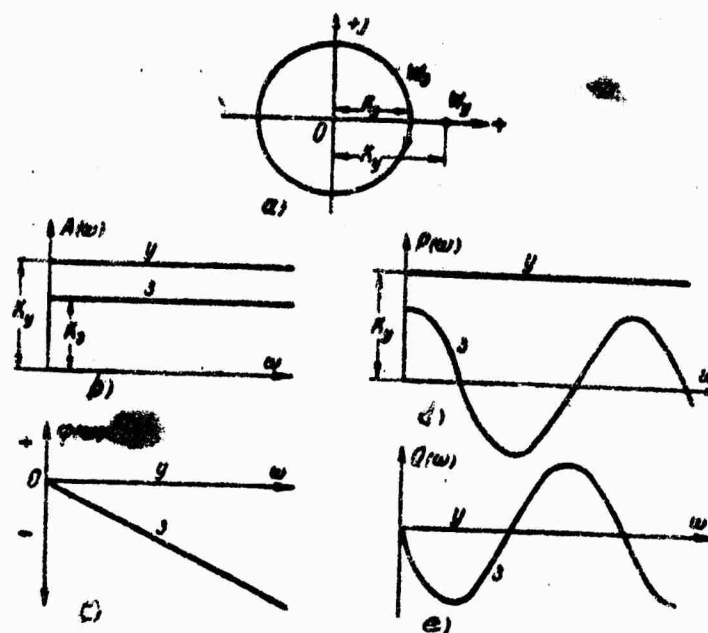
Fig 4-13.   Frequency characteristics of the amplifying
and delay components.

In Figure 4-14 are given the frequency characteristics of the
differentiating and integrating components. When the amplification
factors $k_{-1} = 1/T$ are in agreement, both amplitude-phase character-
istics are mutually inverse. The amplitude-frequency characteristic
of the differentiating component has a linearly increasing graph, and
that of the integrating a hyperbolically falling, which also is pre-
served with accuracy of the sign in the graphs of the imaginary char-
acteristics. The real characteristics of both components are exactly
equal to zero, and the phase-frequency characteristics are horizontal
on the levels $+\frac{\pi}{2}$ and $-\frac{\pi}{2}$.

In Figure 4-15 are arranged the frequency characteristics of the
boosting (ϕ-1), aperiodic and quasi-static first-order components
with consistent amplification factors. The graph with the amplitude-
phase characteristic repeats Figure 4-8 for the mutually inverse char-
acteristics with new amplification factors and expanded on account of
the amplitude-phase characteristic of the first-order quasi-static
component. The remaining graphs are the result of the amplitude-phase
characteristic. We note that the amplitude and imaginary frequency
characteristics of the component K-1 coincide with the analogous char-
acteristics of the aperiodic component, that is, taken separately,
these characteristics do not uniquely determine the type of component.
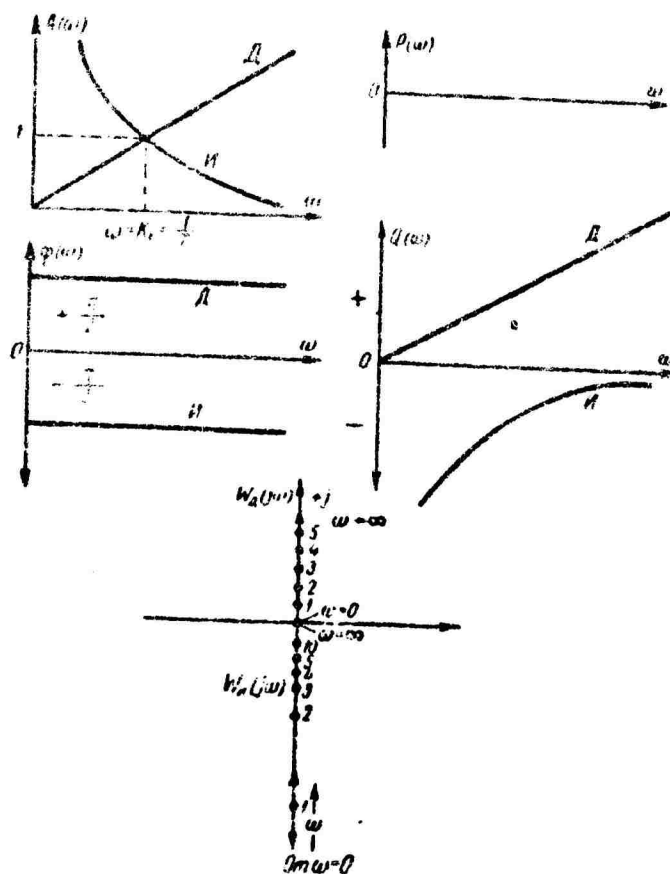
Fig. 4-14. Frequency characteristics of the differentiating and integrating components.

$Д = D$

$К = I$
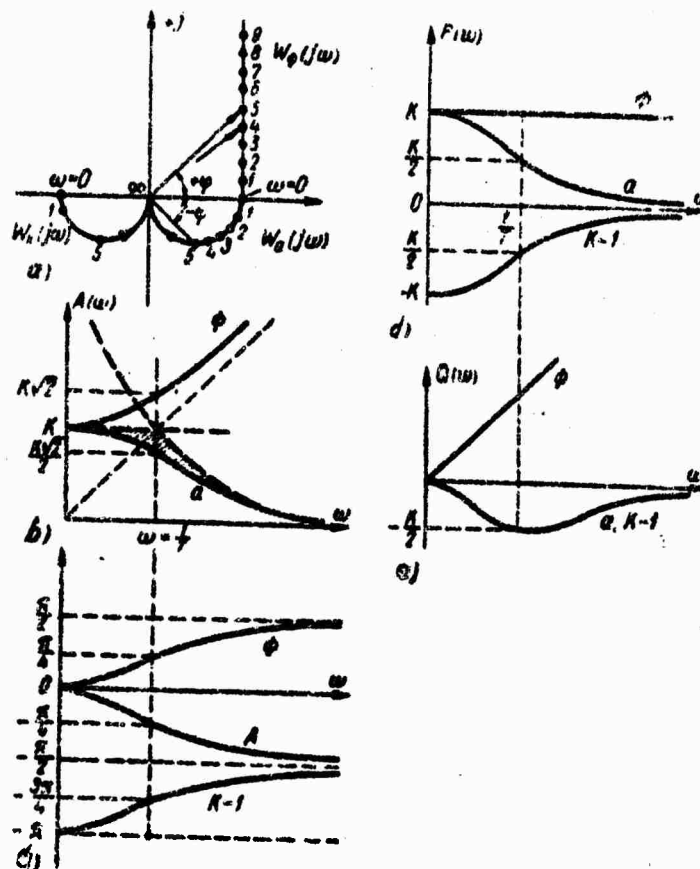
Fig 4-15. Frequency characteristics of first-order components.

In Figure 4-16 are given the frequency characteristics of the following components: second-order boosting (φ-2), oscillating resonance and quasi-static, second order, with consistent amplification factors: $k = k_2 = 1/k_\rho$. The graph of the amplitude-phase characteristic repeats Figure 4-8, illustrating the rule of inversion, but contains additionally the amplitude-phase characteristic of K-2. On the remaining graphs are the scalar characteristics, the majority of which have one or two extremums, the location and values of which are given in the table. The resonance component has break characteristics at the frequency Ω. The quasi-static component of the second order has amplitude-frequency and real frequency characteristics which coincide with the oscillating component and a phase-frequency characteristic that coincides with the second-order boosting component.
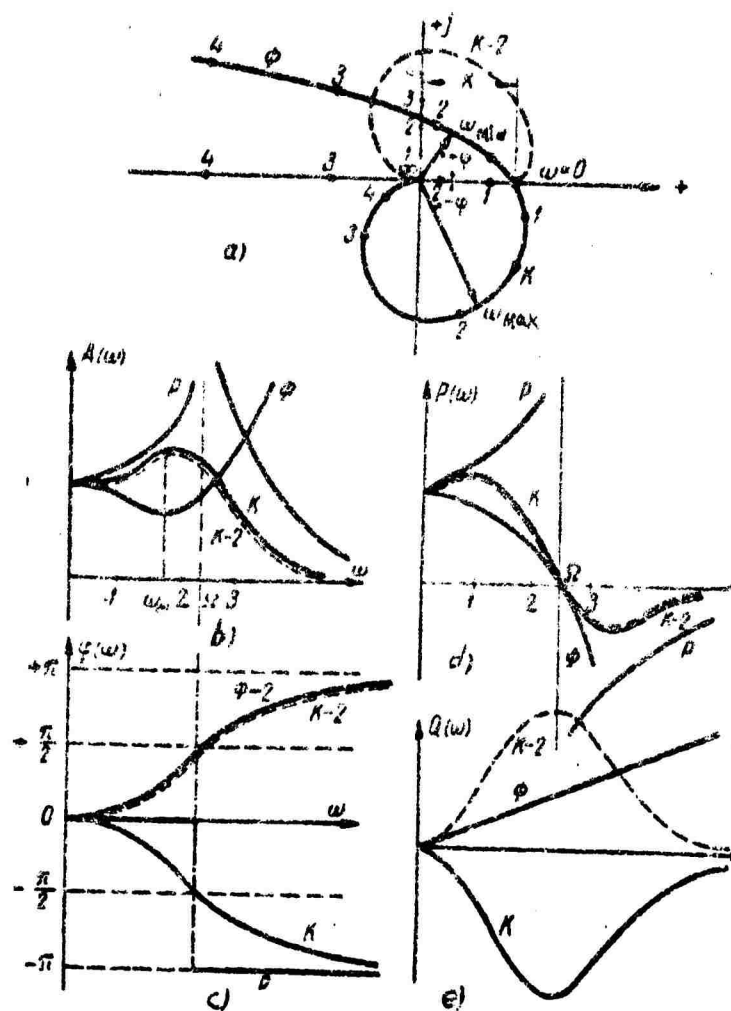
Fig 4-16. Frequency characteristics of second-order components.

4-5. Logarithmic Frequency Characteristics

A. Logarithmic Scales

For frequency characteristics, logarithmic scales are predominantly used, thanks to which the construction of typical amplitude-frequency and phase-frequency characteristics in the combinations of components in a single control system is essentially simplified.

Simplifications are attained as a result of the use not only of

the value ω in the construction of the amplitude-frequency charac-
teristics as the argument x laid out along the axis of the abscissas,
and the logarithm of the ratio of the current value of the frequency
to the basic

$$x = \lg \frac{\omega}{\omega_0}$$ (*

and as the function y laid out along the axis of the ordinates, not
the values of the amplification factor in modulus, but its logarithm

$$y = \lg A.$$ (**)

. The basic frequency ω_0 often is assumed to be equal to 1 sec^{-1}
and it is not possible to write it in formula (*) given here, but as
a result of normalization under the sign of the logarithm the dimen-
sionless value of the ratio remains. Amplification in modulus of A,
which enters into the second formula (**) also is assumed to be di-
mensionless in determination as the ratio of the output amplitude
to the input.

Semi-logarithmic scales are used for the phase-frequency charac-
teristic -- the same logarithm of the ratio of the frequencies along
the axis of the abscissas and of phase in degrees or radians along
the axis of the ordinates.

We will examined the principal advantages of the logarithmic
scales.

Obtaining straight-line characteristics for direct and inverse
power functions. If the amplitude-phase characteristic is reduced
to the straight line $A(\omega) = k(\omega/\omega_0)^n$ or the inverse power func-
tion $A(\omega) = k(\omega/\omega_0)^{-n}$, the construction of such an amplitude-
phase characteristic on ordinary scales requires calculations of the
characteristic by points.

The transition from the function $A(\omega) = k(\omega/\omega_0)^{\pm n}$ to the
relation between the logarithms gives: $\log A = \log k \pm n \log \omega/\omega_0$.
Thus the equation of the straight line $y = c \pm nx$ is obtained in the
system of logarithmic coordinates xOy. This straight line has the
inclination (steepness) $S_x^y = \pm n$ and passes through the point $\log A =$
$= \log k$ at the frequency ω_0.

The construction of such characteristics is elementarily simple.

Vertical displacement of the logarithmic frequency characteristics
udring change of the amplification factor. If the amplitude-phase
characteristic of a certain system $A_1(\omega)$ has been obtained in advance,
and then the constant (for all frequencies) amplification factor k is
introduced into the system, the new characteristic $A_2(\omega)$ is equal to

On natural scales it is necessary to recalculate the old charac-
teristic by multiplying all the ordinates by the coefficient k, if the
change in scale on the axis of the ordinates is not permissible due to
the presence of characteristics of other components or systems being
compared on the same graph.

In the transition to logarithmic characteristics

$$\lg A_2 = \lg k + \lg A_1$$

the new characteristic differs from the old only by the constant number
log k and can be obtained by vertical shift of the former logarithmic
amplitude-frequency characteristic without change of its configuration.

· Horizontal displacement of logarithmic frequency characteristics
during change of the basic frequency. Let us assume that the original
logarithmic amplitude-frequency characteristic has a single basic fre-
quency, that is, $\log A_1 = F(\log \omega)$, or in logarithmic coordinates
$y = F(x)$.

If we now change the basic frequency, the new logarithmic ampli-
tude-frequency characteristic $\log A_2 = F(\log \omega/\omega_0) = F(\log \omega - \log \omega_0)$ in logarithmic rectangular coordinates will differ from the old
logarithmic amplitude-frequency characteristic only by the shift along
the horizontal axis.

This property relates also to semi-logarithmic phase-frequency
characteristics, since at any of their form $\varphi = F_1 \log[\omega/\omega_0]$ the
derived rule of shift of the curves is retained in the logarithmic co-
ordinates $y = F_1(x)$.

The possibility of taking into consideration changes in the ampli-
fication factor k and the basic frequency, the role of which various
coefficients in the equation can play in characteristics of real com-
ponents of systems (usually inversion of the time constants, since
$\omega_0 = 1/T \sec^{-1}$), by vertical and horizontal shifts of the logarith-
mic frequency characteristics permits constructing for unit values of
the coefficients typical models of the logarithmic amplitude-frequency
and phase-frequency characteristics and using them further at any val-
ues of the coefficients k and T, by using the rule of displacement.

Extension of the scale in the region of low frequencies. For ex-
position of the general properties of an automatic control system, for
example by the angle of rotation of the amplitude-phase characteristic
examined in Section 4-3, it often is necessary, on the one hand, to
have a general representation of the frequency characteristics in a
very broad range of frequencies, and on the other, for the automatic
control system it is desirable to represent the course of the charac-
teristics in the region of low frequencies with adequate precision.

Table 4-2 Frequency Characteristics of Components

① Порядок	Наименование звена ②	Комплексный коэффициент усиления $W(j\omega)$ ③	Амплитудно-частотная характеристика ④	
			Формула $A(\omega)$ ⑤	1-й экстремум ⑥
0	Усилительное ⑭	K_y	K_y	—
	Запаздывающее ⑮	$K_9 e^{-j\omega\tau_3}$	K_3	—
	Дифференцирующее ⑯	$j\omega T$	ωT	—
1	Интегрирующее ⑰	$-j\dfrac{K_{-1}}{\omega}$	$\dfrac{K_{-1}}{\omega}$	—
	Форсирующее-1 ⑱	$K_\phi(1+j\omega T)$	$K_\phi\sqrt{1+\omega^2 T^2}$	$\dfrac{0}{K_\phi}$
	Апериодическое ⑲	$\dfrac{K_a}{1+j\omega T}$	$\dfrac{K_a}{\sqrt{1+\omega^2 T^2}}$	$\dfrac{0}{K_a}$
	Квазистатическое-1 ⑳	$\dfrac{K_a}{-1+j\omega T}$	$\dfrac{K_a}{\sqrt{1+\omega^2 T^2}}$	$\dfrac{0}{K_a}$
2	Форсирующее-2 ㉑	$K_\phi(1-\omega^2\tau^2+j2\xi\tau\omega)$	$K_\phi\sqrt{V(\omega)}$	$\dfrac{\frac{1}{\tau}\sqrt{1-2\xi^2}}{2K\xi\sqrt{1-\xi^2}}$
	Колебательное ㉒	$\dfrac{K_a}{1-\omega^2\tau^2+j2\xi\tau\omega}$	$\dfrac{K_a}{\sqrt{V(\omega)}}$	$\dfrac{\frac{1}{\tau}\sqrt{1-2\xi^2}}{\frac{K}{2\xi\sqrt{1-\xi^2}}}$
	Резонансное ㉓	$\dfrac{K\Omega}{\Omega^2-\omega^2}$	$\dfrac{K\Omega}{|\Omega^2-\omega^2|}$	—
	Квазистатическое-2 ㉔	$\dfrac{K_a}{1-\omega^2\tau^2-j2\xi\tau\omega}$	$\dfrac{K_a}{\sqrt{V(\omega)}}$	$\dfrac{\frac{1}{\tau}\sqrt{1-2\xi^2}}{\frac{K}{2\xi\sqrt{1-\xi^2}}}$

Примечания: ㉕

1. В графе „1-й экстремум" в числителе дроби показано местоположение экст|
2. $V(\omega) = (1-\omega^2\tau^2)^2 + 4\xi^2\tau^2\omega^2$.
3. $C = 2\sqrt{1-\xi^2}+\xi$.

Table 4-2   Frequency Characteristics of Components   (Cont'd)

Фазово-частотная характеристика $\varphi(\omega)$ ⑦	Вещественная частотная характеристика ⑧		Мнимая частотная характеристика ⑪	
	Формула $P(\omega)$ ⑨	1-й экстремум ⑩	Формула $Q(\omega)$ ⑫	1-й экстремум ⑬
0	K_y	—	0	—
$-\omega\tau_3$	$K_3 \cos\omega\tau_3$	$\dfrac{0}{K_3}$	$-K_3\sin\omega\tau_3$	$\dfrac{\pi}{2\tau_3}$ $-K_3$
$+\dfrac{\pi}{2}$	0	—	ωT	—
$-\dfrac{\pi}{2}$	0	—	$-\dfrac{K_{-1}}{\omega}$	—
$\mathrm{arctg}\,\omega T$	K_ϕ	—	$K_\phi T\omega$	—
$-\mathrm{arctg}\,\omega T$	$\dfrac{K_3}{1+\omega^2T^2}$	$\dfrac{0}{K_3}$	$-\dfrac{K_3T\omega}{1+\omega^2T^2}$	$\dfrac{\dfrac{1}{T}}{-\dfrac{K_3}{2}}$
$\mathrm{arctg}\,\dfrac{-\omega T}{-1}$	$\dfrac{-K_3}{1+\omega^2T^2}$	$\dfrac{0}{K_3}$	$\dfrac{-K_3T\omega}{1+\omega^2T^2}$	$\dfrac{\dfrac{1}{T}}{-\dfrac{K_3}{2}}$
$\mathrm{arctg}\,\dfrac{2\xi\tau\omega}{1-\omega^2\tau^2}$	$K(1-\omega^2\tau^2)$	—	$2K\xi\tau\omega$	—
$\mathrm{arctg}\,\dfrac{-2\xi\tau\omega}{1-\omega^2\tau^2}$	$\dfrac{K(1-\omega^2\tau^2)}{V(\omega)}$	$\dfrac{\dfrac{1}{\tau}\sqrt{1-2\xi}}{\dfrac{1}{4\xi(1-\xi)}}$	$\dfrac{-2K\xi\tau\omega}{V(\omega)}$	$\dfrac{1}{\tau}\sqrt{1-2\xi+C}$
0 at $\omega<\Omega$; π at $\omega>\Omega$	$\dfrac{K\Omega^2}{\Omega^2-\omega^2}$	—	—	—
$\mathrm{arctg}\,\dfrac{2\xi\tau\omega}{1-\omega^2\tau^2}$	$\dfrac{K(1-\omega^2\tau^2)}{V(\omega)}$	$\dfrac{\dfrac{1}{\tau}\sqrt{1-2\xi}}{\dfrac{1}{4\xi(1-\xi)}}$	$\dfrac{2K\xi\tau\omega}{V(\omega)}$	$\dfrac{1}{\tau}\sqrt{1-2\xi+C}$

1 - Order; 2 - Nomenclature; 3- Complex amplification coefficient $W(j\omega)$; 4 - Amplitude-frequency characteristic; 5 - Formula A (ω); 6 - First extremum; 7 - Phase-frequency characteristic $\phi(\omega)$; 8 - Real frequency characteristic; 9 - Formula P (ω); 10 - First extremum; 11 - Imaginary frequency characteristic; 12 - Formula Q (ω); 13 - First extremum; 14 - Amplifying; 15 - Delay; 16 - Differentiating; 17 - Integrating; 18 - Boosting - first order; 19 - Aperiodic; 20 - Quasi-static, first order; 21 - Boosting, second order; 22 - Oscillating; 23 - Resonance; 24 - Quasi-static, second order; 25 - Notes: In the "First Extremum" column, in the numerator of the fraction is shown the location of the extremum on the axis of frequencies, and in the denominator, its value.

If we use the scales of natural values and select, starting from the necessary accuracy of representation of the low-frequency part, the large scale of frequencies, the same scale must also be preserved for the entire region of changes in frequency, and that is why the graph is obtained in non-compact form and often is in general not realizable in a single scale.

For logarithmic coordinates the scale is automatically reduced in the region of high frequencies.

Actually, if a band equal to a single logarithmic unit is derived for the low-frequency band from ω_0 to $10\,\omega_0$, that is, to the extent of $9\,\omega_0$ in the logarithmic coordinates, since $\log 10\,\omega_0 - \log \omega_0 = 1$, then for the same band of the higher frequencies from $10\,\omega_0$ to $19\,\omega_0$, that is, also to the extent of $9\,\omega_0$, there are derived in the logarithmic coordinates a total of $\log 19\,\omega_0 - \log 10\,\omega_0 = \log 19 - \log 10 = 1.2788 - 1 \approx 0.279$ logarithmic units, etc. Thanks to this the logarithmic frequency characteristics are feasible on relatively small blanks, having at the same time a large scale in the low-frequency band.

Units of measurement of logarithmic coordinates. The following units of measurement are used in technique for logarithmic coordinates: the decade, the octave, the decilog and the decibel (db). The decade and octave are used most frequently for the scales of frequencies, and the decilog and decibel for scales of amplification in amplitude.

A single decade corresponds to a tenfold change in frequency: $\log 10\,\omega - \log \omega = 1$. During a change in frequency of n times the number of decades (dec) is simply equal to the decimal logarithm of the ratio of the frequencies:

$$\lg \eta\omega - \lg \omega = \lg \eta \quad \text{dec}.$$

A single octave (oct) corresponds to a change in the frequency of two times: $\log_2 2\omega - \log_2 \omega = 1$ oct. In decimal logarithmic units of measurement, that is, in decades, this ratio is:

$$\lg 2\omega - \lg \omega = \lg 2 = 0.301 \quad \text{dec}$$

Thus 1 oct = 0.301 dec.

A single decilog is a measurement of amplification one-tenth as large in logarithmic units as a single decade

$$1 \text{ decilog} = 0.1 \text{ dec}.$$

One decibel (db) is a logarithmic unit one-twentieth as large as one decade:

$$1 \text{ db} = 1/20 \text{ dec, or } 1 \text{ dec} = 20 \text{ db}.$$

The generally accepted unit of measurement of intensification of amplitude, the decibel, permits forming relatively small amplifications in whole numbers, which has proved convenient in practice. In natural measurement 1 db corresponds to the increase of intensification of amplitude by 1.12 times, since

$$\lg 1.12 = 0.05 = \frac{1}{20}.$$

We will adopt the convential designations:

$$20 \lg A(\omega) \text{ [db]} = LmA(\omega) = L(\omega). \qquad (4\text{-}34)$$

Figure 4-17 shows a grid of uniform scales of the logarithmic coordinates x and y.

The basic grid is formed by the thicker lines and is figured in logarithmic units, that is, in decades, on the axes Ox and Oy.

The grid for intensification of amplitude (db) is shown by the thinner horizontal lines. In the given case the grid is carried through 10 db and, as noted above, 1 dec corresponds to 20 db. For such a calculation the scale of inclinations of the linear logarithmic amplitude-frequency characteristics, reflecting the power functions of the order of $\pm$ n, will be:

$$S = \pm 20n \quad \text{db/dec} \qquad (4\text{-}35a)$$
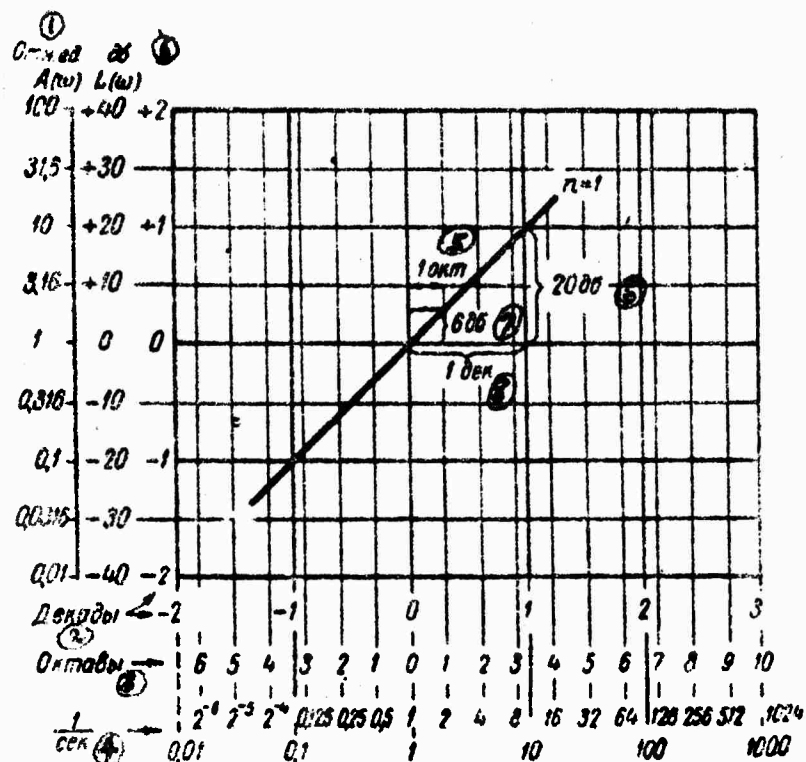
Fig 4-17. Uniform scales of logarithmic coordinates.
1 - Relative units; 2 - Decades; 3 - Octaves; 4 - 1/sec;
5 - oct; 6 - db; 7 - db; 8 - dec.

If we apply this rule for the boundary sections of amplitude-frequency characteristics, determinable by formulas (4-28b) and (4-29b), we get the inclinations of the logarithmic amplitude-frequency characteristics or, more exactly, their asymptotes:

In the region of low frequencies

$$S_{\bullet} = 20\,(\mu - \nu)\ db/dec. \qquad (4\text{-}35b)$$

In the region of high frequencies

$$S_{\infty} = 20\,(m - n)\ \text{db/dec};\qquad (4\text{-}35c)$$

At the intersection of the line 0 db:

of the first asymptote at the point:

$$\omega_0 = \sqrt[\mu - \gamma]{\dfrac{a_\mu}{b_\nu}}\,;\qquad (4\text{-}36a)$$

of the second asymptote at the point:

$$\omega_\infty = \sqrt[m - n]{\dfrac{a_n}{b_m}}\,.\qquad (4\text{-}36b)$$

The scale of octaves is constructed by the finer vertical lines on the same figure. In that calculation of the scales (octaves and decibels) the inclination of the linera characteristics of the power functions becomes:

$$\pm\,20n\cdot 0{,}301 \approx \pm\,6n \quad \text{db/oct}$$

Along with uniform scales of the logarithmic coordinates x and y, on the same figure is given the computation of the scale of frequencies and amplification in natural dimensionless values. The line 0 db corresponds to an amplitude equal to 1; the positive decibels indicate intensification of amplitude, and the negative, weakening. On the scale of frequencies the line 0 dec corresponds to the ratio of the frequencies to the basic, equal to 1; the positive decades and octaves give the increase in frequency, and the negative, the decrease. Of the examined types of computation, in practice computation in $\sec^{-1}$ is used on the axis of frequencies (at a basic frequency of $\omega_0 = 1$ $\sec^{-1}$) and in decibels on the axis of the amplification. In this, on the axis of frequencies a uniform grid of decades is computed in values of $\sec^{-1}$, equal to $10^{\pm N}$, where N are whole numbers, and the scale of frequencies obtained between the decades also is logarithmic, but on the other hand it is possible to calculate the natural values of the frequencies from it.

The scale of the amplification (db) constructed according to the formula

$$L(\omega) = L[\text{db}] = 20\lg L(\omega),$$

does not give the natural amplification; the latter is determined by
the formula

$$A(\omega) = 1.12^{A\,[db]} = 1.12^{L(\omega)} = \lg^{-1}\left[\frac{L(\omega)}{20}\right].$$

Table 4-3 is used for the transition from natural ratios to
decibels.

B. Semi-Logarithmic Amplitude-Phase Grid

Amplitude and phase frequency characteristics of components have
been plotted separately on logarithmic and semi-logarithmic coordin-
ates. Two types of semi-logarithmic grids -- the polar and the rect-
angular -- are used for amplitude-phase characteristics. The polar
grid is shown in Figure 4-18; in it the phase is laid out in the form
of the natural angle and the amplitude is in decibels, counted from
the circle 0 db (the region of negative decibels is limited). On the
same figure the amplitude-phase characteristics of typical components
have been plotted. Let us agree to designate the amplitude-phase
characteristic by the logarithmic amplitude (db) and the natural phase
by the symbol

$$L(j\omega) = L(\omega)\,e^{j\Psi(\omega)}. \qquad (4\text{-}37)$$

The rectangular grid represents an evolution of the polar grid
around the circle 0 db and is given in Figure 4-25 and later.
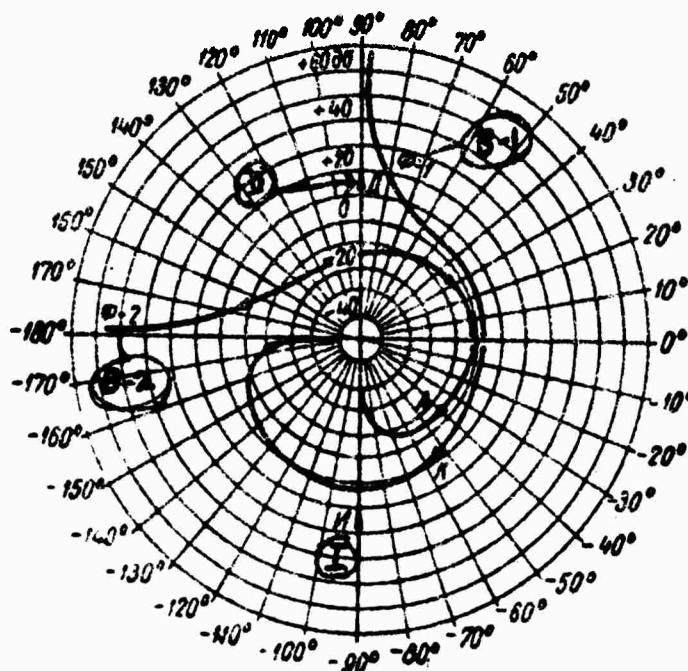
Fig 4-18. The amplitude-phase characteristics of components on
a semi-logarithmic complex plane. D - Differentiating; I - Inte-
grating; A - Aperiodic; B-1 Boosting, first order; (Continued)

C. Representation of Logarithmic Frequency Characteristics
During Cascade Inclusion of Components

In cascade inclusion the output harmonic oscillations of one
component are fed to the input of the following component, etc., as
shown in Figure 4-19.

Each component has a definite amplitude-phase characteristic
equal to the ratio of oscillations on the ouput and input, given in
the symbolic form in (4-16). Let us write out these ratios in the
order of the numbers of the components shown in Figure 4-19.

$$
\begin{aligned}
W_1(j\omega) &= \frac{1_2 e^{j(\omega t + c_2)}}{1_1 e^{j(\omega t + c_1)}} ; \\[6pt]
W_2(j\omega) &= \frac{1_3 e^{j(\omega t + c_3)}}{1_2 e^{j(\omega t + c_2)}} ; \\[6pt]
W_3(j\omega) &= \frac{1_4 e^{j(\omega t + c_4)}}{1_3 e^{j(\omega t + c_3)}} .
\end{aligned}
\qquad (4\text{-}38)
$$

If we multiply the left and right sides of the obtained equali-
ties, cancel the intermediate values and note that the ratio of the
output oscillations $A_4 e^{j(\omega t + \varphi_4)}$ of the circuit to the input oscil-
lations $A_1 e^{j(\omega t + \varphi_1)}$, given in symbolic form, by definition is the
total amplitude-phase characteristic of the entire circuit, we arrive
at an expression for the total amplitude-phase characteristic in the
form of the following product:

$$ W(j\omega) = W_1(j\omega)\, W_2(j\omega)\, W_3(j\omega). \qquad (4\text{-}39) $$

In multiplication of the amplitude-phase characteristics the
moduli also are multiplied, and the phases are added:

$$ A(\omega) = A_1(\omega)\, A_2(\omega)\, A_3(\omega); \qquad (4\text{-}40) $$

$$ \varphi(\omega) = \varphi_1(\omega) + \varphi_2(\omega) + \varphi_3(\omega). \qquad (4\text{-}41) $$

Since multiplication of the amplitudes corresponds to the opera-
tion of summation of their logarithms, then for the circuit in ques-
tion the logarithmic amplitude-frequency characteristics are simply
added:

$$ L(\omega) = L_1(\omega) + L_2(\omega) + L_3(\omega). \qquad (4\text{-}42) $$

For example, let us consider the obtaining of the frequency characteristics of a real differentiating component, of given OFT $W(p) = \tau p/\tau_p + 1$; we will present the amplitude-phase characteristic in the form of the product of the characteristics of the ideal differentiating and aperiodic components:

$$W(j\omega) = j\omega \tau \frac{1}{1 + j\omega T} \cdot$$
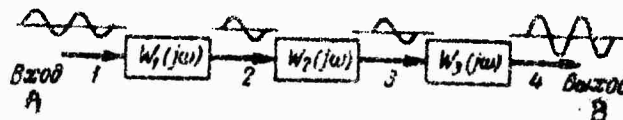
Fig 4-19. Frequency characteristics of a cascade circuit.
A - Input; B - Output.

In Figure 4-20a are plotted the asymptotic logarithmic characteristics of the two components, where $\tau = 0.5$ sec, that is, $\omega_1 = 1/T = 2$ sec^{-1} is assumed for the differentiating component, and $T = 0.01$ for the aperiodic component, or a conjugating frequency $\omega_2 = 100$ sec^{-1}.

If we correspondingly sum the characteristics of the components, we get the characteristics of the real differentiating component, singled out in the same figure by hatching. The real differentiating component, as is evident from the characteristics, practically does not change the amplification in the band of frequencies beyond the conjugating frequency $\omega > \omega_2$. The lead in phase on the conjugating frequency amounts to only $+\frac{\pi}{4}$ and with further increase in the frequency drops to zero.

As a second example let us consider the construction of the characteristics for a system with a second-order transfer function, having two real poles.

This OFT can also be described by the parameters τ and ξ in the form:

$$W(p) = \frac{k}{\tau^2 p^2 + 2\xi\tau p + 1} \cdot$$

but here $\xi > 1$ and the bands are real (see the derivation of formula (3-44)).

Let us present the OFT in the form

$$W(p) = \frac{k\tau^2}{(p\tau + \xi - \sqrt{\xi^2 - 1})(p\tau + \xi + \sqrt{\xi^2 - 1})}.$$

Table 4-2   Relationships between decibels and direct amplitude ratios

Децибел	Отношение амплитуд	Период	Отношение амплитуд	Децибел	Отношение	Децибел	Отношение	Децибел	Отношение
0,0	1,000	5,0	1,778	10,0	3,162	15,0	5,623	10	3,162
0,1	1,012	5,1	1,795	10,1	3,199	15,1	5,689	20	10
0,2	1,023	5,2	1,820	10,2	3,236	15,2	5,754	30	31,62
0,3	1,035	5,3	1,811	10,3	3,273	15,3	5,821	40	100
0,4	1,047	5,4	1,862	10,4	3,311	15,4	5,888	50	316,2
0,5	1,059	5,5	1,884	10,5	3,350	15,5	5,957	60	1000
0,6	1,072	5,6	1,905	10,6	3,388	15,6	6,026	70	$3,162 \cdot 10^3$
0,7	1,084	5,7	1,968	10,7	3,428	15,7	6,095	80	10^4
0,8	1,096	5,8	1,950	10,8	3,467	15,8	6,166	90	$3,162 \cdot 10^4$
0,9	1,109	5,9	1,972	10,9	3,508	15,9	6,237	100	10^5
1,0	1,122	6,0	1,995	11,0	3,548	16,0	6,310	110	$3,162 \cdot 10^5$
1,1	1,135	6,1	2,018	11,1	3,589	16,1	6,383	120	10^6
1,2	1,148	6,2	2,042	11,2	3,631	16,2	6,457	130	$3,162 \cdot 10^6$
1,3	1,161	6,3	2,065	11,3	3,673	16,3	6,531	140	10^7
1,4	1,175	6,4	2,089	11,4	3,715	16,4	6,607		
1,5	1,189	6,5	2,113	11,5	3,758	16,5	6,683		
1,6	1,202	6,6	2,138	11,6	3,802	16,6	6,761		
1,7	1,216	6,7	2,163	11,7	3,846	16,7	6,839		
1,8	1,230	6,8	2,188	11,8	3,890	16,8	6,918		
1,9	1,245	6,9	2,213	11,9	3,936	16,9	6,998		
2,0	1,259	7,0	2,239	12,0	3,981	17,0	7,079		
2,1	1,274	7,1	2,265	12,1	4,027	17,1	7,161		
2,2	1,288	7,2	2,291	12,2	4,074	17,2	7,244		
2,3	1,303	7,3	2,317	12,3	4,121	17,3	7,328		
2,4	1,318	7,4	2,344	13,4	4,169	17,4	7,413		
2,5	1,334	7,5	2,371	12,5	4,217	17,5	7,499		

At bottom of table and key, see next page.

①	②	①	②	①	②	①	②
2,6	1,349	7,6	2,399	12,6	4,266	17,6	7,586
2,7	1,365	7,7	2,427	12,7	4,315	17,7	7,674
2,8	1,380	7,8	2,455	12,8	4,365	17,8	7,762
2,9	1,396	7,9	2,483	12,9	4,416	17,9	7,852
3,0	1,413	8,0	2,512	13,0	4,467	18,0	7,943
3,1	1,429	8,1	2,541	13,1	4,519	18,1	8,035
3,2	1,445	8,2	2,570	13,2	4,571	18,2	8,128
3,3	1,462	8,3	2,600	13,3	4,624	18,3	8,222
3,4	1,479	8,4	2,630	13,4	4,677	18,4	8,318
3,5	1,496	8,5	2,661	13,5	4,732	18,5	8,414
3,6	1,514	8,6	2,692	13,6	4,786	18,6	8,511
3,7	1,531	8,7	2,723	13,7	4,842	18,7	8,610
3,8	1,549	8,8	2,754	13,8	4,898	18,8	8,710
3,9	1,567	8,9	2,786	13,9	4,955	18,9	8,811
4,0	1,585	9,0	2,818	14,0	5,012	19,0	8,913
4,1	1,603	9,1	2,851	14,1	5,070	19,1	9,016
4,2	1,622	9,2	2,884	14,2	5,129	19,2	9,226
4,3	1,641	9,3	2,917	14,3	5,188	19,3	9,226
4,4	1,660	9,4	2,951	14,4	5,248	19,4	9,333
4,5	1,679	9,5	2,985	14,5	5,309	19,5	9,441
4,6	1,698	9,6	3,020	14,6	5,370	19,6	9,550
4,7	1,718	9,7	3,055	14,7	5,433	19,7	9,661
4,8	1,738	9,8	3,090	14,8	5,495	19,8	9,772
4,9	1,758	9,9	3,126	14,9	5,559	19,9	9,886

1 – Decibels; 2 – Amplitude ratio.
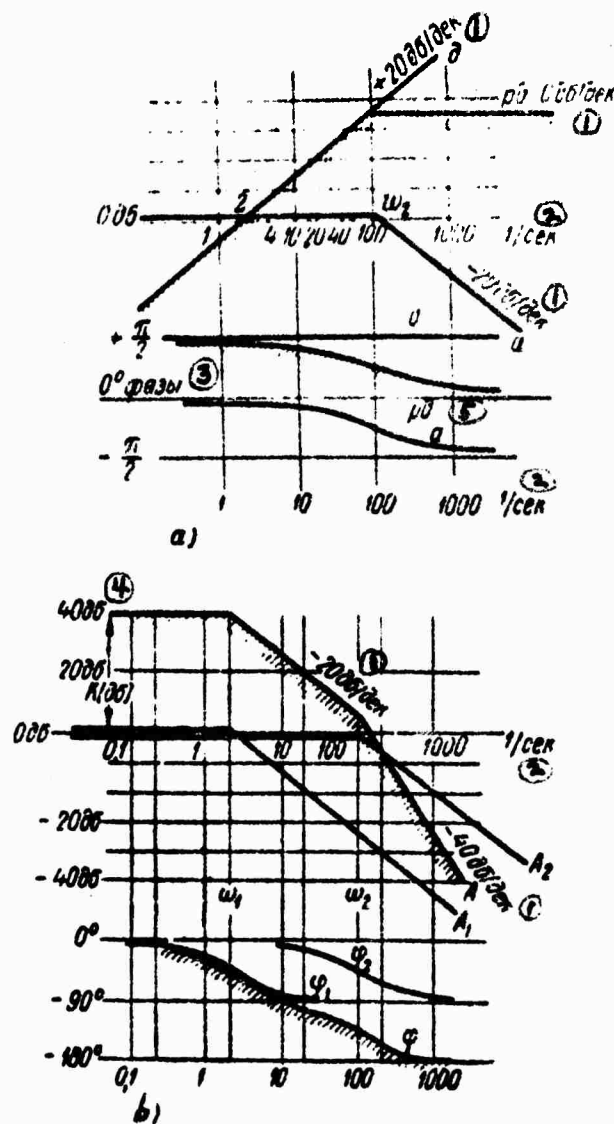
Fig 4-20. Obtaining the frequency characteristic of a cascade
circuit by frequency characteristic elements. a - logarithmic
frequency characteristic of a real differentiating component;
b - logarithmic frequency characteristic of aperiodic compon-
ents connected in in cascade. 1 - db/deo; 2 - 1/sec; 3 - phase;
4 - db; 5 - rd.

If we examine the factors as the OFT's of the aperiodic components, we find the conjugating frequencies of their characteristics:

$$\omega_1 = \frac{\xi - \sqrt{\xi^2 - 1}}{\tau}; \quad \omega_p = \frac{\xi + \sqrt{\xi^2 - 1}}{\tau}.$$

In Figure 4-20b are constructed the asymptotic logarithmic amplitude characteristics for $\omega_1 = 2 \ sec^{-1}$ and $\omega_2 = 100 \ sec^{-1}$, and their summation is performed. If we sum the logarithmic amplitude-frequency characteristic that is horizontal in the band of frequencies $0 - \omega_1$, it has the inclination 20 db/dec in the band of frequencies $\omega_1 - \omega_2$ and the inclination 40 db/dec at frequencies above ω_2.

Summation of the phase characteristics has been performed in the same figure.

When there is a large number of sequentially excluded aperiodic components, after each conjugating frequency the inclination of the total characteristic is increased by 20 db/dec, attaining -20, -40, -60 db/dec, etc.

4-6. Nomograms for Transformations of Frequency Characteristics

A. P, Q Nomograms

Let us examine the conditions of the passage of a control signal, given in the form of harmonic oscillations, through a matching-parallel circuit which has, in accordance with Figure 4-21, the total amplitude-phase characteristic:

$$W(j\omega) = W_1(j\omega) + W_2(j\omega). \qquad (4\text{-}13)$$

The physical meaning of summation of the oscillations on the output is explained by diagram a; the geometric interpretation of the addition of the vectors is given in diagram b.

The total output amplitude and phase are most simply obtained by means of the real and imaginary frequency characteristics of the components:

$$A(\omega) = \sqrt{[P_1(\omega) + P_2(\omega)]^2 + [Q_1(\omega) + Q_2(\omega)]^2}; \qquad (4\text{-}14)$$

$$\varphi(\omega) = arctg \frac{Q_1(\omega) + Q_2(\omega)}{P_1(\omega) + P_2(\omega)}. \qquad (4\text{-}15)$$

If the amplitude-phase characteristics $W_1(j\omega)$ and $W_2(j\omega)$ are

given on a complex plane, then for each point ω according to the scales on the coordinate axes it is easy to count the rectangular coordinates, and the sums of the corresponding coordinates

$$P(\omega) = P_1(\omega) + P_2(\omega); \qquad (4.46)$$

$$Q(\omega) = Q(\omega) + Q(\omega) \qquad (4.47)$$

are used for the construction of a hodograph of the total amplitude-phase characteristic of the circuit by points.
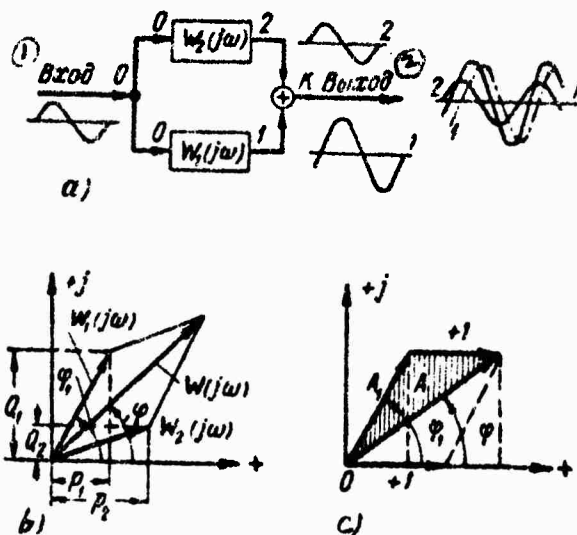
Fig 4-21. Transformation of the frequency characteristics of components in the presence of a matching-parallel circuit diagram. 1 - Input; 2- Output.

If the components are given logarithmic frequency characteristics, expansion into the real and imaginary constituents is conveniently done on semi-logarithmic polar grids (Figure 4-18) or on their evolvent, a semi-logarithmic rectangular grid, shown in Figure 4-22.

The evolution is accomplished in the following manner: in the upper half-plane in Figure 4-18 the 90° line (ray) was left neutral; it and the db scale close to the ray were transferred without change to the development of Figure 4-22; the semi-circle 0 db was straightened, and all the rays perpendicular to it became vertical straight lines in Figure 4-22.
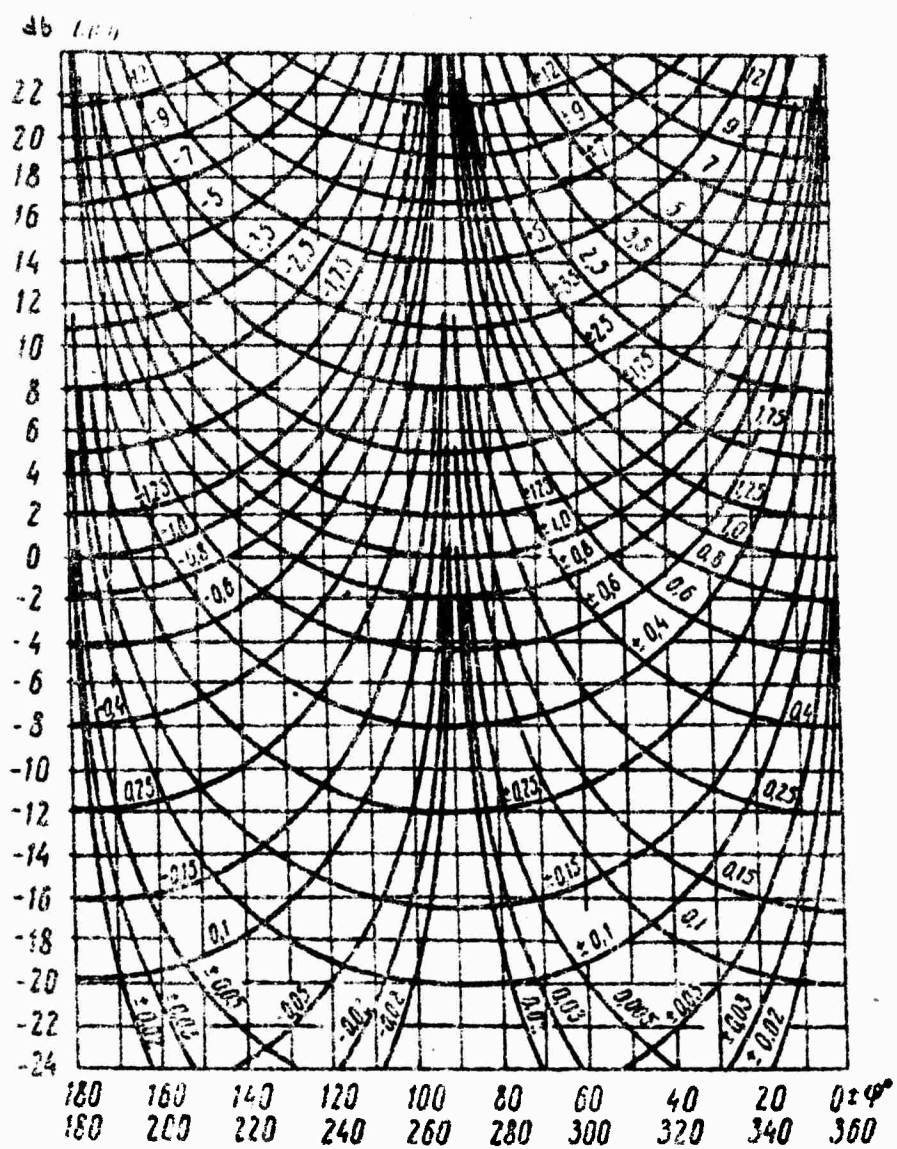
Fig 4-22. P, Q nomogram.

In this supporting rectangular grid, $L_1(\omega)$, φ_1 and $L_2(\omega)$, φ_2 are plotted according to the data for a series of values of frequencies of the point, and when these are joined by smooth curves the amplitude-phase characteristics $L_1(j\omega)$ and $L_2(j\omega)$ of the components are obtained on a semi-logarithmic amplitude-phase plane.

In order to expand $L_1(j\omega)$ and $L_2(j\omega)$ into rectangular coordinates, an additional grid of the isolines $P = c_1$ and $Q = c_2$ is needed. This grid is plotted on the supporting rectangular grid in the form of two sets of curves: peaked for the real and bowl-shaped for the imaginary. The equations of the isolines are very simple.

The real are:

$$L_P(\omega) = Lm\,\frac{P_i}{\cos\varphi} = LmP_i - Lm\cos\varphi; \qquad (4\text{-}48a)$$

and the imaginary:

$$L_Q(\omega) = Lm\,\frac{Q_k}{\sin\varphi} = LmQ_k - Lm\sin\varphi. \qquad (4\text{-}48b)$$

According to these formulas, given for each isoline with a fixed value of P_i or Q_k (these values are written on each isoline of the figure), it is possible by the abscissa φ to determine the ordinate $L(\omega)$ and construct the isolines.

Let us recall that on the polar plane in Figure 4-18 the isolines (4-48) have the form of horizontal and vertical straight lines. In the evolution of the half-plane the edges of the imaginary -- horizontal -- isolines were raised and in Figure 4-22 they became bowl-shaped. The vertical -- real -- isolines were compressed from above in the evolution and diverged at the bottom, forming the peaked isolines in Figure 4-22.

All the isolines are obtained from any isoline of each set by vertical shift. Therefore to expand the range of the db scale the blanks can contract along the vertical by setting the calculation of additional lines in accordance with formulas (4-48).

When a blank is used for the lower half-plane $180° < \varphi < 360°$ the isolines of the imaginary characteristics are assumed to be with negative sign.

The Order of Construction of the Characteristics of a Matching-Parallel Circuit

1. According to the given $L_1(\omega)$ and $\varphi_1(\omega)$, and also $L_2(\omega)$ and $\varphi_2(\omega)$ the amplitude-phase characteristics of components are constructed on a rectangular grid by points for the series of values of

frequency: ω_1, ω_2, $\omega_3 \dots$

2. If we are given any frequency ω_k, corresponding points are found on the curves $L_1(j\omega_k)$ and $L_2(j\omega_k)$ are counted from the real isoline on which those points and calculations of $P_1(\omega_k)$ and $P_2(\omega_k)$ fall; the results are summed:

$$P(\omega_k) = P_1(\omega_k) + P_2(\omega_k).$$

3. The values of $Q_1(\omega_k)$ and $Q_2(\omega_k)$ are counted from the imaginary isolines on which the points of the amplitude-phase characteristic with identical frequency fell, and they are summed:

$$Q(\omega_k) = Q_1(\omega_k) + Q_2(\omega_k).$$

4. The results according to points 2 and 3 need not be written down, and directly on those coordinates on the same blank is constructed one point of the total amplitude-phase characteristic, and on it is written the calculated frequency ω_k.

5. Points 2, 3 and 4 are repeated for the following frequency: ω_γ etc.

If the points of the amplitude-phase characteristic with the calculated frequencies do not fall on the isoline, readings of the $P(\omega_k)$ and $Q(\omega_k)$ are made on the isolines closest to those points by linear interpolation.

The Order of Construction of the Characteristics of
   the Antiparallel Circuit

For the antiparallel circuit given in Figure 4-23 it is convenient to determine at first the inverse amplitude-phase characteristic of the circuit which establishes the connection between the given output harmonic oscillations that are being established and the unknown input oscillations.

If we move from right to left in the circuit in Figure 4-22, we get the inverse amplitude-phase characteristic in the following form:

$$\frac{1}{W(j\omega)} = \frac{1}{W_1(j\omega)} - W_2(j\omega) \qquad (4-49a)$$

From this we proceed to the direct amplitude-phase characteristic:

$$W(j\omega) = \frac{W_1(j\omega)}{1 - W_1(j\omega)W_2(j\omega)} . \qquad (4-49b)$$

--- 308 ---
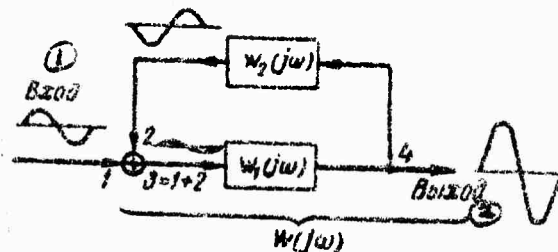
Fig 4-23.   Transformation of the frequency characteristics
in an antiparallel circuit diagram.

1. Input; 2. Output

The result, finally, could be obtained at once by (1-76) in the
substitution of $D = p = j\omega$.

The procedure for construction of the total characteristic of
the circuit differs insignificantly from that stated above:

1. At the given amplitude-phase characteristics of a component
of a direct circuit the sign of the amplification db and the sign of
phase vary, and according to these data of $(-L_1(\omega))$ and $-\psi_1$ the in-
verse characteristic of component No 1 is constructed on the rect-
angular grid; the characteristic of component No 2 is constructed in
the usual manner.

2. The partial real characteristics are found along the P-iso-
lines, and the total real characteristic $P^i(\omega)$ -- on the basis of
their difference, $P_1^i(\omega) - P_2^i(\omega)$.

3. The partial imaginary characteristics are found along the
Q-isolines, and the total imaginary characteristic $Q^i(\omega)$ -- on the
basis of their difference, $Q_1^i(\omega) - Q_2^i(\omega)$.

4. The total characteristic of the circuit $W(j\omega)$ on the grid
of isolines is constructed according to the found coordinates.

5. Since the result, according to formula (4-49a), gives the
inverse characteristic, then for the transition to the straight
line (4-49b) it is necessary to change the sign of the db and phase
on the rectilinear grid to the reverse:

$$L(\omega) = -L^i(\omega);$$
$$\varphi(\omega) = -\varphi^i(\omega).$$

The Order of Construction of the Characteristic of a Circuit
with a Single Negative Feedback

For this case

$$W_2(j\omega) = -1, \quad P_2 = -1, \quad Q_2 = 0.$$

1. Only one characteristic $L_1(j\omega)$ is constructed on the rectangular grid according to the constituents with changed signs:

$$-L_1(\omega) \quad \text{and} \quad -\varphi_1(\omega).$$

2. Unity is added to the real constituents found:

$$P^i(\omega) = P_1^i(\omega) + 1.$$

3. If we find the isoline of the imaginary characteristic $Q_j^i(\omega)$ for a definite frequency, we will seek along that isoline the real isoline intersecting it, with the value $P^i(\omega)$. The point of the total inverse characteristic is determined by the intersection of the isolines, and the entire characteristic $L^i(j\omega)$ by the series of points.

4. For a circuit of data with a direct characteristic, we change the signs of the rectangular scales to $-L(\omega)$ and $-\varphi$.

B.   Nomograms

The principal operation solvable by an φ -nomogram is transformation of the frequency characteristics according to the formula for an anti-parallel diagram with a single negative feedback:

$$\Phi(j\omega) = \frac{W(j\omega)}{1 + W(j\omega)}. \qquad (4\text{-}50)$$

The nomogram given for Figures 4-24 and 4-25 contains a rectangular coordinate grid analogous to the grid in Figure 4-22 for the construction of a hodograph according to the given characteristics of the component $L(\omega)$, $\varphi(\omega)$ and a grid of isolines of amplitude and phase for solution (4-50).

The principle of construction of the isolines is conveniently shown on a very simple operation:

$$K(j\omega) = 1 + W_2(j\omega). \qquad (4\text{-}51\,a)$$

from which on the basis of the inversion it is not difficult to go over to the basic transformation (4-50).

The conditions of summation of the arbitrary vector $W_1(j\omega)$ with a unit vector are explained by Figure 4-21c.

It is easy to obtain a clear solution relative to the parameters of the vector W_1 from the triangle constructed on the investigated diagram:

$$A_1 = \sqrt{1 + A^2 - 2A\cos\varphi}; \qquad (4\text{-}51b)$$

$$\varphi_1 = \text{arctg} \frac{A\sin\varphi}{A\cos\varphi - 1} = \text{arctg} \frac{\sin\varphi}{\cos\varphi - 1/A}. \qquad (4\text{-}51c)$$

If we fix in both formulas the value A, for example, by assuming $A = 1 = 0$ db and varying φ, we get a series of conjugate values of A_1 and φ_1 which are the coordinates of the isoline $L(\omega) = 0$ db = = constant in the coordinate system $L_1(\omega)$, φ_1.

In Figure 4-24a, in the rectangular grid φ_1°, L_1 db, are constructed the isoline $L(\omega) = 0$ db and also two additional "ascending" isolines $L' = -6$ db and $L'' = +6$ db.

If the value of φ° now is fixed in formulas (4-51b) and (4-51c), for example, $\varphi^\circ = 90^\circ$, then by varying A it is possible to calculate the conjugate values L_1 and φ_1 corresponding to the coordinates of the isoline of the constant phase $\varphi = 90^\circ =$ constant. This isoline, and also the additional two "descending" isolines $\varphi' = +60^\circ$ and $\varphi'' = +120^\circ$ are constructed according to the points in the lower half of the nomogram.

For illustration of the rules of application of the nomogram to it, the summation of the two constant vectors is shown:

$$K = 1 + 2e^{j104^\circ} = 1 + R.$$

In order to enter the nomogram for the second vector $\bar{R}$, let us determine the logarithmic amplitude $L = +6$ db and plot the point R (6 db, 104°) on the coordinate rectangular grid. The position of the point is marked by a double circle.

We count the answer (*) in amplitude directly from the isoline which has successfully passed through the examined point $L = 6$ db, and in phase we interpolate the values of the numbers of the closest phase isolines, which gives $\varphi \approx 80^\circ$.

More exact results (in phase) can be obtained by Figure 4-25 and

compared with the geometric summation given in Figure 4-24.

The effectiveness of the application is manifested, naturally, not in the calculation of a single value of the sum, but in large-scale calculations which require for the transformation of the amplitude-phase characteristic $W_1(j\omega)$, given at all frequencies from $\omega = 0$ to $\omega = \infty$, into the new characteristic $K(j\omega)$. As an example of such a transformation by means of a nomogram W on the supporting rectangular grid the amplitude-phase characteristic of the differentiating component $W_1(j\omega) = +j\omega T$ has been constructed, which coincides with the line of the phase $\varphi_1 = 90°$. In the curvilinear grid of isolines it is converted into the characteristic of the boosting component

$$K(j\omega) = 1 + j\omega T.$$

If we now replace the amplitude-phase characteristic $K(j\omega)$ in formula (4-51a) by its inversion:

$$K(j\omega) = \frac{1}{\Phi_*(j\omega)}; \qquad (4\text{-}52a)$$

then we get:

$$\Phi_*(j\omega) = \frac{1}{1 + W_1(j\omega)}. \qquad (4\text{-}52b)$$

In order to perform transformation (4-52b) according to the given $L_1(\omega)$ and φ_1, obviously it is necessary, in accordance with the rule of inversion, to change the sign of the numbers of the output isolines to $-L$ and $-\varphi$, as shown in the diagram $1/1 + W$ in Figure 4-24. The solution of the example of inversion of the geometric sum (*) is given in the same place. Further, we will replace the amplitude-phase characteristic $W_1(j\omega)$ in formula (4-52b) by its inversion:

$$W_1(j\omega) = \frac{1}{W(j\omega)}; \qquad (4\text{-}53a)$$

and then we get formula (4-50), that is,

$$\Phi(j\omega) = \frac{1}{1 + \frac{1}{W(j\omega)}}. \qquad (4\text{-}53b)$$

Summation of the vectors in the denominator can be accomplished according to the diagram $1/1 + W$, which differs from the diagram $1 + W$ by the signs of the numbers of the output values. If we change the signs and numbers of the input scales of the rectangular grid in the initial nomogram $1 + W$ in accordance with the structure of formula (4-53b), we finally get a nomogram for transformation (4-50) or a
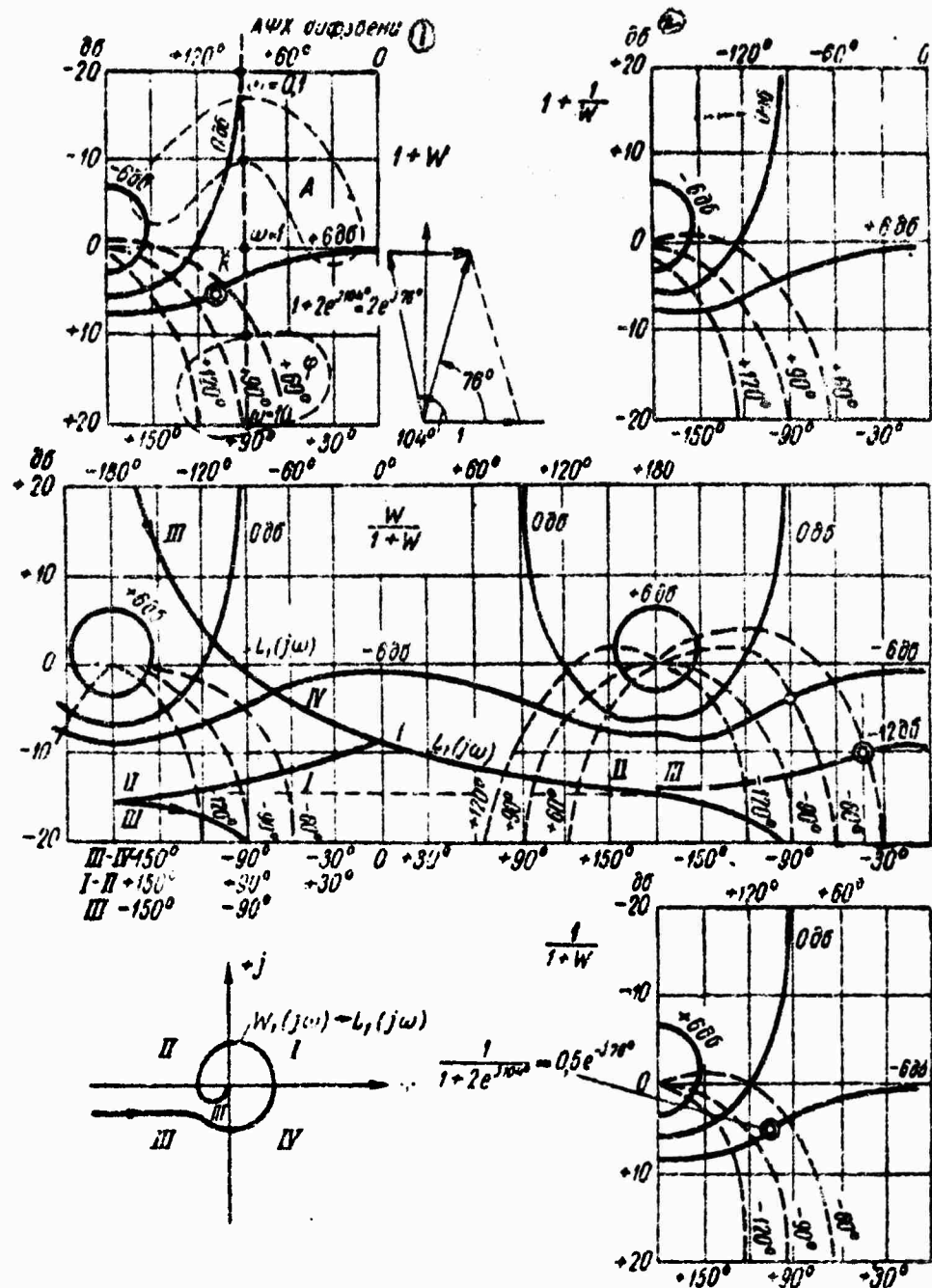
Fig 4-24. Rules of application of a ψ-nomogram. 1 - Amplitude-phase characteristic of the differentiating component; 2 - db.
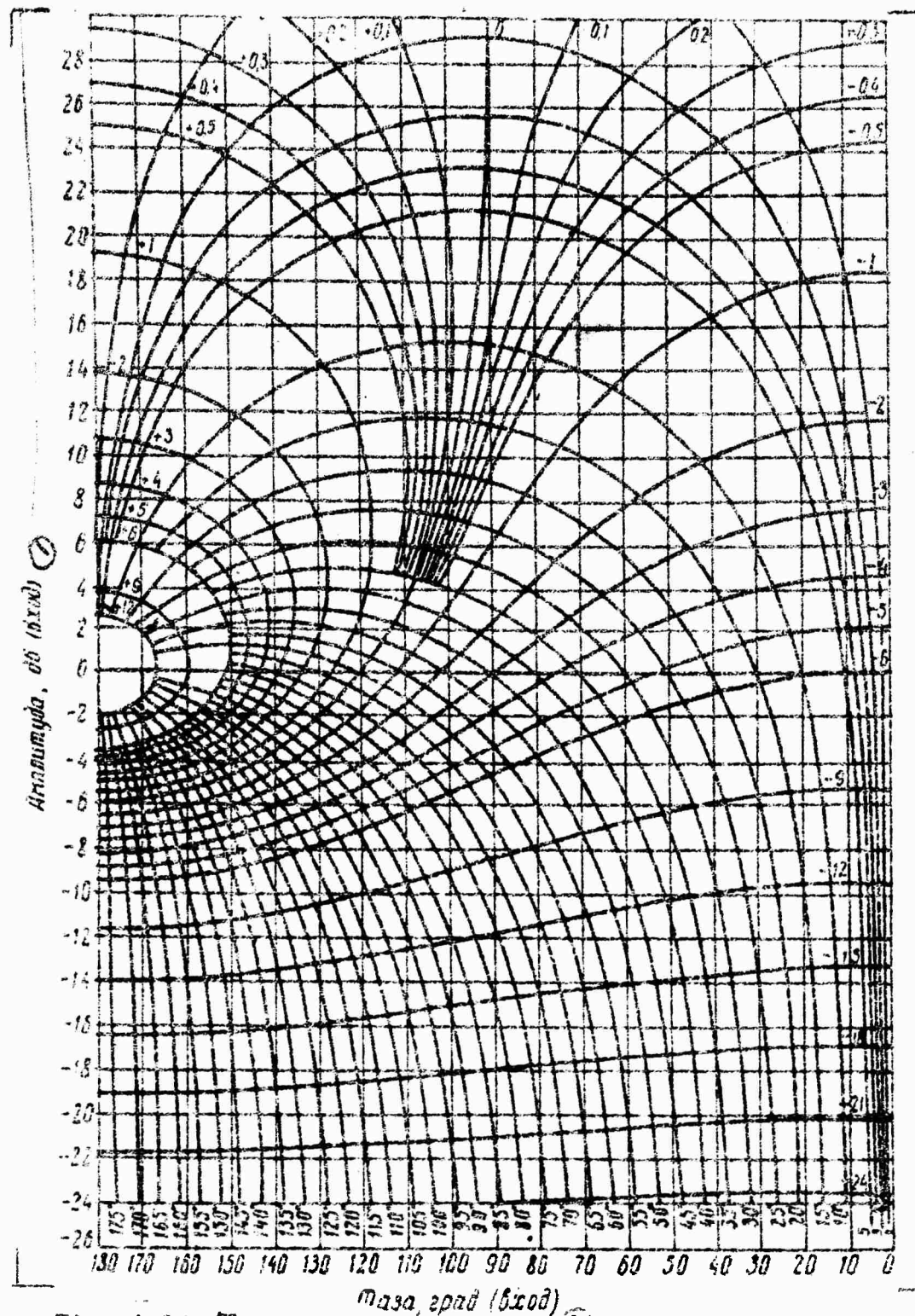
Fig. 4-26. /For caption
and key, see next page./

— 314 —

Fig 4-25. φ-nomogram. 1 - Amplitude, db (input); 2 - Phase, degrees (input).

φ-nomogram, given in Figures 4-25 and 4-24 ($\frac{W}{1+W}$).

If we now accept the φ-nomogram, with its numbering and signs of the input and output scales, as a basis, it is easy to obtain the rules of use of this nomogram for transformations (4-51) - (4-53) of the frequency characteristics.

A summary of the rules of signs in the use of φ-nomograms in Figure 4-25 in various cases is given in Table 4-4.

Table 4-4   Rules of signs for a φ-nomogram (Figure 4-25)

Выходная функция $\textcircled{1}$	Вход W $\textcircled{2}$		Выход $\textcircled{3}$	
	$\delta\delta$ $\textcircled{4}$	$cpad$ $\textcircled{5}$	$\delta\delta$ $\textcircled{4}$	$cpad$ $\textcircled{5}$
$\Phi = \dfrac{W}{1+W}$	$+$	$+$	$+$	$+$
$\Phi_* = \dfrac{1}{1+W}$	$-$	$-$	$+$	$+$
$K = 1+W$	$-$	$-$	$-$	$-$
$K_* = 1+\dfrac{1}{u}$	$+$	$+$	$-$	$-$

1 - Output function; 2 - Input W; 3 - Output; 4 - db; 5 - degrees.

The changed signs of the numbering of the scales for each of the operations according to Table 4-4 are given in the diagrams in Figure 4-24.

Let us dwell additionally on the conditions of the practical use of the basic φ-nomogram.

1. In a region of small amplifications (negative decibels in the lower part of the nomogram) the rectilinear and curvilinear grids approach the input parameters:

$$\lim_{|W|\to 0} \frac{W(j\omega)}{1+W(j\omega)} = W(j\omega)|_{|W|\to 0} \quad (4-54)$$

2. In a region of large amplifications (positive decibels in the upper part of the nomogram) the transformed characteristic approaches in modulus to unity (0 db) at zero phase shift:

$$\lim_{|W| \to \infty} \frac{W(j\omega)}{1 + W(j\omega)} = 1. \qquad (4\text{-}55)$$

This is readily noted in the upper part of the nomogram, where the entire region of change of the input phase is embraced by the isolines of a constant output amplitude close to 0 db.

3. The presence of approximate formulas, given above, permits not increasing the volume of the nomogram beyond the limits of $\pm$ 30 db. As regards the phases, the two quadrants (I and II) given in the nomogram (Figure 4-25) are also sufficient for the entire possible range of changes in phase, since the alteration of the sign of the phase, that is, the transition into quadrants III and IV generally is not reflected on the output amplitude, and in the output phase the sign varies simultaneously with change of the sign of the input phase. Consequently, the nomogram in Figure 4-25 can be symmetrically repeated for quadrants III and IV with change of the sign in the numeral of the phase, or a single half of it can be used, if we recall that in the transition of the input amplitude-phase characteristic into quadrants III and IV it is necessary to change the sign in the numbering of the input and output phase lines; the graph of the transformed characteristic acquires breaks in the second case.

For the complex amplitude-phase characteristic $W_1(j\omega)$, shown below on Figure 4-24, it is necessary to adopt the expanded φ-nomograms, by contracting the blanks of Figure 4-25 and changing the numbering of the scales, as shown in the diagram $\left(W/(1 + W)\right)$ in Figure 4-24. However, it is completely possible to use a single blank in all, as shown on the left side of the same diagram, by constructing the sections of the graph $L_1(j\omega)$ relating to quadrants II and III on the principle of reflection from the boundary lines of the nomogram.

4. In the working up of the data of the experiment carried out in accordance with Figure 4-6b, the amplitude characteristics $L(\omega)$, $L_1(\omega)$ serve as the input into the φ-nomogram, and the phase characteristics $\varphi(\omega)$ and $\phi_1(\omega)$ are determined at their intersection.

4-7. The Complex Spectrum of the Process; One-Sided Fourier Transform

A. Apparatus of a one-sided Fourier transform

The direct and inverse Fourier transforms are given by the formulas:
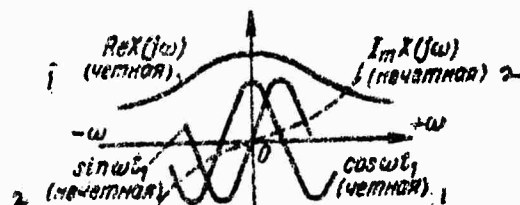
Fig 4-26. Graphs of the functions entering the Fourier
integral. 1 - Even; 2 - Odd.

$$X(j\omega) = \int\limits_{0}^{\infty} x(t)\, e^{-j\omega t}\, dt; \qquad (4\text{-}56a)$$

$$x(t) = \frac{1}{2\pi} \int\limits_{-\infty}^{\infty} e^{j\omega t} X(j\omega)\, d\omega. \qquad (4\text{-}56b)$$

The auxiliary role of this apparatus in control theory is the
same as that of the apparatus of a Laplace transform: to facilitate
analysis of the passage of a signal through linear components and
systems. This can be explained by using once more Figure 3-1. The
direct transformation (4-56a) transfers the controlling initial pro-
cess from the region of the originals into the region of the complex
spectra:

$$x_{in}(t) \leftarrow\rightarrow X_{in}(j\omega). \qquad (4\text{-}57)$$

In addition, the complex spectrum of the controlling process
$X_{in}(j\omega)$ is transformed into the complex spectrum of the output pro-
cess $X_{out}(j\omega)$ by multiplication by the amplitude-phase character-
istic of the component:

$$X_{out}(j\omega) = W(j\omega)\, X_{in}(j\omega), \qquad (4\text{-}58)$$

after which, on the basis of the inverse Fourier transform it is pos-
sible to proceed from the region of the complex spectra to the orig-
inals:

$$X_{out}(j\omega) \leftarrow\rightarrow x_{out}(t). \qquad (4\text{-}59)$$

Formulas (4-56) and (4-58) are the result of the corresponding

317

operational formulas (see Chapter 3) upon substitution of

$$p = j\omega. \qquad (4\text{-}60)$$

To obtain the complex spectrum of the process $X(j\omega)$ it is sufficient to take the Laplace transform of this process $X(p)$ and perform substitution of (4-60); after this we get the complex function of the frequency, given in one of the following forms:

$$X(j\omega) = \operatorname{Re} X(j\omega) + j \operatorname{Im} X(j\omega); \qquad (4\text{-}61)$$

$$X(j\omega) = |X(j\omega)| \, e^{j\psi(\omega)}, \qquad (4\text{-}62)$$

where $\operatorname{Re} X(j\omega)$ is the real spectrum of the process;
$\operatorname{Im} X(j\omega)$ is the imaginary spectrum of the process;
$X(j\omega)$ is the amplitude spectrum of the process;
$\phi(\omega)$ is the phase spectrum of the process.

It can readily be noted that if any process is regarded as the weight function of a certain boosting component or system

$$x(t) = w_x(t), \qquad (4\text{-}63)$$

the concept of the spectrum of that process coincides with that of the frequency characteristic of the boosting component, analytically extended into the region of negative frequencies:

$$X(j\omega) = W_x(j\omega); \qquad (4\text{-}64)$$

$$-\infty \leqslant \omega \leqslant +\infty.$$

The graphs of the spectrum of the processes also are obtained from the graphs of the frequency characteristics given in Figures 4-13 — 4-16.

Let us take, for example, the process in the form of the decreasing exponent

$$x(t) = e^{-ct}. \qquad (4\text{-}65)$$

Corresponding to it is the aperiodic boosting component with the amplitude-phase characteristic

$$W_c(j\omega) = \frac{1/c}{1/c\,p + 1} \bigg|_{p=j\omega} = \frac{1}{c + j\omega}.$$

Thus the complex spectrum is:

$$X(j\omega) = \frac{1}{\sigma + j\omega}.$$ (4-66a)

The real spectrum

$$\text{Re}\, X(j\omega) = \frac{\sigma}{\sigma^2 + \omega^2}$$ (4-66b)

has a graph that coincides with the graph $P(\omega)$ (Figure 4-15 c), but extended by virtue of the evenness of the real spectrum in the region of negative frequencies symmetric with respect to the axis of the ordinates.

The imaginary spectrum

$$\text{Im}\, X(j\omega) = \frac{-\omega}{\sigma^2 + \omega^2}$$ (4-66c)

coincides with the graph $Q(\omega)$ (Figure 4-15e) and is extended in the region of negative frequencies on the basis of the rule of central symmetry relative to the start of the coordinates by virtue of the unevenness of the imaginary spectrum.

The amplitude spectrum

$$|X(j\omega)| = \frac{1}{\sqrt{\sigma^2 + \omega^2}}$$ (4-67a)

in the region of negative frequencies is the analytic extension of graph $A(\omega)$ (Figure 4-15b) according to the rule of axial symmetry, and the phase spectrum $\psi(\omega) = -\text{arctg}\frac{\omega}{\sigma}$ extends the graph of $\psi(\omega)$ (Fig 4-15c) according to the rule of central symmetry.

For the inverse determination of the process according to spectrum it is possible to follow by the operational method the expansion (after determination of the poles) of the complex spectrum into partial spectra of type (4-66a) with subsequent transition according to the tables of elementary representations to the originals. The tables of operational correspondences are readily transformed into tables of spectral correspondences.

But formula (4-56b) likewise permits, in the inverse transformation, going by another method (without calculation of the poles of the spectrum), by being oriented to methods of numerical integration, which is very valuable for engineering practice.

Let us make the following substitutions in formula (4-56b):

$$e^{j\omega t} = \cos \omega t + j \sin \omega t;$$

$$X(j\omega) = \operatorname{Re} X(j\omega) + j \operatorname{Im} X(j\omega);$$

then we get, after rearrangement of the real and imaginary terms:

$$x(t) = \frac{1}{2\pi} \int\limits_{-\infty}^{\infty} [\cos \omega t \operatorname{Re} X - \sin \omega t \operatorname{Im} X +$$

$$+ j (\operatorname{Re} X \sin \omega t + \operatorname{Im} X \cos \omega t)] \, d\omega.$$

Let us consider the character of the change of the integrands in the region of the positive and negative frequencies.

In Figure 4-19 is shown the law of change of functions $\cos \omega t_1$ and $\sin \omega t_1$ for the fixed value $t_1 > 0$. The graphs presented illustrate the independence of the even functions, to which $\cos \omega t_1$ belongs, of the sign of ω and the change of the sign of the uneven function $\sin \omega t_1$ during change of the sign of ω. In the same figure are graphs of the real and imaginary spectra of some arbitrary process, the features of which, independently of the type of process are that the real spectrum is always an even function, since it contains only the even powers $(j\omega)^{2n}$, that is $\pm \omega^{2n}$, and the imaginary spectrum is always an uneven function.

If we examine the integrands in the preceding formula, we can establish that the imaginary part of the subintegral expression on the whole is an uneven function and the integral from it in the limits from $\omega = -\infty$ to $\omega = +\infty$ is equal to zero; for the real part, the integration in the region of positive and negative frequencies gives identical results, and therefore it is sufficient to include only the region of the positive frequencies and to double the result of the integration. With these observations taken into consideration, the expression for the time process assumes the form:

$$x(t) = \frac{1}{\pi} \int\limits_{0}^{\infty} [\cos \omega t \operatorname{Re} X - \sin \omega t \operatorname{Im} X] \, d\omega. \quad (4\text{-}68)$$

If we examine only time processes of the type of the initial functions, that is, those which satisfy the condition $x(t) = 0$ at $t < 0$, it is possible to establish that when any value $t < 0$ is substituted in the preceding formula the result of the integration must be equal to zero, that is, at

$$t_1 \quad -|t|$$

$$\int_0^\infty [\cos(-\omega|t|)\operatorname{Re}X - \sin(-\omega|t|)\operatorname{Im}X]\, d\omega = 0.$$

If we take out the minus in the argument of the uneven function as the symbol of the function, we get the relation between the same terms in the positive arguments, which is valid for all the values of time:

$$\int_0^\infty \cos\omega|t|\operatorname{Re}X\, d\omega = -\int_0^\infty \sin\omega|t|\operatorname{Im}X\, d\omega. \qquad (4\text{-}69)$$

Thus in determining the time process it is sufficient to integrate one of the examined functions and double the result. Finally we get:

$$x(t) = \frac{2}{\pi}\int_0^\infty \operatorname{Re}X(j\omega)\cos\omega t\, d\omega; \qquad (4\text{-}70a)$$

$$x(t) = -\frac{2}{\pi}\int_0^\infty \operatorname{Im}X(j\omega)\sin\omega t\, d\omega. \qquad (4\text{-}70b)$$

The two formulas are of equal value for application.

B. The Transformation of Regular and Irregular Parts of the Process

A direct Fourier transform always uniquely forms the initial process. The difficulties that arise in application of formula (4-56a) to non-damping processes are overcome by the substitution of $j\omega = \sigma + j\omega$, which, when the value of σ is suitably made, makes the integral (4-56a) always convergent. After completion of the integration, which gives the new function $X(\sigma + j\omega)$, the unknown spectrum is determined on the basis of the limiting transition

$$X(j\omega) = \lim_{\sigma \to 0} X(\sigma + j\omega). \qquad (4\text{-}71)$$

Thus, for example, the spectrum of a unit function can be obtained from the spectrum of the exponent (4-66a):

$$X_1(j\omega) = \lim_{\sigma \to 0} X_e(j\omega) = \lim_{\sigma \to 0}\frac{1}{\sigma + j\omega} = \frac{1}{j\omega}$$

It can readily be noted that the introduction of the real indicator of the power σ leads to a Laplace transform and, consequently, the above-indicated limiting transition, as already noted, can be

written directly in the form:

$$X(j\omega) = X(p)|_{p=j\omega}. \qquad (4\text{-}72)$$

The inverse Fourier transform, made according to the engineering formulas (4-70), does not provide unique correspondences between the real or imaginary spectrum and the time process, since the individually taken real spectrum, for example, does not completely contain neutral functions of the form of $\delta_2/t/$, $1/t$, t^2 ... and does not manifest a divergent function. Thus the real spectrum which enters formula (4-66b) can be related both to the damping exponent with negative scale and to the divergent exponent

$$\mathrm{Re}\,X(j\omega) = -\frac{c}{\omega^2 + c^2} \left\{ \begin{array}{l} \rightarrow - e^{-ct} \\ \rightarrow e^{+ct} \end{array} \right.$$

and without information about the properties of the imaginary spectrum it is impossible to determine the process uniquely.

Analogous miscalculations also are possible in the use of only imaginary spectra.

Therefore the engineering method of application of Fourier transforms requires separation of the damping part of the process from the neutral and divergent parts.

If we turn to the conditions of expansion of the total process (3-51a), the damping terms are called a regular part of the process, and the remaining terms, an irregular part.

The regular part of the process uniquely passes through the direct (4-56a) and any of the inverse (4-70a) or (4-70b) Fourier transforms. It is most convenient to subject a separate irregular part to a Laplace transformation.

For example, let us consider the conditions of passage of a regularly varying controlling signal $f(t) \Leftarrow - 1/p^2$ through a component with the QFT

$$W(p) = \frac{b_2 p^2 + b_1 p + b_0}{a_3 p^3 + a_2 p^2 + a_1 p a_0}.$$

In the general Laplace transform of the output process

$$X_{out}(p) = \frac{b_2 p^2 + b_1 p + b_0}{p^2 (a_3 p^3 + a_2 p^2 + a_1 p + a_0)} \qquad (*)$$

the irregular part (forced motion) is separated according to formula (3-39b):

$$X_{out}(p) = \frac{W(0)}{p^2} + \frac{W'(0)}{p} + X_c(p).$$

where

$$W(0) = \frac{b_0}{a_0};$$

$$W'(0) = \frac{a_0 b_1 - b_0 a_1}{a_0^2}.$$

The regular part, in the given case -- the representation of the proper motion -- is found as the remainder of expression (*) after separation of the irregular part:

$$X_c(p) = \frac{b_2 p^2 + b_1 p + b_0}{p^2 (a_3 p^3 + a_2 p^2 + a_1 p + a_0)} -$$

$$- \frac{b_0}{a_0 p^2} - \frac{a_0 b_1 - b_0 a_1}{a_0^2 p} =$$

$$= \frac{a_1 (b_0 a_1 - a_0 b_1) p^2 + [a_2 (b_0 a_1 - a_0 b_1) - a_0 a_3 b_0] p}{a_0^2 (a_3 p^3 + a_2 p^2 + a_1 p + a_0)} +$$

$$+ \frac{a_1 (b_0 a_1 - a_0 b_1) - a_0 a_3 b_0 + a_0^2 b_2}{a_0^2 (a_3 p^3 + a_2 p^2 + a_1 p + a_0)}.$$

Let us determine the output process by the combined formula

$$x_{out}(t) = L^{-1}\{X_n(p)\} + \frac{2}{\pi} \int_0^\infty \operatorname{Re} X_c(j\omega) \cos \omega t\, d\omega \quad (4\text{-}7.3)$$

or

$$x_{ut}(t) = \frac{a_0 b_1 - b_0 a_1}{a_0^2}\, 1(t) + \frac{b_0}{a_0}\, t +$$

$$+ \frac{2}{\pi} \int_0^\infty P_1(\omega) \cos \omega t\, d\omega. \qquad (**)$$

In this example the irregular part was determined very simply, and in the regular part the real frequency characteristic can be

found by the nomograms and the integral in (**) is found by methods of numerical integration without the operation of finding the poles (*), which is very tedious.

In the examined example the first term of (**) does not have a real spectrum and the second has no imaginary, and the use of only one of formulas (4-70) would lead to error.

C. Limiting Theorems

The limiting theorems derived for the Laplace transforms in Section 3-9 are also preserved during transition to a complex spectrum of the regular and irregular processes, if the argument   tends toward 0 and toward ∞. If the graphs of the real and imaginary spectra are examined, and not the complex spectrum, the formulas acquire the form:

$$x[0+] = -\lim_{\omega \to \infty} \omega \operatorname{Im} X(j\omega); \qquad (4\text{-}74a)$$

$$\dot{x}[0+] = -\lim_{\omega \to \infty} \omega^2 \operatorname{Re} X(j\omega); \qquad (4\text{-}74b)$$

$$\ddot{x}[0+] = \lim_{\omega \to \infty} \{\omega^3 \operatorname{Im} X(j\omega) + \omega^2 x[0+]\}; \quad (4\text{-}74c)$$

$$\dddot{x}[0+] = \lim_{\omega \to \infty} \{\omega^4 \operatorname{Re} X(j\omega) + \omega^2 \dot{x}[0+]\}, \quad (4\text{-}74d)$$

that is, only the real terms participate on the right side, and the imaginary automatically are reduced to zero, since the result and the parameters of the process are always real.

A limiting theorem of type (3-53) for the regular process leads, according to determination (3-51a), to the zero result:

$$\lim_{\omega \to \infty} \omega \operatorname{Im} X(j\omega) = 0. \qquad (4\text{-}74e)$$

For the frequently encountered irregular process -- the transient function, the spectrum of which equals:

$$H(j\omega) = \frac{W(j\omega)}{j\omega},$$

the limiting formulas have the form:

$$h(0+) = P(\infty); \qquad\qquad (4\text{-}75a)$$

$$h(0+) = \lim_{\omega \to \infty} \{-\omega Q(\omega)\}; \qquad\qquad (4\text{-}75b)$$

$$\dot{h}(0+) = \lim_{\omega \to \infty} \{-\omega^2 P(\omega) + \omega^2 h(0+)\}; \qquad (4\text{-}75c)$$

$$\ddot{h}(0+) = \lim_{\omega \to \infty} \{\omega^3 Q(\omega) + \omega^3 \dot{h}(0+)\}; \qquad (4\text{-}75d)$$

$$h(\infty) = P(0). \qquad\qquad (4\text{-}75e)$$

4-8. Tabular Methods of Calculation of the Regular and Some Irregular Processes According to the Spectrum

A. The Application of Displaced Functions in the Region of the Spectra

In inverse Fourier transform formulas for the initial functions (4-70) we will simplify the designations to some extent:

$$\left. \begin{aligned} x(t) &= \frac{2}{\pi} \int_0^\infty r(\omega) \cos \omega t \, d\omega; \\ x(t) &= -\frac{2}{\pi} \int_0^\infty i(\omega) \sin \omega t \, d\omega, \end{aligned} \right\} \qquad (*)$$

where $r(\omega)$ is the real spectrum of the unknown process and $i(\omega)$ is the imaginary spectrum of the unknown process, representing a two-sided function of the frequency ω.

It is expedient to digress from the conclusion of formulas (4-70) and use only the final result for the calculation of the process; then the result of the calculations does not change if the spectra are considered the initial functions $r(\omega)$ and $i(\omega)$, and in a number of cases the designation of the displaced functions of the frequency $r(\omega - \omega_0)$ and $i(\omega - \omega_0)$ is required. These functions can be subjected to Laplace transformation:

(see next page)

325

$$R(p) = \int\limits_0^\infty r(\omega)\, e^{-p\omega}\, d\omega;$$

$$I(p) = \int\limits_0^\infty i(\omega)\, e^{-p\omega}\, d\omega.$$

(**)

It can readily be noted that transformations (4-70a) and (4-70b) can be regarded also as Laplace transforms of the spectra along the argument ω with subsequent substitution of $p = jt$ (which forms a bi-spectrum) and separation of the real part or coefficient in the imaginary part. In fact,

$$x(t) = \frac{2}{\pi}\, \mathrm{Re}\left\{\int\limits_0^\infty r(\omega)\, e^{-j\omega t}\, d\omega\right\} =$$

$$= \frac{2}{\pi}\, \mathrm{Re}\left\{R(p)_{p=jt}\right\} = \frac{2}{\pi}\, \mathrm{Re}\left\{R(jt)\right\};$$

(4-76a)

$$x(t) = \frac{2}{\pi}\, \mathrm{Im}\left\{\int\limits_0^\infty i(\omega)\, e^{-j\omega t}\, d\omega\right\} =$$

$$= \frac{2}{\pi}\, \mathrm{Im}\left\{I(p)_{p=jt}\right\} = \frac{2}{\pi}\, \mathrm{Im}\left\{I(jt)\right\}.$$

(4-76b)

And so, in order to calculate the time process, for example, according to the real spectrum, it is necessary:

To adopt the graph of the spectrum as the graph of the initial (displaced) function of the frequency;

To make a Laplace transformation of the initial function along the argument ω;

To substitute p for jt;

To separate the real part of the transform; the latter after multiplication by $\frac{2}{\pi} = 0.637$ also will represent the unknown time process.

Let us apply the obtained rule to the simplest real spectra represented in Figures 4-27 and 4-28.
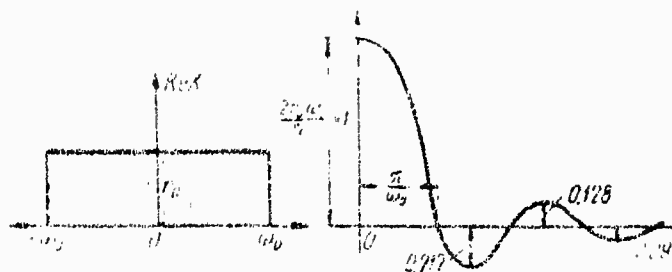
Fig 4-27. A rectangular spectrum and the process corresponding to it.
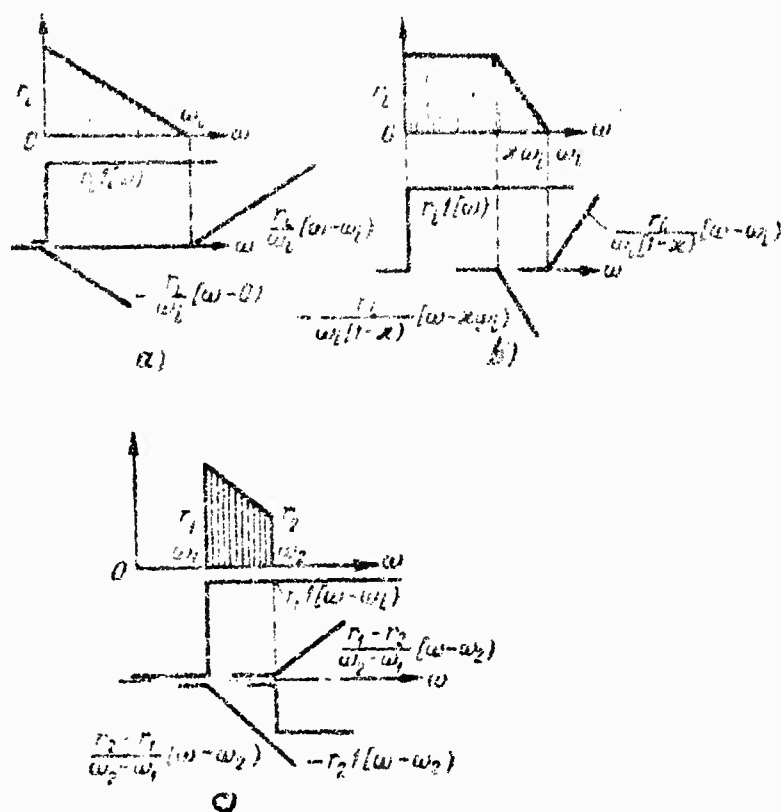
Fig 4-28. Displaced functions in the region of the spectra.

1. A limited rectangular spectrum.

We will consider only the positive frequencies in the symmetric two-sided picture of the spectrum in Figure 4-27 with the band $-\omega_0$ to $+\omega_0$.

Then the spectrum is written in designations of the displaced functions as

$$r(\omega) = r_0 \left\{ 1(\omega) - 1(\omega - \omega_0) \right\}.$$

Its Laplace transform is

$$R(p) = \frac{r_0}{p}(1 - e^{-p\omega_0}).$$

The transform with the imaginary argument $p = jt$ is

$$R(jt) = \frac{r_0}{jt}(1 - \cos\omega_0 t + j\sin\omega_0 t).$$

Its real part is

$$\mathrm{Re}\left\{R(jt)\right\} = \frac{r_0 \sin\omega_0 t}{t}.$$

The process corresponding to the rectangular spectrum is

$$x_0(t) = \frac{2r_0\omega_0}{\pi} \cdot \frac{\sin\omega_0 t}{\omega_0 t}. \tag{4-77}$$

The latter transformation (multiplication and division by ω_0) is performed to obtain the tabular function $\sin\nu/\nu$.

A graph of the obtained time function is represented in the same figure on the right. The period of the sine curve is $2\pi/\omega_0$, the damping occurs inversely proportionally to the first power t, and the values of the first three adjacent amplitudes in fractions of the initial value $2r_0\omega_0/\pi$ are shown on the graph. The initial value of the process turns out to be proportional to the area of the spectrum $r_0\omega_0$.

If the frequency band is increased, for example, is doubled $(\omega_1 = 2\omega_0)$, then firstly, the initial value $4r_0\omega_0/\pi$ increases by two times and, secondly, the period of oscillations decreases to half, that is, the time scale is as it were decreased. Thus the speed of the passing of the time process is proportional to the width of the band of the frequency spectrum (in the given case, the real). This

property, which has been proved for the partial form of the spectrum, generally speaking is also valid for other spectra and agrees with formula (3-5b) for change in the scale of the argument.

As an important property of the obtained process, let us determine the connection between its area and the parameters of the spectrum.

The area of the process is

$$\int_0^\infty \frac{2r_0\omega_0}{\pi} \cdot \frac{\sin\omega_0 t}{\omega_0 t} \, dt = \frac{2r_0}{\pi} \cdot \text{Si}(\omega_0 t)\Big|_0^\infty = r_0,$$

since the integral sine $\text{Si}(\vee)$ has the following limiting values:

$$\text{Si}(0) = 0; \qquad \text{Si}(\infty) = \frac{\pi}{2}.$$

The result is evidence that the area of the process does not depend on the band of the spectrum, that is, during change of ω_0 the area remains constant.

Let us now direct ω_0 toward infinity; then the initial ordinate of the process rises to infinity, and the entire process is contracted close to $t = 0$, having been converted into an impulse. At an amplitude of the spectrum equal to unity, that is at $r_0 = 1$, the area of the process likewise is equal to unity. An infinitely large amplitude, an infinitely small duration and a unit area of the process are characteristics of a unit impulse. Thus an infinite real spectrum of unit height actual gives the original impulse during its "conversion".

2.   A triangle adjacent to the axis of the ordinates.

In the designations adopted for displaced functions, according to Figure 4-23a:

$$r(\omega) = r_i \left\{ 1(\omega) - \frac{(\omega - 0)}{\omega_i} + \frac{(\omega - \omega_i)}{\omega_i} \right\}.$$

The Laplace transform of the spectrum $r(\omega)$ is

$$R(p) = r_i \left\{ \frac{1}{p} - \frac{1}{\omega_i p^2}(1 - e^{-\omega_i p}) \right\}.$$

The transform with the imaginary argument $p = jt$ (dispectrum) is

$$R(jt) = r_i \left\{ \frac{1}{jt} + \frac{1}{\omega_i t^2} (1 - \cos \omega_i t + j \sin \omega_i t) \right\}.$$

Its real part is

$$\text{Re}\left\{R(jt)\right\} = r_i \frac{1 - \cos \omega_i t}{\omega_i t^2} = 2r_i \frac{\sin^2 \dfrac{\omega_i t}{2}}{\omega_i t^2}.$$

The process corresponding to the triangular spectrum is

$$x_3(t) = \frac{r_i \omega_i}{\pi} \left(\frac{\sin \dfrac{\omega_i t}{2}}{\dfrac{\omega_i t}{2}} \right)^2. \qquad (4.78)$$

3. A trapezo' adjacent to the axis of the ordinates (Figure 4-28b) is

$$r(\omega) = r_i \left\{ 1(\omega) + \frac{(\omega - \omega_i) - (\omega - x\omega_i)}{\omega_i (1 - x)} \right\}.$$

The transform is

$$R(p) = r_i \left\{ \frac{1}{p} + \frac{1}{\omega_i (1 - x) p^2} (e^{-\omega_i p} - e^{-x\omega_i p}) \right\}.$$

The real part of the transform with the imaginary argument is

$$\text{Re}\left\{R(jt)\right\} = \frac{r_i}{\omega_i (1 - x) t^2} (\cos x \omega_i t - \cos \omega_i t) =$$

$$= \frac{2r_i}{\omega_i (1 - x) t^2} \sin \frac{\omega_i t}{2} (1 + x) \sin \frac{\omega_i t}{2} (1 - x).$$

The process is

$$x_4(t) = \frac{r_i \omega_i (1 + x)}{\pi} \frac{\sin \dfrac{\omega_i (1 + x) t}{2}}{\dfrac{\omega_i (1 + x) t}{2}} \times$$

$$\times \frac{\sin \dfrac{\omega_j(1-x)t}{2}}{\dfrac{\omega_j(1-x)t}{2}} \qquad (4.79)$$

4. A strip not adjacent to the axis of the ordinates (Figure 4-28c). Analogously to the preceding:

$$
\begin{aligned}
r(\omega) &= r_1 \cdot 1(\omega - \omega_1) - r_2 \cdot 1(\omega - \omega_2) + \\
&\quad + \frac{r_1 - r_2}{\omega_2 - \omega_1}\{(\omega - \omega_2) - (\omega - \omega_1)\}; \\[4pt]
R(p) &= \frac{1}{p}\left(r_1 e^{-\omega_1 p} - r_2 e^{-\omega_2 p}\right) + \\
&\quad + \frac{r_1 - r_2}{(\omega_2 - \omega_1)p^2}\left(e^{-\omega_2 p} - e^{-\omega_1 p}\right); \\[4pt]
\operatorname{Re}\{R(jt)\} &= \frac{1}{t}\left(r_2 \sin \omega_2 t - r_1 \sin \omega_1 t\right) + \\
&\quad + \frac{r_1 - r_2}{(\omega_2 - \omega_1)t^2}(\cos \omega_1 t - \cos \omega_2 t); \\[4pt]
x_{out}(t) &= \frac{1}{\pi}\left\{ \frac{r_2}{t}\sin \frac{\omega_2 - \omega_1}{2}t \times \right. \\
&\quad \times \cos \frac{\omega_2 + \omega_1}{2}t - \frac{r_1 - r_2}{2t}\sin \omega_1 t + \\
&\quad \left. + \frac{r_1 - r_2}{(\omega_2 - \omega_1)t^2}\sin \frac{\omega_1 + \omega_2}{2}t \sin \frac{\omega_2 - \omega_1}{2}t \right\}.
\end{aligned}
\qquad (4.80)
$$

Any complex spectrum can, in separate sections, be replaced by segments of straight lines, after which it can be represented in the form of the sum of the elementary spectra (Figure 4-28 a, b and c). The methodical accuracy of calculations of the processes according to triangular, trapezoidal or band partial spectra is identical and is determined by the degree of approximation of the linear segments to the initial graph of the spectrum.

B. Time Processes Corresponding to "Mosaic" Spectra

A certain continuous real spectrum Re(ω) is given in Figure 4-29a. To determine the corresponding spectrum of the time process it is necessary to go over to elementary figures of the spectrum, for

which it is necessary first of all to approximate the curvilinear spectrum by segments of straight lines in the separate sections, whereupon the extremal sections are best limited to horizontal segments (see graph a).
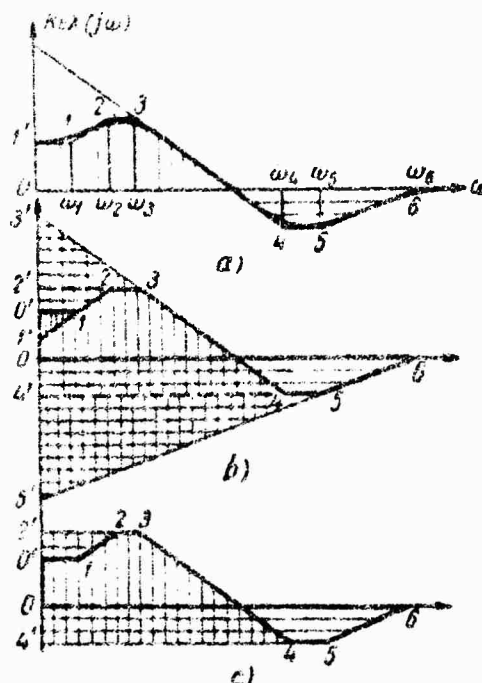
Fig 4-29. Mosaic spectra.

For the band spectrum (Figure 4-28c) inverse transformation formula (4-60) was obtained; if we apply it for each of the obtained bands and sum the partial processes, we can readily obtain the total process:

$$x(t) = \sum_{i=1}^{n} x_{i_n}(t)$$

Formula (4-78) is used for triangular partial spectra (Figure 4-28a). In order to obtain the elementary triangular spectra it is necessary to extend all the segments of the polygonal line to intersection with the axis of the ordinates, as in Figure 4-29b, where the points of intersection are marked with the same numbers (with primes) as the corresponding points of breaks on the polygonal line. The following triangles were obtained as a result of this construction:
4' - 3' - 4; 1' - 2' - 2; 5' - 0 - 6; 1' - 0' - 1; 5' - 4' - 5.

The frequency bands for each triangle are extended from zero to the corresponding frequency of the break, and the initial values of the heights of the triangles are determined by the following segments: +(4' - 3'), -(1' - 2'), -(0 - 5'), +(4' - 5') and +(0' - 1').

The hatching made on Figure 4-29 reflects the signs of the heights. The hatchings different in sign cancel a corresponding area. In the triangle 1' - 0' - 1 an uneven number of hatchings are laid, three in the given case; the sign of this area is determined by the excess hatching (+). In the graphic separation of the given continuous spectrum into elementary constituents during observance of the rule of hatching a picture is obtained which recalls a mosaic, and therefore such spectra will be called mosaic. The six partial spectra obtained, which enter the mosaic, correspond to six partial processes (4-78), the sum of which gives the unknown process:

$$ x(t) = \sum_{i=1}^{n} x_{ia}(t) = \frac{1}{\pi} \sum_{i=1}^{n} r_i \omega_i \left(\frac{\sin \frac{\omega_i t}{2}}{\frac{\omega_i t}{2}} \right)^2. $$

The functions of $(\text{sine } \surd/\surd)^2$ are given in the next to last column of Table 4-5.

To obtain a trapezoidal mosaic it is necessary to enxtend to intersection with the axis of ordinates only the horizontal segments of the polygonal line, as in Figure 4-29c. This construction forms three trapezoids: 4' - 2' - 3 - 4, 0' - 2' - 2 - 1 and 4' - 0 - 6 - 5, with the heights +(4' - 2'), -(0' - 2') and -(0 - 4'), the frequency bands $\omega_1 = \omega_4$, $\omega_{II} = \omega_2$ and $\omega_{III} = \omega_6$ and the parameters

$$ x_1 = \frac{\omega_3}{\omega_4}; \quad x_{11} = \frac{\omega_1}{\omega_2}; \quad x_{111} = \frac{\omega_5}{\omega_6}, $$

which enter (4-79). Upon use of the indicated formula, three partial time processes are obtained which give the total process

$$ x(t) = \sum_{i=1}^{n/2} x_{ib}(t). $$

The functions of sine γ/γ entering $x_{ib}(t)$ in the form of the product are given in Table 4-5.

It can readily be noted that in the use of the band partial processes according to formulas (4-80) the terms entering that formula of the type of sine $\omega_i t/\omega_i t$ for adjacent bands and for horizontal sections cancel one another and in fact the calculations will

be made by the formulas for the trapezoidal mosaic. Thus the calculations according to Figure 4-29, a and c, will be identical if the cancellation is performed in the partial processes.

The calculations according to the diagram of Figure 4-29b give twice as large a number of terms as calculations according to the examined diagram c, but when the table of functions of sine v/v is used the number of selections from the table is kept the same in all cases, and this also determines the approximately identical difficulty of all the methods examined.

The accuracy of these three methods also is identical, since the basic error is determined by the nearness of the polygonal line on graph a to the smooth curve of the spectrum.

If we use the designation Re $X(j\bar{\omega})$ for the piecewise linear graph of the spectrum, we can obtain from formula (4-70a) a formula for calculation of the error:

$$\Delta x (t) = \frac{2}{\pi} \int\limits_{0}^{\infty} [\mathrm{Re}\, X(j\bar{\omega}) - \mathrm{Re}\, X(j\omega)] \cos \omega t \, d\omega.$$

At a constant factor cos $\omega t = 1(t \to 0)$ it is sufficient to provide equality of the excess and deficiency of the areas of the smooth Re $X(j\omega)$ and piecewise linear Re $X(j\bar{\omega})$ graphs.

To increase the accuracy of the calculation close to any given point t_i it is necessary to mutually cancel the sections of the areas weighted proportionally to cos ωt_i. Subsequent calculations of the additional principal errors are not introduced.

It must be noted that although the partial processes obtainable from the mosaic spectra also approach in sum the real process, in particular they do not reflect any real properties of the processes in linear systems with constant coefficients. The actual partial processes can be obtained only on the base of an inverse Laplace transform (on the basis of the theorem of expansion) considered in Chapter 3 and giving typical functions shown in Tables 3-1 and 3-7. The function (sine $\omega_i t/\omega_i t)^2$, given in the next to last column of Table 4-5, is peculiar to linear systems with variable coefficients. But this circumstance does not interfere with obtaining excellent approximation to the processes proceeding in systems with constant coefficients, in the form of the sum of such partial processes.

C. The Use of Tables of Special Functions for the Construction of Time Processes

Tables of $h_x(t)$ functions are used for calculation of processes

333

by spectra along with tables of the functions $(\sin \nu' / \nu)^2$ and $\text{Si } \nu$.

The tables of $h_x(t)$ functions and the method of applying them have been worked out by Professor V V Solodovnikov mainly for determination of transient functions of control systems according to their real frequency characteristics. See very similar tables in [2].

If the transfer function of an automatic control system is $W(p)$, the representation of its transient function is

$$H(p) = \frac{1}{p} W(p).$$

The spectrum of the output process in the given case can be expressed by the real and imaginary frequency characteristics of the automatic control system:

$$H(j\omega) = \frac{1}{\omega} Q(\omega) - j \frac{P(\omega)}{\omega}. \qquad (4\text{-}81)$$

If we use the real characteristic of the automatic control system to obtain the transient function, it is necessary to turn to formula (4-70b), which gives:

$$h(t) = \frac{2}{\pi} \int_0^\infty P(\omega) \frac{\sin \omega t}{\omega} d\omega. \qquad (4\text{-}82)$$

The practical application of this formula is based on the examination of the simplest partial characteristics and their subsequent superposition.

As before, we will consider the rectangular, triangular and trapezoidal real characteristics depicted in Figure 4-30 as the simplest.

It must be recalled that in this figure there are represented, not the real spectra of the processes, but the real characteristics of the automatic control system, which, to obtain the imaginary spectrum of the transient function, must be symmetrically extended in the region of negative frequencies and divided by ω.

The rectangular real characteristic of height p_1 and width ω_1, represented on the left in Figure 4-30a, gives the imaginary spectrum of the transient function $\text{Im } H(j\omega) = p_1 / \omega$.

The process shown in Figure 4-30 a on the right can be determined by the characteristic according to formula (4-82):

Table 4-5. R-Functions and Special Functions

	0.5	0.05	0.10	0.15	0.20	0.25	0.30	0.35	0.40	0.45	0.51	0.75
0.0	0.000	0.000	0.000	0.000	0.000	0.000	0.000	0.000	0.000	0.000	0.000	0.000
0.5	0.138	0.165	0.176	0.184	0.192	0.199	0.207	0.215	0.223	0.231	0.240	0.248
1.0	0.316	0.326	0.349	0.356	0.371	0.386	0.401	0.417	0.432	0.417	0.461	0.476
1.5	0.449	0.469	0.494	0.516	0.538	0.560	0.593	0.603	0.617	0.646	0.665	0.685
2.0	0.572	0.597	0.628	0.656	0.683	0.709	0.681	0.761	0.786	0.810	0.833	0.856
2.5	0.674	0.707	0.739	0.771	0.802	0.833	0.862	0.891	0.917	0.943	0.967	0.985
3.0	0.755	0.790	0.828	0.863	0.856	0.928	0.958	0.986	1.013	1.038	1.061	1.082
3.5	0.783	0.853	0.892	0.928	0.963	0.994	1.024	1.050	1.074	1.095	1.115	1.132
4.0	0.857	0.856	0.938	0.974	1.008	1.039	1.060	1.090	1.107	1.124	1.142	1.122
4.5	0.883	0.923	0.960	0.997	1.029	1.057	1.080	1.100	1.115	1.129	1.138	1.134
5.0	0.886	0.936	0.978	1.012	1.042	1.067	1.087	1.103	1.112	1.117	1.118	1.115
5.5	0.900	0.940	0.986	1.019	1.046	1.067	1.083	1.093	1.095	1.097	1.092	1.083
6.0	0.904	0.942	0.982	1.013	1.037	1.054	1.065	1.070	1.068	1.062	1.051	1.037
6.5	0.904	0.943	0.980	1.009	1.030	1.043	1.050	1.049	1.043	1.033	1.018	1.001
7.0	0.904	0.944	0.979	1.006	1.024	1.035	1.037	1.033	1.023	1.000	0.993	0.975
7.5	0.907	0.945	0.980	1.006	1.019	1.025	1.025	1.017	1.005	0.989	0.974	0.958
8.0	0.916	0.951	0.985	1.008	1.026	1.024	1.021	1.012	0.995	0.981	0.966	0.951
8.5	0.918	0.956	0.988	1.010	1.021	1.022	1.018	1.007	0.992	0.977	0.966	0.949
9.0	0.924	0.965	0.997	1.016	1.025	1.025	1.018	1.006	0.992	0.978	0.970	0.960
9.5	0.932	0.972	1.004	1.022	1.029	1.027	1.019	1.006	0.993	0.982	0.975	0.972
10.0	0.939	0.976	1.009	1.025	1.031	1.027	1.019	1.006	0.993	0.987	0.982	0.985
10.5	0.944	0.985	1.013	1.028	1.033	1.028	1.017	1.005	0.993	0.991	0.987	0.996
11.0	0.947	0.986	1.015	1.029	1.031	1.025	1.014	1.002	0.993	0.991	0.993	1.002
11.5	0.949	0.988	1.016	1.027	1.028	1.021	1.010	0.999	0.991	0.989	0.997	1.006
12.0	0.950	0.988	1.015	1.025	1.024	1.015	1.004	0.994	0.988	0.987	0.997	1.006

12.5	0.950	0.989			0.999	1.010	0.999	0.990	0.986	0.986
13.0	0.950	0.983			0.994	1.005	0.986	0.985	0.987	0.996
13.5	0.950	0.990			0.990	1.000	0.993	0.984	0.986	0.996
14.0	0.952	0.989			0.988	0.997	0.983	0.985	0.994	1.006
14.5	0.954	0.990			0.987	0.996	0.985	0.988	0.996	1.006
15.0	0.956	0.983			0.988	0.995	0.987	0.991	1.000	1.007
15.5	0.959	0.995			0.989	0.995	0.988	0.996	1.004	1.007
16.0	0.961	0.997			0.991	0.995	0.992	0.998	1.007	1.008
16.5	0.964	0.999			0.993	0.995	0.995	1.002	1.009	1.008
17.0	0.965	1.001			0.994	0.995	0.997	1.005	1.010	1.005
17.5	0.966	1.002			0.994	0.995	0.998	1.006	1.010	1.005
18.0	0.966	1.002			0.995	0.995	0.991	1.008	1.010	1.002
18.5	0.966	1.001			0.995	0.994	0.981	1.007	1.009	0.999
19.0	0.967	1.000			0.995	0.992	1.001	1.006	1.006	0.995
19.5	0.967	1.002			0.995	0.991	1.001	1.005	1.004	0.992
20.0	0.967	1.000			0.995	0.991	1.001	1.004	1.002	0.991
20.5	0.968	1.002			0.996	0.991	1.002	1.003	1.001	0.991
21.0	0.969	1.002			0.997	0.992	1.003	1.004	1.001	0.993
21.5	0.970	1.002			0.995	0.992	1.004	1.004	0.997	0.995
22.0	0.971	1.002			1.000	0.993	1.005	1.005	0.997	0.994
22.5	0.973	1.002			1.002	0.995	1.006	1.004	0.995	1.000
23.0	0.974	1.005			1.004	0.996	1.007	1.003	0.996	1.001
23.5	0.975	1.005			1.004	0.998	1.008	1.003	0.996	1.002
24.0	0.975	1.005			1.005	0.999	1.007	1.002	0.997	1.002
24.5	0.975	1.005			1.005	1.000	1.006	1.001	0.997	1.002
25.0	0.975	1.005			1.005	—	1.000	1.000	0.996	1.002
25.5	0.975	1.005			1.004		0.998	0.998	0.996	1.002
26.0	0.000	1.000			1.004		0.997	0.997	0.996	1.002

337

Fig 4-30. Typical real characteristic and transient functions corresponding to them.

$$h(t) = \frac{2p_i}{\pi} \int_0^{\omega_i} \frac{\sin \omega t}{\omega} \, d\omega = \frac{2p_i}{\pi} \, \mathrm{Si} \, \omega_i \, t. \qquad (4\text{-}83)$$

The values of the integral signal Si ν for the argument $\nu = \omega_i t$ are given in the last column of Table 4-5.

The triangular real characteristic shown in Figure 4-30 b on the left forms the imaginary spectrum

$$\mathrm{Im} \, H \, (j\omega) = - p_i \left(\frac{1}{\omega} - \frac{1}{\omega_i} \right).$$

and when integrated according to formula (4-82) gives the process shown in Figure 4-30b on the right:

$$k_0[t] = \frac{2p_i}{\pi}\left[\mathrm{Si}\,\omega_i\,t + \frac{\cos\omega_i\,t - 1}{\omega_i\,t}\right]. \qquad (4\text{-}84)$$

Every function entering the obtained formula has been tabulated, but to accelerate the calculations A A Voronov [3] has proposed a completed table of $h_0^*(\nu)$ functions (see the second column of Table 4-5 of h_x functions). The table has the input argument $\nu = \omega_i\,t$ and was composed for the value $p_i = 1$. To go from the tabulated values of the $h_0^*(\nu)$ functions to the actual values of the partial process it is necessary to divide the argument ν by the value ω_i, and multiply the tabulated values of h_0^* functions by the height of the triangle:

$$t = \frac{\nu}{\omega_i};$$

$$h_{0i}[t] = p_i\,h_0^{\bullet}[t\omega_i].$$

For calculation of the transient function according to the given real frequency characteristic of the automatic control system, first of all a triangular mosaic real frequency characteristic was obtained, analogous to the mosaic spectrum given in Figure 4-29b, and then the tabular h_0^* function was transformed for each tringle by compressing the argument and increasing the ordinates, and all the partial functions were summed:

$$h[t] = \sum_{i=1}^{n} p_i\,h_0^{\bullet}[\omega_i\,t]. \qquad (4\text{-}85)$$

The trapezoidal real characteristic shown on the left in Figure 4-30a is preferably used for calculation of the transient function.

Let us express the frequency of the break of the trapezoid analogously to (4-79) across the band of the entire spectrum ω_i and coefficient χ, less than unity:

$$\omega_{0i} = \chi\omega_i.$$

Then the trapezoid can be divided into two triangles with the following parameters:

$$p_1 = \frac{p_i}{1-\chi}; \quad \omega_1 = \omega_i;$$

$$p_2 = -\frac{p_i\,\chi}{1-\chi}; \quad \omega_{11} = \chi\omega_i$$

Addition of the partial processes (4-84), after transformations, gives:

$$h_v^*(v) \quad h_x^*(\omega_i t) \cdots \frac{2p_i}{v} \left\{ \text{Si } xv + \left| \frac{1}{x} \right| \text{Si } v - \text{Si } xv + \right.$$
$$\left. + \frac{\cos v - \cos xv}{v} \right\} \Big| \Big\} . \tag{4-86}$$

This formula is used at $p_i = 1$ for the construction of the table of h^* functions (the left part of Table 4-5). The table has two inputs: x and $v = \omega_i t$; the h^* function for the triangular real characteristic is a particular case of the h_x^* function at $x = 0$.

In calculating the transient function by the method of V V Solodovnikov, the trapezoidal mosaic characteristic, analogous to the mosaic spectrum given in Figure 4-29, must primarily be constructed according to the given real characteristic of the automatic control system.

Then it is necessary to find, for each trapezoidal characteristic, the ratio of the frequency of the break to the band x_i and enter the part of the h_x^* functions table corresponding to x_i.

In the obtained tabular values it is necessary to compress the argument by taking the new values $t = v/\omega_i$ instead of the tabular argument and the increased value

$$h_i(t) = p_i h_x^*(\omega_i t).$$

instead of the tabular h_x^* function.

A summation of the partial processes is made according to (4-85).

The tables of h_x^* functions can be used for the construction not only of the transient functions of an automatic control system, but of any other time characteristics. For this the so-called reduced frequency characteristic is determined.

We call a reduced frequency characteristic the frequency characteristic of such a fictitious system in which, upon delivery of a unit function on the input, the output process being investigated is excited on the output. Obtaining the reduced (to a given process) frequency characteristic is illustrated in Figure 4-31. If the given process has the representation $X_{out}(p)$, the reduced frequency characteristic of the fictitious system must be

$$\Phi_x(j\omega) = j\omega X_{out}(j\omega). \qquad (4\text{-}87)$$

Actually, in accordance with Figure 4-31, the representation of the input unit step, multiplied by the reduced transfer function, gives the representation of the output process being investigated:

$$X_{out}(p) = \frac{1}{p}\,\Phi_x(p) = \frac{1}{p}\,[p X_{out}(p)].$$

The reduced amplitude-phase characteristic can be expanded into real and imaginary constituents:

$$\Phi_x(j\omega) = P_x(\omega) + j Q_x(\omega) = -\omega\,\text{Im}\,X(j\omega) + j\omega\,\text{Re}\,X(j\omega).$$
$$(4\text{-}88)$$

$$\frac{1}{p} \longrightarrow \boxed{\Phi_x(p) = p X_{out}(p)} \longrightarrow X_{out}(p)$$
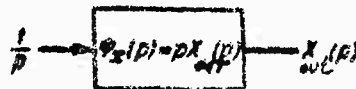
Fig 4-31. For determination of the reduced transfer function.

According to these characteristics, for example, according to the real reduced frequency characteristic, the process being investigated can be constructed. As an example of determination of the time process according to a characteristic reduced to it, let us consider the obtaining of a weight function.

The weight function of a system $\omega(t)$ is determined directly by the spectrum of the transfer function $W(j\omega)$ by the table (sine v/v)^2 but when it is desired to use the table of h_x functions it is necessary according to the representation of the unknown process $W(p)$ to obtain the reduced frequency characteristic by formula (4-87):

$$\Phi_w(j\omega) = j\omega\,W(j\omega) = -\omega Q(\omega) + j\omega P(\omega)$$

and according to the reduced real characteristic $-\omega Q(\omega)$ to seek the transient function of a fictitious system which will be the weight function of the system $\omega(t)$ being investigated.

Thus, as shown above, the initial process can be represented in one of the form:

In a piece-wise-linear approximation of its real spectrum -- in the form of the sum of the partial processes containing the tabular functions of type (sine $v/v)^2$.

In a piecewise-linear approximation of the frequency real characteristic of the system, for which the investigated process is a transient function, in the form of the sum of the partial processes containing tabular h_x/t) functions.

Table 4-6   Typical transformations of the spectra and frequency characteristics in calculation of a process by tables of special functions

Определяемый процесс (1)	Преобразованные спектры или частотные характеристики для расчета процесса (2)	
	при использовании таблиц $\left(\dfrac{\sin v}{v}\right)^2$ (3)	при использовании таблиц h_x (4)
$x(t)$	$\operatorname{Re} X(j\omega)$	$-\omega \operatorname{Im} X(j\omega)$
$h(t)$	$-\dfrac{Q(\omega)}{\omega}$	$P(\omega)$
$w(t)$	$P(\omega)$	$-\omega Q(\omega)$

1 - Process being determined; 2 - Transformed spectra or frequency characteristics for calculation of the process; 3 - During use of (sine $v/v)^2$ tables; 4 - During use of h_x $|v|$ tables.

A summary of the necessary transformations of the spectra or frequency characteristics for the use of these or other tables is given in Table 4-6.

In calculating the processes with use of the method of reduced frequency characteristics it is necessary to convince oneself beforehand whether the process being investigated is regular or contains a constant constituent, in order to use the (sine $v/v)^2$ table in the first case or the h-function table in the second case.

D. Determination of Separate Points of a Transient Function

In practice, along with the investigation of the entire process, it often presents special interest to determine the separate points of the process at given most corresponding moments of time. Among such moments are:

Moments of change of the operating regime of the automatic control system when, before examining the process in a new regime, it is desirable to determine how the preceding process was completed;

Moments of attainment by an automatic control system of extremal points, etc.

For the fixed moment of time $t_1 = \vartheta$, formula (4-82) does not change its form:

$$h(\vartheta) = \frac{2}{\pi} \int_0^\infty P(\omega) \frac{\sin \omega \vartheta}{\omega} d\omega \qquad (*)$$

and its calculation can be done by methods of numerical integration, by taking for the separate intervals $\Delta\omega$ the function $P(\omega)$ by the average value beyond the sign of the integral.

If the interval of the frequencies is included in the limits of ω_i and $\omega_i + \Delta\omega$, the mean value of the real characteristic for that interval equals $P_{ei} = \bar{P}_i$, and the function that has remained under the integral after integration gives the increment of the integral sine:

$$\int_{\omega_i}^{\omega_i + \Delta\omega} \frac{\sin \omega \vartheta}{\omega} d\omega = \Delta_i \operatorname{Si} \omega \vartheta.$$

After this, formula (*) can be replaced by the sum:

$$h(\vartheta) = \frac{2}{\pi} \Sigma \bar{P}_i \Delta_i \operatorname{Si} \omega \vartheta. \qquad (**)$$

The values of the permissible intervals are determined by the period of the function sine $\omega\vartheta/\omega$ and the character of the function $P(\omega)$. The function sine $\omega\vartheta/\omega$ passes through zero at the argument $\omega_\pi \vartheta = \pi$ or at the frequency

$$\omega_x = \nu = \frac{\pi}{\vartheta} \qquad (***)$$

and further at frequencies $k\nu$. We will call ν the half-period of

the function $\sin \omega \nu/\omega$ in the scale of frequencies at fixed $t_1 = \mathcal{F}$.

Let us examine the first case, where the half-period is considerably less than the value of the frequency ω_0, at which the real characteristic passes through zero $/P(\omega_0) = 0/$, and within the limits of the half-period ν the real characteristic varies relatively little and it is possible to assume that $P_{mi} = P(\omega_m)$. These conditions we will call the "case of large t_1 values"; they are illustrated in Figure 4-32 by graph a. Here the entire half-period can be understood as the interval $\Delta\omega$. The increments in the function $\Delta_1 S_1 \omega \mathcal{F}$ during the half-period are given in the rows bearing an asterisk in Table 4-7. If we use their values, formula (**) can be presented in the expanded form:

$$h\,(\theta) = 1.18 P\,(0.5\nu_a) - 0.277 P\,(1.5\nu_a) + 0.163 P\,(2.5\nu_a) -$$
$$- 0.116 P\,(3.5\nu_a) + 0.09 P\,(4.5\nu_a) - 0.074 P\,(5.5\nu_a) +$$
$$+ 0.062 P\,(6.5\nu_a) - 0.054 P\,(7.5\nu_a) + \ldots \qquad (4\text{-}89a)$$

The summation is continued to the output on the declining section of the frequency characteristic, after which the terms of the series begin to decrease especially rapidly. The error from the discarded terms in the alternating series is less than the last discarded term.

Let us examine the second case, where the half-period ν_b and the band of the real characteristic ω_b are close to each other, and call it the "case of small $\mathcal{F}$ values." In Figure 4-32, for the characteristic b it is assumed that $\nu_b = \omega_b$.

The time, determinable by the band of the real characteristic when the axis of frequencies intersects it sharply, turns out to be very close to the time of attainment of the maximum of the transient characteristic t_M, that is

$$t_M \approx \frac{\pi}{\omega_b}.$$

In the relationship between the integrands in formula (4-89a) that are being examined, it is necessary to substitute not the value $P(\omega_m)$ in the center of the half-period ν, but the weighted-mean value of P_i^{m} for the half-period. For this, in Table 4-7, the first two half-periods have been divided by 10 and 5 (depending on the desired accuracy) intervals and the increments of the function $\frac{2}{\pi} Si\,\nu$ have been written in these intervals: the absolute (columns 2 and 4) and the relative in percentages (columns 3 and 5) of the total increment for the first interval (1.18) and the second interval (0.277).

If we use the coefficients given in Table 4-7 for the first half-period, it is possible to write the formula for determination of the

weighted-mean value $\bar{P}_1$ based on five measurements:

$$\bar{P}_1 = 0.331 P(0.1\nu) + 0.290 P(0.3\nu) + 0.215 P(0.5\nu) +$$
$$+ 0.125 P(0.7\nu) + 0.038 P(0.9\nu). \qquad (4\text{-}89b)$$

The weighted-mean value $\bar{P}_2$ for the second interval is determined analogously according to the corresponding tabulated coefficients. These values are substituted in formula (4-89a) in its first two terms. For succeeding half-periods, if we take into consideration the rapid damping of the real characteristics that is usually observed, we can retain the approximate expressions for the increments, determinable by the additional terms of formula (4-89a).

Upon substitution of the weighted-mean value for the first (4-89b) and for the second half-period in formula (4-89a), it is necessary to multiply the result by the coefficients 1.18 or 0.277 or calculate at once the recalculated weighted-mean values according to the absolute increments given in columns 2 and 4.
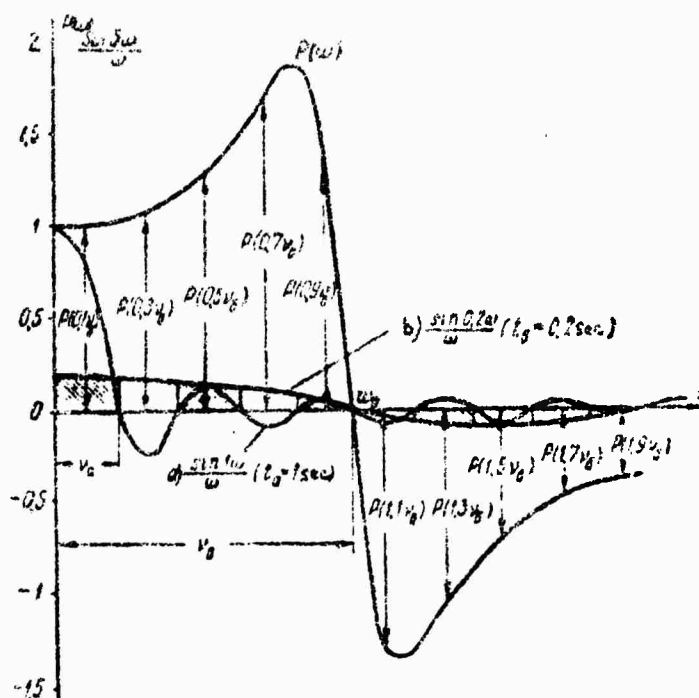
Fig 4-32.   Calculation of separate points of the process by
its real spectrum.

Table 4-7   Increments of the integral sine $\frac{2}{\pi} \Delta \mathrm{Si}\, \nu$

Band of frequencies in fractions of ν (1)	i=10		i=5		Sign (3)
	Number (2)	%	Number (2)	%	
0,0 – 0,1	0,198	16,8	0,390	33,1	+
0,1 – 0,2	0,192	16,3			
0,2 – 0,3	0,180	15,3	0,342	29,0	+
0,3 – 0,4	0,162	13,7			
0,4 – 0,5	0,140	11,8	0,255	21,5	+
0,5 – 0,6	0,115	9,7			
0,6 – 0,7	0,087	7,4	0,147	12,5	+
0,7 – 0,8	0,060	5,1			
0,8 – 0,9	0,034	2,9	0,045	3,8	+
0,9 – 1,0	0,011	0,9			
* 0,0 – 1,0	1,18	100	1,18	100	+
1,0 – 1,1	0,010	3,4	0,035	12,4	—
1,1 – 1,2	0,025	9,0			
1,2 – 1,3	0,036	12,9	0,078	28,1	—
1,3 – 1,4	0,042	15,2			
1,4 – 1,5	0,043	15,6	0,084	30,3	—
1,5 – 1,6	0,041	14,7			
1,6 – 1,7	0,034	12,4	0,059	21,6	—
1,7 – 1,8	0,025	9,2			
1,8 – 1,9	0,016	5,8	0,021	7,6	—
1,9 – 2,0	0,005	1,8			
* 1,0 – 2,0	0,277	100	0,277	100	—
* 2,0 – 3,0	0,163	100	0,163	100	+
* 3,0 – 4,0	0,116	100	0,116	100	—
* 4,0 – 5,0	0,090	100	0,090	100	+
5,0 – 6,0	0,074	100	0,074	100	—
* 6,0 – 7,0	0,062	100	0,062	100	+
7,0 – 8,0	0,054	100	0,054	100	—
* 8,0 – 9,0	0,048	100	0,048	100	+
* 9,0 – 10,0	0,043	100	0,043	100	—
* 10 – 11	0,039	100	0,039	100	+
* 11 – 12	0,035	100	0,035	100	—

1 - Band of frequencies in fractions of ν ; 2 - Number; 3 - Sign.

4-9. Method of Balance of the Spectra for Systems with Variable Parameters

A. The High Frequency Part of the Spectrum of the Output Process

The high frequency part of the spectrum (4-74) is determined by the initial section of the output process. The method of finding the initial values of a process when the variable coefficients are given in the form of a power polynomial was shown in Chapter 3. If the initial sections of the graphs of variable coefficients, independently of the further course of the graph, approximate the simplest functions -- straight lines or parabolas, then the initial values of the output process can be found. For what follows it is necessary to determine the values of only two first initial derivatives $x_{out}^{(l)}(0)$ and $x_{out}^{(l+1)}(0)$ not equal to zero, for which the above-indicated approximation of the coefficients always gives satisfactory accuracy. According to the calculated values of l and $l + 1$ of the derivatives a process of the following type is formed:

$$x_{init}(t) = x^{(l)}(0)\,\frac{|t|^{l}}{l!} + x^{(l+1)}(0)\,\frac{|t|^{l-1}}{(l+1)!} \qquad (4\text{-}90a)$$

and its spectrum is

$$X_{init}(j\omega) = -\frac{x^{(l)}(0)}{(j\omega)^{l+1}} + \frac{x^{(l+1)}(0)}{(j\omega)^{l+2}}. \qquad (4\text{-}90b)$$

In Table 4-8 the real and imaginary spectra of the process are given for various values of l.

If a sufficiently high frequency ω_γ is selected, then at that frequency the spectrum of the entire output process will be close to the spectrum of the initial process (4-90b).

B. Calculation of the Spectrum by the Frequency Bands

If we know the real and imaginary parts of the spectrum of the output process at a single point ω_γ, it is possible to plot them on the graph in Figure 4-33 of the real and imaginary constituents of the spectrum. In order to draw on the graphs not only a single point, but also some segment of the unknown spectrum, let us set a certain interval of frequencies $2\Delta\omega$, sufficiently narrow that it is possible to take into consideration change of the spectrum in that interval linearly.

The linearity of the change presupposes constancy of steepness of the graphs of the real and imaginary spectra. For convenience of calculation made from the region of high frequencies to the region of

l	$l+1$	Re $X_{init}(j\omega)$	Im $X_{init}(j\omega)$	$-S^R$	$-S^I$	$\dfrac{\omega_{v+1}}{\omega_v}$
1	2	3	4	5	6	7
0	1	$-\dfrac{\dot{x}(0)}{\omega^3}$	$-\dfrac{x(0)}{\omega}$	$\dfrac{2\dot{x}(0)}{\omega^2}$	$\dfrac{x(0)}{\omega^2}$	1.5
1	2	$-\dfrac{\dot{x}(0)}{\omega^2}$	$\dfrac{\ddot{x}(0)}{\omega^3}$	$\dfrac{2\dot{x}(0)}{\omega^3}$	$\dfrac{3\ddot{x}(0)}{\omega^4}$	1.5
2	3	$\dfrac{\ddot{x}(0)}{\omega^4}$	$\dfrac{\dddot{x}(0)}{\omega^3}$	$\dfrac{4\ddot{x}(0)}{\omega^5}$	$\dfrac{3\dddot{x}(0)}{\omega^4}$	1.25
3	4	$\dfrac{\dddot{x}(0)}{\omega^4}$	$-\dfrac{x^{(IV)}(0)}{\omega^5}$	$\dfrac{4\dddot{x}(0)}{\omega^5}$	$\dfrac{5x^{(IV)}(0)}{\omega^5}$	1.25

low frequencies, let us introduce the concept of steepness of the decline of the spectra, determinable as the derivatives with reversed sign:

$$S^R = -\frac{d\,\mathrm{Re}\,X_{out}(j\omega)}{d\omega}\,C_1 \qquad (4.91a)$$

$$S^I = -\frac{d\,\mathrm{Im}\,X_{out}(j\omega)}{d\omega}\,C_2 \qquad (4.91b)$$

$$S = S^R + jS^I \cdot \frac{-dX_{out}(j\omega)}{d\omega} = \bar{C} \qquad (4.91c)$$

The values of the real steepness S^R, the imaginary S^I and the complex $\bar{S}$ at the selected interval are assumed to be constant (C_1, or C_2, $\bar{C}$).

If we develop formula (4-91c)

$$\bar{S} = -j\frac{dX_{out}(j\omega)}{d(j\omega)} = -jX'_{out}(j\omega) = -j[X'_{out}(p)]_{p=j\omega} \qquad (*)$$

It can be noted that the condition of linearity of the spectrum is equivalent to constancy of the first derivatives or to equality to zero of all the highest derivatives in the region p, and is analogous to condition (3-22a).

350
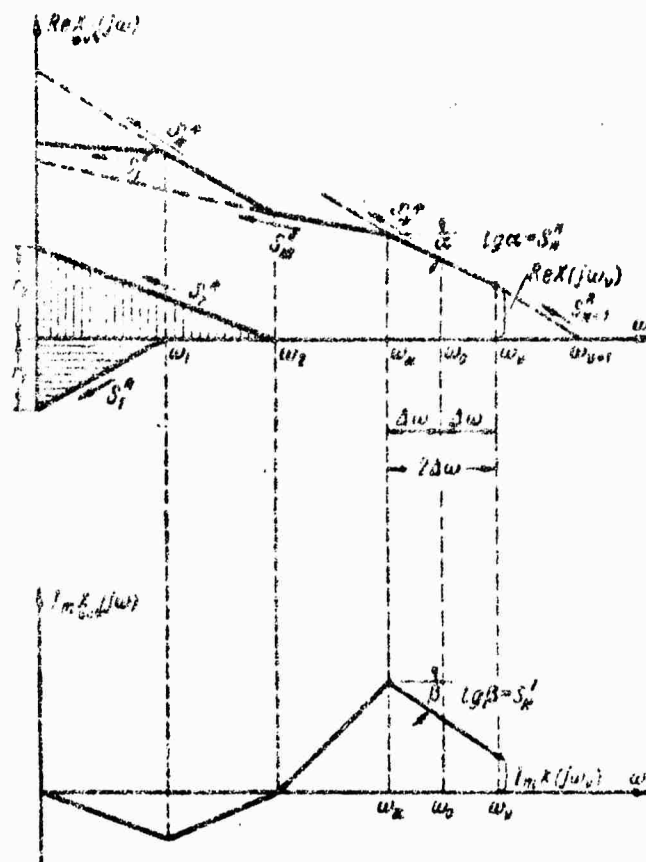
Fig 4-33. Graphic constructions in calculation of the process in a system with variable parameters by the method of balance of the spectra.

As the initial equation in the region p let us adopt an equation with polynomial coefficients, obtained from expression (3-20), if its right side is reduced to a single function:

$$\sum_{i=0}^{n}\sum_{k=0}^{i} (-1)^k a_{ik} \frac{\partial^k}{\partial p^k} \left[p^i X(p)\right] = \Pi(p).$$

If we assume in this equation

$$X^{(k)}(p) = 0 \text{ of which } k > 1,$$

substitute $p = j\omega$ and substitute on the basis of (*)

$$X'(j\omega) = j\overline{S},$$

we get the equation in the region of the spectra of the form:

$$jV(j\omega)\overline{S} + U(j\omega)X(j\omega) = \Pi(j\omega). \qquad (4\text{-}92)$$

where the coefficients in the presence of the spectrum and steepness are combined into the general functions $U(j\omega)$ and $V(j\omega)$, determinable by formulas (3-23 b and c) during substitution of $p = j\omega$.

Balance of the spectra at the frequency ω_y. For the frequency the steepness

$$S_Y = \frac{\Pi(j\omega_y) - U(j\omega_y)X(j\omega_y)}{jV(j\omega_y)} \qquad (4\text{-}93)$$

can be determined from the previously known spectra of the output process $X(j\omega)$ and from formula (4-92).

If we know the steepness, it is possible to calculate the spectrum of the output process at another frequency $\omega_x = \omega_y - 2\Delta\omega$ by the formula for the linear increment

$$X(j\omega_x) = X(j\omega_y) + 2\Delta\omega\overline{S}_Y. \qquad (4\text{-}94)$$

Thus on Figure 4-33 can be constructed: the second points of the components of the output spectrum $X(j\omega)$ and the linear sections between the frequencies ω_y and ω_x. The balance at frequency ω_x permits determining in an analogous way the steepness on the following section of frequencies, etc.

Balance of the spectrum at the frequency ω_0. The accuracy of the calculations can be increased if the equations of balance of the spectra are solved for the center of the frequency bands. Let the average frequency equal ω_0 in the last band. The spectrum at that frequency is unknown, but can be expressed by the steepness and the known spectrum analogously to expression (4-94):

$$X(j\omega_0) = X(j\omega_x) + \Delta\omega\overline{S}_{X0} \qquad (**)$$

If we substitute (**) in equation (4-92), we have:

$$\overline{S}_{X0} = \frac{\Pi(j\omega_0) - U(j\omega_0)X(j\omega_x)}{\Delta\omega U(j\omega_0) + jV(j\omega_0)}, \qquad (4\text{-}95)$$

Usually $\bar{S}_{NO}$ approaches somewhat more exactly the parameters of the unknown spectrum than $\bar{S}_N$, determined by formula (4-93).

The calculation is conducted further by formulas (4-94) and (4-95) and step by step the graphs of the unknown real and imaginary spectra are created.

C. The Transition from the Real Steepness to the Time Process

In the preceding calculations it was necessary all the time to operate with complex steepness of the drop of the spectrum $\bar{S}$, but for transition to a regular process on the basis of an inverse Fourier transform it is sufficient to know only the real steepness S^R. We will use for the construction of the time process the method of partitioning the spectrum into right triangles, one of the legs of which coincides with the axis of ordinates (Figure 4-28a). The steepness of drop for each triangle, or the partial steepness, is determined as the difference of steepness in adjacent bands:

$$
\left.
\begin{aligned}
S_1^R &= S_1^R - S_{11}^R; \\
S_2^R &= S_{11}^R - S_{111}^R; \\
&\cdots \cdots \cdots \cdots \\
S_v^R &= S_N^R - S_{N+1}^R; \\
S_{v+1}^R &= S_{N+1}^R
\end{aligned}
\right\}
\tag{4-96}
$$

On the figure under consideration the first two partial triangles have been constructed, which include the frequency bands $\omega_x = \omega_1$ and $\omega_x' = \omega_2$. At a base of each triangle equal to ω_x and at a partial steepness S^R, the height is

$$
r_x = S_x^R \omega_x.
\tag{***}
$$

The partial process for a triangular spectrum with the parameters r_x, ω_x is determined by (4-78), in which substitution of (***) gives

$$
x_v(t) = \frac{S_v^R \omega_v^2}{\pi} \left(\frac{\sin \frac{\omega_v t}{2}}{\frac{\omega_v t}{2}} \right)^2.
\tag{4-97a}
$$

The total output process is equal to the superposition of the partial processes:

$$x(t) \approx \frac{1}{\pi} \sum_{\lambda=1}^{r+1} S^{R}_{\lambda} \omega^2_{\lambda} \left(\frac{\sin \frac{\omega_{\lambda} t}{2}}{\frac{\omega_{\lambda} t}{2}} \right)^2. \qquad (4.97h)$$

The band width can be varied in the process of calculation; for example, where large values of steepness are expected in the solution, due to closeness to zero of $V(j\omega)$, the bands must be narrowed; during increase of $V(j\omega)$, that is, at $|V(j\omega)| \gg 0$, small values of $|\tilde{S}_x|$ can be expected and the band can be expanded, that is, the process of calculation can be "self-adjusting." For such variations, naturally, there must be preliminary construction of the frequency characteristic $V(j\omega)$ on a complex plane or its constituents (amplitude and phase); logarithmic grids can be used here.

For calculation of the $\nu + 1$-th band the steepness $\tilde{S}_{\nu+1}$ is determined not on the basis of the balance of the spectra, but as the derivative of the spectra of the initial processes, given in Table 4-8, where the spectra are put in the third and fourth columns and their derivatives in the fifth and sixth columns.

Let us assume the tabular value of the steepness to be constant for the entire $\nu + 1$-th band. Since the $\nu + 1$-th band starts at the frequency ω_ν, it is not difficult to determine where the line of the assumed frequency, having passed throught the point $\omega = \omega_\nu$, $\operatorname{Re}(\omega) = \operatorname{Re}(\omega_\nu)$, intersects the axis of the frequencies. The point of intersection gives the frequency $\omega_{\nu+1}$, determinable by the formula

$$\omega_{\nu+1} = \omega_\nu + \frac{\operatorname{Re}(\omega_\nu)}{S^{R}_{\nu+1}}.$$

The ratios of the latter frequency $\omega_{\nu+1}$ to the next to last, $\sim \omega_\nu$, are given in the seventh column of the same table.

Calculations by the hands of the spectra, which are broadly applicable in previously known spectra, is much less labor-consuming than numerical integration directly according to the time of the processes of an oscillating type, since the $2\Delta\omega$ bands selected are broad enough. For the method of balance of the spectra the figure of the spectrum is previously unknown and a polygonal graph of the spectrum is more poorly inserted into an actual smooth spectrum of an unknown process, which forces the frequency bands to be contracted.

If the spectrum at the end of a band (of high enough frequency) is assumed to be equal to zero, and all the intermediate bands are

assigned a width equal to 2δ, the frequencies of the breaks of the graph of the spectrum obtains a single-type expression:

$$\omega_x = 2\kappa\delta \qquad (4\text{-}98)$$

and the total process is determined by the compact formula

$$x(t) = \frac{4\delta^2}{\pi} \sum_{\kappa=0}^{1} \kappa^2 S_\kappa^R \left(\frac{\sin \kappa\delta t}{\kappa\delta t}\right)^2. \qquad (4\text{-}99)$$

D. Use of the Tables of h-Functions

The method of calculation of a process by the tables of h-functions can be applied to an already calculated spectrum, for example, that shown in Figure 4-33; for this, according to Table 4-6, an additional recalculation of the obtained spectrum, in the given case, the imaginary, by the formula $-\omega\,\mathrm{Im}(\omega)$ is required, in order that afterwards the mosaic trapezoids can be separated on the basis of a piecewise-linear approximation and the partial processes sought on a basis of them.

But it is more convenient to seek at once, according to (4-87) the reduced frequency characteristic $j\,X_{out}(j\omega)$ as the solution of the initial operator equation (3-80). Let us introduce into that equation the new argument ω, replace the derivatives according to the imaginary argument by the derivatives according to the real frequency

$$-\frac{\partial}{\partial (j\omega)} = j\,\frac{\partial}{\partial\omega}$$

and, taking designation (4-87) into consideration, recompose equation (3-80);

$$\sum_{i=0}^{n}\sum_{k=0}^{l} a_{ik}\,(j)^k\,\frac{\partial^k}{\partial\omega^k}\,[(j\omega)^{i-1}\Phi_x\,(j\omega)] = \Pi\,(j\omega). \qquad (4\text{-}100a)$$

If we assume in this equation (in view of the future piecewise-linear approximation) in the separate sections

$$\frac{\partial^k}{\partial\omega^k}\,\Phi_x\,(j\omega) = 0 \;\; \text{at} \;\; k > 1$$

and designate

$$-\frac{\partial\Phi_x\,(j\omega)}{\partial\omega} = \vec{S}_\Phi, \qquad (4\text{-}100b)$$

355

we once more obtain an equation of the type of (4-92) in the new designations:

$$V_\Phi(j\omega)\,\overline{S}_\Phi + U_\Phi(j\omega)\,\Phi_\chi(j\omega) = \Pi(j\omega). \quad (4\text{-}100\text{ c})$$

Upon obtaining the complex coefficients $V_\Phi(j\omega)$ and $U_\Phi(j\omega)$ it is possible to be guided by the derivation of formula (3-23c), but in that case it is necessary additionally to take into consideration reduction of the exponent p to unity and the new conditions of differentiation of the lower terms at $i = 0$:

$$\frac{\partial}{\partial\omega}\left[\frac{\Phi_\chi(j\omega)}{\omega}\right] = j\,\frac{\Phi_\chi(j\omega)}{\omega} - \frac{\Phi_\chi(j\omega)}{\omega^2} =$$

$$= -\frac{\overline{S}_\Phi}{\omega} - \frac{\Phi_\chi(j\omega)}{\omega^2};$$

$$\frac{\partial^2}{\partial\omega^2}\left[\frac{\Phi_\chi(j\omega)}{\omega}\right] = \frac{2\overline{S}_\Phi}{\omega^3} + \frac{2\Phi_\chi(j\omega)}{\omega^3}$$

etc.

Moreover, equation (4-100c) is solved analogously to (4-92). As a result the spectra will be obtained from the same elements as in Figure 4-36, but they will be components of the reduced frequency characteristic. The real frequency characteristic is divided into a mosaic of trapezoids, each of which, according to the tables of h-functions, gives a partial output process.

Since all h-functions have a constant constituent, it is natural to resort to these tables only if the output process has a non-damping part. Often it is caused by a stepwise disturbance.

In exactly the same way, expansion of the process according to the functions sine $\omega t/\omega t$ will give a satisfactory result when the process is oscillationally damping, for example reaction on an impulse.

4-10. Analytical Calculation and Modeling of Parametric
Frequency Characteristics of Systems with Variable Parameters

A. Symbolic Method of Calculation

Let us determine the forced reaction of a system described by the algebraized equation of connection (1-6a) at an input action given in the symbolic formula (4-16a) with zero initial phase

$$\chi_{_H}(t) \doteqdot e^{j\Omega t}. \qquad (4\text{-}101a)$$

For systems with constant coefficients such a reaction is found by formula (4-16c) by multiplication of $\chi_{j,H}(t)$ by the time-independent complex transfer coefficient, which is a function of the frequency. In a system with variable parameters the co-factor $W(t, j\omega)$, besides the frequency, depends also on the time:

$$x_{f\text{or}i}(t) \doteqdot W(t, j\Omega)\, e^{j\Omega t} \qquad (4\text{-}101b)$$

and is called the parametric amplitude-phase characteristic of the system (PAPC).

If we substitute the values of (4-101a) and (4-101b) in equation (1-6a):

$$a(t, D)\, W(t, j\Omega)\, e^{j\Omega t} = b(t, D)\, e^{j\Omega t}$$

and take into consideration the properties of the derivative of the exponential function (3-80b), we get by analogy with equation (3-90) a differential equation relative to the PAFC for the parameter t:

$$a(t, D + j\Omega)\, W(t, j\Omega) = b(t, j\Omega). \qquad (4\text{-}102a)$$

If we expand the function $a(t, D + j\omega)$ into a Taylor series, final for the polynomial, by the powers of D:

$$a(t,\, D + j\Omega) = a(t, j\Omega) + \frac{\partial a(t, j\Omega)}{\partial(j\Omega)}\, D + \ldots +$$
$$+ \frac{1}{n!}\, \frac{\partial^n a(t, j\Omega)}{\partial^n (j\Omega)^n}\, D^n$$

and substitute the expansion in (4-102a), carrying all the derivatives to the right side:

$$a(t, j\Omega)\, W(t, j\Omega) = b(t, j\Omega) -$$
$$- \left[\frac{\partial a(t, j\Omega)}{\partial(j\times)}\, D + \ldots + \frac{1}{n!} \cdot \frac{\partial^n a(t, j\Omega)}{\partial(j\Omega)^n}\, D^n \right] W(t, j\Omega).$$
$$(4\text{-}102b)$$

Let us determine the first approximation of the parametric amplitude-phase characteristic by discarding on the right side all the derivatives in time:

$$W_1(t, j\Omega) = \frac{b(t, j\Omega)}{a(t, j\Omega)}. \qquad (4\text{-}102c)$$

The second approximation of the PAPC equals $W_1(t, j\Omega) + W_2(t, j\Omega)$, where $W_2(t, j\Omega)$ is obtained by solution of (4-102b), abbreviated by deletion of the first term on the right side (since the reaction on it has already been obtained), during substitution in the remaining terms of the derivative of the first approximation instead of the derivative $W_2^{(k)}$:

$$W_2(t, j\Omega) = \frac{1}{a(t, j\Omega)} \left[\frac{\partial a(t, j\Omega)}{a(j\Omega)} W_1(t, j\Omega) + \cdots + \frac{1}{n!} \frac{\partial^n a(t, j\Omega)}{a(j\Omega)^n} W_1^{(n)}(t, j\Omega) \right]. \qquad (4\text{-}102d)$$

The third approximation equals $W_1 + W_2 + W_3$; $W_3(t, j\Omega)$ is determined from the equation

$$W_3(t, j\Omega) = \frac{-1}{a(t, j\Omega)} \left[\frac{\partial a(t, j\Omega)}{a(j\Omega)} W_2 + \cdots + \frac{1}{n!} \frac{\partial^n a(t, j\Omega)}{a(j\Omega)^n} W_2^{(n)} \right]. \qquad (4\text{-}102e)$$

The resulting parametric amplitude-phase characteristic in n-th approximation is

$$W(t, j\Omega) = W_1(t, j\Omega) + W_2(t, j\Omega) + W_3(t, j\Omega) + \cdots + W_n(t, j\Omega). \qquad (4\text{-}102f)$$

It can readily be noted that the parametric amplitude-phase characteristic can be obtained from the parametric operator transfer function of system (3-91) during transition from the argument S to the imaginary frequency:

$$S = j\Omega. \qquad (4\text{-}103)$$

Just as in the FOFT the complex argument obtained new designations of S, so in the PAPC the frequency obtains a new designation: Ω. The parametric transfer function naturally can be used both in formula

(3-91) and in the form of (3-81c).

During slow change of the variable coefficients the conditions of transfer of the harmonic actions are successfuly represented by a first approximation of the PAPC (4-102c), and the process of successive approximations rapidly converges.

B. Graphic-Analytical Calculation of a Process at a Single Point

Let us fix in a parametric amplitude-phase characteristic the time at a given point $t = t_1$ = constant and further, by using the properties of the parametric transfer function (3-83c) and substituting $S = j\Omega$, we can obtain a parametric spectrum of the output process:

$$X_{out}(t, j\Omega) = W(t, j\Omega) X_{in}(j\Omega). \qquad (4-104a)$$

The transition from the spectrum to the process along the argument Θ is done by the methods considered above for ordinary spectra, by formulas (4-70a) and (4-70b):

$$X_{out}(t, \theta) = \frac{2}{\pi} \int_0^\infty Re\, X_{out}(t, j\Omega) \cos \Omega\theta\, d\Omega; \qquad (4-101b)$$

$$X_{out}(t, \theta) = -\frac{2}{\pi} \int_0^\infty I_m X_{out}(t, j\Omega) \sin \Omega\theta\, d\Omega, \qquad (4-104c)$$

in which the time t is fixed in the stage of integration, and can be varied after the integration by analytical methods. But the transition to numerical methods of calculation of the process by triangular or trapezoidal mosaic real characteristics and spectra requires the construction of a graph in the region of the frequency for the concrete value t_0 and, consequently, during transition to the partial processes the valid point in them will be only the point corresponding to the argument $\Theta = t_0 - \lambda_{in}$. Therefore, for example, during use of the triangular mosaic and tables of the sine γ/ν functions for each triangle of height r_1 and frequency band Ω_1 from Table 4-6 it is necessary to take for the undisplaced action ($\lambda_{in} = 0$) the argument

$$\gamma_i = \Omega_i t_0. \qquad (\cdot\cdot)$$

The sum of the tabular functions of type (4-78) gives the sought result:

359

$$\dot{x}_{out}(t_0) = \dot{x}_{out}(t_0, \theta)_{\theta = t_0} = \sum_{i=1}^{n} \frac{r_i \Omega_i}{\pi} \left(\frac{\sin \nu_i}{\nu_i} \right)^2. \quad (4\text{-}105)$$

If the same input action is displaced by the value $\mathcal{N}_{in}^0$ relative to the start of change of parameters of the automatic control system, to obtain the reaction at the point t_0 from Table 4-5 it is necessary to select values for

$$\nu_i = \Omega_i (t_0 - \theta_{in}), \quad (**)$$

To obtain the value of the process at another point (t_1) it is necessary to reconstruct the figure of the spectrum Re $X_{out}(t_1, j\Omega)$ since it has the new value of the parameter t_1, to form again the appropriate mosaic, etc.

C. Experimental Taking of the Parametric Amplitude-Frequency Characteristic

The experiment was constructed on the basis of representation of the forced reaction of a component in the form of (4-101b) on the assumption that the proper constituent motions on the output are rapidly damped thanks to the properties of the tested component itself.

The test diagram requires: two examples of homogeneous test components, a pickup of sine and cosine oscillations of infralow frequency, two quadrators -- non-linear blocks which produce on the output the squares of the input voltage, and a summator.

A block diagram of these elements is shown in Figure 4-34. The pickup of the harmonic oscillations shifted by $\frac{\pi}{2}$ can serve as a model of a resonance component, formed in Figure 4-7 on three amplifiers: 1, 2 and 3. The oscillations taken from the output of amplifier 1 cause a reaction in the first specimen of component x_s (t, Ω), which we will conventionally call "sine." The oscillations taken from the output of amplifier 2 cause a reaction in the second specimen of component $x_c(t, \Omega)$, conventionally called "cosine."

At the unit level of the two input harmonics the "sine" and "cosine" reactions, after being raised to the squares and summated, give the square of the sought amplitude of the parametric amplitude-frequency characteristic:

$$A^2(t, \Omega) = X_s^2(t, \Omega) + X_c^2(t, \Omega). \quad (4\text{-}106)$$

The result is obtained in the form of the oscillogram $A^2(t, \Omega_i)$ for a single fixed frequency Ω_i. After taking of the oscillogram the frequency of the pickup is reconstructed and taken $A^2(t, \Omega_k)$ at another frequency. Thus the necessary number of points of the parametric amplitude-frequency characteristic is gathered in the given frequency band.

Selection from the set of graphs of the value of the amplitudes for a fixed t_i gives the parametric amplitude-frequency characteristic $A(t_i, \Omega)$ with fixed t_i and variable Ω, which was used in the preceding formulas of transfer of actions.

Separate taking of an oscillogram of the constituents $x_s(t, \Omega)$ and of the input harmonics $e^{j\Omega t}$ permits finding the phase and later the entire parametric amplitude-phase characteristic $W(t, j\Omega)$.

4-11. Distribution of Power in the Spectrum. Spectral Density

1. The Average Power of the Signal in Time

The average power in the interval $2T$ for any type of signals will be its mean square value, determinable according to Figure 4-35a by the formula

$$P(t) = \frac{1}{2T} \int_{+T}^{-T} x_0^2(t-\tau)\, d\tau = \frac{1}{2T} \int_{-T}^{T} x^2(\tau)\, d\tau. \quad (4\text{-}107)$$
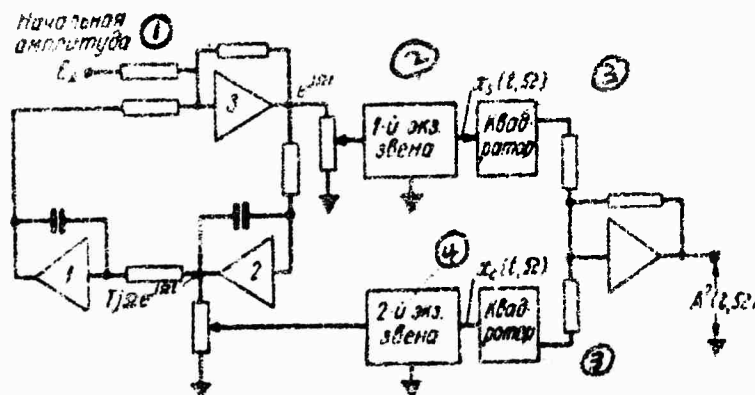
Fig 4-34. Diagram of the experimental arrangement for taking the frequency characteristics of components with variable parameters. 1 - Initial amplitude; 2 - First model of component; 3 - Quadrator; 4 - Second model of component.
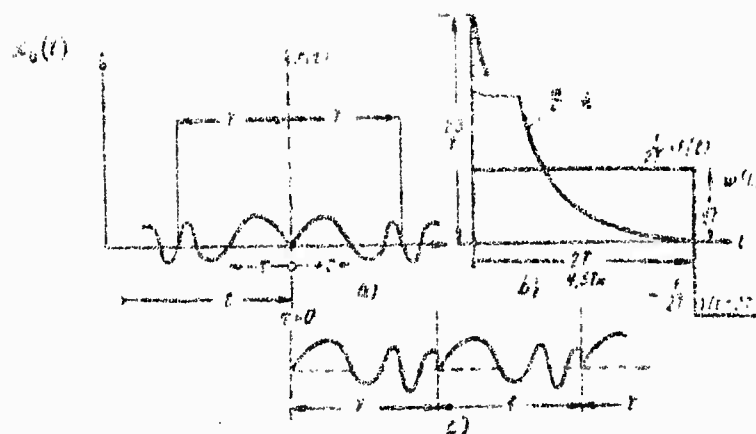
Fig 4-35. Established section of a complex oscillating process and its artificial periodization.

If the signal x is given in the form of electric current, the integral (4-107) actually is equal to the power dispersed by that current at a resistance of 1 ohm. For signals x of another physical nature the term power will be used as a conventional designation of dependence (4-107).

Under the experimental conditions the average power can be manifested by a thermal instrument, the heating of which is proportional to the square of the current: $y = x^2$, and the heat emission of which is proportional to the excess temperature t^o.

The equation of the thermal equilibrium of the instrument is

$$Ct^o + kt' = my,$$ (4-108)

where C is the heat capacity of the instrument, in cal/degree;
   k is the heat emission coefficient, in cal/(deg)(sec);
   m=C,2G is the scalar co-factor, taking into consideration the real resistance of the instrument R and the ratio between the thermal and electric units of power, cal/(sec)(a²).

The aperiodic component can be reduced to standard form:

$$\frac{C}{k} t^o + t' = \frac{m}{k} y$$

or

$$T_{heat}\dot{t}^{\circ} + t^{\circ} = \frac{m}{k}\,y.$$

where $T_{heating} = \frac{C}{k}$ is the time constant of the heating of the instrument.

From this we determine the weight function of the instrument:

$$w\,(t) = \frac{m}{kT_{heat}}\,e^{-\frac{t}{T_{heat}}} = \frac{m}{C}\,e^{-\frac{t}{T_{heat}}} \qquad (4\text{-}100)$$

and the conditions of obtaining the reading of power $P(t)$ on the instrument:

$$P(t) = \frac{m}{C}\int\limits_{0}^{t} e^{-\frac{\tau}{T_{H}}}\,y_0\,(t-\tau)\,d\tau = \frac{m}{C}\int\limits_{0}^{t} e^{-\frac{\tau}{T_{H}}}\,y\,(\tau)\,d\tau.$$

If a considerable interval of time $t \gg T_H$ has passed after switching in of the instrument, the memory of the measuring system of the instrument does not extend to the previous history before $4.6T_H$ (with accuracy to 1%), and the preceding formula can be written as:

$$P_{wt.\,mean}(t) = \frac{m}{C}\int\limits_{0}^{4.6T_H} e^{-\frac{\tau}{T_H}}\,y\,(\tau)\,d\tau. \qquad (4\text{-}111)$$

The result gives the weighted-mean power for the interval $4.6T_H$. The difference between formulas (4-107) and (4-111) is that the first gives the mean power, which also could be attained during the working of an equivalent physical component in a one-sided regime with a weight function of the type

$$w\,[t] = \frac{1}{2T}\,[1\,(t) - 1\,(t-2T)],$$

shown in Figure 4-35b, and the second formula gives the weighted-mean power. In the same figure the exponential weight function is constructed, for which the interval $2T = 4.6T_H$. To equate both weight functions in areas, it is sufficient to assume the initial ordinate of the exponent

$$\frac{m}{C} = \frac{2.3}{T}.$$

For determination of the average power (4-111) at the moment of time t it is most convenient to make the reading of the argument τ during integration, as shown in Figure 4-35a, that is, symmetrically on both sides of the point of the process corresponding to the moment of time t. In that case the function $x(\tau)$ is given as a two-sided function of the argument τ.

2. Two-Sided Fourier Transformation

Some change of the mathematical apparatus worked out for the initial functions is required for the new conditions of assignment of the process.

Let us designate by $X_2(j\omega)$ the two-sided Fourier transformation of the process $x(\tau)$, determined by the formula

$$X_2(j\omega) = \lim_{T\to\infty} X_{2T}(j\omega) =$$

$$= \lim_{T\to\infty} \int_{-T}^{T} x(\tau) e^{-j\omega\tau} d\tau. \qquad (4\text{-}112)$$

Upon substitution of infinite limits of integration, division of the integral into two parts:

$$X_2(j\omega) = \int_{-\infty}^{0} x_t(\tau) e^{-j\omega\tau} d\tau + \int_{0}^{\infty} x_u(\tau) e^{-j\omega\tau} d\tau$$

and substitution of the argument $-\tau = \vartheta$ on the left side:

$$x_t(-\tau) = x_t(\vartheta)$$

we get:

$$X_2(j\omega) = \int_{0}^{\infty} x_t(\vartheta) e^{+j\omega\vartheta} d\vartheta + \int_{0}^{\infty} x_u(\tau) e^{-j\omega\tau} d\tau =$$

$$= X_t(-j\omega) + X_u(j\omega), \qquad (4\text{-}113)$$

that is, the two-sided Fourier transformation X_2 is equal to the sum of the one-sided representation of the right half-branch of the func-

tion and the conjugate one-sided representation of the left half-branch of the function.

For even functions of $x(\tau)$ the representation $X_2(j\omega)$ is real:

$$X_{\text{Re }2}(\omega) = 2\,\text{Re}\,X(j\omega) = 2\int_0^\infty x(\tau)\cos\omega\tau\,d\tau \quad (4\text{-}114)$$

and for uneven functions it contains only the imaginary part:

$$X_2(j\omega) = j2\,\text{Im}\,X(j\omega) = j2\int_0^\infty x(\tau)\sin\omega\tau\,d\tau. \quad (4\text{-}115)$$

We will use further the diagram of representation of the process in the form of even functions. Formula (4-114) gives the possibility of using tables of ordinary (one-sided) Fourier transformation for the two-sided Fourier transformation, by separating the doubled real constituent from them.

The Fourier transformations of certain even functions are given in Table 4-9. The inverse transformation is accomplished by the formula:

$$x(\tau) = \frac{1}{2\pi}\int_{-\infty}^\infty X_2(j\omega)\,e^{j\omega\tau}\,d\omega =$$

$$= \frac{1}{\pi}\int_0^\infty X_{\text{Re }2}(\omega)\cos\omega\tau\,d\omega. \quad (4\text{-}116)$$

3. Relay Theorem for the Energy of the Process

We will proceed from formula (4-107) to a determination of the energy of the Process

$$I_{2T} = \int_{-T}^T x^2(\tau)\,d\tau = \int_{-T}^T x(\tau)\,x(\tau)\,d\tau. \quad (4\text{-}117)$$

Let us replace one of the subintegrands by its expression (4-116) through the two-sided spectrum:

$$I_{2T} = \int_{-T}^T x(\tau)\left\{\frac{1}{2\pi}\int_{-\infty}^\infty X_2(j\omega)\,e^{j\omega\tau}\,d\omega\right\}d\tau.$$

365

Let us change the order of integration:

$$I_{2T} = \frac{1}{2\pi} \int\limits_{-\infty}^{\infty} X_2(j\omega) \left\{ \int\limits_{-T}^{T} x(\tau) e^{j\omega\tau} d\tau \right\} d\omega =$$

$$= \frac{1}{2\pi} \int\limits_{-\infty}^{\infty} X_2(j\omega) X_{2T}(-j\omega) \, d\omega. \qquad (*)$$

If we proceed to the limit $T \to \infty$, we get:

$$I_2 = \frac{1}{2\pi} \int\limits_{-\infty}^{\infty} X_2(j\omega) X_2(-j\omega) \, d\omega =$$

$$= \frac{1}{2\pi} \int\limits_{-\infty}^{\infty} |X_2(j\omega)|^2 \, d\omega.$$

In connection with the evenness of the modulus of the complex spectrum it can be written:

$$I_2 = \frac{1}{\pi} \int\limits_{0}^{\infty} |X_2(j\omega)|^2 d\omega. \qquad (4\text{-}118)$$

If the same derivation is repeated for the initial process, we get:

$$\int\limits_{0}^{\infty} x^2(t) \, dt = \frac{1}{\pi} \int\limits_{0}^{\infty} |X(j\omega)|^2 \, d\omega. \qquad (4\text{-}119)$$

Formulas (4-118) and (4-119) prove the equivalence of integration in time of the square of the signal and integration of the square of the modulus of the complex spectrum in frequency, which also represents the content of the Relay theorem.

Let us determine now the elementary energy in the frequency band from ω to $\omega + d\omega$:

$$dI_2 = \frac{1}{\pi} |X_2(j\omega)|^2 \, d\omega;$$

whence

$$|X_2(j\omega)|^2 = \pi \frac{dI_2}{d\omega}, \qquad (4\text{-}120)$$

that is, the square of the modulus of the complex spectrum characterizes the increase by π times in the steepness of growth of energy of the process in frequency or the energetic density of the spectrum.

Table 4-9 Four Transformation of two-sided even functions

Original $f_q(\tau)$ ①	Изображение $f_q(\omega)$ ②
$e^{-\alpha|\tau|}$	$\dfrac{2\alpha}{\alpha^2+\omega^2}$
$\sin\Omega|\tau|$	$\dfrac{2\Omega}{\Omega^2-\omega^2}$
$\cos\Omega\tau$	$\pi[\delta(\omega-\Omega)+\delta(\omega+\Omega)]$
$\sin(\Omega|\tau|+\varphi)$	$\dfrac{2\Omega}{\Omega^2-\omega^2}\cos\varphi$
$e^{-\alpha|\tau|}\cos\Omega\tau$	$\dfrac{2\alpha(\alpha^2+\Omega^2+\omega^2)}{\omega^4+2\omega^2(\alpha^2-\Omega^2)+(\alpha^2+\Omega^2)^2}$
$e^{-\alpha|\tau|}\sin\Omega|\tau|$	$\dfrac{2\Omega(\alpha^2+\Omega^2-\omega^2)}{\omega^4+2\omega^2(\alpha^2-\Omega^2)+(\alpha^2+\Omega^2)^2}$
$e^{-(\alpha\tau)^2}$	$\dfrac{\sqrt{\pi}}{2\alpha}\,e^{-\left(\frac{\omega}{2\alpha}\right)^2}$
$e^{-(\alpha\tau)^2}\cos\omega\tau$	$\dfrac{\sqrt{\pi}}{\alpha}\left[e^{-\left(\frac{\pi}{2\alpha}\right)^2(\omega-\Omega)^2}+e^{-\left(\frac{\pi}{2\alpha}\right)^2(\omega+\Omega)^2}\right]$
$\delta|\tau|=\dfrac{1}{2}\{\delta(\tau+)+\delta(\tau-)\}$	$1(\omega)$
$1(\tau)$	$\pi[\delta(\omega+)+\delta(\omega-)]$
$|\tau|$	$-\dfrac{2}{\omega^2}$
τ^2	$\pi[\delta(\omega+)+\delta(\omega-)]$

1 - Original $f_{freq}(\gamma)$; 2 - Transformation $P_{freq}(\omega)$

4. Spectral Density of Power

The energy of a process of infinite duration is finite only when the process is damped rapidly enough. If the process is not damped, the integrals (4-118) and (4-119) do not converge. Non-damping pro-

cesses must be analyzed by their power. We will proceed in formula (*), which arises from (4-117) to a determination of the power:

$$P_{av} = \frac{I_{2T}}{2T} = \frac{1}{2\pi} \int_{-\infty}^{\infty} \frac{X_2(j\omega)X_{2T}(-j\omega)}{2T} \, d\omega. \qquad (**)$$

If we turn to the initial formula (4-117) or to the formula of the real instrument measuring the power (4-111), we can determine the value of the interval 2T for which, during its further increase, the average power will vary inconsiderably, and the measuring instrument, by virtue of limited resolution will not perceive the scale of this difference. Then it is possible to proceed to the limit in the right side of formula (**) without disturbing the value of the left side:

$$P_{av} = \frac{1}{2\pi} \int_{-\infty}^{\infty} \lim_{T \to \infty} \frac{|X_{2T}(j\omega)|^2}{2T} \, d\omega =$$

$$= \frac{1}{\pi} \int_{0}^{\infty} \lim_{T \to \infty} \frac{|X_2(j\omega)|^2}{2T} \, d\omega.$$

If we now examine the power in the frequency band

$$dP = \frac{1}{\pi} \lim_{T \to \infty} \frac{|X_{2T}(j\omega)|^2}{2T} \, d\omega,$$

then on the basis of the transformations

$$\lim_{T \to \infty} \frac{|X_{2T}(j\omega)|^2}{2T} = \pi \frac{dP}{d\omega} = S_x(\omega) \qquad (4\text{-}121a)$$

we get the density of power in the spectrum $dP/d\omega$ or -- when it is increased by π times -- the spectral density.

And so the spectral density is equal to the limit of the ratio of the square of the modulus of a two-sided complex spectrum of a process limited to the limits $\pm T$ to the value of the interval during infinite increase of the latter. At the same time the spectral density is equal to the derivative, increased by π times, of the power of the process in frequency, that is the density of power of the spectrum. For a periodic process at frequencies ω_k, short of the frequency of repetition, the limit (4-121a) is found at once from the first period T in accordance with (4-114).

It follows from formula (4-121a) that:

$$dP = \frac{1}{\pi} S(\omega)\, d\omega; \qquad (4\text{-}121\text{b})$$

$$\Delta P = \frac{1}{\pi} \int_{\omega_1}^{\omega_1 + \Delta\omega} S(\omega)\, d\omega. \qquad (4\text{-}121\text{c})$$

5. Periodization of the Process

The mathematical apparatus drawn above with partial application of non-converging integrals and limiting transitions is little suitable for practical calculation of spectral density.

For example, only a limited part of the established section of the process in the interval $0 - T$ proves to be at the disposal of an investigator, as shown in Figure 4-35c. In that case, instead of the real process, it is more convenient to study a model of the process or its calculating diagram. A suitable calculating diagram is obtained in an artificial periodization of the process. In it, as shown in Figure 4-35c, multiple repetition of the sections of the process $0 - T$ makes the process non-damping at any duration, and the symmetric reflection of the right half-branch of the process on the side of the negative arguments τ makes the process even.

Further, if we replace limit (4-121a) by the ratio of the finite increments in the course of the first period, it remains to calculate the amplitudes of the cosine harmonics of the Fourier series according to formulas analogous to (4-114), and to go over to the spectral density of an even process:

$$S(\omega_k) = S\left(\frac{2\pi}{T} k\right) =$$

$$= \frac{2}{T} \left[\int_0^T x(t) \cos \frac{2\pi k}{T} t \, dt \right]^2 = \frac{T}{2} a_{ck}^2. \qquad (4\text{-}122)$$

This formula permits calculating the series of supporting points of the spectral density for frequencies that on the whole are k times greater than the frequency of the periodization

$$\omega_1 = \frac{2\pi}{T}.$$

If the process is recorded on magnetic tape at the segment $0 - T$ and then it is pasted into a ring, the artificial periodized process obtains infinite duration and can be analyzed by measuring instruments,

4-12. The Effective Transmission Band

Let there be at the disposal of the investigator a length section of an established process, transformed into a law of change of voltage in time. Let this voltage pass through a narrow-band filter which has the amplitude-frequency characteristic $A_\phi(\omega)$, shown in Figure 4-36.

The amplitude spectrum on the input of the filter will be designated by $|X_{2_T}(j\omega)|$ and on the output of the filter

$$|Y_{2T}(j\omega)| = A_\phi(\omega)|X_{2T}(j\omega)|.$$
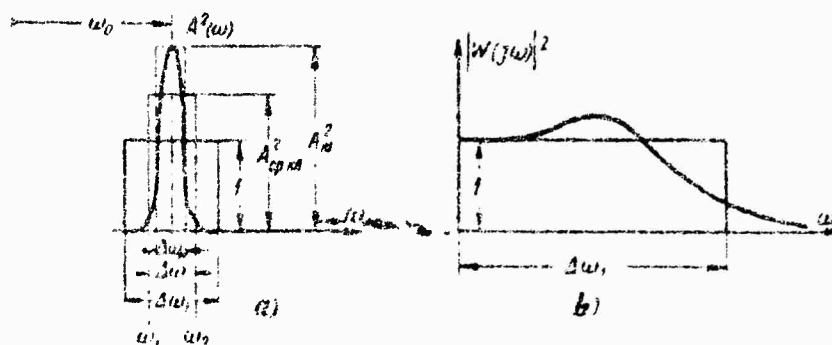
Fig 4-36. Determination of the effective transmission band in a narrow-band filter and in a component with a semi-infinite amplitude-frequency characteristic.

Let us determine the ratio between the spectral densities on the output S_y and input S_x of the filter by using formulas (4-121) and (*):

$$\frac{S_y(\omega)}{S_x(\omega)} = \lim_{T \to \infty} \frac{\dfrac{|Y_{2T}(j\omega)|^2}{2T}}{\dfrac{|X_{2T}(j\omega)|^2}{2T}} = \frac{|X_{2T}(j\omega)|^2 A_\phi^2(\omega)}{|X_{2T}(j\omega)|^2} = A_\phi^2(\omega),$$

whence

$$S_y(\omega) = S_x(\omega)A_\phi^2(\omega). \tag{4-123}$$

Let us use formula (4-121c) for determination of the power on the output of the filter

$$\Delta P_y = \frac{1}{\pi} \int\limits_{\omega_1}^{\omega_1 + \Delta\omega} A_\phi^2(\omega) S_x(\omega) \, d\omega.$$

At the narrow band $\Delta\omega = \omega_2 - \omega_1$ the spectral density in the zone of integration can be assumed to be unchanged and equal to its value in the center of the band $\omega_0 = \dfrac{\omega_1 + \omega_2}{2}$, that is,

$$S_x(\omega) \to S_x\left(\frac{\omega_1 + \omega_2}{2}\right) = S_x(\omega_0),$$

which simplifies the integration

$$\Delta P_y = \frac{S_x(\omega_0)}{\pi} \int\limits_{\omega_1}^{\omega_1 + \Delta\omega} A_\phi^2(\omega) \, d\omega,$$

whence

$$S_x(\omega_0) = \frac{\pi \Delta P_y}{\displaystyle\int\limits_{\omega_1}^{\omega_1 + \Delta\omega} A_\psi^2(\omega) \, d\omega}. \tag{4-124a}$$

The integration in frequency can be made approximately as the calculation of the area of one of the equivalent rectangles shown in Figure 4-36, where the following can serve as a basis:

The actual band of the filter $\Delta\omega$ at the square of the mean square amplitude A_{ms}^2;

The recalculated band of the filter $\Delta\omega_M$, corresponding to the square of the maximal amplitude A_M^2;

The effective transmission band of the filter $\Delta\omega_1$, corresponding to the unit amplitude $A^2 = 1$.

All the rectangles, naturally, have identical area:

$$\Delta\omega_1 \cdot 1^2 = \Delta\omega A_{cp.\kappa B}^2 = \Delta\omega_M A_M^2 = \int\limits_{\omega_1}^{\omega_1 + \Delta\omega} A_\phi^2(\omega) \, d\omega. \tag{4-124b}$$

Further, we will preferably use the effective transmission band, with the introduction of which formula (4-124a) assumes the form:

$$S_x(\omega_0) = \pi \frac{\Delta P_y}{A_{cp.\kappa B}^2 \Delta\omega} = \pi \frac{\Delta P_y}{\Delta\omega_1}. \tag{4-124c}$$

371

If we have calculated the $\Delta \omega$ for the filter and measured with an instrument on the filter output the power in the band ΔP_{in}, it is possible to determine the spectral density of the input process at a single point by the obtained formula on the basis of the experiment:

$$S_x(\omega_0).$$

If we reconstruct the filter at the new band ω_2 to ω_4, by an analogous method we find the spectral density for the following point $\dfrac{\omega_2 + \omega_4}{2}$ and thus we construct the complete graph of the spectral density of the input process.

All the statements made above have been for determined processes which have concrete Fourier transformations. But such a parameter of the process as the power density, especially if it is determined experimentally, is insensitive to changes of phase of the harmonic constituents of the process and little sensitive to partial changes in amplitude, if the average value remains constant. Therefore the estimation of the properties of processes by the spectral density will be used extensively later on (see Chapter 10) for random processes of a definite class.

The effective transmission band serves as a suitable estimate not only of the properties of narrow-band filters but also of ordinary components and control systems. In that case the amplitude-frequency characteristics of the component-system, $W(j\omega)$, have the ordinary form, being extended to a semi-infinite region of frequencies, as shown in Figure 4-36b. The limits of integration are correspondingly extended in formula (4-124b):

$$\Delta \omega_1 = \int_0^\infty |W(j\omega)|^2 \, d\omega. \qquad (4\text{-}125)$$

but as before the area of the semi-infinite graph coincides with the area of the rectangle shown in the same figure, having the height $A^2(\omega) = 1$ and the base $\Delta \omega_1$.

Since the OFT of the component-system serves as a representation of an impulse reaction, that is, the weight function, formula (4-119) for this process can be described by the effective transmission band:

$$I_2 = \int_0^\infty \omega^2 |f| \, d\omega = \frac{1}{\pi} \Delta \omega_1. \qquad (4\text{-}126)$$

For analytical calculation of the effective transmission band

according to the given OFT in the form of a rational function

$$W(p) = \frac{b_m p^m + \ldots + b_1'' p + b_0}{a_n p^n + \ldots + a_1 p + a_0} =$$

$$= \frac{b_m'' p^m + \ldots + b_1'' + b_0''}{p^n + a_{n-1}'' p^{n-1} + \ldots + a_1'' p + a_0''} \qquad (*)$$

it is possible to use formula (3-107b)

$$\frac{\Delta\omega_1}{\pi} = \lim_{p \to 0} \lambda_1 \left| \frac{b_m^2 p + \ldots + b_0''}{p^n + \ldots + a_0''} \right| =$$

$$= \frac{1}{\Delta(0)} \sum_{i=0}^{n} B_i(0)\, \Delta_{ii}(0) \qquad (4\text{-}127)$$

and the method stated in Section 3-14.

In the table presented below are the values of the effective transmission band for automatic control systems which have an order of the OFT not greater than the fourth, expressed by normalized coefficients of the OFT, and likewise for components of not higher than the second order, expressed by the technical parameters of the components. Part of the solutions have been borrowed from the examples of Chapters 2 and 3, and for the calculation of the last two lines use was made of formula (4-127), on the basis of which the table can be extended as needed.

For an OFT of a higher order it is possible to continue the calculations by the same formula or to utilize the prepared table of Phillips and Maclxin (Introduction [5]), compiled at other designations of the OFT coefficients and on the basis of methods of integration in a complex plane. An account of additional methods which do not have a structural direction can be found in the works of P V Bulgakov [4], A A Krasovskiy [5], A A Fel'dbaum [6], I D Moiseyev [7] and other authors.

If the effective transmission band is expressed in cycles per second, then from (4-126) we have

$$\Delta f_1 = \frac{\Delta\omega_1}{2\pi} = \frac{1}{2} I_2 \qquad (4\text{-}128)$$

We will present without derivation one more formula obtained by

Table 4-10 The effective transmission band of linear systems which have rational OTF's of not higher than the fourth order

$F(p)$		$N(p)$	$\frac{3\omega_1}{\pi}$
$\dfrac{1}{p + a_0^u}$	a_0^u	$\dfrac{k}{Tp + 1}$	$\dfrac{k}{a_0}$
$\dfrac{1}{p^2 + a_1^u p + a_0^u}$	$\dfrac{1}{2a_1^u}$	$\dfrac{k}{T^2 p^2 + 2\xi T p + 1}$	$\dfrac{k^2}{4\xi}$
$\dfrac{b_1^u p + b_0^u}{p^2 + a_1^u p + a_0^u}$	$\dfrac{1}{2a_0^u a_1^u}$	$\dfrac{b_0^{u2} a_1^u + b_0^{u2}}{2 a_1^u a_0^u}$	$\dfrac{k^2}{4\xi}$
$\dfrac{1}{(p^2 + a_2^u p^2 + a_1^u p + a_0^u)}$	$\dfrac{b_1^u p + b_3^u}{p^2 + a_1^u p + a_3^u}$	$\dfrac{k(Tp + 1)}{T^2 p^2 + a_1^u p + 1}$	$k^2\left[1 + \left(\dfrac{T}{\tau}\right)^2\right]$
		$\dfrac{a_2^u}{2 a_0^u (a_1^u a_2^u - a_0^u)}$	$\dfrac{k^2}{4\xi}$
$\dfrac{1}{(p^4 + a_3^u p^3 + a_2^u p^2 + a_1^u p + a_0^u)}$		$\dfrac{a_1^u - a_3^u a_0^u}{2 a_0^u (a_1^{u2} + a_0^{u2} a_2 - a_3^u a_2^u a_1^u)}$	

374

us for calculation of the effective transmission band by the OFT (*) with non-normalized coefficients at $m \leqslant n - 1$ and disposition of all the bands in the left half-plane:

$$\Delta f_1 = \frac{\begin{vmatrix} 2(b_0 b_{10} - b_1 b_9 + b_2 b_8 - b_3 b_7 + b_4 b_6) - b_5^2 & \dots a_5\, a_6\, a_7\, a_8\, a_9\, a_{10} \\ 2(b_0 b_8 - b_1 b_7 + b_2 b_6 - b_3 b_5) + b_4^2 & \dots a_3\, a_4\, a_5\, a_6\, a_7\, a_8 \\ 2(b_0 b_6 - b_1 b_5 + b_2 b_4) - b_3^2 & \dots a_1\, a_2\, a_3\, a_4\, a_5\, a_6 \\ 2(b_0 b_4 - b_1 b_3) + b_2^2 & \dots 0\, a_0\, a_1\, a_2\, a_3\, a_4 \\ 2 b_0 b_2 - b_1^2 & \dots 0\, 0\, 0\, a_0\, a_1\, a_2 \\ b_0^2 & \dots 0\, 0\, 0\, 0\, 0\, a_0 \end{vmatrix}}{4a_n \begin{vmatrix} a_{n-1} & a_n & 0 \dots 0 & 0\, 0\, 0\, 0\, 0 \\ 0 & 0 & 0 \dots a_5\, a_6\, a_7\, a_8\, a_9\, a_{10} \\ 0 & 0 & 0 \dots a_3\, a_4\, a_5\, a_6\, a_7\, a_8 \\ 0 & 0 & 0 \dots a_1\, a_2\, a_3\, a_4\, a_5\, a_6 \\ 0 & 0 & 0 \dots 0\, a_0\, a_1\, a_2\, a_3\, a_4 \\ 0 & 0 & 0 \dots 0\, 0\, 0\, a_0\, a_1\, a_2 \\ 0 & 0 & 0 \dots 0\, 0\, 0\, 0\, 0\, a_0 \end{vmatrix}} \cdot (-1)^{n-1}. \qquad (4.129)$$

Bibliography

1. Manukhin A I, Compensation method of taking frequency and amplitude characteristics of linear and non-linear components, Byulleten' tekhnicheskoy informatsii MRTP, 1957, No 2
2. Solodovnikov V V, Topchiyev Yu I and Krutikova O V. Chastotny metod postroyeniya perekhodnykh protsessov (Frequency Method of Construction of Transient Processes), Gostekhizdat, 1955.
3. Voronov A A. Elementy teorii avtomaticheskogo regulirovaniya (Elements of the Theory of Automatic Control), Voyenizdat, 1954.
4. Bulgakov B V. Kolebaniya (Oscillations), GITTL, 1954.
5. Krasovskiy A A. O stepeni ustoychivosti lineynykh system (On the degree of stability of linear systems), No 281, 1948.
6. Fel'dbaum A A Integral criteria of the quality of control, Avtomatika i telemekhanika, 1948, Vol IX, No 1.
7. Moiseyev I D. Quasi-integral derivation of the direct coefficient criterion of asymptotic stability for an ordinary system, Zapiski seminara po teorim ustoychivosti, 1948.

Chapter 5

STRUCTURAL METHODS

5-1. Graphic Representations of Control Systems and
the Principal Forms of Structural Connections

A. Types of Graphic Representations and the Role of
Structural Methods

Structural methods are based on graphic representations:

1) which throw light upon the physical interconnections between the elements of an automatic control systems and their mathematical equivalents;

2) which reflect in the most convenient engineering form the conditions of transmission of control signals and controlling values in the system;

3) which permit carrying out purposeful changes in working up the structure of a control system;

4) which facilitate the mathematical transformations of equations describing the behavior of elements and of the control system as a whole, for preliminary evaluations of the properties of the system and for subsequent complete evaluations.

Graphic representations are very profitably used in the theory of automatic control for the solution of the indicated problems. In using generally accepted methods and developing them in the direction indicated in Chapter 1, we present a brief list of graphic representations of automatic control systems.

1. A block diagram reflects the physical connections between the real elements of a control system which determine the functional and energetic transformations of the signals.

2. A structural diagram takes into consideration the linearized mathematical connections between the mathematical equivalents of the elements -- the components which are determinable by differential equations with constant coefficients. The conditions of transmission of signals by the components have an algebraic description in the region of representations of time processes that have been subjected to Laplace or Fourier transformation.

3. A structural representation extends the application of the structural diagrams to linear systems with variable parameters, while retaining the notation of the conditions of transmission and transformation of signals in the region of time, using the principle of algebraization of differential equations.

4. The adjustment circuit of an electronic model is an instrumental realization of the mathematical dependences established in the initial equations of the control system or in its structural representation, degenerating into a structural diagram for the case of constant coefficients.

The most complex and important problem is the synthesis of the structure of components and of a control system as a whole.

In connection with separate components, structural methods reveal the internal structure of each component, which promotes a very clear understanding of the essence of the processes occurring in the components and permits a proper approach to improvement of the characteristics of a component by the superposition of additional external connections which amplify the useful connections that exist within the component itself or that neutralize the action of undesirable connections.

With respect to the system as a whole, structural methods permit establishing the rationality of the structure of the system from the point of view of solution of the principal problem laid upon it and of compensation for the disturbances acting upon the system.

Academician B N Petrov [1] worked on the creation of a special algebra of structural analysis and synthesis. The elements of structural methods in connection with problems of stability were worked up by A M Mikhaylov (see Chapter 1 [1]) and were shown in very clear form by D I Mar'yanovskiy [2]. A singular interpretation of the problems of structural analysis was given in the work of I I Gal'perin [3], and a number of new designations, terms and theorems on the plane of general theory were advanced.

In Chapter 1 of this book the principal forms of connections were examined and formulas were given for the contraction of single (Figure 1-14) and multiple (Figures 1-1 and 1-2) circuits with a

single input and output without cross connections. On the basis of
the general principles of Chapter 1, and also by using rational oper-
ator and frequency methods, we will proceed to a further development
of structural methods.

B. Multi-Circuit Matching-Parallel Diagrams

At the beginning let us examine circuits without cross connec-
tions, a calculation of which will be made in Sections 5-4, 5-5 and
5-6.

In Figure 5-1a a three-circuit matching-parallel diagram is shown.
It can be contracted into a single complex component, that is, all the
equations of the components can be reduced to a single equation of the
circuit by successive use of formulas for a matching-parallel circuit
with the internal circuit 1, then of formulas of cascade connection
for the direct path of circuit 2, again of formulas of matching-para-
llel connection for the same circuit and analogously for circuit 3.
All these partial transformations are carried out for components with
variable parameters by formulas (1-97), (1-99) and (1-101) and for com-
ponents with constant parameters by the formulas of Chapter 3. Let us
give   the general formula in operator notation:

$$W(p) = B_s(p) + \Pi_s(p)\{B_2(p) + $$
$$+ \Pi_2(p)\{B_1(p) + \Pi_1(p)\}\Pi_{II}(p)\}\Pi_{III}(p). \quad (5\text{-}1)$$

In the diagram a numeration of the circuits and components is
used that is in agreement with the order of the transformations during
the contraction. If we remove the parentheses in (5-1), it is possi-
ble to reduce it to the sum of four terms, and the circuit to four
independent parallel branches.

The formula and diagram are valid for the amplitude-phase char-
acteristics of components during substitution of $p = j\omega$, and likewise
for parametric operator transfer functions and parametric amplitude-
phase characteristics. The transition to a matching-parallel circuit
in a number of cases is applied in the calculation of the amplitude-
phase characteristic according to complex operator polynomials.

Thus, for example, the polynomial

$$R(p) = a_n p^n + a_{n-1} p^{n-1} + a_{n-2} p^{n-2} + \ldots + $$
$$+ a_2 p^2 + a_1 p + a_0$$

can correspond to the general transfer function of the system or to

378

a part of it, its inversion, etc.
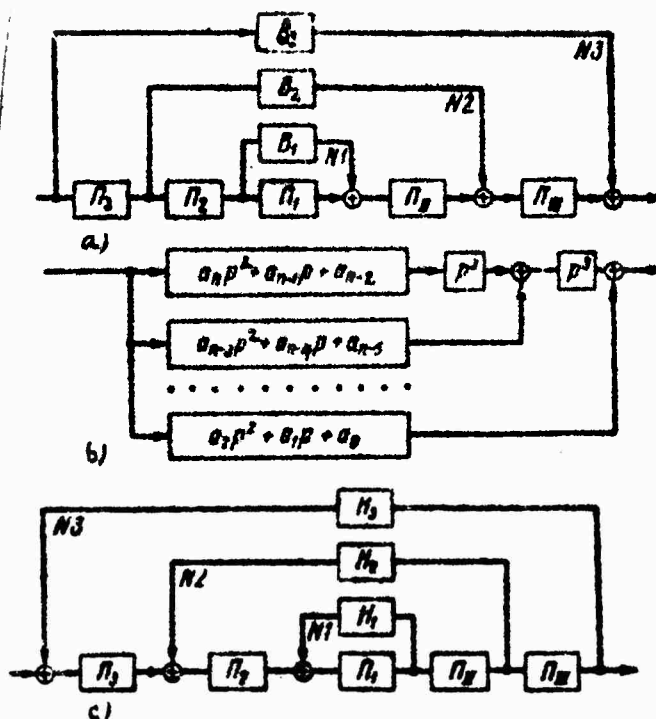
Fig 5-1. Contraction of circuits without cross connections.

In a number of cases it is necessary to calculate frequency characteristics equivalent to that transfer function; then if it is desired to use models it is necessary to factor the polynomial by transfer functions of not higher than the second order, for which models were constructed earlier. Such a factoring is obtained in the grouping of adjacent terms of the polynomial by threes and the removal from brackets of the lowest power for each group of terms:

$$R(p) = a_{n-2} p^{n-2} \left(\frac{a_n}{a_{n-2}} p^2 + \frac{a_{n-1}}{a_{n-2}} p + 1 \right) + \ldots +$$
$$+ a_0 \left(\frac{a_2}{a_0} p^2 + \frac{a_1}{a_0} p + 1 \right).$$

The structural circuit corresponding to this factoring is shown in Figure 5-1b.

Now for the construction of the general frequency characteristic it is sufficient to have models for each trinomial of the type $\tau^2 p^2 + 2\xi\tau p + 1$ or for the binomial $Tp + 1$, to increase the moduli of the logarithmic amplitude-frequency characteristic and phase in accordance with the factors a p^2, and then successively for each trinomial and the sum of the preceding trinomials to apply the nomogram $1 + W(j\omega)$ (Figure 4-28) or the P, Q-nomogram.

The transition to a matching-parallel circuit was used in Chapter 3 (Figure 3-7) to illustrate the role of the poles of the OFT. Such a matching-parallel circuit is equivalent to a cascade circuit obtained in summation of the elements of Figure 3-7, which, upon reduction of the fractions to the common denominator, forms the latter in the form of the derivative of the elementary factors, characteristic for a cascade circuit.

C. The Multi-Circuit Antiparallel Diagram

The contraction of Circuit 5-1c should be done by starting from the internal feedback circuit, subsequently applying the formulas of Chapter 1 for variable or constant coefficients. In the operator form of notation the general OFT of the circuit is most simply obtained on the basis of inversion of the circuit. Actually, the inverse OFT is equal to:

$$\frac{1}{W(p)} = -H_3(p) + \frac{1}{\Pi_3(p)} \left\{ -H_2(p) + \frac{1}{\Pi_2(p)} \times \right.$$
$$\times \left[-H_1(p) + \frac{1}{\Pi_1(p)} \right] - \frac{1}{\Pi_{11}(p)} \left. \right\} \frac{1}{\Pi_{111}(p)} .$$

If we reduce the right side to the common denominator, we find the direct OFT:

$$W(p) = \frac{\Pi_1(p)\Pi_2(p)\Pi_{11}(p)\Pi_3(p)\Pi_{111}(p)}{1 - H_1(p)\Pi_1(p) - H_2(p)\Pi_1(p)\Pi_2(p)\Pi_{11}(p) - H_3(p)\Pi_1(p)\Pi_2(p)\Pi_{11}(p)\Pi_3(p)\Pi_{111}(p)}$$

$$(5 \cdot 2a)$$

If we designate the product of the OFT's of all the components in each open circuit by the general operators:

(see next page)

$$C_1(p) = H_1(p)\,\Pi_1(p);$$

$$C_2(p) = H_2(p)\,\Pi_1(p)\,\Pi_2(p)\,\Pi_{11}(p);$$

$$C_3(p) = H_3(p)\,\Pi_1(p)\,\Pi_2(p)\,\Pi_{11}(p)\,\Pi_3(p)\,\Pi_{111}(p),$$

$$\left.\begin{array}{r}\\\\\\\end{array}\right\}\quad(5\text{-}2\text{b})$$

we get:

$$W_+(p) = \frac{\Pi_1(p)\,\Pi_2(p)\,\Pi_{11}(p)\,\Pi_3(p)\,\Pi_{111}(p)}{1 - C_1(p) - C_2(p) - C_3(p)}.$$

$$(5\text{-}2c)$$

For the case of all negative feedbacks

$$W_-(p) = \frac{\Pi_1(p)\,\Pi_2(p)\,\Pi_{11}(p)\,\Pi_3(p)\,\Pi_{111}(p)}{1 + \sum_{i=1}^{3} C_i(p)}. \quad (5\text{-}2d)$$

If we generalize the result on any number of circuits, we formulate the rule: the general OFT of a multi-circuit diagram with negative non-cross feedbacks is equal to the OFT of a direct channel divided by unity plus the sum of the OFT's of all the open circuits.

The partial case for a single circuit antiparallel diagram

$$W(p) = \frac{\Pi(p)}{1 + C(p)} \qquad (5\text{-}2e)$$

has already been discussed for the algebraized differential polynomial (1-78) and for the amplitude-phase characteristic (4-49).

5-2. Change of the Characteristics of Components by Additional Connections

A. An Aperiodic Component Spanned by a Feedback

1. Proportional Negative Feedback

If the feedback does not contain the operator components

$$H(p) = \pm k_{\text{H}},$$

it is called a proportional positive or negative feedback.

An aperiodic component with the OFT

$$K(p) = \frac{k_\text{п}}{Tp + 1} \,,$$

spanned by a proportional negative feedback, forms the circuit with the complete OFT

$$W_-(p) = \frac{k_\text{п}}{Tp + 1 + k_\text{п}k_\text{н}} \,. \tag{*}$$

Let us divide the numerator and denominator of the fraction by $1 + k_\text{п}k_\text{н}$ and designate

$$T_\text{э} = \frac{T}{1 + k_\text{п}k_\text{н}} \,; \tag{5-3a}$$

$$k_\text{э} = \frac{k_\text{п}}{1 + k_\text{п}k_\text{н}} \,. \tag{5-3b}$$

Then we will obtain a new aperiodic component with the OFT

$$W_-(p) = \frac{k_\text{э}}{T_\text{э}p + 1} \tag{5-3c}$$

with an equivalent amplification factor $k_\text{э}$ and an equivalent time constant $T_\text{э}$. The negative proportional feedback does not change the structure of the aperiodic component, but it decreases the amplification factor and increase the quick operation by reducing the time constant.

2. Proportional Positive Feedback

Let us define the total OFT of the circuit:

$$W_+(p) = \frac{k_\text{п}}{Tp + 1 - k_\text{п}k_\text{н}} \,. \tag{**}$$

As is evident from the obtained formula, the feedback coefficient has an effect on the sign of the free term of the denominator $a_0 = 1 - k_\text{п}k_\text{н}$. Let us consider the three possible cases of the ratio of the values 1 and $k_\text{п}k_\text{н}$, which we will distinguish according to the degree of compensation of the second term ($- k_\text{п}k_\text{н}$) and of the first, unity.

Incomplete compensation. When the compensation is incomplete, that is, at $k_n k_H < 1$, the structure of the component does not change; it remains a stable aperiodic component, but its amplification factor is increased:

$$k_\theta = \frac{k_n}{1 - k_n k_H} \qquad (5\text{-}4a)$$

with simultaneous increase in the time constant:

$$T_\theta = \frac{T}{1 - k_n k_H}, \qquad (5\text{-}4b)$$

that is, with increase of the rapid action.

Overcompensation. In the presence of overcompensation $k_n k_H > 1$ and for preservation of the positive sign in the parameters T_θ and k_θ of the component during transformation of the transfer function (**) the numerator and denominator of the fraction must be divided by the difference $k_n k_H - 1$. Then we get the transfer function of the overcompensated component

$$W_+(p) = \frac{k'_\theta}{T'_\theta p - 1} \qquad (5\text{-}5a)$$

with equivalent time constant and amplification factor

$$T'_\theta = \frac{T}{k_n k_n - 1}; \qquad (5\text{-}5b)$$

$$k'_\theta = \frac{k_n}{k_n k_n - 1}. \qquad (5\text{-}5c)$$

An overcompensated component, as is evident from the formulas, is a quasi-static first-order component.

Complete compensation. Complete compensation is observed in the fulfilment of the precise equality $k_n k_H = 1$. In that case the transfer function (**) assumes the form:

$$W_+(p) = \frac{k_n}{Tp}. \qquad (5\text{-}6)$$

that is, the aperiodic component in the presence of complete compensation by the positive feedback becomes an integrating component.

All the examined transformations become especially clear if the aperiod stable component is considered not as a primary element, but

as a circuit containing an integrating component k_π/Tp, spanned by the proportional negative feedback $1/k_\pi$. Then in the examples considered a supplementary external connection k_H is superposed on the existing internal connection $k_{int} = 1/k_\pi$, as shown in Figure 5-2a. Depending on its value, one degree or another of compensation is observed.

3. Flexible Feedback

If we investigate the case of spanning of an aperiodic component by a feedback on a derivative, called a flexible feedback, it is convenient to present the aperiodic component in the form of a circuit consisting of an amplifying component spanned by an internal negative feedback on the derivative $(T_1/k_\pi)p$, as shown in Figure 5-2b.
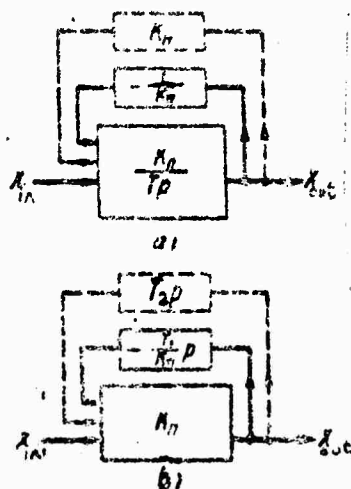
Figure 5-2.   Internal structure of an aperiodic component.

If we superimpose the flexible external feedback $\pm T_2p$ in parallel to the internal, we get:

$$W\,(p) = \frac{k_\pi}{1 + (T_1 \mp k_\pi T_2)\,p}. \qquad (5-7)$$

In the presence of a negative flexible feedback the component remains aperiodic with an increased time constant:

$$T_Q = T_1 + k_\pi T_2.$$

In the presence of a positive feedback the properties of the component depend on the degree of compensation, defined by the difference $T_e = T_1 - k_\pi T_2$.

Incomplete compensation, $k_\pi T_2 < T_1$ leads to increase in the rapid action of the component.

Complete compensation $k_\pi T_2 = T_1$ converts the aperiodic component into an amplifying component.

Overcompensation $k_\pi T_2 > T_1$ makes the component quasi-static (for the last two cases it is necessary to take into consideration additional small time constants -- see Section C).

Negative feedback on the integral. Spanning of an aperiodic component by a feedback with the transfer function $- (k_1/p)$ leads to the OFT of a real differentiating component

$$W(p) = \frac{k_n p}{p(Tp+1) + k_a k_u} , \qquad (5-8)$$

the parameters of which depend on the character of the poles.

B. An Operator Feedback at a Large Amplification
   Factor of the Direct Channel

Let the aperiodic component be spanned by a complex negative feedback

$$W_{fb}(p) = \frac{k_u}{\tau^2 p^2 + 2\xi\tau p^2 + 1} .$$

Then the general OFT of the circuit is reduced to the form:

$$W(p) = \frac{W_n(p)}{1 + W_n(p) W_{o.c}(p)} =$$

$$= \frac{\dfrac{k_n}{Tp+1}}{1 + \dfrac{k_a k_u}{(Tp+1)(\tau^2 p^2 + 2\xi\tau p + 1)}} .$$

Let us now direct the amplification factor of the direct channel toward infinity: $k_\pi \to \infty$; then unity in the denominator can be neglected and the general OFT is simplified:

$$\lim_{k_n \to \infty} W(p) = \frac{1}{W_{f.b}(p)} = \frac{1}{k_u}(\tau^2 p^2 + 2\xi\tau p + 1).$$

(5-9)

And so the general OFT of an antiparallel circuit with a large amplification factor of the direct chanel is roughly equal to the inverse OFT of a circuit with a negative feedback. In the example considered a second-order boosting component was obtained from the oscillating component by the method of circuit inversion. By an analogous method the differentiating and others can be obtained from the integrating component.

C. Extension of the Obtained Results to Other Components.
The Technique of Superposition of Connections.

When the amplifying component k_{π} is spanned by feedbacks the OFT of the circuit can be obtained from analogous formulas for an aperiodic component, by directing the time constant T toward zero.

Thus, according to (5-3c) for the case of a negative feedback we get from (*)

$$k_- = \lim_{T \to 0} \frac{k_n}{Tp + 1 + k_n k_u} = \frac{k_n}{1 + k_n k_u}. \quad (5\text{-}10a)$$

The same result can be obtained directly also by formula (5-2e), but for the case of positive feedback the use of formula (5-2e) is possible only for the case of under-compensation

$$C = k_n k_u < 1.$$

which gives:

$$k_+ = \frac{k_n}{1 - k_n k_u}; \quad (5\text{-}10b)$$

for the case of over-compensation, formula (5-5a) is retained:

$$k_+(p) = \frac{\dfrac{k_n}{k_n k_u - 1}}{\dfrac{T}{am}p - 1}, \quad (5\text{-}10c)$$

where T_{am} is a small time constant of the amplifying component, not taken into consideration when the positive connections are weak, but which can be manifested by deep positive connections, since in that case the amplifying component is put in unusual conditions -- transition across an infinitely large amplification factor and correspond-

ing jump of the output value in the presence of a limited controlling signal.
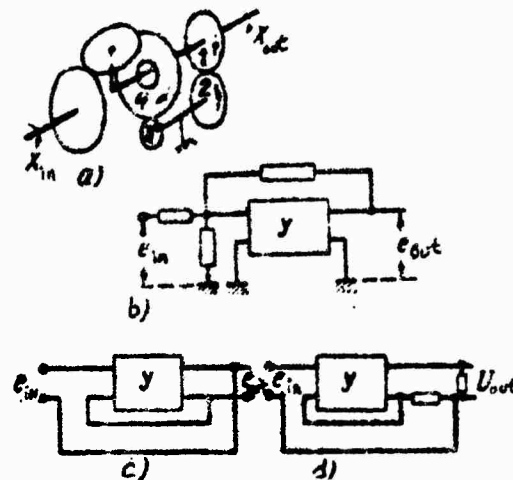
Fig 5-3. Amplifying components spanned by a feedback.

In Figure 5-3 examples are given of the superposition of feedbacks on some amplifying components. In the planetary transmission a the positive feedback is attained through gears 1 - 2, 3 - 4 and a differential; the approximation of the transfer coefficient $i =$ $= i_{1,2} i_{3,4}$ to unity, according to formula (5-10b), unlimitedly increases the transfer number x_{out}/x_{in}, but since the moment of resistance brought to the input shaft increases at the same time, then, starting at a certain moment the transmission is wedged. The value of the circuit is manifested in the inversion of the planetary transmission, when the inverse transfer number can be realized without wedging as small as desired.

For electric amplifiers the superposition of feedbacks is shown in diagrams b, c and d. An exact realization of formulas (5-10a) or (5-5) is observed only on the linear section of the characteristic of the amplifier until the signal falls in the zone of saturation.

2. The Integrating Component

The integrating component can also be considered as an aperiodic component, the internal feedback $1/k_{\pi} = k_i = 0$ of which was taken

as shown in Figure 5-2a. The superposition of the new external connections k_H returns the integrating component k_{-1}/p into the old state by forming, depending on the sign of the connection, a first-order aperiodic component or a quasi-static component

$$W_-(p) = \frac{k_{-1}}{p} = \frac{\dfrac{k_{-1}}{p}}{1 + \dfrac{k_{-1}k_H}{p}} = \frac{\dfrac{1}{k_H}}{\dfrac{1}{c}\,p + 1},$$

(5-11a)

where

$$c = k_{-1}k_H; \quad \frac{1}{c} = T; \qquad (5\text{-}11b)$$

$$W_+(p) = \frac{\dfrac{1}{k_H}}{\dfrac{1}{c}\,p - 1}. \qquad (5\text{-}11c)$$

In Figure 5-4 are examples of the superposition of feedbacks on integrating components of various types. If originally turning of the friction screw a displaced its roller from the center of the disc and caused limited rotation, switching in of voltage on the brush of the motor b caused its rotation at a constant speed and the displacement of its valves determined the rate of movement of the pistons, then after the imposition of negative feedbacks on the angle across the mechanical differential, on the voltage through the feedback potentiometer, upon travel through the arm connections of the first and second type, the components become static-aperiodic. In fact, on the feedback lines the increasing output value is subtracted from the controlling signal until the difference is reduced to zero or to such a small unbalance that the displacement on the output ceases, that is, the constant proportional output value corresponds to a constant controlling signal.

All the examined circuits in the presence of negative feedback have structure e.

3. The Oscillating Component

The general conclusions checked on an aperiodic component are:

Increase in rapid action and reduction of amplification in the presence of negative external feedbacks;

Reduction of rapid action and increase in amplification in the presence of positive feedbacks in the case of under-compensation:

Transition to a quasi-static regime in the presence of overcompensation of a positive connection;

Increase in rapid action in the presence of a positive connection on the first derivative.

These are also preserved for an oscillating component, as well as for many more complex components and control systems.

It is convenient to make a detailed analysis of the changes in the properties of a component for the case of rigid connections by the build-up of a circuit of the type in Figure 1-2, and for flexible connections by increase of the coefficients in the circuit in Figure 1-6. The new values of the parameters of the component thus obtained give exhaustive data on the properties of a component (see Section 3-13).
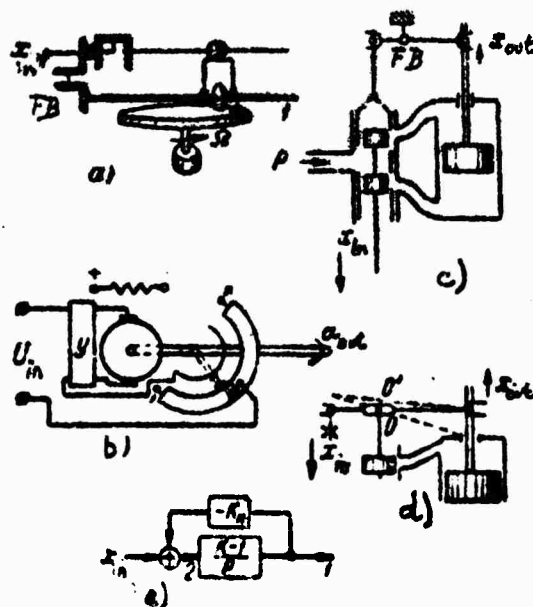
Fig 5-4. The scope of typical integrating feedback components.

D. The Transformation of a Structural Circuit for an Established Regime

If the constant input disturbance on the output of a system corresponds also to a constant output signal, its determination is made

$$W'(0) = W(p)_{p=0}. \qquad (^a)$$

Thus, after proof of the possibility of use of the limiting transition (*) $\big[$see the comments to (3-52), (3-53) and, in more detail, Chapter 11$\big]$ in the structural circuit it is sufficient to assume $p = 0$ in the transfer functions of all the components; by the same token the form of all the transfer functions is essentially simplified, and a number of branches of the structural circuit which contain transfer functions with zeros at the start of the coordinates (containing differential components), are simply eliminated from the circuit.

It is necessary to transform somewhat more carefully the sections of circuits which contain transfer functions with zero poles. Here the established regime is possible only when there is inclusion of similar components with negative feedbacks which form stable circuits (see Chapter 11).

If a component with a zero pole is in a direct circuit of a circuit with negative feedback, as shown in Figure 5-5a, substitution of $p = 0$ is equivalent to an infinite amplification factor of the circuit and on the basis of (5-9) we obtain the general transfer function
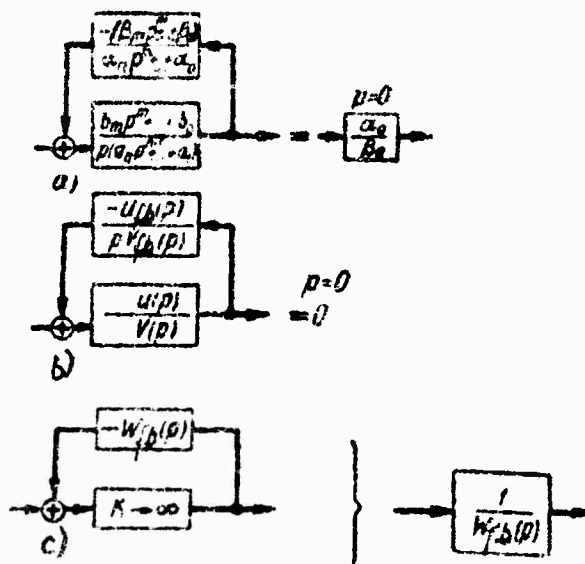
Fig 5-5. Transformation of a structural circuit for an
established regime.

$$W_{i-k}(p) = W_3(p)\,W_1(p). \qquad (5\text{-}13)$$

For the feedback circuit ($W_{i4} \neq 0$) in the same figure, the calculation of the function of the influence is done for given points of the input and output according to the general formula (5-2e), where the components disposed between the point of introduction of the disturbance and the point at which the reaction is investigated are considered the components of a direct circuit, and the remaining components fall into the feedback.
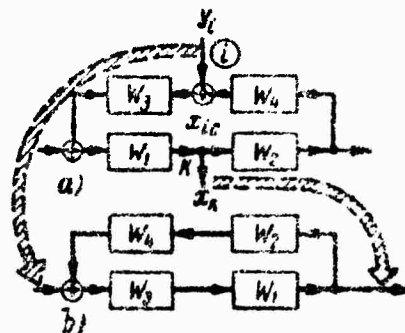
Fig 5-6. Rule of calculation of the conditions of transfer of disturbance.

In the designations of circuit b the function of the effect upon disturbance is

$$\Phi_{ik}(p) = \frac{W_3(p)\,W_1(p)}{1 - W_1(p)\,W_2(p)\,W_3(p)\,W_4(p)} =$$
$$= \frac{W_3(p)\,W_1(p)}{1 - C(p)}. \qquad (5\text{-}14)$$

It is possible to vary the calculation somewhat: by determining at the beginning the product of all the transfer functions of the open loop

$$C = W_1 W_2 W_3 W_4,$$

then finding the transfer function from the given external disturbance Y_i to reaction on the line of the input x_{ic}, but after the summator, that is, in a closed circuit, called the transfer function of the input:

$$\Phi_{ic}(p) = \Phi_*(p) = \frac{X_{ic}(p)}{Y_i(p)} = \frac{1}{1 - C(p)}; \qquad (5\text{-}15a)$$

for transition from reaction on the line of input of the disturbance

x_i to x_k, since the closed state of the system is already taken into consideration, it now is sufficient to use formula (5-13):

$$X_k(p) = W_{i-k}(p) X_{ie}(p). \qquad (5\text{-}15b)$$

For a better representation of the concept "direct channel" at arbitrary points of application of the disturbance and determination of the reaction from it, it is useful to present the system in the form of circuit 5-6b. In this line of input, the disturbance and reaction are transferred to the usual places on the left and right, and the summator for the input of the useful signal is excluded from consideration.

For solution of the problems of control and compensation for the disturbances the structure of the automatic control system is formed on the basis of definite principles. We will proceed to a consideration of them.

2. The Principle of Control of Deviation

In Figure 5-7a is shown a structural circuit of a system of control of deviation, based on utilization of the principle of inclusion of a direct channel of proportional feedback. For the simplest case, where the transfer coefficient in the feedback circuit equals -1, the transfer function of the entire system is

$$\Phi(p) = \frac{W(p)}{1 + W(p)}. \qquad (5\text{-}16a)$$

If we now examine the very simple case of application of disturbance on the output of the circuit, but within the feedback loop, the function of the influence is determined as

$$\Phi_{ie}(p) = \frac{1}{1 + W(p)}. \qquad (5\text{-}16b)$$

It can readily be seen that at a large amplification factor of the direct channel ($W \to \infty$) the influence of the disturbance on the deviation of the output value can be reduced to desired limits, but in principle the process of control proceeds under the influence of the deviation of the controlled value that arises from the action of the disturbance.

For established regimes, if $W(0) = k$, then

$$\Phi(0) = \frac{k}{1 + k}. \qquad (5\text{-}17a)$$

The right side of this formula can be expanded into the series:

$$\Phi(0) = \left(1 + \frac{1}{k}\right)^{-1} = 1 - \frac{1}{k} + \frac{1}{k^2} - \frac{1}{k^3} + \dots$$

(5-17b)

At an infinitely large amplification factor $\frac{1}{k} \to 0$, we get in the limit:

$$\lim_{k \to \infty} \Phi(0) = \Phi_e(0) = 1. \qquad (5\text{-}17c)$$

At a large, but finite amplification factor, the relative deviation of the static transfer coefficient is readily calculated from the series (5-17b), limiting with respect to the first two terms:

$$\frac{\Phi(0) - \Phi_e(0)}{\Phi_e(0)} \approx -\frac{1}{k}, \qquad (5\text{-}17d)$$

that is, the circuit is little sensitive to osciallations of the amplification factor of the direct channel, only if it were to remain large.

3. The Principle of Control of Disturbance

According to this principle it is necessary to measure, not the deviation, but the cause of it, that is, the disturbance, and on the basis of the measured disturbance to work out the compensating signal, adding it at various points of the structural circuit.
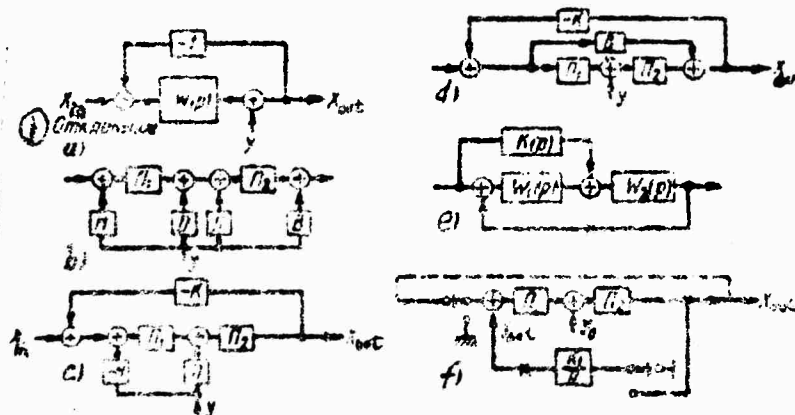
Fig 5-7. Circuits for compensation of disturbances.

1. Deviation

In Figure 5-7b are shown the circuit for input of disturbance through the transfer function $D(p)$ and the compensating circuits; on the line of the input of disturbance, in front along the course of the signal from the point of input of disturbance, and behind, counter to the course of the signal. The transfer functions of the compensating circuits equal $\Pi(p)$, $B(p)$ and $H(p)$ respectively.

The conditions of complete compensation of the action of disturbance are expressed by the following formulas:

$$\Pi(p) = - D(p); \qquad (5\text{-}18a)$$

$$B(p) = - D(p)\,\Pi_1(p); \qquad (5\text{-}18b)$$

$$\Pi_1(p)\,H(p) = - D(p). \qquad (5\text{-}18c)$$

The method requires measurement of each disturbance, the formation of a separate circuit for it, compensation and observance of stability of the compensating elements, due to which it yields to the first method and in the pure form finds very narrow practical application.

4. The Principle of Compensation of Disturbance by Internal Negative Feedbacks

Let us assume that the disturbance, as shown in Figure 5-7c, acts through the input transfer function $D(p)$. If there are no compensating connections ($-H$ and $-K$), the disturbance brings about on the output the reaction

$$\Delta_1 X_{out}(p) = D(p)\,\Pi_2(p)\,Y(p). \qquad (*)$$

If we introduce the proportional negative feedback $-K$ on an arbitrary section of the circuit, provided the connection includes the component with disturbance, we get a new value of the deviation on the output:

$$\Delta_2 X_{out}(p) = \frac{D(p)\,\Pi_2(p)}{1 + C(p)}\,Y(p), \qquad (**)$$

where $C(p) = k\Pi_1(p)\Pi_2(p)$.

If the amplification factor is increased on the local circuit $C(p)$, the absolute error $\Delta_2 X$ of $(**)$ can be made considerably smaller than $\Delta_1 X$ of $(*)$. But since the introduction of the circuit of connection converts the original transfer function of the useful signal $\Pi_1(p)\Pi_2(p)$ into the new OFT, $\Pi_1(p)\Pi_2(p)/1 + C(p)$, likewise reduced

by $1 + C(p)$, the relative increase in the level of the useful reaction on the background of reaction from disturbance is not attained, since

$$\frac{\lambda_{ou}(p)}{\Delta_1 \lambda_x(p)} = \frac{\lambda_{of}(p)}{\Delta_2 \lambda_{of}(p)} = \frac{\Pi_1(p)}{D(p)} \frac{\lambda_{in}(p)}{Y(p)} .$$

Therefore, if a feedback is introduced which reduces the reaction from disturbance and the useful signal, it is necessary at the same time to increase the scale of the input signal.

5. Combination of the Principles of Control of Deviation and Disturbance

Favorable results are attained in the combination of parallel compensating circuits with negative feedback circuits which include the point of application of disturbance.

If the parallel compensating line -H is added in circuit 5-7c, a combination of the method of control of disturbance with a local feedback is obtained.

If a compensation for disturbance is introduced into circuit 5-7d, where the feedback determines the basic properties of the automatic control system, the methods of control of deviation and of disturbance are combined. Thus dominating disturbance usually is eliminated, which facilitates the operation of the principal closed automatic control system and increases its accuracy.

6. The Principle of Compensation for Disturbance in a Closed System by Introduction of a Parallel Connection

In circuit 5-7d, without the parallel connection B, the function of the influence of disturbance is:

$$\Phi_1(p) = \frac{\Pi_2}{1 + \Pi_1 \Pi_1 k} = \frac{D_2}{1 + C_1} . \qquad (*)$$

If the parallel connection B is superimposed, we get the new function of the influence:

$$\Phi_2(p) = \frac{\Pi_2}{1 + C_1 + kB} = \frac{\Pi_2}{1 + C_1 + C_2} . \qquad (**)$$

The ratio of the new function of the influence to the old is determined as

$$\frac{\Phi_2(p)}{\Phi_1(p)} = \frac{1 + C_1(p)}{1 + C_1(p)} = \frac{1 + C_1(p)}{1 + C_1(p) + kB} . \qquad (5-13)$$

By increasing B this ratio can be reduced to the necessary value. It can readily be noted that the desired result is once more provided here by the presence of the main negative feedback. The parallel connection only increased the general effect of amplification of the circuit. Its place of application can be changed; for example, if connection B is applied directly before and after the point of introduction of the disturbance, we get $C_2 = K B \Pi_1 \Pi_2$.

7. The Principle of Combined Control of Open and Closed Cycles

Control of a closed cycle (of deviation) with supplementary introduction of a transformed input signal into the closed system is called combined control.

Let us determine the OFT of circuit 5-7e on the basis of the principle of superposition:

$$\Phi(p) = \frac{W_1(p) W_2(p)}{1 + W_1(p) W_2(p)} + \frac{K(p) W_2(p)}{1 + W_1(p) W_2(p)}. \quad (5\text{-}20a)$$

If the condition

$$K(p) W_2(p) = 1, \quad (5\text{-}20b)$$

is provided, the result

$$\Phi(p) = 1, \quad (5\text{-}20c)$$

is attained, that is, undisturbed transfer of the input with large rapid action is provided, since the feedback circuit in this transfer is not affected and is used only for the suppression of disturbance.

8. The Principle of Removal of the Influence of Disturbances by Periodic Alignments (Automatic "Zeroing")

The method is based on the inclusion in a section of the structural circuit, which has been subjected to the action of constant disturbance, of a short-period negative feedback containing an integrating component.

The principle of operation is illustrated in Figure 5-7f. It is evident from the diagram that along with the basic elements of the direct channel Π_1 and Π_2, between which the application of constant disturbance is assured, there is introduced into the circuit an additional negative feedback circuit is introduced on the integral $-(k_{-1}/p)$ which can be connected in to the principal channel by a switch. In the figure the circuit is depicted in the operating state, when the principal channel is closed and the integrating component has a zero

input or a constant output which compensates the action of disturbance Y_0.

In the state of "alignment" the contacts occupy the vertical position. In that case the input of the direct channel is fixed at zero, and the feedback on the integral is completely connected in.

Let us determine the signal on the output of the integrating component for the position of "alignment":

$$Y_{out}(p) = \frac{-\Pi_2 \dfrac{k}{p}}{1 + \Pi_1 \Pi_2 \dfrac{k_{-1}}{p}} \cdot \frac{Y_0}{p} =$$

$$= -\frac{\Pi_2 k_{-1} Y_0}{p^2 + \Pi_1 \Pi_2 k_{-1} p}, \qquad (5\text{-}21)$$

or for the regime being established we have:

$$Y_{out.est} = -\frac{1}{\Pi_1(0)} Y_0. \qquad (5\text{-}22)$$

In the operating position, when the input of the integrator is fixed at zero, the integrator operates as a remembering device by continuing to introduce into the direct channel the signal $-Y_0/\Pi_1(0)$, which provides compensation for the disturbance according to (5-18c).

Alignment of the circuit always is possible before the start of its operation, when a break of the direct channel is allowable, and in that case the alignment automatically removes such disturbances as the departures from zero of the amplifiers and other elements of the automatic control system. During the time of operation of the system a short-period regime of alignment is allowable only for systems of stabilization, sufficiently inertial that during the time when the direct channel is in the open state the operating regime of the automatic control system will not be substantially disturbed.

5-4. The Rule of Transformation of the Structural Representations and Structural Circuits

A. The transfer of nodes and summators through components with variable and constant parameters

The structural representation and the structural circuit obtainable from it when there is constancy of parameters of the components

can be transformed into a form very suitable for further investigation by very simple methods based on the rules of superposition and single directivity, which permit obtaining from a single structural representation-circuit a series of equivalent structural representation-circuits. We will give graphic explanations for these rules.

In Figure 5-8, diagrams a - d illustrate the equivalence of the input and output signals in the presence of various mutual arrangements of the nodes and summators. The non-equivalent sections of the channel of passage of signals on the circuits are hatched. Thus the mutual permutation of the summators creates an equivalent structure, since the sum does not vary from arrangement of the terms. The equivalence of the structures during mutual permutation of the nodes is based on insensitivity of the unidirectional circuit to changes in load. The displacement of the node by the summator and the reverse require, for equivalence of the structures, the introduction of additional lines of connection, shown in diagrams c and d.

Diagrams e and f illustrate the conditions of transfer of nodes and summators through linear components without disturbance of the equivalence of the transformed structure and the initial circuit shown in the center of the figure. This equivalence of the circuits is noted in the figure by an equal sign. During transfer of a summator across a component in the course of the signal or of a node across a component counter to the course of the signal, doubling components which re-establish a "drop in scale" at the necessary points of the additional channel are introduced into the additional channel. In the transfer of a summator across a component counter to the course of the signal or of a node along the course of the signal, neutralizing components are introduced into the additional channel which eliminate the "excess of scale" of the signal at the necessary points of the additional channel. If the components are not only amplifying but operator, it will be a matter not of scale but of the "drop" and re-establishment of the dynamic estimates.

In diagram e the additional channel was selected in the form of a loop of the boosting connection ϕC (feed of the signal ahead). When the boosting connection includes additional adjacent components and there is the compensation of the dynamic scales indicated above, an equivalence of the signals in provided on the input and output of the boosting component, on the input and output of the entire circuit and on most of the sections of the direct channel. The non-equivalent sections of the channel are hatched. If a closed system is examined instead of a direct channel, then by separating the node and summator for the boosting connection it is possible to reduce them to the input and output of a single component (M), lying on the "opposite" side of the loop (diagram e'). For this component m the boosting is transformed into a feedback. Here the equivalence in the transmission of the signal is disturbed on a rather large section of

399
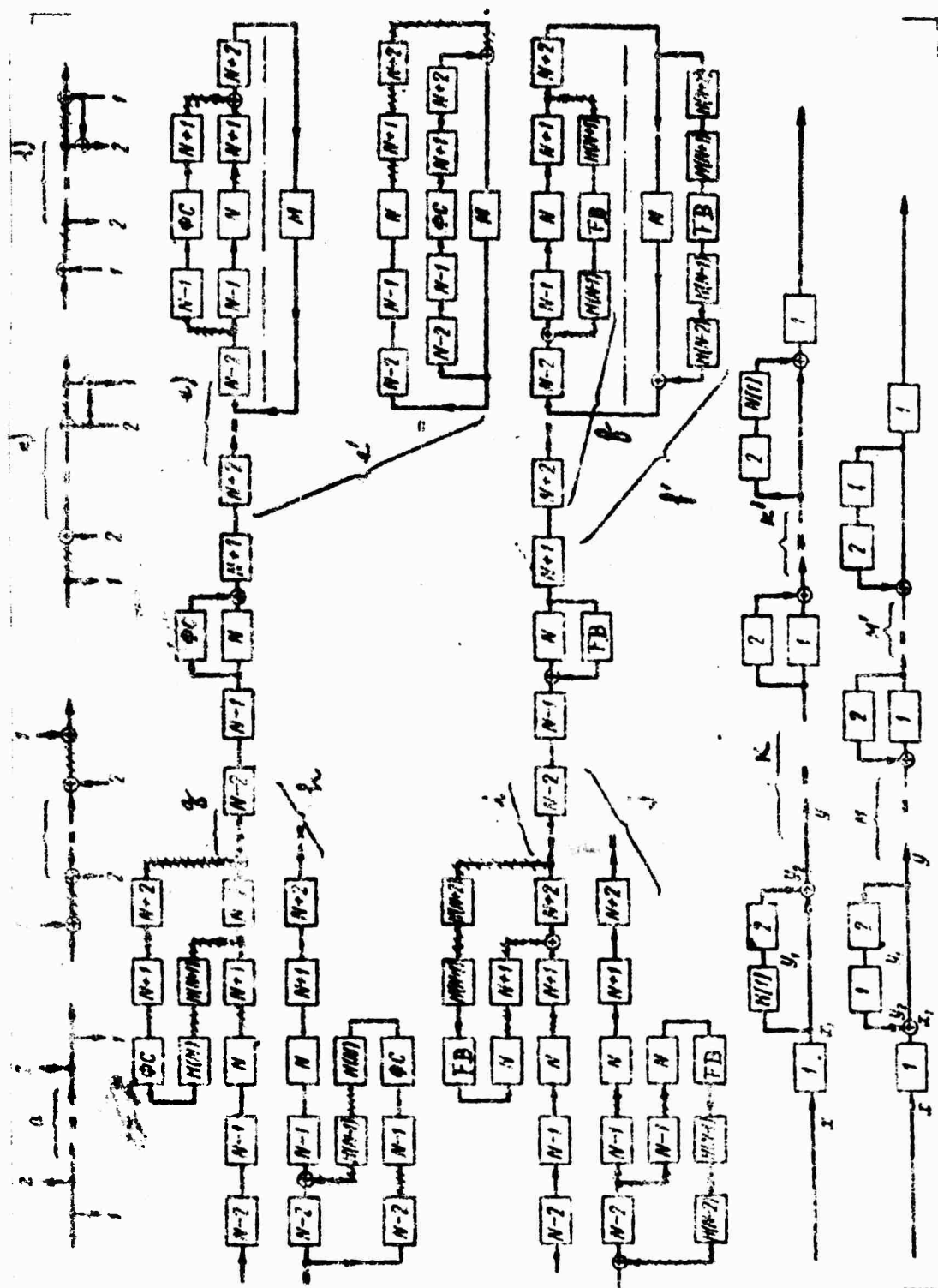
Fig. 5.8. Rules of transfer of nodes and summators.

the direct channel, but in the analysis of a closed circuit as a whole, for example for stability, circuits e, e' and the initial one are equivalents.

The feedback loop FB is examined in circuit f; its extension to adjacent components during observation of the above-indicated compensation creates equivalence of signals on the input and output of the feedback component, on the input and output of the entire circuit, and in a number of sections (unhatched) of the direct channel. If the ends of the feedback line are brought on the input and output of a single component M, located in the general circuit with the remaining components, then for that new component M the equivalent connection will be boosting (circuit f').

Thus, for example, for the stabilization circuit of an airplane around the center of mass (Figure 1-10), the feedback created by aerodynamic damping (extinguishing) moment can be replaced by equivalent boosting according to the conditions of transfer in the component of the autopilot.

In circuits g to j the ends of the boosting and feedback loops, that is, nodes and summators, are transferred to the new components along the open direct channel. The necessary doubling and neutralizing components are connected into the transformed circuits. If we by-pass any circuit along the course of the signal, it can readily be noted that the initial and neutralizing components, for example components $N + 2$ and $H(N + 2)$ in circuit i, are adjacent and mutually neutralized, by forming a single transfer coefficient; in the same way, components $N + 1$ and $H(N + 1)$ become adjacent in the same circuit, and likewise are neutralizing into unity. Thanks to this, equivalence of the initial and transferred circuits is created on the unhatched sections.

The methods of transfers of nodes and summators presented in Figure 5-8 have permitted obtaining a number of new equivalent circuits of the same class as the circuits given in Figures 1-14 and 5-1. The rules of contraction of similar circuits have already been examined above. However, these rules are inapplicable if the circuits contain cross connections. Then methods of transfers of nodes and summators become especially effective which we will examine in more detail separately for constant and variable components.

For components with constant parameters, Figure 5-8 serves as a structural diagram in each square of which can be written the transfer function of a component and its inversion for neutralizing components. In that case the transfer of the nodes and summators across a component is compensated for by the introduction into the side branches of direct (node counter to the course of the signal, summator along the course of the signal) and inverse (node on the signal, summator

counter to the signal) transfer functions of the omitted components. In that case, for circuits g, h, i and j the direct $W_{N \pm 1}(p)$ and

inverse $H\left[W(p)\right] = 1/W_{N \pm 1}(p)$ OFT's of the components, disposed sym-

metrically in the transformed circuit relative to the components ϕc and OC, are mutually cancelled out, and in the recalculation of the boosting connection or feedback, superimposed on the new component, only the direct $W_N(p)$, $W_{N+2}(p)$ and $W_{N-2}(p)$ or the inverse OFT of the original and the new component participate, and the remainder, which have been passed through in the transfer of the connection of the component, have no effect on the conditions of the recalculation, regardless of their number. Let us write out the complete values of the OFT in the transformed connections for each of the examined circuits.

Circuit g:

$$W_{\phi c+2}(p) = W_{\phi c}(p) \frac{W_{N+2}(p)}{W_N(p)} ;$$

circuit h:

$$W_{\phi c-2}(p) = W_{\phi c}(p) \frac{W_{N-2}(p)}{W_N(P)} ;$$

circuit i:

$$W_{fb+2}(p) = W_{fb}(p) \frac{W_N(p)}{W_{N+2}(p)} ;$$

circuit j:

$$W_{fb-2}(p) = W_{fb}(p) \frac{W_N(p)}{W_{N-2}(p)} .$$

Figure 5-8 is a structural representation with non-detailed given by its own equations, for components with variable parameters. If we have written them in the form of the ADP for the direct and neutralizing N-th component in accordance with (1-104), we will always arrive at expressions of the type:

Component N

$$a_N(t, D) x_{ot} = b_N(t, D) x_{in};$$

Component $H[N]$:

$$b_N(t, D) y_{out} = a_N(t, D) y_{in}.$$

In the same way as the constant components, the doubling components are introduced into the transformed connections during transfer of the node against the course of the signal or of the summator along the course of the signal, and the neutralising components during transfer of the node along the course of the signal or of the summator counter to the course of the signal, but the OFT will not be transformed here yet and the algebraized equations according to the rules of Section 1-9 and neutralization of components N and H$\boxed{N}$ are allowable only in the case of insertion into the interval between them of amplifying components which do not differentiate the coefficients into ADP's. The generality of the series of formulations for structural transformations in variable and constant components permitted the rules of transfer of nodal elements to be reduced to a single table.

Table 5-1   Equations of Additional Components that can be Inserted
in a Connection Circuit during Transfer of a Nodal
Element to a New Point of the Main Channel

Условия пере-носи узлового элемента ①	Тип узлового элемента ②	
	Сумматор ③	Узел ④
Переменные коэффициенты ⑤		
По ходу сигнала ⑥	$a(t, D)\, y = b(t, D)\, x$	$b(t, D)\, y = a(t, D)\, x$
Против хода сигнала ⑦	$b(t, D)\, y = a(t, D)\, x$	$a(t, D)\, y = b(t, D)\, x$
Постоянные коэффициенты ⑧		
По ходу сигнала ⑥	$W(p)$	$\dfrac{1}{W(p)}$
Против хода сигнала ⑦	$\dfrac{1}{W(p)}$	$W(p)$

1 - Conditions of transfer of the nodal element; 2 - Type of nodal element; 3 - Summator; 4 - Node; 5 - Variable coefficients; 6 - Along the course of the signal; 7 - Counter to the course of the signal; 8 - Constant coefficients.

The new rules, illustrated by Figure 5-8 and Table 5-1, permit a structural representation of any complexity to be reduced to an equivalent structural representation which allows multiple application of the rules of transformations examined in Section 1-9.

Let us apply these rules at first to relatively uncomplicated transformations of circuits with variable parameters, shown in the lower part of Figure 5-8.

In Figure 5-8 k' and k the transformation of a circuit according to a parallel connection into equivalent circuits is given.

Contraction of the equivalent circuit k requires:

1) cascading of components $H[1]$ and 2, given by equations

$$ b_1(t, D) y_1 = a_1(t, D) x_1 \text{ and } a_2(t, D) y_2 = b_2(t, D) y_1, $$

which after solution of the conditions of agreement with respect to the CADP's $\beta_1(t_1, D)$ and $\beta_2(t, D)$ gives analogously to formula (1-97b):

$$ \beta_1(t, D) a_2(t, D) y_2 = \beta_2(t, D) a_1(t, D) x_1; $$

2) addition of the two-component circuit with a single direct channel on the basis of the equation $y = y_2 + x_1$ or $y_2 = y - x_1$, which gives:

$$ \beta_1(t, D) a_2(t, D) y = [\beta_2(t, D) a_1(t, D) + \beta_1(t, D) a_2(t, D)] x_1 $$

3) cascading of (*) with component 1 again by formulas (1-97).

In Figure 5-8 the transformation of the antiparallel circuit is indicated by m and m'.

Contraction of the equivalent circuit m requires:

1) cascading of components 2 and 1 of the given equations

$$ a_2(t, D) y_1 = b_2(t, D) y \text{ and } a_1(t, D) y_2 = b_1(t, D) y_1. $$

which after determination of the CADP's $\alpha_2(t, D)$ and $\beta_1(t, D)$ gives:

$$ \beta_1(t, D) b_2(t, D) y = a(t, D) a_1(t, D) y_2; $$

2) contraction of the feedback circuit with the single direct channel on the basis of the formula $y_2 = y - x_1$, which gives:

$$[a_2(t, D) a_1(t, D) - \beta_1(t, D) b_2(t, D)] y =$$
$$= a_2(t, D) a_1(t, D) x_1; \qquad (**)$$

3) cascading of (**) with component 1.

Thus the most tedious operation -- finding the CADP's in circuits k and m -- is done only in the cascading of the components, which introduces a certain uniformity into the calculations.

In circuits k' and m' the interaction of the components with the single direct channel is accomplished on the input of component 1, but this leads to results equivalent to those for circuits k and m.

Transformations of a similar type permit preparing matching-parallel and antiparallel circuits with constant components for use of φ-nomograms in frequency analysis.

We will present further examples of the application of the rules of structural transformations in this section for the case of constant parameters.

B. Rules of Contraction of Cross Circuits and Obtaining Equivalent Circuits for Components with Constant Parameters

In Figures 5-9 to 5-12 are shown elementary cross circuits in which additional nodes or summators of the lateral channel, existing in the circuit, hinder the application of the rules.

The general rule for ridding a circuit of nodes or summators is the recommendation to transfer these elements across elements which have the same name -- nodes and summators, since in that case, in accordance with circuits a and b of Figure 5-8 there are no additional branches. However, sometimes, according to the conditions of transformations of complex circuits, it is necessary to violate this recommendation for their elements. Therefore in Figures 5-9 to 5-12 both cases of transfer are examined.

In Figure 5-13 are shown the conditions of transformation of a boosting connection circuit into a circuit of equivalent feedback, superimposed on the same component, in contrast with circuit 5-8e, where the connection was transferred into a new place. The inverse problem is solved in the same place.

In Figures 5-14 to 5-16 are given the equivalent transformations of multi-ray circuits which permit preserving all the input and output rays for subsequent analysis.
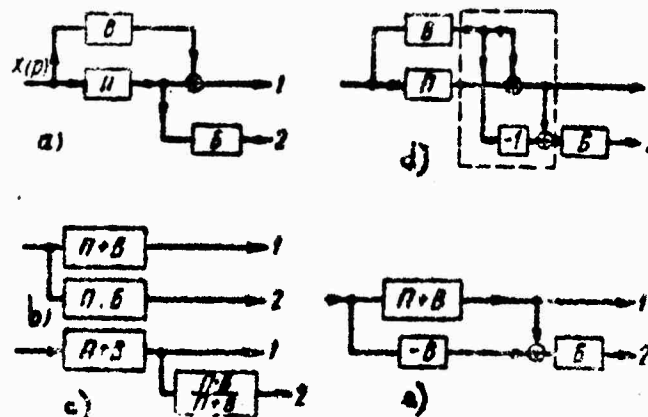
Fig 5-9. Transformations of a structural circuit during
removal of a node from the boosting circuit.
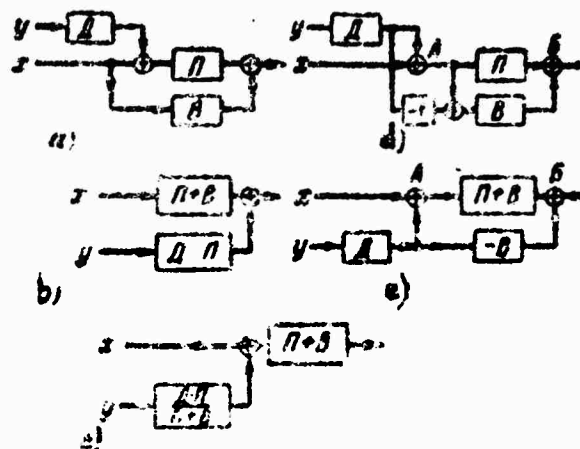
Fig 5-10. Transformations of a structural circuit during
removal of a summator from the boosting circuit.

C. Rules for Resetting of Components with Constant Parameters

In the cascade circuit (Figure 5-17a), the resetting in place
of any components, both adjacent and those separated from each other
by other components, is allowable if there are no nodes and summa-
tors between them, since the product is not changed by resetting of
the factors:

$$\Pi_1 \Pi_2 = \Pi_2 \Pi_1. \qquad (5\text{-}23)$$
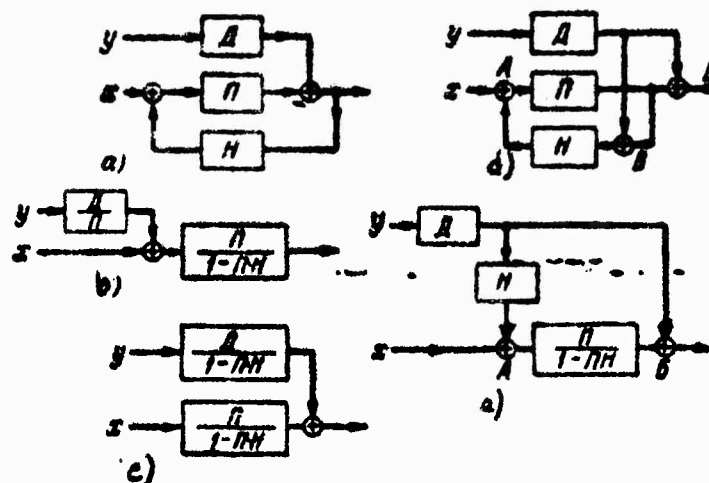
Fig 5-11. Transformations of a structural circuit during removal of a summator from the feedback circuit.
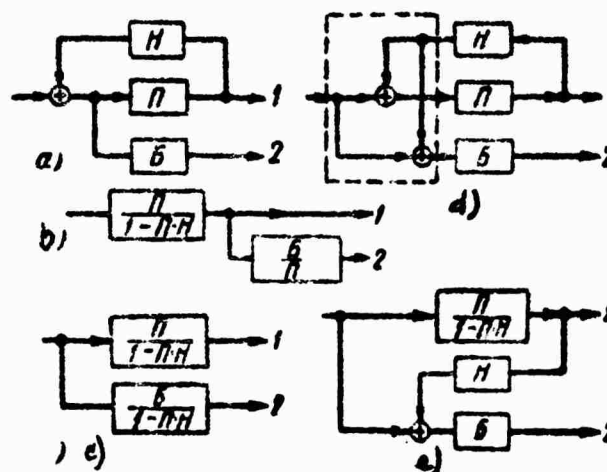
Fig 5-12. Transformations of a structural circuit during removal of a node from the feedback circuit.
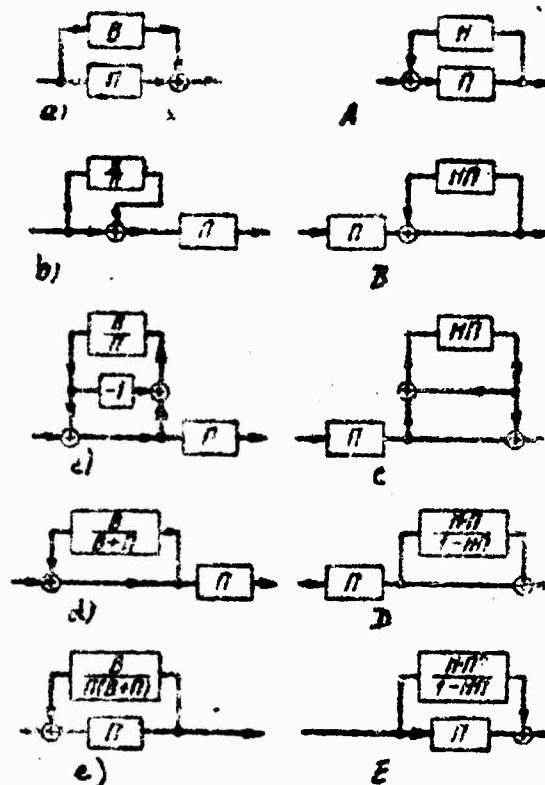
Fig 5-13. Transition from a matching-parallel circuit
to an antiparallel circuit and the reverse.

An equivalent of circuit a is presented in circuit A of the same figure. Here only the total transfer function for the entire line is preserved unchanged; the intermediate controlled values vary here, and if it is necessary to preserve them the transformation cannot be used.

In a circuit with a direct connection (Figure 5-17b), resetting of the transfer function of the direct circuit into the boosting circuit and of the transfer function of the boosting circuit into the direct circuit is allowable, since the sum is not changed by the re-setting of the terms:

$$\varPi + B = B + \varPi. \qquad (5\text{-}24)$$

Circuits b and B are equivalent, but again only for the total transfer function.

In the circuit with the negative feedback c, exchange of places
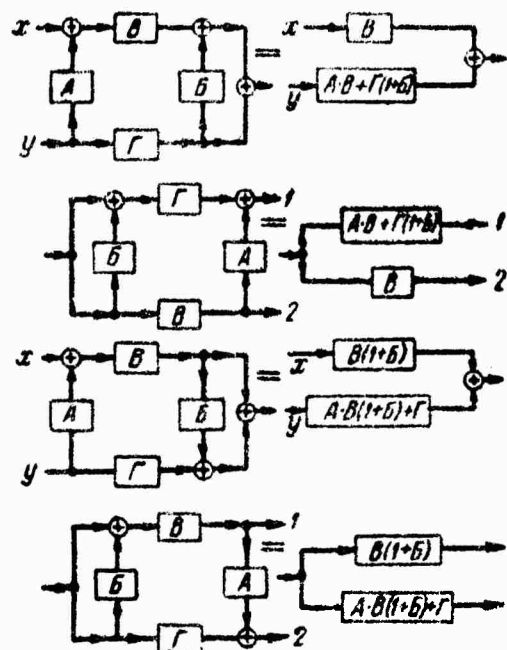
Fig 5-14. Structural transformations of three-ray match-
ing-parallel circuits.

of the components of the direct circuit and components of the feed-
back circuit is allowable during simultaneous inversion of the trans-
fer functions of the components, as shown in circuit C:

$$\frac{\Pi}{1+\Pi H} = \frac{\dfrac{1}{H}}{1 + \dfrac{1}{H}\dfrac{1}{\Pi}} . \qquad (5\text{-}25a)$$

In the circuit with positive feedback d the resetting of the
components from the direct circuit into the feedback circuit must
be accompanied by inversion of the transfer functions and change
of their sign:

$$\frac{\Pi}{1-\Pi H} = \frac{\left(-\dfrac{1}{H}\right)}{1 - \left(-\dfrac{1}{H}\right)\left(-\dfrac{1}{\Pi}\right)} . \qquad (5\text{-}25б)$$

For components with constant parameters, some part of the rules
presented in this Section have been published in the work of Gray-
bill /4/.

408
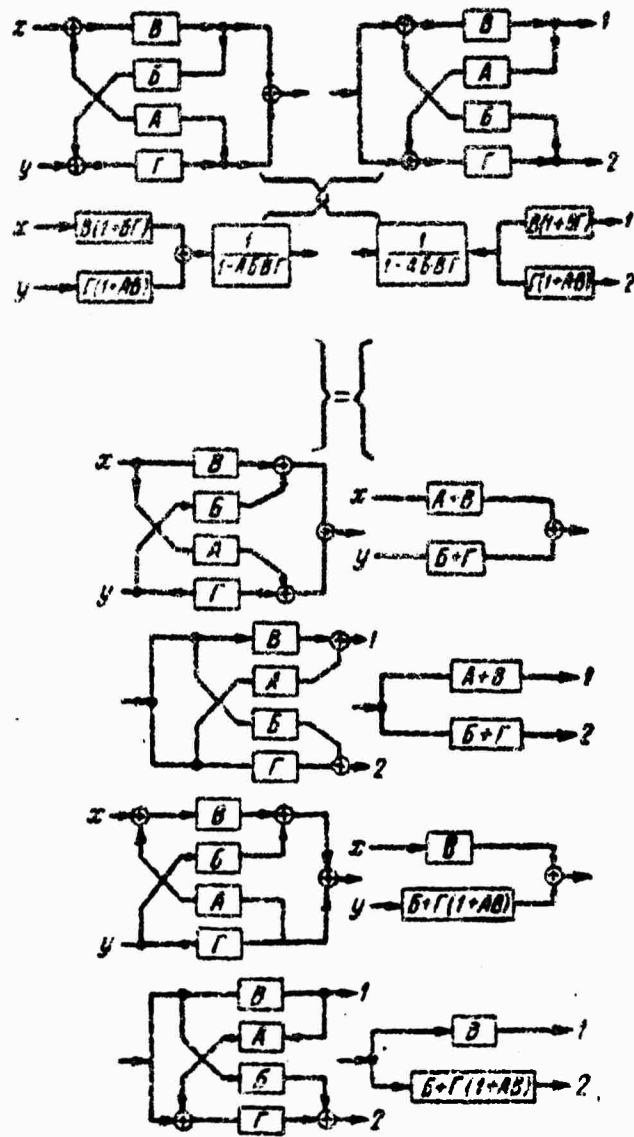
Fig 5-15. Structural transformation of three-ray cross
circuits.
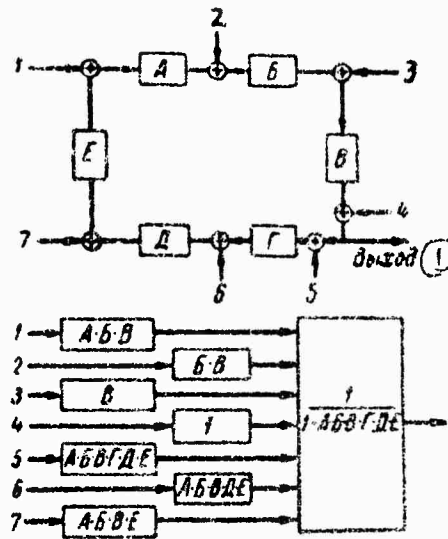
Fig 5-16. Structural transformations of a single-ray circuit. 1. Output
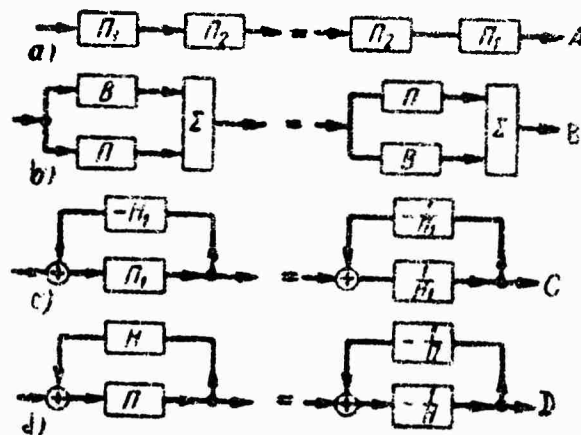
Fig 5-17. Conditions of the resetting of components.

5-5. Structural Representations of Systems of Equations with Variable Parameters

A. The Normal (Canonical) System

A system of n equations with variable coefficients can be written very compactly in the normal form:

$$\dot{x}_q = \sum_{h=1}^{n} a_{qh}(t)\, x_h + y_q \quad (q = 1, 2 \ldots n). \quad (5\text{-}26)$$

Here x_q is the unknown controlled values;

y_q is the known input actions;

$a_{qh}(t)$ is the variable coefficients forming the matrix A.

For a system of three equations the matrix has the form:

$$A = \begin{Vmatrix} a_{11} & a_{12} & a_{13} \\ a_{21} & a_{32} & a_{23} \\ a_{31} & a_{32} & a_{33} \end{Vmatrix}. \quad (5\text{-}27)$$

In Figure 5-18 a structural representation is shown, corresponding to this system, wherein the input value y_3 is introduced only in one (the third) equation: $y_1 = y_2 = 0$, and one (the first) of the unknown values x_1 is considered the principal output value. In the rectangles corresponding to the coefficients, only their numbers are indicated. The disposition of the coefficients in the circuit is assumed to coincide with their disposition in matrix A.

The operations on the given and unknown values are reduced to summation, multiplication by the variable coefficient and integration in accordance with (5-26), where each equation was brought to a conventionally solved form, which permits constructing at once the structural representation by repeating the principles of Figure 1-1 n times. Figure 5-18 can be used for the adjustment of the circuit of the matric electronic model, since all the lines of connection, summation blocks, blocks of variable coefficients and integrators (1/D) are marked in it. For constant coefficients the diagram of the operations coincides with the structural diagram according to which the representations are summated and multiplied by the function 1/p and the constant coefficients.

For generality of approach it is worthwhile also sometimes to present one summary equation of the system in normal form, considering it

as a special case of a system of n equation, where n is the order of the summary equation.
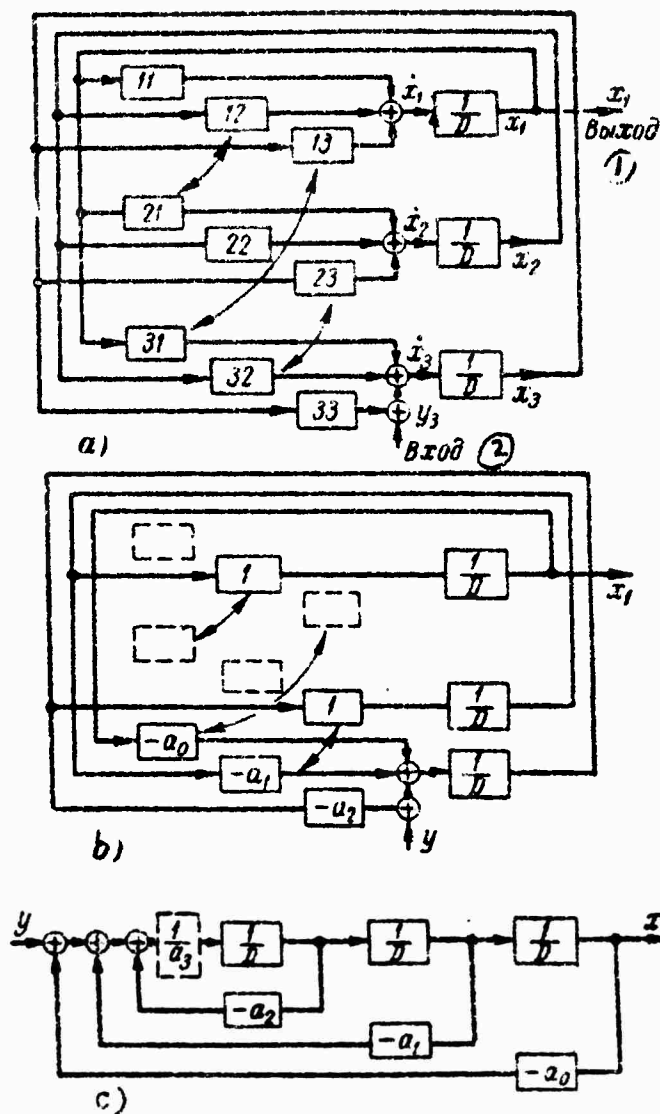
Fig 5-18. Structural representations for a canonical system of equations. 1 - Output; 2 - Input.

Thus, for an equation of the third order

$$\dddot{x} + a_2 \ddot{x} + a_1 \dot{x} + a_0 x = y;$$

by assuming $x = x_1$, introducing the designations $\dot{x}_1 = x_2$ and $\dot{x}_1 = x_2 = x_3$, we get a system of equations and a matrix of the coefficients in the form:

$$\dot{x}_1 = 0 + x_2 + 0;$$
$$\dot{x}_2 = 0 + 0 + x_3;$$
$$\dot{x}_3 = -a_0 x_1 - a_1 x_2 - a_2 x_3 + y;$$

$$A = \left\|\begin{array}{ccc} 0 & 1 & 0 \\ 0 & 0 & 1 \\ -a_0 & -a_1 & -a_2 \end{array}\right\|.$$

This corresponds to the structural representation (b) in the same Figure 5-18, drawn according to a matrix with a number of blank circuits.

The more compact structural circuit c, usually used in practice, in which for generality the unit coefficient $a_3(t)$ is not introduced, is equivalent to circuit b. Considering it a partial case of a circuit reflecting the system of equations is convenient for the subsequent transformations, for example, in transition to RC systems.

Along with the application of modeling of the system of equations (5-26) it is possible to solve on the basis of the method of balance of the partial representations. For this purpose we will replace all the unknown values x_h (h = 1, 2, 3) in the equations by the series (3-25c) and proceed to the representations:

$$\sum_{x=0}^{\infty} \frac{x_1^{(x)}(0)}{p^x} = \sum_{h=1}^{3} \sum_{k=1}^{1} (-1)^k a_{1hk} \frac{\partial^k}{\partial p^k} \sum_{x=0}^{\infty} \frac{x_h^{(x)}(0)}{p^{x+1}};$$

$$\sum_{x=0}^{\infty} \frac{x_2^{(x)}(0)}{p^x} = \quad \text{,} \quad a_{2hk} \quad \text{,} \quad$$

$$\sum_{x=0}^{\infty} \frac{x_3^{(x)}(0)}{p^x} = \quad \text{,} \quad a_{3hk} \quad \text{,} \quad$$

We will find the solution on the output x_1 during excitation of the system by a single impulse on the input $y_3 = \delta[\tau]$, that is, we will find the weight function $w_{31}[\tau, \vartheta]$, by using Table 3-3.

Balance for p^0

Checking balances for the highest powers of p shown equality of the coefficients at their zero, and therefore:

$$x_1(0) = 0;$$
$$x_2(0) = 0;$$
$$x_3(0) = 1.$$

Balance for p^{-1}

$$\dot{x}_1(0) = \sum_{h=1}^{3} a_{1h0} x_h(0) = a_{130};$$

$$\dot{x}_2(0) = \sum_{h=1}^{3} a_{2h0} x_h(0) = a_{230};$$

$$\dot{x}_3(0) = \sum_{h=1}^{3} a_{3h0} x_h(0) = a_{330};$$

the solution is written in the right column, with use of the results of the preceding balance.

414

$$\text{Balance for } p^{-2} \qquad \ddot{x}_1(0) = \sum_{h=1}^{3} [a_{1h1} \dot{x}_h(0) + a_{1h1} x_h(0)],$$

$$\ddot{x}_2(0) = \sum_{h=1}^{3} [a_{2h1} \dot{x}_h(0) + a_{2h1} x_h(0)];$$

$$\ddot{x}_3(0) = \sum_{h=1}^{3} [a_{3h1} \dot{x}_h(0) + a_{3h1} x_h(0)].$$

The further derivatives are determined on the basis of analogous balances, and the lines on the right side are formed from the columns of Table 3-8 with the corresponding power of p at $i = 0$, since on the right sides of the initial equations there are no derivatives.

Let us note that even when it is desired to find only the process x_1 it is necessary to calculate the derivatives from all n processes that enter the formulas of the balances.

E. Block System of Equations

The designations of the ADP adopted in Chapter 1 permit writing systems of linear equations with variable coefficients in a compact form:

$$
\left.
\begin{array}{l}
a_{11}(t, D) x_1 + a_{12}(t, D) x_2 + \ldots \\
\qquad \ldots + a_{1n}(t, D) x_n = b_{11}(t, D) y_1; \\
\quad \ldots \qquad \ldots \qquad \ldots \\
a_{n1}(t, D) x_1 + a_{n2}(t, D) x_2 + \ldots \\
\qquad \ldots + a_{nn}(t, D) x_n = b_{n1}(t, D) y_1.
\end{array}
\right\} \quad (5\text{-}28)
$$

where x_i represents the controlled values on the inputs and outputs of n interconnected blocks; y_1 is the input action; $a_{1k}(t, D)$ is the ADF characterizing the properties of the block. For explanation of the structure, let us limit ourselves to a system of three equations (1-92a). Let us separate in each equation of that system a single controlled value x_1, the index of which coincides with the number of the equation, and the lines

$$
\left.
\begin{array}{l}
a_{11}(t, D) x_1 = \\
\quad -[b_{11}(t, D) y_1 - a_{12}(t, D) x_2 - a_{13}(t, D) x_3]; \\
a_{22}(t, D) x_2 = \\
\quad = [b_{21}(t, D) y_1 - a_{21}(t, D) x_1 - a_{23}(t, D) x_3]; \\
a_{33}(t, D) x_3 = \\
\quad = [b_{31}(t, D) y_1 - a_{31}(t, D) x_1 - a_{32}(t, D) x_2].
\end{array}
\right\} \quad (5\text{-}29)
$$

Then each equation of system (5-29) becomes analogous to equation (1-4a), but with a complicated right side consisting of three groups of terms, each of which has a structural representation similar to b(t,D) in Figure 1-1. The transition on the left sides of system (5-29) to the form (1-11), conventionally solved with respect to x_1, x_2 and x_3, leads to structural representations of the type 1/a(t,D) on the same figure 1-1.

If we preserve the compact form of designation of the ADP and take into consideration the connections between the equations of system (5-29), we arrive at the structural representation shown in Figure 5-19, corresponding to the system of equations (1-92), which is readily developed for system (5-28).
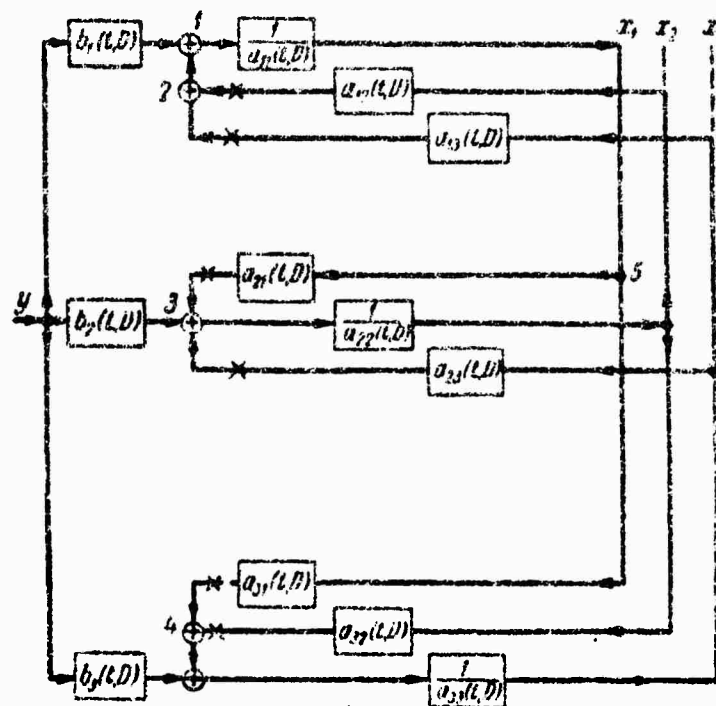
Fig 5-19. Structural representations for a complete system
of equations.

In Figure 5-19 is examined the case of action of only one disturbance y_1, which for generality enters into all the equations of the system.

In a number of practical cases each concrete disturbance can

enter only one equation of the system; then in the remaining equations the right sides are changed correspondingly.

5-6. Structural Equivalents of the Method of Non-Commutative Determinants

A. Convoluted Circuits for Certain Disturbances

Let a series of disturbances, y_1, y_2, and y_3, act on a system of equations describable by equations (5-29), where all of them enter each line of equations (5-29) with their ADP's in the following manner:

$$
\begin{aligned}
\Pi_1 &= b_{11}(t, D)\, y_1 + b_{12}(t, D)\, y_2 + \\
&\quad + b_{13}(t, D)\, y_3; \\
\Pi_2 &= b_{21}(t, D)\, y_1 + b_{22}(t, D)\, y_2 + \\
&\quad + b_{23}(t, D)\, y_3; \\
\Pi_3 &= b_{31}(t, D)\, y_1 + b_{32}(t, D)\, y_2 + \\
&\quad + b_{33}(t, D)\, y_3.
\end{aligned}
\qquad (5\text{-}30)
$$

If the adopted expressions for the right sides of Π_i are introduced into equations (5-29), it is possible to go over to the structural representation of the convoluted system shown in Figure 5-20, obtained on the basis of the method of non-commutative determinants.

The upper ray of circuit a, combined with the right block, form a program of convolution of system of equations (1-92a) or (5-29) into a single equation with respect to $x_n(t)$ during the action of $y_1(t)$ corresponding to notation of the solution in the form of (1-93).

The second ray of circuit a contains in the substituted determinant the new elements $b_{12}(t,D)$, and the determinant of the system, contained in the right block, remains without change. As a result the convoluted equation with respect to x_n and y_2 obtains a new right side. The total reaction on the output x_n from the series of actions is determined by the principle of superposition. If it is necessary to determine the reaction from a single disturbance on a number of outputs of a system of equations x_1, x_2, x_3, then in constructing a solution of type (1-93) it is necessary to substitute the ADP column of the determinant corresponding to the number of the output value x_1. Since the unknown controlled value is not excluded in the expansion of the non-commutative determinants, but remains in the transformations of the latter, then in the general case for various outputs the non-commutative determinants are expanded in various ways. The principal difference will be contained in the conditions of calculation of the new CADP's.
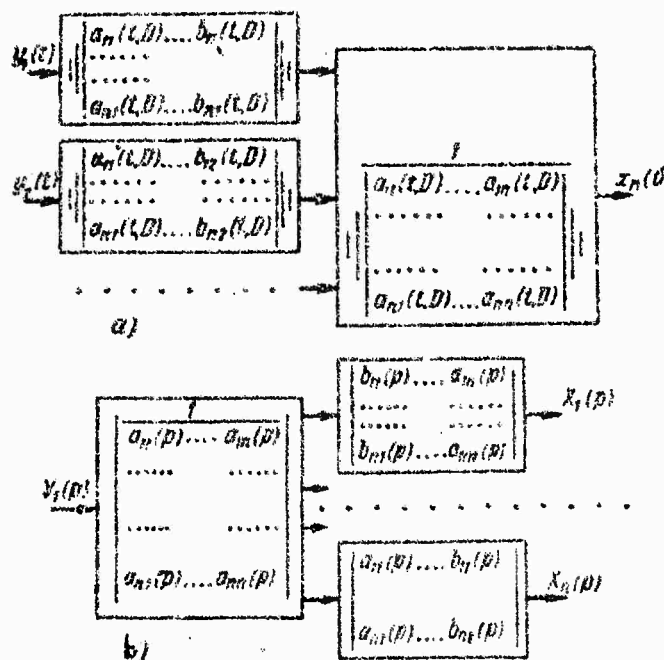
Fig 5-20. Calculation of the action of certain disturbances
on the total output of a system with variable parameters and
of a single disturbance on several outputs for a system with
constant parameters.

Thus, for each new output, circuit a is repeated with other sub-
stituted columns in the determinants of the rays and a new sequence
of expansion of the non-commutative determinants.

For systems with constant parameters it is possible to mention
circuit 5-20b, which illustrates the action of a single disturbance
y_1 on all the outputs x_1, x_2... x_n. In that case the determinant
of the system is expanded identically, independently of the number
of the substituted column in the right side.

An OFT block corresponding to an inverse determinant is shown
in circuit b on the left. Depending on the number of the output
being investigated, a corresponding column is substituted in the
determinant of the right side. In circuit b are shown two operator
blocks for the first and last outputs. In making up circuit b, use
was made of rule (5-23) for the resetting of the OFT, which permit-
ted making the structure very compact.

Each now investigated disturbance y_2, y_3 ... will pass through the operator block with the inverse determinant of the system, and then the blocks containing determinants with columns replaced by the ADP's relating to the given disturbance $b_{12}(p)$, $b_{13}(p)$ ...

B. The Exclusion of Intermediate Controlled Values by the Structural Method

Let the task be to construct a structural representation of a connected system in Figure 5-19 with exclusion of the controlled value x_1.

For compactness of the drawing let us limit ourselves to consideration of a system of three equations.

The sought circuit is constructed on the basis of the first step (1-94b) in the transformation of a non-commutative determinant of the system (1-92a), if one goes over again from it to the abbreviated system of equations (1-92b).

In Figure 5-21 a structural representation of a system which takes into consideration only the controlled values x_2 and x_3 has been constructed according to equations (1-92b). The disposition of the blocks in the figure coincides with the disposition of the coefficients of system (1-92b). As for the circuits in Figure 5-20, the inverse determinants with the ADP after their expansion must be understood in accordance with the right side of Figure 1-1. It is possible to arrive at the structural representation of Figure 5-21 from Figure 5-19 (for three controlled values) by applying the rules considered in Section 5-4 for elementary transformations of structural representations.
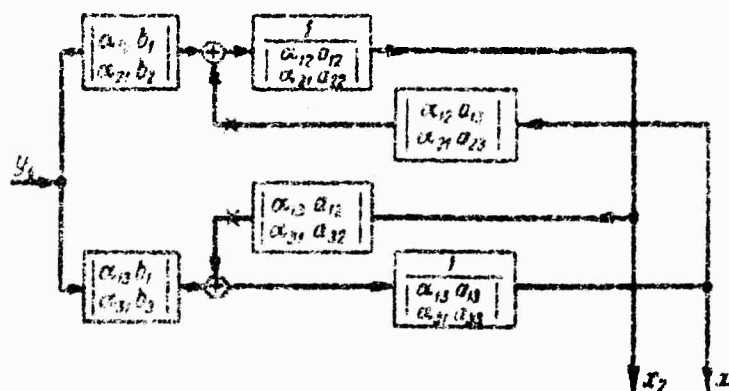
Fig 5-21. Structural representation of a system of equations with a single variable excluded by the analytical method.

A similar transition serves as an excellent example of the application of the mentioned rules, and therefore we will consider it in detail.

Thus, in the structural form presented in Figure 5-19, the exclusion of the controlled value x_1 by the methods of structural transformations is assumed.

The first step is the transfer of the summator 1 of the input action.

In Figure 5-19 we will transfer summator 1 to the outputs of components $b_2(t, D)$ and $b_3(t, D)$. On the way to component $b_2(t, D)$ we have the component $1/a_{11}(t, D)$, the node and the component $a_{21}(t, D)$. On the path to the component $b_3(t, D)$, the same component $1/a_{11}(t, D)$, the node and the component $a_{21}(t, D)$. The transfer goes along the course of the signal, and the components are doubled in accordance with circuits e and g of Figure 5-8 (right sides of the circuits); node 5 is overcome in accordance with rule d, that is, the summators fall into two branches. All this, along with the old blocks of input actions $b_2(t, D)$ and $b_3(t, D)$, retained in circuit 5-22, creates doubling circuits which end in the summators 1' and 1".

The second step is the transfer of summator 2.

We will transfer along the course of the signal summator 2 in Figure 5-19 through block $1/a_{11}(t, D)$; we will replace it by two summators: 2' and 2" during transition through node 5 and will further transfer summator 2' through component $a_{21}(t, D)$ and summator s" through component $a_{31}(t, D)$. In Figure 5-22 the new lines of connection from the controlled value x_2 end in these summators 2' and 2". Since with this value in circuit 5-19 there were connections through blocks $1/a_{22}(t, D)$ and $a_{32}(t, D)$. preserved also in Figure 5-22, the new connections include these blocks with reverse and direct circuits.

The third step is doubling of blocks $a_{13}(t, D)$ and $1/a_{11}(t, D)$.

Through the blocks $a_{13}(t, D)$ and $1/a_{11}(t, D)$ which remain after the first two steps the controlled value x_3 enters, after node 5, block $a_{21}(t, D)$ first and creates a new connection in parallel with component $a_{23}(t, D)$ and, secondly, block $a_{31}(t, D)$, embracing again by a created inverse connection component $1/a_{33}(t, D)$. These connections end on summators 3' and 4' of the transformed circuit 5-22.

For a system of control with constant parameters the structural representation in Figure 5-21 remains completely analogous, but in that case all the ADP's are independent of time $b_i(D)$, $a_{ik}(D)$, and upon substitution of $D = p$ Figure 5-21 goes over into the structural

420
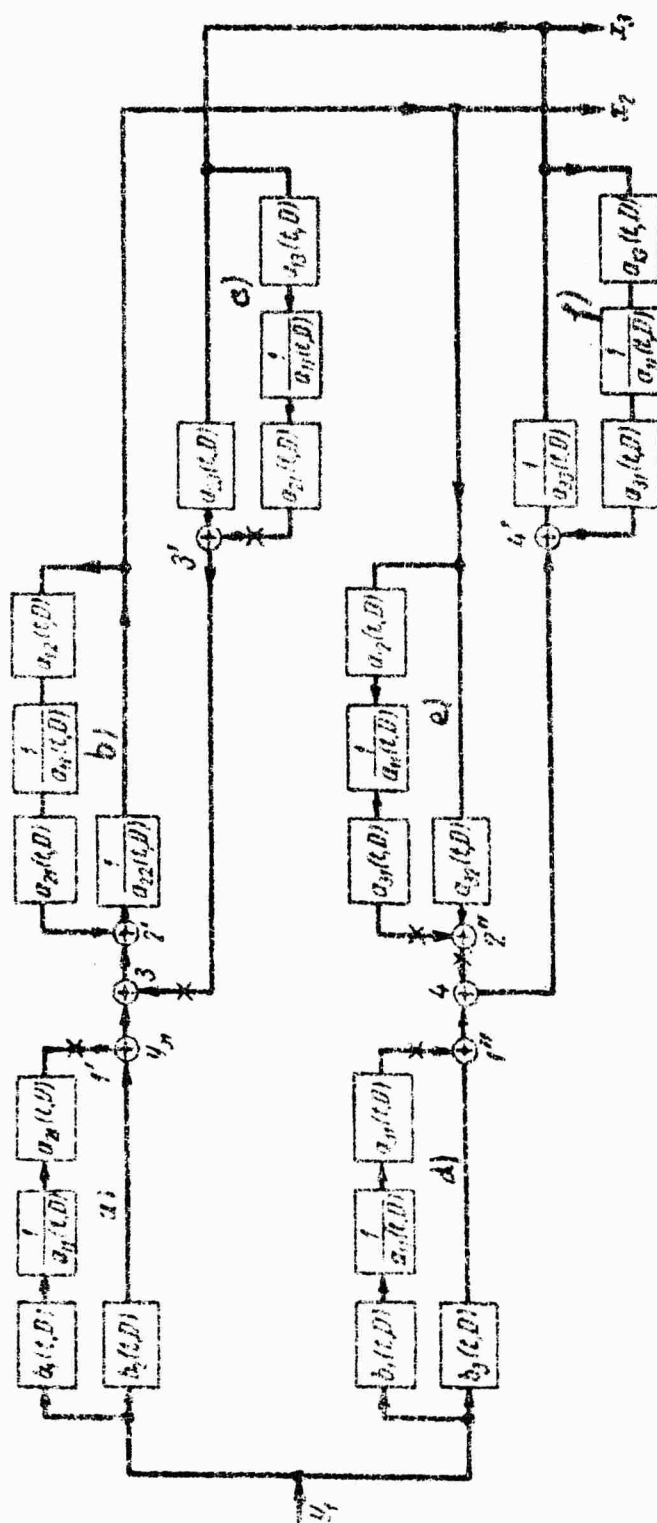
Fig 5-22. Structural representation of a control system with a single variable excluded by the structural method.

circuit.

In the structural circuit the local circuits a - f are readily convoluted into general OFT's equal to

$$A(p) = b_2(p) - \frac{b_1(p)\, a_{21}(p)}{a_{11}(p)} = \frac{1}{a_{11}(p)} \begin{vmatrix} a_{11}(p)\, b_1(p) \\ a_{21}(p)\, b_2(p) \end{vmatrix}.$$
$$(5\text{-}31a)$$

$$\frac{1}{B(p)} = a_{22}(p) - \frac{a_{21}(p)\, a_{12}(p)}{a_{11}(p)} = \frac{1}{a_{11}(p)} \begin{vmatrix} a_{11}(p)\, a_{12}(p) \\ a_{21}(p)\, a_{22}(p) \end{vmatrix}$$
$$(5\text{-}31b)$$

$$B(p) = a_{23}(p) - \frac{a_{21}(p)\, a_{13}(p)}{a_{11}(p)} = \frac{1}{a_{11}(p)} \begin{vmatrix} a_{11}(p)\, a_{13}(p) \\ a_{21}(p)\, a_{23}(p) \end{vmatrix}$$
$$(5\text{-}31c)$$

$$\Gamma(p) = b_3(p) - \frac{b_1(p)\, a_{31}(p)}{a_{11}(p)} = \frac{1}{a_{11}(p)} \begin{vmatrix} a_{11}(p)\, b_1(p) \\ a_{31}(p)\, b_3(p) \end{vmatrix}$$
$$(5\text{-}31d)$$

etc.

In a structural representation with variable ADP's the convolution of the circuits proceeds according to the rules of Section 1-9 with simultaneous solution of the equation of agreement for determination of the CADP

$$a_{12}(t, D),\ a_{21}(t, D),\ a_{13}(t, D),\ a_{31}(t, D).$$

Thus, for example, for the connection between the input value y_1 and the output value of summator 1' of circuit (5-21), y_{1e}, we get the equation

$$a_{12}(t, D)\, y_{1e} = \begin{vmatrix} a_{12}(t, D)\, b_1(t, D) \\ a_{21}(t, D)\, b_2(t, D) \end{vmatrix} y_1. \quad (5\text{-}32)$$

The determinant on the right side of the obtained equation coincides with the determinant written in the block in Figure 5-21; in exactly the same way the determinants obtained during convolution of the circuits in Figure 5-22 coincide with the determinants written in the remaining blocks in Figure 5-21. The additional CADP's $a_{12}(t, D)$ enter all the equations of the blocks and do not complicate system of equations (1-92b) during the formation of the sums on summators 3 & 4.

Thus the structural representations in Figures 5-21 and 5-22 are completely equivalent.

C. Combined Methods of Transformation of Structural Representations and Structural Circuits

In a number of cases it is simpler to make up a structural representation or a structural circuit than to write the complete system of equations of an investigated automatic control system.

The convolution of a structural representation (circuit) passes rather simply to a certain stage until the cross connections are prevented by transformations, and in that case it is possible to continue the transformations on the basis of the method of determinants.

It is possible to obtain a system of equations by the structure of the automatic control system, by writing the equations of all the summators and introducing into the equations only the controlled values on the nodes.

It is necessary to exclude one or several controlled values from the obtained system of equations on the basis of one or several steps in the expansion of the non-commutative determinants.

After any step in analytical transformations it always is possible to turn to a structural representation of the type of Figure 5-21.

Transformations by combined methods are fruitful for automatic control systems both with variable and with constant parameters.

5-7. RC-Structures for Systems of Equations

A. A Canonical System of Equations

The system of equations with variable parameters was characterized by a matrix of coefficients A (5-27).

The conjugate system of equations is characterized by a transposed matrix of coefficients A with changed signs:

$$- A. = \begin{vmatrix} a_{11} & a_{21} & a_{31} \\ a_{12} & a_{22} & a_{32} \\ a_{13} & a_{23} & a_{33} \end{vmatrix}, \qquad (5\text{-}33)$$

on which is composed a homogeneous system of equations for the new function g:

$$\dot{g}_q = -\sum_{h=1}^{n} a_{hq}(t)\, g_h. \qquad (5\text{-}34a)$$

A structural representation of a system with a transposed matrix (5-33) can be obtained in two ways:

1) Resetting of the blocks of coefficients in the structure of a canonical system, as shown by the two arrows in Figure 5-18;

2) exchange of places of the input and output during replacement of the nodes by summators and the reverse, which gives the circuit of Figure 5-23a.

Thanks to preservation of the matric disposition of the blocks of coefficients in the figures it is easy to satisfy oneself that the second way leads to the formation of the sum on the inputs of the integrators according to the elements of the columns, that is, actually transposes the matrix.

Consideration of conjugate systems in problems of automatic control is worthwhile in cases where it is important to know the state of the automatic control system at one given moment of time, for which it is sufficient to find the section of the weight function of the control system at $t = t_1 = \text{constant}$. It turns out that this section is obtained most simply from a solution of the conjugate system of equations under defined boundary conditions. Let us proceed to a determination of those conditions.

Let us multiply both parts of system of equations (5-26) by g_q, of system of equations (5-34) by x_q, and add them. Then on the left side we get the derivative of the product, and on the right side there remains only the transformed sum of the input actions.

$$\frac{d}{dt}\sum_{q=1}^{n} g_q x_q = \sum_{q=1}^{n} g_q y_q. \qquad (*)$$

To obtain a single point of the output reaction $x_c(t_1)$ at the moment of time t_1, we will integrate (*) in the limits $0 - t_1$:

$$\sum_{q=1}^{n} \left[g_q(t_1)\, x_q(t_1) - g_q(0)\, x_q(0) \right] =$$

$$= \sum_{q=1}^{n} \int_{0}^{t_1} g_q(\vartheta)\, y_q(\vartheta)\, d\vartheta, \qquad (**)$$
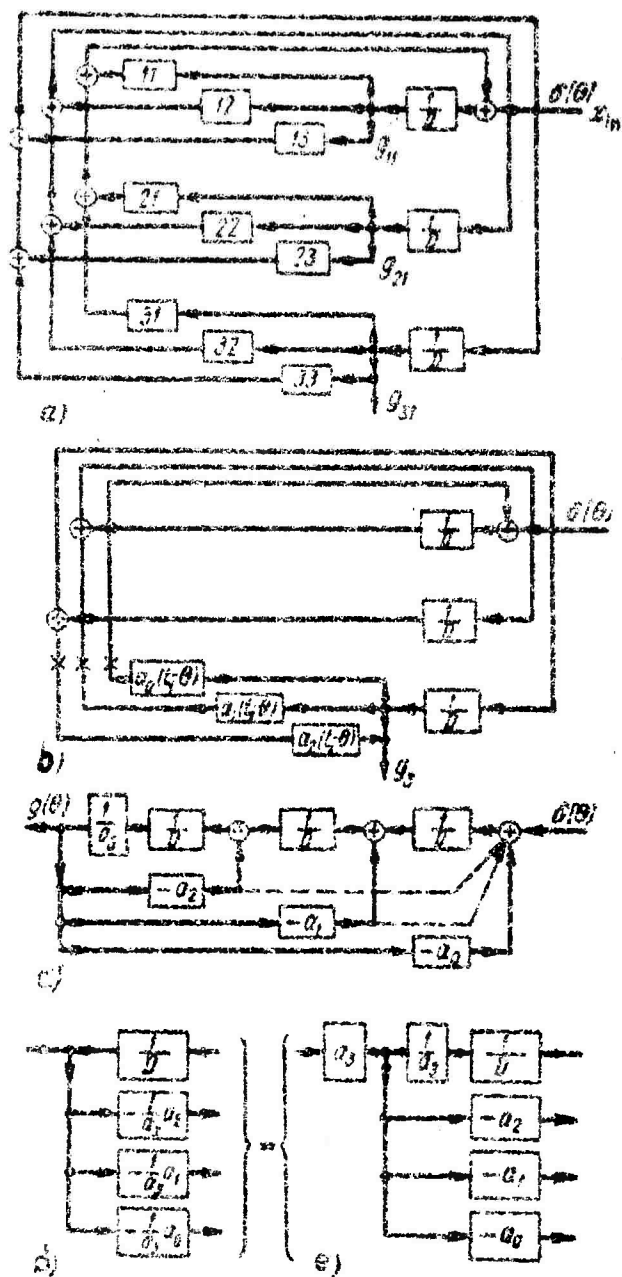
Fig 5-20. Canonical RC-Structures.

where under the sign of the integral the argument is replaced by ϑ, from which the value of the determined integral naturally did not vary.

In order to separate from the groups of x_q variables the solution with respect to any one value of x_e (in Figure 5-18, $e = 1$), it is sufficient to assume

$$g_e(t_1) = 1; \quad g_q(t_1) = 0 \text{ when } q \neq e. \qquad (***)$$

If, in addition, a system not previously excited is examined, for which, in accordance with (5-26)

$$x_q(0) = 0; \quad q = 1, 2 \ldots n, \qquad (****)$$

then integration of equations (**) gives:

$$x_e(t_1) = \sum_{q=1}^{n} \int_0^{t_1} g_{qe}(\vartheta) \, y_q(\vartheta) \, d\vartheta.$$

In order to fix strictly on which input of the structural circuit the disturbance is given and on which output the reaction is to be sought, a double indexation (q for input, e for output) must be introduced into the designation of the sought function g_{qe}.

Each action, for example $y_k(\vartheta)$ at $q = k$, brings about the partial reaction x_{ek} on the output:

$$x_{ek}(t_1) = \int_0^{t_1} g_{ke}(\vartheta) \, y_k(\vartheta) \, d\vartheta.$$

In Figure 5-18, $k = 3$, that is, $y_3 \neq 0$, but $y_1 = y_2 = 0$ and $e = 1$.

If we compare the latter equation with (2-46), it can readily be noted that

$$g_{ke}(\vartheta) = g_{ke}^{\triangledown}(t_1, \vartheta),$$

where according to Table 2-1 the index $\triangledown$ notes the variability of the second argument ϑ, that is, at the same time it is established that the section of the weight function of a system of equations with equations of connection (5-26) with the plane $t_1 = $ constant is a solution along the argument ϑ of conjugate system of equations (5-34a) under conditions (***).

It is possible to assign the value $g_{ka}(t_i) = 1$ to the conjugate system with the structure in Figure 5-23a by supplying the impulse $\delta(\vartheta - t_i)$ to its input at the moment of time t_i. The system is assumed to be unexcited prior to the supplying of the impulse; the time of supplying of the impulse agrees only with the values of the variable coefficients $a_{hq}(t_i)$.

Further calculation of the process $g^{\nabla}(t_1, \vartheta)$ along the argument ϑ is needed in the interval from $\vartheta = t_1$ to $\vartheta = 0$, that is, on the side of diminution of ϑ, and therefore it is worth while introducing the reversed argument $\Theta = t_1 - \vartheta$.

If we go over from the homogeneous system of equations (5-34) to a heterogeneous one containing the impulse on the right side of the n-th equation, introduce the new argument Θ -- reverse-displacement, which varies on the reverse side in relation to the initial argument ϑ, and in addition substitute $a_{hq}(\ ) = a_{hq}(t_1 - \ )$, as well as

$$\frac{\partial g}{\partial \vartheta} = -\frac{\partial g}{\partial \Theta},$$

we get the new system of RC-equations:

$$\frac{\partial g_{li}(t_1, \Theta)}{\partial \Theta} = \sum_{h=1}^{n} a_{hq}(t_1 - \Theta)\, g_{hl}^{*}(t_1, \Theta) + \delta(\Theta);$$

$$(5\text{-}34б)$$

$$\frac{\partial g_{ql}^{*}(t_1, \Theta)}{\partial \Theta} = \sum_{h=1}^{n} a_{hq}(t_1 - \Theta)\, g_{hl}^{*}(t_1, \Theta);$$

$$q = 1, 2 \ldots \neq l,$$

where the index * according to Table 2-1 notes the variability of the second argument $-\Theta$.

The structural circuit for this system of equations at $n = 3$ is given in Figure 5-23a.

In the solution of this system are contained all the weight functions $g_{ql}^{*}/t_1, \Theta)$ from any input to the output $x_{out} = x_1$ in accordance with Figure 5-18, including the unknown function g_{kl}^{*} at $q = k$.

Let us note that the minus signs that exist in accordance with the derivation can be mutually cancelled in the derivatives and in the coefficients of (5-33); therefore the system of equations in the region of the argument Θ has a simply transposed matrix (5-33) with-

out change of the sign. An electronic model can be adjusted according to this circuit. Let the model be realized by the introduction of an impulse on the input of an integrator, the output of which is $g_2/t_1, \Theta)$ (in the given example $g_2 = g_{31}$ is sought and the integrator is used along the line g_1), or previous assignment of the initial condition $g_2/t_1, \Theta) = 1$ directly on the output of the integrator. In that case the blocks of the variable coefficients must be rotated from the moment t_1 to the side of decrease of the argument.

System of equations (5-34b) can be solved by the analytical method of balance of the partial representations. The solution gives the sought section of the weight function along the argument Θ.

If the system of canonical equations under consideration is reduced to a single equation which can be reflected by the structural circuits b and c in Figure 5-18, the RC-system in that case also is obtained by transposition of the matrix of coefficients containing a number of empty (zero) cells.

As also on the complete structural circuit a, the transition to the RC-structure can be attained in two ways. In Figure 5-18b the conditions of resetting of the coefficients are shown by double arrows. In this a portion of the circuits is cancelled out during the replacement of the non-zero coefficient by a zero coefficient (the dotted rectangles), and a portion of the circuits is regenerated during the inverse substitution. Analogously to the complete system, the RC-structure also is obtained during exchange of places of the input and output and replacement of the nodes by summators, as shown in Figure 5-23b.

If the integrators are disposed in a single line, it is possible to go from circuit b to circuit c $(a_3 = 1)$. This also is transposed in relation to circuit c in Figure 5-18, that is, its matrix is changed:

$$A = \begin{Vmatrix} 0 & 0 & -a_0 \\ 1 & 0 & -a_1 \\ 0 & 1 & -a_2 \end{Vmatrix}.$$

Calculation of the additional coefficient $a_3(t)$ is explicable on the example of third-order equations:

$$a_3(t)\,\dddot{x} + a_2(t)\,\ddot{x} + a_1(t)\,\dot{x} + a_0(t)\,x = y. \qquad (*)$$

We will transform it to the normalized form:

$$\ddot{x} + \frac{a_2}{a_3}\ddot{x} + \frac{a_1}{a_3}\dot{x} + \frac{a_0}{a_3}x = \frac{1}{a_3}y \qquad (**)$$

or to the new formula:

$$\ddot{x} + a''_2(t)\ddot{x} + a''_1(t)\dot{x} + a''_0(t)x = y''.$$

for which it has been proved that the RC-system in circuit 5-23b, excited by the single impulse $\delta[\Theta]$, gives the section of the weight function g^*/t_1, $\Theta)$.

Let us now construct the structural circuit according to equation (**). Since the forms of the connections remain the old ones, we will limit ourselves only to consideration of the lines and elements close to the node, as indicated in Figure 5-23d. On the basis of the rules of transformation of structural circuits we will divide the coefficient $1/a_3(t_1 - \Theta)$, common to all three lines, into the individual component and transfer it through the node, which leads to circuit e in the same figure.

Since the final problem is to find the section of the weight function corresponding to equation (*) with the input value y, it is necessary to take into consideration that the single impulse $y[t] = \delta[t - \mathfrak{A}]$ on the right side of equation (*) corresponds to the impulse of the area $1/a_3(\mathfrak{A})$ on the right side of equation (**). If a single impulse is given on the right side of equation (**), the solution will be the relief of the weight function of equation (*) on a scale increased by $a_3(\mathfrak{A})$ times.

Such a change of scale for the sections $\mathfrak{A} =$ constant naturally relates also to the entire relief. In order to return to the sought relief, it is necessary to divide the solution of equation (**) during such action by $a_3(\mathfrak{A})$. On a structural circuit which gives the section of the weight function, this is equivalent to introduction of a component with the coefficient $1/a_3(\mathfrak{A})$, which cancels out the coefficient of the output block of circuit 5-23e and it is reduced to circuit c.

If in this circuit, as shown by the dotted lines, all the connections are now transferred to a single summator, it is possible to write the equation of this summator:

$$\sum_{i=0}^{3} D^i_* [a_i(t_1 - \theta) g^*[t_1, \theta)] = \delta[\theta],$$

which coincides with (2-51a) at $n = 3$.

Thus it has been shown that the general RC-equation (2-51a), obtained in Chapter 2 for a system with a single output and input, is a partial case of an RC system of equations.

B. A Block System of Equations

A Cascade Circuit

Let us write the equation of the blocks in Figure 5-24 in canonical form:

$$\left.\begin{aligned} \dot{x_1} &= a_{11}x_1 + a_{12}x_2; \\ \dot{x_2} &= a_{21}x_1 + a_{22}x_2 + y; \end{aligned}\right\} \tag{5-35}$$

$$\left.\begin{aligned} \dot{x_3} &= a_{33}x_3 + a_{34}x_4; \\ \dot{x_4} &= x_1 + a_{43}x_3 + a_{44}x_4. \end{aligned}\right\} \tag{5-36}$$

Here the blocks selected are not of higher than the second order, which does not disturb the generality of the derivation. The control values x_1 and x_2 are used for the first block, and x_3 and x_4 for the second block, which facilitates a single numbering of the equations in both blocks and unifies the designations of the variable coefficients.

The output value of the first block is designated x_1; it is obtained after integration of the first equation. The input action is introduced into the second equation of the block (in the general case in the last equation of the canonical form for each block).

The output value of the second block is designated x_3; x_1, introduced into the second equation of block (5-36), serves as the action for the second block. Together, (5-35) and (5-36) form a single system of equations of the automatic control system. The matrix of coefficients given in Figure 5-25a was constructed on this system of equations. One can readily note in the matrix a grouping of the coefficients from the equations of each block and separately the coefficient + 1, reflecting the connection between the blocks.

In the transition to the RC-system the matrix is transposed, as shown by arrows in the figure, and equations (5-35) and (5-36) acquire the appearance of (5-34b) in expanded form:

See (5-37) on page 432.

The concretization of the general formula (5-34b) was determined in the given example by the conditions $l = 3$ (since the output value x_3 is determined from the third equation of the system) and $k = 2$
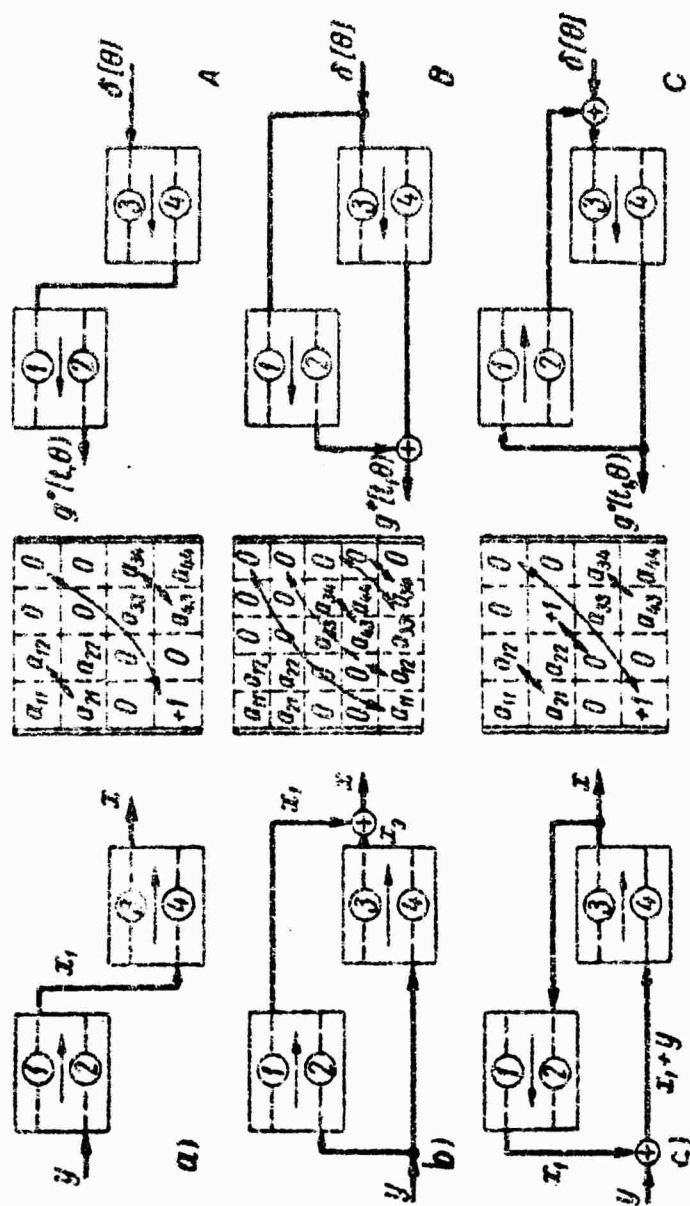
Fig 5-24. The obtaining of block RC-structures.

$$\dot{g}_1^* = a_{11}(t_1 - \theta)\,g_1^* + a_{21}(t_1 - \theta)\,g_2^* + 0 \qquad + g_1^*$$
$$\dot{g}_2^* = a_{12}(t_1 - \theta)\,g_1^* + a_{22}(t_1 - \theta)\,g_3^* + 0 \qquad + 0$$
$$\dot{g}_3^* = 0 \qquad + 0 + a_{33}(t_1 - \theta)\,g_3^* + a_{43}(t_1 - l)\,g_4^* + \dot{s}[\theta]$$
$$\dot{g}_4^* = 0 \qquad + 0 + a_{34}(t - \theta)\,g_3^* + a_{44}(t_1 - \theta)\,g_4^* .$$

$$\text{(5-37)}$$

$$\dot{g}_1^*[t_1,\theta] = a_{11}(t_1 - \theta)\,g_1^* + a_{21}(t_1 - \theta)\,g_2^* + 0 + 0 + \delta[\theta];$$
$$\dot{g}_2^*[t_1,\theta] = a_{12}(t_1 - \theta)\,g_1^* + a_{22}(t_1 - \theta)\,g_2^*;$$
$$\dot{g}_3^*[t_1,\theta] = 0 + \quad 0 \quad + a_{33}(t_1 - \theta)\,g_3^* + a_{43}(t_1 - \theta)\,g_1^* + \dot{s}[\theta];$$
$$\dot{g}_4^*[t_1,\theta] = 0 + \quad 0 \quad + a_{34}(t_1 - \theta)\,g_3^* + a_{44}(t_1 - \theta)\,g_4^* .$$

$$\text{(5-39a)}$$

(since the input action y_2 is given in the right side of the second equation of the system) corresponding to Figure 5-24a. In the RC-circuit of 5-24a, therefore, the impulse is given in the right side of the third equation and the solution $g_2^x(t_1 - \Theta)$ is obtained as a result of integration of the second equation of the RC-system (5-37).

The transformation of the matrix of the entire circuit can be considered as a separate transposition of the matrices in each block and change of the conditions of connection, brought about by the transition of the coefficient of connection + 1 into the first line. This leads to RC-circuit A, where the directions of the signals are changed even in the components formed by the RC ADP together with the ADP.

A Matching-Parallel Circuit

In circuit 5-24b, if it is excited by an impulse, a weight function equal to the sum of the two weight functions of each block is formed on the output x. The series of functions displayed along the argument t forms a relief which also can be considered to consist of two layers of terms. In considering the reaction of the RC-system to the impulse we arrive at the same relief and the same two layers here give sections at variable Θ and constant t_1.

Thus for a matching-parallel circuit the RC-circuit is obtained by a matching-parallel connecting up of the blocks, as shown in diagram B.

Let us write out the initial system of equations of the matching-parallel circuit:

$$\left.\begin{aligned}
\dot{x}_1 &= a_{11}x_1 + a_{12}x_2; \\
\dot{x}_2 &= a_{21}x_1 + a_{22}x_2 + y; \\
\dot{x}_3 &= \qquad\qquad a_{33}x_3 + a_{34}x_4; \\
\dot{x}_4 &= \qquad\qquad a_{43}x_3 + a_{44}x_4 + y; \\
\dot{x}_5 &= a_{51}x_1 + a_{52}x_2 + a_{53}x_3 + a_{54}x_4.
\end{aligned}\right\} \quad (5\text{-}38)$$

where the fifth equation is obtained by differentiation of the equation of external connection $x_5 = x_4 + x_2$ and $\dot{x}_4$ and $\dot{x}_2$ are substituted from the second and third equations. The matrix of coefficients composed on (5-38) is shown in the figure, where the conditions of its transposition are marked by arrows. The transposed system of equations can readily be made up on the matrix:

$$\ddot{g}_1^* = a_{12} g_1^* + a_{21} \dot{g}_2 + 0 + 0 + a_{11} \dot{g}_5 =$$
$$= a_{11}(\dot{g}_1^* + 1) + a_{21} \dot{g}_2 + 0 + 0;$$

$$\ddot{g}_2^* = a_{12} \dot{g}_1^* + a_{22} \dot{g}_2^* + 0 + 0 + a_{12} \dot{g}_5 =$$
$$= a_{12}(\dot{g}_1^* + 1) + a_{22} \dot{g}_2 + 0 + 0;$$

$$\ddot{g}_3^* = 0 + 0 + a_{33} \dot{g}_3 + a_{43} \dot{g}_4 + a_{13} \dot{g}_5 =$$
$$= 0 + 0 + a_{33}(\dot{g}_3 + 1) + a_{43} \dot{g}_4;$$

$$\ddot{g}_4^* = 0 + 0 + a_{34} \dot{g}_3 + a_{44} \dot{g}_4^* + a_{34} \dot{g}_5 =$$
$$= 0 + 0 + a_{34}(\dot{g}_3^* + 1) + a_{44} \dot{g}_4^*;$$

$$\dot{g}_5^* = \delta[\theta].$$

Since the unit function serves as the solution of the fifth equation, it is introduced into the right sides of the equations of the system. But instead of increase by unity of the coordinates g_1^* and g_3^* in all the equations of the system it is sufficient to increase by the single impulse their derivatives in only the first and third equations, which gives:

It is possible to arrive at the same result from g on the basis of the structural transformations.

The final result is obtained as the sum of the two terms:

$$g^*[t_1, \theta] = g_2^*[t_1, \theta] + g_4^*[t, \theta], \quad (5.39b)$$

since the output reaction in system (5-38) is obtained from the two inputs:

$$x_i = x_5 = x_{52} + x_{54}.$$

An Antiparallel Circuit

The equations of the external connections are:

$$y_2 = x_3 = x;$$
$$x_4 = x_1 + y \leftarrow \text{input};$$
$$x_3 = x \leftarrow \text{output}.$$

The complete equation of the circuit with the external and internal connections taken into consideration is:

$$\dot{x}_1 = a_{11}x_1 + a_{12}x_2;$$
$$\dot{x}_2 = a_{21}x_1 + a_{22}x_2 + x_3;$$
$$\dot{x}_3 = \qquad\qquad a_{33}x_3 + a_{31}x_1;$$
$$\dot{x}_4 = x_1 + 0 + a_{33}x_3 + a_{11}x_4 + y.$$

$$(5\text{-}40)$$

Circuit c and the matrix of coefficients were constructed according to this system of equations. Here there are two coefficients of connection (+ 1) in the second and fourth lines. After transposition of the matrix of coefficients the connections go over into the first and third lines, which also determines the conditions of construction of circuit c and the transition to the system of equations of the RC-circuit:

Output After integration

$$g_1 = a_{11}g_1 + a_{31}g_2;$$
$$g_2 = a_{12}g_1 + a_{23}g_2;$$
$$\dot{g}_3 = \qquad g_2 + a_{33}g_3 +$$
$$\qquad + a_{43}g_4 + \delta(9);$$
$$\dot{g}_4 = \qquad\qquad a_{34}g_3 +$$
$$\qquad + a_{11}g_1.$$

$$(5\text{-}41)$$

On the basis of examination of the circuits in Figure 5-24 it is possible to conclude that the transition to RC-systems can be realized not only according to the structural representations detailed to the elementary components, but also according to circuits with enlarged blocks; in that case it is necessary to apply the rules

of transition twice: to the external connections and blocks, and then to the internal connections and elementary components within the blocks.

C. Invariance of the Blocks of Constant Coefficients During Transition to RC-Systems

Let the controlled values x_k, x_{k+1}, x_{k+2} and x_l among the equations of system (5-34) be connected by equations with constant parameters of the following type:

$$\left. \begin{array}{c} a_2 \ddot{x}_{k+2} + a_1 \dot{x}_{k+2} + a_0 x_{k+2} = b_0 x_k + c_0 x_l; \\ \dot{x}_{k+2} = x_{k+1}. \end{array} \right\} \quad (5\text{-}42)$$

Structural circuit a in Figure 5-25 was constructed on the basis of these equations.

In circuit 5-25b the blocks with constant coefficients have been convoluted into a single transfer function with exclusion of the intermediate controlled value x_{k+1}.

If the problem of transition from the basic circuit to the RC-circuit is now posed, then all the branches of the general circuit corresponding to the system of equations (5-34) must be subjected to transformations of a single type -- replacement of the nodes by summators and of the summators by nodes, and alteration of the directions of transfer of the signals. The part of the elements forming circuit 5-25a is transformed in accordance with the indicated rules into the circuit in Figure 5-25c.

If we convolute RC-circuit c, we get the transfer function according to circuit d, which in the operator nucleus coincides with the initial transfer function in circuit b.

If we generalize the obtained results into blocks of constant coefficients of any complexity, we can obtain a number of conclusions that are important for practice:

1. In the writing of systems of equations in canonical form and the construction of the corresponding structural representation of an equation with constant coefficients it is possible to write any order in the convoluted form and assign it on the structural circuit in the form of a general transfer function. In modeling, it is possible to join the real apparatus with the matric model.

2. In the transition to the structural representation of a RC-system the nucleus of the transfer function, excluding the blocks for delivery of the input values for summation, remains unchanged.

436
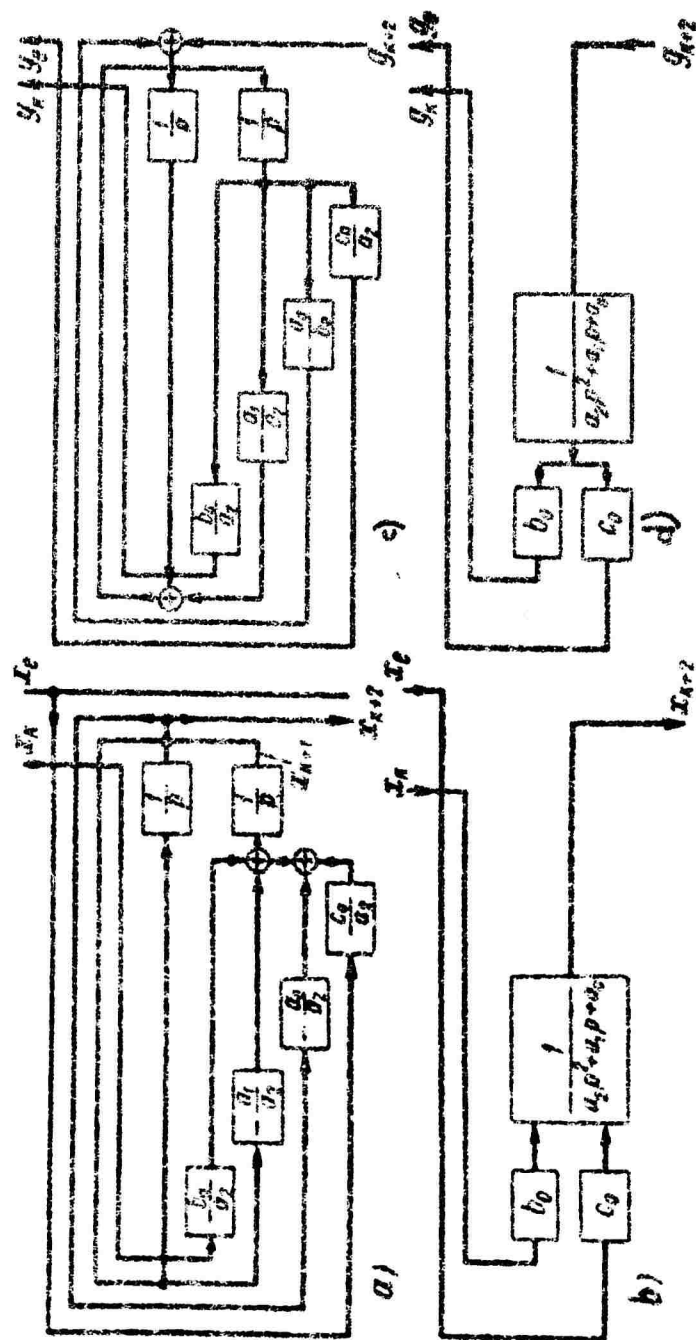
Fig 5-25. Block with constant coefficients in the initial (a and b) and RC-structures (c and d).

3. In modeling, real blocks with constant coefficients operating according to a single-channel principle can be connected into the RC-circuit of the model. A multi-channel real apparatus with summation of some input signals, for example on a magnetic amplifier for the model of the RC-system, is connected in with the use of only one of the input windings of the summating amplifier. The establishment of an equivalent "splitter" is required on the output of the summating amplifier, with scales of signals in the beams corresponding to the scales of the original terms.

D. Variants of Practical Methods of RC-Transformation

If the differential equation of a connection or system of equations is given, describing processes in a control arrangement, the transition to an RC-structure contains the following steps:

Transformation of the equations from the initial form to the RC-form by transition from the initial ADP to the RC ADP or from the initial matrix of coefficients to a transposed matrix;

Obtaining conventional solutions with respect to the highest derivative of the product of the controlled value multiplied by the variable coefficient;

Construction of a structural RC representation in accordance with Figure 2-14.

If the structure of the controlled arrangement is given, the transition to the RC-structure can be carried out by one of the variants which follow, based on the above.

Variant No 1. Structural representation - detailisation.

The places of the input and output are varied, the nodes are replaced by summators and the summators by nodes, and the signal direction is set from the new input to the new output. The structural model can be adjusted according to the RC- circuit.

Variant No 2. Canonical representation.

The blocks of coefficients are reset according to the transposed matrix.

The matric model can be adjusted according to the RC-circuit.

Variant No 3. A block circuit with detailisation within each block.

The places of the input and output of each block and of the

circuit as a whole are changed; the nodes and summators are mutually replaced in the external connections. The direction of signals in the external circuits is set from the new input to the new output. These same transformations are repeated in the internal detailized circuits of the blocks.

Variant No 4. A block circuit with canonical representations in the blocks.

A general matrix of the entire circuit is created. The external connections between the blocks are changed in accordance with the re-arrangement of the connection coefficients in the general matrix of coefficients. The internal connections are changed according to the rules for the transposition of matrixes in each block.

Variant No 5. A circuit with single-channel blocks with constant parameters.

The equations with constant parameters are convoluted into a general equation of the block. In the transition to the RC-circuit, the old input and output of the single-channel block and its equation are preserved. Real apparatus can be connected into the RC model in the form of blocks with constant coefficients.

5-8. Structural Transformations of Systems with Differentiation of the Input Actions

A. The Modeling of Equations with Derivatives on the Right Side

The application of differentiating components in electronic modeling is extremely undesirable due to the unfavorable frequency characteristics and internal noises of such elements. Meanwhile the typical equations (1-1) of control systems contain operations of differentiation on the right side, which leads to the appearance of differentiating blocks in the structural representation in Fig 1-1.

Let us carry out in (1-1) the normalization and limitation of the order (n = 3) necessary for subsequent analysis of the equation:

$$[D^3 + a_2(t)D^2 + a_1(t)D + a_0(t)]x =$$
$$= [b_3(t)D^3 + b_2(t)D^2 + b_1(t)D + b_0(t)]y. \quad (5\text{-}43)$$

This equation corresponds to the structural representations in both Figure 5-26a and in 5-25b (for circuit 5-26b only the input elements which form y_0 are given; the subsequent portion of the circuit contains the integrators and coincides with circuit a).
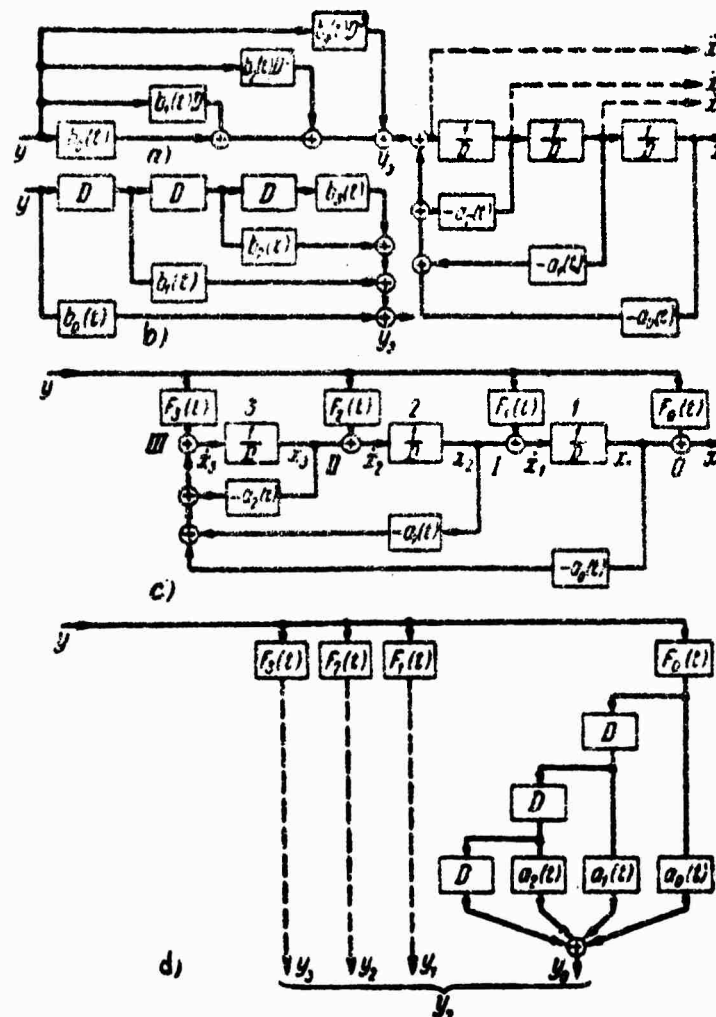
Fig 5-26. Equivalent differentiating components.

If we trace on circuit a the conditions of transformation of the input signal, we note that since the delivery of the signal to the output of the integrator is equivalent to the assignment of the derivative $\dot{y}$ on its input, then*the introduction of the signal y through blocks of variable coefficients $F_i(t)$ on the output of the three integrators is equivalent to the assignment on the input of the derivatives of y up to the third order inclusively. It remains only to bring the form of the functions $F_i(t)$ into agreement with the coefficients of equation (5-43).

*as shown in diagram

For this purpose let us transfer in structural representation c three summators from the outputs of the integrators onto the input of the circuit, that is, let us transform the structural representation c to the form of a.

In circuit 5-26d the conditions of such a transfer are shown in detail for the branch containing the block $F_0(t)$. The transfer proceeds against the course of the signal of the direct channel and along the course of the signal in the feedback circuits, and therefore on the basis of Table 5-1 inverse and doubling components are introduced into the circuits that are formed during the transformation. The number of circuits was determined by the number of nodes across which the summator was transferred, in accordance with the rule of Figure 5-8c.

Thus, for example, if we transfer in circuit c the summator 0 along the direct channel, it is necessary to make a branching at the nodal point x_1. In a left branching the summator 0 is transferred across the integrator counter to the course of the signal, and therefore an inverse component, that is, a differentiator, is introduced in the left branching from $F_0(t)$ in circuit d. Further, summator 0 approaches node x_2, during the transition across which a branching is again created. A second left branching again contains an integrator, during transition across which a second differentiator appears in circuit d, and then during the transfer of the summator 0 across the node x_3, a third differentiator.

The right branching from $F_0(t)$, by overcoming node x_1, obtains a minus sign, and therefore during the transfer of the summator 0 across the block $-a_0(t)$ it is doubled in the right branch of circuit d as positive. Further, summator 0 is transferred to the input of the integrating part of the circuit, that is, beyond summator III, without any sort of transformation. The second right branch also, having obtained the minus sign after node x_2, during transfer of summator 0 across block $a_1(t)$ doubles it in the second branch of circuit d with positive sign. The third right branch contains transfer of summator 0 across block $-a_2(t)$ also with change of sign, which gives the branch $+a_2(t)$ on circuit d.

Differentiating components are contained in the obtained circuit 5-8d. The action of the symbol of short differentiation D^+ on the signal with a variable coefficient $F_0(t)y$ we will decipher in algebraized form (1-82c):

(See next page)

$$D = D_F + D_{in};$$

$$D^2 = (D_F + D_{in})^2 = D_F^2 + 2D_F D_{in} + D_{in}^2;$$

$$D^3 = (D_F + D_{in})^3 = D_F^3 + 3D_F^2 D_{in} +$$
$$+ 3D_F D_{in}^2 + D_{in}^3.$$

If we transmit the signal $F_0(t)y$ across all the components of circuit d, we get the first constituent of the equivalent signal on the input of the circuit:

$$y_0 = \{[D_F^3 + 3D_F^2 D_{in} + 3D_F D_{in}^2 + D_{in}^3] +$$
$$+ a_2(t)(D_F^2 + 2D_F D_{in} + D_{in}^2) +$$
$$+ a_1(t)(D_F + D_{in}) + a_0(t)\} F_0(t) y. \qquad (*)$$

For the block $F_1(t)$ of circuit c, development analogous to d gives three branches with transforming components:

$$D^2, \ a_2(t) D \text{ and } a_1(t),$$

which permits determining the second constituent of the equivalent signal on the input:

$$y_1 = \{D_F^2 + 2D_F D_{in} + D_{in}^2 + a_2(t)(D_F + D_{in}) +$$
$$+ a_1(t)\} F_1(t) y. \qquad (**)$$

For block $F_2(t)$ the development has two branches: D and $a_2(t)$ and the third constituent of the equivalent signal is equal to:

$$y_2 = [D_F + D_{in} + a_2(t)] F_2(t) y. \qquad (***)$$

Transformations are not required for block $F_3(t)$ and it is possible to obtain at once the fourth constituent of the input signal:

$$y_3 = F_3(t) y. \qquad (****)$$

The total equivalent input signal equals:

$$y_e = y_0 + y_1 + y_2 + y_3.$$

If we compare formulas (*) to (****) with (5-43), we determine the sought connection between the variable coefficients in circuits a and b on the basis of the balance of functions in the presence of identical derivatives of the signal:

$$b_3(t) = F_0(t);$$

$$b_2(t) = 3\dot{F}_0(t) + a_2(t)F_0(t) + F_1(t);$$

$$b_1(t) = 3\ddot{F}_0(t) + 2a_2(t)\dot{F}_0(t) + a_1(t)F_0(t) +$$
$$+ 2\dot{F}_1(t) + a_2(t)F_1(t) + F_2(t);$$

$$b_0(t) = \dddot{F}_0(t) + a_2(t)\ddot{F}_0(t) + a_1(t)\dot{F}_0(t) +$$
$$+ a_0(t)F_0(t) + \ddot{F}_1(t) + a_2(t)\dot{F}_1(t) +$$
$$+ a_1(t)F_1(t) + \dot{F}_2(t) + a_2(t)F_2(t) + F_3(t). \quad (5\text{-}44)$$

The problem -- finding the functions of $F_i(t)$ -- can also be solved analytically. For this, let us renumber all the integrators in circuit c from right to left and use these same numbers in the subscripts of the output values on the integrators -- x_i and their derivatives -- the input values $\dot{x}_i$; then we get the system of equations:

$$\begin{aligned}
\dot{x}_3 &= -a_2(t)x_3 - a_1(t)x_2 - a_0(t)x_1 + F_3(t)y; \\
\dot{x}_2 &= x_3 && + F_2(t)y; \\
\dot{x}_1 &= x_2 && + F_1(t)y; \\
\dot{x} &= x_1 && + F_0(t)y,
\end{aligned} \quad (5\text{-}45)$$

which is a canonical system with an additional last equation. Let us convolute this system of equations, containing the unknown values x_3, x_2, x_1 and x into a single equation with regard to x by utilizing the designation of the non-commutative determinants:

(See next page)

443

$$
\begin{Vmatrix}
a_2(t) + D & a_1(t) & a_0(t) & 0 \\
1 & -D & O & 0 \\
0 & 1 & -D & 0 \\
0 & 0 & 1 & -1
\end{Vmatrix} x =
$$

$$
= \begin{Vmatrix}
\cdots & F_3(t) \\
\cdots & -F_2(t) \\
\cdots & -F_1(t) \\
\cdots & -F_0(t)
\end{Vmatrix} y. \qquad (5\text{-}46)
$$

The first step in the expansion of this determinant changes only the first two lines; since in the given case the consistent ADP's coincide with the initial ADP's, we write the result of the transformations at once:

$$
\begin{Vmatrix}
-a_2(t)D - D^2 - a_1(t) & -a_0(t) & 0 \\
1 & -D & 0 \\
0 & 1 & -1
\end{Vmatrix} x =
$$

$$
= \begin{Vmatrix}
\cdots -a_2(t)F_2(t) - F_2'(t) - F_2(t)D - F_3(t) \\
\cdots \qquad\qquad -F_1(t) \\
\cdots \qquad\qquad -F_0(t)
\end{Vmatrix} y.
$$

The second step likewise proceeds in a simple enough manner, since only the right side is complicated, where the symbol of differentiation is replaced by the sum $D = D_F + D_x$, which gives:

$$
\begin{Vmatrix}
a_0(t) + a_1(t)D + a_2(t)D^2 + D^3 & 0 \\
 & \\
1 & -1
\end{Vmatrix} x =
$$

$$
= \begin{Vmatrix}
\cdots a_2(t)\dot{F}_1(t) + a_2(t)F_1(t)D + \ddot{F}_1(t) \\
+ 2\dot{F}_1(t)D + F_1(t)D^2 + a_1(t)F_1(t) + \\
+ a_2(t)F_2(t) + \dot{F}_2(t) + F_2(t)D + F_3(t) \\
- F_0(t)
\end{Vmatrix} y.
$$

The third step permits obtaining:

$$[a_0(t) + a_1(t)D + a_2(t)D^2 + D^3]x$$

$$= \{a_0(t)F_0(t) + a_1(t)F_0(t) + a_1(t)F_0(t)D +$$

$$+ a_2(t)\dot{F}_0(t) + 2a_2(t)\dot{F}_0(t)D + a_2(t)F_0(t)D^2 +$$

$$+ \ddot{F}_0(t) + 3\ddot{F}_0(t)D + 3\dot{F}_0(t)D^2 + F_0(t)D^3 +$$

$$+ a_2(t)\dot{F}_1(t) + a_2(t)F_1(t)D + \dot{F}_1(t) +$$

$$+ 2\dot{F}_1(t)D + F_1(t)D^2 + a_1(t)F_1(t) +$$

$$+ a_2(t)F_2(t) + \dot{F}_2(t) + F_2(t)D + F_3(t)\}y. \quad (5\text{-}47)$$

If we equate the coefficients at identical powers of D^i on the right sides of the obtained equation and (5-43), we get the solution with respect to the sought functions of $F_i(t)$, which we write in Table 5-2.

If the order of the right side m of equation (5-43) is greater than the order of its left side n, then m - n differentiating components cannot be successfully excluded by the method examined above. But such a relation os the orders m > n is unnatural to real power control systems, since in that case the reaction on the input step must contain impulses for the creation of which infinitely large power is required on the output. In fact, the impulses or other processes with a steep front manifest small time constants which are not taken into account. It is necessary to introduce them into the initial equations of a control system, raising its order at the most to m = n.

If it is necessary to have in the circuit or model not only the output signal but also its derivatives, the latter are readily found on the inputs of the integrators of the direct channel of circuit a and can be deduced from the lines of the inputs for further utilization.

In the practice of electronic modeling the signals containing derivatives of the output value are used, for example, for control of the electromechanical blocks of a model, and assure decrease in the dynamic errors of those blocks.

If the input signal is formed as a result of the solution of

Table 5-2 Equivalents of differentiating components for equations from the first to the third order

$F_i(t)$	$n = 1$	$n = 2$	$n = 3$
$F_0(t)$	$b_1(t)$	$b_2(t)$	$b_3(t)$
$F_1(t)$	$b_0(t) - \dot{b}_1(t) - a_0(t)b_1(t)$	$b_1(t) - a_1(t)b_2(t) - 2\dot{b}_2(t)$	$b_2(t) - a_2(t)b_3(t) - 3\dot{b}_3(t)$
$F_2(t)$	—	$b_0(t) - a_0(t)b_2(t) +$ $+ a_1(t)[2\dot{b}_2(t) - b_1(t) + a_1(t)b_2(t)] +$ $+ \dot{a}_1(t)b_2(t) - \dot{b}_1(t) + \ddot{b}_2(t)$	$b_1(t) - [3\ddot{F}_0(t) + 2\dot{F}_1(t)] -$ $- a_2(t)[2\dot{F}_0(t) + F_1(t)] - a_1(t)F_0(t)$
$F_3(t)$	—	—	$b_0(t) - [\dddot{F}_0(t) + \ddot{F}_1(t) + \dot{F}_2(t)] -$ $- a_2(t)[\ddot{F}_0(t) + \dot{F}_1(t) + F_2(t)] -$ $- a_1(t)[\dot{F}_0(t) + F_1(t)] - a_0(t)F_0(t)$

the "input signal equation" on separate blocks of the generator of
the input signal (the sine-shaped signal is formed on two integrat-
ing blocks, a polynomial of the n-th order requires n integrators,
etc), then if we include the blocks of the input signal generator in
the general circuit, we can take down the necessary derivatives of
the input signal from the inputs of the integrators of the input sig-
nal generator.

C. An RC-Structure for a Single Equation with Differentiation
    of the Input Actions

In Figure 2-14 an RC-structure was presented for the general
equation (1-4a). But if a structural representation is prepared for
subsequent modeling of an RC system, the differentiators in Figure
2-14a are inapplicable. They can be removed from the circuit by the
method of structural transformations in the region of the argument
Θ, just as was done for the direct circuit in the region of the ar-
gument t.
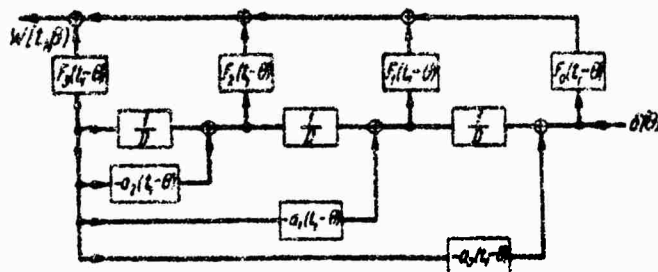
Fig 5-27. RC structures for a single equation with differ-
entiating components.

But it is simpler to take the prepared structure in Figure 5-26c,
which does not have differentiating blocks, and to perform on it an
RC transformation of the circuit, which leads to the new RC-structure
shown in Figure 5-27 and suitable for modeling.

D. An RC-Structure for Systems of Equations with
    Differentiation of the Input Actions

Let the input actions in a system of equations given in canon-
ical form be differentiated, multiplied by the variable coefficients
$b_{ik}(t)$ and assigned to each equation of the system. Let us consider
this complex case on the example of the three equations:

$$
\left.
\begin{aligned}
Dx_1 &= a_{11}x_1 + a_{12}x_2 + a_{13}x_3 + \\
&\quad + (b_{11} + b_{12}D + b_{13}D^2)\, y; \\
Dx_2 &= a_{21}x_1 + a_{22}x_2 + a_{23}x_3 + \\
&\quad + (b_{21} + b_{22}D + b_{23}D^2)\, y; \\
Dx_3 &= a_{31}x_1 + a_{32}x_2 + a_{33}x_3 + \\
&\quad + (b_{31} + b_{32}D + b_{33}D^2)\, y.
\end{aligned}
\right\}
\qquad (5\text{-}48)
$$

If we designate the derivatives of the input value by the new symbols:

$$
y = y_1;
$$
$$
\dot{y} = y_2;
$$
$$
\ddot{y} = y_3
$$

we reduce the functions of the input actions $\Pi_1(t)$, $\Pi_2(t)$ and $\Pi_3(t)$ to the form

$$
\left.
\begin{aligned}
b_1(t,\ D)\, y &= \Pi_1(t) = \\
&= b_{11}(t)\, y_1 + \dot{b}_{12}(t)\, y_2 + b_{13}(t)\, y_3; \\
b_2(t,\ D)\, y &= \Pi_2(t) = \\
&= b_{21}(t)\, y_1 + \dot{b}_{22}(t)\, y_2 + b_{23}(t)\, y_3; \\
b_3(t,\ D)\, y &= \Pi_3(t) = \\
&= b_{31}(t)\, y_1 + b_{32}(t)\, y_2 + b_{33}(t)\, y_3,
\end{aligned}
\right\}
\qquad (5\text{-}49)
$$

which permits all the coefficients to be given in the form of the matrix:

$$
B_{hq} =
\begin{Vmatrix}
b_{11} & b_{12} & b_{13} \\
b_{21} & b_{22} & b_{23} \\
b_{31} & b_{32} & b_{33}
\end{Vmatrix}.
\qquad (5\text{-}50)
$$

The structural representation of system of equations (5-48), shown in Figure 5-25a), repeats the disposition of the coefficients in the matrix of the input actions B_{hq} (5-50) -- the left side of the figure and in the matrix of coefficients of the system A_{hq} (5-27) -- the right side of the figure.

The solution of system of equations (5-48) can be replaced by the sum of the solutions

$$\Pi_i(t) = b_{iq}(t, D)\,y = \sum_{q=1}^{3} b_{iq}(t)\,D^{q-1}y; \quad (5\text{-}51a)$$

$$\left\|\begin{vmatrix} D - a_{11} & -a_{12} & -a_{13} \\ -a_{21} & D - a_{22} & -a_{23} \\ -a_{31} & -a_{32} & D - a_{33} \end{vmatrix}\right\| x_{3h} =$$

$$= \left\|\begin{vmatrix} -------- & 0 \\ \overline{\begin{matrix} \text{line} \\ h \end{matrix}} & \Pi_i(t) \\ -------- & 0 \end{vmatrix}\right\|_{h=i=1,\,2,\,3} ; \quad (5\text{-}51b)$$

$$x = x_3 = \sum_{h=1}^{3} x_{3h}. \quad (5\text{-}51c)$$

In the present case it is assumed that a solution is sought with respect to the output value $x_3 = x$; therefore the third column has been substituted in the non-commutative determinant of the right side.

In the sum (5-51c) the terms x_{31}, x_{32} and x_{33} are constituents of the general solution x_3 from the actions $\Pi_h(t)$ given in the h-th column (h = 1, 2, 3).

In the investigation of other solutions of system (5-48), for example x_1 and x_2, the first or second column of the determinant on the right side (5-51b) is correspondingly substituted.

If the input action is given in the form of a single displaced impulse $y = \delta[t - \vartheta]$, equations (5-51b) are transformed:

$$\left\| \begin{matrix} D - a_{11}(t) & -a_{12}(t) & -a_{13}(t) \\ -a_{21}(t) & D - a_{22}(t) & -a_{23}(t) \\ -a_{31}(t) & -a_{32}(t) & D - a_{33}(t) \end{matrix} \right\| g_{3h}[t,\vartheta] =$$

$$= \left\| \begin{matrix} ---------- \; 0 \\ \hline \begin{array}{cc} \text{line} \\ h \end{array} \quad \delta[t-\vartheta] \\ \hline ---------- \; 0 \end{matrix} \right\| ; \qquad (5\text{-}52a)$$

$$w_{3h}[t,\vartheta] = \sum_{q=1}^{3} (-1)^{q-1} \frac{\partial^{q-1}}{\partial \vartheta^{q-1}} [b_{hq}(\vartheta) g_h[t,\vartheta]];$$

$$\qquad (5\text{-}52b)$$

$$w_s[t,\vartheta] = \sum_{h=1}^{3} w_{3h}[t,\vartheta]. \qquad (5\text{-}52c)$$

The subscripts 3h are attached to the partial weight functions g_{3h} and w_{3h}. In the reduced partial weight functions g_{3h} the subscript h designates the line in which, according to the right side of Figure 5-28a, the impulse is assigned on the input of the integrator.

The transition to the RC system changes the analytical connections only in equations (5-52a), instead of which it is necessary to obtain equations for the partial reduced weight functions of the argument Θ. The equations for $g_{3h}[t_1,\Theta]$ are derived from the initial system (5-48) upon replacement of the initial matrix of coefficients A_{hq} by the transposed matrix A_{qh}^{*} during assignment of the impulse $\delta[\Theta]$ only on the right side of the third line (from which solution x_3 was obtained in the initial system) and during variation of the subscript h -- the number of the line.

The remaining equations, (5-52b) and (5-52c), for the transition from the partial reliefs to the complete relief of the weight function are transferred into the region of the argument Θ by elementary transformations:

$*(5-33)$
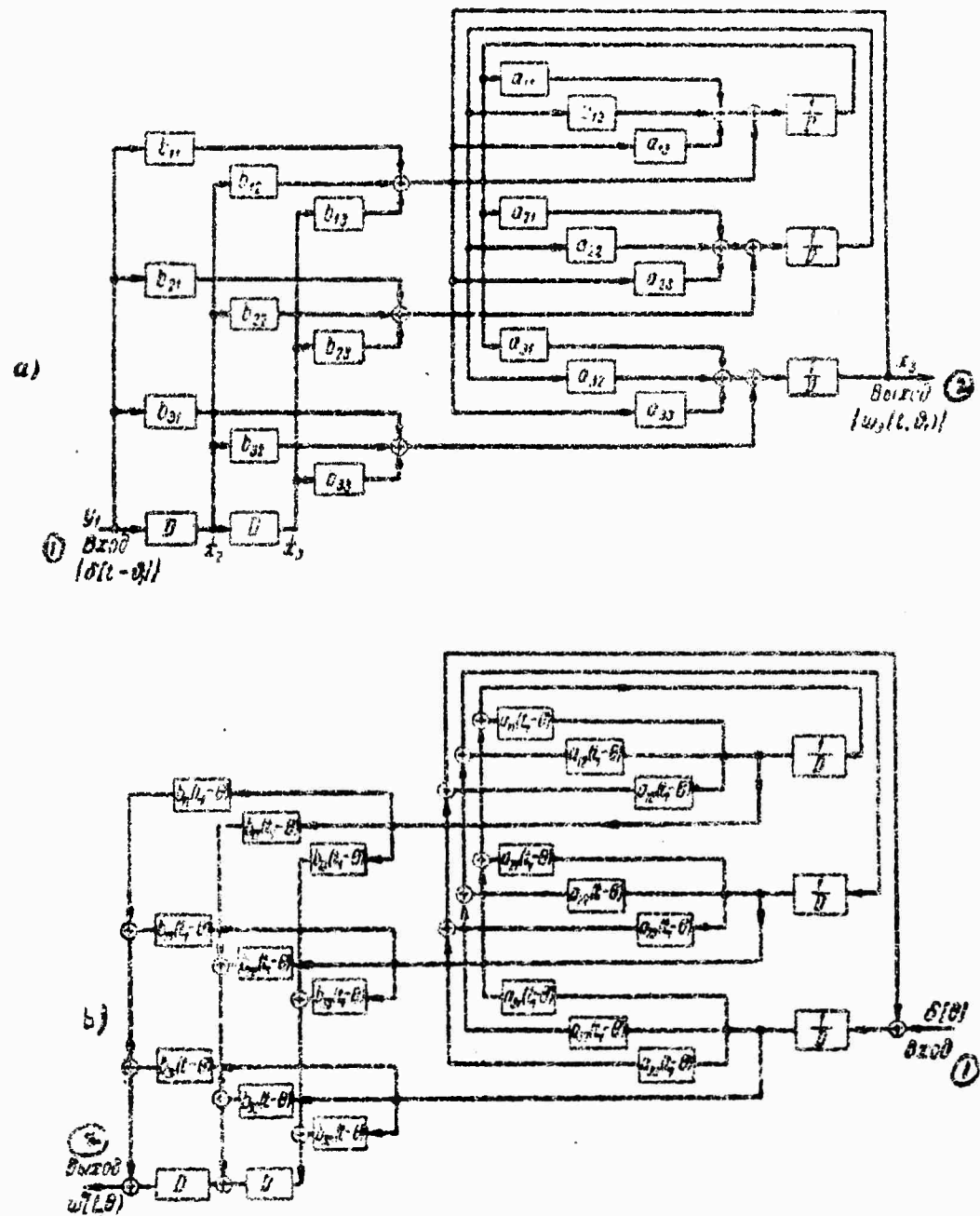
Fig 5-23. The initial structure (a) and RC-structure (b) for a system of equations with differentiation of the input actions. 1 – Input; 2 – Output.

And so we get a group of equations of the RC-system:

$$-\frac{\partial}{\partial\vartheta}=\frac{\partial}{\partial\theta}\;;\;\;\vartheta=t-\theta.$$

$$
\begin{vmatrix}
D^* - a_{11}(t_1 - \theta) & -a_{21}(t_1 - \theta) & -a_{31}(t_1 - \theta) \\
-a_{12}(t_1 - \theta) & D^* - a_{22}(t_1 - \theta) & -a_{32}(t_1 - \theta) \\
-a_{13}(t_1 - \theta) & -a_{23}(t_1 - \theta) & D^* - a_{33}(t_1 - \theta)
\end{vmatrix}
\dot{g}_3[t_1,\;\theta] =
$$

$$
= \begin{vmatrix}
\cdot & \cdot & \cdot & \text{column} \\
& & & 3 \\
\cdot & \cdot & \cdot & \\
\cdot & \cdot & \cdot & \delta[\theta]
\end{vmatrix}_3 \;;\quad (5\text{-}53a)
$$

$$w^*_{3h}[t_1,\;\theta] = \sum_{q=1}^{3} D_*^{q-1}[b_{hq}(t_1 - \theta)\,g^*[t_1,\;\theta]];\quad (5\text{-}53b)$$

$$\dot{w}_3[t_1,\;\theta] = \sum_{h=1}^{3} w^*_{3h}[t_1,\;\theta],\quad\quad (5\text{-}53c)$$

$$h = 1,\;2,\;3.$$

For expansion of the determinant a the last transformed column must be column h.

The structural representation of a RC-system is shown in Figure 5-28b.

The right side of the circuit has the coefficients a_{hq}, disposed according to the matrix A_{hq}, but since in circuit b, in comparison with circuit a, an exchange of the inputs and outputs and of the nodes and summators has been made, the matrix A_{hq} has been transposed for the input $\delta[\theta]$. The left side of circuit b realizes transformations (5-53b) and (5-53c).

The coefficients of the input actions in circuit b have been arranged, just as in circuit a, in accordance with the matrix B_{hq}. But since a RC transformation was performed in circuit b, the actual matrix proves to have been transposed:

$$B_{qh} = \begin{Vmatrix} b_{11} & b_{21} & b_{31} \\ b_{12} & b_{22} & b_{32} \\ b_{13} & b_{23} & b_{33} \end{Vmatrix},\quad\quad (5\text{-}54)$$

Which reflects the new conditions of summation of the products on the input of the differentiators, obtainable from composition of (5-53b) and (5-53c):

$$w'_3 [t_1, \ 9] = \sum_{h=1}^{3} D^{h-1}_* \sum_{q=1}^{3} b_{hq} (t_1 - 9) \ g_{3q} [t_1, \ 9)].$$

$$(5-55)$$

Thus the rule of RC transformation of a detailized structure a coincides in the given case with the rule of transposition of the matrix of the left and right sides and redistribution of the connections between the elements of the structural representations of the left and right sides on that basis.

For block circuits with enlarged structure the RC transformation is done in two steps:

According to the external connections in the general matrix of the entire circuit or on the basis of RC transformation of the circuit;

According to the internal connections on the basis of transposition of the internal matrices of the components and the input actions with the differentiating elements or on the basis of RC transformation of the internal circuits.

5-6. Partial Transformations of Structural Circuits at Given PO?T's of the Variable Components

According to the terminology stated at the beginning of the chapter, a structural circuit illustrates laplace or Fourier transformations of representations of a signal, which is reduced to multiplication of the representation by operator or complex function. It; moreover, to branching on the nodes and to addition on the summators. For the CFT's of constant components the operations of multiplication of the direct and inverse CFT's and of their addition are used. In other worms, if the CFT of the elements is known, it is always easy to get the CFT of the entire circuit.

For components with variable parameters the representation of the input signal is transformed into the representation of the output signal likewise by multiplication of the POFT of the component, but if we know the POFT of the separate components, it is as a rule impossible to obtain the general POFT of the entire circuit by the above-indicated very simple algebraic operations, and consequently there is no structural circuit with algebraic transformations of the representations of signal for variable systems, except in particular cases on which we will dwell briefly.

For circuit 5-24b the general POFT is equal to the sum of the POFT's of the parallel components:

$$W(t, s) = W_1(t, s) + W_2(t, s). \qquad (5\text{-}56)$$

A Cascade Circuit of Initial Constant and Subsequent Variable Components

For circuit 5-24a, after RC transformation, the impulse in the region Θ is given on the input of a variable component, the POFT of which is found by successive approximation from the equations

$$
\begin{aligned}
&[D_*^\gamma a_n(t-\theta) + \ldots + a_0(t-\theta)] g_2^*[t, \theta] = \delta[\theta], \\
&w_2^*[t, \theta] = [D_*^m b_m(t-\theta) + \ldots + b_0(t-\theta)], \\
&g_*^*[t, \theta], \quad w_2^*[t, \theta] \div W_2(t, s).
\end{aligned}
\qquad (*)
$$

Then for a constant component in the region of the argument $w_2^*(t, \Theta)$ serves as the input and the weight function of the entire circuit $w^*(t, \Theta)$ as the output, connected by the equation

$$
\begin{aligned}
(a_\nu D_*^\nu + \ldots + a_0) w^*[t, \theta] = \\
= (\beta_\mu D_*^\mu + \ldots + \beta_0) w_2^*[t, \theta].
\end{aligned}
\qquad (**)
$$

If we make a Laplace transformation of $(**)$, we get

$$
\begin{aligned}
W(t, s) &= \frac{\beta_\mu s^\mu + \ldots + \beta_0}{a_\nu s^\nu + \ldots + a_0} W_2(t, s) = \\
&= W_1(s) W_2(t, s), \qquad (5\text{-}57)
\end{aligned}
$$

where

$$
W_1(s) = \frac{\beta_\mu s^\mu + \ldots + \beta_0}{a_\nu s^\nu + \ldots + a_0}
$$

represents the OFT of the constant component.

A Cascade Circuit of an Initial Constant Component and Subsequent Amplifier with a Variable Amplification Factor

This partial case proceeds from the preceding, wherein equation (*) assumes the form:

$$w_2 [t, \ \theta) = k (t - \theta) \, \delta [\theta] = k (t) \, \delta [\theta].$$

Whence instead of equation (**) we get

$$(a_\nu D_s^\nu + \ldots + a_0) \, w [t, \ \theta) = $$
$$= (\beta_\mu D_s^\mu + \ldots + \beta_0) \, k (t) \, \delta [\theta]$$

If we make a Laplace transformation of the result at fixed t, we have:

$$W [t, \ s) = k (t) \, W_1 (s). \qquad (5\text{-}58)$$

A Cascade Circuit of a Boosting Constant and Subsequent Variable Components

The arbitrary input signal $x_{in} (t)$, exciting the variable component, must be subjected to Laplace transformation:

$$X_{in} (p) = \frac{\beta_\mu p^\mu + \ldots + \beta_0}{a_\nu p^\nu + \ldots + a_0}. \qquad (5\text{-}59a)$$

Then the formation of the output reaction can be represented as obtaining the weight function of a cascade circuit consisting of a forming (first) component, an excited impulse and a variable (second) component.

If we assume

$$X_{in} (s) = W_\Phi (s) = W_1 (s), \qquad (5\text{-}59b)$$

on the basis of formula (5-57) we arrive at the relationship

$$X_{out} (t, \ s) = X_{in} (s) \, W_2 (t, \ s). \qquad (5\text{-}59c)$$

Thus, just as for constant components, a derivation of the connection between the representations can be obtained not only on the equation of convolution [see the derivation of formula (3-83c)], but also on the given differential equations which determine the conditions of formation of the signal (5-59a) from the impulse and the

conditions of transmission of the signal by the component.

The parametric process

$$x_{out}[t, \theta] \div X_{out}(t, s) = W_{\phi}(s) W_{x}(t, s) = W_{\phi x \theta}(t, s)$$

can be understood as the weight function

$$w[t, \theta] \div W_{\phi x \theta}[t, s),$$

which has its relief in the space of the coordinates t, $\vartheta = t - \theta$, w. The section of this relief along the argument θ gives a series of output reactions at the moment t_1 on the homogeneous action x_{in}, but with different displacement $\vartheta_{in} = t_1 - \theta$.

A Cascade Circuit of an Input Amplifier with Variable Coefficients and a Subsequent Constant Component

Let the variable coefficient be exponentially increasing:

$$k(t) = e^{+\sigma t}. \tag{5-60a}$$

After RC transformation of the cascade circuit the constant component excited by the impulse generates a reaction on the argument θ:

$$w'_2[\theta] \div W_2(s), \tag{5-60b}$$

which is multiplied by the reversed coefficient:

$$w[t, \theta] = e^{\sigma(t-\theta)} w_2[\theta] = e^{\sigma t} \{e^{-\sigma \theta} w_2[\theta]\}. \tag{5-60c}$$

If we make a Laplace transformation of (5-60c) at fixed t, according to Table 3-1 we get:

$$W(t, s) = e^{\sigma t} W_2(s + \sigma). \tag{5-60d}$$

Let us examine also the case where a variable coefficient is assigned to a more complex function k(t), but after reverse of the argument it decomposes into the sum of the products of the arbitrary functions of time and the tabular functions of reverse-displacement:

$$k\left(t-\theta\right)=\sum_{k=1}^{l} f_k\left(t\right) a_k\left(\theta\right), \qquad (5\text{-}61a)$$

where the a_k -functions coincide with the functions presented in Table 3-1 or are obtained from them on the basis of linear transformations. Then, if we make a Laplace transformation of the weight function of the circuit

$$w\left[t,\ \theta\right]=\sum_{k=1}^{l} f_k\left(t\right) a_k\left(\theta\right) w_2\left[\theta\right] \qquad (5\text{-}61b)$$

along the argument θ, we get the general POFT in the form

$$W\left(t,\ s\right)=\sum_{k=1}^{l} f_k\left(t\right) \Lambda_k\left\{W_2\left(s\right)\right\}, \qquad (5\text{-}61c)$$

where the form of the Λ_k transformations is determined from Table 3-1.

A Cascade Circuit of Two Constant Components and an Intermediate Amplifier with a Variable Amplification Factor

Let the output constant component be given an OFT of the form

$$W_2\left(s\right)=\frac{\beta_m s^m+\ldots+\beta_0}{a_n s^n+\ldots+a_0} \qquad (*)$$

In the transition to an RC circuit the input impulse will be supplied on the output component and bring about a reaction determinable by the representation $(*)$:

$$W_2\left(s\right)\div w_2\left[\theta\right]. \qquad (**)$$

Let the variable coefficient $k(t)$ after RC transformation be reduced to the form of (5-61a); then upon multiplication of the process along the argument θ by the variable on θ coefficient (5-61b), the representation of process $(*)$ undergoes lambda transformation and is brought to the form of (5-61c). It remains now to take into consideration the first constant component, which has become the output component in the RC circuit, according to (5-57):

$$W(t, s) = W_1(s) \sum_{k=1}^{l} f_k(t) \Lambda_k \{W_k(s)\}. \quad (5\cdot62)$$

For more complex circuits containing components with variable parameters the algebraic transformations over the POFT's, used in structural circuits, prove insufficient to obtain the POFT of the entire circuit. Here the methods of transformations of OFT's in the structural circuits must be combined with methods of transformation of the ADP's in structural representations.

The general method of transformation of equations written in algebraized form, stated in Chapter 1, permits going from equations of the components to equations of the system as a whole and then finding by successive approximation the POFT of the system by its RC equation.

For a system with variable parameters, operating a limited interval of time and estimable by its state only at the end of that interval t_k, the partial operator function of transfer composed for the given input and output is an exhaustive characteristic of all the properties of the system. Therefore, in spite of calculating difficulties, it always is necessary to strive toward calculation of the parametric operator function of transfer.

5-10. Structural Representation of Linear Equations For the Determination of Quadratic Forms

As was shown in Section 2-10 for an equation with variable parameters of the first order and in Section 5-14 for equations of higher orders with constant parameters, in the composition of a linear differential equation for quadratic estimation of a process a canonical system of equations is formed.

The structural representation of such a system will be analogous in form to Figure 5-18; see additional features in Chapter 3 /4/. The construction of such circuits requires reduction of all the equations of components with variable parameters into a single equation of the control system, which leads to very tedious calculations. The representation of the input actions in the circuit likewise is very much complicated in the development of the right side of the general equation of the system.

If the block structure of the control system is preserved, the structure of quadratic form for such assignment of the linear connections can be constructed even without reduction to a single equation of the system, but then the input actions become especially complicated. The calculation of the input actions in a block circuit is

done on the basis of determination of the initial values of the reactions of each block. A general approach to the calculation of block circuits was given in Section 5-5; examples of calculation of the initial conditions were examined in Chapter 3, with use of Table 3-3. For analysis of the quadratic forms when a single equation of a control system with a right side is given, an example of calculation of the initial conditions was given in Chapter 1 [5].

V N Zakharov, Cand Tech Sci, Docent, has communicated to us regarding an analogous analysis that has been made for an unconvoluted system of equations. In it the problem of recalculation of variable parameters is taken up, but on the other hand the diagrams of the calculation and assignment of the input actions strongly expand. But such a problem falls in the circle of questions of structural analysis, since it permits studying the formation of quadratic estimates of an entire system inside each of its elements.

Bibliography

1. Petrov B N. On the construction and transformation of structural circuits, Izvestiya OTN AN SSSR (News of the Academy of Sciences USSR, Technical Sciences Section), 1945, No 12.
2. Mar'yanovskiy, D I. The stability of linear systems of automatic control, Elektrichestvo (Electricity), 1946, No 9.
3. Gal'perin I I. Sintez sistem avtomatiki (Synthesis of Systems of Automation), Gosenergoizdat, 1960.
4. Graybill, G P. Transformations of block diagrams, El Engineering, 2, 11, 1951.

PART II

CHARACTERISTICS OF TYPICAL ELEMENTS USED IN THE AUTOMATIC
REGULATION OF POWER EQUIPMENT AND IN AUTOMATIC CONTROL SYSTEMS

CHAPTER 6

pp186-207   BLOCK DIAGRAMS OF ELECTRICAL MACHINES

6-1. SELF-EXCITED GENERATORS USING A RHEOSTAT IN THE FIELD
      CIRCUIT

1. Circuits, Principles of Operation

The circuit of a [self-excited] generator is shown in
Fig. 6-1(a).   The generator is driven at a speed Ω by a prime
mover. The field winding has an ohmic resistance R_f and an induc-
tance L_f. A control rheostat R_c is inserted in series with the
field and is used to vary the generator voltage in the course of
the regulation process.

The field may be separately energized, as in separately
excited generators, or it may be connected in shunt with the arma-
ture circuit, as in self-excited generators. We shall use the
following symbols in the generator armature circuit: armature
winding ohmic resistance R_a and load ohmic resistance R_L: the
latter will fluctuate as the number of terminals in the network
varies (the inductance of the armature circuit will be considered
later).

2. No-load Operation of the Generator

The mesh equation for the armature circuit can be
written

$$(R_f+R_c)I_f+L_f(dI_f/dt) = U_f$$

Inasmuch as the present discussion assumes stable gen-
erator operation, we can consider incremental departures of the
controlled variables from their nominal values at the particular
operating condition being considered and write

$$\ast - 3$$

$$(R_{\rm m} + R_{y0})\,\Delta I_{\rm m} + I_{\rm m,0}\Delta R_y + L_{\rm m}\frac{dI_{\rm m}}{dt} = \Delta U_{\rm m}.$$

$$\mathrm{m} = f \quad y = c$$

Using operator notation and solving for $\Delta I_f(p)$, we can rewrite the above expression as follows

$$\Delta I_{\rm m}(p) = \frac{1}{L_{\rm m}p + R_{\rm m} + R_{y0}}\,[\Delta U_{\rm m}(p) - I_{\rm m,0}\Delta R_y(p)].$$

$$(6\text{-}1)$$

In computing the armature emf from the excitation current, we make use of the magnetization [saturation] curve of the generator. The slope S_I^E at the operating point gives the rate of increase of the generated emf as a function of the excitation current and we have

$$\Delta E(p) = S_I^E \,\Delta I_{\rm m}(p).\qquad(6\text{-}2)$$

From the relationship described by equations (6-1) and (6-2), the left portion of the block diagram in Fig 6-2(a) may be readily constructed. We now proceed to build up the block diagram.

3. Full-load Operation of the Generator

When a load current I_j flows in the armature, the generated emf is reduced as a result of the brush contact drop, the armature IR drop, and the armature reaction.

Fig 6-1(c) shows the variation of brush-contact drop with load current for a Type ED-32 generator. It may be seen from the figure that at currents above 80 amps the brush contact drop shows little variation and approaches a value of 2 volts. When considering incremental departures of the brush-contact drop, the variation of the latter may be considered equivalent to a resistance the value of which is determined by the slope of the curve at the operating point, i.e., $R_{be} = S_I^b$. For $I \approx 0$, the slope has the value 1 volt / 20 amp. = 0.05 ohms; as the current increases, the slope decreases to 0. When the generator is operated at nominal current values of the order of 100 amps, $R_{be} = 2(\partial\Delta U_b/\partial I)$ is negligibly small.

The demagnetizing effect of the armature reaction in unsaturated machines is produced by the demagnetizing armature ampere-turns $w_d I_a$. The latter result from a [forward] shift of the brushes from geometrical neutral in noninterpole machines. In interpole machines the shift of the brushes from geometrical neutral may be the result of careless assembly or of vibration

481

during operation.

The calculation of the armature demagnetizing ampere turns is elementary. It is sufficient to calculate the equivalent field current from the ampere-turn ratio

$$I_{af} = -(w_d/w_f)I_a$$

and to add it to the [nominal] field current

$$I_{f\Sigma} = I_f - (w_d/w_f)I_a$$

The reduced field current I_{fr} is used in determining the operating point on the saturation curve. As shown on Fig 6-1(b), the procedure for using the no-load saturation curve in the calculation of the terminal voltage [at a full-load point] consists in subtracting from the emf corresponding to the reduced field current the voltage drop in the armature and the brush-contact drop $2 \Delta U_b$, provided that the latter is not negligible. The shaded triangle in the figure is called the short-circuit triangle of the generator. [TN: two such triangles are shown].

The relation derived above remains unchanged when incremental departures from the nominal values of the variables are introduced:

$$\Delta I_{w\Sigma} = \Delta I_{w} - \frac{w_d}{w_w} \Delta I_{a}. \tag{6-3}$$

The relations derived above remain valid when saturation is present in the circuit, in which case they describe only one of the effects of the armature reaction. It should be noted that notwithstanding the fact that the slope S_f^0 must be read from the no-load saturation curve at the displaced operating point corresponding to the reduced excitation current $I_f - (w_d/w_f)I_a$, at high saturations this shift in operating point will have very little effect on the slope and the resulting change in voltage will be negligibly small.

The second effect of the armature reaction in saturated machines operates independently of the presence of demagnetizing armature ampere-turns and is superimposed on the demagnetizing effect. The second effect of the armature reaction results from
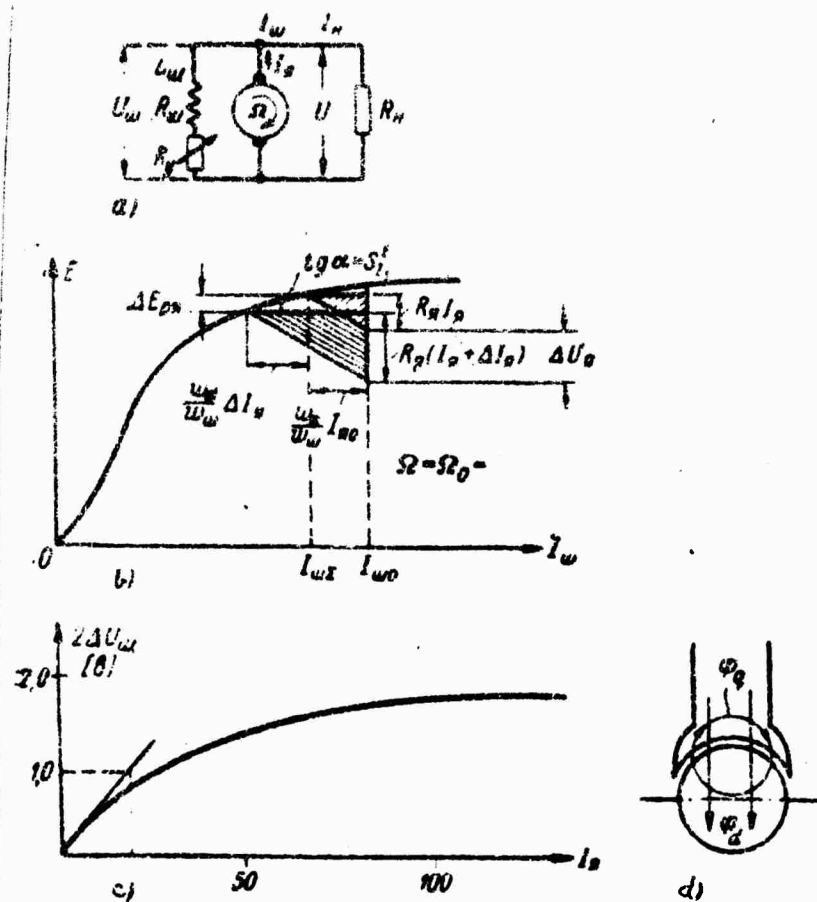
Fig. 6-1. Circuit and Characteristics for a d-c Generator
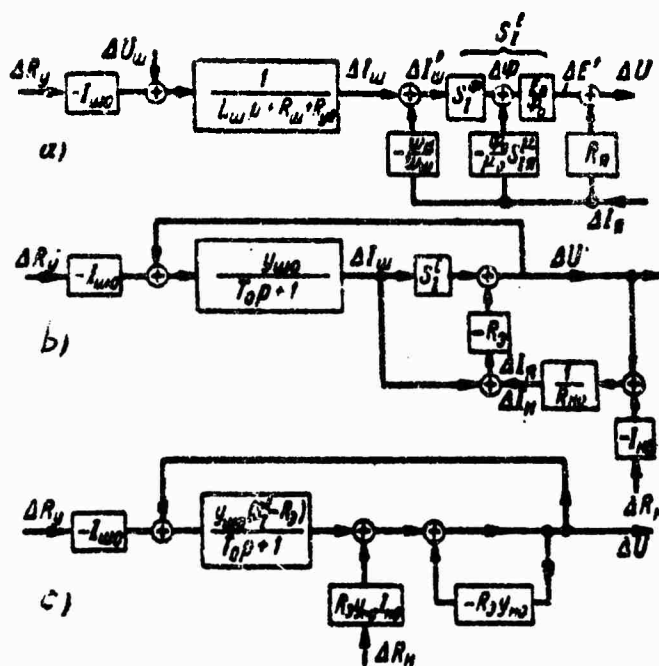
Fig 6-2. Block Diagrams for a Shunt-Wound Generator Using a
Rheostat in the Field Circuit

the fact that the armature reaction sets up a magnetic flux at
right angles to the main pole flux as shown in Fig 6-1(d); the
flux produced by the cross-magnetizing effect in part shares the
path of the main-pole flux. When the armature reaction ampere-
turns oppose the ampere-turns of the main-pole field, their dif-
ference [sic] falls on the straight portion of the magnetization
curve, and an effective decrease in flux is observed. When the
effects of the above-indicated groups of ampere-turns reinforce
each other, their sum falls on the flat portion of the magneti-
zation curve, and the increase in flux is insignificant. The
variation of the resultant magnetic flux may be expressed in
terms of an average permeance of the complete magnetic circuit.

We shall use the symbol $\mu(I_a)$ for the effective main-
pole flux permeance and the symbol μ_o for its value at the op-
erating point on the magnetization curve (the notation used is
customarily reserved for the permeability; however, there is no
possibility of introducing confusion inasmuch as the ratio of
the permeances used is equal to the ratio of the average permea-
bilities for the complete magnetic circuit). The effective field
flux is then given by the relation

$$\phi_d = \phi(I_{fr})[\mu(I_a)/\mu_o]$$

On introducing incremental departures we have

$$\Delta\Phi_d = S_I^\phi \Delta I_{wr} - \frac{\Phi_o}{\mu_o} S_{I_a}^\mu \Delta I_a. \qquad (6\text{-}4$$

Equations (6-3) and (6-4) are used in building up the
block diagram in Fig 6-2(a). Equation (6-3) is used to run a
feedback channel from the armature current channel ΔI_a to the
nominal field current channel.

For the evaluation of equation (6-4), a channel for
the [effective main field] flux $\Delta\phi_d$ is required in the block
diagram. The latter is readily obtained by splitting the calcu-
lation of armature voltage from the nominal field current into
two steps. In the first step the flux is computed from the field
current:

$$\Delta\Phi = S_I^\phi \Delta I_{wr}: \qquad (6\text{-}5)$$

In the second step the armature voltage is computed from the flux:

$$\Delta E = \frac{E_a}{\Phi_a} \Delta\Phi.$$ (6-6)

The quantity S_f^ϕ represents the slope of the graph giving the variation of field flux with field current. Its evaluation does not require the construction of additional graphs, since it can be obtained from the saturation curve of the generator (Fig 6-1(b)) by the relation

$$S_f^\phi = \frac{\Phi_a}{E_a} S_f^\prime.$$ (6-7)

Having provided in the block diagram for a channel representing the field flux, we connect to it a feedback branch from the armature current channel; this branch contains the element

$$-(\Phi_a / \mu_0) S_a^k$$

and represents the change in the field current produced by the saturating effect of the armature reaction.

The quantity $S_{IR}^{\mu\mu}$ represents the slope of the curve giving the variation of the effective main-pole flux permeance as a function of the armature current. Such a curve can be constructed from the full-load (saturation) curve of the generator, excluding the effect of other factors.

Let us now write the mesh equation for the armature circuit. The shortest form of the equation is obtained when the reduced armature emf E' resulting from the operation of the various factors discussed above is introduced into the equation; written in incremental form, the latter becomes

$$\Delta U = \Delta E' - \Delta I_a R_a.$$ (6-8)

The branch corresponding to the reduced emf was

previously entered in the block diagram, and all that remains to be done is to subtract from it the IR drop in the armature, which is taken off the armature current channel. This operation completes the construction of the block diagram in Fig 6-2(a); additional elements will be described in the block diagram shown in Fig 6-2(b) in order to provide a clearer understanding of the sequence of transformations and of the "buildup" of block diagrams.

We shall begin by noting that the feedback elements

$$-(w_d/w_f) \text{ and } -(\phi_0/\mu_0)S_{Ia}^{\mu}$$

are equivalent in their effect and produce a voltage drop proportional to the armature current. They can therefore be combined with the element R_a. This transformation is effected by moving the two summing points in the righthand portion of the block diagram in Fig 6-2(a) to the ΔU channel and by combining the transfer functions of the parallel branches.

$$R_e = R_a + \frac{E_0}{\mu_0} S_{I_a}^{\mu} + \frac{w_d}{w_{w}} S_f^E. \qquad (6\text{-}9)$$

The sum of the coefficients is designated as the equivalent resistance of the armature and is shown as such in the block diagram in Fig 6-2(b).

We now proceed to the analysis of the operating conditions of an actual self-excitation circuit. These conditions are as follows.

The armature current is equal to the sum of the load current I_L and the field current I_f:

$$\Delta I_a = \Delta I_g + \Delta I_f \qquad (6\text{-}10)$$

The incremental departure of the armature voltage ΔU forms the input field voltage (when the equations are written in incremental form):

$$\Delta U = \Delta U_f \qquad (6\text{-}11)$$

The above supplemental equations make possible the addition of one forward and one feedback loop to the block diagram in Fig 6-2(b). Finally, the change in load current can be expressed in terms of changes in the load resistance and in the load voltage. On introducing incremental deviations into the total-variables

$$I_{\ell}R_{\ell} = U$$

we obtain the following incremental equation:

$$R_{\ell o}\,\Delta I_{\ell} + I_{\ell o}\,\Delta R_{\ell} = \Delta U$$

which can be solved for ΔI_{ℓ} to give

$$\Delta I_{11} = -\frac{1}{R_{\eta 0}}\left(\Delta U - I_{110}\Delta R_{11}\right) \qquad (6\text{-}12)$$

On the basis of equation (6-12) we add two functions, $(1/R_{\ell o})$ and $-I_{\ell o}$, and one summing point to the block diagram in Fig 6-2(b). The resulting block diagram forms the basis for the analysis of the controlled system under discussion, and we therefore will proceed to transform it into a form more convenient for our analysis without introducing additional elements.

We begin by introducing a number of new symbols:

$T_0 = L_{fo}/(R_f + R_{oo})$, the time constant of the field circuit.

$Y_{fo} = 1/(R_f + R_{oo})$, the nominal admittance of the complete field circuit.

$Y_{\ell o} = 1/R_{\ell o}$, the nominal admittance of the load circuit.

Next, the summing point $\Delta I_{u} = \Delta I_{g} + \Delta I_{f}$ is moved to the left past as is the summing point for the ΔR_g input channel (rearrangement of summing points and combination of cascade elements). The takeoff branch from the ΔU channel is fed back into the right-hand portion of the block diagram.

Finally, the forward loop $b\gamma = n_e$ is combined with the aperiodic element, and the changes in the functions produced by the rearrangement of summing points are entered in the block diagram. The result is the block diagram shown in Fig 6-2(c).

We obtain the analysis of the simplified block diagram by forming the open-loop response function from the transfer functions of the forward and feedback elements.

$$C(p) = \frac{Y_{u0}(S_I^E - R_3)}{(T_e p + 1)(1 + R_3 Y_{H0})} \qquad (6\text{-}13$$

$\omega' = f \quad 3 = e \quad H = l$

The open-loop [static] gain is given by

$$C(0) = \frac{Y_{u0}(S_I^E - R_3)}{1 + R_3 Y_{H0}} \qquad (6\text{-}14$$

Inasmuch as the generator under discussion is not connected to an external power supply, the condition of self-excitation must be met in the course of its operation.

The condition of generation or self-excitation reduces to the application of positive feedback, which is the case, and to the attainment of an open-loop gain greater than unity. In the case under discussion, this condition is equivalent to stating that

$$Y_{fo}(S_I^E - R_e)/(1 + R_e Y_{lo}) > 1$$

or
$$\left. \begin{array}{c} \\ \\ S_I^E > R_{fo}(1 + R_e Y_{lo}) + R_e \end{array} \right\} \qquad (6\text{-}15)$$

i.e., self-excitation requires that the slope of the saturation curve of the machine

$$S_I^E = dE/dI_f \quad (\text{ohms})$$

exceed the sum of the total ohmic resistance of the field circuit multiplied by the coefficient $(1 + R_e Y_{lo})$, representing the effect of the load, and of the equivalent armature resistance.

The straight portion of the saturation curve shown in Fig 6-1(b) has the steepest slope, and for that portion of the curve condition (6-15) should hold unconditionally. The low value of the slope of the curve at the origin is not determinant for the conditions of self-excitation inasmuch as it is overridden by the residual magnetism of the machine.

Self-excitation ends when the following relationship between the total variables

$$I_f R_f = U(I_f, I_g)$$

is satisfied. The above relationship is used in the determination of the nominal operating point on the curve and is examined in greater detail in Chapter 13 during the discussion of nonlinear methods.

In discussing the relationships between the incremental departures from the nominal values, it should be noted that because of the saturation -induced decrease in S_f^E the inequality (6-15) usually is not satisfied at the operating point for the steady-state case.

When the equality

$$S_f^E = R_{mg}(1 + R_g Y_{g0}) + R_g$$

is satisfied exactly in the neighborhood of the operating point, the response of the generator will be astatic [nonstationary] since $a_0 = 0$ in the denominator of the transfer function which is derived below (Equation (6-16)).

When the inequality (6-15) is satisfied in the neighborhood of the operating point, the response of the generator is considered to be quasi-static.

The addition of an automatic voltage regulator would give satisfactory results over the full range of conditions discussed above.

Let us now construct the transfer function on the input signal, using the block diagram in Fig 6-2(c):

$$W_y(p) = -\frac{I_{m0} C(p)}{1 - C(p)} =$$

$$= \frac{-I_{m0} Y_{m0}(S_f^E - R_g)}{(T_e p + 1)(1 + R_g Y_{H0}) - Y_{m0}(S_f^E - R_g)}. \quad (6\text{-}16)$$

Let us also construct the transfer function on the extraneous input signal:

$$W_H(p) = \frac{R_g Y_{H0} J_{H0}(T_e p + 1)}{(T_e p + 1)(1 + R_g Y_{H0}) - Y_{m0}(S_f^E - R_g)}. \quad (6\text{-}17)$$

For the static regulation of the generator in accordance with the formulas derived above, we may set $p = 0$ and obtain the [static] gain on the input signal.

$$W_y(0) = \frac{-I_{\mu\mu0}Y_{\mu\nu0}(S_I^E - R_s)}{1 + R_s Y_{\mu0} - Y_{\mu0}(S_I^E - R_s)} \qquad (6\text{-}18)$$

and the [static] gain on the extraneous signal

$$W_\mu(0) = \frac{R_s Y_{\mu0} I_{\mu0}}{1 + R_s Y_{\mu0} - Y_{\mu0}(S_I^E - R_s)}. \qquad (6\text{-}19)$$

As may be seen from the formulas, compared to separately excited generators, self-excited generators show a greater gain on the input signal because of the difference term in the denominator. Thus an increase in field current resulting from a decrease in the control resistance R_c is reinforced by an increase in I_f resulting from an increase in output voltage, and vice versa. The overall result is an increased sensitivity of the system to variations in the reference input ΔR_c. A second result obtained by letting the inequality (6-15) approach an equality, is the achievement of a very high gain.

On the other hand, self-excitation also leads to an increase in the gain on the extraneous signal compared to that observed in separately excited generators, since the drop in the output voltage caused by an increase in load current is simultaneously aggravated by a drop in field current. When the extraneous signal is fed in as ΔR_f rather than as ΔI_f, the coefficient $1/(1+R_c Y_{f0})$ reduces the effect of the extraneous signal, since the increase in the [field] current is counteracted by a simultaneous drop in generator [armature] voltage.

4. Compound-wound Generators

When the operation of the closed-loop voltage-regula-
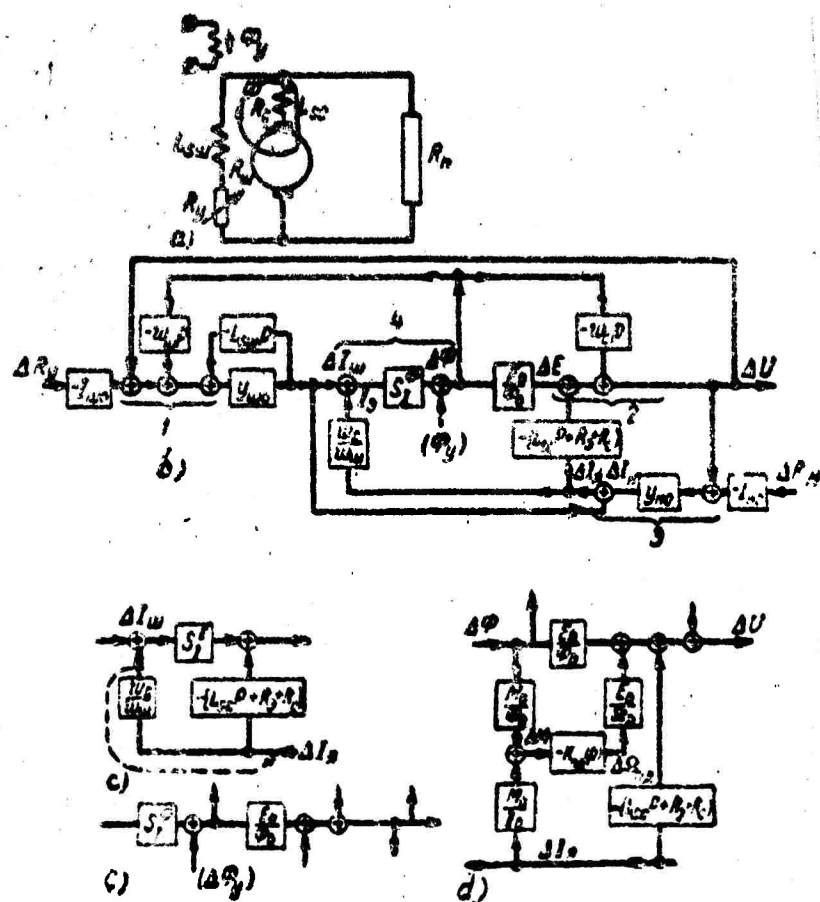
Fig 6-3. Circuit and Block Diagrams for a Compound Generator
Using a Rheostat in the Field Circuit

tion system of the generator is based on the deviation from the
reference input signal, improved performance and a reduction in
the effect of the basic disturbance, fluctuations in the load
current, can be achieved by making the disturbance the actuating
signal. In the case under discussion this condition is achieved
by compounding the generator.

The circuit of a compound-wound generator using a
so-called "long shunt" connection is shown in Fig 6-3(a). We shall
now analyze the principle of operation of such a machine.

A comparison with the circuit of Fig 6-1(a) shows that
the only difference between a compound-wound generator and a
shunt-wound generator is the addition of a series winding with an
ohmic resistance R_s and a leakage inductance L_{ss} near the operat-
ing point. The presence of two flux-linked windings makes it nec-
essary to treat separately in the discussion of circuit processes
the mutual inductance flux ϕ linking both windings, as shown in
Fig 6-3(a), and the leakage flux which is expressed in terms of
the leakage self-inductances.

On the basis of the above discussion, the leakage self-
inductance of the shunt winding is introduced in the place of the
total field inductance L_f appearing in Fig 6-1.

When the new notation is used and increments are con-
sidered, the mesh equation for the shunt winding takes the form

$$(R_f + R_{co}) \Delta I_f + I_{fo} \Delta R_c + L_{sf} \Delta \dot{I}_f + w_f \Delta \dot{\phi} = \Delta U$$

When the sum of the nominal resistances in the shunt circuit
is expressed by a single symbol $R_{f_0} = R_f + R_{co}$ and the above equa-
tion is solved for ΔI_f, an equation very similar to equation
(6-1) but containing a greater number of regulated variables is
obtained:

$$\Delta I_{\text{ш}}(p) =$$

$$= \frac{1}{L_{\text{sш}} p + R_{\text{ш}0}} [\Delta U(p) - I_{\text{ш}0} \Delta R_y(p) - w_{\text{ш}} p \Delta \Phi(p)]. \quad (6\text{-}20)$$

Equation (6-20) can be used to describe the deviation.

To obtain the armature emf, we make use of the satura-
tion curve of the generator. The shape of the curve will be as

473

in Fig 6-1(c), but the magnetizing ampere-turns are now obtained by summing the ampere-turns of the shunt and series windings:

$$(aw)_\Sigma = (aw)_f + (aw)_s$$

Since the no-load curve in Fig 6-1 was constructed as a function of I_f, it is convenient to rewrite the above expression in the following form

$$\Delta (aw_\Sigma) = w_f(\Delta I_f + (w_s/w_f) \Delta I_a)$$

The quantity in brackets represents a fictitious current in the shunt winding, the magnetizing effect of which is equivalent to that of the currents flowing in the shunt and series windings. Substituting this equivalent current in Equation (6-5), we obtain the relation

$$\Delta\Phi = S_f^\Phi \left(\Delta I_m + \frac{w_c}{w_w} \Delta I_s \right). \qquad (6\text{-}21)$$

$$c = s$$
$$w = f$$
$$s = a$$

In attempting to establish the relationship between a variation in current and the corresponding change in terminal voltage, one must take into account that in addition to the quantities which constitute the equivalent resistance R_e of the armature circuit appearing in Equation (6-8), in the case under discussion the armature circuit includes a series winding which has an ohmic resistance R_s, a leakage self-inductance L_{ss}, and w_s turns linked by the mutual inductance flux Φ. When allowance is made for these terms and incremental departures are considered, the following equation is obtained

$$\Delta U = \Delta E - [(R_e + R_s) \Delta I_a + L_{ss} \Delta \dot{I}_a + w_s \Delta \dot{\phi}]$$

Rewriting the above expression in operator notation, we obtain

$$\Delta U (p) =$$
$$= \Delta E - [(R_s + R_c + L_{sc}p) \Delta I_a (p) + w_c p \Delta\Phi(p)]. \qquad (6\text{-}22)$$

$$I_e \cdot I_s \qquad I_a$$

Using Equations (6-20) through (6-22) and Equations (6-7) through (6-11), the block diagram for a compound-wound generator has been constructed as shown in Fig 6-3(b). The block diagram retains all the elements appearing in the block diagram in Fig 6-2(b). In addition, two [feedback] branches have been added representing the mutual inductance $\Delta \phi$ and the total equivalent exciting current

$$I_e = I_f + w_s/w_f)I_a$$

and some of the transfer functions have been made more complex.

From this block diagram the transfer functions on the input signal and on the disturbance can be derived. We shall supplement the method used in reducing the block diagrams in Fig 6-2 by deriving the required transfer functions by the transformation of systems of equations discussed in Chapter V.

We shall begin by rewriting the equations expressing the relationships between the controlled variables. [TN: The Russian text does not appear to make a distinction between manipulated and controlled variables]. We shall write all stimuli on the righthand side of the equations. The controlled variables shall be written in fixed sequence on the lefthand side of the equations. When a particular equation does not contain one of the controlled variables, a zero is entered in its place.

It should be noted that if all of the enumerated controlled variables are retained in the equations, the system of equations will consist of six equations and its determinant will be of order 6, which makes the subsequent computations rather cumbersome. It is therefore convenient to reduce the number of equations by the elimination of selected controlled variables by the method of substitution.

A decrease in the rigor of the method by the occurence of random transformations in the course of the substitution can be avoided by adopting the convention that controlled variables which appear in no more than two equations will be excluded from the system. In the system under discussion ΔE and ΔI_g are such variables.

The block diagram can be very helpful in the elimination of controlled variables of the type described above. In effect, all system equations are input-output ratios about summing points or the branches of the block diagram. For a controlled [manipulated] variable to appear in only two system equations, it is necessary and sufficient that the channel assigned to that variable in the block diagram be an output of only one preceding element and an input to only one following element, i.e., the channel assigned

_ 475 _

to the controlled variable must not have takeoff (branch) points.

Thus the initial system of equations can be constructed in the form of input-output ratios involving only [output] variables which have takeoff points on their channels. On the basis of the foregoing analysis we have for the system under discussion:

$$(L_{sш}p + R_{ш0})\,\Delta I_{ш}(p) + w_{ш}p\Delta\Phi(p) + 0 - \Delta U(p) =$$
$$= -I_{ш0}\Delta R_y(p);$$

$$0 + \left(\frac{E_ь}{\Phi_ь} - w_c p\right)\Delta\Phi(p) -$$
$$- (L_{sc}\,p + R_я + R_c)\,\Delta I_я(p) - \Delta U(p) = 0,$$

$$\Delta I_{ш}(p) + 0 - \Delta I_я(p) + Y_{н0}\Delta U(p) = I_{н0}Y_{н0}\Delta R_н(p);$$

$$S_I^\Phi \Delta I_{ш}(p) - \Delta\Phi(p) +$$

$$+ S_I^\Phi \frac{w_c}{w_{ш}}\,\Delta I_я(p) + 0 = 0.$$

ш = f   у = с   я = н   ч = k   с = s

The summing points involved in the above equations are indicated by the numbers under the brackets in Fig 6-5(b).

The determinant of the system is

$$\Delta(p) =$$

$$= \begin{vmatrix} L_{sш}p + R_{ш0} & w_{ш}p & 0 & -1 \\ 0 & \dfrac{E_ь}{\Phi_ь} - w_c p - R_я - R_c - L_{sc}p & -1 \\ 1 & 0 & -1 & Y_{н0} \\ S_I^\Phi & -1 & S_I^\Phi \dfrac{w_c}{w_{ш}} & 0 \end{vmatrix}$$

(6-23a)

475

The determinant obtained has no more than one zero in any row or column with the result that the labor involved in the reduction of the determinant is not apt to be affected much by the choice of the elements of a particular row or column for the expansion of the determinant. However, from the point of view of the utilization of the intermediate computations in the subsequent discussion, we shall expand the determinant in terms of the elements of the fourth column:

$$\Delta(p) = \begin{vmatrix} 0 & \dfrac{E_0}{\Phi_0} - w_c & -R_a - R_c - L_{sc}p \\ 1 & 0 & -1 \\ S_I^\Phi & -1 & S_I^\Phi \dfrac{w_c}{w_m} \end{vmatrix} -$$

$$- \begin{vmatrix} L_{sm}p + R_{m0} & w_m p & 0 \\ 1 & 0 & -1 \\ S_I^\Phi & -1 & S_I^\Phi \dfrac{w_c}{w_m} \end{vmatrix} - \quad (6\text{-}234)$$

$$- Y_{m0} \begin{vmatrix} L_{sm}p + R_{m0} & w_m p & 0 \\ 0 & \dfrac{E}{\Phi_0} - w_c p & -R_a - R_c - L_{sc}p \\ S_I^\Phi & -1 & S_I^\Phi \dfrac{w_c}{w_m} \end{vmatrix}.$$

When the third-order determinants in Equations (6-25b) are reduced by the application of general rules, we obtain

$$\Delta(p) = R_a + R_c - S_I^\Phi \frac{E_0}{\Phi_0}\left(1 + \frac{w_c}{w_m}\right) +$$

$$+ R_{m0} + Y_{m0}R_{m0}\left(R_a + R_c - \frac{w_c}{w_m}\frac{E_0}{\Phi_0}S_I^\Phi\right) +$$

$$+ p\left\{L_{sc} + w_c S_I^\Phi + \frac{w_c^2}{w_m}S_I^\Phi + L_{sm} + S_I^\Phi(w_m + w_c) + \right.$$

$$+ Y_{m0}\left[R_{m0}\left(L_{sc} + \frac{w_c}{w_m}S_I^\Phi w_c\right) + \right.$$

$$+ (R_a + R_c)(L_{sm} + S_I^\Phi w_m) - L_{sm}S_I^\Phi \frac{E_0}{\Phi_0}\cdot\frac{w_c}{w_m}\bigg]\bigg\} +$$

$$+ p^2 Y_{m0}\left(L_{sm}L_{sc} + L_{sm}\frac{w_c^2}{w_m}S_I^\Phi + L_{sc}w_m S_I^\Phi\right).$$

We can now write an expression for $\Delta(p)$ using the standard notation for the coefficients of the lefthand side of the differential equation of the system:

where

$$\Delta(p) = a_2 p^2 + a_1 p + a_0, \qquad (6 \cdot 23\,c$$

$$a_0 = (R_s + R_c)(1 + Y_{110}R_{110}) +$$

$$+ R_{110} - S_I^E \left[1 + \frac{\omega_c}{\omega_{111}}(1 + Y_{110}R_{110}) \right];$$

$$a_1 = L_c + L_{111} + 2\omega_c S_I^\Phi + Y_{110}\left[R_{110}L_c + \right.$$

$$\left. + (R_s + R_c)L_{111} - L_{s111}S_I^E \frac{\omega_c}{\omega_{111}} \right]; \qquad (6 \cdot 23\,d$$

$$a_2 = Y_{110}(L_{s111}L_{sc} + L_{s111}M_c + L_{sc}M_{111}).$$

The sum of the leakage self-inductance of the shunt winding L_{sf} and of the mutual inductance of that same winding $S_I^\Phi w_f$ which appears in the above equations can be replaced by the total inductance:

$$L_f = L_{sf} + S_I^\Phi w_f = L_{sf} + M_f$$

Analogously the sum of the leakage self-inductance of the series winding L_{ss} and of its mutual inductance $(S_I^\Phi w_s/w_f)w_s$ constitutes the total inductance of the series winding:

$$L_s = L_{ss} + S_I^\Phi (w_s/w_f)w_s = L_{ss} + M_s$$

The inductances are best evaluated in terms of the time constants of the windings under discussion:

$$T_{fo} = L_f/R_{fo} \text{ and } T_s = L_s/R_s$$

Let us now construct the substituted determinant for the evaluation of the input signal:

$$\Delta_1(p) =$$

$$= \begin{vmatrix} L_{\text{SM}} + R_{\text{M0}} & w_{\text{M}}p & 0 & -I_{\text{M0}} \\ 0 & \dfrac{E_\bullet}{\Phi_\bullet} - w_c p & -R_s - R_c - L_{\text{SC}}p & 0 \\ 1 & 0 & -1 & 0 \\ S_j^\bullet & -1 & S_j^\bullet \dfrac{w_c}{w_{\text{M}}} & 0 \end{vmatrix} .$$

This determinant can be reduced to a third-order determinant which has been previously evaluated in the course of the evaluation of the determinant of the system (cf. the first of the three determinants appearing in Equations (5-25a)).

Using the results obtained above, we can immediately write a general expression for the transfer function on the input signal in terms of operator polynomials:

$$W_y(p) = \frac{b_{y1} + b_{y0}}{a_2 p^2 + a_1 p + a_0} = \frac{\Delta_1}{\Delta} . \qquad (6\text{-}24a)$$

where the coefficients of the denominator are given by Equations (5-25d) and the coefficients of the numerator have the values

$$b_{y0} = I_{\text{M0}} \left[S_j^E \left(\frac{w_c}{w_{\text{M}}} + 1 \right) - (R_s + R_c) \right] : \left.\begin{array}{c}\\ \\ \end{array}\right\}$$
$$b_{y1} = -(L_c + w_c S_j^\bullet) I_{\text{M0}}. \qquad (6\text{-}24b)$$

When the condition $a_0 > 0$ is satisfied, the static gain may be calculated from the transfer function:

$$W_y(0) = \frac{I_{m0}\left[S_f^E\left(\frac{w_c}{w_m} + 1\right) - \right.}{(R_s + R_c)(1 + Y_{n0}R_{m0}) + R_{m0} -}$$

$$\frac{\left. - (R_s + R_c)\right]}{- S_f^E\left[1 + \frac{w_c}{w_m}(1 + Y_{n0}R_{m0})\right]} = \frac{b_0}{a_0}.$$

As in the case of the simplified block diagram with the transfer function given by Equation (6-16), an increase in gain can be achieved first by increasing the magnitude of b_0 by increasing the slope of the no-load curve and the admittance of shunt [sic] and armature windings, and second, by decreasing the value of the coefficient a_0.

By letting a_0 approach zero from above, the generator response can be made very sensitive to changes in the input signal. The result is a static system operating near the boundary of self-excitation.

When $a_0 = 0$, the system acquires transient characteristics which in a number of cases have valuable practical applications. The above condition can be developed as follows

$$S_f^E\left[1 + \frac{w_c}{w_m}(1 + Y_{n0}R_{m0})\right] =$$
$$= (R_s + R_c)(1 + Y_{n0}R_{m0}) + R_{m0}.$$

whence we have

$$S_f^E = \frac{(R_s + R_c)(1 + Y_{n0}R_{m0}) + R_{m0}}{1 + \frac{w_c}{w_m}(1 + Y_{n0}R_{m0})}. \qquad (6\text{-}25)$$

It can be readily seen from Equation (6-25) that for $w_s = 0$ and $R_s = 0$, i.e., when the series winding is eliminated, the equation reduces to Equation (6-16) for a shunt-wound generator.

If the contribution of the shunt winding is to be minimized in Equation (6-25), both sides of the equation should be multiplied by w_c/w_f and the admittance Y_{f0} should be used in the place of the corresponding resistance R_{f0}. We then obtain

$$S^E_{I_{\text{ш}}} \frac{w_c}{w_{\text{ш}}} = S^E_{I_c} =$$

$$= \frac{(R_s + R_c)(Y_{\text{ш}0} + Y_{\text{н}0}) + 1}{\left(1 + \dfrac{w_{\text{ш}}}{w_c}\right) Y_{\text{ш}0} + Y_{\text{н}0}},$$

where $S^E_{I_{\text{ш}}}$ is the slope of the saturation curve for the current in the series winding.

Setting $Y_{f0} = 0$, we obtain the condition for astatic [nonstationary] operation of a series-wound generator:

$$S^E_{I_c} = R_s + R_c + R_{\text{н}0}. \qquad (6\text{-}26)$$

When $a_0 > 0$, the system acquires quasi-static characteristics.

The conditions $a_0 \gtrless 0$ are identical with the conditions for self-excitation of the machine. Generally speaking, it matters little whether the excitation approaches linearity as a function of the time ($a_0 = 0$) or exponentially ($a_0 < 0$), in view of the fact that the use of these concepts [sic] in the linear theory is justified only for small deviations of the controlled variables from their nominal values. When the deviations of the controlled variables become significant, nonlinear methods of analysis have to be substituted for linear methods of analysis; nonlinear techniques are discussed in Chapter 13. Hence in the discussion of self-excitation, it will be sufficient to establish that the coefficient passes through zero in the region of negative values.

Let us write the determinant for the transfer function on the extraneous signal, which is input in the form of changes in the load resistance ΔR_ℓ:

$$\Delta_s(p) =$$

$$\begin{vmatrix} L_{sm}p + R_{m0} & w_m p & 0 & 0 \\ 0 & \dfrac{E_0}{\Phi_0} - w_c p - R_s - R_c - L_{sc}P & 0 \\ 1 & 0 & -1 & +I_{H0}Y_{H0} \\ S_I^{\Phi} & -1 & S_I^{\Phi}\dfrac{w_c}{w_m} & 0 \end{vmatrix}$$

For a drive motor shaft reduced to ... disturbance signal ... in which the previously ... disturbance ... variable ... of the motor part of the system, the ... a useful signal which the transfer function of the extraneous variable ... ... for ... ... of polynomials:

$$W_H(p) = \frac{\Delta_2(p)}{\Delta(p)} = \frac{b_{H2}p^2 + b_{H1}p + b_{H0}}{a_2 p^2 + a_1 p + a_0}, \qquad (6\text{-}27a)$$

... the coefficients in the denominator are given in Equation ... the following relations can be readily obtained for the coefficients in the numerator:

$$\left. \begin{aligned} b_{H0} &= I_{H0}Y_{H0}R_{m0}\left[(R_s + R_c) - \frac{w_c}{w_m}S_I^E\right]; \\ b_{H1} &= I_{H0}Y_{H0}\left[R_{m0}L_c + (R_s + R_c)L_m - L_{sm}S_I^E\frac{w_c}{w_m}\right]; \\ b_{H2} &= I_{H0}Y_{H0}[L_{sm}L_{sc} + L_{sm}M_c + L_{sc}M_m]. \end{aligned} \right\} \qquad (6\text{-}27b)$$

For a constant disturbance the static gain is ... over

$$W_H(0) = \frac{b_{H0}}{a_0} =$$

$$= \frac{I_{H0}Y_{H0}R_{m0}\left(R_s + R_c - \dfrac{w_c}{w_m}S_I^E\right)}{(R_s + R_c)(1 + Y_{H0}R_{m0}) + R_m - S_I^E\left[1 + \dfrac{w_c}{w_m}(1 + Y_{H0}R_{m0})\right]}.$$

It will be immediately apparent that an increase in the susceptibility of the system to changes in the input signal achieved through a reduction in the value of a_o simultaneously leads to an increase in the susceptibility of the system to load disturbances. A distinguishing feature of the transfer function described above is its ability to allow a decrease in the effect of load disturbances by decreasing the value of the coefficient b_o in the numerator, since the latter contains a difference of two terms as known in Equations (6-27b).

When the two terms are made equal, the system will be insensitive to a constant disturbance. Thus the condition

$$S_I^E = \frac{\omega_{III}}{\omega_c}(R_s + R_c) \qquad (6\text{-}28)$$

determines the optimum setting for regulation on a constant disturbance.

The block diagram in Fig 6-3(c) gives a better illustration of the principle of regulation on the extraneous input. The block diagram reproduces a section of the block diagram in Fig 6-3(b).

An examination of the block diagram shows that the effect of the series winding is structurally equivalent to regulation on the disturbance with feedback of the compensating effect. Equation (6-28) is a particular case of the general equation for this type of compensation (5-18c) which was derived in the preceding chapter. Of course, full compensation cannot be achieved in the case under discussion because of differences in the transient processes in the circuits having the transfer functions:

$$F_1 N = S_I^E(w_s/w_f) \text{ and } D(p) = L_{ss}p + R_e + R_s$$

Nevertheless, for a constant disturbance in the steady-state condition, the effect of the load current is eliminated.

The discussion of self-excited 1- and 2-winding generators [shunt- and compound-wound generators, respectively] presented above illustrates how the method of structural analysis can be used in the investigation of control systems. Starting with the simplest possible block diagram, the method permits the stepwise introduction of additional elements to account for complications introduced in the process or for previously neglected factors.

If the inductance of the armature winding were to be taken into account, the value of the coefficient L_{BB} in the block diagram would have to be increased.

The addition of a third, independently excited field to the generator, illustrated in Fig 6-3(a) makes it possible to regulate the generator output voltage by adjusting the external control flux ϕ_c.

The new reference input can be readily introduced into the block diagram by the insertion of an additional summing point on the $\Delta\phi$ branch in Fig 6-3(b). Fig 6-3(d) reproduces a section of the block diagram in Fig 6-3(b) showing the connections required for the introduction of the new reference input.

The substituted determinant for the evaluation of the transfer function on the new reference input can be written as follows:

$$\Delta_s(p) =$$

$$= \begin{vmatrix} L_{sw}p + R_w & w_w p & 0 & 0 \\ 0 & \dfrac{E_s}{\Phi_s} - w_c p & -R_s - R_c - L_{sc}p & 0 \\ 1 & 0 & -1 & 0 \\ S_I^\phi & -1 & S_I^\phi \dfrac{w_c}{w_w} & -1 \end{vmatrix}$$

The above determinant can be reduced to a third-order determinant which can be expanded to give the coefficients of the numerator of the required transfer function:

$$b_{\phi 0} = \frac{E_s}{\Phi_s} R_{w0};$$

$$b_{\phi 1} = -R_{w0}w_c + (R_s + R_c)w_w + \frac{E_s}{\Phi_s}L_{sw};$$

$$b_{\phi 2} = L_{sw}w_c + L_{sc}w_w$$

The general form of the transfer function can be expressed in the form of a fraction:

$$W_{\Phi_Y}(p) = \frac{\Delta_3(p)}{\Delta(p)} = \frac{b_{\Phi 2}p^2 + b_{\Phi 1}p + b_{\Phi 0}}{a_2 p^2 + a_1 p + a_0}, \qquad (6\text{-}29)$$

We shall give the expanded-form expression only for the static gain at $p = 0$:

$$W_{\Phi}(0) = \frac{\dfrac{E_0}{\Phi_0}}{(R_a - R_c)(Y_{m0} + Y_{n0}) + 1 - S_i^E \left[Y_{m0} + \dfrac{w_c}{w_m}(Y_{m0} + Y_{n0}) \right]}$$

By assigning values to the coefficients in the denominator, such as to make the system operate on the boundary of self-excitation, we can achieve an extremely high gain on the control flux. This property has found practical application in design of special machines operating on the boundary of self-excitation (Regulex). The circuit in Fig 6-3(a) with the extra field added, can be readily adapted to shunt-wound and series-wound generators operating on the boundary of self-excitation. For shunt-wound generators a rheostat is inserted in the circuit of the shunt winding. For series-wound generators, an adjustable shunt-resistance is used.

The current in the control field, and hence also the strength of the field, are computed by solving additional equations. The latter are used in building up the block diagram for the system and make the determinant of the system more complex.

5. Corrections Required by the Speed Regulation of the Prime Mover

If one were to take into account that a change in generator load produces a change in the torque and hence also in the speed of the prime mover, there results a requirement for the introduction of a new controlled variable Ω or of its increment $\Delta\Omega$ in the system of equations and in the block diagram.

In the generator equations a change in the speed of

the prime mover will affect the generator voltage. Whereas previously the voltage was computed from the curve (Fig 6-1(b)) expressing the variation of the voltage as a function of the field current alone at $\Omega = \Omega_o = $ const, i.e., as a single-valued function of the magnetic flux, in accordance with the relation

$$E = \frac{E_o}{\Phi_o} \Phi.$$

the voltage now has to be computed in terms of the effective speed, i.e., as a function of two manipulated variables:

$$E = \frac{E_o}{\Omega_o \Phi_o} \Omega\Phi.$$

When the above relation is rewritten in incremental form, we have

$$\Delta E = \frac{E_o}{\Phi_o} \Delta\Phi + \frac{E_o}{\Omega_o} \Delta\Omega. \qquad (6\text{-}30)$$

The introduction of the manipulated variable $(E_o/\phi_o)\Delta\Omega$ into the block diagram requires the insertion of an additional summing point on the ΔU branch.

In order to compute the value of $\Delta\Omega$, the characteristic regulation curve of the prime mover and the change in torque must be known.

The torque can be determined from the product of the armature current and the magnetic flux and from the generator efficiency η, using the following expression:

$$M \, [\kappa\Gamma \cdot M] = \frac{0{,}102 \Phi I_a}{\eta} = M_o \Phi I_a. \qquad (6\text{-}31)$$

Once again rewriting the expression in incremental form, we have

$$\Delta M = \frac{0{,}102}{\eta} (\Phi_o \Delta I_a + I_o \Delta\Phi) =$$

$$= M_o \left(\frac{\Delta\Phi}{\Phi_o} + \frac{\Delta I_a}{I_o} \right). \qquad (6\text{-}32)$$

Fig 6-3(e) shows the additions which must be made to the block diagram to reflect the effect of the regulation of the prime mover in accordance with equations (6-30) and (6-32).

We shall use the symbol $K_{pm}(p)$ to represent the transfer function of the prime mover which expresses the effect of a change in torque on the speed. An expanded-form expression for this transfer function will be derived in Section 6-2. If we set $p = 0$, $K_{pm}(0)$ will represent the slope of the mechanical characteristic [speed-torque curve] $\Omega = f(m)$ of the prime mover. The negative sign of the transfer function follows from the fact that the speed decreases as the load increases.

The block diagram in Fig 6-3(e) illustrates the linearized handling of the factors introduced by the consideration of the characteristics of the prime mover.

The increase of the load current along the path $I-M-\Omega-U$ lowers the generator voltage by a factor of

$$M_o K_{pm}(0) E_o / I_o \Omega_o$$

In a steady-state condition the above coefficient is equivalent to an additional resistance in the armature circuit. On forming the sum of this and the other resistances in the armature circuit, we obtain an effective resistance for that circuit combining the ohmic contribution and that made by the regulation of the prime mover:

$$(R_a)_\phi = R_s + R_c + \frac{M_o E_o}{I_o \Omega_o} K_{n.a}(0). \qquad (*)$$

In addition, in a steady-state condition the drop in the speed of the prime mover must be reflected in a lowering of the value of the coefficient E_0/Φ_0 to an effective value

$$\left(\frac{E_o}{\Phi_o}\right)_\phi = \frac{E_o}{\Phi_o} - \frac{M_o E_o}{\Phi_o \Omega_o} K_{n.a}(0)$$

$$= \frac{E_o}{\Phi_o}\left[1 - \frac{M_o}{\Omega_o} K_{n.a}(0)\right]. \qquad (**)$$

484

In the derivation of Equations (∗) and (∗∗), the branch containing K_{pg} was split in accordance with the rules for the manipulation of block diagrams and both components are taken in account in the merger with the parallel branches R_e and E_0/Ω_0.

6-2. DUAL-FEED DIRECT-CURRENT ELECTRIC MOTORS

1. A Control Scheme Using Separate Excitations with Allowance for the Inductance of the Armature Circuit

A general circuit for an electric motor using both series-resistance and field control is shown in Fig 6-4. We shall make use of the method of gradually building up the block diagram for the system and initially set $U_a = U$ and $U_f =$ const. In addition, the series winding will be left out of the discussion. However, the possibility of the development of inductance in the armature circuit from other causes shall be expressed by setting the coefficient $L_{ss} = L$.

We shall now write a series of incremental equations which will be used in the construction of the block diagram.

The equation for the armature circuit is

$$(Lp+R_A)\Delta I_a(p) + \Delta E(p) = \Delta U(p)$$

Solving for $\Delta I(p)$, we have

$$\Delta I(p) = (1/R_a)/(Tp+1)[\Delta U(p) - \Delta E(p)]$$

The relationship between [armature] current and torque at constant field flux is given by

$$\Delta M(\omega) = M_0 \Delta I/I_0$$

The torque equation, i.e., the equation of dynamic equilibrium, can be written:

$$(Jp+s_\Omega^M)\Delta\Omega(p) + \Delta M_\ell(p) = \Delta M(p)$$

The above equation can be solved conditionally for $\Delta\Omega(p)$ to give:

$$\Delta\Omega(p) = \frac{1}{(Jp)}\ [\Delta M(p) - \Delta M_\ell(p) - s_\Omega^M \Delta\Omega(p)]$$

The dependence of the counter-emf on the speed at constant flux is given by the relation

$$\Delta E(p) = E_0 \Delta\Omega/\Omega_0$$

— 485—
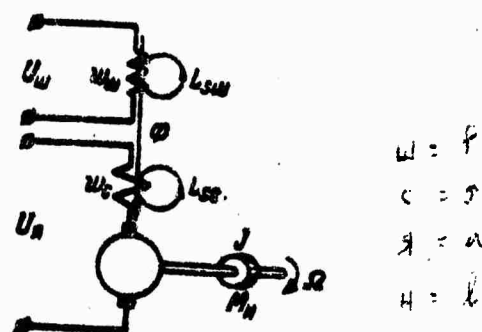
Fig 6-4. Circuit for a Compound d-c Motor
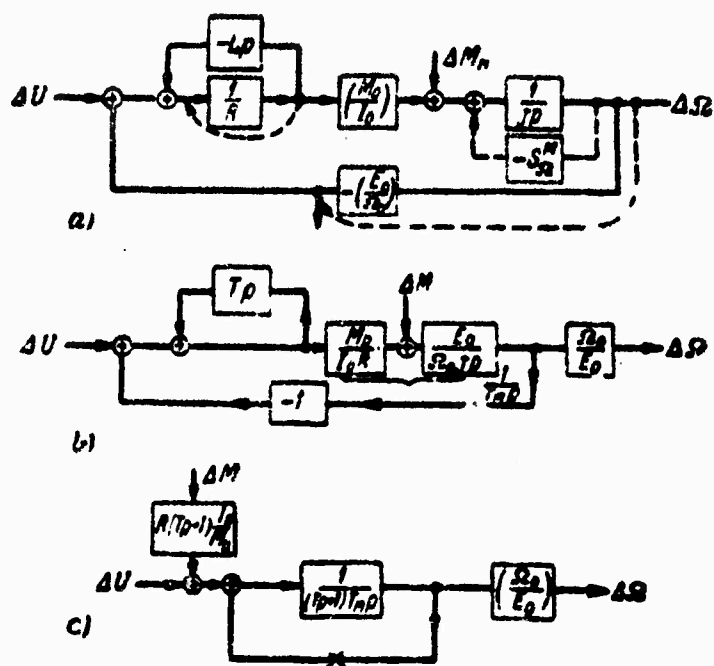
Fig 6-5. Block Diagrams for a [Compound] d-c Motor Using Armature Control

The expanded equations derived above were used in the construction of the block diagram shown in Fig 6-5(a), which depicts the required interconnections. In actual practice, the feedback loop $-S_{\Omega}^{M}$ around the intergrating element, representing the viscous friction in air or in some other medium, can be neglected compared to the contributions of other elements in the system (particularly that of the counter emf E_0/Ω_0), and the integrating element $1/Jp$ can be discussed without taking into account this feedback loop. However, the integrating element is not "free", since it is included in a negative feedback loop which contains a "stiff" component, the effect of which is to tranform the integrating element into an aperiodic element.

The loop gain for the rigid feedback loop containing the integrating element can be obtained by forming the product of the transfer functions of the elements in the loop;

$$k_{-1} = \frac{1}{R} \cdot \frac{M_\bullet}{I_\bullet} \cdot \frac{1}{J} \cdot \frac{E_\bullet}{\Omega_\bullet}.$$

[TN: In the above expression the subscript "a" of the armature resistance R_a has been incorrectly dropped in the text; in addition, the motor armature reactance has been ignored].

We shall call the reciprocal of the loop gain

$$T_M = \frac{JR}{\left(\frac{M_\bullet}{I_\bullet}\right)\left(\frac{E_\bullet}{\Omega_\bullet}\right)} \tag{6-33}$$

the electromechanical time constant. Introducing the above notation and the time constant for the armature circuit $T = L/R$ into the block diagram in Fig 6-5(a), and transforming the latter by moving the takeoff point for the Lp branch ahead of element $1/R$ and the takeoff point for the $\Delta\Omega$ branch ahead of element E_0/Ω_0, we obtain the block diagram shown in Fig 6-5(b). Fig 6-5(c) shows the final reduction of the block diagram to a form for which the closed loop transfer function on the input signal can be written as follows in expanded form:

$$W_U(p) = \frac{\dfrac{\Omega_\bullet}{E_\bullet}}{TT_M p^2 + T_M p + 1}. \tag{6-34a}$$

490

Inasmuch as the transfer function obtained is that of a second-order control system, velocity transients can develop when the damping ratio ξ (see Table 1-2) is less than unity,

$$\xi = \frac{T_M}{2\sqrt{TT_M}} = \frac{1}{2}\sqrt{\frac{T_M}{T}} < 1, \text{ i. e. } T > \frac{T_M}{4}.$$

If we set $T = 0$ in Fig 6-5(b) and move the control voltage feed channel to the torque branch [past element $M_O/I_O R$], we have from Equation (6-34a)

$$W_U(p) = \frac{M_\bullet}{RI_\bullet} \cdot \frac{R/\Omega_\bullet}{E_\bullet M_\bullet (T_M p + 1)} = M_U^n \frac{1/S_\Omega^M}{T_M p + 1}. \quad (6-34b)$$

We shall now derive the transfer function on the load torque. Wishing to use Equation (6-34b), we shall move the disturbance feed channel backward to the input summing point. This requires the addition of the reciprocal of the overall transfer function of the omitted [passed-over] elements.

$$R(Tp + 1)\left(\frac{I_\bullet}{M_\bullet}\right).$$

in series with the disturbance feed channel.

Taking into account the above addition, we can write the desired transfer function as follows:

$$W_M(p) = \frac{R(Tp+1)\left(\frac{I_\bullet}{M_\bullet}\right)\left(\frac{\Omega_\bullet}{E_\bullet}\right)}{(Tp + 1)T_M p + 1}. \quad (6-35a)$$

The coefficient $1/M_0$ can be factored out of the above expression:

$$W_M(p) = \frac{(Tp+1)RI_0 \frac{\Omega_0}{E_0}}{(Tp+1)T_M p + 1} \cdot \frac{1}{M_0}. \qquad (6\text{-}35b)$$

Multiplication of the disturbing torque by the right-hand side of the above operator transfer function transforms the disturbing torque into a torque ratio. $\Delta M_*/M_0 = \Delta M_*$.

It is also convenient to define the relative change in speed $\Delta \Omega_* = \Delta \Omega / \Omega_0$. The gain in terms of the transfer function relating the relative speed change to a relative change in torque will then have the value

$$W_M(0)_* = RI_0/E_0 \qquad (6\text{-}36)$$

2. Speed-Torque Characteristics of Electric Motors Using Field Control

We shall now pass to the discussion of the regulation characteristics of electric motors using field control. Initially we shall find it convenient to treat the field flux as an input and to derive the corresponding relationships. These will be used in constructing the basic block diagram which will then be gradually built up by taking into account specific methods of controlling the field flux with different types of excitation of the electric motor.

Thus if the total field flux $\overset{\rightarrow}{\Phi}$ is considered to be independent of the number of windings and of the winding scheme used in the motor, the torque of the electric motor will be proportional to the product of armature current and field flux:

$$M = \left(\frac{M_0}{I_0 \Phi_0} \right) I \Phi.$$

[TN: Subscript "a" not used for armature parameters].

If increments are used, we obtain an expression analogous to equation (6-32):

─ 492 ─

$$\Delta M = \left(\frac{M_o}{I_o \Phi_o} \right) (I_o \Delta \Phi + \Phi_o \Delta I) =$$

$$= M_o \left[\frac{\Delta \Phi}{\Phi_o} + \frac{\Delta I}{I_o} \right], \qquad (6\text{-}37a)$$

where

$$\left(\frac{M_o}{I_o \Phi_o} \right) = M_{y_I} \qquad (6\text{-}37b)$$

is the torque gradient (kg-m/amp-volts-sec).

The block diagram is shown in Fig 6-66a); the portion of the diagram corresponding to the relations derived above is enclosed within the dotted lines.

The buildup of the block diagram is carried out by the addition of elements expressing the dependence of the change in armature current on other controlled [manipulated] variables.

The equation for the armature current can be written

$$I = \frac{1}{R} \left[U - \left(\frac{E_o}{\Phi_o \Omega_o} \right) \Phi \Omega \right], \qquad (6\text{-}38)$$

where $(E_o / \Phi_o \Omega_o)$ gives the volts of counter-emf produced per unit flux-speed product.

Introducing increments, we obtain

$$\Delta I (p) = \frac{1}{R} \left[\Delta U (p) - E_o \left(\frac{\Delta \Phi}{\Phi_o} + \frac{\Delta \Omega}{\Omega_o} \right) \right]. \qquad (6\text{-}39)$$

— 493 —

Equation (6-39) has been used in constructing the upper portion of the block diagram in Fig 6-6(a).

All that remains to be done is to establish the relationship between an increment in torque and an increment in angular velocity [motor speed]. Such a relationship has already been established and can be written as follows in operator notation:

$$\Delta\Omega(p) = \frac{1}{Jp}\left[\Delta M_{\text{\emph{д}}}(p) - \Delta M_{\text{\emph{н}}}(p)\right].$$

The above relation was used in inserting the last forward element in the feed forward channel in the block diagram shown in Fig 6-6(a).

From the block diagram obtained we shall derive only one transfer function on the input signal, which we shall consider to be an increment in magnetic flux $\Delta\Phi(p)$. We shall temporarily neglect the extraneous input signals, i.e., changes in the armature supply voltage $\Delta U(p)$ and changes in the load torque $\Delta M_\ell(p)$, and we shall proceed to transform the block diagram. The first transformation is shown in Fig 6-6(b) and consists in moving the upper summing point downward beyond the element $-E_0 R I_0$ [TN: Actually three elements are involved] into coincidence with the lower summing point.

The right portion of the reduced block diagram contains an integrator with rigid negative feedback compensation. The time constant T_M of that loop is equal to the reciprocal of the open loop gain

$$T_M = \frac{J I_0 \Omega_0 R}{M_0 E_\bullet}. \qquad (6-40)$$

The gain of the resultant aperiodic element is equal to the reciprocal of the feedback channel gain

$$k_a = \frac{R I_0 \Omega_0}{E_\bullet}.$$

We shall find it convenient to simplify the notation by combining the elements in the feedback channel. The result is the block diagram shown in Fig 6-6(c).

We can now simply write down the closed-loop transfer function [on the input signal]

494
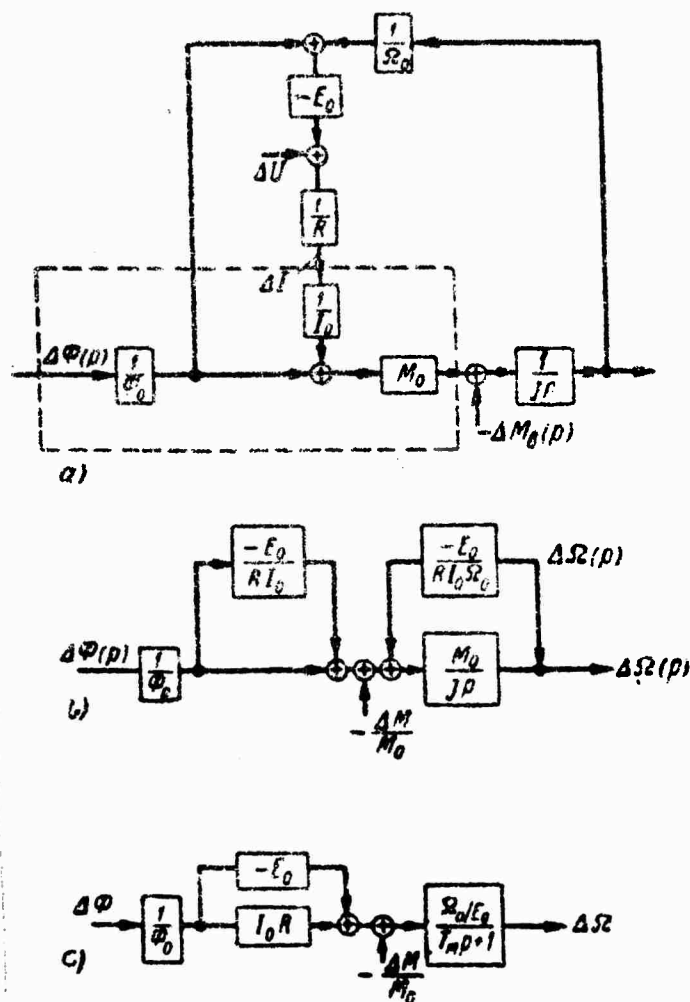
Fig 6-6. Block Diagram Illustrating the Conditions for the Regulation of a [Compound d-c] Motor Using Field Control

[TN: The factor RI_0 is missing from the numerator of the transfer function of the last element on the right in the reduced diagram in Fig 6-6(c).]

$$W_\Phi(p) = \frac{(I_\bullet R - E_\bullet)\frac{\Omega_\bullet}{E_\bullet}}{T_M p + 1} \cdot \frac{1}{\Phi_\bullet} \cdot \qquad (6\text{-}41)$$

The term $1/\Phi_o$ has been factored out to indicate that a change in magnetic flux $\Delta\Phi$ must be converted to a relative change in flux $\Delta\Phi/\Phi_o$. This eliminates the need for the determination of the absolute value of Φ_o, which is usually not given in standard electric motor catalogues.

An analysis of the transfer function described by Equation (6-41) or of the lefthand portion of the block diagram in Fig 6-6(c) shows that the sign of the transfer function is determined by the difference

$$I_\bullet R - E_\bullet.$$

If the nominal IR drop of the armature is expressed as the difference between the impressed circuit voltage and the motor-generated voltage, i.e., if we write

$$I_\bullet R = U_\bullet - E_\bullet,$$

the [closed-loop] transfer function can ce written in the form

$$W_\Phi(p) = \frac{(U_\bullet - 2E_\bullet)\frac{\Omega_\bullet}{E_\bullet}}{T_M p + 1} \cdot \frac{1}{\Phi_\bullet} \cdot \qquad (6\text{-}42)$$

On the basis of the relation derived above, the following conclusions may be formulated:

If the nominal operating conditions of the electric motor ($\Phi = \Phi_o$, $E = E_0$, $\Omega = \Omega_0$) are such that the counter-emf is less than one-half of the impressed circuit voltage, an increase in the field flux will result in an increase in motor speed.

493

If the nominal counter-emf is greater than one-half the impressed circuit voltage, an increase in the field flux will lead to a reduction in the speed of the electric motor.

Thus at low speeds and during startup, the sign of the transfer function will be positive.

Practical application of the positive transfer function, i.e., the use of field control during startup or at low speeds, requires the insertion of considerable starting resistances, sometimes even barretters, in the armature circuit, since the current-limiting effect of the counter-emf is small under these conditions. When starting resistances are not used, given the standard characteristics of commercial electric motors operated under conditions of speed stabilization, the counter-emf will be greater than one half the voltage impressed on the armature circuit, and the "flux-speed" transfer function will take on a negative sign which deserve special notice:

$$W_\Phi(p) = -\frac{(2E_0 - U_0)\dfrac{\Omega_0}{E_0}}{T_M p + 1} \cdot \frac{1}{\Phi_0}. \qquad (6\text{-}43)$$

To obtain the transfer function on the load torque, it is sufficient to limit our analysis to the second feedback loop in Fig 6-6(b), for which the transfer function may be written as follows

$$\frac{\dfrac{\Omega_0 I_0 R}{E_0}}{T_M p + 1}$$

Inasmuch as the feed channel for the disturbing torque has been moved ahead of the element M_0 [cf. Fig 6-6(a)], the above transfer function must be divided M_0. The resulting transfer function can be written

$$W_M(p) = -\frac{\left(\dfrac{\Omega_0}{E_0}\right)\left(\dfrac{I_0}{M_0}\right)R}{T_M p + 1}. \qquad (6\text{-}44a)$$

We shall find it convenient to factor out the coefficient $1/M_0$ in Equation (6-44a):

$$W_M(p) = -\frac{\dfrac{\Omega_0}{E_0} RI_0}{T_M p + 1} \cdot \frac{1}{M_0} . \qquad (6\text{-}44b)$$

We can now first express the disturbing torque as a torque ratio [percent change]

$$\Delta M_* = \frac{\Delta M}{M_0} ,$$

which, as may be seen from the transfer function, leads to the following relative change in speed in the steady state:

$$\Delta\Omega_* = \frac{\Delta\Omega}{\Omega_0} = \frac{RI_0}{E_0} \Delta M_* . \qquad (6\text{-}45)$$

The proportionality constant relating a percent change in torque to a percent change in speed is the ratio of the IR armature drop to the nominal counter-emf. For greater rigidity [sic] of the characteristics, this ratio must be made smaller.

3. A Generalized Block Diagram for Compound-Wound Electric Motors Using Various Control Schemes

We shall return to a discussion of the generalized circuit of an electric motor having a separately excited shunt winding and a series winding. As shown in fig 6-4, a disturbing torque M_L is applied to the shaft of the electric motor by a load having a reduced moment of inertia J.

The block diagram of a compound electric motor is the adjoint of the block diagram for a compound generator given in Fig 6-3. It follows that the generator and motor equations for corresponding channels are analogous in many respects, though the input and output variables differ in a number of cases [sic]. We shall therefore retain the notation used for the controlled variables in the generator block diagram discussed in Section 6-1.

Mesh Equations for the Shunt Winding. When the excitation current is regulated by varying the resistance of the shunt winding circuit, the relations between the currents and voltages in the circuit are expressed by Equation (6-20). When the resistance is kept constant ($\Delta R_2 = 0$), the equation is simplified

498

slightly:

$$(L_{sf}p + R_f)\,\Delta I_f(p) = \Delta U_f(p) - w_f\, p\, \Delta \phi\,(p) \qquad (6\text{-}46)$$

Equivalent Exciting Current Flowing in the Shunt Winding. We shall consider the basic saturation curve of the machine to be given in terms of the shunt winding. When a series field is present, the graph must be entered with an equivalent current

$$\Delta I_e = \Delta I_f + (w_s / w_f)\,\Delta I_a \qquad (6\text{-}47)$$

Total Field Flux. The total field flux is computed from the slope of the saturation curve

$$\Delta \phi = s_I^{\phi}\,\Delta I_e \qquad (6\text{-}48)$$

Mesh Equation of the Armature Circuit. We shall use Equations (6-22) as a basis and rewrite it in a form more convenient for the computation of $\Delta I_a(p)$; in addition, we shall use the symbol R_{Σ} to represent the total [ohmic] resistance of the armature circuit:

$$(L_{ss}p + R_{\Sigma})\,\Delta I_a(p) = \Delta U(p) - \Delta E - w_s\, p\, \Delta \phi \qquad (6\text{-}49)$$

Change in Counter-emf. Inasmuch as the electric motor operates under variable speed conditions, we shall Equation (6-30):

$$\Delta E = E_0 \left(\frac{\Delta \Phi}{\Phi_0} + \frac{\Delta \Omega}{\Omega_0} \right). \qquad (6\text{-}50)$$

In addition, inasmuch as the solution reduces to the regulation of the variables $\Delta \phi$ and ΔI_a, we can make use of the following equations which were derived for the electric motor:

For the change in torque

$$\Delta M(p) = M_0 \left[\frac{\Delta \Phi(p)}{\Phi_0} + \frac{\Delta I_a(p)}{I_0} \right]. \qquad (6\text{-}51)$$

For the change in speed

$$\Delta \Omega(p) = \frac{1}{Jp} [\Delta M(p) - \Delta M_r(p)]. \qquad (6\text{-}52)$$

439
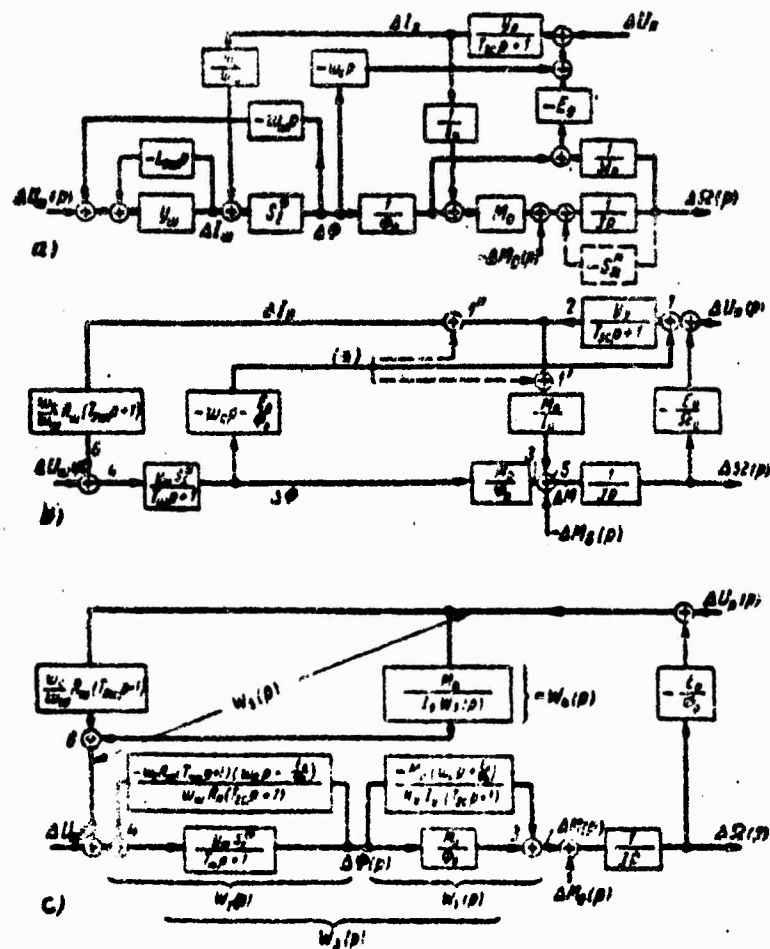
Fig 6-7. Block diagrams for the Compound [d-c] Motor Using Two-Channel Control

[TN: The transfer function $-E_0/\Phi_0$ should read $-E_0/\Omega_0$ in the righthand portion of Fig 6-7(c)].

Equations (6-47) through (6-52) were used in constructing the generalized block diagram for an electric motor shown in Fig 6-7(a). The block diagram has many features in common with the block diagrams constructed for the compound generator and the compound electric motor shown in Figs 6-5 and 6-6, respectively.

We shall now carry out a number of transformations of the block diagram in order to establish the time constants of the various loops in the scheme.

In proceeding with the determination of the time constant of the field loop, we note that the flexible feedback loops $w_f p$ and $L_{sf} p$ around the power elements S_I^ϕ and $(1/R_f) = Y_f$, respectively, act in parallel and consequently can be combined. To this end we first move the feed channel containing the element w_s/w_f in the lefthand portion of Fig 6-7(a) to the input of the diagram, as shown in Fig 6-7(b). In so doing, we multiply the transfer function of the element w_s/w_f by the reciprocal of the overall transfer function of the passed-over elements, obtaining the new transfer function $w_s R_f (T_{sf} p + 1)/W_f$, which is entered in the block diagram in Fig 6-7(b) ($T_{sf} = L_{sf}/R_f$, the time constant of the field winding referred to the leakage flux).

We can proceed to combine the element $L_{sf} p$ with the element $w_f p$. However, the transfer function of the latter [former] must first be multiplied [divided] by S_I^ϕ as the takeoff branch is moved forward past the latter element. Following this rearrangement we can add the two elements to obtain

$$L_{sf} p + w_f S_I^\phi p = (L_{sf} + w_f S_I^\phi) p$$

Since $S_I^\phi = \partial \phi / \partial I$, the multiplication of S_I^ϕ by the number of [shunt] turns yields the self-inductance of the shunt winding referred to the main-pole flux. The sum of the latter quantity and of the leakage self-inductance constitutes the total self-inductance of the shunt winding.

$$L_{f0} = L_{sf} + w_f S_I^\phi .$$

The time constant of the shunt winding referred to the total field flux thereby becomes

$$T_f = L_f / R_f$$

When the above-established notation is taken into account, the transfer function of the element $Y_f = 1/R_f$ enclosed by the feedback loops discussed above becomes $Y_f/(T_f p + 1)$. In the block diagram this element has been combined with the adjoining

element $\delta \overset{\phi}{I}$.

Transferring our attention to the righthand portion of Fig 6-7(a), we move the output of the element $1/\Omega_0$ to the feed channel for the input signal ΔU_a, past the element E_0. The overall transfer function for the branch E_0/Ω_0 is entered in the righthand portion of Fig 6-7(b).

Finally, we combine the adjoining elements $1/\Phi_0$ and E_0 in the block diagram in Fig 6-7(a). Before combining these elements we must first rearrange the intervening branch and summing points. The branch point is moved backwards, thus introducing the function $1/\Phi_0$ in series with the branch, while the summing point is moved ahead, thus changing the transfer function of the $1/I_0$ branch to E_0/I_0. The resulting changes are shown in Fig 6-7(b).

The parallel branches w_{sp} and $E_0/\overset{\cdot}{\Phi}_0$ in Fig 6-7(a) have been combined into a single element having the transfer function $-(w_{s}t+E_0/\Phi_0)$, as shown in Fig 6-7(b).

The block diagram in Fig 6-7(b) has undistorted [sic] for the regulated variables $\triangle \phi$, ΔM, and ΔI_a; in addition, the block diagram has input and output channels [sic]. From the block diagram a number of **judgments** concerning the operating characteristics of the system can be made. However, before doing so we shall find it convenient to remove the cross-over branch terminating at summing point 1.

We shall first move the branch ahead of the integrating element to point 2. The transfer function for the cross-over branch is then given by

$$ -\frac{w_c p + \dfrac{E_0}{\Phi_0}}{R_a(T_{sc}\,p+1)} \qquad (*) $$

It is further necessary to move the summing point past the takeoff point in the direction of signal flow with a resultant shift of the element(s) in the branch and the formation of two equal branches with the indicated transfer function ($*$), terminating at summing points 1' and 1", as shown by the broken lines in the diagram.

Next, we move summing point 1' to point 3. This re-arrangement requires the insertion of the function M_0/I_0 in series with the branch, the transfer function of which now becomes

$$-M_0(w_s p + E_0/\Omega_0)R_a I_0(T_{ss}p+1)$$

This transfer function has been entered on the rearranged branch in the block diagram in Fig 6-7(c).

The presence of two parallel branches of opposite sign between the $\Delta\phi$ and ΔM channels indicates that the sign of the overall transfer function on the input signal can be controlled by adjusting the gains in the two parallel branches. When the two branches are combined into a single branch, the transfer function of the latter relating a change in torque to a change in flux becomes

$$W_1(p) = \frac{\Delta M(p)}{\Delta\Phi(p)} = -\left[\frac{\Phi_0 w_c p + E_0}{R_a I_0(T_{sc}p+1)} - 1\right]\frac{M_0}{\Phi_0}. \quad (6\text{-}53)$$

$$\mathcal{R} = \omega \quad c = s$$

In a steady-state condition ($p = 0$)

$$\Delta M/\Delta\phi = -(M_0/\phi_0)[(E_0/I_0 R_a)-1]$$

and all deductions concerning the rule of signs coincide with the deductions made from the analysis of Equations (6-41) and (6-42).

We now move summing point 1" to point 4. The transfer function of the crossover branch is then given by

$$-\frac{w_c R_m (T_{sm}p+1)\left(w_c p + \frac{E_0}{\Phi_0}\right)}{w_m R_s(T_{sc}p+1)}.$$

$$\omega = f$$

The result of the above rearrangement is to introduce a feedback loop around the aperiodic element, and we can write for the closed-loop transfer function

$$W_2(p) =$$

$$= \frac{Y_{tu}S_I^{\bullet}w_{tu}R_{a}(T_{sc}p+1)}{w_{tu}R_{a}(T_{sc}p+1)(T_{tu}p+1)+w_cS_I^{\bullet}(T_{su}p+1)\left(w_cp+\frac{E_{\bullet}}{\Phi_{\bullet}}\right)}.$$

When the above transfer function is combined with that
of the adjoining element $W_1(p)$. the resultant overall transfer
function is given by the Equation (6-54).

$$W_3(p) = W_1(p)W_2(p) =$$

$$= \frac{-M_{\bullet}Y_{tu}S_I^{\bullet}w_{tu}(\Phi_{\bullet}w_cp+}{I_{\bullet}\Phi_{\bullet}[w_{tu}R_{a}(T_{tu}p+1)(T_{sc}p+1)+}$$

$$\frac{+E_{\bullet})-R_{a}I_{\bullet}(T_{sc}p+1)]}{+w_cS_I^{\bullet}(T_{su}p+1)\left(w_cp+\frac{E_{\bullet}}{\Phi_{\bullet}}\right)]}. \qquad (6\text{-}54)$$

Next, we move summing point 5 to point 6 and insert
the reciprocal of the overall transfer function of the passed-over
elements in series with the branch. The resultant overall trans-
fer function for the branch can be written

$$W_4(p) = M_o/I_oW_3(p) \qquad (6\text{-}55)$$

Equation (6-55) can be combined with the overall
transfer function of the parallel branch terminating at summing
point 6.

In the block diagram [Fig 6-7(c)] the transfer function
of the combined parallel branches is labelled $W_4(p)$ in conformity
with the notation used for the cascade element [sic]. The ex-
panded form of transfer function $W_5(p)$ is given by Equation
(6-56).

$$W_5(p) = -\frac{R_{tu}}{w_{tu}}\frac{Y_{a}}{T_{sc}p+1}\times$$

$$\times\left[\frac{w_{tu}R_{a}(T_{tu}p+1)(T_{sc}p+1)+}{S_I^{\bullet}[\Phi_{\bullet}w_cp+E_{\bullet}-}\right.$$

$$\left.\frac{+w_cS_I^{\Phi}(T_{su}p+1)\left(w_cp+\frac{E_{\bullet}}{\Phi_{\bullet}}\right)}{-R_{a}I_{\bullet}(T_{sc}p+1]}-w_c(T_{su}p+1)\right]. \quad (6\text{-}56)$$

an analysis of the two parallel branches referred to above shows that they both are in a feedback relation to the integrating element $1/Jp$. The interplay of the signs of the component elements of transfer function $W_4(p)$ is such that the overall sign of the function is negative, and it therefore constitutes a negative feedback loop. The element $w_s R_f(T_s p+1)/w_f$ introduces a positive feedback signal or reduces the effect of the negative feedback loop. This arrangement increases the sensitivity of the scheme to changes in excitation voltage but simultaneously also increases the effect of torque disturbances on the speed error, i.e., the mechanical characteristic [mekhanicheskaya kharakteristika: speed-torque curve?] of the electric motor is thereby made "softer". When the direction of the flux in the series winding is reversed, i.e., the electric motor is made "anticompound," the sensitivity of the scheme to field control is reduced and the mechanical characteristic is made "stiffer."

For armature control of the electric motor, the feedback loop around the integrating element contains only the element $-E_0/\Omega_0$, from which the overall gain is computed to be Ω_0/E_0. The overall transfer function of the armature voltage feed channel $W_5(p)$ has no effect on the system transfer function in the steady state, though the overall system stability is retained.

Thus the block diagram constructed in Fig 6-7(c) can be represented as a single loop scheme. The closed loop transfer function can then be written

$$C(p) = \frac{1}{Jp}\left(-\frac{E_0}{\Omega_0}\right)W_5(p)\,W_4(p).$$

Using the transfer function notation introduced above, we can write the overall transfer function (Equation (5-15)) for the determination of the actuating signal at the disturbance input summing point or the relative transfer function [actuating signal ratio].

$$\Phi_a(p) = \frac{1}{1+C(p)}. \tag{6-57}$$

[TN: The sign convention followed here appears to contradict that followed in Equation (6-16)].

We can easily write the transfer functions on the two input signals as well as the transfer function on the extraneous signal.

The transfer function on the control field voltage can be written

$$\Phi_{U_m - \varrho}(p) = \frac{W_1(p)}{Jp\left[1 + C(p)\right]}. \qquad (6\text{-}58)$$

[TN: From Figs 6-7(c) it would appear that $W_3(p)$ should have been used in the numerator; cf. Equation (6-58) below].

The transfer function on the armature voltage becomes

$$\Phi_{U_A - \varrho}(p) = \frac{\Omega_0}{E_0} \cdot \frac{C(p)}{1 + C(p)}. \qquad (6\text{-}59)$$

[TN: A negative sign in front of the factor Ω_0/E_0 has been dropped].

The transfer function on the disturbing torque is given by

$$\Phi_{M - \varrho}(p) = \frac{-1}{Jp\left[1 + C(p)\right]}. \qquad (6\text{-}60)$$

[TN: Incorrect sign; cf. Fig 6-7(c)]

From the above transfer functions the static gains for a step input can be calculated:

$$\Phi_{U_m - \varrho}(0) = -\frac{\Omega_0 S_I^\Phi (E_0 - I_0 R_a)}{R_m E_0 \left(\Phi_0 + S_I^\Phi I_0 \dfrac{w_c}{w_m}\right)}; \qquad (6\text{-}58a)$$

$$\Phi_{U_A - \varrho}(0) = \frac{\Omega_0}{E_0}; \qquad (6\text{-}59a)$$

$$\Phi_{M - \varrho}(0) = -\frac{R_a I_0 \Omega_0 \left(1 + \dfrac{w_c}{w_m} S_I^E I_a\right)}{M_a E_0 \left(1 + \dfrac{w_c}{w_m} S_I^E \dfrac{I_0}{E_0}\right)}. \qquad (6\text{-}60a)$$

[TN: The symbol J_a in the numerator of Equation (6-60a) has not been defined previously].

The essential steady-state characteristics of the scheme have been discussed in the course of the analysis of the intermediate block diagrams. The equations presented above merely provide a more rigorous confirmation of deductions previously stated.

A more detailed descriptions of the properties of electric machines by classical methods can be found in contemporary textbooks (Ref 1 and 2) and in the literature on the regulation of machines (Ref 3). Structural methods [block diagram analysis] also make it possible to formulate a number of additional problems in a readily visualized format. Tensor analysis (Ref 4) is another method of fairly broad applicability offering similar possibilities. However, experience cited in Ref 5 indicates that this latter method is not nearly as graphic.

6-5. DYNAMOELECTRIC AMPLIFIERS-THE AMPLIDYNE

The circuit for the system under discussion is shown in Fig 6-8(a). A load having a static torque M_l and a reduced moment of inertia J is driven by a separately excited electric motor, the armature field of which is controlled by the amplidyne output.

The amplidyne has a control field with a resistance R_{co} and a total inductance L_{co}, a short-circuited set of primary brushes having a resistance R_q and an inductance L_q (including an auxiliary series winding), and a set of secondary brushes set on an axis at right angles to the axis of the primary short-circuited brushes. In the circuit formed by the secondary brushes should be included the [effective] armature resistance R_e and the inductance L_d of the armature along the longitudinal axis [sic], as well as the resistance R_k and the inductance of the compensator winding which is shunted by the rheostat ρ_k. The distributed character of the compensator winding, which is a mirror image [opposes] the armature winding, and the provision of a variable shunt resistor make possible the complete compensation of the armature reaction along the longitudinal axis [i.e., resulting from the load current], with the result that the flux linking the windings can be neglected (in the case of incomplete compensation, this flux must be taken into account by the introduction of additional elements into the block diagram).

We shall now proceed to write the equations for the various circuits in the system under discussion.

For the ohmic resistance of the control winding

507
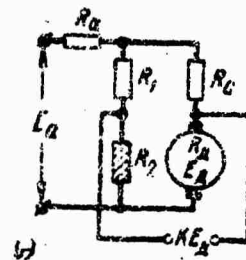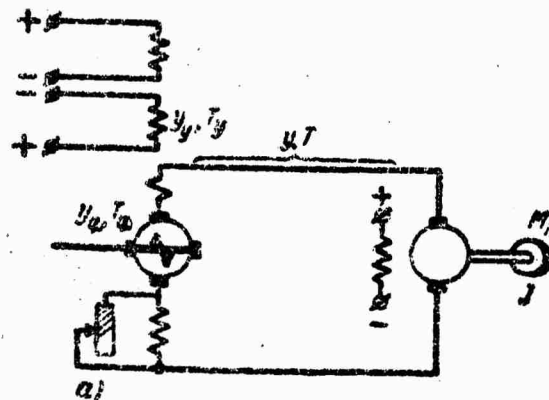
Fig. 6-8. Electrical circuit for controlling a
d-c motor with the aid of a dynamoelectric
amplifier (amplidyne)

a) amplidyne-motor circuit; b) circuit for taking off
the counter emf of the motor.

circuit of the amplidyne, we can write $R_c = 1/Y_c$; the time constant for the circuit can then be written $T_c = L_c/R_c$. With the introduction of this notation, the equation for the exciting current becomes

$$I_y(p) = \frac{Y_y}{T_y p + 1} U_y(p). \qquad (6\text{-}61).$$

$$y = c$$

The relationship between the current in the control field winding (exciting current) and the emf E_q in the short-circuited armature winding of the amplidyne can be determined from the corresponding saturation curve. Following rectification of the unsaturated portion of the curve up to E_{q0} and I_{c0}, the following approximate relation can be established:

$$E_q = \frac{E_{q0}}{I_{y0}} I_y = S_i^{E_q} I_y. \qquad (6\text{-}62)$$

The voltage equation for the short-circuited primary circuit can be written as follows:

$$E_q(p) = (R_q + L_q p) I_q(p).$$

It should be noted that for the amplidyne as for the generator with only one set of brushes described in Section 6-1, we must determine the equivalent resistance of the circuit formed by the short-circuited primary brushes. This equivalent resistance, in addition to the armature IR drop, the brush-contact drop, and the IR drop in the auxiliary series winding also includes the demagnetizing effect of the armature reaction. The latter effect can be quite large as a result of the design of the magnetic circuit of the amplidyne. More complete information will be found in Ref 6.

The inductance shown in the preceding formula likewise represents a summation of the contributions of the internal and external parts of the circuit set up by the short-circuited primary brushes.

When the preceding equation is solved for $I_q(p)$ in operator form we have

$$I_q(p) = \frac{Y_{q3}}{T_q p + 1} E_q(p). \qquad (6\text{-}63)$$

$\vartheta = \ell$

We now proceed to compute the emf at the secondary brushes from the current flowing in the short-circuited windings, which sets up the armature cross field. The functional relationship between the exciting current and the emf is given by the saturation curve $E_a = f(I_q)$. Rectifying the latter over the initial branch from 0 to E_0 and I_{q0}, we obtain the relation

$$E_a = \frac{E_0}{I_{q0}} I_q = S_{Iq}^E I_q. \qquad (6\text{-}64)$$

Next, we set up the overall voltage equation for the main circuit composing the amplidyne and motor.

$$E_a(p) = E_m(p) + I(p)(R + Lp)$$

In the above equation we have again used the total ohmic resistance of the circuit formed by the amplidyne, motor, and connecting leads; the inductance used likewise represents the sum of the contributions of the circuit components. We shall find it convenient to solve the above equation conditionally for the main-circuit current:

$$I(p) = \frac{Y}{Tp+1} [E_a(p) - E_a(p)]. \qquad (6\text{-}65)$$
$$\underset{m}{\downarrow}$$

When the magnetic flux in the electric motor is held constant, the torque can be readily calculated from the current:

$$M = \frac{M_0}{I_0} I = K_I^M I. \qquad (6\text{-}66)$$

In the absence of a viscous friction torque, the speed of the motor can be computed from the torque with allowance for disturbing torque M_ρ:

510

$$\Omega(p) = \frac{1}{Jp} [M(p) - M_H(p)]. \qquad (6\text{-}67)$$

The system of equations is completed by writing the equation for the calculation of the counter-emf of the motor from the speed:

$$E_A = \frac{E_0}{\Omega_0} \Omega = K_0^E \Omega. \qquad (6\text{-}68)$$

Using the equations derived above, the block diagram in Fig 6-9 was constructed. In the case under discussion the number of branches between regulated variables is minimal [sic] and the block diagram obtained contains only one loop. In this form [Fig 6-9(a)] the block diagram does not take into account the mutual inductance of the windings in the primary and secondary circuits. However, given ideal compensation of the various magnetic fluxes, which is after all precisely the reason for the insertion of a control shunt rheostat across the compensating winding, the block diagram under discussion represents a fairly close approximation to real systems and is frequently used in the form shown.

We now return to Fig 6-8. Whenever it becomes necessary for a given application to measure the counter-emf of the electric motor during operation, the measurement can be carried out with the bridge circuit shown in Fig 6-8(b). The resistances in the various arms of the bridge are proportional, i.e., $R_S/R_m = R_1/R_2$, and hence the emf of the amplidyne E_a does not affect the voltage of the bridge. When the counter-emf of the motor is inserted in a bridge arm loaded by resistance R_a, it is transmitted to the terminals amplified by the gain K of the bridge:

$$KE_A = \frac{R_c(R_a + R_1 + R_2) + R_a R_1}{(R_1 + R_2)R_a + (R_a + R_1 + R_2)(R_2 + R_c)} E_a.$$

The possibility of experimentally determining the quantity KE_m appearing in the block diagram permits the further utilization of the variable E_m as a regulated [manipulated] variable when new elements are added to the system. It should be noted

511

that a variable [signal] proportional to the speed Ω or E_m could be obtained from a tachometer generator mounted on the shaft of the electric motor. The latter method produces a more accurate value of Ω inasmuch as in the bridge scheme discussed above only ohmic resistances were taken into account in establishing the bridge balance; however, the use of a tachometer generator complicates the mechanical part of the system.

From the block diagram in Fig 6-9(a) we can write the transfer function from the [amplidyne] field input to the speed of the driven motor

$$W_e(p) = \frac{Y_y S_{I_y}^E Y_q S_{I_q}^E \frac{1}{K_{\Omega}^E}}{(T_y p + 1)(T_q p + 1)[(Tp + 1)T_M p + 1]} \qquad (6-69)$$

and the transfer function on the disturbing load torque

$$W_M(p) = \frac{\frac{R(Tp + 1)}{K_6^E K_I^M}}{(Tp + 1)T_M p + 1}, \qquad (6-70)$$

where

$$T_M = \frac{JR}{K_I^M K_{\Omega}^E}.$$

We shall now take up a number of additional factors affecting the operation of the motor-amplidyne set and to the corresponding buildup of the block diagram.

We shall examine first the case of incomplete compensation of the secondary field. Let ΔwI be the difference between the cross-magnetizing armature ampere-turns and the compensating winding. The equivalent additional exciting current in the control winding calculated from the ampere-turn ratio is

$$\frac{\Delta w}{w_y} I.$$

The total equivalent magnetizing current flowing across the ~~~~~~~~~~~~~~~~ primary circuit of the amplidyne is given

$$I_{y.s} = I_y + \frac{\Delta w}{w_y} I. \qquad (6\text{-}71)$$

$$y: c \qquad \vartheta : c$$

For the determination of the total secondary flux we introduce the symbol S_I^Φ for the slope of the curve giving the variation of the secondary flux as a function of the current in the short-circuited windings.

$$\Phi_d = S_I^\Phi I_{y.s} \qquad (6\text{-}72).$$

For the calculation of the emf generated between the primary brushes at constant speed, it is sufficient to introduce the constant E_{qo}/Φ_{do}. We then have

$$E_q = \frac{E_{q0}}{\Phi_{d0}} \Phi_d. \qquad (6\text{-}73)$$

The determination of the new quantities appearing in Equation (6-72) and (6-73) does not require the recording of special experimental curves. All of these quantities can be computed from the magnetization curve for the primary circuit. The slope of that curve is given by

$$S_I^e = S_I^\Phi \frac{E_{q0}}{\Phi_{d0}}.$$

The determination of the equivalent magnetizing current, secondary flux, and primary emf in accordance with Equations (6-72) and (6-73) is reflected in the block diagram in Fig 6-9(b). The block diagram contains new elements and an additional feedback branch from the channel for the main circuit current.

The block diagram also shows additional branches taken off the secondary flux channel. The dependence of the secondary flux not only on the control field current but on a number of additional factors as well requires us to account separately for the changes in the emf of the control winding produced by changes in the secondary flux. The mesh equation

513
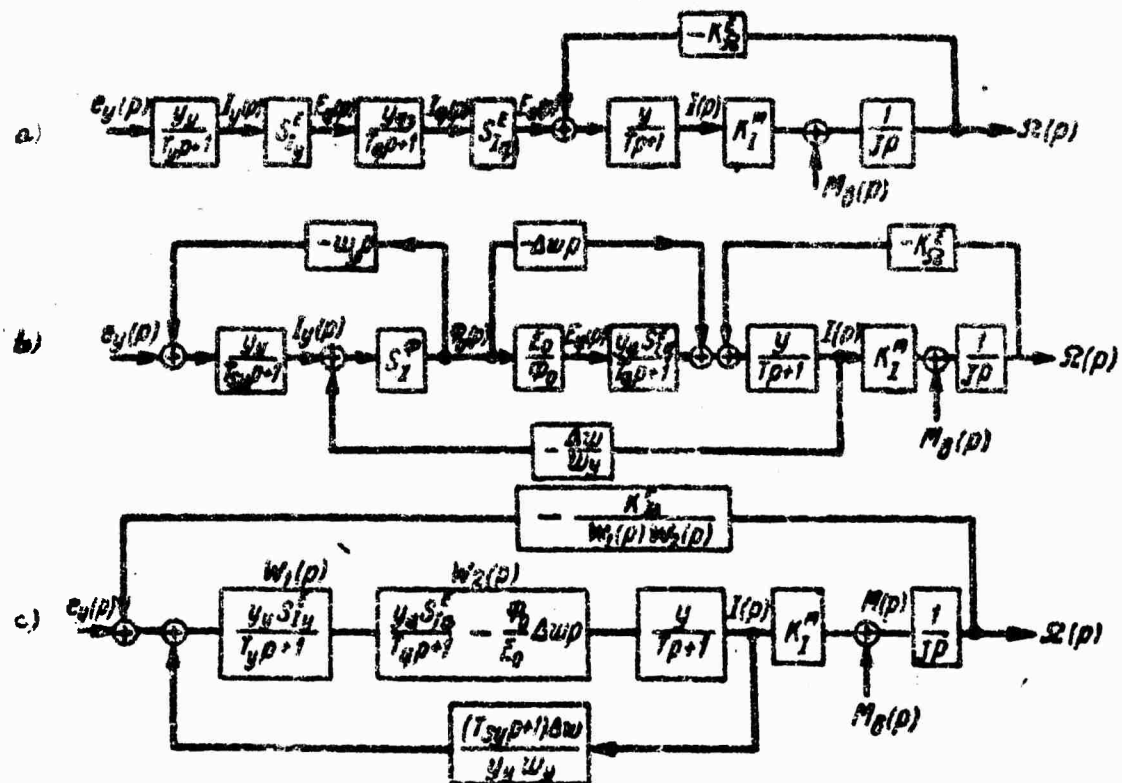
Fig 5-9. Block Diagrams of Control Systems for Electric Motors Using a Dynamoelectric Amplifier

for the control circuit is thereby made somewhat more complicated compared to Equation (6-61):

$$e_c(p) = (L_{sc}p + R_c)I_c(p) + w_c p \Phi_d(p)$$

Solving the above equation for $I_c(p)$, we have

$$I_y(p) = \frac{1}{L_{sy}p + R_y} [e_y(p) - w_y p \Phi_d(p)]. \qquad (6\text{-}74)$$

$$y = c$$

The above relationships are expressed in the block diagram given in Fig 6-9(b). The symbols L_{sc} and $T_{sc} = L_{sc}/R_c$ represent the leakage self-inductance and the time constant of the control winding, respectively.

We note immediately that such a distribution of the self-inductances is useful only in the intermediate stage of investigation. Once the conditions for current feedback in the diagram shown in Fig 6-9(b) have been determined, it will be found convenient to move the summing point in the control current channel to the input of the system, as shown in the block diagram in Fig 6-9(c). The feedback transfer function thereby takes on a more complex form

$$(T_{sc}+1) \Delta w / Y_c w_c$$

Bearing in mind the relationship

$$L_{sc} + S_I w_c = L_c$$

discussed in Section 6-1, we reintroduce in the feed-forward branch the initial total inductance and the initial time constant T_c.

Changes in the secondary field can also affect the emf balance in the main [amplidyne-driven motor] circuit inasmuch as an additional emf is impressed upon the circuit by the contribution of the noncompensated turns to the secondary flux

$$\Delta E(p) = -\Delta w p \Phi_d(p). \qquad (6\text{-}75)$$

This emf has also been entered in the block diagram in Fig 6-9(b). In the preceding discussion we have already mentioned transformations of the block diagram in Fig 6-9(b) and the partial reduction of that diagram to the block diagram shown in Fig 6-9(c). We now continue these transformations.

515

First, the two branch points in the Φ_d channel are moved beyond element E_0/Φ_c. We can write for the combined transfer function of the elements up to the branch point [sic]

$$W_1(p) = \frac{Y_y S_{Iq}^E}{T_y p + 1}.$$

$$y = c$$

The overall transfer function for the modified feed forward loop to the right of the branch point is given by

$$W_2(p) = \frac{Y_q S_{Iq}^E}{T_q p + 1} - \frac{\Phi_0}{E_0} \Delta w\, p.$$

It will be found convenient to move the feedback branch $-\kappa^E$ backward to the input to the system. The transfer function for the branch will thereby be transformed as follows

$$-\frac{\kappa_0^E}{W_1(p)\, W_2(p)}.$$

The above transformations were used in constructing the block diagram shown in Fig 6-9(c), which does not contain crossed branches and has undistorted channels for the regulated variables. The reduced block diagram permits the easy determination of the desired transfer functions, both on the reference input and on the disturbance.

We first proceed to the determination of the transfer function for the internal positive feedback loop:

$$\Phi_{12}(p) = \frac{Y_y Y S_{Iy}^E \left[Y_q S_{Iq}^E - \right.}{(T_y p + 1)(T_q p + 1)(T p + 1) - Y S_{Iy}^E (T_{zy} p + 1) \times}$$

$$y = c$$

$$\frac{-\dfrac{\Phi_0}{E_0} \Delta w_1 (T_q p + 1)\, p]}{\times \left[Y_q S_{Iq}^E - \dfrac{\Phi_0}{E_0} \Delta w_1 (T_q p + 1)\, p \right] \dfrac{\Delta x}{w_1}}. \qquad (6\text{-}76)$$

The above transfer function characterizes the operation of the amplidyne as a generator with a load which does not produce a counter-emf ($K^E = 0$).

It is important to note that for

$$\frac{\Delta w}{w_y}\bigg|_{y\,=\,c} = \frac{RR_q}{S_{Iy}^E S_{Iq}^E} \tag{6-77}$$

the free term in the denominator vanishes ($a_o = 0$) and the amplidyne takes on the characteristics of an astatic element. For

$$\Delta w/w_c > RR_q/S_{Ic}^E S_{Iq}^E$$

the free term takes on a negative sign, and the system becomes quasi-static. When either condition (6-77) or the condition

$$\Delta w/w_c < RR_q/S_{Ic}^E S_{Iq}^E$$

is fulfilled, the equivalent element can be used as a component of a more complex system for which the necessary stability conditions discussed in Chapter 11 must be assured.

The overall transfer function of the system on the reference input [control ratio] is given by

$$\Phi_e(p) =$$

$$= \frac{Y_y Y S_{Iy}^E K_I^M \times}{pJ\left\{(T_y p + 1)(T_q p + 1)(T p + 1) - Y S_{Iy}^E (T_{sy} p + 1) \times \frac{\times\left[Y_q S_{Iq}^E - \dfrac{\Phi_e}{E_e}\,\Delta w \times\right]}{\times\left[Y_q S_{Iq}^E - \dfrac{\Phi_e}{E_e}\,\Delta w (T_q p + 1) p\right] \dfrac{\Delta w}{w_y}\right\} + } + \dfrac{\times (T_q p + 1) p\Big]}{+ Y K_Q^E K_I^M (T_q p + 1)(T_y p + 1)}} \tag{6-78}$$

When the system is in a steady state, the static gain for a constant reference input is given by

$$\Phi_e(0) = \frac{Y_y S_{ly}^F Y_q S_{lq}^E}{K_\Omega^E} = \frac{S_{ly}^E S_{lq}^E}{K_\Omega^E R_y R_q}. \qquad (6\text{-}79)$$

The transfer function on the disturbing torque is given by

$$\Phi_M(p) =$$

$$= \frac{\{(T_y p + 1)(T_q p + 1)(T p + 1) - Y S_{ly}^E (T_{sy} p + 1) \times}{p J \Big\{ (T_y p + 1)(T_q p + 1)(T p + 1) - Y S_{ly}^E (T_{sy} p + 1) \times}$$

$$\frac{\times \Big[Y_q S_{lq}^E - \frac{\Phi_q}{E_q} \Delta x \times}{\times \Big[Y_q S_{lq}^E - \frac{\Phi_q}{E_q} \Delta x (T_q p + 1) p \Big] \frac{\Delta x}{w_y} \Big| +}$$

$$\frac{\times (T_q p + 1) p \Big] \frac{\Delta x}{w_y} \Big\}}{+ Y K_\Omega^E K_I^M (T_y p + 1)(T_q p + 1)} \qquad (6\text{-}80)$$

The disturbance static error coefficient is given by

$$\Phi_M(0) = \frac{1 - Y Y_q S_{ly}^E S_{lq}^E \frac{\Delta x}{w_y}}{Y K_I^M K_\Omega^E}. \qquad (6\text{-}81)$$

It is important to note that when condition (6-77) is satisfied, $\Phi_M(0) = 0$ and a constant load torque has absolutely

518

no effect on the steady state speed of the electric motor.

It must be borne in mind that the passage to the limits in (6-79) and (6-81) by setting p = 0 is justified only for stable systems.

The block diagram in Fig 6-9(a), representing the motor-amplidyne circuit, can also be used to represent the circuit of a motor-generator set as well as a quadratic motor-generator scheme [exciter-type regulation method]. In the latter type of scheme control is effected by varying the field voltage of the exciter, the field of the power generator is connected across the exciter armature, and the generator supplies power to the working motor. Though the block diagram is very similar to that in Fig 6-9(a), the response time of an actual exciter-type regulation system is considerably increased as a result of the increase in the value of the time constant of the second stage, in which the low-inductance primary circuit of the amplidyne is replaced by the multiple-turn excitation field of the power generator.

The block diagram for one stage of the motor-generator set [sic] will not contain one set of leftmost elements in Fig 6-9(a).

The conclusions presented above were based on the assumption that the speed of the driving motor which is mechanically coupled to the amplidyne will remain constant. However, in the presence of variations in the load torque, the requirement for a rigorously constant speed is equivalent to requirement of an infinitely large motor rating, which is impossible. We shall apply a method analogous to that developed in Section 6-2 to the investigation of this question.

Let a disturbance in the form of a change in torque ΔM_β be impressed upon the working motor. This will result in a change in practically all the regulated variables, since they are all interrelated, as can be seen from the block diagram.

We shall consider first the changes in the armature current ΔI and in the primary flux $\Delta \Phi_q$, inasmuch as the product of these quantities determines the electromagnetic inertia of the amplidyne.

We can compute the change in the torque of the driving motor from Equation (6-92), derived for a single-stage generator. We note that the efficiency of the amplidyne will be smaller inasmuch as this parameter reflects all ohmic losses in the windings (other than the control winding) as well as all mechanical losses.

519

$$\Delta M_{\text{и}} = \frac{0,102}{\eta} (\Phi_{q0}\Delta I + I_q \Delta \Phi_q). \qquad (6\text{-}82)$$

$I_{\text{ДМ}}$ (driving motor)

To determine the effect of the disturbing torque on the speed of the driving motor, we shall make use of the disturbance transfer function of the latter. We shall assume that the speed-torque characteristic of the driving motor is linear over the range involved and that the transfer function closely approximates Equation (6-35). To simplify the calculation, we shall neglect the time constant determined by the self-inductance of the armature circuit. We then have

$$K_{\text{и}}(p) = \frac{-R_{\text{н}}I_{\text{и}.0}\dfrac{\Omega_{\text{и}0}}{E_{\text{и}0}}\dfrac{1}{M_{\text{н}0}}}{T_{\text{и}}p + 1} = \frac{-K_{\text{и}}}{T_{\text{и}}p + 1}. \qquad (6\text{-}83)$$

The fluctuation in the speed of the amplidyne, which is computed from the relation

$$\Delta \Omega_{\text{и}}(p) = K_{\text{и}}(p)\,\Delta M_{\text{и}}(p),$$

will induce additional voltage changes in both stages. These changes can be computed by formulas analogous to Equation (6-30). When these additional changes are taken into account, the total variations in emf [in the two stages] can be written as follows:

$$\Delta E_q = S^E_{I_y}\Delta I_y + \frac{E_{q0}}{\Omega_{\text{и}.0}}\,\Delta \Omega_{\text{и}}; \qquad (6\text{-}84)$$

$$\Delta E = S^E_{I_q}\Delta I_q + \frac{E_q}{\Omega_{\text{и}.0}}\,\Delta \Omega_{\text{и}}. \qquad (6\text{-}85)$$

The block diagram in Fig 6-10 reproduces the feed-forward channel of the diagram in Fig 6-9(а). In addition, the block diagram in Fig 6-10 has been built up by the inclusion of elements corresponding to Equations (6-82) through (6-35).

We begin by providing in the diagram a channel for the

520

new regulated variable $\Delta \Omega_{DM}(p)$ representing the variation in the speed of the driving motor (left lower portion of the diagram), from which the increases in emf amplified by the elements E_{qo}/Ω_{DMo} and E_o/Ω_{DMo} are fed to appropriate points on the feed-forward channel.

To obtain $\Delta \Omega_{DM}(p)$, we introduce an element equivalent to the driving motor, to the input of which are fed the load torque change components from the $\Delta I(p)$ and $\Delta \Phi_q(p)$ channels, amplified by the elements Φ_{qo} and I_o, respectively. The coefficients $0.102/\eta$ is included in the element representing the motor.

It will be readily seen that the new branches in Fig 6-10 have negative signs compared to Fig 6-9 [sic]. The overall effect is the decrease in the gain change following an increase in the reference input made necessary by the drop in the speed of the driving motor.

For the load torque, on the other hand, the additional branches result in an increase in gain in the feedback loop around the integrating element $1/Jp$. The result is au increase in the overall gain on the disturbance.
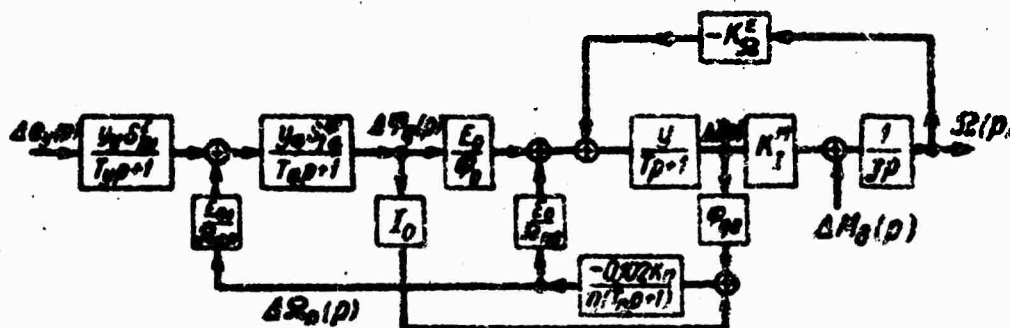

Fig 6-10. Block Diagram of a Regulating System Using a Dynamo-electric Amplifier and Taking into Account the Limited Power of the Prime Mover Driving the Dynamo-electric Amplifier

Ω = driving motor (DM)

521

From the block diagram in Fig 6-10, all necessary transfer functions can be obtained by the application of relatively simple transformations. The diagram contains only one cross-over branch from the $\Delta \phi_0(p)$ channel to the summing point; this branch can be readily eliminated by moving the summing point beyond the branch point in the direction of signal flow. We shall not present these formulas, being of the opinion that the construction of the block diagram is equivalent to the derivation of all transfer functions.

By way of an auxiliary equation, we shall introduce a simplified relationship, by means of which the driven motor torque corresponding to a constant driving motor torque can be computed. The relationship is based on the ratio of the power output of the two motors when they are operated at constant speed:

$$M_s = \frac{M_8}{\gamma_2} \frac{\Omega}{\Omega_n}. \qquad (6\text{-}86)$$

$$^{DM(driving\ motor)}$$

The efficiency γ_2 in Equation (6-86) takes into consideration losses in the driving motor, main circuit, and in the amplidyne.

It should be noted that the block diagram for the motor-amplidyne system given in Fig 6-9 is based on the linearization of the saturation curves. In the case of the amplidyne, these characteristics, generally speaking, deviate little from linearity with the result that the analytical procedure described above can be applied to the evaluation of both incremental and total variables, including the change in sign of the reference input and its passage through zero.

The block diagram in Fig 6-10 has been constructed on the basis of the linearization of the principal nonlinearities which are usually present in the form of the product of two regulated variables. It follows that care must be exercised in using this diagram only for relatively small deviations.

6-4. DIRECT-CURRENT AND ALTERNATING-CURRENT TRANSFORMERS

1. Basic Parameters

As components of automatic control systems, transformers are used in both d-c and a-c service.

We shall discuss the operation of a d-c transformer

with dual feed from two sources supplying voltages U_I and U_2. The circuit for this transformer is shown in Fig 6-11(a). From the consideration of this general case, we shall later find it easy to pass to a consideration of simpler particular cases.

In the circuit diagram in Fig 6-11(a), the primary (w_1) and secondary (w_2) windings coupled by the mutual inductance flux Φ are arbitrarily drawn separately. The leakage fluxes are expressed in terms of the leakage self-inductances $L_{1\,s}$ and $L_{2\,s}$. The [total] inductances shown in the figure also include the inductances $L_1 \ell$ and $L_2 \ell$ of the primary and secondary circuits, respectively. We thus can write

$$L_1 = L_{1\,s} + L_1 \ell \quad ; \quad L_2 = L_{2\,s} + L_2 \ell$$

The ohmic resistances r_1 and r_2 of the two windings are likewise arbitrarily separated and added to the ohmic resistances $r_1 \ell$ and $r_2 \ell$ of the primary and secondary circuits, respectively, so that we have:

$$r_I = r_1 + r_1 \ell \quad ; \quad r_{II} = r_2 + r_2 \ell$$

The mesh equations for the transformer circuits are given by:

$$I_1 r_1 + L_1 \dot{I}_1 + w_1 \dot{\Phi} = U_1;$$

$$I_2 r_{II} + L_2 \dot{I}_2 + w_2 \dot{\Phi} = U_2.$$

Solving the above equations conditionally for the primary and secondary currents, respectively, we have:

$$I_1(p) = \frac{1}{L_1 p + r_1} [U_1(p) - w_1 p \Phi(p)]; \quad (6\text{-}87a)$$

$$I_2(p) = \frac{1}{L_2 p + r_2} [U_2(p) - w_2 p \Phi(p)]. \quad (6\text{-}87b)$$

The total coupling magnetic flux can be determined from the sum of the ampere-turns

$$\Phi = \frac{0.4\pi}{R_\mu} A w_1 = S_{aw}^{\Phi} A w_1.$$

523

Expanding the expression for the ampere-turns, we have

$$\Phi = S_{aw}^{\Phi}(w_1 I_1 + w_2 I_2). \qquad (6\text{-}87c)$$

Equations (6-87a) through (6-87b) were used in constructing the block diagram shown in Fig 6-11(b). By appropriate transformations of the block diagram, transfer functions for either direction of signal flow can be obtained. In carrying out the transformations, we shall make use of the following notation:

The mutual inductances of the primary and secondary windings, given by

$$L_{1M} = w_1^2 S_{aw}^{\Phi}; \quad L_{2M} = w_2^2 S_{aw}^{\Phi};$$

The total inductances, given by

$$L_I = L_1 + L_{1M}; \quad L_{II} = L_2 + L_{2M},$$

The mutual inductance, expressed by

$$M = w_1 w_2 S_{aw}^{\Phi} = \sqrt{L_{1M} L_{2M}}.$$

We further note in the block diagram in Fig 6-11(b) the presence of two [feedback] loops sharing a common channel S_{aw}. We shall construct the open-loop transfer functions $C_1(p)$ and $C_2(p)$ for these loops, which we shall have occasion to use in the discussion which follows.

When the time constants, representing the ratio of the self-inductances to the resistances, are labelled with the subscripts of the former, the following equations are obtained:

$$\left.
\begin{aligned}
C_1(p) &= \frac{Y_1 w_1^2 S_{aw}^{\Phi} p}{T_{s1}p + 1} = \frac{\frac{1}{r_1} L_{1M} p}{T_{s1}p + 1} = \frac{T_{1M} p}{T_{s1}p + 1}; \\[2ex]
C_2(p) &= \frac{Y_{11} w_2^2 S_{aw}^{\Phi} p}{T_{s2}p + 1} = \frac{\frac{L_{2M}}{r_{II}} p}{T_{s2}p + 1} = \frac{T_{2M} p}{T_{s2}p + 1}.
\end{aligned}
\right\} \qquad (6\text{-}88)$$

We now pass to the determination of the transfer

524
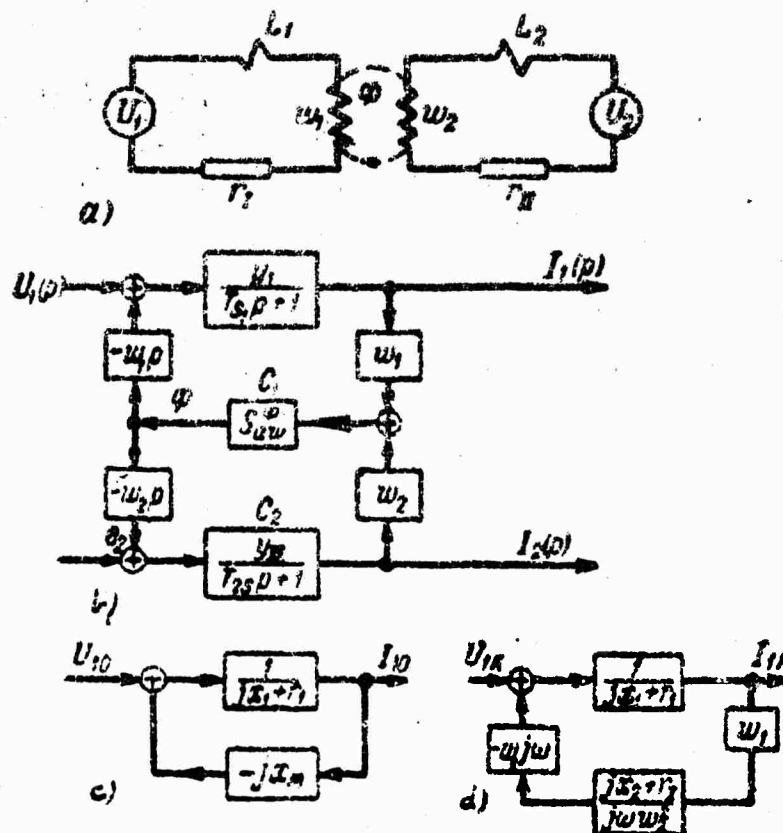
Fig. 6-11. Circuit and Block Diagrams for a Transformer with Independent Dual Feed

functions for the transformer.

2. The Operator Self-Admittance of the Primary Circuit

The self-admittance of the primary circuit defines the relationship between the voltage and the current in that circuit:

$$Y_{11}(p) = \frac{I_1(p)}{U_1(p)} = \frac{\dfrac{Y_1}{T_{s1}p + 1}}{1 + \dfrac{Y_1\omega_1^2 p}{T_{s1}p + 1} \cdot \dfrac{S_{aw}^*}{1 + C_2}} \, ,$$

or

$$Y_{11}(p) = \frac{Y_1(T_{11}p + 1)}{(T_{11}p + 1)(T_{s1}p + 1) + (T_{s2}p + 1)T_{M1}p} \, . \qquad (6\text{-}89)$$

Analogously the self-admittance of the secondary circuit is given by

$$\frac{I_2(p)}{U_2(p)} = Y_{22}(p) =$$

$$= \frac{Y_{11}(T_1p + 1)}{(T_1p + 1)(T_{s2}p + 1) + (T_{s1}p + 1)T_{M2}p} \, . \qquad (6\text{-}90)$$

3. Transfer Admittances

The transfer admittance between the primary and secondary circuits is given by

$$Y_{12}(p) = \frac{I_2(p)}{U_1(p)} =$$

$$= \frac{-Y_1Y_{11}Mp}{(T_1p + 1)(T_{s2}p + 1) + (T_{s1}p + 1)T_{M2}p} \, . \qquad (6\text{-}91)$$

526

and the transfer admittance between the secondary and primary circuits is given by

$$Y_{21}(p) = \frac{I_2(p)}{U_2(p)} =$$

$$= \frac{-Y_1 Y_{11} M p}{(T_{11}p + 1)(T_{s1}p + 1) + (T_{s2}p + 1) T_{M1}p} \qquad (6-92)$$

The equations derived above show that structurally the self-admittances are real second-order driving elements. The transfer admittances, on the other hand, correspond to real differential elements.

The block diagram in Fig 6-11(b) can also be used in the analysis of a number of a-c operating conditions

4. Experimental Determination of No-Load Operating Characteristics for a-c Conditions

The complex admittance for a-c conditions can be determined by setting $p = j\omega$ in the overall operator transfer function. To save space, we shall not carry out these substitutions in Equations (6-89) through (6-92), inasmuch as they are fairly straightforward. Instead, we shall introduce a number of simplified relationships.

For no-load operation ($U_2 = 0$ and $Y_2 = 0$), the loop C_2 can be neglected. The remaining feedback loop C_1 is represented by the block diagram shown in Fig 6-11(c). We shall find it convenient to determine the no-load operator impedance rather than the corresponding admittance. To compute the open-circuit operator impedance, it will be sufficient to add the feedback transfer function to the inverse of the transfer function for the feed-forward branch:

$$Z_{1x,x}(p) = w_1^2 S_{aw}^\bullet p + \frac{T_{s1}p + 1}{Y_1} =$$

$$= (L_{1M} + L_{1s}) p + r_1,$$

Rewriting the above expression in complex notation, we have

527

$$Z_{1\kappa,x}(j\omega) = r_1 + j\omega(L_{1M} + L_{1s}) = r_1 + j(x_1 + x_{M1}), \quad (6\text{-}93)$$

where $x = \omega L$.

For relatively small values of r_1 and x_1, L_{1M} can be determined experimentally. L_{2M} can be similarly determined for the secondary winding . The mutual inductance M is obtained from the geometric mean of the last two quantities:

$$M = \sqrt{L_{1M}L_{2M}}$$

For more accurate computation the hysteresis loss and the eddy current loss must also be taken into account by introducing an active component [sic] in the open-circuit admittance.

5. Experimental Determination of the Short-Circuit Impedance

In the treatment of the short-circuited condition ($r_{2f} = 0$; $L_{2f} = 0$), it is customary to neglect the exciting current ($I_1 w_1 + I_2 w_2 \approx 0$). However, in order to retain a finite secondary current, it is postulated that S_{gw}^ϕ approaches infinity. This permits the retention in the block diagram of the necessary regulated variables.

However, when the gain in the feed-forward branch of loop G_1 is increased without limit, the enclosed loop transfer function will be nearly equal to the feedback transfer function, i.e., in the case under discussion, $(L_{G2} p + R_2)/w_1^2 p$, as shown in Fig 6-11(d).

On forming the sum of the complex feedback gain and of the reciprocal of the forward-element gain, we obtain the [complex] short-circuit impedance:

$$Z_{\kappa 1} = r_1 + jx_1 + \left(\frac{w_1}{w_2}\right)^2 (r_2 + jx_2). \quad (6\text{-}94)$$

The second term on the right in the above equation represents the complex impedance of the secondary circuit converted to primary terms. The conversion factor is inversely proportional to the square of the transformation ratio, which is given by $(x_2/x_1)^2$.

6. Driving Point Impedance in the Primary Circuit for A-C Conditions

The driving point impedance in the primary circuit can be determined either from the complete block diagram in Fig 6-11(b), looking from left to right, or directly by taking the reciprocal of the complex admittance given by Equation (6-89):

$$Z_{11}(p) = r_1 + jx_1 + \left(\frac{w_1}{w_2}\right)^2 \frac{jx_{2M}(r_{II} + jx_2)}{jx_{2M} + (r_{II} + jx_2)}. \qquad (6\text{-}95)$$

From the above equation, the nature of the corresponding circuit can be readily deduced. The circuit contains a complex impedance $Z_1 = r_1 + jx_1$, followed by two parallel branches with impedances $Z_{2M} = jx_{2M}$ and $Z_2 = r_{II} + jx_2$, weighted inversely proportional to the square of the ratio of transformation. The circuit corresponds to the generally accepted equivalent circuit for transformers.

From Equation (6-95) the short-circuit impedance (6-94) can be obtained by setting $x_{2M} = \infty$ and $r_{II} = r_2$. By setting $r_{II} + jx_2 = \infty$ in Equation (6-95), the open-circuit impedance (6-93) is obtained.

As noted above, the block diagram in Fig 6-11(a) can be used as a basis for the discussion of various transformer connection schemes. Let us examine a transformer with an open secondary circuit. The block diagram in Fig 6-11(b) will then contain only the loop C_1, and the output secondary emf can be tapped off the $w_2 p$ branch.

The transfer function for the transformer under these conditions is given by

$$W_{U-e_2}(p) = $$
$$= -\frac{Y_1 w_1 w_2 S_{av}^{\bullet} p}{(T_{e1}p + 1)(1 + C_1)} = -\frac{w_2}{w_1} \cdot \frac{T_{M1}p}{(T_1 p + 1)}. \qquad (6\text{-}96)$$

The above transfer function describes a real driving element. To make this element approximate the ideal element described in Chapters 1-4, r_1 must be increased with the resultant decrease in the time constant T_1. This results in a simultaneous drop in gain corresponding to $T_{M1} = L_{M1}/r_1$. For a-c conditions $/W/$ approaches w_2/w_1.

7. Dual Feed from a Common Source

We shall proceed to the discussion of the modified circuit shown in Fig 6-12.

In this case both transformer windings are connected to the same source which generates a voltage U_1.

We now introduce the notation $U_i(p)$ for the input voltage, which is fed in between the two input summing points. The block diagram expressing the transfer characteristics of the transformer from $U_i(p)$ to the primary current will coincide with the block diagram shown in Fig 6-11(b), except for the common feed channel as shown in Fig 6-12(b). From the latter block diagram the desired transfer functions can be readily derived. Thus the transfer function from U_i to the primary current is given by

$$Y_{Ui_1}(p) = Y_{11}(p) + Y_{21}(p),$$

When the values of the variables from Equations (6-69) through (6-92) are substituted in the above expression, we obtain

$$Y_{Ui_1}(p) = \frac{Y_1 [T_{11}p + 1 - Y_{11}Mp]}{(T_{11}p + 1)(T_{s1}p + 1) + (T_{s2}p + 1)T_{M1}p} \cdot \quad (6\text{-}97a)$$

When the secondary winding of the transformer is connected as shown in Fig 6-12(c), the transfer function takes on a new value expressed by

$$Y_{Ui_1}(p) = \frac{Y_1 [(T_{11} + Y_{11}M) p + 1]}{(T_{11}p + 1)(T_{s1}p + 1) + (T_{s2}p + 1)T_{M1}p} \cdot \quad (6\text{-}97b)$$

When the resistance $R_M + L_M p$ of the common circuit segment shared by the two windings is small, the transfer functions derived above can be used as shown and referred to the source voltage by setting $U_1 = U_i$.

When the impedance of the common circuit segment must be taken into account, the input voltage must be related to the source voltage (actuating signal ratio) as follows

$$U_{av}(p) = U_1(p) - (R_u + L_u p)[I_1(p) + I_2(p)].$$

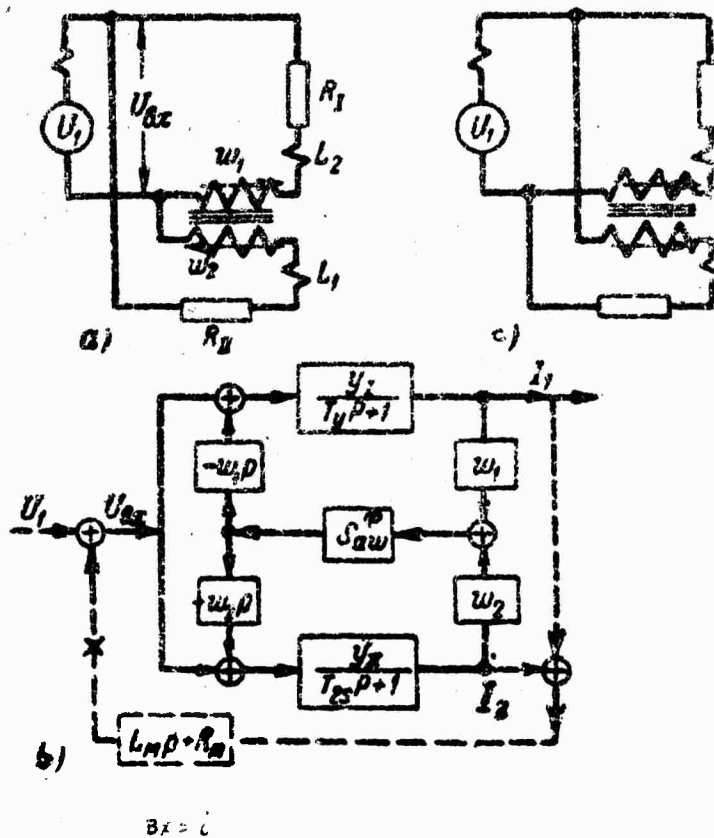The above equation enables us to build up the block

Fig. 6-12. Circuit and Block Diagrams for a Transformer with Dual Feed from the Same Source.

diagram in Fig 6-12(b) by the introduction of additional elements,
as shown by the dotted lines; the result of the summation is the
establishment of a feedback loop which reduces the supply voltage
(see Chapter 8).

6-5. ELECTRIC MOTORS WITH INERTIAL DAMPERS

We shall now examine the changes in the dynamic prop-
erties of an electric motor produced by the application of an
inertial damping torque in addition to the load torque. The con-
struction of the damper is shown schematically in Fig 6-13(a).
In the righthand portion of the figure is shown a freely rotating
rotor with permanently magnetized poles, having a moment of in-
ertia J_D. The rotor fits inside an aluminum or copper can which
is attached to the shaft of the motor.

We shall now determine the torque applied by the
damper to the shaft of the motor. If we let Ω_M be the speed of
the motor and Ω_D, that of the damper rotor, the magnitude of the
electromagnetic torque resulting from the interaction of the
permanent magnet poles with the eddy currents in the walls of the
can can be assumed to be proportional to the difference in speeds:

$$M_{\Delta} = S_{\Delta\Omega}^M (\Omega_M - \Omega_D),\qquad (6.98a)$$

where $S_{\Delta\Omega}^M$ is the proportionality constant.

When the speeds are equal, eddy currents and hence
also a [damping] torque are absent.

In general, the speeds are not equal, and the torque
equation for the electric motor can be written

$$J_M \dot{\Omega}_M + S_\Omega^M \Omega_M + M_{OM}' + S_{\Delta\Omega}^M(\Omega_M - \Omega_D) = M_U^P U. \quad (6.98b)$$

where S_Ω^M is the torque gradient of the electric motor
   J_M is the moment of inertia of the motor
   M_{OM} is the friction torque
   M_U^P is the starting torque gradient [sic]

The reaction produced by the electromagnetic torque

532
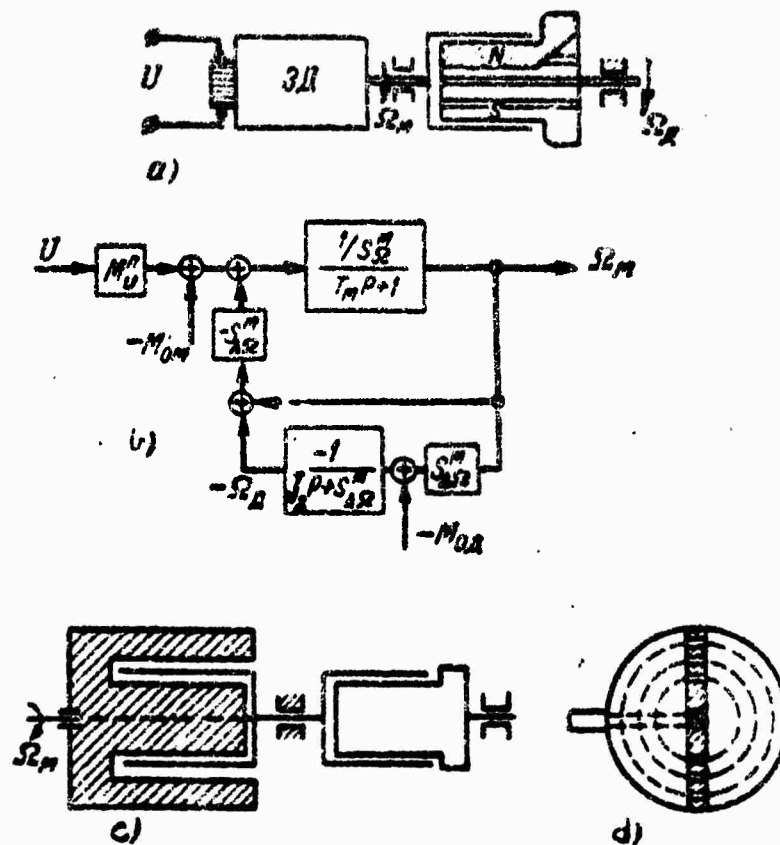
Fig. 6-13. Electromechanical and block diagrams
for electric drive using inert damper

is balanced by the inertial and internal friction torques in the damper:

$$S_{\Delta\Omega}^M (\Omega_M - \Omega_A) = J_A \dot{\Omega}_A + M_{OA}, \qquad (6.98c)$$

Introducing operator notation, we can rewrite Equations (6-98b) and (6-98c) as follows:

$$\Omega_M (p) = \frac{1/S_\Omega^M}{T_M p + 1} \left[M_U^E U (p) - \right.$$
$$\left. - M_{OM} (p) - S_{\Delta\Omega}^M [\Omega_M (p) - \Omega_A (p)] \right], \qquad (6.98d)$$

where $T_M = J_M / S_\Omega^M$ is the time constant of the electric motor. In addition, we have

$$\Omega_A (p) = \frac{S_{\Delta\Omega}^M \Omega_M (p) - M_{OA}(p)}{J_A p + S_{\Delta\Omega}^M}. \qquad (6.98e)$$

The last two equations were used in the construction of the block diagram shown in Fig 6-13(b). The feed-forward channel in the block diagram corresponds to the normal motor configuration without a damper (Equation (6-94b)). The introduction of the additional elements shown is necessitated by the inclusion of the damper.

For the determination of the transfer function from U to Ω_M, we first combine the feedback elements into a single element having a transfer function $H(p)$:

$$\left(\quad J_A p + S_{\Delta\Omega}^M \right) \quad J_A p + S_{\Delta\Omega}^M$$

Using the function derived above, the overall operator transfer function [control ratio] can be readily obtained:

$$W_{U\Omega}(p) = \frac{M_U^{\Pi}}{S_\Omega^M} \frac{T_\Omega p + 1}{(T_M p + 1)(T_\Omega p + 1) + \frac{J_A}{S_\Omega^M} p}, \quad (6\text{-}99a)$$

where $T_D = J_D/S_{\Omega}^M$ is the time constant of the damper.

The inclusion in the numerator of the operator control ratio of the transfer function for a driver element, $T_D p + 1$, improves the frequency response of the electric motor by reducing the phase lag over a given frequency range. As will be seen in subsequent chapters, this reduction in phase lag has a beneficial effect on the properties of the closed system which includes the electric motor under discussion.

To achieve maximum utilization of the positive properties of the scheme, the moment of inertia, i.e., the time constant of the motor, must be reduced in every possible way. The simplest method of implementing this principle constructionally is to make use of two-phase asynchronous shell-type motors, shown diagramatically in Fig 6-13(c). For relatively small values of the time constant T_M, Equation (6-99a) simplies to the following expression:

$$W_{U\Omega}(p) \approx \frac{M_U^{\Pi}}{S_\Omega^M} \frac{T_A p + 1}{\left(T_A + \frac{J_A}{S_\Omega^M}\right) p + 1}. \quad (6\text{-}99b)$$

A similar set of equations and a similar block diagram are obtained when the electromagnetic damper shown in Fig 6-13(a) is replaced with a mercury damper, shown in Fig 5-13(d). As before a braking torque is absent when the speeds of rotation of the shell and of the mercury are equal and no relative displacement of the mercury takes place. When a difference in speed appears, the mercury flows into the shell through openings in the partition; this flow sets up a viscous friction and a resulting torque, which in the first approximation is proportional to the difference in speeds.

LITERATURE CITED

1. Petrov, G. N., *Elektricheskiye mashiny*, [Electrical Machines], Gosenergoizdat, 1956.

2. Piotrovskiy, L. M., *Elektricheskiye mashiny*, [Electrical achines], Gosenergoizdat, 1955.

3. Meyerov, M. V., *Osnovy avtomaticheskogo regulirovaniya elektricheskikh mashin* [Fundamentals of Automatic Regulation of Electrical Machines], Gosenergoizdat, 1952.

4. Kron, *Primeneniye tenzornogo analiza v elektrotekhnike* [The Application of Tensor Analysis to Electrical Engineering Problems], Gosenergoizdat, 1951 (First published in Elec Eng, 1940).

5. Shatalov, A. S., *Analiz raboty asinkhronnoy mashiny s kondensatorami s tenzornom izlozhenii (generatornyye i dvigatel'-nyye rezhimy)* [Tensor Analysis of the Operation of an Asynchronous Machine with Condensers (Generator and Motor Conditions)], Dissertation, Novocherkassk Industrial Institute imeni S. Ordzhonikidze, 1941.

6. Ettinger, Ye. L., and Reyngol'd, Yu. R., The Experimental Investigation of the Dynamic Characteristics of Electromechanical Amplifiers and the Determination of Their Parameters, *Elektrichestvo* (Electricity), No 3, 1956

BLOCK DIAGRAMS OF ELECTRONIC AUTOMATIC CONTROL SYSTEM ELEMENTS

7-1.   Negative Feedback D-c Amplifiers

A simplified circuit for a vacuum-tube negative-feedback
d-c amplifier is shown in Fig 7-1(a). The circuit diagram clari-
fies the construction of the equipment used in the block diagrams
shown in Fig 1-9. However, the main purpose of the present dis-
cussion is not the establishment of the external connections but
rather the structural analysis of the amplifier. We therefore
begin by considering a single input signal E_1 impressed on the
grid of the amplifier through the input resistance r_1. In addi-
tion to the input resistance, the grid circuit includes the feed-
back resistance r_0 and the grid leakage resistance r_2 (in the
notation used in Fig 1-9(a), $r_{n+1} = r_2$).

The amplified voltage is measured at the output resis-
tance R_0; the load resistance R_ℓ is connected across R_0 and the
source U_1. The plate voltage of the tube is equal to the sum of
the voltages of the two sources: $U_a = U_1 + U_2$. The division of
the plate supply into two parts is a condition imposed by the
balancing requirements. The choice of operating point along the
linear portion of the tube characteristic is determined by the
grid bias voltage U_g.

Let us first examine the balancing of the amplifier.

According to the circuit shown in Fig 7-1(a), the out-
put voltage is determined by the difference:

$$E_0 = U_1 - IR_0. \qquad (7\text{-}1)$$

The object of the balancing of the amplifier is the
determination of the current $I = I_0$ for which a zero output volt-
age, $U_1 - I_0 R_0 = 0$, is obtained when $E_1 = 0$. Inasmuch as under
these conditions the voltage produced by source U_1 is completely
balanced by the voltage drop $I_0 R_0$, the only active voltage in the
plate circuit is U_2, which assures the flow of the necessary cur-
rent.

During balancing, the following constant voltage values
are set:

$$U_1 = U_{10}; \; U_2 = U_{20}; \; U_g = U_{g0}; \; E_2 = E_{20}$$

The above voltages are determined by the corresponding mesh cur-
rents required to assure the condition $E_1 = 0$ and $E_0 = 0$.

537

In the discussion which follows we shall cover only incremental departures of voltages and currents from their balancing values.

In our calculations we shall use the circuit shown in Fig 7-1(b), on which are entered only incremental values [of the above variables], denoted by lower case letters. The voltage e_0 is determined from the relation $e_2 = E_2 - E_{20}$; the voltages e_1 and e_0 are identical with the voltages E_1 and E_0, inasmuch as the former are measured from zero.

By way of analogy with equations (1-56) through (1-63), as well as directly from Fig 7-1(b), we obtain the following relationships:

$$i_1 = \frac{1}{r_1}(e_1 - e_2);\qquad (7\text{-}2a)$$

$$i_0 = i_1 - i_2;\qquad (7\text{-}2b)$$

$$e_2 = i_0 r_0 + e_0;\qquad (7\text{-}2s)$$

$$i_2 = \frac{1}{r_2} e_2;\qquad (*)$$

$$e_0 = -ke_2.\qquad (**)$$

The block diagram shown in Fig 7-1(c) has been constructed on the basis of the above equations. Equations (7-2a) through (7-2c) represent the actuating ratios about summing points 1,2,3; Equations (*) and (**) each express the amplifying characteristics of an element [sic].

By moving summing point 3 to the input of the diagram, we can reduce the internal feedback loop terminating at summing point 2, obtaining $r_0 r_2/(r_0 + r_2)$. We can thereupon reduce the direct feedback loop terminating at summing point 1 and obtain:

$$r_0 r_2/(r_0 r_1 + r_0 r_2 + r_1 r_2)$$

The above-indicated transformations lead to the block diagram shown in Fig 7-1(d), which in addition to the reference input signal shows the disturbances which are active in the real circuit; these disturbances are the results of voltage imbalances which are smoothed during balancing. The following types of instabilities must be taken into account:

(1) Instability of the plate supply voltage ΔU_1;
(2) Drift of the grid voltage ΔE_2 due to changes in

(3) Instability of grid bias voltage Δv_g;

(4) Voltage drop produced in the output resistance by the load current

$$\Delta v_4 = I_\ell R_o$$

The above-enumerated instabilities give rise to corresponding errors $\varepsilon_i (i = 1, 2, 3, 4)$ in the output of the amplifier, which distort the transfer characteristics of the latter. We shall now analyze the conditions for the transmission of the reference input signal and the effect of each disturbance (instability) type on the amplifier output.

0. The gain on the useful signal [control ratio] is obtained by reducing the block diagram in Fig 7-1(d) for the input e_i and the output e_0:

$$\Phi_o = \frac{e_0}{e_i} = \frac{-r_0 r_1}{\frac{1}{k}(r_0 r_1 + r_0 r_2 + r_2 r_3) + r_1 r_3} . \qquad (7\text{-}3a)$$

For large values of the amplification factor, the above expression reduces to

$$\Phi_0' = -\frac{r_0}{r_1} . \qquad (7\text{-}3b)$$

If the usually small value of the admittance $1/r_2$ is neglected in Equation (7-3a), Equation (1-61) is obtained. It is important to note that the gain remains unchanged during fluctuations of the amplification factor of the tube.

1. The change in gain due to the instability of the plate supply voltage ΔU_4 is given by

$$\Phi_4 = \frac{z_1}{\Delta U_4} = \frac{r_0 r_1 + r_0 r_2 + r_1 r_3}{r_0 r_1 + r_0 r_2 + r_1 r_3 (1 + k)} . \qquad (7\text{-}4a)$$

For large values of the amplification factor, the above expression reduces to

$$\Phi_1' = \frac{r_0 r_1 + r_0 r_2 + r_1 r_2}{r_1 r_2 k}. \qquad (7\text{-}4b)$$

When the admittance $1/r_2$ is neglected, the above expression simplifies to

$$\Phi_1'' = \frac{r_0 + r_1}{r_1 k}. \qquad (7\text{-}4c)$$

For large values of the amplification factor q, the above instability has an insignificant effect on the operation of the amplifier.

2. The change in gain due to drift of the grid voltage ΔE_2 is given by

$$\Phi_2 = \frac{s_3}{\Delta E_2} = -\frac{r_0 r_1 + r_0 r_2 + r_1 r_2}{\frac{1}{k}(r_0 r_1 + r_0 r_2 + r_1 r_2) + r_1 r_2}. \qquad (7\text{-}5a)$$

For large values of the amplification factor, the above expression reduces to

$$\Phi_2' = -\frac{r_0 r_1 + r_0 r_2 + r_1 r_2}{r_1 r_2}; \qquad (7\text{-}5b)$$

For large values of the resistance r_2, we obtain

$$\Phi_2'' = -\frac{r_0 + r_1}{r_1}. \qquad (7\text{-}5c)$$

3. The change in gain due to drift of the grid bias voltage ΔU_S coincides with the overall gain on the useful signal:

$$\Phi_3 = \frac{s_3}{\Delta U_{cM}} = \Phi_0; \qquad (7\text{-}6a)$$

$$\Phi_3'' = \Phi_3' = -\frac{r_0}{r_1}. \qquad (7\text{-}6b)$$

4. The change in gain due to the load current I_l is obtained by multiplying the change in gain due to the instability

540

$$\Phi_4 = \frac{e_4}{I_H} = \frac{e_4}{R_\text{B} I_H} R_\text{B} = R_\text{B} \Phi_1. \qquad (7\text{-}7)$$

In view of the fact that the amplification factor appears in the numerator of Equations (7-4), the change in gain due to the load current as expressed by Equation (7-7) will be small. Notwithstanding the high values of the resistance R_O (10-20 kilohms) characteristic of vacuum-tube circuits, the amplifier has a low impedance output inasmuch as Equation (7-7) may be considered to express the resistance opposed to the load current by the active circuit of the amplifier. For $r_o = r_1$, that resistance is $k/2$ times smaller than the nominal value of the positive impedance.
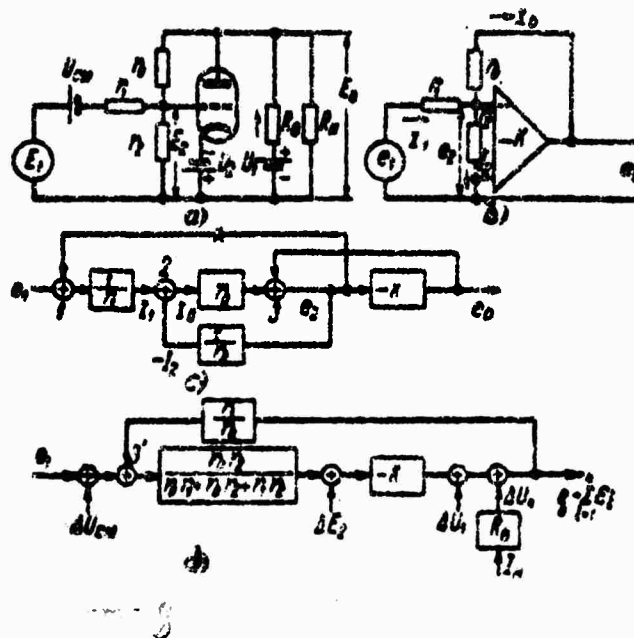

Fig 7-1.   D-c Amplifier.

Legend: (a) electric circuit for a single stage;
(b) circuit used in calculations; (c) (d) block
diagrams

It can be seen from Equations (7-3), (7-4), and (7-7) that an increase in the value of the amplification factor k has a favorable effect on a series of properties of the circuit. A d-c amplifier (DCA) therefore is usually designed in accordance with the 3-stage scheme shown in Fig 7-2(a). The overall amplification factor for this configuration is

$$-k = (-k_1)(-k_2)(-k_3)$$

and can attain values of $/k/ = 50,000$ or higher.

It will be readily noted that whenever it is desired to increase the number of stages, the total number of stages used must be odd. This requirement arises from the fact that the sign of the gain must be negative if negative feedback is to be imposed by the simple method illustrated in the figure.

It can be seen from Fig 7-2(a) that the circuit for the last stage is identical with that shown in Fig 7-1(a). In the earlier stages the feed conditions are modified as follows: additional plate supplies U_4 and U_6 are used together with additional grid bias supplies U_3 and U_5. The grid bias voltages required for interstage coupling are provided by resistances r_{g1} and r_{g2}. The sources U_4, U_6, U_3, and U_5 are combined; in the circuit diagram they are shown separately in the interest of clarity.

The first-stage tube has an auxiliary right half [twin triod] which contains a low resistance in the plate circuit. The right half of the tube is used to stabilize the operation of the left half of the tube. When the drift of the [left] grid voltage is replaced by an equivalent voltage ΔU_g impressed on the common cathode circuit, the compensation of the latter can be effected by the application of the so-called parametric method. The method consists in generating a current increase ΔI in the common cathode circuit such that the voltage drop across the cathode resistance $R_1 + R_2$ balances the voltage equivalent to the drift of the left grid voltage:

$$\Delta U_g = \Delta I (R_1 + R_2) \tag{*}$$

For constant operation of the left half of the tube, the current increase ΔI must be produced entirely in the right half of the tube, the corresponding change in grid voltage is given by

$$\Delta U_g - R_1 \Delta I$$

The above change in grid voltage is readily translated into a current change by means of the tube slope:

$$\Delta I = S(\Delta U_9 - R_1 \Delta I). \qquad (**)$$

Substituting for ΔU_0 its value from Equation ($*$), we obtain the relation between the resistance R_2 and the slope of the tube required for parametric compensation:

$$S = \frac{1}{R_2}. \qquad (7\text{-}8)$$

The balancing procedure used for the three-stage circuit in Fig 7-2 is analogous to that used for the circuit shown in Fig 7-3. Since for $e_1 = 0$ and $s = 0$ the currents must be 0 [sic], the incremental values of the variables coincide with their total values, and the calculation of the circuit in Fig 7-2 can be carried out on the basis of the equivalent circuit shown in Fig 7-1(b) with the following structural transformations.

Let us consider separately the effect of drift due to changes in the grid voltage of each of the three tubes of the three-stage amplifier without parametric compensation. For this purpose we must divide element -K into three elements: $-K_1$, $-K_2$, and $-K_3$, as shown in Fig 7-2(b); the drift voltages for each of the three stages: ΔE_1, ΔE_2, and ΔE_3 are introduced between the stages. The drift at the amplifier output is readily computed from the equation

$$a_1 + a_2 + a_3 = $$
$$= \frac{(r_0 r_1 + r_2 r_3 + r_1 r_2)(-k\Delta E_2 + k_1 k_2 \Delta E_1 - k_2 \Delta E_3)}{r_0 r_1 + r_0 r_2 + r_1 r_2 (1 + K)}. \qquad (7\text{-}9a)$$

It goes without saying that the effects of drift are most serious in the first stage inasmuch as the disturbance is applied to the input of a high-gain element. The effect of drift in the first stage can be decreased by the introduction of additional stage ahead of the first tube, as indicated in the block diagrams shown in Fig 7-2(c) and 7-2(d). The amplification factor of the element introduced ahead of the disturbance in block diagram (c) is K_4; in block diagram(d), the amplification factor is readily computed to be $1+K_4$ [sic] following rearrangement of the summing points.

By making use of the principle that the closed-loop characteristic is merely equal to the inverse of the feedback characteristic when the open-loop gain is large, we can derive a series of transfer functions relating the values of the voltage drift at the output and input terminals of the DCA.

For an uncompensated DCA we have

$$-\frac{e_2}{\Delta E_2} = \frac{r_1 + R_2}{r_1} = 1 + \Phi_0'. \qquad (7 \cdot 9b)$$

Compensation according to block diagram (c) gives:

$$\frac{e_3}{\Delta E_3} = \frac{1 + \Phi_0'}{K_4} . \qquad (7 \cdot 9c)$$

Compensation according to block diagram (d) gives:

$$\frac{e_4}{\Delta E_2} = \frac{1 + \Phi_0'}{1 + K_4} \approx \frac{1 + \Phi_0'}{K_4} . \qquad (7 \cdot 9d)$$

For sufficiently large values of K_4 (usually 300 and larger), the last two equations are practically identical and give a marked reduction in drift: K_4 times greater than that expressed by Equation (7-9b).

We shall now indicate a method for the practical realization of drift compensation according to scheme (d). The additional amplifier K_4 obviously must be essentially drift-free. This is generally true of a-c amplifiers, in which the use of the coupling condensers or transformers eliminates drift of the direct output component. The additional amplifier is connected as shown in block diagram (e), where:

The d-c voltage between mixing point 1 and the ground is sent to the modulator M;

The a-c output from the modulator is amplified by the a-c amplifier K_4 and fed to a demodulator;

The demodulator converts the a-c voltage to a d-c voltage;

The output of the demodulator is connected to the input of the DCA: the grid of the second (righthand) half of the [input] stage is frequently used for this purpose; the voltage impressed on this grid must be of opposite polarity to that impressed on the lefthand grid;

The source of drift in the scheme under discussion is shown in the form of a generator ΔE_2.

544
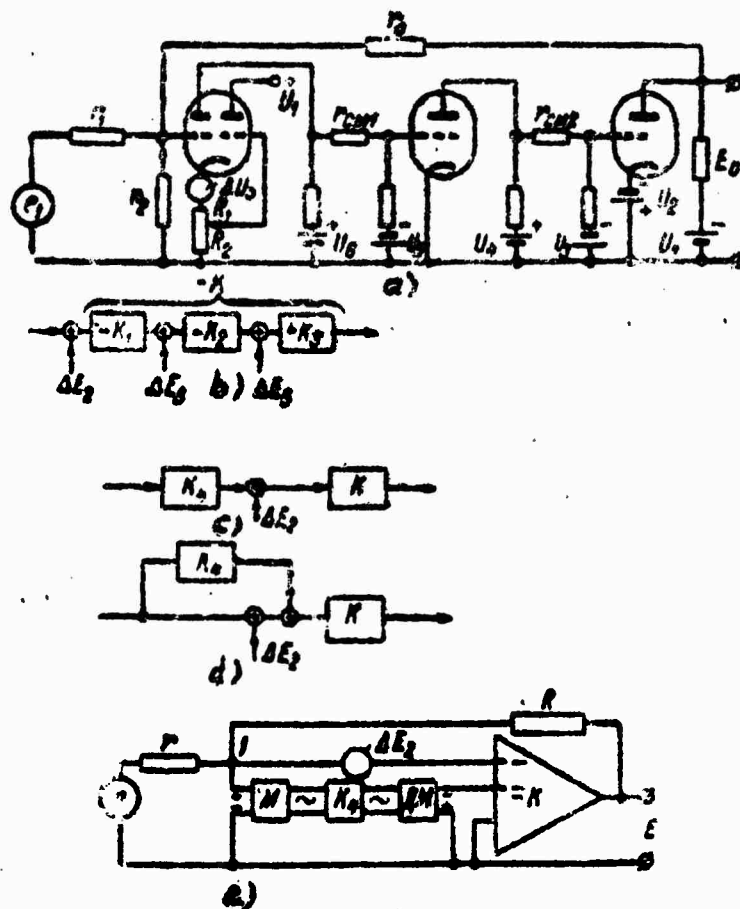
Fig. 7-2.   Three-stage d-c amplifier

The modulator and demodulator are usually executed in the form of synchronous [single-tuned] circuits. The amplification factor K_4 includes both the a-c amplification and the transfer functions of the modulator and of the demodulator.

The amplification introduced by the auxiliary amplifier in the transmission of the control voltage affects the open-loop gain; since, however, the open-loop gain already was large prior to the introduction of the auxiliary amplifier, the properties of the closed DCA [sic] are essentially unmodified, and the transfer function of the DCA is determined by Equation (7-3b) as before. If anything, the accuracy of Equation (7-3b) is enhanced.

It should be noted that the use of a modulator and demodulator reduces the bandwidth of the auxiliary amplifier. Block diagram (c), in which only the control signal passes through the auxiliary amplifier, is therefore preferable to block diagram (d) and its practical implementation expressed by circuit diagram (e), both of which retain the unit gain branch in the main channel [sic] and in which the overall open-loop gain cannot drop below the value of K. It follows that the basic DCA relation expressed by Equation (7-3b) remains valid. For more detail on the compensation circuit used, see Ref 1.

7-2. Magnetic Amplifiers

Fig 7-3 shows one of the magnetic amplifier circuits which have found practical application. The magnetic amplifier under discussion consists of a connected magnetic system of Ш-shaped cores [sic], on which are mounted the d-c and the a-c windings.

The d-c windings, of which there can be any number when the amplifier is operated as a summing element, take up two of the cores. The a-c winding, of which there usually is only one, is separated into two equal coils, each mounted on a separate core in such a way that their fields oppose each other. This arrangement prevents interaction of odd-harmonic induced magnetic flux with the d-c windings.

Let us designate the currents in the d-c windings by I_1, I_2, and I_3, and the number of turns in the windings by w_1, w_2, w_3 and w_4. The system of d-c windings can be considered as a multiple-winding transformer.

We can now write an expression for the overall constant component of the magnetic flux:

$$\Phi = F(w_1 I_1 + w_2 I_2 + w_3 I_3 + w_4 I_4)$$

546

On introducing increments into the above equation, we obtain

$$\Delta\Phi = S^{\Phi}_{no} \, (w_1\Delta I_1 + w_2\Delta I_2 + w_3\Delta I_3 + w_4\Delta I_4) \qquad (7\text{-}10a)$$

The constant component of the magnetic flux, which determines the degree of saturation of the cores, and the magnitude of the load current flowing for a given value of the a-c source voltage and a given set of values for the resistances in the d-c circuit and in the a-c circuit, including the resistance of the rectifying bridge, are related by a function $I = f(\Phi)$. The latter function is frequently represented in the form of the graph shown in Fig 7-3(b).

On introducing increments, we have:

$$\Delta I = K^I_{\Phi}\Delta\Phi. \qquad (7\text{-}10b)$$

The majority of investigations of the operation of magnetic amplifiers are based on the above-presented approximation assumption concerning the presence of an amplifying element which relates changes in the constant component of the flux to changes in the d-c output current, with a transfer function K^I_{Φ} (ref 2). Under this assumption the magnetic amplifier is treated as a current generator ($R_A \ll R_o$).

The consideration of the rectified current as an output variable of the magnetic amplifier is in complete accord with normal practice. However, in a number of cases the inputs to the magnetic amplifier are given not in the form of currents but in the form of voltages U_1, U_2, U_3.

The relationship between the voltages and the currents is the same for all circuits. When the latter include only ohmic resistances, the relationship is expressed as follows:

$$U_1 = R_1 I_1 + w_1\dot{\Phi}.$$

Introducing increments into the above equation and solving it conditionally for the current, we have

$$I_1(p) = Y_1 [U_1(p) - w_1 p\Delta\Phi(p)]. \qquad (7\text{-}10c)$$

Equations (7-10a) through (7-10c) were used in constructing the block diagram shown in Fig 7-3(c). When the circuits of the d-c windings contain reactances other than those linked by the main flux in the windings, aperiodic elements must be substituted in the diagram for the amplifier elements $1/R_1 = Y_1$ [sic].

Let us determine the voltage-current transfer function for one of the windings, e.g., the second; the remaining transfer functions are obtained in a similar manner. We begin by moving all summing points to the input of element Y_1 and all mixing points, to the output of element K_ϕ^I, i.e., to the exit of the block diagram. The forward transfer function then becomes:

$$\Pi = Y_1 w_1 S_{am}^\phi K_\phi^I,$$

The feedback loop contains three parallel branches with an overall transfer function

$$H(p) = -\frac{w_1 p}{K_\phi^I} - \frac{w_2^2 Y_2 p}{w_1 Y_1 K_\phi^I} - \frac{w_3^2 Y_3 p}{w_1 Y_1 K_\phi^I} =$$

$$= -\frac{w_1^2 Y_1 + w_2^2 Y_2 + w_3^2 K_3}{Y_1 w_1 K_\phi^I}.$$

Reduction of the feedback loop yields the transfer function:

$$W_{UI}(p) = \frac{Y_1 w_1 S_{am}^\phi K_\phi^I}{1 + S_{am}^\phi (w_1^2 Y_1 + w_2^2 Y + w_3^2 Y_3)}.$$

The product of S_{am}^ϕ by the square of the number of turns is equal to the self-inductance of the corresponding winding with respect to the coupling flux. The latter, when divided by the ohmic resistance (or multiplied by the admittance), gives the time constant, e.g.:

$$T_1 = \frac{S_{am}^\phi w_1^2}{R_1}. \tag{*}$$

In addition, the product

$$w_1 S_{am}^\phi K_\phi^I = K_{y1}$$

gives the dimensionless gain of the magnetic amplifier from the current flowing in the control winding [primary circuit] to the rectified d-c output current. In terms of these values, the

— 548 —

$$W_{U1}(p) = \frac{Y_1 K_{y1}}{1 + \frac{1}{3}(T_1 + T_s + T_s)p} \,. \qquad (7\text{-}11)$$

It can be seen from Eq (7-11) that notwithstanding the fact that in the determination of the transfer function with respect to the voltage U_1 the remaining voltages were set equal to zero, the loops remained closed with a resulting increase in the overall time constant in the transfer function represented by Equation (7-11). We note that the numerators of the transfer functions for the various windings are identical inasmuch as the time constant for the process in the coupled system is independent of the point of application of the disturbance.

The circuit represented in Fig 7-3 shows an additional winding 4 which has not been discussed. This winding is connected in series with the output circuit, and the direction of the magnetic field produced by it coincides with that of the controlling magnetic flux. Such a winding is designated as a positive feedback connection. The open-loop transfer function for the corresponding loop in the block diagram is given by

$$K_{y4} = K_{\phi}^l S_{aw}^{\Phi} w_4 \qquad (7\text{-}2)$$

In the presence of the above positive feedback loop, the amplification factor of the magnetic amplifier takes on the value

$$K_y = \frac{K_{y1}}{1 - K_{y4}} \,. \qquad (7\text{-}12)$$

The positive feedback loop is introduced simultaneously into each of the loops in the block diagram, thereby increasing the value of the coefficients of S_{aw}^{Φ} in Equation (7-11) and the time constants of the corresponding loops expressed by Equation ($*$) by a factor of $1/(1-K_{y4})$:

$$T_i' = \frac{T_i}{1 - K_{y4}} \,. \qquad (7\text{-}13)$$

Thus by the use of positive feedback as expressed by Equation (7-12), the gain of the amplifier can be raised to any level. However, the ratio of the gain to the time constant remains independent of the range of feedback:

$$\frac{K_y}{T_1'} = \frac{K_{\bullet}^I R_1}{w_1}. \qquad (7\text{-}14)$$

When the load voltage supply operates in the neighborhood of the nominal current I_0, the feedback ampere-turns under conditions of zero input signals will produce an initial magnetization $w_4 I_0$, which is indicated in Fig 7-3(b).

In the absence of initial magnetization, the amplifier is insensitive to the polarity of the input signal, i.e., d-c current amplification will be produced regardless of the sign of the reference voltage. This feature is undesirable in ACS requiring a reversal capability.

Initial magnetization and positive feedback can be achieved without the use of additional windings, by allowing the d-c component of the current to flow through the a-c winding. This requires a special rectification circuit (Fig 7-4).

In the scheme under discussion the circuit of the a-c winding includes half-wave rectifiers; the current produced by these rectifiers is in the form of pulses, as shown on the right in Fig 7-4. By suitably redesigning the winding connections, the constant components of both currents and the corresponding fluxes are added; the result is a magnetization proportional to the output current. The a-c components (first harmonic) are in phase opposition with resulting zero interaction of the a-c circuit with the other windings.

The d-c current supplied to the load is subjected to full-wave rectification. The block diagram is identical with that shown in Fig 7-3. A more detailed analysis of the states of the circuits of the magnetic amplifier during each half period is given in Ref 3.

7-3. Linear Accelerometers

Fig 7-5(a) shows a schematic diagram of a device used in measuring linear accelerations or an accelerometer. The device measures longitudinal acceleration when the frame moves in a direction of change of the coordinate x_y, measured from any arbitrary fixed reference point. The accelerometer comprises a number of moving parts with a combined mass m which is concentrated primarily in the inertial mass which moves with negligible static friction along the guide pins. The linear displacement can be measured from a zero position on a scale. The linear displacement of the inertial mass is opposed by a spring of stiffness S_x^F. The rate of displacement of the inertial mass relative to the frame is

limited by a dashpot of damping coefficient S_v^F.

The equation of motion of the movable part of the device for the coordinates selected can be written as follows:

$$m(\ddot{x}_s - \ddot{x}_y) + S_V^F \dot{x}_s + S_x^F x_s = 0$$

or

$$(mp^2 + S_V^F p + S_x^F) X_s(p) = mZ(p),$$

where

$$Z(p) = p^2 X_y(p)$$

Thus the transfer function for the accelerometer can be written

$$W(p) = \frac{X_s(p)}{Z(p)} = \frac{m}{mp^2 + S_V^F p + S_x^F}, \qquad (7\text{-}15)$$

The above transfer function is characteristic of second-order elements. The corresponding gain is given by $k = m/S_x^F$ and is used in calibrating the acceleration scale. The block diagram corresponding to Equation (7-15) is given in the upper portion of Fig 7-5(b) (above the dividing line).

For small sizes of the orifices of the dashpot, the compressibility of the air will affect the operation of the accelerometer. An analysis of that effect is given below.

Assuming linearization of the coefficients, the compressibility of the air in the cylinder can be represented by the schematic diagram shown in Fig 7 5(c). The diagram shows a second, fictitious piston connected to the main piston by a spring which represents the compressibility of the air. The space between the fictitious piston and the end of the cylinder is assumed to be filled with an incompressible fluid.

If we let y represent the distance between the fictitious and the main pistons, we find that the discharge volume will be proportional to the difference $x-y$ in the strokes of the main and the fictitious pistons, respectively (in the diagram the pistons are assumed to move to the left). It follows that the fluid resistance which is developed is proportional to the rate of change of the above difference, or

$$F_V = S_V^F(\dot{x} - \dot{y})$$

Thus the introduction of fluid resistance affects only
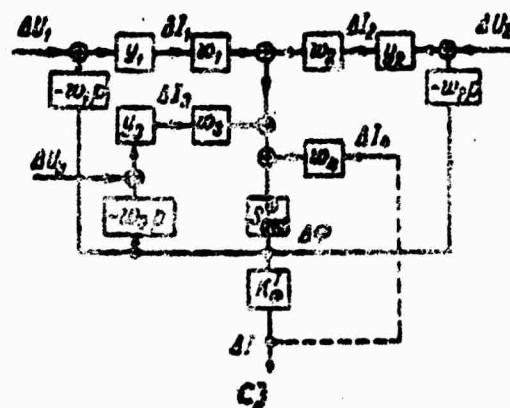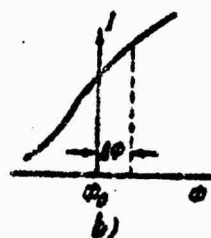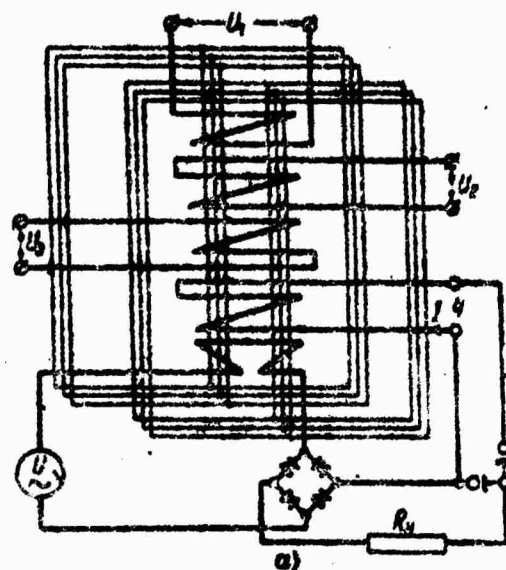
Fig. 7-3. Circuits and static characteristic
of magnetic amplifier

limited by a dashpot of damping coefficient S_V^f.

The equation of motion of the movable part of the device for the coordinates selected can be written as follows:

$$m(\ddot{x}_s - \ddot{x}_y) + S_V^f \dot{x}_s + S_x^f x_s = 0$$

or

$$(mp^2 + S_V^f p + S_x^f) X_s(p) = mZ(p),$$

where

$$Z(p) = p^2 X_y(p)$$

Thus the transfer function for the accelerometer can be written

$$W(p) = \frac{X_s(p)}{Z(p)} = \frac{m}{mp^2 + S_V^f p + S_x^f}. \qquad (7\text{-}15)$$

The above transfer function is characteristic of second-order elements. The corresponding gain is given by $k = m/S_x^f$ and is used in calibrating the acceleration scale. The block diagram corresponding to Equation (7-15) is given in the upper portion of Fig 7-5(b) (above the dividing line).

For small sizes of the orifices of the dashpot, the compressibility of the air will affect the operation of the accelerometer. An analysis of that effect is given below.

Assuming linearization of the coefficients, the compressibility of the air in the cylinder can be represented by the schematic diagram shown in Fig 7-5(c). The diagram shows a second, fictitious piston connected to the main piston by a spring which represents the compressibility of the air. The space between the fictitious piston and the end of the cylinder is assumed to be filled with an incompressible fluid.

If we let y represent the distance between the fictitious and the main pistons, we find that the discharge volume will be proportional to the difference xsy in the velocities of the main and the fictitious pistons, respectively (in the diagram the pistons are assumed to move to the left). It follows that the fluid resistance which is developed is proportional to the rate of change of the above difference, or

$$F_V = S_V^f(\dot{x} - \dot{y})$$

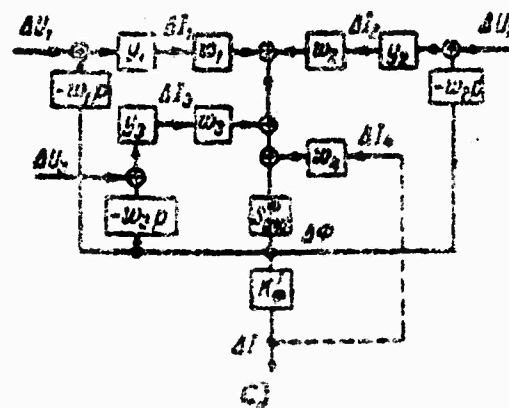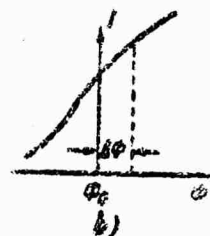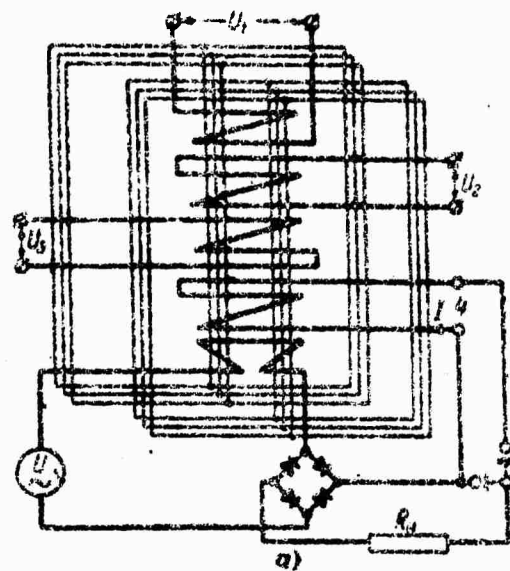Thus the introduction of fluid resistance affects only

551

Fig. 7-3. Circuits and static characteristic
of magnetic amplifier

Finally, we have

$$W(p) = \frac{X_s(p)}{Z(p)} = \frac{m\,\dfrac{1}{mp^2}}{1 + \dfrac{H(p)}{mp^2}} =$$

$$= \frac{m(S_V^F p + S_y^F)}{mp^2(S_V^F p + S_y^F) + S_V^F(S_x^F + S_y^F)p + S_x^F S_y^F},$$

or

$$W(p) = \frac{\dfrac{m}{S_x^F}\,(Tp + 1)}{\dfrac{mp^2}{S_x^F}\,(Tp + 1) + S_V^F\left(\dfrac{1}{S_x^F} + \dfrac{1}{S_y^F}\right)p + 1}, \quad (7\text{-}16)$$

where

$$T = \frac{S_V^F}{S_y^F}.$$

The numerator of Equation (7-16) differs from that of Equation (7-5) [sic] by the presence of the additional factor $Tp+1$, which corresponds to the transfer function of the driver element. The presence of that factor improves the frequency response of the accelerometer by introducing phase advance in a given frequency band.

Accelerometers with Electric 'Springs.' The action of the spring in generating a force which opposes the motion of the main mass can be duplicated by an electric circuit. The principle underlying the construction of such circuits will be examined below, using the construction of the 'pendulum' accelerometer shown in Fig 7-6(a) as an example.

Let us picture an electric motor with its armature shaft attached to two vertical supports while the housing is free to rotate through an angle α under the action of a torque produced by the effect of linear acceleration on an unbalanced mass m. As the housing turns, it moves the arm of the potentiometer. The resulting voltage e is amplified to a value U and causes a current I to flow through the armature of the electric motor.

The current in turn interacts with the constant field and produces an electromagnetic torque which opposes the motion of the housing and increases in proportion to the angular displacement. The situation is completely analogous to that which would have resulted if we had coupled the housing to the frame by means of a

spring.

We can now pass to the quantitative evaluation of the conditions of operation of the device. The torque equation can be written:

$$J\ddot{a} + S_\Omega^M \dot{a} + gL \sin a + S_I^M I = mLZ \cos a, \qquad (7\text{-}17)$$

where J is the combined inertia of all rotating parts;

S_Ω^M is the viscous friction torque gradient (when a is used);

g is the weight of the unbalanced part;

S_I^M is the electromagnetic torque gradient;

L [sic]; see Eq (7-19)] is the radius of travation of the of the unbalanced mass.

In calculating the current, we must take into account that the voltage in the armature circuit consists of two terms, the amplifier output voltage $K_y a$ and the counter-emf of the armature, which contributes to the increase in braking torque and in the current, i.e., we have

$$U = K_y a + K_\Omega \dot{a}.$$

When the inductance of the armature circuit is L and its resistance R, the current can be calculated from the following equation:

$$L\dot{I} + RI = K_y a + K_\Omega \dot{a}. \qquad (7\text{-}18)$$

For small angular displacements of the housing, we can set $\sin \alpha = \alpha$ and $\cos \alpha = 1$ in Equation (7-17). Rewriting the latter in operator notation, we obtain

$$a(p) = \frac{1}{Jp^2}[mlZ - (S_\Omega^M p + gl)\,a(p) - S_I^M I(p)]. \qquad (7\text{-}19)$$

Equation (7-18) can likewise be rewritten in operator notation to give:

$$I(p) = \frac{\frac{1}{R}}{Tp+1}(K_y + K_\Omega p) a(p) \qquad (7\text{-}20)$$

Equations (7-19) and (7-20) were used in constructing the block diagram shown in Fig 7-6(b). Reduction of upper [feedback] loop gives:

$$\frac{1}{Ip^2 + S_\Omega^M p + gl}.$$

Reduction of the entire block diagram yields the following transfer function from the acceleration to the angular displacement:

$$W_{za}(p) = \frac{mlR(Tp+1)}{R(Tp+1)(Ip^2 + S_\Omega^M p + gl) + S_I^M(K_\Omega p + K_y)}.$$

$$(7\text{-}21a)$$

and from the acceleration to the current:

$$W_{zi} = \frac{ml(K_\Omega p + K_y)}{R(Tp+1)(Ip^2 + S_\Omega^M p + gl) + S_I^M(K_\Omega p + K_y)}.$$

$$(7\text{-}21b)$$

For the steady-state condition we have

$$W_{za}(0) = \frac{mlR}{Rgl + S_I^M K_y};$$

$$(7\text{-}22)$$

$$W_{zi}(0) = \frac{mlK_y}{Rgl + S_I^M K_y}.$$

$$(7\text{-}23)$$

Thus the current is proportional to the acceleration and the acceleration can be measured with an ammeter inserted in the armature circuit.

To assure that the angular displacement of the housing is actually small and to prevent the degradation of the proportionality of t measurements by torque effects from unbalanced components and y other factors, it is sufficient to raise the amplifier gain K_y. We then have

$$W_{za}(0) = \frac{mlR}{S_I^M K_y} \to 0;$$

$$(7\text{-}24)$$

$$W_{zi}(0) = \frac{ml}{S_I^M}.$$

$$(7\text{-}25)$$

Small angular displacements make pointless the use of motors designed for continuous rotation. As a rule, such displacements are produced by special limited-stroke torque motors

of the type of electromechanical relays. Information on the construction of block diagrams for other types of elements can be obtained from Ref 4.

7-4. Gyroscopic Elements

Two Degrees of Freedom Gyroscope. Fig 7-7(a) is a schematic representation of the construction of a two degrees of freedom gyroscope. When the base of such a gyroscope turns through an angle ψ, a torque is applied to the inner gimbal; the space orientation of that torque is such as to tend to make the orientation of the angular momentum vector coincide with the angular velocity vector of the base. The magnitude of the torque is equal to the product of the angular momentum H by the angular velocity of the base:

$$M = H\psi$$

As a result of the effect of the above-described torque, the internal gimbal begins to turn about the axis Oy. The rotation of the gimbal is restrained by a spring and a dashpot. The capillary size of the orifices in the dashpot requires the compressibility of air be taken into account. We now define the following variables:

J is the moment of inertia of the movable components about the axis Oy;

S_α^M is the change in angular momentum produced by the restraining spring per unit angular displacement α of the gimbal;

$S_{\Delta q}^M$ is the change in angular momentum resulting from variations in the compressibility of air;

S_Ω^M is the change in angular momentum resulting from variations in the fluid resistance of the dashpot outflow.

Using the above notation, we can write the motion equation of the system:

$$\left\{ Jp^2 + S_\Omega^M p \left[1 - \frac{S_\Omega^M p}{S_\Omega^M p + S_{\Delta q}^M} \right] + S_\alpha^M \right\} a(p) =$$
$$= Hp\psi(p),$$

From the above equation a block diagram can be constructed which in many respects is analogous to that shown in Fig 7-5(b).
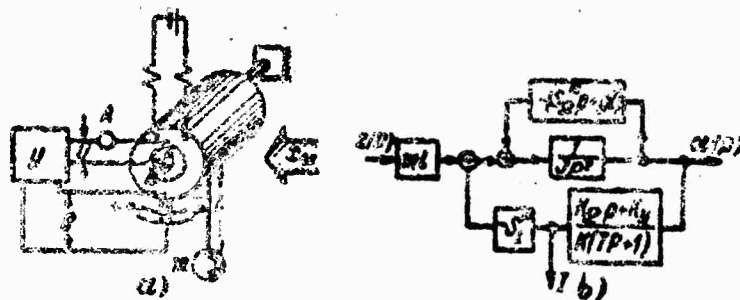
Fig 7-6.   Pendulum Accelerometer with Electric Feedback
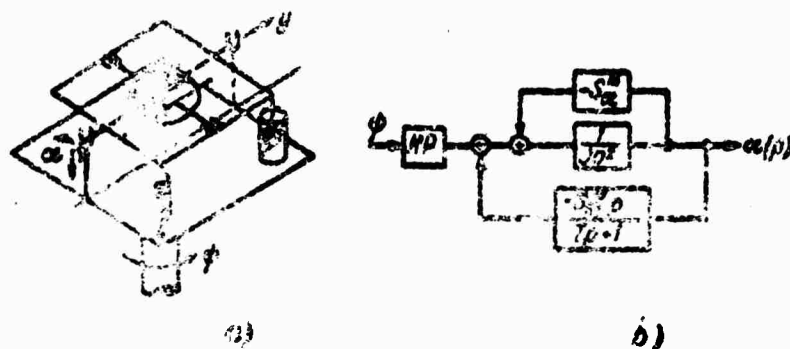
Fig 7-7.   Two Degrees of Freedom Gyroscope

As in the derivation of Equation (7-16), we determine the components of the overall feedback loop

$$-K_{a.e}(p) = S_a^M + \frac{S_\Omega^M p}{Tp+1},$$

feedback

where $T = S_\Omega^M / S_{\Delta\alpha}^M$ is the time constant of the dashpot.

The equations derived above were used in constructing the block diagram shown in Fig 7-7(b), in which the two components of the feedback loop are shown separately.

The transfer function of the device is given by

$$W_{\psi a}(p)_h =$$

$$= \frac{\dfrac{H}{S_a^M}(Tp+1)p}{\dfrac{J}{S_a^M}(Tp+1)p^2 + S_\Omega^M\left(\dfrac{1}{S_{\Delta a}^M} + \dfrac{1}{S_a^M}\right)p + 1}. \qquad (7\text{-}26)$$

It can be noted from Equation (7-26) that the device performs as a pickoff for the velocity ψ ($b_0 = 0$, $a_0 \neq 0$) and is called a rate gyroscope.

If the spring is disconnected, the upper feedback loop in the block diagram must be removed. The transfer function will then be of the form:

$$W_{\psi a}(p) = \frac{\dfrac{H}{S_\Omega^M}(Tp+1)}{\dfrac{J}{S_\Omega^M}(Tp+1)p + 1}. \qquad (7\text{-}27)$$

When operated in accordance with Equation (7-27), the device is used as an angular position pickoff. By analogy with Fig 7-6, an 'electric spring' could be used, in which case the operations of connecting and disconnecting the spring would be performed by switches in electric circuits.

Three Degrees of Freedom Gyroscope. We shall analyze the operation of the mechanism of Fig 7-8(a), in which the suspension of the external and internal gimbals is such that the system as a whole can precess about the axes Ox and Oy.

If we assume the system to be approximately linearized, we can write the following system of equations for small angular displacements α and β about the axes Oy and Ox, respectively:

$$J_x\ddot{\beta} + S_{\Omega x}^M\dot{\beta} + H\dot{\alpha} = M_x; \quad \Big\}$$
$$J_y\ddot{\alpha} + S_{\Omega y}^M\dot{\alpha} - H\dot{\beta} = M_y. \quad \Big\} \qquad (7\text{-}28)$$

where J_x and J_y are the moments of inertia of the movable system about the axes Ox and Oy;

$S_{\Omega x}^M$ and $S_{\Omega y}^M$ are the damping torque gradients resulting from natural viscous friction in air or produced by special dashpots;

M_x and M_y are the disturbing torques along the same axes;

H is the angular momentum of the gyroscope.

The terms $H\dot{\alpha}$ and $-H\dot{\beta}$ in the torque equations represent the precession torques which determine the interaction of motions about both axes. We recall that in the preceding example, the torque $H\dot{\psi}$ was the basic input in the torque equation.

Equations (7-28) were used in constructing the block diagram shown in Fig 7-9(b). The block diagram is constructed in the form of a closed loop.

The open-loop transfer function is given by

$$C(p) = \frac{H^2}{(J_x p + S_{\Omega x}^M)(J_y p + S_{\Omega y}^M)}.$$

The actuating signal ratio is given by

$$\frac{1}{1 + C(p)} = \frac{(J_x p + S_{\Omega x}^M)(J_y p + S_{\Omega y}^M)}{(J_x p + S_{\Omega x}^M)(J_y p + S_{\Omega y}) + H^2}. \qquad (7\text{-}29)$$

We shall now list a number of transfer functions:

The transfer function from the torque M_y to the angle α is

$$W_\alpha(p) = \frac{1}{1 + C(p)} \frac{1}{p(J_y p + S_{\Omega y}^M)} =$$

$$= \frac{J_x p + S_{\Omega x}^M}{p[(J_x p + S_{\Omega x}^M)(J_y p + S_{\Omega y}^M) + H^2]}. \qquad (7\text{-}30)$$

The transfer function from the torque M_y to the angle β is

$$W_\beta(p) = \frac{\frac{C(p)}{Hp}}{1 + C(p)} = $$

$$= \frac{+H}{p[(J_x p + S_{\Omega x}^M)(J_y p + S_{\Omega y}^M) + H^2]}. \qquad (7\text{-}31)$$

An examination of the expression derived for the open-loop transfer function shows that in the absence of damping $(S_{\Omega x}^M = S_{\Omega y}^M = 0)$, we have:

$$C_0(p) = \frac{H^2}{J_x J_y p^2}.$$

i.e., two integrating elements are obtained. The addition of a negative feedback loop around these elements yields an oscillatory element which produces an oscillatory response with an angular frequency

$$\omega_0 = \frac{H}{\sqrt{J_x J_y}}.$$

In the case of a free gyroscope this angular frequency is called the nutation frequency. Damping leads to the attenuation of the nutation frequency. The attenuation conditions are readily determined by inspection of the denominator of the right-hand member of Eq (7-29) or of the corresponding terms in Equations (7-30) and (7-31), which can be reduced to the denominator of the transfer function of the oscillatory element.

Gyro Stabilizer. The addition of an 'electric [electro-mechanical] spring' to the free gyroscope mechanism discussed above would give it the capability of performing as a stabilizer.

Fig 7-9(a) shows a three degrees of freedom gyroscope with a disturbing force F_y applied to its external gimbal. The disturbing force produces a torque M_y which tends to rotate the gimbal about the axis 0_y. The rotation is opposed by the electromechanical spring, consisting of an electric motor coupled to the same axis 0_y, which produces a torque of opposite sign to the disturbing torque. The electric motor is controlled via an amplifier by a potentiometer which produces a voltage proportional to the angular displacement
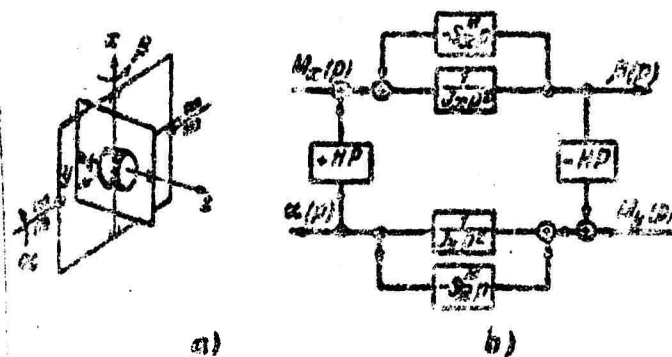
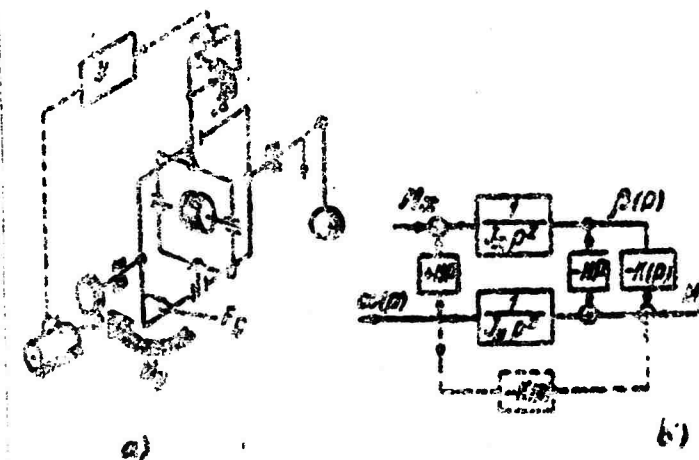Fig 7-8. Three Degrees of Freedom Gyroscope.

Fig 7-9. Gyro Stabilizer

If we designate the transfer function of the electric motor from the angle β to the torque along the axis O_y by $K(p)$, a new block diagram can be obtained by adding to Fig 7-9(b) a new element, $-K(p)$, in parallel with element $-Hp$ between the β and M_y channels. The new block diagram is shown in Fig 7-9. In the interest of simplicity, the damping torques represented by $S^M_{\Omega x}$ and $S^M_{\Omega y}$ have been neglected. The transfer function from the disturbing torque to the angular displacement of the stabilized gimbal is given by

$$W_a(p)_1 = \frac{J_x p}{J_x J_y p^2 + H [K(p) + Hp]} . \quad (7\text{-}32a)$$

If in addition steps are taken to attenuate the drift of the gyroscope and the results of these steps are reflected in the transfer function $K(p)$ so that $K(0) \neq 0$, the constant disturbing torque in the steady-state condition is given by

$$W_a(0)_1 = 0, \quad (7\text{-}32b)$$

i.e., the disturbing torque does not displace the gimbal from its reference position.

It may be desired to feed back the characteristic angular displacement [sic] of the stabilized gimbal. It will then be necessary to mount the potentiometer on the Oy axis and to measure the angles between the gimbal and the pendulum. The solid $-K(p)$ branch shown in the block diagram will then have to be replaced with the channel shown by a dotted line. In the latter case the transfer function from the disturbing torque to the angular displacement becomes

$$W_a(p)_2 = \frac{J_x}{J_x [J_y p^2 + K(p)] + H^2} . \quad (7\text{-}32c)$$

For a constant disturbing torque in the steady-state condition, we have

$$W_a(0)_2 = \frac{J_x}{J_x K(0) + H^2} , \quad (7\text{-}32d)$$

i.e., a change in orientation of the stabilized gimbal is unavoidable.

When the damping torques $S^M_{\Omega x} \beta$ and $S^M_{\Omega y} \alpha$ are taken into account, Equations (7-32) take on a slightly more complex form:

$$W_a(p)_1 = \frac{J_x p + S_{\Omega x}^M}{p(J_x p + S_{\Omega x}^M)(J_y p + S_{\Omega y}^M) + H[K(p) + Hp]};$$

$$\tag{7-33a}$$

$$W_a(0)_1 = \frac{S_{\Omega x}^M}{HK(0)};$$

$$\tag{7-33b}$$

$$W_a(p)_3 = \frac{J_x p + S_{\Omega x}^M}{(J_x p + S_{\Omega x}^M)[p(J_y p + S_{\Omega y}^M) + K(p)] + H^2 p};$$

$$\tag{7-33c}$$

$$W_a(0)_3 = \frac{1}{K(0)}.$$

$$\tag{7-33d}$$

As before for small values of $S_{\Omega x}^M$, the result computed by Equation (7-33b) is more favorable than that computed from Equation (7-33d). This conclusion can be modified only by an artificial increase in the damping.

It should be noted that the use of a pickoff connected to a pendulum which can introduce additional disturbances due to its characteristic vibrations presents a number of drawbacks. In addition, the first scheme discussed assures limited motion of the system about the more sensitive Ox axis.

Literature Cited

1. Gederbaum, I. and Salaban, P., Automatic Compensation of Drift in d-c Amplifiers [Back translated], Rev Scient Instr, 26, No 8 (1958)

2. Storm, Magnetic Amplifiers, Izd Inostr Lit, 1957

3. Rozenblat, M. A., Magnitnyye usiliteli [Magnetic Amplifiers], Izd 'Sov radio,' 1956

4. Chistyakov, N. I., Aviatsionnyye pribory [Airborne Instruments], Oborongiz, 1957

5. Kuznetkov, N. T., Teoriya avtomaticheskogo regulirovaniya [Theory of Automatic Control], Oborongiz, 1957

CHAPTER 8

STRUCTURAL ANALYSIS AND SYNTHESIS OF ELECTRIC CIRCUITS

8-1. Two-Terminal Networks

1. Transfer Functions of Elementary Two-Terminal Networks

Special electric circuits, sometimes referred to as filters, are frequently used in the main channel and in the auxiliary loops of automatic control systems in order to modify the system frequency response for the purpose of achieving specified figures of merit.

The basic element of an electric circuit is the two-terminal network, characterized by a single quantity, the admittance or the impedance which it introduces between a pair of terminals. When a current is made to flow between the terminals of a two-terminal network by connecting them to a source of power, a corresponding voltage drop will be produced. The notation used in describing the above quantities is shown in Fig 8-1.
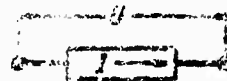
Fig 8-1. Electrical Circuit of a Two-Terminal Network

Inasmuch as in the context of the present discussion elements of electric circuits are considered as components of automatic control systems, we shall find it convenient to apply to them the concept of the operator transfer function. This requires us to identify inputs and outputs among the quantities under discussion.

When the current flowing through the two-terminal network is considered as the input and the corresponding voltage as the output, the concept of the operator transfer function coincides with the definition of the (transfer) operator impedance.

$$W_1(p) = \frac{U(p)}{I(p)} = Z(p). \qquad (8 \cdot 1)$$

When the input to the filter is taken as a voltage, and the output from it, a current, the transfer function for the two-terminal network (in terms of the image quantities) is expressed by the operator admittance:

$$W_2(p) = \frac{I(p)}{U(p)} = Y(p). \qquad (8 \cdot 2)$$

The relationship between the admittance and the impedance is expressed by the well-known relation

$$Z(p) = \frac{1}{Y(p)}. \qquad (8 \cdot 3)$$

By way of example, transfer functions for idealized two-terminal networks specified as pure resistances, pure capacitances, and pure inductances are listed in Table 8-1. These examples will assist us in effecting the transition to the discussion of more complex cases.

TABLE 8-1

OPERATOR ELEMENTS OF ELECTRIC CIRCUITS

ELEMENT	$Z(p)$	$Y(p)$
Ohmic resistance	R	$1/R$
Capacitance	$1/Cp$	Cp
Inductance	Lp	$1/Lp$

2. Two-Terminal Networks Connected in Series

The diagram in Fig. 8-2 shows a circuit built up of two-terminal sections in series. In practice, the inputs to such circuits as a rule are voltages, and the ouputs, currents. The overall transfer function of the network therefore is identical

with the transfer admittance:

$$Y(p) = \frac{1}{Z_1(p) + Z_2(p)}. \qquad (8\text{-}4a)$$

Dividing both numerator and denominator by $Z_1(p)$ and replacing the reciprocal of the impedance by the corresponding admittance, we obtain

$$Y(p) = \frac{Y_1(p)}{1 + Y_1(p) Z_2(p)}. \qquad (8\text{-}4b)$$

The general properties of the circuit are sufficiently adequately expressed by Equation (8-4a). However, Equation (8-4b), which reflects the terminal characteristics of the circuit, brings out additional internal relationships in the circuit on the basis of which the structural properties of the circuit can be determined. In effect, if the operator functions Y_1 and Y_2 are treated as transfer functions of unidirectional elements, Equation (8-4b) can be used in constructing the block diagram shown in Fig 8-2(b), which represents a feedback network comprising a forward element Y_1 and a feedback element Z_2.

When the input to the network is taken as a current and the output from it as a voltage, the impedance function is obtained from the simple relation:

$$Z(p) = Z_1(p) + Z_2(p). \qquad (8\text{-}4c)$$

The transformation of the electric circuit into an equivalent block diagram makes possible the application of structure analysis techniques in the treatment of electric circuits common to several Automatic Control System (ACS) elements.

When the frequency response characteristics of the elements are known, e.g., in the case under discussion, the frequency-response transfer function of the complex impedance $Z_1(j\omega)$ and of the complex admittance $Y_1(j\omega)$ the overall frequency response of the circuit can be obtained not only in the P-plane in the nomogram in Fig 8-2 but also from the $j\omega$-nomogram in Fig 8-3, following the transformation of Equation (8-4b) into the form

$$Y(j\omega) = Y_2(j\omega) \frac{Y_1(j\omega) Z_2(j\omega)}{1 + Y_1(j\omega) Z_2(j\omega)} \cdot$$

Whenever a negative feedback loop has to be added around an element in an ACS, the action can be economically duplicated by the introduction of an equivalent series impedance $Z_2(p)$ in an electric network in the same ACS.

When it is desired to remove a negative feedback loop from a circuit, and it is found impossible to effect that removal by a direct modification of the circuit in question, the loop can be compensated for by the addition of a positive feedback loop around some other element of the ACS, provided that the second loop is equivalent to the first in terms of the algebra of block diagrams.

We shall illustrate the last of the above-named methods by giving some examples of its operation. Fig 8-3(a) shows an electric circuit $Y_1(p)$, $Z_2(p)$ which is coupled to an amplifier; the input to the latter is the current flowing in the circuit. When the problem is formulated in terms of the compensation of the negative feedback loop in the circuit without at the same time modifying the circuit, the solution is obtained by the addition of a positive feedback branch from the amplifier output to the input of the circuit as shown in Fig 8-3(a), where

$$H_1(p) = \frac{Z_2(p)}{K},$$

or by closing an internal feedback loop around the amplifier as shown in Fig 8-3(b), where

$$H_2(p) = H_1(p) \frac{Y_1 p}{1 + Y_1(p) Z_2(p)} =$$
$$= \frac{Y_1(p) Z_2(p)}{K[1 + Y_1(p) Z_2(p)]} \cdot \quad (*)$$

The block diagram in Fig 8-3(b) can also be used to determine the amplifier feedback loop which is equivalent to the feedback loop in the circuit and, conversely, the circuit feedback loop which is equivalent to the amplifier feedback loop:
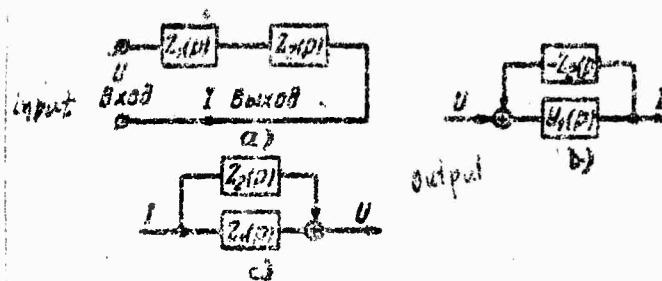
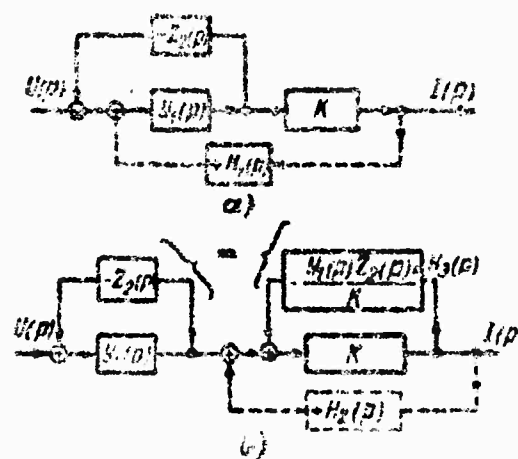Fig 3-2. Electric and Block Diagrams of a Circuit Consisting of Series-Connected Two-Terminal Sections

Fig 8-3. Structural Methods for the Compensation of Internal Negative Feedback Loops in Circuits

$$H_3(p) = \frac{Y_1(p) Z_2(p)}{K} ; \qquad (^{**})$$

$$Z_2(p) = \frac{H_3(p) K}{Y_1(p)} . \qquad (^{***})$$

We note that

$$H_2(p) \neq H_3(p), \qquad (^{****})$$

since after the shift of the $-Z_2(p)$ loop to a new element in the K channel, the section of the block diagram between $Y_1(p)$ and K does not correspond to a real circuit (see the shaded portions in Fig 5-5(c)). It follows that the compensating loop cannot be introduced directly in accordance with Equation (***) [sic] and requires the prior evaluation of Equation (*).

In Fig 5-4(a) the circuit is represented by the field of a generator and the amplifier, by the generator [armature]. The input is represented by the exciting current, and the output, by the armature voltage. Inductance and resistance are inseparable properties of the field winding; however, since they interact as series-connected simple two-terminal networks, we can set:

$$Y_1(p) = \frac{1}{Lp} ; \quad Z_2(p) = R.$$

The transfer admittance of a network of pure inductances is of the same form as the transfer function of an integrating element and as such cannot be used to represent a resistance, including the internal resistance of the winding. Since the effect of the internal resistance of the winding is represented by a negative feedback loop, as shown in Fig 8-4(b), this effect can be cancelled by the application of positive voltage feedback from the generator output. The setting of the voltage divider is determined from the following condition

$$S_l^E \frac{r}{r_f} = R.$$

The above condition is equivalent to the condition for self-excitation of the generator. Standard generator designs do not permit the use of voltage dividers and require full coupling of the field winding.

Following the introduction of the positive feedback loop, the overall transfer function of the two-terminal network and generator combination is given by

$$W_r(p) = \frac{S_l^E}{Lp}.$$

Instead of a current, one output from two series-connected two-terminal networks may be a voltage drop across one of the resistors in the circuit. In the latter case a voltage amplifier rather than a current amplifier is used. The principles on which the above-discussed transformation of the block

571

diagrams was based remain unchanged.

Let us turn our attention to the scheme shown in Fig 3-4(c), which contains a RC-circuit and a voltage amplifier. We set:

$$Y_1 = \frac{1}{R}; \; Z_2(p) = \frac{1}{Cp}.$$

When capacitance coupling is used, the overall transfer function for the scheme is of the same form as that of an aperiodic element, discussed in the preceding chapters. However, we shall represent this transfer function as the product of two operators: the transfer admittance of the circuit and the transfer impedance of the elementary two-terminal network represented by the condenser.

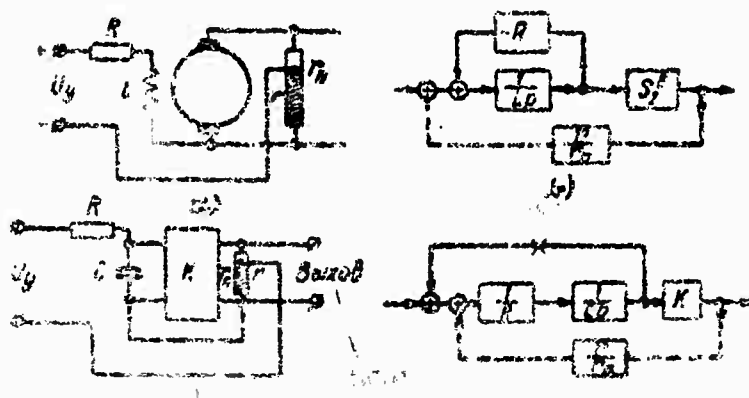$$W_c(p) = \frac{\frac{1}{R}}{1 + \frac{1}{RCp}} \cdot \frac{1}{Cp}$$

Fig 3-4. Feedback Compensation in RL and RC Circuits

In the scheme just described the condenser by itself acts as an integrating element, but its integrating characteristics are suppressed by the feedback loop in the first term representing the admittance of the circuit.

Fig 8-4(d) shows the block diagram for the scheme, including the generator and the takeoff point for the output voltage feedback. The feedback is negative. The feedback loop can be compensated by the addition of a positive feedback loop from the amplifier output, through a voltage divider, back to the input to the circuit, provided that the condition $K(r/r_f) = 1$ satisfied. When this is the case, the overall operator transfer function for the scheme becomes:

$$W_c(p) = \frac{1}{RCp} = \frac{1}{Tp}.$$

Such integrators have been used   in electronic modelling by L. I. Gutenmakher (Ref 1). Though simple to construct, these integrators require a high degree of gain stability.

3. Two-Terminal Networks Connected in Parallel

Fig 8-5(a) shows a circuit consisting of two two-terminal networks connected in parallel and having operator admittances $Y_1(p)$ and $Y_2(p)$. The overall admittance of the parallel network is given by the sum of the admittances of the branches:

$$Y(p) = Y_1(p) + Y_2(p) \tag{8-5a}$$

The above equation can be generalized to include any number of parallel branches.

The block diagram in Fig 8-5(b), from which the overall admittance can be obtained, closely resembles the electric circuit. When the block diagram is constructed from the impedance function

$$Z(p) = \frac{1}{Y_1(p) + Y_2(p)} = \frac{Z_1(p)}{1 + Z_1(p)Y_2(p)}, \tag{8-5b}$$

the structure obtained is in the form of a feedback loop, as shown in Fig 8-5(c). However, it must be noted that the block diagram thus obtained reflects the state of the electric circuit

573

only between the terminals indicated and whereas the block dia-
gram, being unidirectional, permits the buildup of the elements,
the electric circuit upon the addition of new impedances will be
transformed into one of a very different type.

4. Two-Terminal Networks Connected in Series-Parallel

A network containing series- and parallel-connected
two-terminal networks represents a combination of the networks
discussed in the preceding sections and is usually characterized
by its impedance function, which is equal to the sum of the im-
pedances of the meshes containing parallel-connected admittances:

$$Z(p) = \frac{1}{Y_1(p) + Y_2(p)} + \frac{1}{Y_1'(p) + Y_2'(p)} + \ldots \quad (8\text{-}6)$$

Fig 8-5(d) shows a circuit built up of series-parallel
connected simple two-terminal networks. For this example $Y_1(p) = 1/R_i$, $R_2(p) = C_i(p)$, and the total impedance is given by

$$Z(p) = \frac{R_1}{C_1 R_1 p + 1} + \frac{R_2}{C_2 R_2 p + 1} + \ldots \quad (8\text{-}7)$$

The block diagram in Fig 8-5(e) has been constructed
from elementary networks on the basis of Equation (8-6) and of
the transformation indicated in Equation (8-5b). From the block
diagram, the total impedance of the circuit can be obtained.

5. Ladder Filter Networks Built Up of Two-Terminal Sections

The name given this type of network is derived from
its configuration, which is shown in Fig 8-5(f). The individual
two-terminal networks in the block diagram are numbered from right
to left and are represented by their operator admittances $Y_{2n}(p)$
or by their operator impedances $Z_{2n-1}(p)$. Using this notation,
a general formula for the admittance of the complex two-terminal
network can be readily obtained:

$$Y(p) = \cfrac{1}{Z_1 + \cfrac{1}{Y_2 + \cfrac{1}{Z_4 + \cfrac{1}{Y_5 + \cfrac{1}{Z_4 + \cfrac{1}{Y_5 + \cfrac{1}{Z_2 + Z_1}}}}}}} \quad (8\text{-}8a)$$

594

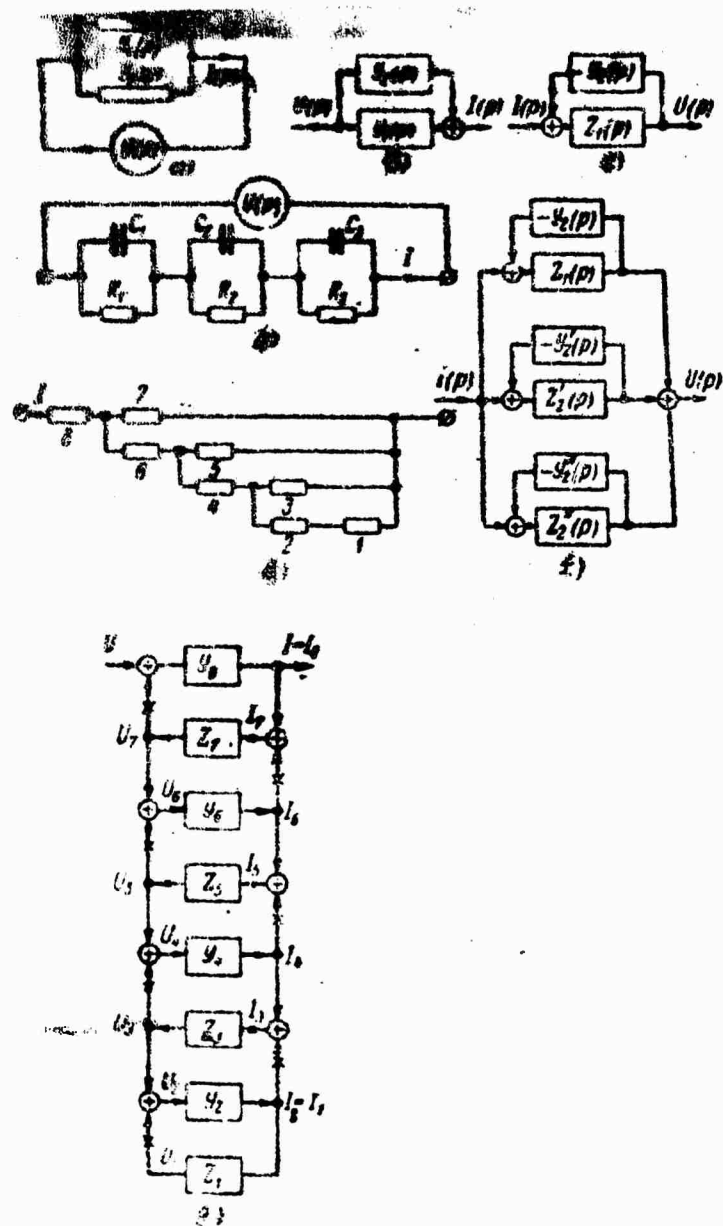Fig 6-5.   Electric Circuits Built Up of Two-Terminal Networks.

Legend: (a) Parallel connection; (d) Series-parallel
                [.....] .. .. connection;
              (b, c, e, f) Block Diagrams for above circuits,
              respectively.

The denominator of the righthand term of the above equation is equal to the total impedance of the complex two-terminal network:

$$Z(p) = Z_0 + \cfrac{1}{Y_1 + \cfrac{1}{Z_0 + \cfrac{1}{Y_3 + \cfrac{1}{Z_1 + \cfrac{1}{Y_3 + \cfrac{1}{Z_2 + Z_1}}}}}} \qquad (8\text{-}8v)$$

For the determination of the general properties of the network, the equations obtained above are reduced to the usual form by complexing the numerator and denominator; however, the effect of the properties of the various elements of the network are more directly visualized by using the untransformed equations. The effect is even more graphic when the block diagram in Fig 8-5(g) is used in the place of the electric circuit in Fig 8-5(f). The block diagram is constructed from a series of simple equations.

The nodal current equations are given by

$$I_{2n-1} = I_{2n} - I_{2n-2}; \quad n = 1, 2, 3, 4 \qquad (8\text{-}8c)$$

(righthand portion of the diagram) [sic].

The branch voltage equations are given by

$$U_{2n} = U_{2n+1} - U_{2n-1} \qquad (8\text{-}8d)$$

(lefthand side of the diagram). The transfer characteristics of the elements are given by

$$I_{2n} = Y_{2n}U_{2n}; \quad U_{2n+1} = Z_{2n+1}I_{2n+1} \qquad (8\text{-}8e)$$

The reduction of the block diagram in Fig 8-5(d), starting with the lower meshes, readily leads to equation (8-8a). In addition, when the [output] error $\triangle Z_k$ in one of the resistances in the network is known, the voltage error in the corresponding element of the ladder, $I_k \triangle Z_k$, can be computed. When this error is inserted in the block diagram, its effect on the output error of the two-terminal network can be evaluated.

3. Operator Transfer Functions of Complicated Two-Terminal Networks

The elements inserted between the terminals of an

electric circuit can be connected in a variety of ways. The typical connections discussed above can be made more complex; as the number of internal loops between terminals increases, the two-terminal network becomes a multiple-mesh network. However, in the absence of internal sources of emf in the network, the latter remains passive. Overall impedance and admittance functions can be calculated for any multiple-mesh two-terminal network. The first step in the calculation is the application of the basic rules for the transformation of networks (Figs 8-2 through 8-5). In the case of intersecting circuits [lattice networks], it is sometimes useful to perform the transformation from wye to the equivalent delta and vice versa. Finally, multiple-mesh networks can always be treated by the general methods involving the solution of mesh and nodal equations, using matrix symboletry (Ref 2) to abbreviate the notation.

We shall now pass to the determination of the impedance function for the complex two-terminal network shown in Fig 8-6(a). The righthand portion of the circuit contains two stars [wyes] which cannot be combined in view of the differences in the leg impedances and the resulting difference in potential at points O' and O''. We shall therefore transform these wye connections into equivalent deltas.

The formulas for the wye-delta transformation are as follows:

$$\left. \begin{array}{l} Y_{12} = \dfrac{Y_{01}Y_{02}}{Y_{01} + Y_{02} + Y_{03}} ; \\[2mm] Y_{13} = \dfrac{Y_{01}Y_{03}}{\Sigma Y} ; \quad Y_{23} = \dfrac{Y_{02}Y_{03}}{\Sigma Y} . \end{array} \right\} \qquad (8.9)$$

The resultant transformations are indicated in the circuit diagram in Fig 8-6(A).

To facilitate the application of the formulas, legs of the same type in the starting diagram in Fig 8-6(a) are labelled with the same letters, and differences in their impedances are denoted by the number of primes used. Substitution of these impedances in the formulas (8-9) gives the admittances of

577

the sides of the delta connection:

$$Y'_{12}, \ Y''_{12}; \quad Y'_{13}, \ Y''_{13}; \quad Y'_{23}, \ Y''_{23}.$$

Inasmuch as the elements obtained are connected in pairs to like nodes, the summation of their admittances yields the total admittances of the sides of the delta connection shown in fig 8-6(b):

$$Y_{\mathrm{I,\,II}} = Y'_{12} + Y''_{12}; \quad Y_{\mathrm{I,\,III}} = Y'_{13} + Y''_{13};$$

$$Y_{\mathrm{II,\,III}} = Y'_{23} + Y''_{23}.$$

Following the combination of the impedances of the parallel branches in the diagram shown in Fig 8-6(b), we shall find it expedient to transform one of the deltas, e.g., the one on the left (including all of the bridge arm), into a wye. The formulas for the delta-wye transformation are as follows:

$$\left.\begin{array}{c} Z_{\mathrm{I0}} = \dfrac{Z_{12}Z_{13}}{Z_{12} + Z_{23} + Z_{13}}; \\[2ex] Z_{\mathrm{II0}} = \dfrac{Z_{12}Z_{23}}{\Sigma Z}; \quad Z_{\mathrm{III0}} = \dfrac{Z_{13}Z_{23}}{\Sigma Z}. \end{array}\right\} \qquad (8\text{-}10)$$

The notation used in the above formulas is clarified by the circuit shown in Fig 8-6(a). When the above transformation is carried out, the circuit shown in Fig 8-6(c) is obtained; this circuit can be readily reduced further to a single imped- ance Z(p) (Fig 8-6(d)):
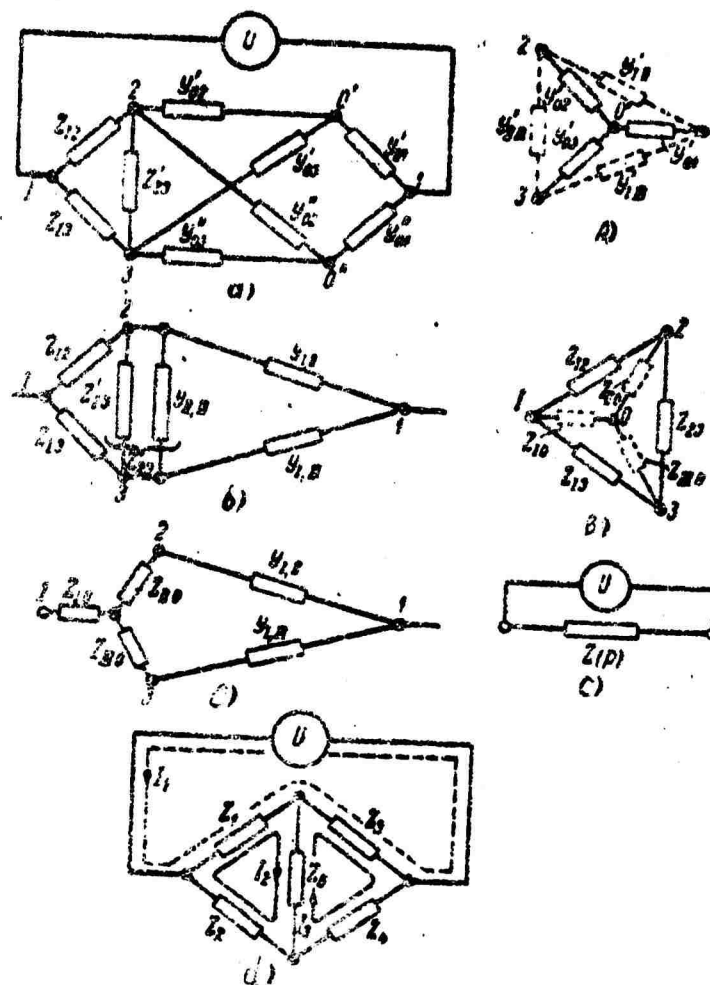
Fig. 6-6. Conversion of a Compound Two-
terminal Circuit

$$Z\ p) = Z_{\text{I}|} + \cfrac{1}{\cfrac{1}{Z_{\text{II}9} + Z_{\text{I II}}} + \cfrac{1}{Z_{\text{II}6} + Z_{\text{I III}}}} . \qquad (^\circ)$$

We can now insert the values of the intermediate parameters into Equation (✕). We shall now examine in greater detail the frequently encountered bridged network. The latter was obtained in the form shown in Fig 8-6(b) but will be rewritten as shown in Fig 8-6(*) in order to simplify the indexing of the leg impedances.

The impedance function of the bridged two-terminal network in Fig 8-6(e) can be written

$$Z(p) =$$

$$= \frac{Z_5(Z_1 + Z_2)(Z_3 + Z_4) + Z_1 Z_3(Z_2 + Z_4) + Z_2 Z_4(Z_1 + Z_3)}{Z_5(Z_1 + Z_2 + Z_3 + Z_4) + (Z_1 + Z_3)(Z_2 + Z_4)} .$$

$$(8\text{-}11)$$

We shall now proceed to transform the circuit in Fig 8-6(e) into the circuit shown in Fig 8-6(f) by the mesh current method. To do so, we must introduce as intermediate variables the current and voltage of the source U connected to the terminals of the two-terminal network, even though we only wish to obtain the impedance function for the network.

The individual meshes and the positive direction of flow of the mesh currents I_1, I_2, and I_3 are indicated in the circuit shown in Fig 8-6(e).

The number of independent meshes is always one greater than the difference between the number of branches and the number of nodes. In the example under discussion, this rule gives 6-4+1 = 3 meshes.

We can now write the system of impedance equations expressing the voltage balance in each mesh:

$$U = I_1(Z_1 + Z_2) \quad\quad + I_2 Z_1 \quad\quad\quad + I_3 Z_2$$
$$0 = I_1 Z_1 \quad\quad + I_2(Z_1 + Z_3 + Z_5) \quad\quad - I_3 Z_5$$
$$0 = I_1 Z_2 \quad\quad\quad - I_2 Z_5 \quad\quad + I_3(Z_3 + Z_4 + Z_5)$$

The determinant of the above system of equations is given by

$$\Delta(p) =$$

$$= \begin{vmatrix} Z_1 + Z_2 & Z_1 & Z_2 \\ Z_1 & Z_1 + Z_3 + Z_5 & -Z_5 \\ Z_2 & -Z_5 & Z_3 + Z_4 + Z_5 \end{vmatrix},$$

or in expanded form,

$$\Delta(p) = Z_5(Z_1 + Z_2)(Z_3 + Z_4) + Z_1 Z_3(Z_2 + Z_4) + $$
$$+ Z_2 Z_4(Z_1 + Z_3).$$

Solving the above system of equations for I_1, we have

$$I_1(p) = \frac{U(p)}{\Delta(p)} \begin{vmatrix} Z_1 + Z_3 + Z_5 & -Z_5 \\ -Z_5 & Z_3 + Z_4 + Z_5 \end{vmatrix} =$$
$$= \Delta U \frac{Z_3(Z_1 + Z_2 + Z_3 + Z_4) + (Z_1 + Z_3)(Z_3 + Z_4)}{\Delta(p)}$$

On forming the ratio of $I_1(p)$ to $U(p)$, we obtain the admittance function for the bridged two-terminal network in accordance with Fig 8-1:

$$Y(p) =$$

$$= \frac{Z_3(Z_1 + Z_2 + Z_3 + Z_4) + (Z_1 + Z_2)(Z_3 + Z_4)}{Z_4(Z_1 + Z_2)(Z_3 + Z_4) + Z_1 Z_2(Z_3 + Z_4) + Z_3 Z_4(Z_1 + Z_2)}.$$

$$(8\text{-}12)$$

The result is verified by comparing it with Equation
(8-11). Thus the application of the general method has yielded
a solution to a relatively simple problem, as we might have ex-
pected from the very formulation of the problem [sic].

The system of equations discussed above can also be
represented in terms of a block diagram. An analysis of the
block diagram corresponding to the three simultaneous equations
indicates that a large number of additional problems arising in
the investigation of four-terminal networks can be solved by the
application of block diagram algebra or analytically, on the
basis of Equation (8-12).

We shall now specify the conventions used in writing
the determinant for the multiple-mesh two-terminal network and
describe some of the properties of that determinant.

Since the rows of the determinant are formed from the
coefficients of the lefthand sides of the mesh equations, and
the number of each column corresponds to the subscript of the
current associated with the respective coefficient, the follow-
ing rules hold:

The diagonal elements of the determinant are equal
to the self-impedances of the associated meshes.

The remaining elements of the determinant represent
coupling factors [mutual impedances] which indicate
the impedance [branch] Z_{ik} in which a current I_k
(k = column index) in an adjoining mesh produces a
voltage drop which is included in the i-th equa-
tion (i = row index).

The usual convention is to assign double subscripts to
the individual branches. The intersection of the row and column
thus indicated fixes the position of the element. The determi-
nant for the system can then be written as follows:

$$\Delta(p) = \begin{vmatrix} Z_{11} & Z_{12} & Z_{13} \cdots \\ Z_{21} & Z_{22} & Z_{23} \cdots \\ Z_{31} & Z_{32} & Z_{33} \cdots \\ \cdots & \cdots & \cdots \end{vmatrix}. \qquad (8\text{-}13)$$

Inasmuch as the impedance Z_{ik} weighting the contribution of the k-th current to the i-th mesh equation is identical with the impedance Z_{ki} weighting the contribution of the i-th current to the k-th mesh equation, i.e., $Z_{ik} = Z_{ki}$, the determinant (8-13) is always symmetric. This property can be verified by constructing the determinant for the bridged two-terminal network discussed above.

When the equally general method of nodal voltages [nodal equations] is used, the coefficients in the system of equations which is obtained represent the nodal self- and mutual admittances. The [transfer] impedance of the two-terminal network can be calculated directly from the determinant of the latter system of equations.

It should be noted that both the nodal and mesh methods yield systems of equations containing a minimum number of unknowns. However, these unknowns, e.g., the mesh currents for interior meshes, are obtained in the form of algebraic sums of real branch currents. In addition, the impedances which are the elements of determinant (8-12) [sic] likewise represent complicated expressions. Finally, the same impedance appears in more than one rows of the determinant.

The representation of real branch currents and real voltage balances in each of the branches of the system of equations [sic] or of the block diagram constructed on the basis of that system of equations requires that the number of equations be equal to the number of meshes, including external meshes [terminations?]. The order of the determinant of the system will be increased thereby; however, the determinant will contain a set of zero coefficients, since not all of the equations are dependent.

By way of an example, we shall write the system of nodal equations for the bridged two-terminal network (fig 8-6e)). The current in the external circuit will be designated by I,
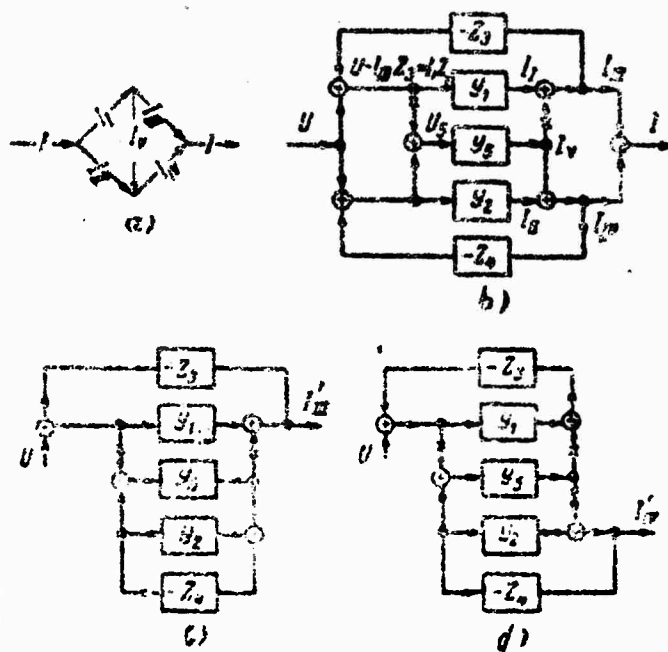
Fig 8-7.   Block Diagram for a Bridged Two-Terminal Network

while the branch currents will be labelled with an index corresponding to the number of the impedance in the branch, i.e., we have: I_I, I_{II}, I_{III}, I_{IV}, and I_V. The Roman numerals are introduced to avoid confusing the branch currents with the mesh currents. The positive direction of flow for each current is shown in Fig 8-7(a).

From Kirchhoff's first and second law, we obtain one of the possible configurations of the system of equations:

$$I_1 Z_1 + I_{III} Z_3 = U;$$
$$I_{II} Z_2 + I_{IV} Z_4 = U;$$
$$I_1 Z_1 + I_V Z_5 = I_{II} Z_2;$$

$$I_{III} = I_1 - I_V;$$
$$I_{IV} = I_{II} + I_V;$$

$$I = I_{III} + I_{IV}.$$

The coefficients of the six unknown branch currents in the above equations are the branch impedances and ±1. These coefficients become the elements of the determinant of the system; the form of the coefficients indicates the type of coupling: an impedance indicates a coupling circuit, whereas a coefficient of unity indicates a node.

The starting equations thus have been reduced to elementary simplicity, even though their number has increased, and the equivalent block diagram can now be readily constructed. In constructing the block diagram shown in Fig 8-7, we use first the equations having coefficients of unity. From those equations the current sums in the righthand side of the block diagram in Fig 8-7(b) have been constructed by connecting the appropriate branch current channels to the summing points at which the algebraic sum of the currents is formed. When all the current channels and voltage input channels are shown, the additional connections in the lefthand side of the block diagram in Fig 8-7(b) can be readily constructed from the remaining voltage balance equations, which can be rewritten in conditional form:

$$I_1 = Y_1 (U - I_{III} Z_3);$$
$$I_{II} = Y_2 (U - I_{IV} Z_4);$$

$$I_V = Y_5 (I_{II} Z_2 - I_1 Z_1).$$

The simplicity of the operation involved permits the construction of the block diagram directly from the electric circuit diagram, even without first writing the system of equations.

As an example of a particular solution which can be
obtained, we shall determine the admittance of the two-terminal
network by carrying out appropriate reductions of the block dia-
gram shown.

Inasmuch as the output current is the sum of two
terms, and the voltage is impressed on the network at two
points, we shall use the principle of superposition and express
the overall admittance function as a sum of four terms:

$$Y(p) = Y'_{III} + Y''_{III} + Y'_{IV} + Y''_{IV}.$$

where
Y'_{III} is the admittance function from the first
voltage input point to the current I'_{III} in accordance
with block diagram (c);

Y''_{III} is the admittance function from the second volt-
age input point to the current I''_{III} in accordance
with a block diagram which is symmetric to block
diagram (d) [sic];

Y'_{IV} is the admittance function from the first voltage
input point to the current I'_{IV} in accordance with
block diagram (d);

Y''_{IV} is the admittance function from the first voltage
input point to the current I''_{IV} in accordance with a
block diagram which is symmetric to block diagram
(c) [sic].

The separate analysis of block diagrams (c) and (d)
permits the ready reduction of these diagrams and the quick
evaluation of Y_{III} and Y_{IV}. When I_1 is replaced with Y_2 and Z_3
with Z_4 in Y_{III}, Y_{IV} is obtained. An analogous substitution
procedure yields Y_{III} from Y_{IV}.

We now write the expressions for the above admittance
functions obtained by the reduction of block diagrams (c) and
(d) and on the basis of the above substitutions:

$$Y'_{III} = \frac{Y_3(1 + Z_4 Y_2 + Z_3 Y_1) +}{Y_3[Z_3 + Z_3 Z_4(Y_1 + Y_2) + Z_4] + 1 +}$$
$$\frac{+ Y_1(1 + Z_3 Y_2)}{+ Z_3 Y_1 + Z_4 Y_2 + Z_3 Z_4 Y_1 Y_2},$$

$$Y''_{III} = \frac{- Y_3}{Y_3[Z_3 + Z_3 Z_4(Y_1 + Y_2) + Z_4] + 1 +}$$
$$+ Z_3 Y_1 + Z_4 Y_2 + Z_3 Z_4 Y_1 Y_2$$

$$Y'_{IV} = \cfrac{-Y_s}{Y_s\,[Z_s + Z_sZ_s\,(Y_1 + Y_s) + Z_s] + 1 + }$$
$$\phantom{Y'_{IV} = } \overline{ + Z_sY_1 + Z_sY_s + Z_sZ_sY_1Y_s }$$

$$Y''_{IV} = \cfrac{Y_s\,[(Y_1 + Y_s)\,Z_s + 1] + }{Y_s\,[Z_s + Z_sZ_s\,(Y_1 + Y_s) + Z_s] + 1 + }$$
$$\cfrac{+ Y_s\,(1 + Z_sY_1)}{+ Z_sY_1 + Z_sY_s + Z_sZ_sY_1Y_s}.$$

The sum of the above partial functions gives the overall admittance function:

$$Y\,(p) = \cfrac{Y_s\,(Y_1 + Y_s)\,(Z_s + Z_s) + }{Y_s\,[Z_s + Z_s + Z_sZ_s\,(Y_1 + Y_s)] + 1 + }$$
$$\cfrac{+ Y_1Y_s\,(Z_s + Z_s) + Y_1 + Y_s}{+ Z_sY_1 + Z_sY_s + Z_sZ_sY_1Y_s}.$$

It can be readily seen that on replacing Y_1, Y_2, and Y_3 with their reciprocals, i.e., $1/Z_1$, $1/Z_2$, and $1/Z_3$, we obtain Equation (8-12).

8-2. STRUCTURAL ANALYSIS OF FOUR-TERMINAL NETWORKS

1. Dual-Feed Operation

A four-terminal network is an autonomous electric circuit which may contain any number of meshes and has four accessible terminals, as shown in Fig 8-8(a). A four-terminal network is designated active if one of its component meshes contains a source of electromotive force; in the absence of such a source, the network is designated passive. We propose to apply the method of structure analysis to the study of passive four-terminal networks which are inserted along with two-terminal networks between generators, and to build up the elementary block diagrams obtained.

The interfacing of the four-terminal network with the line circuits implies the possibility of the simultaneous impression of two voltages U_1 and U_2 on the four-terminal network; these voltages cause currents I_1 and I_2 to flow between the respective pairs of terminals. We shall find it convenient to begin the study of the operation of four-terminal networks with a discussion of the general case from which we can then proceed to a discussion of particular cases.

The above-described operating conditions for four-terminal networks are encountered in ACS in which a four-terminal network feeds the control winding of a magnetic amplifier, the field of an uncompensated amplidyne, and other magnetic systems in which an extraneous signal is used to induce an emf in the secondary circuit of the four-terminal network. As will be apparent from the discussion which follows, the operation of a four-terminal network under these conditions has many traits in common with the operation of a transformer which couples two independent circuits, which was discussed in Chapter 6.

If a four-terminal network which has its input terminals connected to a source of emf contains n meshes, short-circuiting the output terminals through a second source of emf results in the establishment of an additional mesh. The total number of meshes in the network thereby becomes $K_2 = n+1$.

Fig 8-8(a) shows a four-terminal network which has K_2 = 3+1 = 4 meshes. In writing equations for such systems, the input mesh is always given the subscript 1 (current I_1) and the output mesh, subscript 2 (current I_2). The positive direction for the mesh currents is assumed to be clockwise. In addition, terminals 1 and 3 are assumed to be positive. Since the positive directions of current and voltage do not coincide in the output

mesh, the impressed voltage U_2 is introduced with a minus sign.

The solution of a system of equations of the type

$$
\left.
\begin{aligned}
U_1 &= I_1 Z_{11} + I_2 Z_{12} + \cdots \\
-U_2 &= I_1 Z_{21} + I_2 Z_{22} + \cdots \\
0 &= I_1 Z_{31} + I_2 Z_{32} + \cdots \\
&\;\;\cdots\cdots\cdots\cdots\cdots\cdots\cdots \\
0 &= I_1 Z_{n+1,1} + I_2 Z_{n+1,2} + \cdots
\end{aligned}
\right\} \quad n+1
$$

reduces to the construction of the system determinant Δ_{n+1} and its minors $-\Delta_n^{12}$, Δ_n^{22} and Δ_n^{11}, Δ_n^{21}. The input and output currents are then given by the following equations:

$$
\left.
\begin{aligned}
I_1 &= \frac{\Delta_n^{11}}{\Delta_{n+1}} U_1 + \frac{\Delta_n^{21}}{\Delta_{n+1}} (-U_2); \\
I_2 &= \frac{\Delta_n^{12}}{\Delta_{n+1}} U_1 + \frac{\Delta_n^{22}}{\Delta_{n+1}} (-U_2)
\end{aligned}
\right\} \quad (8\text{-}14)
$$

The coefficients of the voltages in the righthand sides of Equations (8-14) are equivalent to admittances and can not only be evaluated analytically, but also determined experimentally.

In effect, Equations (8-14) express the superposition of the short-circuit current I_1' produced by source 1 at the terminals of source 2 and of the short-circuit current I_1'' produced by source 2 at the terminals of source 1, i.e., $I_1 = I_1' + I_1''$. Similarly $I_2 = I_2' + I_2''$. The tests which follow are designed on the basis of the above discussion.

Test for the Short-Circuit Impedance at the Input Terminals. The test is set up as indicated in Fig 8-8(b) and gives the value of the short-circuit impedance at the input terminals Z_{1k} or of its reciprocal, the short-circuit admittance at the input terminals:

$$
Y_{1k} = \frac{\Delta_n^{11}}{\Delta_{n+1}}. \quad (8\text{-}15)
$$

Test for the Short-Circuit Impedance at the Output Terminals. The test is set up as shown in Fig 8-8(c) and gives the value of the short-circuit impedance at the output terminals or of the corresponding admittance

$$Y_{2k} = \frac{\Delta_n^{22}}{\Delta_{n+1}}. \qquad (8\text{-}16)$$

Determination of the Short-Circuit Transfer Admittance. The test is set up according to Figs 8-8(b) or 8-8(c). The current through the short-circuited terminals is measured. When the impressed voltages are equal, the current values recorded with the two setups will be equal because of the reciprocity principle (symmetric determinants). The ratio of the current to the impressed voltage gives the desired admittance

$$Y_{mk} = I_1 k / U_2 k = I_2 k / U_1 k$$

which is given by

$$Y_{mk} = \frac{\Delta_n^{21}}{\Delta_{n+1}} = \frac{\Delta_n^{12}}{\Delta_{n+1}}. \qquad (8\text{-}17)$$

In the course of the tests described above, only single measurements were made on four-terminal networks containing ohmic resistances. In the case of operator four-terminal networks, the admittance or impedance frequency response transfer functions are recorded in the frequency space of the ACS in which the circuit under investigation is used.

The substitution of the notation introduced above in Equations (8-14) transforms the latter as follows:

$$\left. \begin{array}{l} I_1 = Y_{1k}U_1 + Y_{mk}(-U_2) \\ I_2 = Y_{mk}U_1 + Y_{2k}(-U_2) \end{array} \right\} \qquad (8\text{-}18)$$

We shall now represent the coefficients in Equations (8-18) by the impedances of the T network equivalent to the four-terminal network (Fig 8-8(d), without subscripts).

When the short-circuit tests according to diagrams are applied to the T network shown in diagram (d), the following values are obtained for the impedances:

$$Z_{1k} = Z_1 + \frac{Z_2 Z_3}{Z_2 + Z_3} = \frac{Z_1 Z_2 + Z_1 Z_3 + Z_2 Z_3}{Z_2 + Z_3};$$

$$Z_{2k} = Z_2 + \frac{Z_1 Z_3}{Z_1 + Z_3} = \frac{Z_1 Z_2 + Z_1 Z_3 + Z_2 Z_3}{Z_1 + Z_3};$$

$$Z_{mk} = Z_{1k}\frac{Z_3 + Z_2}{Z_2} = Z_{2k}\frac{Z_1 + Z_3}{Z_1} =$$

$$= \frac{Z_1 Z_2 + Z_1 Z_3 + Z_2 Z_3}{Z_3}$$ (8-19a)

The corresponding admittances are given by:

$$Y_{mk} = \frac{Z_3}{Z_1 Z_2 + Z_1 Z_3 + Z_2 Z_3};$$

$$Y_{1k} = \frac{Z_2 + Z_3}{Z_3} Y_{mk};$$ (8-19b)

$$Y_{2k} = \frac{Z_1 + Z_3}{Z_3} Y_{mk}.$$

The inverse problem can also be solved, i.e., the impedances Z_{1e}, Z_{2e}, Z_{3e} of the branches of the T network can be evaluated from the given coefficients Y_{1k}, Y_{2k}, Y_{mk}:

$$Z_{1s} = \frac{Y_{2k} - Y_{mk}}{Y_{1k}Y_{2k} - Y_{mk}^2};$$

$$Z_{2s} = \frac{Y_{1k} - Y_{mk}}{Y_{1k}Y_{2k} - Y_{mk}^2};$$ (8-20)

$$Z_{3s} = \frac{Y_{mk}}{Y_{1k}Y_{2k} - Y_{mk}^2}.$$

As far as the relationships between the input and output voltages and currents are concerned, the circuit defined by Equations (8-20) is fully equivalent to the multiple mesh four-terminal network, the parameters of which are defined by Equations (8-15) through (8-17). The circuit defined by Equations (8-20) is therfore called the equivalent T network.

The no-load transfer functions can be expressed in terms of the parameters of the equivalent network or of the coefficients of the original system of equations (8-18). In effect, we obtain directly from diagram (c):

$$W_{1s} = \frac{Z_{3s}}{Z_{1s} + Z_{3s}}; \quad W_{2s} = \frac{Z_{3s}}{Z_{2s} + Z_{3s}}.$$

Substituting the values of the Z's from Equations (8-20), we have

$$W_{10} = \frac{Y_{mk}}{Y_{2k}}; \quad W_{30} = \frac{Y_{mk}}{Y_{1k}}. \tag{8-21}$$

Block Diagram for Dual-Feed Operation. The behavior of a four-terminal network can be completely described under all conceivable operating conditions in terms of only three parameters, e.g., the short-circuit impedances Z_{1k}, Z_{2k}, and Z_{mk}. When this approach is used and additional parameters of the four-terminal network are expressed in terms of the basic parameters, an insufficiently clear formulation of the dependence of these other parameters on the basic parameters is obtained.

The interdependence of the various modes of operation of the four-terminal network is best brought out by the methods of structure analysis.
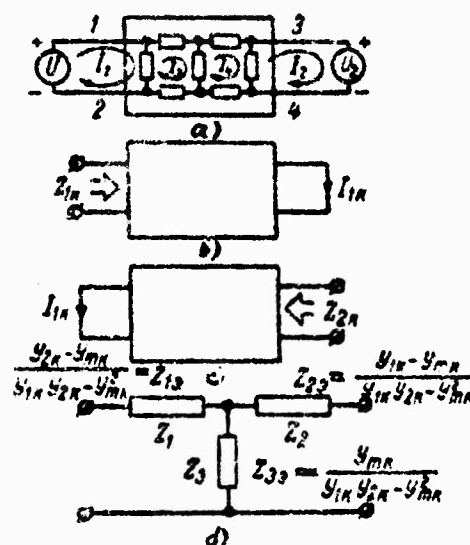

Fig 8-8.   Electric Circuits of Four-Terminal Networks

Legend: (a) dual-feed operation: (b) operation with output terminals short-circuited; (c) operation with input terminals short-circuited; (d) equivalent T network

Fig 8-9 shows a number of block diagrams which represent the various operating modes of four-terminal networks.

Diagram (a) shows the electrical connections and is given for the purpose of repeating the notation and rules concerning signs which were used in Equations (8-18).

Block diagram (b) was constructed directly from Equations (8-18), the coefficients in which now become transfer functions for unidirectional elements. The rule concerning the sign of the secondary voltage is reflected in the "reversal" of the U_2 input channel.

The above arrangement permits the analysis of the positive coefficients of Equations (8-18), which are characteristic of these equations by virtue of their physical nature [sic]. As an example, we shall examine the components of current I_1, I_1', the short-circuit current at the output terminals produced by source 1, and I_1'', the short-circuit current at the input terminals produced by source 2. The directions of flow of the component currents when both feed voltages are positive are indicated in diagram (a). In the interest of simplicity, we shall assume that the four-terminal network is given in the form of an equivalent T network.

The current components will then effectively subtract. If the direction of the current I_1' is taken to be positive, a negative sign must be obtained for the second component, assuming the line voltage to be positive; this is achieved in the block diagram by the reversal of the U_2 channel. Similar considerations also apply to the components of current I_2.

Taking into account the Internal Resistance of the Sources of emf. When the two pairs of terminals of a four-terminal network are connected to different sources of emf, e.g. E_1 and E_2 having internal resistances Z_{E_1} and Z_{E_2}, respectively, the discussion of the network parameters must take into account the following obvious relationships:

$$U_1 = E_1 - I_1 Z_{E_1}$$

$$U_2 = E_2 - I_2 Z_{E_2}$$

Using the above relationships, block diagram (b) can be readily built up and transformed into block diagram (c) by the addition of the indicated feedback loops. When the summing points and branch points are removed from the feedback loops in block diagram (c) by the application of the rules of algebra of
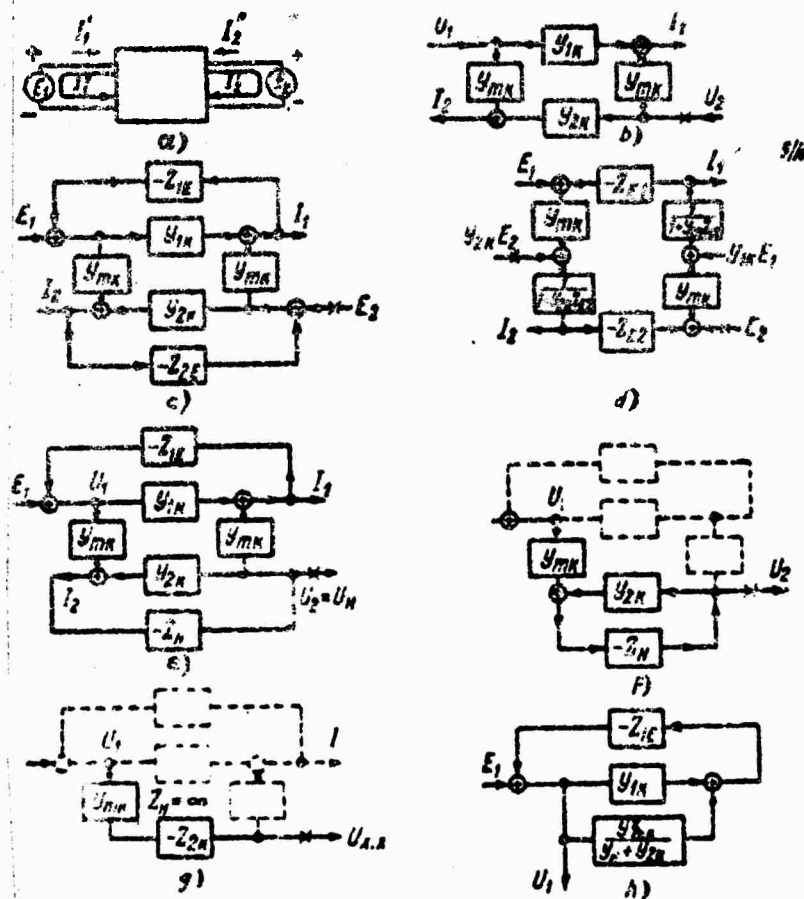
Fig 8-9. Electric Circuit and Block Diagrams for a General Four-Terminal Network

block diagrams, including the rule concerning duplexed channels, the block diagram shown in Fig 8-9(d) is obtained.

On the basis of this general scheme, an analytical relationship similar to that expressed by Equations (8-18) can again be derived, this time between the currents and the emf's instead of the voltages:

$$I_1 = aE_1 + m(-E_2); \quad I_2 = b(-E_2) + mE_1. \quad (8\text{-}22)$$

Before proceeding to the determination of the coefficients of the equations from the block diagram, we shall write the product of the open-loop transfer functions [overall open-loop transfer function]:

$$C = \frac{Z_{E1} Z_{E2} Y_{mk}^2}{(1 + Z_{E1} Y_{1k})(1 + Z_{E2} Y_{2k})};$$

In addition, we must take into consideration the direction of signal flow and the number of inputs to the scheme; we then obtain:

$$a = \frac{1}{1-C} \times$$

$$\times \left[\frac{Y_{1k}}{1 + Y_{1k} Z_{E1}} - \frac{Y_{mk}^2 Z_{E2}}{(1 + Y_{1k} Z_{E1})(1 + Y_{2k} + Z_{E2})} \right] =$$

$$= \frac{Y_{1k} + Z_{E2}(Y_{1k} Y_{2k} - Y_{mk}^2)}{1 + Y_{1k} Z_{E1} + Y_{2k} E_{E2} + Z_{E1} Z_{E2}(Y_{1k} Y_{2k} - Y_{mk}^2)};$$

$$b = \frac{1}{1-C} \times$$

$$\times \left[\frac{Y_{2k}}{1 + Y_{2k} Z_{E2}} - \frac{Y_{mk}^2 Z_{E1}}{(1 + Y_{1k} Z_{E1})(1 + Y_{2k} Z_{E2})} \right] =$$

$$= \frac{Y_{2k} + Z_{E1}(Y_{1k} Y_{2k} - Y_{mk}^2)}{1 + Y_{1k} Z_{E1} + Y_{2k} Z_{E2} + Z_{E1} Z_{E2}(Y_{1k} Y_{2k} - Y_{mk}^2)};$$

$$m = \frac{1}{1-C} \times$$

$$\times \left[\frac{Y_{mk}}{1 + Y_{2k}Z_{E2}} - \frac{Y_{1k}Y_{mk}Z_{E1}}{(1 + Y_{1k}Z_{E1})(1 + Y_{2k}Z_{E1})} \right] =$$

$$= \frac{Y_{mk}}{1 + Y_{1k}Z_{E1} + Y_{2k}Z_{E2} + Z_{E1}Z_{E2}(Y_{1k}Y_{2k} - Y_{mk}^2)}$$

2. Four-Terminal Networks Connected to a Single Source

Full-Load Operation. We shall set $E_2 = 0$ in the block diagram shown in Fig 8-9(c) and eliminate the summing point previously used for the introduction of the input E_2. The impedance of the external circuit can now be designated as the load impedance, i.e., we can make the substitution $Z_{E2} = Z_L$ in the block diagram. Finally, we shall include in the outputs of the block diagram in addition to the currents, the output voltage of the four-terminal network, $U_2 = I_2 Z_L$. Inasmuch as the diagram contains the channel $-I_2 Z_L$, the sign of data taken off this channel is changed.

The transformations indicated above lead to the diagram shown in Fig 8-9(e). The internal connections in that diagram are identical with those shown in diagram (c), and we can therefore apply to it the general transformation leading to diagram (d), excluding the provision for an input channel for E_2 and the corresponding summing points [sic] and substituting a takeoff branch $+U_2 = U_L$. The modifications just described permit the study of complex operating conditions in networks containing two impedances in the supply circuit and in the load circuit. We can again make use of Equation(8-22) retaining the coefficients a and m but dropping the terms containing E_2, i.e., we have

$$I_1 = aE_1 \; ; \quad I_2 = mE_1 \tag{8-23}$$

If one is interested only in the relationship between the output and input voltages, the elements used in forming the [input] voltage from emf E_1 can be dropped from diagram (e); the resultant block diagram is shown in Fig 8-9(f). Upon reduction, block diagram (f) yields the following transfer function:

$$W_u = \frac{Y_{mk}Z_H}{1 + Y_{2k}Z_H} = \frac{Y_{mk}}{Y_{2k}} \cdot \frac{C_H}{1 + C_H}. \tag{8-24}$$

$$H = L$$

We shall derive the above equation directly from the electric circuit shown in Fig 8-10(a), in which the product of the functions in the smaller [sic] loop in the block diagram shown in Fig 8-9(e)

$$C_\text{н} = \frac{Z_\text{н}}{Z_{2\text{к}}} = Z_\text{н} Y_{2\text{к}} = \frac{Y_{2\text{к}}}{Y_\text{н}} \qquad (8\text{-}25)$$

$$\text{н} = \ell$$

is designated as the relative load impedance.

In the derivation we shall make use of the theorem of the equivalent generator [reciprocity theorem] and construct the circuit shown in Fig 8-10(b), which is identical with circuit (a) in terms of loading conditions. The voltage of the equivalent generator introduced in the load circuit in Fig 8-10(b) is set equal to the open-circuit voltage of the four-terminal network and is distributed over the load impedance and the short-circuit impedance of the four-terminal network.

It follows that the overall transfer function of the loaded four-terminal network can be represented as the product of the no-load transfer function expressed by Equations(8-21) and the transfer function of a network consisting of two-terminal sections connected in series:

$$W(p) = \frac{Z_\text{н}}{Z_\text{н} + Z_{2\text{к}}} W_\bullet(p),$$

or

$$W(p) = \frac{Z_\text{н} Y_{2\text{к}}}{1 + Z_\text{н} Y_{2\text{к}}} W_\bullet(p) = \frac{C_\text{н}}{1 + C_\text{н}} W_\bullet(p). \qquad (8\text{-}26)$$

For small values of the short-circuit input impedance, the function in Equation (8-26) approaches unity, and the no-load transfer function is not distorted. As Y_ℓ increases, the distortion of the no-load transfer function becomes significant and usually operates to decrease the modulus of the transfer function. Equation (8-26) can be represented by the diagram

597

shown in Fig 8-10(c), which contains a 'rigid' [direct] negative feedback loop.

When the type of block diagram is established, nomograms can be used to compute the frequency response of the four-terminal network at progressively higher load levels and structural changes required for the elimination of undesirable system effects can be noted.

When the four-terminal network and load consist of purely ohmic elements, the inclusion of the load operates to decrease the no-load transfer constant of the four-terminal network, a condition which must be viewed as a negative factor. When operator elements are present, the multiplication of the no-load transfer function by an additional factor gives a new operator transfer function with a corresponding change in frequency response, which can be made to operatre in the desired direction.

The effect of the additional factor is most clearly observed on the inverse of the transfer function given by Equation (8-26):

$$\frac{1}{W(p)} = \frac{1}{W_0(p)}(1 + Y_H Z_{2k}) = \frac{1 + 1 C_H}{W_s(p)}.$$
$$H = \ell$$

Inclusion of the Impedance of the Feed Circuit. We shall now use Fig 8-9(h) to discuss the effect of the impedance of the input circuit [input termination] on the transition from emf E_1 to the [input] voltage. For the solution of this special question, we transform block diagram (e) into diagram (h), in which only the E_1 input channel and the U_1 channel are retained; the latter channel is now considered the output.

The remaining parallel [feedback] loops in the diagram represent the input [driving point] admittance of the network:

for the loaded four-terminal network, we have

$$Y_{1s} = Y_{1k} - \frac{Y_{mk}^2}{Y_H + Y_{2k}} = \frac{Y_{1k}(Y_{11} + Y_{m2} - Y_{mk}^2}{Y_H + Y_{2k}}; \quad (8-27a)$$

for the no-load [open-circuit] condition, we have

$$Y_{1a} = Y_{1k} - \frac{Y_{mk}^2}{Y_{2k}} = \frac{Y_{1k}Y_{2k} - Y_{mk}^2}{Y_{2k}} . \qquad (8\text{-}27b)$$

the overall feedback transfer function in diagram (h) is given by

$$C_{EN} = \frac{Y_{1k}(Y_N + Y_{2k}) - Y_{mk}^2}{Y_N + Y_{2k}} Z_{E1}, \qquad (8\text{-}28a)$$

$$N = 0$$

and the voltage reduction coefficient [actually the transition loss is given by

$$K_E = \frac{1}{1 + C_{EN}} =$$

$$= \frac{1 + Z_{2k}Z_N}{(1 + Z_N Y_{2k})(1 + Z_{E1} Y_{1k}) - Y_{mk}^2 Z_{E1} Z_N} . \qquad (8\text{-}28b)$$

We have thus expressed the quantities used in the above equations in terms of the basic parameters of the four-terminal network.

It goes without saying that the voltage reduction coefficient can also be obtained from the generalized block diagram (c) by bringing together the two E_1 inputs at a single point, thereby obtaining

$$E_1\left(1 - \frac{Y_{1k}Z_{E1}}{1 + Y_{1k}Z_{E1}}\right) = \frac{1}{1 + Y_{1k}Z_{E1}} E_1 .$$

Insertion of the above sum in the loop [sic] gives

$$K_E = \frac{1}{1 - C} \cdot \frac{1}{1 + Y_{1k}Z_{E1}} .$$
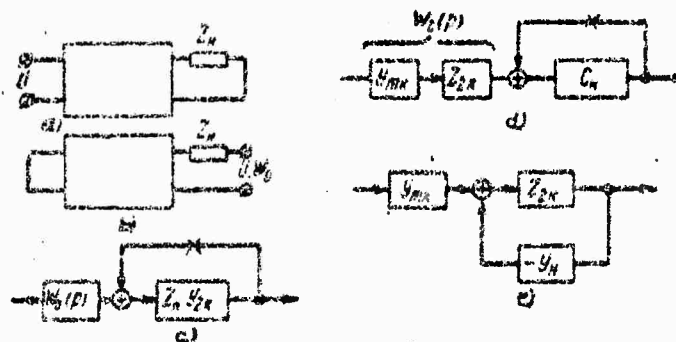
Fig 8-10. A Four-Terminal Network Coupled to a Load

Legend: (a) electric circuit; (b) design diagram
based on Thévenin's theorem; (c), (d), (e)
block diagrams

No-Load Operation. If we let Z_y in Fig 8-9(b) ap-
proach infinity, the transfer function of the negative feedback
loop will be equal to the inverse of the feedback characteristic.
The transfer function thus obtained, $-(1/Y_{2k}) = -Z_{2k}$, is shown
in the no-load [open-circuit] block diagram in Fig 8-9(g).

The no-load transfer function is readily derived from
the diagram:

$$W_o(p) = Y_{mk} Z_{2k} = \frac{Y_{mk}}{Y_{2k}}. \tag{8-29}$$

The representation of the no-load operator transfer
function as the product of two terms, represented by Equation
(8-29), has already been illustrated in Fig 8-10(d). Such a
representation of the operator transfer function permits the
transformation of diagram (d) into diagram (e) by moving the
feedback channel ahead of element Z_{2k}. Diagram (e) will be
frequently referred to in the course of the discussion which
follows.

The no-load operator transfer functions for a group
of simple four-terminal networks can be derived directly from
the corresponding electrical circuits. Some typical examples
are shown in Fig 8-11.

Circuit (a) illustrates the general case of no-load operation.

Circuit (b) represents a general L-type four-terminal network; circuits (c) and (d) represent general T- and π-type four-terminal networks, respectively. All of these four-terminal networks have identical no-load transfer functions, derived from the formula giving the ratio of the impedances in the voltage divider

$$W_e(p) = \frac{Z_2}{Z_1 + Z_2} \qquad (8.30)$$

Circuit (e), which has a square configuration, has a similar transfer function inasmuch as the input impedance Z_3 (as in the case circuit (d)) is not involved in the voltage distribution. The latter function is discharged exclusively by the circuit comprising impedances 1'-2-1''.

If we represent the sum of the impedances in the horizontal sides of the square by a single symbol

$$Z_1 = Z_1' + Z_1''$$

we obtain an expression identical with Equation (8-30) for the transfer function of the voltage divider.

The inclusion of impedances 5' and 5 does not change the transfer function. However, if the square circuit is extended by the inclusion of additional meshes, a ladder-type four-terminal network is obtained, the transfer function of which will be more complex.

For the determination of the transfer function of the ladder-type four-terminal network shown in Fig 8-11(f), it will be found convenient to number the impedances from right to left. The self-impedances [sic] in each mesh are labelled with the same numerals and distinguished by the number of primes shown. The sum of the self-impedances is written without primes:

$$Z_2 = Z_2' + Z_2''; \quad Z_4 = Z_4' + Z_4''; \text{ etc.}$$

It will be found convenient to consider the ladder-type four-terminal network as a multi-sectioned voltage divider. The first mesh impresses a fraction $Z_2/(Z_1 + Z_2)$ of the voltage on impedance Z_3; the voltage across Z_3 in turn is a fraction of the voltage across Z_5; etc. The voltage drop in each mesh is

determined by the ratio of the sum of the impedances remaining in the circuit after the given mesh to the sum of these imped- ances and the self-impedance of the given mesh.

Since all of the above-indicated impedances are con- tributed by ladder-type two-terminal networks, we can obtain the required transfer function by multiplying together the in- dividual impedance ratios:

$$
W_3(p) = \frac{Z_1}{Z_1 + Z_2} \cdot \frac{\dfrac{1}{\dfrac{1}{Z_3} + \dfrac{1}{Z_1 + Z_2}}}{Z_4 + \dfrac{1}{\dfrac{1}{Z_3} + \dfrac{1}{Z_1 + Z_2}}} \times
$$

$$
\times \frac{\dfrac{1}{\dfrac{1}{Z_3} + \dfrac{1}{Z_4 + \dfrac{1}{\dfrac{1}{Z_3} + \dfrac{1}{Z_1 + Z_2}}}}}{Z_6 + \dfrac{1}{\dfrac{1}{Z_5} + \dfrac{1}{Z_4 + \dfrac{1}{\dfrac{1}{Z_3} + \dfrac{1}{Z_1 + Z_2}}}}}. \quad (8\text{-}31a)
$$

Each of the terms in Equation (8-31a) can be reduced to a proper fraction with the result that the preceding equa- tion takes the form:

$$
W_3(p) = \frac{Z_1}{Z_1 + Z_2} \cdot \frac{Z_3(Z_1 + Z_2)}{Z_3(Z_1 + Z_2) + Z_4(Z_1 + Z_2 + Z_3)} \times
$$

$$
\times \frac{Z_5[Z_3(Z_1 + Z_2) + }{(Z_1 + Z_2)[Z_3(Z_1 + Z_2) +}
$$

$$
\frac{+ Z_4(Z_1 + Z_2 + Z_3)]}{+ Z_4(Z_1 + Z_2 + Z_3)] + \ldots + Z_5 Z_6 (Z_1 + Z_2 + Z_3)} \quad (8\text{-}31b)
$$

It will be noted that the denominators and numerators of successive pairs of terms in Equation (8-31b) cancel. The final equation obtained for any number of meshes will contain

in the denominator the product of impedances connected in paral-
lel; the numerator of the same expression will contain only the
denominator of the last term.

We present the following special cases:

for a two-mesh network, we have

$$W_2(p) = \frac{Z_1 Z_3}{Z_3(Z_1 + Z_2) + Z_4(Z_1 + Z_2 + Z_3)};$$ (8-31c)

for a three-mesh network, we have

$$W_3(p) = \frac{Z_1 Z_3 Z_5}{(Z_3 + Z_4)[Z_3(Z_1 + Z_2) + Z_4(Z_1 + Z_2 + Z_3)] + Z_4 Z_5(Z_1 + Z_2 + Z_3)}$$ (8-31f)
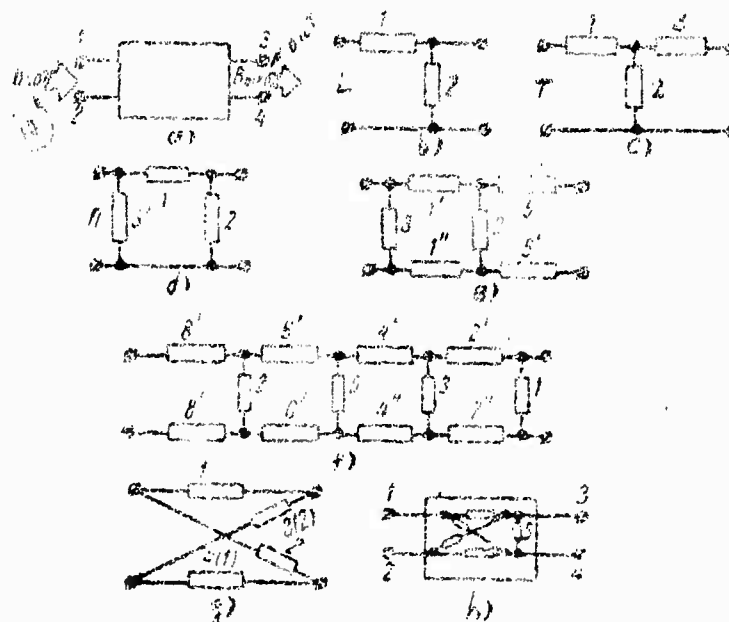

Fig 8-11. Simple Circuits for Four-Terminal Networks Used in
the Derivation of the No-Load Operator Transfer
Function

The transfer function for a network containing a large number of meshes can be obtained by the application of the basic Equation (8-31a) and of the following recursion formula which makes use of the simple equations presented above:

$$\frac{1}{W_{n+1}} = \frac{Z_{2n+1} + Z_{2n+2}}{Z_{2n+1}} \cdot \frac{1}{W_n} +$$
$$+ \frac{Z_{2n+2}}{W_{n-1}} \left(\frac{1}{Z_{2n-1}} + \frac{1}{Z_{вxn}} \right). \qquad (8\text{-}31\,e)$$

It will be readily noted that following the combination of the even-numbered impedances, the ladder network shown in Fig 8-11(f) reduces to the ladder network in Fig 8-5(c) when the output from the ladder is considered to be the voltage drop U across impedance Z_4. It follows that the block diagram 8-5(c) is fully adequate for the representation of the transfer characteristics of ladder-type four-terminal networks if the U_1 channel is considered the output channel. This can be easily confirmed by carrying out the reduction of the block diagram between the input channel and the above-indicated output channel; the result should be Equation (8-31c).

The circuit shown in Fig 8-11(g) represents a lattice or bridge network. It will be found convenient to consider it as two voltage dividers having legs 1-3 and 2-4 connected together. The transfer function is obtained as the difference of two transfer function of the type described by Equation (8-30):

$$W_\bullet(p) = \frac{Z_3}{Z_1 + Z_3} - \frac{Z_4}{Z_2 + Z_6} = \frac{Z_2 Z_3 - Z_1 Z_4}{(Z_1 + Z_3)(Z_2 + Z_4)}.$$
$$(8\text{-}32a)$$

When the impedances in opposing legs are equal, $Z_3 = Z_2$ and $Z_4 = Z_1$, and the network becomes symmetric.

To avoid repeating the figure, the symmetry conditions are entered in parentheses in the circuit. The no-load transfer function then becomes:

$$W_\bullet(p) = \frac{Z_2 - Z_1}{Z_2 + Z_1}. \qquad (8\text{-}32\,b)$$

The circuit in Fig 8-11(h) differs from circuit (g) by the inclusion of the additional impedance Z_5, connected diagonally across the bridge. This change introduces considerable modifications in the order of derivation of the transfer function. The situation is relieved somewhat by the fact

that the lattice network under discussion if expanded would coincide completely with the bridged network shown in Fig 8-5(e).

When the last-indicated network is operated as a four-terminal network, the output voltage produced by the mesh currents I_2 and $-I_3$ (from Equation (8-11(h))is taken off impedance Z_5.

Using the results from the analysis of this network when operated as a two-terminal network, the transfer function for the four-terminal network can be computed:

$$W_e(p) = \frac{Z_5(I_2 - I_3)}{U_{BX}} =$$

$$= Z_4 \frac{- \begin{vmatrix} Z_1 & -Z_5 \\ Z_3 & Z_5 + Z_4 + Z_5 \end{vmatrix} - \begin{vmatrix} Z_1 & Z_3 + Z_2 + Z_5 \\ Z_3 & -Z_5 \end{vmatrix}}{\Delta_n},$$

$BX = U_n$

Expansion of the above determinant gives:

$$W_e(p) = \frac{Z_1 Z_3 - Z_2 Z_4}{Y_5[Z_1 Z_2(Z_3 + Z_4) + Z_3 Z_4(Z_1 + Z_2)] + \cdots \atop \qquad \cdots + (Z_1 + Z_3)(Z_2 + Z_4)} \qquad (8-33)$$

The above example shows that the solution of multiple-mesh four-terminal networks requires the application of more general computational procedures.

The transfer function for a four-terminal network can be obtained by the method of mesh equations as follows:

Find within the four-terminal network the shortest path involving impedances $Z_k, \ldots, Z_m$, linking the output terminals;

Establish the relationship between the mesh currents used in constructing the system of equations and the branch currents flowing through the impedances $Z_k, \ldots, Z_m$; this relationship can be expressed in the form of the conditional sum

$$I_N = \sum_{i=1}^{S_l} I_i.$$

where the number of component mesh currents S_i and their signs in the expression for each branch current are determined from the diagram (in turn, the mesh currents entering the above summation are computed from the system of equations by the general formula $I_i = (\Delta_{n-1}^i / \Delta_n) U_{in}$);

Determine the sum of the branch voltages

$$\sum_{N=k}^{m} I_N Z_N$$

and divide that sum by the input voltage to obtain the operator no-load transfer function in terms of the above-discussed quantities:

$$W_0(p) = \frac{1}{\Delta_n} \sum_{N=k}^{m} Z_N \sum_{i=1}^{S_i} \Delta_{n-1}^i \tag{8-34}$$

When the internal circuit [sic] of the four-terminal network linking the output terminals contains only one imped-ance, Equation (8-34) will contain only one term

$$W_0(p) = \frac{Z_k}{\Delta_n} \sum_{i=1}^{S_i} \Delta_{n-1}^i \tag{8-35}$$

Such a case was discussed in the course of the calcu-lation of circuit (h). It goes without saying that in the con-struction of the system of equations one can always select the system of mesh currents which is most convenient for the subse-quent computations. When the method of nodal voltages is used, the input voltage must be introduced as one of the voltages used in the system of equations and the solutions must be ex-pressed in terms of the input voltage and in the form of deter-minantal ratios.

When the expanded system of equations in terms of the nodal currents is used, one obtains immediately the real cur-rents and the corresponding real voltage drops in the chain of impedances connecting the output terminals. In the block dia-gram which is equivalent to the complete system of equations [sic], new desirable outputs can always be indicated; reduction of the diagram in terms of these new outputs then gives directly the desired transfer function.

Thus the transfer function expressed by Equation (8-35)

can be obtained from the block diagram for the bridged network given in Fig 8-7 by selecting the channel for the voltage drop expressed by the product of current I_y and impedance z_7. This channel forms the input to element Y_8. Reduction of the diagram between the input U_{in} and the output U_5 gives the transfer function expressed by Equation (8-53), bypassing the solution of the system of equations.

3. Three-Terminal Networks

When homopolar input and output terminals of the four-terminal network are bridged, e.g., if the pair 2-4 is short-circuited and the pair 1-3 is connected through an operator impedance, the block diagram shown in Fig 8-12(a) is obtained. We note that short-circuiting terminals 2-4 makes them equipotential.

The analysis of circuits of the type described above is of considerable practical importance, since in the majority of four-terminal networks discussed so far, terminals 2-4 are at the same potential because of the internal circuit [etc]. The L-, T-, and π-type four-terminal networks shown in Fig 8-11 and the ladder network shown in Fig 8-5(c) are of that type. It was noted above that the terminated ladder network shown in Fig 8-11(e) has the same transfer characteristics as the [corresponding] unterminated network when $z_1 = z_1' + z_1''$. Inasmuch as the latter network has fewer elements, it is to be preferred and should be used.

Finally, 'single-wire' circuits, in which the ground always acts as the second terminal, are widely used. The transformation of the mesh voltages in such networks is always performed in terms of the equivalent three-terminal network.

Four-terminal networks having their terminals 3 and 4 short-circuited are represented by the block diagram in Fig 8-12 (b). In such four-terminal networks the provision of an additional connection between the upper terminals through the impedance z_y' makes it possible to obtain any desired transfer characteristic.

The potential difference between the bridged homopolar terminals 1-3 is given by the expression:

$$U_d = U_{in} - U_c$$

Using the above expression, the transfer function from the input voltage to the potential difference between

terminals 1-3 can be written as follows:

$$W_{BO}(p) = 1 - W_a(p).$$

If impedance Z_B is now inserted between the homopolar terminals, the side circuit will be placed under load and the loaded form of the transfer function defined above is given by the following equation, based on Equation (8-26):

$$W_B(p) = \frac{C_B}{1+C_B}[1 - W_a(p)].$$

The relative impedance of the bridge arm is given by the expression

$$C_B = Z_B/Z_{2k}$$

As may be seen from circuit (c), the short-circuit impedance at terminals 1-3 is identical with the basic short-circuit imped-ance Z_{2k} of the four-terminal network at the output terminals, thereby eliminating the need for any further analysis of the original network.

We now return to the original voltage balance equation

$$U_o = U_{in} - U_B$$

From the above relation a new expression can be readily obtained for the basic transfer function of the three-terminal network when the load is applied to the homopolar terminals:

$$W(p) = 1 - \frac{C_B}{1+C_B}[1 - W_a(p)],$$

or

$$W(p) = \frac{1}{1+C_B} + \frac{C_B}{1+C_B}W_a(p). \qquad (8-34a)$$

It follows that the loading of the homopolar terminals of a four-terminal network has the same effect on the no-load transfer function as the application of a direct load and intro-ducing additional term $1/(1+C_B)$; the block diagram for the four-terminal network (diagram (d)) is augmented by a parallel

(forward) long.

When bridging the homopolar terminals of a loaded four-terminal network, Equation (8-36a) must be referred to the full-load transfer function $W(p)$ for the four-terminal network; in addition, the load circuit must be taken into account in the determination of Z_{2k}. Since the load is connected in parallel with Z_{2k} in the short-circuit test, the new short-circuit admittance corresponding to diagram (e) is given by $Y_{2k}+Y_\ell$, and the relative impedance of the bridge arm becomes

$$c\frac{r}{8} = Z_\ell(Y_{2k}+Y_\ell)$$
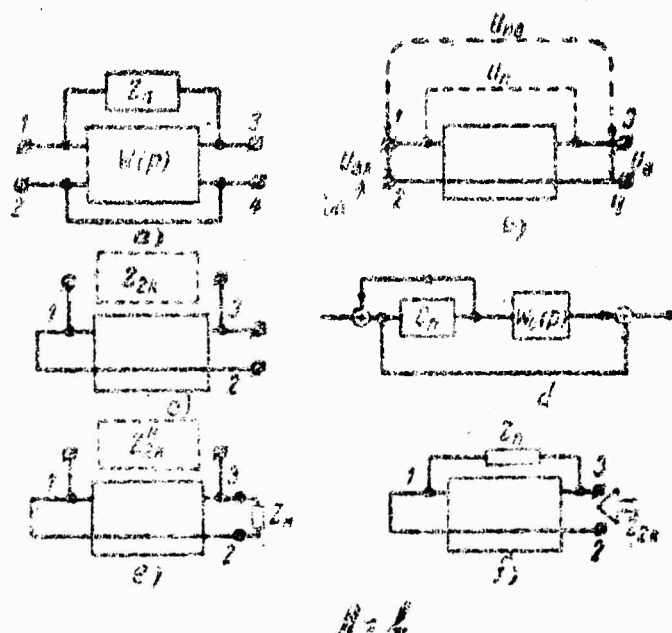
Fig 8-12. Circuits for Three-Terminal Networks
Legend: (a) working electric circuit for a three-terminal network; (b) schematic representation of the impressed voltages; (c), (e), (f) experimental setups for the determination of the short-circuit impedance; (d) block diagram for a three-terminal network with the load applied across the bridge arm.

When the above-indicated changes are implemented, the full-load transfer function for a four-terminal network with a

supplemental bridge arm [sic] takes on the form:

$$W_{HR}(p) = \frac{1}{1 + C_n^H} + \frac{C_n^H}{1 + C_n^H} W_H(p). \quad (8\text{-}36\text{o})$$

$$H = \mathcal{L} \quad H = \hat{B}$$

If in addition to the load applied to the homopolar terminals, the four-terminal network discussed above also receives a direct load, its transfer function according to Equation (8-36a) is multiplied by the standard factor expressed by Equation (8-26):

$$W'_{nn}(p) = \left[\frac{1}{1 + C_n} + W_o(p) \frac{C_n}{1 + C_n} \right] \cdot \frac{C'_H}{1 + C'_H}, \quad (8\text{-}37)$$

where

$$C'_k = z_i (Y_{2k} + Y_B)$$

We shall now discuss some examples of very simple bridged three-terminal networks.

The L-type RC circuit shown in Fig 8-13(a) without the bridged arm has the transfer function of a real differential element

$$W_1(p) = T_1 p / (T_1 p + 1)$$

Such an element will not transmit a constant signal; when such a signal is required, it is sufficient to add the bridge arm R_1.

Using the circuit shown, we obtain the following relative impedance for the bridge arm:

$$C_B = R_1 (T_1 p + 1) / r_1$$

The complete transfer function for the circuit is that of a real driving element:

$$W_H(p) = \frac{1 + R_1 C_p}{1 + R_1 C_1 p + \dfrac{R_1}{r_1}} = r_1 \frac{R_1 C_1 p + 1}{r_1 R_1 C_1 p + R_1 + r_1}, \quad (8\text{-}38\text{a})$$

We note that the time constant in the denominator is smaller than in the starting equation.

We now build up circuit (a) by coupling to its output an L-type RC circuit and proceed to recompute the transfer function on the basis of Equation (8-37). The load has an impedance

$Z_y = r_2 + 1/C_2 p$; the output short-circuit admittance of the first
stage is given by

$$Y_{2k} = r_1^{-1} + R_1^{-1} + C_1 p$$

The relative admittance of the load is given by

$$\frac{(r_2 C_2 p + 1)(r_1 + R_1 + r_1 R_1 C_1 p)}{r_1 R_1 C_2 p} = C_H'.$$

Using the above relation in expanding the value of the
correction factor $C_H'/(1+C_H')$ and substituting the expanded value
of that factor in the expression for the transfer function, we
obtain:

$$W_b(p) = \frac{r_1(R_1 C_1 p + 1) r_2 C_2 p}{r_1 R_1 C_2 p + (r_2 C_2 p + 1)(r_1 + R_1 + r_1 R_1 C_1 p)}.$$

$$(8.38\,b)$$

The above transfer function also fails to assure the
transmission of a constant signal through the network. We shall
therefore analyze the conditions for the introduction of an ad-
ditional bridge arm, as shown in diagram (c).

In our analysis we shall start with the four-terminal
network shown in diagram (b) and assume that the transfer func-
tion given by Equation (8-38b) corresponds to the no-load trans-
fer function of the new four-terminal network. We have for Y_{2k}:

$$Y_{2k} = \frac{1}{Z_{2k}}$$
$$= \frac{r_1 + R_1 + r_1 R_1 (C_1 + C_2) p + r_2 C_2 p (r_1 + R_1 + r_1 R_1 C_1 p)}{r_2 [r_1 + R_1 + r_1 R_1 (C_1 + C_2) p]}$$

and for the relative impedance of the side circuit:

$$C = \frac{R_2 [r_1 + R_1 + r_1 R_1 (C_1 + C_2) p + r_2 C_2 p (r_1 + R_1 + r_1 R_1 C_1 p)]}{r_2 [r_1 + R_1 + r_1 R_1 (C_2 + C_1) p]}$$

$$(8.38\,c)$$

From Equation (8-36a) we have:

$$W_c(p) = [W_6(p) C + 1] \frac{1}{1+C}.$$

Following a series of transformations, the above expression
gives the transfer function for the circuit shown in diagram (c).

$$W_c(p) = \frac{\{R_1 R_2 r_1 C_1 C_2 p^2 + r_1 [R_2 (C_1 + C_2) + }{R_1 R_2 r_1 r_2 C_1 C_2 p^2 + [R_1 r_2 C_2 (R_1 + r_1) + R_2 r_1 R_1 (C_1 +}$$

$$\frac{+ R_1 C_2] p + r_1 + R_1\} R_2}{+ C_2) + R_1 r_1 r_2 (C_1 + C_2)] p + (r_1 + R_1)(r_2 + R_2)}. \qquad (8\text{-}38a)$$

The above transfer function describes a second-order real driver element. By adjusting the resistances R_1 and R_2, the network can be made to yield desired values of the various coefficients, within certain limits.

Diagram (d) in Fig 8-13 likewise represents a second-order driver element. Its transfer function can be conveniently obtained by considering two four-terminal networks of the type described in diagram (a) to be connected in tandem. For high values of the impedance of the second stage, the overall transfer function is approximately equal to the product of the transfer functions expressed by Equation (8-38a) with corresponding values of the parameters of the functions [sic]. This result is discussed in greater detail in the following paragraph.

We now pass to the derivation of the transfer function for the circuit shown in Fig 8-13(e). Prior to the addition of the bridge arm, we have from Equation (8-31o)

$$W_o(p) = \frac{r_1 r_2 C_1 C_2 p^2}{r_1 r_2 C_1 C_2 p^2 + [C_2 r_1 + C_1 (r_1 + r_2)] p + 1}$$

and from Equation (8-8a):

$$Y_{pp} = \frac{r_1 r_2 C_1 C_2 p^2 + [r_1 (C_1 + C_2) + r_1 C_1] p + 1}{r_1 r_1 (C_1 + C_2) p + 1},$$

When the resistance R of the side circuit is taken into account, the relative impedance of the load inserted between the loudspeaker terminals is given by:

$$C = \frac{R}{r_1} \frac{r_1 r_2 C_1 C_2 p^2 + [r_1 (C_1 + C_2) + r_1 C_1] p + 1}{r_1 C_1 + C_2) p + 1},$$

From Equation (8-36a) we have:

$$W_d(p) = r_1 \frac{r_1 C_1 C_2 p^2 + r_1 (C_1 + C_2) p + 1}{r_1 [r_1 (C_1 + C_2) p + 1] + R_1 [r_1 r_1 C_1 C_2 p^2 + \\ + [r_1 (C_1 + C_2) + r_2 C_2]] p} \quad (8\text{-}38\,e)$$

The consumption of power at the input of the circuit is frequently limited by introducing an input-resistance R_0 as shown for a type "a" circuit in Fig. 8-13,f. The effect of the additional resistance on the voltage-division coefficient (8-28) is the same as if it were a resistance in the source of supply E_1. The K_E for a given four-terminal network is computed from its short-circuiting resistances. The K_E-value of above circuits can be computed directly by the circuit-conversion method, or from the equations which have been obtained for similar circuits.

The transfer function for circuit f, will be:

$$W_a(p) = \frac{r_1 (R_1 C_1 p + 1)}{(R_0 + r_1) R_1 C_1 p + R_0 + r_1 + R_1} \quad (8\text{-}38\,f)$$

8-3. FOUR-TERMINAL NETWORKS IN NON-UNIDIRECTIONAL CIRCUITS

1. Cascade Connection of Non-Unidirectional Four-Terminal Networks.

Fig. 8-14,a shows an electrical cascade connection of four-terminal networks with an output terminal of each preceding cascade connected to the input terminal of the next one and a load connected to the extreme cascade.

Electrical or block-diagram cascadings are both alike; the coincidence is misleading because the former contains non-unidirectional units whose transfer function changes with a load connected to the output. All these features can be noted in the complex block-diagram b of the same figure.

Let us start with the extreme cascade to trace the structure of this diagram. Its transfer properties from voltage U_1 to the voltage across the load are fully determined from the block-diagram 8-10,a. This diagram is repeated

In the right side of the chain of blocks of Fig.8-14,b; the
only exception are the upper indexes of the resistances and
admittances which have been changed to have them correspond
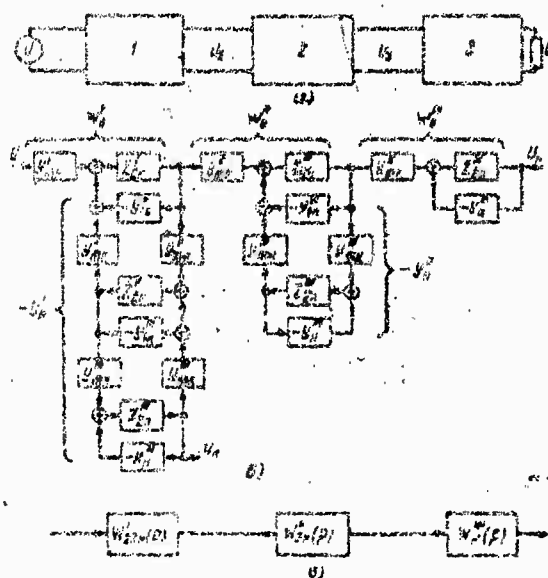with the number of the cascade.

Fig. 8-14. Electrical cascade connection of
non-unidirectional four-terminal networks
and its equivalent block diagrams

The conditions required to obtain a transfer from the
voltage U_2 to voltage U_3 for the second cascade are shown
in the middle section of the chain of blocks b. It repeats
in the direct channel the conditions required to transfer
the extreme cascade, but the indexing of the resistances is
changed to indicate the number of the cell, also the load-
admittance Y'_L of the second cascade has a more complex
representation. For the second cascade, this load is rep-
resented by the entire third cascade. However, its input-
admittance from voltage U_2 to current I_2 is fully determined
between these lines in block-diagram 8-9,c (the effect of
Z_2 is not taken into account). Having this diagram take the
place of Y'_L in the chain of blocks (Fig.8-14,b), changing

the places of Z''_{2k} and Y''_ℓ in the feedback circuit, using
their inverse values in accordance with the rules on struc-
tural analysis (5-25b), and designating all parameters with
the indexes of the third cascade will give us a broad rep-
resentation of the admittance -- Y''_ℓ.

The direct channel of the preceding block-diagrams is
repeated for the third cascade with a new indexing for the
parameters Y'_{mk} and Z'_{2k} and for the admittance Y'_ℓ. It is
decoded with the aid of the parameters of the second and
third cascades, including the terminal load, as shown in
the left part of the chain of blocks b. The right part of
the block-diagram was formed as a corollary, although its
formation is not required because all of its elements are
repeated in the left part of the figure, including the out-
put value of U_ℓ.

In a locked form each cascade receives its operator
transfer function W^i according to equation (8-26), its
block-diagram assumes the form of c, and the overall oper-
ator transfer function of the chain is reduced to one of
the following forms:

$$W(p) = W^i_{2k}(p)\,W^{ii}_{2k}(p)\,W^{iii}_p(p), \qquad (8-34a)$$
$$\mu = \ell$$

where the indexes denote the elements forming the load, or

$$W(p) = W^i_0(p)\,W^{ii}_0(p)\,W^{iii}_0(p)\,\frac{1}{1+C^i_{2k}} \times$$
$$\times \frac{1}{1+C^{ii}_{2k}} \cdot \frac{1}{1+C^{iii}_k} \qquad (8-34b)$$

In many cases it is convenient when using the last
equation to multiply the no-load operator transfer function
followed by taking into account the correcting factors
$$\frac{1}{1+C^i(p)}.$$

Let us consider an example of application of the
derived equations for a chain of L-shaped four-terminal
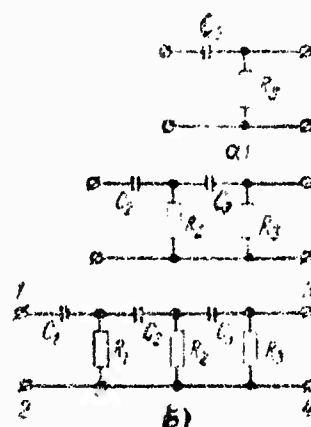networks shown in Fig. 8-15.

615

Fig. 8-15. Cascade of L-shaped four-terminal networks
for computing the operator transfer function by the
method of building up the block diagram

According to diagram a, the transfer function of the
third location, is

$$W'_{36}(p) = \frac{R_3}{R_3 + \frac{1}{C_3 p}} = \frac{T_3 p}{T_3 p + 1} = W_a(p); \quad (8\text{-}40a)$$

the input resistance of the third location, is

$$Z''_{11} = R_3 + \frac{1}{C_3 p} = \frac{T_3 p + 1}{C_3 p};$$

$$\beta = k$$

the no-load transfer function of the second cascade, is

$$W_{26}(p) = \frac{T_2 p}{T_2 p + 1};$$

the output short-circuit resistance of the second cascade,
is:

$$Z_{2k} = \frac{R_2}{T_2 p + 1};$$

the relative load resistance for the second cascade, is

$$C_2 = \frac{Z_k''}{Z_{2k}''} = \frac{(T_3 p + 1)(T_2 p + 1)}{R_2 C_3 p}.$$

Hence, the overall transfer function of the two-cascade circuit b, is

$$W_b(p) = \frac{T_3 p \, T_2 p}{(T_3 p + 1)(T_2 p + 1)} \cdot \frac{C_2}{1 + C_2},$$

or

$$W_b(p) = \frac{T_2 T_3 p^2}{T_2 T_3 p^2 + (T_2 + T_3 + R_2 C_3) p + 1} \qquad (8\text{-}40b)$$

The load for the 1st cascade is found from diagram b. Since the latter can be now regarded as a ladder-type of a two-terminal network, similar to equation (6-8b) we obtain:

$$Z_k' = \frac{1}{C_2 p} + \cfrac{1}{\cfrac{1}{R_2} + \cfrac{1}{\cfrac{1}{C_3 p} + R_2}} =$$

$$= \frac{T_2 T_3 p^2 + (T_2 + T_3 + R_2 C_3) p + 1}{C_2 p [(T_3 + R_2 C_3) p + 1]}.$$

$$N = \xi$$

The relative load resistance of the 1st cascade, is:

$$C_1 = \frac{Z_k'}{Z_{2k}'} = \frac{(T_1 p + 1)[T_2 T_3 p^2 + (T_2 + T_3 + R_2 C_3) p + 1]}{R_1 C_2 p [(T_3 + R_2 C_3) p + 1]}.$$

and the transfer function of the three-cascade circuit c, is

$$W_c(p) = W_b(p) W_{1b}(p) \frac{C_1}{1 + C_1},$$

$$W_c(p) = \frac{T_1 T_2 T_3 p^3}{T_1 T_2 T_3 p^3 + (T_1 T_2 + T_2 T_3 + T_1 T_3 + R_1 C_3 T_2 + R_2 C_3 T_1 + R_1 C_3 T_2) p^2 + (T_1 + T_2 + T_3 + R_2 C_3 + R_1 C_2) p + 1} \qquad (8\text{-}40c)$$

For simple inter-cascade couplings, the above design of a multi-cascade circuit by taking into account the load of each cascade may prove to be more labor-consuming than a complete design of the entire electrical circuit.

For example, if the entire circuit is regarded as a single ladder of a four-terminal network, the final equation (8-40c) can be also obtained from equation (8-31c). However, a cascade-by-cascade computation provides many valuable intermediate results. In addition, an application is found for cascade circuits with a given band of frequencies where a cascade having a certain resistance is followed by a cascade having a considerably larger resistance. In such a case, the correcting terms C/1+C approach unity and the overall transfer function of the circuit becomes equal to the product of the no-load transfer functions:

$$ W(p) = W_{10}(p) W_{20}(p) W_{30}(p) $$

The simplestway to disclose such a condition is by the cascade-by-cascade method.

Circuits, as the ones examined in Fig. 8-15, are in wide use due to their differentiating properties which, in many cases, provide a desirable phase-lead. True, the terms of the denominator become more effective as the frequency increases and gradually reduce the phase to zero, but for a definite frequency band the desirable effect remains intact.

In order to include such filters into the direct channel of the control system, it is necessary to provide a parallel path for the constant component of the signal by adding other links, or by changing somewhat the circuits of the loop by methods analysed in the next paragraph.

2. PARALLEL WORK OF NON-UNIDIRECTIONAL
FOUR-TERMINAL NETWORKS ON A COMMON LOAD

Under examination is the electrical diagram 8-16.s. To change it to a block-diagram it is necessary to specify the voltage across the load:
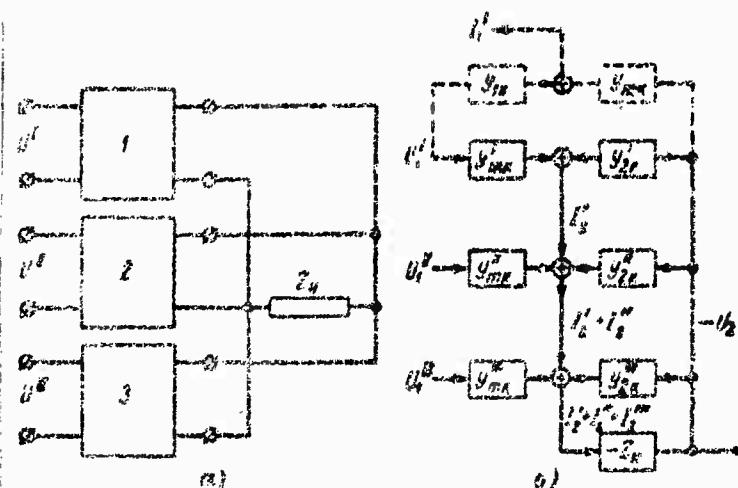
$$ U_2 = I_y Z_y ; $$

Fig. 8-16. Electrical diagram of non-unidirectional
four-terminal networks connected in parallel with
a common load and its equivalent block-diagram

each four-terminal network will then have a dual supply and,
according to the block-diagram 8-9,b, will consume a current
I_1^j and will generate a current I_2^j. So as not to obscure
the diagram, it is reproduced fully in Fig. 8-16,b for the
first four-terminal network and only for the secondary cir-
cuits of the remaining networks. Next, it remains to add up
the secondary currents and obtain the current of the load:

$$I_{_H} = \sum_{j=1}^{3} I_2^j$$

from which we can easily change to the voltage across the
load:

$$U_2 = Z_H \sum_{j=1}^{3} I_2^j$$

$$H = 1$$

The last equation enables us to close the block-
diagram b as shown in the figure.

The diagram shows that the voltage across the load is

equal to the sum of all responses from each of the input voltages acting through its operator transfer function:

$$U_k(p) = \sum_{j=1}^{3} W^j(p) U_j(p).$$

(8-41a)

Each operator transfer function is determined by looking the block-diagram:

$$W^j(p) = \frac{Z_n(p) Y_{mk}^j(p)}{1 + Z_n(p) \sum_{k=1}^{3} Y_{kk}^j(p)}$$

(8-41b)

For input voltages coming from a common source whose internal resistance must be taken into consideration, it is necessary to form circuits for the primary currents in each of the four-terminal networks, as was done in the first network, to add up these currents: $I_1 = \sum_{j=1}^{3} I_j$ and to create in the circuit an additional loop through Z_{B1}, as in Fig. 8-9,b.

The block-diagrams are obtained in a similar manner for the subsequent coupling circuits of the four-terminal networks and for the feedbacks.

8-4. FOUR-TERMINAL NETWORKS IN CIRCUITS CONTAINING AMPLIFIERS

A. D-c Amplifier with Four-Terminal Network in the Circuit.

The method of connecting is shown in Fig. 8-17. Under consideration is a special form of a four-terminal network with inter-connected terminals, i.e. a three-terminal network. Assume that $W_0(p)$ is the no-load transfer function of the three-terminal network. It is loaded in this circuit with the resistance Z_2 and, therefore, the transfer function is to be corrected by multiplying it by the factor:

$$\frac{C}{1+C} = \frac{Z_1 Y_{2k}}{1+Z_1 Y_{2k}}.$$

An inspection of the work performed by the parts of the D-c amplifier shows that the input part ends by forming a current and, therefore, the voltage transfer function must be divided by Z_1 which makes it possible to multiply everything by the transfer function of the second part of the direct-current amplifier Z_0, which provides:

$$W(p) = -W_0(p) \frac{Y_{2k}(p) Z_0(p)}{1+Y_{2k}(p) Z_1(p)}. \qquad (8-49a)$$

The transition in the block-diagram b from voltage to current is obtained by transferring the unit to the C-loop (Fig. 8-10,c).
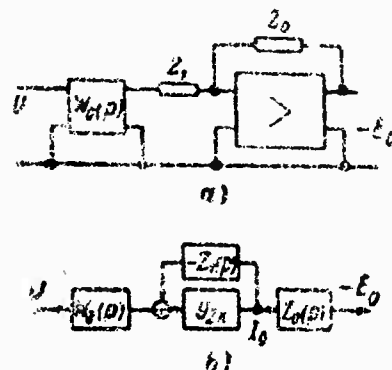

Fig. 8-17. Electrical and block-diagram methods of connecting four-terminal networks to the input circuit of D-c amplifier

If Z_1 is larger than Z_{2k} it will simplify the equation of the transfer function:

$$W(p) = W_e(p) \frac{Z_e(p)}{Z_1(p)}.$$ (8-42b)

2. FOUR-TERMINAL NETWORK IN THE FEEDBACK
CIRCUIT OF D-c AMPLIFIER

The connection of a T-shaped four-terminal network to the feedback of the amplifier is shown in Fig. 8-18,a. As shown in the electrical diagram, the feedback with the existing polarities of the circuits is supplied also with current I_3 from the grounded branch, which increases the transfer ratio. It is more convenient to compute the transfer function by using the block-diagram b, instead of the electrical diagram.
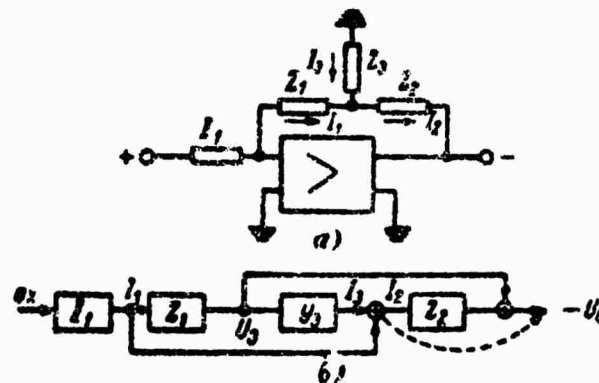

Fig. 8-18. Electrical and block diagrams of
D-c amplifier and T-shaped four-terminal
in the feedback circuit

The current $I_1 = Y_1 U_{1n}$ is first to be determined from the data available in the input circuit. The feedback circuit is here regarded as one that generates a current. The current I_1 creates along the resistance Z_1 a voltage drop U_1 which is equal also to U_3:

$$U_3 = U_1 = Z_1 I_1$$

The additional current is determined from the voltage:

$$I_3 = U_3 Y_3$$

The coefficients of admittance and resistance which enter the above equations are written in the block-diagram as the transfer functions of the unidirectional components located along one chain of blocks.

Next, we add up the currents in unit $I_2 = I_1 + I_3$, which is represented in the block-diagram by a respective coupling line and a summator.

The voltage drop along the resistance Z_2 is computed from equation $U_2 = Z_2 I_2$ and the link Z_2 is introduced into the block-diagram.

Adding up the voltages across the resistances Z_1 or Z_3 and Z_2, we obtain the output voltage $U_{out} = U_3 + U_2$.

Into the block-diagram are introduced a second line and a second summator. The diagram thus obtained has no cross connections and, after the carry over of one summator, it is readily looked to furnish the transfer function of the circuit:

$$W(p) = Y_1 [Z_2 + Z_1 (1 + Y_3 Z_3)]$$

or

$$W(p) = \frac{Z_1 Z_2 + Z_1 Z_3 + Z_2 Z_3}{Z_1 Z_3} . \qquad (8\text{-}43a)$$

This equation, when expressed as an admittance, has the form of:

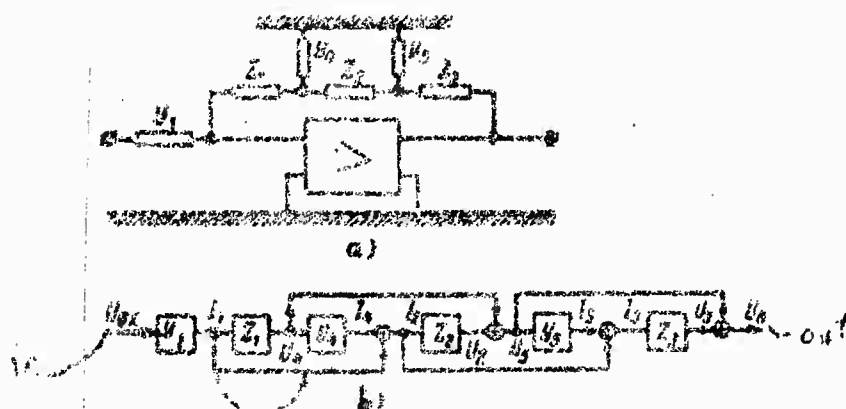$$W(p) = \frac{Y_1 (Y_1 + Y_2 + Y_3)}{Y_1 Y_3} . \qquad (8\text{-}43b)$$

Fig. 8-19. Electrical and block diagrams of
feedback circuit with D-c amplifier and
ladder-type four-terminal network.

Let us analyze still another circuit having a four-
terminal network in the feedback circuit (Fig. 8-19).

This is a complex circuit having, in addition to the
current generated by the input admittance Y_1, two more
currents supplied by admittances Y_4 and Y_5. In this case,
however, the block-diagram has a very simple make up and,
therefore, we will start at once to mark the links of the
block-diagram and the coupling lines:

link Y_1 for generation of current $I_1 = Y_1 U_1$;
link Z_1 for transition to voltage-drop $U_2 = U_4 = I_1 Z_1$;
link Y_4 to obtain additional current $I_4 = Y_4 U_4$;
coupling and summator to form current $I_2 = I_1 + I_4$;
link Z_2 for transition to voltage drop $U_2 = I_2 Z_2$;
coupling and summator to obtain voltage $U_5 = U_4 + U_2$;
link Y_5 to obtain the second additional current
$$I_5 = Y_4 U_5;$$
coupling and summator to obtain current $I_3 = I_2 + I_5$;
link Z_3 to determine the voltage drop $U_3 = Y_3 Z_3$;
coupling and summator to determine the output voltage
$$U_{out} = U_5 + U_3.$$

The carry-over places of the nodal points are marked in the block diagram b so, that the carry-over can take place only through identical nodal points and links. After this it is easy to convolute the diagram and to obtain the following transfer function:

$$W(p) = Y_1 Z_1 Z_2 [Y_1 + Y_3 + Y_4 + Y_5 + Z_2 (Y_1 + Y_4) \times$$
$$\times (Y_3 + Y_5)]. \qquad (8\text{-}44a)$$

Writing the expression for this function in term of admittances, we have:

$$W(p) = \frac{Y_1 [Y_3 (Y_1 + Y_3 + Y_4 + Y_5) + (Y_1 + Y_4)(Y_3 + X_5)]}{Y_1 Y_2 Y_2}.$$
$$(8\text{-}44c)$$

3. DEVELOPING THE PRINCIPLES OF ELECTRONIC MODELLING

The D-c amplifier shown in Fig. 1-9 served together with impedances and capacitances to obtain integrating, scaling, and adding components of an electronic model. The number of integrating amplifiers in the electronic model was determined by the order of the modelled equation, and the number of the other amplifiers -- by the relationship between the terms of the equation.

The introduction into the amplifier circuit of somewhat more complex four-terminal and two-terminal networks synthesized in accordance with a specified operator transfer function can reduce considerably the number of units contained in the model, although it involves the loss of universality for the principle of setting-up an equation from typical elements, and each equation will require a special method of modelling.

We will cite certain examples of expanding the transfer properties of a direct-current amplifier by including in its circuit a slightly more complex two-terminal network.

The RL portion of the direct-current circuit provides an admittance-function and, consequently, also a transfer function for the direct-current amplifier, which corresponds to the following aperiodic component:

$$Y(p) = \frac{1}{R_1 + L_1 p}; \quad W(p) = \frac{\dfrac{R_0}{R_1}}{Tp + 1};$$

the part in the feedback circuit made up of R and C connected in parallel, will give us:

$$Z_0(p) = \frac{1}{\dfrac{1}{R_0} + C_0 p}; \quad W(p) = \frac{\dfrac{R_0}{R_1}}{R_0 C_0 p + 1}.$$

Table 8-2

Transfer functions of D-c amplifiers

Resistance of input circuit \ Feedback resistance	R_0	$\dfrac{1}{C_0 p}$	$L_0 p$
R_1	$\dfrac{R_0}{R_1}$	$\dfrac{1}{R_1 C_0 p}$	$\dfrac{L_0}{R_1} p$
$\dfrac{1}{C_1 p}$	$R_0 C_1 p$	$\dfrac{C_1}{C_0}$	$L_0 C_1 p^2$
$L_1 p$	$\dfrac{R_0}{L_1 p}$	$\dfrac{1}{L_1 C_0 p^2}$	$\dfrac{L_0}{L_1}$

A series-parallel chain of such cells forms the function of resistance (8-7). Placed in the feedback, it provides an identical (at $B_1 = R_1$) transfer function. Based on the theorem of factoring (see Ch. 3), any fraction-rational transfer function with real poles can be formed in this manner in the left half of the plane. A similar effect is produced by series-parallel diagram in the input circuit made up of the same elements. The transfer proper-

ties of D-c amplifiers with elementary two-terminal networks are shown in Table 8-2.

8-5. THE SYNTHESIS OF TWO-TERMINAL NETWORKS

1. Initial Data

The very simple electrical circuits encountered in automatic control systems in form of power-driven circuits for supplying current to control (excitation) windings, control lines, etc., are synthesized by following natural logical reasons evolving primarily from the necessity of providing a connection between the individual parts of the automatic control system. The initial data for such an elementary synthesis consist of: length of line, current for the load, heating conditions, voltage of the line, and the insulation-breakdown voltage.

The problem becomes more complex when dealing with automatic control systems containing correcting circuits designed (together with other components of the control system) to create for the system a common operator transfer function that would enable the automatic control system to operate under specified conditions with a performance of specified quality.

The question of reasonable requirements for the over-all transfer function of automatic control systems is by itself a complex problem and will be considered in the next chapters, but it can be noted, even now, that an automatic control system consisting only of power, amplifying, and connecting components has, as a rule, a transfer function which is entirely different from a needed one and, in the majority of cases, it is required to have correcting components, the transfer functions of which can correct the transfer function of the automatic control system.

Therefore, the initial data required to synthesize electrical circuits must include the transfer function of the circuit, or its frequency characteristics.

2. Synthesis by the Table Method

Among the books on electrical and radio-engineering subjects there is a very rich supply of information hand-books on two-terminal and four-terminal networks (see /3/).

A circuit that is most suitable for the specifications can be selected from a set of tables containing various circuits of two- and four-terminal networks with respective transfer functions and frequency characteristics. Because it would be rather difficult to expect a complete agreement between the table characteristics and the specifications, therefore, the next step for the synthesis is to introduce purposeful changes in the design of the electrical circuit.

The text of the preceding paragraphs of this chapter had for its particular object to illustrate the various methods of translating: the calculation of series connected resistances in two-terminal networks, and the calculation of direct and side loads in four-terminal networks. All these methods received a diagramatic interpretation, which disclosed the appearance of other direct, cascade, and feedback circuits; in translating the frequency characteristics, extensive use can be made of the nomograms cited in Ch. 4 and the calculations become more illustrative than with other methods, with the matrix $[A]$ method, for example.

3. Synthesis of series-parallel circuits of two-terminal networks

Assume for the synthesis the following function of the resistance of a two-terminal network:

$$Z(p) = \frac{b_2 p^2 + b_1 p + b_0}{a_2 p + a_1 p + a_0}. \qquad (8\text{-}45a)$$

Let us resolve the transfer function into partial components by using the methods described in Ch. 3.

For this, since both the numerator and the denominator have the same power, we will first separate the constant component

$$Z(p) = \frac{b_2}{a_2} +$$

$$+ \frac{\left(b_1 - a_1 \frac{b_2}{a_2}\right) p + b_0 - a_0 \frac{b_2}{a_2}}{a_2 p^2 + a_1 p + a_0}; \qquad (8\text{-}45b)$$

secondly, let us determine the roots of the denominator
(the poles of the function)

$$z_1 = -\xi \text{ и } z_2 = -\eta$$

and, thirdly, let us determine the coefficients at the
partial functions, which yields:

$$Z(p) = \frac{b_2}{a_2} + \frac{\left(b_0 - a_0\frac{b_2}{a_2}\right) - \left(b_1 - a_1\frac{b_2}{a_2}\right)\xi}{a_2(\eta - \xi)[p + \xi]} +$$
$$+ \frac{\left(b_0 - a_0\frac{b_2}{a_2}\right) - \left(b_1 - a_1\frac{b_2}{a_2}\right)\eta}{a_2(\xi - \eta)[p + \eta]}. \qquad (8\text{-}45c)$$

The first term of the obtained function is a non-
operator and can be physically obtained in form of an ohmic
resistance $R_1 = b_2/a_2$. The second term can be physically
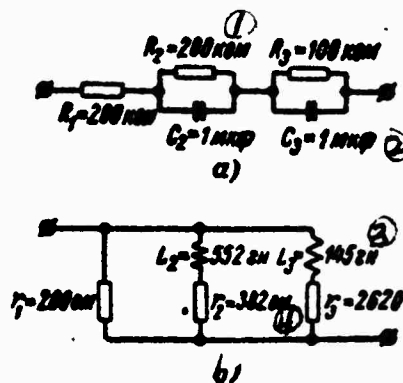realized in form of a parallel RC-circuit.

Fig. 8-20.   Series and parallel structure of
synthesized two-terminal network
key: 1) kilo-ohm; 2) microfarads; 3) henry; 4) ohms

In fact, the resistance of such a cell, is:

$$Z_2(p) = \cfrac{1}{C_2 p + \cfrac{1}{R_2}} = \cfrac{\cfrac{1}{C_2}}{p + \cfrac{1}{R_2 C_2}}.$$

Equating it with the second partial function, we get the values of the capacitance and of the resistance:

$$C_2 = \cfrac{a_2(\xi - \eta)}{\left(b_1 - a_1\dfrac{b_2}{a_2}\right)\xi - \left(b_0 + a_0\dfrac{b_2}{a_2}\right)};$$

$$R_2 = \cfrac{b_0 - a_0\dfrac{b_2}{a_2} - \left(b_1 - a_1\dfrac{b_2}{a_2}\right)\xi}{\xi a_2(\eta - \xi)}.$$

Also, an identical cell is formed in accordance with the third partial function:

$$C_3 = \cfrac{a_2(\xi - \eta)}{b_0 - a_0\dfrac{b_2}{a_2} - \left(b_1 - a_1\dfrac{b_2}{a_2}\right)\eta};$$

$$R_3 = \cfrac{b_0 - a_0\dfrac{b_2}{a_2} - \left(b_1 - a_1\dfrac{b_2}{a_2}\right)\eta}{\eta a_2(\xi - \eta)}.$$

Fig. 3-20,a shows a circuit of a two-terminal network and the capacitances and resistances for a resistance-function (3-45a)with the following values of the coefficients:

$$Z(p) = \frac{2\cdot 10^5 (p^2 + 25p + 125)}{p^2 + 15p + 50} =$$

$$= \frac{2\cdot 10^5 (p + 6,9)(p + 18,1)}{(p + 5)(p + 10)} =$$

$$= 2\cdot 10^5 \left(1 + \frac{5}{p + 5} + \frac{5}{p + 10}\right)$$

Let us note thal all zeros and poles of the realized resistance-function are at the left and follow one another; also, that the root of the denominator is the one located nearest to the imaginary axis.

In fact, let us write all zeros ($\emptyset$) and poles (P) in the order with which the module increases:

$$P_1 = -5; \quad O_1 = -6.9; \quad P_2 = -10; \quad O_2 = -18.1.$$

The follow-one-another conditions obtained in the special example are general for all circuits of this class and are known as the conditions for physical realization.

Let us now have a given admittance-function to be realized for a two-terminal network. Let us write it in the same form as in (8-45a) but use new coefficients (α and β) instead of the old a and b.

$$Y(p) = \frac{\beta_2 p^2 + \beta_1 p + \beta_0}{\alpha_2 p^2 + \alpha_1 p + \alpha_0} . \qquad (8\text{-}46)$$

Here we can again perform a resolution into partial functions which would be fully identical with the one in (8-45b). The result, however, should be now treated as a scheme for admittances. Therefore, the first term of the resolution without operators is assumed to be equal to the ohmic admittance:

$$\frac{\beta_2}{\alpha_2} = Y_1 = \frac{1}{R_1} = \frac{1}{\frac{\alpha_2}{\beta_2}} .$$

The second and third partial admittances in simple two-terminal networks can be realized only in form of RL-circuits, because we have in this case:

$$Y_2(p) = \frac{1}{L_2 p + R_2} = \frac{\frac{1}{L_2}}{p + \frac{R_2}{L_2}} .$$

Equating the coefficients in the partial functions and in the admittance of the circuit we will obtain the values of the parameters of the electrical diagram b:

$$L_4 = \frac{a_2(\xi - \eta)}{\left(\beta_1 - a_1\frac{\beta_2}{a_2}\right)\xi - \left(\beta_3 + a_0\frac{\beta_1}{a_2}\right)};$$

$$R_5 = \frac{\xi a_2(\eta - \xi)}{\beta_0 - a_0\frac{\beta_2}{a_2} - \left(\beta_1 - a_1\frac{\beta_2}{a_2}\right)\xi};$$

$$L_2 = \frac{a_2(\xi - \eta)}{-\left(\beta_1 - a_1\frac{\beta_2}{a_2}\right)\eta + \beta_0 + a_0\frac{\beta_1}{a_2}};$$

$$R_3 = \frac{\eta a_2(\xi - \eta)}{\beta_0 - a_0\frac{\beta_2}{a_2} - \left(\beta_1 - a_1\frac{\beta_2}{a_2}\right)\eta}.$$

In this diagram are written the values of the imped-
ances and inductances for the following values of the coef-
ficients of the admittance-function:

$$Y(p) = \frac{p^2 + 30p + 200}{200(p^2 + 25p + 125)} =$$

$$= \frac{(p + 10)(p + 20)}{200(p + 6,9)(p + 18,1)} =$$

$$= \frac{1}{200}\left(1 + \frac{3,62}{p + 6,9} + \frac{1,37}{p + 18,1}\right).$$

Here we have again: all roots at the left and a root
with a minimum module as a pole. The poles and the zeros
follow one another: P_1, O_1, P_2, O_2, therefore, the admit-
tance-function is physically realizable.

It should be noted that the case under consideration
is a two-terminal network for which $Z(p) = 1/Y(p)$ and the
zeros and poles of any and, consequently, of both functions
follow one another, such network can be realized only in
form of one of the diagrams of Fig. 8-20, i.e., only by one
function of admittance or resistance which has a pole by
virtue of the root having a minimum module. Only under this

condition can the coefficient of p in the numerator of the operator function $(b_1/a_2 = -|0_1+0_2|)$ and the free term in the numerator $(b_0/a_2 = 0_1 0_2)$ be larger than the identical coefficients of the denominator; also, when the numerator is divided by the denominator in changing to a proper fraction, only under the above condition will the remainder be with a plus sign and, therefore, can be realized in form of an impedance or admittance.

The numerical example of Fig.8-20 illustrates the the rule that the impedance-function realized in diagram a will, upon inversion, result in an admittance-function that is unrealizable in diagram b, because the minimum module contains zero, although the inversion did not disrupt the sequence of the roots. To illustrate an example where a realization takes place, a new admittance-function was used with zeros $0_1 = -10$ and $0_2 = -20$, where the minimum module has again a pole $P_1 = -6.9$.

Therefore, from the operator point of view, diagrams a and b cannot be equivalent. An equivalency, however, can be obtained for a certain frequency.

For example, for a constant component $(p = 0)$ the condition required for equivalency is:

$$R_1 + R_2 + R_3 = \cfrac{1}{\cfrac{1}{r_1} + \cfrac{1}{r_2} + \cfrac{1}{r_3}} = \frac{r_1 r_2 r_3}{r_1 r_2 + r_1 r_3 + r_2 r_3}.$$

For high frequencies $(p \to \infty)$ the condition for equivalency is $R_1 = r_1$.

It is readily noted that due to the rapid increase in capacitance it is difficult to make diagram a become low-ohmic by retaining the time-constant of the circuit, and to have diagram b become high-ohmic because of the excessive increase in inductance.

4. Synthesis of Two-Terminal Ladder Networks

Let us use again a specified transfer function of resistance in form of function (8-45a). After the proper fraction is separated, it can be written in form of a sum

of an ohmic and an operator resistance (8-45b):

$$Z(p) = R_1 + Z_2(p). \qquad (8\text{-}47a)$$

Using the identity

$$Z_2(p) = \frac{1}{Y_2(p)} \qquad (8\text{-}47b)$$

and transforming the operator function of admittance:

$$Y_2(p) = \frac{a_2 p^2 + a_1 p + a_0}{\left(b_1 - a_1 \frac{b_2}{a_2}\right) p + \left(b_0 - a_0 \frac{b_2}{a_2}\right)} =$$

$$= \frac{a_2 p^2 + a_1 p + a_0}{C_1 p + C_0} = \frac{a_2}{C_1} p + \frac{\left(a_1 - C_0 \frac{a_2}{a_1}\right) p + a_2}{C_1 p + C_0}. \qquad (8\text{-}47c)$$

which, after the numerator is divided by the denominator
and after the separation of the first remainder, resolves
into a sum of two admittances:

$$Y_2'(p) + Y_3(p) \qquad (8\text{-}47d)$$

one as an elementary admittance in form of capacitance Cp,
the other as the complex admittance $Y_3(p)$.

Using again the identity

$$Y_3(p) = \frac{1}{Z_3(p)} \qquad (8\text{-}47e)$$

and transforming as before the function of resistance:

$$Z_3(p) = \frac{C_1 p + C_0}{\left(a_1 - C_0 \frac{a_2}{a_1}\right) p + a_0} = \frac{C_1 p + C_0}{d_1 p + d_0} =$$

$$= \frac{C_1}{d_1} + \frac{C_0 - a_0 \frac{C_1}{d_1}}{d_1 p + a_0}. \qquad (8\text{-}47f)$$

The last function resolves again into two parts

$$Z'_3 + Z_4 \qquad (8\text{-}47_g)$$

one of which is a strictly ohmic part $R = C_1/d_1$, and the other is the operator Z_4. Finally, we proceed from the function of resistance to the function of admittance:

$$Y_4(p) = \frac{1}{Z_4(p)} = \frac{d_1}{C_0 - a_0 \frac{C_1}{d_1}} p + \frac{a_0}{C_0 - a_0 \frac{C_1}{d_1}}. \qquad (8\text{-}47_h)$$

Combining all equations (8-47) into one, we obtain the equation of the ladder circuit:

$$Z(p) = \frac{b_2 p^2 + b_1 p + b_0}{a_2 p^2 + a_1 p + a_0} = R_1 + \cfrac{1}{C_2 p + \cfrac{1}{R_3 + \cfrac{1}{C_4 p + \cfrac{1}{R_5}}}},$$

$$(8\text{-}48a)$$

where

$$R_1 = \frac{b_2}{a_2}; \quad C_2 = \frac{a_2}{b_1 - a_1 \frac{b_2}{a_2}};$$

$$R_3 = \frac{\left(b_1 - a_1 \frac{b_2}{a_2}\right)^2}{a_1\left(b_1 - a_1 \frac{b_2}{a_2}\right) + a_2\left(b_0 - a_0 \frac{b_2}{a_2}\right)};$$

$$C_4 = \frac{a_1}{C_0 - a_0 \frac{C_1}{d_1}}; \quad R_5 = \frac{C_0 - a_0 \frac{C_1}{d_1}}{a_0}$$

The electrical diagram of Fig. 8-21 is based on the equation derived for the resistance. The numerical values of the ohmic resistances and capacitances are given for the transfer function which served for the drawing of diagram 8-20,a. These numerical values can be best computed by direct division:

$$
\begin{array}{c|c}
p^2 + 25p + 125 & p^2 + 15p + 50 \\
\underline{p^2 + 15p + 50} & 1 \text{ (resistance } R_1) \\
 10p 75 &
\end{array}
$$

$$
\begin{array}{c|c}
p^2 + 15p + 50 & 10p + 75 \\
\underline{p^2 + 7.5p} & \overline{0.1p} \\
 7.5p + 50 & \text{(admittance } C_2p)
\end{array}
$$

$$
\begin{array}{c|c}
10p + 75 & 7.5p + 50 \\
\underline{10p + 66.67} & \overline{1.33} \\
 8.33 & \text{(resistance } R_3)
\end{array}
$$

$$
\begin{array}{c|c}
7.5p + 50 & 8.33 \\
& \overline{0.9p + 6} \\
& \text{(admittance } C_4p + 1/R_5)
\end{array}
$$

Let us multiply all resistances by the common factor $2 \cdot 10^5$ and divide the admittances by the same coefficient:

$R_1 =$ 200 kilo-ohms ; $C_2 =$ 0.5 microfarads

$R_3 =$ 266 "   " $C_4 =$ 4.5   "

$R_5 =$ 33.3 "   "

Consequently, the series-parallel circuit of RC cells has an equivalent in form of a ladder circuit of the same elements. The transition from one circuit to the other is effected by computations with the aid of the function of resistance $Z(p)$.

— 656 —

If it is an admittance-function of a type (8-46) two-terminal network, the mathematical transformations required to obtain a result in form of a ladder fraction remain the same, except that the first separated term β_2/α_2 will be an ohmic resistance and the second separated term γ_2/C_1 will be an operator resistance realized by an ideal inductance. The next separated terms will be: an ohmic resistance, an inductance, etc.

Taking these changes into consideration, we obtain the following equation of the transformations:

$$Y(p) = \frac{\beta_2 p^2 + \beta_1 p + \beta_0}{\alpha_2 p^2 + \alpha_1 p + \alpha_0} = \frac{1}{R_1} + \cfrac{1}{L_2 p + \cfrac{1}{\cfrac{1}{R_3} + \cfrac{1}{L_4 p + R_5}}}.$$

(8-48b)

where

$$R_1 = \frac{\alpha_2}{\beta_2}; \quad L_2 = \frac{\alpha_2}{\beta_1 - \alpha_1 \frac{\beta_2}{\alpha_2}};$$

$$R_3 = \frac{\alpha_1 \left(\beta_1 - \alpha_1 \frac{\beta_2}{\alpha_2}\right) + \alpha_2 \left(\beta_0 - \alpha_0 \frac{\beta_2}{\alpha_2}\right)}{\left(\beta_1 - \alpha_1 \frac{\beta_2}{\alpha_2}\right)^2};$$

$$L_4 = \frac{d_1}{C_0 - \alpha_0 \frac{C_1}{d_1}}; \quad R_5 = \frac{\alpha_0}{C_0 - \alpha_0 \frac{C_1}{d_1}}.$$

Fig. 8-21. Two-terminal networks synthesized
into a ladder structure

key: 1) kilo-ohms, 2) microfarads.

The inclusion of R and L in accordance with the ob-
tained equation is shown in Fig. 8-21,b. This diagram also
contains the numerical values of the parameters for the
function of admittance which was used for drawing the 8-20b
diagram. Again, direct division is more convenient for the
computation of the parameters:

$$\frac{\dfrac{p^2 + 30p + 200}{p^2 + 25p + 125}}{5p + 75} \quad \Bigg| \quad \frac{p^2 + 25p + 125}{1 \ (\text{admittance } 1/R_1)} \ ;$$

$$\frac{\dfrac{p^2 + 25p + 125}{p^2 + 15p}}{10p + 125} \quad \Bigg| \quad \frac{5p + 75}{0.2p \ (\text{resistance } L_2 p)} \ ;$$

$$\frac{\dfrac{5p + 75}{5p + 62.5}}{12.5} \quad \Bigg| \quad \frac{10p + 125}{0.5 \ (\text{admittance } 1/R_3)} \ ;$$

$$10p + 125 \quad \Bigg| \quad \frac{12.5}{0.8p + 10 \ (\text{resistance } L_4 p + R_5)}.$$

The common coefficient 1/200 in the equation for the admittance is taken into account by increasing all resistances 200 times, which yields:

$$R_1 = 200 \text{ ohms}; \quad L_2 = 4 \text{ henrys}$$

$$R_3 = 400 \text{ ohms}; \quad L_4 = 160 \text{ henrys}$$

$$R_5 = 2,000 \text{ ohms}.$$

Ladder circuits can reflect only those functions of resistance or admittance which comply with the analysed conditions required for physical realization.

5. Synthesis of Two-Sided Ladder Structure of Two-Terminal Networks

Let the function of admittance of a two-terminal network be again given as:

$$Y(p) = \frac{a_2 p^2 + a_1 p + a_0}{b_2 p^2 + b_1 p + b_0}.$$

The result of dividing the polynoms (located from left to right in order of diminishing powers) produced a ladder structure that can be called a "left ladder structure".

If the polynoms are now located in reverse order, a division is still possible, one stage of which with a separation of a remainder is shown below:

$$Y(p) = \frac{a_0 + a_1 p + a_2 p^2}{b_0 + b_1 p + b_2 p^2} = \frac{a_0}{b_0} +$$

$$+ \frac{\left(a_1 - \frac{a_0}{b_0} b_1\right) p + \left(a_2 - \frac{a_0}{b_0} b_2\right) p^2}{b_0 + b_1 p + b_2 p^2} =$$

$$= \frac{a_0}{b_0} + \frac{1}{\dfrac{b_0 + b_1 p + b_2 p^2}{C_1 p + C_2 p^2}} = Y_1 + \frac{1}{Z_2(p)}.$$

The conversion of the last term in a form expressed through a resistance makes it again possible to perform a division in the range of resistances and separate the remainder:

$$Y(p) = \frac{a_0}{b_0} + \cfrac{1}{\cfrac{b_0}{C_1 p} + \cfrac{\left(b_1 - \frac{b_0}{C_1}C_2\right)p + b_2 p^2}{C_1 p + C_2 p^2}}$$

$$= Y_1(p) + \frac{1}{Z_2(p) + Z_3(p)}.$$

The result of these operations and its continuation produce a right ladder structure. However, if the further operations are discontinued, the last remainder $Z_3(p)$ is reduced by p, the polynoms are again located from left to right, and if the division is completed as required by a left structure

$$Z_3(p) = \frac{b_2 p + b_1}{C_2 p + C_1} = \frac{b_2}{C_2} + \frac{d_1'}{C_2 p + C_1}.$$

where

$$b_1' = b_1 - \frac{b_0}{C_1}C_2; \quad d_1 = b_1' - \frac{b_2}{C_2}C_1.$$

all these will result in a two-sided ladder structure. At this, the term $Z_2 = b_0/C_1 p$ in the range of resistances will be reflected by the capacitance connected in series with the remaining circuit Z_3. Introducing the designations for the capacitances and the ohmic resistances we will obtain a complete equation for the new structure:

$$Y(p) = \frac{1}{b} + \cfrac{1}{C_1 p + K_1 + \cfrac{1}{C_2 p + \frac{1}{R_0}}}, \qquad (8\text{-}40a)$$

where

$$R_1 = \frac{b_0}{a_0}; \quad C_2 = \frac{C_1}{b_0}; \quad R_3 = \frac{b_2}{C_2}; \quad C_4 = \frac{C_2}{d_1}; \quad R_5 = \frac{d_1}{C_1}.$$

The make-up of the two-sided ladder-diagram 8-21,c is based on equation (8-49a). The numerical values of the capacitances and resistances correspond to those in diagram "a" and were obtained by direct division:

<div align="center">

right structure

$$\frac{\dfrac{50 + 15p + p^2}{50 + 10p + 0,4p^2}}{5p + 0,6p^2} \quad \left| \quad \frac{125 + 25p + p^2}{0,4\left(\text{admittance } \frac{1}{R_1}\right)}; \right.$$

$$\frac{\dfrac{125 + 25p + p^2}{125 + 15p}}{10p + p^2} \quad \left| \quad \frac{5p + 0,6p^2}{\dfrac{25}{p}\left(\text{resistance } \dfrac{1}{C_2 p}\right)}; \right.$$

left structure

$$\frac{\dfrac{p + 10}{p + \dfrac{50}{6}}}{\dfrac{10}{6}} \quad \left| \quad \frac{0,6p + 5}{\dfrac{10}{6}\ (\text{resistance } R_2)}; \right.$$

$$\frac{0,6p + 5}{\dfrac{10}{6}} = 0,36p + 3 \quad \left(\text{admittance } Cp + \frac{1}{R_3}\right).$$

</div>

As the division was completed, all resistances were multiplied and all capacitances were divided by $2 \cdot 10^5$ so as to comply with the specified conditions.

The introduction of another stage of right division can change the form of equation (8-49a), in which case it will assume the following form:

$$Y_1(p) = \frac{1}{R_1} + \cfrac{1}{C_2 p + \cfrac{1}{\cfrac{1}{R_2} + \cfrac{1}{\cfrac{1}{C_4 p} + R_3}}} \,, \quad (8.49b)$$

where R_1 and C_2 are determined as in the preceding case, and:

$$R_3 = \cfrac{b_1 - \dfrac{b_0 C_2}{C_1}}{C_1}; \quad C_4 = \cfrac{C_1 - \cfrac{C_1 b_2}{b_1 - \dfrac{b_0}{C_1} C_2}}{b_1 - \dfrac{b_0}{C_1} C_2};$$

$$R_5 = \cfrac{b_2}{C_2 - \cfrac{C_1 b_2}{b_1 - \dfrac{b_0}{C_1} C_2}}.$$

This equation corresponds to diagram c. The numerical computation for it changes beginning with the third stage and results in new parameters:

$$\begin{aligned}
&\frac{5 + 0.6p}{5 + 0.5p} \left| \frac{10 + p}{0.5 \left(\text{admittance } \dfrac{1}{R_1} \right)} \right. ; \\[2mm]
&\frac{10 + p}{0.1p} \left| \frac{0.1p}{\dfrac{100}{p} + 10} \right. \\[2mm]
&\hspace{3cm} \left(\text{resistance } \dfrac{1}{C_4 p} + R_3 \right).
\end{aligned}$$

which were written in the diagram after they were multiplied by $(2 \cdot 10)$.

It should be noted that diagram 8-20,a and diagrams "a", "o", and "d" in Fig. 8-21 are fully equivalent and have a common function of resistance

$$Z(p) = \frac{b_2 p^2 + b_1 p + b_0}{a_2 p^2 + a_1 p + a_0}.$$

or, for the analysed numerical example

$$Z(p) = \frac{2 \cdot 10^5 (p^2 + 25p + 125)}{p^2 + 15p + 50} =$$
$$= \frac{2 \cdot 10^5 (p + 6.9)(p + 18.1)}{(p + 5)(p + 10)}.$$

At this, while the realization of "left" ladder-structures was possible for functions of resistance or for functions of admittance with a pole of a minimum module, the realization of "right" ladder-structures is also possible for functions having a zero of a minimum module, provided the rule on the alternation of zeros and poles is retained.

Since the admittance in the same two-terminal network is equal the inverse of resistance, therefore, the pole of a minimum module that was present in the function of resistance corresponds to the minimum zero in the function of admittance and the realization of equivalent structures is possible for both equations: a "left" structure for resistance and a "right" ladder-structure for admittance. This can be easily discovered from the performed numerical computation.

The transfer function that was used in above examples was a function of the second order; the method of synthesis however, is valid also for functions of higher orders.

8-6. SYNTHESIS OF FOUR-TERMINAL NETWORKS

1. Synthesis of Unloaded Four-Terminal Networks

Only the simple four-terminal networks used in cir-
cuits of voltage dividers will be covered in this analysis.

Four-terminal networks shaped as an inverted letter L.
Let us realize a transfer function in form of:

$$W_e(p) = \frac{U(p)}{V(p)} = \frac{b_2 p^2 + b_1 p + b_0}{a_2 p^2 + a_1 p + a_0} = \frac{b_2 (p + \delta)(p + \eta)}{a_2 (p + \sigma)(p + \gamma)}$$

(8-30a)

It is written in several forms, including one in form
of a product making it necessary to determine in advance
the zeros $-\delta$, $-\eta$ and the poles $-\sigma$, $-\gamma$ of the transfer
function.

The L-shaped diagram in Fig. 8-11,b has a transfer
function of (8-30) which will be written again and used for
further transformations:

$$W(p) = \frac{Z_1(p)}{Z_1(p) + Z_2(p)}.$$

The problem consists of finding such resistance-
functions of two-terminal networks Z_1 and $Z_1 - Z_2$ whose ratio
would equal the ratio of the numerator and denominator of
the given transfer function. The methods of forming L-shaped
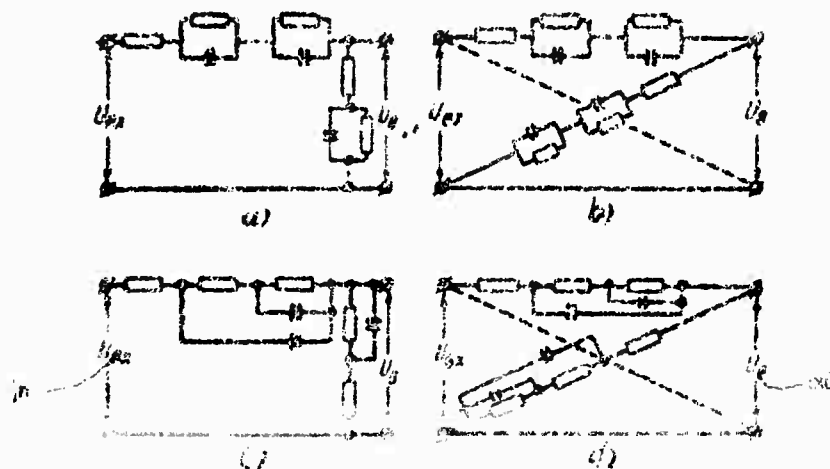diagrams from simple cells are shown in Fig. 8-22.

Fig. 8-22.   Synthesized L-shaped and bridge
four-terminal networks

As it follows from this formulation, it is not advisable to equate directly the numerators and denominators of the voltage-divider equation and of the transfer function, because it leads to relationships than cannot be realized by passive diagrams.

The ratio between the numerator and denominator of the transfer function will not be changed by dividing both by the same operator function $Q(p)$, which we will call the basic function:

$$W(p) = \frac{U(p)}{V(p)} = \frac{\dfrac{U(p)}{Q(p)}}{\dfrac{V(p)}{Q(p)}} . \qquad (8\text{-}50b)$$

Equating the new numerator and denominator with the cited resistances, we obtain:

$$\left.\begin{array}{l} Z_1(p) + Z_2(p) = \dfrac{V(p)}{Q(p)}; \\[2ex] Z_1(p) = \dfrac{U(p)}{Q(p)}; \quad Z_2(p) = \dfrac{V(p) - U(p)}{Q(p)} . \end{array}\right\} \qquad (8\text{-}50c)$$

The basic function is given in form of a polynom of the same order as the transfer function, so the obtained equations may be written in the expanded form:

$$Z_1(p) = \frac{b_2 p^2 + b_1 p + b_0}{q_2 p^2 + q_1 p + q_0} ,$$

$$Z_2(p) = \frac{(a_2 - b_2) p^2 + (a_1 - b_1) p + a_0 - b_0}{a_2 p^2 + q_1 p + q_0}$$

The roots of the basic function should alternate with both the roots $U(p)$ and the roots $U(p) - V(p)$. This condition reduces the number of conditions required for the physical realization of the two-terminal networks.

The two-terminal networks are computed from the obtained equations and are included as in diagrams a and b of Fig. 8-22.

Bridge-shaped four-terminal networks. The bridge diagram of Fig. 8-11,g has, if the arms are symmetrical, a transfer function (8-32b) of $W(p) = Z_2 - Z_1/Z_2 + Z_1$, which is obtained as the difference between the transfer functions of two voltage dividers.

Equating the numerator and denominator of equation (8-50b) with the difference and the sum of the resistances:

$$Z_2 - Z_1 = \frac{U}{Q}; \quad Z_2 + Z_1 = \frac{V}{Q}.$$

we obtain:

$$Z_1(p) = \frac{V(p) - U(p)}{2Q(p)}; \quad Z_2(p) = \frac{V(p) + U(p)}{2Q(p)};$$

or, for the transfer function of the second order:

$$Z_1(p) = \frac{(a_2 - b_2) p^2 + (a_1 - b_1) p + a_0 - b_0}{2(q_2 p^2 + q_1 p + q_0)}$$

$$Z_2(p) = \frac{(a_2 + b_2) p^2 + (a_1 + b_1) p + (a_0 + b_0)}{2(q_2 p^2 + q_1 p + q_0)}$$

The basic function in this diagram should have roots which alternate with both the roots $V - U$ and with $V + U$. The problem is again reduced to the realization of two-terminal networks and is to be solved by the methods which were described above; depending on the method, the diagrams of the four-terminal networks assume the form of diagrams o and 3 of Fig. 8-22. The broken lines in the figure indicate the symmetrical branches of the bridge.

If the bridge or L-shaped diagram cannot be used for the realization of the transfer function $W = U/V$, it is necessary to check whether the same function can be realized with an altered gain factor

$$KW(p) = \frac{KU(p)}{V(p)}.$$

At this, the differences encountered in equations in form of V - U are reduced to a form of V - KU and can be always made to be positive. A change in the gain factor of four-terminal network is compensated by other amplifying components of the automatic control system.

2. Synthesis of Loaded Four-Terminal Networks

If we follow Gillemin [5], we assume for the primary function of a loaded four-terminal network a load with a resistance equal to one ohm (8-24), i.e. $Z_\rho = R_\rho = 1$ ohm; in this case the equation will assume the form of:

$$W_1(p) = \frac{Y_{mk}}{1 + Y_{2k}} . \qquad (8\text{-}51a)$$

To reduce the given transfer function (8-50a) to a form comparable to expressions of (8-51a), the polynom of the denominator is divided by breaking up the coefficients into two parts:

$$V(p) = a_2 p^2 + a_1 p + a_0 = (a_2 + q_2) p^2 + (a_1 + q_1) p + $$
$$+ a_0 + q_0 = (a_2 p^2 + a_1 p + a_0) + (q_2 p^2 + q_1 p + q_0) = $$
$$= V_1(p) + Q(p).$$

The transfer function can be then reduced to form:

$$W(p) = \frac{U(p)}{V_1(p) + Q(p)} = \frac{\dfrac{U(p)}{Q(p)}}{1 + \dfrac{V_1(p)}{Q(p)}} . \qquad (8\text{-}51b)$$

Equating the numerators and denominators of equations (8-51a) and (8-51b), we obtain

$$\left.\begin{aligned}
Y_{2k} &= \frac{V_1(p)}{Q(p)} = \frac{a_2 p^2 + a_1 p + a_0}{q_2 p^2 + q_1 p + q_0} ; \\
Y_{mk} &= \frac{U(p)}{Q(p)} = \frac{b_0}{q_2 p^2 + q_1 p + q_0} + \\
&\quad + \frac{b_1 p}{q_2 p^2 + q_1 p + q_0} + \frac{b_2 p^2}{q_2 p^2 + q_1 p + q_0} .
\end{aligned}\right\} \qquad (8\text{-}51c)$$

Based on the obtained equation, the function of the secondary, short-circuit, admittance is the first to be realized, mostly in form of a ladder structure. For this, let us proceed from admittance to resistance by using the equation (8-48a):

$$Z_{2k}(p) =$$

$$= \frac{q_2 p^2 + q_1 p + q_0}{c_2 p^2 + c_1 p + c_0} = R_1 + \cfrac{1}{C_2 p + \cfrac{1}{R_3 + \cfrac{1}{C_4 p + \frac{1}{R_5}}}}.$$

$$(8-51b)$$

The diagram corresponding to the obtained equation was already cited in Fig. 8-21; however, since the diagram will be used in this example for two conditions, therefore, it will be drawn in a form more convenient for the subsequent transformations, as shown in Fig. 8-23,a.
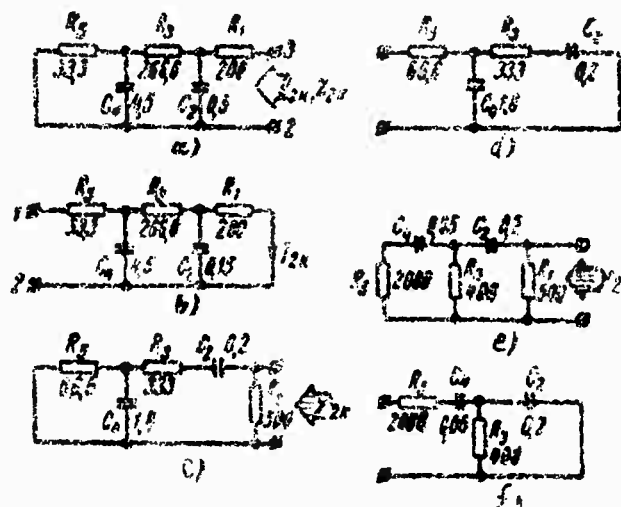
Fig. 8-23. Intermediate diagrams to synthesize loaded ladder-type of four-terminal networks

The drawn diagram can be converted into a four-terminal network by opening any place and by designating the new terminals as terminals 1 and 2. For the consequent operations it is convenient to have it open at the left, in which case, the transfer function of the mutual (short-circuit) admittance of the circuit $Y_{mk}(p)$ will have, from U_3 to I_{2k}, a numerator in form of a constant number and a denominator which will be the same as in the function of the secondary (short-circuit) admittance Y_{2k}, because in the same circuit the denominator for any transfer function is equal to the common determinant of the system.

Consequently, we obtain a function of the mutual admittance of the short-circuiting

$$Y'_{mk}(p) = \frac{b'_0}{q_2 p^2 + q_1 p + q_0} = \frac{b'_0}{Q(p)} \ .$$

Paying attention to equation (8-51c) we note that $Y_{mk}(p)$ contains a term identical with the one which was here obtained. It is suggested that the subsequent terms should be formed as two-sided ladder diagrams having the same secondary short-circuit admittance $Y_{mk}(p)$.

The two-sided two-terminal ladder networks which realize an admittance-function of the second order are shown in diagrams c and d of fig. 8-21. They are all equivalent to diagram 8-23,a when R and C are determined from the coefficients of the operator functions, as required by the described equations.

The same two-terminal networks serve to form the Y_{2k} of the synthesized four-terminal network and are shown in fig. 8-23,c and d.

Let us express the admittance-function Y_{2k} for these diagrams in term of the following electrical parameters:

$$Y_{2ka} = \frac{C_2 C_4 R_5 R_2 p^2 + [C_2 (R_2 + R_5) + C_4 R_5] p + 1}{C_2 C_4 R_1 R_5 R_2 p^2 + \{R_1 [C_2 (R_2 + R_5) + C_4 R_5] + C_4 R_5 R_5\} p + R_1 + R_2 + R_5}$$

$$Y_{2ka} =$$

$$= \frac{C_2 C_4 R_5 (R_1 + R_2) p^2 + [C_2 (R_1 + R_2 + R_5) + C_4 R_5] + 1}{R_1 \{C_2 C_4 R_5 R_5 p^2 + [C_2 (R_2 + R_5) + C_4 R_5] p + 1\}};$$

$$Y_{2ka} = \frac{C_2 C_4 (R_2 R_1 + R_5 R_1 + R_1 R_5) p^2 + (R_1 C_2 + R_5 C_4 + R_5 C_4 + R_5 C_4) p + 1}{R_1 \{R_1 R_5 C_2 C_4 p^2 + [C_2 R_4 + C_4 (R_2 + R_5)] p + 1\}}$$

Replacing the electrical parameters with their expression in term of the coefficients of the function of admittance by using for each diagram its own equation will, naturally, result in the following identities:

$$Y_{2k}(p) = Y_{2ka} = Y_{2ka} = Y_{2ka} = \frac{a_1 p^2 + a_1 p + a_2}{q_1 p^2 + q_1 p + q_0} \quad (8\text{-}52)$$

We will now try to find out what can be expected from the same diagrams in the matter of forming a mutual short-circuit admittance. This matter was already analysed for diagram 8-2),a by changing to diagram b; in the same manner let us proceed from diagram c to diagram d, and from diagram e to diagram f.

Let us express the sought functions in terms of the electrical parameters of the circuit. Since the diagrams a, c, and e are of the ladder type, it will be expedient to make use of the already derived equations (8-31b) and (8-31a) for two and three cells. For the transition from transfer function of the voltage to the transfer function of the admittance with the designations shown in Fig. 8-11,f, it is necessary to divide the function W(p) by the output resistance of the last L-shaped cell, i.e.,
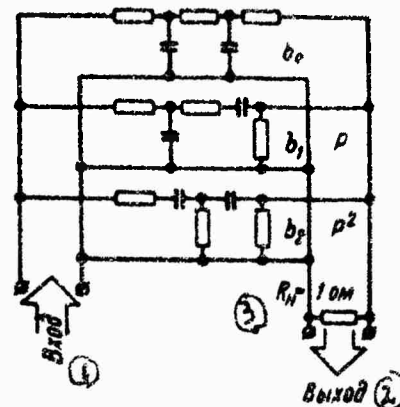
$$Y_{12}(p) = \frac{W(p)}{Z_1}$$

Fig. 8-24. Synthesized ladder-type loaded
four-terminal network
key: 1) input; 2) output; 3) load resistance
in ohms.

In view of the specific features of the short-circuit
diagrams of Fig. 8-23 containing no output resistance, the
value of Z_1 after the above division should be considered
as equal to zero. In which case the equations for the
mutual admittance of the short-circuited ladder-diagram
will assume the following form:

for two cells:

$$Y_{mk_2}(p) = \frac{Z_3}{Z_3 Z_2 + Z_4(Z_2 + Z_3)};\qquad(8\text{-}53a)$$

for three cells:

$$Y_{mk_3}(p) =$$

$$= \frac{Z_3 Z_5}{(Z_5 + Z_6)[Z_3 Z_2 + Z_4(Z_2 + Z_3)] + Z_3 Z_4(Z_2 + Z_3)} \cdot (8\text{-}53b)$$

Let us remember that the resistances in these equat-
ions are numbered as follows: the Z_{2n-1} odd resistances of
the vertical connectors are numbered from right to left,

beginning with $Z_1 = 0$, and the Z_{2n} even resistances of the horizontal lines in the L-cells have the same sequence.

Using the first equation for diagrams d and f, and the second for diagram b of Fig. 8-23, we obtain:

$$Y_{mk_0} = \frac{1}{Q(p)} ; \qquad (8\text{-}54)$$

$$Y_{mk_1} = \frac{R_1 C_1 p}{Q(p)} ; \qquad (8\text{-}55)$$

$$Y_{mk_2} = \frac{R_1 R_2 C_2 C_4 p^2}{Q(p)} . \qquad (8\text{-}56)$$

A comparison between (8-54) to (8-56) with equations (8-49c) and identities (8-52) shows that the denominator of the obtained mutual admittance-functions coincides with the the denominator of the synthesized mutual admittance-function of (8-49c), while the numerators have the required content of 1, p, p^2; therefore, it is possible by connecting the elementary diagrams in parallel to obtain the required transfer function and to match the coefficients or the scales of the items of addition.

We will first match the relative values of the coefficients inside the function of mutual admittance. Based on above, the required function has the form:

$$Y_{mk} = \frac{b_0}{Q(p)} + \frac{b_1 p}{Q(p)} + \frac{b_2 p^2}{Q(p)} .$$

and the realized function at

$$Y_{2k_0} = Y_{2k_1} = Y_{2k_2} = Y_{2k}$$

will be:

$$Y_{mk_0} = \frac{b_0'}{Q(p)} + \frac{b_1' p}{Q(p)} + \frac{b_2' p^2}{Q(p)} .$$

$$\psi = \text{fractnl}$$

It is readily noted that this example is a special case of a parallel circuit of Fig. 8-16 with computations performed in accordance with the scales of equation (8-41b).

Let us change the admittance Y_0 by $(b_0/b'_0)\lambda$ times as compared with the factual:

$$Y'_0 = Y_{o\Phi} \frac{\iota_\bullet}{b'_0} \lambda. \qquad (8-57)$$

$\dot{\Phi}$ - factual

In this case the remaining partial admittances should be recalculated as follows, in order to retain the relative conformity of the coefficients inside equation (8-49c):

$$Y'_1 = Y_{1\Phi} \frac{b_1}{b'_1} \lambda; \qquad (8-58)$$

$$Y'_2 = Y_{2\Phi} \frac{b_2}{b'_2} \lambda. \qquad (8-59)$$

An increased mutual admittance of the circuit is obtained by increasing the admittances of all its units:

$$R' = \frac{R}{K\lambda}; \quad C' = CK\lambda.$$

This leads to a proportional increase in admittances Y_{2ki} and, therefore, by connecting the circuits in parallel we obtain the overall admittance:

$$\cdot_{2k\Phi} = Y'_{2k0} + Y'_{2k1} + Y'_{2k2}.$$

The overall admittance, however, was matched at the beginning of the computations with the load resistance R_L assumed to be equal to one ohm, therefore, it cannot be changed. Equating the sum of admittances to the required value, we obtain the following condition:

$$Y_{2k} = Y_{0k} \left(\lambda \frac{b_0}{b_0'} + \lambda \frac{b_1}{b_1'} + \lambda \frac{b_2}{b_2'} \right)$$

required to determine λ:

$$\lambda = \frac{1}{\dfrac{b_0}{b_0'} + \dfrac{b_1}{b_1'} + \dfrac{b_2}{b_2'}}. \qquad (8.40)$$

The value of λ also determines the ratio between the actual and required transfer function of the four-terminal network:

$$W_\phi(p) = \lambda W(p). \qquad (8.41)$$

BIBLIOGRAPHY

1. Gutenmakher, L.I. - Elektricheskiye modeli. Izd. AN SSSR (Electrical models. Published by AS USSR), 1949.

2. Baysv, N.A. and Udalov, A.P. - Lektsii po teorii tsepey s sosredotochennymi elementami (Lectures on the theory of circuits with concentrated units), Svyaz'izdat, 1955.

3. Teumin, I.I. - Spravochnik po perekhodnym elektricheskim protsessam (Handbook on transient electrical processes), Svyaz'izdat, 1952.

4. Taft, V.A. - Osnovy metodiki rascheta lineynykh elektricheskikh tsepey po zadannym ikh chastotnym kharakteristikam (Fundamentals of the methods of designing linear electrical circuits based on their required frequency characteristics), Izd. AN SSSR, 1954.

5. Korrektiruyushchiye tsepi v avtomatike (Correcting circuits in automation). Symposium of translated articles edited by M.Z. Litvin-Sedov, IL, 1954.

CHAPTER 9

ELECTRICAL CIRCUITS AND BLOCK-DIAGRAMS OF TYPICAL AUTOMATIC CONTROL SYSTEMS

9-1. STRUCTURE OF STABILIZING FOLLOW-UP AND CONVERTING SYSTEMS

As shown in Chapter 5, a closed structure is the best structure for steady transmission of programmed actions and for simultaneous reduction of the effects caused by most of the disturbances; special attention, therefore, will be given to such structures as they apply to various typical systems.

Let us start with a general analysis of conditions required for closing various types of control systems.

The conditions required for closing can be shown by a simple diagram, such as Fig. 9-1,a, if the nature of the input actions and the methods of their introduction into the system are not taken into consideration.

The direct channel of the control system in this diagram contains all units including the units of the controlled object which are subjected to controlled disturbances (changes). The crossed wires of the electrical line are purposely shown to emphasize the negative sign of feedback. Negative feedback imparts to the circuit a property of self-adjustment, because a positive deviation of the output is transmitted to the input of the direct channel with a minus sign and is followed by a reduced output, and vice-versa. This property of self-adjustment makes it possible to use various components in closed systems, including astatic and even quasi-astatic components, although a closed circuit, as such, contains a natural channel for the circulation of deviations and special methods described in Chapter 11 must be employed to take care of these deviations.

Let us proceed from diagram 9-1,a which shows no input actions to actual systems of various types.

Stabilizing Systems. The structure of a system for stabilizing at a given (zero) value is shown in Fig. 9-1,b.
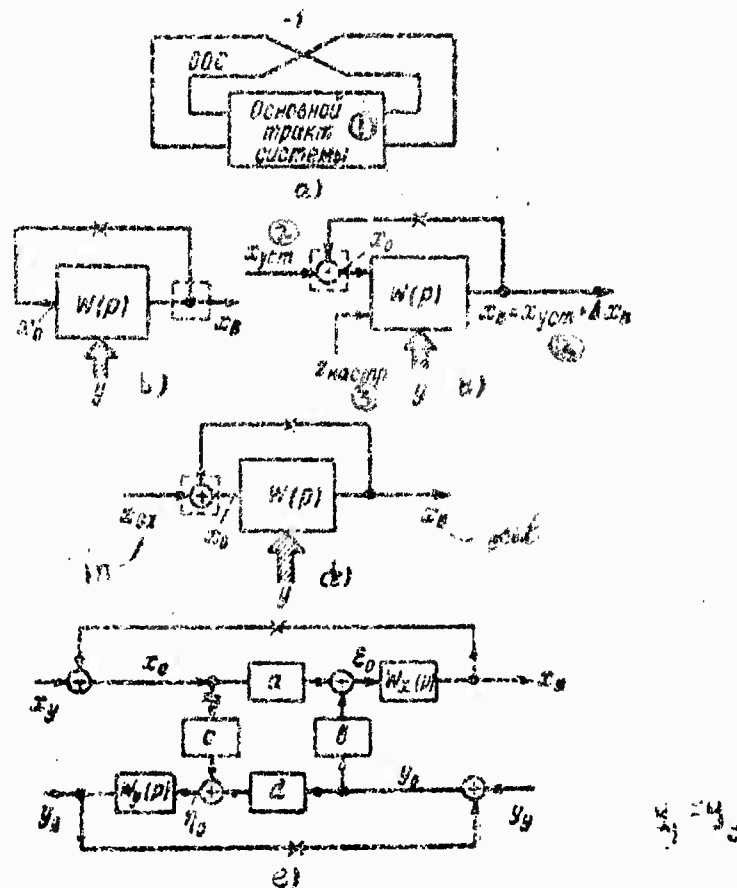
Fig. 9-1. Structure of closed stabilizing and follow-up systems

key: 1)main channel of the system; 2) setup; 3) adjusted.

This type includes, for example, a system stabilizing the bank of a plane which must be kept at zero.

An actual system must obviously contain a unit (an inclinometer or gyroscope) to measure directly the output value (the bank) and to introduce into the stabilizing direct channel a controlling signal having an opposite sign and proportional to the output value, or

$$x_0 = -x_{out} \qquad (9-1)$$

Disturbances may appear in any component of the stabilizing system and are shown in the diagram by a common arrow "y". In examinining a stabilizing system, the main attention is given to the transfer functions of disturbance-to-output.

The structure of a system for stabilizing near the setup, or near the nominal output value x_{set}, is shown in diagram c, where the unit must measure the difference between the nominal and actual values of the output, or

$$x_0 = x_{set} - x_{out} \qquad (9-2)$$

and to supply this difference to the direct channel of the stabilizing system and to dampen the deviations from the reference (setup) value. However, if x_0 equals zero, one of the components of the system must be first adjusted to some intermediate value that would assure a nominal setup value during nominal disturbances. The additional constant value of the adjustment is shown in the diagram as a separately introduced value of Z_{adj}. The adjustment may be performed at any place of the system. For example, for a generator controlled as in diagram 6-3,a, the nominal voltage can be be adjusted for a given current of the load, as follows:

by specifying the required magnetization obtained from an additional winding ϕ_y:

by controlling the resistance of the rheostat;

by changing the pressure exerted by the carbon rods of the voltage regulator.

Since the values of both Z_{adj} and x_{set} are constants, the control performed as required by the variable component will proceed in the same manner as in diagram b, namely, $x_0 = -\Delta x_{out}$ is to be reduced to zero.

F o l l o w - u p   s y s t e m s. The structure of a follow-up system (for both programmed control and for reproduction) is shown in diagram d, which contains the actual input and output values x_0 and x_{out} with the difference between them determined by a measuring unit, which difference is

$$x_0 = x_c - x_{out} \qquad (9\text{-}3)$$

to be used to furnish the direct channel of the system with the motion that reduces this difference to zero.

In all examined cases, the absolute value of the controlling action is equal to the error of the automatic control system and differs only in sign.

c o n n e c t e d   s y s t e m s. If two connected automatic control systems are reproducing the values x_c and y_c, each one of them operates in accordance with the principle of reducing to zero the similar (9-3) differences

$$x_\bullet = x_y - x_g; \quad y_\bullet = y_y - y_{g'} \qquad (9\text{-}4a)$$

The conditions required for coupling are determined by the effect of the unbalance of one and other systems on the formation of the signals ξ_0 and η_0 in both systems. Let us cite a very simple form of the controlling signal for the controllings signals as a linear function of the unbalances:

$$\xi_0 = ax_\bullet + by_\bullet; \quad \eta_\omega = cx_\bullet + dy_\bullet. \qquad (9\text{-}4\text{6})$$

Fig. 9-1,e is a block-diagram drawn in accordance with equations (9-4); the amplifying components a and d are included in the direct channel of each system to amplify the gain factor of the system without changing its operating conditions, as compared, for example, with the isolated system shown in diagram 9-1,d.

The amplifying components b and c effect a mutual coupling between the systems. Let us note that in case the own coupling of each system must be negative, the mutual couplings may form in certain cases a positive feedback, as for example, when the coupling coefficients (b and c > 0) shown in the diagram are both positive. In such a case, as it follows from the structural analysis (see Ch.5), the gain factor of the circuit of efficient automatic control systems must be limited to a value of +1.

As an example of a connected system is an airplane equipped with an autopilot with mutually dependent banking

and yawing channels /1/. Certain connected systems used in computing devices will be analysed in section 9-5.

C o n v e r t i n g   s y s t e m s.   Let us now proceed with the analysis of the structure of converting systems which operate in accordance with a specified linear mathematical function.

Besides the solution of the mathematical problem of conversion, the requirements of the system also include, as a rule, boosting the signal intensity, suppression of the effect of disturbances, etc. Without such requirements there is no sense of forming a complex control system, as in such a case it would be sufficient to use electrical circuits or typical components without combining them into a single system.
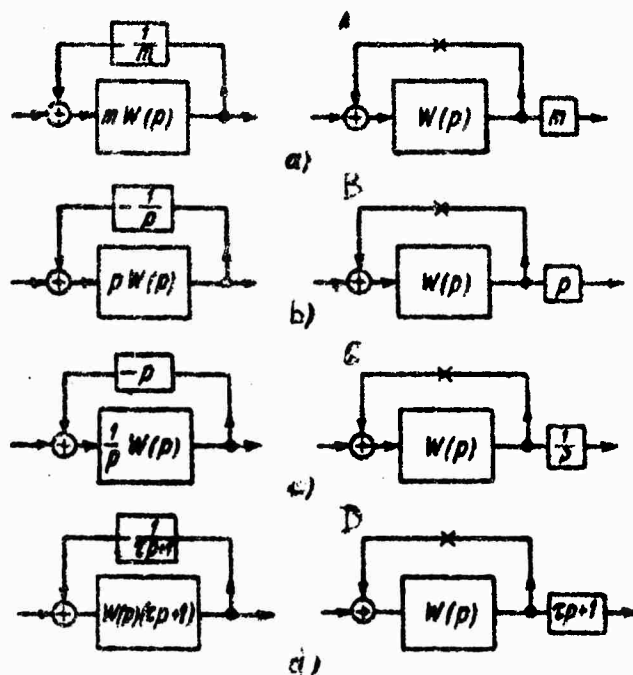
Fig. 9-2. Structure of converting systems.

Fig. 9-2 shows block-diagrams of converting systems

which take into consideration all of above requirements. The block-diagrams at the right illustrate the method of solving separately the problems of power amplification by creating a separate reproducing closed automatic control system and the problems connected with the conversion of a programmed action in accordance with a specified rule, following its amplification by installing at the output of the reproducing system amplifying, differentiating, integrating, forcing, and similar components.

The solution of conversion problems must be reflected as a form of forced motion in the system. In case of a separately-acting structure it is sufficient to check the errors of reproduction of the closed systems by the methods described in Ch.11.

The uncompensated errors of the forced motion of a reproducing system are the errors at the input of the converting part. The scaling component A will increase these errors m-times. The differentiating component B will differentiate them; in this case the precision of the entire system will not be affected by the constant component of the error of the reproducing part.

With a constant component present in the input-error, the integrating component C, on the contrary, will produce an accumulating error at the output.

In solving the problem of forestalling D, the forcing component can be considered from the standpoint of converting the errors as a sum of the amplifying and differentiating components with the coefficient of t.

The basic defect of a separately-acting structure is the inability of taking off any significant power from the output of the operating components. Only a scaling component of, for example, the reducing gear type is able to retain the power of the output device (shaft) of a reproducing system; if the mathematical part of the problem is accurately performed, all remaining components possess a small output-power and the action upon them of disturbances in form of a load results in additional errors. In many cases a series of errors can be prevented by changing the places of the operating and reproducing parts.

Let us analyse the solution of the same problems of conversion of the programmed action with the aid of a system having a closed structure, as shown at the left of Fig. 9-2.

The transition from a separately-acting to a unified structure is accomplished by carrying the assembly through the converting units according to the course taken by the signal. At this the transfer function of the converting unit is introduced into the direct circuit, and its inverse -- into the feedback circuit.

As a result of the technical execution of such conversions, the converting unit with its inverse transfer function is applied to the no-load feedback circuit where it operates at high precision as, for example, electrical circuits operate under compensating conditions. The output of the entire circuit represents a high-power output of the direct channel with load-type disturbances mostly damped. In the majority of cases there is no need of making the direct channel too complex because, when its gain factor is large, the overall transfer function will (irrespective of its operator transfer function) come nearer to the inverse value of the operator transfer value of the feedback circuit, as was earlier illustrated by equation (5-9). For example, such units as "p" can be excluded from the direct channel of diagram b which, naturally, will require a re-calculation of the error.

9-2. GENERATOR-VOLTAGE STABILIZATION METHODS

The operating principles governing the control of the voltage of D-c generators are illustrated in Fig. 9-3,a. The generator operates with a certain load connected to the bus-bars shown at the left of the diagram. The voltage of the generator is determined mainly by the current flowing through its excitation winding; therefore, either the voltage across the excitation winding, or the excitation current, or any other item affecting the excitation current can serve as the control signal of the system. The voltage across the bus-bars should be regarded as the output.

The circuit can be open provided the state of the excitation-circuit does not depend on the voltage across the bus-bars. In this case, the voltage across the bus-bars located along the negative-feedback line (OOC) is supplied to the input of the system -- to a unit regulating the excitation-current.

Certain principles affecting the regulator will be reviewed in detail to determine whether the basic equation (9-2) for stabilizing near the set control point in a sys-

tem having the structure shown in Fig.9-1,c can be applied
for this particular circuit.

REGULATOR WITH A STANDARD SOURCE OF REFERENCE VOLTAGE.
One of the circuits that can be applied for the regulator is
shown in Fig.9-3,b. The input value in a regulator of this
type is represented by the voltage of the standard source:
x_{in} = U_{st} . From this voltage must be subtracted the vol-
tage U_g across the buses of the generator which is supplied
to it along the line of the negative feedback (OOC in dia-
gram a). The difference between these voltages, e = U_{st}-U_g,
which according to equation (9-2) is the controlling signal,
is supplied to the amplifier's input. It is the amplified e
that determines the generator's excitation-current.
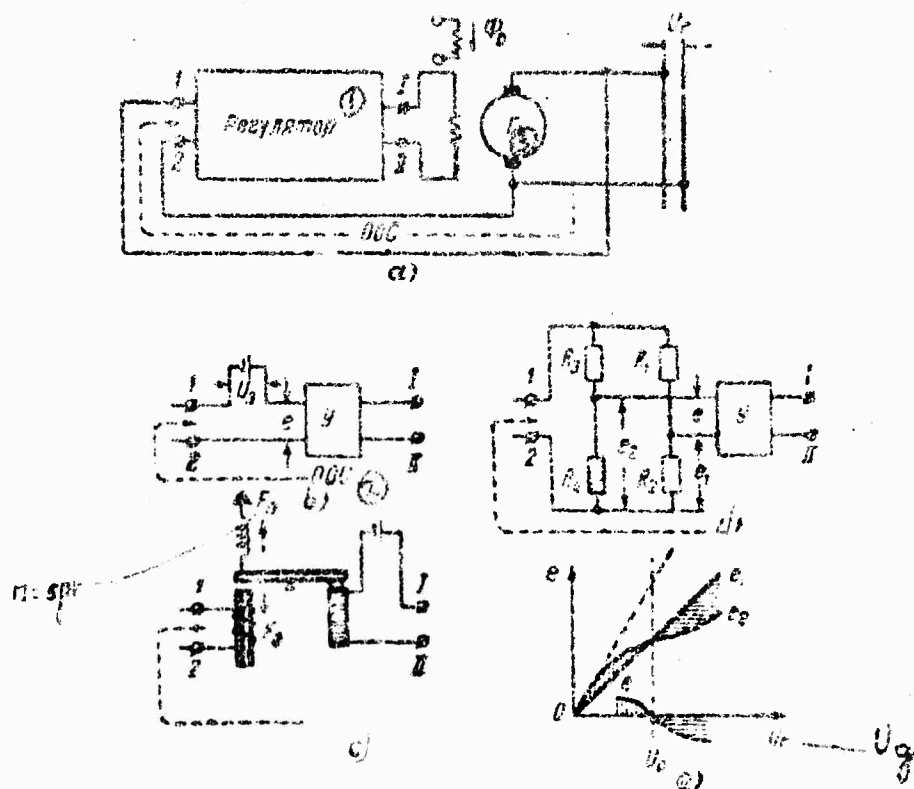
Fig. 9-3. Electrical circuit of systems for
stabilizing the voltage of D-c generators.

key: 1) regulator; 2) negative feedback; 3) generator

Both the standard voltage and the initial excitation-current selected during the initial tuning of the circuit must assure for the specified load a nominal voltage equal to $U_{st} = U_{nom} + f(R_{ar}I_{ar\ nom})$. In an open circuit any change in the load ΔI_ℓ would have caused an additional voltage drop of $\Delta U = -R_{ar}\Delta I_\ell$, but in a closed system any change in the voltage across the buses along the line OOC will be transmitted to the regulator where, in this case, it will change the difference $U_{st} - U_g$, which will accordingly vary the excitation-current that compensates the effect of the disturbance.

For example, if the load-current is increased ($\Delta I_\ell > 0$), it will also increase the difference $U_{st} - U_g$ and the excitation-current will become larger. This demonstrates the self-adjusting property of a closed system. An increase in the standard voltage by $f(R_{ar}I_{ar\ nom})$ can be avoided in the case of a two-winding generator where the tuning can be accomplished by the initial flux Φ_0.

An electromechanical design of a regulator which is used more frequently is shown in Fig.9-3,c. Here the voltage across the buses is changed by the attraction of an electromagnet which weakens the pressure of the spring against the carbon rod, increasing thereby its resistance and reducing the current of the excitation circuit. The latter can be supplied either by an independent source, as shown on the drawing, or it can be connected to the buses of the generator.

It should be regarded in this case that the input-value x_{set} shown in the block-diagram 9-1,c is the voltage depending on the spring-tension F_{spr}, the initial value of which is set for the specified voltage during the tuning. The output voltage can be also transformed to match the force of the electromagnet. The difference between these forces due to a disturbance causing the voltage to deviate from the control point determines the regulation process, i.e. the self-adjustment of the system. In case of small deviations, a proportionality is established between the force-increments and the voltage-increments; therefore, the voltage proportional to the initial tension of the spring can be regarded as the input of the system, and the voltage across the buses -- as the output. The voltage-difference, i.e., the controlling signal with the same proportionality factor acquires more force to change the resistance of the carbon rod and, finally to change the excitation current (see also Fig. 1-3).

Diagram 4 shows a regulator with a nonlinear bridge. The voltage across the generator buses is supplied along the line OOC to the vertical diagonal of the bridge and from the horizontal diagonal is taken off the voltage to the amplifier which supplies the excitation circuit. The right side of the bridge contains the linear elements R_1 and R_2, consequently, as shown by the straight line e_1 in curve e, a change in voltage across the buses will bring a proportional change in the voltage across the resistances of this branch: $e_1 = (R_2/R_1 + R_2)U_g$.

The left branch of the bridge contains one linear element R_3 and a nonlinear element R_L which is shaded on the diagram. Let us assume that the resistance of the nonlinear element increases with the decrease in voltage. Then, the ratio $R_L/R_3 + R_L$, which determines the share of the voltage across the nonlinear elements in terms of the full voltage, will increase with the decrease in voltage across the buses and vice versa (see curve e_2).

The input-voltage of the amplifier is equal to the difference between the voltages e_2 and e_1 across the R_L and R_2 elements. As shown by the curve, this difference is equal to zero at voltage $U_g = U_o$ and it changes its sign depending on the sign of the voltage-increment across the buses.

It is possible, therefore, to find in this circuit an implicitly specified input-value U_0 from which is subtracted the actual voltage across the buses, so that the difference is converted into the output-voltage of the bridge. The increment-steepness of the output-voltage of the bridge S is proportional to the difference between the increment-steepness of the voltages across the linear and nonlinear elements and serves as the gain factor of the bridge:

$$e = \left(\frac{R_4}{R_3 + R_4} - \frac{R_2}{R_1 + R_2} \right) U_g = S\Delta U.$$

In conclusion, a general remark about the polarity of the controlling signal should be stated for circuits shown in this . The polarity of the signal should be such that the changes caused by it in the system would serve to compensate the effect of external disturbances. A wrong polarity of the signal leads the system away from the operating point and makes it inefficient. Such an error can be

readily eliminated, however, by switching the ends of the electrical circuits b and d, and by moving the carbon rod to the opposite arm of the lever in circuit c.

For a dynamic analysis of stabilizing systems it is necessary to have a block diagram of the complete closed automatic control system containing both the object to be regulated and a voltage regulator. A block-diagram of the regulated object -- a self-excited D-c generator -- has been already shown in Fig. 6-1,d. It is repeated in the lower part of Fig. 9-4, where the input is represented by the change in resistance of the excitation-circuit ΔR_c and the output -- by the change in armature voltage ΔU.

K: steepness
n. left
$\gamma = e$
ℓ
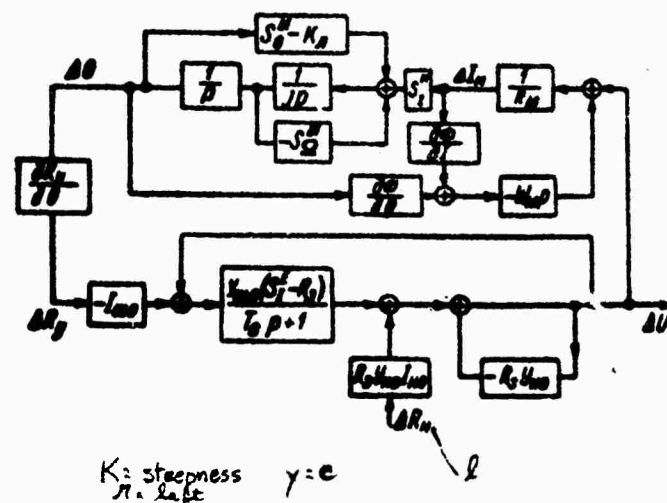
Fig. 9-4. Block-diagram of voltage stabilizer
with voltage-amplification regulator

Let us prepare the data on the structure of the regulator's circuit which is needed to close the direct channel of the feedback circuit through the voltage regulator. We will base the data on equation (1-25), according to which is formed the section between ΔI_m and $\Delta\theta$ in the upper part of Fig. 9-4. The missing relationship between ΔU and ΔI is determined from the equation for the circuit of the winding of the electromagnet having a number of turns ω_m and a resistance R_m:

$$I_M R_M + w_M \dot{\Phi}_M = U.$$

Using the Laplace representations and the increments, we obtain:

$$\Delta I_M(p) = \frac{1}{R_M}[\Delta U(p) - \omega_M p \Delta \Psi_M(p)] \qquad (*)$$

It remains only to determine the increment of the magnetic flux. Since the latter depends on the current I_m and on the angle of rotation θ (which depends on the gap) of $\Phi(I,\theta)$, the increment expressed with linear approximation is written as follows:

$$\Delta \Phi = \frac{\partial \Phi}{\partial I} \Delta I_M + \frac{\partial \Phi}{\partial \theta} \Delta \theta. \qquad (**)$$

The motion of the lever changes the pressure against the carbon rods, the resistance of which varies as per the rule of $R_c(\theta)$. Giving consideration to the increments in resistance, we obtain the last missing equation:

$$\Delta R_y = \frac{\partial R_y}{\partial \theta} \Delta \theta.$$

which together with equations (*) and (**) enables us to make the final closing of the circuit's structure.

A more extensive review of stabilization methods can be found in /2/.

9-3. STABILIZATION OF FREQUENCY AND SPEED OF ROTATION WITH THE AID OF ELECTRIC MACHINES

The general principle governing the construction of a closed speed-stabilizing system is illustrated in Fig. 9-5,a; the speed of the output shaft of the electric motor is evaluated by a certain electric pickup which acts upon the regulator along the line OOC and causes it to change the current in the excitation-winding of the motor or of its armature which, in its turn, restores the specified speed affected by some disturbance.

The simplest electric pickup of the speed is a centrifugal contact regulator; when the speed exceeds the setup

value, the regulator closes the movable contact to shunt a
part of the resistance of the excitation-winding circuit;
this increases the excitation-current and is followed by a
reduced speed. A simplified form of an electric circuit of
such a regulator is shown in Fig. 9-5,b.(the armature is
here connected through an additional resistance to the
network and is not regulated).

Another widely used type of an electric speed-pickup
is a D-c tachogenerator which generates a voltage that is
proportional to the rotary speed of the shaft.

The circuit of a regulator using a tachogenerator is
shown in Fig.9-5,c. The voltage from a standard (reference)
source serves as the input for this method of stabilization;
the required part of U_{st} (of a definite polarity), which is
proportional to the nominal /rated/ speed, is taken off the
source with the aid of a potentiometer. From this voltage
is deducted the voltage of the tachogenerator U_{tg} which is
supplied along the OOC-line and is related to the speed of
the output-shaft by the same proportionality factor; the
voltage-difference, $e = U_{st} - U_{tg}$, which is equal to the
controlling signal, is amplified and provides the armature
with the current necessary to overcome the load-moment.

When the load on the motor shaft is undergoing further
changes, the voltage-difference will provide a compensating
moment having the same sign as the disturbance.

High-power systems employ dynamoelectric amplifiers
which feed the armature-circuit of the electric motor. In
such cases the excitation-circuit is connected to the net-
work and is not regulated. Low-power systems employ elec-
tronic tube amplifiers or magnetic amplifiers connected to
excitation-winding. At this, the armature-circuit is con-
nected directly to the network with the aid of a limited
resistance -- a barretter /balast resistor/.

If a more powerful D-c generator replaces the tacho-
generator in diagram c leaving the rest of the circuit un-
changed, such a system could be regarded as a voltage
stabilizer for this generator. Unlike as in Fig. 9-3, the
voltage would be stabilized by changing the rotary speed of
the generator with the excitation-current remaining constant.

Serving as an electrical speed-pickup in Fig.9-5,d
is a A-c synchronous generator whose voltage and frequency
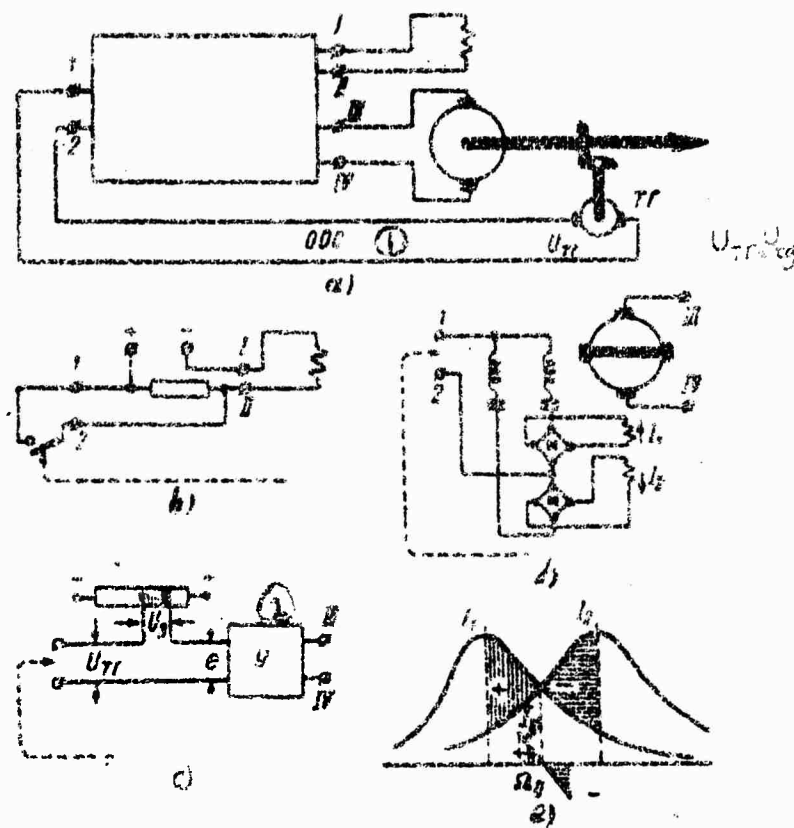are proportional to the speed of the output-shaft.

Fig. 9-5. Circuits for stabilization of
speed of electric motors

key: 1) OOC - negative feedback; 2) amplifier.

The voltage of the synchronous generator is supplied
along the OOC-line to two resonant circuits of the regulator.
The rectifiers installed in these circuits supply the two
control-windings of the dynamoelectric amplifier. Diagram e
illustrates the dependency of the rectified currents I_1 and
I_2 on the frequency or on the speed, which is proportional
to the frequency. The curves are shifted towards each other
because the selected resonant frequencies differ in each
circuit. In accordance with the electrical circuit, the
controlling current, I_c, is represented by the difference
between the currents of these circuits: $I_c = I_1 - I_2$. At a
speed Ω_g, which corresponds to the point of intersection

of the curves in the diagram, the controlling current is equal to zero; a deviation from this speed will cause the appearance of a controlling current which reflects the sign of the deviation and is proportional to it, provided the deviation is small. In its function of changing the frequency, the steepness S' with which the control-current is increasing is equal to the difference between the steepness with which the currents in both resonant circuits are increasing.

Based on the curves and circuits of this example, the speed Ω_0 should be regarded as the input, and the actual speed Ω as the output. The difference obtained from equation (942) is transformed into the controlling current $I_0 = (\Omega_0 - \Omega)S_\Omega$ with a steepness of S'_Ω. Also, a change in the controlling current serves to regulate the voltage of the dynamoelectric amplifier and brings about a change in the speed of the electric motor in order to compensate for the undesired speed caused by outside disturbances, such as a load-moment.

If the voltage of a synchronous generator instead of the speed of the shaft of the motor is used as the output, then this system can be called a system of stabilizing the frequency.
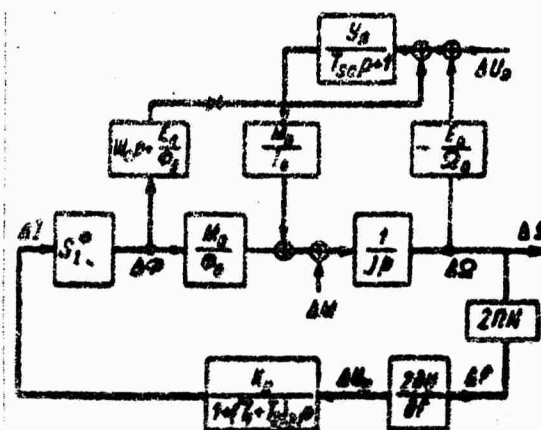

Fig. 9-6. Block-diagram of frequency stabilizer with magnetic amplifier and two-channel control of the motor

We will now examine the complete block-diagram for one version of speed stabilization. Such a diagram is shown in Fig. 9-6 for a two-channel control of a motor, where the control is effected along the lines of the excitation and armature circuits with the aid of a measuring device in form of a resonant bridge and a magnetic amplifier for the subsequent amplification.

The resonant bridge of the type shown in Fig.9-5,d will not act upon the dynamoelectric amplifier, but will affect the magnetic amplifier whose circuit is shown in Fig. 7-3. The voltage in one of the bridge circuits will depend on the input-voltage U_g and on the frequency f, i.e., $U_c = U(U_g, f)$. Taking the increments into account, we obtain:

$$\Delta U_{y1} = \frac{\partial U}{\partial U_r} \Delta U_r + \frac{\partial U}{\partial f} \Delta f. \qquad (*)$$

The windings 1 and 2 in the circuit of the stabilizer run opposite each other, therefore, the obtained increments of currents and fluxes in the windings are to be subtracted. It is convenient to perform this subtraction in advance, in form of voltages; then, the first members in equation (*) having the same sign for the derivatives of both circuits of the bridge will be reduced, while the second members with derivatives differing in signs will be doubled. Finally, the doubled increment of the voltage will be:

$$\Delta U_y = 2 \frac{\partial U}{\partial f} \Delta f.$$

The lower block of the diagram illustrates the obtaining of the control-voltage increment; the increment in the frequency is found from the speed-increment proportional to the number of pair of poles of generator N and to coefficient 2. The magnetic amplifier for the two input-windings is shown in a block-diagram smaller than the one shown in Fig.7-3,c; the current-increment ΔI is found at its output. The block-diagram for the two-channel controlled motor has been copied from Fig. 6-7 and, since the magnetic amplifier is regarded as a generator of current, i.e., it is assumed that its output-resistance is high, therefore, all lines in in the block-diagram of Fig. 6-7 which involve the formation of current are discarded, except the line from the magnetic amplifier. In the same manner is simplified the formation

of the magnetic flux of the motor which is connected with the current-increment by the simple relationship $\Delta\Phi = S_i \cdot \Delta l$, which was taken into account in the block-diagram.
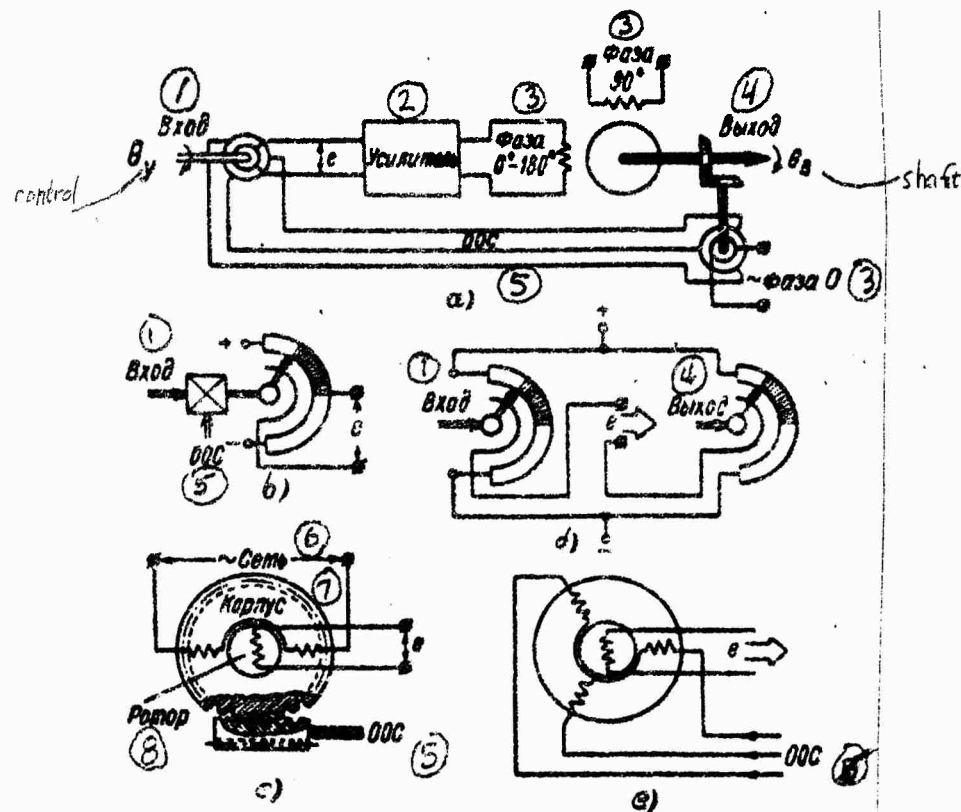

Fig. 9-7. Electrical circuits of measuring units of follow-up systems

key: 1) input; 2) amplifier; 3) phase; 4) output;
5) negative feedback; 6) network; 7) housing;
8) rotor.

The remaining elements of the block-diagram 6-7 are left unchanged. The stabilization is concerned with a speed which is near the rated /nominal7 -- high -- speed of the motor, at which the counter-emf exceeds one-half the voltage across the armature. In such a case, a predominant imprtance

in the system is attached to the path shown in the block-
diagram by thick lines forming the loop of the negative
feedback.

The block-diagram also shows the conditions required
to control the armature-voltage and the conditions required
to introduce disturbances from the moment of the load.

Several circuits in Fig. 9-6 are left unconvoluted,
which makes it possible to build up easily the system by
introducing additional units and loops when perfecting the
principles governing the control.

This scheme can serve as a basis for a detailed
dynamic investigation of the system with the aid of methods
described in the following chapters.

9-4. POWER-DRIVEN FOLLOW-UP SYSTEMS

Of the three categories of automatic control systems
the follow-up category is the most variegated for its
structure, types of drives, amplifiers, converters, and its
range of power. Fig. 9-7,a illustrates one of the types of
a follow-up system designed to assure the coincidence of
the angles of rotation of both the input and output shafts,
or a continuous follow-up of the output shaft after the
input shaft.

The input in electromechanical follow-up systems is
the angle of rotation θ_o of the controlling shaft. For the
output value is taken the angle of rotation θ_{ah} of the
adjusting shaft. The latter is supplied along the COC-line
to the input to be matched with the angle of the turn and
to form the unbalanced values according to equations (9-3).

The angular value of the error is usually converted
into an electric voltage which, after its amplification, is
used for the electric motor which turns the adjusting shaft
and with it the pickup in the circuit of the negative feed-
back to compensate for the error.

Serving as a servomotor driving the output-shaft in the
diagram a is a two-phase, a-c motor with a short-circuited
rotor, one of its windings with a phase-shift of 90 degrees
obtained with the aid of a capacitor in the supply circuit
of the winding or in the circuit of the amplifier of the
supply-voltage is connected to an uncontrolled network.

The second winding receives an amplified difference-signal with a phase shift of 0 or 180 degrees, depending on the unbalance required to compensate for the mismatch between the direction of the motor's rotation.

It was already mentioned that the direct path of a follow-up system may be constructed in different ways, but the principles governing the closing of a negative feedback follow-up system as in block-diagram 9-1,d can be considered without taking into consideration the units of the direct path. Let us describe these principles.

FEEDBACK WITH THE AID OF A MECHANICAL DIFFERENTIAL (Fig. 9-7,b). If the feedback is made to be mechanical with the aid of an additional shaft, it will require the use of a mechanical differential to perform the operation of subtracting the input and output angles. A mechanical differential servings as a summator was already mentioned in chapter 1 (see Fig. 1-8); however, in this follow-up system with its electric motor it is expedient not only to perform a subtraction and obtain also a difference in form of an angle of rotation, but also to convert this difference into an electric signal of the error. As one of such converters can be served by a potentiometer shown in diagram b. Its wiper rotates to cover the mismatch angle and from this wiper is taken off with the aid of a current-removing ring the controlling voltage between the wiper and the mid point of the potentiometer. The ultimate mismatch angle and the ultimate angle of rotation of the potentiometer wiper, both of which are determined by constructional limitations, should be made to agree by introducing inter-mediate transfer numbers.

MECHANICAL FEEDBACK USING A CONVERTING UNIT WITH A MOVABLE HOUSING AND A ROTOR (Fig. 9-7,c). The subtraction of the angles of rotation can be performed by both a mechanical differential and by other means, provided the obtained difference between the angles is not applied to a separate shaft, but is immediately converted into an electric voltage. For this purpose use is made of the difference between the angles of rotation of the housing and rotor of the pickup resulting from their related motions, provided the housing and the rotor are made to rotate respectively by the driven and driving shafts.

A pickup of this type is shown in diagram c; it is a rotary transformer with a single-phase winding on the housing (stator) and a rotor. The housing of the pickup is

rotated by the driven shaft, and the driving shaft rotates the rotor. The drawing illustrates the relative position of the windings when both shafts are in a matched position. In such a case, the rotor winding is perpendicular to the axis of the magnetic flux created by housing winding which is connected to the network, so that the control signal taken off the first winding is equal to zero.

The relative position of the housing and rotor windings remains unchanged during a matched rotation of both shafts (the connection of the windings with outside sources and other terminals is by means of contact rings and wipers) and the error-signal remains equal to zero. As a mismatch $\Delta\theta$ appears between the angles of rotation by the shafts, one of the windings will turn at an angle $\Delta\theta$ with respect to the other and, with a sinusoidal distribution of the magnetic flux of the primary (stator) winding, the voltage of the secondary winding will be $e = U_0 \sin\Delta\theta$. For small mismatches, the error-signal changes linearly: $e = U_0 \Delta\theta$.

It should be noted that the principle on which is based the use of relative rotation of two parts to disclose an error-signal can be applied also to pickups of other designs. For example, it is possible to obtain an error-signal without using a mechanical differential gear simply by placing the potentiometer-plate on a rotary housing which is rotated by the driven shaft and connect the wiper with the driving shaft and take off the output voltage between the wiper and the mid-point, as in diagram b.

ELECTRICAL FEEDBACK WITH POTENTIOMETERS (diagram d). According to the method illustrated in diagram b, the subtraction of the angles of rotation of two shafts was first performed and was followed by conversion of the difference into an electrical voltage made by one potentiometer. For this it was necessary to move the OOC-shaft from the driven to the driving shaft and use a separate mechanism -- a differential.

In the majority of cases it is more convenient to change the order of the conversion, namely, first to convert the angles of rotation of both shafts into an electrical voltage with the aid of two separate potentiometers, then to subtract one voltage from another, as shown in diagram d. The subtraction of the voltages is obtained by the circuit itself without using additional units. The feedback in this case is effected by the conductors and it connects the driven with the driving shafts over a large distance.

Such systems are known as remote potentiometric follow-up systems.

ELECTRICAL FEEDBACK WITH SELSYNS (diagrams a and e). The last of the analysed methods of using feedback can be better explained by examining the principles illustrated in diagram e. Really, according to diagram e, the driven shaft turned the housing of the pickup and, with it, the axis of the magnetic flux created by the winding of the stator. But it is possible to turn the magnetic flux at a required angle without rotating the housing and to do it also at a distance with the aid of a special type of pickup -- a selsyn.

Diagram e shows the connection of the windings of a single selsyn, while diagram a shows the connection of two selsyns for creating a OOC /negative feedback7. As shown in diagram e, the stator of the selsyn has a three-phase winding which, according to diagram a, are interconnected by a three-wire line. The rotor of the selsyn has a single-phase winding, one of which is connected to the network to supply current to the circuit, while the second is used for taking off the signal of the error.

The single-phase winding of the selsyn connected to the network creates a variable magnetic flux directed along the axis of the winding. This magnetic flux induces in the three-phase winding of the stator a emf which brings about a flow of secondary current in the phases of the selsyns and through the three-wire line. The intensity of each current and its created demagnetized magnetic flux can be determined either analytically or with the aid of geometric plottings (projections); it is important, however, to know not the individual fluxes, but the direction of the overall demagnetizing flux from all three phases.

The law of Lenz provides a simple method to determine the direction of the overall demagnetizing flux. Really, if the demagnetizing flux is viewed as a reaction of a complex electromagnetic system to the only disturbance represented by the variable magnetizing flux, therefore, the overall demagnetizing flux must be directed just opposite the direction of the magnetizing flux, i.e., along the axis of the rotor winding.

If the rotor of the selsyn connected to the network is turned at a certain angle, the axis of the demagnetizing flux will also turn at the same angle.

Let us examine the process in the second selsyn. The same currents flow through both the three phases of the second selsyn and through the phases of the first selsyn, therefore, its magnetic flux will have the same direction. The turning of the rotor of the selsyn with a single-phase winding connected to the network will also turn the magnetic flux in the second selsyn. Now, if with the shafts in matched positions, a single-phase winding is installed in the second selsyn perpendicular to the magnetic flux, as was already done in diagram c, then, just as in diagram c, the error-signal in form of voltage e will be determined by the mismatch between the shafts.

Hence, one selsyn specifies the angle of rotation for the magnetic flux, the three-wire line "transports" this direction of the magnetic flux to the second selsyn and, finally, an error-signal is produced in the latter. For the operation by this method it is entirely unimportant whether the three-phase and the single-phase windings are located on the stator or rotor, or which of the selsyns must be connected to the network and from which of the selsyns to take off the error-signal; these questions do not affect the principle of adding a negative feedback and are solved in a form more convenient from the construction viewpoint.

If the input potentiometer in diagram d is eliminated and the control is effected directly by the input-voltage U_c, the principle of reducing the voltage-unbalance to zero will remain the same and, with the scale of the output potentiometer equal to $K_2 = U_2/x_{in\ max}$ e/rad, the statics of the system is described by equation

$$U_y = K_2 x_a \ \text{или} \ x_a = \frac{1}{K_2} U_y.$$

Such an automatic control system, which converts the input-voltage into a proportional rotation of the shaft, is known as an automatic voltage-adjusting system. With a measuring unit containing different converting elements between the unbalance and, respectively, between the input and output, the automatic control system may provide the follow-up of an output value of one physical dimension ... example, the shaft watches the controlling voltage, the voltage watches the controlling pressure, etc.

If voltages U_1 and U_2 of different intensities are supplied to the potentiometers of the same diagram d, the statics of the system will be determined by equation

$$\frac{U_1}{x_{max}} x_y = \frac{U_2}{x_{max}} x_B$$

or

$$K_1 x_y = K_2 x_B$$

from which

$$x_B = \frac{K_1}{K_2} x_y = \frac{U_1}{U_2} x_y = m x_y.$$

This is the simplest way of solving the problem of scaled dimensionless conversion, the block-disgram of which was discussed in analysing Fig. 9-2,a.

The mathematical description of the operation of a follow-up system is not greatly complicated by the presence of measuring units, because in the majority of cases they are characterized by a static transmission factor. The dynamic part of the problem is determined by the composition of the direct channel of the automatic control system.

The operating conditions of measuring units become complicated when dealing with high-precision systems where, besides the main channel -- the channel of coarse readings -- shown in Fig. 9-7 which assures the coincidence of the input and output axes with a precision Δ equal to the error of the instrument parts, there is also a second controlling channel with a similar unbalance-pickup but connected with the input and output shafts with increased transmission ratios i, which reduce i-times the instrument errors of the measuring units. In such a case, the automatic control system, in case of a large mismatch, operates along the coarse control-channel and, after the mismatch is reduced to a small value, the commutation circuit containing either contact or contactless nonlinear parts changes the operation of the automatic control system to control with precision. while the latter case is subjected to a dynamic investigation, because the coarse mismatch is readily evaluated by the ultimate requirements specified for the assembly of the automatic control system (see Chapter 12).
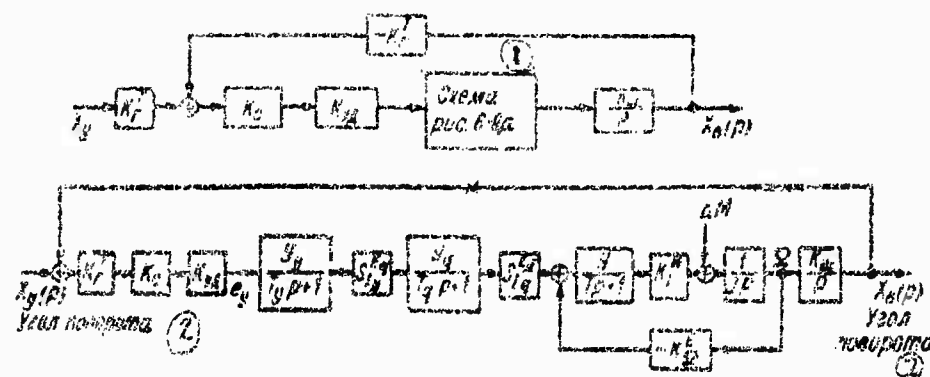
Fig. 9-8. Block-diagram of a follow-up system
with a dynamoelectric amplifier

key: 1) block-diagram of Fig. 6-9,a; 2) angle of rotation.

Several features are brought about also by supplying
the measuring units with an alternating current, because
the supply frequency serves to excite all units of the
automatic control system and to change their transmission
properties in accordance with the controlling action which
acts only with infra-low frequencies. It especially affects
the transfer properties of electrical loops. The work of
such systems with precision obtained by modulating the sig-
nal is described in Chapter 14; the study here will concern
the automatic control systems with preliminary specified
electric loops which operate with a rectified D-c, while
the remaining electromechanical units practically do not
respond to the supply-frequency of the pickups because of
their inertness. A dynamic description of the work of such
an automatic control system can take into account only the
controlling signal even when the pickups operate on A-c.
Taking this into consideration, Fig. 9-8,a shows a block-
diagram of a follow-up system containing a dynamoelectric
amplifier (an amplidyne). It is based on the block-diagram
6-9,a for a compensated amplidyne with a motor but it has
in addition new blocks which are characterized by the fol-
lowing transmission properties:

$K_u = k_{shr}$ - transmission ratio between motor shaft and
        load shaft;

$\frac{K_\omega}{P} \cdot k_{shr}/p$ — the operator transfer function of the meter;

$k\frac{T}{C} \cdot k_0^D$ — transmission ratio from coarse to precise reading (usually equal to 20,60,31);

$k_c \cdot k_s$ — transmission factors of pickup and receiving selsyns, volts/radians;

$K_{y\mu} \cdot k_{ad}$ — gain factor of amplifier-demodulator;

a loop of the main feedback has been also introduced in the diagram.

By decoding the structure of the amplidyne-meter block and carrying the summator to the left through the component k_0^D, we proceed from the diagram 9-8,a to diagram b which can be used for the subsequent analysis of the automatic control system operating with precision.

9-5. FOLLOW-UP SYSTEMS OF COMPUTING DEVICES

A. DIRECT SOLUTIONS

Certain functions performed by computers are partially explained by the converting systems shown in Fig. 9-2. The type of problems solved by special computers /4/ is, of course, much larger than those shown in Fig. 9-2. Among the simplest of the problems is to obtain a specified function

$$Z = F(x) \qquad (*)$$

with x as the argument.

A similar function is obtained by functional converters having one input FC-1 which differ in design and in output power. Besides the type of the function F, the design is mostly influenced by the physical nature of the input and output values. The most widely used versions of the design contain either a mechanical M or electrical E input and output. The various combinations involving the magnitudes of the input and output values are covered by the following: M-M, M-E, E-M, and E-E, where the first letter indicates the nature of the input value, and the second letter -- of the output.

The M-E combination for a sinusoidal functional dependence was considered in chapter 4 (Fig. 4-3). The E-E

combination is used by FC-1 in nonlinear electronic models.

Simple problems of the type similar to (*) can be solved directly. In such cases the FC-1 is combined with the follow-up system as shown in diagrams A-D of Fig.9-2, i.e., the block m of diagram A is replaced with a suitable FC-1, and the follow-up system provides either an amplified input-signal, specifies this signal at a distance, or in case of different pickups, it changes the physical magnitude of the control-signal in accordance with the design of the pickup.

With such an arrangement, the dynamic part of the conversions is effected by a linear follow-up system, while the FC-1 provides only the specified static conversion (*).

In case the function performed by the FC-1 requires a further conversion of the physical magnitude or a further amplification of power, the follow-up system is to be installed after the FC-1. Then, at the output of the FC-1 only a more complex control-signal is received by the follow-up system, but its dynamics are to be investigated by linear methods, as before.

B. METHOD OF INVERSE FUNCTIONS

The method of inverse functions is illustrated by the diagrams of Fig. 9-2, a-d. If the coefficient of the direct channel is large, the operator transfer function of the feedback is transformed into a reciprocal or inverse operator transfer function of the system:

$$\Phi(P) = \frac{1}{W_{o.c}(P)} = H\,[W_{o.c}(P)].\qquad (**)$$

The right part of equation (**) made use of also of the designation H for the neutralizing operation (see Table 5-1) which, for linear constant operators, coincides with the inverse operator transfer function.

The method of inverse functions is also generally used in functional conversions. Really, if the component −1/m of the feedback in Fig. 9-2,a is replaced by a FC-1 with a conversion function of $Z = F(x_{in})$, the unbalance of the system will be determined by equation:

$$x_0 = x_c - z = x_c - F(x_{out}).$$

With an astatic direct channel under steady condition we have $x_0 = 0$, and we obtain at the output of the system as whole

$$x_{out} = M \; F(x_{out}). \qquad (9-5)$$

Here, the right side for neutralizing the given function $F(x)$ provides an inverse function, as for example, for $\sin x \longrightarrow$ arc $\sin z$, etc.

Certain systems which operate by the method of inverse functions are shown in figs. 9-9 and 9-10.

1. AUTOMATIC TACHOMETER

The other features of diagram 5-4,a are shown with more details in Fig. 9-9,a. The direct channel of the system includes an output-shaft connected with a transmission ratio of $k_d = 1/2$ to the gears of the measuring unit (a differential) and a screw combined with a nut having a pitch h, which determines the transmission ratio of the screw

$$k_s = h/2\pi$$

and the overall transmission ratio of the direct channel

$$k_{tr} = h/4\pi = k_d k_s$$

The disk of the friction integrator located in the feedback rotates with a constant speed Ω_M which determines the operator transfer function of the integrator from l (the displacement of the roller with r_0 as its radius, or the input) to the angle of the roller's rotation (output)

$$W_1(p) = \Omega_M/r_0 p$$

Both the roller and the measuring differential have a transmission ratio of 1; therefore, the overall operator transfer function of the feedback is:

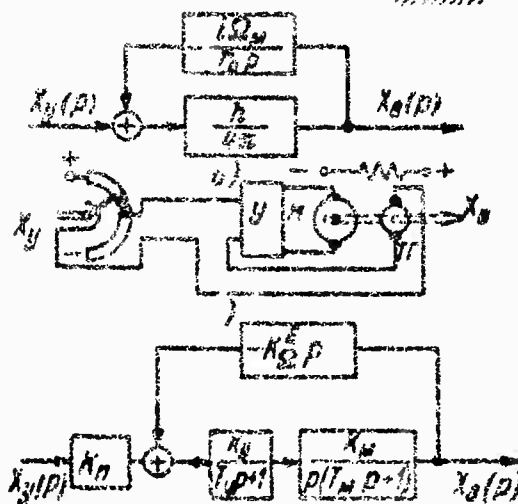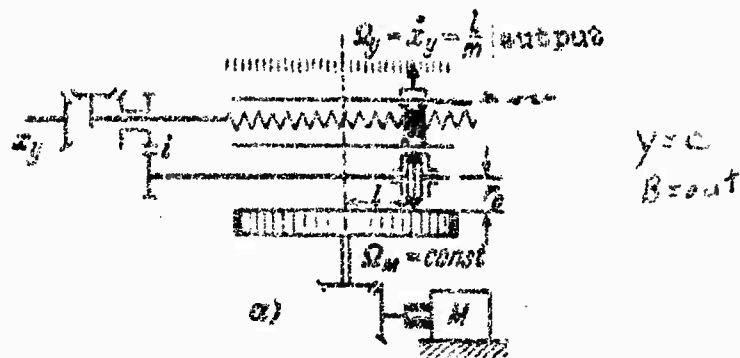$$W_{oc}(p) = \frac{i\Omega_u}{r_s p}. \qquad (9-6a)$$

Fig. 9-9. Diagrams illustrating the transmission
by the method of inverse functions

The closing of the loop by a negative feedback, as in
diagram b, yields the overall operator transfer function of
the automatic tachometer

$$\Phi(p) = \frac{k_n}{1 + k_n W_{o.c}(p)} = \frac{h r_o p}{4 \pi r_o p + h \Omega_M}, \quad (9.6b)$$

With the roller rotating at a constant speed of Ω_{e0}, the input, i.e., the control signal will be represented as follows:

$$X_y(p) = \frac{\Omega_{y0}}{p^2};$$

the output-value (the nut or roller displacement) will have the following representation:

$$L(p) = X_y(p)\Phi(p) = \frac{hr_a\Omega_y}{p\left(4\pi r_a p + hi\Omega_M\right)}$$

and the stabilized operating conditions of the system will be found from equation (3-53) as:

$$l_{yeT} = \lim_{t \to \infty} l(t) = \frac{r_b}{i\Omega_M}\cdot\Omega_{y0}. \qquad (9\text{-}6c)$$

Therefore, if a linear scale is used to mark the position of the nut of the automatic tachometer, it will also measure the rotary speed of the input-roller with a scale $m = \frac{r_b}{i\Omega_M}$, determined by the right side of equation (9-6c).

Since the operator transfer function (9-6b) corresponds to a real differentiating component, therefore, the reading with an accuracy of one percent can be accomplished only at the lapse of $4.6T$, where the time constant T is related to the parameters of the tachometer by the following relationship:

$$T = \frac{4\pi r_a}{hi}. \qquad (9\text{-}6d)$$

The actual operator transfer function of the system (9-6b) can come near the feedback operator transfer function (9-6a), only when the gain factor of the direct channel is infinitely large.

2. INTEGRATING DRIVING SYSTEM

The automatic control system shown in the electrical circuit of Fig. 9-9,c has a measuring unit consisting of different elements, since the input-voltage is formed on the potentiometer with a transfer ratio of $K_u = U_p/X_{max}$, while the feedback-voltage is formed on the tachogenerator with an operator transfer function $W_{fb}(p) = K_2^E p$. The direct channel consists of an amplifier with a gain factor K_{am} and T_{am} as its time-constant, and of a drive with an operator transfer function $W_{m}(p) = K_m/p(p_m p+1)$. The block-diagram 6 has been drawn with the electrical circuit c as a basis. If the value of the unbalance is small, we have a close coincidence between the representations $K_u X_{in}(p) \approx$ $\approx K_2^E X_{out}(p)$, from which the approximate operator transfer function of the entire system is:

$$\frac{X_o(p)}{X_i(p)} \approx \frac{K_n}{K_2^E p}$$

(9.7)

i.e., the system has integration properties, and a definite speed can be assigned to the output-shaft by placing the input-shaft in different positions and, due to the presence of feedback, the speed is little affected by disturbance.

3. ARC SINE CONVERTER

Fig. 9-10,a illustrates the automatic adjustment of the input voltage with a sine FU-1 [single-input functional converter] introduced in form of a cam between the motor shaft and the potentiometer of the feedback. Let us read the angle of rotation of the cam as the angle between the point corresponding to the apogee and the perigee; on the drawing it is $\varphi = 90°$. With an eccentricity a with respect to driving worm gear, the cam displaces the potentiometer wiper of the feedback by a distance $2 \cdot e \sin$ from the center. If the maximum voltage taken off the potentiometer .... and the transmission ratio between the cam and the motor-shaft is 1, the overall feedback voltage will be:

$$U_{\text{o.c}} = U_n \sin i x_{\text{в}}. \qquad (9\text{-}8a)$$

Comparing it with the input-voltage when the unbalance is zero, we obtain the static equation:

$$U = U_n \sin i x_{\text{в}}.$$

from which it follows that:

$$x_{\text{в}} = \frac{1}{i} \arcsin \frac{U}{U_n}, \qquad (9\text{-}8b)$$
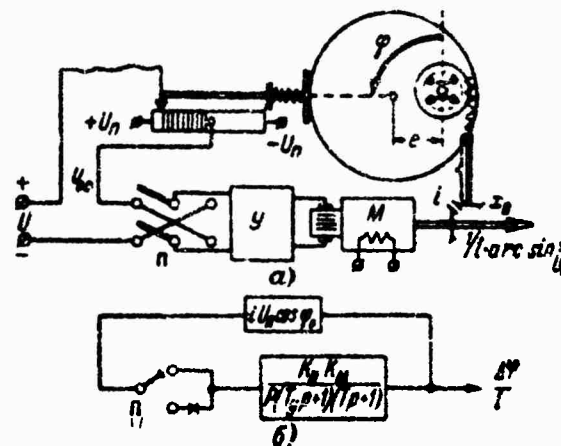
which corresponds to the general equation (9-5).

Fig. 9-10. Electromechanical and block diagrams
of an arc sine converter built by the
method of inverse functions

A block-diagram for this automatic control system can be obtained only if it is based on the principle of linearization. For this purpose we assign to the input a specific

value U_s and calculate for it the corresponding output from the following equation of the statics:

$$x_{pc} = \frac{1}{T} \arcsin \frac{U_s}{U_n}$$

The feedback is linearized as in equation (1-26) near the point corresponding to the solution and is reduced to the fixed transfer ratio:

$$K_{pc} = TU_n \cos Tx_{s.o} = TU_s \cos \varphi_o$$

The direct channel has the amplifier and the motor with a linear operator transfer function and, together with the feedback, it forms the block-diagram 9-10,b. It should be classified as a method of stabilization near zero, since the increment-deviation Δx_{out} from zero (for a fixed input) should be for any reason suppressed by the negative feedback. Because the function $\cos \varphi$ changes the sign, in order to retain the sign "minus" for the system, as a whole, it is necessary that in quadrants II and III, the amplification sign in the direct channel should be opposite to the amplification sign in quadrants I and II; a polarity switch P is introduced for this purpose in the direct channel. It is installed in advance in a position which corresponds to the quadrant in which a solution is sought, or it is switched automatically by a cam located at the borders of quadrants I and II and also at the border between quadrants III and IV.

It should be noted that, since the function arc sin z is multiple-valued, the same multiple-valued feature will be retained by the transfer control system equipped with automatic switching, because both the negative sign of the feedback and the stability of the solution are assured for both positions φ and $T-\varphi$. A solution in the spurious quadrants $\varphi + 90°$ and $\varphi + 180°$ will be unstable, because it will make the feedback positive and the motor will move the load into a zone of stable solution. The stability of the solution we have discussed only assures the requirements derived that the overall feedback must have a negative sign. This requirement must be absolutely fulfilled, as it helps to single reliably the summation circuit with its self-adjusting static property; it does not, however, disclose the dynamic properties of the automatic control system, which

a correct commutation reflects only the conditions required to obtain a stable solution. The conditions adequate for this purpose are discussed in Chapter 10.

Of the three examples of the method of inverse functions, this method proves to be better than the direct solution method in a case where the FC-1 with an inverse function is simpler than a direct FC-1, and a load overcome by the motor is present at the output of the system.

C. METHOD OF IMPLICIT FUNCTIONS APPLIED FOR ONE EQUATION

Let the required value z enter the following complex equation:

$$F_1(z, x, y \ldots) + F_2(z, x, y \ldots) + \ldots + F_n = 0, \quad (9\text{-}9a)$$

from which it is impossible, or extremely difficult, to determine z in explicit form. In such a case, the circuit of the transfer control system is built as in Fig. 9-11,a, where all terms of equation (9-9a) are shaped as functional blocks in which the unknown function of z also serves as the input, just as other specified values of x and y, with a corresponding function F_1, F_2, ...F_n serving as the output of each block. The output functions of the blocks are added and, if the the unknown $z \neq z_0$ is incorrectly stated in the equation and causes an error, the overall error is given a reverse sign to control the driver which corrects $\tilde{z}$ until the unbalance is reduced to zero.

Since this method provides an implicit form of solution of (9-9a) for the transfer control system in so far as z is concerned, this method is known as the method of implicit functions.

A transfer control block diagram is obtained by writing equation (9-9a) as a general function

$$F(z, x, u) = 0, \quad (9\text{-}9b)$$

finding   z on the equation   g of the specified
input values of x_0, y_0, and linearizing the conditions for obtaining the error in equation (9-9b) near the fixed point x_0, y_0, z_0:

$$\Delta F = \frac{\partial F}{\partial z}\bigg|_{\substack{x=x_0 \\ u=u_0 \\ z=z_0}} \Delta z = \sum_{i=0}^{n} \frac{\partial F_i}{\partial z} \Delta \qquad (9\text{-}9c)$$

Structure b is obtained by introducing a standard direct channel -- an amplifier and a driver. It coincides with diagram 9-10,b because the method of inverse functions is a specific case of the method of implicit functions. The condition necessary for a stable solution is again represented by the formation of an overall negative feedback. If preference is given to the expanded diagram a, it is necessary for the linearization of all functional blocks to obtain a negative feedback from the sum of the partial derivatives, although the individual partial derivatives may have any sign. For an unstable solution, we will switch the polarity of the direct channel.

The method of implicit functions is also applied in a case when the specified direct solutions are not suitable for the blocks of the transfer control system. Let us examine, for example, a direct problem to obtain an arc tangent for the components specified in form of voltages:

$$\beta = \operatorname{arctg} \frac{U_y}{U_x}. \qquad (9\text{-}10a)$$

The geometrical concept of this problem is illustrated in Fig. 9-11,c where the rectangular coordinates are given as voltages and are used to determine the direction to a point in these coordinates.

The direct solution involves operations which are not convenient to perform, such as division with a quotient varying in the operating zone within $\pm\infty$, and finding the arc tangent with an infinitely varying argument. All these cannot be obtained with the aid of the blocks of the transfer control system and, therefore, it is expedient to change to a solution by the method of implicit functions by transcribing equation (9-10a) which will give us:

$$\operatorname{tg}\beta = \frac{\sin\beta}{\cos\beta} = \frac{U_y}{U_x}$$

or

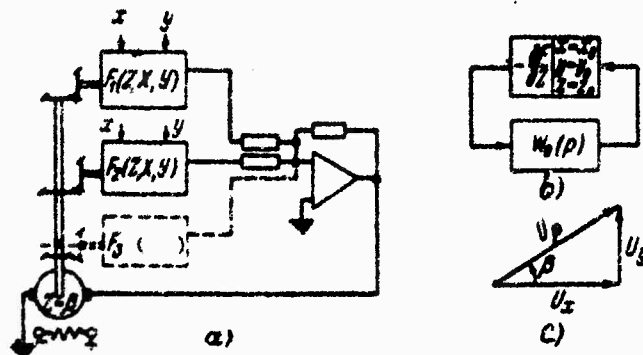$$F(\beta, x, y) = -U_y \cos\beta + U_x \sin\beta = 0. \qquad (9\text{-}10b)$$

Fig. 9-11. Electromechanical and block diagrams
for transfer control systems using the method
of implicit functions of one variable

The diagram is a repetition of Fig. 9-11,a, except
that the blocks F_1 and F_2 are replaced by sine and cosine
potentiometers which are supplied, respectively, by voltages
U_x and U_y with motor β driving the wipers.

The error-voltage is determined by equation (9-10b),
the linearization of which yields the feedback coefficient:

$$\frac{\partial F}{\partial\beta} = U_y \sin\beta + U_x \cos\beta. \qquad (9\text{-}10c)$$

Taking the geometric sum of the voltages outside the
parentheses, we obtain:

$$\frac{\partial F}{\partial\beta} = \sqrt{U_x^2 + U_y^2}\,(\sin^2\beta + \cos^2\beta) = +\sqrt{U_x^2 + U_y^2}. \qquad (9\text{-}10d)$$

Because the feedback sign is always unchanged, a block
correctly built in any of the quadrants will provide the

conditions necessary for stability in all quadrants without taking any other steps. In using such methods, the practice is to pay attention to the gain factor drop along the loop when the geometric sum $\sqrt{U_x^2 + U_y^2}$, is diminishing, because the system becomes less sensitive when this sum approaches zero. This drop is compensated by an amplifier having a variable gain factor introduced in function $U_x - U_y$.

D. METHOD OF IMPLICIT FUNCTIONS APPLIED TO SYSTEMS OF RELATED EQUATIONS

A linear system of two related equations

$$\varphi_1(x, y, f_1) = ax + by + f_1 = 0, \qquad (9\text{-}11a)$$

$$\varphi_2(x, y, f_2) = cx + dy + f_2 = 0 . \qquad (9\text{-}11b)$$

where x and y are unknown and f_1 and f_2 are the specified input-values, is solved by the method of implicit functions with the aid of an electromechanical diagram shown in Fig. 9-12.a. Just as in case of one unknown, each equation is set up by computer elements which, serving as input-values, contain both the specified parameters f_1 and f_2 as well as the unknown x and y. Each equation forms its own closed loop in the circuit of the transfer control system with the outputs consisting of error $\Delta\varphi_1$ for equation (9-11a) and $\Delta\varphi_2$ for equation (9-11b); each error causes one of the follow-up systems to go into action and adjust the value of x,y in order to eliminate the error and bring it nearer to the solution of x,y.

Since after the substitution the system of equations

$$x \rightarrow \tilde{x}, \; y \rightarrow \tilde{y}, \; \varphi_1 \rightarrow \Delta\varphi_1, \; \varphi_2 \rightarrow \Delta\varphi_2.$$

remains linear, therefore, all values undergo a Laplace transformation by taking into consideration the transfer functions of the follow-up systems, results in a new system of equations with the following representation.

$$\Delta \varphi_1(p) W_y(p) = [a\widetilde{X}(p) + b\widetilde{Y}(p) +$$

$$+ F_1(p)] W_y(p) = -\widetilde{Y}(p); \qquad (9\text{-}12a)$$

$$\Delta \varphi_2(p) W_x(p) = [c\widetilde{X}(p) + d\widetilde{Y}(p) +$$

$$+ F_2(p)] W_x(p) = -\widetilde{X}(p). \qquad (9\text{-}12b)$$

This system of equations corresponds to the block-diagram b. Compared with a power-driven control system, the specific features of a transfer control system are that the relation between the channels are specified not by the properties of the automatic control system, but by the designer of the transfer control system. For example, instead of using the accepted method of having error $\Delta \varphi_2$ to excite driver X and error $\Delta \varphi_1$ to excite driver Y, it is possible to re-address the effect of the errors to other drivers; the system of equations (9-12) would then change in the following manner:

$$\Delta \varphi_1(p) W_x(p) = [a\widetilde{X}(p) + b\widetilde{Y}(p) +$$

$$+ F_1(p)] W_x(p) = \widetilde{X}(p); \qquad (9\text{-}13a)$$

$$\Delta \varphi_2(p) W_y(p) = [c\widetilde{X}(p) + d\widetilde{Y}(p) +$$

$$+ F_2(p)] W_y(p) = -\widetilde{Y}(p). \qquad (9\text{-}13b)$$

With the effect of the input actions excluded, these equations correspond to the block-diagram 9-1,d, where the new components (located along the horizontal sides of the central square of the drawing) are enclosed by feedbacks.

As before, a negative feedback is the first necessary condition for the stability of the solution of the system of equations. Now, however, this condition applies to two loops, each corresponding to each of the equations of the

system (9-11). Since the sign of all terms of equations can always be changed simultaneously and arbitrarily, let us agree that our basic form of writing will be one that takes into account the consequent method of solving equations for transfer control systems and, depending on whether the accepted method of solution applies to (9-12) or to (9-13), positive signs will be given to coefficients of the unknown values located simultaneously in the left and right parts of the equations, i.e., to the unknown values which are to be adjusted by the drivers.
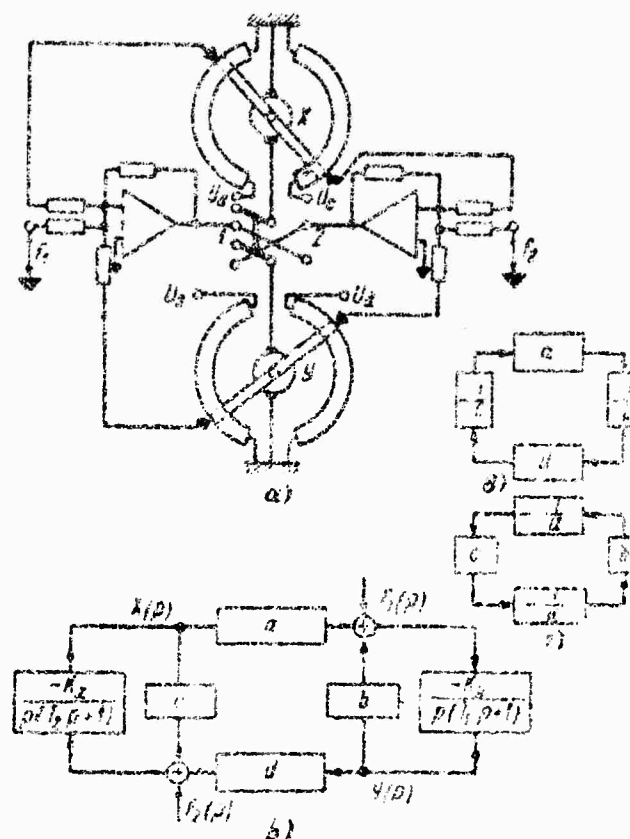
Fig. 9-12. Circuit and block-diagram of transfer control system for solving a system of linear equations containing two unknowns

If the investigation of the automatic control system is confined enly to its own motion, the lines of the input values can be eliminated in Fig. 9-1,e as in diagram b and, if the gain factors of the direct channel sections containing the follow-up systems $W_x(p)$, $W_y(p)$ are large, the over-all transfer functions of the loops can be replaced by the inverse values of the feedback coefficients 1/b, 1/c for equations (9-12) and by 1/a, 1/d for equations (9-13). The The folded block-diagrams of the transfer control system employed for the solution of equations (9-11) by assigning the errors to different drivers are shown in Fig.9-12,c,d.

Multiplying all coefficients contained in the loop, will give us the gain factor of the open system in diagrams c and d:

$$W_2(0) = \frac{ad}{bc} ; \qquad (9\text{-}14a)$$

$$W_1(0) = \frac{bc]}{ad} . \qquad (9\text{-}14b)$$

The second necessary condition for the stability of the solution follows from the analysis of the open system and is reduced to limiting this coeffient to a value not exceeding +1, i.e.,

$$W(0) < +1; \qquad (9\text{-}15a)$$

otherwise it will disrupt the stability of the solution, as shown by the investigation in Chapter 5 with the amplifying component in equations (5-10b and 5-10c) as an example. If $W(0)$ is negative, the inequality (9-15a) will be satisfied at any combination of the coefficients. If $W(0)$ is positive, the second necessary condition for stability of the solution leads to the following censequences:

from equation (9-14a)

$$bc > ad; \qquad (9\text{-}15b)$$

and from equation (9-14b)

$$ad > bc \quad or \quad \begin{vmatrix} ab \\ cd \end{vmatrix} > 0. \qquad (9\text{-}15c)$$

The electrical circuit in 9-12,a is provided with a switch to address the errors in accordance with conditions required by (9-15b) and (9-15c). The general rule for the construction of a commutation circuit can be stated as follows: the product of the feedbacks own coefficients [b,e in (9-12) and a,d in (9-13)] must be larger than the product of the mutual feedbacks.

An analysis of the conditions required for accuracy shows that, even with $W(0) < 1$ which fulfills the second condition for a stable solution at any addressing, it is expedient to change the addressing of the errors with the equations (9-15b) and (9-15c) for the moduli of the coefficients serving as a guide. In addition to commutation measures to provide adequate conditions for stability, this method also requires several measures based on a dynamic analysis (see Ch. 11).

We will now examine the functional system of equations

$$\varphi_1(x, y, f_1) = 0; \qquad (9\text{-}16a)$$
$$\varphi_2(x, y, f_2) = 0. \qquad (9\text{-}16b)$$

The principle of constructing a diagram for the solution of a transfer control system remains the same, but the method of linearization alone provides an adequately simple method of forming the errors. Upon selecting any method of addressing the errors to the drivers, for example, one similar to equations (9-13a) and (9-13b), we will express the equations for the automatic control system in deviations Δx, Δy for a selected point with the solution of x_0, y_0 at f_{10} and f_{20}:

$$\left[\frac{\partial \varphi_1}{\partial x} \Delta X(p) + \frac{\partial \varphi_2}{\partial y} \Delta Y(p) \right] W_x(p) = -\Delta X(p) \quad (9\text{-}17a)$$

$$\left[\frac{\partial \varphi_2}{\partial x} \Delta Y(p) + \frac{\partial \varphi_2}{\partial y} \Delta Y(p) \right] W_y(p) = -\Delta Y(p) \quad (9\text{-}17b)$$

Based on the first necessary condition for stability of the solution, the functions in equations (9-16) are to be always written with signs that will make positive the

— 694 —

partial derivatives of the variable which is adjusted by
the driver to which the error is addressed:

$$\frac{\partial \varphi_1}{\partial x} > 0; \quad \frac{\partial \varphi_2}{\partial y} > 0: \qquad (9\text{-}18)$$

then, the first condition is satisfied due to the negative
sign in the right parts of equations (9-17).

The second condition required for stability of the
solution is written in form of a Jacobian:

$$\begin{vmatrix} \dfrac{\partial \varphi_1}{\partial x} & \dfrac{\partial \varphi_1}{\partial \mu} \\[2mm] \dfrac{\partial \varphi_2}{\partial x} & \dfrac{\partial \varphi_2}{\partial y} \end{vmatrix} > 0. \qquad (9\text{-}19)$$

If the Jacobian is negative, the addressing of the
errors must be changed. As a good example of application
of commutation measures to provide the necessary conditions
for stability of the solution can be served by the task of
plotting a vector with an unknown module ϱ and phase ϑ with
given coordinates X and Y, which is illustrated by the
diagram of Fig. 9-11,c. From this diagram we compose such
equations that will make simple to obtain a solution by the
method of implicit functions:

$$\varphi_y (\varrho, \vartheta, y) = \rho \sin \vartheta - Y = 0; \qquad (9\text{-}20a)$$

$$\varphi_x (\varrho, \vartheta, x) = -\rho \cos \vartheta + X = 0. \qquad (9\text{-}20b)$$

Since the partial derivatives are as follows:

$$\frac{\partial \varphi_y}{\partial \rho} = \sin \vartheta; \quad \frac{\partial \varphi_y}{\partial \vartheta} = \rho \cos \vartheta;$$

$$\frac{\partial \varphi_x}{\partial \rho} = -\cos \vartheta; \quad \frac{\partial \varphi_x}{\partial \vartheta} = \rho \sin \vartheta,$$

and it is assumed that the error in equation a is to be
addressed to driver ρ and the error in equation b -- to
driver β , therefore, the equations (9-20) are written so
as to comply with the rule of signs for the first quadrant.
The Jacobian system of equations (9-20) made up from the
calculated derivatives is reduced to a simple form:

$$\begin{vmatrix} \sin\beta & \rho\cos\beta \\ -\cos\beta & \rho\sin\beta \end{vmatrix} = \rho(\sin^2\beta + \cos^2\beta) = \rho.$$

The polarity of one or of both drivers should be
changed in quadrants II, III, and IV to obtain again a
similar Jacobian.
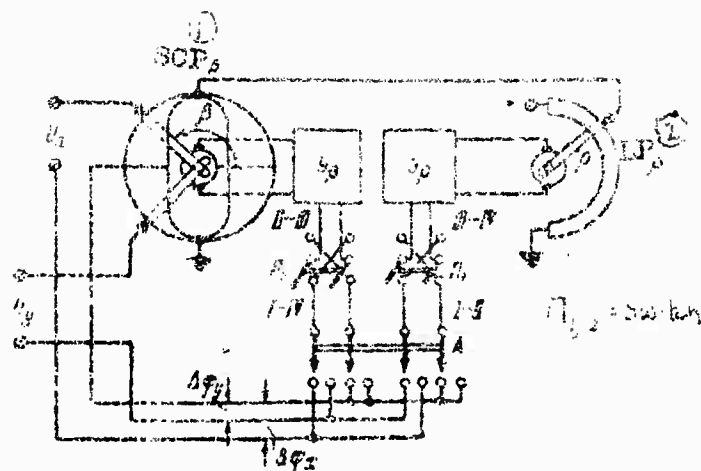
Fig. 9-13. Circuit of transfer control system
for solving the problem of plotting
a vector with given coordinates

key: 1) Sine-cosine potentiometer; 2) linear
potentiometer.

Since the modulus of the vector is always positive,
therefore, the accepted addressing of the errors can be
retained for all four quadrants.

Fig. 9-13,a shows an electromechanical diagram of a
transfer control system for equations (9-20), where the

input rectangular coordinates of the vector are given in
form of voltages proportional to their geometric dimensions,
while the sought ρ and β are in form of proportional to
them angles of rotation of the driver shafts. The linear
potentiometer LP_ρ supplies a voltage proportional to ρ and
the voltages proportional to the products of $\rho\sin\beta$ and
$\rho\cos\beta$ are taken off the wipers of the sine-cosine potent-
iometer SCP_β. The switches SW_1 and SW_2 are provided for
commutation of the inside loops when the signs change for
the coefficients in the quadrants; these switches are
similar to the switch shown in Fig. 9-10. The diagram
shows the numbers of the quadrants in which the negative
feedback is retained when the switches SW_1 and SW_2 are at
their lower position, also the numbers of the quadrants in
which, due to the change of sign of the feedback, it is
necessary to move the switches into the upper position.

A similar constant-addressing system, however, will
have a variable amplification in the inside feedback loops,
with a module varying from zero to unity according to the
variation of the sine and cosine coefficients. A small
amplification along the loop, as illustrated in ch.5, will
make the disturbance to produce a large effect on the
automatic control system, i.e., to the appearance of large
errors in the solution. In order to confine the harmonic
part of the gain factor to $1 - \frac{V^2}{5}$, it is expedient to
re-address the errors in the middle quadrants, i.e. at
angles equal to:

$$\beta = 45^\circ (2n + 1)$$
$$n = 0, 1, 2, 3.$$

An additional commutation device shown in Fig. 9-13
in form of switch A is provided to effect the re-addressing.
If the re-addressing of the errors complies with the condit-
ions required for accuracy, the position of the switches
SW_1 and SW_2, which provide the first necessary condition
for a stable solution, must be again calculated according
to the sign of the inside feedback loops. The results of
the calculations are presented in the table.

Table 9-1

Switching in coupled follow-up systems required to
comply with conditions for stability and accuracy

zone of β	address and polarity
$-45°(+315°)-+45°$	$+\Delta\varphi_x \to \beta;\quad -\Delta\varphi_y \to \varphi$
$+45°-135°$	$+\Delta\varphi_x \to \beta;\quad +\Delta\varphi_y \to \beta$
$+135°-225°$	$-\Delta\varphi_x \to \beta;\quad +\Delta\varphi_y \to \varphi$
$+225°-315°(-45°)$	$-\Delta\varphi_x \to \beta;\quad -\Delta\varphi_y \to \beta$

Since the switching in all commutations take place as
functions of angle β, it is performed automatically with a
so-called quadrant-switch. The complex commutation which
has been analysed is applied in cases where the load on the
supply-voltages U_x and U_y is inadmissible.

Commutation measures do not remove the necessity of
dynamic checking whether the conditions for stability are
adequate by using the methods described in Chapter 11. A
similar method of analysis can be also used for systems of
three equations which are encountered by computers /5/.

D. UNCOUPLING FOLLOW-UP SYSTEM FOR
SOLVING SYSTEMS OF EQUATIONS

Complex commutation measures similar to those analysed
above can be avoided by isolating from the overall signals
which control the drivers only that component which has to
do with the deviations from the solution (of the root) of
the unknown which is adjusted by the given driver.

Let us write the general form for the equations of
the unbalance.

$$\Delta \varphi_1 = \frac{\partial \varphi_1}{\partial x} \Delta x + \frac{\partial \varphi_1}{\partial y} \Delta y; \qquad (9\text{-}21a)$$

$$\Delta \varphi_2 = \frac{\partial \varphi_2}{\partial x} \Delta x + \frac{\partial \varphi_2}{\partial y} \Delta y. \qquad (9\text{-}21b)$$

Solving this system with respect to Δx and Δy, we obtain:

$$\Delta x \begin{vmatrix} \dfrac{\partial \varphi_1}{\partial x} & \dfrac{\partial \varphi_1}{\partial y} \\[2mm] \dfrac{\partial \varphi_2}{\partial x} & \dfrac{\partial \varphi_2}{\partial y} \end{vmatrix} = \Delta \varphi_1 \frac{\partial \varphi_2}{\partial y} - \Delta \varphi_2 \frac{\partial \varphi_1}{\partial y} = k_1 \Delta x; \qquad (9\text{-}22a)$$

$$\Delta y \begin{vmatrix} \dfrac{\partial \varphi_1}{\partial x} & \dfrac{\partial \varphi_1}{\partial y} \\[2mm] \dfrac{\partial \varphi_2}{\partial x} & \dfrac{\partial \varphi_2}{\partial y} \end{vmatrix} = \Delta \varphi_2 \frac{\partial \varphi_1}{\partial x} - \Delta \varphi_1 \frac{\partial \varphi_2}{\partial x} = k_2 \Delta y. \qquad (9\text{-}22b)$$

Fig. 9-14 indicates the conditions required to transform the unbalance-voltages by multiplying them by respective coefficients and by addition. Multiplication, of course, requires special block, for example, potentiometers and other devices. Complete uncoupling of an automatic control system is obtained by realizing accurately the calculated coefficients which enter the equations (9-22) and generally is assured only for small deviations.

Averaging the coefficients and maintaining them as constants simplifies the method but results only in a partial uncoupling. Adequately simple methods of uncoupling are obtain by solving the problem of plotting a vector by the compensation method. In this case the unbalances must undergo sine-cosine transformations, just as the adjusted values, which makes it possible to apply homogeneous transformations for the method.

The principles governing the uncoupling have been demonstrated by computing devices and can be also employed for certain coupled automatic control systems.
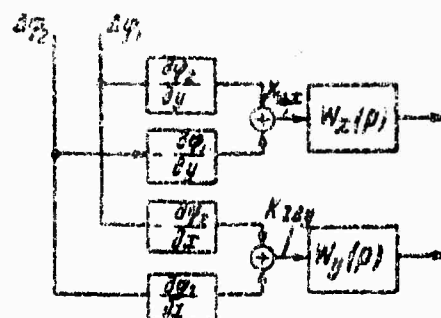
Fig. 9-14.   Section of block-diagram illustrating
conditions for transforming unbalances to
eliminate inter-coupling in two-channel
automatic control systems

BIBLIOGRAPHY

1. Krasovskiy, A.A.- O dvukhkanal'nykh sistemakh
avtomaticheskogo regulirovaniya s antisimmetrichnymi svya-
zami (On two-channel automatic control systems with anti-
symmetrical coupling), Avtomatika i telemekhanika (Auto-
tomation and Remote Control), 1957, No 2.

2. Khokhlov, A.F. - Teoriya i tekhnicheskoye prime-
neniye avtomaticheskikh ustroystv (Theory and technical
application of automatic devices), Mashgiz, 1959.

3. Iosif'yan, A.G., Kagan, B.M., and Sheremet'yevskiy,
N.M. - Teoriya amplidino-sel'sinnoy sinkhronno-sledyashchey
sistemy (Theory of amplidyne-selsyn synchronous follow-up
system), Elektrichestvo (Electricity), 1946, No 3.

4. Dobrogurskiy, S.O., Titov, V.K., and Kazakov, V.
A. - Schetno-reshayushchiye ustroystva (Computing devices),
Oborongiz, 1959.

5. Presnukhin, L.N., Seretrovskiy, L.A., and Yudin,
D.B. - Osnovy teorii i proyektirovaniya priborov upravleniya
(Fundamentals of the theory and design of control devices),
Oborongiz, 1960.

ANALYSIS AND SYNTHESIS OF LINEAR CONTINUOUS CONTROL SYSTEMS

Chapter 10

pp 257 - 297   PRECISION OF FORCED MOTION

10-1. General Definition of Forced Motion and its Errors

Output motion arises in control systems as a consequence of input signals, such as program data x_y and disturbances $y_1, y_2, \ldots, y_1$. Transmission of the signal from the input to the output takes place in accordance with transfer functions which vary for the program input and for each disturbance with different application points.

We denote by

$\Phi(p)$ the basic control signal transfer function;

$\Phi_i(p)$ the disturbance effect function.

Let us in the first place examine forced motion in control systems since when designing them their basic structure is determined precisely by the assigned relation between the program signal and the forced output motion component. The present Chapter deals with these problems.

The proper motion of control systems is investigated in the following Chapter where we also expound the methods for reducing its effect on the system's steady-state operation. This enables us to discuss forced motion problems separately.

Forced output motion of control systems is defined
according to a general procedure described in Chapter 3.
It consists in expanding OTF in series near the point
p = 0 and accounting for a specific number of input
derivatives. For the program input and the transfer
function corresponding to it, the formula for forced
motion takes the form: $x_{out}(t) = \Phi(0) x_{in}(t) + \Phi'(0) \dot{x}_{in}(t) +$

$$+ \frac{\Phi''(0)}{2!} x(t) + \dots \quad (10\text{-}1a)$$

Forced response to any disturbance is defined in
a like fashion: $x_{bi}(t) = \Phi_i(0) y(t) + \Phi'_i(0) \dot{y}_i(t) +$

$$+ \frac{\Phi''_i(0)}{2!} \ddot{y}_i(t) + \dots \quad (10\text{-}1b)$$

The transfer functions $\hat{\Phi}(p)$ and $\hat{\Phi}_i(p)$ used in the
formulas above are real transfer functions for control
systems and are defined in a general form as relations
of operator polynomials

$$\Phi(p) = \frac{\varkappa_m p^m + \dots + \varkappa_1 p + \varkappa_0}{\mu_n p^n + \dots + \mu_1 p + \mu_0}, \quad (10\text{-}2)$$

where the number of terms depends on the complexity of
the system.

In the synthesis of control systems one usually
knows the desired or standard transfer function which
determines the prescribed character of the conversion
of $\hat{\Phi}(p)$.

There exist various conversion problems for program
signals. Below we cite some of them together with the
corresponding standard transfer functions.

702

① Задача копирования: $\Phi_s(p)=1$;

② задача изменения масштаба:
$$\Phi_s(p)=m;$$

③ задача дифференцирования:
$$\Phi_s(p)=p;$$

④ задача интегрирования: $\Phi_s(p)=\dfrac{1}{p}$;

⑤ задача линейного упреждения:
$$\Phi_s(p)=1+\tau_y p;$$

⑥ задача параболического упреждения:

$$\Phi_s(p)=1+\tau_y p+\frac{\tau_y^2}{2!}p^2$$

(10-3)

Key: 1) reproduction problem; 2) scale conversion
problem; 3) differentiation problem; 4) integration
problem; 5) linear lead problem; 6) parabolic lead
problem.

The difference between the real and standard
transfer functions brings about the program conversion
error. To determine this error we introduce the <u>con-
cept of the error transfer function</u>:

$$\Phi_s(p)=\Phi(p)-\Phi_s(p). \qquad (10\text{-}4a)$$

As a rule, for disturbances the desired influence
function equals zero since any disturbance is bound to
additionally distort the real conversion of the program
signal:

$$\Phi_{ei}(p)=\Phi_i(p)-0=\Phi_i(p). \qquad (10\text{-}4b)$$

Thus the control system error consists in a
disparity between the real and standard transfer
functions for the program which brings about a non-
zero error transfer function, and disturbances acting
through non-zero disturbance transfer functions. In

703

accordance with the above, the general expression for the error takes the following form:

$$E_z(p) = \Phi_s(p) X_m(p) + \sum_{i=1}^{n} \Phi_i(p) Y_i(p). \quad (10\text{-}5a)$$

We expand the right-hand side of this formula in the series (10-1) and find:

$$\varepsilon_z(t) = \Phi_s(0) x_{in} + \Phi'_s(0) \dot{x}_{in} + \frac{\Phi''_s(0)}{2!} \ddot{x}_{in} + \ldots;$$
$$\ldots + \sum_{i=0}^{n} \left[\Phi_i(0) y_i + \Phi'_i(0) \dot{y}_i + \frac{\Phi''_i(0) \ddot{y}_i}{2!} + \ldots \right]. \quad (10\text{-}5b)$$

The coefficients for the controlled quantities and their derivatives in the right-hand side of the formula obtained are called error coefficients.

As an example let us investigate the errors in the conversion of a control signal by a real differentiator with a transfer function $\Phi(p) = mp/(Tp + 1)$ for a standard OTF $\Phi_s(p) = mp$. In this case the error transfer function and its derivative in zero are

$$\Phi_s(p) = \frac{mp}{Tp+1} - mp = -\frac{mTp^2}{Tp+1};$$
$$\Phi_s(0) = 0; \quad \Phi'_s(0) = 0;$$
$$\frac{\Phi''_s(0)}{2} = -mT; \quad \frac{\Phi'''_s(0)}{3!} = mT^2,$$

and the differentiation error takes the form of the following series

$$\varepsilon(t) = m(-T\ddot{x}_{in} + T^2\dddot{x}_{in} - \ldots).$$

Conversion systems operating by inversion of the negative feedback OTF $K_{fb}(p)$ (Fig. 5-5b and 9-2) have a standard OTF $1/K_{fb}(p)$ and a real OTF $W(p)/(1+W(p)K_{fb}(p))$, the conversion error OTF amounting to

$$\Phi_s(p) = \frac{W(p)}{1+W(p)K_{fb}(p)} - \frac{1}{K_{fb}(p)} = \frac{-1}{1+W(p)K_{fb}(p)}. \quad (10\text{-}6)$$

By expanding the OTF obtained in a series it is possible to evaluate the conversion errors which depend on the input signal derivatives.

Table 10-1 gives the values of the error transfer function computed by formula (10-4) for the general expression of the real transfer function (10-2) and particular forms of standard transfer functions (10-3). The third column gives the conditions for the reduction to zero of the first term of forced error. These conditions amount to selecting two or three minor coefficients of the transfer function and are in most cases easily realizable when designing or adjusting control systems.

Below will be given the conditions for compensating the higher-order terms of the error series for a particular case. In the meantime let us look into the analysis of the lowest term.

The coefficient $\Phi_\varepsilon(0)$ is a factor of proportionality between input signal and error. If it is not equal to zero, then the error increases linearly as the input signal increases.
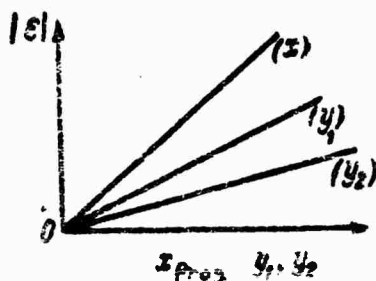
Fig. 10-1. Chart of static errors proportional to control signal x_c and disturbances y_i.

Table 10-1

Error Transfer Functions of Conversion Systems Expressed by OTF Coefficients of a Closed Loop Control System

(1) Standard transfer function	(2) Error transfer function	(3) Conditions for compensating the first term of error $\theta_q(0) = 0$
1	$\dfrac{\ldots(a_1 - \mu_1)p + a_0 - \mu_0}{\ldots \mu_1 p + \mu_0}$	$a_0 = \mu_0$
m	$\dfrac{\ldots(a_1 - m\mu_1)p + a_0 + m\mu_0}{\ldots \mu_1 p + \mu_0}$	$a_0 = m\mu_0$
p	$\dfrac{\ldots(a_1 - \mu_0)p + a_0}{\ldots \mu_1 p + \mu_0}$	$a_0 = 0$
$\dfrac{1}{p}$	$\dfrac{\ldots(a_0 - \mu_1)p - \mu_0}{(\ldots \mu_1 p + \mu_0)p}$	$\mu_0 = 0$ $a_0 = \mu_1$
$1 + p\tau$	$\dfrac{\ldots(a_1 - \mu_1 - \tau\mu_0)p + a_0 - \mu_0}{\ldots \mu_1 p + \mu_0}$	$a_0 = \mu_0$
$1 + p\tau + \dfrac{\tau p^2}{2}$	$\dfrac{\ldots(a_1 - \mu_1 - \tau\mu_0)p + a_0 - \mu_0}{\ldots \mu_1 p + \mu_0}$	$a_0 = \mu_0$

Key: 1) standard transfer function; 2) error transfer
functions; 3) conditions for compensating the first
term of error $\theta_q(0) = 0$.

Figure 10-1 shows the error modulus variation curves
for the reaction of an input signal such as a program
or a disturbance. With a steady program input, in-
creased disturbance brings about a drop in the output
quantity (since the errors have prevailingly a negative
sign), for example, the slowing down of an electric

motor with increasing load torque. Such characteristics are called static characteristics, and the control systems with $\Phi_1(0) \neq$ or $\Phi_z(0) \neq 0$ are said to have static disturbance or program signals. If the first term of the series of an error transfer function of a program or disturbance equals zero $[\Phi_z(0) = 0$ or $\Phi_1(0) = 0]$, then there is no staticism and the control system is said to be an astatic system of the first, second or ν -th order depending on the number of terms equalling zero. The number ν is said to be the astatic order of the control system.

In order that function $\Phi_z(p)$ or its derivatives equal zero when substituting $p = 0$, it is obviously necessary that the OTF of the error have a zero root of the multiplicity factor , i.e., that it be reduced to the form

$$\Phi_{\varepsilon}(p) = \frac{V_\nu(p)}{M(p)} p^\nu, \tag{10-7a}$$

where $V_\nu(0) \neq 0$ and $M(0) \neq 0$.

In this case, according to formula (3-56)

$$\left.\begin{aligned} &\Phi_{\varepsilon}^{(k)}(0) = 0; \quad k = 0, 1, 2 \ldots \nu - 1; \\ &\frac{\Phi_{\varepsilon}^{(\nu)}(0)}{\nu!} = \frac{V_\nu(0)}{M(0)} = \frac{v_\nu}{\mu_0} ; \\ &\frac{\Phi_{\varepsilon}^{(\nu+1)}(0)}{(\nu+1)!} = \left[\frac{V_\nu(p)}{M(p) p} - \frac{V_\nu(0)}{M(0) p}\right]_{p=0} = \\ &= \frac{\mu_0 v_{\nu+1} - \mu_1 v_\nu}{\mu_0} \quad \text{etc.} \end{aligned}\right\} \tag{10-7b}$$

Thus, the exponent ν in formula (10-7a) which defines the number of terms equalling zero in the error series, i.e., the astatic order of the control system, is equal

707

to the multiplicity factor of the zero root of the numerator (zero) in the error OTF.

Generally speaking, one and the same control system may have a different astatic order for the control signal and for the disturbances applied at different points of the block diagram.

A like analysis can be carried out also for the disturbance transfer function (10-4b) if in the control system we use, e.g., the principle of disturbance control with different-parallel circuit compensation 5-7,b. In this case the OTF for the error from the i-th disturbance amounts to

$$\Phi_{ei}(p) = [\Pi(p) - \Pi(p)]\Phi_i(p). \qquad (10\text{-}8a)$$

The astatic order required is obtained by function $\Phi_i(p)$ analyzed like (10-7), or by the difference $\Pi(p) - \Pi(p)$ if it contains operators. Condition

$$\Pi(0) - \Pi(0) = 0 \qquad (10\text{-}8b)$$

turns the system into an astatic one after the i-th disturbance. In this case, however, we should consider the possibility of the appearance of a static error in the control system because of the instability of the parameters of channels $\Pi(0)$ and $\Pi(0)$.

Let channel Π be unstable. We write the relation between the transfer coefficient $\Pi(0)$ of this channel and some primary parameters α, β, γ (e.g., temperature, pressure, insulation conditions, etc.):

$$\Pi = f(\alpha, \beta, \gamma).$$

in which case with variations (instabilities) of these

parameters $\Delta\alpha$, $\Delta\beta$, $\Delta\gamma$ total instability of the transfer
coefficient on the basis of general precision theory
$\begin{bmatrix} 2 \end{bmatrix}$ is

$$\Delta\varLambda = \frac{\partial f}{\partial a}\,\Delta a + \frac{\partial f}{\partial \beta}\,\Delta\beta + \frac{\partial f}{\partial\gamma}\,\Delta\gamma$$

and the static value of disturbance influence function is

$$\Phi_{ai}(0) = \left(\frac{\partial f}{\partial a}\,\Delta a + \frac{\partial f}{\partial \beta}\,\Delta\beta + \frac{\partial f}{\partial\gamma}\,\Delta\gamma\right)\Phi_i(0). \quad (10\text{-}8c)$$

Thus we have outlined three basic classes of control
system errors:

Errors in the transmission of the control signal
due to OTF deficiencies, i.e., because of its deviation
from standard OTF;

Errors from disturbances resulting from a non-zero
disturbance influence function;

Errors from parameter instability or decompensation
in disturbance control circuits.

If the signal engendering the error is harmonic,
e.g., $x_c = \sin\omega t$, then with the aid of the first group
of terms in the right-hand side of formula (10-8b) we
can obtain the expression for the harmonic error in the
form of the following series:

$$A_i \sin(\omega t + \varphi_i) = \left| \Phi_i(0) - \Phi_a''(0)\frac{\omega^2}{2!} + \right.$$
$$\left. + \Phi_a^{(IV)}(0)\frac{\omega^4}{4!}\ldots \right| \sin\omega t + \omega\left[\Phi_i'(0) - \right.$$
$$\left. - \Phi_i'''(0)\frac{\omega^2}{3!} + \Phi_a^{(IV)}(0)\frac{\omega^4}{5!}\ldots \right]\cos\omega t. \qquad (10\text{-}9a)$$

The series of functions $\sin\omega t$ and $\cos\omega t$ correspond
to real parts $P_{\varepsilon}(\omega)$ and imaginary parts $Q_{\rho}(\omega)$ of a complex
transfer function of error $\Phi_{\varepsilon}(j\omega)$:

$$P_i(\omega) = \Phi_i(0) - \Phi_a''(0)\frac{\omega^2}{2!} + \Phi_a^{(IV)}\frac{\omega^4}{4!} - \ldots; \quad (10\text{-}9b)$$

709

$$Q_z(\omega) = \omega \left[\Phi_z'(0) - \Phi_z''(0) \frac{\omega^2}{3!} + \Phi_z^{(V)} \frac{\omega^4}{5!} - \ldots \right] \quad (10\text{-}9c)$$

For infralow frequencies $(\omega \leqslant 1 \text{ sec}^{-1})$ in the series it suffices to use a small number of the first terms when computing the harmonic error for one assigned frequency or in computing the low-frequency part of the complex error spectrum by the general formula

$$E(j\omega) = \Phi_z(j\omega) X_y(j\omega) = [P_z(\omega) +$$
$$+ jQ_z(\omega)] X_y(j\omega). \quad (10\text{-}9d)$$

10-3. Transfer Functions and Connection Equations of Standard Static and Astatic Servomechanisms

A. Classification of OTF of a Standard Servomechanism with Constant Parameters

The diagram of a standard control system (simulator) is shown in Fig. (10-2a).

In various cases of control signal and disturbance transmission analysis, along with the transfer function of the open system $W(p)$ the OTF of the closed system must also be investigated. The designations of these functions and the conditions for obtaining them by means of OTF interconversion are given in Table 10-2.
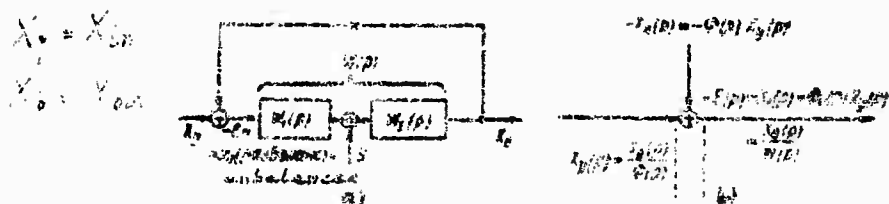
Fig. 10-2. Block diagram of a standard control system and representations of signals on the rays of the basic adder.

The tabular relations are obtained by means of structural transformations and can be easily checked as input adder equations. Figure 10-2,b separately shows the portion of the block diagram a near the adder and gives the designations of signals on the adder rays through the control and output signals.

We introduced in the Table an OTF, $\Phi_*(p)$, called relative OTF since it is equal to the relation between the OTF of a closed and an open system.

The relative OTF for simulators differs from the OTF of error $\Phi_\varepsilon(p)$ only by the sign:

$$\Phi_*(p) = -\Phi_\varepsilon(p); \qquad (10\text{-}10a)$$

in the case of converting systems such a coincidence does not exist.

As we see from Table 10-2 the basic and relative OTF complement each other up to one unit. This simplifies interconversion of corresponding frequency-response characteristics and processes on the output line and the error line.

Thus, for the transient function on the output line $h[t]$ and on the error line $h_\varepsilon[t]$ we have:

$$-h_\varepsilon[t] = 1 - h[t]. \qquad (10\text{-}10b)$$

Similar simple relations can be easily established on the basis of data from Table or Fig. 10-2 between direct and inverted OTF of open and closed systems:

$$\frac{1}{\Phi(p)} = \frac{1}{W(p)} + 1. \qquad (10\text{-}11a)$$

$$\frac{1}{\Phi_*(p)} = 1 + W(p) \qquad (10\text{-}11b)$$

Table 10-2

Relations Between OTF of a Standard Control System
(Simulator)

(1)	OTF sought	(2) OTF included in interconversion formulas			
(2) Name	(7) designation	$\Phi(p)$	$\Phi_x(p)$	$W(p)$	$\Phi \cdot W \cdot \Phi$
(3) basic control signal OTF of closed system	$\Phi(p)$	$\times$	$1 - \Phi_x(p)$	$\dfrac{W(p)}{1 + W(p)}$	$\Phi_x(p) W(p)$
(4) relative OTF	$\Phi_x(p)$	$1 - \Phi(p)$	$\times$	$\dfrac{1}{1 + W(p)}$	$\dfrac{\Phi(p)}{W(p)}$
(5) OTF of open systems	$W(p)$	$\dfrac{\Phi(p)}{1 - \Phi(p)}$	$\dfrac{1 - \Phi_x(p)}{\Phi_x(p)}$	$\times$	$\dfrac{\Phi(p)}{\Phi_x(p)}$
(6) disturbance influence function	$\Phi_v(p)$	$\dfrac{\Phi(p)}{W_x(p)}$	$\Phi_x(p) W_x(p)$	$\dfrac{W_x(p)}{1 + W(p)}$	$\times$

Key: 1) OTF sought; 2) name; 3) basic control signal OTF
of closed system; 4) relative OTF; 5) OTF of open
systems; 6) disturbance influence function; 7) designation;
8) OTF included in interconversion formulas.

$$\frac{1}{W(p)} = \frac{1}{\Phi(p)} - 1 \qquad (10\text{-}11c)$$

These simple relations or tabular formulas enable
us, if instead of the closed system OTF (10-2) we take
the OTF of an open system:

$$W(p) = \frac{U(p)}{V(p)} = \frac{u_m p^m + \cdots + u_1 p + u_0}{v_n p^n + \cdots + v_1 p + v_0}, \qquad (10\text{-}12)$$

to express by coefficients u_j, v_i all of the remaining
OTF and define the conditions for obtaining OTF of the
error (10-10a) with varying astatic order. These con-
ditions for $i = 0$, 1, 2 are tabulated in Table 10-3
which develops the particular result ($\Phi_v = 1$) of the
more general table 10-1.

Table 10-3

Expressions of OTF and Their Limits By Open System. Coefficients U_j, V_j.

① графа	② Порядок астатизма по управляющему воздействию		
	$\nu_y = 0$	$\nu_y = 1$	$\nu_y = 2$
$W(p)$	$\dfrac{U_m p^m + \ldots + U_1 p + U_0}{V_n p^n + \ldots + V_2 p^2 + V_1 p + V_0}$	$\dfrac{U_m p^m + U_1 p + U_0}{V_n p^{n-1} + \ldots + V_2 p^2 + V_1 p}$	$\dfrac{U_m p^m + \ldots + U_1 p + U_0}{V_n p^{n-2} + \ldots + V_2 p^2}$
$W(0)$	$\dfrac{U_0}{V_0} = K_0$	∞	∞
$\lim_{p \to 0} [p^\nu W(p)]$	$\dfrac{U_0}{V_0} = K_0$	$\dfrac{U_0}{V_1} = K_{-1}$	$\dfrac{U_0}{V_2} = K_{-2}$
$\Phi(p)$	$\dfrac{U_m p^m + \ldots + U_1 p + U_0}{V_n p^n + \ldots + (V_m + U_m) p^m + \ldots + V_0 + U_0}$	$\dfrac{U_m p^m + U_1 p + U_0}{V_n p^n + \ldots + (V_1 + U_1) p + U_0}$	$\dfrac{U_m p^m + \ldots + U_1 p_0^2 + U_0}{V_n p^n + \ldots + (V_2 + U_2) p^2 + U_1 p + U_0}$
$\Phi(0)$	$\dfrac{U_0}{U_0 + V_0} = \dfrac{K_0}{1 + K_0}$	1	1
$\Phi_x(p)$	$\dfrac{V_n p^n + \ldots + V_0}{U_n p^n + \ldots + (U_m + V_m) p^m + \ldots + U_0 + V_0}$	$\dfrac{(V_n p^{n-1} + \ldots + V_1) p}{V_n p^n + \ldots + (U_1 + V_1) p + U_0}$	$\dfrac{(V_n p^{n-2} + \ldots + V_2) p^2}{V_n p^n + \ldots + (U_2 + V_2) p^2 + U_1 p + U_0}$
$\lim_{p \to 0} \left[\dfrac{1}{p^\nu} \Phi_x(p) \right]$	$\dfrac{V_0}{U_0 + V_0} = \dfrac{1}{1 + K_0}$	$\dfrac{V_1}{U_0} = \dfrac{1}{K_{-1}}$	$\dfrac{V_2}{U_0} = \dfrac{1}{K_{-2}}$

Key: 1) OTF; 2) Order of control signal astaticism.

713

We can easily see that to obtain ν-th astatic order
for control signals it suffices to have in the direct
path of the control system free integrators (not com-
prised by follow-ups).

Figure 10-3 shows block diagrams a, b with free
integrators in the straight path of the control system,
and diagram c with an integrator enclosed in a negative
follow-up which transforms it into an aperiodic unit
and deprives the circuit of astatic properties ($\nu = 0$)
for control action if the remaining elements of the
direct path are also static.

E. Computing the Gain of Open Control Systems With
   Assigned Constant Error.

Depending on the order of astaticism ν, each system
has only one mode of operation with a constant error. In
fact, if we investigate only the first term of the
right-hand side of formula (10-5a) and substitute into
the OTF of the astatic system (10-7) we have

$$X_y = X_{in} \qquad -E(p) = X_y(p)\,\frac{V_y(p)}{M(p)}\,p^\nu. \qquad (10\text{-}13a)$$

The constant error $\xi_y = \lim_{t\to\infty}\xi_y(t)$ can be found on
the basis of an equivalent transition to limit (5-53)
from formula (10-13a) in the case of a control signal
proportional to the ν-th power of time:

$$X_y(p) = \frac{x_y^{(\nu)}(0)}{p^{\nu+1}} + \cdots \frac{x_y^{(\nu)}(0)}{p^{\nu}}. \qquad (10\text{-}13b)$$

In this case constant error equals

$$-\xi_y = x_y^{(\nu)}(0)\,\frac{V_y(0)}{M(0)}. \qquad (10\text{-}13c)$$
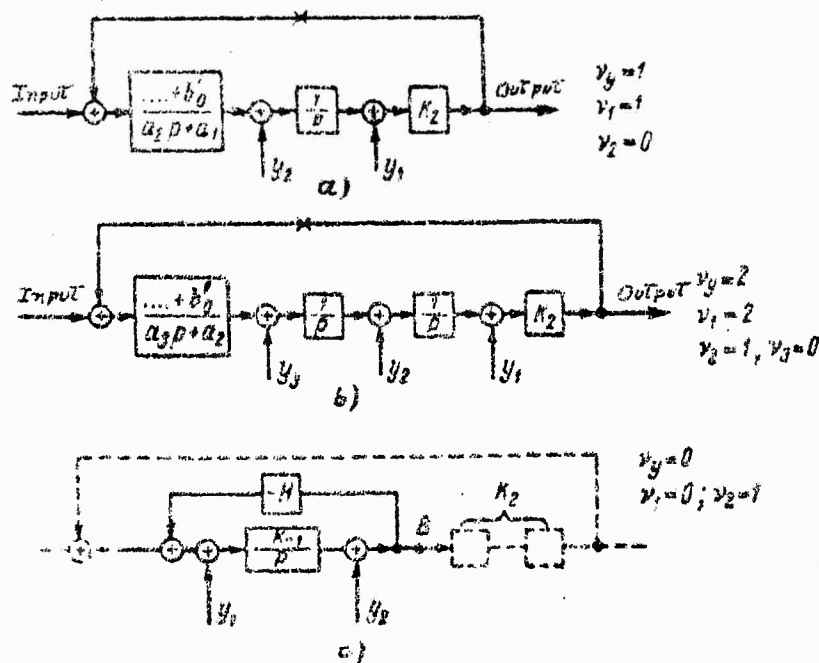
Fig. 10-3.   Systems of varying astatic order for control
signal ν_c and disturbances ν_i.

Passing to a simulator with standard properties
(10-10a), the constant error can be expressed in a
different fashion:

$$X_\gamma = X_{\angle n} \qquad -\varepsilon_\gamma = x_y^{(\nu)}(0)\lim_{p\to 0}\left[\frac{1}{p^\nu}\,\Phi_\varepsilon(p)\right]. \qquad (10\text{-}13d)$$

The limits in the latter formula have been computed
and can be found in the last line of Table 10-3.

If we express $\Phi_\varepsilon(p)$ by the OTF of an open-loop
system we have:

$$-\varepsilon_\gamma = x_y^{(\nu)}(0)\lim_{p\to 0}\frac{1}{p^\nu + p^\nu W(p)} \qquad (10\text{-}14a)$$

For static systems where $\gamma = 0$, constant errors
arise in the case of steady-level step input signals
that equals

$$-\varepsilon_0 = x_{y0}\,\frac{1}{1+W(0)} = \frac{x_{y0}}{1+K_\varepsilon}. \qquad (10\text{-}14b)$$

_715_

In the case of astatic systems, constant error arises under one of the following conditions: constant speed, i.e., uniform starting ($\dot{y} = 1$), constant acceleration ($\ddot{y} = 2$), etc., and is defined by the formula

$$X_y : X_{in} \qquad -\varepsilon_\nu = x_y^{(\nu)}(0) \frac{1}{\lim_{p \to 0}[p^\nu W(p)]} = \frac{x_y^{(\nu)}(0)}{K_{-\nu}} \qquad (10\text{-}14a)$$

The limiting values of $\lim_{p \to 0}\left[p^\nu W(p)\right]$ are given in the third line of Table 10-3. They are equal to the amplification factors of the straight path $K_{-\nu}$, the subscript denoting the dimension $\sec^{-\nu}$; K_0 $\sec^0$ is the static amplification factor; K_{-1} $\sec^{-1}$ is the velocity-error constant; K_{-2} $\sec^{-2}$ is the acceleration error constant.

Constancy of the error brings about the coincidence of all the derivatives of the input and output signals:

$$X_B : X_{out} \qquad x_y^{(k)}(t) = x_{in}^{(k)}(t); \quad k > 0, \qquad (10\text{-}15a)$$

while for static control servomechanisms with step input signals it results in a simple relation between the input and output coordinates:

$$x_{in} = \frac{K_0}{1 + K_0} x_{y0}. \qquad (10\text{-}15b)$$

As a consequence, the constant error can be computed by means of derivatives or coordinates of the input as well as the output processes: $\dot{y}_y = 0$ – the static error

$$-\varepsilon_0 = \frac{x_{in}}{K_0} = \frac{x_{in}}{1 + K_0}; \qquad (10\text{-}16a)$$

$\dot{y}_y = 1$ – the velocity error

$$-\varepsilon_1 = \frac{x_B(0)}{K_{-1}} = \frac{\dot{x}_1}{K_{-1}}; \qquad (10\text{-}16b)$$

$\ddot{y}_y = 2$ – acceleration error

$$-\varepsilon_2 = \frac{\ddot{x}_B}{K_{-2}} = \frac{\ddot{x}}{K_{-2}}, \qquad (10\text{-}16c)$$

motion $|\varepsilon|$ the required amplification factor of the
straight path is computed by the inverted formulas
(10-16) in substituting into them the maximum values
of coordinates and derivatives $x^{(\nu)}$. This corresponds
to the most disadvantageous modes of operation. Thus
we have:

Static amplification constant

$$K_0 = \frac{x_{s\,max}}{|\varepsilon_0|};$$ (10-17a)

Velocity-error constant

$$K_{-1} = \frac{x_{max}}{|\varepsilon_1|}.$$ (10-17b)

Acceleration-error constant

$$K_{-2} = \frac{x_{max}}{|\varepsilon_2|}.$$ (10-17c)

Examples

1. A d-c amplifier with negative feedback with
$R_1/R_0 = 1$, $U_{Bm} = 100$ v, $\varepsilon_U = 0.004$ v. $U_g = \varepsilon_U/2 = 0.002$ v
(see Chapter 7).

$$K_0 = 100/0.002 = 50,000.$$

2. System with one integrator. Peak velocity
$x_m = 0.5$ rad/sec; $|\varepsilon_1| = 0.001$ rad.

$$K_{-1} = 0.5 \text{ sec}^{-1}/0.001 = 500 \text{ sec}^{-1}$$

3. System with two integrators. Maximum accelera-
tion $\ddot{x} = 5$ degrees/sec^2 ; $|\varepsilon_1| = 0.05°$.

$$K_{-2} = 5 \text{ degrees/sec}^2/0.05 \text{ degrees} = 100 \text{ sec}^{-2}.$$

It should be noted that the errors computed take
account only of one, forced component with a specific
law of motion. More complex laws of motion engender
additional errors.

Constant errors of forced motion and amplification

factors of control systems are easily determinable experimentally by measuring the angle, the speed or acceleration in open systems with a constant control signal assigned from outside.

Let us note that when carrying out this test with a closed-loop control system with the aim of determining the constant error of, e.g., a system with an astaticism of second order, we must feed into it an equally accelerated motion generated usually by two cascade-connected integrators - friction integrators (Fig. 5-4a) for mechanical input and integrating amplifiers (Fig. 1-9e) for electric input. Open control systems with astaticism of second order are by themselves generators of equally accelerated motion, for the analysis of which it suffices to have an angular accelerometer.

6. Disturbance Astaticism ν_1

The general analytic definition of astaticism is given by formula (10-7) into which we substitute the OTF for disturbance (10-4b). Let us now define the structural symptoms of disturbance astaticism. We go back to Fig. 10-3 and determine the OTF for disturbances applied at various points of the diagram a, b, c.

Diagram a

$$\Theta_1(p) = \Theta_e(p) K_2 = \frac{a_1 p + a_1}{t_1 + t_1 \gamma \gamma + t_5} K_\mu p.$$

We juxtapose this formula and (10-7) and set:
$\nu_1 = 1$, as well as γ_y:

$$\Phi_2(p) = \Phi_1(p)\frac{K_2}{p} = \frac{a_2 p + a_1}{\ldots(a_1+b_1)p + b_0}K_2,$$

whence $\nu_2 = 0$.

Diagram b

$$\Phi_1(p) = \frac{\ldots a_3 p + a_2}{\ldots b_1 p + b_0}K_2 p^2; \quad \nu_1 = 2 = \nu_y;$$

$$\Phi_2(p) = \frac{\ldots a_3 p + a_2}{\ldots b_1 p + b_0}K_2 p; \quad \nu_2 = 1;$$

$$\Phi_3(p) = \frac{\ldots a_3 p + a_2}{\ldots b_1 p + b_0}K_2; \quad \nu_3 = 0.$$

Diagram c

$$\Phi_1(p) = \frac{K_{-1}K_2}{p + K_{-1}H + K_1 K_2}, \quad \nu = 0, \text{ as well}$$
$$\text{as} \quad \nu_y;$$

$$\Phi_2(p) = \frac{K_2 p}{p + K_1 H + K_{-1}K_2}; \quad \nu_2 = 1.$$

Thus, the order of disturbance astaticism differs
in the general case from that of input signal astaticism
by the control signal: $\nu_y \neq \nu_1$. The presence of in-
tegrators in the straight path may, in the case of a
disadvantageous position of the disturbance application
point turn out to be useless for creating disturbance
astaticism (disturbance y_2 in diagram a, and disturbance

y_3 in diagram b) and, conversely, a control system with a static control signal may turn out to be astatic for disturbances applied inside the integrator (diagram c, disturbance y_2).

We generalize the above results into the following formulation of the structural symptom of astaticism order: the order of disturbance astaticism is equal to the number of integrators only in a negative feedback circuit with a given disturbance and does not depend upon the number of integrators between the disturbance application point and the output where the disturbance error is measured.

This rule holds also for control signals since the point where errors are removed is next to the input adder (see Fig. 10-2) while in the error CTF the entire straight path becomes a feedback circuit.

D. Algebraized and Operator Equations of Open and Closed Control Systems

If the straight path of a control system contains elements with variable parameters then its equation can be written

$$x_3 = x_{out} \qquad v(t, D)\, x_3 = u(t, D)\, x_1. \qquad (10\text{-}18a)$$

In the case of standard feedback shown in Fig. 10-2, we add to (10-18a) the equation of the measuring element

$$
\begin{aligned}
x_y &= x_{in} \\
x_3 &= x_{out}
\end{aligned}
\qquad
- \varepsilon = x_1 = x_y - x_3. \qquad (10\text{-}18b)
$$

Equations (10-18a) and (10-18b) are solved simultaneously and yield a result analogous to (1-102b) but with different designations of ADP coefficients:

$$X_\beta = X_{out} \qquad [u(t,\ D) + v(t,D)]\, x_s = u(t,\ D)\, x_y. \qquad (10\text{-}18c)$$
$$X_y = X_{in}$$

The same convolution is true also for diagrams with constant parameters which yield, in analogy to the algebraized equation (1-77a), the operator equation

$$[U(p) + V(p)]\, X_s(p) = U(p)\, X_y(p). \qquad (10\text{-}18d)$$

In summing ADP in formulas c and d, we sum the coefficients of the left side $v(t, D)$ and right side $u(t, D)$ of the original equation (10-18a). Summary coefficients can be denoted by the new symbol μ_i and determined in the same way as the coefficients in the formula (1-102b):

$$\left. \begin{array}{c} \mu_i(t) = u_i(t) + v_i(t) \quad \text{and} \quad \mu_i = u_i + v_i \\[4pt] \text{for} \quad i \leqslant m; \\[6pt] \mu_{m+k}(t) = v_{m+k}(t) \quad \text{and} \quad \mu_{m+k} = v_{m+k} \\[4pt] \text{for} \quad n > m. \end{array} \right\} \qquad (10\text{-}19)$$

The designations of coefficients u, v, μ different from those in Chapter 1 were introduced to distinguish them from the coefficients of the equations of units (a, c) from which the coefficients for full equations of the system are formed.

The equation for the error is derived from Eq. (10-18a) by substituting

$$x_s = x_y - x_n \qquad (10\text{-}20a)$$

which, by analogy with (1-103b), yields

$$X_1, X_{1s} \qquad [u(t,D)+v(t,D)]\,x_1 = v(t,D)\,x_y. \qquad (10\text{-}20b)$$

For the case of constant coefficients we use formulas (1-72) from which we can easily pass to operator equations:

$$[U(p)+V(p)]\,X_1(p) = V(p)\,X_y(p). \qquad (10\text{-}20c)$$

By expanding the ADP in Eq. (10-20b) considering the summation of coefficients (10-19) we find:

$$v_n(t)\,x_1^{(n)} + \ldots + [v_m(t)+u_m(t)]\,x_1^{(m)} + \ldots +$$
$$+ [v_1(t)+u_1(t)]\,x_1 + [v_0(t)+u_0(t)]\,x_1 = \qquad (10\text{-}20d)$$
$$= v_0(t)\,x_y + v_1(t)\,\dot{x}_y + \ldots + v_n(t)\,x_y^{(n)}.$$

To have an astatic system, i.e., a system yielding zero forced error as a response to a steady input signal $x_y = 1(t)$ it suffices to have $v_0(t) = 0$, hence $\nu_y = 1$. If $v_0(t) = 0$ and $v_1(t) = 0$, then $\nu_y = 2$, and so on.

When the straight path is described by a system of operator equations with respect to the quantities x_{11}, $x_{12}, \ldots, x_{1n} = x_1$ and the input action is taken account of only in the first equation, then by analogy with (5-28) and Fig. 5-19 we find the block diagram shown in Fig. 10-4 and the solution

$$\begin{vmatrix} a_{11}(p) \ldots a_{1n}(p) \\ \cdot\;\cdot\;\cdot\;\cdot\;\cdot\;\cdot\;\cdot\;\cdot \\ a_{n1}(p) \ldots a_{nn}(p) \end{vmatrix} X_s(p) =$$
$$= \begin{vmatrix} a_{11}(p) \ldots b_1(p) \\ \cdot\;\cdot\;\cdot\;\cdot\;\cdot\;\cdot\;\cdot\;\cdot \\ a_{n1}(p) \ldots 0 \end{vmatrix} X_1(p). \qquad (10\text{-}21a)$$

Closing condition (10-18b) will affect in this problem only the first equation, and the coupling equation for a closed control system in operator form can be written:

$$X_y = X_{in}$$
$$X_\beta = X_{out}$$

$$\begin{vmatrix} a_{11}(p) \ldots b_1(p) + a_{1n}(p) \\ \cdots \cdots \cdots \cdots \\ a_{n1}(p) \ldots a_{nn}(p) \end{vmatrix} X_s(p) = \qquad (10\text{-}21b)$$

$$= \begin{vmatrix} a_{11}(p) \ldots b_1(p) \\ \cdots \cdots \cdots \\ a_{n1}(p) \ldots 0 \end{vmatrix} X_y(p).$$

This equation can be rewritten with respect to error $-\mathcal{E} = x_1$:

$$\begin{vmatrix} a_{11}(p) \ldots b_1(p) + a_{1n}(p) \\ \cdots \cdots \cdots \cdots \\ a_{n1}(p) \ldots a_{nn}(p) \end{vmatrix} X_1(p) =$$

$$= \begin{vmatrix} a_{11}(p) \ldots a_{1n}(p) \\ \cdots \cdots \cdots \\ a_{n1}(p) \ldots a_{nn}(p) \end{vmatrix} X_y(p). \qquad (10\text{-}21c)$$

Conditions for compensating the control signal error can be written in the form

$$\begin{vmatrix} a_{11}(p) \ldots a_{1n}(p) \\ a_{21}(p) \ldots a_{2n}(p) \\ \cdots \cdots \cdots \\ a_{n1}(p) \ldots a_{nn}(p) \end{vmatrix} = 0 \qquad (10\text{-}21d)$$

or

$$\begin{vmatrix} a_{11}(p) \ldots b_1(p) + a_{1n}(p) \\ a_{21}(p) \ldots a_{2n}(p) \\ \cdots \cdots \cdots \cdots \\ a_{n1}(p) \ldots a_{nn}(p) \end{vmatrix} = \infty. \qquad (10\text{-}21e)$$

In the following we investigate some characteristic applications of the mathematic result thus obtained.

1. Obtaining zero value for the determinant (10-21d) from the proportionality of elements of operator polynomials in two of its lines.

Suppose the elements of the first and last lines are proportional:

$$\frac{a_{11}(p)}{a_{n1}(p)} = \frac{a_{12}(p)}{a_{n2}(p)} = \ldots = \frac{a_{1n}(p)}{a_{nn}(p)} = c.$$

This means that in the circuit shown by bold lines in Fig. 10-4 the product of OTF of the elements will

723

amount, prior to its closing, to

$$k = -a_{1n}(p)\frac{1}{a_{11}(p)}\left[-a_{n1}(p)\right]\frac{1}{a_{nn}(p)} =$$

$$= \frac{a_{1n}(p)\,ca_{11}(p)}{a_{11}(p)\,ca_{1n}(p)} = +1$$

and after closing

$$\frac{1/a_{11}(p)}{1-k} = \frac{1/a_{11}(p)}{1-1} = \infty.$$

considering the compensation for negative signs in the feedback, OTF between X_{11} and b_1X_1.
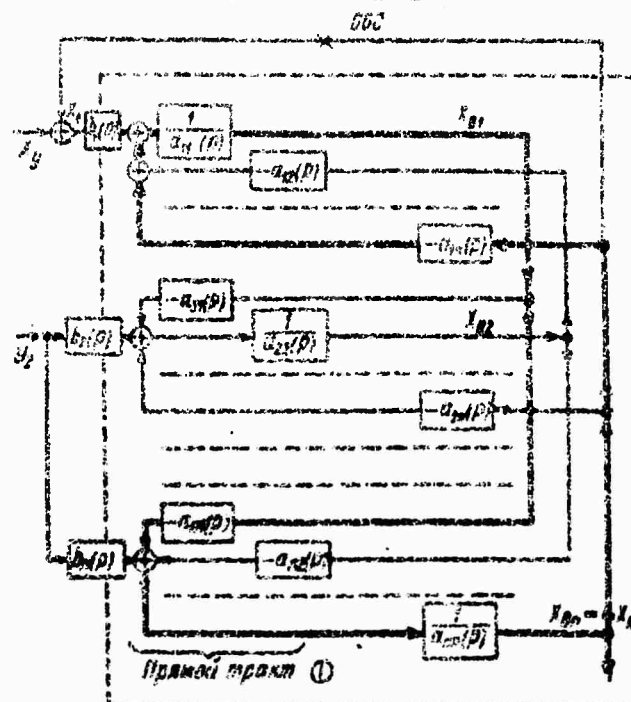
Fig. 10-4. Block diagram of an automatic control system with complex straight path described by a system of equations.
Key: 1) straight path.

Thus, technological measures amount to an infinite increase of the amplification factor of the straight

path on account of local positive feedback.

2. **Obtaining zero value for determinant (10-21d) from the proportionality of elements in two of its columns.**

Suppose the ADP of the first and second column are proportional. We trace in Fig. 10-4 the circuit containing the elements $-a_{12}(p)$, $1/a_{11}(p)$, $-a_{21}(p)$ and $1/a_{22}(p)$. The product of these OTF equals unity, and feedback has a positive sign. After closing we obtain an infinite amplification between signals X_{11} and X_{12}, i.e., a new variant of positive feedback.

3. **Infinite increase of the value of determinant (10-21e).** The same results are obtained with increasing operator polynomial $b_1(p)$, contained in the determinant under investigation, or increasing amplification factor of element $b_1(p)$ in the block diagram in Fig. 10-4.

4. **Astaticism.** If $a_{ik}(p)$ and $b_1(p)$ are operator polynomials and some of them do not contain the lowest terms $p^{\nu-i}$, then p^{ν} is a common multiplier of the higher terms. If such co-factors are common to the entire line or the entire column of determinant (10-21d), then they are taken out from the sign of the determinant and its equality to zero is attained not in the general form but in a steady state for $p = 0$. Inasmuch as the value of the determinant under study coincides with polynomial $V(p)$ of the entire system, astaticism is determined according to formulas (10-7).

If $a_{ik}(p)$ and $b_1(p)$ are operator fractions, i.e., OTF of real units, then to obtain $V(p)$ of the system we

725

must after expansion of the determinants in Eq. (10-31a) reduce them to a common denominator.

Let us now investigate the case of assigning signal Y_2 to two equations of the system, the second and the n-th through the CTF $b_2(p)$ and $b_n(p)$, as shown diagrammatically in Fig. 10-4 and in the analytic form below:

$X_1 = X_{in}$
$X_2 = X_{out}$

$$a_{11}(p)X_{n1} + a_{12}(p)X_{n2} + \ldots + a_{1n}(p)X_{nn} =$$
$$= -b_1(p)X_{nn};$$

$$a_{21}(p)X_{11} + a_{22}(p)X_{12} + \ldots + a_{2n}(p)X_{nn} =$$
$$= b_2(p)Y_2;$$

$$\ldots \ldots \ldots \ldots \ldots \ldots \ldots \ldots \ldots \ldots \ldots \ldots \ldots \ldots \ldots \ldots = 0$$

$$a_{n1}(p)X_{n1} + a_{n2}(p)X_{n2} + \ldots + a_{nn}(p)X_{nn} =$$
$$= b_n(p)Y_2$$

Here the closure condition ($x_1 = -x_{out}$) of the first equation has already been considered. Response to disturbances at the system's output is, in the given case, the error of the system. By substituting $X_{out} = -X_2$ we find the equation

$$
\begin{vmatrix}
a_{11}(p)a_{12}(p)\ldots a_{1n}(p) + b_1(p) \\
a_{21}(p)a_{22}(p)\ldots a_{2n}(p) \\
\ldots \ldots \ldots \ldots \ldots \ldots \\
a_{n1}(p)a_{n2}(p)\ldots a_{nn}(p)
\end{vmatrix} E_2 =
\begin{vmatrix}
a_{11}(p)a_{12}(p)\ldots 0 \\
a_{21}(p)a_{22}(p)\ldots b_2(p) \\
\ldots \ldots \ldots \ldots \ldots \\
a_{n1}(p)a_{n2}(p)\ldots b_n(p)
\end{vmatrix} Y_2 \qquad (10\text{-}31c)
$$

We see that the determinant on the right equals

$$b_n(p) \begin{vmatrix} a_{11}(p) \ldots a_{1,n-1}(p) \\ \cdots \cdots \cdots \cdots \cdots \\ a_{n-1,1}(p) \ldots a_{n-1,n-1}(p) \end{vmatrix}$$

$$- b_2(p) \begin{vmatrix} a_{11}(p) \ldots a_{1,n-1}(p) \\ a_{31}(p) \ldots a_{3,n-1}(p) \\ \cdots \cdots \cdots \cdots \cdots \\ a_{n,1}(p) \ldots a_{n,n-1}(p) \end{vmatrix} = 0 \qquad (10\text{-}21g)$$

by properly choosing the parameters of the system, makes it invariant with respect to the given disturbance, i.e., irrespective of the changes of Y_2, errors engendered by it invariably equal zero. Thus we have achieved the principle of disturbance regulation the error of which is defined by formulas (10-8).

A further complication of the conditions for feeding signals to systems consists in examining the case of simultaneous effect of control signal $X_y = Y_1$ and disturbances $Y_2, \ldots, Y_n$ along independent paths with OTF $b_i(p)$; then the equation for the error from the complex of signals takes the form:

$$- \begin{vmatrix} a_{11}(p) \ldots a_{1n}(p) + b_1(p) \\ a_{21}(p) \ldots a_{2n}(p) \\ \cdots \cdots \cdots \cdots \\ a_{n1}(p) \ldots a_{nn}(p) \end{vmatrix} E_1 =$$

$$= \begin{vmatrix} a_{11}(p) \ldots b_1(p) X_y(p) \\ a_{21}(p) \ldots b_2(p) Y_2(p) \\ \cdots \cdots \cdots \cdots \\ a_{n1}(p) \ldots b_n(p) Y_n(p) \end{vmatrix} \qquad (10\text{-}21h)$$

Conditions of mutual compensation of errors from various signals are as follows:

$$\begin{vmatrix} a_{11}(p) \ldots b_1(p) X_y(p) \\ a_{21}(p) \ldots b_2(p) Y_2(p) \\ a_{n1}(p) \ldots b_n(p) Y_n(p) \end{vmatrix} = 0. \qquad (10\text{-}21i)$$

If we apply the mathematical result obtained to
control technique, then for each new combination of
signals new values for system parameters must be chosen.

The conditions established above can be derived from
the general principles devised by Academician V. S.
Kulebakin and his school /Bibl. 1/ for designing invariant
systems.

For systems of equations with variable parameters
the equations of closed-loop control systems , for
output signals (10-21b) and for unbalance signals (minus
error) (10-21c) remain valid but in the form of non-
abelian determinants

$$
\left\| \begin{array}{c} a_{11}(t,\ D) \ldots b_1(t,\ D) + a_{1n}(t,\ D) \\ \cdots \cdots \cdots \cdots \cdots \cdots \\ a_{n1}(t,\ D) \ldots a_{nn}(t,\ D) \end{array} \right\| X_y(t) =
$$

$$
= \left\| \begin{array}{c} \ldots b_1(t,\ D) \\ \cdots \cdots \cdots \\ \ldots 0 \end{array} \right\| X_y(t); \quad (10\text{-}22a)
$$

$$
\left\| \begin{array}{c} a_{11}(t,\ D) \ldots b_1(t,\ D) + a_{1n}(t,\ D) \\ \cdots \cdots \cdots \cdots \cdots \cdots \\ a_{n1}(t,\ D) \ldots a_{nn}(t,\ D) \end{array} \right\| X_1(t) =
$$

$$
= \left\| \begin{array}{c} \ldots a_{1n}(t,\ D) \\ \cdots \cdots \cdots \\ \ldots a_{nn}(t,\ D) \end{array} \right\| X_y(t). \quad (10\text{-}22c)
$$

Equations (10-21, c-i) can be assigned in the same
form but expansion of non-abelian determinants has to
be carried out according to the specific rules expounded
in section 1-2.

10-3. Computation and Compensation of Forced Motion Errors

1. Definition of Series Terms of Forced Motion Errors

In Section 10-2 we examined some particular solutions of the problem of determining constant errors of forced motion and how to reduce them by properly choosing the required amplification constant. An overall general solution requires computation of all the necessary terms of series (10-5b).

Let us compute only the error in the reproduction of the control signal (program); for the disturbances the procedure remains the same, only the OTF changes. If we take the relative OTF as the basic one, then the expansion of the reproduction error in a series takes the form:

$$x_1(t) = -e(t) = \Phi_*(0)\, x_y + \Phi'_*(0)\, \dot{x}_y +$$

$$X_y = X_{in}$$

$$+ \Phi''_*(0)\, \frac{\ddot{x}_y}{2!} + \ldots = C_{\nu 0} x_y + C_{\nu 1} \dot{x}_y + C_{\nu 2} \ddot{x}_y +$$

$$+ C_{\nu 3} \dddot{x}_y + \ldots \qquad (10\text{-}23)$$

The series coefficients are called error coefficients; in their designation $C_{\nu i}$ we used a double subscript; the first, ν, corresponding to the astaticism order according to which the number of lowest terms of the series changes, and the second, i, corresponding to the order of the input signal derivative. If the relative OTF is defined by the open system parameters according to Table 10-3 the error coefficients are also expressed in terms of these parameters. Their values

are tabulated in Table 10-4 which also gives the amplification factor of the open system

$$k = \frac{u_s}{v_s} = \frac{u_0}{\mu_0}.$$

The most efficient way of computing the error coefficients is by means of formulas (10-7b). Following is their application for the case $\nu = 1$.

$$C_{10} = \Phi_s(0) = 0;$$

$$C_{11} = \frac{\Phi_s(p)}{p}\bigg|_{p=0} = \frac{v_1}{\mu_0} = \frac{1}{k_{-1}};$$

$$C_{12} = \frac{\Phi_s(p) - C_{11}p}{p^2}\bigg|_{p=0} = \frac{V(p)\mu_0 - M(p)v_1 p}{p^2 v_0 M(p)}\bigg|_{p=0};$$

with any complexity of the polynomials $V(p)$ and $M(p)$ in the products above it suffices to select only those terms containing p^2. After cancellation from the denominator we have:

$$C_{12} = \frac{v_2 v_0 - \mu_1 v_1}{u_0 v_0} = \frac{v_2 k_{-1} - u_1}{u_s v_{-1}} = \frac{1}{k_{-2}}.$$

Computation of

$$C_{13} = \frac{\Phi_s(p) - C_{11}p - C_{12}p^2}{p^3}\bigg|_{p=0}$$

will require the selection in the numerator of only those terms containing p^3, and so on.

The coefficient can also be determined by continuously dividing the numerator of the CLF by its denominator with simultaneous expansion of the elements in ascending powers p (first terms: v_0 and μ_0).

2. Compensation of Forced Motion Errors in Input Value Operations

Suppose the actual transfer function of a control system is a fraction

—750—

Table 10-4

Forced Motion Error Coefficients Through Amplification
Factors and Parameters of Open Control System Equation

① Формула алгоритма	② Коэффициенты C_i	③ Формула
	$C_{00} = \Phi_1(0)$	$\dfrac{1}{1+K_0}$
	$C_{01} = \Phi'_0(0)$	$\dfrac{K_0 V_1 - U_1}{V_0(1+K_0)^2}$
$=0$	$C_{02} = \dfrac{\Phi''_0(0)}{2!}$	$\dfrac{(U_2 K_0 - U_3)(U_0 + V_0) - (U_1 K_0 - U_1)(U_1 + V_1)}{V_0^2(1+K_0)^3}$
	$C_{03} = \dfrac{\Phi'''_0(0)}{3!}$	$\dfrac{\{1+K_0\}\{(1+K_0)(U_3 L_1 - V L_2 + 3V_0(V_3 K_0 - U_3)\} - 4(U_2 + U_3)(U_2 K_0 - U_2)\}}{3V_0^2(1+K_0)^4}$ $-$ $\dfrac{(U_1 K - U_1)\left[2(1+K_0)(U_2 + V_2) - \dfrac{3}{V_0}(U_1 + V_1)^2\right]}{3V_0^2(1+K_0)^4}$

Table 4 continued.

$C_{10} = \Phi_1(0)$	0	$\nu = 1$
$C_{11} = \Phi_1'(0)$	$\dfrac{1}{K_{-1}}$	
$C_{12} = \dfrac{\Phi_1''(0)}{2!}$	$\dfrac{V_2 K_{-1} - U_1}{U_0 K_{-1}} \cdot \dfrac{1}{K_{-1}^2}$	
$C_{13} = \dfrac{\Phi_1'''(0)}{3!}$	$\dfrac{U_0[(V_2 U_1 - V_1 U_2) - 2V_1(V_2 + U_2) + 3U_0 V_3 - U_2(V_1 + U_2)]}{3U_1 K_{-1}^3} - \dfrac{3(U_1 + V_1)[U_0 V_2 + V_1(U_1 + V_1)]}{3V_1 K_{-1}^3}$	
$C_{20} = \Phi_2(0)$	0	$\nu = 2$
$C_{21} = \Phi_2'(0)$	0	
$C_{22} = \dfrac{\Phi_2''(0)}{2!}$	$\dfrac{1}{K_{-2}}$	
$C_{23} = \dfrac{\Phi_2'''(0)}{3!}$	$\dfrac{V_3 K_{-2} - U_1}{V_2 K_{-2}^2}$	

Key: 1) Astaticism order; 2) Coefficients; 3) Formulas.

732

$$\Phi(p) = \frac{U(p)}{M(p)}.$$

We let the input value through a dynamic system with transfer function $K(p)$ and subject it to a transformation such that the aggregate transformations of the signal by the dynamic system and the basic control system be equivalent to the standard transfer function $K(p)\Phi(p) = \Phi_s(p)$. Hence we determine the OTF of the correcting dynamic system: $K(p) = \frac{\Phi_s(p)}{\Phi(p)} = \frac{M(p)}{U(p)}\Phi_s(p)$.

For $\Phi_s = 1$ we have:
$$K(p) = \frac{1}{\Phi(p)} = \frac{1}{\Phi(0)} + \left[\frac{1}{\Phi(0)}\right]' p +$$
$$+ \left[\frac{1}{\Phi(0)}\right]'' \frac{p^2}{2!} + \cdots = \frac{1}{\Phi(0)} - \frac{\Phi'(0)}{\Phi^2(0)} p -$$
$$- \frac{\Phi(0)\Phi''(0) - 2\Phi'^2(0)}{\Phi^3(0)} \cdot \frac{p^2}{2!} + \cdots \qquad (10\text{-}24)$$

The solution found in the form of a p power series enables us to consider in a simple fashion the compensation conditions with an input signal of varying complexity.

Let the input be represented by curve 1 in Fig. 10-5, i.e., during basic time, except the hatched intervals, the input value is constant at varying levels. In this case $\dot{x}_y = \ddot{x}_y = \ldots = 0$ and the correcting transfer function degenerates into the correction factor :
$$\beta = \frac{u_c + u_o}{u_o} = \frac{1 + K_o}{K_o}. \qquad (10\text{-}25)$$

In most systems with various characteristics the input value can be easily increased at a prescribed ratio β. Some design solutions are shown in Fig. 10-6.
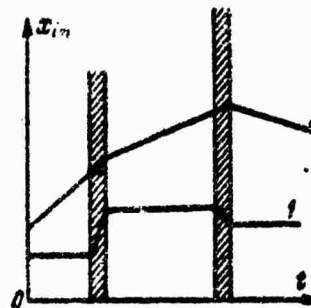
Fig. 10-5.   Constant level and constant rate processes in operation zones.
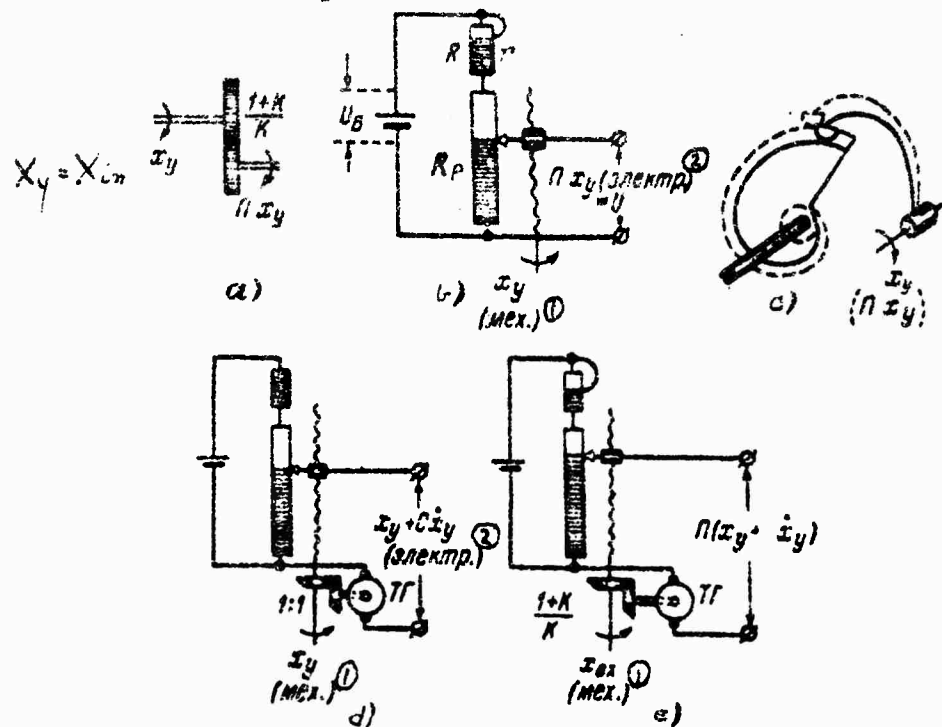
Fig. 10-6.   Correction for staticism and rate error with mechanical and electric control signals.
Key: 1) (mech.); 2) (elec.);

In diagram a with mechanical elements the input value is assigned in the form of the deflection angle of a shaft.   The input value scale is increased in this

base of a pinion drive with a transmission ratio
$(1 + K_0)/K_0$.

In diagram b the input value corresponds to voltage taken off from a potentiometer brush. If we denote by R_p the resistance of the potentiometer plate, and by R the total resistance of an additional (control) rheostat, then with a fully inserted rheostat maximum output voltage of the potentiometer is

$$U_{_M} = U_0 \frac{R_p}{R_p + R} .$$

If the control rheostat is only partially inserted, as shown in the Figure, then with rheostat resistance r maximum output voltage of the potentiometer is

$$U_{_{Ml}} = U_0 \frac{R_p}{R_p + r} .$$

In order to have the input voltage amplification factor exactly equal to the correction factor, i.e., $\prod = (R_p + R)/(R_p + R)$, it suffices to introduce resistance r in the control rheostat:

$$r = \frac{R - R_p(\prod - 1)}{\prod} .$$

Diagram c has a cam shaft as a starter. To compensate the statisism of the control system operated by it, it suffices to change the variable part of all its radius-vectors $\prod$ times, as shown in the Figure by the dashed line.

Earlier it was said that similar corrections are applicable to most control systems. For stabilizers corrections of this type are introduced when tuning regulators of potentiometers, adjusting springs of measuring devices, etc. For program control systems, closest to the idea of a permanent program comes diagram c

where instead of a profiled eccentric a profiled potentiometer can be used. For servosystems, diagrams a, b, etc., can be used.

Thus, the elimination of staticism does not necessarily require the designing of astatic systems; the same result can be reached by introducing corrections in static control systems. The correction method, however, has also its drawbacks consisting, as we can see from Fig. 10-6, in that the correction factor introduced has a constant magnitude (a "hard" correction factor) such as, e.g., the gear ratio of a pinion drive, whereas it is computed by the formula in Table 10-4 comprising the amplification constant of open control systems the constancy of which can, in the general case, not be warranted.

In fact, the straight path of control systems may comprise electron tubes, magnetic, electromechanical and other amplifier units of electric circuits and electromagnetic elemnts with nonlinear properties, etc. The transmission properties of these elements may depend on temperature, the magnitude of feed voltage including filament voltage of electron tubes, constancy of electric and mechanic loads, and so on. If we denote the numerical characteristic of these parameters by β_i, then if the value of the parameter (e.g.. temperature) changes by the quantity $\Delta \beta_i$, the correction factor must change by the quantity $\Delta \Pi = \partial \Pi / \partial \beta_i$. If, on the other hand, we are dealing with a "hard" correction factor, then the

formula obtained determines a new coefficient of decom-
pensation error. Such an error may turn out to be sub-
stantial. In an electric pickup operating according to
the principle of diagram b, periodic adjustments can
eliminate decompensation errors which then will arise
only in the intervals between adjustments.

Astatic systems are free of such errors. Moreover,
astatic systems not only reproduce the useful signal
faultlessly but eliminate permanent output disturbances
of the integrator. Static systems with compensation are
not protected against additional disturbances.

Let us now investigate the operation of control
systems with inputs where we must consider the rate of
change of input value $\dot{x}_{in}$ but may disregard acceleration
and the highest time derivatives $\ddot{x}_{in} \approx 0$ according to
curve 5 in Fig. 10-5. In this case, in formula (10-24)
we consider the terms containing zero and first power of

p:
$$K(p) = \frac{1}{\Phi(0)} \left[1 - \frac{\Phi'(0)}{\Phi(0)} p \right] \cdots$$

$$= \frac{1 + K_a}{K_0} \cdot (1 + Tp) \ldots \qquad (10\text{-}26a)$$

For the astatic system $\Phi(0) \approx 1$ the correction formula
is simplified:

$$K(p) = 1 + Cp. \qquad (10\text{-}26b)$$

Figure 10-8d shows one of the possible diagrams for
introducing such a correction in the form of electric
voltage; input value x_y is taken as voltage from a
continuously moving potentiometer brush while the
rate of change of input value with the required coefficient

C is obtained in the form of voltage of a tachogenerator set in motion by the same shaft driving the potentiometer brush. Aggregate voltage proportional to the sum $x_y + Cx_y$ fed to the input of the control system which lags behind (errs) by the quantity $C_1\dot{x}_y$, and thus a basically accurate prescribed input value is produced.

For static systems, along with increasing the scale of the input value by a factor of Π according to (10-26a), constant correction for speed is multiplied by the same factor Π. This can be achieved according to diagram e of the same figure or by other means.

The corrected total signal for a static control system is in this case

$$\Pi\left(x_{in} + T\dot{x}_{in}\right).$$

If the variable character of speed has to be considered, i.e., if we have to consider the essential values of the second and highest derivatives $\dddot{x}_{in}, \ddot{x}_{in}$, then in a similar fashion we can calculate the corrections also for higher derivatives. In this case the electric circuit for the input of corrections must be provided with devices for the repeated differentiation of the input signal. If the input signal changes by some transcendental function ($e^{-\alpha t}$, arc tan $\underline{at}$...), then the correction formulas become complex and their realization is difficult. An exception are program control systems with preassigned programs such as, e.g., the one shown in Fig. 10-6 c in the form of a profiled potentiometer, or other devices. Inasmuch as

738

In this case the deflection angle of the cam is a
function of time, and the corrections for rate, accelera-
tion, etc., are also functions of time, they can all be
computed and summed beforehand if the correction series thus
formed is convergent and the variation of the working
radii of the cam has been considered.

5. Compensation of Forced Motion Errors in the Output Value Function

The difficulties arising in a number of cases when
evaluating the error and also when introducing
corrections in the input value function of control systems
have forced us to investigate other methods of evaluating
errors.

To establish the relation between the error and the
output value we turn to Fig. 10-2, b and write the re-
lation

$$X_c(p) = - E(p) = \frac{1}{W(p)} X_{out}(p). \qquad (10\text{-}27)$$

which has already been used.

We expand the function $1/W(p) = W_i(p)$ in a series,
pass from images to originals and find a formula for
the error analogous in its structure to formula (10-23)
but with other coefficients, viz.:

$$X_0(t) = - \epsilon(t) = W_i(0) x_{out} +$$
$$+ W_i'(0) \dot{x}_{out} + \frac{W_i''(0)}{2!} \ddot{x}_{out} \ldots \qquad (10\text{-}28)$$

Compared with (10-23) this formula offers advan-
tages for complex laws of motion only in those cases
where the numerator $W(p)$ is elementary and the inverted

function $W_1(p)$ is simple. We investigate the case where the transfer function of an open control system has a zero-order numerator, i.e.,

$$W(p) = \frac{u_0}{v_n p^n + \ldots + v_1 p + v_0}.$$ (10-29)

Inasmuch as the inverted function

$$W_i(p) = \frac{v_n}{u_0} p^n + \frac{v_{n-1}}{u_0} p^{n-1} + \ldots + \frac{v_1}{u_0} p + \frac{v_0}{u_0}$$

has in this case a finite number $(n + 1)$ of terms all being powers of p, the number of coefficients of the error different from zero is also limited:

$$\left. \begin{array}{c} W_i(0) = \frac{v_0}{u_0} \\ \cdots \cdots \cdots \\ W_i^{(n)}(0) = n! \frac{v_n}{u_0} \end{array} \right\} n+1.$$

Hence for such control systems the error formula, and, consequently, the correction formula resulting from it will have, irrespective of the complexity of the law of motion, a finite number of terms exceeding by no more than unity the order of the control system's transfer function.

Let us examine, e.g., the simplest transfer function of an astatic control system in its open form,

$$W_1(p) = \frac{k_{-1}}{p}.$$

Its inversion is

$$W_{i1}(p) = \frac{p}{k_{-1}}.$$

The error coefficients in (10-28) are:

$$W_i(0) = 0; \ W_i'(0) = \frac{1}{k_{-1}}.$$

For the simplest static control system with transfer function $W_2(p) = k_0 / (Tp + 1)$ the inverted quantity $W_{i2}(p) = T/k_0 \times p + 1/k_0$ and the error coefficient

$$-740-$$

amount to

$$W_{i2}(0) = \frac{1}{k_s}; \quad W'_{i3}(0) = \frac{T}{k_s}.$$

The errors computed by the methods mentioned determine also the corrections which can be introduced at the output or the input of the control system.

When introducing corrections at the system's output the typical measures to be taken are similar to those examined earlier in Fig. 10-6. The corrected output value is defined for this method of introducing corrections by the formula

$$x_{corr}(t) = x_{out}(t) + W_i(0)\,x_{out}(t) +$$

$$+ W'_i(0)\,\dot{x}_{out}(t) + \frac{W''_i(0)}{2!}\,\ddot{x}_{out}(t) + \dots \qquad (10\text{-}50)$$

For the two simplest control systems of the first order investigated: astatic

$$x_{corr} = x_{out}(t) + \frac{1}{k_{-1}}\,\dot{x}_{out}(t)$$

and static

$$x_{corr} = x_{out}(t)\left(1 + \frac{1}{k_s}\right) + \frac{T}{k_s}\,\dot{x}_{out}(t)$$

the compensation of the rate error is shown in Fig.10-7,a relative to the case where the corrected value must be obtained in the form of voltage, and additional voltage is derived from the tachogenerator. Other diagrams may also be suggested, e.g., without tachogenerator but with immediate voltage differentiation by means of electric circuits.

If, in addition to compensating the rate error, we also have to compensate staticism, then, like in Fig. 10-6e, we must increase the feed voltage of the potentiometer. But unlike the compensation diagram at

the input, voltage of the tachogenerator at the output is determined only by the coefficient T/k_0.

a)

b)

c)
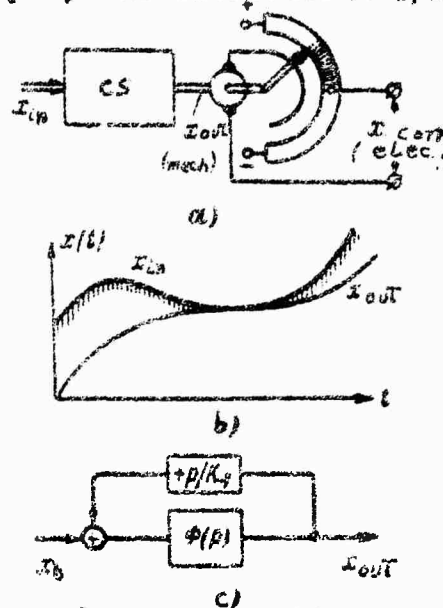
Fig. 10-7. Diagram for compensating rate errors in the output value function.

When introducing corrections at the system's input, proceeding from the definition of the error as a difference between output and input of a control system, the input value required must be computed according to formula

$$x_{in}(t) = x_{out}(t) + W_i(0) x_{out} +$$

$$+ W_i'(0) \dot{x}_{out} + W_i'' \frac{\ddot{x}_{out}}{2!} + \dots$$

(10-31)

If the prescribed law of input value variation is known beforehand, as this is the case in program control systems, then the corrections can be computed preliminarily and introduced at the input.

For example, for the simplest astatic system of first order the correction consists only of one term

742

proportional to the rate of change of the output value -

$(1/k_{-1})\ \dot{x}_{out}$. Figure 10-7, b shows an arbitrary though preliminarily assigned pattern of variation of output value $x_{out}(t)$ to which the correction $+(\dot{x}_{out}/k_{-1})$ is added. The input curve thus obtained can be used for designing a control gear feeding the system's input.

In those cases where the parameters of the output process can be computed during the regulation process itself, which is possible if output motion is governed by a specific, preliminarily formulated hypothesis (hypothesis of steady motion, motion according to the law $\omega = \tan \Omega t$, etc.,), corrections can also be applied at the control system's input. Thus, this method can be employed not only with systems with one preassigned program, but also with systems operating according to a specific hypothesis. Although motion within the limits of a specific hypothesis encompasses a wider circle of processes than motion by one single program, motion according to a hypothesis should, nevertheless, be understood not as a random law of motion but rather as the totality of various programs not exceeding the limits of the hypothesis.

A compensation of errors by this method with a random law of motion could presumably be devised by connecting the control system's output and input. Indeed, if for the investigated astatic system of first order, with the aid of a tachogenerator or by other means we determine the rate of change of output value and feed it with

743

4

coefficient $+ (1/k_{-1})$ to the system's input, then, as shown in the block diagram 10-7, c we should theoretically have a control system of first order operating "faultlessly" with any law of motion. This we can check by transforming the transfer functions: we have $W(p) = k_{-1}/p$, hence $\Phi(p) = k_{-1}/(p + k_{-1})$; encompassing by positive feedback $+ (f/k_{-1})$ yields:

$$\frac{k_{-1}}{p + k_{-1} - p} = \frac{k_{-1}}{k_{-1}} = 1,$$

i.e., the control system reproduces accurately the input value at the output.

Thus, compensation of forced motion errors by means of superposing positive feedbacks is possible but the new closed-loop system must be thoroughly checked for all the quality factors and, above all, stability.

In practice, positive feedbacks are used for partial error compensation. The technique of superposing feedbacks on closed control systems is simplified if we employ the method of structural analysis. In fact, if we bear in mind that the closed control system with transfer function $\Phi(p)$ shown in Fig. 10-7 c has a standard structure we can, by transferring onto Fig. 10-8 the complementary adder through the system's basic measuring element and by changing places of the output nodes, insert the correction feedback in the control system's straight path.

Further, by transferring the adder and the node

744

through the elements of the forward circuit and correcting accordingly the error transfer function we can transfer the positive feedback to any element of the system.
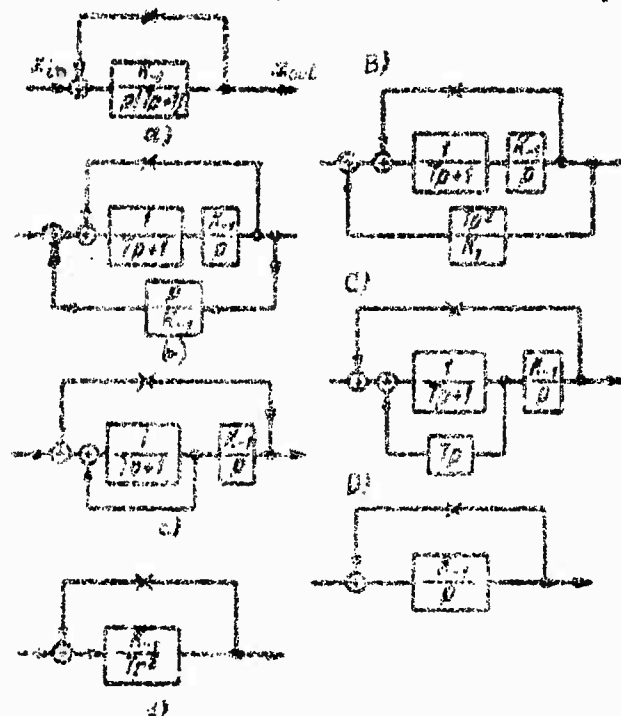
Fig. 10-8. Examples of error compensation by positive feedbacks.

Partial compensation of forced motion errors can be explained as the development of the compensation example investigated above.

Suppose that according to Fig. 10-8 a the forward circuit has a transfer function $W_1(p) = k_{-1}/p(Tp + 1)$ which is closer to real conditions than an ideal integrating element. Series (10-28) for the error in this case consists of two terms:

$$\varepsilon(p) = \frac{1}{k_{-1}} \dot{\eta} + \frac{T}{k_{-1}} \ddot{x} \qquad (10-33)$$

$$W_{11}(0) = -\frac{Tp^2 + p}{k_{-1}} \; ; \; W_{11}(0) = 0;$$

$$W'_{11}(p) = \frac{2Tp + 1}{k_{-1}} \; ; \; W'_{11}(0) = \frac{1}{k_{-1}} \; ;$$

$$W''_{11}(p) = \frac{2T}{k_{-1}} \; ; \; W''_{11}(0) = \frac{2T}{k_{-1}} \; .$$

Let us assign the first problem, viz., compensate the rate error alone. To do this it suffices to connect the output and input of the positive feedback with the transfer function

$$H_1(p) = \frac{p}{k_{-1}} \; .$$

Application of such a connection is shown in Fig. 10-8,b; further, in diagrams c and d, feedback is transferred to the aperiodic element of the forward circuit owing to which the aperiodic element is relieved of an identical inner feedback but with an inverted sign and becomes an integrator. The aggregate transfer function of the forward circuit $W_2(p)$ corresponds now to a system with second-order astaticism:

$$W_2(p) = \frac{k_{-1}}{Tp^2} = \frac{k_{-2}}{p^2} \; .$$

We can easily see that the correeponding error coefficient in formula (10-28) equals zero since

$$W_{21}(p) = \frac{T}{k_{-1}} \, p^2; \; W'_{21}(p) = \frac{2Tp}{k_{-1}} \; ; \; W'_{21}(0) = 0.$$

The control system's structure obtained satisfies the problem of eliminating the rate error, although the closed system as a whole has a transfer function of the resonance element which is evidence of natural undamped oscillations existing in the system. In order that this system be operative, additional measures are required which will be dealt with in the following chapter.

We proceed now to the second problem, viz., compensating only the Acceleration error, i.e., the second term in formula (10-32). To this end we introduce the transfer function

$$H(p) = \frac{T}{K_{-1}} p^2.$$

in the positive output feedback with input.

By applying this connection as shown in Fig. 10-8 B and performing the structural conversions connected with the transfer of the node and the adder we pass to circuit C. If according to Fig. 1-6 we represent the internal structure of the aperiodic element in the form of an amplifier covered by flexible negative feedback we see that the internal negative feedback is compensated by the external positive feedback, as a result of which we simply have an amplifying element whose amplification factor in the given case equals unity.

The aggregate transfer function of the forward circuit is reduced to the form $W_2(p) = k - 1/p$ as shown in circuit d. Inasmuch as $W_{12}(p) = p/k_{-1}$ the second term in the error formula, $W''_{24}(0)\, \ddot{x}_{out}/2!$, is in our case actually equal to zero. Thus the system as a whole is found to be fully operative.

4. <u>Compensation of the Higher Terms in the Series of Forced Motion Error in the Function of the First Term of the Series</u>

Let us go back to formula (10-22). This formula represents the magnitude of the error and, at the same

time, determines that control signal which must be at
the input of the forward circuit with transfer function
$W_1(p)$ so as to satisfy at the output the prescribed law
of motion $x_{out}(t)$. This signal in accordance with the
basic structure of closed control systems is the difference
between the input and output values. If complementary ele-
ments are introduced in the forward circuit, then it is
sufficient to obtain the difference equal only to the
first term of the error series; the remaining terms of
the series can be formed from the first term by differ-
entiating it.

Depending upon the astatic order of system ν in
formula (10-28) the ν first terms are absent. The re-
maining terms of the series, of course, remain and yield
altogether an input signal x_n for the straight path
$W_1(p)$ such that it excites at the output the output pro-
cess required. If now we complicate the straight path
$W_2(p) \, W_1(p)$ by introducing after the adder the additional
factors $W_2(p)$, then on the unchanged elements of the
straight channel $W_1(p)$ the input signal can still be
represented by series (10-28) although it no longer is
equal to the unbalance. If we transform that series in
such a way that all the subsequent terms of the series
can be expressed by the first term x_ν, we find the
following formulas for computing the required input
signal of the basic portion of the straight path
$W_1(p)$:

For static control systems $(x_\nu = x_0)$

_748_

$$x_{3x0} = x_0 + W_1(0) W_{1f}'(0) \dot{x}_0 +$$

$$+ \frac{W_1(0)}{2!} W_{1f}''(0) \ddot{x}_0 + \ldots; \qquad (10\text{-}33a)$$

for control systems with first-order astaticism

$(x_3 = x_1)$

$$x_{4,01} = x_1 + \frac{W_{1f}''(0)}{2! W_{1f}'(0)} \dot{x}_1 +$$

$$+ \frac{W_{1f}'''(0)}{3! W_{1f}'(0)} \ddot{x}_1 + \ldots; \qquad (10\text{-}33b)$$

for control systems with second-order astaticism

$(x_3 = x_2)$

$$x_{4,02} = x_2 + \frac{W_1'''(0)}{3 W_{1s}''(0)} \dot{x}_2 +$$

$$+ \frac{W_1^{(IV)}(0)}{3 \cdot 4 W_{1f}''(0)} \ddot{x}_2 + \ldots \qquad (10\text{-}33c)$$

Thus, if the first term of the series is formed as a difference between input and output values, then the remaining signal components can be found by increasing this difference by means of differentiating it and adding derivatives to its original value. To this end, between the output of the basic adder in the block diagram and the input of elements with transfer function $W_1(p)$ there must be connected in parallel with the main channel such differentiators which would warrant differentiation with the multiplicity required and with an amplification factor determined from formulas (10-33a) – (10-33c).

Figure 10-9 shows the connection of complementary differentiators into the straight path of the control system and gives the position of the error and the control signal. Owing to the connection of new links the

aggregate transfer function of the open system has
changed and taken the form

$$W(p) = W_1(p) W_2(p) = (1 + Tp + m^2 p^2 + \quad (10\text{-}34)$$
$$+ \tau^3 p^3 \ldots) W_1(p).$$
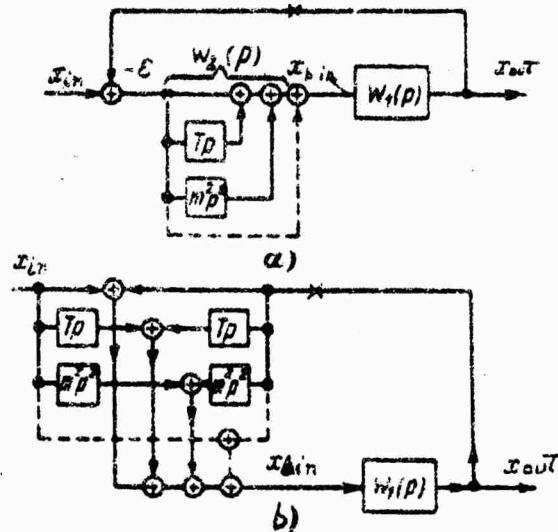
Fig. 10-9. Compensation of the second and last terms of
error series.

Quantities T, m^2, τ^3, which may be called <u>correction
factors</u>, are included in formulas (10-33); their expressions
by the transfer function of the open system and its
coefficients are tabulated in Table 10-5.

We can easily ascertain that total error of the new
system with straight path $W_1(p)$ $W_2(p)$ (10-34) is
actually equal to the first term in the series of the
error of the original system $W_1(p)$.

Technical solution of the introduction of additional
terms usually amounts to inserting forcing elements into
the straight channel. As a rule, the error signal appears
in the form of electric voltage and the link takes the
form of an electric circuit. It should be borne in

find that passive circuits do not yield ideal forcing and compensation of the higher terms of the error is only approximate.

In a number of cases instead of the circuit a (Fig. 10-9) it is expedient to employ the circuit b equivalent to it. It is readily obtainable by means of structural transformations if the nodes of circuit a are placed in front of the signal input after taking them across the basic adder and then double the operating links placing them into each new branch. Moreover, the design principle of circuit b can be easily understood if we differentiate the basic formula for the error:

$$- \dot{\varepsilon}(t) = \dot{x}_n - \dot{x}_c \qquad (10-35)$$

Consequently, instead of directly determining the error derivative we can determine the derivatives of output and input values and then substract them. Precisely this is being done in circuit b for derivatives of any multiplicity.

Let us apply this method to the already investigated astatic system with transfer function of the forward circuit $W_1(p) = k_1/p(Tp + 1)$. Let us assume that the rate error existing in this system will be compensated by one of the methods expounded and let us try to eliminate the acceleration error.

In a system with first-order astaticism the control signal is formed in this case according to formula (10-33b) which has only two terms in its right-hand side. The

the section and the input of the system investigated

is

$$-\frac{\left[\dfrac{1}{W(0)}\right]''}{2\left[\dfrac{1}{W(0)}\right]'} = \frac{2T}{2} = T.$$

Table 10-5

Correction Factors for the Compensation of the Higher
Terms of the Error Series

① Коэффициенты	$\nu = 0$	$\nu = 1$	$\nu = 2$
T — $T(V)$	$W(0)\left[\dfrac{1}{W(0)}\right]'$	$\dfrac{\left[\dfrac{1}{W(0)}\right]''}{2!\left[\dfrac{1}{W(0)}\right]'}$	$\dfrac{\left[\dfrac{1}{W(0)}\right]'''}{3\left[\dfrac{1}{W(0)}\right]''}$
$T(V_i, U_0)$	$K_0\dfrac{v_1}{u_0}$	$K_{-1}\dfrac{v_2}{u_0}$	$K_{-2}\dfrac{v_3}{u_0}$
m^2 — $m^2(W)$	$\dfrac{W(0)}{2!}\left[\dfrac{1}{W(0)}\right]''$	$\dfrac{\left[\dfrac{1}{W(0)}\right]'''}{3\left[\dfrac{1}{W(0)}\right]'}$	$\dfrac{\left[\dfrac{1}{W(0)}\right]^{(IV)}}{3\cdot4\left[\dfrac{1}{W(0)}\right]''}$
$m^2(V_i, U_0)$	$K_0\dfrac{v_2}{u_0}$	$K_{-1}\dfrac{v_3}{u_0}$	$K_{-2}\dfrac{v_3}{u_0}$
τ^2 — $\tau^2(W)$	$\dfrac{W(0)}{3!}\left[\dfrac{1}{W(0)}\right]'''$	$\dfrac{\left[\dfrac{1}{W(0)}\right]^{(IV)}}{4\left[\dfrac{1}{W(0)}\right]'}$	$\dfrac{\left[\dfrac{1}{W(0)}\right]^{(V)}}{3\cdot4\cdot5\left[\dfrac{1}{W(0)}\right]''}$
$\tau^2(V_i, U_0)$	$K_0\dfrac{v_3}{u_0}$	$K_{-1}\dfrac{v_4}{u_0}$	$K_{-2}\dfrac{v_5}{u_0}$

Key: 1) coefficients.

The differentiator with this coefficient is joined
up parallelly with the main channel, as shown in Fig.
10-10, a where together with the direct path it forms
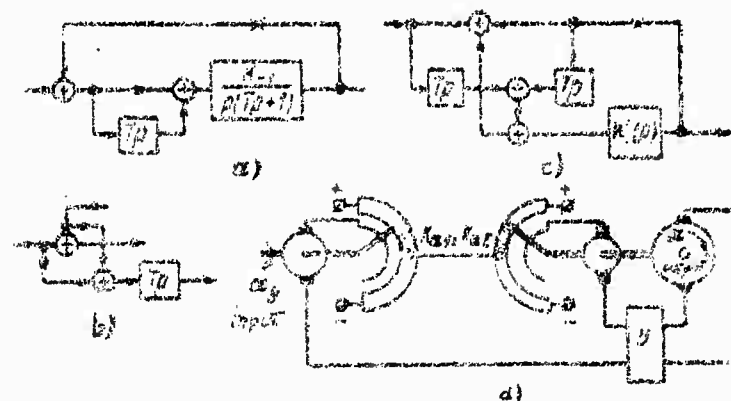
Fig. 10-10. Circuits of a control system compensated for control signals.

By transferring the node from the direct path through the adder against the course of the signal according to the rules of structural analysis, as shown in circuit b, and then, doubling the link, we obtain circuit 10-10, c. The validity of these transformations can be easily verified by juxtaposing the signals in the direct path of the old and the new system.

We now pass from the block diagram to the electric circuit of the control system, as shown in Fig. 10-10,d.

Input and output values in the given case are the deflection angles of the shafts α_{v} and α_{out}. The displacement angle between these shafts is measured as voltage between two potentiometers connected against each other whose brushes are connected with the shafts by means of

corresponding and equal transfer numbers. The difference
between the rates of both shafts is defined as the
difference in the voltage of the two tachogenerators
connected with them. Thus, four voltages participate
in the formation of the control signal. Since the sum
does not change if the addends change places, these
voltages can be summed following any sequence but with
a strict compliance with the signs. The diagram shows
one of the possible summation versions which is most ex-
pedient for designing.

Let us remind the reader that although the form of
the elements used in the circuit may lead us to conclude
that the circuit operates according to the principle of
equating angles and velocities, it has nevertheless a
fundamental rate error inversely proportional to the
amplification factor of the open control system but in
it is compensated the error of output acceleration. The
higher error coefficients are equal to zero since in the
example investigated the transfer function of the forward
circuit has a second-order denominator with a zero-order
numerator.

It was assumed until now that potentiometers and
tachogenerators on the input and output shafts have
identical voltage scales, yet if we remove this restric-
tion then, by utilizing the same circuit, we can also
eliminate the rate error of the system.

The rate error or first term of formula (10-33 b)
also did not change after forcing was introduced. It

_754 _

is important to note that the rate error coefficient in
the output function according to formula (10-28) coin-
cides with the rate error coefficient in the input func-
tion according to formula (10-23). This property is re-
tained for the first terms of error series of all asta-
tic systems.

Thus, we can compensate this error in both input and
output functions with identical coefficients. Let us use
the compensation method in the input function. It is
necessary in this case to assign the input value of a
magnitude greater than its nominal value times the error
magnitude. Inasmuch as the input value is in the last
analysis assigned in the form of voltage, error voltage
equal to $\dot{x}_{in}/K_{-1}$ must be added to it.

This error voltage can be obtained at the input
tachogenerator. If in accordance with the conditions for
compensating the error of acceleration the tachogenerator
is required to yield a voltage proportional to $T\,\dot{x}_{in}$ at
a scale adjusted to that of the output tachogenerator
then, if we also solve the problem of compensating the
rate error, we must ensure that the generator produces
an aggregate voltage proportional to the quantity

$$\left(T + \frac{1}{K_{-1}}\right)\dot{x}_{in}.$$

Tachogenerator voltages must also be adjusted to
the potentiometer voltages. To do this the following
conditions have to be followed: voltage taken from the
tachogenerator brushes (at the output) at a rotation of
its rotor equalling n rad/sec must be T times greater

than voltage taken from the potentiometer when its brush from zero position turns by an angle corresponding to the deflection angle of the tachogenerator shaft n rad. The scale of the potentiometers as well as the amplification factor of the amplifier and the electric motor are part of the aggregate amplification factor of the open system k_{-1}.

Circuits of this kind for systems with more complex denominators of the transfer function can considerably improve the accuracy of data transmission. At the same time it will be shown in Chapter 11 that forcing has a positive effect upon the stability of control systems.

Yet, if noises are present in the program signal, then they are increased by differentiators in direct proportion with frequency and the performance of compensated systems must under these conditions be very thoroughly investigated.

5. Errors of Control Systems with Quasistatic Elements

In systems with quasistatic elements computation of error coefficients leads to some specific results.

Let us examine, e.g., a very simple system having only one quasistatic element of first order in the forward circuit. The transfer function of the open control system for this case is

$$W(p) = \frac{k}{Tp - 1} ;$$

the basic transfer function of the closed system is

$$\Phi(p) = \frac{k}{Tp + k - 1}$$

and the relative transfer function is

$$\Phi_v(p) = \frac{Tp - 1}{Tp + k - 1}.$$

Examination of the basic transfer function leads us to conclude that if condition $k > 1$ is fulfilled, then the system as a whole behaves as an aperiodic link, i.e., by an appropriate choice of coefficients its natural oscillations can be damped at any arbitrary rate.

From the examination of the relative transfer function we can find the coefficients of forced motion error:

$$\Phi_v(0) = -\frac{1}{k - 1};\qquad\qquad (10\text{-}36\ a)$$

$$\Phi_v'(0) = \frac{kT}{(k - 1)^2}\qquad\qquad (10\text{-}36\ b)$$

and so on,

Comparison of the obtained results with error coefficients of static control systems given in Table 10-4 for $u_1 = 0$ and $v_1/\tau_0 = T$ show that qualitatively new phenomena are the changing sign of the static error and a certain increase in the rate error which is negligible with great k.

We can easily show that if we want to have a rate error with advancing sign we must also have a quasi-static transfer function of the open system but with a coefficient v_1 with a negative sign.

We can combine the astatic properties of control systems which warrant zero statisism with the leading sign of the rate error; to this end the forward circuit

requires integrating and quasistatic links. For example, we can practically realize a transfer function of the open system of the form

$$W(p) = \frac{k(Tp+1)}{p(\tau p - 1)} = \frac{kTp + k}{\tau p^2 - p} \cdot$$

The relative transfer function in this case amounts to

$$\Phi_*(p) = \frac{\tau p^2 - p}{\tau p^2 + (kT - 1)p + k} \cdot$$

The error coefficients for this system are

$$\Phi_*(0) = 0; \quad \Phi'_*(0) = -\frac{1}{k} \cdot$$

Thus, we have obtained a control system with a rate error with an advancing sign.

In the given case, in addition to the two assigned links we have introduced in the transfer function of the forward circuit a forcing link of first order with transfer function $Tr + 1$, and only owing to a selection of sufficiently great values of the amplification factor and forcing time constant $kT > 1$ have we warranted the required damping of natural motion with an oscillatory character.

Thus, a fundamental characteristic of quasistatic control servomechanisms is negative staticism or rate error coefficient, i.e., a positive (leading) error. In most cases it in undesirable to have either a positive or a negative error (overshot - undershot in artillery, etc.), and the positive sign of the error cannot be regarded as a merit, but in individual cases through a change in the sign of the error we can obtain a compensation of errors of various signs. Let us examine this

_758_

8. Mutual Error Compensation for Several Control Systems in Cascade Connection

If the output of any control system is joined up with the input of a subsequent system, as shown in Fig. 10-11, and both are independent closed systems, then the errors of the first and the second system will be summed. In this case, at least to compensate staticism, it is expedient to take one static system and the other quasi-static and coordinate the amplification factors of the open systems so as to satisfy the equality of the absolute values of errors $1/(1 + k_0) = 1/(k - 1)$ whence $k = k_0 + 2$.

In a like fashion we can ensure compensation of the system's rate error with first-order astaticism by connecting it with the output of a control system having in the forward circuit one integrating and one quasistatic sections of first order.
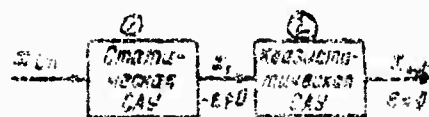
Fig. 10-11. Coupling of a static and a quasistatic system for staticism compensation.

Key: 1) static control system; 2) quasistatic control system.

10.-4. Systems Self-Tuning to Input Signals Assigned in the Form of Transcendental Functions

Let there be assigned an input signal in the form of

$$X_{in}(p) = \frac{U_1(p)}{(p+\eta)(p-\theta)+\Omega^2} . \qquad (10\text{-}37)$$

If the parameters in the denominator η, θ, Ω are not all simultaneously equal to zero, then the original $x_y(t)$ can be reduced to the following transcendental functions:

1) $\theta = 0, \Omega = 0$ - descending exponential curves;

2) $\eta = 0, \Omega = 0$ - ascending exponential curve for $U_1(p) = pU_0(p)$;

3) $\eta = -\theta = \sigma$ - damped harmonic oscillations;

4) $\eta = -\theta = -\chi$ - divergent harmonic oscillations;

5) $\eta = \theta = 0$ - sustained harmonic oscillations.

Expansion of these functions in series does not always yield a good approximation of the sum of the first terms of the series with the general function, and the methods for computing and compensating errors studied in the preceding section may turn out to be ineffective. For this reason we shall now seek new ways for solving the compensation problem.

Let us form the straight path of a control system in the form OTF $W(p)$ containing the same poles as representation (10-37) of the input signal:

$$W(p) = \frac{U_2(p)}{[(p+\eta)(p-\theta)+\Omega^2]V(p)} ; \qquad (10\text{-}38 \text{ a})$$

then relative OTF for a standard control system

with selected straight path will be:

$$\Phi_e(p) = \frac{[(p+\eta)(p-\theta)+\Omega^2]V(p)}{U_1(p)+[(p+\eta)(p-\theta)+\Omega^2]V(p)}. \qquad (10\text{-}38\ b)$$

Representation of the error excited by the signal (10-37) will then be simpler:

$$-E(p) = \frac{V(p)U_1(p)}{U_1(p)+[(p+\eta)(p-\theta)+\Omega^2]V(p)}, \qquad (10\text{-}38\ c)$$

since the denominator of the input signal representation is canceled by the numerator of the relative OTF of the control servomechanism.

In this case the problem of reducing to zero the forced motion error is solved by selecting the variable elements of the open control system $U_2(p)$ and $V(p)$ contained in the OTF denominator (10-38 c) so that the closed control system be steady. In fact, input process (10-37) with fixed poles for any scale of partial processes determined by the numerator $pU_0(p)$ does not change the character of the system's natural motion determined by poles $E(p)$ (10-38 c) since $U_1(p)$ is not part of the denominator of (10-38 c) and in a steady control system the steady-state error approaches zero with time $(t \to \infty)$:

$$-s_F = \lim_{p \to 0} pE(p) = 0.$$

Introduction in the invariable part of the OTF of an open control system of cofactors containing denominators of the form (10-37) is equivalent to introducing in the real straight path sections such that their weight functions coincide with an accuracy up to a constant measure with the representation of the input function.

Thus, for the parameter variants of formula (10-37 [...])

—781 —

investigated above we need to introduce in the system
only one of the following sections:

1) aperiodic section with time constant $T_1 = 1/\eta$;

2) quasistatic section of first order with time
constant $T_2 = 1/\mathcal{R}$;

3) oscillating section with conventional time
constant

$$\tau_1 = \frac{1}{\sqrt{\sigma^2 + \Omega^2}}$$

and relative damping

$$\xi_1 = \frac{\sigma}{\sqrt{\sigma^2 + \Omega^2}};$$

4) quasistatic section of second order with para-
meters

$$\tau_2 = \frac{1}{\sqrt{\varkappa^2 + \Omega^2}} \quad \text{and} \quad \xi_2 = \frac{\varkappa}{\sqrt{\varkappa^2 + \Omega^2}};$$

5) resonant section with oscillation frequency

$$\omega_0 = \frac{1}{\tau_0} = \Omega.$$

The physical significance of faultless operation
of similar systems with an input signal coinciding in
character with the system's tuning consists in the
fact that the system's straight channel automatically
generates an output process which differs at the be-
ginning of the system's operation from the input process
only by measure m which becomes equal to the measure
of the input signal during the transition process when
the error until the instant of its damping t_{damp} forms
the input signal indispensable for the straight path:

$$M_0 = m = \int_0^{t_{damp}} \varepsilon(t)\, dt. \qquad (10\text{-}39)$$

Further the straight channel operates without
"consuming" the error signal until the input signal does
not change its measure or sign while maintaining

unchanged poles in its representation. After a time interval t_{damp} following the change of the input signal the system will again perform without errors.

Such systems are considerably more flexible than control systems, even with a high order of astaticism. Thus, e.g., for an exponential increasing input process the role of high-order derivatives in the expansion of the input process in a series increases continuously, and an even greater number of integrators does not reduce the forced motion error to zero whereas one quasistatic section in the forward circuit with a time constant coordinated with the pole of input process $(T = 1/\alpha)$) eliminates completely the forced error. In a like fashion the installation in the straight channel of a resonant section permits the control system to faultlessly reproduce the input harmonic oscillations of one complete frequency coinciding with the tuning of the section.

If in addition to transcendental functions the input signal also contains a constant component, then an integrating section is introduced in the straight channel owing to which the control system becomes astatic ($\nu = 1$) and operates faultlessly with a compound signal. Thus, by introducing into the straight path several investigated sections simultaneously we can immediately compensate several error components excited by the input process.

Compound input processes can also be reproduced

783

faultlessly if in the system's straight channel we place a computer adjusted beforehand to produce a process of the required form in response to a unit pulse. Also in this case the actual error signal is determined automatically according to formula (10-39), and after t_{damp} the error is removed.

All what has been said above about the compensation of control signal errors applies in an equal measure to any disturbance, but the sections adjusted by disturbance poles for each given disturbance must be included in the feedback circuit.

When an input process or a disturbance have a representation with changing poles, a preliminary introduction into the straight channel of the control system (or into the negative feedback loop for disturbance) of the generating sections with all the possible parameters of the input process becomes impossible. If, however, we still keep to this compensation method then we must use the electronic models of generating sections discussed in chapters 1 and 4 (Figs. 1-6 and 4-7). In such circuits the amplification factors of direct links and feedbacks change easily, and this has a desirable effect on section parameters.

The model's parameters can be adjusted automatically: first, on the basis of the analysis of parameters of the process generated, and, second, by measuring the error modulus. Suppose, e.g., that we automate the frequency retuning process of a resonant section.

The first stage, that of single-valued self-tuning, is accompanied by: measuring of the frequency of the input process and the generating section frequency, detecting the frequency unbalance and forming a command to the motor or any other executive component to change the model parameters (resistances in the section circuits) in a strictly determined, i.e., single-valued, direction.

The second stage, scanning , begins with an arbitrary joining up of the motor which changes the resistances in the model circuits. If the error increases, then the motor is reversed and it keeps the rotation direction imparted to it until the next change of sign of the derivative of the error variation process envelope.

10-5. Combined Control Systems

Closed type circuit control with additional input of converted input signals into the closed circuit is called combined control.

Its block diagram is shown in Fig. 10-18 a; it is repeated from Fig. 5-7,a. By structural transformations we can from circuit a derive a new circuit b and c. The latter can be referred to the class of system with compensation at the input, hence new terms need not be introduced.

But if block diagram a reflects with sufficient accuracy the actual (nonconverted) sections in the system, then it is possible that the representation of its working principle as the operation of two systems, an open one with transfer function K(p) and a closed one

785

with transfer function of the straight path
$W(p) = W_1(p) W_2(p)$, will make the system's synthesis
more apparent.

The aggregate transfer function of a combined system
of the type investigated is given by formula (5-20 a).

According to (10-4a) we find the transfer function
of the error:

$$\Phi_s(p) = \Phi(p) - 1 = \frac{K(p) W_2(p) - 1}{1 + W(p)}. \qquad (10\text{-}40a)$$
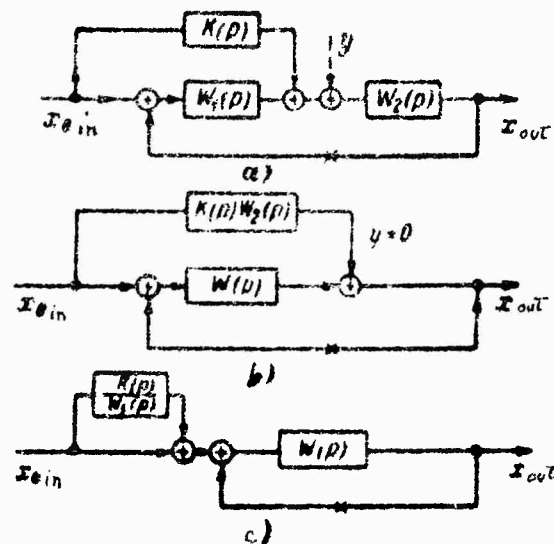
Fig. 10-12. Converted block diagram of combined control.
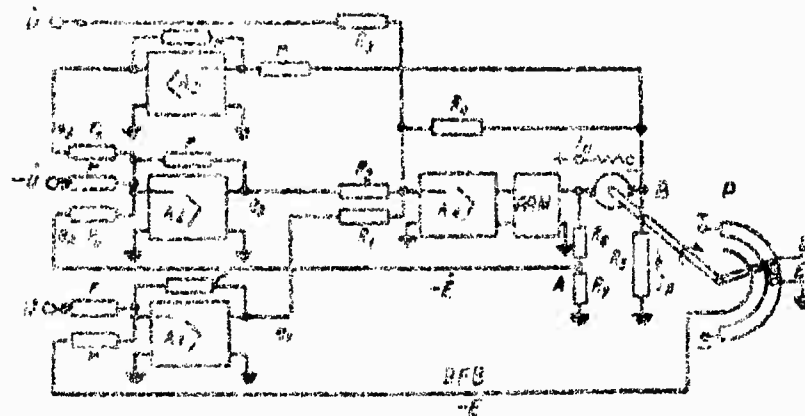
fig. 10-13. Electric circuit of an electromechanic
RDU unit of an electronic model.

We can easily see that in fulfilling condition
(5-20 a);

$$K(p)W_2(p) = 1, \qquad (10-40\ b)$$

we can obtain a fully compensated system. Moreover,
insofar as the standard transfer function $\Phi_s(p) = 1$
is warranted by the open system with an additional
section $W_2(p)$, the closed system has to take care only
of eliminating deviations in the transfer function of
the open control system and prevent additional dis-
turbances. Obviously since the open control system
operates with a control signal independent of the out-
put, the combined control system can attain very high
operation rates on account of the open system.

Let us examine as an example of combined control
the diagram of a dynamic unit RDU-1 shown in Fig. 10-13.
The unit is designed to control the voltage U obtained

from an electronic model in the form of the deflection angle of the motor shaft and the platform connected with it.

Basic feedback (BFB) is effected through a potentiometer : from which is taken the voltage proportional to the deflection angle of the shaft α :

$$E = K_t a,$$

where K_t is the transfer constant of the potentiometer and the reducer, in v/rad.

The algebraic sum of voltages $U - E = e_1$ appearing at the summing amplifier A_1 controls the system's straight channel and is reduced by it to zero owing to which the required static properties of the entire unit

$$E = U \quad \text{or} \quad a = \frac{U}{K_T}.$$

are ensured.

Additional compensating rate coupling is effected by subtracting on amplifier A_2 the rate of change of input voltage obtained also from the electronic model $\dot{U}$ and the motor emf proportional to the shaft rotation rate.

In its turn the motor emf is taken between points A and B of the bridge circuit consisting of anchor resistance R_4 and external resistances R_5, R_6, R_7. When balancing the bridge $R_6/R_7 = R_2/R_5$ on the diagonal AB the output voltage component of the power amplifier PA equals zero and only the component proportional to the emf of E is retained (see analogous amplidyne circuit, Chapter 6, Figs. 6-8, b). Inasmuch as the voltage at points A and B are assigned with respect to earth to obtain their distance in parallel summation circuits

employ. In d-c amplifiers the sign of one of the
voltages must be changed. This has been done with
voltage e_b at the output of   inverting amplifier A_3.
Thus, at the output of A_2 there forms a voltage

$$e_s = \ddot{U} - k(e_a - e_b) = \ddot{U} - \dot{E}.$$

Open circuit control is effected by feeding into
the system's closed circuit a signal proportional to the
second derivative $\ddot{U}$ of the line shown in the upper
part of Fig. 10-12.

Thus, except for the complementary signal of the
second derivative, circuit 10-12 has the same four
control signals (start U, $\dot{U}$ and operation $\ddot{U}$, $\dot{E}$) as
in Fig. 10-10, c and d, although the design of the
done units is substantially different.

Let us now investigate the amplifying and power
channels of the unit. The former consists of amplifier
A_4 with a large voltage amplification factor (80,000)
continuing into power amplifier PA which forms current
through the anchor of the motor and resistance R_5.
Voltage U_5 on R_5 through feedback resistance R_4 is fed
to the input of A_4.

Thus, the operating principle of d-c current am-
plifiers with negative feedback has not been disrupted
in this case since by inserting into the straight channel
an additional cascade PA only increases the accuracy of
the formula of the summing amplifier which for the
signals studied has the form:

$$- U_5 = R_4 \left(\frac{e_1}{R_1} + \frac{e_2}{R_2} + \frac{U}{R_3} \right) =$$

$$= \frac{R_4}{R_1} \left(e_1 + \frac{R_1}{R_2} e_2 + \frac{R_1}{R_3} \right)$$
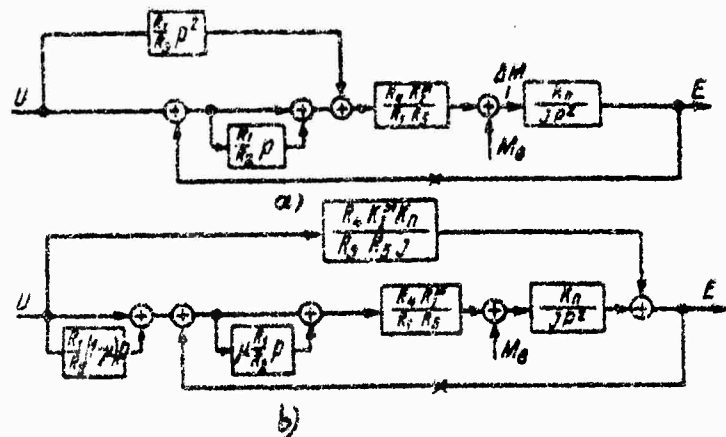
Fig. 10-14. Block diagram of electrodynamic unit.

Elimination of the effect of counter emf on the motor's operation is one of the chief merits of the circuit investigated and increases considerably its accuracy.

The presence in the closed circuit of an amplifier of the motor emf does not interfere with the transfer properties of the amplifier since the emf may be regarded as an additional disturbance applied to the circuit after a large amplification factor.

All further transformations of voltage U_5 are standard: from voltage we pass to current

$$I = \frac{U_5}{R_5};\tag{**}$$

by introducing the designation of momentum coefficient K_I^M for direct excitation current we find the motor's moment:

$$M_d = K_I^M I;\tag{***}$$

we exclude the possible resistance moment ΔM_d (disturbance) and determine the excessive moment:

$$\Delta M = M_y - M_L; \qquad (****)$$

by double integration of the ratio of excessive moment to moment of inertia we find the deflection angle of the rotor shaft:

$$a(\rho) = \frac{1}{\rho^2} \cdot \frac{\Delta M(\rho)}{J}.$$

The block diagram of the unit has been designed according to the formulas denoted by asterisks and also according to control signal formation equations in Fig. 10-14,a. Some structural transformations were carried out in the block diagram.

From circuit 10-14,a we can easily pass to circuit b equivalent to that shown in Fig. 10-10, b. In so doing we obtain condition(10-40 b) for faultless reproduction of the input signal in the absence of additional disturbances:

$$\frac{R_1 R_2^y K_t}{R_1 R_2 J} = 1. \qquad (10-41)$$

The circuit can be easily tuned according to this formula by choosing the appropriate resistances for the input circuits of the amplifier. We introduce into the final formulas a limited number of adjustable resistances; all the other resistances in the circuits denoted by r are assumed to be mutually identical, this fact determining the single aggregate amplification factor for A_1, A_2, A_3 and facilitating the writing of the formulas.

To compute the measures of U and $U_s - A_5$ on A_1 (considering that from the rate of motor Ω to the rate of voltage change in the principal channel (on potentiometer P) there is a transfer factor K_t, and in channel A_2 we have

a product of transfer factors: K_Ω^E, the motor emf coeffi-
cient, and K_B, the bridge transfer coefficient) resistances
$r_a = r_b$ should be chosen according to formula

$$\frac{r_a}{r} = \frac{r_b}{r} = \frac{K_\Omega^E K_B}{K_T}.$$

If $r_a = r_b$ is taken $1/\mu$ ($\mu < 1$) times greater than
recommended in the formula, as shown in circuit b,
inner forcing will decrease by a factor of μ but there
will instead arise outer forcing $1 + R_1/R_2 (1 - \mu)p$.

It can be used for compensating the component of
disturbance moment M_D proportional to rate.

As noted above, the closed part of the control
system fights additional disturbances, and although the
disturbance input point has an unfavourable position
the extensive adjustment possibilities (Bibl. 3) warrant
an exact operation of the unit up to $0.1 - 0.2^\circ$ with
harmonic oscillations at frequencies of $0.02 - 1.00$ cps.

Internal forcing for the given circuit is compulsory
($\mu > 0$) since otherwise the closed circuit forms a
resonant section and the circuit cannot operate.

From the general theory and from the example investi-
gated we can see that combined circuits with models or
computers make it possible to attack the problem of
eliminating errors not only of forced motion of the
assigned class but also total errors $\varphi (p) \to 0$.

10-6. Compensation of Disturbance Errors

The theoretical side of the problem remains the

same as when investigating errors of program motion;
in using the formulas derived it will be necessary,
however, to replace input by disturbance and error
transfer function or relative transfer function by
disturbance influence function. Forced motion errors
due to disturbances in linear systems are algebraically
summed with program performance errors.

Let us cite as an example the technical realization
of the principles of compensating forced motion error
due to disturbance.

We examine the electric circuit of a control system with
amplidyne shown in Fig. 10-15,a.

$a)$

$b)$
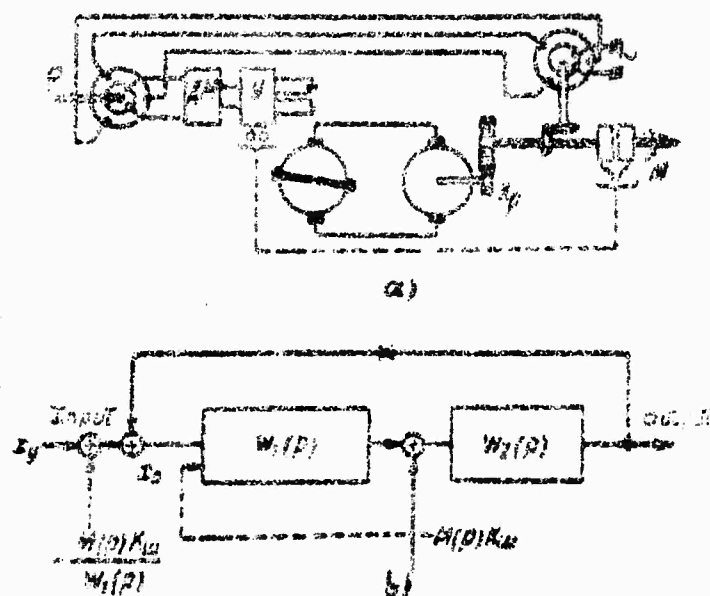
Fig. 10-15. Compensation circuit for load moment
disturbance.

In this circuit the measuring element and the

793

fundamental feedback are selsyns according to Fig. 9-6.
Unbalance between the input and output shafts is simul-
taneously transformed by the measuring element (selsyn)
into a-c voltage of phase 0 or 180° depending upon the
sign of the unbalance angle.

Unbalance voltage is fed to the demodulator where
it is rectified maintaining, however, the polarity
corresponding to the unbalance sign. From the amplifier
output the amplified signal is fed to the amplidyne
control coil. We investigate the amplidyne's operation
under conditions of total compensation of demagnetizing
longitudinal flow, as shown in block diagram 9-8, b.
This circuit has a feedback from counter emf of the
motor; it is convenient to transfer it through the sections
and the adder to feed disturbance to the moment line
and carry out investigations somewhat later, and first
study the sections of the straight channel up to the
moment application point and beyond.

If we multiply all the coefficients and section
transfer functions given in Figs. 9-8, we obtain a
transfer function from the control signal to disturbance-
moment input line

$$W_1(p) = \frac{K_r^T K_c K_{ya} Y_v S_{l_y}^{E_q} Y_q S_{l_q}^{E_d} Y K_l^M}{(T_y p + 1)(T_q p + 1)(T p + 1)}$$

or

$$W_1(p) = \frac{K'}{(T_y p + 1)(T_q p + 1)(T p + 1)}, \qquad (10\text{-}42\ a)$$

where

$$K' = K_r^T K_c K_{ya} Y_y S_{l_y}^{E_q} Y_q S_{l_q}^{E_d} Y K_l^M. \qquad (*)$$

This transfer function is shown in the wrapped
block diagram in Fig. 10-15, b.

Transition from excess moment to electric motor rotation rate is given by function $1/Jp$, but this section is enveloped by converted feedback with transfer function $\dfrac{K_g^E Y K_j^M}{Tp+1}$, hence aggregate transfer function moment-rate is:

$$\frac{\dfrac{1}{Jp}}{1 + \dfrac{K_g^E Y K_j^M}{Jp(Tp+1)}} = \frac{Tp+1}{Jp(Tp+1) + K_g^E Y K_j^M}.$$

Further, considering the transfer function of the kinematic section and reducer k_{sh}/p, we find the transfer function of the disturbance-output portion of the straight channel

$$W_2(p) = \frac{K_{ni}(Tp+1)}{[Jp(Tp+1) + K_g^E Y K_j^M]p}, \qquad (10\text{-}42\,b)$$

shown in block diagram 5-8, b.

Further, we must apply between sections $W_1(p)$ and $W_2(p)$ the disturbance moment whose magnitude reduced to the motor shaft equals $M(p) K_{sh}$ and investigate the standard closed   control system.

The complete transfer function of the open system

$$W(p) = W_1(p) W_2(p) =$$

$$= \frac{K_{-1}}{(T_y p + 1)(T_g p + 1)(c^2 p^2 + 2\zeta\tau p + 1)p} \qquad (10\text{-}43)$$

has a common amplification factor

$$K_{-1} = K'K'' \ \sec^{-1},$$

where

$$K'' = \frac{K_{ni}}{K_g^E Y K_j^M}. \qquad (**)$$

The control system obtained has a first-order program input astaticism since the integrator is included in the feedback for the program error transfer function (from x_y to x_0) and is static with respect to disturbance

since the integrator is not comprised in the feedback of
disturbance influence function (disturbance transfer
function).

To determine the required amplification factor of
the open control system for the assigned error ε_p of
program performance at maximum rate $\dot{x}_{mr}$ we use formula
(10-17 b).

Example 2 for $\dot{x}_{mr} = 0.5$ rad/sec and $\varepsilon_p = 0.001$ rad,
solved on p. 263, yields the required value of the am-
plification factor $K_{-1} = 500$ sec^{-1}. Suppose that for
the control servomechanism investigated we have adopted
precisely this value of the open system amplification
factor.

Now let us investigate the disturbance error. We
determine the relative transfer function of the control
system studied:

$$\Psi_*(p) = \frac{(T_y p + 1)(T_q p + 1)(\tau^2 p^2 + 2\xi\tau p + 1)p}{(T_y p + 1)(T_q p + 1)(\tau^2 p^3 + 2\xi\tau p + 1)p + K_{-1}} . \quad (10\text{-}44\ a)$$

We then pass to the disturbance influence function:

$$\Phi_u(p) = \Phi_*(p) W_a(p) =$$

$$= \frac{(T_y p + 1)(T_q p + 1)(Tp + 1)K''}{(T_y p + 1)(T_q p + 1)(\tau^2 p^3 + 2\xi\tau p + 1)p + K_{-1}} . \quad (10\text{-}44\ b)$$

Steady-state disturbance error for a constant re-
tarding moment is $\quad e_u = \frac{-K''}{K_{-1}} K_w M = -\frac{K_w M}{K'} =$

$$= -\frac{K_w M}{K_r^T K_c K_{ya} Y_y S_{l_y}^{Eq} Y_q S_{l_q}^{Ed} Y K_f^M} . \quad (10\text{-}44\ c)$$

If the maximum value of the moment is determined
and that portion of total error which it is permissible
to have from disturbance is also determined, then from
formula (10-44 c) we can derive the required value of

$$K' = \frac{K_M M}{\varepsilon_M} \quad [kГ \cdot м/rad]. \qquad (10\text{-}45\,a)$$

Thus, e.g., with the same allowance for error $\varepsilon_M = 0.001$ and the magnitude of the reduced load moment $K_M M = 0.1$ kg m

$$K' = 0.1/0.001 = 100 \text{ kg m/rad.}$$

the second amplification factor with a total coefficient $K_{-1} = 500$ sec^{-1} then amounts to

$$K'' = 500 \text{ sec}^{-1}/100 \text{ kg m/rad} = 5 \text{ (rad/sec/kg m).}$$

We can easily note that it is expedient to create the greater part of the total amplification factor before the disturbance application point in order that it be included in the feedback for the closed circuit "disturbance-output". Let us also note that for the diagram investigated, in the closed circuit "disturbance-error line" the direct link contains an integrator while the feedback contains the static section $W_1(p)$.

In steady state the disturbance influence factor is equal to the inverted feedback coefficient:

$$\Phi_v(0) = \frac{1}{W_1(0)}. \qquad (10\text{-}45\,b)$$

This rule was used in formula (10-44 c).

In a number of cases, for the purpose of unifying the computation or errors from program and from disturbance, it is expedient to transfer the disturbance to the circuit's input. Such a transfer is shown in the block diagram by the dashed line, and the converted disturbance is written:

$$\ldots \ldots \frac{K_M M(p)}{K_1(p)} \ldots \ldots$$

Subsequently all the errors can be computed as in the case of program input.

The disturbance effect can also be inhibited by introducing corrections proportional to the disturbance measured. To do this we need an additional measuring element which determines the magnitude of the disturbance and feeds into the circuit the compensation on the basic of disturbance control method.

In the electric circuit investigated the moment may be measured by an elastic joint with a resistance transducer or a variable inductor. It is expedient to feed the measured signal to the input of the amplifying circuit, as shown in Fig. 10-15, a by the dashed lines (Bibl. 4).

Tuning conditions for the compensating line are given by formulas (5-18); decompensation error is defined by formula (10-8 c).

We remind that Chapter 6 deals also with disturbance adjustment methods by means of overcompensating amplidyne. This requires no additional measuring elements.

10-7. Precision of Control Systems with Variable Parameters

Differential equations (10-20 d) or (10-22 b) give in their algebraized form a connection between control signal and error signal in a closed system:

$$\mu(t, D)\, x_1(t) = v(t, D)\, x_n(t). \qquad (10\text{-}46\ a)$$

Let us investigate variable systems operating only during a limited time interval and whose accuracy is measured at the end of this interval t_K. Given the value of t_K from the direct equation (10-45 a) we can pass to the R-S-equation

$$X_y > X_{in} \qquad \mu(D', t_K - \theta)\, g'_s(t_K, \theta) = \delta(\theta), \ \atop w'_s(t_K, \theta) = v(D^*, t_K - \theta)\, g^*_s(t_K, \theta), \quad (10\text{-}46 \ b)$$

set up with respect to the weight function on the error line $w_s(t_K, \theta)$ changing along argument θ with fixed t_K. The function determined by this equation becomes the kernel of the convolution equation

$$-x(t_K) = x_y(t_K) = \int^{t_K} w'_s(t_K, \theta)\, x_y(t_K - \theta)\, d\theta. \quad (10\text{-}46 \ c)$$

In order that the curve of the error excited by constant input

$$x_y(t) = x_y(0) = \text{const.}, \qquad (10\text{-}47 \ a)$$

at the instant of time $t = t_K$ pass exactly through zero it suffices to fulfill the condition

$$\int^{t_K} w'_s(t_K, \theta)\, d\theta = 0. \qquad (10\text{-}47 \ b)$$

With an input signal changing linearly

$$x_y(t) = x(0) + \dot{x}(0)\, t, \qquad (10\text{-}48 \ a)$$

in addition to satisfying condition (10-47 b), another condition

$$\int_0^{t_K} \theta w'_s(t_K, \theta)\, d\theta = 0. \qquad (10\text{-}48 \ b)$$

has to be fulfilled for a precise reproduction at the instant $t = t_K$.

For a signal in the form of the polynomial

$$x_y(t) = \sum \frac{x^{(i)}(0)}{i!}\, t^i \qquad (10\text{-}49 \ a)$$

a faultless reproduction at the instant t_K is attained

799

If the following series of conditions is met:

$$\int_\delta^{t_k} \theta^i x_a(t_k, \theta) \, d\theta = 0; \quad i = 0, 1, 2 \ldots n. \qquad (10\text{-}49\ b)$$

For some particular relations between input process derivatives $x_y^{(i)}(0)$ we can compensate the error by means of nonzero values of integrals (10-49 b) with different signs.

Relations (10-47) — (10-49) also hold for control systems with constant parameters if the weight function is taken to depend only upon one argument. This result will be used below (see Table 12-2). We continue our investigation of the accuracy of control systems with variable parameters with the aid of more explicit methods.

We determine $\Phi(t_k, S)$ from equation (10-46 b) following the method of successive approximations of AOTF discussed in Chapter 3; then according to formula (3-83 c) the error takes the form:

$$X_y = X_{in} \qquad E(t_k, S) = \Phi_a(t_k, S) X_y(S). \qquad (10\text{-}50\ a)$$

We expand $\Phi(t_k, S)$ in a series and obtain a result analogous to the series employed in (3-85 a):

$$\Phi_a(t_k, S) = \Phi_a(t_k, 0) +$$
$$+ \Phi_a'(t_k, 0) S + \Phi_a''(t_k, 0) S^2 \ldots$$

or in accordance with (3-85 b) for the unbiased output process

$$\varepsilon(t_k) = \Phi_a(t_k, 0) x_y(t_k) + \Phi_a'(t_k, 0) \dot{x}_y(t_k) +$$
$$+ \Phi_a''(t_k, 0) \frac{\ddot{x}_y(t_k)}{2!} + \ldots \qquad (10\text{-}50\ b)$$

If the input process retains its form but shifts by a quantity $\mathfrak{D}_e$, then formula (3-85 a) should be used.

By analogy with automatic control systems with constant

coefficients the variable system is said to be astatic
at point t_K if the lower order terms of the right hand
side of (10-50 b) will be equal to zero. As before, the
order of astaticism will coincide with the number of
low-order terms of series (10-50 b) equalling zero.
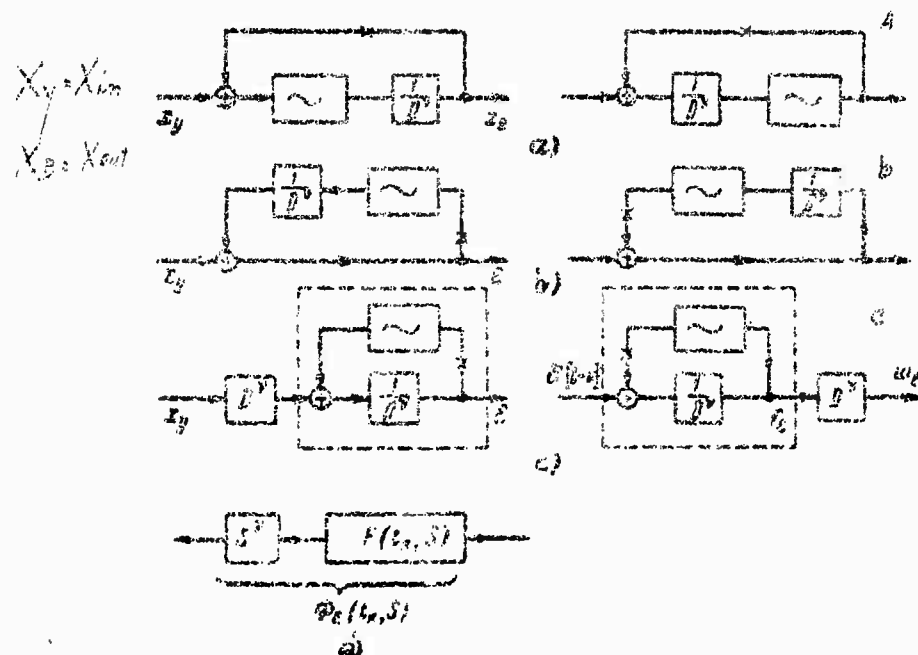
Fig. 10-15. Block diagrams of astatic and static
control systems with variable parameters

Conditions for obtaining a control system with
variable parameters astatic at point t_K are analogous
to conditions (10-7 a) and amount to forming an ADE
of the form

$$\Phi_{st}(t_x, S) = F(t_x, S) S^\gamma$$

(10-50 c)

Let us now proceed to derive the structural con-
ditions for obtaining astatic systems. Figure 10-16, a
shows the diagram of a control system with variable

parameters into the straight channel of which ν integrators have been introduced. By means of structural transformations we can from diagram a obtain diagram b which shows in a more explicit fashion the way errors are obtained, and diagram c in which after transferring the adder in a direction opposite to the path of the signal the conditions for input signal differentiation are determined.

If for the variable straight channel equation (10-18 a) is given, then the weight function of the circuit framed in diagram c by a dashed line, can be determined from equation

$$\left\| \begin{array}{ccc} 0 & v(t, D) & -u(t, D) \\ 1 & 0 & -D \\ 1 & 1 & 0 \end{array} \right\| f_{\epsilon} =$$
$$= \left\| \begin{array}{cccc} \cdot & \cdot & \cdot & 0 \\ \cdot & \cdot & \cdot & 0 \\ \cdot & \cdot & \cdot & 1 \end{array} \right\| \delta[t - \theta], \qquad (10\text{-}51\ a)$$

which, like equations (1-100) and (1-101), can be reduced to the form

$$\mu(t, D) f_{\epsilon} = v(t, D) \delta[t - \theta]. \qquad (10\text{-}51\ b)$$

Now we pass to R-S equations

$$\mu(D^*, t - \theta) \varphi_{\epsilon}^{*} = \delta[\theta]; \\ f_{\epsilon}^{*} = v(D^*, t - \theta) \varphi_{\epsilon}. \qquad (10\text{-}51\ c)$$

and by solving them by successive approximations we can determine the ACTF for that part of the circuit $F(t_y, S)$. Further, on the basis of formula (5-57) we pass to block diagram d and to the aggregate ACTF for the error, which coincides with (10-50 c).

system's straight channel, as shown in diagram A, converted diagrams B and C do not allow us adopt simple procedures on the basis of formulas (5-50) - (5-62) given in Chapter 5 for obtaining the aggregate AOTF of the circuit for a certain $K(t_k, \theta)$.

In fact, in the B-S system (7) corresponding to diagram c there will be at the input of the variable unit a pulse of $(\nu + 1)$ -th order $\delta^{\nu}(\theta) = \delta^{\nu}(t-\theta)$. Knowing the solution

$$f_k^*(t, \theta) = f_k^*(t, t-\theta)$$

of equations (10-51 c) with an input pulse of first order, and differentiating these equations with respect to the second argument (t) in a like fashion as (8-80), we can find the solution of the B-S system (7) also for high-order input pulses, and find that the representation of this reaction along argument θ.

Then the AOTF for diagram c will be

$$\Phi_{c}(t, S) = L\left\{\left[\frac{\partial}{\partial t^{\nu}}[f_k^*(t, t-\theta)]\right]_{\theta=t-s}\right\}. \quad (*)$$

In the general case the result will be longer lead to the solution of (10-50 c). For qualitative conclusions we need not resort to complex transformations but may turn directly to circuits a or A and circuits c or C derived from them. For circuit c the input signal is differentiated and its constant, rate, etc., (ν in all) components do not excite the system and do not generate errors, i.e., with the establishment of integrators at the output of the system's straight channel the automatic control system

becomes astatic. In circuit C even a steady input
signal can excite a complex reaction in the variable
system which, in the general case, subsequent differ-
entiation will not succeed in eliminating and the
system does therefore not acquire astatic properties.

Thus, in variable systems the establishment of
integrators in the negative feedback circuit for a
given disturbance (or in the straight channel for the
control signal) provides the automatic control system
with astatic properties only if the integrators are
placed at the output of the variable part, i.e., the
variable section is equivalent to the disturbance
force.

10-8. Statistical Precision Estimate According to The System of Random Variables

A. Definition of Disturbances with Random Scale

If one and the same automatic control system is
used repeatedly and each time the system is switched
in the disturbances acting upon it are checked, then
the results of this control can be systematized and
on their basis we can obtain type laws of the varia-
tion of disturbances with time. Some standard curves
of variation changes are shown in Fig. 10-17.
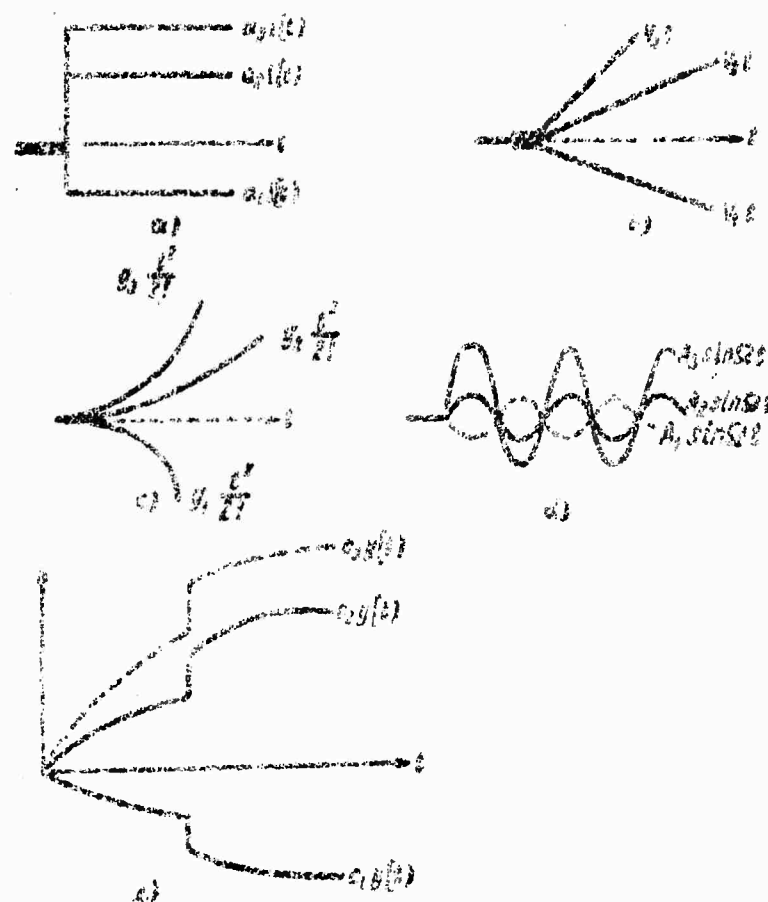
Fig. 10-17. Random-scale processes.

If the nature of the causes bringing about disturbances remains unchanged during a series of connections of one and the same automatic control system or during a mass connection of control systems of the same type of design and transfer functions, then the shape of the curve of disturbances characteristic for an actual type of control system will be recurrent. As a rule, however, the disturbance level changes from test to test and its concrete value for a given

test cannot be predicted although the possible limits of its changes can apparently be estimated.

Such processes will be called determined in shape but random in scale.

In diagram a the stepped form of process a $1[t)$ is determined, whereas the height of step a is arbitrary.

In diagram b there is determined the linearity of disturbance increase with time vt but rate v is random.

In diagram c we have a determined uniformly accelerated law of disturbance increase with time $gt^2/2$, while the magnitude of acceleration g is arbitrary.

In diagram d the harmonic law of concrete frequency $A \sin \Omega t$ is determined but its amplitude A is random.

In diagram e the complex form of process cy(t) is determined but its scale c is arbitrary.

Thus, in all the examples above the random factors are determined by only one quantity - the scale.

Random quantities (variables) have the following statistical characteristics:

$$c \begin{cases} \overline{c} - \text{statistical mean;} \\ D_c - \text{dispersion} \end{cases}$$

Having available data on the concrete magnitude of scale c_j in j-th test we can easily determine the statistical mean value of the scale for N tests:

$$\overline{c} = \frac{\sum_{j=1}^{N} c_j}{N}. \tag{10-52 a}$$

If we increase the number of tests to infinite, statistical mean value approaches mathematical expectation.

$$-786-$$

$$M[c] = \lim_{n \to \infty} \overline{C}. \qquad (10\text{-}52\ b)$$

If in all the measurements of c_j we exclude the statistical mean value of scale $\overline{C}$, we obtain a series of so-called centralized values of the random quantity (variable):

$$c_{j0} = c_j - \overline{C} \quad (j = 1, 2 \ldots N). \qquad (10\text{-}52\ c)$$

or more exactly:

$$c_{j0} = c_j - M[c]. \qquad (*)$$

The mean value of the square of centralized random variables is called measure of dispersion:

$$D_c = \frac{\sum_{j=1}^{N} c_{j0}^2}{N - 1}. \qquad (10\text{-}52\ d)$$

Reducing the denominator of the formula by unity is due to the necessity of introducing a correction for the limitation of the number of tests $N \neq \infty$ where mathematical expectation is not equal to the statistical mean, and formulas (*) and (10-52 c) do not coincide.

The positive value of the square root from the dispersion is equal to the mean square magnitude of the measure:

$$\sigma_c = \sqrt{D_c}. \qquad (10\text{-}52\ e)$$

All of the above statistical estimates are interesting only if we have a large-scale utilization of the control system investigated under single-type conditions and when the mean results characterize the efficiency of the plant serviced by the automatic control system. When we speak, e.g., of the mean accuracy of automatic control systems used by the industry for the

production of specific goods, we determine the mean value of scraps. When we speak of the mean accuracy of automatic control systems for military installations we evaluate their combat efficiency, for example, as a whole for the military operation or even for the entire war, the ammunition consumed, etc.

Such an approach makes it possible to study the statistical model of the phenomenon rather than investigate the actual conditions under which disturbances arise, conditions which break down into a large number N of actual tests. And since it suffices to have only two statistical characteristics $\bar{C}$ and D_c for the entire set, it obviously makes sense to intentionally roughen the data on disturbances subordinating them to the system adopted for studying the phenomenon. In the present section we investigate the system of random variables -measures with determined disturbance form. Other methods are also possible if they rely upon practical working conditions of actually operating control servomechanisms.

B. Statistical Estimates of Forced Motion Errors in Control Systems

Random scale disturbances shown in Fig. 10-17, a-d excite the control system with a prescribed error weight function $w_\varepsilon(t)$ or $w_\varepsilon^*[t, \theta)$ corresponding to OTF $\Phi_\varepsilon(p)$ or ACTF $\Phi_\varepsilon(t, S)$ and bring about specific processes to occur on the error line. We investigate control

systems such that under the effect of those disturbances the error change process becomes steady-state, i.e., the error takes on a constant value or constant amplitude for harmonic response.

a) Steady-state (positional) error of static control systems ($\nu = 0$).

A determined process $a_j 1(t)$ with a concrete j-th measure a_j engenders the steady-state error

$$\varepsilon_{0j} = \Phi_\varepsilon(0) a_j \qquad (10\text{-}53a)$$

By performing a statistical processing of the series of single-type connections of the control system for j, i.e., by applying formula (10-53a) to both sides of Eq. (10-53a) we find the statistical mean of the steady-state error:

$$\bar{\varepsilon}_0 = \Phi_\varepsilon(0) \bar{a} \qquad (10\text{-}53b)$$

By applying formulas (10-58 c, d) to both sides of Eq. (10-53a) we find the dispersal n of the steady-state error:

$$D_{\varepsilon_0} = \Phi_\varepsilon^2(0) D_a \qquad (10\text{-}53c)$$

a) Steady-state rate error of control system with astatism of first order ($\nu = 1$)

The determined relation between type b process (Fig. 10-14) with concrete rate value v and the error engendered by it in a system with first-order astatism is the following

$$\varepsilon_{1j} = \dot{\Phi}_\varepsilon(0) v_j \qquad (10\text{-}54a)$$

After statistical processing of the first series we obtain, similarly to formula (10-53), a relation between the statistical characteristics of the source ...

789

of input disturbance and the system's output error:

$$\overline{E}_1 = \Psi'_s(0)\overline{V};\qquad (10\text{-}54b)$$

$$D_{s1} = \Phi'^2_s(0)D_y.\qquad (10\text{-}54c)$$

c) Steady-state acceleration errors of control systems
with astaticism of second order ($\nu = 2$)

Analogous conclusions hold also for that response.

The determined relation is

$$\epsilon_{2i} = \frac{1}{2}\Phi''_s(0)g_i.\qquad (10\text{-}55a)$$

The relations between the statistical characteristics
of input acceleration and the output error of the control
system are

$$\overline{E}_2 = \frac{\Phi''_s(0)\overline{g}}{2};\qquad (10\text{-}55b)$$

$$D_{s2} = \frac{\Phi''^2_0(0)D_g}{4}.\qquad (10\text{-}55c)$$

d) Forced harmonic error

The determined relationship between input ampli-
tudes and actual test error takes the form:

$$A_{si} = |\Phi_s(j\Omega)|A_{yi}.\qquad (10\text{-}56a)$$

The relation between amplitude characteristics
can be derived from the determined relation (10-56a):

$$\qquad (10\text{-}56b)$$

$$\overline{A}_s = |\Phi_s(j\Omega)|\overline{A}_y;$$

$$D_{As} = |\Phi_s(j\Omega)|^s D_{Ay}.\qquad (10\text{-}56c)$$

C. Statistical Estimates of Control System Errors at
an Assigned Point t_k

We investigate the more general process of disturbance
variation (Fig. 10-17, b). If its values, derivatives of
harmonic amplitudes approach asymptotically a constant
limit, then processes a-d ensue from process e as par-

790

ticular cases but processes a way also not approach the par-
ticular cases above; in the last analysis the method of
statistical investigation remains the same.

For a practical test for j-th process value the error
at the assigned point t_k can be determined by the determined
equation of integral coupling for control system with
constant parameters:

$$e_j(t_k) = c_j \left\{ \int_0^{t_k} w_s(\theta) y(t_k - \theta) d\theta \right\} \quad (10\text{-}57\text{a})$$

and for the case of variable parameters

$$e_j(t_k) = c_j \left\{ \int_0^{t_k} w_s^*(t_k, \theta) y(t_k - \theta) d\theta \right\} \quad (10\text{-}57\text{b})$$

In both formulas the result of the integration
placed in braces does not depend upon the measure and is
reduced to the constant coefficient, i.e., the determined
relation in the example investigated is analogous to those
examined earlier; similarly, we derive from here the re-
lation between statistical characteristics of the input
measure and the error at a prescribed instant:

$$F(t_k) = \left\{ \int_0^{t_k} \ldots \right\} F.$$
$$\quad (10\text{-}57\text{c})$$

$$D_s(t_k) = \left\{ \int_0^{t_k} \ldots \right\}^2 D_y \quad (10\text{-}57\text{d})$$

where under the integrals are introduced weight functions
for the case of constant coefficients $v(\theta)$ and variables
$v(t_k, \theta)$.

These relations can also be expressed by representa-
tions and CTF or AOFS.

$$\overline{E}(t_k) = \overline{C} \left\{ L^{-1}[\Phi_s(p) Y(p)], \, t_k \right\}$$
$$D_s(t_k) = D_s \left\{ L^{-1}[\Phi_s(p) Y(p)], \, t_k \right\} \quad (10\text{-}57\text{e})$$

791

$$\overline{E}(t_\kappa) = \overline{C}\{L^{-1}[\Phi_\bullet(t_\kappa, S)Y(S)]_{\theta=t_\kappa-\theta_y}; $$
$$D_s(t_\kappa) = D_c\{L^{-1}[\Phi_\bullet(t_\kappa, S)Y(S)]^2_{\theta=t_\kappa-\theta_y}. \tag{10-57f}$$

D. Predictions

With only a few tests available, limit (10-52b) can obviously not be exactly fulfilled. This, of course, has no effect upon the accuracy of the above conclusions regarding the relation between the statistical characteristics of the disturbance measure and the control system error. These relations will remain unchanged if we use mathematical expectation of the measure and the error instead of the statistical mean, and the exact value of dispersion instead of only the measure of dispersion. However, to forecast errors, knowledge of only the two statistical characteristics mentioned above is not sufficient; we must also have data relative to the law of distribution of the random variable.

Most widespread among the distribution laws is the normal law, called Gauss law. It has the following expression for the differential distribution curve, i.e., probability density:

$$f(s) = \frac{1}{\sqrt{2\pi\sigma}} e^{-\frac{s-M[s]}{2\sigma^2}}. \tag{10-58a}$$

If we know the parameters σ, $M\left[\varepsilon\right]$ of the normal distribution law we can forecast the probability of an error arising within the assigned limits $-(\xi/_\alpha)$ to $+(\xi/_6)$ ...ing to the formula

792

$$2\Phi\left(\frac{\xi}{\sigma}\right) = \frac{1}{2\pi\sigma}\int_{-\xi/\sigma}^{+\xi/\sigma} f(s)\,ds. \qquad (10\text{-}58c)$$

Thus, e.g., the probability of an error ξ in the zone $\pm[\xi] \pm 3\sigma_a$ is determined in the table of Φ-functions (Bibl. 5) by the following figure:
$2\Phi(\xi/\sigma) = 2 \times 0.4986 = 0.9973$.

Inasmuch as the probability of exceeding that zone is regarded as very small, $100(1 - 0.9973) = 0.27\%$, the virtually maximum and minimum probable errors to be expected are computed for the case of determined relation (10-58a) by the formulas:

$$\xi_{max} = M[a]\,\Phi_a(0) + 3\Phi_a(0)\,s_a; \qquad (10\text{-}59a)$$

$$\xi_{min} = M[a]\,\Phi_a(0) - 3\Phi_a(0)\,s_a. \qquad (10\text{-}59b)$$

For the other determinant relations (10-54)-(10-57) in the formulas obtained the system coefficient $\Phi_a(0)$ is replaced by another coefficient.

For the case that several disturbances with random measures representing non-connected random variables act upon the system we have to apply separately the formula of algebraic summation of mathematical expectations or statistical means and the formula of geometric summation of mean square errors. For the simplest case (10-53) we find the formulas

$$M[a] = \sum_{i=1}^{k}\Phi_i(0)\,M[c_i] \qquad (10\text{-}60a)$$

$$s_a = \sqrt{\Phi_1^2(0)\,s_{c1}^2 + \Phi_2^2(0)\,s_{c2}^2 + \dots \Phi_k^2(0)\,s_{ck}^2} \qquad (10\text{-}60b)$$

If the measures of all the disturbances are distributed normally, then prediction of the aggregate maximum probable error is done according to formulas analogous

793

to (10-59):

$$\bar{\varepsilon}_{max} = \sum_{i=1}^{k} \Phi_i(0) M[c_i] + 3 \sqrt{\sum_{i=1}^{k} \Phi_i^2(0) \sigma_c^2}. \quad (10\text{-}60c)$$

Occasionally prediction amounts to determining the mean error E which limits the accuracy range within which fall 50% of the test connections of control systems. From the table of function $\Phi(\xi/\sigma)$ for normal distribution law we can easily determine the relation between the mean error and the mean square error for a probability value 0.5:

$$E = 0,675\sigma.$$

If for a control system we have determined the limiting value of an error such that if it is exceeded the task assigned to the controlled member is not fulfilled, then prediction may be directed to computing the required (nominal plus excessive) number of connections of the control system in order to have the probability of fulfilling the task approach unity. Insofar as each connection of the control system is associated, e.g., with energy consumption, the prediction may wind up with computing the probable aggregate energy consumption needed for fulfilling the task. In military engineering such a problem can be, e.g. the calculation of ammunition consumption.

Probability predictions can obviously not be checked against a limited number of connection tests; their validity becomes apparent only in the case of mass tests or when predicting errorsbe it only in one test, provided they are engendered by a large number of various independent

794

disturbances (formulas (10-60)).

10-9. Statistical Accuracy Estimates by the Method of Random Functions

1. Statistical Definition of Disturbances as Random Processes

A. Non-stationary Random Process. Along with the relatively simple definitions of disturbances investigated above, in practice we frequently deal with disturbances in the form of random processes in the case of repeated control system connections. In diagram a of Fig. 10-18 we have curves showing concrete processes of disturbance variations for individual control system connections. These processes will be called characteristics of the random process.

Each characteristic is denoted, as this is done also with other functions of time, by a small letter with a subscript corresponding to the number of the process:

$$y_1(t); \; y_2(t), \ldots$$

The totality of these characteristics is denoted by $Y(t)$ which is said to be a random function or a random process.

The random function $Y(t)$ can, in turn, be regarded as a certain statistical representation of the totality of the possible characteristics. It is defined as follows:

795

$Y(t)$ $\begin{cases} y_i(t_k) & \text{-totality of random variables;} \\ \bar{Y}(t) & \text{- statistical mean of random functions;} \\ \xi & \text{- dispersion of random variable;} \\ K_y(t_1, t_2) & \text{- correlation function.} \end{cases}$
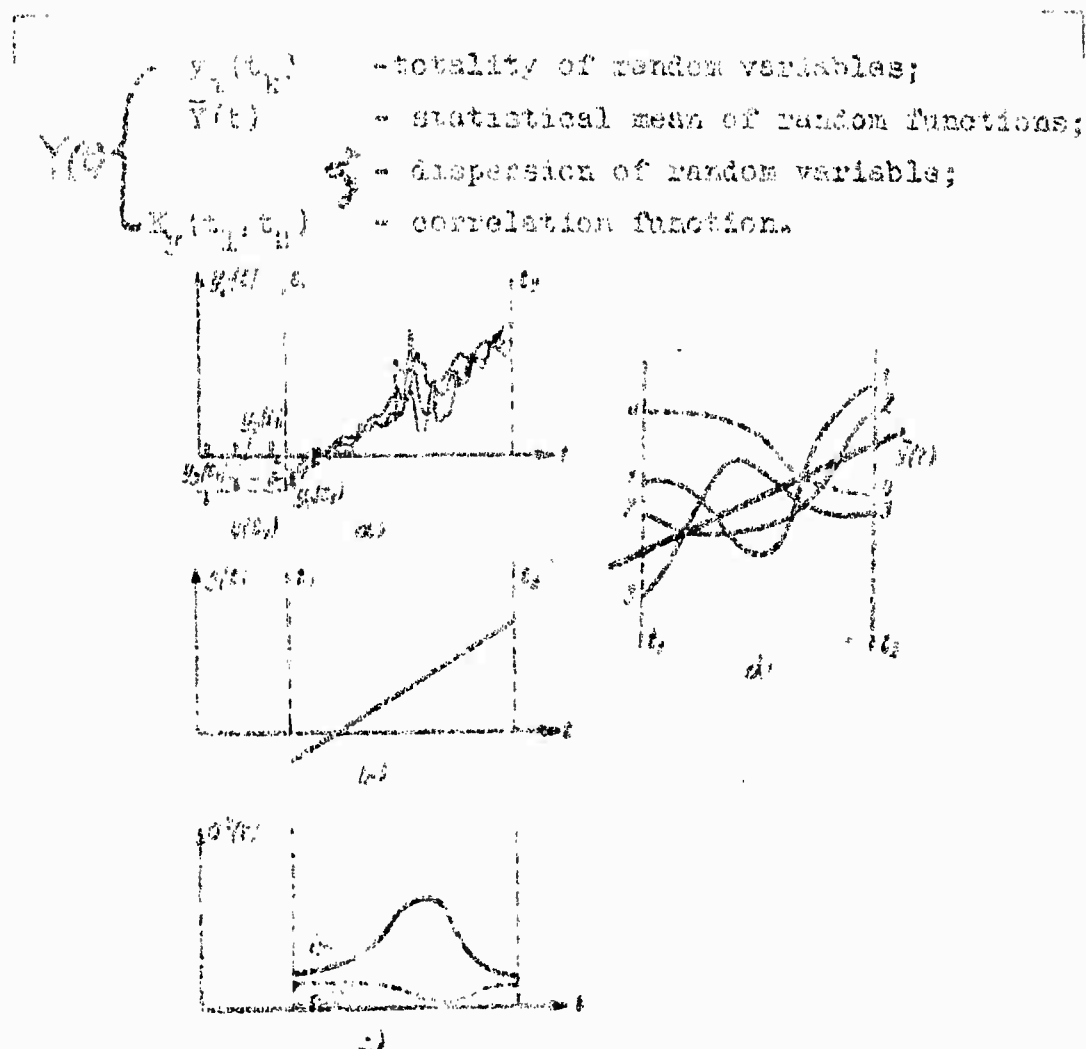
Fig. 10-18. Characteristics of random processes.

To determine the statistical mean of the random function we must assign individual instants of time t_k and seek the statistical mean (10-52a) of the totality of random variables

$$\bar{Y}(t_k) = \frac{\sum_{i=1}^{N} y_i(t_k)}{N} \qquad (10\text{-}52a)$$

In carrying out calculations for instants of time $t_1, t_2 \ldots$ we can find a curve $\bar{Y}(t)$, e.g., diagram b

790

plotted on the basis of the realizations of diagram a
in Fig. 10-18.

To determine the dispersion of the random function
we use a similar procedure of plotting the curve by
points computed by formula (10-52 d):

$$D_y(t_\kappa) = \sigma_y^2(t_\kappa) = \frac{\sum_{i=1}^{N}[y_i(t_\kappa) - \overline{Y}(t_\kappa)]^2}{N-1}. \qquad (10\text{-}61b)$$

The curve of the disturbance dispersion variation
c has been plotted in the same figure on the basis of
diagram a. We can easily note that the dispersion curve
reaches its peak at a point where realization dispersion
is maximal.

In determined processes with random measure we also
used estimates of the form (10-52) similar to the charac-
teristics of random process (10-61), but in the latter
case these characteristics are insufficient and to fully
evaluate the random process we introduce an additional
characteristic, the random process correlation function.
The need for studying the new characteristic of the random
process, viz., its correlation function, arises in connec-
tion with the formulation of the problem of transforming
by the control system the random process characteristics,
e.g., dispersion of a disturbance assigned as a random
process, into an output error dispersion.

Such a transformation can obviously not be reduced
to multiplying each point of the input disturbance disper-
sion curve by some constant factor as this has been done
for random variables. Indeed, if we investigate, e.g.,

797

input disturbance realization curves shown in Fig.10-18,a
and assume that in   the central part of the curve,
disturbance variation frequencies are considerably
higher than at its edges we can obtain for control
systems with great inertness an abrupt reduction of
high-frequency input oscillations and a considerably
lesser smoothening of low-frequency components at the
output. In this case the output dispersion curve may
turn out not only to be unproportional to the input
dispersion curve but even completely opposite to it.

In fig. 10-18, c the input dispersion curve is
drawn with a solid line, whereas the possible output
dispersion curve is shown with a dashed line.

Thus, the approach from preceding positions
based on the investigation of individual independent
points, is inapplicable to random processes since in
the latter case there is a connection between values
at neighboring points of the process which is all
the greater the smaller the interval between the points.
The measure of this connection is the correlation
function.

The correlation function of random processes is
understood to be the statistical mean of products of
measured values for various instants of time:

$$K(t_1, t_2) = \frac{\sum_{i=1}^{N} [y_i(t_1) - \bar{Y}(t_1)][y_i(t_2) - \bar{Y}(t_2)]}{N-1} \qquad (10-81c)$$

Definition of the correlation function for one
pair of points is shown in diagram d where are marked

the individual realizations of processes 1-4 and the
signs of deviations from the statistical mean Y(t).
We can note that realizations 1-3 have the same signs
at the ends of the interval investigated and when
summing according to formula (10-61c) they ensure the
accumulation of the sum. If the connectivity of pro-
cesses over the interval $\tau = t_2 - t_1$ is steady, then,
as a result of summing on the interval τ we find a
concrete number which is all the greater the smaller
the number of exceptions (of the type of realization 4).

Such computations for all points of the process
can be tabulated as follows:

t_K	t_1	t_2	. . .
t_1	$K(t_1, t_1)$	$K(t_1, t_2)$	. . .
t_2	—	$K(t_2, t_2)$	. . .
. . .	. . .	. . .	. . .

From this table we can plot the contour of the corre-
lation function.

Thus, an analytic and a tabular definition of the
correlation function are possible.

By definition (10-61c) the correlation function
is symmetric with the diagonal of the Table, hence it
suffices to fill in only one-half of that Table. The
diagonal of the Table where $t_1 = t_2$ yields the follow-
ing dispersion value

$$\sigma^2(t) = K(t, t).$$

799

[In fact, with $\tau_1 = \tau_2$ formulas (10-61b) and (10-61c)]
coincide.

3. Stationary Random Process. If for identical time
intervals $\tau = t_2 - t_1$ the correlation functions coincide
independently of the location of the interval shown in
Fig. 10-18,d, i.e.,

$$K(t_i, t_i + \Delta t) = K(\Delta t); \quad K(t_i, t_i + 2\Delta t) = K(2\Delta t),$$

where Δt is the step of the Table, then such a correlation
function has a simpler form $K(\tau)$ and a reduced computa-
tion table, and is said to be the correlation function
of a stationary random process.

The concept of stationary random processes is in
many things analogous to that of undamped steady-state
determined processes. Indeed, as we move with time along
the series of realization curves of random processes in
statistically processing them according to formulas
(10-61a) and (10-61b) changes in the results are not
expected, i.e.,

$$\bar{F}(t) = \bar{F} = const.; \quad \sigma_i^2(t) = \sigma_i^2 = const.;$$
$$K(t_i, t_j) = K(t_j, t_i) = K(\tau). \qquad (10-62)$$

The independence of statistical characteristics
(10-62) from time is taken to be the symptom of the
stationary state of a random process.

For stationary random processes, on the basis of
ergodic hypothesis we proved the equivalence of a
statistical processing of a set of processes by series
and by instructed product of a set with time. Hence
instead of formulas (10-61) for $N \to \infty$ we can for $T \to \infty$

write the equivalent formulas:

$$\tilde{Y}(t) = \frac{1}{2T} \int_{-T}^{T} y(t)\, dt;$$

$$(10\text{-}63a)$$

$$y_0(t) = y(t) - \tilde{Y}(t);$$

$$(10\text{-}63b)$$

$$\mathfrak{s}_y^2 = \frac{1}{2T} \int_{-T}^{T} y_0^2(t)\, dt;$$

$$(10\text{-}63c)$$

$$(10\text{-}63d)$$

$$K_y(\tau) = \frac{1}{2T} \int_{-T}^{T} y_0(t)\, y_0(t-\tau)\, dt.$$

In contrast to series-averaged quantities, the time-averaged quantities in (10-63) are denoted by $\sim$ on the top.

Definition of the correlation function by the integral equation (10-63d) in the domain of argument permits us to pass readily into the region of bilateral Fourier transforms: $K_y(j\omega) = \int_{-\infty}^{\infty} K_y(\tau)\, e^{-j\omega\tau}\, d\tau =$

$$= \lim_{T\to\infty} \int_{-\infty}^{\infty} \left\{ \frac{1}{2T} \int_{-T}^{T} Y(t)\, Y(t+\tau)\, dt \right\} e^{-j\omega\tau}\, d\tau.$$

We change the order of integration with respect to t and τ and place under the integral the unit factor $1 = e^{j\omega t} e^{-j\omega t}$ distributing the cofactors between two integrands in the right-hand side:

$$K(j\omega) = \lim_{T\to\infty} \frac{1}{2T} \int_{-\infty}^{\infty} Y(t)\, e^{j\omega t} \times$$

$$\times \left\{ \int_{-T}^{T} Y(t+\tau)\, e^{-j\omega(t+\tau)}\, d\tau \right\} dt.$$

We introduce the intermediate argument $r = t + \tau$, proceed in the same way as when deriving formula (4-118) and find

$$K(j\omega) = \lim_{T\to\infty} \frac{1}{2T} |Y_T(j\omega)|^2.$$

[ōF, on the basis of formula (4-121a)

$$K(j\omega) = S(\omega).$$ (10-64)

Thus, spectral density is equal to the Fourier transform of the correlation function of random stationary processes. Consequently, after having statistically processed the aggregate of realizations or one protracted realization and obtained the correlation function we can pass from it to spectral density.

In practice, in order to perform the transformation of (10-64), taking account of the evenness of the correlation function $K(\tau) = K(-\tau)$ which warrants that the imaginary part of the formula be equal to zero, we determine only its real part (4-114)

$$S(\omega) = 2\int_0^\infty K(\tau)\cos\omega\tau d\tau.$$ (10-65)

Computations can be carried out by the approximate procedures discussed in Chapter 4 or analytically by approximating the correlation function expedient for integrating by a dependence chiefly among those given in Table 4-9.

Thus, the random stationary process can be defined either by correlation functions or by spectral density. Another important characteristic of the stationary process is dispersion. The correlation function is a more general characteristic of random processes since dispersion reflects only the initial ordinate of the correlation function curve:

$$D_y = \sigma_y^2 = K(0).$$ (10-6?)

If in formula (10-64) we pass to the original on the basis of the inverse Fourier transform we find the

802

expression of the correlation function through spectral density:

$$K(\tau) = \frac{1}{\pi} \int_0^\infty S(\omega) \cos \omega \tau \, d\omega \qquad (10\text{-}67a)$$

and from formula (10-66) the connection between dispersion and the surface of spectral density curve

$$D_y = \sigma_y^2 = \frac{1}{\pi} \int_0^\infty S(\omega) \, d\omega. \qquad (10\text{-}67b)$$

C. Definition of input process by the white noise system.
An idealized stationary random process with constant spectral density:

$$S_n(\omega) = N^2 = const, \qquad (10\text{-}68)$$

is said to be "white noise". Its curve expands from zero frequency to an infinitely large frequency $0-\infty$.

We find the correlation function for white noise from an inverted Fourier transform according to Table 4-9:

$$K_n(\tau) = \frac{N^2}{2} \left(\delta[\tau +] + \delta[\tau -] \right) = N^2 \delta[\tau]. \qquad (10\text{-}69)$$

White noise dispersion can be computed only for a limited frequency band $\omega_0 \div \omega_0 + \Delta\omega$; in this case it is equal to

$$D_\Delta = \frac{N^2 \Delta\omega}{\pi}. \qquad (10\text{-}70a)$$

If we compute dispersion directly from formula (10-69) for $\tau = 0$ we find its value to be infinitely great in accordance with the height of the ideal pulse:

$$D_n = K_n(0) = \infty. \qquad (10\text{-}70b)$$

We can obtain the same result also from formula (10-67b) by infinitely widening the frequency band $\Delta\omega$. This is evidence of the fact that a white noise of

803

finite level cannot be practically achieved on an
infinite band since this would require a noise generator
of infinite power. But if the disturbance is defined for
a control system with a limited frequency passband, then
the part of the input spectrum beyond the cutoff fre-
quency of the control system does virtually not affect
the system at all. Hence from the viewpoint of esti-
mating the final result, that is, the system's error,
the investigation of the system's response to noise with
infinite band or noise with a finite band slightly
exceeding the passband of the control system yields
practically identical results. It is obvious, however,
that an isolated investigation (without control systems)
of a random effect with limited or infinite frequency
bands leads to completely different estimates of the
dispersion of the effect proper (10-70a) or (10-70b).

The term "white noise" was coined in analogy to
white light spectrum which contains all the frequency
harmonics in a band visible to the eye.

8. Effect of White Noise on Control Systems

A. Description of experimental investigation methods.
It is natural that testing conditions are approximated
as closely as possible to actual working conditions of
a control system. Since under actual service conditions
the control system is under the effect of random pro-
cess realization, the experimental procedure imitating
real operating conditions of control systems is called

the <u>realization method.</u>

Statistical laws, however, reveal themselves only
if we average a large number of tests, and since
practically this number is always limited the realiza-
tion method may turn out not to be satisfactory since
the deviations of experimental data from those expected
theoretically may be great. Let us remind the reader
that ideal white noise is virtually unachievable and
tests can be conducted only with a certain amount of
approximation. On the other hand, if we determine
experimentally only the weight function of a control
system, the passage from a determined weight function
to statistical noise characteristics can be achieved
quite easily by analytical means. This can be taken
into account during testing. In the latter case tests
are conducted according to the so-called <u>weight function</u>
<u>method.</u>

Let us now take a closer look at the two methods.

<u>Realization method.</u> A noise generator in the form
of a slowly rotating drum filled with small metal balls
creating random variable conductance between the walls
and the axis of the cylinder can generate a noise in the
frequency band from $\omega = 0$ to $\Delta\omega = 10$ sec^{-1}. Possible
irregularities in the spectrum of such a generator are
balanced by a filter, as shown in Fig. 10-19,a.

If the power (mean square time value) of the signal
generated equals ΔP, the spectral density level taken
to be constant in the $\Delta\omega$ frequency band according to
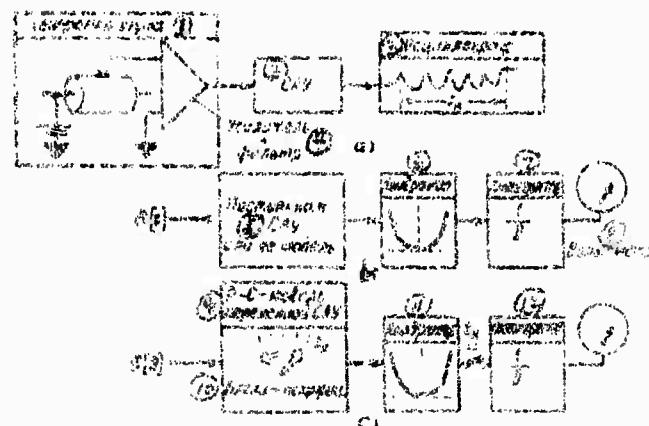
Fig. 10-19. Statistical simulation by the realization
method and the weight function method.
Key: 1) noise generator; 2) control system; 3) oscillo-
graph; 4) amplifier + filter; 5) constant control
system or its model; 6) squarer; 7) integrator; 8) volt
meter; 9) R-S model of a variable control system;
10) coefficient units; 11) squarer; 12) integrator.

(4-124c) amounts to

$$ N^2 = \varkappa \frac{\Delta P}{\Delta \omega}. \qquad (10\text{-}71a) $$

Each time the a noise generator connected in the
test with the input of the nonexcited control system
is switched on there occurs a new process of error
variation. The variety of processes at the output
(error line) is due in the first place to the scattering
of initial pulses (half-waves) at the instant of
switching on the noise generator, and in the second
place to various accumulation conditions for the output
response excited by the noise at the instant t_k accord-
ing to the convolution equation.

The first reason causes the process at the system's

output to be always nonstationary, at any rate until
the moment when the reaction to the initial pulse fades
away; the second reason yields with stationary input
a stationary output for control systems with constant
parameters and a nonstationary output for systems with
variable parameters. Hence, in the general case, for
statistical processing of test results we have to:

Find a set of noise error variation oscillograms;

Choose in each oscillogram the required instant
of time and from a set of graph ordinates find the
error dispersion.

Processing of oscillograms for time is permissible
only in the case of control systems with constant
parameters and a sufficiently rapidly damping weight
function. In this case the dispersion or mean power
of the error as a stationary process can be given by
an indicating instrument after the damping time of the
system's weight function and the averaging time of the
instrument itself (see Section 4-12) have elapsed. The
statistical processing for time is also permissible
for certain classes of processes where the only non-
stationary (variable with time) element is the statis-
tical mean $\overline{Y}(t)$ if it is singled out according to the
methods expounded in Chapter 12.

Weight function method. We investigate the condi-
tions for statistical processing of a series of error
change processes to determine the error's dispersion:

$$D_{\text{вых}}(t) = \frac{1}{N}\sum_{j=1}^{N} e_j(t)\, e_j(t) = \qquad (*)$$

$$= \frac{1}{N}\sum_{j=1}^{N}\int_0^t\int_0^t \omega_{ij}^*(t,\theta) y_j(t-\theta) \times$$

$$\times \omega_{ij}^*(t,\xi) y_j(t-\xi)\, d\xi d\theta.$$

The right-hand side of the formula is obtained by substituting the output value e in the j-th realization by its expression by means of the j-th signal y_j and the system's weight function for the given signal.

The series averaging operation can be inserted under the integral where only the quantities with subscripts of the j-th realization are being averaged. Averaging of signal noise realizations yields:

$$\frac{1}{N}\sum_{j=0}^{N} y_j(t-\theta) y_j(t-\xi) = \qquad (**)$$

$$= K(\xi-\theta) = N^2\delta(\xi-\theta).$$

We join the above formulas, $(*)$ and $(**)$ and define:

$$D_{\text{вых}}(t) = N^2\int\int \omega_{ij}^*(t,\theta)\, \omega_{ij}^*(t,\xi)\,\delta(\xi-\theta)\, d\xi d\theta.$$

First we integrate with respect to ξ and use the filtering properties of pulse (δ-function):

$$D_1(t) = N^2\int \omega_{ij}^*(t,\theta)\,\omega_{ij}^*(t,\theta)\, d\theta = \qquad (10\text{-}72a)$$

$$= N^2\int \omega_{ij}^{*2}(t,\theta)\, d\theta.$$

The same conclusion for control systems with constant parameters yields a similar result:

$$D_{\text{вых}}(t) = N^2\int_0^t \omega_{ij}^2(\theta)\, d\theta = \qquad (10\text{-}72b)$$

$$= N^2\int_0^t \omega_{ij}^2(t)\, dt.$$

Thus, noise dispersion at a prescribed point accumulates as the integral (multiplied by the noise level) of the square of the weight function along argument θ (reverse displacement) for variable systems and along argument t for steady systems.

Formulas (10-72a) and (10-72b) are valid for the diagrams of the test by the weight function method shown in Fig. 10-19, b and c. According to diagram a the pulse or equivalent initial conditions (2-60b) excite the prescribed control system or its direct model with constant parameters. At the system's output the signal is squared and integrated, and is read on the measuring device in the form of a dispersion which the hand of the voltmeter approaches at the rate at which the weight function damps.

According to diagram c for control systems with variable parameters tests are conducted only with R-S system models. Excitement and sampling conditions are the same as those of diagram b, but the integrator is disconnected at the instant t_k in order to discontinue any further growth of the result.

The process of noise dispersion variation can also be replaced by modeling of the transfer function which reflects the quadratic evaluation of the process according to Section 3-13.

D. Spectral methods. If the weight function of a control system with constant parameters virtually damps for a time t_{damp}, the steady-state value of noise

809

[dispersion
$$D_{\varepsilon\,SS} = D_{\nu n}(t)|_{t\to\tau_{max}} = N^2 \int_0^\infty w^2(\theta)\,d\theta. \qquad (*)$$

can be determined by formula (10-72b).

We pass from integrating with respect to time to integrating with respect to spectrum (4-119) and find:

$$D_{\varepsilon\,SS} = \frac{N^2}{\pi} \int_0^\infty |\Phi_\varepsilon(j\omega)|^2\,d\omega. \qquad (10\text{-}73a)$$

For an analogous transformation of formula (10-72a) we must ascertain beforehand that for a given finite instant of time the analytic continuation of the cut of the weight function along argument θ damps sufficiently rapidly with

$$\theta > t_k, \ i.\ e.\ w(t,\theta)|_{\theta > t_k} \to 0.$$

Then in the left-hand side of the formula and in the kernel of the integral on the right parameter t_k is retained while the integration limits become semi-infinite and integration with respect to argument θ can be replaced by integration with respect to parametric spectrum, which yields

$$D_{\nu n}(t) = \frac{N^2}{\pi} \int_0^\tau |\Phi_\varepsilon(t_k, j\omega)|^2\,d\Omega. \qquad (10\text{-}73b)$$

The main difficulty in using this formula to state and determining the AOSF $\Phi_\varepsilon(t_k,\theta)$ inasmuch as the method for successive integration of Laguerre polynomials is given on the basis of formulas (3-107a) – (3-107c); in chapter 4 are given a Table 4-10 of particular cases and the general formula (4-129).

Some circuits for which the AOSF is obtainable with

relative simplicity are investigated in Section 5-9. For these circuits we can also easily compute the noise dispersion by spectral methods.

a) A cascade circuit of a stationary input unit and a subsequent amplifier with variable amplification factor have the AOTF (5-58) in common. Applying to it formula (10-73b) we have

$$D_{\varepsilon n}(t) = \frac{N^2 K(t)}{\pi} \int_0^\infty |\Phi_1(j\Omega)|^2 d\Omega. \qquad (10\text{-}74a)$$

b) A cascade circuit of an input amplifier with an exponentially growing amplification factor and subsequent stationary unit with a common AOTF (5-60d). In this case the formula of noise dispersion (10-73b) takes the form

$$D_{sn}(t) = \frac{N^2 e^{2st}}{\pi} \int_0^\infty |\Phi_2(s + j\Omega)|^2 d\Omega. \qquad (10\text{-}74b)$$

c) A similar cascade circuit but with a complex amplification factor which after reversing the argument breaks up into a sum of functions of θ (5-61a), which reduces the general AOTF of the circuit to the form (5-61c), transforms input noise and output dispersion according to formula

$$D_{sn}(t) = \frac{N^2}{\pi} \int_0^\infty \left| \sum_{k=1}^i f_k(t) \Lambda_k \{W_2(j\Omega)\} \right|^2 d\Omega. \qquad (10\text{-}74c)$$

d) For a circuit of two steady links with an analogous variable coefficient between them when dispersion arises we can use formula (5-62):

$$D_{\varepsilon n_1}(t) = \frac{N^2}{\pi} \int_0^\infty |W_1(j\Omega)|^2 \left| \sum_{k=1}^i f_k(t) \Lambda_k \{W_2(j\Omega)\} \right|^2 d\Omega. \quad (10\text{-}74d)$$

3. Effect on Control Systems of Stationary Disturbances With Assigned Spectral Density

A. The case of white noise. Let the spectral density of a stationary response be assigned analytically $S_y(\omega)$ or graphically. Suppose that Y is, in turn, the response of a constant pulsed filter with OTF $W_f(r)$ excited by white noise ξ of unit level (Fig. 10-20,a).
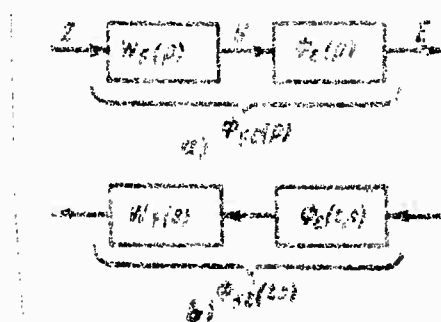
Fig. 10-20. Block diagram for inserting pulsed filters in control systems with constant and variable parameters.

Then, according to form la (8-180), we have:

$$S_y(\omega) = |W_f(j\omega)|^2$$

whence the filter's PAF equals

$$A_f(\omega) = \sqrt{S_y(\omega)} \tag{10-75}$$

By selecting a steady filter with a phase-amplitude characteristic approaching the rated one, we can approximately or exactly determine the OTF of the filter

$$W_f(p) = \frac{b(p)}{a(p)} \tag{10-76a}$$

or its algebraized equation of coupling

$$a(D)y = b(D)z. \tag{10-76b}$$

Further, if the filter is joined into one circuit with the system, for the case of a control system with constant parameters we find a unit OTF

$$\frac{E(p)}{Z(p)} = \Phi_{f\varepsilon}(p) = W_f(p)\Psi_\varepsilon(p). \qquad (*)$$

A system with OTF $\Phi_{f\varepsilon}$ (p) excited by white noise of unit level has the same output response as a system with OTF Φ (p) excited by a random process with prescribed spectral density. This enables us to analyze the unit system by experimental or mathematical methods expounded for the case of input white noise. If we substitute, e.g., (*) into (10-73) we find:

$$D_{\iota x} = \frac{1}{\pi} \int_0^\infty |W_f(j\omega)|^2 |\Psi(j\omega)|^2 \, d\omega. \qquad (10\text{-}77a)$$

For systems with variable parameters tests by the realization methods are conducted with the same filter at the output, while tests by the weight function method require that a filter be placed at the output of the R-S system.

In the case of analytical computations by spectral methods, an AOTF of the unit system of the form (5-57) should be substituted into formula (10-77b), as shown in Fig. 10-20,b. This yields

$$D_{\iota x}(t) = \frac{1}{\pi} \int_0^\infty |W_f(j\Omega)|^2 \Phi_\varepsilon(t, j\Omega)|^2 d\Omega. \qquad (10\text{-}77b)$$

1. Spectral methods. If in formulas (10-77) we go back to the prescribed spectral density of the input signal we find on the basis of relation (4-122) formulas for converting the output spectral density to the input

and the conditions for determining the output dispersion on the error line without involving the equivalent filter.

Thus, for systems with constant parameters we have an output spectral density

$$S_s(\omega) = |\Phi_e(j\omega)|^2 S_y(\omega) \qquad (10\text{-}78a)$$

and an input dispersion

$$D_{sS} = \frac{1}{\pi} \int_0^\infty |\Phi_s(j\omega)|^2 S_y(\omega)\, d\omega. \qquad (10\text{-}78b)$$

Likewise, for systems with variable parameters we find a parametric input spectral density

$$S_s(t,\Omega) = |\Phi_s(t, j\Omega)|^2 S_y(\Omega) \qquad (10\text{-}79a)$$

and an output dispersion at a fixed point

$$D_{sS}(t) = \frac{1}{\pi} \int_0^\infty |\Phi_e(t, j\Omega)|^2 S_y(\Omega)\, d\Omega. \qquad (10\text{-}79b)$$

C. _Correlation analysis_. If we pass from assigned spectral density to disturbance correlation function

$$K_y(\tau) = \frac{1}{\pi} \int_0^\infty S_j(\omega) \cos \tau \tau\, d\omega,$$

we can compute the correlation function of the system's output error by processing the series of output processes

$$K_s(\tau, t) = \frac{1}{N} \sum_{i=1}^N s_i(t)\, s_{i}(\,\cdot\,)\ (\,\cdot\,). \qquad (*)$$

Here we examine the general case valid for variable and constant control systems. In a system with variable parameters we express the output process on the basis of the equation of integral coupling and substitute it into (*):

814

$$K_z(\tau, t) = \frac{1}{N} \sum_{i=1}^{N} \int_0^\infty w_i(t, \xi) \, y_i(t -$$

$$- \xi) \, d\xi \int_0^\infty w_i(t + \tau, \eta) \, y_i(t - \eta + \tau) \, d\eta =$$

$$= \frac{1}{N} \sum_{i=1}^{N} \int_0^\infty \int_0^\infty w_i(t, \xi) \, w_i(t + \tau, \eta) \times$$

$$\times y_i(t - \xi) \, y_i(t - \eta + \tau) \, d\eta \, d\xi.$$

The series averaging operation can be placed under the sign of a double integral to yield

$$K_y(\tau + \xi - \eta) = \frac{1}{N} \sum_{i=1}^{N} y_i(t - \xi) \, y_i(t - \eta + \tau).$$

With the aid of this result we definitely find

$$K_z(\tau, t) = \int_0^\infty \int_0^\infty K_y(\tau + \xi - \eta) \, w_i(t, \xi) w_i(t + \tau, \eta) d\xi d\eta: \quad (10\text{-}80)$$

and assuming that $\tau = 0$ we find the output dispersion

$$D_z(t) = \int_0^\infty \int_0^\infty K_y(\xi - \eta) \, w_i(t, \xi) w_i(t, \eta) \, d\xi \, d\eta. \quad (10\text{-}81)$$

Further, if we replace the correlation function by a pulse we can find formula (10-72a). Thus, the correlation method is a duplication of the spectral methods.

4. Effect on Control Systems of Nonstationary Disturbances

A. Passing through the system of the statistical mean. An example of characteristics of the nonstationary random process is shown in Fig. 10-14,e. To simplify the description of its passage through the system, each charac-

In passing through the system the disturbance characteristic engenders at the output an error variation process characteristic which can be determined by the formula

$$\varepsilon_i(t) = L^{-1}\{\Phi_s(p) L[y_i(t)]\}. \qquad (10\text{-}82)$$

Here the image-obtaining operation is written in an intermediate form, which makes it possible to determine the order in which the statistical mean was obtained. Indeed, once the statistical mean has been found by formula (10-81a) the summation operation can be placed within the brackets of formula (10-82) since all the subsequent transformations are linear:

$$\bar{E}(t) = L^{-1}\left\{ \Phi_s(p) L\left[\frac{\sum_{i=1}^{N} y_i(t)}{N} \right] \right\}.$$

Hence, in analogy with (10-59), we have

$$\bar{E}(t) = L^{-1}\{\Phi_s(p) L[\bar{Y}(t)]\}, \qquad (10\text{-}83)$$

where $L[\bar{Y}(t)]$ is a Laplace transform of the statistical mean of the random function reflecting input disturbances.

It should be noted that after processing a large number of random function characteristics, the statistical mean becomes a concrete function (Fig. 10-18b) which characterizes specific objective conditions for defining disturbances and, as long as these conditions do not change, the graph reflects a nonrandom function which

as any time graph, can be subjected to a Laplace transformation.

Thus, the statistical mean of a random function

according to the disturbance influence function, bringing about a response of the control system in the form of a statistical mean of the output error.

Once the statistical mean of the output error has been found and subtracted from all the output characteristics we find centered characteristics which may be subjected to further statistical analysis.

B. Passage of correlation function through the system. By the methods investigated in the preceding section when deriving formula (10-80) we can obtain a formula which links the input and output functions of the correlation

$$K_\epsilon(t_1, t_2) =$$

$$= \int_0^{t_1} w_\epsilon(t_1, \xi) \, d\xi \int_0^{t_2} w(t_2, \eta) \times \qquad (10\text{-}84)$$

$$\times K_y(t_1 - \xi, t_2 - \eta) \, d\eta.$$

Setting $t_1 = t_2 = t$ in this formula we determine the output dispersion

$$D_\epsilon(t) = K(t, t).$$

C. Structural methods. In this more complex case, as well as in the preceding examples, the solution of the statistical problems by experimental or analytical methods becomes considerably more explicit if the input signal is formed by a variable filter from a noise or stationary signal.

Further, the filter equation is combined with the principal system equation and is studied for the case of excitation by ordinary signals. Thus, structural

817

methods, such as shaping elements, structural R-S transformations, etc., are widely applied also to statistical problems.

D. The case of a control system acted upon by a determined control signal of random scale and with stationary disturbance. If any of the input signals determined in shape among those shown in Fig. 10-17 is fed to the control device of the system from real measuring devices, then the useful component is bound to be subjected to measuring device noises or disturbances of another kind. For a linearly increasing useful signal the possible shape of the summation signal is found in Fig. 10-21, a:

$$y_c = K_y + y. \qquad (*)$$

We investigate the case where such a transient problem can be studied with the aid of stationary methods. We assign to a closed-loop system acted upon by the summation signal $(*)$ an astaticism of second order $(\nu = 2)$. Then with forced motion the useful signal does not generate errors and on the unbalance line we only have a response to a disturbance which it is expedient to evaluate by the spectral density $S_c(\omega)$ readily definable by the prescribed spectral density $S_y(\omega)$ of the input disturbance

$$S_c(\omega) = |\Phi_x(j\omega)|^2 S_y(\omega) =$$
$$= \frac{1 \cdot S_y(\omega)}{|1 + W(j\omega)|^2}.$$

$$(10.85a)$$

Beginning with a certain frequency above the system's passband, the phase-amplitude characteristic of open-loop systems has a modulus considerably smaller than unity $|W(j\omega)| \ll 1$ and formula (10-85a) takes the simplified form

$$S_0(\omega) = S_y(\omega), \qquad (10\text{-}85\text{b})$$
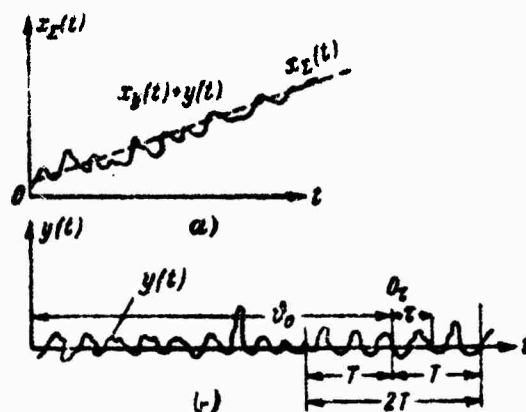
Fig. 10-21. Process with superimposed disturbances and disturbance released on the unbalance line

i.e., at high frequencies we can obtain from the output of the system's measuring device a noise signal separated from the useful signal.

At the system's principal output the noise signal has another spectral density:

$$S_\epsilon(\omega) = S_n(\omega) = |\Phi(j\omega)|^2 S_y(\omega). \qquad (10\text{-}86)$$

Inasmuch as the useful signal has an optimum per-

formulas at any rate level, we calculate by (10-84) only the spectral density of the error.

In a like fashion we can separate the disturbance also from determinant useful signals of another shape, provided the control system is designed according to the self-tuning principle expounded in Section 10-4.

In this case the spectrum on the unbalance line will, as before, be determined by the exact formula (10-85a) or the approximate formula (10-85 b), while the output error spectrum is defined by formula (10-86).

The methods cited in this Chapter permit the solution of a certain minimum required number of problems relating to the statistical theory of precision of control systems. A further development of these questions reaches beyond the scope of this book insofar as it leads to the creation of specialized works on the statistical theory of automatic control [Introduction, Bibl. 1, 4 and 7].

BIBLIOGRAPHY

1. Teoriya invariantnosti i eyё primeneniye v avtomaticheskikh ustroystvakh (Invariance Theory and Its Application to Automatic Devices), Academy of Sciences of the Ukrainian SSR, Department of Technical Sciences, Proceedings of the Meeting, Kiev 16-20 Oct. 1958, Reports of Academicians V. S. Kulebakin, A. Yu. Ishlinskiy, B. N. Petrov, 1959, Moscow.

2. Bruyevich N. O., Tochnost' mekhanizmov (Accuracy of Mechanisms), Mashgiz, 1950.

3. Pitcher, L. N., Ob odnom tipe sledyashchikh sistem ...

s korrektiruyushchimi vozdeystviyami (On One Type of Servomechanisms with Corrective Actions), Avtomatika i Telemkhanika (Automation and Telemechanics), 1956, No. 3.

4. Ivakhnenko A. G., Elektroavtomatika (Electroautomation), GITTL UkSSR, 1954.

5. Venttsel' Ye. S., Teoriya veroyatnostey (Theory of Probabilities), Fizmatgiz, 1958.

ASYMPTOTIC STABILITY

11-1. Indices of Asymptotic Stability

A linear automatic control system is said to be
asymptotically stable if its response to any determined
input signal approaches with time only the forced com-
ponent while the free output process component damps.

Only in this case can the rules for calculating
and compensating forced motion errors, examined in the
preceding Chapter, be applied to the system's output
process as a whole.

It was shown in Section 3-8 that a control system's
inherent motion is also formed of its partial weight
functions, the conditions defining the input signal
affecting only the scale of partial functions, hence
the stability is affected only by the control system's
inherent properties assigned by its weight function or
by the OTF.

The steadiness signs of a control system become
evident if such processes as weight functions are com-
puted beforehand or the OTF poles are determined for
a closed-loop system. These signs are then called
indices of stability. In view of the fact that the
requirement of asymptotic stability for control systems
is not a strict one since damping time is not determined
and may be infinitely great, stability signs can be
detected even without calculating the processes or

determine OTF poles on the basis of examining the relations between the coefficients of the equation of coupling or the properties of the system's frequency hodographs. But in these cases the stability symptoms are already implicit and are called stability _criteria_.

Following are several formulations of control systems stability _indices_, all of them stating one and the same fact but from different viewpoints.

1. A control system is said to asymptotically stable if its weight function damps:

$$\lim_{t \to \infty} \omega(t) = 0. \tag{11-1a}$$

2. A control system is asymptotically stable if all partial weight functions have exponential factors with negative exponents:

$$\omega(t) = \sum_{i=0}^{n} f_i(t) e^{-|z_i| t} \tag{11-1b}$$

3. A control system is asymptotically stable if all the roots of the characteristic equation of the closed system have negative real parts:

$$M(z_i) = 0; \quad \mathrm{Re}(z_i) < 0; \quad i = 1, 2 \ldots n. \tag{11-1c}$$

4. A control system is asymptotically steady if all the poles of the OTF of the closed system are lying in the left-hand half of a complex plane, as shown in Fig. 11-1.
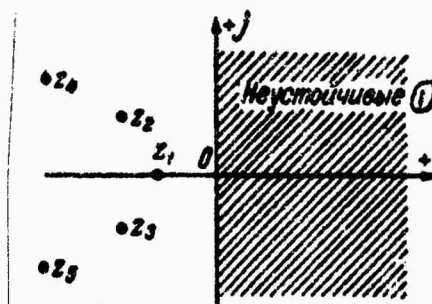
Fig. 11-1. Possible distribution of roots of a
characteristic equation in a complex plane.
Key: 1) transient.

Formulations of implicit signs or stability
criteria require preliminary proof, and the following
sections of this Chapter are devoted to this subject.

11-2. Necessary and Sufficient Stability Criteria.

Limiting Criterion in the Field of Representations.

Let us find the properties of a control system's
weight function when condition

$$\lim_{p \to 0} p\Phi(p) = 0. \tag{11-2}$$

is fulfilled.

On the basis of (3-52) we see that this condition
warrants the absence among partial weight functions of
neutral-polynomial processes, but it can by no means
confirm or refute the damping of the weight function
as a whole (11-1a).

Thus the limiting criterion in the field of representations is only a necessary but not a sufficient stability criterion.

Criterion of Positive Coefficients for Equations of First and Second Order.

In the characteristic equation of first order

$$M_1(z) = 0 \quad \text{or} \quad \mu_1 z + \mu_0 = 0 \; ;$$

both coefficients are positive:

$$\left. \begin{matrix} \mu_1 \\ \mu_0 \end{matrix} \right\} > 0, \qquad\qquad (11\text{-}3a)$$

then the sole root of this equation is real and negative:

$$z_1 = -\frac{\mu_0}{\mu_1} \, , \;$$

which is the stability coefficient of (11-2c).

If in the characteristic equation of second order $M_2(z) = 0$ or $\mu_2 z^2 + \mu_1 z + \mu_0 = 0$ all three coefficients are positive:

$$\left. \begin{matrix} \mu_0 \\ \mu_1 \\ \mu_2 \end{matrix} \right\} > 0, \qquad\qquad (11\text{-}3b)$$

then both roots of the equation

$$z_{1,2} = -\frac{\mu_1}{2\mu_2} \pm \sqrt{\frac{\mu_1^2}{4\mu_2^2} - \frac{\mu_0}{\mu_2}} \; ,$$

always have a negative real part. In fact, positive coefficients μ_1 and μ_2 warrant a negative sign of the first term. If the second term is imaginary, it affects in no way the real part of complex roots; if the second term is real, then the positive coeffi-

cients μ_0 and μ_1 under the radical sign warrant that its modulus be smaller than that of the first term and, hence, both real roots have a negative sign.

Thus, the criterion of positive coefficients of the characteristic equation of a closed system of first (11-3a) and second (11-3b) order is for these systems $(n \leqslant 2)$ a necessary and sufficient stability criterion.

Criterion of Positive Coefficients for Equations of High Order $(n \geqslant 3)$.

We examine a characteristic equation of n-th order $M_n(z) = 0$ and assume that some of its roots are real, i.e.,

$$I_m(z_i) = 0, \; i = 1, 2 \ldots k. \tag{*}$$

With positive coefficients

$$\mu_i > 0; \; i = 1, 2 \ldots n$$

it is obvious that only a negative real root can turn the sum of terms of the characteristic equation into zero.

Thus the existence of positive coefficients in a characteristic equation warrants that all of its real roots are negative. However, the criterion of positive coefficients contains no information as to the sign of the real parts of complex roots of the same equation. Consequently, we are dealing here only with a necessary but not with a sufficient stability criterion. The particular cases (11-3a) and (11-3b) are, as a whole, encountered very rarely. Let us therefore proceed to investigate more general sufficient stability criteria.

11-8. I. A. Vyshnegradskiy's Stability Criterion

While studying the dynamics of a steam engine governor in 1876, the renowned Russian scientist Ivan Alekseyevich Vyshnegradskiy gave with respect to the equation of third order a mathematically and technically well-founded stability criterion /Bibl. 1/.

He investigated a system of third order whose characteristic equation written in the designations adopted in this book has the form:

$$\mu_3 p^3 + \mu_2 p^2 + \mu_1 p + \mu_0 = 0. \qquad (*)$$

By the criterion of positive coefficients we determine that the system has no aperiodic transient processes.

Further, we check the possibility of undamped oscillations arising in the system investigated. A symptom of undamped oscillations in the system are purely imaginary roots of the characteristic equation $z_{1,2} = \pm j\omega$. We substitute one of these roots into the characteristic equation under study:

$$\mu_0 - \mu_2 \omega^2 + j(\mu_1 \omega - \mu_3 \omega^3) = 0.$$

In order that the complex function equal zero, we must equate to zero its real and imaginary parts individually, i.e.,:

$$\mu_0 - \mu_2 \omega^2 = 0; \quad \omega(\mu_1 - \mu_3 \omega^2) = 0.$$

We can eliminate frequency from these two equations and find the relation between the coefficients of the characteristic equation at which undamped oscillations are possible in the system.

From the second equation after reduction by ω (we investigate the case of $\omega \neq 0$) we find:

$$\omega^2 = \frac{\mu_1}{\mu_3}.$$

If we substitute this value of ω^2 into the first equation we find $\mu_0 - (\mu_2 \mu_1 / \mu_3) = 0$, whence

$$\mu_1 \mu_3 = \mu_0 \mu_2. \tag{11-4}$$

Consequently, if the product of the mean coefficients of a third-order characteristic equation is equal to the product of extreme coefficients, then undamped oscillations are observed in the control system, which is to say that it finds itself on the boundary of stability.

This boundary divides all third-order systems into two classes, viz., stable and unstable ones. On one side of the boundary we have all the systems with, say, the left-hand side of equation (11-4) greater than the right-hand side; on the other side of the boundary we find the systems in which the right-hand side of equation (11-4) is greater.

To determine which side of the boundary corresponds to stable systems let us diminish the coefficient μ_3; then two roots of the third-order system (*) will approach the roots of the second-order system which, with positive coefficients of the characteristic equation, are always on the left side. There remains a third root, but inasmuch as it is one, it is real, and inasmuch as the coefficients are positive, the root is negative. Thus, the region of the smallest

permissible values of μ_3 for which the left-hand side
of (11-4) is greater than the right side, corresponds
to the stability region, hence the inequality

$$\mu_1\mu_2 > \mu_0\mu_3 \qquad (11-5)$$

is evidence, if fulfilled, of the stability of the
system.

Condition (11-5) is precisely the Vyshnegradskiy
stability criterion which can be worded as follows:

If a third-order system satisfies the criterion of
positive coefficients and, moreover, the product of
mean coefficients of the characteristic equation is
greater than the product of extreme coefficients, then
such a system is said to be stable.

Thus, without calculating the roots of the charac-
teristic equation but only by investigating the relation
between its coefficients we can gather exhaustive in-
formation relative to the system's stability. This
fact is evidence of the importance of Vyshnegradskiy's
criterion, all the other criteria investigated in the
following are aimed at the solution of the same problem.

Vyshnegradskiy's hyperbola. Besides discovering
the stability criterion, Vyshnegradskiy has also de-
rived the proper engineering approach for its applica-
tion. It is a fact that the simultaneous selection of
four coefficients μ_0, μ_1, μ_2, μ_3 of the charac-
teristic equation is all the more difficult as with
such a number of variables graphical methods may not
be used. Vyshnegradskiy reduced the third-order equa-
tion with four parameters to an equation with two

parameters.
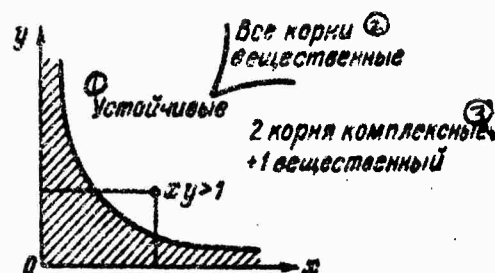
Fig. 11-2. I. A. Vyshnegradskiy's hyperbola.
Key: 1) stable; 2) all roots are real; 3) 2 complex
roots + 1 real root.

We divide all the terms of the original charac-
teristic equation by the smallest coefficient μ_o :

$$\frac{\mu_3}{\mu_0} p^3 + \frac{\mu_2}{\mu_0} p^2 + \frac{\mu_1}{\mu_0} p + 1 = 0$$

and perform the substitution

$$z = \sqrt[3]{\frac{\mu_2}{\mu_0}} p, \quad i.e. \quad p = \sqrt[3]{\frac{\mu_0}{\mu_2}} z;$$

then we have

$$z^3 + xz^2 + yz + 1 = 0, \tag{11-6a}$$

where

$$x = \frac{\mu_2}{\sqrt[3]{\mu_0 \mu_3^2}}; \quad y = \frac{\mu_1}{\sqrt[3]{\mu_0^2 \mu_3}}.$$

The stability boundary for the given equation co-
incides with that of the initial equation and is

$$xy = 1. \tag{11-6b}$$

This link between the system's parameters on the
boundary of stability is graphically expressed by an

equilateral hyperbola, as shown in Fig. 11-8. The
region above the curve (not hatched in the Figure) is
the region of stability since there $xy > 1$; the hatched
area is obviously the region of instability.

Vyshnegradskiy divided the stability region into
a subregion of aperiodic processes corresponding to
all three real roots of the characteristic equation,
which is achieved if the relation between the coeffi-
cients is

$$x^2 y^2 - 4 (x^3 + y^3) + 18 xy - 27 > 0. \qquad (11-8c)$$

11-4. Limiting Amplification Factor

We see from Section 11-3 that, beginning with
third-order systems, stability is affected not only
by the sign of the coefficients of the characteristic
equation but also by their magnitude. The coefficients
of the characteristic equation are, in turn, determined
by the technical parameters of the system, and, in
most cases, most interesting are precisely the relations
between the system's technical parameters with which
the system finds itself on the boundary of stability.

One of the most important technical parameters
of closed-loop control systems is the amplification
factor of the direct path (of an open-loop system);
let us investigate its effect upon stability by
utilizing formula (11-5) for systems no higher than
third order.

As a first example let us examine a static system,

containing in the linear network three aperiodic units,
as shown in the block diagram of Fig. 11-3,a. Let the
overall amplification factor of the linear network be
$K = K_1 K_2 K_3$, and the time constants of the aperiodic
unit satisfy a geometric progression with denominator
m, i.e., $T = T$; $T_2 = mT$; $T_3 = m^2 T$. As an example of
a real control system with such parameters we may take
an automatic voltage stabilizer with three amplifiers
and a standard source. Diagram b of the same figure
shows for simplicity all the three amplifiers in the
form of separate excitation oscillators.
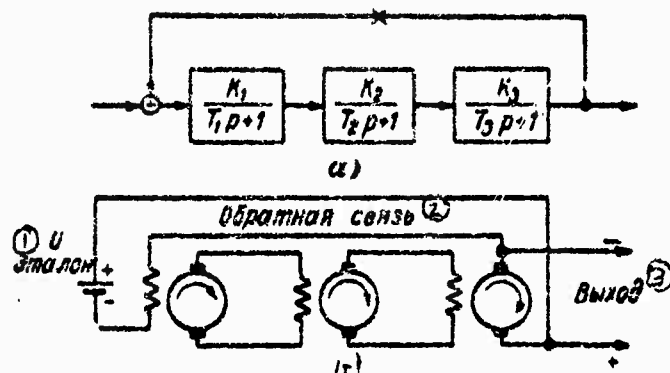
Fig. 11-3. Block diagram and electric circuit of a
voltage stabilizer (third-order static system, n = 3)
Key: 1) standard voltage; 2) feedback; 3) output.

We set up the transfer function for the open-loop
system:

$$W(p) = \frac{K}{(Tp + 1)(mTp + 1)(m^2 Tp + 1)},$$

and then the relative transfer function of the closed-loop control system:

$$\Phi_s(p) = \frac{(Tp+1)(mTp+1)(m^2Tp+1)}{(Tp+1)(mTp+1)(m^2Tp+1)+K}$$

The characteristic polynomial of the closed control system after reduction of similar terms takes the form:

$$m^3T^3p^3 + (m+m^2+m^3)T^2p^2 +$$
$$+ (1+m+m^2)Tp + 1 + K = M(p).$$

We apply the Vyshnegradskiy stability criterion and find the stability conditions for the system investigated in the form:

or

$$m(1+m+m^2)^2 T^3 > m^3T^3(1+K),$$

$$\left(\frac{1}{m}+1+m\right)^2 > 1 + K.$$

The stability boundary is given by the following value of the amplification factor:

$$K_A = \left(m+1+\frac{1}{m}\right)^2 - 1. \qquad (11\text{-}?)$$

As the limit of the gain is exceeded, the control system becomes unstable. The numerical dependence of limit gain upon the ratio of adjoining time constants $m = T_2/T_1 = T_3/T_2$ is given in Table 11-1 taken from /Bibl. 2/ of Chapter 5.

The structure of the formula for limit gain is such that identical results are obtained by substituting into it the greater or the inverted value, i.e., and by value m; for this reason the Table has two primary for m

Table 11-1

Boundary Values of Parameters of Third-Order Static
System

①Отношение постоянных времени m		②Предельный коэф-фициент усиления $K_{\text{пред}}$
1	1,0	8
2	0,5	11,3
5	0,2	37,4
8	0,125	82,3
10	0,1	123
20	0,05	443
.40	0,025	1 681
100	0,01	10 201

Key: 1) ratio of time constants m; 2) limit gain K_{lim}

The limiting amplification factor determines the
utmost performance accuracy of a closed-loop system.
Thus, with constant disturbance applied at any point
of the closed system the portion of the residual error
forming on the disturbance input line is defined by
the value of the relative transfer function of the
closed control system with p = 0, which in the given
case amounts to $\Phi_*(0) = 1/(1 + k)$.

In the specific case for m = 1, i.e., for
identical time constants of all the three aperiodic
units, limit gain according to the Table equals 8
while the residual error portion $\Phi_*(0) = 1/(1 + 8)$,

that is, one-ninth or 11% of the constant disturbance applied.

If the magnitude of the error is excessive, it can be reduced, as we see from the formula for $\Phi_x(0)$, by increasing the gain of the linear network. With the assigned time constant ratios, however, this leads to the loss of stability.

Thus, there exists a contradiction between the accuracy requirements and stability requirement. This contradiction, as it ensues from the dialectic method, is one of the reasons for the development of automatic control systems aimed at the creation of perfect systems and new calculation methods.

These methods will to some extent be elucidated below. In the meantime, however, on the basis of Table 11-1 and of the formulas investigated we can come up with the following recommendation: in increasing the accuracy of automatic control systems by raising the gain of the direct circuit, to maintain stability it is expedient to increase n, i.e., "separate" as far as possible the time constants of the aperiodic sections comprised in the direct circuit.

As the second example let us investigate another third-order astatic control system. Its structure is shown in Fig. 11-14, and we can see that its direct circuit contains two aperiodic sections with time constants T_1 and T_2, and the integrating component.
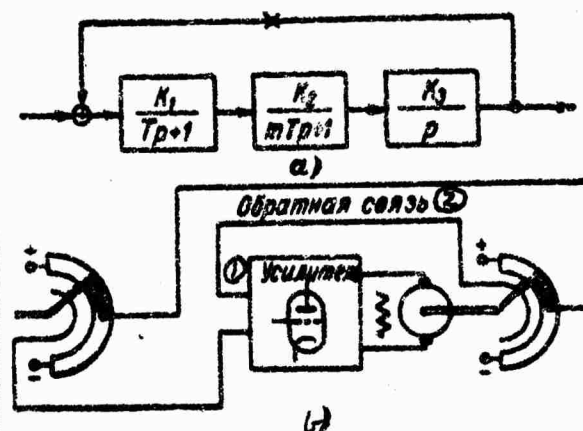
Fig. 11-4. Block diagram and electric circuit of potentiometer servo (third-order system, n = 3 with astaticism ν = 1).
Key: 1) amplifier; 2) feedback.

In practice, such a structure may be encountered e.g., in a control system with a potentiometer-type transmitter, an amplifier being an aperiodic section, and an electric motor being a combination of an aperiodic and integrating component. The electric circuit of the device is shown under b in the same figure.

We write the transfer function of the open-loop system and the relative transfer function of the same closed-loop system:

$$W(p) = \frac{K_{-1}}{p(Tp+1)(mTp+1)};$$

$$\Phi_{\ast}(p) = \frac{p(Tp+1)(mTp+1)}{p(Tp+1)(mTp+1)+K_{-1}}.$$

The characteristic polynomial of the closed-loop

856

control system is reduced to the form:

$$mT^2 p^3 + T(1+m) p^2 + p + K_{-1} = M(p).$$

Hence the Vyshnegradskiy stability criterion:

$$T(1+m) > K_{-1} mT^2,$$

or

$$1 + m > K_{-1} mT.$$

Limit gain with which the control system finds itself on the boundary of stability is

$$K_{-1 lim} = \frac{1+m}{Tm}, \qquad (11-8a)$$

Investigation of the formula obtained shows that for great values of m, when $(1+m)/m \to 1$, the formula can be reduced to the form

$$K_{lim} = \frac{1}{T}, \qquad (11-8b)$$

i.e., rate gain cannot be greater than the inverse value of the smallest time constant; for small values of m, when $(1+m)/m \to 1/m$, the formula is reduced to the form

$$K_{lim} = 1/mT, \qquad (11-8c)$$

Once again the coefficient is limited by the inverse value of the smaller (mT) time constant. Hence we may draw this following simple recommendation for control systems of the given type: reduce the smaller time constant.

If the quantity m is prescribed, then the amplification factor is limited by the quantity $K_{-1 lim}$; if this value is exceeded the system becomes unstable.

On the other hand, this gain is inversely proportional to the static error coefficient $\varphi_i(0) = 1/K_{-1}$.

and to reduce the rate error it is desirable to increase
the gain of the direct circuit.

Thus, also in astatic systems the requirement of
accuracy and that of stability contradict each other.

This contradiction is inherent also in systems of
higher order, yet in complex systems the stability
boundary can be connected with the amplification factor
in a non-single-valued fashion. Occasionally, this
leads to a limitation of the amplification factor for
reasons of stability both from the maximum as well as
from the minimum side.

11-5. The Hurwitz Stability Criterion.

Requested by the renowned Czech specialist in
the field of governors and regulators Aurel Stodola,
the professor of Zurich University, A. Hurwitz, devised
in 1895 an analytical stability criterion which holds
true for systems of any order.

Let us expound the rules for utilizing the Hurwitz
criterion on the basis of a characteristic fifth-order
equation.

1st stage. With the coefficients of the
characteristic equation of n-th order we set up a
square diagram of n x n cells. First we write along
the diagonal of the diagram all the coefficients of
the equation in ascending order of their numbers
according to the system "upwards and from right to left"
beginning with μ_0 (at the bottom) and ending with

μ_{n-1}, i.e., in the same way as these coefficients are arranged in the characteristic equation proper, and μ_n next to μ_{n-1}:

System
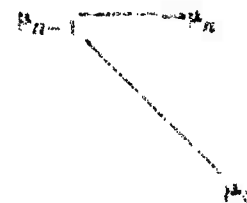
Then, in the order determined by the first row, the remaining cells are filled with coefficients so as to have the coefficients along the diagonal follow the natural order of numbers given by their subscript.

μ_4	μ_5	0	0	0
μ_2	μ_3	μ_4	μ_5	0
μ_0	μ_1	μ_2	μ_3	μ_4
0	0	μ_0	μ_1	μ_2
0	0	0	0	μ_0

i.e., from left to right. Whenever the ordinal numbers are smaller than zero or greater than n, zero is written into the cells of the diagram.

2nd stage. From the table obtained we set up

839

determinants from the first to n-th order, each smaller determinant being the diagonal minor of the next higher determinant:

$$\Delta_1 = \mu_4; \quad \Delta_2 = \begin{vmatrix} \mu_4 & \mu_5 \\ \mu_2 & \mu_3 \end{vmatrix}; \quad \Delta_3 = \begin{vmatrix} \mu_4 & \mu_5 & 0 \\ \mu_2 & \mu_3 & \mu_4 \\ \mu_0 & \mu_1 & \mu_2 \end{vmatrix};$$

$$\Delta_4 = \begin{vmatrix} \mu_4 & \mu_5 & 0 & 0 \\ \mu_2 & \mu_3 & \mu_4 & \mu_5 \\ \mu_0 & \mu_1 & \mu_2 & \mu_3 \\ 0 & 0 & \mu_0 & \mu_1 \end{vmatrix}; \quad \Delta_5 = \mu_0 \Delta_4.$$

3rd stage. We check the sign of the coefficients of the characteristic equation and all the determinants.

We can formulate the Hurwitz stability criterion as follows: <u>A system is said to be stable if all the coefficients of the characteristic equation are positive, and all the diagonal determinants from the first to n-th order set up according to the table of coefficients</u>

$$\begin{rcases} \mu_i > 0; \qquad \Delta_j > 0; \\ i = 0, 1, 2 \ldots n; \quad j = 1, 2 \ldots n. \end{rcases} \qquad (11\text{-}9)$$

<u>are positive as well.</u>

Fulfillment of the criterion of positive coefficients enables us not to calculate the first and last determinants for systems of any order.

For a third-order system the diagram of coefficients has the form

$$
\begin{array}{cc|c}
\mu_2 & \mu_3 & 0 \\
\hline
\mu_0 & \mu_1 & \mu_2 \\
\hline
0 & 0 & \mu_0
\end{array}
$$

Its diagonal determinants are

$$
\Delta_1 = \mu_2; \quad \Delta_2 = \begin{vmatrix} \mu_0 & \mu_3 \\ \mu_0 & \mu_1 \end{vmatrix}; \quad \Delta_3 = \mu_0 \Delta_2.
$$

The condition that the first and last determinants be positive coincides with the criterion of positive coefficients, and that of the second determinant with the Vyshnegradskiy criterion.

An analytic criterion of stability whose proof closely approaches the one above but is written in a different form was worked out in 1873-1877 by E. J. Routh.

The system is unstable if any of the inequalities (11-9) changes.

The system is on the boundary of stability if any among the determinants (11-9) equals zero. To determine the stability boundary the one but last determinant

$$
\Delta_{n-1} = 0. \tag{11-10}
$$

is usually employed in the first place.

As an example, we apply the Hurwitz criterion to evaluate the stability of two interconnected systems whose block diagram is shown in Fig. 9-1, e. It was noted in Chapter 9 that systems with intrinsic coupling coefficients $a = \cos\gamma$, $d = \cos\gamma$ and mutual coupling coefficients $b = \sin\gamma$, $c = -\sin\gamma$ are frequently

encountered in practice. For this reason it is pre-
cisely such systems that we are going to study. We
assume that the transfer functions of the direct paths
for the quantities x and y consist of aperiodic and
integrating components:

$$W_x(p) = \frac{K_x}{p(T_x p + 1)} ;$$

$$W_y(p) = \frac{K_y}{p(T_y p + 1)} .$$

In checking for stability, the lines of input and
output values shown in diagram 9-1,e may be disregarded:
then, following the rules of circuit convolution, we
can easily determine the transfer functions of locally
closed systems in the direction of the signal acting
upon the circuit:

$$\Phi_x(p) = \frac{-W_x(p)}{1 + a W_x(p)} = \frac{-K_x}{p(T_x p + 1) + K_x \cos \gamma} ;$$

$$\Phi_y(p) = \frac{-W_y(p)}{1 + d W_y(p)} = \frac{-K_y}{p(T_y p + 1) + K_y \cos \gamma} .$$

The aggregate transfer function of an open system
with negative feedback is

$$W(p) = -bc\Phi_x(p)\Phi_y(p) =$$

$$= \frac{K_x K_y \sin^2 \gamma}{[p(T_x p + 1) + K_x \cos \gamma][p(T_y p + 1) + K_y \cos \gamma]} .$$

It was shown in Chapter 10 that if we assign any
input or output to a closed automatic control system

the characteristic polynomial will always be the same;
in the given case it takes the form

$$U(p) + V(p) = T_x T_y p^4 + (T_x + T_y) p^3 +$$
$$+ [1 + (K_x T_y + K_y T_x) \cos \gamma] p^2 +$$
$$+ p (K_x + K_y) \cos \gamma + K_x K_y.$$

Since the polynomial is of fourth order, the
Hurwitz diagram is a square 4 x 4:

$T_x + T_y$	$T_x T_y$	0	0
$(K_x + K_y) \cos \gamma$	$1 + (K_x T_y + K_y T_x) \cos \gamma$	$T_x + T_y$	$T_x T_y$
0	$K_x K_y$	$(K_x + K_y) \cos \gamma$	$1 + (K_x T_y + K_y T_x) \cos \gamma$
0	0	0	$K_x K_y$

If the variation of the angle γ is limited to
the I and IV quadrants, then all the coefficients
of the characteristic equation are positive and
we can proceed to checking the positiveness of
the diagonal determinants made up from the diagram
obtained.

We begin with the second-order determinant:

$$\Delta_2 = \begin{vmatrix} T_x + T_y & T_x T_y \\ (K_x + K_y)\cos\gamma & 1 + (K_x T_y + K_y T_x)\cos\gamma \end{vmatrix} =$$

$$= (T_x + T_y) + (T_x^2 K_y + T_y^2 K_x)\cos\gamma.$$

Under the conditions given here it is always positive $\Delta_2 > 0$.

We pass now to the development of the third, in our example one but last, determinant:

$$\Delta_3 = \begin{vmatrix} T_x + T_y & T_x T_y & 0 \\ (K_x + K_y)\cos\gamma & 1 + (K_x T_y + K_y T_x)\cos\gamma & T_x + T_y \\ 0 & K_x K_y & (K_x + K_y)\cos\gamma \end{vmatrix} =$$

$$= (K_x T_y^2 + K_y T_x^2)(K_x + K_y)\cos^2\gamma +$$

$$+ (T_x + T_y)(K_x + K_y)\cos\gamma - (T_x + T_y)^3 K_x K_y.$$

Analysis of the conditions for which $\Delta_3 > 0$ makes it possible to determine the relations between the system's parameters permissible from the viewpoint of stability. We undertake this analysis to obtain more compact formulas and assume for simplicity that both interconnected systems have in the direct path identical amplification factors and time constants, i.e.,

$$K_x = K_y = K; \quad T_x = T_y = T.$$

In this case

$$\Delta_3 = 4K^2 T^3 \cos^2\gamma + 4KT\cos\gamma - 4K^2 T^2,$$

or

$$= 4KT[\cos\gamma - KT(1 - \cos^2\gamma)].$$

Condition $\hat{\Delta}_3 > 0$ amounts to

$$KT < \frac{1}{\sin\gamma\,\mathrm{tg}\,\gamma}.$$

i.e., a limitation for gain is imposed upon the system, which, of course, reduces its accuracy. Limited time constants are also imposed upon the system, and this requires the introduction of elements with a quicker response if the system is to be operating (stable) with a coupling determined by trigonometric functions of angle γ.

11-8. A. V. Mikhaylov's Stability Criterion

In 1936 the Soviet scientist Aleksandr Vasil'yevich Mikhaylov proposed to evaluate the stability of automatic control systems by the deflection angle of the characteristic vector (see Chapter 1 /Bibl. 17/).

A characteristic vector is said to be a function of complex variables obtained by substituting the variable $j\omega$ rather than p into the system's characteristic equation.

For a closed system the characteristic vector, in the following to be called the Mikhaylov characteristic vector or M-vector is

$$M\,(j\omega) = \mu_n\,(j\omega)^n + \ldots + \mu_3\,(j\omega)^3 +$$
$$+ \mu_1\,(j\omega) + \mu_0. \qquad (11\text{-}11)$$

If, by assigning various values to ω, by points
or patterns with the aid of the ϕ-th nomogram or P,
Q-nomogram (see Chapter 4) we trace out in a complex
plane a curve, this curve will be called the Mikhaylov
hodograph.

Mikhaylov's criterion can be basically formulated
as follows: <u>For a system to be asymptotically stable
it is necessary and sufficient that when frequency
changes from zero to infinity the Mikhaylov charac-
teristic vector turn in a positive direction towards
the number of quadrants equal to the order of the
characteristic equation</u>

$$\mathcal{P}_{M_{SS}} = n\,\frac{\pi}{2}. \qquad (11\text{-}12)$$

The author himself and the commentators have
suggested various proofs of the Mikhaylov criterion,
the best among them being based on general relation-
ships between the shape of frequency-response curves
and the character of zeroes and poles of the transfer
function (see Chapter 4).

In the given case we investigate the deflection
angle not of the real frequency-response curve but of
a certain analytically assigned complex vector. Ine -
much as its expression has only a numerator, the
root designations given in Table 4-1 can be changed,
leaving out the division into numerator and denomi-
nator roots ("n" and "d") and denote by means of
... ... given case t... ... ... belong to
the characteristic equation of a closed system.

Thus, for a characteristic Mikhaylov polynomial
we have:

l_M - number of left roots;

r_M - number of right roots;

i_M - number of intermediate roots.

Then, in analogy with formula (4-32), we find the
general expression for the deflection angle of the
M-vector

$$\varphi_M = \frac{\pi}{2}(l_M - r_M) = \frac{\pi}{2}(n - 2r_M - i_M). \qquad (11-13)$$

The particular expression (11-13) is obtained if
we are dealing only with left roots: $l_M = n$; $r_M = 0$;
$i_M = 0$. We can easily note that a stable system has
the greatest among the possible hodograph deflection
angles.

In Figure 11-5,a are given Mikhaylov hodographs
for the static third-order system dealt with in Section
10-4. The curve on the left begins for $\omega = 0$ with
the value $\mu_0 = 1 + K$; the number of positive quadrants
passed by it is equal to the order of the equation
($n = 3$) and, consequently, the system is stable.
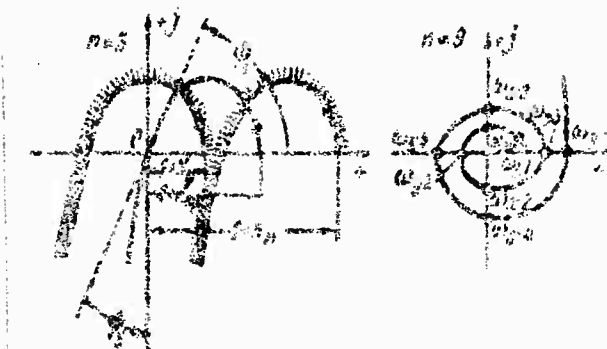
Fig. 11-5. Mikhaylov hodograph.

By increasing the amplification factor only the free turn changes in the characteristic polynomial, and only when the gain reaches limit value determined by formula (11-7) the curve will shift to the right without being deformed and will pass through the origin of coordinates if we move the initial point $(\omega = 0)$ by a distance $1 + K_{lim}$ from the origin of coordinates. Calculation of the hodograph deflection angle according to the rules established in Chapter 4 for characteristics with neutral zeroes (angle before the tangent + angle after the tangent) yields $\varphi_M = \psi_1 + \psi_2 = +1$ quadrant; hence with the aid of formula (11-13) $1 = 3 - i_M$ we can determine the number of intermediate roots $i_M = 2$ which turn out to be two, thus being evidence of the existence of two imaginary conjugate roots and one real root on the right.

If the gain increases further, the curve moves right by the quantity $\mu = 1 + K_n$, the deflection angle becomes $\varphi_M = -1$ quadrant, hence the system becomes unstable. We calculate the number of roots on the right $-1 = 3 - 2r_M$ by formula (11-13). It is found to be two, i.e., there are two conjugate complex roots (degenerate imaginary) on the right and, as usual, one real root $r_M = 2$, $\ell_M = 1$ on the left.

For equations of higher orders the characteristic covers a larger number of quadrants. In Fig. 11-5,b the system with $n = 9$ is stable since $\varphi_M = +9$ quadrants.

Rotation of the characteristic vector $M(j\omega)$ brings

about an alternation of the points of intersection of
the hodograph with the real and imaginary axes. If the
real part of the characteristic vector is denoted by
$X_M(\omega)$ and its imaginary part by $Y_M(\omega)$, i.e., if
we set

$$M(j\omega) = X_M(\omega) + jY_M(\omega), \qquad (11\text{-}14a)$$

then when the hodograph intersects the real axis at
some frequency ω_y condition $Y_M(\omega_y) = 0$ is fulfilled,
whereas when the hodograph intersects the imaginary
axis the second condition $X_M(\omega_x) = 0$ is fulfilled.

Inasmuch as the hodograph of the M-vector of
a stable automatic control system traverses n quadrants
it intersects the coordinate axes n times. i.e.,
equations $X_M(\omega) = 0$ and $Y_M(\omega) = 0$ must have together
n real positive roots, that is, frequencies of inter-
section points:

$$\omega_{x1}, \omega_{x2}, \dots, \omega_{y1}, \omega_{y2}.$$

A correct rotation of the vector is warranted
only by an alternation of the intersected axes; con-
sequently, between any two roots of one equation,
e.g., $Y_M(\omega) = 0$, there must exist a root of the second
equation $X_M(\omega) = 0$, i.e., the roots of both equations
must alternate to;

$$\omega_{y1} < \omega_{x1} < \omega_{y2} < \omega_{x2} < \omega_{y3}. \qquad (11\text{-}14b)$$

The condition for alternating roots (frequencies)
obtained from equating to zero the real and imaginary
parts of the characteristic complex vector appears to
be the mathematical condition for the minimum of the

The Mikhaylov criterion can also be applied to investigating closed-loop automatic control systems. In this case the characteristic vector is written

$$V(j\omega) = v_n p^n + \ldots + v_1 p + v_0. \qquad (11\text{-}15)$$

We denote the roots of the characteristic equation of the open system by the subscript v: the left ones l_v, the right ones r_v and the intermediate ones i_v.

For the deflection angle of the v-vector of an open system we find a formula analogous to (11-13):

$$\varphi_v = \frac{\pi}{2}(l_v - r_v) = \frac{\pi}{2}(n - 2r_v - i_v). \qquad (11\text{-}16)$$

Calculation of the deflection angle of the v-vector of open automatic control systems might be required for inferences regarding the stability criteria always of closed systems. As for the evaluation of the stability of an open system proper, it has to be said that although it can be performed in the same way as this was done for closed automatic control systems according to a formula analogous to (11-12), the result of such an evaluation taken separately is of little value and may even lead to misunderstandings since a stable open system can, after joining up, become unstable in a closed state and, conversely, a neutral or unstable open system occasionally results in a stable closed control system with good accuracy properties, as shown in Chapter 10.

Rules for matching. This rule adds a great deal of clearness to the problem of evaluating stability by hodographs /Bibl. 2/. It is based on the principle of a one-to-one correspondence between curves in the argument plane (the plane of the roots in Fig. 11-1) and in the plane of the characteristic function of this complex argument $M(p)$. Until now this correspondence was used only for the purely imaginary argument $j\omega$ where to each point on the positive imaginary semiaxis in the plane of the argument in Fig. 11-1 there corresponded a specific point on the hodograph of the M-vector in the half-plane of the function of Fig. 11-5. Moreover, if the system is on the boundary of stability, the corresponding root in the root plane is situated on the imaginary semiaxis, and when with changing frequencies hits this point, in the function plane the hodograph passes through the origin of coordinates.

If now in the argument plane we outline any other motion line and pass through another root, then the hodograph of vector $M(p)$ will again traverse zero in the function plane.

Finally, if in the argument plane we enclose by the outline any root then, accordingly, in the function plane the hodograph of vector $M(p)$ will enclose the origin of coordinates.

On the basis of the latter property let us draw out in the argument plane a contour comprising the entire imaginary axis and the semicircumference with infinitely great radius. This contour encompasses the entire

of the hatched half-plane in Fig. 11-1. Let us note
that the hatched area lies right of the basic contour
- the imaginary positive semiaxis, as we move towards
increasing frequency.

In the half-plane of function $M(j\omega)$ we should
therefore expect that the hodograph of the M-vector will
enclose the origin of coordinates if in the equation
there are right roots enclosed in the argument plane,
and will not enclose the origin of coordinates if right
roots do not exist.

Like in the argument plane, the encompassed region
should be considered the part of the half-plane situated
right of the M-vector hodograph as we move towards in-
creasing frequencies.

The hodograph's right side is hatched, as shown in
Fig. 11-5.

Thus, if the origin of coordinates occurs into the
hatched region on the right of the Mikhaylov hodograph,
the system is unstable. Conversely, if the origin of
coordinates lies in the unhatched region, the system is
stable.

Thus:

Hatching of the Mikhaylov hodograph answers the
question as to the automatic control system's stability,
i.e., whether or not there exist roots on the right of
the characteristic equation;

Passing through the origin of coordinates by the
hodograph is evidence that the system finds itself on the

boundary of stability, i.e., it is evidence of the
existence of intermediate roots;

Finally, juxtaposition of the deflection angle
available and that calculated by formula (11-13) for
all cases makes it possible to establish the number of
roots of various kind; let us remind the reader that
the roots of the characteristic equation are poles of
the transfer function of a closed system.

Boundary of stability. The condition for finding
the system on the boundary of stability, besides its
graphical definition, viz., passage of the M-vector
hodograph through the origin of coordinates, can also
be defined analytically and be reduced to the simul-
taneous equating to zero of the real and imaginary
components of the characteristic vector, i.e., to the
presence of a root common to two equations:

$$X_M(\omega) = 0 \; {}^{and} \; Y_M(\omega) = 0. \qquad (11\text{-}17)$$

Evaluation of stability by the Mikhaylov criterion
for automatic control systems with delay components. A
delay component with the OTF $K_d e^{-\zeta_d p}$ inserted in one of
the system's circuits introduces into the characteristic
polynomial new elements with operator factors of the
form $e^{\pm \zeta_d p}$ where the sign of the exponent depends
upon the place of the delay component in the block
diagram and on the subsequent algebraic transformations
of the OTF.

We investigate the case where the characteristic
polynomial is written

853

$$M(p, \tau_d) = e^{\tau_d p} Q(p) + R(p),$$

$Q(p)$ and $R(p)$ are polynomials of n-th and m-th order, respectively, and $e^{+\tau_d p}$ is reduced to a polynomial of infinite order:

$$e^{\tau_d p} = 1 + \tau_d p + \frac{\tau_d p^2}{2} + \frac{\tau_d p^3}{3!} + \cdots$$

If we construct a hodograph $M(j\omega \tau_d)$, its total deflection angle φ_M will always be infinite because of the properties of the delay component, and to catch the variation of this angle for a limited number of quadrants with the appearance of roots on the right side of the characteristic equation is only possible if we juxtapose two hodographs, $M(j\omega)$ and $M(j\omega, \tau_d)$, but the alternation conditions of the roots are easily controllable by means of one hodograph, $M(j\omega, \tau_d)$.

A. V. Mikhaylov's methods, and especially the evaluation of the deflection angles of complex vectors, are a useful contribution to the development of control theory. With the aid of these methods Mikhaylov and a number of other scientists were able to give a strict and clear elucidiation of stability conditions, to analyze the behavior of frequency-response characteristics in accordance with the character of zeroes and poles of the transfer function, and so on.

When directly using the Mikhaylov stability criterion, however, the M-vector hodograph can only be constructed analytically; in the general case it cannot be taken experimentally inasmuch as the complex Mikhaylov vector does not reflect the entire transfer function of an automatic control system but only its $\ldots$

11-7. Nyquist's Stability Criterion

In 1932 the American scientist and radio engineer H. Nyquist formulated a criterion for the stability of amplifiers with negative feedback based on the investigation of the phase-amplitude characteristic of open circuits /Bibl. 9/. Nyquist's method turned out to be quite expedient when applied to automatic control systems where frequency-response characteristics of open circuits are fairly easily constructed by means of patterns or determined experimentally, hence it became quite widespread.

The criterion was proved by the author himself on the basis of the relation between the variation of argument $p = j\omega$ and function $W(j\omega)$ in a complex plane, with the aid of Cauchy's "Principle of Arguments". Soviet scientists (Ya. Z. Tsypkin and others) showed, however, that proofs based on the Mikhaylov principle are clearer especially for astatic automatic control systems. The method for investigating frequency-response characteristics have been fully determined in Chapter 4 of this book and it will be maintained for the following.

Let us now expound Nyquist's criterion on the basis of this method.

1. Boundary of Stability.

A phase-amplitude characteristic $W(j\omega)$ has been constructed in a complex plane $+$, $+j$ (Fig. 11-6). For what follows the shape of the characteristic is irrelevant, but we shall note, however, that the characteristic shown in this figure refers to a static automatic control system.
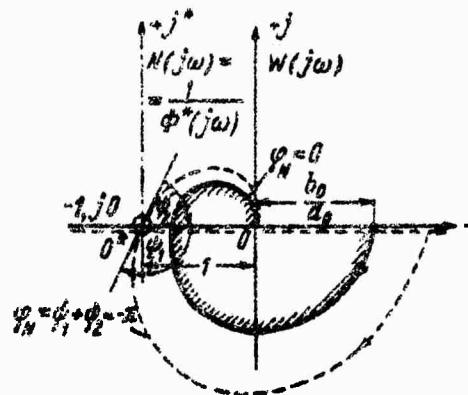
Fig. 11-6. Nyquist hodograph.

By changing the gain of the open circuit or other parameters of the control system we can deform the PAC so as to have it pass through the point -1, j0, as shown by the dashed line in the drawing.

Compared with other points of the complex plane of function $W(j\omega)$, the point -1, j0 has a specific peculiarity. In fact, passage of the PAC of an open control system $W(j\omega_{\pi})$ at a certain frequency ω_{π} through this point is evidence of the fact that at this frequency the direct path of the system shows a gain equal to unity with a phase shift of 180°. It suffices to recall that the direct path is closed by a negative

follow-up which again changes by 180° the phase of output oscillations and feeds them to the input with the same amplitude, hence we can see that such a system has all the conditions for the existence of undamped oscillations at the frequency ω_{qy}.

Thus, if the phase-amplitude characteristic of an open automatic control system passes through the point -1, j0, then the closed system finds itself on the boundary of stability. The analytic expression for the stability boundary is

$$W(j\omega_\tau) = -1. \qquad (11\text{-}16)$$

By expanding the expression for $W(j\omega)$ through the system's parameters we find the relation between these parameters characteristic for the boundary of the stability region.

2. PAC Deflection Angle of an Open Automatic Control System with Respect to Point -1, j0

We see from the foregoing that a shift of the PAC with respect to point -1, j0 on account of changes in the system's parameters leads it from the boundary into the region of stability or instability. Thus, for the following we must investigate the behavior of the characteristic precisely with respect to point -1, j0. To do this it is most expedient to translate the origin of coordinates to this point, i.e., displace the imaginary axis to the left by unity. In the drawing the new origin of coordinates is denoted by 0^* and the

new coordinate axes are shown by a dash-and-dot line.

The PAC equation of the new coordinate system can be written

$$1 + W(j\omega) = 1 + \frac{U(j\omega)}{V(j\omega)} = \frac{U(j\omega) + V(j\omega)}{V(j\omega)}.$$

The sum 1 + W will be called N-vector (Nyquist vector).

We continue the transformations and reduce the preceding formula to the form:

$$1 + W(j\omega) = \frac{M(j\omega)}{V(j\omega)} = N(j\omega), \qquad (11\text{-}19)$$

where we have the M-vector of the closed system in the numerator and the V-vector of the open system in the denominator. In such a form the characteristic can be investigated for the deflection angle on the basis of formula (4-32). We retain the designations of the roots of the characteristic polynomial M(p) of the closed automatic control system and of the roots of the characteristic polynomial V(p) of the open system adopted in formulas (11-13) and (11-16); then the expression for the deflection angle of the N-vector (1-19) can, on the basis of formula (4-32), be written

$$\varphi_N = \frac{\pi}{2}(l_M - r_M - l_V + r_V).$$

Since the order of the characteristic polynomials of closed and open automatic control systems with $m < n$ (this being the case most of the time) is identical and equal to n, we can rewrite the above formula:

$$\varphi_N = \frac{\pi}{2}(i_V + 2r_V - i_M - 2r_M). \qquad (11\text{-}20)$$

3. Stability Conditions

For an automatic control system to be stable, the right and intermediate roots $r_M = 0$ and $i_M = 0$ must be absent; in this case from formula (11-30) we obtain the expression for the criterion of stability

$$\varphi_{\text{изб}} = \frac{\pi}{2}(i_o + 2r_o).$$

(11-31a)

Thus, _a closed system is stable if with frequency changing from zero to infinity the N-vector has a deflection angle (measured in terms of full numbers of quadrants) equal to the sum of the number of intermediate roots and the twofold number of right roots of the characteristic equation of an open automatic control system, or the PAC of an open automatic control system has the same deflection angle with respect to point -1, j0._
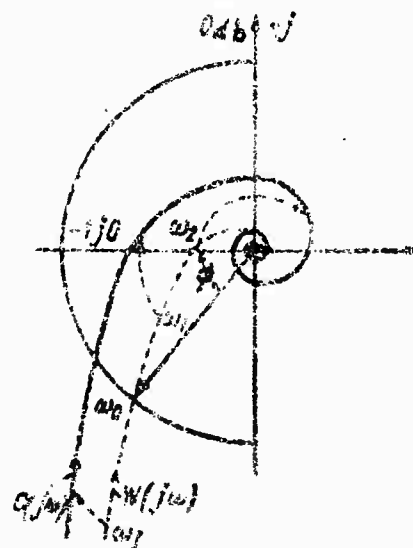
Fig. 11-7. PAC hodograph of an open system with delay component.

If the characteristic equation of an open system has no right or intermediate roots (because of the absence of the zero pole such a system must be static), i.e., $r_v = 0$ and $i_v = 0$, then the stability condition can be written in a simpler form:

$$\varphi_{N\,st.} = 0. \qquad (11\text{-}21b)$$

The PAC of such a system is shown in Fig. 11-7 by the solid line. For such characteristics the Nyquist criterion has a simpler formulation: a closed system (with the limitations for the direct path mentioned above) is stable if the PAC of an open automatic control system does not enclose the points -1, j0.

Thus, with the aid of hodograph $W(j\,\omega)$ we calculate the angle φ_W and with its aid on the basis of formula

$$\varphi_W \quad \frac{\pi}{2}\left(m - n + i_V + 2r_V - i_l - 2r_l\right)^*$$

we find the pole singularities of $W(p)$. Further, according to the same hodograph W. we calculate the angle φ_N and determine the stability conditions.

4. Stability of Automatic Control Systems with Delay Components.

If a multicircuit automatic control system has a delay component with transfer function $e^{-p\tau_d}$, while the remaining components form a transfer function amounting to the polynomial ratio $U(p)/V(p)$, then the system has to be opened at the input of the delay component. In this case the total transfer function of

860

the open [...] will be used as the product of transfer
functions of the form:

$$C(p) = e^{-p\tau} W(p). \qquad (11\text{-}22)$$

To this transfer function there corresponds a complex
amplification factor, the hodograph of which is shown in
Fig. 11-7. It is expedient to construct the hodograph
first without considering lag, i.e., to construct the
PAC $W(j\omega)$ in the first place, and then take account of
the effect of the delay component. The PAC $W(j\omega)$ is
shown in the same drawing by a dashed line. The complex
amplification factor of the delay component is equal to
$e^{-j\omega\tau_d}$, i.e., the component has a unit PAC (for any
other amplification factor it is more convenient to con-
sider it in $W(j\omega)$) and a phase shift proportional to
the frequency $\varphi(\omega) = -\omega\tau_d$.

Hence to obtain the final PAC from the hodograph
$W(j\omega)$ each vector of frequency ω_i must, without changing
the modulus, be turned by an angle $-\omega_i\tau_d$. This
procedure was performed in the Figure; it leads to the
fact that in the region of high frequencies the deflec-
tion angle becomes very great and as the frequency
approaches infinity the modulus characteristic approaches
zero with an undetermined phase performing an infinite
number of rotations.

Having a PAC of a system without lag, we determine
the limit of the lag at which the automatic control
system with a delay component will find itself on the
boundary of stability. If the hodograph of a system
without lag intersects the circumference of unit

amplitude at a frequency ω_o then, in order that the PAC of a system with lag pass through the point -1, j0 the vector $W(j\omega)$ must turn in a negative direction by an angle $\psi = \omega_o \tau_d$.

Thus, with delay time equalling

$$\tau_{d.lim} = \frac{\psi}{\omega_o},\tag{11-23}$$

the automatic control system is on the boundary of stability.

With a delay smaller than $\tau_{d.lim}$ the system is stable, and with one greater than $\tau_{d.lim}$ the control system is unstable.

If the delay component is enclosed by the local feedback $K_H(p)$, and this circuit comprises also other components $K_p(p)$, then the local OTF of the direct path can be written

$$\frac{K_p(p)\, e^{-p\tau_3}}{1 + K_H(p)\, K_p(p)\, e^{-p\tau_3}} = \frac{K_p(p)}{e^{p\tau_3} + K_H(p)\, K_p(p)}.$$

Consideration of the additional elements of the direct path $K(p)$ leads to the general OTF:

$$W(p) = \frac{K_p(p)\, K(p)}{e^{p\tau_3} + K_H(p)\, K_p(p)}$$

and to the function of the N-vector

$$N(p) = 1 + W(p) =$$

$$= \frac{e^{p\tau_3} + K_p(p)\, [K_H(p) + K(p)]}{e^{p\tau_3} + K_H(p)\, K_p(p)} =$$

$$= \frac{U_1(p)\, e^{p\tau_3} + U_2(p)}{V_1(p)\, e^{p\tau_3} + V_2(p)} = \frac{M(p)}{V(p)}.\tag{11-24}$$

862

Here $U_1(p)$, $U_2(p)$, $V_1(p)$, $V_2(p)$ are polynomials of
limited order, and $e^{p\tau_d}$ is a polynomial of infinite order.
However, the difference between the orders of the
numerator (11-24) and the denominator is finite since
it is determined by the difference of the orders of
polynomials $U_1(p)$ and $V_1(p)$. Hence the deflection
angles of the N-vector are limited and can be used
under the stability conditions mentioned above, but
the construction of hodograph (11-24) is more complex
than (11-12).

5. Evaluation of Stability with Feedbacks

If instead of a standard negative feedback an
automatic control system has a more complex feedback
circuit, then all of the above methods for evaluating
stability require some additional explanations although
they are basically applicable to such a system.

Figure 11-8 shows the block diagram of the system
with direct circuit transfer function $W(p)$ and feed-
back circuit transfer function $H(p)$. To study the
stability of the closed system irrespective of the
position of the output and input we have to use the
transfer function of the entire open system which, in
this case, equals $C(p) = W(p)H(p)$, and undertake the
subsequent analysis according to its hodograph.
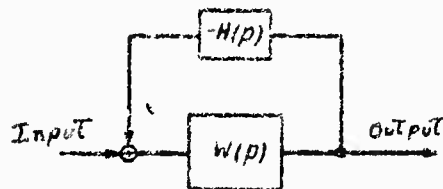
Fig. 11-8. Block diagram with nonstandard feedback.

Some particular conclusions relative to the properties of the system can be obtained not only from function $C(p)$ but also from the component transfer functions.

Thus, e.g., the stability boundary for such systems can be found from the equation

$$C(j\omega_{x}) = W(j\omega_{x}) H(j\omega_{x}) = -1, \qquad (11\text{-}25)$$

whence

$$W(j\omega_{x}) = -\frac{1}{H(j\omega_{x})}.$$

If the feedback without being unitary is still a follow-up with an amplification factor H, then the stability boundary can be found from the equation

$$W(j\omega_{x}) = -\frac{1}{H}.$$

If we compare this equation with that of the stability boundary of a standard automatic control system (11-18) we see that in the given case the role of a singular point is played by the point with coordinates $-1/H$, $j0$, relative to which we must now consider the passage of the hodograph of vector $W(j\omega)$.

For example, for a static system with direct circuit transfer function $W(p)$ and feedback circuit

864

-H to be stable it is necessary that the point $-1/H$, jc be not encircled by the N-vector hodograph.

11-8. Methods for Evaluating the Stability of Closed Automatic Control Systems by the Hodograph of an Open System, Not Requiring the Knowledge of the Character of the Poles of W(p)

1. Method of Calculating the Difference of N- and W-vector Deflection Angles

The deflection angles of N- and W-vectors were defined above by formulas (11-20) and (*). If we subtract the letter from the former we have

$$\varphi_N - \varphi_W = \frac{\pi}{2}(n - m + i_U + 2r_U - i_M - 2r_M). \qquad (11\text{-}26a)$$

The stability condition of open automatic control systems ($i_M = r_M = 0$) leads to the necessary quantity of the difference angle:

$$(\varphi_N - \varphi_W)_{SS} = \frac{\pi}{2}(n - m + i_U + 2i_U). \qquad (11\text{-}26b)$$

If we displace the origin of coordinates by -1, the construction of the W-hodograph results automatically in that of the N-hodograph and all the necessary angles can easily be defined from the PAC of the open automatic control system since its zeroes i_U and r_U are known.

If the numerator U(p) has only left roots, then the stability condition takes a simpler form:

$$(\varphi_N - \varphi_W)_{SS} = \frac{\pi}{2}(n - m). \qquad (11\text{-}26c)$$

The roots z_i of the characteristic polynomial convert the OTF of the open system into a minus unit since according to Table 10-2

$$W(p) = \frac{\Phi(p)}{1 - \Phi(p)} = \frac{U(p)}{M(p) - U(p)}$$

and, inasmuch as $M(z_i) = 0$,

$$W(z_i) = \frac{U(z_i)}{0 - U(z_i)} = -1.$$

Owing to this property, if in the root plane right of the trajectory $j\omega (0 \leqslant \omega \leqslant \infty)$ there are the roots $M(z_i) = 0$, in the plane of function $W(j\omega)$ right of the hodograph W there must lie the point -1, $j0$.

Checking for stability amounts to hatching on the right the hodograph $W(j\omega)$ and to detecting the point -1, $j0$ outside of the hatched area.

But besides the connection with the M-vector, the hodograph $W(j\omega) = U(j\omega)/V(j\omega)$ is also subjected to the effect of its proper zeroes and poles on the position of the PAC: the zeroes on the right orient hatching towards the origin of coordinates, the poles on the right orient hatching of the W hodograph in the opposite direction, and so on. The uncertainty in the determination of the M-hodograph properties arises if there exists simultaneously an equal number of right roots and poles $W(p)$; in this case the evaluation of the stability of a closed automatic control system from the hatching of the $W(j\omega)$-hodograph may be erroneous

/Bibl. 4/ since there exist for the time being no general rules for determining the indefiniteness /Bibl. 4/.

For the remaining cases, prevailingly applied in practice, the method of hatching the $W(j\omega)$ hodograph appears to be valid and is worth being applied because of its elementary simplicity /Bibl. 2/.

11-9. Generalization of A. V. Mikhaylov's Criterion of Stability

The characteristic Mikhaylov polynomial can be detected in the denominator of all the transfer functions of a closed automatic control system. In Chapter 10 we brought the following standard transfer functions of a closed system: basic $\Phi(p)$, relative $\Phi_*(p)$, disturbance transfer function $\Phi_i(p)$.

The transfer function of an open system does not directly contain a Mikhaylov polynomial but a simple transformation $1 + W(p)$ amounting to the translation of the origin of coordinates leads, as shows formula (11-19), to a function containing the Mikhaylov polynomial in the numerator.

Thus, in all the above transfer functions in passing to phase-amplitude characteristics the influence of the M-vector will become noticeable. This vector has specific deflection angles which can be easily found for stable and unstable closed automatic control systems.

But the clear picture of the deflection of the

867

M-vector proper when using more complex phase-amplitude characteristics becomes obviously obscured by the appearance of additional angles from complex functions comprised in the PAC formulas in addition to the M-vector.

Yet, when generalizing the Mikhaylov method it appears to be possible to evaluate stability according to any phase-amplitude characteristic of the system derived from the above transfer functions on the basis of the calculation of the deflection angle of this characteristic, proceeding from deflection angles included in the PAC of the M-vector and other complex functions.

1. Evaluation of Stability from Relative PAC

From the expression for a relative transfer function given in Table 10-2 we pass immediately to the phase-amplitude characteristic

$$\Phi_.(j\omega) = \frac{V(j\omega)}{M(j\omega)} \; .$$

We determine the deflection angle of the relative PAC in a fashion similar to that of the preceding angles:

$$\varphi^{\cdot} = -\frac{\pi}{2}(l_V - r_V - l_M + r_M);$$

With equal order of the polynomials of the numerator and the denominator we have:

$$\varphi' = -\frac{\pi}{2}(i_V + 2r_V - i_M - 2r_M). \qquad (11\text{-}27a)$$

For a stable closed automatic control system we

determine the required deflection angle of its relative PAC:

$$\varphi'_{SS} = -\frac{\pi}{2}(i_V + 2r_V).\tag{11-27b}$$

2. Evaluation of Stability by Inverted Relative Phase- Amplitude Characteristics (IRPAC)

It is easier to construct the inverted relative PAC (10-11b) than the direct relative PAC, hence we formulate the proved criterion for the hodograph of the inverted relative PAC (IRPAC). Obviously the deflection angle of the IRPAC of a stable closed system will differ from (11-27b) only by the sign:

$$-\varphi^*_{SS} = \frac{\pi}{2}(i_V + 2r_V).\tag{11-27c}$$

Thus, a closed system is stable if, when the frequency changes from zero to infinity, the IRPAC has a positive deflection angle with a number of quadrants traversed by the characteristic equal to the sum of the intermediate poles and doubled number of right poles of the open system.

If condition (11-27c) is not fulfilled, it might be useful to ascertain not only the existence of a nonsteady state in the automatic control system but also to determine the character and the number of the right poles of the closed system. To do this we use formula (11-27a) with its sign changed for the inverse characteristic:

$$-\varphi^* = \frac{\pi}{2}(i_V + 2r_V - i_M - 2r_M).$$

Calculation by this formula and juxtaposition
with the deflection angle of the actual IRPAC give
an answer to the questions posed. For example, in
Fig. 11-6 φ^* equals $\psi_1 + \psi_2 = -\mathcal{T}$; whence for $i_V = 0$
and $r_V = 0$ we have

$$-2 = -i_M, \quad or \quad i_M = 2.$$

3. Evaluation of Stability by PAC of an Open Automatic
Control System

The IRPAC graph of a closed automatic control
system is obtained from the PAC graph of an open system
by a simple displacement of the latter by unity along
the real axis. For this reason in Fig. 11-6 the plane
with coordinate axes shown with dash-and-dot lines is
designated as the plane of function $1/\phi_*(j\omega)$.

Thus, the graph plotted in Fig. 11-6 in the coor-
dinate system with the axes represented by solid lines
are PAC of the open system, while in the coordinate
system with dash-and-dot axes they are IRPAC of the
same, though closed system.

It is obvious that on the strength of this coinci-
dence the deflection angles of the open-system PAC with
respect to point -1, j0 coincide with the deflection
angles of the IRPAC of the closed system with respect
to the origin of coordinates 0^*. The same deflection
angles were obtained in deriving the Nyquist stability
criterion ($\varphi^* = \varphi_N$) which thus becomes a particular
case of the generalized Mikhaylov criterion.

870

It is useful to underscore this fact so it be clear that the stability of a closed system is evaluated by the characteristics of the closed system. The drawing of PAC of _open_ automatic control systems in utilizing the Nyquist criterion is but an intermediate operation since when shifting the origin of coordinates to the point -1, j0 we obtain the IRPAC of the _closed_ system.

4. Evaluation of Stability by Basic PAC of a Closed Automatic Control System

The PAC of a closed automatic control system is expressed by the formula

$$\Phi(j\omega) = \frac{U(j\omega)}{M(j\omega)} = \frac{W(j\omega)}{N(j\omega)}.$$ (11-28a)

The expression for a full deflection angle of the basic PAC of a closed system is obtained like Eq. (11-28a):

$$\psi_o = -\frac{\pi}{2}(i_0 + 2r_0 - i_M - 2r_M + n - m).$$

The deflection angle for a stable automatic control system must be

$$\psi_{o_{3s}} = -\frac{\pi}{2}(i_0 + 2r_0 + n - m).$$ (11-28b)

5. Stability of Closed Automatic Control Systems with Mutually Inverted Transfer Functions

Earlier we investigated examples of real frequency-response characteristics of control systems in which the transfer function of the direct circuit the order of the denominator polynomial is always greater than that

of the numerator. For the force transmission of
control signals this limitation is quite natural since
in feeding to the input of the direct circuit a constant
step already with a numerator and a denominator of equal
order in the transfer function the expansion of the OTF
contains a constant term, i.e., an instantaneous trans-
mission of this step to the output must be assured,
whereas if the order of the numerator exceeds that of
the denominator, pulses must be observed at the system's
output, which is not feasible from a power engineering
point of view.

Yet, in electric circuits such relationships be-
tween the order of the numerator and that of the denomina-
tor of the transfer function of the direct circuit are
possible, and their connection by means of a negative
follow-up directly or through amplifiers is possible
as well. This was dealt with in Chapter 7. There may
arise the question of the stability of the closed cir-
cuit which is solved, as in the examples investigated,
by determining the deflection angle of the characteristic
$1/\varphi_*(j\omega) = N(j\omega)$.

If the order of the numerator in a transfer function
of an open system is equal to that of its denominator,
then the characteristic terminates on the real axis
since $W(j\infty) = b_n/a_n$. When evaluating stability such
a characteristic has no singularities.

If the order of the denominator is smaller than
that of the numerator of a transfer function of an
open system, then its PAC proceeds to infinity. In this

case the IRFAC takes the form

$$\frac{1}{\hat{W}_v(p)} =$$

$$= \frac{b_m p^m + \ldots + b_{n+1} p^{n+1} + (a_n + b_n) p^n + \ldots + (a_0 + b_0)}{a_n p^n + \ldots + a_0}. \qquad (11\text{-}29)$$

If all the poles of the open system are left ones, then the condition for stability for such systems in a closed state will be the IRFAC deflection angle relative to the origin of coordinates 0* or the FAC deflection angle of the open automatic control system with respect to the point -1, $j0$ measured in terms of quadrants equal to the difference between the order of numerator and denominator polynomials of the transfer function of the open system:

$$\varphi_{v.ss} = -\varphi_{ss}^{*} = \frac{\pi}{2} (m - n). \qquad (11\text{-}30)$$

Figure 11-9 shows the FAC W_1 for the case $m = n + 3$ and their inversion W_2.
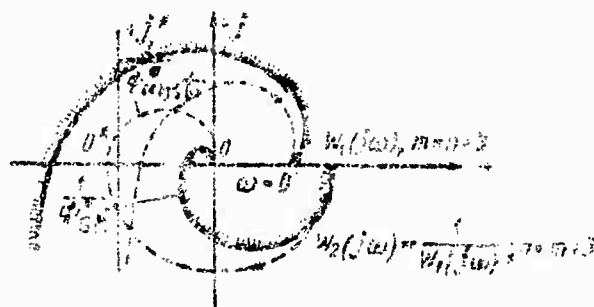
Fig. 11-4. Hodographs of mutually inverted FAC of an open system.

The characteristic $W_1(j\omega)$ drawn in a solid line has a positive deflection angle +3 quadrants with respect to point -1, j0. The IRPAC has the same deflection angle with respect to its origin of coordinates 0*. The closed system is therefore stable. For an unstable system of the same order the characteristic is drawn with a dashed line, and its deflection angle is -1 quadrant. Both characteristics proceed towards infinity in the third quadrant in the direction of the negative imaginary semi-axis. Characteristics W_2(solid line and dashed line) refer, respectively, to a stable and unstable closed automatic control system according to (11-21b) and (11-20).

Characteristic of systems (m > n) is the change in the respective location of stable and unstable characteristics with respect to the point -1, j0. In stable systems, however, the point -1, j0 never falls into the hatched region.

In the given case the inversion method enables us to draw the following conclusion: if in the direct circuit of a closed system the transfer function $W_1(j\omega)$ is substituted by the inverse $W_2 = 1/W_1$, the stability of the closed system undergoes no change. Hence, in evaluating the stability we may plot in the plane $W(j\omega)$ either the hodograph $W(j\omega)$ or the hodograph $1/W(j\omega)$ depending upon what is most convenient for the purposes of the investigation.

In two closed automatic control systems with open transfer functions $W(j\omega)$ and $1/W(j\omega)$ not only the stability indices but also the nature of transfer

874 _

processes coincide. Indeed, if we determine the full transfer function of the second system

$$\Phi_{z}(p) = \frac{\frac{1}{W(p)}}{1 + \frac{1}{W(p)}} = \frac{1}{1 + W(p)} = \Phi_{1_z}(p), \qquad (11\text{-}31)$$

it turns out to be equal to the relative transer function of the first system

$$\Phi_{z}(p) = \Phi_{1_z}(p). \qquad (11\text{-}32)$$

Consequently, the transfer process at the output of one system coincides with the process on the error line of the second system:

$$x_{out}(t) = x_{o1}(t).$$

The transfer functions of both closed systems complement each other up to unity:

$$h_{2}(t) = 1 - h_{1}(t),$$

i.e., if one system copies with an amplification equalling unity ($h_{1\ st} = 1$), then the other system does not transmit the steady signal $h_{2\ st} = 0$ (the case of real differentiation).

The weight functions of these systems differ only by the sign and by the initial pulse $w_{2}(t) = \delta(t - w_{1}\ t)$, while in steady-state their moduli coincide $\left| w_{2}(\infty) \right| = \left| w_{1}(\infty) \right|$.

11-10. Stability Evaluation of Multicircuit Automatic Control Systems by Logarithmic Characteristics

If we use the method of logarithmic characteristics in its full extent with all the facilitating transformations

of the characteristics by nomograms, the stability of
multicircuit automatic control systems may be investi-
gated in several stages.

This makes it possible to establish more clearly
the role played by each circuit in the formation of
right-hand poles in the open control system and devise
means for eliminating them if the system as a whole
cannot be stabilized at once.
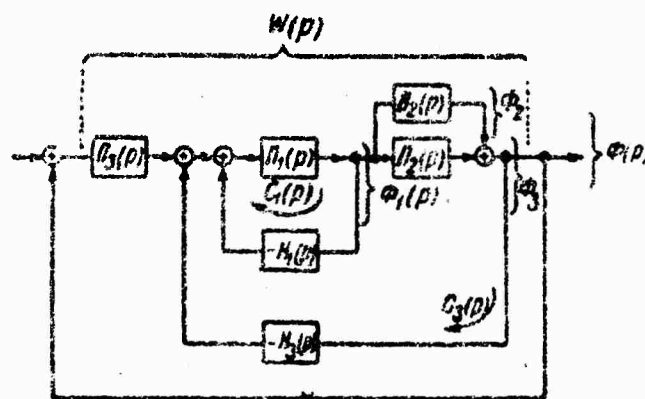
Fig. 11-10.   Evaluating the stability of multicircuit
automatic control systems

We investigate the multicircuit automatic control
system shown in Fig. 11-10. We perform a successive
convolution of the circuit and plot the general
frequency-response characteristic, focusing our
attention on the information required for a subsequent
evaluation of the control system's stability.

1st circuit. The circuit characteristics
$C_1(p) = a_1(p) \prod_1 (p)$ are found by summing the LAFC and

876

and PFC of the components $H_1(p) = \beta_1(p)/\alpha_1(p)$ and $\Pi_1(p) = b_1(p)/a_1(p)$. We fix the singularities at the poles of $H_1(p)$ and $\Pi_1(p)$: $r_{\alpha 1}$, $i_{\alpha 1}$; r_{a1}, i_{a1}. We contract the circuit by the $\overset{\circ}{\Phi}_{*1}$ nomogram (Fig. 4-28): $\overset{\circ}{\Phi}_{*1}(j\omega) = 1/(1 + C_1(j\omega)) = V_1(j\omega)/M_1(j\omega)$. Information about the roots r_{M1}, i_{M1} of the $M_1(p)$ polynomial is gathered from the properties of the open circuit $C_1(j\omega)$. By summing the LAFC and PFC of the obtained $\overset{\circ}{\Phi}_{*1}(j\omega)$ with characteristics $\Pi_1(j\omega)$ we obtain "transmission" frequency-response characteristics of the first circuit $\overset{\circ}{\Phi}_1(j\omega) = \Pi_1(j\omega)\overset{\circ}{\Phi}_{*1}(j\omega)$ and full data about the singularities of poles $\overset{\circ}{\Phi}_1(p)$:

$r_{M1} = r_{M1} + r_{a1}$; $i_{M1} = i_{M1} + i_{a1}$.

   2nd Circuit. The "transmission" frequency-response characteristics of a coparallel circuit

$$\Phi_2(p) = B_2(p) \mid -\Pi_2(p) = \frac{\beta_2(p)}{\alpha_2(p)} + \frac{b_2(p)}{a_2(p)} = $$
$$ = \frac{\alpha_2(p)\beta_2(p) + \alpha_2(p)b_2(p)}{\alpha_2(p)a_2(p)} = \frac{l_2(p)}{N_2(p)} $$

are obtained from the P, Q-nomogram (Fig. 4-25), and we fix the singularities of the poles $\overset{\circ}{\Phi}_2(p)$:

$r_{MII} = r_{\alpha 2} + r_{a2}$; $i_{MII} = i_{\alpha 2} + i_{a2}$.

   3rd Circuit. The open circuit is formed by the following elements: $C_3(p) = \overset{\circ}{\Phi}_1(p)\overset{\circ}{\Phi}_2(p) \times H_3(p) = U_3(p)/V_3(p)$ and has singularities in the roots of $V_3(p)$ (poles): $r_{V3} = r_{M1} + r_{MII} + r_{\alpha 3}$; $i_{V3} = i_{M1} + i_{MII} + i_{\alpha 3}$. where $H_2(p) = \beta_3(p)/\alpha_3(p)$. The logarithmic frequency-response characteristics of the three units are summed to form $C_3(j\omega)$. By the

Φ_* nomogram we find the relative LFC of the closed circuit $\Phi_{*3}(j\omega) = 1/(1 + C_3(j\omega)) = V_3(j\omega)/M_3(j\omega)$. By the $C_3(j\omega)$ hodograph we determine the singularities of the poles of $M_3(p)$: r_{M3} and i_{M3}. The "transmission" frequency-response characteristics of the circuit are found by summing LFC $\Phi_{*3}(j\omega)$ and $\Phi_1(j\omega)\Phi_2(j\omega)$ according to the formula $\Phi_3(j\omega) = \Phi_{*3}(j\omega) \times \Phi_1(j\omega)\Phi_2(j\omega)$ $V_{III}(j\omega)/M_{III}(j\omega)$. The singularities of the poles of $\Phi_3(p)$ are easily singled out: $r_{MIII} = r_{M3} + r_{M1} + r_{MI}$; $i_{MIII} = i_{M3} + i_{M1} + i_{MI}$.

4th degenerative feedback circuit. The open system has an OTF $C_4(p) = W(p) = \prod_3(p)\Phi_3(p) = b_3(p)/a_3(p)\Phi_3(p)$. The singularities of its poles are found taking account of what preceded: $r_V = r_{MIII} + r_{a3}$; $i_V = i_{MIII} + i_{a3}$. All this makes it possible to evaluate the stability of a closed automatic control system by the LAFC and PFC $W(j\omega)$ on the basis of the rules expounded in Section 11-7. To calculate the deflection angles of vectors in the complex plane near the origin of coordinates we can use directly semilogarithmic PFC, while for the calculation of the deflection angles of the same vectors with respect to the point -1, $j0$ we must analyze both the PFC and LAFC and single out the number of intersections by the phase characteristic of the line 180° at an amplitude greater than 0 db.

11-11. Practical Methods for Stabilizing Unstable Systems

1. Purpose of Method. Stability Margin.

The overall purpose of measures for ensuring the stability of automatic control systems is determined by the aim, namely, carry the system from a nonsteady state across the stability boundary into the stable region.

Passage across the stability boundary is effected by changing the engineering parameters of the control system's elements and its block diagram. Hence complex control systems may have a great number of engineering parameters affecting the system's stability; the search for optimum solutions is usually associated with a large number of alternate calculations.

Carrying the system across the boundary of stability is by itself not a sufficient measure, on the strength of possible fluctuations in the engineering parameters of the system during its operation, and owing to the fact that because of the approximateness of engineering calculations a system with a stable design cannot fulfill practical requirements if its parameters are such that it finds itself close to the boundary of stability. However, the main drawback of stable systems close to the stability boundary appears to be in the abrupt drop in control quality. Hence there arises the perfectly legitimate requirement of not only ensuring the stability of automatic control systems but also of creating a specific stability margin, i.e., the system must be

sufficiently remote from the boundary of stability.

Let us note in addition that the solution of the problem of stability of automatic control systems and the creation of the required margin of stability must not impair the system's accuracy.

The complex solution of these problems is dealt with in Chapter 12.

How to apply the measures for ensuring the above stability indices, as well as the evaluation of the results obtained can be decided on the basis of analytic or frequency criteria of stability.

In the given Section we are going to deal only with frequency stability criteria.

The measures for carrying the system across the stability boundary far enough from it into the stability region become clearer if we resort to frequency criteria of stability and to a number of rules established while determining these criteria.

The boundary of stability in the plane of the PAC of an open system appears in the form of a boundary characteristic of each of the systems investigated, passing across the point -1, j0. The stability margin in the PAC plane has a visual-geometric character consisting in the receding of the points on the PAC investigated from the boundary point -1, j0. This receding is expediently measured in a polar coordinate system in terms of phase and radius-vector or the logarithm of modulus ratio (in decibels), and by introducing respectively the notions of phase and amplitude margins

for stable systems.

A phase margin is said to be the angle between the direction of the real negative semiaxis and the PAC vector of an open automatic control system whose modulus equals unity, i.e., 0 db:

$$\psi = \pi - \varphi(\omega_0).$$ (11-55a)

The amplitude margin is said to be the modulus of the vector of the same PAC placed along the negative real semiaxis, expressed in decibels:

$$L(\omega_{\varkappa}) = 20 \lg |W(j\omega_{\varkappa})|.$$ (11-33b)

Figure 11-11 shows a circular arc of unit radius 0 db which subtends the angle 2ψ. The system has a phase margin ψ^0 if the PAC of the open system intersects the circumference 0 db on the boundaries of the hatched sector.

In the same figure, against the negative real semiaxis are plotted points corresponding to margins and amplitudes equal in magnitude (decibels) and different in signs. A stable system has an amplitude margin $L(\omega_{\varkappa})$ if the PAC of the open system intersects the negative real axis at one of the two points on the boundaries of the hatched sector. In such a control system deviations of the gain from rated value towards the margin are permissible without impairing the system's stability.

Let us investigate two stable closed control systems with an OTF of the open loop $W_1(p)$ and $1/W_1(p) = W_2(p)$.

If for one of the systems, e.g., the first one, the phase margin has a positive sign, then it is negative for the second one. The signs of the amplitude margin for both automatic control systems vary in

exactly the same fashion. In terms of absolute magnitude
both indices of the systems investigated are identical,
as shown in Fig. 11-11.
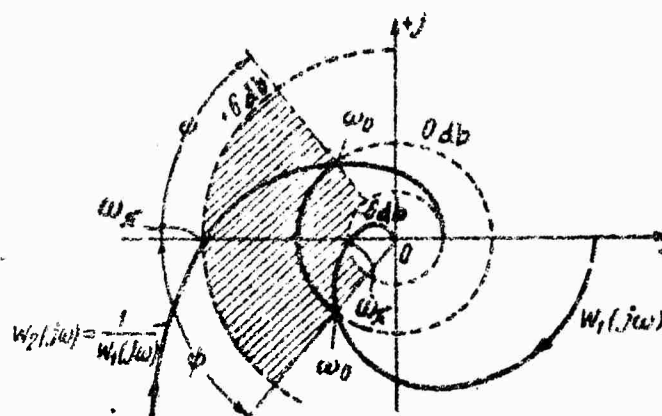
Fig. 11-11. Designation of phase and amplitude margins
in a complex plane.

For each individual system the characteristic moves
away from the boundary of stability only with a specific
sign of the stability margin. Rostral characteristics
may have two signs for the amplitude margin. The proper
signs are determined on the basis of general stability
evaluations.

Phase and amplitude margins can be clearly read
on the decibel-log-frequency and the phase characteristic
shown in Fig. 11-12. The phase margin is equal to the
difference between 180° and phase magnitude at a transi-
tion frequency of the AFC across the line of 0 db. The
amplitude margin is equal to the amplitude magnitude
in decibels at a passage frequency of the phase charac-

teristic across the phase line of 180°.
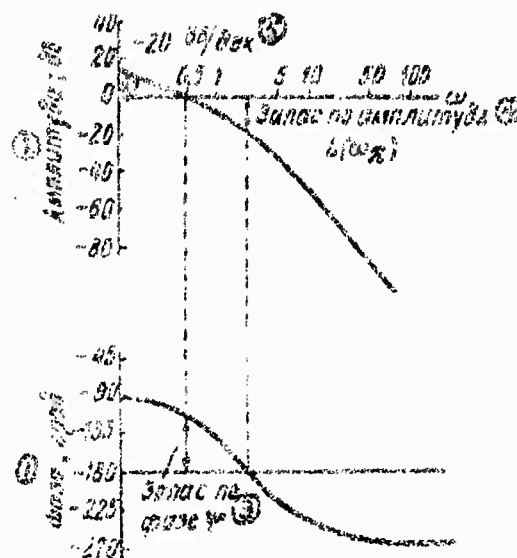
Fig. 11-12. Phase and amplitude gains marked on
logarithmic frequency-response curve
key: 1) phase, degrees; 2) amplitude, db; 3) phase
margin; 4) amplitude margin; 5) db/dec.

The logarithmic frequency-response curves plotted
in Fig. 11-12 refer to the astatic three-circuit auto-
matic control system already investigated in Section
11-4. Its block diagram was shown in Fig. 11-4. The
amplitude characteristic can be replaced by asymptote
segments with an inclination of -20 db/dec at low
frequencies, -40 db/dec after the first tracking
frequency $\Omega_1 = 1/T_1$, and -60 db/dec after the second
tracking frequency $\Omega_2 = 1/T_2$. The phase response is
constructed with the aid of patterns. The phase
margin for the particular case $T = 1$ and $a = 0.2$

amounts to about 70°, the amplitude margin to about
20 db.

It should be recalled that the gain of the integrator
K_{-1} is quantitatively equal to the frequency at the
point of intersection of the asymptote of the initial
segment with the line of 0 db (see Chapter 4), hence in
the given system we have a velocity error constant
$K_{-1} = 0.5 \text{ sec}^{-1}$. Judging from the magnitude of the
amplitude margin, it can be increased ten-fold, i.e.,
brought up to 5 sec^{-1}.

In the following these very rough calculations
will be compared with analytic evaluations. For
automatic control systems differing from the one in-
vestigated by their structure, in the case of several
points of intersection with the line 0 db or phase 180°
the margin has to be determined several times. In so
doing, the sign of the margin must be evaluated correctly.

On the basis of the frequency evaluations of
stability investigated and of the stability margin we
can devise a number of engineering measures by which
to ensure the indices desired.
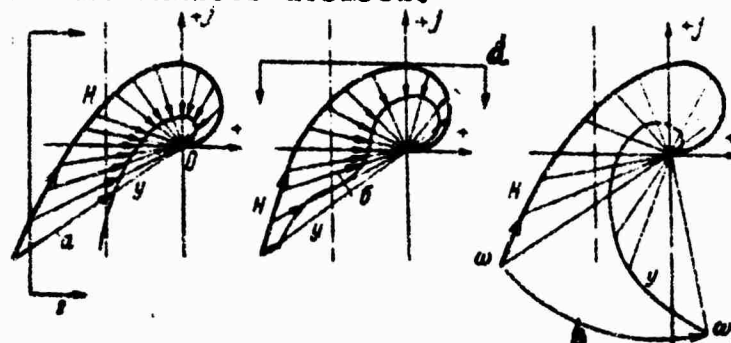
Fig. 11-13. General principles of deformation of the
PAC of an open system for stabilizing a closed automatic
control system.

Let in Fig. 33-43 be given the PAC of an open
system which is unstable when closed. Stability will
be ensured in the given case by shifting characteristic
W to the right of point -1, j0 and by its further
displacement for attaining the stability margin required.

Deformation of the PAC can be performed by the
following methods:

a) By reducing the modulus of vectors W at all
frequencies;

b) By reducing the modulus of vectors W in a
frequency band yielding a phase close to -180°, i.e.,
by means of a selective decrease of the modulus;

c) By turning the entire PAC without changing its
modulus in the given case in a positive direction, or,
in the direction of passage across the stability
boundary, or by turning a part of the characteristic
in the frequency band desired (selective turn);

d) By displacing the PAC points in a direction
assigned by additional vectors;

e) By combining the methods enumerated.

The above methods can be achieved as follows:

By a cascade connection of the new element into
the direct circuit of the control system or by replacing
some elements of the direct circuit by elements with
the same gain but improved dynamic characteristics;

By introducing parallel forcing couplings by means
of joining up with the direct circuit in parallel with
the existing elements some additional elements, or by
inserting new forcing elements containing parallel arms

in its inner structure;

By introducing feedbacks enclosing one element or a group of elements of the direct circuit.

These procedures are worth being thoroughly investigated.

2. Cascade Connection of New Elements into the Direct Circuit

By connecting into the direct circuit of a control system a new amplifying component with a gain less than unity, one achieves a reduction of the modulus of the PAC vectors at all frequencies through a proportional decrease in the total gain of the open system. This method needs no particular elucidations, yet it stands in contradiction with accuracy requirements and its application is in many cases limited. When inserting into the direct circuit an operator element it must be selected among a number of elements having a lead for the turning of the system's PAC according to method "c" or having a dropping amplitude-phase characteristic in the required frequency band in accordance with method "b".

3. Substitution of Elements in the Direct Circuit

Let the transfer function of an open automatic control system be assigned in its general form: $W_1(p)$. In the chain of elements of the direct circuit we separate out a group of elements which remain unchanged,

$\Pi_1(p)$, and a second part — an element or a group of elements $\Pi_2(p)$ subject to replacement, as shown in the block diagram of Fig. 11-14. The aggregate transfer function of the direct circuit is equal to the product of transfer function components:

$$W_1(p) = \Pi_1(p)\,\Pi_2(p).$$
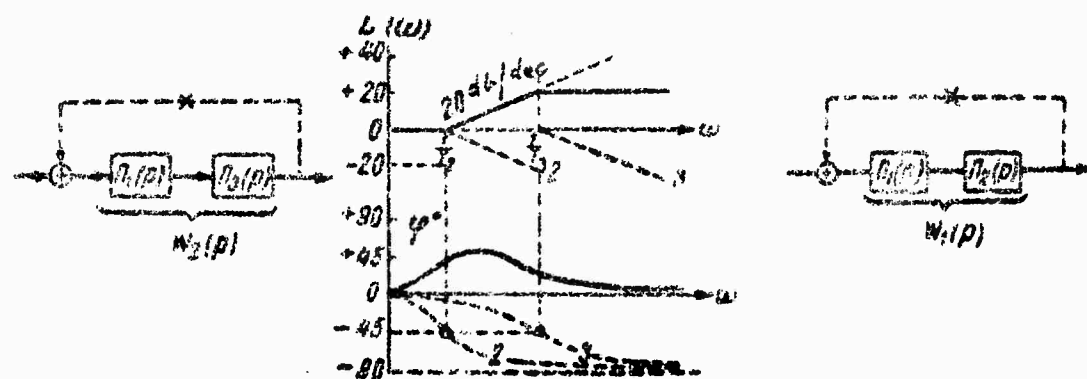
Fig. 11-14. Stabilization by replacing elements of the direct circuit

If now instead of the element with transfer function $\Pi_2(p)$ we insert a new element with transfer function $\Pi_3(p)$, then the aggregate transfer function of the direct circuit will be

$$W_2(p) = \Pi_1(p)\,\Pi_3(p).$$

The relation between the new and the old transfer functions of the direct circuit can be reduced to the following form:

$$W_2(p) = W_1(p)\frac{\Pi_1(p)}{\Pi_2(p)} = W_1(p) K(p). \qquad (11\text{-}34)$$

The formula above makes it possible to determine the PAC of the new system from the original PAC. To do this, all of the complex vectors of the fundamental PAC must be multiplied by the complex correction factor

$$K(j\omega) = \frac{\Pi_1(j\omega)}{\Pi_2(j\omega)}. \qquad (11\text{-}35)$$

In this case the PAC changes its modulus by $\left|K(j\omega)\right|$, while the phase of each vector turns by the phase of the correction factor. These PAC deformations may turn out to be useful for ensuring stability or increasing the stability margin.

Suppose that in a system the aperiodic component is being replaced by an identical component but with a smaller constant of time; then $\Pi_2(j\omega) = 1/(1 + j\omega T_2)$; $\Pi_2(j\omega) = 1/(1 + j\omega T_2)$, and the complex correction factor can be defined as the relation

$$K(j\omega) = \frac{\dfrac{1}{1 + j\omega T_1}}{\dfrac{1}{1 + j\omega T_2}} = \frac{1 + j\omega T_2}{1 + j\omega T_1}.$$

The last transformation in the formula derived need not be performed if we evaluate the PAC deformation by the logarithmic characteristics of the components, which in the given case appears to be most expedient.

In Fig. 11-14 the dashed lines 2 and 3 show the logarithmic characteristics of the aperiodic components

with unit gain. The amplitude characteristics are given here in their asymptotic form, and the break of the horizontal portion of a component with a greater constant of time T_2 at the tracking frequency $1/T_2$ takes place earlier than the break of a characteristic with a constant of time T_3 and tracking frequency $1/T_3$. The phase responses are traced with the aid of patterns through points -45^0 at their tracking frequencies.

By subtracting from the characteristics of the third component those of the second one we obtain the aggregate characteristics shown in the Figure by a solid line.

From the phase characteristic of the correction factor we can establish that a decrease in the constant of time of the aperiodic component introduces in the PAC a lead at all frequencies, and especially in the frequency band from $1/T_2$ to $1/T_3$ where the leads may attain 45^0 and more. This represents a merit of the given correction method.

A drawback of the method investigated consists in a simultaneous increase in amplitude at high frequencies by

$$20 \lg \frac{T_2}{T_3} \, |db|.$$

The relatively small phase lead and the increase in amplitude make it possible by replacing the components by uniform components with improved dynamic characteristics to ensure the stability only for those systems which are comparatively close to the boundary

of stability; in more complex cases additional measures are required which we discuss below.

4. Insertion of Coparallel Forcing Circuits.

We divide the transfer function of the direct circuit of system W_1 into cofactors Π_1, Π_2, Π_3; Π_1 and Π_3 being transfer functions of components with invariable operating conditions, and Π_2 being a transfer function of components enclosed in the direct circuit.

If the direct circuit is joined up with the basic system in the way shown in the block diagram of Fig.11-15,a, and if it has a transfer function B, then the transformed transfer function takes the form:

$$W_3(p) = \Pi_1(p)[\Pi_2(p) + B(p)]\Pi_3(p) =$$
$$= W_1(p) + \Pi_1(p)\Pi_3(p)B(p).$$

(11-36)
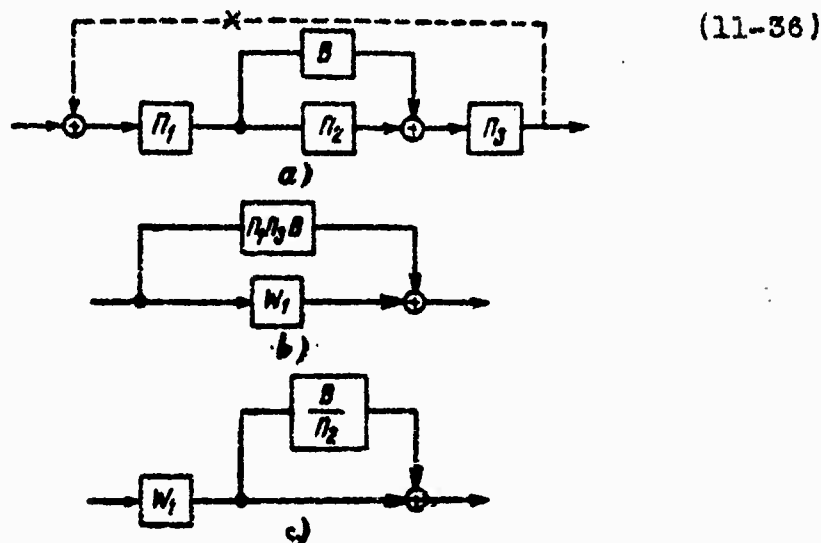
Fig. 11-15. Coparallel stabilizing circuits.

The second form of the right-hand side of the equation obtained reflects the second version b of the block diagram shown in the Figure above and obtained from the first circuit by shifting the node against the path of the signal and the adder along it.

Circuit c and the transformation formula for the characteristics

$$W_2(p) = W_1(p)\left[1 + \frac{B(p)}{\Pi_2(p)}\right].\tag{11-37}$$

can be found analytically and by structural methods.

Thus, the new PAC $W_2(j\omega)$ can be found by joining to the original PAC $W_1(j\omega)$ the vector

$$\Lambda(j\omega) = \Pi_1(j\omega)\, B(j\omega)\,\Pi_3(j\omega)\tag{11-38}$$

or by multiplying $W_1(j\omega)$ by the complex correction factor

$$K(j\omega) = 1 + \frac{B(j\omega)}{\Pi_2(j\omega)}.\tag{11-39}$$

It is better to perform the addition of vectors in a complex plane, while the characteristics are more expediently multiplied with the aid of logarithmic characteristics.

Let us take a closer look at the additional vector $\Lambda(j\omega) = \Pi_1(j\omega)\, B(j\omega)\,\Pi_3(j\omega)$. In those cases where it is expedient to shift the PAC of an open system to the right and turn it in a positive direction in order to obtain stability or to increase the stability margin, the additional vector must have a phase close to zero or within the limits of the fourth quadrant with an

891

undesirable passage to the third quadrant in a band of
frequencies close to the natural oscillations of a
system on the stability boundary.
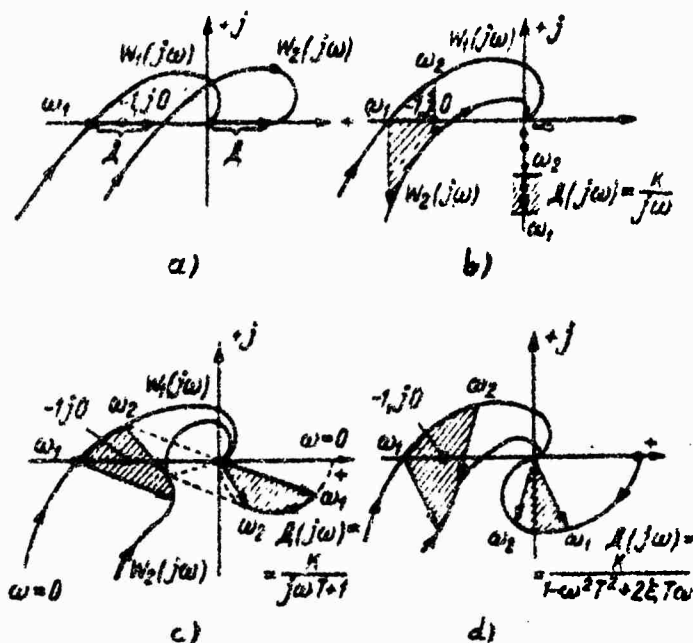
Fig. 11-16. Transfer of the PAC of an open system into
the stability region by inserting a coparallel circuit

Figure 11-16 shows some typical additional vectors
$Д$ $(j\omega)$ and their effect upon the PAC.

Diagram a investigates a purely real and positive
vector $Д(j\omega) = Д$. By adding to the PAC W_1 a vector
constant in magnitude and direction we obtain a PAC W_2
shifted to the right by the quantity $Д$. We can easily
see that stability can in the given case always be
ensured.

In diagram b the additional vector is taken
purely imaginary and negative but with a variable

modulus of the type of an integrating component $\Delta(j\omega) =$
$K_1/j\omega$. Its hodograph coincides with the negative
imaginary semiaxis. It is shown in the diagram, and on
the hodograph there is separately marked the band of
frequencies close to the system's natural frequency.
The diagram has also additional vectors for limiting
frequencies ω_1 and ω_2; these vectors push downward
the corresponding points of the PAC W_1. After per-
forming constructions of this kind for all points
we obtain a new PAC W_2. Passage across the stability
boundary can in this example always be ensured provided
we choose the modulus of the additional vector greater
than the imaginary frequency-response characteristic
at frequency ω_2, i.e., $\left|\Delta(j\omega_2)\right| > \mathrm{Im}\, W_1(j\omega_2)$.

In diagram c we study an additional vector of the
type of an aperiodic component whose hodograph falls
entirely into the fourth quadrant: $\Delta(j\omega) = K/(1+j\omega T)$.
The region hatched in the diagram corresponds to the
frequency $\omega_1 - \omega_2$ near the system's natural frequency.
The addition of vectors $\Delta(j\omega_1)$ and $\Delta(j\omega_2)$ to the
PAC W_1 is performed following the rule of vector
summation. After carrying out similar constructions
for all points of the graph, we obtain a new PAC.
It should be noted that in the frequency band $\omega_1 - \omega_2$
the hodograph W_1 can be carried across the stability
boundary in the shortest direction, and this makes it
possible, if the additional vector is situated in
the fourth quadrant, to ensure the stability of an
automatic control system with a relatively small gain

In the parallel circuit.

In diagram d we investigate a second-order additional vector of the type of an oscillatory component

$$\Delta(j\omega) = \frac{K}{1 - \omega^2 T^2 + j2\xi\tau\omega}.$$

From the fourth quadrant its hodograph passes into the third quadrant. If we again introduce the limiting frequencies ω_1 and ω_2 we can easily note that as long as the additional vector is in the fourth quadrant the displacement of the PAC W_1 occurs in a favorable direction, whereas when the additional vector passes into the third quadrant, only the imaginary vector component displaces the PAC W_1 in a required direction (downward) while the real part of the additional vector leads the PAC W_1 away in an undesirable direction (to the left). Although in the example studied in the diagram stability is attained, if the vector phase $\Delta(j\omega)$ approached π in the third quadrant then, to obtain the required imaginary component the gain in the subsidiary loop should be chosen excessively great, which is not always feasible.

By analogous diagrams we can show that when finding the additional vector in the first quadrant a useful displacement can be achieved only by its real part, while when finding the additional vector in the second quadrant the system cannot be carried across the stability boundary whatever the gain of the parallel arm.

If we determine the frequency at which the additional vector taken from a corresponding point of the PAC or its continuation passes through the point -1,j0,

we can easily calculate the minimum gain of the parallel
circuit at which the system finds itself on the boundary
of stability. In diagram b, e.g., the limiting gain of
the subsidiary arm is equal to the adopted gain K_{-1} re-
duced by the ratio $\text{Im } W(j\omega_2)/\Pi(j\omega_2)$. For the other
diagrams this calculation is performed on the basis of
analogous geometric relations.

The aggregate subsidiary vector Π contains as a
cofactor the transfer functions $\Pi_1(p)\Pi_3(p)$ of the
elements of the system's direct circuit and, moreover,
newly inserted elements with the transfer function
$B(p)$. The choice of subsidiary elements depends, of
course, on the character of components already available
in the direct circuit. Let us investigate some possible
choices of subsidiary elements in accordance with the
type of elements of the control system's main circuit
not covered by the direct parallel circuit.

The parallel circuit does not cover the amplifying
component alone. In this case $\Pi_1\Pi_3$ is a constant
number and the recommendations relative to the aggre-
gate subsidiary vector $\Pi(j\omega)$ are referred now to the
vector of the parallel branch $B(j\omega)$. Hence it is
expedient to have the parallel direct circuit in the
form of a rigid direct circuit with amplifying com-
ponents, or in the form of an astatic circuit with
integrating elements and aperiodic components, or a
group of components satisfying the phase requirements
of the subsidiary vector.

It should be noted that a parallel circuit with

such a wide coverage of nearly all the elements of the direct circuit must to some extent duplicate the functions of the latter. For example, if the elements covered are assigned the task of increasing the power, then the parallel branch must solve an analogous problem if a summation of the parallel branches according to the block diagram in Fig. 11-15 is to be achieved.

Let us investigate, e.g., the direct circuit of a powerful electromechanical system shown in Fig. 11-17. The control input in the form of the deflection angle of the input shaft brings about the displacement of electrical, mechanical, hydraulic . or other similar elements of the speed variator of a powerful electric motor driving the output shaft. The principal energy flow is conveyed to the output shaft from the electric motor which overcomes the load moment.
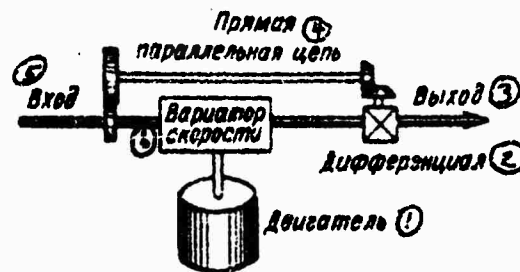
Fig. 11-17. Mechanical rigid coparallel circuit.
Key: 1) motor; 2) differential; 3) output; 4) direct parallel circuit; 5) input; 6) speed variator

If now we apply to the speed variator a direct rigid circuit in the form of a shaft branching out at the input from the main path and joined with the

output shaft by means of a mechanical differential, then the moment on the parallel circuit shaft will be determined by the output moment calculated inversely proportional to the transmission figures of the differential and subsequent transmissions. The required moment at the input shaft is determined in a like fashion.

Diagrams similar to that shown in Fig. 11-17 are used in direct circuits of control systems closed by man (operator). In this case the direct circuit ensures the stability of sufficiently complex closed systems.

Application of direct circuits in electric circuits, especially with the aid of amplifiers, is carried out with fewer limitations and was dealt with in Chapter 8. In this case, however, the result of summing signals in parallel branches to convert them into the output value of a relatively powerful system requires the insertion of a number of subsidiary elements which, as a rule, are more complex than nonstorage amplifiers. But such a system exceeds the scope of the case investigated and will be discussed subsequently.

Thus, stability is theoretically always attained if all the operator components of the direct circuit are covered by a parallel circuit which is made rigid. In practice, however, such a coupling is usually not achievable for power engineering considerations.

The parallel circuit does not cover elements with a transfer function higher than second order. When standardizing the varieties of direct circuits, we refer to the given case all the elements forming

transfer functions $\Pi_1(p)\,\Pi_3(p)$ which have the PAC in the lower half-plane. Such elements include the integrating, aperiodical, cascade circuits with two aperiodic components, the oscillating component, etc.

If at all frequencies the vector $\Pi_1(j\omega)\,\Pi_3(j\omega)$ is in the lower half-plane, then when forming the additional vector $\Delta(j\omega)$ there are various possibilities of choosing transfer function $B(j\omega)$.

The parallel circuit may be rigid: $B(j\omega) = B$; in this case the subsidiary vector $\Delta(j\omega)$ ensures the drop of the system's aggregate PAC and it suffices to choose in the required frequency band a large gain of the parallel branch in order to warrant the stability of the closed automatic control system. For a more favorable effect on the PAC W_1 the subsidiary vector $\Delta(j\omega)$ must in the frequency band close to the natural frequency of the system's undamped oscillations be in the fourth quadrant.

The parallel circuit must give a phase lead if the hodograph $\Pi_1(j\omega)\,\Pi_3(j\omega)$ passes into the third quadrant at an undesirable frequency band, i.e., $B(p)$ must contain differentiating components.

Only very rarely does the parallel circuit yield a phase lag resulting from the insertion into it of integrating and aperiodic components, if the vector $\Pi_1(j\omega)\,\Pi_3(j\omega)$ has itself a small lag in the required frequency band.

The parallel circuit does not cover all the operator

components of the system. In this case only the system's amplifying elements are covered by the direct circuit, i.e., $\Pi_2(j\omega) = \overline{\Pi}_2$, and in a particular case the coefficient Π_2 may also be equal to unity. Then the subsidiary vector becomes equal to $W_1(j\omega)B(j\omega)$. If we bear in mind that in relatively complex automatic control systems the FAC of the direct circuit $W_1(j\omega)$ has a considerable lag then, in order to form the subsidiary vector $\Pi_4(j\omega) = W_1(j\omega)B(j\omega)$ close to the real positive semiaxis or situated in the fourth quadrant, vector $B(j\omega)$ must have a considerable lead, i.e., differentiating elements must be inserted in the parallel branch.

All of the recommendations relative to the additional vector $\Pi_4(j\omega)$ remain in force also for the given case, but their realization is studied more conveniently if we proceed from the block diagram shown in Fig. 11-15. In that diagram with $\Pi_2 = 1$ or $\Pi_2 = $ const and by utilizing differentiating elements as $B(p)$, the entire right-hand side of the system from the node to the adder may be regarded as one forcing element. The deformation of the FAC $W_1(j\omega)$ is conveniently regarded as the result of inserting in the control system's direct circuit of a subsidiary forcing element (an element with a derivative).

We denote the transfer function of the forcing element as

$$K(p) = 1 + \frac{B(p)}{\Pi_2} = k(1 + 2\xi\tau p + \tau^2 p^2);$$

then the new FAC $W_2(j\omega)$ is derived from the old $W_1(j\omega)$

by multiplying it by the correction factor $K(j\omega)$:

$$W_2(j\omega) = W_1(j\omega) K(j\omega).$$

As already noted, the simplest way of investigating the PAC deformation from multiplication is with the aid of logarithmic frequency-response characteristics.

In Chapter 4, Fig. 4-16 and Table 4-2, are given logarithmic amplitude and phase characteristics of ideal forcing elements of first and second order. First-order elements yield a phase lead up to 90^0, and second-order elements up to 180^0 although at the assigned frequency it is actually possible to obtain considerably smaller terms of the PAC W_1 in the positive direction.

In ideal forcing elements of first order we add to the decibel -log-frequency of the control system's direct circuit the asymptotic broken characteristic of the component; to the phase characteristic we add the component's phase traced out following a pattern.

For real first-order forcing elements with the transfer function

$$K(p) = \frac{T_1 p + 1}{T_1 p + 1}, \text{ where } T_1 > T_2,$$

the logarithmic characteristics coincide with the characteristics of Fig. 11-14. It is interesting to note here that if characteristics 3 of Fig. 4-14 coincide with the characteristics of the aperiodic part of the real forcing element $1/(T_2 p + 1)$, and characteristics 2 are inverse with respect to the actually forcing part $1 + T_1 p$, then the insertion into the system of an element with such characteristics is equivalent to the —

899

replacement of one aperiodic element by another one
with a smaller constant of time. This was discussed
under No.5 of the present Section.

For the ideal and real forcing element of second
order we use their logarithmic characteristics obtained
from the data in Chapter 8 and add it to the basic
characteristics of the control system's direct circuit
in order to obtain the desired result.

The general principle of introducing phase lead
was already shown in diagram 11-18, c.

Parallel circuits increasing the accuracy of forced
motion. It was noted in Chapter 10 that insertion into
the main path of a control system of integrating com-
ponents eliminates the static error in the case of one
component, the rate error in the case of two components,
etc. This holds also true if the integrating component
is inserted into the parallel circuit.
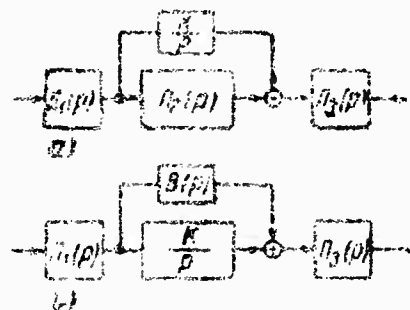
Fig. 11-18. Integrating coparallel circuit.

Figure 11-18,a shows an integrating component

connected in parallel with a group of elements of the direct circuit with the transfer function $\Pi_2(p)$. Such an insertion is occasionally called _forwarding the integral_. We can easily note that the general transfer function of the new open system

$$W_2(p) = \Pi_1(p)\left[\Pi_2(p) + \frac{K}{p}\right]\Pi_3(p)$$

after reducing all the terms to a common denominator has a zero pole, i.e., the system as a whole becomes astatic. This property is noticeable also without mathematical transformations. Indeed, with $p \to 0$ it suffices that one term of the transfer function, namely, K/p, tend to infinity and that the power transfer function also approach infinity. This fact determines its astatic properties. It is assumed that the system is comprised in the classes of systems investigated and that its transfer function, as well as the principle part of its $\Pi_1(p)\Pi_3(p)$ have no differentiating properties, i.e., transmit a constant signal.

From the viewpoint of raising the stability, the transfer forward of the integral is favorable only if the vectors $\Pi_1(j\omega)\Pi_3(j\omega)$ are located in the range of "dangerous" frequencies within the fourth quadrant when the aggregate subsidiary vector

$$\Pi(j\omega) = \frac{\Pi_1(j\omega)\,K_1\Pi_3(j\omega)}{j\omega}$$

remains in the lower half-plane. For complex PAC these recommendations must be made more precise.

If the integrating component connected in parallel

with any portion of the direct circuit ensures the creation of an astatic system, then the following corollary also holds true: if in an astatic automatic control system the integrating component is covered by a direct parallel circuit, then the astatic properties of the control system are not disrupted. Thus, in diagram b of the same figure the transfer function $S(p)$ can be chosen within a sufficiently wide range without restrictions as to static accuracy.

Parallel connection of differentiating elements can be easily investigated from the viewpoint of accuracy if the circuit is reduced to a forcing circuit by structural methods. As was established in Chapter 10, a correctly computed forcing may cancel all the terms in an error series except the first one. For static systems and systems with first-order astaticism an exact compensation of higher-order terms of the error series simultaneously solves also the problem of the stability of a closed automatic control system since forcing removes the inertness from a number of elements in the direct path transforming in the ideal case a static system into a system of zero order, and a system with first-order astaticism into a first-order system, which are doubtless stable with positive coefficients.

For systems with second-order astaticism the ideal compensation of higher order terms of the error series leads the closed system to a resonance component transfer function, and stability can be ensured only by additional forcings (besides those already used) to remove the error

components.

Thus, for stabilization by means of forcing the requirements of accuracy and stability are not in contradiction, but, on the contrary, are solved simultaneously.

This stabilization method, however, should not be overrated. Ideal forcing makes the system excessively "rigid" by forcing it to operate under great overloads. Moreover, the differentiating elements contained in the parallel branches increase considerably the amplitude of high-frequency disturbances whenever they occur under actual service conditions (see Chapters 10 and 12).

5. Feedback Insertion

Degenerative feedbacks are highly efficient means for increasing stability. To formulate the recommendations as to where and what kind of feedback to apply to elements of a direct circuit, we investigate a sufficiently general case shown in Fig. 11-19. Here, as in the preceding examples, the direct circuit of an automatic control system with transfer function W_1 is divided into three cascade-connected groups of elements with transfer functions $\Pi_1(p)$, $\Pi_2(p)$ and $\Pi_3(p)$. Feedback is applied to the element with the transfer function $\Pi_2(p)$. In the system this element is the second on the signal's path but since in a cascade system the position of the elements may be changed without changing the transfer function, the conclusions obtained hold for any point where the feedback is applied.

outlines is found to lack clearness at first.

The influence of feedback will become more obvious if we proceed to investigate inverse characteristics. Indeed, we have for them from formula (11-41)

$$\frac{1}{W_2(j\omega)} = \frac{1}{W_1(j\omega)}[1 + \Pi_2(j\omega) H(j\omega)] =$$
$$= \frac{1}{W_1(j\omega)} + \frac{H(j\omega)}{\Pi_1(j\omega)\Pi_2(j\omega)}. \qquad (11\text{-}42)$$

Thus, the initial inverse PAC of an open control system shifts, if feedback is applied, by the magnitude of the ratio of feedback vectors to the parts in the circuit not covered by feedback.

Which shift of the inverse characteristic should then be considered favorable from the viewpoint of attaining stability?

To answer this question we investigate one of the standard inverse PAC of the direct circuit $1/W_1(j\omega)$ corresponding to an unsteady closed automatic control system, as shown in Fig. 11-20. If the basic PAC of an unsteady system enclosed the point -1, j0, then the inverse PAC of an unsteady system does, on the contrary, not enclose this point and to ensure stability we must deform the old inverse PAC so as to have the new inverse PAC encompass this point, i.e., in both cases the point -1, j0 has to pass into the unhatched area.

Thus, in a band of frequencies close to that of the natural oscillations of the system, the subsidiary vector $\Delta(j\omega) = H(j\omega)/\Pi_1(j\omega)\Pi_2(j\omega)$ must be in the left-hand half-plane (in the second or third quadrant). For PAC close to the characteristics shown

in the Figure the most favorable quadrant is found to
be the second one.

The effectiveness of various types of feedback
$H(p)$ depends to a great extent on the transfer function
of elements $\Pi_1(p)\Pi_3(p)$ not covered by the feedback.
This must be borne in mind when investigating into this
problem.

Follow-up. The application of degenerative follow-up
to individual components and elements was investigated
in Chapters 5-7. We remind the reader that degenerative
follow-up reduced the constant of time of aperiodic com-
ponents and simultaneously reduced the gain, transformed
astatic components into static ones, and so on.
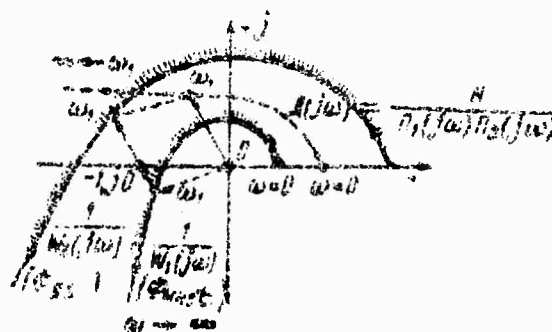
Fig. 11-20. Passage of the inverse PAC into the stability
region on account of feedback vector

As already noted, all these measures are conveniently
investigated with the aid of logarithmic frequency-response
characteristics. In many cases they ensure stability on
account of a reduced phase lag, a partial decrease of the
gain, a reduced number of integrating elements, etc.

All this can be successfully analyzed on the direct
PAC or its logarithmic component.

Inverse PAC permit a stricter determination of the
effectiveness of degenerative follow-ups depending on
the transfer function of the components not covered by
it.

With a zero-order function $\Pi_1(p)\Pi_3(p)$, when the
follow-up does not cover the amplifying components alone,
the subsidiary vector $H/\Pi_1\Pi_6$ is real and positive and,
hence, the degenerative follow-up displaces the inverse
PAC to the right, which is unfavorable for the stability
of most systems. This can be readily determined if we
consider that the direct circuit is entirely enclosed by
the degenerative follow-up; by adding a second follow-up
to it increases the gain of the system and, if the system
was unstable, this, as a rule, makes things even worse. An
exception are systems unstable in the open state, with
high-order astaticism ($\nu = 3$) or systems with rostral
PAC where occasionally it is expedient to increase the
gain within certain limits.

If we change the sign of coefficient H, then the
component -H placed in the degenerative feedback circuit
forms a positive feedback. In so doing, vector Δ receives
the required displacement to the left, but the positive
follow-up disrupts the relations in the fundamental de-
generative follow-up of the control system. In fact, in
the reproducing system $K_{fb} = 1$, after application of
positive feedback $K'_{fb} = 1 - \dfrac{H}{\Pi_1\Pi_3} = \dfrac{\Pi_1\Pi_3 - H}{\Pi_1\Pi_3}$
is transformed and the transmission number of the control

907

system in a steady state changes:

$1/X'_{cm} = \Pi_1 \Pi_3/(\Pi_1 \Pi_3 - H)$. This is inadmissible. With a mutual compensation of components 1 and $H/\Pi_1 \Pi_3$ the control system becomes open, i.e., in a number of cases it becomes neutral ($\nu > 0$) or unsteady ($r_\nu > 0$).

With a first-order function $\Pi_1 \Pi_3(p)$ the inverse characteristic $H/\Pi_1 \Pi_3(j\omega)$ is located in the first quadrant and the degenerative follow-up which displaces the inverse PAC upward and to the right is ineffective for common systems.

With a second-order function $\Pi_1 \Pi_3$ its inverse characteristic $H/\Pi_1(j\omega)\Pi_3(j\omega)$ is in the first and second quadrants, as shown by the dashed line in Fig. 11-20. If the critical frequencies occur in the left branch of the PAC $1/\Pi_1(j\omega)\Pi_3(j\omega)$, then the degenerative follow-up operates effectively. In the same figure as an example is shown an inverse PAC of the direct circuit of a static third-order system $1/W_1(j\omega)$ unstable in the closed state. If the degenerative follow-up covers only one aperiodic component, i.e., a first-order component, then the remaining components will be of second order. Their inverse characteristic is also shown by a dashed line in Fig. 11-20. With a gain of feedback elements $H = 1$ summation of the characteristics $1/W_1(j\omega)$ and $H/\Pi_1(j\omega)\Pi_3(j\omega)$ yields the characteristic $1/W_2(j\omega)$ which corresponds to a control system with a specific stability margin. The gain required by the feedback circuit can be established by the modulus of the

additional vector which passes through the point -1, j0, and changes in accordance with the gain of the feedback circuit. A minimum gain corresponds to the displacement of the PAC exactly to the point -1, j0 at any frequency ω_1, i.e., to a shift of the system on the boundary of stability; any further increase of the gain in the feedback circuit creates the margin desired.

<u>With higher orders of function</u> $\Pi_1(j\omega) \Pi_3(j\omega)$ coverage of the remaining components by the follow-up becomes ineffective, since the subsidiary vector withdraws to the lower half-plane.

<u>Flexible degenerative feedback.</u> A degenerative first-derivative feedback encompassing the entire system except the amplifying components is effective only for systems with an inverse PAC of a specific shape. In fact, under the conditions mentioned, the subsidiary vector is $\Pi_1(j\omega) = j\omega\tau / \Pi_1 \Pi_2$ and displaces the inverse PAC only upward. This can ensure stability only for inverse PAC whose real component passes left of the point -1, j0, i.e., on condition that

$$\left| \mathrm{Re}\, \frac{1}{W_1(j\omega)} \right|_{min} < -1.$$

Figure 11-21 shows such a system where the inverse characteristic of the direct circuit passes left of the point -1, j0 and stability is warranted by a rising characteristic. The gain of the flexible negative feedback circuit τ sec required for attaining the stability boundary is determined by the vector modulus $j\omega_1\tau / \Pi_1 \Pi_3$ at a
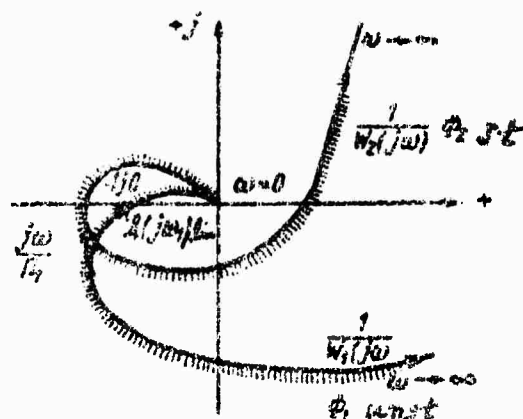
Fig. 11-21.   Effective stabilization of first-derivative
negative feedback

frequency ω_1 at which the inverse PAC passes through the
point -1, j0.   A gain greater than limit ensures the
stability margin desired.

The flexible degenerative feedback network becomes
more effective if we eliminate it from the circuit of
the aperiodic element.   In this case $\Pi_1 \Pi_3 (j\omega) \approx$
$K/(1 + j\omega T_1)$, the additional vector equals
$j\omega \tau (1 + j\omega T_1)$ and its greater part is located in the
second quadrant, acting effectively in accordance with
the case shown in Fig. 11-20.

With non-encompassed elements of a higher order the
derivative feedback leads the subsidiary vector into the
lower half-plane and stability is not attained.

Second-derivative negative feedback. When a second-
derivative negative feedback encompasses all the operator
elements of the direct circuit, the subsidiary vector
becomes equal to $-\tau^2 \omega^2 / \Pi_1 \Pi_3$, i.e., it shifts the
entire inverse characteristic to the left.

This shift is quite favorable for attaining stability, hence second-derivative feedback is a powerful stabilizer with the aid of which we can virtually stabilize any unstable system after properly selecting the required circuit gain τ^k of the flexible degenerative feedback circuit.

The effectiveness of second-derivative degenerative feedbacks drops and is reduced to zero if it does not cover all of the operator elements, when because of the transfer function $1/\Pi_1(j\omega)\Pi_3(j\omega)$ the subsidiary vector is led into the lower half-plane.

<u>Effect of feedback circuits on the accuracy of forced motion.</u> As a rule all feedback circuits increase forced motion errors. This can be strictly proved analytically by determining the error coefficients of the closed system transfer function for various forms of feedback circuits. Here we shall confine ourselves to qualitatively evaluating the errors on the basis of operating circuits.
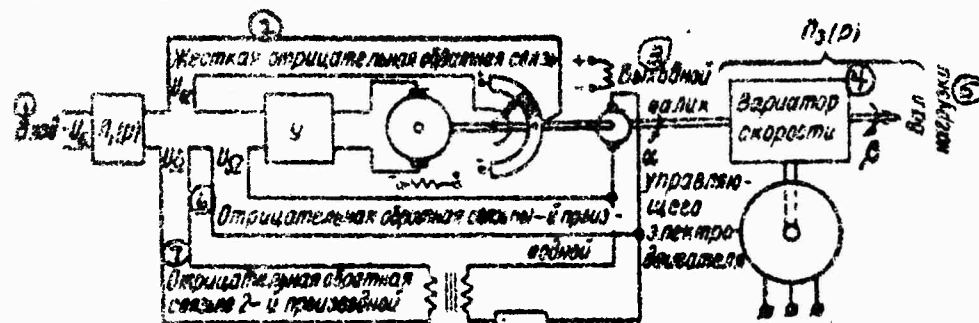
Fig. 11-22. Practical methods for applying stabilizing feedbacks. Key: 1) input; 2) degenerative follow-up; 3) output shaft of control electric motor; 4) speed variator; 5) load shaft; 6) first-derivative degenerative feedback; 7) second-derivative degenerative feedback.

Figure 11-82 shows various methods of applying follow-up circuits and flexible feedback circuits to an electromechanical system. We investigate the direct path of a system whose input is given by a minus error signal $-U_g$ and the output is given by the deflection angle of the shaft of the actuating mechanism; the degenerative feedback and subsidiary elements of the closed control system are not shown in the diagram. Feedback covers a specific section of the direct circuit from the output shaft which controls the speed variator of the electric motor to the amplifier input. Elements with transfer function $\Pi_1(p)/\Pi_g(p)$ are not encompassed.

Degenerative follow-up is achieved in the form of voltage taken from the potentiometer, proportional to the deflection angle of the output shaft $U_\alpha = K_\alpha^U \alpha$ and fed to the amplifier input. The amplification factor of the follow-up circuit is a scale factor which establishes the proportionality between the angle and the voltage K_α^U v/rad.

We can easily see that if to overcome the load resistance moment prior to the insertion of the feedback circuit a certain error signal was required, then after the insertion of the feedback circuit the error signal must be increased in order to eliminate the feedback voltage U_α.

If the transfer function of the portion of the direct circuit prior to being encompassed by the feedback circuit had the form $U(p)/pV(p)$, then after

encompassing by the degenerative follow-up circuit the new transfer function is

$$\frac{\dfrac{U(p)}{pV(p)}}{1+\dfrac{K_a^U U(p)}{pV(p)}}=\frac{U(p)}{pV(p)+K_a^U}.$$

This result shows that the astatic system has become static, i.e., a new error (staticism) has arisen which did not exist earlier. If the system was already static then, after insertion of the follow-up circuit, its staticism increases.

A flexible degenerative first-derivative feedback is achieved in the diagram investigated by installing a techogenerator producing a voltage proportional to the rotational speed of the control electric motor $U_\Omega = T\Omega$. Consequently, operation of the control electric motor requires in addition to the error signal needed to overcome the resistance moment in the variator, an additional error voltage value to cover the voltage of the tachogenerator.

Thus, the regulating system of the control motor has an increased rate error.

The flexible second-derivative degenerative feedback is achieved in the given circuit by feeding voltage from the tachogenerator to the primary coil of the transformer, while emf of the secondary coil is fed to the amplifier input. The magnitude of secondary emf with constant acceleration of the shaft of the control electric motor is proportional to that acceleration: $U = \mathcal{T}^2(d^2/dt^2)$. Consequently, with

913

equally accelerated motion at the amplifier input,
besides all the other error signal components we also
need an additional error voltage component to compensate
the transformer emf. Thus, the system investigated has
an increased error from the acceleration of the control
electric motor. Now, if we consider the OTF of the
variator $U_3(p)/pv_3(p) = \Pi_3(p)$, then in the total system
the order of astaticism increases by unity as compared
to the regulating system of the control electric motor
with corresponding error variation.

Feedback engineering. Feedback circuits are joined
with the output of usually sufficiently powerful auto-
matic control systems. The signal is fed to the input
of the direct circuit amplifier. Hence feedback en-
gineering is considerably more advantageous than direct
circuit engineering.

8. Structural Method for a Total Solution of the
   Stabilization Problem

If a stabilizing circuit is applied in a fashion
more complex than those investigated under No. 3-5 above,
the new circuit can always be reduced to one of the
standard ones by the method of structural transformations.

Designers have wide possibilities for choosing a
new stabilizing circuit or changing the properties of
any component in the existing circuits proceeding from
the condition of measuring by transmitters the inter-
mediate controlled values and from the conditions for
their summation required for the application of circuits

Let there be assigned a multicircuit system whose block diagram is shown in Fig. 11-10. It is planned to solve the correction problem with respect to the term H_1.

We open the branch containing H_1 and expand the block diagram to the form shown in Fig. 11-23 which is more convenient for subsequent transformations. The minus sign of H_1 refers to the feedback shown in the Figure by a dashed line.
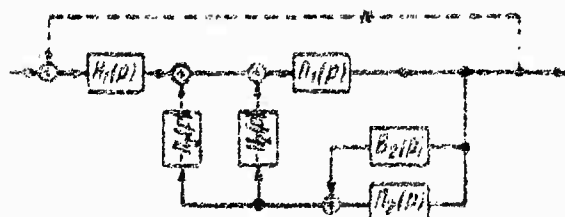
Fig. 11-23. Structural transformations of a complex stabilizing circuit shown in Fig. 11-18 into a cascade circuit.

The transfer function of the open system is

$$C(p) = H_1(p) \times$$
$$\times \frac{\Pi_1(p)}{1 + \Pi_1(p)[\Pi_2(p) + \Pi_2(p)][\Pi_3(p) + \Pi_3(p)]}.$$

Insofar as the transfer function of the variable element is comprised in the transfer function of the open system as a cofactor, after constructing the FAC of the open system $C(j\omega)$ any further correction

can be undertaken according to the methods set forth in No. 3.

Let us note that the amplitude margin obtained by the PAC $G(j\omega)$ shows permissible changes in the coefficient of the entire system including the changing element. The same can be said about the available phase shift.

It must be pointed out that after unlocking any circuit we can find the gain margin for each component of the system in a like fashion.

If the parameters of the control system's elements are unstable, calculation of phase and amplitude margins for various unlocking conditions of the block diagram yields fairly complete information as to the margins available in the system and the sections critical from the viewpoint of stability loss.

Application of the structural method for solving the stabilization problem makes it possible to unify calculations and to do away with the heterogeneity between graphical structures and analytical calculations observed in the methods expounded earlier.

In the given Section we investigated both types of stabilizing devices which basically affect advantageously the systems with sufficiently simple PAC. For systems with more complex, especially rostral, PAC the investigation method remains the same but of course, the conclusions may be completely opposite from the viewpoint of selecting concrete feedback elements.

The effect of circuits on the accuracy holds basically true for systems with PAC of any type, and increased errors should be fought by one of the methods expounded in Chapter 10. Regenerative feedback circuits, of course, increase the accuracy and can even be applied in individual special cases but their effect is unfavorable as regards stabilization; they increase the constants of time of aperiodic elements, occasionally increase the order of astaticism of the system and create inner quasistatic elements in the direct circuits; in the latter case the question of the desirability of shifting the inverse characteristic is reappraised in accordance with the deflection angle of the N-vector required by stability conditions.

We investigate as an example the multicircuit system shown in Fig. 9-1, e which was analyzed for coupling coefficients in the form of trigonometric functions of angle γ in Section 11-5.

We write the transfer function of the system unlocked along the coupling circuit, taking the constants of time and the gains to be identical for both interlocking systems:

$$W(p) = \frac{K^2 \sin^2 \gamma}{(Tp^2 + p + K \cos \gamma)^2} .$$

We determine the frequency at which the PAC intersects the negative real semiaxis from the condition of equality to zero of the real part of the square root from the denominator

$$-T\omega_c^2 + K\cos\gamma = 0; \qquad x_R^2 = \frac{K\cos\gamma}{T}.$$

At this frequency the PAC is real and amounts to

$$W'(j\omega_R) = -\frac{K^3\sin^2\gamma}{\dfrac{K\cos\gamma}{T}} = -KT\sin\gamma\,\mathrm{tg}\gamma.$$

With respect to the boundary of stability $W(j\omega_R) = 1$ we have an amplitude margin

$$L(\omega_R) = -20\lg KT\sin\gamma\,\mathrm{tg}\gamma.$$

Similar results were obtained also in Section 11-5 but here we determine more rapidly and clearly the possibilities of the system or the measures necessary especially for the interrelationship loop. If the breaking of the closed system were effected at any local circuit, we could see the restrictions on the parameters of the inner couplings of each interconnected control system, and so on.

11-12. Analytical and Frequency Methods for Constructing Stability Regions

At the beginning of the foregoing Section the moving away from the stability boundary was evaluated in the form of two generalized parameters, viz., phase margin and amplitude margin. If we evaluate the margin by more concrete control system parameters comprised directly in the coefficients of the equations of coupling, then the preceding method ceases to be clear

and we require a more precise definition of the role played by the parameters under study.

In low-order equations the definition of individual parameters is performed quite easily.

Let us investigate, .e.g., a third-order equation. Stability can be evaluated according to the Vyshnegradskiv criterion which establishes the required relations between the coefficients of the characteristic equation of the closed system (11-5). On the basis of this criterion we can easily show that to bring this system into the stability region we must increase the product of the mean coefficients of the characteristic equation $\mu_1 \mu_2$ and reduce the product of the limit coefficients $\mu_0 \mu_3$.

It is expedient to give the concept of stability margin or the moving away from the stability boundary determined by Eq.(11-5) a relative evaluation:

$$x = 20 \lg \frac{\mu_0 \mu_3}{\mu_1 \mu_2},\qquad(11\text{-}43)$$

where x is the coefficient product margin.

Indeed, according to Eq.(11-4) with a ratio of coefficients $\mu_0 \mu_3$ and $\mu_1 \mu_2$ equalling unity the system is on the boundary of stability and the margin equals zero, and the smaller this coefficient ratio, the greater the "remoteness" from the stability boundary expressed in negative decibels.

If we evaluate the change of any one coefficient, e.g., μ_0 (its magnitude not affecting that of the

[remaining coefficients), then on the basis of Eq.(11-4)
we can easily find the critical value of this coefficient
μ_5 lim at which the system finds itself on the boundary
of stability;

$$\mu_{6,lim} = \frac{\mu_1 \mu_2}{\mu_3} .$$

Obviously the moving away of the actual value of
the coefficient from the critical value (towards the
decreasing side) will favorably affect the increase in
stability margin for this coefficient and it may be
given the following evaluation

$$x_0 = 20 \lg \frac{\mu_6}{\mu_6 \, lim} \quad db,$$ (11-44)

where x_0 is the margin for coefficient μ_6.

The coefficients of the characteristic equation
depend upon the technical parameters of the system.
In particular, for the system shown in Fig. 11-4 with
the characteristic equation

$$mT^3 p^3 + T(1+m) p^2 + p + K_{-1} = 0$$

the equation coefficient μ_0 is equal to the gain of
the open system K_{-1} and is linked with the system's
other parameters m and T for the stability boundary by
the formula (11-8).

We can easily see that if we introduce the loga-
rithmic evaluation of the margin for coefficient
$\mu_0 = K_{-1}$ (11-44) it coincides with the frequency
evaluation (11-33,c) for the amplitude margin.

The concept of a stability region for one parameter
is graphically shown by the position of a point charac-

terizing the value K_{lim} on the line μ_0. Figure 11-24,a
shows the line μ_0 and on it is marked the point K_{lim}.
The line segment $0 - K_{lim}$ is the stability region, and
segment $K_{lim} - \infty$ is the instability region on the line
investigated.
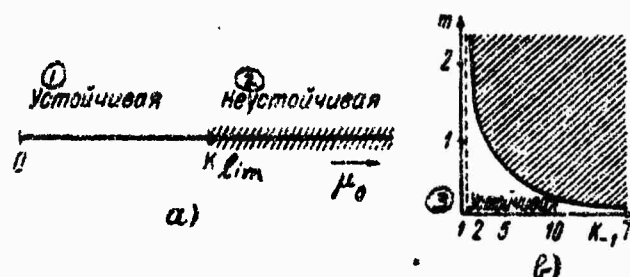
Fig. 11-24.   Stability regions for one (a) and two (b)
              parameters
Key: 1) stable; 2) unstable; 3) stable.

Let us now investigate the structure of the stability
region for two parameters.

In the third-order equation given above these
parameters investigated will be, in the first place,
again the gain K_{-1} and, in the second place, the ratio
of time constants m.   The analytic relation between
them is defined by the boundary of stability (11-8 a)
and is reduced to the form

$$K_{-1}T - \frac{1+m}{m} = 0.$$

By assigning various values to m with fixed T we
can derive from this equation the corresponding values
of K_{-1}. The curve of this relation is plotted in
Fig. 11-24,b where for the generality of the curve the

product $K_{-1}T$ is plotted against the abscissa.

The curve obtained divides the parameter plane into two regions, an unstable one (hatched) and a stable one (without hatching). The concrete values of the parameters m and K_{-1} of the real system in the parameter plane yield the image point: by its distance from the boundary of stability we can judge of the system's stability margin.

Analytical calculations relative to the construction of stability regions are in a number of cases facilitated by the introduction of an intermediate parameter. Thus, e.g., if we define the boundary of stability according to Mikhaylov, then such intermediate parameter will be the frequency.

Let us now proceed to expounding the frequency methods based upon the generalized method of D-partioning according to Yu. I. Neymark /Bibl. 6/.

We investigate the relatively complex case of constructing stability regions by two parameters, ξ and η, which enter into the characteristic equation with the first terms in the form of cofactors with operator polynomials of any order

$$M(p) = \xi Q(p) + \eta P(p) + R(p) = 0. \qquad (11\text{-}45)$$

We write the stability boundary equations:

$$X_M(j\omega) = a(\omega)\,\xi + b(\omega)\,\eta + r(\omega) = 0; \\ Y_M(j\omega) = c(\omega)\,\xi + d(\omega)\,\eta + s(\omega) = 0. \qquad (11\text{-}46)$$

922

In separating the real part from the imaginary one, parameters ξ and η remain, as before, in the form of linear cofactors although the ω-polynomials have another form, viz., a, b, c, d, r, s.

The system of equations thus obtained can be solved with respect to ξ and η:

$$\xi = - \frac{\begin{vmatrix} r(\omega) & b(\omega) \\ s(\omega) & d(\omega) \end{vmatrix}}{\begin{vmatrix} a(\omega) & b(\omega) \\ c(\omega) & d(\omega) \end{vmatrix}};$$

$$\eta = - \frac{\begin{vmatrix} a(\omega) & r(\omega) \\ c(\omega) & s(\omega) \end{vmatrix}}{\begin{vmatrix} a(\omega) & b(\omega) \\ c(\omega) & d(\omega) \end{vmatrix}}. \qquad (11\text{-}47)$$

All the remaining parameters of the system, except ξ and η, are taken to be defined and invariable, hence the formulas obtained yield a solution in terms of the frequency function. If the functional frequency relationships are relatively simple, then frequency is eliminated from both solutions and we obtain a stability boundary equation in the plane of parameters ξ and η:

$$f(\xi, \eta) = 0. \qquad (11\text{-}48)$$

Elimination of frequency is optional. We can by assigning various frequency values obtain from both formulas (11-47) bounded values of parameters ξ and η, and construct graph (11-48) in accordance with them.

As an example let us repeat the investigation of the stability regions of a system examined above $(K_{-1} = \xi; \; m = \eta)$. For it the characteristic Mikhaylov vector has the following expression:

$$M(j\omega) = mT^3 (j\omega)^3 + T(1 + m)(j\omega)^2 + j\omega + K_{-1}.$$

The real and imaginary components are

$$X_{M}(j\omega) = K_{-1} - T\omega^2(1 + m);$$
$$Y_{M}(j\omega) = \infty - mT^3\omega^3.$$

Thus, the coefficients of standard equations (11-46) amount to

$$a(\omega) = 1; \quad b(\omega) = - T\omega^2; \quad r(\omega) = - T\omega^2;$$
$$c(\omega) = 0; \quad d(\omega) = - T^3\omega^3; \quad s(\omega) = \omega.$$

In the given case, even without resorting to the solution in terms of determinants (11-17), we can immediately obtain:

$$m = \frac{1}{(\omega T)^2}; \quad K_{-1} = T\omega^2 + \frac{T\omega^3}{(\omega T)^2} = \frac{(\omega T)^2 + 1}{T}.$$

It suffices to eliminate ω from both equations to arrive at the form (11-48). Of course, the result of elimination will lead to the analytical function obtained earlier for the system investigated and plotted in Fig. 11-27,b. We shall therefore bring a circumstantial calculation without eliminating ω. To this end we must change ω and compute the adjoining values for m and K_{-1}. This has been done in Table 11-2, where, for convenience, ωT has been taken as the input value.

If according to the last two columns of the Table we trace a curve, it will coincide with that shown in Fig. 11-27,b since we are dealing with one and the same system.

In the examples studied the analytical relation

Table 11-2

Calculation of the Boundary of Stability for a Third-Order System

ωT	$K_{-1}T$	m
0	1	∞
1	2	1
2	5	0,25
3	10	0,11
5	26	0,04
10	101	0,01

between K_{-1} and m is established without difficulty, and we can calculate at once only the two last columns of the Table, but for more complex systems the introduction of the intermediate parameter ω is sometimes absolutely compulsory.

Above we expounded the method for constructing the boundary of stability. To establish which region belongs to stable systems and which to unstable ones we require only one check for the system's stability at any one point interior to the region.

Frequency methods. Frequency methods for calculating stability regions are based upon the construction in a complex plane of function hodographs obtained from stability boundary equations according to Mikhaylov, and on the application to these hodographs of appropriate evaluations taken from frequency stability

criteria.
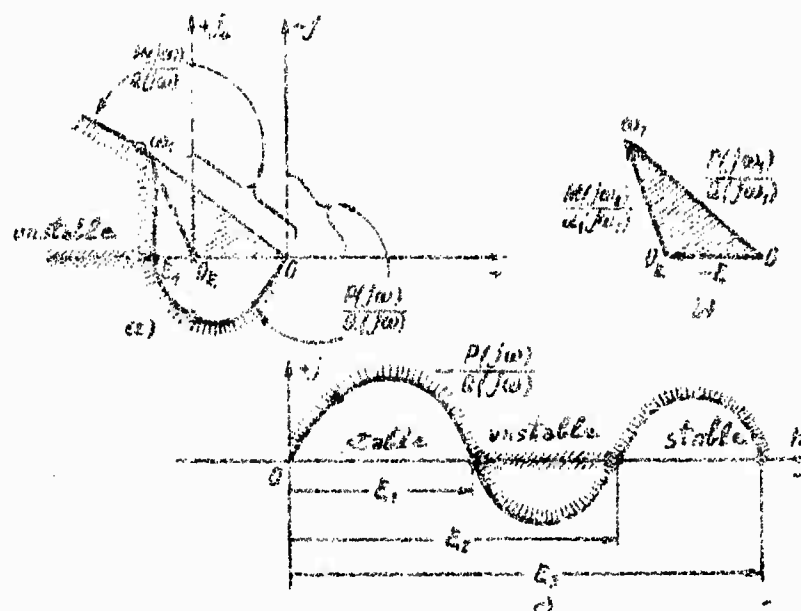
Fig. 11-25. Determination of the stability region for one parameter by the frequency method

Tracing of a hodograph for determining the stability region for one parameter. Let there be assigned a characteristic Mikhaylov vector the equation of which comprises the varying parameter ξ in the first term as a cofactor with a part of complex terms:

$$M(j\omega) = P(j\omega) + \xi Q(j\omega).$$

We could construct a series of Mikhaylov hodographs for various partial values of ξ and determine by the deflection angle at which values of ξ the system is stable; thus we would obviously also determine the stability region, but this method is evidently cumbersome.

926

To reduce the volume of constructions we transform the characteristic vector and divide both parts of the preceding equation by the cofactor with ξ:

$$\frac{M(j\omega)}{Q(j\omega)} = \xi + \frac{P(j\omega)}{Q(j\omega)}. \qquad (11\text{-}49)$$

Now we trace out in a complex plane the hodograph of function P/Q as shown, e.g., in Fig. 11-25,a; it does not depend upon ξ, hence the plotting for the system investigated is performed only once.

As for the calculation of various ξ, the aggregate vector $\xi + P(j\omega)/Q(j\omega)$ is found from a hodograph already plotted by shifting the origin of coordinates to the left along the real axis by the quantity $-\xi$. This is also shown in the Figure by the general hodograph a and the vector triangle b constructed for one point ω_1.

Let us now find to what is equal the deflection angle of the plotted hodograph $P(j\omega)/Q(j\omega)$ with the shifted origin of coordinates O_ξ, i.e., with respect to the end of segment $-\xi$.

We denote this angle by φ_ξ, and note from the drawing that it is equal to the deflection angle of the vector $M(j\omega)/Q(j\omega)$. This vector contains in the numerator the M-vector with the deflection angle φ_M, and in the denominator it has the complex function $Q(j\omega)$ whose deflection angle we denote by $\varphi_q = q(\pi/2)$. We can now write the relation sought:

$$\varphi_\xi = \varphi_M - \varphi_q. \qquad (11\text{-}50)$$

For values of ξ in the stability region the deflection angle of vector M/Q must be

$$\varphi_{i_{35}} = -\frac{\pi}{2} \cdot (n-q).$$

(11-51)

Now there remains, by shifting the point O_ξ, i.e., by changing ξ, to check the correspondence between the deflection angles obtained and the stable angle (11-51).

Parameter ξ is the quantitative expression of any technical factor of an operating system, hence it is always real; also, it is always taken positive ; should there appear a minus sign in front of $\xi Q(j\omega)$, we shall always refer it to the cofactor $Q(j\omega)$. Thus, the new origin of coordinates will slide along the negative real semiaxis. The stability conditions (deflection angle) remain obviously invaried as long as the origin of the moving coordinate system does not coincide with the point of intersection of the real axis with the hodograph $M(j\omega)/Q(j\omega)$.

The value of ξ will in this case obviously correspond to the stability boundary since with $M(j\Omega)/Q(j\Omega) = 0$ and $Q(j\Omega) \neq \omega$ we obtain $M(j\Omega) = 0$.

Thus, hodograph $P(j\omega)/Q(j\omega)$ divides the line ξ, i.e., the negative real semiaxis into two regions. In order to determine which of them is stable we have to compute by the above formula the deflection angle of hodograph $P(j\omega)/Q(j\omega)$ with respect to the point O_ξ located in any one region.

As an example we carry out a circumstantial investigation of the third-order system with parameter

m examined above. The characteristic polynomial is in this case expediently written

$$P(j\omega) + \xi Q(j\omega) =$$
$$= -T\omega^2 + j\omega + K_{-1} - mT\omega^2(jT\omega + 1).$$

Here
$$P(j\omega) = K_{-1} - T\omega^2 + j\omega;$$
$$Q(j\omega) = -T\omega^2(1 + j\omega T);$$
$$\xi = m.$$

we form the operator function

$$\frac{P(p)}{Q(p)} = \frac{Tp^2 + p + K_{-1}}{Tp^2(Tp + 1)}$$

and the complex vector

$$\frac{P(j\omega)}{Q(j\omega)} = \frac{K_{-1} - \omega^2 T + j\omega}{-T\omega^2(1 + j\omega T)} .$$

corresponding to it.

The hodograph constructed according to this PAC equation approaches that shown in Fig. 11-25,a.

We now determine the deflection angle of this vector with respect to point 0, required for the stability of the automatic control system.

The polynomial $Q(p) = Tp^2(1 + Tp)$ has a zero multiple root which determines the constant component in the direction of the vectors, and only one left-hand root which actually affects the rotation of the hodograph when frequency changes. Consequently

$$\varphi_q = \frac{\pi}{2}; \quad q = 1.$$

We use formula (11-51) and bearing in mind that n = 3 we find

$$\varphi_{\xi_{ss}} = \frac{\pi}{2}(3-1) = \pi.$$

Such a deflection angle results when ξ is located right of the boundary. When ξ increases and crosses over left of the boundary, the deflection angle becomes equal to $-\widetilde{\eta}$. The difference $-2\widetilde{\eta}$ between the actual angle and the required one is evidence of the existence of two right-hand poles in the closed automatic control system. Thus, we hatch the segment of the axis from $-\infty$ to the boundary of stability on which the values of ξ yield unsteady modes of operation.

Let us note that in the given example the polynomial $Q(p)$ has no right-hand roots[1], hence the rule for hatching the hodograph of vector $M(j\omega)$ is also applicable to the hodograph of vector $M(j\omega)/Q(j\omega)$. Consequently, the deflection angles may be ignored, and after constructing the hodograph $P(j\omega)/Q(j\omega)$ we may directly apply to it the right-hand hatching which will immediately reveal the unstable part of the real axis, since when ξ passes into this region the zero points of vectors $M(j\omega)/Q(j\omega)$ and $M(j\omega)$ get into the hatched region.

Occasionally it is more expedient to construct the hodograph of vector $-(P(j\omega)/Q(j\omega))$ rather than

_____

[1] if $Q(p)$ had a right-hand root then, by developing the indeterminacy according to (11-49), we find that the rule can be infringed only if there simultaneously exists a right-hand root also in $P(p)$.

that of vector $+(P(j\omega)/Q(j\omega))$. The change in the sign does not change the direction of the vector's rotation, it merely carries all the points of the hodograph symmetrically on to the other side of the center 0. In so doing, all the preceding rules do not change and ξ is plotted against the positive side of the real axis, which appears to be clearer than plotting ξ against the negative side of the semiaxis.

Thus, construction of instability regions for one parameter amounts to plotting the hodograph of vector $-(P(j\omega)/Q(j\omega))$, as shown in Fig. 11-25,c, and hatching on the right which automatically separates out the instability regions on the real axis. There may be several such regions (see diagram c). If the polynomial $Q(j\omega)$, which is a cofactor with ξ, has right-hand roots the rule of hatching may be infringed; then the type of zones is determined by calculating the deflection angles φ_ξ.

It can be easily shown that the Nyquist criterion is the consequence of a more general frequency method of constructing a stability region for one parameter [Bibl. 6]. To do this, from the polynomials U(p) and V(p) constituting the OTF of the open system, we factor out the lower-order terms, u_0, v_0 (or v_y), form from their ratio the amplification factor $k = u_0/v_0$ and denote the polynomials normed with respect to the lowest term by $u^n_0(p)$ and $v^n_0(p)$; then we have

$$W(p) = \frac{u_0^n(p)}{\frac{1}{k} \, v_0^n(p)} = k W_0^n(p).$$

For the closed automatic control system we determine the characteristic polynomial

$$M(p) = \frac{1}{k} \, v_0^n(p) + u_0^n(p),$$

whence

$$\frac{M(p)}{v_0^n(p)} = \frac{1}{k} + W_0^n(p).$$

Suppose the graph 11-25,a does coincide with the hodograph $W_0^n(j\omega)$ of a control system.

In constructing this hodograph it will cut off on the negative real semiaxis according to Fig. 11-25,a a segment $0\,c_1$ by which we determine the boundary amplification factor

$$k_{bound} = \frac{1}{0c_1}.$$

The actual amplification factor can in the given case be taken only greater than k_{bound}. In this case the hodograph $k W_0^n(j\omega) = W(j\omega)$ will pass with respect to the point -1, j0 as this is required by the Nyquist stability criterion for $\nu = 2$.

Construction of hodographs for determining the stability region for two parameters. Again we investigate the characteristic equation (11-45). We pass to the Mikhaylov vector, and by dividing it by $Q(j\omega)$ we reduce it to the form

$$\frac{M(j\omega)}{Q(j\omega)} = \xi + \eta\frac{P(j\omega)}{Q(j\omega)} + \frac{R(j\omega)}{Q(j\omega)}. \qquad (11-52)$$

We construct the hodograph of vector $-(R(j\omega)/Q(j\omega))$ and, in the same complex plane, the hodograph of $P(j\omega)/Q(j\omega)$.

With $\eta = 1$ the beginning of vector $-(M(j\omega)/Q(j\omega))$ will be at the point O_* obtained by geometric summation of vectors $(\xi + 1)(P(j\omega)/Q(j\omega))$ and its end at the hodograph $-(R(j\omega)/Q(j\omega))$. The boundary of stability is found when the point O_* hits the hodograph $-(R(j\omega)/Q(j\omega))$.
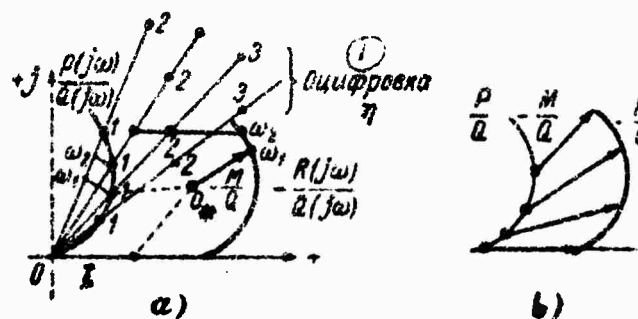
Fig. 11-26. Determination of the stability region for two parameters by the frequency method.
Key: 1) marking

Figure 11-26 shows for the general case sections of the hodograph $-(R(j\omega)/Q(j\omega))$ and $P(j\omega)/Q(j\omega)$, and for a random value of ω_1 the point O_* has been formed. The limiting values of ξ for carrying the system on the stability boundary are obtained by simply measuring the horizontal segment between the hodograph $-(R(j\omega)/Q(j\omega))$ and $P(j\omega)/Q(j\omega)$ provided that the frequencies coincide at the point where both hodographs

intersect the horizontal straight line. Of course, such
points must be found beforehand.

Thus, for one value $\eta = 1$ there can be found an
appropriate value ξ corresponding to the boundary of
stability. A change in η results in a proportional
change of all the vector radii of hodograph $P(j\omega)/Q(j\omega)$.
It is pointless to retrace this hodograph for new η,
it suffices instead to mark on the central rays the
position of the points of the changed hodograph for
integral values of η, as shown in the Figure.

Having such prepared rays with markings of η, as
well as the frequencies marked on the hodographs
$P(j\omega)/Q(j\omega)$ and $-(R(j\omega)/Q(j\omega))$, the bounded values
of parameters ξ and η corresponding to the boundary
of stability can be found in the following fashion.

From any point of hodograph $-(R(j\omega)/Q(j\omega))$ with
a certain frequency ω_2 we draw a horizontal straight
line until it intersects that ray which has the same
frequency ω_2 for hodograph $P(j\omega)/Q(j\omega)$. The length
of the segment between hodograph $-(R(j\omega)/Q(j\omega))$ and
the ray is equal to ξ; marking of the ray at the point
where it is intersected by the horizontal straight line,
determined by linear interpolation, yields the bounded
value of η.

By repeating this procedure we can accumulate the
epadic values of ξ and η by which we trace the curve of
the stability boundary in the plane of these parameters.

The character of the regions bounded by the

stability boundary curve is determined by calculating the deflection angles of the vector $M(j\omega)/Q(j\omega)$. Since the position of the point O_* changes with changing frequency, this vector has a moving origin. The character of the zone must therefore be checked for any specific point ξ, η.

The simplest procedure is to check whether the point $\xi \neq 0$, $\eta = 0$ belongs to the stable zone. In this case we simply use the formulas for the deflection angle derived for one parameter (11-51) or the rule of hatching.

Somewhat more complex is the checking of the appurtenance to the stable zone of the point $\xi = 0$, $\eta \neq 0$. If, in particular, we take $\eta = 1$ for this case, then the difference between vectors $-(R(j\omega)/Q(j\omega))$ and $P(j\omega)/Q(j\omega)$ equal to $-(M(j\omega)/Q(j\omega))$ can be seen in Fig.11-26 without additional constructions.

By tracing the deflection angle of this difference vector, as shown in Fig. 11-26 b, we establish the magnitude of the angle $\varphi_{\xi\eta} = \varphi_{01}$.

In analogy with expression (11-50) we write for this angle:

$$\varphi_{\xi\eta} = \varphi_M - \varphi_q. \tag{11-53}$$

If the point $\eta = 1$, $\xi = 0$ investigated by us falls into the stability region, then a condition analogous to (11-51)

$$\varphi_{\xi\eta\,ss} = \frac{\pi}{2}(n - q). \tag{11-54}$$

must be fulfilled.

As an example we again take the characteristic

equation investigated, which we write in the form

$$\eta\, P(p) + \xi Q(p) + R(p) =$$
$$= K_{-1} + mTp^2(Tp+1) + p(Tp+1).$$

Here

$$\eta = K_{-1};\quad P(p) = 1;\quad \xi = m;$$
$$Q(p) = Tp^2(Tp+1);\quad R(p) = p(Tp+1).$$

We write out the required polynomial relations and the complex functions corresponding to them:

$$\frac{R(p)}{Q(p)} = \frac{1}{Tp};\quad -\frac{R(j\omega)}{Q(j\omega)} = +\frac{j}{\omega T};$$

$$\frac{P(p)}{Q(p)} = \frac{1}{Tp^2(Tp+1)};\quad \frac{P(j\omega)}{Q(j\omega)} = -\frac{1}{\omega^2 T(1+j\omega T)}.$$

In Fig. 11-27 there is plotted a hodograph $(R(j\omega)/Q(j\omega))$ which coincides with the positive imaginary semiaxis, and on it the frequencies are numbered. In the second quadrant there is a hodograph $P(j\omega)/Q(j\omega)$ with its own frequency numbering. In the upper diagram, through points of hodograph P/Q corresponding to frequencies 0.3; 0.4; 0.5; 1 sec^{-1} rays have been traced on which is given the numbering $\eta = K_{-1}$. Here $K_{-1} = 1$ at the intersection of the ray with hodograph P/Q, and further the unit radius-vector is plotted along the ray for a number of times given by the numbering.

In the bottom diagram are repeated all the hodographs mentioned, with a twenty-fold magnification. This made it possible to cover also the high-frequency
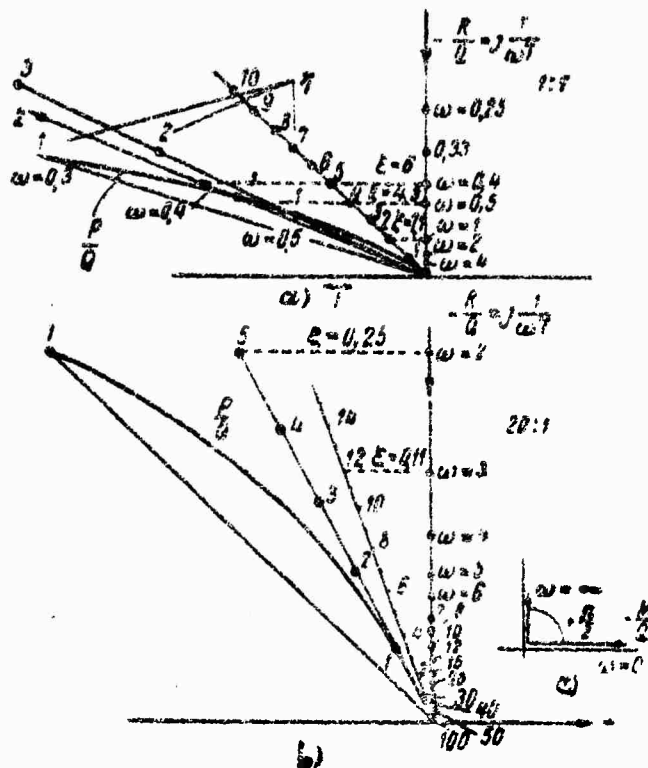
Fig. 11-27. Construction of a stability region for
two parameters in a complex plane

part. Additional rays with numbering are traced in the
bottom drawing through points of hodograph P/Q corre-
sponding to frequencies $\omega = 2$ sec^{-1} and $\omega = 3$ sec^{-1}.

Upon completion of the preparatory work we traced
horizontal dashed lines from hodograph $-(R(j\omega)/Q(j\omega)) =$
$= j/\omega T$ to the rays so that the frequencies of the rays
and the points of intersection of the horizontal straight
lines with hodograph R/Q be identical. Direct measuring
of the segments and interpolation by numbering scales
of the rays yield proportional values of ξ and η. Thus,
for frequency $\omega = 1$ we have: $m = 1$; $K_{-1} = 2$,; for $\omega = 2$
we have $m = 0.25$; $K_{-1} = 5$. We can easily see that these

937

values as well as the complementary ones shown in the
Figure, give the boundary of stability in the plane of
parameters K, m which coincides with the curve in Fig.
11-24.

Now there remains only to verify the character of
the regions.

We check the region in which the point $\eta = 1$, $\xi = 0$
lies.

In Fig. 11-27 the vector difference $-(R(j\omega)/Q(j\omega)) - (P(j\omega)/Q(j\omega))$ has the phase 0^0 with $\omega = 0$, and the
phase $+90^0$ with $\omega = \infty$; total turn $= +\Pi/2$, which is
characteristic for vector $M(j\omega)/Q(j\omega)$ of a stable
system with n = 2 (because of m = 0) and q = 1.

All the above constructions were carried out in a
complex plane. Yet, also here we can successfully apply
logarithmic characteristics and nomograms for their
transformation utilizing polynomial structures in the
form of sums of trinomials.

Final calculations by special nomograms are par-
ticularly convenient when determining the boundary of
stability for two parameters. To do this we need a
P, Q-nomogram containing a semilogarithmic rectangular
net "φ [degrees] - A [db]" (the rectilinear net in

Fig. 11-26) and a superimposed net of isolines of
real and imaginary characteristics corresponding to
the rectangular net.

The characteristics $-(R(j\omega)/Q(j\omega))$ and
$P(j\omega)/Q(j\omega)$ are plotted onto the processed rectangular

Fig. 11-28. Construction of stability region by logarithmic
             P, Q-nomogram.

net with isolines. It is borne in mind that the charac-
teristics are also obtained by means of logarithmic
nomograms.

Further, the determination of the bounded values
ξ and η is quite simple:

On the curves $-(R(j\omega)/Q(j\omega))$ and $P(j\omega)/Q(j\omega)$ we
mark the points with identical frequencies (ω_1 in the
Figure);

_ 939 _

We single out the "imaginary" isoline which passes through the point a_1 of characteristic $-(R(j\omega)/P(j\omega))$ (Im_1 in the drawing);

We measure the vertical segment between the point ω_1 on the characteristic P/Q and the singled-out "imaginary" isoline; in terms of decibels this segment is equal to one parameter η db;

We determine the numeration of the "real" isolines running through the point ω_1 on the characteristic $-(R/Q)$, and through the point obtained on the isoline Im_1 at the end of segment η. In the Figure the isolines are denoted by Re_1 and Re_2; the difference between their numberings in natural numbers yields the second parameter $\xi = Re_1 - Re_2$.

Constructions on the logarithmic net are analogous to those in Fig. 11-26; an increase in the modulus of vector R/Q by η times (Fig. 11-26) is equivalent to a shift of the characteristic P/Q by $\eta\overline{[db]}$ (Fig.11-28); Measuring of the horizontal segment ξ (Fig. 11-26) is equal also to determining the difference between the real components of vectors $-(R/Q)$ and $\eta(P/Q)$ (Fig. 11-28).

To increase the gain scale the nomogram in Fig. 4-28 is enlarged by gluing together blanks along the vertical.

11-16. Stability of Systems with Variable Parameters

For automatic control systems with variable parameters operating a limited time interval the concept of asymptotic stability is virtually useless although cases

940

can be pointed when such evaluations are applied also
to such systems.

The case of slowly changing coefficients. Suppose
the magnitude of coefficients affect the processes in
the system, whereas the rate of change of the coefficients
(and high-order derivatives) have no effect on the charac-
ter of the processes. Then the checking of automatic
control systems for asymptotic stability with fixed
(frozen) values of coefficients, especially if it is per-
formed repeatedly for a number of characteristic points
(instants of time on the work interval) virtually
guarantees the damping of the control system's intrinsic
motion even under conditions of really changing coeffi-
cients. If the control system is designed with constant
tuning of the inner circuits, it is convenient to carry
out the calculations for asymptotic stability by con-
structing stability regions for variable parameters.

Utilization of parameteric phase-amplitude characteris-
tics of closed control systems. When applying formulas
(10-73) and (10-74) for calculating noise dispersion
by integrating the square modulus of PPAC there was
specifically mentioned the need for a sufficiently
rapid damping of the corresponding parametric weight
function beyond $\theta > t_k$. This condition is equivalent
to an asymptotic stability along argument θ of a system
with a PPAC

$$\Phi(t_\kappa, j(\Omega) \quad \text{or AOTF} \quad \Phi(t_\kappa, s) = /$$
$$= \frac{U(t_\kappa, s)}{M(t_\kappa, s)}$$

Inasmuch as the parameter in these functions is time t_k and it is fixed at the point of observation, stability is evaluated by the usual methods with the Mikhaylov polynomial

$$M(t_\kappa, s)/$$

or Mikhaylov vectors

$$M(t_\kappa, j\Omega) = \text{denominator} \ [\Phi(t_\kappa, j\Omega)] \qquad (11\text{-}55)$$

and Nyquist vectors:

$$N(t_\kappa, j\Omega) = \frac{M(t_\kappa, j\Omega)}{M(t_\kappa, j\Omega) - U(t_\kappa, j\Omega)}$$

The required damping rate is attained with suitable stability margins.

Bibliography

1. Academician A. A. Andronov and Associate Member I.I. Voznessenskiy, O rabotakh D. K. Maksvella, I. A. Vyshnegradakogo i A. Stodola v oblasti teorii regulirovaniya mashin, (On the Works of J. K. Maxwell, I. A. Vyshnegradakiy and A. Stodola in the Field of Theory of Engine Control), Klassiki nauki (Classics of Science), Press of the Academy of Sciences of the USSR, 1949.

2. Malotkov G. P., Paper Delivered at the IAT Seminar of the Academy of Sciences of the USSR, 1955.

3. Nyquist, Regeneration Theory, Bell System Techn. Journ., Vol. 11, January 1932.

4. Dzung, Avtomaticheskoye regulirovaniye, (Automatic Control), Collection of Materials of the Conference in Crenfield, IL, 1954, p. 37.

5. Lavrent'yev M. A. and Shabat B. V., Teoriya funktsiy kompleksnogo peremennogo, (Theory of Functions of Complex Variables), Fizmatgiz, 1958.

6. Neymark, Yu. I. Ustoychivost' linearizovannykh sistem (Stability of Linearized Systems), 1949.

SYNTHESIS OF LINEAR AUTOMATIC CONTROL SYSTEMS AND COM-
PUTING FILTERS

pp 336 - 366

12-1. General Cases of the Synthesis of Control Systems

Synthesis or shaping is one of the fundamental
stages in the design of control systems which ensure
optimum dynamic and accuracy performance of the system
together with the controlled member.

Optimum mathematical solutions are obtained by
seeking the maxima or minima of functions of one or
a number of parameters or by seeking the best possible
functions by variation methods. This requires that
from the overall stock of methods and formulas of
automatic control theory there be chosen the most
effective synthesis problems best suited for a clear-
cut solution. In most cases these problems determine
the entire structure of fundamental works on control
theory, for example, those mentioned in the introduc-
tion /Bibl. 1-8/. In the present book we elucidate
only structural and frequency solutions of the synthesis
problem based upon data from the literature and works
of this author.

As any stage of technical designing, the synthesis
of a control system cannot always be performed according
to one preassigned sequence. As a rule, the solution
of each individual problem does not only determine the
character of the solution of subsequent problems but
it frequently forces us to revise recommendations which

were already adopted. Hence optimum technical solutions are reached, as a rule, on the basis of many different calculations.

However, for the general case of the synthesis of control systems we can, none the less, outline a specific sequence of measures which should possibly be complied with unless there arise some special requirements having top priority and which, consequently, disrupt the adopted sequence of synthesis measures.

Following are the main stages in the synthesis of control systems in the general case.

1. Formulation of the Task.

Greatest attention is devoted in the formulation of the task to the determination of the necessary characteristics of the controlled member and to setting forth the initial requirements to the quality of control advanced by the controlled member and the ultimate problem solved by it.

It may appear that the characteristics of the controlled member must always be preassigned by the organization designing or manufacturing the member proper. Yet, these characteristics required for designing the control system are occasionally so specific that in a number of cases they have to be determined by the engineer designing the control system. Moreover, the designer of the control system may set up counter-requirements relating to the object's characteristics which are then changed accordingly. It should be noted

945

that the best results are obtained when jointly designing the controlled member and its control system.

The control quality indices required initially are based upon the design characteristics of the controlled member and on the conditions for solving the fundamental problem assigned to the controlled member. Most important, as a rule, is to warrant maximum accuracy under conditions of specific responses and in the presence of random disturbances. When examining the quality of the transfer process, greatest attention is devoted to its duration and to the magnitude of the first maximum of the transfer function, viz., overshoot. For such an analysis of the oscillating component see Chapter 3(Fig. 3-11 and 12).

Subsequently the quality indices are refined by the restrictions applied to the processes in the system by all its concrete elements.

2. Selection of a Power (Actuating) Element

The actuating element is organically connected with the controlled member. If there is assigned the mechanical displacement of the member, then the actuating element can be, e.g., a motor - electric, hydraulic, pneumatic, etc.

The problems concerning the coordination of the characteristics of the motor with the load characteristics are usually solved by methods developed by the theory of drive or, for electric motors, by the theory of electrical drive, an independent branch of science closely associated with automatic control theory (see, e.g., [Bibl. 1]. Let us now briefly review the fundamental problems.

The power of the motor is chosen in accordance with
the load considering losses in transmission and power
used for accelerating inertial parts. For constant duty
with constant load, rated power of the motor is always
set greater than load power. For short-time duty or
recurring short-time operation, rated power of an
electric motor capable of short-time overloads must be no
less than the power equivalent to thermal heating con-
ditions but it may be less than heat load power.

Power equivalent to heating with constant magnetic
flux and rate of the electric motor is equal to
RMS load power. Under more complex duties one usually
seeks RMS armature current and proceeds from there to
power equivalent to heating.

Nominal rate of the motor is coordinated with the
maximum rate at the load shaft by the ratio i. For
considerations of weight and size it is expedient to
have high-rate electric motors. For the linear displace-
ment of mechanisms and occasionally also for limited
deflection angles, hydraulic and pneumatic piston
engines and draft electromagnets with limited run
and direct transmission to the load mechanism are em-
ployed. The motor's rate margin compared with design
magnitude is taken up to one and a half fold:

$$\Omega_{mot\ rate} = 1.5 \frac{\Omega_{Load\ m.}}{i} \qquad (*)$$

from overtaking conditions. If the control system has
specified short-time drive forcing, the margin in terms

947

of nominal data may be ignored.

The moment of the motor is equal to the sum of load moment, multiplied by ratio i and divided by transmission efficiency η, and dynamic moments required for the start of inertial load parts with moment of inertia J_n and the motor proper with moment of inertia of the rotor J_o:

$$M_m = i\left(\frac{M_\ell}{\eta} + J_\ell \dot{\Omega}_m i\right) + J_m \dot{\Omega}_m \qquad (**)$$

In the above formulas (*) and (**):

The ratio is understood to be gain of the reducer (amplifying component) equal to the ratio of output rate (load) to motor rate;

Angular load acceleration is expressed by the angular acceleration of the motor shaft $i\dot{\Omega}_m$, and in calculations for the preliminary selection of the motor it is determined for the assigned starting time t up to maximum rate

$$\dot{\Omega}_m = \frac{\Omega_{m.d.}}{t};$$

Efficiency is considered only in the transmission of the static moment assumed to be inhibiting with any rotation direction of the motor; in the transmission of the dynamic moment $(J_n \dot{\Omega}_m i)$ efficiency may either be ignored or the dynamic moment should be divided by it for the case of starting, and multiplied by it for the case of braking;

Moments of inertia occurring at various spots (in the motor, the load, intermediate transmissions) are

usually reduced to the motor shaft to form a reduced
moment of inertia

$$J = \sum_k J_k i_k^2 .$$

With this designation the formula of moment (**)
takes the form:

$$M_m = \frac{i M_2}{\eta} + J \dot{\Omega}_m . \qquad (^{***})$$

The nominal moment of the motor in case of constant
loads must be no less than the value given above. Short-
time peaks of the moment can be overcome by the motor
with a lesser nominal moment owing to the capacity of
most electric motors to withstand approximately double
overloads also by means of special measures to force
the mode of operation provided that the equivalent
heating moment does not exceed nominal values.

The optimum reducer must with a prescribed aggre-
gate ratio add a minimum boost at the reduced moment of
inertia of the inertial masses of its own gears. Minimum
calculations show /Bibl. 2/ that it is convenient to
obtain the assigned i with several pairs of gears rather
than with one. Worm gear and other irreversible reducers
are not recommendable because of possible jams when
braking the driving gear, and great inertial mass of the
drive.

3. Selection of Control Methods

The basic control methods are: deflection control

949

method, disturbance control method and the combined method.

In servosystems and program control systems the deflection control method prevails; frequently the compound disturbance method, i.e., the combined method is applied.

Along with the two other methods, stabilization systems frequently use the disturbance control method.

4. Selection of the Structure of Control Systems

This design control stage comprises the selection of the system's astaticism order, the number of circuits in a closed system and the elements consituting the circuit, the selection of direct circuits and their componenls. Of course, the structure of a control system depends greatly upon the control method chosen.

5. Ensuring the Quality Indices Relative to a Control System's Forced Motion

First of all one determines the gain required by accuracy conditions considering to perform a larger program and to overcome the prevailing regular disturbance.

In static control systems the gain is determined both by the constant components of the program and all the disturbances as well as by the variable components varying uniformly, with equal acceleration, etc.

In control systems with first-order astaticism the gain no longer depends upon the constant components of the program and disturbances applied at the output

of the integrating element.

In control systems with second-order astaticism the gain does not depend upon uniformly varying components of the program and disturbances applied at the output of two integrating elements. Disturbance constants at the output of the first integrating element do also not affect the gain. Thus, e.g., a load moment on the shaft of the actuating motor does not affect the control system's forced motion if in the preceding elements there exists a second integrating element in a system with second-order astaticism. The system's order of astaticism and gain determine the slope of the low-frequency portion of the decibel-log-frequency and the point at which it intersects the zero db line.

For harmonic program and disturbance components at a fixed frequency the role similar to that of the integrating element is played by the resonance element tuned to the same frequency.

Quality indices connected with forced motion under the effect of stationary random disturbances are defined, as is seen from Chapter 10, by relation (10-66) between the disturbance spectrum and the amplitude-frequency characteristic of the closed system for the disturbance. If in the general case of design control the task of obtaining optimum resistance to disturbances (regarded in the following as special cases) is not assigned, then on the basis of Fig. 12-1 it is still possible to draw conclusions as to a favorable or un-favorable mutual position of the disturbance spectrum

$(S\omega)$ and the AFC of a closed system $A(\omega)$ and take them into consideration when solving subsequent synthesis problems.
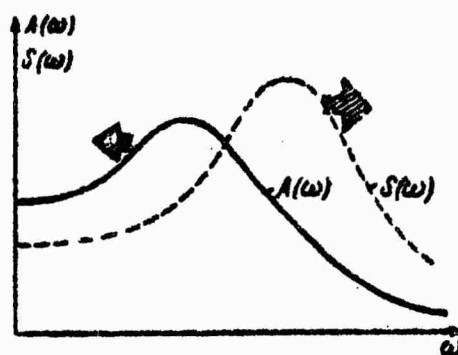
Fig. 12-1. Directions of desirable shifts of AFC of a closed system and of the spectral density of input disturbances in design control

An obviously unfavorable position of the AFC of a closed control system is that where the AFC peak coincides with that of the disturbance spectrum; in this case an increase in noise level should be expected at the output.

A favorable position of the AFC peak is to the right or to the left of the disturbance spectrum peak, as shown in the Figure investigated. With a considerable drop in the curves as one moves away from the peak zone it is expedient to draw apart as far as possible the peaks of the AFC and the disturbance spectrum along the frequency axis in the directions shown in the Figure.

6. Selection of the Types and Designs of the Elements
of the Control System's Direct Path and Principal
Circuits

The principal elements to be selected are: **the**
measuring device, **the amplifying and intermediate**
coupling elements.

The main specification of the measuring device is
to ensure static and dynamic accuracy.

The amplifying elements must amplify the signal
received from the measuring device:

by the regulated "reference" quantity in accordance
with the value calculated for **warranting the prescribed**
accuracy of forced motion;

By power, **in accordance with load from the controlled**
member proper **and exterior load with respect to the**
controlled member, **which may be regarded as disturbance.**

While amplifying the control signal there may arise
the need of measuring the physical dimension and **the**
character of the reference quantity; intermediate ele-
ments are employed for this **purpose.**

7. Warranting the Quality Indices Relative to the Control
System's Natural Motion

This stage of design control can be elucidated best
with the aid of frequency-response characteristics of
an open control system.

If we hold to this criterion, then design control
should aim at obtaining frequency-response characteristics
with favorable margin values. Figure 12-8 shows

logarithmic characteristics of an open system. In the case where the direct circuit has no singularities, a favorable feature is the shift of the amplitude characteristic to the left and the phase response to the right or the shift of the PAC downward owing to a decrease in gain, and the shift of the phase characteristic upward by creating a phase lead.
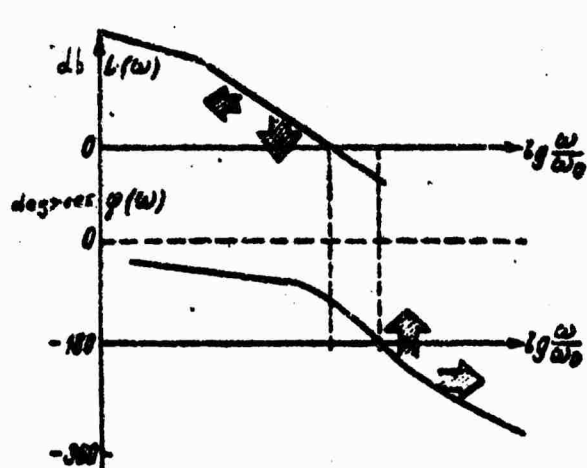
Fig. 12-2. Directions of desirable shifts of frequency-response characteristics of an open system in design control

Occasionally these measures are in contradiction with other quality criteria, e.g.:

A reduction of cutoff frequency leads to a reduction of quick response [see (4-83)];

A reduction in gain increases the error, which forces us to introduce in the frequency-response characteristics the selective changes discussed in Chapter 11.

Synthesis on the basis of the damping criterion proceeds from the assumption that damping time of the

954

overall transient process of a control system coincides with the damping time of the system's partial weight function having the greatest time constant T_M:

$$\tau_{damp} = D T_M.$$

Introduction in the OTF of a closed control system of artificial divergence

$$\sigma = \frac{1}{T_M} = \frac{D}{T_{damp}}$$

$$(*)$$

can transform (mathematically) a stable system with the weight function

$$L^{-1}\{\Phi(p)\} = w(t)$$

into a system with artificial divergence and a new weight function

$$L^{-1}\{\Phi(p-\sigma)\} = w(t) e^{+\sigma t},$$

which may remain damped with $\sigma < 1/T_M$, may become divergent with $\sigma > 1/T_M$ and become neutral with $\sigma = 1/T_M$ (*). The "system with artificial divergence $\Phi_\sigma(p) = \Phi(p-\sigma)$" representing this weight function will be stable, unstable and on the stability boundary, respectively. The latter stage can be easily revealed by means of the Mikhaylov stability criterion applied to this closed system $\Phi(p-\sigma)$, or the Nyquist stability criterion applied to the open system

$$W(p-\sigma) = \frac{\Phi(p-\sigma)}{1-\Phi(p-\sigma)}.$$

The frequency-response characteristics of the direct circuit of systems with artificial divergence are derived from the frequency-response characteristics

of the components of the control system's elements whose transfer functions $K_1(p)$, $K_2(p)$,... are respectively replaced by displaced OTF $K_1(p-\sigma)$, $K_2(p-\sigma)$,...

Although with the above transformations the weight of the partial component with greater damping time does not become apparent, yet, owing to the simplicity of the method it is used in design control and amounts to constructing the frequency-response characteristics of the direct circuits AFC and PC, but of the artificial system (with induced divergence of the weight function); moreover, in the synthesis process it suffices to take the artificial system to the boundary of stability. Thus, in many cases the synthesis of the sy tem can be carried out on the basis of attaining the frequency-response characteristics desired.

8. Providing for Optimum Transient Process With Restricted Maximum Acceleration

We investigate the operating conditions of a stepped input. Let the starting conditions be known, then maximum stepped input can be taken as $x_m1[t)$. Let there also be a restriction for maximum acceleration $\ddot{a}_m$: this restriction may depend on the permissible overloads of the controlled member as well as on the permissible overloads of the elements of the control system proper. We can easily show that the smallest working time of the control system's input step is attained with complete utilization of its acceleration capacities, i.e.. with

Starting at maximum acceleration up to the middle of the path $x_m/2$ and subsequent maximum retarding on the second half of the part. Such a process is shown in Fig. 12-3,a. Diagram b shows the necessary law of acceleration variation.
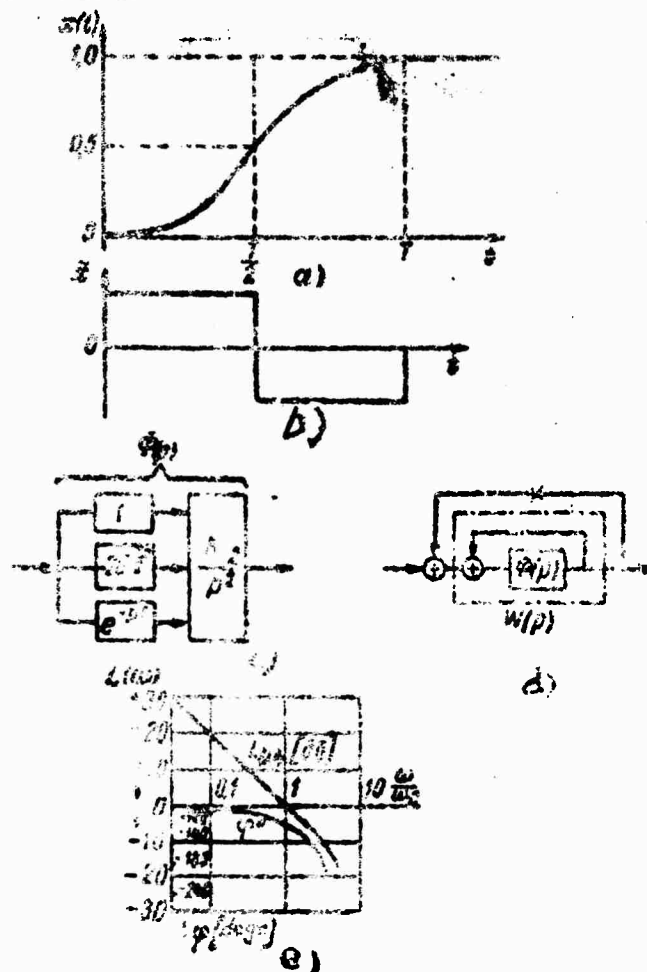
Fig. 12-3. Characteristics of a control system with maximum quick-response and restricted acceleration

From these graphs we can synthesize the control system's block diagram.

To do this we write the expression for graph x in terms of displaced functions:

$$\ddot{x}(t) = \ddot{a}_m \left\{ 1\,(t) - 2 \cdot 1 \left[t - \frac{T}{2} \right) + 1\,(t - T) \right\}.$$
(12-1a)

With a unit ouput step the graph proportionally decreases $\ddot{x}(t)/x_m$, this relation being equal to the weight function derivative of the control system sought:

$$\dot{w}(t) = \frac{\ddot{x}(t)}{x_m} = K_{-2} \left\{ 1\,(t) - 2 \cdot 1 \left[t - \frac{T}{2} \right) + \\ + 1\,(t - T) \right\}.$$
(12-1b)

We now pass to representations, and by dividing by p we obtained the OTF

$$\Phi(p) = \frac{K_{-2}}{p^2} \left(1 - 2e^{-\frac{Tp}{2}} + e^{-Tp} \right).$$
(12-1c)

Indeed, to warrant a constant acceleration at the output with a stepped input, we need two integrating elements with a total gain

$$K_{-2} = \frac{\ddot{a}_m}{x_m}.$$

To change the acceleration sign at the instant $t_1 = T/2$ and to obtain a zero value for acceleration at the instant $t_2 = T$ we require two delay components with delays $T/2$ and T, i.e., with transfer functions $-2e^{-Tp/2}$ and e^{-Tp}. The delay, amplifying and integrating components are inserted according to block diagram c of the same Figure.

We can easily check that during the time interval $0 - T/2$ only the signal $+ 1 \times x_m$ is fed through the amplifying component to the input of the integrating components. During the time interval $(T/2) - T$ there exists at the input of the integrating elements a sum of two signals from the amplifying component and the first delay component:

$$(1-2)\,x_m = -1 \cdot x_m. \qquad (12\text{-}2)$$

In the interval $T - \infty$ the summed signal from three components equals zero:

$$(1-2+1)\,x_m = 0.$$

Since the signal at the input of the integrating elements is equal to acceleration, we can easily see that the preset acceleration graph $\ddot{z}$ is actually achieved.

Thus we have obtained a system with an open structure which theoretically ensures the faultless transmission of a constant input program since $\Phi(0) = K_{-2}(T^2/4)$, and for $T = 2/\sqrt{K_{-2}}$ we have the condition indispensable for any servosystem, viz., $\Phi(0) = 1$ $\int$ the limit is expanded after repeated differentiation of the numerator and the denominator (12-1c) for p_7. Yet, inasmuch as such a control has an absolutely unstable performance, zero drift is unavoidable; hence instead of a theoretically accurate open structure we have to create a system virtually close to it by the transfer function but with a closed structure.

Diagram d of the same Figure shows the passage to the structure desired. From the simultaneous application

959

of regeneration and degeneration the total transfer
function $\phi(p)$ does not change, but if we consider the
part framed by the dashed line to be the control system's
direct circuit, we can form it first exactly according
to formula

$$W(p) = \frac{\Phi(p)}{1 - \Phi(p)} = \frac{K_{-2}\left(1 - 2e^{-\frac{Tp}{2}} + e^{-Tp}\right)}{p^2 - K_{-2}\left(1 - 2e^{-\frac{Tp}{2}} + e^{-Tp}\right)},$$

$$(12\text{-}3)$$

and then also approximately.

The degree of approximation will be evaluated by
the frequency-response characteristics. In the given
case the frequency-response characteristic of the direct
circuit or of the open control system is

$$W(j\omega) = \frac{\frac{4}{T^2}\left(1 - 2e^{-j\frac{\omega T}{2}} + e^{-j\omega T}\right)}{-\omega^2 - \frac{4}{T^2}\left(1 - 2e^{-j\frac{\omega T}{2}} + e^{j\omega T}\right)} \cdot (12\text{-}4)$$

The above problem was studied by V. V. Solodovnikov.
He obtained a logarithmic frequency-response characteristic
which he called optimum It is shown in diagram e. The
main features of this characteristic are as follows:
cutoff frequency $\omega_c = 2/T$; inclination in the center
frequency band -20 db/dec.

Let us note that optimality is evaluated here by
the absence of overshoot and by a minimum regulating
time equal for maximum input to

$$T = \frac{2}{\sqrt{K_{-2}}} = 2\sqrt{\frac{x_m}{a_m}}. \qquad (12\text{-}5)$$

If the input decreases $(x_1 < x_m)$, performance acceleration decreases as well, $\ddot{a}_1 = K_{-2}\, x_1 = \ddot{a}_m(x_1/x_m)$, but control time remains unchanged:

$$T_1 = 2\sqrt{\frac{x_1}{\ddot{a}_1}} = 2\sqrt{\frac{x_1 x_m}{\ddot{a}_m x_1}} = \frac{2}{\sqrt{K_{-2}}} \quad (12\text{-}6)$$

and the system's acceleration capabilities are not fully exploited. Their full exploitation with a stepped input of any magnitude is possible in systems with nonlinear circuits.

However, if conditions of maximum input prevail, a linear realization of the above system is also possible. Its synthesis must aim at obtaining an optimum frequency-response characteristic with its new indices: cut-off frequency $\omega_c = 2/T$ and an inclination in the center frequency band of -20 db/dec.

V. V. Solodovnikov (see Chapter 1 /Bibl. 1/, uses these indices also for the synthesis of control systems not only by preset control time but also by preset overcontrol. On account of the link between overcontrol and the peaks of the real characteristic on the one hand, and between the real characteristic of a closed control system and amplitude and phase responses of an open system on the other hand, there is established the required phase margin which prevents the real characteristic of the closed control system from attaining peaks of undesirable values. Additional nomograms make it possible to establish quite simply for standard control systems the character of the

frequency response desired.

9. Synthesis of Compensating Networks

If by satisfying the requirement of forced and
natural motion we established the approximate charac-
ter of the frequency response desired and if, after
selecting the power units and the compulsory coupling
elements, we determined the frequency responses of
the unaltered element, then the difference between the
frequency response desired and the response of the
unaltered element must be completed by correcting
networks.

In Chapter 11 we discussed various methods of
operating stabilizing networks to ensure stability.
In solving the synthesis problem with prescribed
frequency response these methods remain the same.
We expand the sequence of the synthesis of a cascade-
connected stabilizing device to which, as is shown
in Section 11-10, any correction network can be re-
duced.

As the desired frequency response of a servo-
system we can take in the first approximation the
frequency response of an oscillatory component which
satisfies the prescribed qualitative indices.

A favorable frequency response during operation
with disturbances is that of the oscillatory component
with the value $\xi = (\sqrt{2}/2) = 0.707$ since, as is seen
from Table 4-2, the AFC of the component has no peaks

and decreases monotonically as frequency rises. Overshoot for this value of ξ according to formula (3-19), $\delta_u = e^{-\pi} = 0.043$, is also comparatively small. With preset control time, which we take to be the damping time of the oscillation component up to 1% of maximum amplitude, the relative control time τ of the element is (Table 1-2)

$$\tau = \xi T = \frac{\xi T_{contr}}{4.6} = 0.15 T_{contr}.$$

The values desired for ξ and τ can also be determined proceeding from other considerations. For example, if with maximum stepped variation of the input value x_m the rate of the transient function is limited by the saturation of the actuating element, then, inasmuch as maximum rate of the transient function is equal to the peak of the weight function determined by formula (3-42 c) for $X_v(p) = p$ whence we find τ_1, and further by (3-43 a) for $K = 1$

$$x_m h_m = x_m \cdot w(t_m) = \frac{x}{\tau \sqrt{1 - \xi^2}} e^{\sqrt{1-\xi^2}},$$

we find the values for ξ from condition

$$\xi = f(w, \tau).$$

The values of ξ and τ selected by one or the other method refer to closed systems, but from the characteristics of a closed control system we can easily pass to those of an open system.

Suppose the control system is static and its gain is chosen according to the conditions of accuracy indispensable to compensating the constant

963

disturbance. Then, in the closed state, the transfer function of a servosystem reduced to the form of the transfer function of an oscillatory element, takes the form:

$$\Phi(p) = \frac{\frac{K}{1+K}}{\tau^2 p^2 + 2\xi\tau p + 1} . \qquad (12\text{-}7a)$$

The transfer function of the open system is

$$W(p) = \frac{K}{(1+K)(\tau^2 p^2 + 2\xi\tau p + 1) - K} =$$

$$= \frac{K}{(\tau\sqrt{1+K})^2 p^2 + 2(\xi\sqrt{1+K})(\tau\sqrt{1+K})p + 1} . \qquad (12\text{-}7b)$$

From the parameters obtained

$$\tau_{open} = \tau_3\sqrt{1+K} \quad \text{and} \quad \xi_{open} = \xi_3\sqrt{1+K}$$

with a given k we construct the desired characteristic of the open system.

If the control system has a first-order astaticism, then the desired transfer function of the closed system is

$$\Phi(p) = \frac{1}{\tau^2 p^2 + 2\xi\tau p + 1} \qquad (12\text{-}8a)$$

and that of the open system is

$$W(p) = \frac{1}{p(\tau^2 p + 2\xi\tau)} = \frac{\frac{1}{2\xi\tau}}{p\left(\frac{\tau}{2\xi}p+1\right)} . \qquad (12\text{-}8b)$$

The desired characteristic of the open system is constructed to gauge for the aperiodic component and is increased by the characteristic of the integrating component. Since gain $k_{-1} = 1/2\,\xi\tau$ affects the accuracy of linearly changing disturbance, indices ξ and τ may be revised.

For additional changes of some characteristics of the second-order component we can complicate the numerator of the ODF /Bibl. 3/.

Thus, the qualitative indices desired are first achieved in a system of lower order, e.g., of second order where : they can easily be linked with the shape of frequency-response characteristics, and then these characteristics are taken as the desired ones when synthesizing systems of higher order.
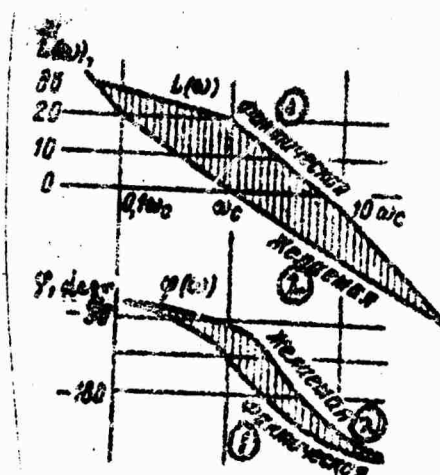
Fig. 12-4. Frequency-response curves of a stabilizing network
Key: 1) actual; 2) desired

Let there be assigned the desired logarithmic frequency-response curves $L_1(\omega)$ and $\varphi_1(\omega)$, and the characteristics of the actually available unalterable element $L_2(\omega)$ and $\varphi_2(\omega)$ shown in Fig. 12-4.

The differences between them

$$L(\omega) = L_1(\omega) - L_2(\omega) \quad \text{and} \quad \varphi(\omega) = \varphi_1(\omega) - \varphi_2(\omega)$$

are hatched in the diagram. These differences are precisely the required frequency responses of serial correcting units.

Following the methods expounded in Chapter 8, the synthesis of an electric circuit can be performed either directly by the characteristics of the correcting networks or by the transfer functions constructed from approximated characteristics.

If the passive network is physically unachievable, part of its functions should be transferred to active components or a solution should be sought in the form of a network in another line. Deviation of the characteristic obtained from the desired one changes the prescribed qualtitative indices of a control system.

This is the pattern of solutions for the synthesis problem in the general case. Below we shall investigate some special cases of the synthesis of control systems with more rigid requirements as to noise stability.

12-2. Statistical Synthesis of Control Systems

1. Mean-Root-Square Error (MRSE) From Two Groups of Signals

We investigate such control systems which are acted upon simultaneously by a useful signal and a disturbance. The control system designed on the basis of general synthesis principles does not suppress all of the input signal reproduction errors because of its

limited order of astaticism and because of the existence
of a specific passband resulting from the OTF of the
PAC error of a closed system for the case that a useful
signal is assigned in the form of a random process.

The signal reproduction errors (dynamic errors) and
disturbance effect errors (fluctuation errors) form
two groups. In the following we shall consider only
those cases where these two groups are independent, that
is, when the square of the aggregate mean-root-square
error is obtained by summing the dispersion of both
error groups without introducing cross-correlation
functions.

Practice and calculations show that various para-
meters of the control system variously affect the
components of the aggregate MRSE. For example, in-
creasing gain of an open system reduces the dynamic
error and increases the fluctuation error, and so on.
Under such circumstances synthesis must obviously be
aimed at finding a value for gain (or any other vary-
ing parameter) for an assigned control system design
or, in the more general case, for any control system
design such that it would warrant a minimum aggregate
MRSE from the two error groups.

2. Input is a Polynomial and Disturbances Are White
   Noise

Let the useful signal be reduced to an adequately
simple form:

$$x = a + bt \qquad (12\text{-}9a)$$

The control system is taken to be astatic with a simple transfer function of the direct circuit

$$W(p) = \frac{K_{-1}}{p(Tp+1)} .$$
(12-9b)

The statistical data relative to the useful signal are

$$\overline{b}_{\text{init}} = 0; \ D_b \neq 0.$$

According to (10-54 c) the rate dispersion of the useful signal is transferred to the output by means of multiplication by the square of the second error coefficient:

$$D_1 = \Phi_\bullet'^2(0) D_b = \frac{1}{K_{-1}^2} D_b .$$

To calculate the effect of white noise we have to find the fundamental transfer function of a closed control system

$$\overline{\Phi}(p) = \frac{K_{-1}}{p(Tp+1) + K_{-1}} = \frac{1}{\frac{T}{K_{-1}} p^2 + \frac{1}{K_{-1}} p + 1} .$$

From Table 4-10 for $K = 1$, $a_0 = 1$ we find the effective passband of the second-order element:

$$\Delta\omega_1 = \frac{\pi}{2a_1} = \frac{\pi K_{-1}}{2} .$$

and by formula (10-70a) we determine the noise dispersion

$$D_n = \frac{N^2}{2} K_{-1}.$$

Assuming that noise and useful signal are not correlated we determine the aggregate dispersion:

$$D_t = D_1 + D_n. \qquad (12\text{-}10)$$

or for the example under study

$$D_1 = \frac{D_b}{K_{-1}^2} + \frac{N^2 K_{-1}}{2}. \qquad (12\text{-}11)$$

Thus, the gain of the direct circuit reduces the dispersion of the first error group D_1 and increases that of the second group D_n.

Optimum gain is defined from the condition

$$\frac{\partial D_t}{\partial K_{-1}} = 0. \qquad (12\text{-}12)$$

By extending the solution of the example we find:

$$\frac{\partial D_t}{\partial K_{-1}} = \frac{2D_b}{K_{-1}^3} + \frac{N^2}{2} = 0, \quad or \quad K_{-1 opt} = \sqrt[3]{\frac{4D_b}{N^2}}.$$

Minimum dispersion is

$$D_{1\,min} = \sqrt[3]{\frac{N^4 D_b}{16}} + \sqrt[3]{\frac{N^4 D_b}{2}} = \sqrt[3]{\frac{27 N^4 D_b}{16}}.$$

$$(12\text{-}13)$$

Thus, by adopting the direct circuit gain found by calculation we attain a minimum MRSE for all the inserts of the given system. If the control system services single-action objects (military objects), we reach a minimum of aggregate dispersion for all the launchings of one-type objects (minimum aggregate dispersion for the entire operation or even for the

entire war).   Minimum error dispersion leads to minimum consumption of objects.

3.   The Effective Signal Is a Polynomial, The Disturbance Has a Complex Spectrum

The expression for aggregate dispersion of a control system with first-order astaticism is

$$D_s = \Phi_s'^2 D_b + \frac{1}{\pi} \int_0^\infty S_{out}(\omega) \, d\omega. \qquad (*)$$

If the changing parameter q is defined in formula (*), e.g.:

$$D_s = \Phi_s'^2 (p, q)_{p=0} D_b + \frac{1}{\pi} \int_0^\infty F(q) S_1(\omega) \, d\omega,$$

$$(12\text{-}14)$$

then with a limited synthesis, when only this parameter q is optimized, its optimum value is found from a condition analogous to (12-12):

$$\frac{\partial D_s}{\partial q} = 0. \qquad (12\text{-}15)$$

In the right-hand side of formula (12-14) integration can be performed once, e.g., with a unit cofactor F(q). This yields the constant coefficient

$$Q = \frac{1}{\pi} \int_0^\infty S_1(\omega) \, d\omega, \qquad (12\text{-}16)$$

and condition (12-15) with simple functions F(q) can be found analytically:

$$\frac{\partial D_s}{\partial q} = -\frac{\partial}{\partial q}[\Phi'^2(0,q)D_b + F(q)Q] =$$

$$= -\frac{\partial}{\partial q}\Phi'^2(0,q)D_b + \frac{\partial F(q)}{\partial q}Q = 0; \quad (12\text{-}17)$$

whence we determine q_{opt}.

In more complex cases integration should be performed graphically, carrying out a number of alternate calculations to find the optimum.

4. Effective Signal and Disturbance Are Given As Spectral Densities

An effective input signal may have a more complex statistical task than that discussed under No. 3. If the signal is stationary then, as a rule, it is given in terms of spectral density.

Suppose, e.g., that an effective signal has always a determined magnitude (modulus) a and an indeterminate sign, the average number of sign changes per second amounting to μ. Spectral density of such a signal is reduced to the form:

$$S_\chi(\omega) = \frac{2a^2\mu}{\omega^2 + 4\mu^2}. \qquad (*)$$

If a disturbance is inserted together with the effective signal and is also defined in terms of spectral density $S_n(\omega)$, and if the effective signal and the disturbance are not correlated, then spectral density of the error in the reproduction of the output signal according to standard function $\Phi_d(p)$ with a transfer function of the real system $\Phi(p)$ is

$$S_e(\omega) = |\Phi_s(j\omega) - \Phi(j\omega)|^2 S_\chi(\omega) + |\Phi(j\omega)|^2 S_n(\omega).$$

(12-18)

For control purposes the standard function has a simpler form: $\Phi_s = 1$; then

$$S_e(\omega) = |1 - \Phi(j\omega)|^2 S_\chi(\omega) + |\Phi(j\omega)|^2 S_n(\omega).$$

(12-19)

We can easily see that by changing the system's transfer function we can influence the spectral density of the error and the magnitude of the mean-root-square resulting from integration of spectrum $S_e(\omega)$ in semi-infinite limits.

If we take a look at the integration of the spectral density of the error we can easily notice that for any narrow frequency band $\Delta\omega$ the prescribed spectral densities $S_\chi(\omega)$ and $S_n(\omega)$ can be regarded as constant numbers; likewise, we can consider constant within the band the unknown value of the complex transfer function $\Phi(j\omega)$ sought for. To determine the minimum of the integral of the error's spectral density it suffices to ensure the minimum of its growth in each band.

Minimum conditions without considering the physical feasibility of the system are found from Eq. (12-18) by differentiating it with respect to real $P(\omega)$ and imaginary $Q(\omega)$ with the frequency-response characteristics of the system sought for:

$$\frac{\partial S_e}{\partial P} = -2[1 - P(\omega)]S_\chi(\omega) + 2P(\omega)S_n(\omega) = 0;$$

$$\frac{\partial S_e}{\partial Q} = 2Q(\omega)S_\chi(\omega) + 2Q(\omega)S_n(\omega) = 0.$$

Hence

$$\mathring{Q}(\omega) = 0 \text{ and } D(\omega) = \Phi(j\omega) = \frac{S_Y(\omega)}{S_X(\omega) + S_{N}(\omega)}. \qquad (**)$$

The singularity of formula (**) will be shown in a simple example. Let the useful signal have a spectral density (*) with unit parameter $S_X(\omega) = 1/(\omega^2 + 1)$, and the noise have a plane spectrum of level N^2.

According to formula (**) we find

$$\Phi(j\omega) = \frac{1}{N^2\omega^2 + 1 + N^2}. \qquad (***)$$

Although this result and the conclusion are temptingly simple, the conclusion did not take account of the fact that spectral densities are Fourier transforms of even bilateral correlation functions while the unknown PAC $\Phi(j\omega)$ is a Fourier transform of the system's initial weight function, hence formula (**) yields results which cannot be achieved physically. Indeed, the PAC (***) could be derived from the transfer function $\Phi(p) = 1/(1 + N^2 - p^2 N^2)$, but the latter yields an unstable system.

The conditions for minimizing dispersion considering physical feasibility [Bibl. 5] make it possible to determine the PAC of an optimum control system in the form

$$\Phi(j\omega) = \frac{1}{2\pi\Psi(j\omega)} \int_0^\infty e^{-j\omega t}\, dt \int_{-\infty}^{\infty} \frac{S_X(\omega)}{\Psi(-j\omega)} e^{j\omega t}\, d\omega,$$

$$(12\text{-}20)$$

where $\Psi(j\omega)$ is an auxiliary function obtained from spectral density:

$$[\Psi(j\omega)]^2 = \Psi(j\omega)\,\Psi(-j\omega) = S_X(\omega) + S_n(\omega).$$

$$(12\text{-}21a)$$

Accordingly, for minimum error value we find a new expression in terms of spectral density:

$$\xi_{min.}^2 = \frac{1}{\pi}\int_0^\infty [S_X(\omega) - |\Phi(j\omega)|^2 S_\varsigma(\omega)]\,d\omega,\qquad (12\text{-}21b)$$

where $\varphi = x + x_n$.

Continuing the solution of the above example taken from $/\text{Bibl. }5/$ we calculate according to Eq. (12-20):

Aggregate spectral density:

$$S_X(\omega) + S_n(\omega) = \frac{1}{\omega^2 + 1} + N^2 = \frac{1 + N^2 + N^2\omega^2}{1 + \omega^2} =$$

$$= \frac{(\sqrt{1+N^2} + j\omega N)(\sqrt{1+N^2} - j\omega N)}{(1 + j\omega)(1 - j\omega)};$$

auxiliary function

$$\Psi(j\omega) = \frac{\sqrt{1+N^2} + j\omega N}{1 + j\omega}$$

and optimum complex transfer function of a control system

$$\Phi(j\omega) = \frac{1}{(N + \sqrt{1+N^2})(\sqrt{1+N^2} + j\omega N)}\,.$$

In the given example the PAC calculated coincides with the PAC of the aperiodic element and, obviously, differs from (***).

If the useful signal and the disturbance are applied at different points, these points can be joined by means of structural transformations. Transformation of the spectral density of the disturbance when transferring the point of its application must be directly proportional

(transfer along the path of the signal) to the square of
the modulus of the PAC of the elements skipped or in-
versely proportional (transfer against the path of the
signal) to the square of the modulus of the PAC of the
elements passed.

The optimum PAC thus obtained is used for the
synthesis of real control systems by the methods dis-
cussed earlier, but approximation of the real system
to the optimum one is usually performed not in a part
of the structure but by the minimum reference value of
the error (12-21b).

Indeed, as we can see from the example above, even
such a usually steady parameter as the transfer coeffi-
cient of a closed control system determined by perfor-
mance conditions of constant initial installations,
etc., depends in optimum systems on the disturbance
level, that is, when this level changes the transfer
coefficient is bound to change as well.

Obviously, the control systems most convenient
from an operational viewpoint are those with constant
tuning to a unit gain in a closed state. Then by
choosing the appropriate order of astaticism the
constant components as well as those changing with
time according to polynomial law, will be worked by
the system faultlessly irrespective of their magnitude
which may be a random quantity. This, however,
corresponds already to new information regarding the
useful signal which we discuss separately.

12-5. Synthesis of Computing Filters Operating in A Limited Time Interval

1. Hypothesis of the Change of the Effective Signal in the Prescribed Interval

Computing filters can be designed proceeding from the theory of closed control systems or from that of open circuit, chiefly electric networks. But in this case the elements of the computing circuit must have a high instrumental accuracy, and construction of the electric circuit must be based upon a specific mathematical formula which takes account of the prescribed transformation of the input signal and its assumed properties. Thus one may compensate for the loss of self-regulation and disturbance stability inherent in closed control systems.

If the input signal is fed in a complex form where against the noise background the properties of the effective component are not checked directly, we have to formulate a hypothesis of changes occurring to the useful signal in the form of some preset law.

In the present Section we investigate cases where the effective signal changes according to a law expressed by the power polynomial

$$x = x_0 + (t - t_0)\dot{x}_0 + \frac{(t - t_0)^2}{2!}\ddot{x}_0 \dots, \qquad (12\text{-}22)$$

To start with we shall study constant signals and such uniformly changing with time.

In many cases, however, one cannot count on preserving for a long time the law (12-22) in the effective component. For example, when a radar is tracking a moving target (an aircraft) the latter may maneuver, and this will obviously complicate the law of coordinate variation (12-22).

High-speed aircraft, however, have specific restrictions placed upon their maneuverability. Accordingly, in the case of formation flying or mass raids, maneuverability is restricted and, finally, the task performed by the aircraft (bombing, terrain photography, etc.) places at specific time intervals considerable restrictions upon the aircraft's maneuverability.

Thus, on the one hand we have a number of factors of random character which change the law (12-22) while, on the other hand, there exists a number of factors limiting these changes. It is on the basis of these factors that, relying chiefly upon data from experience, we can formulate well-founded hypotheses regarding the law of effective signal variation over a limited time interval. For the example with the aircraft cited above the hypothesis most frequently applied is that of uniformly changing Cartesian coordinates of the aircraft during observation time or during the flight of the shell when firing against enemy aircraft.

In a simpler example, e.g., in a system in the form of a filter smoothening the pulsations of rectified a-c, we should hold to the hypothesis of a constant effective signal. With varying load and a relatively

high resistance of the source and the rectifier, input
voltage at the filter will also change; thus, the hypothe-
sis formulated holds true for a limited time interval.
The problem of determining the effective signal against
a noise background according to the hypothesis accepted
is said to be the smoothing problem. If in the synthesis
of a smoothing filter there is attained a minimum mean-
root-square deviation of the effective signal determined
from the actual aggregate signal (with disturbances), then,
according to the terminology in /Bibl. 6/, this is said
to be mean-root-square smoothing.

2. Mean-Root-Square Smoothing Assuming that the Effective
   Signal is Constant Over a Prescribed Time Interval

Mathematical solution of the problem. Let the law of
aggregated input signal variation be assigned in the form
of the curve shown in Fig. 12-5 reflecting the history of
the process up to the current instant of time t. The task
is to reproduce the effective signal during the current
instant of time t, but by utilizing the history of the
process.

In the first place, we formulate a hypothesis on
the constancy of the effective signal during observation
time T. This hypothesis is corroborated by the shape of
the curve shown. But the curve studied reflects only one
realization of the random process, hence before performing
mathematical operations and synthesizing the system ex-
pected to operate repeatedly according to the formulas
obtained for various realizations of the random process,—

we must ascertain that this curve is standard from the statistical viewpoint. Thus, observing the conditions cited, we have the hypothesis

$$x_{h}(t) = a = \text{const.} \qquad (12\text{-}23)$$

In Fig. 12-5 this hypothesis is represented in the form of a straight line horizontal over the interval T. The degree to which this hypothesis corresponds to the real curve will be evaluated by the square criterion

$$l_{2T} = \int_{0}^{T} [x(t-\tau) - a]^{2} d\tau. \qquad (12\text{-}24)$$

Minimum conditions of the criterion

$$\frac{\partial l_{2T}}{\partial a} = -2 \int_{0}^{T} [x(t-\tau) - a] d\tau = 0,$$

will be considered optimum, hence

$$a = \int_{0}^{T} \frac{1}{T} x(t-\tau) d\tau. \qquad (12\text{-}25)$$
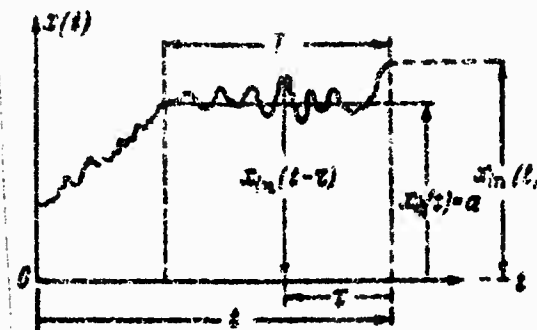
Fig. 12-5. Input process for smoothing filters.

979

It is obvious that the arithmetic mean satisfies the minimum mean-root-square error.

Synthesis of smoothing systems. Suppose we design a real system operating according to (12-25), i.e., a system which after input of signal $x_0(t)$ produces upon expiration of time T the output quantity a. The system may be regarded as determined once its weight functions, transfer functions, block diagram or frequency-response characteristics have been defined. By any of these indices we can form an ideal or an approximate system, and it is frequently convenient to evaluate the degree of approximation by various indices, hence we shall bring a number of them below.

The weight function of a system operating according to formula (12-25) can be defined by juxtaposing this equation and the standard equation of integral coupling (2-49). Coefficient 1/T in Eq. (12-25) can be regarded as the weight function sought for if, in order to coordinate the limits of integration (0 - t and 0 - T), we bound its existence domain by the interval 0-T, as shown in Fig. 12-6,a and expressed by the formula

$$w(t) = \frac{1}{T}\{1(t) - 1(t - T)\}.$$ (12-26)

The system's transient function is found by integrating the weight function. It is shown in diagram b of this figure and is expressed by the formula

$$h(t) = \frac{1}{T}\{t \cdot 1(t) - (t - T) \cdot 1(t - T)\}.$$ (12-27)
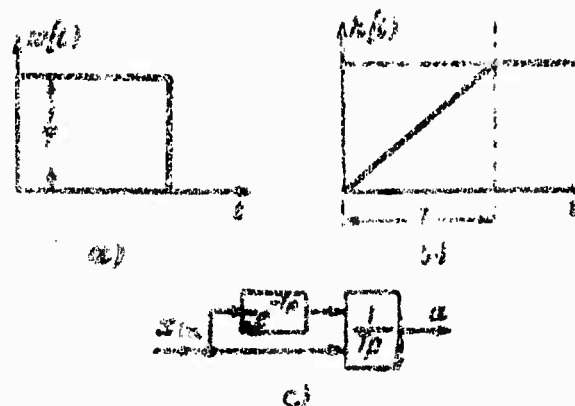
Fig. 18-6. Time responses and block diagram of a filter with mean square averaging of the effective signal over a limited interval.

Over the interval 0-T it has a constant slope, whereas further on it runs horizontally.

The block diagram is constructed according to the OTF which is a transform of the weight function

$$\Phi(p) = \frac{1 - e^{-pT}}{Tp}.$$

(18-28)

We can see from the formula that the block diagram comprises delay and integrating components shown in diagram c of the same figure.

Formation of the transient function can be easily followed on the diagram. In fact, if we feed into the circuit a unit signal it produces at the output of the integrating component a uniform growth of the output value at a rate 1/T equal to the tangent of the dip angle of diagram b. Further, after T sec the delay

component also lets through the unit signal but with inverted signs so that at the output of the integrating element there is a zero signal and integration ceases while the output value remains at unit level $h_{st} = 1/T$ $T = 1$.

The block diagram can also be drawn in a different fashion by transforming the circuits through structural analysis.

In analyzing the circuits in Fig. 12-3,c it was noted that open systems with integrating elements may, under service conditions, turn out to be unstable. Thus, e.g., zero drift of the integrating amplifier results in the distortion of the horizontal portion of the transfer characteristic investigated, and so on.

The system becomes more stable if we close it by the method shown in Fig. 12-3,d. At any rate, we can easily obtain that the steady-state value of the transient function be equal to unity owing to unit negative follow-up. Equivalence of the transient function over the inclined portion can be attained approximately by replacing the straight line by exponents. This will be circumstantially investigated in Section 12-4 below.

The <u>frequency-response characteristics</u> of the smoothing system are found from the transfer function (12-28):

$$\Phi(j\omega) = \frac{1}{\omega T} \left[\sin \omega T - j(1 - \cos \omega T) \right], \qquad (12\text{-}29\text{a})$$

the amplitude-frequency characteristic is

$$A(\omega) = \frac{1}{\omega T} \sqrt{\sin^2 \omega T + (1 - \cos \omega T)^2} = \frac{\sin \frac{\omega T}{2}}{\frac{\omega T}{2}};$$
(12-29 b)

The phase characteristic over the frequency interval $0 - (2\pi/T)$ is

$$\varphi(\omega) = -\text{arctg}\, \frac{1 - \cos \omega T}{\sin \omega T} = -\frac{\omega T}{2},$$
(12-29 c)

The last two characteristics are shown in Fig. 12-7. The amplitude-frequency characteristic gives a clear idea of the smoothing of purely sinusoidal disturbances at various frequencies.
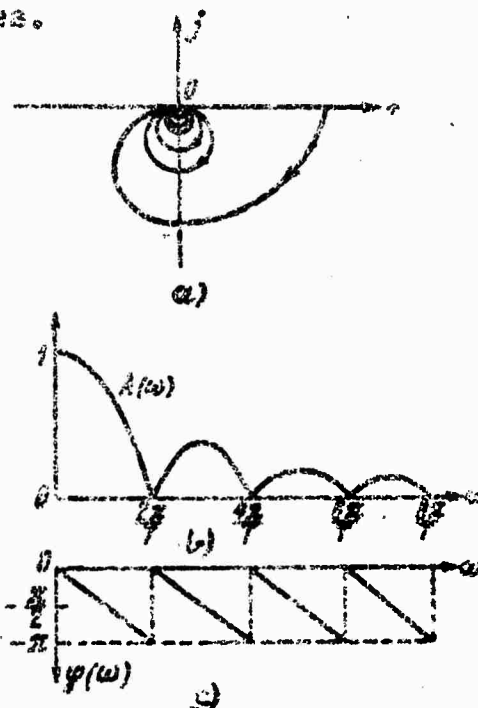
Fig. 12-7. Frequency characteristics of a filter with mean-square averaging over a limited interval

If we synthesize a system of the closed type, then the equivalent characteristics of its direct circuit are found in analogy with (12-3):

$$W(j\omega) = \frac{\Phi(j\omega)}{1 - \Phi(j\omega)} = \frac{1 - e^{-j\omega T}}{j\omega T - 1 + e^{-j\omega T}} \cdot$$

$$(12\text{-}30)$$

For calculation we can use the nomograms given in Chapter 4 writing transformation (12-30) in the form $-W(j\omega) = -\left[\Phi(j\omega)\right]/(1 + \left[-\Phi(j\omega)\right]$ and considering phase shift at $\widetilde{\Pi}$ in the input and output values.

We should aim at achieving these characteristics when synthesizing systems according to the general method expounded under No. 1 of the present Chapter.

Considerations regarding the choice of the time interval. The greater the time interval T, the better the filtration of sign-changing disturbances from a steady effective signal since according to (12-25) there takes place a mutual damping of sign-changing disturbances. This fact can also be easily noted from the amplitude-frequency characteristic (12-29 b) according to which sinusoidal disturbances are smoothed in proportion to the quantity $1/\omega T$.

Yet, the smoothing time T is also the time required by the system to become operating, as we can see from the example of the transient function. Only upon expiration of time T from the moment the system has been switched on, the result corresponds to the sought for value a. Thus, as the smoothing interval increases, the response of the system is slowed down.

If the operating conditions of a system are such

984

that it can be switched on in advance and the long time re-
quired by it to become operating do not affect its
performance, we have still to consider the errors of
the hypothesis proper in the form of a polynomial with
a limited number of terms. Thus, e.g., in Fig. 12-5 we
see that by increasing the smoothing interval the hypothesis
of the constancy of the effective signal will lead to an
error in the moving coordinate since the encompassing
of the dropping portion by the integrating band (12-25)
reduces the output value and the current instant of time,
which is not justified by the subsequent course of the
process. These considerations bound the smoothing in-
terval.

In the approximate synthesis of a closed system with
prescribed power and actuating elements of the direct
circuit minimum time is frequently due to certain pro-
perties (constants of time) of the unalterable component.

3. Mean-Square Smoothing Assuming a Uniform Change of
   the Effective Signal Over A Prescribed Time Interval.

The realization of the random process close to the
hypothesis formulated is shown in the initial portion of
Fig. 12-5.

The mathematical formation of the hypothesis over
the interval T counted from the current instant back-
ward, i.e. from $\tau = 0$ to $\tau = T$, is as follows:

$$x_n = a - b\tau. \qquad (12\text{-}31)$$

The square integral criterion

$$I_{2T} = \int_0^T [x(t-\tau) - a + b\tau]^2 \, d\tau \qquad (12\text{-}32)$$

gives an estimate of the approximation of the recti-
linear hypothesis to the actual curve over the interval
0-T.

We can easily see that the minimum of I_{2T} is associated
both with the choice of the final value of the coordinate
according to hypothesis a and with the choice of the
slope of straight line b, i.e., with a choice of the
rate of variation of the coordinate according to the
hypothesis. The required analytical conditions for the
minimum of a function with two variables

$$\frac{\partial I_{2T}}{\partial a} = 0 \text{ and } \frac{\partial I_{2T}}{\partial b} = 0$$

lead to the equations

$$\frac{\partial I_{2T}}{\partial a} = -2\int_0^T [x(t-\tau) - a + b\tau]\, d\tau = 0;$$

$$\frac{\partial I_{2T}}{\partial b} = +2\int_0^T [x(t-\tau) - a + b\tau]\, \tau \, d\tau = 0.$$

It is obvious that the function I_{2T} investigated has
no maximum, and the conditions set forth are also suffi-
cient for the determination of the minimum.

We single out the terms which can be integrated in the
preceding equations, leave the more complex functions
under the integral sign and obtain

$$aT - \frac{bT^2}{2} = \int_0^T x(t-\tau)\,d\tau;$$

$$\frac{aT^2}{2} - \frac{bT^3}{3} = \int_0^T x(t-\tau)\,\tau\,d\tau.$$

We solve this system of equations with two unknowns a and b by the method of determinants

$$a = \frac{\begin{vmatrix} \int_0^T x(t-\tau)\,d\tau & -\frac{T^2}{2} \\[2mm] \int_0^T x(t-\tau)\,\tau\,d\tau & -\frac{T^3}{3} \end{vmatrix}}{\begin{vmatrix} T & -\frac{T^2}{2} \\[2mm] \frac{T^2}{2} & -\frac{T^3}{3} \end{vmatrix}} =$$

$$= \frac{-T^2\left[\frac{T}{3}\int_0^T x(t-\tau)\,d\tau - \frac{1}{2}\int_0^T x(t-\tau)\,\tau\,d\tau\right]}{-\frac{T^4}{12}};$$

$$b = \frac{\begin{vmatrix} T & \int_0^T x(t-\tau)\,d\tau \\[2mm] \frac{T^2}{2} & \int_0^T x(t-\tau)\,\tau\,d\tau \end{vmatrix}}{-\frac{T^4}{12}} =$$

$$= \frac{-6\left[2\int_0^T x(t-\tau)\,\tau\,d\tau - T\int_0^T x(t-\tau)\,d\tau\right]}{T^4}.$$

The final results are conveniently written in the following form where all the constant numbers are under the integral sign:

$$a = \int\limits_0^T \frac{4T - 6\tau}{T^2} x(t - \tau)\, d\tau; \tag{12-33}$$

$$b = \int\limits_0^T 6\frac{T - 2\tau}{T^3} x(t - \tau)\, d\tau. \tag{12-34}$$

The first formula serves as the mathematical basis for a reproducing system smoothing disturbances according to the hypothesis of uniform effective signal variation; the second formula is the basis for constructing a differentiating system operating according to the same hypothesis. Let us now take a look at the technical features of these systems.

Reproducing System. The system's weight function exists only within the limit from $\tau = 0$ to $\tau = T$, and its time curve is shown in Fig. 12-8.a. The analytical expression of the weight function has in its base the value of the integrand of formula (12-33), but it is somewhat complicated owing to the need of reflecting the limited boundaries of the representation. To this end graph a is conveniently represented in the form of a sum of four elementary graphs, viz., stepped 1 and linearly dropping 2 functions without delay, and stepped 3 and linearly increasing 4 functions with delay according to the formula

$$w(t) = \frac{2}{T}\left\{\left(2 - 3\frac{t}{T}\right)\cdot 1(t) + \right.$$

$$\left. + \left(1 + 3\frac{t-T}{T}\right)1(t-T)\right\}.\qquad (12\text{-}35)$$

a)

b)

c)
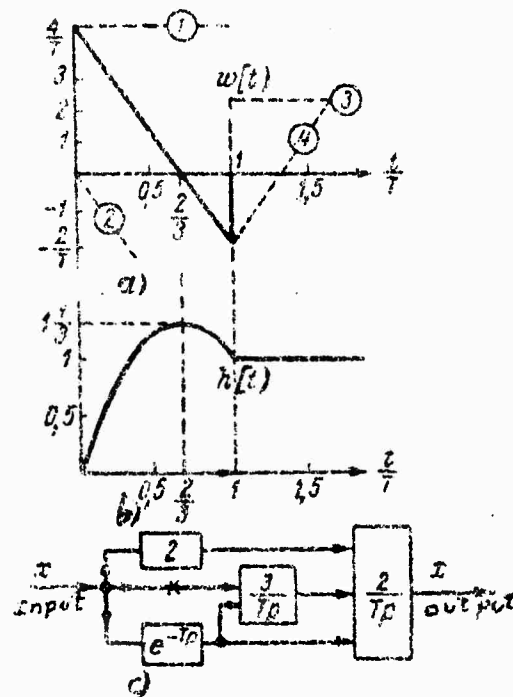
Fig. 12-8. Time responses and block diagram of a filter with mean-square moving over a limited interval according to the hypothesis of uniform effective signal variation.

The transient function obtained from integrating the weight function has the following analytical expression:

$$h(t) = \left\{\left[4\frac{t}{T} - 3\left(\frac{t}{T}\right)^2\right]\cdot 1(t) + \right.$$

$$\left. + \left[2\frac{t-T}{T} + 3\left(\frac{t-T}{T}\right)^2\right]\cdot 1(t-T)\right\}\qquad (12\text{-}36)$$

and is shown in diagram b in the same Figure.

The transient function has a peak at the instant

$t_m/T = 2/3$ and amounts to $h_m = 4/3 = 1.33$. Thus, a re-
producing system optimal from the viewpoint of disturbance
smoothing has a relatively high overshoot which amounts to
33%.

The transfer function is derived from the weight
function

$$\Phi(p) = \left\{ 2 - \frac{3}{Tp} + \left(1 + \frac{3}{Tp}\right) e^{-Tp} \right\} \frac{2}{Tp}. \quad (12-37)$$

The block diagram c is constructed according to the
transfer function with a minimum number of elements.

On the block diagram we can easily follow the passage
of signals through the system. For example, a unit input
pulse passes during an instant of time $t = 0$ only along
the upper line, and according to Fig. 2-2, b the integrating
element yields a jump of the output coordinate $4/T$. At
the same time at the output of the other integrating ele-
ment there is a jump $-3/T$, that is, we establish immediate-
ly the rate of output value variation which, considering
the gain of the principal integrating element, is equal
to $-6/T^2$. Thus, the output value changes in accordance
with diagram a. After T sec the delay component lets
through the input pulse thus bringing about a jump of the
output coordinate $2/T$; at the same time the output of the
second integrating element is cancelled owing to which
the coordinate and its variation rate take on zero values
at the output. Passage of the transient function can be
observed in a like fashion.

The block diagram obtained can be realized as an
electronic model with a special delay component and

Integrators. In actually operating control systems it is again expedient to pass to the closed circuit on account of the approximate realization of the system. To this end we bring below the frequency-response characteristics of an optimum system as well as those of the direct path of a closed system obtained in the same way as formula (12-29):

Phase-amplitude characteristic:

$$\Phi(j\omega) = \frac{2}{j\omega T}\left[2 + \frac{j\beta}{\omega T} + \left(1 - \frac{j\beta}{\omega T}\right)e^{-j\omega T}\right];$$

(12-38 a)

Amplitude-frequency characteristic (Fig. 12-9):

$$A(\omega) = \frac{2}{\omega T} \times$$

$$\times \sqrt{5 + \frac{18}{\omega^2 T^2} + 2\sqrt{\left(4 + \frac{9}{\omega^2 T^2}\right)\left(1 + \frac{9}{\omega^2 T^2}\right)} \times}$$

$$\times \cos\left(\arctan\frac{3}{2\omega T} + \arctan\frac{3}{\omega T} + \omega T\right);$$

(12-38 b)
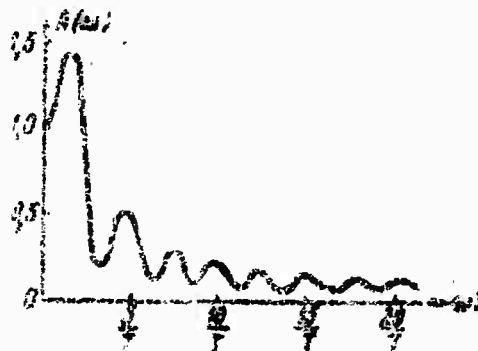
Fig. 12-9. Amplitude-frequency characteristic of a smoothing filter for a uniformly changing effective signal (according to hypothesis).

Phase characteristic:

$$\varphi(\omega) = \operatorname{arctg} \frac{\operatorname{Im} \Phi(j\omega)}{\operatorname{Re} \Phi(j\omega)} ; \qquad (12\text{-}38\ c)$$

Phase-amplitude characteristic (12-30) of the direct path of a standard closed control system

$$W(j\omega) = \frac{2\left[2 + j\frac{3}{\omega T} + e^{-j\omega T}\left(1 - j\frac{3}{\omega T}\right)\right]}{j\omega T - 2\left[2 + j\frac{3}{\omega T} + e^{-j\omega T}\left(1 - j\frac{3}{\omega T}\right)\right]} . \qquad (12\text{-}39)$$

It is useful to note that control systems designed according to the hypothesis of uniformly changing effective signals will, of course, control with the greatest accuracy also a hypothetically steady signal. If, instead, we use a simple system for more complex signals, systematic errors will be unavoidable.
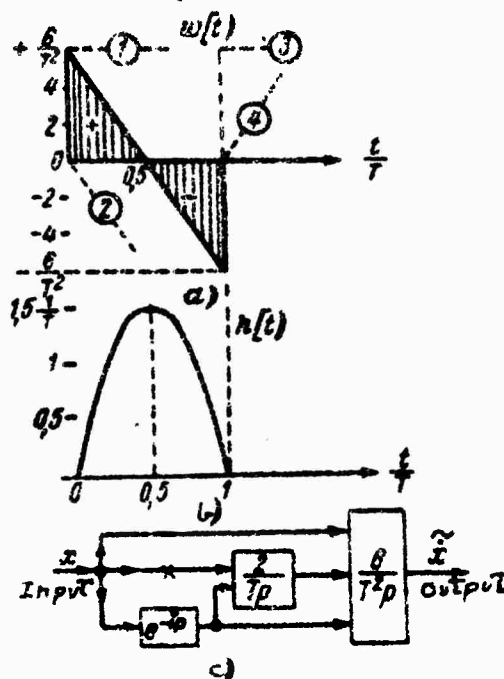
Fig. 12-10. Time responses and block diagram of a differentiating-smoothing filter for uniformly changing effective signal (according to hypothesis).

Differentiation system. Systems operating according to (12-34) have a weight function existing over a limited time interval and shown in Fig. 12-10,a. The analytic expression of the function is

$$w(t) = \frac{6}{T^2}\left\{\left[1 - 2\frac{t}{T}\right]\cdot 1(t) + \right.$$
$$\left. + \left[1 + 2\frac{(t-T)}{T}\right]\cdot 1(t-T)\right\}. \qquad (12-40)$$

Each term of this function may be regarded as an individual elementary, initial (1, 2) and delay (3, 4) function in accordance with the numbers applied to the dashed straight lines shown in the figure.

For the transient function we bring diagram b and the following formula:

$$h(t) = \frac{6}{T}\left\{\left[\frac{t}{T} - \left(\frac{t}{T}\right)^2\right]\cdot 1(t) + \right.$$
$$\left. + \left[\frac{t-T}{T} + \left(\frac{t-T}{T}\right)^2\right]\cdot 1(t-T)\right\}. \qquad (12-41)$$

Of course it ends with zero since differentiation of a constant signal yields a zero result, but in smoothing systems this result is attained only after a lapse of time T. The final zero value of the transient function depends upon the zero value of the graph area of weight function a.

With t = T/2 the transient function has a maximum h_m = 3/2T.

The system's transfer function is

$$\Phi(p) = \left\{1 - \frac{2}{Tp} + \left[1 + \frac{2}{Tp}\right]e^{-Tp}\right\}\frac{6}{T^2 p} \qquad (12-42)$$

Its block diagram is shown in Fig. 12-10, c. Here

the operator components are the same as in Fig. 12-8, but the gains are changed.

We follow on the block diagram the formation of the weight function. Input pulse at the output of the principal integrating element brings about a jump of $+ (6/T^2)$ as well as a jump at the output of the second integrator of $-2/T$ which, converted to the output value rate, is equal to $-12/T^3$. It is with this deviation from the value $6/T^2$ that the output value begins to change according to diagram a. After a lapse of T sec the pulse is repeated by the delay component, the output coordinate and the rate of its change being reduced to zero.

The frequency responses of the differentiating-smoothing system are as follows:

Phase-amplitude characteristic

$$\Phi(j\omega) = \frac{-j6}{\omega T^2}\left[1 + I\frac{2}{\omega T_s} + e^{-j\omega T}\left(1 - \frac{2j}{\omega T}\right)\right];$$

$$(12\text{-}43 \text{ a})$$

Amplitude-frequency characteristic

$$A(\omega) = \frac{12}{\omega T^2}\sqrt{1 + \frac{4}{\omega^2 T^2}}\cos\left(\text{arctg}\frac{2}{\omega T} + \frac{\omega T}{2}\right).$$

$$(12\text{-}43 \text{ b})$$
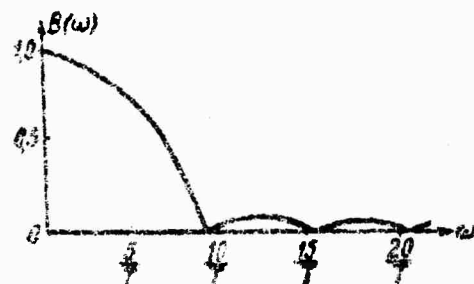
Fig. 12-11. Rate B(w) amplitude-frequency characteristic of a differentiating-smoothing filter
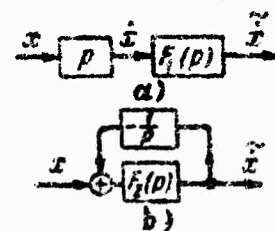
Fig. 12-12. Block diagrams of a differentiating-smoothing system.

394

Figure 12-11 shows a characteristic

$$B(\omega) = \frac{A(\omega)}{\omega} = \frac{12}{\omega^2 T^2} \sqrt{1 + \frac{4}{\omega^2 T^2}} \times$$

$$\times \cos\left(\text{arctg}\,\frac{2}{\omega T} + \frac{\omega T}{2}\right),$$

(12-43 c)

more interesting for a differentiating system from a physical viewpoint. This characteristic represents the ratio of output amplitude (the output being measured in terms of rate) to the amplitude of disturbance variation rate at the input ωA_{in}.

When passing from the structure of optimum systems to real closed-loop systems with increased operational stability we can take out seuprately the differentiating component, as shown in Fig. 12-12, a, and supplement it with a smoothing system with transfer function $F_1(p)$, $F_1(0)$, being equal to 1. Then we have the instantaneous value of derivative x at the output of the differentiating component, and the smoothed value of derivative $\dot{x}$ at the output of the smoothing system.

Design control of a smoothing system can be carried out by approaching the frequency-response characteristics

$$F_1(j\omega) = \frac{\Phi(j\omega)}{j\omega}.$$

If the smoothing portion is closed , then with the aid of the frequency-response characteristic $F_1(j\omega)$ obtained we can following the methods expounded above /see formula (12-30)7 find the frequency-response characteristic of the direct circuit. Of course the synthesis of the system can be carried out by approaching the optimum not only in the region of frequency-response curves but

also at transient functions.

Systems with block diagram b shown in the same Figure also have differentiating-smoothing properties. With a prescribed frequency characteristic for the entire system (12-43 a) the characteristic of the direct circuit is determined by the formula

$$F_2(j\omega) = \frac{j\omega \Phi(j\omega)}{j\omega - \Phi(j\omega)} \; .$$

It is precisely for this characteristic that we should strive in the synthesis of similar systems.

Predictor systems. If a system is assigned the task of reproducing not the current value of the input coordinate but its probable value after a prescribed constant time interval τ_{pr}, then, as noted in Section 10-1, the working formula of the system must be written

$$x_y = x + \dot{x}\tau_{pr}$$

if the input signal changes uniformly.

Under disturbance conditions the predicted value has to be found only for the effective signal, hence the preceding formula takes the form:

$$\tilde{x}_y = \tilde{x} + \dot{\tilde{x}}\tau_{pr} \qquad (12\text{-}44)$$

With greater prediction time it is particularly important to have well-smoothed rate values.

Above we had the block diagrams of the smoothing and differentiating systems; if their transfer functions are conditionally denoted by $\tilde{1}$ and $\tilde{p}$ then the block diagram of the predictor system takes the form shown in Fig. 12-13,a.
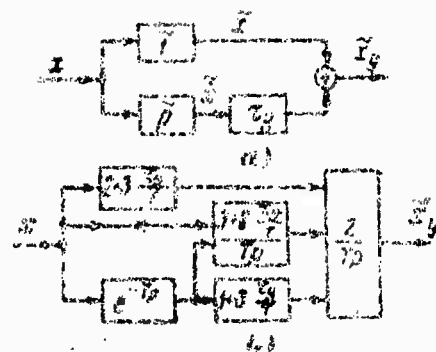
Fig. 12-13. Block diagrams of predictor system for uniformly changing effective signal.

It is expedient to synthesize the real system according to this block diagram if it is required to have a separate prediction time unit for operational, economical or design reasons.

If such a requirement is not advanced, then, bearing in mind the fact that the operator elements coincide in the circuits shown in Figs. 12-8 and 12-10, only one specimen of such elements is required and we need only changing the gain in the corresponding arms, i.e., superimpose the block diagram in Fig. 12-8 on that in Fig. 12-10 with a scale increased τ_{pr} times. Then we obtain the diagram b shown in Fig. 12-13.

The aggregate transfer function of the predictor system is derived analytically from formulas (12-37) and (12-42):

$$\Phi(p) = \left[2 - \frac{2}{Tp} + \left(1 + \frac{3}{Tp}\right) e^{-Tp} \right] \frac{2}{Tp} -$$

$$- \left[1 - \frac{2}{Tp} + \left(1 + \frac{2}{Tp}\right) e^{-Tp} \right] \frac{6}{Tp}$$

997

and can be reduced to a form convenient for comparison with the block diagram in Fig. 12-13, b:

$$\Phi(p) = \left\{ 2 + \frac{3\tau_y}{T} - \frac{3 + 6\frac{\tau_y}{T}}{Tp} + \right.$$

$$\tau_y = \tau_{pr}$$

$$+ \left[1 + 3\frac{\tau_y}{T} + \frac{3 + 6\frac{\tau_y}{T}}{Tp} \right] e^{-Tp} \left. \right\} \frac{2}{Tp} . \qquad (12\text{-}45)$$

As is seen from block diagram a, the transient and frequency characteristics of the predictor system are obtained by summing characteristics already obtained earlier taking into consideration coefficient τ_{pr}.

Automatic storage units. If a system has the moving coordinate and the rate determined earlier, once interval T has elapsed we may cease to receive information regarding the input signal and reproduce it from the data $\tilde{x}(t_o)$ and $\dot{\tilde{x}}(t_o)$ produced by the storage system according to the formula for the linearly changing effective signal

$$x_A(t) = \tilde{x}(t_o) + \dot{\tilde{x}}(t_o)(t - t_o) \dots \qquad (12\text{-}46)$$

According to this formula we design the structural-operative diagram in Fig. 12-14 which, along with operator elements, has also an equipment for switching networks and control as well as two storage elements S.

Normal operation (reproduction of the input coordinate) is performed by the smoothing system $\tilde{1}$, the remaining networks are in this case disconnected with the output; the integrating element is enclosed by a follow-up with great gain which eliminates the initial conditions
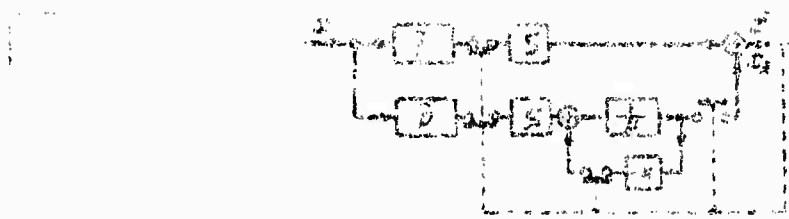
Fig. 18-14. Structural-operative diagram of an automatic
storage device with uniformly changing effective signal

on the element's output. Normal operation lasts no less
than the smoothing time interval after the expiration of
which we have the correct value of the effective signal
at the system's output, and the smoothed rate of its
change at the output of element p which "charges" the
rate storage element.

Automatic conditions are characterized by a posi-
tion of contact opposite to that shown in the Figure.
The connection of the system with the input signal is
severed, the integrating element is released of feed-
back and receives as a stepped input the prepared rate
value $\dot{x}$ by which the second term of formula (18-16) begins
to perform immediately. The first term of that formula
is taken off the storage coordinate element.

Message to the automatic coordinate rather than
to the actual one is performed in those systems where a
temporary suppression of the effective signal by dis-
turbances is possible; then the automatic device makes
it possible not to stop the system's operation and to
prepare it for the subsequent reception of the effec-
tive signal when it arises again.

With a stationary useful signal it is occasionally

expedient to pass to the automatic coordinate if the disturbance level has a tendency to rise. One should bear in mind, however, the defficiencies of the hypothesis put into the automatic device, control the difference between the input and the automatic output values periodically eliminating this difference by means of corrections or by repeatedly taking back the system to normal operating conditions. As a storage element conserving at the output the last value prior to the switching off of the input it is convenient to use integrating elements of various modifications.

4. Mean-Square Smoothing and Complex Hypotheses Regarding Changes in the Effective Signal Over a Prescribed Time Interval

A more complicated hypthesis, provided it maintains the form of the polynomial (12-22) as before, does not change the synthesis method of smoothing system. Beginning with equation (12-31) these considerations hold true for hypotheses of any complexity.

Let us investigate, e.g., the hypothesis of equally accelerated effective signal variation of a prescribed time interval. By introducing variable τ this hypothesis can be written

$$x_h = a - b\tau - \frac{c\tau^2}{2!} . \tag{12-47}$$

The square criterion

1000

$$I_{2f} = \int_0^T \left[x(t-\tau) - a + b\tau + \frac{c\tau^2}{2!} \right]^2 d\tau \qquad (12\text{-}48)$$

is now a function with three variables, a, b, and c, and the conditions for its minimum are determined for the three partial derivatives $\partial I_{2f}/\partial a$, $\partial I_{2f}/\partial b$ and $\partial I_{2f}/\partial c$. being equal to zero. These conditions are written in the form of a system of three equations:

$$aT - \frac{bT^2}{2} - \frac{cT^3}{2\cdot 3} = \int_0^T x(t-\tau)\, d\tau;$$

$$\frac{aT^2}{2} - \frac{bT^3}{3} - \frac{cT^4}{2\cdot 4} = \int_0^T x(t-\tau)\, \tau\, d\tau;$$

$$\frac{aT^3}{3} - \frac{bT^4}{4} - \frac{cT^5}{2\cdot 5} = \int_0^T x(t-\tau)\tau^2\, d\tau.$$

The solutions take the form:

$$a = \int_0^T \left(\frac{9}{T} - \frac{36\tau}{T^2} + \frac{30\tau^2}{T^3} \right) x(t-\tau)\, d\tau;$$

$$b = \int_0^T \left(\frac{36}{T^2} - \frac{192\tau}{T^3} + \frac{180\tau^2}{T^4} \right) x(t-\tau)\, d\tau;$$

$$c = 2\int_0^T \left(-\frac{30}{T^2} + \frac{180\tau}{T^4} - \frac{180\tau^2}{T^5} \right) x(t-\tau)\, d\tau.$$

On the basis of these equations we can synthesize the following systems: smoothing, differentiating-smoothing and double differentiating-smoothing (that is, a system determining the effective signal acceleration).

Weight Functions and OTF of Smoothing Filters

Table 12-1

① serial number of hypothesis	② output value	③ weight function	④ OTF	⑤ noise dispersion σ^2
0	x	$\frac{1}{T}\{1[t]-1[t-T]\}$	$\frac{1}{pT}(1-e^{-pT})$	$\frac{N^2}{T}$
1	x	$\frac{2}{T}\left\{\left(2-3\frac{t}{T}\right)\cdot1[t]+\left(1+3\frac{t-T}{T}\right)\cdot1[t-T]\right\}$	$\frac{2}{pT}\left[2-\frac{3}{pT}+e^{-pT}\left(1+\frac{3}{pT}\right)\right]$	$\frac{4N^2}{T}$
	$\dot{x}$	$\frac{6}{T^2}\left\{\left(1-2\frac{t}{T}\right)\cdot1[t]+\left[1+\frac{2(t-T)}{T}\right]\cdot1[t-T]\right\}$	$\frac{6}{pT^2}\left[1-\frac{2}{pT}+e^{-pT}\left(1+\frac{2}{pT}\right)\right]$	$\frac{12N^2}{T^3}$
2	x	$\frac{3}{T}\left\{\left(3-12\frac{t}{T}+10\frac{t^2}{T^2}\right)\cdot1[t]-\left[1+8\frac{(t-T)}{T}+10\frac{(t-T)^2}{T^2}\right]\cdot1[t-T]\right\}$	$\frac{3}{pT}\left[3-\frac{12}{pT}+\frac{20}{p^2T^2}-e^{-pT}\left(1+\frac{8}{pT}+\frac{20}{p^2T^2}\right)\right]$	$\frac{9N^2}{T}$
	$\dot{x}$	$\frac{12}{T^2}\left\{\left(3-16\frac{t}{T}+15\frac{t^2}{T^2}\right)\cdot1[t]-\left[2+14\frac{t-T}{T}+15\frac{(t-T)^2}{T^2}\right]\cdot1[t-T]\right\}$	$\frac{12}{pT^2}\left[3-\frac{16}{pT}+\frac{30}{p^2T^2}-e^{-pT}\left(2+\frac{14}{pT}+\frac{30}{p^2T^2}\right)\right]$	$\frac{192N^2}{T^3}$
	$\ddot{x}$	$\frac{60}{T^3}\left\{\left(-1+6\frac{t}{T}-6\frac{t^2}{T^2}\right)\cdot1[t]+\left[1+6\frac{(t-T)}{T}+6\frac{(t-T)^2}{T^2}\right]\cdot1[t-T]\right\}$	$\frac{60}{pT^3}\left[-1+\frac{6}{pT}-\frac{12}{p^2T^3}-e^{-pT}\left(-1-\frac{6}{pT}-\frac{12}{p^2T^2}\right)\right]$	$\frac{720N^2}{T^5}$

Key: 1) serial number of hypothesis; 2) output value;
3) weight function; 4) OTF; 5) noise dispersion.

$$\tilde{x}_{y'} = \tilde{x} + \tilde{\dot{x}}\tau_{p,r} + \tilde{\ddot{x}}\frac{\tau_{pr}^2}{2!}; \qquad (12\text{-}49)$$

Accordingly, its block diagram is also more complex.

The automatic storage device must operate in analogy with formula (12-46) according to the following equation:

$$x_{A} = \tilde{x}(t_{o}) + \tilde{\dot{x}}(t_{o})(t - t_{o}) + \tilde{\ddot{x}}(t_{o})\frac{(t - t_{o})^2}{2!}.$$

$$(12\text{-}50)$$

Its structural-operative diagram must now have three storage devices for the coordinate, rate and acceleration, and three integrators for rate integration and double acceleration integration.

5. Systematic Errors of Optimum Smoothing Filters

If the input signal is disturbance-free and has only a regular component exactly coinciding with the hypothesis inserted in the system, the minimum of the integral-square criterion for the smoothing filter will be attained when the input and output processes coincide, i.e., when the integral criterion equals zero: $I_{2T} = 0$.

Since this minimum condition is utilized in the following for designing linear reproducing systems, these optimum filters have essentially a zero systematic error. When synthesizing on the basis of the method expounded, this feature of a system is attained, so-to-speak, automatically.

Systematic errors arise when the input signal is changed according to a sign more complex than the hypothesis inserted in the filter, or in the case of various deviations from optimum characteristics. It is computed by the usual methods (see Chapter 10).

12-4. Synthesis of Computing Filters in Parallel Structures

The synthesis method discussed in Section 12-3, based on obtaining optimum block diagrams and characteristics, makes it possible to design a system which must necessarily contain a delay component, and which has an open structure. The exact realization of such a circuit is apparently expedient only for certain devices containing computing units, while in most cases only an approximate synthesis can be obtained which despite some deviations from optimum characteristics yields elements and block diagrams more convenient for the actual realization of systems.

It must be noted, however, that if deviations from exact conditions of minimum mean-root-square error are permissible in those cases where the magnitude of that error in the function of the system parameters changes but slightly, the hypothesis itself, the time interval T and other factors are assigned approximately, (and such conditions are prevailing in practice), deviations from the principle of obtaining a zero systematic error may not be regarded as permissible.

However, for complex laws of input coordinate

variations, especially in those cases where there is
assigned the task of complete investigation of these
laws, e.g., the successive solution of the problem of
prediction, the automatic reproduction of data available
in the system's "memory" etc., the conditions for ob-
taining a zero systematic error determine a number of
restrictions applied to the characteristics of the syn-
thesized system.

As was shown in Section 12-3, in the case of exact
design control these conditions are automatically rea-
lized by optimum filters; in the case of approximate
synthesis they have to be considered separately.

1. Conditions for Obtaining a Zero Systematic Error

This problem was already investigated in Chapter 10
but we come back on it in order to give a number of
additions. Suppose the input process contains only
the regular component expressed by the power polynomial
(12-22). If the linear system has the transfer function
$\Phi(p)$, then the output process is defined by formula
(10-1):

$$x_{ou\overline{t}} = \Phi(0)\, x_{u} + \overline{\Phi}(0)\, \dot{x}_{in} +$$
$$+ \frac{\Phi'(0)}{2!}\, \ddot{x}_{in} + \frac{\Phi''(0)}{3!}\, \dddot{x}_{in} + \ldots$$

For a faultless reproduction of the coordinate it
is obviously necessary that conditions

$$\Phi(0) = 1; \ \Phi^{(i)}(0) = 0; \ i \neq 0.$$

be fulfilled.

For a faultless reproduction of any derivative, e.g. the i-th, conditions

$$\frac{\Phi^{(i)}(0)}{i!} = 1; \quad \Phi^{(i)}(0) = 0; \; i \neq 1.$$

must be fulfilled.

These conditions are given in an expanded form in the first half of Table 12-2. It is important to note that the number of restricting conditions is equal to the number of terms of the power polynomial (the hypothesis), including the free term.

Occasionally it is more convenient to refer these bounding conditions to the system's weight function rather than to the OTP. The appropriate recalculation is carried out on the basis of operator relations known from the foregoing.

Suppose we have $\Phi(p) \rightarrow w(t)$; $\Phi'(p) \rightarrow -t w(t)$, etc. By integrating with a variable upper limit in the time range we obtain the transforms:

$$\frac{1}{p} \Phi(p) \div \int_0^t w(t) \, dt;$$

$$\frac{1}{p} \Phi'(p) \div - \int_0^t w(t) \, t \, dt.$$

The integrals on the right-hand side of the relation are functions of time. To find their boundary with $t \rightarrow \infty$ it suffices to apply the theorem of the connection of the function limit with its transform, which yields:

Table 12-2

Limitation Imposed Upon the OTF and the Weight Function of a Linear Filter Faultlessly Reproducing the Input Signal and its Derivatives

(1)	(2) Ограничения в передаточной функции			(3) Ограничения в весовой функции		
x	$\Phi(0)=1$	$\Phi'(0)=0$	$\Phi''(0)=0$	$\int_0^\infty w(t)\,dt=1$	$\int_0^\infty w(t)\,t\,dt=0$	$\int_0^\infty w(t)\,t^2\,dt=0$
x .	$\Phi(0)=0$	$\Phi'(0)=1$	$\Phi''(0)=0$	$\int_0^\infty w(t)\,dt=0$	$\int_0^\infty w(t)\,t\,dt=-1$	$\int_0^\infty w(t)\,t^2\,dt=0$
x :	$\Phi(0)=0$	$\Phi'=2!$	$\Phi''(0)=0$	$\int_0^\infty w(t)\,dt=0$	$\int_0^\infty w(t)\,t^2\,dt=2!$	$\int_0^\infty w(t)\,t^2\,dt=0$
x :;	$\Phi(0)=0$	$\Phi'=0$	$\Phi''(0)=3!$	$\int_0^\infty w(t)\,dt=0$	$\int_0^\infty w(t)\,t^3\,dt=0$	$\int_0^\infty w(t)\,t^3\,dt=-3!$

$$\Phi(0) = \int_0^\infty w(t)\,dt; \quad \Phi'(0) = -\int_0^\infty w(t)\,t\,dt.$$

Thus, the values of the OTF and its derivatives for p = 0 are quantitatively equal to the weight function graph area , the weight function "first-order moment" $(w\left[\frac{t}{s}\right]t)$, etc., respectively.

In accordance with the problem being solved, these functions or moment areas must be equal to zero or one of them must be equal to a constant number, as this is tabulated in the second half of the Table.

Table 18-3 gives a concrete definition of the general conditions (10-47) - (10-49) derived earlier.

The data obtained therein can be fully utilized for the third-order hypothesis. For hypotheses of lower order the number of input parameters to be determined as well as the number of restrictions decrease, hence the size of the Table decreases, as is shown by the angular lines.

We can easily check that for optimum systems discussed in Section 12-3 all of these restrictions are actually fulfilled automatically.

2. Synthesis of a Filter of a Parallel Network with Preset Types of Elements

We investigate the OTF of a filter to be synthesized consisting of the sum of several partial transfer functions with variable coefficients:

$$\Phi(p) = K_1 f_1(p) + K_2 f_2(p) + K_3 f_3(p) + \ldots \quad (12\text{-}51)$$

The parallel network corresponding to this formula is shown in Fig. 12-15. To solve the synthesis problem which in the given case amounts to determining the coefficients K_i we must have a number of partial functions equal to the number of the terms of the hypothesis, and we must ensure the linear independence of all the partial functions.
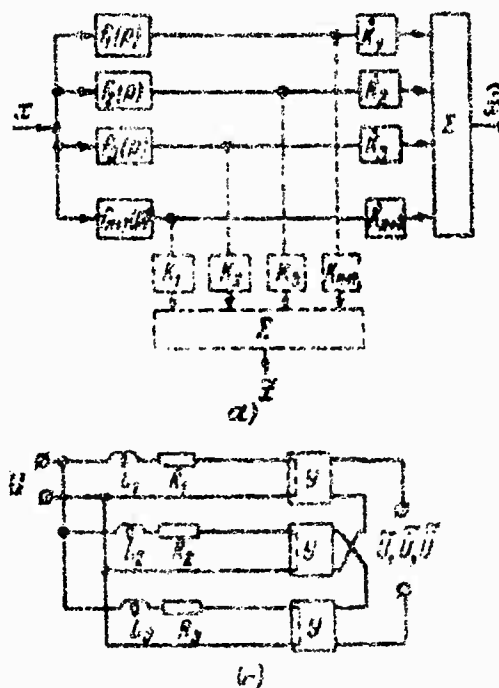
Fig. 12-15. Parallel networks of a smoothing and differentiating-smoothing filter synthesized from preset elements.

To determine the coefficients of partial transfer functions we use the restrictions applied to systems with zero systematic errors. Suppose, e.g., the system is designed to determine the rate $\dot{x}$ of the input process reduced to the second-order hypothesis (equally accelerated motion). From the second row of Table 12-2 we write out the first three bounding conditions in accordance with the order of the hypothesis, and represent the transfer function in the form of a sum of three partial functions (12-51) whose coefficients are marked with points in order to denote that the system is designed to determine the first derivative of the input law:

$$\dot{K}_1 f_1(0) + \dot{K}_2 f_2(0) + \dot{K}_3 f_3(0) = 0;$$
$$\dot{K}_1 f_1'(0) + \dot{K}_2 f_2'(0) + \dot{K}_3 f_3'(0) = 1;$$
$$\dot{K}_1 f_1''(0) + \dot{K}_2 f_2''(0) + \dot{K}_3 f_3''(0) = 0.$$

The solution of this system of equations with respect to coefficient $\dot{K}_1$ has the form:

$$\dot{K}_1 = \frac{\begin{vmatrix} 0 & f_2(0) & f_3(0) \\ 1 & f_2'(0) & f_3'(0) \\ 0 & f_2''(0) & f_3''(0) \end{vmatrix}}{\begin{vmatrix} f_1(0) & f_2(0) & f_3(0) \\ f_1'(0) & f_2'(0) & f_3'(0) \\ f_1''(0) & f_2''(0) & f_3''(0) \end{vmatrix}}. \qquad (12\text{-}52)$$

For the subsequent coefficients $\dot{K}_2$, $\dot{K}_3$ other columns are replaced in the determinant which we find in the numerator.

Suppose that the partial OTF were chosen in the form of transfer functions of aperiodic elements with different constants of time, i.e.:

$$f_1(p) = \frac{1}{T_1 p + 1}; \quad f_2(p) = \frac{1}{T_2 p + 1};$$

$$f_3(p) = \frac{1}{T_3 p + 1}.$$

Then we have

$$f_1(0) = 1; \qquad f_2(0) = 1; \qquad f_3(0) = 1;$$

$$f_1'(0) = -T_1; \qquad f_2'(0) = -T_2; \qquad f_3'(0) = -T_3;$$

$$f_1''(0) = 2T_1^2; \qquad f_2''(0) = 2T_2^2; \qquad f_3''(0) = 2T_3^2.$$

Formula (12-52) for the partial OTF chosen takes the form:

$$\dot{K}_1 = \frac{-\begin{vmatrix} 1 & 1 \\ 2T_2^2 & 2T_3^2 \end{vmatrix}}{\begin{vmatrix} 1 & 1 & 1 \\ T_1 & T_2 & T_3 \\ T_1^2 & T_2^2 & T_3^2 \end{vmatrix}} =$$

$$= \frac{T_3^2 - T_2^2}{T_1 T_2 (T_2 - T_1) + T_2 T_3 (T_3 - T_2) + T_1 T_3 (T_1 - T_3)}.$$

The aggregate transfer function of a differentiating, smoothing system operating according to the second-order hypothesis, after determination of all the coefficients

is reduced to the form:

$$w(p) = \frac{\frac{T_3^2 - T_1^2}{T_1 p + 1} - \frac{T_3^2 - T_1^2}{T_2 p + 1} + \frac{T_3^2 - T_1^2}{T_3 p + 1}}{T_1 T_3 (T_3 - T_1) - T_2 T_3 (T_3 - T_2) + T_1 T_2 (T_1 + T_3)}.$$

All the characteristics of the system can be constructed according to the transfer function.

If the aperiodic elements have an intrinsic gain m_1, m_2, m_3, it suffices when designing the block diagram of Fig. 12-15, to insert in each arm only the gain missing with respect to rated gain, which we determine by the formula

$$K_{12} = \frac{b_1}{m_1}, \qquad (12-55)$$

Further calculations showed how to obtain a system for determining input signal variation rate; the block diagram for this case is shown in Fig. 12-15, a in the part drawn with solid lines. We can easily see that in designing a moving system which reproduces the input signal maintaining the same hypothesis, we can maintain the same partial OTF merit, changing the coefficients. Since in fig. 12-15 there is designed with dashed lines an additional portion to the principal diagram a which enables us to obtain the smoothed signal $\dot{x}$. A similar addition with new coefficients could be inserted in the same system to obtain smoothed acceleration $\ddot{x}$.

Let us take a look at some systems with parallel circuits developed by this author in 1949-1951. It

should be noted that for power systems parallel diagrams can hardly be considered expedient since the power units and amplifiers have to be duplicated for each network. For this reason we shall confine ourselves to electric circuits where the duplication of certain parts of the circuit encounters no difficulties.

Resistor-Inductance circuits. A resistor-inductance circuit L, R is an aperiodic element if as the input value we take voltage and the output value we take current with a gain 1/R and a constant of time $T = L/R$.

A series of such circuits connected to terminals to which is fed voltage U smoothed according to the accepted hypothesis, forms the electric circuit b similar in design and operation to block diagram a. Summation of currents or of the voltage drops created by them on the ohmic resistances for the independent operation of individual arms and the possibility of changing the sign of the summands require the insertion of decoupling amplifiers. Suppose that the system uses magnetic amplifiers with a gain between input current and output voltage equal to m_i. Then the gain of each amplifier with selected L_i and R_i (coefficients specific according to the above formulas for partial transfer functions K_i) can be calculated according to the formula

$$ m_i = K_i R_i. $$

By combining the gains we can read from the system's

output the smoothed values of input voltage as well as of its first and second derivatives.

Resistor-Capacitor circuits. A resistor-capacitor circuit RC is also an aperiodic element if we take as the input value the voltage at the circuit and as the output value the voltage at the capacitor; the gain of the element is equal to unity (m = 1) and the constant of time T = RC.

We investigate the simple case of input voltage variation according to first-order hypothesis (uniform variation) which enables us to obtain electric circuits with decoupling amplifiers. For this case the CTF of the synthesized system (12-51) can be written

$$\Phi(p) = \frac{K_1}{T_1 p + 1} + \frac{K_2}{T_2 p + 1} . \qquad (12\text{-}54 \ a)$$

From a formula analogous to (12-52) we find the coefficients for partial transfer functions of the smoothing system:

$$K_1 = \frac{\begin{vmatrix} 1 & 1 \\ 0 & -T_2 \end{vmatrix}}{-\begin{vmatrix} 1 & 1 \\ T_1 & T_2 \end{vmatrix}} = \frac{T_2}{T_2 - T_1} ;$$

$$K_2 = -\frac{\begin{vmatrix} 1 & 1 \\ -T_1 & 0 \end{vmatrix}}{T_2 - T_1} = -\frac{T_1}{T_2 - T_1} .$$

The aggregate CTF of the smoothing system is

$$\Phi(p) = \frac{\frac{T_2}{T_2 - T_1}}{T_1 p + 1} - \frac{\frac{T_1}{T_2 - T_1}}{T_2 p + 1} = \frac{(T_1 + T_2) p + 1}{(T_1 p + 1)(T_2 p + 1)} . \ (12\text{-}54 \ b)$$

Figure 12-15 shows an electric circuit designed according to the formulas obtained. The first circuit requires a gain greater than unity; it forms at the system's input by setting the input amplifier or by reducing the system to a lower scale.

In the second circuit the gain must be reduced with respect to T_1/T_2 (it is borne in mind that $T_2 > T_1$). This is done by installing at the input a voltage divider. Voltage at the output will be equal to the difference of potentials of points shown in the diagram or to the difference in voltage at the capacitor of both circuits.
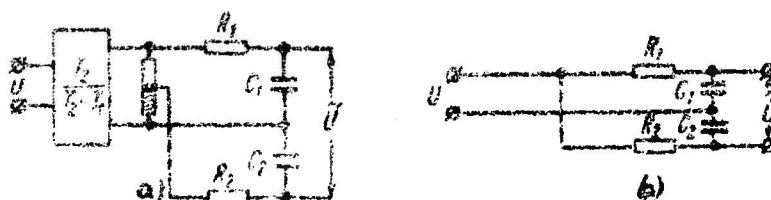
Fig. 12-16. Smoothing filters with successive summation of voltages of partial components.

Let us now find the coefficients for partial transfer functions of a differentiating-smoothing system. Again we use a formula of the type (12-52):

$$K_1 = \frac{\begin{vmatrix} 0 & 1 \\ 1 & -T_2 \end{vmatrix}}{-(t_2 - T_1)} = \frac{1}{T_2 - T_1};$$

$$K_2 = \frac{\begin{vmatrix} 1 & 0 \\ -T_1 & 1 \end{vmatrix}}{-(T_2 - T_1)} = \frac{1}{T_2 - T_1}.$$

The aggregate OTF of the differentiating-smoothing system is

$$\Phi(p) = \frac{1}{T_2 - T_1}\left(\frac{1}{T_1 p + 1} - \frac{1}{T_2 p + 1}\right) =$$

$$= \frac{p}{(T_1 p + 1)(T_2 p + 1)}. \qquad (12\text{-}55)$$

In the given case the gains of both networks are equal in magnitude, they are, in fact, equal to unity ($K_1 = K_2 = 1$) and differ only in the sign, hence the electric circuit b turns out to be quite simple.

Thus, the circuits in Fig. 12-13 can be designed quite easily owing to the fact that only two transfer functions having different signs are included in the general formula.

If the number of partial OTF is greater than two, voltage summation requires the utilization of decoupling amplifiers: either one amplifier per each arm, as shown in Fig. 12-15, or with a number of amplifiers reduced to no less than one-half when pairing networks with gains of different signs on the basis of principles relating to Fig. 12-16.

Current summation enables us to reduce the number of amplifiers to one or two irrespective of the number of transfer functions.

Passage in a resistor-capacitor circuit to an output value in the form of current will be investigated on the basis of two elementary diagrams.

Circuit with parallel capacitor. (Fig. 12-17,a). Its transfer admittance can be written on the basis of data from Chapter 8 where similar circuits were discussed:

$$Y(p) = \frac{\frac{1}{R}}{rCp + 1 + \frac{r}{R}} = \frac{1}{RrCp + r + R} .$$

Its gain is $m = 1/(r + R)$; its constant of time $T = RrC/(R + r)$. When designing a circuit with several partial OTF we first define the constants of time of aperiodic elements and define by them in accordance with the formulas above the coefficients of partial transfer functions K_i. Further, bearing in mind the possibility of subsequent amplification, we design the electric circuits with amplification factors m_i proportional to the calculated coefficients of partial transfer functions:

$$m_i = \frac{K_i}{a} \; ohm^{-1}.$$

If resistance r is given, we find R from the load conditions of the input voltage source for a certain m. There remains to determine the magnitude of capacitor C from the constant of time T. With $r \ll R$ calculations are simplified.

The cells a thus calculated are connected to the summing dc amplifier DCA, as shown in diagrams b or c in Fig. 12-17.

Diagram b has an input voltage divider and one input
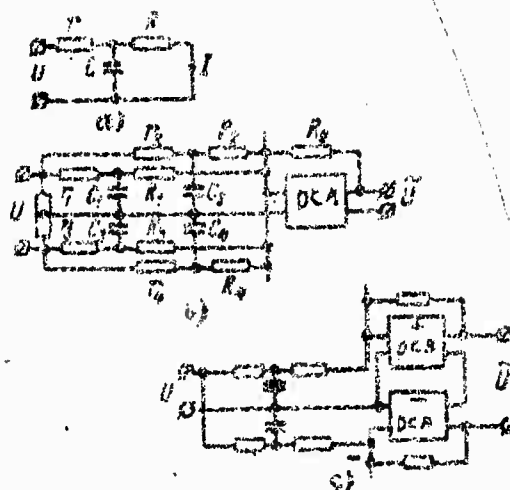
Fig. 12-17. Smoothing circuits with parallel voltage summation of partial elements

amplifier has connected with the grid of the first cascade, hence all the circuits with positive coefficients are connected between the upper terminal and the middle point of the voltage divider, while all the circuits with negative coefficients are inserted between the bottom terminal and the middle point.

The circuit currents are summed (considering the signs) on the bus virtually without errors since the DCA equivalent resistance between the grid and earth is quite small.

The amplifier output voltage is equal to the sum of currents multiplied by feedback resistance $\tilde{u} = R_0 \sum I_i$. The magnitude of R_0 governs the final gain of the system according to condition $a = R_0$.

In circuit c the input voltage divider has been

dispensed with, hence the circuits with positive coeffi-
cients are connected to one DCA and those with negative
coefficients to the other. Difference voltage is obtained
owing to the corresponding circuit diagram of their output
terminals.

Circuit with series capacitor (Fig. 12-18,a). Its
operator admittance is

$$f(p) = Y(p) = \frac{Cp}{Tp + 1}.$$

If we form the general transfer function from partial
functions of a similar form, we can easily note that
after factoring out the overall factor p, the complete
transfer function (2-51) can be written

$$\Phi(p) = p \left[\frac{K_1}{T_1 p + 1} + \frac{K_2}{T_2 p + 1} + \frac{K_3}{T_3 p + 1} + \cdots \right]. \tag{12-56}$$

We can see from the formula that a diagram with
similar circuits is always differentiating because of
the first collector, and that by varying the magnitude
and sign of the coefficients K_i within the brackets we
may give it additional properties, viz., a simply sub-
sidiary smoothing or a reiterated differentiation and
smoothing.

Thus, analysis of differentiating-smoothing diagrams
with circuits with series capacitors is performed accord-
ing to formulas for aperiodic elements bearing in mind
that each circuit has its proper amplification factor

1020
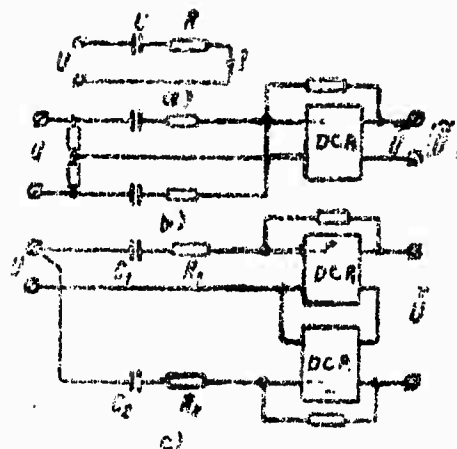
Fig. 12-18. Differentiating-smoothing diagrams with parallel current summation of partial elements.

$C_i = m_i$ and that the differentiating circuit coefficients are found from the formulas of the smoothing diagram, the coefficients of the double differentiating diagram are found from the formulas of the single differentiating diagram, and so on.

The circuits are joined up with the DCA, as shown in diagrams b and c of the same Figure.

Measuring diagrams with two-frame galvanometer. In testing control systems one has in many cases to check a number of derivatives in motion processes. Thus, e.g., there exists a widespread method of testing control systems by means of data units rotating with constant acceleration. A system with second-order astaticism tested in the open state with a constant step fed into it will have at the output under steady-state conditions an equally accelerated motion. Obviously, other examples can also be adduced.

Measuring of higher order derivatives, inasmuch as
they are assumed to be constant, can be sufficiently
accurately performed with an indicating instrument,
whereas variable quantities have to be recorded on an
oscillograph. Examination of diagrams b and c in Figs.
12-17 and 12-18 shows that the correctness of the signs
of various summands has to be especially ensured. When
measuring with a device, the magnitude of the various
signs is best evaluated with the aid of a two-frame
galvanometer.
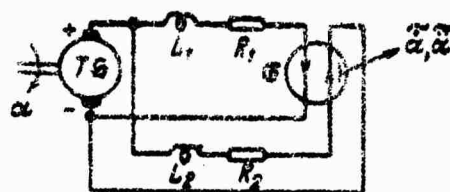
Fig. 12-19. Circuit diagram of a two-frame galvanometer
for measuring rotation speed or angular acceleration
according to the hypothesis of equally accelerated rota-
tion.

Let us investigate an actual circuit with such a
device, as shown in Fig. 12-19. Here the circuits are
calculated following the general rules already mentioned
when studying Fig. 12-15.

A two-frame galvanometer is a summing element of the
moments created by the currents of both frames. Since
the deflection angle of the moving system of the galva-
nometer, kept at zero by a spring, is proportional to
the moment and the latter is proportional to the current,

the deviation of the pointer is in the final analysis proportional to the sum of currents considering their signs.

By using two circuits and varying their coefficients we can form a smoothing diagram and a differentiating-smoothing diagram.

In the first place, considering a differentiating tachogenerator, the pointer of the instrument deviates in proportion to rotation speed of the input shaft, whereas in the second place its deviation is proportional to the shaft's acceleration. The system's parameters should be calculated according to formulas analogous to (12-54) and (12-55).

5. Fundamental Characteristics of Systems with Parallel Diagrams

Above we synthesized diagrams according to one property, viz., that of processing without systematic error the preassigned derivative under steady-state conditions with an established hypothesis of input variation. However, other characteristics of these systems are also important. Let us take a look at them now.

The time required by the system to become operating is equal to the time required by the system to terminate its natural motion. For intrinsic processes having exponential cofactors, damping time can be considered to be $B \sim 4.6\ T_{max}$, where T_{max} is the greatest constant of

time of the parallel arm.

In those cases where the exponent with the slowest damping has a small coefficient, the damping of that exponent may, with prescribed accuracy, not define the damping of the entire process, hence it has to be calculated more carefully.

Smoothing properties. The time to become operating also determines the actual duration of the weight function. In determining the output by the equation of integral coupling with exponential weight function, integration beyond the limit 4.6 T yields, as a rule, a negligible integral gain which, under the given circumstances, may be ignored. But over the interval from $\tau = 0$ to $\tau = 3-4.6$ T the weight function, changing relatively slowly, determines when integrating sign-changing disturbances their mutual elimination to a specific degree. Consequently, here, as in systems with limited observation time discussed in Section 12-3, conditions for smoothing disturbances improve with increasing starting time and observation time.

But if the smoothing of disturbances by systems with an established time interval (with a delay component) above was called optimum, the smoothing with arbitrary components (if we hold to the old positions of optimum evaluation) can no longer be called optimum. Earlier it was shown, however, that systems with parallel block diagrams can be synthesized from elements with random

characteristics. Thus, there always remains the possibility of choosing the partial characteristics such that their sum be close to the optimum characteristics.

Thus, e.g., the parabolic characteristic shown in Fig. 12-8 as optimal for differentiating and smoothing with the hypothesis of uniform input signal variation, must be considered sufficiently remote from the difference of two damping exponents which can be easily obtained when performing an inverse Laplace transformation over the OTF (12-58). But with four exponents we can approximate the parabola with considerably greater accuracy. Consequently, when obtaining transfer function (12-55) we must complicate the partial transfer functions reducing each of them to the sum of two functions of aperiodic elements.

A good approximation to the parabola is attained with partial OTF with even roots of the form $f(p) = a/(Tp + 1^2)^2$.

Frequency-response curves having the OTF of filters we can easily plot their frequency-response curves. But whereas the systems with a preset time interval T had specific frequency-response curves and there was a point in studying them separately (Section 12-3), the frequency characteristics of parallel diagram with standard elements can be easily traced out following transfer functions (12-54) and (12-55) on the basis of data from the preceding chapters, especially from Chapter 4, hence we shall
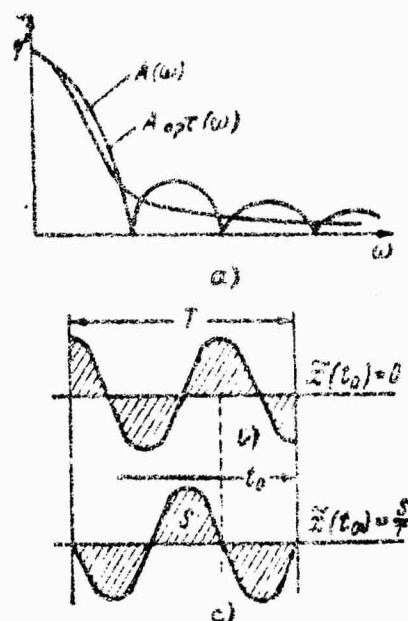
Fig. 12-20. Amplitude-frequency characteristics of a
simplest optimum smoothing filter with a bounded in-
terval and an aperiodic element; time graphs explaining
the conditions for obtaining the characteristics.

We plot in Fig. 12-20 the amplitude-frequency charac-

teristic of one aperiodic element with a gain equal to

unity. This element, according to Table 12-2, is a

smoothing system for a constant signal according to

hypothesis. Onto the same diagram we transfer from

Fig. 12-7 the amplitude-frequency characteristic of the

optimum system, taking interval T equal to the three-

fold time constant of the exponent.

Table 1

Noise Dispersion at the Output of Certain Control Systems
Made Up of Aperiodic Elements

(1) Formula number	(2) Переключная функция	(3) Шумовая дисперсия
12.54а	$\dfrac{(T_1 + T_2)\,p + 1}{(T_1 p + 1)(T_2 p + 1)}$	$\dfrac{N^2}{(T_2 - T_1)^2}\left(\dfrac{T_2^2}{2T_1} + \dfrac{T_1^2}{2T_2} - \dfrac{2T_1 T_2}{T_1 + T_2}\right)$
12.55	$\dfrac{p}{(T_1 p + 1)(T_2 p + 1)}$	$\dfrac{N^2}{2(T_1 + T_2)}$
12.54б	$\dfrac{K_1}{T_1 p + 1} + \dfrac{K_2}{T_2 p + 1}$	$N^2\left(\dfrac{K_1^2}{2T_1} + \dfrac{2K_1 K_2}{T_1 + T_2} + \dfrac{K_2^2}{2T_2}\right)$

Key: 1) formula number; 2) transfer function; 3) noise dispersion.

This comparison shows that in a certain frequency band the optimum system smoothes disturbances less efficiently than the aperiodic element. This fact is easily explainable. If, e.g., the preassigned interval comprises precisely an odd number of harmonic disturbance periods, then the mean value of the effective signal determined by the method of least squares ranges from zero to the magnitude of the disturbance half-

wave area divided by the interval, as shown in diagrams
b and c of Fig. 12-20.

It is obvious that for the given concrete frequency
interval T is evidently unsuitable and the concept of
optimality must be revised. Thus we arrive at the
frequency analysis of the input signal component; in
this case, in the presence of data relative to the input
spectrum, synthesis of the control system should be
performed according to the method expounded earlier,
whereas in the case of computing filters one should
resort to specialized literature /Bibl. 6/.

It appears useful to stress the conditionality of
the choice of interval T in optimum systems and the
absurdity of aiming at an excessively exact reproduc-
tion of optimum characteristics. Apparently, the peaks
and drops of optimum frequency characteristics need
not necessarily be reproduced.

Noise Dispersion. If we have the frequency charac-
teristic or the weight function of systems of various
types, we can compare their properties also by the noise
dispersion at the output. For systems with preset smooth-
ing interval, the noise dispersions are given in Table
12-1, while for systems with preassigned aperiodic
elements investigated in the given Section, the noise
dispersions are tabulated in Table 12-3.

In calculating noise dispersion we can use the
effective passbands of analogous elements given in
Table 4-10, or formula (4-129).

Systematic errors with a complicated input. If the
input is complicated in comparison with the hypothesis
in the system, e.g., if the order of the input polynomial
becomes greater by unity than the order of the hypothesis,
then in (10-1) there appears the additive term

$$a(t) = \frac{\Phi_{(0)}^{(n+1)}}{(n+1)!} x_h^{(n+1)}, \qquad (12-57)$$

which according to synthesis conditions is not cancelled
and becomes the systematic error of this system propor-
tional to the value of the highest derivative.

4. Transformations of Parallel Diagrams.

Above we studied systems with parallel diagrams which,
in the field of electric circuits, computing and measuring
devices, afford specific practical advantages. The main
value of these solutions, however, consists in obtain-
ing the system's block diagram in the simplest fashion.
Having one variant of the block diagram, and availing
ourselves of structural analysis methods, it can always
be transformed into another one more convenient for
technical realization. The general methods of structural
transformation were expounded in Chapter 5, hence here
we shall deal only with specific examples.

Series (cascade) diagrams. We study the transition
from the parallel diagram in Fig. 12-13,a to the cascade
diagram following the example of systems operating
according to first-order hypothesis. For a smoothing
system the transfer system is given by formula (12-54)

in its expanded form suitable for designing parallel diagrams (diagram a in Fig. 12-21) as well as in its transformed form (right-hand side of the formula) which we write as follows

$$\Phi(p) = [(T_1 + T_2)p + 1]\frac{1}{T_1 p + 1} \cdot \frac{1}{T_2 p + 1} \cdot (12\text{-}58)$$

Thus we see that the system can be made up of three cascade-connected elements: a forcing element and two aperiodic elements with different constants of time, as is shown in Fig. 12-21, b.
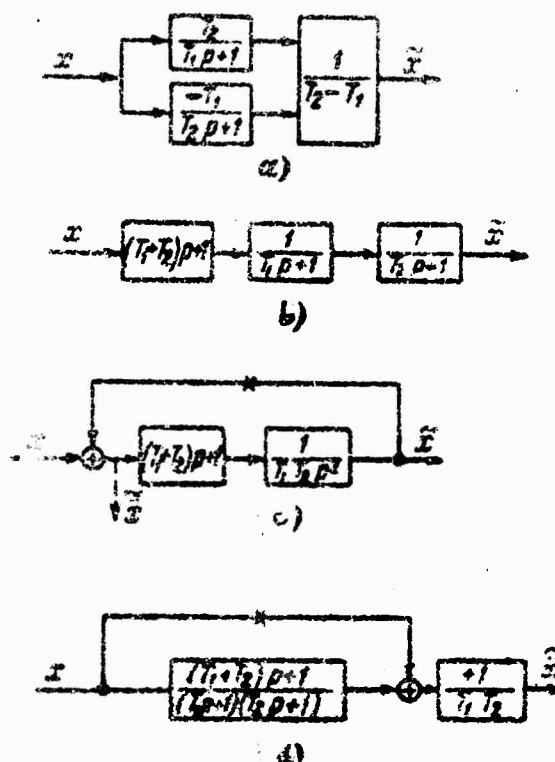
Fig. 12-21. Passage from parallel diagram of a computing filter to cascade and closed diagrams.

Likewise, a differentiating-smoothing system according to the right-hand side of formula (12-35) instead of a parallel diagram can be represented by a cascade circuit diagram of three elements: a differentiating one and two aperiodic elements.

Closed diagrams. We determine with the aid of formula (12-54) the direct circuit of a standard closed-loop system:

$$W(p) = \frac{\frac{(T_1 + T_2)p + 1}{(T_1 p + 1)(T_2 p + 1)}}{1 - \frac{(T_1 + T_2)p + 1}{(T_1 p + 1)(T_2 p + 1)}} = \frac{(T_1 + T_2)p + 1}{T_1 T_2 p^2}. \quad (12-59)$$

Block diagram c in Fig. 12-21 was constructed according to the formula obtained. We can easily note that we have obtained a result which was already established in Chapter 10 for the standard closed control system, namely: to obtain a zero rate error the system must have a second-order astaticism, i.e., it must have two integrating elements in the direct circuit. The existence in Formula (12-59) and in the diagram of a first-order forcing element in addition to two integrating elements ensures the preassigned flow of natural motion processes in the form of the sum of two exponents with pre-established constants of time.

The problem of stability does not arise at all with respect to diagram c, since the system is known to be stable (see diagram a).

The problem of quality can be regarded in exactly the same way, since if we hold to the damping criterion

when evaluating quality, it has already been realized to
the desired extent when choosing the starting time for
diagram a.

In point of fact, things amount here to the synthesis
of control systems by the prescribed roots of the charac-
teristic equation of closed systems.

Reduced diagrams. We have already shown that to
determine the smoothed value of the highest derivative
in an n-th order hypothesis for a parallel diagram we
need $n + 1$ linearly independent elements. Let us now
use formula (12-57) for the system's systematic error
with an input exceeding the order of the hypothesis by
unity. For reproducing (smoothing) systems the error
formula is given in Chapter 10:

$$\epsilon(t) = X_{\text{вх}}(t) - x(t).$$

Passing to the operator form and using formula
(12-57) we find

$$p^{n+1} X(p) = \frac{(n+1)!}{\Phi_{(0)}^{(n+1)}} [\Phi(p) - 1] X(p).$$
(12-60)

Thus, the highest derivative in the law of $(n + 1)$-th
order can be obtained by using a smoothing system operating
according to n-th order hypothesis if from the output
value we subtract the input value and multiply the
difference by the coefficient $(n + 1)! / \Phi^{(n+1)}(0)$.

Figure 12-21 shows the block diagram d which corresponds

331

to these operations, and the transfer function used is that of a smoothing system operating according to the first-order hypothesis. We have:

$$n + 1 = 2; \quad \Psi(0) = -2T_1 T_2$$

and

$$\frac{(n+1)!}{\Phi^{(n+1)}(0)} = -\frac{1}{T_1 T_2}.$$

In the principal channel of the diagram under study the transfer function is written in a transformed form. If we expand it and represent it by a parallel diagram a we can easily see that only two operator elements are taken up in the diagram instead of three required according to the methods above to determine the smoothed value of the second derivative.

The principal channel can also be replaced by diagram c. In this case the result $\tilde{x}$ at a changed scale can be read from the adder output.

The aggregate transfer function of the entire system d

$$\Phi_d(p) = \left[\frac{(T_1 + T_2)p + 1}{(T_1 p + 1)(T_2 p + 1)} - 1 \right] \frac{-1}{T_1 T_2}$$

$$= \frac{p^2}{(T_1 p + 1)(T_2 p + 1)}$$

proven that it is correct to regard this system as a double differentiating one.

Analysis of the frequency-response curves of this system may occasionally show that the smoothing properties, determined by the terms of the denominator, are inadequate. In this case one can always go back to

the three-component diagram. The desired degree of
smoothing, however, can also be attained in a reduced
diagram by increasing the constants of time if the input
signal spectrum places no special requirements upon the
shape of frequency characteristics.

Passage from block diagrams to technical realization
yields in many cases technically interesting solutions.
Thus, e.g., if in a circuit with galvanometer (Fig. 12-19)
we have one purely ohmic network with a resistance equal
to that of the second network, then the network with
resistance forms a negative direct circuit and the
aggregate OTF amounts to

$$\frac{\frac{1}{r}}{Tp+1} - \frac{1}{r} = -\frac{\frac{T}{r}p}{Tp+1},$$

i.e., the galvanometer operates as a differentiator.

The examples investigated give us an idea of the
possible trends to be followed in the synthesis of
various linear dynamic devices. Together with the
principles of the synthesis of electric circuits
discussed in Chapter 8, the procedures described here
disclose virtually inexhaustible possibilities for
finding various technical solutions of which the
most economical ones should be chosen.

Comparison of the accuracy of performance of
similar devices under noise conditions can be effected
on the basis of the output dispersion given for some
systems in Table 12-1.

If input disturbances are not given by white noise

but have a complex form of spectral density function
affecting the useful signal in the form of polynomials,
then optimum conditions are bound to change accordingly
/Bibl. 8/.

12-5. Synthesis of Control Systems With Variable Parameters

In the present Chapter we solved the synthesis problem
only for elements with constant parameters, but a number
of solutions can be generally applied also to systems with
variable parameters by using parametric weight functions
instead of weight functions with one argument, and
AOTF instead of OTF where there existed an analogy in
the accuracy analysis.

Of course, there arises a number of additional
peculiarities. Thus, e.g., in synthesizing constant
systems it appeared to be desirable that the transient
process in the control system approach that in the
oscillating component with OTF (12-7a) or (12-8a). For
systems with variable parameters such a synthesis may
also turn out to be desirable, but its realization will
require the insertion of stabilizing circuits with
variable tuning or of self-tuning filters.

Solution of the problem of statistical synthesis
of a variable system where the effective signal is
given as a polynomial and the disturbances as white
noise requires that we use the system's AOTF instead
of (12-9b), and minimum dispersion at the output is
obtained only at an actually fixed instant of time t_k.

To obtain a variation of dispersion with time in the synthesis of variable systems optimum over a certain time interval requires a considerable complication of the system of equations investigated as compared with the system's initial equations. This method is discussed by us in /Bibl. 4/ and Chapter 3.

In most cases analytical calculations of control systems with variable parameters are quite difficult and can only be achieved with the aid of computers.

The problem of synthesizing an optimum system amounts in this case to a trial and error method varying the parameters of the control system whose equations are set up on an electronic model.

Optimization of control system parameters to obtain a minimum of the criterion chosen, e.g., of the aggregate, can also be achieved by automatic "analyzers" connected with an electronic model or a digital computer /Bibl. 7/.

BIBLIOGRAPHY

1. Andreyev V. P. and Sabinin Yu. A., Osnovy elektro-privoda, (Fundamentals of Electric Drive), Gosenergoizdat, 1959.

2. Chestnat G. and Mayer R., Proyektirovaniye i raschet sledyashchikh sistem i sistem regulirovaniya, (Design and Calculation of Servosystems and Control Systems) Vol. II. Gosenergoizdat, 1959, p. 130.

3. Kirby M. and Beaumariage D., Otnositel'naya ustoychivost' zamknutykh sistem, (Relative Stability of Closed Systems), Part II. IL, 1953.

4. Meyerov M. V., Sintez struktur sistem avtomaticheskogo regulirovaniya vysokoy tochnosti, (Synthesis of High-Precision Automatic Control Systems), Fizmatgiz, 1959.

5. Solodovnikov V. V., Statisticheskaya dinamika lineynykh sistem avtomaticheskogo upravleniya (Statistical Dynamics of Linear Control Systems), Fizmatgiz, 1960.

6. Stanislavskiy B. I., Osnovy teorii elektricheskikh schetno-reshayushchikh ustroystv, (Fundamentals of the Theory of Electric Computing Devices), Oborongiz, 1948.

7. Fel'dbaum A. A., Vychislitel'nyye ustroystva v sistemakh avtomaticheskogo upravleniya (Computing Devices in Control Systems), Fizmatgiz, 1960.

NONLINEAR AND SPECIAL AUTOMATIC CONTROL SYSTEMS

Chapter 13

AUTOMATIC CONTROL SYSTEMS WITH NONLINEAR COMPONENTS
(pp. 367 - 387)

13-1.   Static Characteristics of Nonlinear Components
and the Methods Used for Their Transformation

A nonlinear component, for which the relationship
between the input and output is expressed by the following
functional form

$$x_{out} = f(x_{in}), \tag{13-1}$$

which involves no operations for a mathematical analysis,
is known as a nonlinear component of the zero-order, or as
a nonlinear amplifying component. The static characteristic
(13-3) of a nonlinear, zero-order component is a universal
relationship that determines the relation between the input
and output values for both the steady state (as implied by
the name of the characteristic) and during the variation
of these values with respect to time.

If the relationship of a nonlinear component is given
by a differential equation containing no nonlinear terms,
then depending on the order of the first derivative in the

equation for this relationship, the component is known as a nonlinear component of the first order, second order, etc. The static characteristic of type (13-1) for stable nonlinear components of an order other than zero reflects the relation between the input and output values only during their state of stability.

The static characteristics of nonlinear components are represented by a variety of types and, therefore, we will examine only their typical features and classification.

We will first make a distinction between single-valued and multiple-valued static characteristics of nonlinear components.

Single-valued characteristics contain only one output-value for each value of the input, while multiple-valued characteristics contain (over their entire range, or in individual sections) output values which are determined not only by the numerical value and the sign of the input value, but also by the direction of its change.

Single-valued characteristics are shown in Fig. 13-1.

In its turn, we will subdivide the single-valued characteristics according to their properties near zero and near the maximum value of the input. In accordance

with these indications we will distinguish the following
features of these characteristics: their zone of insensi-
tivity and their saturation.

If, while the controlling signal increases from zero,
the output-value does not begin to change at once but only
upon reaching a certain minimum input-value of $\frac{\delta}{2}$, then
the nonlinearity acquires the property of a nonsensitive
zone and may be represented, for example, by curves 1, 2,
and 3 of Fig. 13-1,a.

If a limited increase in input-value is observed when
the values of the controlling signal are large, then the
nonlinearity is represented by characteristics typified by
4, 5, and 6 of Fig. 13-1,b.

Both a nonsensitive zone and saturation may be observed
in the same characteristic typified by 7 and 8 of Fig. 13-1,c.

The appearance of similar characteristics in circuits
containing iron is determined by the ability of the magnetic
circuit to reduce its magnetic permeability down to a com-
paratively small value (permeability of air) while the
induction increases. In the case of electron tubes, the
final section of a static characteristic is influenced by
the limited emission of the cathode when the temperature

remains unchanged. In such cases, the term "saturation", therefore, reflects the physical nature of the phenomenom.
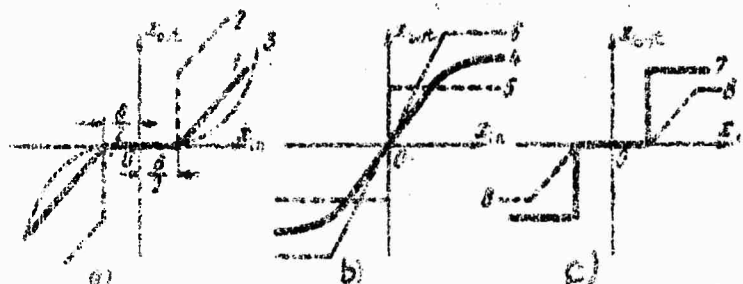
Fig. 13-1. Single-valued characteristics
of nonlinear components.

a) with a zone of insensitivity; b) with saturation;
c) combined.

Static characteristics which differ physically but are of nearly the same nature contain regulating systems whose units are provided with restrictors for:

linear displacement in piston engines, in linear acceleration-pickups, etc.;

angle of rotation in measuring and servo-units;

pressure, consumption, etc.

The effect of all such restrictors is that, starting from the value set for the output, the static characteristic

becomes a horizontal line which, as a rule, bends at the
point of restriction, as shown by the broken line 6 of the
same figure.

The single-valued characteristic 7 of a relay also
belongs to the saturation type and bends at right angles
at the point of restriction.

Multiple-valued characteristics are shown in Fig. 13-2.
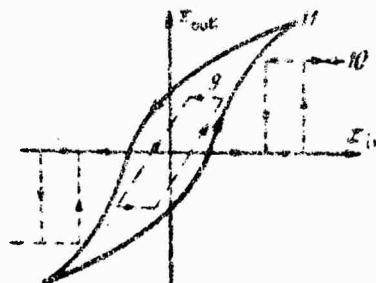
Fig. 13-2.   Multiple-valued characteristics of
nonlinear components.

An analysis of characteristics located near zero and in
zone of large values will again lead to the conceptions
describing an insensitive zone and saturation. It may add
to the multiple-valued significance of a characteristic.

Multiple-valued characteristics are intrinsic in such
linearities as "free-play" or backlash 9, multiple-valued
relay 10, and "hysteresis" 11.

Let us examine certain actual units possessing typical nonlinearities and shown in Fig. 13-3.
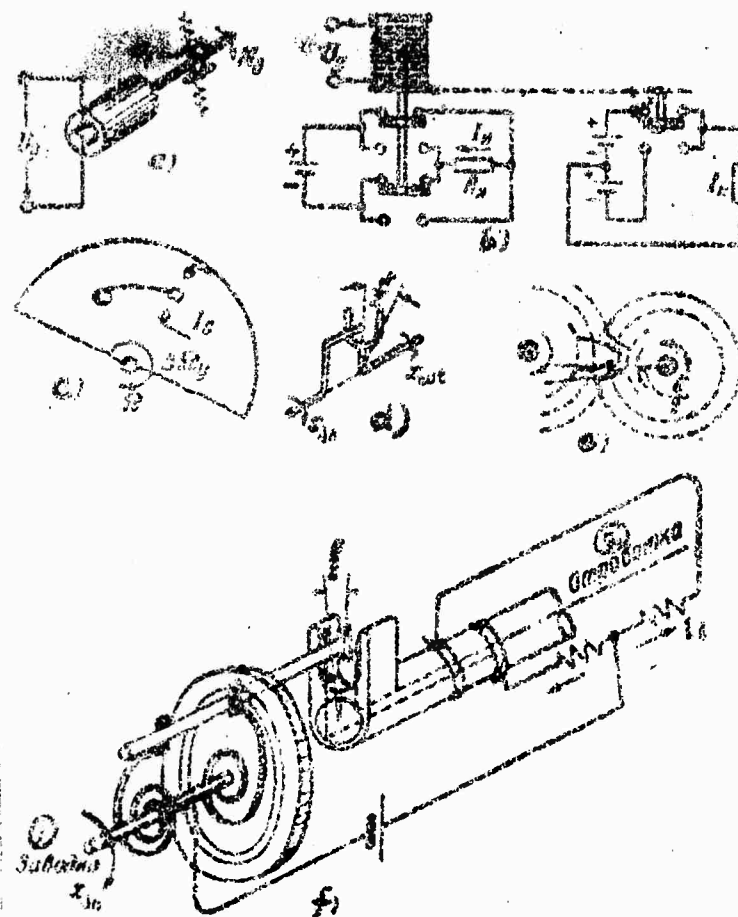
Fig. 13-3. Typical units with nonlinear characteristics. key: 1) winding up; 2) final adjustment.

Dry-friction motor (Fig. 13-3,a). The dry friction is due to the load on the motor shaft or possibly to the friction of its wipers. As the electromagnetic torque of

the motor increases in a linear manner, its excess torque in
the voltage function is reduced by the amount of torque
lost by dry friction and varies in accordance with the non-
linear characteristic 1 represented by a solid line in Fig.
13-1,a, i.e., in accordance with a characteristic having an
insensitive zone.

As long as the input voltage does not exceed the pickup
voltage designated in the diagram by $\frac{\delta}{2}$, the motor shaft
will remain at rest and the network will not respond to the
control signal. If a blocking voltage exists at the input
of an electronic tube amplifier,   an insensitive zone will
be likewise present in the characteristic as long as the
input voltage does not exceed the blocking voltage.

Relay amplifier (Fig. 13-3,b). Depending on its design,
a relay amplifier may have various typical nonlinearities in
the characteristic which links the control signal (voltage or
current in the winding) with the output value (current of the
load) commutated by the contacts of the relay.

Saturation - restriction. The principal feature of a
relay characteristic as shown in Fig. 13-1,c by line 7 is
its rectangular appearance.

The current in the load is strictly limited by the
value of the battery voltage and by the resistance of the

load: in the above circuit it may have a fixed positive value, a negative value usually equal to the first, or it may be equal to zero.

In simplified commutation the current is limited to two values: positive and zero; in such a case, the operation of a relay-amplifier is based on the "yes-no" principle.

The zone of insensitivity. A relay-amplifier will not switch-on the contacts as long as the input-voltage does not exceed the pickup-voltage.

Multiple-valued form - electrical backlash. If the permeance of a magnetic circuit of a relay where the normally open contacts are switched-on (for example, when the core is pulled-in) differs substantially from the permeance when the contacts are switched-off, then the pickup-voltage will also differ from the release-voltage, i.e., the characteristic will assume a multiple-valued form. The multiple-valued characteristic 10 of a relay is shown in Fig. 13-2.

The contact-pickup of a centrifugal speed regulator (Fig. 13-3,c). It also has a typical relay-characteristic with a small insensitive zone. In order to reduce it to the form of 7 shown in Fig. 13-1,c, it is necessary to assume that the zero input-value is the average speed-value when the contact is at the middle position. Taking into account the sagging of the spring after the contacts are closed

1065

will bring it to characteristic 10 of Fig. 13-2.

Transmissions with mechanical backlash (Fig. 13-3,d-f).
Static characteristics with backlash are shown by the dash-
and-dot line 9 of Fig. 13-2. The specific features of the
backlash are exposed near zero and during the reverse.

Provided that only one-half of the backlash exists at
its initial position in transmissions using a dog (d) or
gears (e) with a backlash $\frac{\delta}{2}$ expressed in angular units,
then the output-shaft will remain motionless over the range
of $\frac{\delta}{2}$ while the input-shaft moves away from zero in any
direction and will remain motionless until the proper back-
lash is selected.

The transmission continuity of the section is also
disrupted during the reverse movement until the dog (d) will
pass from one side of the yoke to the other, or until the
tooth of the driving gear (e) will disengage itself from
one of the teeth of the driven gear and will become engaged
with a tooth located on the opposite side. This event will
cause in characteristic 9 of Fig. 13-2 the appearance of
horizontal "Shelves" which are typical for a backlash. This
characteristic, generally speaking, may be extended to any
value of the input by maintaining the slope of the linear
parts and the size of the horizontal shelves, because the
rotary motion itself is not limited by the size of the angle.

The diagram (1) shows a contact device KP which serves to control the current in the windings of the motor and is designed to turn the "final adjustment" shaft immediately after the winding-up shaft begins to rotate. The contact-part of this device always contains a mechanical backlash. Similar KP devices are always provided with a flexible connection between the driving and driven parts to avoid breaks and to accumulate an input value for a stationary motor. In the figure, the flexible connection is shown in form of two-sided spiral springs.

Unlike the "backlash" type of characterics, the "hysteresis type of characteristic, which is also multiple-valued, has smooth transitions, unless special measures are taken for its rectification.

Additional special features of nonlinear characteristics. Among the additional properties of static characteristics are usually present: the symmetry or asymmetry of characteristics in the region of positive and negative values of the input, steepness of characteristics increasing from the initial section to saturation, number of bends, etc. These special features are best to analyse not in their general form, but using concrete examples of components employed by the ACS. An example of a static characteristic depending on two arguments was analysed in chapter 1-4.

Let us proceed with the problem of transforming static characteristics of several jointly-operating nonlinear components or, as a specific case, of nonlinear and linear components included in typical ACS /Automatic Control System/ circuits.

1. Cascade Connection of Components

The scheme used in cascading nonlinear components is illustrated in Fig. 13-4,a. Each component has its own static characteristic (13-1) reflected by the functions $F_1(X_{1n})$, $F_2(X_1)$, $F_3(X_2)$ -- the functions of the input argument.

The general static characteristic will be represented by the following expression:

$$x_{out} = F_3 \{F_2 [F_1 (x_n)]\}. \qquad (13\text{-}2)$$

which can be read as function F_3 of function F_2 of function F_1, because the expressions in the parentheses play each time the role of a new argument.

2. Nodal Nonlinear Elements

Before proceeding to matching-parallel and counter-parallel types of schemes that are to follow later, it is necessary to note that unlike the case of cascading these schemes include the presence of nodal elements.

The angle of the forked node is the same in linear and nonlinear systems. However, a summator in nonlinear schemes

represents only a specific case of a nonlinear bous with two inputs.

Fig. 13-4. Structural transformation of cascade, matching-parallel, and nodal schemes with nonlinear components.

Note: X_B = X input
Y_B = X output

A general case of a nonlinear node with two inputs is illustrated by scheme (b) in Fig. 13-4. If the nodal component provides a functional transformation of two arguments of form

$$x_{out} = \varphi(\xi, \eta) \qquad (13\text{-}3)$$

and if functions $\xi = f_1(x)$ and $\eta = f_2(y)$ enter as arguments at the input, then at the output will be obtained a function φ of a function in the form of

$$x_{out} = \varphi[F_1(x), F_2(y)]. \qquad (13\text{-}4a)$$

Examples of application of this formula are given in schemes c) and d).

Among the widely used nodal nonlinear components is the multiplying component

$$\varphi(\xi, \eta) = \xi\eta.$$

In fact, the torque of the electric motor was regarded in the preceding examples as the product of the current by the flux, or the emf as the product of the velocity by the flux, etc. In this case the equation for a nodal element assumes the form of

$$x_{out} = F_1(x) F_2(y); \qquad (13\text{-}4b)$$

The simplest form of a function of two variables is their sum:

$$\varphi(\xi, \eta) = \xi + \eta$$

which will provide a linear summator instead of a nonlinear nodal element:

$$x_{out} = F_1(\xi) + F_2(\eta) \qquad (13\text{-}4)$$

3. Matching-parallel Connection of Nonlinear Components

Scheme (e) shows the general case of matching-parallel connection of nonlinear components with a nonlinear nodal element.

If the static characteristics of the parallel branches are equal to $F_1(X_{in})$ and $F_2(X_{in})$ when the nodal element performs a transformation according to function $\varphi(\xi, \eta)$ then the full static characteristic of the scheme will be:

$$x_{out} = \varphi[F_1(x_{in}), F_2(x_{in})] \qquad (13\text{-}5a)$$

If a summator serves as the nodal element, then the overall static characteristic of the scheme (with characteristics of parallel branches remaining unchanged) will be:

$$x_{out} = f_1(x_{in}) + f_2(x_{in}) \qquad (13\text{-}5b)$$

Let $\varphi(\xi, \eta)$ represent the function of two input arguments ξ and η. If the known function φ is now used to determine one of the arguments, ξ for example, it will be necessary to introduce the designation of the inverse function for this argument:

$$\xi = H_\varphi^\xi(\varphi, \eta).$$

The inverse function neutralizes the action of the given function, forming according to argument ξ a transfer coefficient equal to unity:

$$H_\varphi^\xi[\varphi(\xi, \eta), \eta] = \xi. \tag{1346}$$

and forming according to argument η a transfer coefficient equal to zero, as shown in scheme (1). If the function of the two arguments x and y are in form of a contour in a Cartesian space x, y, φ, then the inverse function is obtained by using simple geometrical sense: intersecting the contour by plane $y = $ constant, the abscissa x is found along the ordinate φ.

Examples:

$$1. \quad \begin{cases} \varphi(x, y) = xy; & H_\varphi^x(\varphi, y) = \varphi \dfrac{1}{y}; \\[2mm] H_\varphi^x[\varphi(x), y] = xy \dfrac{1}{y} = x. \end{cases}$$

$$2. \quad \begin{cases} \varphi(x, y) = \sin(x + y^2); & H_\varphi^x(\varphi, y) = \arcsin \varphi - y^2. \\[2mm] H_\varphi^x[\varphi(x, y), y] = \arcsin[\sin(x + y^2)] - y^2 = x. \end{cases}$$

4. Neutralization and Duplication
of Nonlinear Components

Two cascade-connected nonlinear components (Fig. 13-4,f) will neutralize each other if the neutralizing function $H_F(\xi)$ is an inverse function with respect to the transforming function of the first component.

Examples: 1. $F(x) = \sin x$; $\quad H_F(F) = \frac{1}{\sin}\left[F(y)\right] = x$.

2. $F(x) = x^2$; $H_F(F) = \sqrt{F(x)} = x$.

A neutral circuit has only one transfer coefficient

$$H_F[F(x)] = x. \qquad (13\text{-}6a)$$

Thanks to the introduction of the concept of a neutralizing component it is easy to formulate the rule on the transfer of a simple node through a nonlinear component according to the course taken by the signal, which is shown by scheme g) of the same figure. Such a transfer should be accompanied by introduction of a neutralizing component into the displaced branch.

The transfer of a simple node through a nonlinear component contrary to the course of the signal leads to the appearance of a duplicating nonlinear component, as shown in scheme (h).

Nodal nonlinear components capable of functional transformation of two input arguments can also be neutralized.

The concept of a neutralizing component is applied in scheme (k) to transfer a simple node through a functional node according to the course taken by the signal. The equivalence of transformed and initial circuits is obtained by intoducing into the displaced branch a neutralizing component $H_\phi^z(\xi, \eta)$.

Scheme (ℓ) shows the transfer of a simple node through a functional node contrary to the course taken by the signal; in this case, into the transferred branch is introduced a duplicating component $\phi(\xi, \eta)$.

5. COUNTER-PARALLEL CONNECTION OF NONLINEAR COMPONENTS
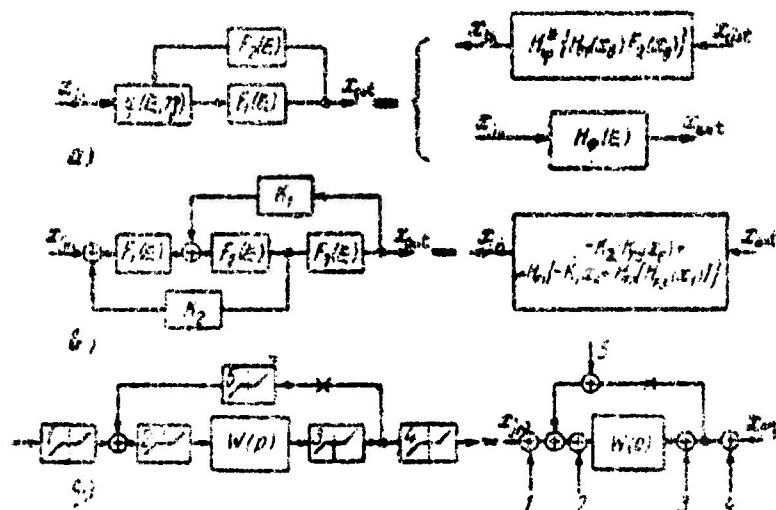
Fig. 13-5. Structural transformations of counter-parallel circuits with nonlinear components.

Scheme (a) of Fig. 13-5 shows a feedback circuit, or a counter-parallel circuit with nonlinear elements, including nodal parts. For static characteristics of the straight branch F_1, feedback circuit F_2, and formula for the nodal element $\varphi(\xi, \eta)$, the overall static characteristic of the circuit employing above functions can be obtained, first, in the implicit form of:

$$x_{out} = F_1\{\varphi[x_{in}, F_2(x_{out})]\};\qquad (13\text{-}7a)$$

secondly, by employing designations for inverse, i.e., neutralizing functions $H_\varphi^\xi(F_2, \varphi)$, $H_{F1}(\xi) = H_{F1}(x_{out})$, it is here possible to obtain an explicit solution with respect to input value:

$$x_{in} = H_\varphi^\xi\{H_{F1}(x_{out}), F_2(x_{out})\}. \qquad (13\text{-}7b)$$

Finally, if the right member of (13-7b) is taken as a single function of one argument (x_{out}), then, thirdly, the solution with respect to x_{out} can be expressed by an overall inverse function:

$$x_{out} = H_\varphi(x_{in}). \qquad (13\text{-}7c)$$

If the connection is superimposed through a simple linear summator, instead of an addition-formula the inverse function will become a formula of subtraction:

$$x_{in} = H_{F1}(x_{out}) - F_2(x_{out}). \qquad (13\text{-}7d)$$

Feedback is frequently made to be linear, i.e.,

$$F_2(y) = K_H x_3$$

In which case the preceding equation for the static characteristic of the scheme is simplified to:

$$x_3 = \mathscr{P}_1(x_N) - K_H x_3 \qquad (13.7a)$$

The equations obtained for application to schemes for connecting nonlinear components mentioned in Figs. 13-4 and 13-5 make it possible, on one hand, to analyse the connected nonlinear units and, on the other, can be used to synthesize a given functional relationship from the available nonlinear elements. Such a problem frequently appears in development of automatic computing devices. Given a set of typical functional (nonlinear) elements, it is possible to expand to a large extent the class of reproduced functions (static characteristics) with the aid of such elements taken from schemes cited in Fig. 13-4, or by using more complex schemes. For example, the scheme of Fig. 13-5,b with intersecting connections can be regarded as a complex scheme for which we can write at once the general function:

$$x_3 = \mathscr{P}_1(x_N) + H_{3!}\{-K_1 x_3 x_N\} \qquad (13.8)$$

Let us note that as in the case of linear systems of Fig. 13-4, more complex similar schemes can be also named

as functional structural schemes. They serve as a graphic example of mathematical relationships obtained during the transformation of regulated values in control systems. From a functional structural scheme it is possible to proceed to its technical realization and, vice versa, given an actual nonlinear ACS device it is possible to construct its functional structural scheme. These possiblities are also observed in linear structural schemes.

The intrinsic distinction of nonlinear circuits is that the principle of superposition cannot be applied for them; this makes it obvious that it is inadmissible to apply the methods of structural transformations of types involving the carry of summators, convolution of circuits, etc., if these operations involve nonlinear elements. On the other hand, the entire linear part of ACS is transformed on the structural circuit, as before, which makes it possible to simplify the circuit by separating the sections containing those nonlinearities which cannot be simplified.

In conclusion we will examine the statics of a typical follow-up system, the different circuits of which contain components having a zone of insensivity, as shown in Fig. 13-5,c. Let us assume that the system is connected, but is at rest after the final adjustment of the input signal and only one of the mentioned nonlinearities is present in it.

Let us find the static index-error of the system due
to this nonlinearity. For this purpose we will replace the
component with an insensitive zone by a signal equal to one-
half of the fork of symmetrial insensitive zone (as shown on
the right side of the drawing), because to overcome the zone
of insensitivity requires such an "expense of signal" which,
in the final analysis, brings about the error.

If one-half of the zone of insensitivity along the
i-signal is designated by δ_i and the error caused by it in
the output is Δ_i, then, based on the linear theory of con-
ditions required to carry-over errors to the output of the
system, it is not difficult to write the following equations:

$$\Delta_1 = \frac{W(0)}{1 + W(0)}\, \delta_1 \tag{13-9a}$$

$$\Delta_2 = \frac{W(0)}{1 + W(0)}\, \delta_2 \tag{13-9b}$$

$$\Delta_3 = \frac{1}{1 + W(0)}\, \delta_3 \tag{13-9c}$$

$$\Delta_4 = \delta_4 \tag{13-9d}$$

$$\Delta_5 = \frac{W(0)}{1 + W(0)}\, \delta_5 \tag{13-9e}$$

For static systems with large amplifying factors we have that $W(0) \to \infty$, or that for astatic systems $W(0) = \infty$, and that errors 1,2,4, and 5 coincide with the actions of δ_1, i.e., the zone of insensitivity is fully carried-over to the output and the error Δ_3 becomes equal to zero.

For irreversible movements and when the controlling and output values begin to change from zero, the nonlinearity of the backlash type makes its appearance in the same manner as the zone of insensitivity. Consequently, from the standpoint of static accuracy, a backlash is harmless in output circuits until the point of superposition of feedback and causes errors in the feedback circuit, beyond it at the output and at the input.

6. GRAPHICAL METHODS OF CONSTRUCTION OF STATIC CHARACTERISTICS OF CONNECTED NONLINEAR COMPONENTS

For the cascade method of connecting nonlinear components as in scheme (a) of Fig. 13-4, the overall static characteristics of components given in form of curves is obtained more simply by locating the curves in such a manner that the axis of the ordinates of the first curve x_1 serves as the axis of the abscissa of the second curve; the ordinate axis of the second curve becomes the axis of the abscissa of the third curve, etc. In this case the equation (13-2) is attained by a simple graphical construction.

In fact, let us locate (as shown in Fig. 13-6) the first curve in the first quadrant with axes $X_{in} = X_o$ and X_1; the second curve -- in the second quadrant with axes X_1 and X_2; the third curve -- in the third quadrant with axes X_2 and X_{out}. These axes correspond to the numbers for the controlled values in Fig. 13-4,a.

Let us select an arbitrary input-value of $X_o = a$ and lay it off on the first curve. At this point, the ordinate of the curve $F_1(a) = b$ is the argument for the second curve. This value of argument (b) enters the second curve to find the next function $F_2(b) = c$ which will serve as the argument for the third curve with which we finally find $F_3(c) = X_{out}$ which is to be carried over to the 4th quadrant. Plotting is repeated in the same manner to plot in the 4th quadrant the overall static characteristic with X_{in} and X_{out} as coordinates.

It is useful to remember that in the presence of a back-lash or saturation (even in one of the cascade-connected components) these features will be also repeated in the overall static characteristic.

If only two (instead of three) components are cascade-connected, we have $F_3 = 1 X_2$ and in the 3rd quadrant we simply draw the bisector B of a right angle (Fig. 13-6) which is used for turning the plotted lines. This bisector can be regarded also as the characteristic of a linear component with a gain factor equal to unity.

13-1
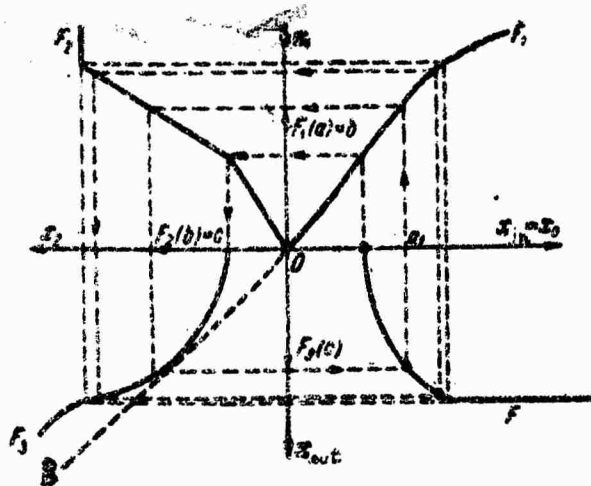
Fig. 13-6. Graphic construction of a static
characteristic for the cascade-method of
connecting nonlinear components.

Graphic constructions for matching-parallel schemes are
illustrative only if a linear summator is used as a nodal
unit. According to equation (13-5b) the problem in such a
case is reduced to a graphic summation of two characteristics
plotted on common axes X_{in} and X_{out}. An example of such an
addition of characteristics with a zone of sensitivity and
with saturation is shown in Fig. 13-7. It is not difficult
to note that when these features are intrinsic for only one
of the parallel components, they will not appear in the
overall characteristic.

Graphic constructions for counter-parallel schemes are
also effective only when a linear summator is present. In
such a case, use is made of equation (13-7d).

An inverse function is obtained from the curve of the basic function by changing the role played by the axes of the abscissas and ordinates.
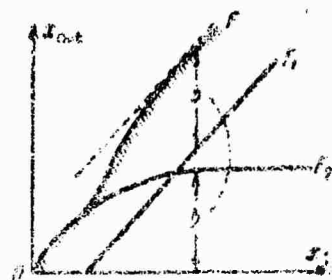
Fig. 13-7. Graphic construction of a static characteristic for a matching-parallel scheme for connection of nonlinear components.

Therefore, the concept of graphic construction is near to that of Fig. 13-7; the difference is that instead of addition of the ordinates of the curves it performs a subtraction of their abscissas. We will examine the construction of a static characteristic of a counter-parallel scheme by using a specific example of an electric circuit with nonlinear as elements.

Let us consider an electric circuit (Fig. 13-8,a) containing a supply (e), a load resistance (r) which changes when connections are made for consumers demand, and a stabilized supply of current for the resistance of a baretter which increases with the increase of the current in accordance with the functional dependency R(I).

The current in the circuit under examination is found by using the equation

$$I = \frac{e}{R(I) + r}.\qquad (*)$$

It is possible to prove that the obtained expression is an exceptional case of the general equation (13-7a); however, desiring to obtain an explicit solution, we will reduce at once the obtained equation to the form of (13-7d) by taking into account the fact that the input value is here regarded as the load-resistance

$$r = \frac{e}{I} - R(I).\qquad (**)$$

With this equation it is easy to construct the functional structural scheme (b) of Fig. 13-3, where in the nonlinear components is recorded the generalized argument ξ which then assumes concrete values. For the inverse function $z = \frac{e}{I}$, which is recorded in (**), we will get a straight function $I = \frac{e}{z}$ which in this case is given analytically and is to be constructed in the first quadrant of the equation (dotted line

The nonlinear function of the feedback circuit $R(I)$ is given by a curve in the same quadrant drawn by dotted line. The difference of (**) on the curve is shown for point $I=a$, $r=r(a)$. This value is carried to the lower quadrant for

the same abscissa Ixa and is used for drawing the curve
$x = F(I)$ which is the static characteristic of the entire
system.

If I_{max} and I_{min} are the given allowable limits for the
change in current, then without a baretter the allowable
changes in the load-resistance are limited by one value Δr
which is obtained from the dotted curve. When a baretter is
present it can be seen from the overall static characteristic
that these limits are increased to Δr_a and the resistance r
can now change from zero to Δr_b.

It is necessary to note that while both functions in the
structural scheme (b) are shown with positive signs, their
steepnesses differ with the sign and, therefore, a transition
accompanied with increments results in a circuit with a
negative feedback. But, before the increments take place, it
is first necessary to perform the above constructions in
order to determine the "working" point.

If a linear "ballast"-resistance is included instead of
a nonlinear baretter, the control zone along r for the
limits specified for change of current is also expanded, but
to a lesser degree.

By reducing also the variations of the current caused
by the change in supply-voltage, the baretter makes it pos-
sible to use larger allowances for these variations when

— 1083 —

the limits of current variations are given. For the input value e and output value I it is convenient to rewrite the equation (*) as follows:

$$I = \frac{1}{r}[e - R(I)I]. \qquad (***)$$

With this equation it is easy to construct the functional structural scheme c (Fig. 13-8). The static characteristic of such a scheme is obtained by construction or by calculation by using the following equation:

$$e = I[r + R(I)].$$

Circuits with positive proportional feedback represent an isolated case of counter-parallel schemes. Let us examine them separately by using technical examples about which we know from the preceding chapters.

The generator with positive feedback. Let us examine the static characteristic of a self-excited generator with a simultaneous control of excitation. The electrical circuits were analysed in detail in Chapter 6, but the method of linearization which was used there required a preliminary finding of the working point on the characteristic, the construction of which we will now proceed to perform.

Let the relationship between the emf of the generator and the excitation-current be specified by the characteristic of the idle-run $E(I)$, the curve of which is drawn
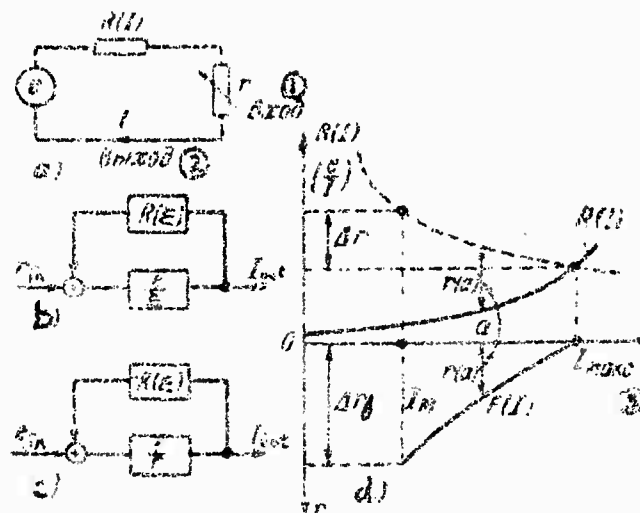
Fig. 13-8. Characteristics of a counter-parallel
structure exemplified by a scheme for a baretter,
key: (1) input; (2) output; (3) maximum.

in Fig. 13-9. Since the excitation current is $I = \frac{E \pm e}{r}$,
then the full equation for the static characteristics assumes
the form of:

$$E = F_1\left(\frac{E + e}{r}\right) = E(I).$$

The equation thus obtained makes it possible to construct
the functional structural scheme (a, in Fig. 13-9). For the
construction of the static characteristic of the scheme it is
possible either to redraw the curve $E(I)$ by dividing its
coordinates by r, or to change the appearance of the linear

part of the structural scheme by reducing it to the form of scheme (b) where the partial current $i = \dfrac{e}{r}$ containing no feedback serves as the input of the nonlinear part which is enclosed by feedback.

For the new input i and output E, the equation for the static characteristic of the scheme, is:

$$E = F_1\left(i + \frac{E}{r}\right),$$

or in form of (13-7d), it is

$$i = H_{F1}(E) - \frac{1}{r}\, E. \qquad (*)$$

With this equation it is very simple to determine graphically the static characteristic of the scheme.
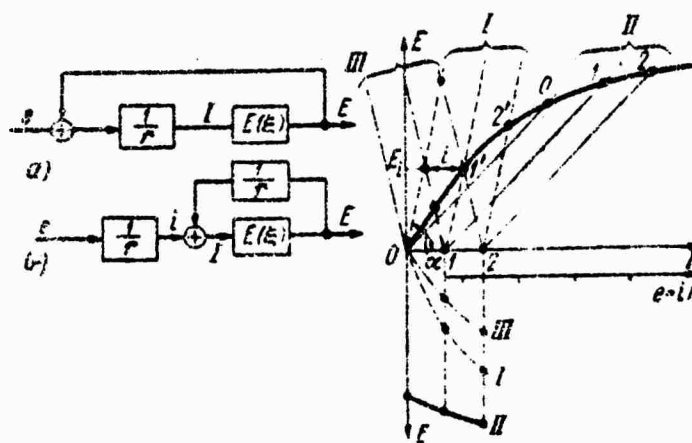
Fig. 13-9. Characteristics of a structure with positive proportional feedback as exemplified by a scheme for a saturated d-c generator.

3

Really, from the beginning of the coordinates let us draw a straight line $\frac{I}{r}-E$, i.e., a straight line sloping at angle α with respect to the axis OI, where $\tan \alpha = r$ and assuming any value for E_1 we determine the current as the difference along the horizontal line between the idle-run characteristic and the straight line $\frac{I}{r}-E$.

Drawn in Fig. 13-9 is a family of straight I, the left straight line of which corresponds to zero current; the above construction is then performed. The order of construction can be changed by handling first the partial current "i" and drawing from the corresponding point on the abscissa-axis a straight line running parallel to the zero-current line and by finding the intersection of this line with the idle-current characteristic, the ordinate of which equals the sought emf.

On the drawing under consideration are shown the points where the family of dotted lines intersect the idle-run characteristic ($0,1'$, $2'$) and the corresponding emf's are transferred to the lower part of the curve where the characteristic I is drawn by a dotted line in the coordinates i,E. It is convenient to replace at once the scale "i" with the scale $\frac{i}{r}$, in which case the curve I in these coordinates will turn out to be the sought static characteristic of the scheme.

If the conductance $\frac{1}{r}$ of the excitation-circuit is now increased, it will reduce respectively the slope of the

Straight lines and there will appear new points where these lines intersect the idle-run characteristic, as for example, the points 0, 1, and 2 for the II-family of straight lines. The static characteristic **II** is drawn for these points by a solid line in the lower part of the drawing. For a zero input voltage there is present a definite emf which is proven by the presence of the generator's self-excitation.

The conditions required for self-excitation are provided by the graphic construction, namely, the slope of the straight lines "r" must be less than the initial steepness of the idle-run characteristic, or

$$r < S_{I_a}^E.$$

The static characteristic thus obtained (II) has the "relay" features with a typical abrupt jump of the output value near the zero. A jump in the opposite direction is observed during the change of the input voltage, which is reduced by hysteresis.

The case of a generator contacted by a negative feedback is illustrated on the same drawing by a family of straight lines III. For a negative feedback the straight lines $\frac{E}{r}$ are inclined in an opposite direction with respect to the ordinate axis, as compared with the straight lines corresponding to a positive feedback. The construction of the static characteristic was performed by the above method.

The characteristic of a circuit with negative feedback is shown on the drawing by curve III drawn by a broken line.

As can be seen from the graphic plottings, the superimposition of negative feedback serves to narrow the range of changes undergoing by the output value.

If a linearity of the saturation type is under consideration, then by reducing the range of output changes to the initial section, the negative proportional feedback will, as a rule, rectify or linearize the nonlinear characteristic. A similar linearization is employed in practice: if necessary power amplification is provided, the decrease in output value as obtained above will be subsequently compensated by other amplifying components and the ACS, as a whole, will become nearly linear.

Magnetic amplifier with positive feedback. The electrical circuit was treated in Chapter 7. The equation for its static characteristic can be written in form of:

$$I_{ai} = F_a(w_a I_a + w_{fb} I_{ai})$$

The structural functional scheme which corresponds to this equation is drawn in Fig. 13-10. The latter also shows the plotting of the characteristic of the output current I of the amplifier contained in the function of the overall number of ampere-turns.
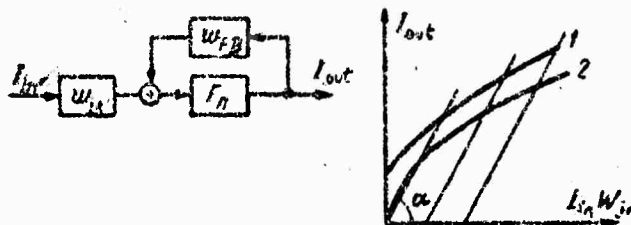
Fig. 13-10. Structure and static characteristics
of a magnetic amplifier with positive feedback.

Let us return to the form written in (13-7e), namely,
$w_{in}I_{in} = H_{f_{\pi}}(I_{out}) - w_{f.b.} I_{out}$. To have it plotted, let us draw
a straight line from the beginning of the coordinates and
draw it at an angle a, which is determined from the fol-
lowing condition:

$$tg\, \alpha = \frac{1}{w_{f.b}}.$$

Assuming different values for the input ampere-turns we
draw a family of straight lines and we find the output cur-
rent in the points where the lines intersect the characteristic
I. The plotting is the same as in 13-9.

The condition required for the self-excitation of a mag-
netic amplifier in a balanced circuit with a characteristic

$$(S'_{ax})_o > \frac{1}{w_{f.b}}$$

is also similar to the conditions required for the self-excitation of a generator.

As the feedback number of ampere-turns increases we have, however, that at $\omega_{f.b} < \dfrac{1}{(S^{I}_{a\omega})_o}$ there is a continuous increase in steepness of the static characteristic of a balanced magnetic amplifier. As the number of ampere-turns goes beyond $\dfrac{1}{(S^{I}_{a\omega})_o}$, the magnetic amplifier will acquire the characteristic of relay 5 (Fig. 13-2,b).

In a magnetic amplifier with an uncompensated initial current (characteristic 1), the positive feedback also acquires larger input-values; the relay section, however, is obtained upon closing the output circuit at any value of $\omega_{f.b}$.

For a cross-circuit scheme shown in Fig. 13-5,b, the static characteristic is graphically constructed in accordance with the rule for plotting characteristics of cascade and parallel schemes. It should be based on equation (13-8) and, for a given X_{out}, the plotting should be performed as in Fig. 13-6 but in reverse order and by adding the linear function $K_1 X_{out}$ and the inverse function $K_2 \Pi_{F_3}(X_{out})$ in the corresponding quadrants.

In conclusion let us examine the structural functional scheme for a linear rotary transformer (LRT) which is used in control systems as a linear voltage-pickup with a limited

angle of rotation of the shaft. Fig. 13-11,a shows one of the modifications of connecting the LRT windings. The primary winding is connected to an a-c circuit having a frequency of f cycles and in the secondary circuit it excites a current of the same frequency which is defined as the sum of the emf's divided by the sum of the resistances:

$$I_\text{н} = \frac{\Sigma E_{2i}}{\Sigma Z_i}.$$ (a)

For an approximate analysis we will take into account only two emf's, or E_{21}, induced in the secondary winding by the longitudinal flux of the stator:

$$E_{21} = E_{10} \sin \theta,$$ (b)

and emf E_{22} induced in the secondary winding by the transverse flux of the stator and proportional to the current of the load flowing through this winding:

$$E_{22} = - k_I^E I_\text{н} \cos \theta.$$ (c)

The influence of the remaining emf's of self-induction and mutual induction of the LRT windings is compensated to a certain extent by the demagnetizing action of the second winding of the LRT rotor which is connected with a constant resistance the value of which is selected during the tuning of the circuit.
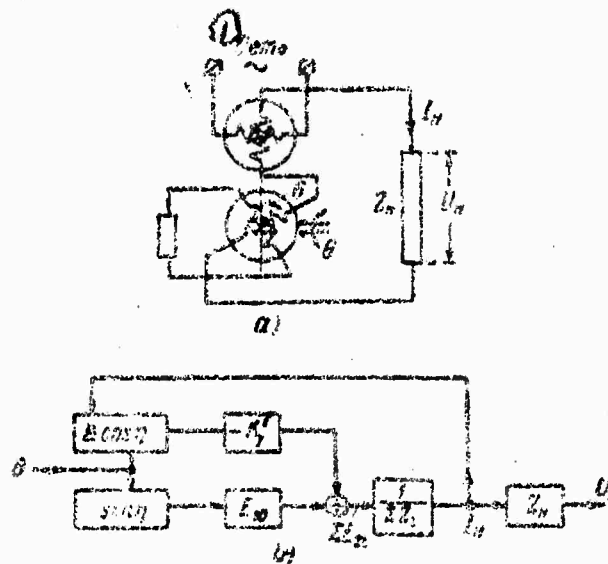
Fig. 13-11. Electrical and structural-functional circuit of a linear rotary (LRM) transformer.

1. Supply line

It remains to add to above equations the conditions required to proceed from the current to the load-voltage:

$$U_n = I_n Z_{n9} \qquad \text{(d)}$$

after which it is easy to draw the structural-functional scheme (b) of the same drawing. The left part of the diagram contains the functional elements with one input equal to $\sin\eta$ and two inputs $\xi \cos\eta$. For the partial values of the generalized arguments of the nonlinear components η and ξ, the actual blocks of the circuit contain, respectively, the real signals θ and I_n.

The structural scheme makes it possible to discern the

qualitative side of the conditions required to transmit
the input value -- the angle of rotation. At small angles
of rotation, the main(lower) route of the scheme provides
a practically linear transmission of the angle, since

$$\lim_{\eta \to 0} \frac{\sin \eta}{\eta} = 1.$$

At this, the feedback exerts a maximum reduction of the
transmission factor, since $\lim_{\eta \to 0} \cos \eta = 1$.

The transmission factor decreases with the increase of
the angle of rotation, since the sinusoidal characteristic
in the first quadrant is similar to a characteristic with
saturation, but because of it, the negative feedback also
decreases ($\cos \eta < 1$) and this aligns the overall characteristic
and makes it nearly linear.

The convolution of the structural scheme, or the trans-
formation of equations (a) - (d) results in:

$$U_{\text{н}} = \frac{Z_{\text{н}} E_{\text{то}} \sin \theta}{\Sigma Z_i \left(1 + \frac{k_j^F}{\Sigma Z_i} \cos \theta\right)} . \tag{13-10a}$$

The best rectification of the characteristic is obtained
at:

$$\frac{k_j^E}{\Sigma Z_i} = \varkappa = 0,54 \tag{13-10б}$$

and provides a deviation from linearity of no more than

13-2. FREQUENCY CHARACTERISTICS OF A NONLINEAR COMPONENT AT THE FIRST HARMONIC

1. QUALITATIVE EVALUATIONS

Let us consider the passage of harmonic oscillations

$$x_{in} = A \sin \omega t$$

through the ACS elements having nonlinear static characteristics.

The transformation of the input sinusoidal signal by a nonlinear component in accordance with the equation

$$x_{out} = F[A \sin \omega t]$$

can be illustrated by the functional structural scheme of Fig. 13-12,a, where the input value ωt passes through a nonlinear (sinusoidal) component, a linear amplifying component with an amplifying factor A, and through the main nonlinear component $F(\xi)$. The reconstruction of the static characteristics to achieve nonlinearity with an insensitive zone is shown as scheme "b" of the same drawing, and fully corresponds to the rules for transformation of characteristics of a cascade scheme as shown in Fig. 13-6.

The resulting output process for the value of amplitude A_1 is shown in the fourth quadrant of the curve of

Fig. 13-12,b in form of the sinusoid's shaded areas. If the input amplitude varies, the new process at the output is to be found by using the same plotting, but changing the slope of the straight line in the second quadrant so as to make it correspond with the new amplitudes A_2, A_3, etc.

As shown in drawing "b", the zone of insensitivity at zero values leads to the appearance of zones of stagnation in the output oscillations; these become smaller as the amplitude increases.

Next, the same Fig. 13-12 shows various characteristics of other types of nonlinearities and their respective harmonic processes. Let us examine their features:

c) saturation; this leads to cutting-off the tops of the sinusoids of output oscillations;

d) progressive nonlinearity (solid line) $\frac{dX_{out}}{dX_{in}} > 0$ and $\frac{d^2X_{out}}{dX^2_{in}} > 0$; this leads to sharper output oscillations and approaches the "zone of insensitivity" type as a limit; in saturated electromagnetic circuits the sinusoidal voltage causes the flow of a similar current; degressive nonlinearity (dotted line) $\frac{dX_{out}}{dX_{in}} > 0$, but $\frac{d^2X_{out}}{dX^2_{in}} < 0$ serve to "dull" the sinusoid and approaches "saturation" type as a limit;

e) hysteresis - mechanical backlash; it cuts off the top of the sinusoid and shifts it in accordance with the phase;
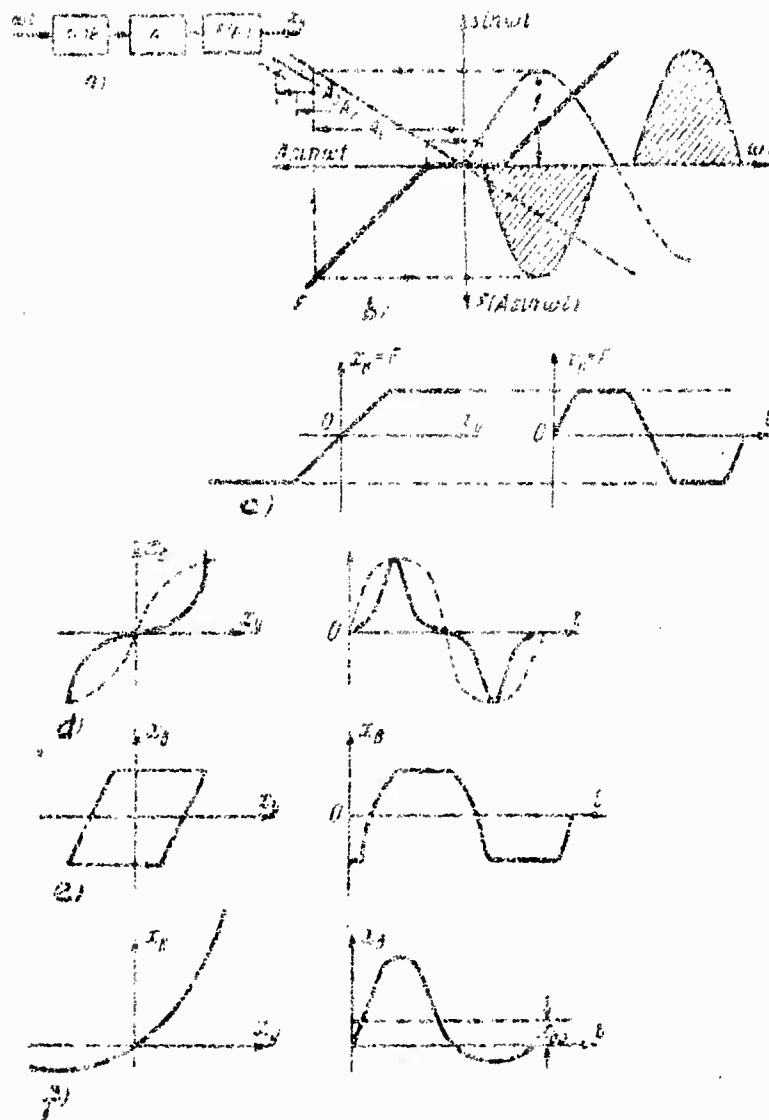
Fig. 13-12. Transformation of input harmonic
oscillations by a nonlinear component

$x_\beta = x_{output}$
$x_j = x_{input}$

f - asymmetric nonlinearity; it deforms the input oscillations and exposes a constant component X_{out_0} found by using equation

$$X_{out} = \frac{1}{2\pi} \int_0^{2\pi} F(A \sin \omega t) \, d(\omega t) =$$

$$= \frac{1}{2\pi} \int_0^{2\pi} F(A \sin \varphi) d\varphi. \qquad (13\text{-}10 \text{ c})$$

2.   HARMONIC COMPONENTS OF OUTPUT OSCILLATIONS

We will examine mainly the symmetric nonlinearities for which the output oscillations can be laid out in the series:

$$X_{out}(t) = A_1 \sin \omega_1 t + A_2 \sin 2\omega_1 t + \ldots + \\ + B_1 \cos \omega_1 t + B_2 \cos 2\omega_1 t + \ldots$$

Let us write the equations required to find the amplitudes for the sine and cosine components of the first harmonic:

$$A_1 = \frac{1}{\pi} \int_0^{2\pi} X_{out}(t) \sin \omega_1 t \, d(\omega_1 t) =$$

$$= \frac{1}{\pi} \int_0^{2\pi} F(A \sin \varphi) \sin \varphi \, d\varphi; \qquad (13\text{-}11a)$$

$$B_1 = \frac{1}{\pi} \int_0^{2\pi} X_{out}(t) \cos \omega_1 t \, d(\omega_1 t) =$$

$$= \frac{1}{\pi} \int_0^{2\pi} F(A \sin \varphi) \cos \varphi \, d\varphi. \qquad (13\text{-}11b)$$

The equations for the remaining harmonics are also well known but their use will become unnecessary if one is to be guided by the methods of N.M. Krylov, N.N. Bogolyubov [1] or by the method of L.S. Gol'dfarb based on nearly the same principles of analysis of oscillations in nonlinear systems.

The most convenient form of writing the equations of (13--11) is the second in which integration is based on angle φ.

In the simple cases of calculation of integrals it is possible to obtain a final result in form of known functions, which will be illustrated below; generally, however, when a nonlinear function is given in form of a curve it is necessary to employ grapho-analytical methods which lead to measuring the curves with a planimeter.

Let us examine the method of transformation of curves for the subsequent planimeter operation [4 and 5].

3. DETERMINATION OF THE SINUSOIDAL COMPONENT

Let us rewrite the equation (13-11a) for a single-valued symmetric characteristic in form of

$$A_1 = \frac{4}{\pi} \int_1^0 F(A \sin \varphi)\, d(\cos \varphi) \qquad (*)$$
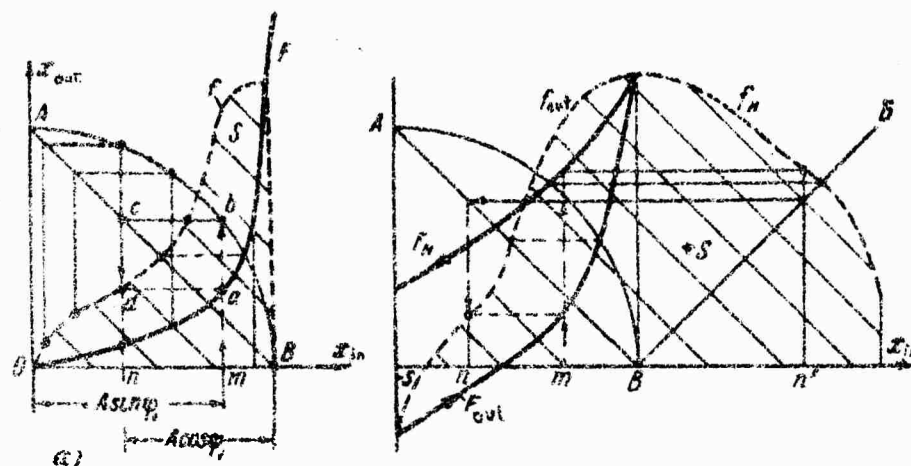
Fig. 13-13. Graphic determination of the amplitude of
a sinusoidal component of an harmonic
at the output of a nonlinear unit.

For a multiple-valued characteristic of hysteresis-type,
the equation will assume the form of:

$$A_1 = \frac{2}{\pi} \int_{-1}^{0} F(A \sin \varphi)\, d(\cos \varphi) + \qquad (**)$$

$$+ \frac{2}{\pi} \int_{0}^{1} F(A \sin \varphi)\, d(\cos \varphi)$$

If the given nonlinear characteristic is redrawn by using
the coordinates $\cos\varphi$, F, the area S of such a curve is just
the one that will provide the results of integration of (*)
and (**).

In Fig. 13-13,a is shown the given   nonlinear

characteristic and plotted, additionally, are one-fourth of
a circle with a radius equal to the given amplitude of the
input harmonic oscillation and the chord AB which makes an
angle of $45°$ with the coordinate axes.

We replot the characteristic F in the following
manner:

Let us select on the x_y-axis an arbitrary point $m(x_1 = Om)$; the value of $\sin \varphi_1$ at this point is obviously

$$\sin \varphi_1 = \frac{x_1}{A} = \frac{1}{A} Om.$$

Let us determine the value of $\cos \varphi_1$ which corresponds
to the same angle φ_1, for which we will draw from point m
a perpendicular line to AB until it intersects the circle at
point b; next, from point b we will proceed along the
horizontal to point c on the chord and from it -- to
point n on the x_n-axis. In view of the parallel manner of
shifting and the slope of the chord at an angle of $45°$, we get
three equal lengths: $mb = nc = \cos \varphi_1 A$. Hence, point n in
the system of coordinates shown on the right side of the
device and having the beginning of the coordinates at point
B will provide the new abscissa for the curve nB.

The ordinate of the static characteristic remains the
same as in point m where it equals the length ma set off on
the perpendicular mb of the static characteristic F. After
shifting point a on the perpendicular nc, we get.

$$nd = am = F(A \sin \varphi_1).$$

By plotting in the same manner for a series of points we will get a replotted curve f shown by dotted line on the same drawing.

Let us mark the shaded area on the drawing enclosed by the coordinate-axes and the replotted characteristic S and this will give us:

$$A_1 = \frac{4}{\pi A} S. \qquad (13\text{-}12a)$$

For an "hysteresis-type" of nonlinearity the manner of obtaining the replotted characteristic is illustrated by the curve b on the same drawing. For the ascending branch F_{ascend} the characteristic f_{ascend} is here similar to the preceding case, but the shaded area has a negative section, while for the descending branch F_{desc} by using an additional bisector of the right angle Bb, it is convenient to develop the transformed characteristic f_{desc} to the right of point B. By designating the total area which is enclosed on the drawing by the transformed characteristic and the horizontal axis and by taking into account the signs of the areas, and designating it as $S_{ascend} + S_{desc}$, we will obtain the following sinusoidal component for the amplitude:

$$A_1 = \frac{2}{\pi A} (S_{ascend} + S_{desc}). \qquad (13\text{-}12b)$$

Only one value of the amplitude of the sinusoidal component is obtained in this manner. All plottings must be performed anew when the input amplitude changes. For certain types of characteristics, however, such plottings may not prove to be too burdensome.

Let us examine an example of plotting the relationship between the amplitude of input oscillations and the amplitude of the sine-components of output oscillations for the relay characteristic F shown on Fig. 10-14 with one-half of the zone of insensitivity and height h of the step.

For the case under consideration, all transformations of the characteristic F will also be in "steps" with h as the height of the step, but of different width. The beginning of the step is found by plotting one-fourth of a circle for each amplitude of input oscillations, drawing to it a chord, and shifting the same length along each circle corresponding to the chord and, again, constructing on the abscissa-axis in accordance with Fig. 10-14. In this manner were obtained points 1, 2, 3, and 4 for the input amplitudes equal to $A_1 = O1'$, $A_2 = O2'$, $A_3 = O3'$, and $A_4 = O4'$. The transformed characteristic has come to an end upon reaching the abscissa-value equal to the input amplitude at points 1', 2', 3', and 4'.

The second area, for example, for the input amplitude $OA' = q$ is equal to the area of a rectangle with height h

and base 11'; for the amplitude $02' = A_2$, the base is equal to 22', etc.

Taking advantage of equation (13-12a), the sought amplitude is found from the curve:

$$A_{11} = \frac{4h}{\pi} \cdot \frac{11'}{0I'}; \quad A_{12} = \frac{4h}{\pi} \cdot \frac{22'}{02'}, \text{ etc.}$$

Plotted in this manner in the lower part of the drawing is a curve drawn in a solid line which reflects the relation between the input and output (sinusoidal) amplitudes.
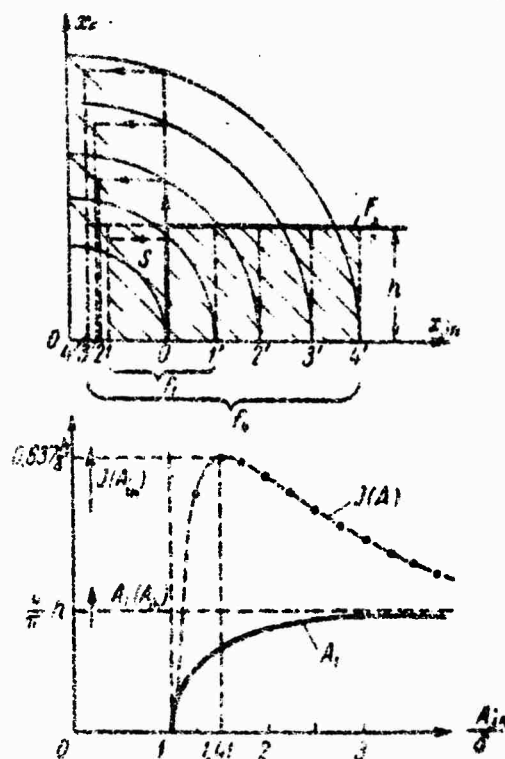
Fig. 13-14. Graphic determination of the sine-component of the first harmonic and of the equivalent transmission-factor of a relay unit.

Instead of the above graphic plottings, the integration of equation (*) can be performed also in a numerical manner. For this purpose we will divide the interval of changes in the variable $\cos \varphi$, which is used for integration, for example, into ten equal parts, i.e. we will assume that $\cos \varphi = 1.0$; 0.9 .... 0.1; 0. To avoid the replotting of the static characteristic, let us find the sine values of these same angles

$$\sin \varphi = \sqrt{1 - \cos^2 \varphi} = 0;\quad 0.436;\dots 0.995;\quad 1.0.$$

On Fig. 13-15 is drawn a nonuniform scale for $\sin \varphi$, which corresponds to the uniform scale for $\cos \varphi$ with the latter divided into ten parts; also, then an arbitrary point are drawn "rays" which, based on proportional recalculation, make it possible to use this scale for any value of the input amplitude, for example, the value $A_M = 0.1'$ shown on the same drawing. Having a given input amplitude and finding the values of the static characteristic for the marked points F_0, F_1, ... F_{10}, the sought area and output amplitude can be next found from the Simpson equation:

$$A_1 = \frac{2}{15\pi}[F_0 + F_{10} + 4(F_1 + F_3 + F_5 + F_7 + F_9) + \\ + 2(F_2 + F_4 + F_6 + F_8)].\qquad (15\text{-}15)$$
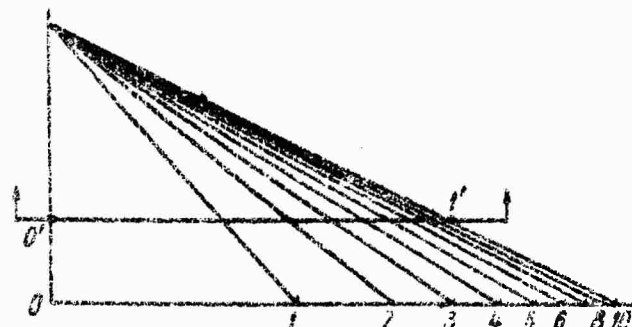
Fig. 13-15. Simple conversion of a sine-scale

4. DETERMINATION OF THE COSINE COMPONENT

While finding B_1 by using equation (13-11b), it is easy to note that in the interval from $\left(-\frac{\pi}{2}\right)$ to $\left(+\frac{\pi}{2}\right)$ the cofactor in the subintegral expression is positive, while in the interval from $\left(+\frac{\pi}{2}\right)$ to $\left(-\frac{\pi}{2}\right)$ the cofactor is negative; therefore, for a single-valued static characteristic the cosine component of the first harmonic is equal to zero.

If the characteristic is multiple-valued, i.e. it belongs to the "hysteresis" type, there will appear a cosine component. For its determination we will use equation (13-11b), in which case it is expedient to divide it into two parts in accordance with the zones of change in sign of $\cos \varphi$ and, in addition, to introduce the function of $\cos \varphi$ under the sign of the differential:

$$B_1 = \frac{1}{\pi} \int\limits_{\varphi = -\frac{\pi}{2}}^{\varphi = \frac{\pi}{2}} F(A \sin \varphi)\, d \sin \varphi -$$

$$(***)$$

$$- \frac{1}{\pi} \int\limits_{\varphi = -\frac{\pi}{2}}^{\varphi = \frac{3}{2}\pi} F(A \sin \varphi)\, d \sin \varphi.$$

It is easy to note that the integrals have the shape
of area in the coordinates of $\sin \varphi$, F, and since for each
given input amplitude the static characteristic in the inter-
val $\pm A_m$ appears to be drawn in the coordinates $A_m \sin \varphi_1, F$,
it means that there is no need of replotting it. The dif-
ference between the integrals $(***)$ is equal to the
area enclosed between the descending and ascending branches
of the static multi-valued characteristic, which is
shaded on Fig. 12-16 and is designated by C. Taking this
designation into account, the amplitude of the cosine com-
ponent is determined by equation

$$B_1 = \frac{1}{\pi A_m} C. \quad (13\text{-}14)$$

If the numerical method of integration is used to find
the area, then dividing, for example, into ten parts

any half of a symmetric hysteresis loop, the expression
for the amplitude of a first sinusoidal harmonic will be in form:

$$B_1 = \frac{1}{15\pi}\left\{(F_{desc} - F_{asc})_0 + 4[(F_H - F_B)_1 + \right.$$
$$+ (F_H - F_B)_3 + (F_H - F_B)_5 + (F_H - F_B)_7 + (F_H - F_B)_9] +$$
$$+ 2[(F_H - F_B)_2 + (F_H - F_B)_4 + (F_H - F_B)_6 +$$
$$\left. + (F_H - F_B)_8] + (F_H - F_B)_{10}\right\}. \qquad (13\text{-}15)$$

$F_H = F_{descending}$

$F_B = F_{ascending}$
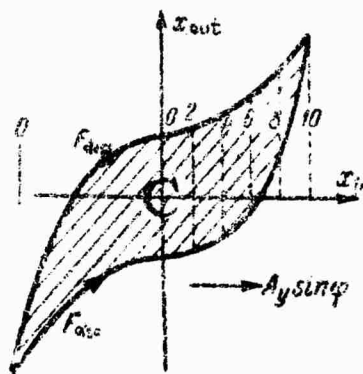
Fig. 13-16. Graphic determination of the cosine-component of the first harmonic of a nonlinear unit.

5. EQUIVALENT COMPLEX GAIN FACTOR

Let us use the operator-form for writting the conditions for the passage of the first harmonic through a nonlinear component.

Let the process at the input be given in form of:

$$X_{in}(p) = \frac{A\omega}{p^2 + \omega^2}.$$

e will put the representation of the process at the output in form of:

$$X_{out}(p) = \frac{A_1\omega + B_1 p}{p^2 + \omega^2}.$$

The ratio between the output representation and that of the input is called the operator equivalent transmission factor of a nonlinear component $f(p,A)$ and is determined by the equation

$$f(p, A) = \frac{A_1}{A} + \frac{B_1}{A}\cdot\frac{p}{\omega}. \qquad (13\text{-}16)$$

In particular, $p = j\omega$, we obtain an equivalent complex gain factor:

$$f(jA) = g(A) + jb(A). \qquad (13\text{-}17a)$$

In the last written form, the dependence on frequency has reduced, but the coefficient g remained complex, as noted in the current. Let us not miss the components of a complex equivalent gain factor.

The real part of a complex equivalent gain factor is:

$$g(A) = \frac{A_1}{A} = \frac{2}{\pi A}\left[\int_0^\theta (E_{out} + E_a)\,d(\cos\varphi)\right]. \qquad (13\text{-}17b)$$

The imaginary part of an equivalent complex gain factor is:

$$b(A) = \frac{B_1}{A} = \frac{2}{\pi A}\left[\int_0^1 (F_{desc} - F_{asc})\, d(\sin\varphi)\right]. \qquad (13\text{-}17c)$$

The module of a equivalent complex gain factor is:

$$|J(jA)| = \sqrt{g^2 + b^2}. \qquad (13\text{-}17d)$$

The phase of an equivalent complex gain factor is:

$$\varphi(A) = \operatorname{arctg}\frac{b}{g}. \qquad (13\text{-}17e)$$

The calculation of parameters of an equivalent complex gain factor can be performed by using the equations (13-17), either by direct integration, or by making preliminary use of the obtained values of the output amplitude of the first harmonic and dividing them by the amplitude of the input oscillations.

Thus, for example, by dividing the ordinate of curve A_1 shown by a solid line on Fig. 13-14 by the values of the input amplitudes (by the abscissa of each point) we will get the dotted curve $J(A)$ which characterizes the change in the real part of the equivalent complex gain factor which, in this example of a single-valued characteristic, coincides with its module.

The analytical expression in this example for $J(A)$ is

alis: fairly simple, since in the interval from $\varphi =$ ___

= arc sin $\frac{\delta}{\lambda}$ to $\varphi = \frac{\pi}{2}$, we have that $F_a = F_{a1c} = 0$ and is

obtained from equations (14-17b) and (13-17a):

$$z(\lambda) = -\frac{4h}{\pi\lambda} \int_{\varphi = \arcsin\frac{\delta}{\lambda}}^{\varphi = \frac{\pi}{2}} d\cos\varphi =$$

$$= \frac{4h}{\pi\lambda} \sqrt{1 - \left(\frac{\delta}{\lambda}\right)^2} = /(\lambda),$$

since $\delta \lambda' = 0$.

Based on the analytical expression it is easy to obtain the derivation of $\frac{\delta}{\lambda} = \sqrt{\frac{2}{3}}$ and the value of $0.77\frac{h}{\delta}$ for the maximum value of the coefficient. For an infinite increase of the wavelength $\lambda(\delta\delta)$, the modulus of the coefficient has zero for limit.

The ... for the elements of the matrix coefficients matrix can be called ... the ... the elements of a non-linear distortion. However, while the amplitude characteristic ... elements depended on the frequency, ... called the amplitude-frequency characteristic (AFCh), which is no ... in frequency in all cases with static nonlinear ... and there ... so, the only ... dependency of the modulus $J(\lambda)$ on the amplitude of input oscillations; ... will ... dependency of the modulus of J-amplitude characte-]

teristic (MJACh). Similarly, for the real, imaginary, and phase characteristics we will use respectively the following abbreviations: ReJACh, ImJACh, and PhJACh.

The real (ReJ) and the imaginary (ImJ) amplitude characteristics may be represented by separate curves, for example, by type of curves drawn on Fig. 13-14; both MJA and PhJACh can be also represented by separate curves, although it is possible to represent these characteristics by a single plotting on a complex plane.
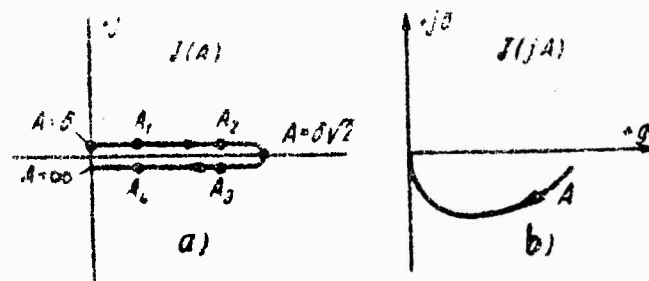
Fig. 13-17. Typical plottings of equivalent complex gain-factors of nonlinear units.

Fig. 13-17 shows examples of plotting amplitude characteristics on a complex plane for single-valued a and for multiple-valued b (hysteresis) static characteristics. The single-valued characteristics yield no imaginary components and are entirely located on real axes and, therefore, it is necessary to show separately both the ascending and descen-

ating branches of the characteristic, each point of which
has its own value for the amplitude of input oscillations.

6. EXPERIMENTAL DETERMINATION OF FREQUENCY-
CHARACTERISTICS OF A NONLINEAR UNIT
AT ITS FIRST HARMONIC

We will examine only those electrical-measurement
devices,which are suitable for taking down the frequency-
characteristics of the components in which the input and out-
put signals are given in form of d-c voltage. It is assumed
that components with other physical properties should for ex-
perimental purposes be provided with transitory devices, such
as electric voltage transmitters, or the test should cover not
the units, but their electronic models.

For taking down the frequency-characteristics at the
first harmonic, the nonlinear units may be connected to
additional linear filters, or by units as shown in Fig. 13-18a,
which eliminates all harmonics higher than the first.

A. Circuit with Low-Frequency Passive Filter

The step-ladder type of filter shown in diagram a has an OTF
in form of

$$W_b(p) = \frac{1}{(T_1 p + 1)(T_2 p + 1)(T_3 p + 1)} \quad (13\text{-}18a) \qquad (13\text{-}18a)$$

where $T_i (i = 1,2,3)$ are time-constants determined by the

methods described in Chapter 6. If the values of the time constants are decreasing with the increase of their numbers, then the slope LACHKh of the linear filter changes with the increase of frequency by 29 decibels/dek each time it passes through the tracking frequency. The properties of a nonlinear static unit do not depend on the frequency, therefore, it is always possible during the experiment to select a frequency that is larger than the last tracking frequency ω_0; in this case *the* amplitude of the second harmonic at the output of linear filter will be smaller than the amplitude of the first harmonic by 6n decibels provided the input levels are the same.
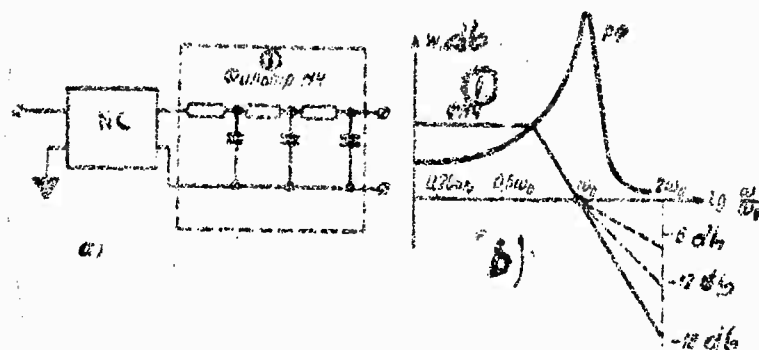
Fig. 13-18. Electric circuit for filtering higher harmonics of a nonlinear unit and LAFCh filters

(1) low-frequency filter

Fig. 13-18,b shows the linear amplitude-frequency characteristic (LAFCh) of a similar low-frequency filter

(1-97) and the suppression coefficients of the second har-
monic by a filter are shown in Table 13-1 for a various
number of cells (n).

Table 13-1

Suppression Coefficients of the Second
Harmonic by a Filter of the n-th order

n	$20 \log \frac{A_2}{A_1}$ decibels	$\frac{A_2}{A_1}$ relative units
1	~ 6	0.5
2	~ 12	0.25
3	~ 18	0.125
4	~ 24	0.625
5	~ 30	0.3125

Beginning with n=4, the share of the second harmonic in
the output-voltage of the filter (and more so of the higher
harmonics under equal conditions) becomes less than 6.25% and
the frequency characteristics of a nonlinear unit together
with the filter can be determined by a device described in
chapter 4 for linear components (Figs. 4-3 to 4-6), but unlike
the linear problem, it is not the frequency that should serve
as the variable input-value, but the amplitude of the input-
oscillations. If $|W(jA, \omega_0)|$ designates the overall modulo-
amplitude characteristic of the nonlinear component (NC) —
filter circuit at frequency ω_0 and $\varphi(A, \omega_0)$ designates the
overall phase-amplitude characteristic of the same circuit,
then the characteristics of the nonlinear component (NC) are
obtained by recalculation of the simple equations:

_1115_

$$\text{MJACh } J(jA) = \frac{|W(jA, \omega_0)|}{|W_{L-FF}(j\omega_0)|} ; \qquad (13-18b)$$

$$\text{PhJACh } \phi(A) = \varphi(A, \omega_0) - \varphi_{L-FF}(\omega_0). \qquad (13-18c)$$

If it is desirable to eliminate the phase-shift $\varphi\varphi(\omega_0)$ introduced by the filter, it is possible for one frequency to select the parameters of a complex filter in such a manner that the hodograph $W(j\omega_0)$ will exactly intersect the real axis. The introduction into the experiment of a low-frequency filter will, of course, other errors due to the inaccurate assumptions of frequency for amplitude and phase errors of the filter, etc.

B. Circuits with Resonant Filters

It is more convenient to replace a low-frequency filter with a resonant filter having a LAFCh (linear amplitude-frequency characteristic) shown in Fig. 13-18,b and designated as RF.

Then, at a resonant frequency ω_0, the importance of the first harmonic compared to the higher harmonics will grow as fast as the rate with which the resonance peak decreases. This makes it possible to disregard the higher harmonics when taking down the frequency characteristics NO of nonlinear components and resonant filters by using the methods developed for linear units, or by selecting a proper threshhold of sensitivity for the measuring device.

1097

Filter characteristics are separated from the overall characteristics in accordance with (13-18).

G. Active Method for Taking Down Frequency Characteristics

The scheme employed for a generator of sustained oscillations (see Fig. 4-7) can be used in experimenting with taking down the frequency characteristics of a non-linear component NC . An NC replacing the linear component in this scheme will cause the transient processes to proceed in a more complex manner. In fact, the equivalent complex transfer coefficient NC $J(jA)$ depends on the amplitude of the input oscillations and, therefore, at diverging or damped oscillations $J(jA)$ may become automatically equal to an arbitrary potentiometer setting (for example, g' for a single valued nonlinearity) and the input-amplitude of the NC may assume a certain specific value A'. Thus can be found g', A', one of the points of the characteristic. Changing the potentiometer setting to g'' will provide the scheme with a new value A'' for the amplitude of input oscillations corresponding to the point g'', A'' of the required characteristic.

The second NC-harmonic appears in the linear tract with a reduced amplitude after the first integrator $\dfrac{A_2 r_c}{r_1 2 \omega T_1}$ and after the second integrator $\dfrac{A_2 r_c}{r_1 2 \omega^2 T_1 T_2}$ and can be largely reduced by a scaled resistance r_1.

If the oscillations in the experiment have no self-restoring tendencies with respect to amplitude, it is then possible to change the polarity of both the NC and that of the potentiometer.

13-3. SELF-OSCILLATIONS IN SYSTEMS WITH NONLINEAR COMPONENTS

1. Qualitative Analysis of Nature of Processes in Nonlinear Automatic Control Systems (ACS)

In analysing the natural movements of linear ACS we introduced the concepts of a steady system with damped natural oscillations, of a nonsteady ACS with diverging natural oscillations, and of a system at the border of stability with oscillations of a definite amplitude brought about by initial influences and remaining unchanged only when the influences are of constant nature.

An entirely new regime — that of self-oscillations — is possible in a nonlinear ACS. Similar to the linear borderline of stability it is also characterized by a steady oscillating state, but the amplitude of oscillations is due entirely to the properties of the system and do not depend (to a certain limit) on the initial disturbances.

The state of self-oscillation is reached by ACS automatically, either as a limit-state called the limit-cycle, or it departs from this state, i.e., the limit-cycle in a

nonlinear systems may be steady or nonsteady which, in its turn, affects the aforementioned definitions given to the properties of ACS as a whole. Let us examine this question in detail and illustrate it with curves shown in Fig. 13-19.
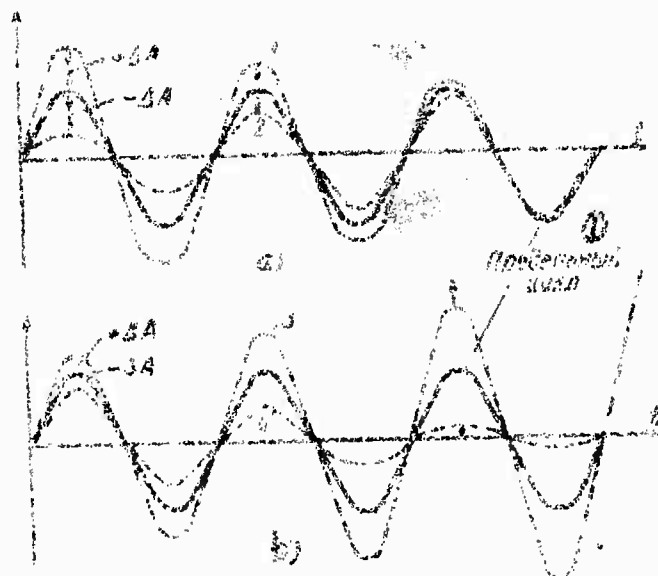
Fig. 13-19. Time-curves for steady and nonsteady limit-cycles (1) limit-cycle

A steady limit-cycle (curve "a") is of such nature that when the first amplitude of the main process (thick line) is undergoing a change due, for example, to a disturbance, the disturbed process will again approach the limit-cycle at any sign of the deviation.

The nature of a nonsteady limit-cycle (curve "b") is

such that any deviation of the amplitude of the limit-cycle will subsequently cause the process to finally depart from the limit-cycle. The process becomes divergent for a positive deviation of the amplitude; with a negative deviation of the amplitude the process tends towards zero.

The appearance of a limit-cycle with a definite amplitude and indications of steadiness change somewhat the concept of the steadiness of a system as a whole. Really, if in a linear system a tendency to reduce the amplitude is observed at any value of the amplitude of oscillations, the system is steady and the motion will end with a complete attenuation. In case of a nonlinear system, however, the reduction of the amplitude may end not with a zero, but with a limit-cycle, i.e., the system as a whole will remain as a self-oscillating system. The same duality is observed for diverging oscillations; the latter may either increase continually, or end with a limit-cycle.

Therefore, the concept of steadiness or nonsteadiness of a system as a whole is tied up with the value of the amplitude of oscillations as compared with the amplitude of the limit-cycle, or with the type of the limit-cycle itself, and this is illustrated by the table below.

A workable nonlinear ACS may, generally, have no limit-cycles and, in such a case, should be steady in all working

ranges; in certain systems, however, it is possible to have
steady limit-cycles characterized by the allowable values
of the amplitude and frequency of self-oscillations.

Table 13-2

Possible (from Standpoint of Steadiness)
Processes in Nonlinear ACS

Type of limit-cycle	The system as a whole	Curve Fig. 13-19
Steady	Steady "in the large"	1
	Nonsteady "in the small"	2
Nonsteady	Nonsteady "in the large"	3
	Steady "in the small"	4
Absent	Steady or nonsteady	--

Consequently, the investigation of the natural motion
of a nonlinear system is essentially reduced to the inves-
tigation of the limit-cycle.

2. Conditions for the Applicability of the Harmonic-Balance Method

Let us examine a very simple transformed structural
scheme of a closed ACS shown in Fig. 13-20 in which all linear
components are reduced by the method of structural analysis
to one element with a complex function $W(j\omega)$, while all non-
linear elements are replaced by a single element with an
equivalent static coefficient of RS $J(A_j)$. Since it is the
self-oscillation regime that is under investigation, the

input and output lines are excluded from the scheme, but
the obtained network remains, as a rule, the network of
negative feedback (it changed the phase of the output sig-
nal by 180°).
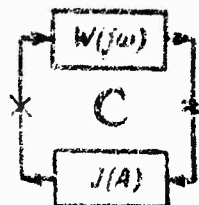
Fig. 13-20. Closed ACS with one nonlinear component.

The harmonic-balance method is based on taking into
account the circulation of only the first harmonic in a
closed network. Actually, at the output of a nonlinear com-
ponent in a regime of self-oscillation we should expect a
periodic curve of complex form containing the higher har-
monics, i.e., the nonlinear element appears to serve as a
generator of higher harmonics. Being closed through the net-
work of the feedback, the higher harmonics enter again the
input of the nonlinear element and change its state (into
saturation, etc).

Since the characteristics of the   linear part of the
control system are nearly the same as the characteristics of
a low-frequency filter, the conditions required for it to
suppress the second and higher harmonics which are generated
by нэ coincide with the conditions described in Table 13-1.
The higher the order of the denominator ОFP of the linear

part as compared with the order of the numerator, the more effective is the filtration of the harmonics.

The smaller the role played by the second and higher harmonics, the more accurate is the harmonic-balance method. Its average accuracy is usually estimated as 10-15%.

The harmonic-balance method is based on the work of Soviet scientists, N.M. Krylov and M.N. Bogolyubov, who, in 1932, applied equivalent linearization for the investigation of the swaying of electrical machines and, later, for other fields of technology. [1]

Let us bear in mind that the equivalent or harmonic linearization differs essentially from the linearization based on the first term of the Taylor series which was employed in the preceding chapters. In harmonic linearization it is assumed, on one hand, that the sinusoidal oscillation at the output correspond to the sinusoidal oscillations at the input of a nonlinear component which, strictly speaking, constitutes the linearization (actually, the output oscillations are not sinusoidal, but contain higher harmonics which are rejected) but, on the other hand, between the amplitudes of the input oscillations and the first harmonic of the output oscillations is retained a functional -- nonlinear relationship.

Having the relation between the input and output of a

nonlinear element with respect to the first harmonic given
in form of a curve or analytically, also having the con-
ditions for closing which, according to Fig. 13-20, make it
possible to connect the input and output oscillations of a
nonlinear element by means of the equation for the linear
part, it becomes possible to compose, first, an equation
for balancing the amplitudes and for balancing the phases
and, secondly, an equation for balancing the real (sinusoidal)
and imaginary (cosinusoidal) components. Both the amplitude
and the frequency of self-oscillations is determined by sol-
ving any of these systems of equations. If the appearance
of a limit-cycle is possible in a ACS, its steadiness becomes
apparent later.

The aforementioned method were further developed by the
works of the Soviet scientists, including those that can be
applied in problems dealing with the theory of control. In
the field of graphic-analytical solutions with the use of an
amplitude-phase balance and criteria of stability resembling
the Nyquist criterion we can mention the work of prof. L.S.
Gol'dfarb which he published beginning with 1940 [2,3]

In the field of analytical solutions which made it pos-
sible to cover a wider range of problems by using the balancing
of real and imaginary characteristics and criteria of stability
based on the criterion of Mikhaylov, the method of harmonic-
balance was substantially advanced by the work of the

3. Finding Periodic Solutions by the method of Amplitude-Phase Balance

Let us return to the scheme for a nonlinear ACS shown on drawing 13-20.

Let APhCh be the given amplitude-phase characteristic of the linear part $W(j\omega)$ which is drawn with the aid of logarithmic templates. Let us transfer it to a complex plane (Fig. 13-21) where the natural angles are retained for recording the phase and a concentric logarithmic net is drawn with a scale in decibels and the circle 0 db is distinguished by a thicker line.

The linearized APhCh of the entire open system will be obviously represented by the following product:

$$C(j\omega, A) = W(j\omega) J(A). \qquad (13\text{-}19a)$$

The limit-cycle of the real system corresponds to the borderline of stability of the linearized system, which is observed in passing the linearized APhCh through points 1, j0, i.e., at $C(j\omega_\pi, A_\pi) = -1$, or at

$$W(j\omega_p) J(A_p) = -1. \qquad (13\text{-}19b)$$

1106

The obtained complex equality, which we will call the amplitudic-phase balance, can provide the balance of amplitudes at both ends of the open system

$$|W(j\omega_p)| = \left|\frac{1}{J(A_p)}\right| \qquad (13\text{-}19c)$$

and the condition for balancing the phases at the same ends, according to Fig. 13-20

$$\varphi_W(\omega_p) = \pi - \varphi_J(A_p). \qquad (13\text{-}19d)$$
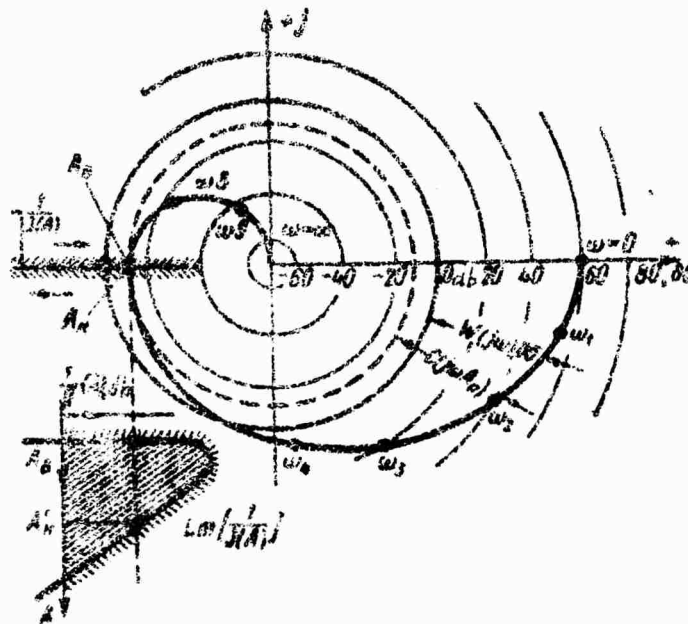
Fig. 13-21. Graphic calculation on a complex plane of a limit-cycle for a single-valued nonlinearity.
Note: $A_H = A$ descending
$A_B = A$ ascending

For a graphic solution of equations (13-19) and for finding the amplitude and frequency of the limit-cycle we will draw on the same Fig. 13-21 an inverse MNACh of the nonlinear part with a phase changed by π, i.e., the characteristic $-\dfrac{1}{J(A)}$.

.We examine a case of a single-valued nonlinearity, where

$$b(A) = 0 \text{ and } J(A) = g(A), \text{ i.e., } \frac{1}{J(A)} = \frac{1}{g(A)}.$$

The entire characteristic $\dfrac{1}{J(A)}$ of such a nonlinearity coincides with the real axis. For an example we will take the curve J shown in dotted line on Fig. 13-14. Its inverse, if recalculated on a logarithmic scale, will occupy a section on the negative real semiaxis from the circle $-\infty$ db to the circle $- 20 \log d_{max}$ db, and again, to $+\infty$ db. In order to separate the ascending branch from the descending one (Fig. 13-21), the ascending branch is shaded at the top with a slope in one direction while the descending branch is shaded with a slope in another direction. Since each branch has its own amplitude-value, the entire curve $\dfrac{1}{J(A)}$ was reproduced below on a logarithmic scale to have it better illustrated and the same shading was reproduced there as the shading on the complex plane..

At the points of intersection of the amplitude-phase characteristic of the linear part $w(j\omega)$ and of the inverse

MJA characteristic of the nonlinear part, we have

$$\left| \frac{1}{J(A_p)} = | W(j\omega_p)|, \right.$$

i.e., we retain the condition (13-19c) for balancing the amplitudes; just as we retain the condition (13-19d) for balancing the phases, since $\varphi_J = 0$ and $\varphi_W(\omega_p) = \pi$.

Therefore, subtracting from the curves the values of frequency ω_π and of amplitudes $A_\pi = A_{asc}$ and $A'_\pi = A_{desc}$, we get the sought parameters of the limit-cycles. Here are possible two limit-cycles with amplitudes A_{asc} (ascending branch) and A_{desc} (descending branch) and the same single frequency . It remains to determine which of these cycles is stable.

The stability of the limit-cycle is checked by drawing a linearized APhCh of an open system (13-19) for fixed values of A_π. For this purpose it is sufficient in this example to increase all radii-vectors of APhCh $W(j\omega)$ by multiplying them by $g(A_\pi)$. With a logarithmic net where the modulo is given decibels it is sufficient to increase all radii-vectors by $Lm \, g(A_\pi) \, [db]$, since it follows from expression (13-19a) that:

$$\left| Lm \, | C(j\omega, A_p)| = Lm \, |W(j\omega)| + \right. \qquad (13\text{-}20) \\ + Lm \, |g(A_p)|.$$

It is obvious, however, the same result can be obtained by leaving APhCh unchanged and by displacing in the opposite direction the entire numerical representation of the

concentric net of decibels by the amount of $\log(A_p)$. Here, the new line 0 db will pass exactly through the point of intersection of the amplitude-phase characteristic and of the inverse MPACh. The new circle 0 db is shown by a dotted circle in the drawing under examination.

Consequently, due to the application of the logarithmic concentric net, AMACh of the linear part $w(j\omega)$ which is drawn with respect to the main line 0 db serves at the same time as linearized AMACh of the open system with respect to line 0 db passing through the point of intersection of the characteristics of linear and nonlinear parts $G(j\omega, A_p)$ shown in fig. 13-21 and passing through point 0 db, W, i.e., $(-1, j0)$ in the new numerical representation of the scales, which is typical for a limit-cycle.

In order to evaluate the stability of the limit-cycle we will increase artificially the amplitude of the limit-cycle by a small value bringing it up to the value of $A_p - \delta A$ and we will see how the change in the gain factor of the nonlinear part, which was brought about by this increment, will affect the stability of the linearized system.

Let us examine the limit-cycle with an amplitude $A_\pi = A_{asc}$ at the ascending branch $g(A)$. An increase in amplitude to the value of $A_{asc} + \delta A$ will in this case lead to a change in the linearized AMACh of the open system:

$$C(j\omega, A_{n.c} + \delta A) = W(j\omega) g(A_{n.c} + \delta A). \qquad (13\text{-}21)$$
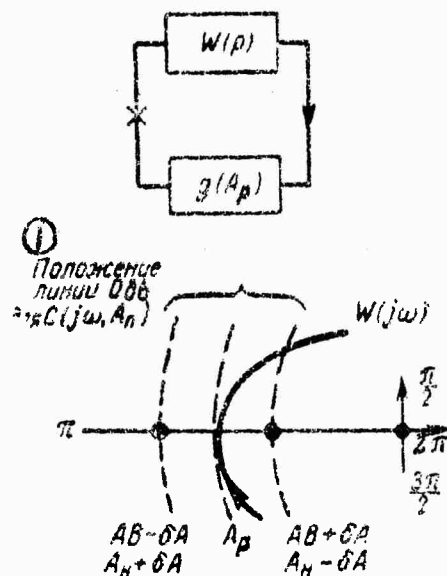
Fig. 13-22. Finding the stability of a
limit-cycle of a static ACS with
a single-valued nonlinearity
(1) Position of line $0\delta b$ for $C(j\omega, A_p)$

There is no need to plot the curve, a change in the
numerical representation on the logarithm-paper will
suffice. Let us trace very carefully the displacement of
point 0db, $P(-1, j0)$. If the amplitude gets a positive
increment, the point 0 db on the ascending branch will move
to the right, as shown in the lower part of Fig. 13-22. If
the transfer-function $W(p)$ has no special features, it means
that the shift of point 0db, $p(-1, j0)$ inside the network

1111

signifies a shift to the region of instability, or a further
increase for the amplitude, as shown by curve 3, Fig. 13-19.
As the amplitude decreases to the value of $A_{asc} - \delta A$, the
point 0 db, W of the new characteristic $C(j\omega, A_{asc} - \delta A)$ will
appear outside the network, or in the region of stability
and the oscillation will reduce their amplitude due to the
attenuation, as in curve 4 of Fig. 13-19. Therefore, the
limit-cycle at amplitude A_{asc} on the ascending branch $g(A)$ is
unstable.

Let us now examine the limit-cycle for amplitude A_{desc} on
the descending branch $g(A)$. An increase in amplitude to the
value $A_{desc} + \delta A$ will, in characteristic $C(j\omega, A_{desc} + \delta A)$, shift
the point 0 db, W outside the network, or to the region of
stability (see shaded area, Fig. 13-21) This indicates a sub-
sequent decrease of amplitude, as in curve 1 of Fig. 13-19.
In characteristic $C(j\omega, A_{desc} - \delta A)$, the decrease in amplitude
to the value $A_{desc} - \delta A$ shifts the point 0 db, W inside the
network, or into the region of instability and the oscil-
lations increase as in curve 2 of Fig. 13-19 approaching the
limit-cycle. Therefore, a limit-cycle with an amplitude A_{desc}
and a frequency ω_p is stable.

Let us note that in determining the stability of a
limit-cycle, the examination of the frequency characteristic

$$C(j\omega, A_p + \delta A) = W(j\omega)g(A_p + \delta A),$$

actually means that under investigation is the stability of
a certain fictitious linear system (Fig. 13-22) whose direct
circuit contains an operator-component $W(p)$ and an ampli-
fying component $g(A_p)$.

However, with the aid of such fictitious system we dis-
close only the direction of the next change in δA, since
simultaneously with a change in δA there is also a change
in the characteristic of the fictitious system which (for a
stable limit-cycle) approaches the characteristic $C(j\omega, A)$
when $\delta A \rightarrow 0$ and moves away from it when δA increases in
an unstable limit-cycle.

Let us conclude the analysis of a specific relay-type
of nonlinearity having a zone of insensitivity by citing
still another conclusion.

If the obtained limit-cycle has an amplitude A_p and a
frequency ω_p which are acceptable for the normal operation
of the controlling object, then the automatic control system
/ACS/, as a whole, is a fairly efficient device. The dis-
ruption of an unstable limit-cycle, although unavoidable, is
no danger for the system because, in such a case, the ampli-
tude either approaches zero as a limit, or is limited by the
amplitude-value of the second stable limit-cycle.

Nonlinearity of the same type, however may affect in
an entirely different manner the efficiency of the ACS

1113

containing a more complex linear part.

Let us examine the characteristic of the linear part
of the system which is shown in Fig. 13-23 and which has an
astaticism of the third order. Such a characteristic may
be obtained also for systems with lower orders of astaticism,
if during the theoretical analysis in accordance with the
conditions required to separate the nonlinear element it
becomes necessary to disrupt the inside follow-up type of
feedback that enclose the integrating components.

For such a system, the region of instability (we speak of
the location of point 0 db, π) is identified by the shading
on the drawing (if other features are present, use is made
of the rule for angle of rotation to find the stable region).
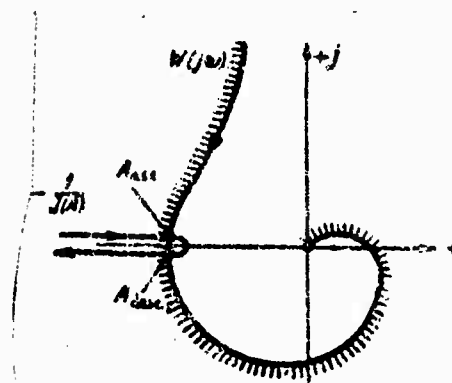
Fig. 13-23. Finding the stability of the limit-cycle
of ACS having an astaticism of the third order
and one nonlinear component.

The same characteristic of the nonlinear component is used as in Fig. 13-21. The intersection of both characteristics produce the amplitudes of the limit-cycles A_{desc} and A_{asc} and the frequency ω_p. Examining now the amplitude A_{asc} at the ascending branch $g(A)$ we see that its increase shifts the point 0 db, π to the region of stability, i.e., that the oscillations again return to the limit-cycle, while a decrease in amplitude shifts the point 0 db, π into the region of instability, i.e., the amplitude begins to increase while returning again to the limit-cycle. It means that the limit-cycle is stable on the ascending branch $g(A)$.

With the second value for the amplitude A_{desc}, its increase shifts the point 0 db, π to the unstable region, while its decrease shifts the point to the stable region, i.e., the limit-cycle is unstable.

Such a system can operate efficiently only within the range of disturbances that end with a stable limit-cycle, provided that its amplitude and frequency are acceptable for the controlling object. The disruption of a stable cycle the shift of oscillations in point A_{desc}, ω_p, while the effect of the disturbance continues, leads to an unlimited increase of the amplitude, which causes the system to operate inefficiently.

It is not difficult to note in an examination of the stability of a limit-cycle that in this case it is also

— 1115 —

an examination of a fictitious linear system (Fig. 13-22), since the evaluation of stability made it necessary to use linear criteria. The use of linear criteria is advisable because of their universal application and the stability of a limit-cycle for a single-valued nonlinearity should be always evaluated by adhering to the following standard method:

1) plot the amplitude-phase characteristic $\overline{A\varphi\angle C_h}$ and mark by shadings the location-region of point -1, $j0$ (0 db, π) that corresponds to the unstable linear system which is closed through an amplifying component;

2) plot the inverse amplitude characteristic of the nonlinear element with the phase of $\overline{AJC_h}$ changed by π;

3) it provides a positive increment for the input amplitude of the nonlinear element, as compared with the amplitude of the limit-cycle which is obtained at the intersection of the linear and nonlinear characteristics.

If while moving along the amplitude characteristic of the nonlinear element we arrive at the nonshaded region $O(j\omega, A_p)$, when there is a positive increment in the amplitude as compared with the amplitude of the limit-cycle, it will mean that the limit-cycle is stable; the crossing into the shaded region results in an unstable limit-cycle, i.e., the limit-cycle will be of the same nature as the region (stable or unstable). The plotting can be done on paper with either uniform or logarithmic divisions.

We will now consider the case of "hysteresis-type" of multiple-valued nonlinearity.

We will plot again an inverse, negative (with phase shifted by π), complex amplitude-characteristic of the non-linear component. Fig. 13-24 shows an inverse, negative, complex characteristic that corresponds to the multiple-valued characteristic located in the first quadrant ($g > 0$, $b > 0$).

Next we plot again the amplitude-phase characteristic of the linear part and the parameters of the limit-cycles A_p, ω_p, and A'_p, ω'_p are found at the points where the characteristics of the linear and nonlinear parts intersect each other.

The complex equivalent gain factor of the nonlinear component is equal, for example, at point A'_p, ω'_p is:

$$J(jA'_p) = g(A'_p) + jb(A'_p)$$

/For hysteresis-characteristic we have $b(A'_p) < 0$; or a lagging phase/. Since the condition for an amplitude-phase balance $W(j\omega_p) = -\dfrac{1}{J(jA_p)}$ is fulfilled, therefore the non-linear component provides for amplitude A_p exactly the necessary conditions for the limit-cycle of characteristic $W(j\omega_p)$ in both the phase and change of its amplitude.

In investigating the stability of the limit-cycle by using linear criteria, it is again necessary to examine the fictitious linear system in which the nonlinear component
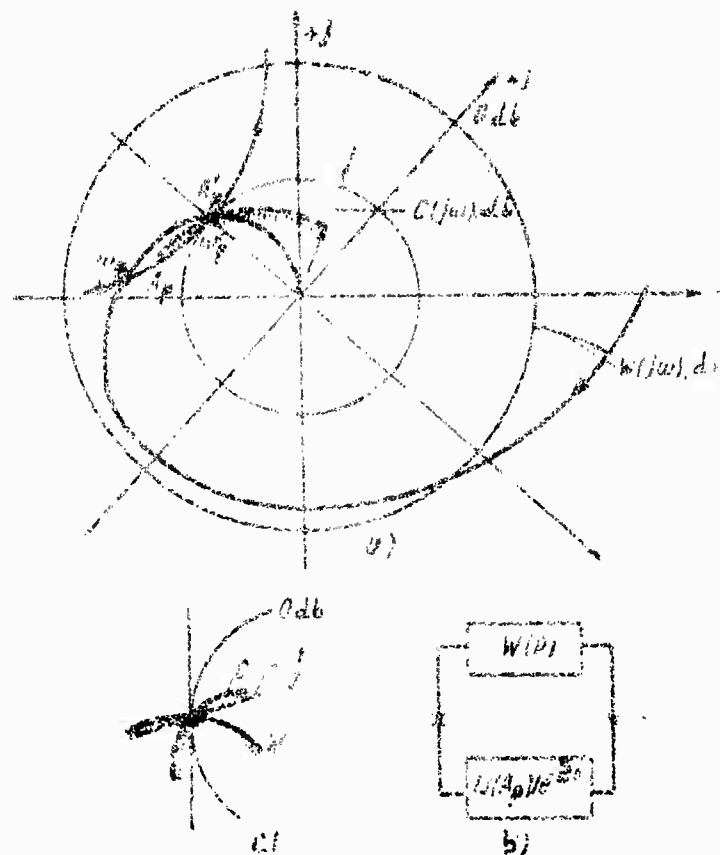
Fig. 17-24. Graphic analysis on a complex plane
of parameters of a limit-cycle of a nonlinear
component with a multiple-valued
static characteristic.

Let us note that the nonlinear component (by creating at
frequency ω_p and amplitude A_p a phase-shift φ_p and gain-factor
of amplitude $|J(jA_p)|$ along the first harmonic) does not

change these parameters when the frequency changes. Such linear components do not exist. An approximate equivalence can be obtained, for example, by using a lagging component with the following transfer function:

$$K(p) = |J(jA_p)| e^{-\frac{\varphi_p}{\omega_p} p}. \qquad (13\text{-}22)$$

In this case the gain factor is unchanged and is in full agreement with the coefficient of the nonlinear component $|J(jA_p)|$ and the phase can be matched only at the frequency of the limit-cycle at $p = j\omega_p$. Continuing with this method of discussion, we reduce the problem to an investigation of the stability of the fictitious linear system "b" (Fig. 13-24) with a transfer function of the open system

$$C(p) = W(p) |J(jA_p)| e^{-\frac{\varphi_p}{\omega_p} p}. \qquad (13\text{-}23)$$

To plot the AFCh of an open fictitious system, we will turn the coordinate axis and will shift the designations of the circle 0 db, as shown in Fig. 13-24. At this, in the new reading system, the characteristic $W(j\omega)$ will pass through point 0 db, π, i.e., at this point it will coincide with the characteristic $C(j\omega)$. At the subsequent points the cofactor $e^{-j\frac{\varphi_p \omega}{\omega_p}}$ will create an additional turn of the characteristic by an angle:

$$\Delta\varphi = \varphi_p \left(1 - \frac{\omega}{\omega_p} \right) = \varphi_p \frac{\Delta\omega}{\omega_p}. \qquad (13\text{-}24)$$

Specifically, the initial section $\omega_{\#\#}$ will turn by an angle φ_β without changing the modulo. Since the borderline of stability is already determined, it sufficient to plot only a small section of the changed characteristic near the point 0 db,π, which is done in Fig. 13-24.

Let us shade on the change characteristic the region of instability for point 0 db,π, determined by means of linear criteria and let us increase the amplitude by δA. Then the nonlinear element contained in the OFP will have a new equivalent linear image:

$$K_1(p) = |J(A_\beta + \delta A)| e^{-\frac{\xi_\beta}{\omega_\beta} p} e^{\frac{\xi_\varphi}{\omega_\beta} p}.$$

To avoid replotting of hodograph $C_1(j\omega)$, it is sufficient to shift the point (0 db,π) along the characteristic $-\frac{1}{J(A)}$. At this, it will not only change the position of circle 0 db, similar to Fig. 13-22, but it will also turn the real axis. The shift of point (0 db,π) during the increase in the amplitude of the limit-cycle from the region of instability to the region of stability along the linear equivalent testifies, as before, to the stability of a limit-cycle of a nonlinear system.

A direct evaluation of the region of stability by means of hodograph $W(j\omega)$ may not coincide with a similar evaluation by means of godograph $C(j\omega)$ in a case illustrated by Fig.

1120

13-24, where the hodograph $-\dfrac{1}{J(A)}$ passes between the characteristics π and C near the point 0 db, π.

Instead of an equivalent lagging component, during the examination of the stability of a limit-cycle NC of the hysteresis-type, the $(\delta < 0)$ can be substituted by an equivalent aperiodic component

$$K(p) = \frac{K}{Tp+1} = \frac{|J(A_p)|^2}{g(A_p) - b(A_p)\dfrac{p}{\omega_p}}.$$

For analytical calculations it is convenient to retain the substitution in (13-16).

4. Finding Periodic Solutions by the Method of Balancing Real and Imaginary Characteristics

Let us represent the transfer function of the linear part of the system as the ratio of polynoms: $W(p) = \dfrac{U(p)}{V(p)}$. From this follows the expression for the amplitude-phase characteristic:

$$W(j\omega) = \frac{U(j\omega)}{V(j\omega)}.$$

The complex amplitude characteristic for the examined static nonlinearities we obtain in form of a complex binom.

The amplitude-phase balance for the assumed designations can be written in form of :

$$-\frac{V(j\omega_p)}{U(j\omega_p)} \cdot g(A_p) + jb(A_p).$$

It is easy to proceed from the amplitude-phase balance to the balance of the real and imaginary characteristics:

$$\left|-\operatorname{Re}\left[\frac{V(j\omega_p)}{U(j\omega_p)}\right]=g(A_p); \quad -\operatorname{Im}\left[\frac{V(j\omega_p)}{U(j\omega_p)}\right]=b(A_p).\right.$$

(13-25)

The amplitude-phase balance can be also written in the following form

$$\left| X(A_p, \omega_p) + jY(A_p, \omega_p) = 0, \right. \qquad (13\text{-}26)$$

By concentrating all members in the left part of the equality, where

$$\left.\begin{array}{l} X(A_p, \omega_p) = \operatorname{Re} V(j\omega_p) + g(A_p)\operatorname{Re} U(j\omega_p) - \\ \qquad - b(A_p)\operatorname{Im} U(j\omega_p); \\ Y(A_p, \omega_p) = \operatorname{Im} V(j\omega_p) + b(A_p)\operatorname{Re} U(j\omega_p) + \\ \qquad + g(A_p)\operatorname{Im} U(j\omega_p). \end{array}\right\}$$

(13-27a)

Then, the balance of the real and imaginary parts will be written in form of:

$$\left| X(A_p, \omega_p) = 0; \quad Y(A_p, \omega_p) = 0. \right. \qquad (13\text{-}27b)$$

The solution of equations (13-25) and (13-27) is usually performed graphically. If an explicit solution with respect to any of the unknown values of A_p or ω_p can be obtained from both equations, then by changing the second value it is easy to plot in Cartesian coordinates the geometrical locus of

the points in form of curves shown in Fig. 13-25. The
intersection of these curves yields a point having the
values of A_p and ω_p which satisfy both equations of the
system. Only the coordinates of the point of intersection
are the ones that have a definite technical meaning as the
parameters of self-oscillation, since in this case, both
A_p and ω_p satisfy both equations of the system of (13-27).
The remaining points of both curves have no technical
meaning and there would be no necessity of plotting the
curves if the system of equations is to be solved
analytically.
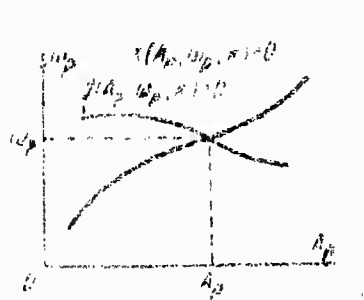
Fig. 13-25. Calculation of parameters of a
limit-cycle by the method of balancing
real and imaginary characteristics.

The curves under investigation may intersect at several
points; if so, the investigation of the stability of the
limit-cycle must be performed very carefully.

If the curves do not intersect, it means that there

are no self-oscillations in the system. Such a regime was
indicated in the last line of Table 13-1. If the absence
of a limit-cycle makes the system as a whole stable, then
it makes sense to strive for it by trying to obtain definite
values of the parameters of the system, namely, the gain
factor, time constants, etc. If any of the parameters is
designated by K and the dependency on it of the equations
of the system is expressed in form of

$$X(A_p, \omega_p, K) = 0; \quad Y(A_p, \omega_p, K) = 0, \quad (13\text{-}38)$$

then, by assuming a number of values for the parameter K
and solving for each value a system of equations (the
graphic method calls for the plotting of two curves of
Fig. 13-25) it is possible to find the borderline of
stability along parameter K, i.e., such of its limit-value
at which self-oscillations do not yet appear. The same data
may furnish the values of parameter K at which self-
oscillations may exist, but their amplitude will not step
outside the permissible value, or their frequency will be
equal to the specified frequency.

The solution of such problems by no means removes the
question of determining the stability of the limit-cycle.

As before, we will determine the stability in a
simplified manner based on linear criteria and this makes

1124

"It necessary to employ a linearized system. Let us do the the substitution of a nonlinear multiple-valued element by a sufficiently simple linear equivalent in form of the component in (13-16). The characteristic equation of a closed ACS will assume in this case the form of:

$$V(p) + U(p)\left[g(A_p) + \frac{b(A_p)}{\omega_p}\,p\right] = 0. \quad (13\text{-}29)$$

This equation makes it easy to obtain an expression for plotting the hodograph of Mikhaylov:

$$M(j\omega,\,A_p) = V(j\omega) + U(j\omega)\left[g(A_p) + j\omega\,\frac{b(A_p)}{\omega_p}\right].$$

The plotting of the hodograph may be carried out by calculating the real and imaginary components:

$$\left.\begin{aligned}
X_{\text{м}}(\omega,\,A_p) &= \operatorname{Re} V(j\omega) + g(A_p)\operatorname{Re} U(j\omega) - \\
&\quad - \frac{\omega}{\omega_p}\,b(A_p)\operatorname{Im} U(j\omega); \\
Y_{\text{м}}(\omega,\,A_p) &= \operatorname{Im} V(j\omega) + g(A_p)\operatorname{Im} U(j\omega) + \\
&\quad + \frac{\omega}{\omega_p}\,b(A_p)\operatorname{Re} U(j\omega).
\end{aligned}\right\} \quad (13\text{-}30)$$

Let us note that, compared with equations of (13-27a) (which, it is true, have an entirely different significance), here will appear additional cofactors $\frac{\omega}{\omega_p}$ when the coefficient is $b(A_p)$. At $\omega = \omega_p$, however, the conditions

1125

$[X(A_p, \omega_p) = 0$ and $Y(\omega_p, A_p) = 0$ coincide with the conditions $X_2(\omega_p, A_p) = 0$ and $Y_2(\omega_p, A_p) = 0$, therefore, the hodograph of Mikhaylov must pass through the beginning of the coordinates which indicates the finding of an equivalent linearized system at the borderline of stability.

In order to pass judgement on the stability of the limit-cycle based on the method used to furnish proof, it is again necessary to impart to the amplitude of the self-oscillations a certain increment δA, obtain new values for the coefficients of the nonlinear component $g(A_p + \delta A)$, $b(A_p + \delta A)$, and verify the stability of the linear equivalent system using the following hodograph of Mikhaylov:

$$M(j\omega, A_p + \delta A) = V(j\omega) + G(j\omega)\left[g(A_p + \delta A) + \right.$$

$$\left. + j\omega \frac{b(A_p + \delta A)}{\omega_p} \right]$$

There is no need to plot the hodograph itself, since small shifts in the hodograph at small changes in parameters have been thoroughly analysed in chapter 4 for the hodograph (4-39). It remains only to substitute the real "V" and the imaginary "U" parts of the equation (4-35,a) with the components of Mikhaylov's vector (13-30) and consider the amplitude "A" as the parameter subject to variations. In such case, the condition for increasing the angle of rotation of Mikhaylov's hodograph by $+180°$ with respect to

the borderline hodograph will be, as in (4-33,b), written in the Jacobian form of:

$$
\left|
\begin{array}{cc}
\dfrac{\partial X_M(\omega,\ A)}{\partial A} & \dfrac{\partial X_M(\omega,\ A)}{\partial \omega} \\[2ex]
\dfrac{\partial Y_M(\omega,\ A)}{\partial A} & \dfrac{\partial Y_M(\omega,\ A)}{\partial \omega}
\end{array}
\right|_{\substack{A=A_p \\ \omega=\omega_p}} > 0,
\qquad (13\text{-}31)
$$

where the partial derivatives can be developed as follows:

$$
\left(\frac{\partial X_M}{\partial A}\right)_p = \operatorname{Re} U(j\omega_p)\left(\frac{dg}{dA}\right)_p - \operatorname{Im} U(j\omega_p)\left(\frac{db}{dA}\right)_p;
$$

$$
\left(\frac{\partial Y_M}{\partial A}\right)_p = \operatorname{Im} U(j\omega_p)\left(\frac{dg}{dA}\right)_p + \operatorname{Re} U(j\omega_p)\left(\frac{db}{dA}\right)_p;
$$

$$
\left(\frac{\partial X_M}{\partial \omega}\right)_p = \frac{d}{d\omega}\operatorname{Re} V(j\omega_p) + g(A_p)\frac{d}{d\omega}\operatorname{Re} U \times (j\omega_n) -
$$
$$
- b(A_p)\left[\frac{\operatorname{Im} U(j\omega_p)}{\omega_p} + \frac{d}{d\omega}\operatorname{Im} U(j\omega_p)\right];
$$

$$
\left(\frac{\partial Y_M}{\partial \omega}\right)_p = \frac{d}{d\omega}\operatorname{Im} V(j\omega_p) + g(A_p)\frac{d}{d\omega}\operatorname{Im} U(j\omega_p) +
$$
$$
+ b(A_p)\left[\frac{\operatorname{Re} U(j\omega_p)}{\omega_p} + \frac{d}{d\omega}\operatorname{Re} U(j\omega_p)\right].
$$

The appearance of the last terms in functions $\dfrac{\partial X}{\partial \omega}$ and $\dfrac{\partial Y}{\partial \omega}$ is due entirely to the nature of the additional equivalent linear component. If the nonlinearity is single-valued, we have that $b = 0$ and all equations become substantially simplified.

If the linear equivalent of the system present at the borderline of stability had no right-handed poles in its OTF but had only left-handed and two neutral poles, then the increase of the angle of rotation of the vector by $+\pi$ indicates the stability of the linear equivalent. With the same limitations, the positive nature of the Jacobian (13-31) serves as a criterion of the stability of the limit-cycle.

5. Phase-Balance in the case of Single-Valued Nonlinearities

If several single-valued nonlinearities are included in a one-circuit (according to the nonlinear elements) closed network together with linear elements, then the structural scheme of the system is usually reduced to the form shown in Fig. 13-26,a. In this case the transfer functions of all linear elements in the span between the nonlinearities are united and form the operators $W_1(p)$, $W_2(p)$, and $W_3(p)$ and in the spans between the nonlinearities the scheme may contain parallel branches and feedbacks. The nonlinear elements are specified by their static characteristics which serve to determine the coefficients of harmonic linearization $g_1(A)$, $g_2(A)$, and $g_3(A)$.

Since single-valued nonlinearities do not produce a phase-shift, therefore, to determine the frequency of the

self-oscillations it is sufficient to examine the phase-characteristic of the linear portion. The overall phase-frequency characteristic of all linear elements of an open system is determined in accordance with the simplified structural scheme of Fig. 13-26,b by using the equation:

$$\varphi(\omega) = \varphi_1(\omega) + \varphi_2(\omega) + \varphi_3(\omega) \qquad (13\text{-}32)$$

made
and is usually ∧ with templates for typical components. The frequencies ω_p, ω'_p, ω''_p, ... which furnish the phase-balance

$$\varphi(\omega_p) = \pi, \qquad (13\text{-}33)$$

are the frequencies of limit-cycles.

Let us now find the amplitude of the limit-cycle. With a known frequency ω_p, the linear elements have the gain factors along the amplitude $A_1(\omega_p)$, $A_2(\omega_p)$, $A_3(\omega_p)$ .... (amplitude-phase characteristics at frequency ω_p). Being constant numbers, they can be included into the amplitude-characteristics of the nonlinear components in form of cofactors for the output values, which will only change the scale of the nonlinear component.

Such a unification of characteristics has been carried out in the scheme of Fig. 13-26,c. To plot the overall amplitude-characteristic of an open system with a frequency ω_p, use can be made of the same method which was used to

obtain the static characteristicof components which were
included in a cascade manner, as illustrated in Fig. 13-5.
A similar plotting was made for Fig. 13-27, but plotted in
quadrants I, II, and III were not the static characteristics,
but the amplitude characteristics of nonlinear components
(of the same type as on Fig. 13-24, for example). Concerning
the overall amplitude characteristic that was obtained in
this manner in quadrant IV, the points of intersection with
the bisector of this quadrant are to be determined. At
these points is observed a equality between the input and
output amplitudes of the open system and, consequently, the
gain factor is equal to unity, or the condition required to
balance the amplitudes is observed when the amplitudes are
respectively equal to A_p and A_p'. The plotting is repeated
for the frequencies ω_p', ω_p'', ...

The method that was examined provides a satisfactory
accuracy only if filtering properties are present in each
of the linear components which are enclosed between the
nonlinearities.
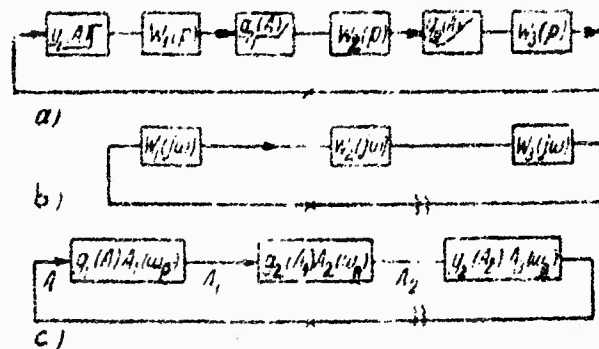
Fig. 13-26. Structural-functional scheme for automatic control system /ACS/ with three single-valued nonlinearities; for calculations by the phase-balance method.
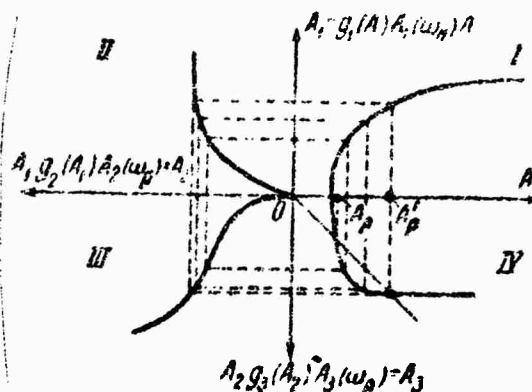
Fig. 13-27. Graphic determination of the amplitude of a limit-cycle for three single-valued nonlinearities separated by filters.

13-4. Control Processes for Nonlinear Systems

The making-up of control-processes for nonlinear
components requires the use of methods employed in numerical
integration. Certain nonlinearities disrupt the linkage of
the ACS-networks by means of nonlinear components /NC/;
for example, we have the zone of insensitivity which acts
to unlock the system in the region of small deviations, or
the relay-characteristic -- for increments in the range of
large values. In such cases an unlocked system without NC is
obtained either by the operator-method or by the frequency-
method until the desired process is found to be outside the
above NC-zones. If, after this, the NC connects the circuit
and breaks it again for increments, a similar method is used
to obtain the next part of the process that will match the
preceding one.

A review of other methods employed in analysis of
processes in nonlinear automatic control systems is outside
the scope of structural methods described in this work and,
therefore, will be omitted.

A most complete description of approximation methods for
investigation of transient processes in nonlinear systems is
furnished by the corresponding member AS USSR, Ye.P. Popov
[37].

BIBLIOGRAPHY

1. Krylov, N.M. and Bogolyubov, N.N. - <u>Vvedeniye v nelineynuyu mekahniku</u> (Introduction to Nonlinear Mechanics). Kiev, Gostekhizdat, 1937.

2. Gol'dfarb, L.S. - <u>Tezisy doklada na soveshchanii po teorii regulirovaniya</u> (These of the Report at the Conference on Theory of Control), published by the AS USSR, 1940.

3. Gol'dfarb, L.S. - <u>O nelineynosti reguliruyemikh system</u> (Concerning the Nonlinearity of Controlled Systems). <u>Byulleten' VEI</u> (Bulletin of the All-Union Electrotechical Institute), 1941, No 3.

4. Shatalov, A.S. - <u>Graficheskoye opredeleniye pervoy garmoniki toka po krivoy namagnichevaniya</u> (Graphic Determination of the First Harmonic of the current with the Aid of a Magnetization Curve), <u>Elektrichestvo</u> (Electricity) 1941, No 1.

5. Shatalov, A.S. - <u>Nekotoryye voprosy garmonicheskovo analiza</u> (Certain Problems in Analysis of Harmonics), <u>Izvestiya Novocherkasskogo Industrial'nogo Instituta imeni Ordzhonikidze</u> (Reports of the Novocherkassk Industrial Institute imeni Ordzhonikidze), 1941, No 13.

6. Popov, Ye.P. - Uchet vliyaniya nelineynostey pri raschete sledyashchikh sistem (Taking into Account the Effect of Nonlinearities in Design of Follow-up Systems), Avtomatika i Telemekhanika (Automation and Telemechanics), 1953, No 6.

7. Popov, Ye.P. and Pal'tov, I.P. - Priblizhennyye metody issledovaniya nelineynykh avtomaticheskih sistem (Approximation Methods of Investigation of Nonlinear Automatic Systems), Fizmatgiz, 1960.

Chapter Fourteen

CONTROL SYSTEMS WITH AMPLITUDE MODULATION

(pp 367-408)

14.1 PHYSICAL PRINCIPLES IN OPERATION
OF ELECTROMECHANICAL SYSTEMS WITH
AMPLITUDE MODULATION

A. Measuring Systems

It is convenient to examine certain properties of sys-
tems with amplitude modulation, first, by taking as an
example simple measuring schemes, such as shown in Fig. 14-1.

Scheme "a" illustrates a remote-control method for the
angle of rotation of shaft $\xi(t)$ with the aid of a pointer-
type of measuring instrument. The transmission of data is
done by an alternating current; the measuring instrument in
this case is of the electrodynamic type, for example, an
electrodynamic wattmeter.

Let the angle of rotation of the shaft be equal to $\xi(t)$
and the angle is converted by a linear potentiometer with
a scale of U_ρ/ε_M of the voltage

$$u(t) = \frac{\sqrt{2}U_\rho}{\varepsilon_M} \, \varepsilon(t) \sin \Omega t. \qquad (14\text{-}1)$$

The voltage formed in this manner retains the frequency

of the network, but its amplitude changes in proportion to
the angle of rotation of the shaft, i.e., the voltage of
the network had its amplitude modulated by the law governing
the change of the angle. The potentiometer in this scheme
serves as a mechanical modulator. The voltage taken off
enters the voltmeter-winding of the wattmeter, while the
current-winding is connected through a limiting resistance
to the network and   through it flows(without change in
amplitude) a current

$$I(t) = \sqrt{2}\,I \sin(\Omega t - \varphi_I), \qquad (14\text{-}2)$$

where φ_I is the possible phase-shift between the current and
the voltage in the windings of the wattmeter, which is due
to the incomplete similarity of the supply circuits.

As it is known [1] , the readings of the wattmeter will be
proportional to the operating values of the current and vol-
tage and to the cosine of the angle between them:

$$P = UI \cos \varphi_I = \left(\frac{U_o I}{k_y} \cos \varphi_I \right) \epsilon(t) \qquad (14\text{-}3)$$

In the right side of the obtained equation are sub-
stituted the operating values of the current and voltage
taken from the right sides of equations (14-1) and (14-2),
while all constant parameters are enclosed in parentheses
and form a coefficient of proportionality between the angle

of the shaft's rotation and the angle of rotation of the
wattmeter's pointer measured in units of the power scale.

Therefore, the equation (14-3) contains no more the
voltage carrier-frequency of (14-1) but converts only the
envelope of the voltage of (14-1), or the demodulated vol-
tage of the potentiometer. In this example, the wattmeter
acts as an electromechanical demodulator.

Demodulation differs from ordinary rectification
(detection) by retaining the information on the sign of the
modulating rule. In fact,/the shift of the potentiometer's
wipers to its lower half changes the angle of the phase
between the current and voltage of the wattmeter by 180°, and
since $\cos (\varphi + 180^\circ) = - \cos \varphi$, the wattmeter's pointer will
in this case deviate from zero in a direction opposite to
that of the voltage recordings for the upper half of the
potentiometer. Therefore, in (14-3) the coefficient enclosed
in parentheses should be considered as being constant in
value and sign, and the change in sign refers to the the
modulating angle of rotation during its moving away from
the middle of the potentiometer.

The simple scale-connection in (14-3) between the
modulating and demodulating processes is valid only during
the slow rotation of the shaft and by disregarding the vib-
rations of the pointer. These assumptions will be given an

_ 1136 _

exact evaluation later and, to understand the physical meaning or the operation of a modulating scheme, it is fairly convenient to continue to use equation (14-3) without making it more complex now.
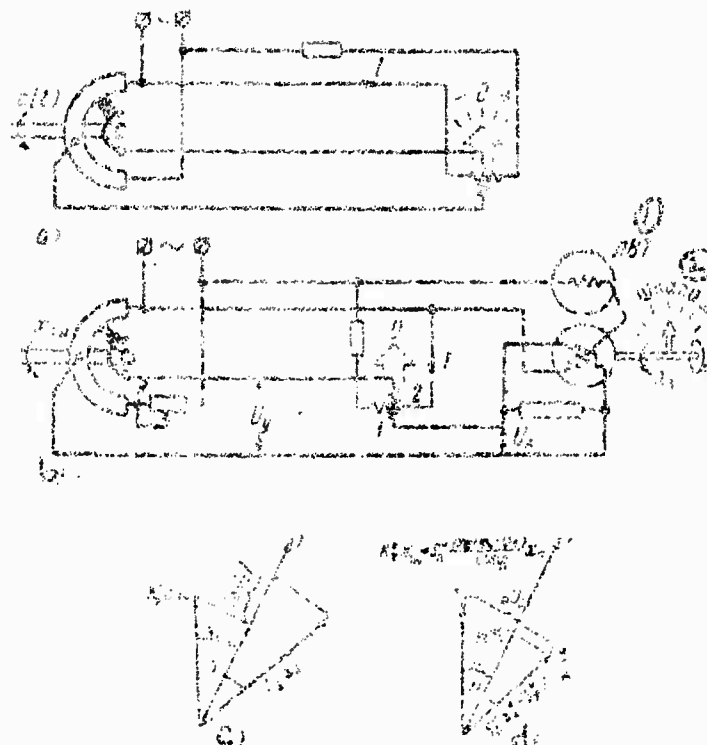
Fig. 14-1. Circuits and vector diagrams of measuring systems with amplitude modulation.
Key: 1) Linear rotary transformer (LRT); 2) scale.

The diagram in Fig. 14-1,b illustrates the compensation method of remote control of the angle of rotation of the input-shaft. The voltage which is proportional to the angle

of rotation of the input shaft $\frac{U_n}{x_{yu}} x_y = K_x^u x_u$, is here com-pared with the voltage which is proportional to the angle of rotation of the compensating shaft that is connected to the recording scale; a linear rotary transformer LVT serves here as a converter of the angle into a voltage (Fig. 13-5). The voltage U_K of the LVT is tied-up with its angle of rotation by a steepnes $S_x^u = \Delta U/\Delta x$. Bringing it to the operating value of the voltage, we will get the following expression for instantaneous values:

$$u_K(t) = \sqrt{2}\, S_x^u\, x_k(t) \sin(\Omega t - \varphi_K). \qquad (14\text{-}4)$$

Therefore, there are two modulators in this scheme: the potentiometer operating in accordance with equation (14-1) provided $\xi[t]$ is replaced by $X[t]$ and $U_n/\mathcal{E}_M$ is replaced by K_x^u , also the LRT /Linear Rotary Transformer/ which operates in accordance with equation (14-4). The difference between the voltages determined by this equation is:

$$\Delta u(t) = \sqrt{2} \left\{ S_x^u x_k(t) \sin(\Omega t - \varphi_K) - K_x^u x_y(t) \sin \Omega t \right\} \qquad (*)$$

and is supplied to the first winding of the wattmeter.

If the second winding of the wattmeter has, as before, flowing through it the current (14-2), then, according to the vector-diagram b, the readings of the instrument are determined by the difference of two "powers":

$$\Delta \Pi - I \Delta u_c = I \left\{ S_x^u x_K(t) \cos(\varphi_x - \varphi_I) - \\ - K_x^u x_y^0(t) \cos \varphi_I \right\}. \qquad (14\text{-}5)$$

The parentheses enclose the difference Δu_c, which is well illustrated by the vector-diagram "c" as the difference between the projections of the voltages in the direction of the vector of the wattmeter's current. For the wattmeter to show zero, it is necessary to equalize the values of these projections (as shown in diagram "d") by turning during the measuring process the shaft of LRT by an angle x_y^0, which will furnish the following condition:

$$x_K^0(t) = \frac{K_x^u \cos \varphi_I}{S_x^u \cos(\varphi_K - \varphi_I)} x_y(t). \qquad (14\text{-}6a)$$

If the recording on the compensation-scale is to correspond to the measured angle of rotation of the shaft

$$x_K^0(t) = x_y(t). \qquad (14\text{-}6b)$$

it is sufficient for the specified phase-shifts to match the potentiometer scale with the steepness of the LRT

$$K_x^u = \frac{\cos(\varphi_K - \varphi_I)}{\cos \varphi_I} S_x^u \qquad (14\text{-}6c)$$

The stability of the examined compensation scheme

depends entirely on the constancy of the phase-shifts which, at the appearance of reactance-components in the circuit's resistance, depend mainly on the constancy of the frequency. The shift in phases is periodically compensated by trimming the scales with the aid of a regulating rheostat R connected in series with the potentiometer.

In the scheme balanced according to equations (14-6), only the cosine-component of the mismatch ΔU_c is subjected to damping, but, as shown in diagram "d", the sine-component ΔU_s continues to circulate in the wattmeter's circuit, since the vector-difference of the voltages $\overline{U}_1$ and $\overline{U}_2$ is perpendicular to the direction of the current's vector and, as per diagram "d", is equal to:

$$\Delta U_s = x_y [K_x^u \sin \varphi_j + S_x^u \sin (\varphi_k - \varphi_j)],$$

or, according to (14-6c), is equal to:

$$\Delta U_s = \frac{S_x^u x_y \sin \varphi_k}{\cos \varphi_j}. \qquad (14\text{-}7)$$

The same result can be easily obtained analytically. Therefore, the pointer of the wattmeter in a compensation-scheme is set at zero, not because the mismatch of the modulus is equal to zero, but because the vector of the mismatch is perpendicular to the vector of the wattmeter's second winding.

1140

B. Single-Channel Follow-Up Systems

Fig. 14-2 shows a follow-up system in which the mismatch obtained in a mechanical differential in form of an angle of rotation of the shaft $\xi(t)$ modulates the amplitude of the network voltage in the inductor. The modulated voltage increases and enters the first movable winding of the wattmeter's relay. The network current flows in the second winding of the relay and the relay, as a whole, operates as a wattmeter serving as a modulator, but the movable winding frame is not connected to the pointer, but to the controlling slide valve of the hydraulic or the pneumatic system (GM). The subsequent part of the ACS is now operating with a demodulated signal and requires no special analysis.

If, for example, the ACS completes a transient function, the mechanical mismatch at the output shaft of the differential varies as in curve "b" of the same drawing. In this case, the modulated mismatch voltage is shown by curve "c" where the envelope "b" is filled with the carrier frequency of the network with the phase varying by 180° each time the output winding of the inductor passes through the position at which it is perpendicular to the exciting magnetic flux. The voltage-frequency of the supply network usually belongs to the category of low frequencies (tens and, occasionally, hundreds of cycles) and the frequency of oscillations

of the ACS shafts belongs to the infra-low group of fre-
quencies (units and fractions of a cycle).

The performance of a specified controlling shift in
ACS is accomplished upon receipt of information on the mis-
match, or when there is a phase-shift of its cosine-component
to zero.

Fig. 14-2,d shows a potentiometer-inductor follow-up
system in which the modulating part coincides with the mea-
suring system of Fig. 14-1,b and uses for a demodulator a
tube-circuit also known as a phase-discriminator. The plate
supply of the phase-discriminator is obtained from the a-c
voltage of the network delivered through a shaping device
(FE) (limiter) which imparts a rectangular shape to each half-
wave of the voltage.

With such a plate supply, the plate current in each tube
will for the duration of the positive half-wave of the plate
voltage contain a constant component I_0 and a variable com-
ponent proportional to the network voltage $I_M \sin(\omega t + \varphi)$.
Since the grid voltage has a common phase-shift with res-
pect to the network voltage φ and, also, the grids of both
tubes are mutually shifted in phase by $180°$, the difference
of the currents of both tubes during the operating half-
period will be equal to

$$i_1 - i_2 = [I_0 + I_M \sin(\omega t + \varphi)] - [I_0 - I_M \sin(\omega t + \varphi)] =$$
$$= 2I_M \sin(\omega t + \varphi).$$

Multiplying this difference by the value of the output resistance we will get the voltage across the output terminals $(i_1 - i_2)R$. The capacitor connected to the output terminals is charged by this voltage and, during one-half period of operation of the circuit, maintains at the terminals an average voltage which is determined by integration during the half-period and averaged for the period:

$$U_{av} = \frac{2RI_M}{2\pi} \int_0^\pi \sin(\omega t + \varphi)\, d(\omega t) = \frac{2RI_M}{\pi} \cos\varphi. \qquad (14\text{-}8)$$

Here it is assumed that the plate-voltage of the phase-discriminator coincides in phase with the voltage of the potentiometer, therefore, the projection axis in the vector diagrams (similar as in Figs. 14-1,c and d) will coincide with the vertical line and, instead of angles φ_1 and φ_2 there will remain the only angle φ. The performance by AOS of the specified angle will end with $\varphi = 90^\circ$, when in equation (14-8), $\cos\varphi = 0$, or when the mismatch vector is perpendicular to the vector of the plate voltage.

The conditions for tuning the follow-up system obeys the equations (14-8) at $\varphi_1 = 0$, since the follow-up system only automates the measuring scheme of fig. 14-1,b.

In Fig. 9-7,a was shown a scheme of a follow-up system with measuring parts made of selsyns and with a two-phase actuating motor. The two selsyns , just as the single

— 1143 —

Inductor with a mechanical differential as in scheme of fig. 14-2,b serves as modulators. As the demodulator, it is the two-phase electric motor itself which during the period develops an average starting torque depending on cos φ, where φ is the phase-shift of the control-voltage with respect to the voltage located at the exact quadrature with the voltage in the excitation winding (B.2).
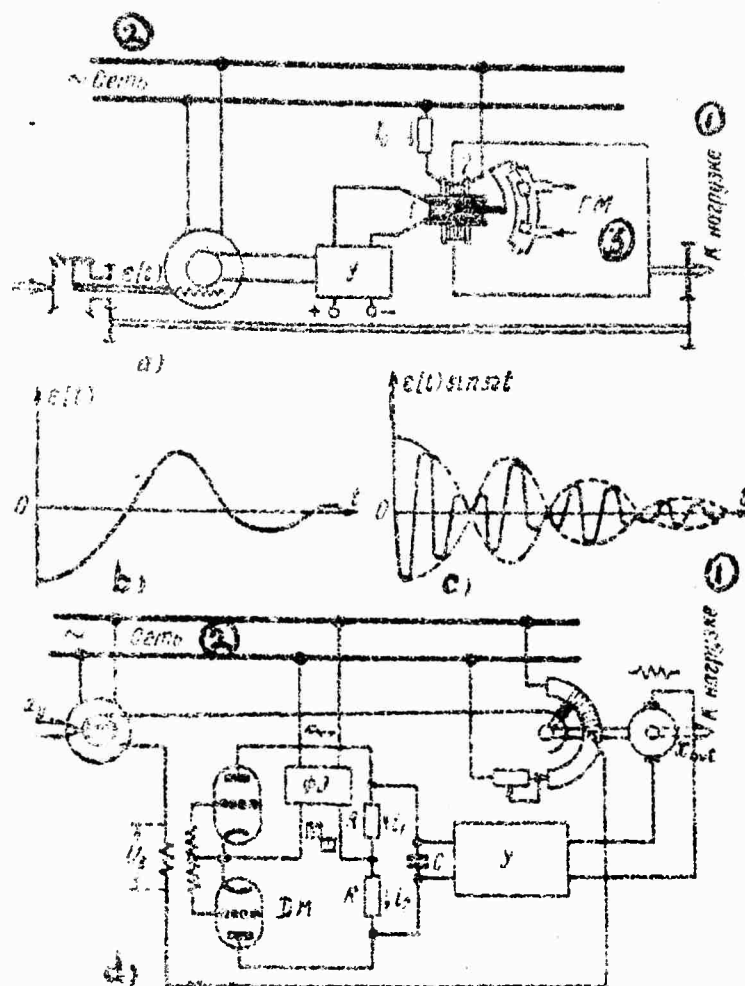
Fig. 14-2. Circuits of follow-up systems with electromechanical and electronic demodulators and curves for the processes.
(1) to the load; (2) network; (3) GM)

C. Two-Channel (Vector) Follow-up Systems

Fig. 14-3,a shows the measuring part of a tridimensional follow-up system of a typical radar station for tracking a target (B. 3).

The target is continually swept by beams of high-frequency electromagnetic energy ; the antenna receives the signals reflected from the target which, after rectification, acquire a definite level of reception. To indicate the location of the target-bearing with respect to the axis of the antenna and the subsequent preparation of command for opening the antenna in a vertical and horizontal planes, the lobe of the radiation pattern rotates (scans),with the aid .of a movable oscillator moving about the paraboloid of the antenna, over a conical surface having a comparatively small opening of 2ν.

This causes the target to be radiated with a periodically changing intensity, except when the bearing of the target coincides with the axis of the antenna, in which case the radiation level is constant (see point 1 in Fig. 14-3,b).

For an arbitrary position of the target typified by angle φ in the image-plane b for point 2, the reflected signal will have a maximum level when the axis of the oscillator passes the plane 012 and will have a minimum level when the oscillator makes one-half of a turn. During the inter-

mediate position the signal will vary in accordance with an almost sinusoidal law with the phase of the sinusoid equal to angle φ in the image-plane b between the vertical diameter in this plane and the bearing for the present position of the target. The high-frequency signal in the radar's receiver is demodulated and freed of its constant level. In Fig. 14-2,c is shown the variable component of the signal before the last stage of demodulation by two electronic blocks connected as in scheme "d".

In this scheme the demodulators have a plate-current supply that is similar to the current-supply of the demodulator in scheme of Fig. 14-2,d; however, the demodulator DM_c gets a rectangular voltage which is in phase with the signal when the target plane coincides with the plane of the axis of the antenna's paraboloid, while the demodulator DM_s receives a voltage with a phase shifted by 90° from that of the first, as shown in U_c and U_s. In connection with this, and similar to equation (14-8), the following voltages appear as in diagram "e) at the output of the demodulators:

$$\Delta U_c = K_1 \cos \varphi; \qquad (14\text{-}9a)$$
$$\Delta U_s = K_2 \sin \varphi. \qquad (14\text{-}9b)$$

The reduction of these mismatches to zero can be, of course, accomplished by individual azimuth and elevation follow-up systems.
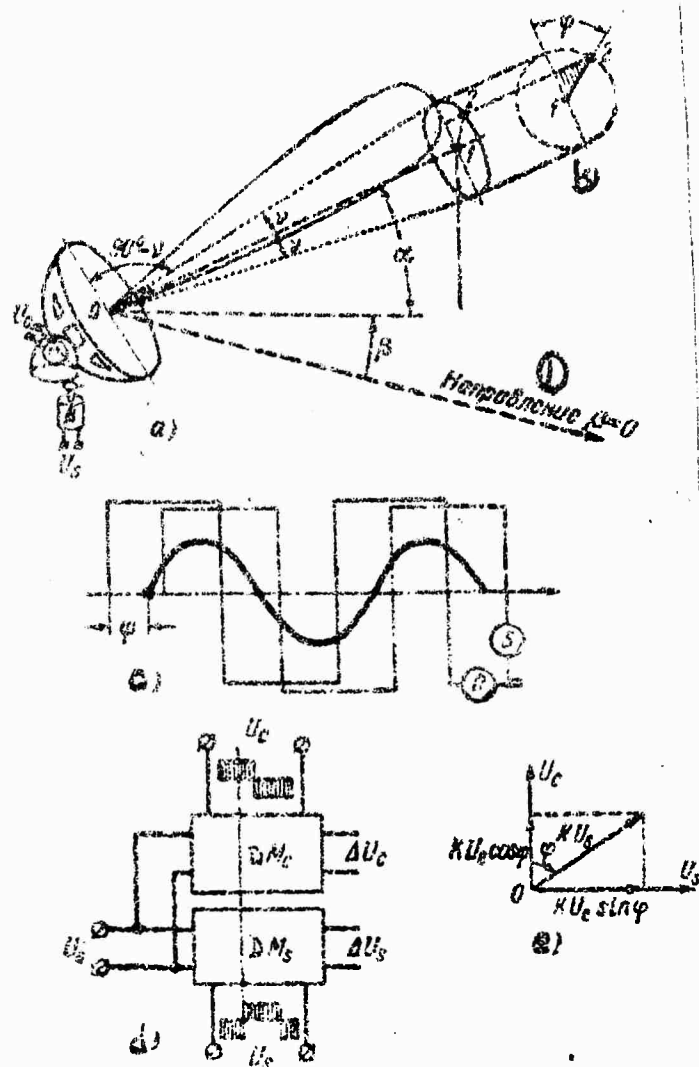
Fig. 14-3. Two-channel, three-dimensional radar follow-up system.

a) scheme for tracking of azimuth and elevation; b) position of target in image-plane; c) curve of the envelope of the reflected signal in the background of the reference voltages of the demodulators; d) connection of the sine and cosine demodulators; e) diagram for the resolution of mismatch vector over the coordinate axes: 1) bearing.

upon receiving the signal ΔU_e, the ACS for elevation
changes the position of the axis of the antenna's paraboloid
with respect to the horizon and reduces the unbalancing ΔU_e
to zero. The azimuthal ACS unfolds the paraboloid into a
horizontal plane and erases the unbalance ΔU_g. Both ACS
devices operate individually; the interconnection between
the channels arrives at the appearance of additional phase-
shifts between the voltages and will be analysed in Sec.14-3

In Fig. 14-4, the principle governing the two-channel
vector-demodulation is made clear by an automatic vector-
reader. Let us assume an input voltage U_e in which the module
φ and the phase β have a definite geometrical meaning, namely,
the distance to the object, the direction to the object, or
as in scheme "c", the geometrical sum of several distances.
In such cases, the values of φ and β should be obtained by
mechanical scales of compensating devices which are consider-
ably more accurate than the pointer-instruments, such as a
voltmeter and phasemeter. For this purpose use is made of a
method of decoding the vector which contains two demodulators
DM_e and DM_g whose plate-circuits are fed by a phase shifter
with a shift of phase by $90°$, a compensation potentiometer
the supply of which is made to be in phase with that of DM_e,
and the motors of the follow-up systems φ and β with suitable
amplifying devices.
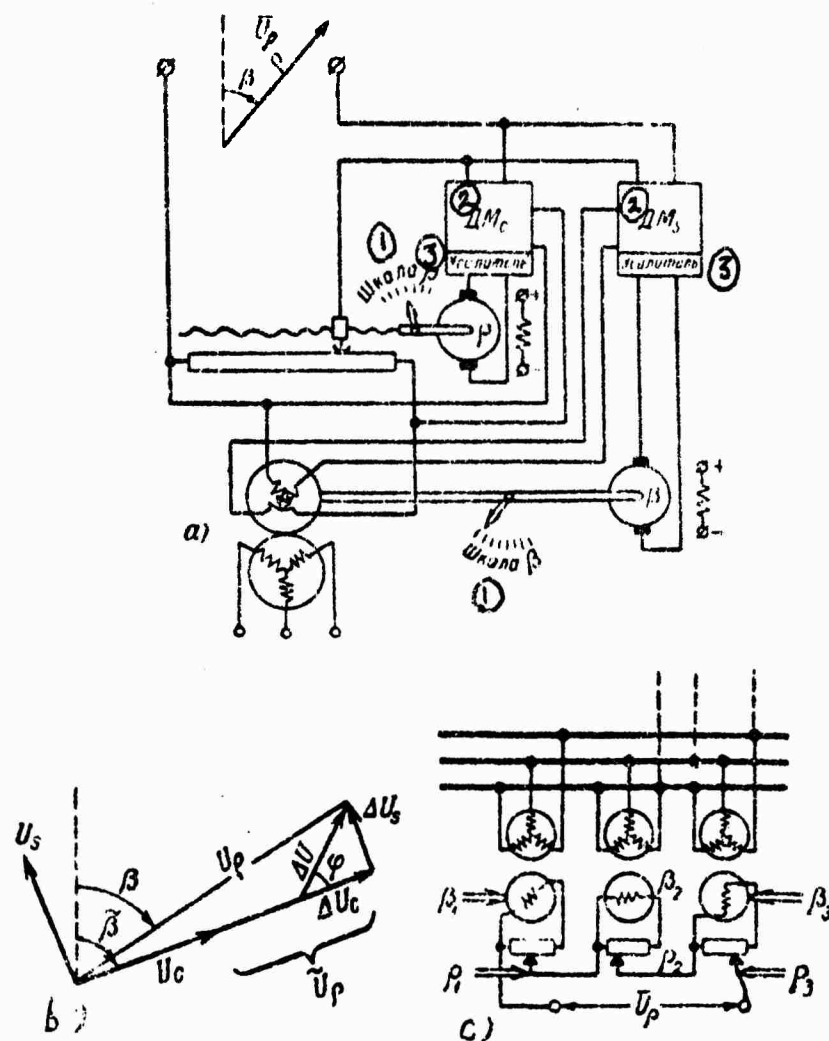
Fig. 14-4. Electrical Circuit and voltage-
diagrams of an automatic vector-reader.

(1) scale; (2) demodulator DM; (3) amplifier.

During an arbitrary rotation of the shafts $\widetilde{\rho}$ and $\widetilde{\beta}$, the compensating vector has an amplitude $\widetilde{\rho}$ and a phase $\widetilde{\beta}$ which differ from the desired ρ and β which brings about the

appearance of the voltage of the unbalance ΔU that can be easily determined by using the vector diagram "b" of Fig. 14-a.

The demodulators separate from this vector projections to the vector of the plate-voltages $\Delta U_c = K_1 \cos$, $\Delta U_s = K_2 \sin$.

If the voltage ΔU_c is amplified and fed to the motor ρ, while the voltage ΔU_s feeds the motor β, the latter will cause the rotation of the potentiometer wiper and the rotor of the phase-shifter which are connected to the shafts ρ and β and will change the compensating voltages of the module and phase, and will reduce the unbalances to zero. After this performance is complete, the result can be read on the mechanical scales of ρ and β. If no consideration is given to other circumstances to be mentioned later, the operation of the follow-up systems along ρ and β is not affected by small deviations because the vectors ΔU_c and ΔU_s are both orthogonal.

In the examples thus far examined and also in other technical applications, amplitude modulation is employed due to their following favorable features:

1) The inducting parts can be made without contacts, with low friction, and highly reliable.

2. The alternating current can be amplified more simply and without drift.

3. An AM signal may furnish vector information.

- 1750 -

14-2. DYNAMIC ANALYSIS OF SINGLE-CHANNEL ACS WITH MODULATORS, AMPLIFIERS, AND DEMODULATORS

1. Methods of Operator and Frequency Analysis Based on the General Theory of Linear ACS with Variable Parameters

According to Fig. 14-2,a the process of modulation can be described as a multiplication of the input signal $\varepsilon[t)$ by the voltage varying sinusoidally with time, and the process of demodulation -- as a repeated multiplication of the modulated voltage by the sinusoidal current to obtain a product proportional to the torque in the movable·system of the wattmeter. These operations in the field of time can be reflected in the field of representations by using the method of λ-conversion described in Chapter 3 in analysing a structural network with variable coefficients, as shown in Fig. 14-5.

Amplitude modulation (AM)

Representation of the input process

$$\varepsilon[t) \leftarrow\div E(p) \qquad (14\text{-}10a)$$

after passing through the block of the variable coefficient, $\cos \Omega t$ is converted to form

$$X(p) = L\{\varepsilon[t)\cos\Omega t\} = \operatorname{Re} E(p+j\Omega) \qquad (14\text{-}10b)$$

$$X(p) \quad \frac{1}{?}\,[F(p + j\Omega) + G(p - j\Omega)] \qquad (14\text{-}10a)$$
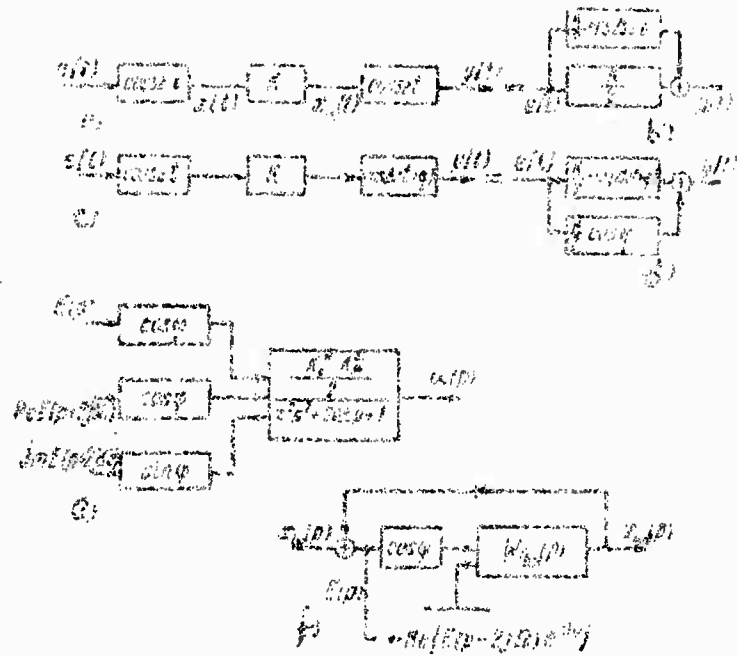
Fig. 14-5. Structural representation of open and closed single-channel AGC with amplitude modulation

By proceeding from the Laplace representation to spectra

$$X(j\omega) = \frac{1}{?}\,\{G[j(\omega + \Omega)] + F[j(\omega - \Omega)]\}, \qquad (14\text{-}11)$$

It is easy to note that the spectrum of the AM signal is equal to one-half of the sum of the spectra of the original process displaced by $\pm\Omega$, i.e., by the frequency of the change in the variable coefficient. When the original

process contains only one harmonic

$$\varepsilon(t) = \sin \omega t, \qquad\qquad (14\text{-}11b)$$

the AM process consists of two harmonics — of the total and differential frequencies:

$$x(t) = \frac{1}{2} [\sin(\omega + \Omega)t + \sin(\omega - \Omega)t]. \qquad (14\text{-}11c)$$

Inertialess Amplification

The further passage of the AM signal along the network of Fig. 14-5,a does not change its properties, but changes only the scale, which forms a new signal $x_{in}(t)$ which has the following representation:

$$X_{in}(p) = \frac{K}{2} [E(p + j\Omega) + E(p - j\Omega)]. \qquad (14\text{-}12)$$

Synchronous and Cophased Demodulation

The representation at the output of the demodulator is tied up with the representation of the input process by the equation (14-10b) for new symbols:

$$Y(p) = \frac{1}{2} [X_{in}(p + j\Omega) + X_y(p - j\Omega)]. \qquad (14\text{-}13a)$$

The substitution of values $X_{in}(p)$ from the preceding equations will result in:

— 1153 —

$$Y(p) = \frac{K}{4} \{ \text{Re } E(p + 2j\Omega) + E(p) \}, \qquad (14\text{-}13b)$$

or

$$Y(p) = \frac{K}{2} E(p) + \frac{K}{4} \{ E(p + 2j\Omega) + E(p - 2j\Omega) \} \qquad (14\text{-}13c)$$

From (14-13b) it simple to obtain the process at the output of the demodulator DM:

$$y(t) = \frac{K}{2} e(t) + \frac{K}{2} e(t) \cos 2\Omega t. \qquad (14\text{-}13d)$$

Consequently, at the output of DM are retained the original signal e(t) which endured only the amplification $\frac{K}{2}$ and its envelope which is filled with the double frequency of the network, i.e., that the network of Fig. 14-5,a can be replaced with the equivalent network "b" with an equivalent amplifier and modulator of the double frequency $\frac{K}{2} - \frac{K}{2}$ cos 2Ωt. The equivalence of the circuits "a" and "b" can be written in the form of equation

$$M_1 \cdot V \cdot DM_1 = \frac{1}{2} (V + M_2) \qquad (14\text{-}13e)$$

In changing to spectra we substitute $p = j\omega$ and from from (14-13e) we obtain the equation

$$Y(j\omega) = \frac{k}{2} E(j\omega) + \frac{k}{4} \{ E[j(\omega + 2\Omega)] + $$
$$+ E[j(\omega - 2\Omega)] \}. \qquad (14\text{-}14a)$$

in which the undistorted input spectrum is present with a scale of $\frac{k}{2}$ and the input spectrum with frequencies shifted by $\pm 2\Omega$.

For the sinusoidal input signal with a single frequency $\sin \omega t$, at the output of m.U. DM network are obtained the signals of the main harmonic and of the total and differential side frequencies:

$$y(t) = \frac{k}{2} \sin \omega t + \frac{k}{4} [\sin(\omega + 2\Omega)t + \sin(\omega - 2\Omega)t].$$
$$(14\text{-}14b)$$

Synchronous Demodulation with a Phase Shift.

The network "c" in Fig. 14-5 illustrates a more general case of a signal passing through m.U. DM when DM is brought to the block of the periodic coefficient with its phase shifted with respect to block M. Resolving the coefficient DM into its components:

$$\cos(\Omega t + \varphi) = \cos \varphi \cos \Omega t - \sin \varphi \sin \Omega t,$$

we obtain the conditions for the transmission of the images by this block:

$$Y(p) = \frac{\cos \varphi}{2} \left[X_{\kappa}(p + j\Omega) + X_{\kappa}(p - j\Omega) \right] +$$

$$+ \frac{\sin \varphi}{2j} \left[X_{\kappa}(p + j\Omega) - X_{\kappa}(p - j\Omega) \right] \qquad (14\text{-}15a)$$

and by the entire circuit:

$$Y(p) = \frac{k \cos \varphi}{2} E(p) + \frac{k}{2} \operatorname{Re} E(p + 2j\Omega) \cos \varphi -$$

$$\left. - \frac{k \sin \varphi}{2} \operatorname{Im} E(p + 2j\Omega). \right\} \qquad (14\text{-}15b)$$

The same equation can be written in a transformed form:

$$Y(p) = \frac{k \cos \varphi}{2} E(p) + \frac{k \cos \varphi}{4} \left[E(p + 2j\Omega) + \right.$$

$$+ E(p - 2j\Omega) \left] - \frac{k \sin \varphi}{4j} \left[E(p + 2j\Omega) - E(p - 2j\Omega) \right]. \right.$$

$$(14\text{-}15e)$$

From equation (14-15b) it is not difficult to obtain the process (original) at the output:

$$y(t) = \frac{k \cos \varphi}{2} e(t) + \frac{k}{2} (\cos \varphi \cdot \cos 2\Omega t - \sin \varphi \cdot \sin 2\Omega t) e(t).$$

or

$$y(t) = \frac{k \cos \varphi}{2} e(t) + \frac{k}{2} e(t) \cos (2\Omega t + \varphi).$$

$$(14\text{-}15d)$$

To this equation corresponds the structural network "d" of fig. 14-4, from which follows the equivalence of the operations $M \cdot g \cdot \mathfrak{M}_{j\varphi}$ and $(M_{\varphi} - M_{2\varphi}) \frac{1}{2}_{c}$ with taking into account the phase shift, which we will write in the form

of the following symbolic equation:

$$M_1 U.D M_{1\varphi} = \frac{k}{2}(Y \cos \varphi + M_{2\varphi}).$$ (14-15e)

Therefore, the output signal of the circuit copies the the input signal with an amplification of $\frac{k}{2} \cos \varphi$ and to it is added the envelope of the input signal filled with a double frequency with a phase shift φ.

In changing to spectra, we obtain the following from equation (14-15c):

$$Y(j\omega) = \frac{k \cos \varphi}{2} E(j\omega) + \frac{k \cos \varphi}{4} \{E[j(\omega + 2\Omega)] +$$

$$+ E[j(\omega - 2\Omega)]\} + \frac{k \sin \varphi}{4j} \{E[j(\omega + 2\Omega)] - E[j(\omega - 2\Omega)]\}.$$

(14-16a)

One harmonic $\varepsilon(t) = 1 \cdot \sin \omega t$ creates at the output:

$$y(t) = \frac{k \cos \varphi}{2} \sin \omega t +$$

$$+ \frac{k}{2}(\cos \varphi \cdot \cos 2\Omega t + \sin \varphi \cdot \sin 2\Omega t) \sin \omega t,$$

or

$$y(t) = \frac{k}{2} \{\cos \varphi \cdot \sin \omega t + \sin [(\omega + 2\Omega)t - \varphi] +$$

$$+ \sin [(\omega - 2\Omega)t + \varphi]\}$$ (14-16b)

-- three items (for addition): main, total, and differential frequencies with a phase shift.

2. Dynamics of a Measuring Open System with an Electromechanical Demodulator (Wattmeter, Wattmeter-Relay)

Let us compose in accordance with the electrical circuit of Fig. 14-1,a a structural diagram shown in Fig 14-5,d which is needed for the analysis. For this purpose and with the specified amplitude of the current $\sqrt{2I}$ in the wattmeter winding connected to the network and the amplitude of the current in the control-winding equal to $\dfrac{\sqrt{2U_n \varepsilon}}{R\varepsilon_M}$ (by disregarding the inductance of the control winding), we will proceed to the amplitude of the torque

$$M = k_\varepsilon^M \varepsilon = \frac{2IU_n k_{12}^M}{R\varepsilon_M}\, \varepsilon. \qquad (14\text{-}17a)$$

The value of the fraction in the right side will be exactly equal to the gain factor $\overset{M}{K}_\varepsilon$ between ε and the torque at the output of the electromechanical demodulator which is present in the equation (14-15b).

Next, this torque will act upon the movable system of the wattmeter or of the wattmeter-relay in which the value $\overset{\alpha}{K}_M$ is in inverse proportion to the rigidity of the spring and determines the stabilized rotation of coil per unit of torque, while the parameters τ and ξ, which are determined as the parameters of the system described in Ch. 1, affect the dynamics of the coil. Taking these factors into account, it

1158

Is possible to write the OTP from the torque to the angle
of rotation as:

$$\frac{\alpha(p)}{M(p)} = \frac{k_M^a}{\tau^2 p^2 + 2\xi\tau p + 1} \cdot \tag{14-17b}$$

Putting the common coefficient $\frac{k}{2}$ out of the parentheses
in the right part of equation (14-15b) and adding it the
single OTP after the demodulator, we obtain a block in the
right side of the structural diagram of fig. 14-15e with a
following OTP:

$$W(p) = \frac{k_a^M k_M^a}{\tau^2 p^2 + 2\tau p + 1} \cdot \tag{14-17c}$$

In accordance with equation (14-15b) we will reform the
left part of the diagram in form of three influences, by
placing in individual blocks the coefficients that do not
depend on the influences.

Let us figure out the transient function for the system
under consideration. We will take the input influence in
form of a single step $\xi(t) = 1(t)$; in this case it will be
represented by $\frac{1}{p}$, while the representation with the
displaced argument is divided easily into the real and
imaginary components:

$$\frac{1}{p + 2/\Omega} = \frac{p}{p^2 + 4\Omega^2} - j\frac{2\Omega}{p^2 + 4\Omega^2} \cdot$$

The overall input influence for anoscillating component will be:

$$Y(p) = \frac{\cos \varphi}{p} + \frac{p \cos \varphi - 2\Omega \sin \varphi}{p^2 + 4\Omega^2} , \qquad (14\text{-}17d)$$

or

$$Y(p) = \frac{2(p^2 \cos \varphi - p\Omega \sin \varphi + 2\Omega^2 \cos \varphi)}{p(p^2 + 4\Omega^2)} . \qquad (14\text{-}17e)$$

The overall representation for the angle of rotation of the coil has a cumbrous written form:

$$\alpha(p) = \frac{2(p^2 \cos \varphi - p\Omega \sin \varphi + 2\Omega^2 \cos \varphi) k_\varepsilon^v k_M^\alpha}{p(p^2 + 4\Omega^2)(\tau^2 p^2 + 2\xi\tau p + 1)} , \qquad (14\text{-}17f)$$

however, by dividing the writing of the input influence (14-17d) among the components with different polarities, it is not difficult to proceed from the representation to the forced motion of the coil, using for this purpose the equations (3-35b) and (3-37) of Ch. 3:

$$\alpha(t) = k_\varepsilon^v k_M^\alpha \cos \varphi \cdot 1(t) + \left(\frac{\cos \varphi}{2\Omega} D - \sin \varphi \right) \times$$

$$\frac{k_\varepsilon^v k_M^\alpha}{[1 - (2\Omega\tau)^2]^2 + 4\xi^2\tau^2 (2\Omega)^2} \sin \left[2\Omega t - \operatorname{arctg} \frac{2\xi\tau (2\Omega)}{1 - (2\Omega\tau)^2} \right] .$$

$$(14\text{-}18a)$$

It is convenient to specify the input influence in convolute form (14-17d) to compute the component of its own motion. The intermediate computations:

$$Y \left(\frac{-\xi + i\sqrt{1 - \xi^2}}{\tau} \right) =$$

$$\ldots \ldots \omega(1+2c^2\Omega^2)+\Omega\sin\varphi - \gamma\sqrt{1-\xi^2}(2\xi\cos\varphi+\Omega\sin\varphi)$$
$$\overline{(\Omega^2-\xi^2)^2-4\Omega^2\xi^2)+\gamma^2(1-\xi^2(\Omega^2-1+4\xi^2\Omega^2)}$$

make it possible to employ equation (3-42d) and obtain as
a result:

$$a_z(t) = \frac{k_2^{xy}k_4^{yl}}{\gamma^2(1-\xi^2)} \times$$

$$\times \sqrt{\operatorname{Re}^2\gamma\left(\frac{-\xi+j\sqrt{1-\xi^2}}{\xi}\right)+\operatorname{Im}^2\gamma\left(\frac{-\xi+j\sqrt{1-\xi^2}}{\xi}\right)} \times \qquad (14\text{-}18b)$$

$$\times e^{-\frac{\Delta t}{\tau}}\sin\left[\frac{t}{\tau}\sqrt{1-\xi^2}+\operatorname{arctg}\frac{\operatorname{Im}\gamma\left(\frac{-\xi+j\sqrt{1-\xi^2}}{\xi}\right)}{\operatorname{Re}\gamma\left(\frac{-\xi+j\sqrt{1-\xi^2}}{\xi}\right)}\right]$$

Just as in the case of forced motion of Fig. 14-18a,
we have in the component of its own motion a mildly mani-
fested second harmonic when the modulation-demodulation
frequency is considerably larger than $\frac{1}{\tau}$ because the coef-
ficients in harmonic processes are small, also, the principal
figure of the output process is determined by the influence
specified for the upper tract of Fig. 14-5,e.

3. Dynamics of a Closed ACS with an Electromechanical Demodulator

Let us draw a structural diagram which corresponds to the electrical circuit of Fig. 14-2,a. In the straight path of the structural diagram running from the block M.DM we will retain only the upper path of the diagram in Fig. 14-5,d, and will regard the additional influences as individual disturbances. The block of the hydraulic motor will be described by a general OFP which will include the additional coefficients of the M.U.DM-block. Upon closing with a standard negative feedback we obtain the structural diagram of Fig. 14-5,b).

An approximate account of the second harmonic which accompanies the M.DM-process is possible in form of an individual disturbance, provided it is intensely filtered by the ACS elements which follow the DM. In this case, there is practically no second harmonic in the feedback and the system is not closed by it. In a ACS with AM, the process $\varepsilon(t)$ computed without taking into account the second harmonic is further utilized for another given influence $.\mathrm{Re}\{E(p+2j\Omega)e^{-j\varphi}\}$, which serves to determine the oscillation-amplitudes of the different elements of the straight path. In certain cases the oscillations have a favorable effect on the ACS elements, for example, by removing the dry friction.

$$\Delta U_e = k_1 \cos \gamma \Delta \alpha - k_2 \sin \gamma \Delta \beta; \qquad (14\text{-}20a)$$

$$\Delta U_g = k_3 \cos \gamma \Delta \beta + k_4 \sin \gamma \Delta \alpha. \qquad (14\text{-}20b)$$

Now it is not difficult at all to prepare a structural diagram shown by Fig. 14-6,b. It is formed by following the general rules for constructing the structure of related systems, as illustrated by Fig. 9-1,d. In addition to the trigonometrical functions, the gain factors introduced by the blocks M.U.DM are included in the OTF of the follow-up systems $W_\alpha(p)$ and $W_\beta(p)$.

The diagram 14-6,b serves to investigate the accuracy and stability of the closed system. It should be remembered that a similar system with simple OTF's of follow-up systems has been investigated earlier for stability with the aid of the criterion proposed by Gurvitz (Sec.II-5) Since the OTF became more complex, the investigation of stability by the frequency-methods is to be preferred.

The second harmonic introduced by the demodulation process can be accounted for as due to the additional influences $\mathrm{Re}\{\Delta \alpha(p + 2j\Omega) e^{-j(\varphi+\tau)}\}$, $\mathrm{Re}\{\Delta \beta(p + 2j\Omega) e^{-j(\varphi+\tau)}\}$, which are supplied to the summators of the structural diagrams.

For the automatic vector-reader, the scheme of which is illustrated in Fig. 14-4, the conditions for establishing

relationships for small deviations are similar to the pre-
ceding scheme and are determined by the phase-shift between
the pedestal voltage of the cosine-demodulator and the supply
voltage of the compensating potentiometer. In the presence
of a shift γ, shown in the vector-diagram "c", the
demodulators release signals similar to (14-19a) and (14-19b):

$$\Delta U_c = \Delta U \cos \varphi \cdot \cos \gamma - \Delta U \sin \varphi \cdot \sin \gamma; \qquad (14\text{-}21a)$$

$$\Delta U_s = \Delta U \sin \varphi \cdot \cos \gamma + \Delta U \cos \varphi \cdot \sin \gamma. \qquad (14\text{-}21b)$$

Deviations from the specified modulus and angle of com-
pleted vector are, as before, determined with the aid of the
undistorted diagram of Fig. 14-4,b and are:

$$\Delta U_p = \Delta U \cos \varphi; \qquad (14\text{-}22a)$$

$$U_p \Delta \beta = \Delta U \sin \varphi. \qquad (14\text{-}22b)$$

Substituting in the equations of (14-21) the values of
the true unbalances from the equations of (14-22), we obtain:

$$\Delta U_c = \Delta U_p \cos \gamma - U_p \Delta \beta \sin \gamma; \qquad (14\text{-}23a)$$

$$\Delta U_s = U_p \Delta \beta \cos \gamma + \Delta U_p \sin \gamma. \qquad (14\text{-}23b)$$

By accepting the OFP of the follow-up systems after the
demodulators in a relatively simple form of $W_p(p) = \dfrac{k_p}{p(Tp+1)}$;
$W_\beta(p) = \dfrac{k_\beta}{p(Tp+1)}$, where the gain factors of the
demodulators are included in the numerators of the OFP's,
except for their functional part we obtain all data needed

1166

to construct the structural diagram shown in Fig. 14-6,d.

The appearance (due to the cofactor) of a variable gain factor along the network U_ρ affects the properties of the process, the accuracy of the vector performance, and the stability.

When the program for changing of U_ρ is specified, the investigation of the processes is carried out based on the theory dealing with systems with variable parameters.

The accuracy of the phase performance is verified for the least value of the modulus ρ. Near the zero-modulus, the system is practically unworkable, unless special steps are taken to equalize the common gain factor.

The stability of the system is verified with the modulus having fixed limit-values by means of conventional methods of the linear theory which is applicable for small increments.

14-4. Filters and Correcting Circuits for AM Signals

Under consideration is a conversion network shown in Fig. 14-7,a in which a linear filter characterized by an OFP of $W_\phi(p)$ is included in the section between M and DM. We will call such a scheme as a M.F.DM scheme.

To obtain the overall OFP of the network it is necessary to use equation (14-10c) and proceed from it to the

representation of the signal at the output of the filter:

$$X_{B\phi}(t) = \frac{1}{2} W_\phi(p)[E(p+j\Omega) + E(p-j\Omega)] \qquad (14\text{-}24)$$

Substituting the obtained result in the equation for synchronous and cophased demodulation (14-13a) will give us:

$$X_{B\phi}(p) = \frac{1}{4}\{E(p)[W_\phi(p+j\Omega) + W_\phi(p-j\Omega)] +$$
$$+ W_\phi(p+j\Omega)E(p+2j\Omega) + W_\phi(p-j\Omega)E(p-2j\Omega)\}. \qquad (14\text{-}25a)$$

or, after elementary conversions:

$$X_{B\phi}(p) = \frac{1}{2}E(p)\,\mathrm{Re}\,W_\phi(p+j\Omega) +$$
$$+ \frac{1}{2}\,\mathrm{Re}\,[W_\phi(p+j\Omega)E(p+2j\Omega)]. \qquad (14\text{-}25b)$$

$$X_y = X_{in}$$

$$X_B = X_{out}$$
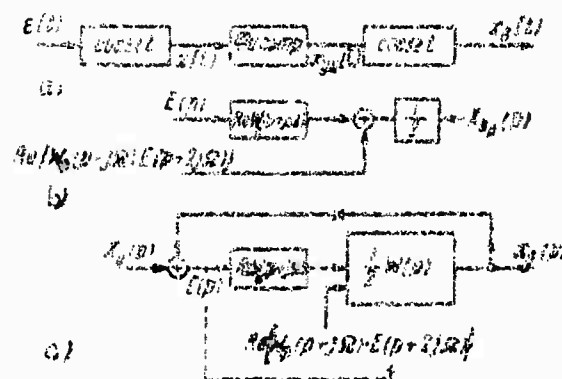
Fig. 14-7. Operating conditions for an operator-filter with a AM signal.

a, b - scheme and structure of an open system, c - structure of a closed system.

The structural diagram for equation (14-25b) is drawn in Fig. 14-7,b. It takes into account the conditions for transmission of the envelope of the effective signal and for generation of the spurious component reflected by the second group of terms in the right part of the equation.

In going over to spectra it is convenient to use the equation (14-25a), from which it follows:

$$X_{\text{мод}}(j\omega) = \frac{1}{4} E(j\omega) \{ W_\phi [j(\omega + \Omega)] + W_\phi [j(\omega - \Omega)] \} +$$

$$+ \frac{1}{4} \{ W_\phi [j(\omega + \Omega)] E[j(\omega + 2\Omega)] + W_\phi [j(\omega - \Omega)] E[j(\omega - 2\Omega)] \}.$$

$$(14-26)$$

In a closed control system, the error-spectrum prior to modulation usually contains a limited band, beyond which appear the frequencies of the pedestal voltages and, therefore, the second group of terms is relatively small. Upon the signal passing through the straight path of the control system, the high-frequency component reduces sharply its amplitude and, for this reason, in the structural diagram of ACS of Fig. 14-7,c it is possible to account for the closing of the system only along the envelope of the effective signal, namely, the first terms in (14-25b) for representing the signals according to Laplace and in (14-26) for representation according to Fourier.

For effective conversion, the envelope filter should, in its turn, have a pass band exceeding the sum of the

The design of a closed AGS of the type shown in Fig. 14-7,c takes into account an equivalent OFP of the filter along the envelope:

$$W_l\,(p) = \frac{1}{2}\,\mathrm{Re}\,W_\phi\,(p + j\Omega) =$$

$$= \frac{1}{4}\,[W_\phi\,(p + j\Omega) + W_\phi\,(p - j\Omega)] \qquad (14\text{-}27)$$

For an equivalent OFP or an equivalent AFCh

$$W_l\,(j\omega) = \frac{1}{2}\,\mathrm{Re}\,W_\phi\,[j\,(\omega + \Omega)] =$$

$$= \frac{1}{4}\,\{W_\phi\,[j\,(\omega + \Omega)] + W_\phi\,[j\,(\omega - \Omega)]\} \qquad (14\text{-}28)$$

there are general requirements which appear when designing correcting circuits; usually these are requirements for a phase-advance, but the transition from requirements for an equivalent OFP to requirements for a real circuit is in this case rather difficult. Let us explain it by using one example.

Real Differentiating Component

We use the OFP of a real component $W_\phi\,(p) = \frac{p}{Tp + 1}$ to determine according to equation (14-27) the equivalent OFP:

$$W_1(p) = \frac{1}{2} \, \text{Re} \, \frac{p + j\Omega}{Tp + 1 + j\Omega T} =$$

$$= \frac{Tp^2 + p + \Omega^2 T}{T^2 p^2 + 2Tp + 1 + \Omega^2 T^2} \, . \qquad (14\text{-}29\text{a})$$

It is seen from the equation that the phase-advancing properties inherent in a real differentiating component at low frequencies are lost in this case, because, upon the decrease of the frequency of the signal $p = j\omega = 0$, the component becomes nearer to an amplifying component:

$$W_1(0) = \frac{\Omega^2 T}{1 + \Omega^2 T^2} \, . \qquad (14\text{-}29\text{b})$$

When the time-constant is reduced to zero, i.e., in a transition to an ideal differentiating component, the м.F.DM network, although retaining the differentiating properties for the envelope, removes in this case the filtering properties for the carrier frequency of the network itself and it loads extensively the path of the demodulator and of the following elements until it becomes suppressed.

Even more loaded turns out to be the input of the demodulator, because during the diferentiation the derivative along the carrier frequency will, naturally, exceed considerably the derivative along the envelope, which serves only as an effective component. The oscillations of the carrier

frequency are the cause of substantial changes in the
transmission properties of a-c networks (4), but in low-
power systems an application is found for stabilization by
using an alternating current   (5).

BIBLIOGRAPHY

and Kalantarov, P. L.,

1. Neyman, L.R./- Teoriya tsepey peremennogo toka,
Teoreticheskiye osnovy elektrotekhniki, sh II (Theory of
a-c Circuits, Theoretical Principles of Electrical Engi-
neering, Part II), Gosenergoizdat, 1959.

2. Chechet, Yu.S. - Dvukhfaznyye asinkhronnyye dvigateli
(Two-phase asynchronous motors), Gosenergoizdat, 1955.

3. Nasonnyye amerikanskiye i angliyskiye radiolokatsi-
onnyye stantsii (American and British ground radar stations),
Voyenizdat, 1947.

4. Shramko, L.S. - Korrektiruyushchiye elementy
peremennogo toka, t.2, ch.II, Osnovy avtomaticheskogo
regulirovaniya (Correcting elements of alternating
current, v.2, part II, Principles of Automatic Control)
edited by V.V. Solodovnikov.

5. Sobubik, A. - Stabilizatsiya servomekhanizmov na
nesushchey chastote (Stabilization of servomechanisms for
the carrier-frequency), Mekhanika, 2nd and 3rd issues, 1960.

INTERMITTENT CONTROL SYSTEMS

(pp. 39?-406)

15-1. STRUCTURE OF FOLLOW-UP SYSTEMS
WITH PULSE ELEMENT

Fig. 15-1,a shows one of the most widely used pulso-type of follow-up systems. It contains a negative feedback that is typical for follow-up systems and in its straight path it has a pulse element PE and a linear continuous part LCP

The pulse element allows the passage of the control signal only during limited intervals of time, which is due usually to the special features present in the design of measuring parts. The specific work of an pulse element, however, does not change the qualitative description of the principles governing the operation of a follow-up system. In fact, in case of a mismatch between the input and output values, the LCP containing the conversion, amplifying, and actuating elements does not change the value of the output. At the appearance of a mismatch, the PE allows the intermittent passage of the control signal into the LCP and its power-part begins to move in the direction orientated to compensate for the mismatch.

The qualitative evaluation of the operating conditions of a ACS with a PE. namely, its sensitivity, precision,

properties of transient processes, and stability, becomes naturally complex and requires a more detailed explanation.

Before proceeding with such an analysis of intermittent control systems we will first examine certain examples which explain the field of application of such systems and the favorable results obtained thereby.
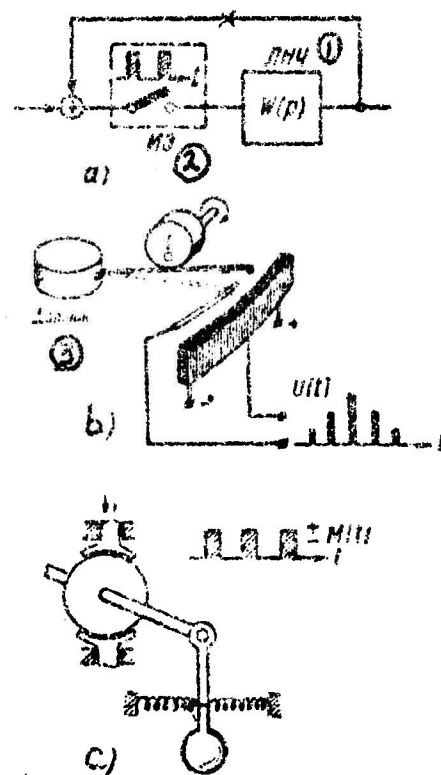
Fig. 15-1. Control system with pulse-element.
a - the general structure; b - intermittent removal of signal from potentiometer transmitter; c - creation of an intermittent friction torque in the oscillating system.
key: 1) Linear continuous part (LCP); 2) pulse-element (PE); 3) transmitter or pickup.

1. Discrete Inflow of Information

In certain cases, a continuous inflow of information related to the input value is not possible. In scanning the air-space by an omnidirectional radar station, for example, the data on each airplane will arrive at a short radiated section only once each time the antenna completes one revolution.

If the information obtained by the omnidirectional (plan-position) radar station is used for tracking the airplane with more accurate radar facilities or optical sighting devices, the follow-up systems of these devices will operate in a regime of intermittent control, but it will, however, solve the problem on tracking.

2. Relief of Pickups

Most of the pickups of physical values, such as direction (gyroscopes), acceleration (accelerometers), pressure (membranes, etc., furnish to the ACS the results of measurement in form of voltages and, for this purpose, it is accomplished by having, for example, the potentiometer wiper or other transient device move away from the sensing element of the pickup. The friction between the wiper and the plate of the potentiometer may reduce substantially the precision of the pickup. However, if the potentiometer wiper is pressed

against the plate not continuously, but intermittently for a short duration of time with the aid of a cylinder on an eccentric axis having a uniform rotation which is shown schematically in Fig. 15-1,b, or by means of a chopper bar used for automatic recording potentiometers, the pickup will be relieved during the pause and will assume its true position and this will make it possible to obtain the result in form of a voltage present during the operating interval of time. Therefore, a regime of intermittent control makes it possible, in this case, to improve the static precision of the pickup.

3. Damping with the Aid of Dry Friction

By applying intermittently the torque of dry friction to the shaft of the measuring system shown in Fig. 15-1,c, it is possible to damp effectively the oscillations of the sensing element without reducing the precision of its set-up during the pause. The structure of such a system of intermittent control will differ from that shown in scheme "a" of the same drawing, but even here the possibility of applying a simple mechanical damping device appeared only due to the transition to intermittent control.

4. Discrete Transmission of Data

For remote transmission it is worthwhile to convert

the continuous control signals into intermittent ones, because it is possible in such a case to use one channel for a simultaneous transmission of several values by having the operating intervals to be used for transmission of one value during the pause in transmission of the second value.

3. Use of Digital Control Machines

The processing of information on complex mathematical relationships received from the ACS pickups for the solution of problems on self-tuning, optimization, three-dimensional control, etc. can be realized in a control process only by high-speed digital computers(HDC). The introduction of such a machine into the ACS network is equivalent to an introduction of a pulse-element, since a solution from a TsVM is received intermittently.

15-2. STATIC AND TIME CHARACTERISTICS OF A PULSE-ELEMENT

a) Porosity

A pulse-element can be compared to a key which, intermittently and for a short time, allows the passage of a control signal and, during the remaining time of the period, opens the ACS circuit along the line of the control signal.

Let us use the same designations as in Fig. 15-2,a:

b - for the operating interval, in seconds;

T — for the period of recurrence of pulses, in seconds;

T - b — the pause, in seconds.

The ratio between the effective interval of time and the period of recurrence of pulses is known as porosity and its designation is:

$$\gamma = \frac{b}{T} = b_* \qquad (15 \cdot 1)$$

The asterisk in the index of the right side of the equality is used to designate the porosity or the relative effective interval in fractions of the period of recurrence of pulses (T); it was also used earlier for all relative values.

b) The Gain Factor

The pulse-element of a type shown in Fig. 15-1,b serves to convert the continuous mismatch signal $\xi(t)$ specified in form of a mechanical angle of rotation of the shaft into a stepped discontinuous function of the voltage variation $U(t)$ shown in Fig. 15-2,a below the curve for the change in angle. For this second curve, the voltage is laid-off along the axis of the ordinate.

The ratio between the height of step h_s of the voltage and the ordinate of the curve of the angle at the beginning of the effective interval h_y is equal to the gain

1176

factor of the pulse-element:

$$k_p = \frac{h_s}{h_y}. \qquad (15\text{-}2a)$$

The gain factor of a linear PE is constant and is equal to the steepness in the slope $\operatorname{tg}\varphi$ of the static characteristic of a pulse-element shown in Fig. 15-2,b:

$$k_p = \operatorname{tg}\varphi = \frac{dh_s}{dh_y}. \qquad (15\text{-}2b)$$

The steepness of curve "b" is not constant for a non-linear pulse-element (PE)
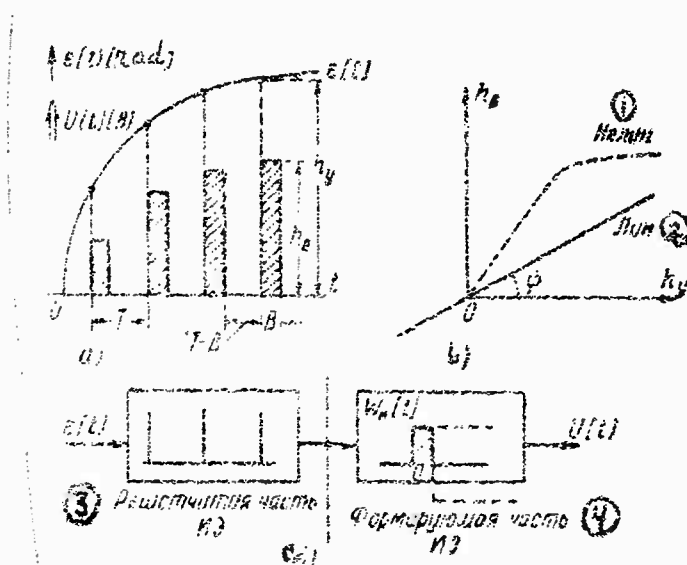
Fig. 15-2. Time and static characteristics of PE.

(1) Nonlinear; (2) linear; (3) latticed part of PE. (4) Shaping part of PE.

For a mathematical description of conditions required for transforming a continuous signal by means of a pulse-element it is useful to attribute to the latter certain fictitious intermediate properties which, together with the subsequent properties of the element, describe correctly its transmitting properties as a whole and, when taken separately, make it easier during the analysis to perform the mathematical conversions. We will explain the aforementioned fictitious intermediate properties separately for the two provisory parts of PE the lattice and shaping which are shown in Fig. 15-2,a.

The lattice part of PE is described as a block of the variable coefficient whose graph degenerates into a lattice of single displaced pulses which form an infinite sequence (pulse train) with a pulse-repetition period T:

$$L[t] = \delta[t] + \delta[t - T] +$$
$$+ \delta[t - 2T] + \ldots = \sum_{m=0}^{\infty} \delta[t - mT]; \quad (15-3a)$$

We will call the sequence (15-3a) as the lattice of single pulse (LSP); its provisory designation is by a symbol of a unit-scale with the sign of the lattice $\underline{\bot}$ written in front.

If a continuous function $\xi(t)$ passes through the

latticed part of FE then, based on the rule for multipli-
cation of pulses by a continuous function (2-10a), the
pulses in the lattice acquire a variable scale (area) which
is equal to the value of the function during the moment of
the pulse's existence:

$$\perp \varepsilon (t) = \sum_{m=0}^{\infty} \varepsilon (mT) \delta (t - mT).$$ (15-3b)

The sequence (15-3b) will be known as LVP -- the lattice
of the variable with the scale used for the pulses; the scales
are given as values of functions in each cycle, while the
latticed shape is again marked in the left part by the symbol
$\perp$ of the lattice of the pulse.

Since the information concerning the type of the functional
part of the process is included in the coefficients during
the occurrence of pulses, it is possible to write separately
the sequence of these coefficients:

$$\varepsilon (nT) = \varepsilon (0), \quad \varepsilon (T), \varepsilon (2T) \ldots$$ (15-3c)

which is known as (LF) -- the latticed function. The latticed
function itself is deprived of energy and is unable to excite
real components. It is widely used in mathematical des-
criptions of given processes as the envelope of the scales
of cyclic pulses.

The writing of scales is substantially simplified by introducing t_* as the designation for the relative time, which is calculated as an integral number of cycles:

$$t_* = \frac{t}{T} = n. \qquad (15\text{-}4)$$

In substituting $t = Tt_*$ it is expedient not to fix the scale of argument t_* in the writing, but to place it a new form of the function; this requires the use of other indexes in form of asterisks for the function of the relative argument:

$$\varepsilon(t)_{t=nT} = \varepsilon(nT) = \varepsilon^*(t_*) = \varepsilon^*(n), \qquad (15\text{-}5a)$$
$$n = 0, 1, 2, \ldots$$

The lattice of single pulses in a relative time and the lattice of variable pulses are both also written in a more complete form:

$$1)[n] = \delta[n] + \delta[n-1] + $$
$$+ \delta[n-2] \ldots = \sum_{n=0}^{\infty} \delta[n-m] \qquad (15\text{-}5b)$$

$$1s^*[n] = \sum_{m=0}^{\infty} s^*[m]\delta[n-m] \qquad (15\text{-}5c)$$

1132

d) The Shaping Part of a Pulse-Element

The shaping part of the pulse element (PE) makes it possible to change from the fictitious pulses introduced in the latticed part to the true output response of the PE. If the actual response of PE is represented in Fig. 15-2,a, where during each cycle there is a response in form of a rectangle with a height equal to the value of the latticed function multiplied by the gain factor of PE, then, by dividing this graph by the ordinate of the latticed function during any cycle, we obtain the weighting function of the shaping part shown in Fig. 15-2,c. Its analytical expression has the form of:

$$w_p[t] = k_p \{1[t] - 1[t - \gamma T]\}. \qquad (15\text{-}6a)$$

The writing of the weighting-function for the relative time is simplified as follows:

$$w_p[n] = k_p \{1[n] - 1[n - \gamma]\}. \qquad (15\text{-}6b)$$

The investigated type of weighting-function of the PE shaping part is typical in design of the measuring element shown in Fig. 15-1,b, when the low-power pickup is unable to overcome the friction of the wiper pressing against the potentiometer and the wiper remains in its initial position during the effective cycle. It is always possible to use a certain average weighting function of the PE shaping

part to give an exact or approximate description of the more complex conditions required to shape the response of the pulse-element. For example, with a drop of information within the range of the effective cycle, from $z^q(n)$ to zero, then according to the linear rule the weighting function of the forming part of the pulse-element will get a new expression:

$$w_\text{m}[t] = k_c \left\{ 1\,[t] - \frac{[t-0]\,{-}\,[t - \gamma\Omega]}{\gamma^2} \right\}. \qquad (15\text{-}6c)$$

Other types of weighting functions, all of which must end during the effective interval, will also contain "shift" (lagging) features, while in other respect they can be subjected to the same analysis, just as the weighting functions of the real components of an automatic control system (ACS).

15-3. APPLICATION OF LAPLACE TRANSFORM FOR THE LATTICE OF VARIABLE PULSES (LVP)

As noted in Ch. 3, the merit of the Laplace transform, which serves as a basis for transforming the discontinuous pulse-functions of time into analytical functions within the range of argument "p", acquires even a larger importance in its application to latticed pulse-processes, because it makes it possible to express the infinite series /sequences/ in a closed form. Let us explain it with typical examples.

Representation of the Lattice
of Single Pulses (LS^E)

Using the Laplace transform for the lattice (15-3a), we obtain:

$$L\{\lfloor\rfloor(t)\} = \sum_{m=0}^{\infty} e^{-mTp}$$

The right side contains the sum of the terms of a geometrical progression with its first term $e^0 = 1$ and a denominator e^{-Tp}; it can be written in a closed form:

$$L\{\lfloor\rfloor(t)\} = \frac{1}{1 - e^{-Tp}}. \qquad (15\text{-}7)$$

Representation of Lattice of Pulses
with Exponential Decline of Scale

$$\varepsilon(t) = e^{-at}$$

Substituting the given form of the function in the sequence (15-3b) and using the Laplace transform, we get:

$$L\{\lfloor\rfloor e^{-at}\} = \sum_{m=0}^{\infty} e^{-amT} e^{-mTp}.$$

To change it into a closed form we use again the equation for the sum of a geometrical progression:

$$\mathcal{L}\left\{ 1 e^{-\gamma t} \right\} = \frac{1}{1 - e^{-T(p+\alpha)}} \,. \qquad (15\text{-}e)$$

Representation of Lattice of Pulses
with cosinusoidal Change of Scale

$$\varepsilon[t] = \cos \Omega t$$

Let us carry out certain transformations in the written form of the given equation:

$$e[t] = \text{Re } e^{-i\Omega t}.$$

We can now use the previous result (15-8) to obtain the L-transformation:

$$\mathcal{L}\left\{ 1 \cos \Omega t \right\} = \text{Re } \frac{1}{1 - e^{-T(p + i\Omega)}}$$

$$= \text{Re } \frac{1}{1 - \cos \Omega T e^{-Tp} + j \sin \Omega T e^{-Tp}}$$

We finally obtain:

$$\mathcal{L}\left\{ 1 \cos \Omega t \right\} = \frac{1 - \cos \Omega T e^{-Tp}}{1 - 2 \cos \Omega T e^{-Tp} + e^{-2Tp}} \qquad (15\text{-}0)$$

Representation of Lattice of Pulses
with Linear Increase of Scale

$$\varrho(t) = t$$

$$L\{\perp t\} = \sum_{m=0}^{\infty} n_i T e^{-mTp}.$$

In this case it is necessary to separate the sum of the geometric progression and find the Λ-transformation that must be performed for the progression in order to reduce it to the form of the right side of the obtained equation. Such a transformation obviously requires a differentiation of "p":

$$L\{\perp t\} = -\frac{\partial}{\partial p} \sum_{m=0}^{\infty} e^{-mTp}.$$

By convolution of the sum under the sign of the derivative, we obtain:

$$L\{\perp t\} = \frac{\partial}{\partial p} \frac{1}{1 - e^{-Tp}} = \frac{Te^{-Tp}}{(1 - e^{-Tp})^2}. \quad (15.10)$$

Λ-Transformation of LSP Representation for a More
Complex Rule for Changing the Scale

It is sufficient to obtain in the closed form the representation of one of the lattices of single pulses (LSP) in order to obtain from it (during a functional change of the lattice-scale by a single linear transformation Λ in the

1187

range of argument "p") a representation of any lattice of variable pulses (LVP) from the common equation:

$$F^\perp(p) = L\left\{ 1_* (t) \right\} = A\left\{ \frac{1}{1 - e^{-Tp}} \right\}, \quad (15\text{-}11)$$

provides the class of functions ε is within the number of coefficients shown in Table 3-1.

The form of A-transformation for each type of coefficient-functions is given in Table 3-1.

If the rule for changing the scale of pulses is broken up into the sum of the function table:

$$\varepsilon_\Sigma (t) = c_1 \varepsilon_1 (t) + c_2 \varepsilon_2 (t) + \dots \quad (15\text{-}12a)$$

then the representation of such a LVP is in the form of the linear form obtained from a A-transformations of the LVP-representations, which correspond to each function in the sum of (15-12a):

$$E_\Sigma^\perp (p) = L\left\{ 1_* \varepsilon_\Sigma (t) \right\} = c_1 \lambda_1 \left\{ \frac{1}{1 - e^{-Tp}} \right\} +$$
$$+ c_2 \lambda_2 \left\{ \frac{1}{1 - e^{-Tp}} \right\} + \dots \quad (15\text{-}12b)$$

If the rule for changing the scale of pulses is reduced to a product of the table-functions:

$$\varepsilon_\Pi (t) = \varepsilon_1 (t)\, \varepsilon_2 (t)\, \varepsilon_3 (t) \quad (15\text{-}13a)$$

then the representation of such a LVP is obtained from the LVP-representation by a successive application to it of

Λ_t-transformations which correspond to each function that is present in the product of (15-13a):

$$E_n^{\perp}(p) = L\left\{\perp e_n(t)\right\} = \lambda_3\left\{\lambda_2\left[\lambda_1\left(\frac{1}{1 - e^{-Tp}}\right)\right]\right\}.$$

$$(15\text{-}13_b)$$

If the rule for changing the scale of pulses contains single functions of type $1(t - n_3T)$, which are biased by an integral number of cycles n_3, then the first term in the geometrical progression corresponding to the representation of ISP will assume the value of e^{-n_3Tp} and the entire sum will change respectively:

$$L\left\{\perp 1(t - n_3T)\right\} = \frac{e^{-n_3Tp}}{1 - e^{-Tp}}.$$

$$(15\text{-}14a)$$

In any other functions, the introduction of lagging will also change in exactly the same manner the first term of the geometrical progression which will make it possible to take out the e^{-n_3Tp} sign from the Λ-transformation and obtain the following result:

$$L\left\{\perp x(t - n_3T)\right\} = e^{-n_3Tp}\lambda_t\left\{\frac{1}{1 - e^{-Tp}}\right\}.$$

$$(15\text{-}14_b)$$

It is easy to check the general methods used for transformation of ISP representations with (15-8) - (15-10) as examples and use them for other cases.

We emphasize that the transformation of the continuous process of LVP is a linear transformation,
for which the principle of superposition is valid, we will show that all LVF obtained above can be generated by a linear system with constant parameters excited by an initial pulse.

Since the generating system is excited by a pulse, the representation of the generating process coincides with the OFP of the system and it is easy to construct the structure of the system by using the OFP.

In Fig. 15-3,a is drawn the structural scheme of a system that generates the weighting function specified by the OFP (15-7) which, for the construction, was taken as the relative OFP of a closed ACS with a positive feedback

$$\Phi_z(D) = \frac{1}{1 - W(p)}$$

From this it follows that with a single straight path, the OFP of the feedback circuit is equal to $1 + e^{-Tp}$ just as shown on the drawing.

For OFP of (15-8), the feedback loop is formed from two links:

$$W(p) = 1 + e^{-Tp}$$

-- an amplifying and lagging links, which are shown in the diagram of Fig. 15-3,b.

For OFP of (15-9), the feedback appears to be branched out in a complex manner;

$$\left| W(p) = + e^{-Tp} (2 \cos \Omega T - e^{-Tp}). \right.$$

The input signal is shaped in form of the sum of signals taken from two points, as shown in diagram "c".
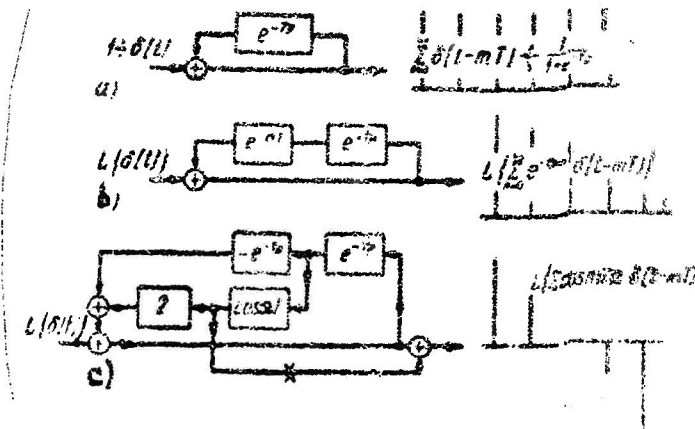
Fig. 15-3. Structural schemes for generators of lattices of variable pulses (LVP).

the writing of LVP-representations can be shortened substantially by designating a typical function in the range of argument "p" by a new intermediate argument:

$$z = e^{+Tp}. \qquad (15\text{-}15)$$

In such a case, the representation for LVP as in (15-7) to (15-9) with an argument z assume the form of:

$$L^z\{\lfloor\!\lfloor 1(t)\}\} = \frac{z}{z-1}; \qquad (15\text{-}16)$$

$$L^z\{\lfloor\!\lfloor e^{-at}\} = \frac{z}{z-e^{-aT}}; \qquad (15\text{-}17)$$

$$L^z\{\lfloor\!\lfloor \cos\Omega t\} = \frac{z^2 - z\cos\Omega t}{z^2 - 2\cos\Omega T z + 1}. \qquad (15\text{-}18)$$

For a biased ISP, instead of (15-14a), we get:

$$L^z\{\lfloor\!\lfloor 1(n - n_s T)\} = \frac{z^{1-n_s}}{z-1}. \qquad (15\text{-}19)$$

These L^z-representations for the above, as well as other processes are located in the third line of Table 15-1.

15-4. TRANSFER PROPERTIES OF OPEN ACS WITH PULSE ELEMENTS

As was noted earlier, the fictitious LVP process from the output of the latticed part of the pulse element enters

its shaping part. The we use the weighting function of the weighting part (15-6,a) to determine its   :

$$W_\phi (p) = \frac{1 - e^{-TP}}{p} \; .$$

(15-20)

Next follows the linear continuous part $\underline{/LCP/}$ with the operator transfer function $\underline{/OTF/}$ given as $W_t (p)$.

As shown in the structural representation in Fig. 15-4,a, the input signal of the open system $e(t)$ passes through the latticed part of the pulse element PE and, depending on the form of the function $e(t)$, acquires the representation (15-11) which is determined in accordance with Table 15-1.

After the transition to representations, a further analysis of the conditions required to transfer the signal becomes an elementary task, namely, it is sufficient to multiply the representation of the signal by the OTF of the subsequent elements which are included in a cascade manner in order to obtain a representation for the output process:

$$X_{out}(p) = \lambda_e \left\{ \frac{1}{1 - e^{-TP}} \right\} \cdot \frac{1 - e^{-TP}}{p} W_t (p) .$$

(15-21a)

The original can be obtained by using the inverse Laplace transform:

$$x_{out}(t) = L^{-1}\{X_{out}(p)\}.$$
$$(15\text{-}21b)$$

However, it is not possible to obtain from the equation (15-21a) the OTF of the entire circuit "a" shown on the drawing, and to obtain it in form of:

$$W(p) = \frac{X_{out}(p)}{E(p)}.$$

The difficulties present in this case are in general typical for all ACS with variable parameters. They can be overcome in this particular case, if instead of analysing the continuous output process, an analysis is made of its corresponding LVP. Then, the representative scheme in Fig. 15-4,b will serve as the starting one for the analysis. The purpose of the analysis will be to determine the OTF of the circuit in form of a ratio between the representations of the NPI of the output and input processes:

$$W^{\perp}(p) = \frac{L\{L x_{out}(t)\}}{L\{L e(t)\}} = \frac{V^{\perp}_{out}(p)}{E^{\perp}(p)}.$$
$$(15\text{-}22)$$

It is not difficult to prove in a fairly common form that such a OTF exists. In fact, the first pulse in the series (15-3c) at the output of the

circuit of Fig. 15-4,b excites an LVP /lattice of variable pulses7

$$L_1 \omega(t) = \epsilon(0) \sum_{m=0}^{\infty} \omega(mT) \delta[t - mT] \div \epsilon(0) W^{\perp}(p);$$

k ∔ first pulse excites a   LVP

$$L_{k+1} \omega(t) = \epsilon(kT) \sum_{m=1}^{\infty} \omega(mT) \times$$

$$\times \delta[t - (m+k)T] \div \epsilon(kT) e^{-kTp} W^{\perp}(p).$$

and the sum of all pulses in the series (15-3b) excites the overall output response of the circuit "b"

$$L x_{out}(t) = L_{\Sigma} \omega(t) = \sum_{k=1}^{\infty} L_k \omega(t).$$

Proceeding to the representations, we obtain equation

$$X_{out}^{\perp}(p) = W^{\perp}(p) \sum_{k=1}^{\infty} e^{-kTp} \epsilon(kT) = W^{\perp}(p) E^{\perp}(p). \quad (15\text{-}23)$$

from which follows the equation of (15-22).

3196
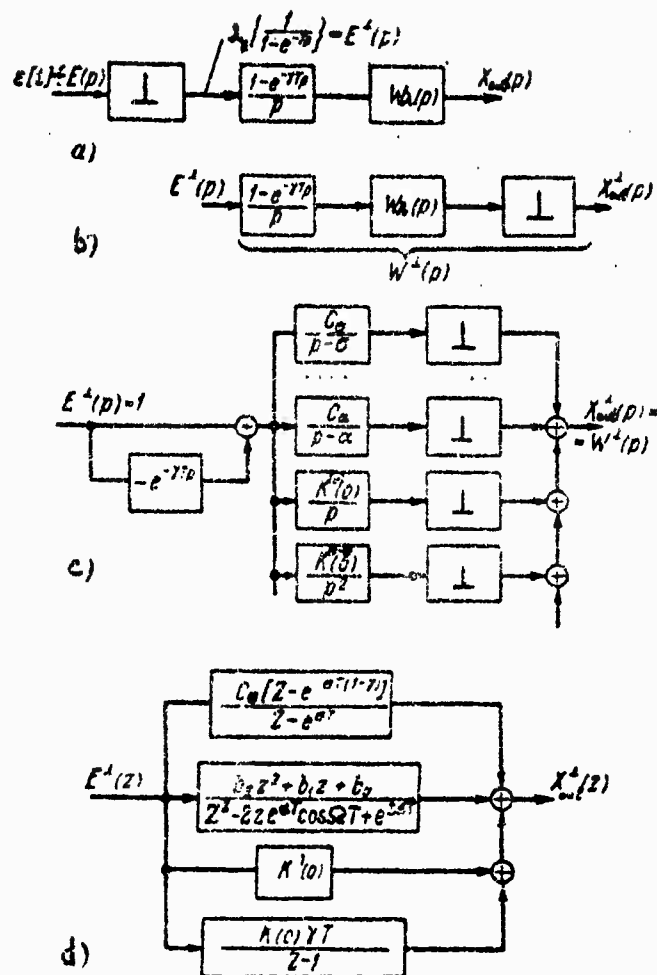
Fig. 15-4. Structural schemes and transformations
of open systems with one pulse-element /PE7.

To calculate the OTF of circuit "b", it is obviously
sufficient to supply to the input of the circuit not the
series of pulses, but only one undisplaced pulse; that will
make the $L\!V\!/\!\rho$-representation at the output to serve as the
sought OTF of the circuit.

Therefore, the calculation of the desired OTF can be reduced to a calculation of the typ-representation. Such calculations have been performed in [5-] for envelopes of the simplest type. To take advantage of these calculations, it is necessary to break up such a complex process as the complete weighting function of circuit "b" into partial weighting functions of the simplest type.

It is convenient to perform the division into elements by basing it on the resolution of a part of the OTF of the circuit $\dfrac{W_i(p)}{p}$ into the sum of the OTF's of the elementary components.

Let the OTF of the linear continuous part be given as a series of ratios between the polynoms and functions in identically coinciding forms:

$$ W_i(p) = \frac{U_i(p)}{V_i(p)\,p^\nu} = \frac{K(p)}{p^\nu} = \frac{U_i(p)}{V_i(p)}. $$

Then, by adding to it the denominator of the OTF of the shaping part of the $p f$, we obtain the characteristic equation

$$ p^{\nu+l}V_i(p) = 0, $$

from which we determine the roots (zero values):

$$ p_1 = 0,\; p_2 = 0,\ldots, p_{s+1} = 0 $$

where ν is the order of the astaticism of LCP and the complex values of $p_{s1} = e_1 = e_1 + j\Omega$, $p_{s2} = e_1 - j\Omega$,

1198

degenerate in certain cases into purely real $p_{20} = \sigma$.

Based on the rules described in Ch. 3, the coefficients
of the resolution are determined from the roots and the
entire OTF of the circuit "b" assumes the following analytical
form at $k_n = 1$:

$$W_L(p) = (1 - e^{-\gamma \tau p}) \left\{ \sum_{a=1}^{k} \frac{\frac{U_L(p_a)}{V_L'(p_a)}}{p - p_a} + \frac{k(0)}{p^{\nu+1}} + \right.$$

$$\left. + \ldots + \frac{k^{(\nu-1)}(0)}{(\nu-1)! \, p^2} + \frac{k^{(\nu)}(0)}{\nu! \, p} \right\} . \tag{15-24}$$

Fig. 15-4,c shows after the first summator to the left
the resolution $\dfrac{W_L(p)}{p}$ into elementary components at $\nu = 1$.
The coefficients written in the blocks of the drawing to
correspond to equation (15-24) are equal to:

$$C_{a_0} = \frac{U_L(z_0)}{V_L'(z_0)} ; \quad C_{a1} = \frac{U_L(z_1 + j\Omega)}{V_L'(z_1 + j\Omega)} =$$

$$= \operatorname{Re} C_{a1} + j \operatorname{Im} C_{a1} ;$$

$$C_{a2} = \frac{U_L(z_1 - j\Omega)}{V_L'(z_1 - j\Omega)} = \operatorname{Re} C_{a2} - j \operatorname{Im} C_{a2} .$$

The input pulse will create in the circuit "c" two
pulses: $\delta[t]$ without a delay and $\delta[t - \gamma \tau]$, which
excite the branched-out circuit.

1199

Let us first analyse a pulse acting without delay.

Components whose OTF is $\dfrac{C\sigma}{p-\sigma}$, where σ is a real number, give rise to the process $C_{0}e^{\sigma t}$, for which the representation of LVP is found by using equation (15-8):

$$X_{\sigma}^{1}(p) = \frac{C_{\sigma}}{1-e^{-T(p-\sigma)}}. \qquad (15\text{-}25a)$$

Components whose OTF is $\dfrac{\operatorname{Re}C + j\operatorname{Im}C}{p-\sigma_{1}-j\Omega}$ have the LVP found formally by using a similar equation:

$$X_{21}^{1}(p) = \frac{\operatorname{Re}C + j\operatorname{Im}C}{1-e^{-T(p-\sigma-j\Omega)}} =$$
$$= \frac{\operatorname{Re}C + j\operatorname{Im}C}{1-e^{-T(p-\sigma)}\cos\Omega T + je^{-T(p-\sigma)}\sin\Omega T}, \qquad (*)$$

but it must be treated together with the LVP representation of the component with a conjugate OTF :

$$X_{22}^{1}(p) = \frac{\operatorname{Re}C - j\operatorname{Im}C}{1-e^{-T(p-\sigma+j\Omega)}} =$$
$$= \frac{\operatorname{Re}C - j\operatorname{Im}C}{1-e^{-T(p-\sigma)}\cos\Omega T - je^{-T(p-\sigma)}\sin\Omega T}, \qquad (**)$$

Then in the overall response (**) and (*) it is possible to get rid of the imaginary component contained in the representation for LVP

$$X_{a12}^{\frac{1}{2}}(p) = \frac{2\left[(1-e^{-T(p-\sigma)}\cos\Omega T)\,\mathrm{Re}\,C + \right.}{1-2e^{-T(p-\sigma)}\cos\Omega T +}$$

$$\frac{\left. + e^{-T(p+\sigma)}\sin\Omega T\cdot\mathrm{Im}\,C\right]}{+ e^{-\sigma T(p-\sigma)}}. \qquad (15\text{-}25\text{b})$$

At $\mathbf{v} = 1$, for a component with OTF of $\dfrac{K'(0)}{p}$ we obtain according to equation (15-7):

$$\left|X_{01}^{\frac{1}{2}}(p) = \frac{K'(0)}{1-e^{-Tp}}\right. . \qquad (15\text{-}25\text{c})$$

For a component with OTF of $\dfrac{K(0)}{p^2}$ we use equation (15-10) which will give us:

$$\left|X_{02}^{\frac{1}{2}}(p) = \frac{K(0)\,Te^{-Tp}}{(1-e^{-Tp})^2}\right. . \qquad (15\text{-}25\text{d})$$

We will now analyse the effect exerted on the same circuit by a delaying pulse $\delta\left[t - \gamma T\right]$.

The delay of the input pulse with respect to cyclic pulses of the output lattice is equal to γT. As long as we have $0 < \,\, < 1$, then regardless of the value of γ, the first pulse will be absent in the output LVP and only the second pulse will have time enough to become shaped, therefore, in equations (15-14) we have always that $n_3 = 1$. However, the value of the weighting function at the time of arrival

for the second and subsequent pulses will now depend on the value of γ and will form the following series:

$$\omega_i[T(1-\gamma)],\ \omega_i[T(2-\gamma)]\ldots\omega_i[T(m-\gamma)]$$

Writing a similar series for the function $\varepsilon[t-\gamma T]$ we obtain a lattice of pulses with a variable scale with the following representation for the lattice:

$$L\{z_i[t-\gamma T]\}=\sum_{m=1}^{\infty}\{\varepsilon[T(m-\gamma)e^{-mTp}]\}\quad(15\text{-}26a)$$

By resolving the envelope into a series arranged according to the degrees of $\tau-T$, we obtain:

$$\ldots\varepsilon[T-\gamma T]+\varepsilon'[T-\gamma T](t-T)+\\+\varepsilon''[T-\gamma T]\frac{(t-T)^2}{2!}+\ldots$$

substituting this series in (15-16,a) we obtain the following intermediate equation:

$$L\{z_i[t-\gamma T]\}=e^{-Tp}\left\{\varepsilon[T-\gamma T]-\varepsilon'[T-\gamma T]\frac{\partial}{\partial p}+\right.\\\left.+\frac{\varepsilon''[T-\gamma T]p^2}{2!}\cdot\frac{\partial^2}{\partial p^2}+\ldots\right\}\frac{1}{1-e^{-Tp}}$$

and the final equation representing the lattice of variable pulse $[t-\gamma T]$ shifted inside the first time-cycle:

1202

$$L\left\{\perp_x[t-\gamma T]\right\}=e^{-Tp}\left\{\frac{\epsilon[T-\gamma T)}{1-e^{-Tp}}+\right.$$

$$\left.+\frac{\epsilon'[T-\gamma T)\,Te^{-Tp}}{(1-e^{-Tp})^2}-\frac{\epsilon''[T-\gamma T)\,T^2(e^{-Tp}+e^{-2Tp})}{2!\,(1-e^{-Tp})^3}+\cdots\right\}.$$

$$(15\text{-}26b)$$

Applying this equation for the envelope in form of a function raised to a power, for example, $(t-\gamma T)^2$, gives us:

$$L\left\{\perp[t-\gamma T)^2\right\}=e^{-Tp}\left\{\frac{(1-\gamma)^2\,T^2}{1-e^{-Tp}}+\frac{2(1-\gamma)\,T^2e^{Tp}}{(1-e^{-Tp})^2}+\right.$$

$$\left.+\frac{T^2(e^{-Tp}+e^{-2Tp})}{(1-e^{-Tp})^3}\right\}.$$

It is convenient to use this equation for envelopes in form of polynoms having a limited number of derivatives. For exponential envelopes $e^{\alpha[t-\gamma T)}$ the shift does not give rise to new functions, but changes only the scale of the first term $e^{\alpha T(1-\gamma)}$; this makes it possible to obtain the representation for the exponent from equation (15-8) or from (15-14b) which is shifted inside the first time-cycle and use it for the real and complex exponents α:

$$L\left\{\perp e^{\alpha[t-\gamma T)}\right\}=\frac{e^{-Tp}e^{\alpha T(1-\gamma)}}{1-e^{-T(p-\alpha)}}.\qquad(15\text{-}26c)$$

Consequently, for components with representations of undelayed $\iota V p$, after the introduction of delay inside the the first time-cycle, the described equations (15-25a-d)

1203

make it possible to obtain respectively new equations:

$$X^{\downarrow}(p,\ \gamma) = \frac{C_0 e^{-T} e_C {}^{0T(1-\gamma)}}{1 - e^{-T(p-s)}};\qquad (15\text{-}27a)$$

$$X_{\alpha/2}^{\downarrow}(p,\ \gamma) =$$

$$= \frac{2\left[e^{-2T(p-s)}\operatorname{Re} Ce^{-j2jT} - e^{-T(p-s)}\operatorname{Re} Ce^{j\Omega(1-\gamma)}\right]}{1 - 2e^{-Tp(p-s)}\cos\Omega T + e^{-2T(p-s)}} - T]$$

$$(15\text{-}27b)$$

These two equations use the rule set forth in (15-26c);
the first uses it directly and the second — by direct and
inverse substitution of harmonic functions by exponential ones.

Next come:

$$X_{01}^{\downarrow}(p,\ \gamma) = \frac{K'(0) e^{-Tp}}{1 - e^{-Tp}};\qquad (15\text{-}27c)$$

$$X_{3}^{\downarrow}(p,\ \gamma) = \frac{(1-\gamma)e^{-Tp}TK(0)}{1 - e^{-Tp}} + \frac{K(0)Te^{-\gamma Tp}}{(1 - e^{-Tp})}\qquad (15\text{-}27d)$$

These two equations correspond to the first and to the
first two terms of the dependence (15-26b) by taking into
account the coefficients $K(0)$ and $K'(0)$ at $\gamma = 1$.

The unification of the difference between the OTF's(as
determined by the equations (15-25) and (15-27)) into one
component makes it possible to obtain a OTF of a new

1204

structural scheme "d" which consists only of matching - parallel circuits. All OTF of the circuits are written on the drawing in form of $\mathbb{Z}$-transformations (see (15-15) ; in this case, a single $zOTF$ of the circuit has the following analytical expression:

$$
\begin{aligned}
W^\perp(z,\,\gamma) = &\sum_{\sigma_l}^{\sigma_k} \frac{C_\sigma\,[z - e^{T\sigma(1-\gamma)}]}{z - e^{\sigma T}} + \\
&+ \frac{2z^2\,\mathrm{Re}\,C - 2z\,\{e^{\sigma(1-\gamma)T}\,\mathrm{Re}\,[Ce^{-j\Omega(1-\gamma)T}] + e^{\sigma T}\,\mathrm{Re}[Ce^{j\Omega T}]\} +}{z^2 - 2z e^{\sigma T}\cos\Omega T} \\
&\frac{+ 2e^{\sigma T(2-\gamma)}\,\mathrm{Re}\,[Ce^{-j\Omega\gamma T}]}{+ e^{2\sigma T}} + \\
&+ K'(0) + \frac{K(0)\gamma T}{z - 1}\,. \tag{15-28}
\end{aligned}
$$

The structural scheme and the analytical expression in (15-28) are given in a non-convolute form to retain the clearness in the necessary inverse transformations from a single OTF to the primary weighting function (the original).

The role of $zOTF$ in $\mathbb{Z}$-representations is the same as in conventional representations, i.e.,

$$
X_{out}^\perp(z) = X_{in}^\perp(z)\,W^\perp(z). \tag{15-29}
$$

If the output process of the entire scheme W_1 is again admitted to the next input of component W_{II} having a latticed-pulse output, then, by applying to the second component the equation (15-23) for the conditions required for transfer

1205

$$X_{11}^+(z) = \left\{ X_{A}^+(z) W_{11}^+(z) \right\} W_{11}^+(z) \dots W_{11}^+(z) W_{R}^+(z) X_{A}^+(z). \quad (15\text{-}30)$$

The same method, if applied to any structural scheme
containing linear components $W(p)$ having the latticed part
of the pulse-element at the output, makes it possible to
prove without difficulty ⌢ also the validity of
more general rules of structural transformation for pulse
systems. For example, an iterated circuit of five blocks,
each containing a "component + latticed part of W" shown in
Fig. 15-5,a, is transformed according to the general rules
into scheme A which, in its turn, is easy to convolute
according to equation (15-30) and results in a single ZOTF
as the product of the ZOTF of three blocks.

Let us note that scheme "a" has mainly a methodic value;
it illustrates the ability to develop the structural methods
also in the field of pulse systems when using ACS containing
several synchronous-copassed pulse elements, in which case
the problem dealing with structural transformations has a
very simple solution. This simple way of obtaining the ZOTF
of the entire scheme from the ZOTF of individual blocks is
immediately disrupted as soon as the pulse elements are
eliminated in the intervals between the components. For
example, the following operations must be performed to find

a single z-OTF [Operator transfer function] of scheme "b",
even for such a simple two-component scheme as the one shown
in Fig. 15-5,b:

to find all (N_1) poles of $W_1(p)$;

to find all (N_2) poles of $W_{II}(p)$;

to resolve the products $W_I(p)W_{II}(p)$ into very simple
fractions W_k based on the obtained poles;

to determine the partial z-OTF for each $W_i(p)$;

to add up all partial z-OTF.

In this case, out of all above calculations performed
to determine the z-OTF of individual blocks of very simple
schemes, only the first two operations can be used with
a certain degree of success.

Returning back to the beginning of this *section*, let
us remember that in order to analyse the processes taking
place in an isolated open circuit containing one pulse-
element it is entirely unnecessary to determine the overall
z-OFP of the entire circuit, because all properties of the
processes are described by equations (15-21a) and (15-21b).
The transfer properties for the lattices of variable pulses
become of value when additional sections containing new
pulse-elements are added to the circuit or, what is extremely
important, when closing an open system with proportional
feedback.

1207
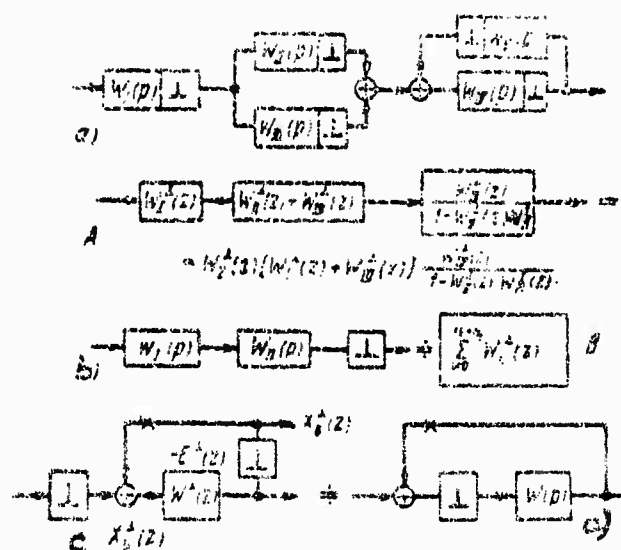
Fig. 15-5. Block-diagrams for ACS with several PE; also their cited and not cited schemes.

15-5. z-TRANSFER FUNCTIONS AND ACCURACY OF CLOSED ACS CONTAINING A PULSE-ELEMENT

Fig. 15-5,c shows a typical arrangement of a closed ACS containing a PE /pulse-element7. To make it easier to analyse the system, it is expedient to transfer the summator through the latticed part of the PE, as shown in scheme "c". The pulse-element can be taken to the linear components containing variable parameters, for which the rules for structural transformation have been proven in Ch. 5. In this case, use is made of the rule on duplicating the PE during the transfer of the summator through the PE in accordance with the course taken by the signal.

The following new points can be marked in the obtained diagram C. $X_{in}^{\perp}(z)$ for the input, $X_{out}^{\perp}(z)$ for the output, and $E^{\perp}(z)$ for removal of error, so that the subsequent calculations may be performed only to represent $\angle YP$, while the scheme with zOTF is fully suitable for typical structural transformations, because it contains "separable" PE.

In accordance with the scheme we write the following relationships:

the equation to determine the error or the conditions required for closing:

$$E^{\perp}(z) = X_{out}^{\perp}(z) - X_{in}^{\perp}(z); \qquad (15\text{-}31)$$

for the principal zOTF:

$$\Phi^{\perp}(z) = \frac{W^{\perp}(z)}{1 + W^{\perp}(z)}; \qquad (15\text{-}32)$$

for the relative zOTF (zOTF of the error):

$$\Phi_{\bullet}^{\perp}(z) = \frac{1}{1 + W^{\perp}(z)}. \qquad (15\text{-}33)$$

Let us remember that the zOTF of the open system that is present in the last two equations includes the OTF of the linear continuous part and the shaping part of PE, which taken together are designated by $W(p)$ and then by by $W^{\perp}(z)$.

1209

The subsequent calculation of $W^\perp(s)$ is by resolution of $W(p)$ into elementary components of type shown in (15-25a - d) and (15-27a - d) followed by uniting the partial functions in accordance with equation (15-28), which will give us:

$$W^\perp(z) = \frac{u_m z^m + \ldots + u_1 z + u_0}{v_n z^n + \ldots + v_1 z + v_0}, \qquad (15\text{-}34)$$

where the coefficients u_i and v_j are constant and a part of them depends on γ; the order of the denominator n is equal to the order of the initial OTF $W(p)$ without taking into account the zero-terminal of the shaping part of the pulse-element, while the order of the numerator m is in most cases less than the order of the numerator ($m < n$).

It is not difficult to proceed from the algebraic form of (15-34) to the similar forms for specifying the ZOTF of a closed ACS, both the principal and relative, determined by equations (15-32) and (15-33):

$$\Phi^\perp(z) = \frac{u_m z^m + \ldots + u_1 z + u_0}{\mu_n z^n + \ldots + \mu_1 z + \mu_0}; \qquad (15\text{-}35)$$

$$\Phi^\perp_\varepsilon(z) = \frac{v_n z^n + \ldots + v_1 z + v_0}{\mu_n z^n + \ldots + \mu_1 z + \mu_0}. \qquad (15\text{-}36)$$

The new coefficients μ_i of a closed z-OTF are connected with the coefficients z-OTF of an open ACS for typical

1228

conditions required for closing through the standard relationship of:

$$\mu_i = u_i + v_i \tag{15-37}$$

Based on the derived equations it is possible to show a number of properties possessed by pulsing ACS which were studied earlier for continuous linear systems.

Astatic Pulse-Systems

Let us write the expression for the error in form of z-representations:

$$- E^\perp(z) = \Phi_c^\perp(z) X_y^\perp(z) \tag{15-38}$$

and assume that the input effect in the envelope of LVP has an exponential relationship

$$x_y(t) = (t)^{\nu-1}; \tag{15-39a}$$

$$X_y^\perp(z) = \frac{U_x(z)}{(z-1)^\nu}. \tag{15-39b}$$

While decoding the contents of the polynom of the numerator in the representation of $U_x(z)$ it is important to pay attention to the denominator of the representation, the terminals of which determine the nature of the process.

If in the content of the representation of the output

1211

process, namely, the error in (15-38), there will be present components with terminals z=1, then, depending on whether these terminals are multiples, the error being the original process will be characterized by the undamped lattices of the values having envelopes in form of constant, linear, quadratic, or exponential functions.

These components of the error can be avoided by introducing terms into the numerator z OTF of the error $\Phi_\delta^\perp(z)$ which coincide with the terminals of the input effect:

$$\Phi_\delta^\perp(z) = \frac{V_\delta(z)(z-1)^\nu}{M(z)}. \qquad (15\text{-}40)$$

In this case, the coinciding binoms in (15-39b) and (15-40) will become abridged in the product (15-38) and undamped LTF will not be observed during the forced motion of the pulsing ACS along the error-line. The absence of undamped LTF in the natural action of the ACS is established by checking the system for stability, which will be the subject of the next paragraph.

An ACS which reproduces without an error the input signal in form of a polynom is called an ACS with astatic control action. The order of astaticism is a multiple of the single terminal in the OTF of the error of a closed ACS.

Since the numerator in OTF of the error (15-36) coincides with the denominator in OTF of a straight path (15-3a),

1212

the order of the astaticism of a closed ACS is also a
multiple of the single terminal of the $ОПF$ of an open
system. In observing the conditions for shaping $W^{\downarrow}(z)$ in
accordance with equation (15-28) it is easy to note that all
cascade-connected integrating components that were present
in the straight path are reduced after the resolution into
parallel-connected components and, after the convolution of
equation (15-28), or after reducing all of its terms to a
common denominator, it retains all terminals of the parallel
components.

Hence, the order of astaticism is also equal to the
number of integrating components in the $U^T P$ of the linear
continuous part of an open system. Let us note that one
integrating component introduced in the $O ПF$ of the shaping
part of the pulse-element does not create the $(\nu=1)$ astati-
cism because, judging from the analysis of a parallel cir-
cuit, it shapes not the sequence of pulses in the weighting
function, but only one input pulse with an effort of $K'(0)$,
$\left[\text{the term next to the last in (15-28)}\right]$. Just as in this
case, in common with the single integrating component, the
ЛНCh which shapes the integrating component in the equation
for the difference $\left[\text{the last term in (15-28)}\right]$ also does not
increase the astaticism.

Let us rewrite the ADC errors in equation (15-24) into a series arranged according to the powers of $z - 1$:

$$Q(z) = Q_1(z) + Q^1(z)(z-1) + \frac{Q^{11}(z-1)^2}{2!} + \ldots (16\cdot1)$$

and let us analyse the action of the operator $(z - 1)^k$ upon the input signal $x_y[t]$.

For $k=1$, we have a conformity of

$$(z-1)X^1(z) = [x(t+T) - x(t)] \qquad (*)$$

Adding up in any m-th path the IVP obtained in the right side of the conformity will give us the difference in values at a point $x[(t-T)]$, which is equal to

$$x[(m+1)T] - x[mT] = \Delta x[mT] = Tx^1[mT]$$

Consequently, the difference in IVP of (*) displaced by a small interval (one ti s-cycle in this case) makes a new IVP, the envelope of which varies as the derivative from the primary rule and has an additional scale t:

$$(z-1)X^1(z) + T \perp x[t] \qquad (16\cdot2)$$

For $n=2$, the initial conformity is somewhat more complex, but again, it is reduced to simpler

$$(z-1)^2 X^1(z) = (z^2 - 2z + 1)X^1(z) =$$
$$= [z^2 - z - (z-1)]X^1(z) =$$
$$+ [[x[t+2T] - x[t+T]] - [x[t+T] - x[t]]] \qquad (**)$$

For the scale of the m-th pulse we will apply the rule
for obtaining the first difference in the brackets and the
second difference between the parenthesss:

$$[x(t + 2T) - x(t + T)] - [x(t + T) - x(t)] =$$
$$= T\dot{x}(t + T) - T\dot{x}(t) \approx T^2 \ddot{x}(t).$$

The analysis of the scale of an arbitrary pulse of the
lattice shows that the envelope of the difference (**)
varies with the second derivative of the initial process
increased by T^2 times:

$$(z - 1)^2 X^{\perp}(z) \div T^2 \perp \ddot{x}(t) \qquad (15\text{-}42b)$$

Based on similar transformations, for the present value
of "z", we obtain:

$$(z - 1)^k X^{\perp}(z) \widetilde{\div} T^k \perp x^{(k)}(t). \qquad (15\text{-}42c)$$

having obtained a group of conformities (15-42a - c), it
is not difficult to proceed (by taking into account the (15-41)
resolution) from the equation of the error in z-representations
to the error conceived as a time-process:

$$-\perp z(t) = \Phi_z^{\perp}(1) \perp x_y(t) + \Phi_z^{\perp'}(1) \perp \dot{x}_y(t) +$$
$$+ \Phi_z^{\perp''}(1) \frac{\perp \ddot{x}_y(t)}{2!} + \ldots \qquad (15\text{-}43)$$

The obtained series determines the components of a ACS error from the coordinate of the envelope, from its velocity, acceleration, and from any first derivatives, in case there is a damping of its natural motion. Let us remember that the point $z=1$, near which was performed the resolution of (15-41), corresponds to $p=0$ which, in its turn, corresponds to $t \to \infty$ in terms of time.

The coefficients of the series (15-43) are called the coefficients of the error. The smaller are the values of the derivatives in the input-process and their corresponding coefficients of error, the higher is the accuracy of the ACS.

The error in a stabilized regime is calculated from each k-th derivative in the envelope of the input-process and is performed according to the single-type equation:

$$- \varepsilon_{iM} = \frac{x^{(i)}_M \cdot \Phi_1^{(m_i)}(1)}{m!}.$$ (15-44a)

The overall error of the forced motion is determined by an algebraic sum of errors from each derivative, if the maximums coincide:

$$- \varepsilon_M = \sum_{(i=)}^{i} \varepsilon_{iM}.$$ (15-44b)

and by summing up statistically in more complex cases. If the given maximum is $x^{(i)}_{iM}$ and the allowable value of the

1216

component of the error from this derivative is $\mathcal{E}_{i \; addit}$, the required coefficient of error is calculated by using the inverse equation of (15-44a):

$$\frac{m!}{\Phi^{\perp(m)}_*(1)} = \frac{X^{(i)}_M T^{-i}}{|\mathbf{s}_{i \; addit}|} . \tag{14-44 c}$$

Referring to the conditions required for shaping the OFP of the error, it is possible to establish that all coefficients of error are decreasing with the increase in the gain factor of a straight path, just as in case of continuous ACS.

15-6.   THE ASYMPTOTIC STABILITY OF ACS CONTAINING A PULSE-ELEMENT

Indicators of Stability

The pulse-system is aymptotically stable if the RPI of the weighting function of a closed ACS has a damping envelope.

The weighting function, as a process, contains a number of components; their representations may be reduced to the elementary types expressed by equations (15-16) to (15-19), if, by using the characteristical equation $M(z) = 0$ of a closed ACS obtained from the z OTF of (15-35) or (15-36), we find the roots of z_i; $i = 1, 2, \ldots . n$.

The root $z_1 = 1 \cdot e^0$ forms during the resolution of $M(z)$ into cofactors a binom $z - 1$ and, during the resolution of $\Phi^4(z)$ into simple fractions, it forms a representation of type (15-16), the original for which is served by $REI(sic)$

The root $z_2 < 1$ yields a partial representation of the type of (15-17) and LVP with a damping according to $\sigma = \frac{1}{T} \ln |z_2|$.

The root $z_3 > 1$ results in a representation which is similar to the latter to (15-17) and in a LVP with an exponentially increasing envelope.

At $z_4 = 1$, the complex roots $z_4 = \alpha \pm j\beta$ result in processes having the form of LVP with a representation of the type as in (15-18), where the envelope changes harmonically in the original without damping. Damping requires that $|z_4| < 1$ and, respectively, $|z_4| > 1$ leads to harmonically increasing envelopes of LVF, in accordance with (15-18).

In order to obtain the damping of the overall LVP envelope of the weighting function, it is obviously necessary that all partial envelopes should become damped. Hence, as an indicator of asymptotic stability in the range of argument "z" will be the following condition:

$$|z_i| < 1; \; i = 1, 2, \ldots, n, \qquad (15-46a)$$

i.e., the moduli of all roots must be less than unity, or all roots of the polynom $M(z)$ must be within the circle with a radius equal to unity.

If the relationship of (15-15) is taken into account for the transition from the range covered by "z" to the range covered by "p", then by using the root $z_i = \text{Re } z_i + j\text{Im } z$ we can calculate its equivalent $p_i = \text{Re } p_i + j \text{ Im } p_i$.

The condition $z_i = e^{+ Tp_i} = e^{T(\text{Re } p_i + j \text{ Im } p_i)}$ serves to find the real and imaginary components:

$$\text{Re } z_i = e^{T \text{ Re } p_i} \cos(T \text{ Im } p_i);$$
$$\text{Im } z_i = e^{T \text{ Re } p_i} \sin(T \text{ Im } p_i),$$

from which

$$\text{Im } p_i = \frac{1}{T} \text{arctg} \frac{\text{Im } z_i}{\text{Re } z_i};$$
$$\text{Re } p_i = \frac{1}{T} \ln |z_i|.$$

The condition $|z_i| < 1$ means that the logarithm in the last equality is negative and that as an indicator of stability may be served by the negative feature of the real part of the root p_i of the function $M^{\perp}[z(p)] = 0$:

$$\text{Re } p_i < 0, \; i = 1, 2, \ldots, n, \qquad (15\text{-}45b)$$

which coincides with the indicator of stability of linear continuous systems.

1219

By substituting $p = j\omega$ in (15-15) and by varying the frequency from 0 to $\frac{\pi}{T}$ it is possible to draw a hodograph of the vector $z(j\omega)$ having the shape of a semicircle with a unit-radius and formed by a left (positive) rotation.
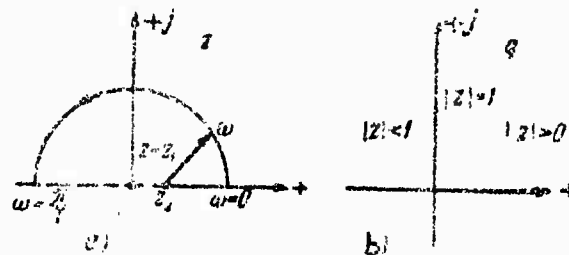
Fig. 15-6. Planes of roots z_i and q_t used to determine the criterion of stability.

As shown in Fig. 15-6.a, the vector of the difference $z - z_i$ within the above range of frequency-variation turns over two quadrants in a positive direction if z_i is located inside the unit-radius circumference and has a zero overall rotation, if the root z_i is located outside the unit-radius circumference. If the roots $z_i = \alpha \pm j\Omega$ are complex conjugates, then we have in mind the average angle of rotation that involves each of the two roots --

with a positive and negative imaginary part. Since the polynom $M^1(z)$ breaks up into the product of difference-vectors, the hodograph of vector $M[z(j\omega)]$ at the same range of frequency variations will obtain an angle of rotation that is equal to the sum of angles of rotation of the elementary vectors.

Since the location of the roots with respect to the unit-circumference is controlled by the angle of rotation of the overall vector for a known order of n of the polynom $M[z(j\omega)]$, it will also control the asymptotic stability. A closed ACS containing a pulse-element has an asymptotic stability, if the analogue of Mikhaylov's vector $M^1[z(j\omega)]$ during the variation of frequency from zero to $\frac{\pi}{T}$ is rotated in a positive direction by 2n quadrants:

$$\varphi M^1_{stability} = \pi n.$$ (15-46)

An Analogue for the Nyquist Criterion

Acriterion of stability -- an analog for the Nyquist criterion -- is readily obtained by taking advantage of the rules for continuous linear systems developed in Ch. 11 and by the considerations that were taken into account when evolving the analogue for Mikhaylov's criterion (15-46). According to this criterion, a closed ACS containing a pulse-element will be stable if, during a frequency-variation from

1221

θ to $-\frac{\pi}{2}$, the hodograph of function $N^{\ast}[z(j\omega)]$ will turn

about point 1.5 by an angle consisting of:

$$\psi_{\text{stability}}^{\ast} = \pi(l_p + 2r_p) \qquad (15\text{-}47)$$

where a_p is the number of roots of polynom $N^{\ast}(z) = 0$ that
$\qquad$ resides with respect to the unit-circumference;

$\qquad \omega_p$ is the number of neutral, i.e., located along the
$\qquad$ unit-circumference, roots of the polynom $N^{\ast}(z) = 0$
$\qquad$ which is included in the denominator of $(15\text{-}2\xi)$.

Analytical Criteria of Stability

The substitution

$$q = \frac{z+1}{z-1} \qquad (16\text{-}48)$$

converts the unit-circumference into an axis γ (ω) of the
plane q. The finding of vector z_i inside the unit-
circumference is equivalent to finding q_i in the left half
of the plane, therefore, the polynom $N^{\ast}[z(q)] = 0$ is also
suitable for the criteria of Hurwitz, Raus, and Vyshnegradskiy,
but as before, these criteria refer to a closed ACS con-
taining a pulse-element.

The analysis properties of pulse-systems disclose to a
fair degree the possibilities of a mathematical device for a
Z-transformation and of structural methods for the new class

1242

of special control systems of significant importance, in view of the introduction into control-circuits of digital computers which operate in an intermittent regime of supplying solutions (B.5 and 3).

The similarities traced between pulse-systems and continuous linear systems make room for other evaluations of ACS /Automatic Control systems/ from different viewpoints described in preceding chapters; it refers to a larger extent also to pulse-systems.

A fundamental analysis of pulse systems was carried out by Doctor of Technical Sciences, winner of the V.I. Lenin Prize, prof. Ya.Z. Tsypkin (B.1), by Doctor of Technical Sciences, V.P. Perov (B.2). An interesting generalization of z-transformations based on the Stiltt'es integral is is presented in the work of H.A. Holm (B.4)

BIBLIOGRAPHY

1. Tsypkin, Ya.Z. - Teoriya impul'snykh sistem (Theory of Pulse Systems), Fizmatgiz, 1958.

2. Perov, V.P. - Staticheskiy sintez impul'snykh sistem (Static Synthesis of Pulse Systems), published by Sovetskoye Radio (Soviet Radio), 1950.

3. Pospelov, G.S. - Sistemy impul'snovo regulirovaniya (Pulse-Control Systems), Sbornik "Avtomaticheskoye upravleniye i vychislitel'naya tekhnika" (Symposium "Automatic Control and Computer Engineering", No 3, Mashgiz, 1959.

4. Kuo, B.C. - z-transformation, Bell System Technical Journal, January 1958.

5. Tou, J.T. - Digital and Sample Data Control Systems, McGraw Hill Book Company, New York, 1959.

LIST OF TABLES

[According to Chapter and Section; e.g. Chap 1, Sec. 1 = 1]

- E N D -